UNITED STATES DEPARTMENT OF THE INTERIOR

GEOLOGICAL SURVEY

PROCEEDINGS OF

CONFERENCE X

EARTHQUAKE HAZARDS ALONG THE WASATCH AND SIERRA-NEVADA FRONTAL FAULT ZONES

Convened Under Auspices of

NATIONAL EARTHQUAKE HAZARDS REDUCTION PROGRAM

29 July 1979 – 1 August 1979

OPEN-FILE REPORT 80-801

This report is preliminary and has not been edited or reviewed for conformity with Geological Survey standards and nomenclature. The views and conclusions contained in this document are those of the authors and should not be interpreted as necessarily representing the official policies, either expressed or implied, of the United States Government. Any use of trade marks in this publication is for descriptive purposes only and does not constitute endorsement by the U. S. Geological Survey.

Menlo Park, California

1980

CONFERENCES TO DATE

Conference I	Abnormal Animal Behavior Prior to Earthquakes, I Not Open-Filed
Conference II	Experimental Studies of Rock Friction with Application to Earthquake Prediction Not Open-Filed
Conference III	Fault Mechanics and Its Relation to Earthquake Prediction Open-File No. 78-380
Conference IV	Use of Volunteers in the Earthquake Hazards Reduction Program Open-File No. 78-336
Conference V	Communicating Earthquake Hazard Reduction Information Open-File No. 78-933
Conference VI	Methodology for Identifying Seismic Gaps and Soon-to-Break Gaps Open-File No. 78-943
Confernece VII	Stress and Strain Measurements Related to Earthquake Prediction Open-File No. 79-370
Confernece VIII	Analysis of Actual Fault Zones in Bedrock Open-File No. 79-1239
Conference IX	Magnitude of Deviatoric Stresses in the Earth's Crust and Upper Mantle Open-File No. 80-625
Conference X	Earthquake Hazards Along the Wasatch and Sierra-Nevada Frontal Fault Zones Open-File No. 80-801

Open-File Service Section
Branch of Distribution
U.S. Geological Survey
Box 25425
Federal Center
Denver, Colorado 80225

UNITED STATES

DEPARTMENT OF THE INTERIOR

GEOLOGICAL SURVEY

PROCEEDINGS OF CONFERENCE X

EARTHQUAKE HAZARDS ALONG THE WASATCH SIERRA-NEVADA FRONTAL FAULT ZONES

Convened Unver Auspices of

NATIONAL EARTHQUAKE HAZARDS REDUCTION PROGRAM

29 July 1979 - 1 August 1979

Organizers

R.E. Anderson
U.S. Geological Survey MS 966
Box 25046, Denver Federal Center
Denver, Colorado 80225

Alan Ryall
Seismological Laboratory
University of Nevada, Reno
Reno, Nevada 89557

Robert A. Smith
University of Utah
Department of Geological & Geophysical Sciences
Salt Lake City, Utah 84112

Convener
Jack F. Evernden
U.S. Geological Survey
Menlo Park, California 94025

Open-File Report 80-801

Compiled by
Pamela D. Andriese

This report is preliminary and has not been edited or reviewed for conformity with Geological Survey standards and nomenclature. The views and conclusions contained in this document are those of the authors and should not be interpreted as necessarily representing the official policies, either expressed or implied, of the United States Government. Any use of trade names and trademarks in this publication is for descriptive purposes only and does not constitute endorsement by the U.S. Geological Survey.

Menlo Park, California

1980

TABLE OF CONTENTS

Introduction i

Earthquake Studies Along the Wasatch Front, Utah: Network Monitoring, Seismicity, and Seismic Hazards

W.J. Arabasz, R.B. Smith, and W.D. Richins 1

Seismicity Related to Structure and Active Tectonic Processes in the Western Great Basin, Nevada and Eastern California

J.D. VanWormer and Alan Ryall 37

Design Earthquake Magnitudes for the Western Great Basin

David B. Slemmons 62

Earthquake Hazards Mapping in the Reno-Carson City Area, Nevada

Dennis T. Trexler 86

Prediction of Seismic Intensities on the Wasatch Fault

Gary Clow and Jack Evernden 109

Liquefaction Potential Maps for Land Use Planning in Utah

Loren R. Anderson, Jeffrey R. Keaton and William J. Gordon 153

Research to Define the Ground Shaking Hazard Along the Wasatch Fault Zone, Utah

W.W. Hays, R.D. Miller, and K.W. King 172

Estimation of Maximum Magnitude and Recommended Seismic Zone Changes in the Western Great Basin

Alan Ryall and J.D. VanWormer 181

Quaternary Faulting in Utah

Larry W. Anderson and Darryl G. Miller 194

Recurrence of Surface Faulting and Moderate to Large Magnitude Earthquakes on the Wasatch Fault Zone at the Kaysville and Hobble Creek Sites, Utah

F.H. Swan, III, David P. Schwartz, and Lloyd S. Cluff 227

Estimating the Probability of Occurrence of Surface Faulting Earthquakes on the Wasatch Fault Zone, Utah

Lloyd S. Cluff, Ashok S. Patwardhan and Kevin J. Coppersmith 276

Patterns of Late Quaternary Faulting in Western Utah and an Application in Earthquake Hazard Evaluation

R.C. Bucknam, S.T. Algermissen, and R.E. Anderson 299

A Feasibility Study of Earthquake Prediction Using Temporal Variations in Seismic Velocity Along the Wasatch Front from Quarry-Blast Monitoring

R.B. Smith, G. Zandt, and J.E. Gaiser 315

Anomalous Patterns of Earthquake Occurrence in the Sierra Nevada-Great Basin Boundary Zone

Alan Ryall and Floriana Ryall 348

State of Stress in the Western United States

Mary Lou Zoback and Mark Zoback 359

Seismotectonic Regionalization of the Great Basin, and Comparison of Moment Rates Computed from Holocene Strain and Historic Seismicity

Roger W. Greensfelder, Frederic C. Kintzer and Malcolm R. Somerville 433

Tectonic and Geomorphic Evolution of the Black Rock Fault, Northwestern Nevada

R.L. Dodge and L.T. Grose 494

Problems in Lake Bonneville Stratigraphic Relationships in the Northern Sevier Basin Revealed by Exploratory Trenching

Alan P. Krusi and Roy H. Patterson 509

The Status of Seismotectonic Studies of Southwestern Utah

R. Ernest Anderson 519

New Interpretations of Lake Bonneville Stratigraphy and Their Significance for Studies of Earthquake-Hazard Assessment Along the Wasatch Front

William E. Scott 548

Soil Stratigraphy as a Technique for Fault Activity Assessment in the Carson City Area, Nevada

John W. Bell and Robert C. Pease 577

Patterns and Rates of Recurrent Movement Along the Wasatch-Hurricane-Sevier Fault Zone, Utah During Late Cenozoic Time

W.K. Hamblin and M.G. Best 601

Fission-Track Dating in the Wasatch Mts., Utah: An Uplift Study

C.W. Naeser, Bruce R. Bryant, M.D. Crittenden, Jr. and M.L. Sorensen 634

Slip Vectors on Faults Near Salt Lake City, Utah, From Quaternary Displacements and Seismicity

T.L. Pavlis and R.B. Smith 647

Crustal Flexure and Earthquake-Generating Stress Along the Wasatch Front, Utah

George Zandt 654

INTRODUCTION

On 29 July - 1 August 1979, a conference on "Earthquake Hazards Along the Wasatch and Sierra-Nevada Frontal Fault Zones" was held at Alta, Utah. The conference was the tenth in the continuing series sponsored by the Earthquake Hazards Reduction Program.

The purpose of this summary is to highlight the important results presented in the twenty-five papers published in this volume. The results fall into two categories: (1) contributions to earthquake hazards and risk assessment, (2) recommendations of principal targets for future research.

CONTRIBUTIONS

Sierra-Nevada Front -- Improved epicenter location in the Sierra Nevada-Great Basin boundary zone, which includes the Reno-Carson City urban area, identifies zones of seismic activity that appear to be associated with specific fault segments, or their terminations or intersections with other structures. In some areas, seismicity appears to be concentrated in zones of dispersed faulting or in zones of active volcano-tectonic processes. In some cases, zones of seismic quiescence correlate with areas of deformation by warping or the location of shallow magma reservoirs. Earthquake hazards mapping in the Reno-Carson City area, combined with soil stratigraphic studies and studies of trenches excavated across fault traces, has led to the identification of several faults that are interpreted to have had surface rupture during Holocene time. Estimates of recurrence times for surface rupture for individual faults in this area vary from 2,000 to 6,000 years. Instrumental data give an average return period of 31 years for earthquakes with $M_L \geq 7.2$ in the western Great Basin, and a re-rupture time of 7,000-10,000 years for individual fault segments capable of generating such earthquakes.

A comparison of historic seismicity with strain rates estimated from late Quaternary faulting and geodetic data indicates relatively higher seismic hazard for a zone along the Sierra Nevada frontal fault system (including the Reno-Carson City area), compared with other subprovinces in the region. Probabilistic estimates that emphasize historic seismicity give incorrect results for the western Great Basin -- in particular, current seismic zone maps show the Sierran frontal fault system as a zone of relatively low hazard, whereas it may have higher potential for major earthquakes than any other zone in the Basin and Range province.

In a discussion of spatial-temporal patterns of earthquake occurrence, it was pointed out that seismicity spread from the aftershock zone of the 1932 Cedar Mountains earthquake into the impending rupture zone of the 1954 Fairview Peak earthquake prior to the main shock. In the Sierran frontal zone, a one-year period of quiescence in 1977-1978 was followed by an abnormally high occurrence of moderate earthquakes (M_L 3.5-5.5) along the entire zone during late 1978 and the first half of 1979. The nature and significance of changes in seismicity patterns needs to be better understood.

Wasatch front--Earthquake activity along the Wasatch front is generally confined to the upper 20 km and suggests a decrease in frequency with depth--90 percent of the focal depths are shallower than 10 km. The geographic distribution patterns of epicenters are uneven and are difficult to correlate with mapped faults. The distribution patterns are relatively stable over the period 1962-1978.

Rates of current earthquake recurrence in the Wasatch front area can be estimated fairly accurately for magnitudes up to about 5.0 using instrumental data from 1962-1978, but extrapolations to higher magnitudes are problematical. If data from the complete earthquake catalogue (1850-1978) are used, they indicate return periods for the Wasatch front area (92,810 km^2) of 22 to 25 years for $M_L \geq 6.0$, 111 to 115 years for $M_L \geq 7.0$, and 232-263 years for $M_L \geq 7.5$. To estimate the probability of a future large earthquake on the Wasatch fault zone, the importance of documenting elapsed times since rupture as well as recurrence intervals of surface faulting on individual segments was emphasized. For example, one can argue that the probability of an earthquake exceeding M_S 7.5 on the Wasatch fault during the next 50 years may be as high as 50%, if two segments of the fault have not ruptured during the past 2,000 years.

Specific segments of the Wasatch fault have been persistently aseismic since 1962 and clearly mark areas of unusually low earthquake activity within a broadly active seismic zone and along a major geologically active structure. The space-time pattern of seismicity along the Wasatch fault, including the existence of persistently aseismic segments, suggests the separate activation of discrete segments of the fault several tens of kilometers long and the potential for future large earthquakes along individual segments.

The Wasatch fault zone contains abundant geomorphic evidence of youthful deformation. Studies of trenches excavated across two segments of it indicate average recurrence times for surface rupture associated with moderate-to-large magnitude earthquakes ($M_S \geq 6.5$) ranging from 500 to 1,000 years at Kaysville and 1,500 to 2,400 years at Hobble Creek. Recurrence times on unstudied segments may be longer. The Wasatch fault may be composed of 6 to 10 segments, and the recurrence times for rupture on the entire fault is clearly shorter than on any one segment. For the entire fault, the values based on geologic data approach the value of a few hundred years for return periods estimated from the historic earthquake data. Holocene slip rates estimated from the two trenched segments are larger by factors of 3 to 4 than long-term uplift rates of 0.4 mm/year estimated from fission-track analysis of apatite grains collected from a broad range of elevations in the uplifted block. Using geologic data together with information from seismic moments, return periods of M_L 7.0-7.5 earthquakes were calculated to be 240-500 years along the Wasatch front and 165-330 years for the state of Utah--consistent with return rates calculated from trenching and b-value estimates.

On the basis of recent geomorphic studies, fault scarps in alluvium of western Utah can be assigned to Holocene and pre-Holocene categories with reasonable certainty. These assignments combined with other data, such as recurrence times estimated from trenches across the Wasatch fault, provide a basis for redefining the seismic source zones in western Utah and assessing the implication of long-term characteristics of large-magnitude earthquake activity, as indicated by the geologic record, on the use of short-term historic data for seismic hazard studies. As an example, if the redefined source zones are used in a probabilistic analysis of maximum accelerations expected along the Wasatch Front in the vicinity of Salt Lake City, estimated maximum accelerations are about three times those obtained by Algermissen and Perkins in the calculation of their hazard map of the United States.

Research to define the ground shaking hazard along the Wasatch front has shown that ground response varies greatly with the type and thickness of unconsolidated materials as compared with the response of rock. Comparison of ratios of velocity spectra between rock and alluvium in the period ranges of most interest in risk analysis suggests that ground response at sites on thick saturated alluvium such as exists beneath large parts of the Salt Lake City area can be ten times greater than at adjacent rock sites. There is also a potential for amplification of low-frequency shear waves by the alluvium-bedrock interface.

Seismic intensities predicted for model earthquakes representing 10-, 20-, and 60-kilometer breaks on the Wasatch fault in the Salt Lake City area are used to estimate dollar losses to wood-frame construction and total loss by doubling the losses to wood-frame construction. The estimated total loss, which does not include losses due to slumping, liquefaction, fire, or dam failure, for Salt Lake City, Provo, and Ogden are $124 million for a 10-km break, $234 million for a 20km break, and $498 million for a 60-km break.

RECOMMENDATIONS

Considerable time was devoted to identification and discussion of topics and areas where future research should be focused. Time did not allow for the priority ranking of the identified research by concensus.

1. An increased effort is needed in developing scaling laws for Great Basin intensity data and for establishing more precise intensity-magnitude-acceleration relations and seismic attentuation laws for the Great Basin.

2. A major deficiency in Great Basin seismology is the lack of a modern network of strong-motion accelerometers. A long-term commitment to obtain strong motion data in the Great Basin is badly needed. A group should be convened to decide on areal priorities for instrumentation based on the most likely next large earthquakes.

3. A better understanding of ground motion variability in geologic settings of the Great Basin is badly needed. A group should be convened to develop specific recommendations for an experiment near the Nevada Test Site. Down-hole P- and S-wave velocity measurements are needed in basin areas that have contrasting stratigraphic and hydrologic characteristics.

4. There is a critical need for long-term multidisciplinary geologic and geophysical commitment to understanding the physical nature and significance of contrasts in the distribution of earthquakes along specific fault zones such as the Wasatch and Sierran Fronts, both of which are characterized by active and quiescent segments. The commitment should include multi-method geophysical study of the subsurface geometry of key fault segments. Complementary geologic studies should be made of the long-term behavior of the same fault segments using techniques such as trench excavations, geomorphic analysis, fission-track analysis, and tectonic framework studies. The commitment should also include an increased effort to determine if the "Nevada seismic zone" is truly unique within the Great Basin.

5. There is a need for increased effort along the Wasatch Front to produce special-purpose strip maps that contain all available information that can be judged to be of use to local governments in earthquakes hazard mitigation.

6. A one-year commitment to produce a draft revision of the national seismic risk map is acknowledged. To meet this commitment, a group should be convened for the purpose of deciding what parameters and hypotheses will go into building the map and what statistical approach will be taken.

7. Throughout all of the above recommendations, there is an implied definite need for the basic data provided by regional and local seismic network operations. Any effort to reduce capability in this area should be resisted and efforts to modernize through digital recording and to increase capability should be supported.

8. A topic that received no specific recommendations, possibly because of a general awareness of current budget constraints, but is of great importance is the need for improved knowledge of the relationship between fault behavior and crustal structure. Contemporary tectonic activity in and adjacent to the Great Basin is closely tied to variations in crustal structure. The depth distribution of faulting is probably controlled by varying degrees of crustal ductility. Seismic sounding techniques may be useful to the extent that contrasts in elasticity may be associated with contrasts in rheology.

9. Budget constraints and the demands of users for short-term risk assessment call for a strategy for future research. Efforts should be increased to determine the most likely locations of the next large earthquakes. Preliminary results indicate that space-time patterns of seismicity combined with other estimates of return periods may foretell large earthquake occurrences in this region. Hence, continued earthquake monitoring is essential. Research must also include accurate dating of faulting and aim toward an understanding of fault geometry and kinematics of earthquakes that occur in an intraplate extensional regime different than that of California.

Earthquake Studies Along the Wasatch Front, Utah: Network Monitoring, Seismicity, and Seismic Hazards

by W. J. Arabasz
R. B. Smith
W. D. Richins

Abstract

The Wasatch Front area of north central Utah occupies an active segment of the Intermountain seismic belt that is characterized by late Quaternary normal faulting and high seismic risk. This paper summarizes new earthquake information for the Wasatch Front area, derived from telemetered seismic arrays operated by the University of Utah since October 1974, and implications for the evaluation of earthquake hazards in this area. Revised earthquake data from a skeletal statewide network for 1962 to 1974 substantiate the pattern of recent seismicity. Important features of this pattern include diffuse but locally intense seismicity throughout a 200-km-wide zone, roughly centered on the major N-S Wasatch fault zone, and persistent quiescence along major sectors of the Wasatch fault. Space-time patterns of seismicity on the Wasatch fault suggest separate activation of discrete segments of the fault several tens of kilometers long and the potential for future large earthquakes along individual segments.

Introduction

Since October 1974, telemetered seismic arrays of high-gain short-period stations have been operated by the University of Utah in the Intermountain seismic belt (ISB) for assessing earthquake hazards, for studying the feasibility of earthquake prediction, and for basic seismological research. Nearly 60 stations are now centrally recorded at the University of Utah campus in Salt Lake City providing regional coverage of the ISB from 44°N, south of Yellowstone National Park, to 27°N, in southernmost Utah (Figure 1). This paper is basically a progress report summarizing new earthquake information specifically for the Wasatch Front area of north-central Utah--the most densely populated segment of the ISB, and hence the area of densest station coverage (43 stations). In this paper we emphasize seismicity and implications of new data for the evaluation of earthquake hazards in this area. Elsewhere in this volume, Smith et al. present detailed data from quarry-blast monitoring relevant to earthquake prediction in this same area, and Zandt discusses possible implications of seismicity in the Wasatch Front area in terms of a viscoelastic model of crustal deformation. For additional information on earthquake studies in the Utah region, we refer the reader to a recent volume edited by Arabasz, Smith, and Richins (1979).

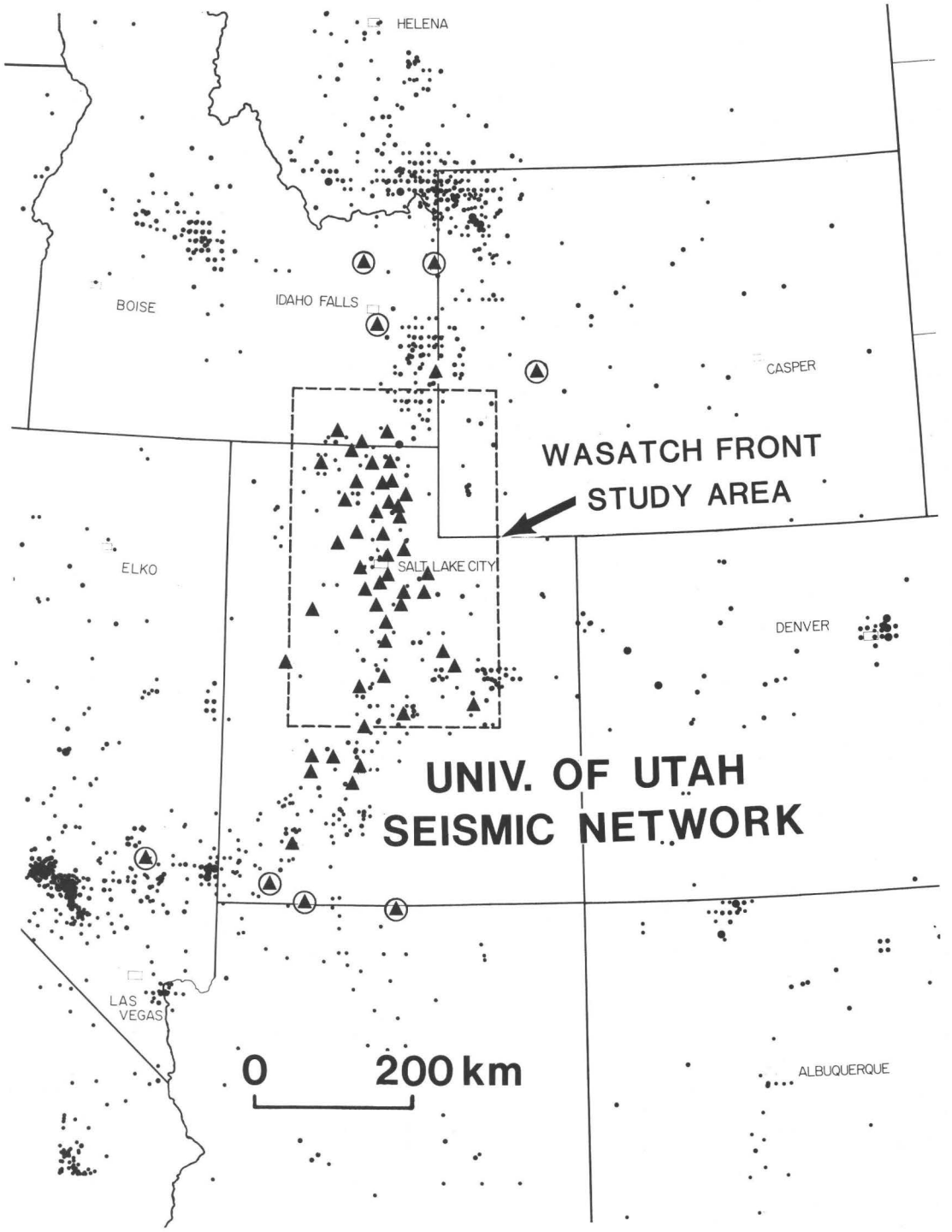

Fig. 1. Index map relating study area of this report and seismograph stations (triangles) of the University of Utah telemetered seismic network to regional earthquake epicenters (small circles) of the Intermountain seismic belt. Epicenter map after Smith (1978). Circumscribed triangles indicate stations owned and operated by other agencies but centrally recorded by the University of Utah.

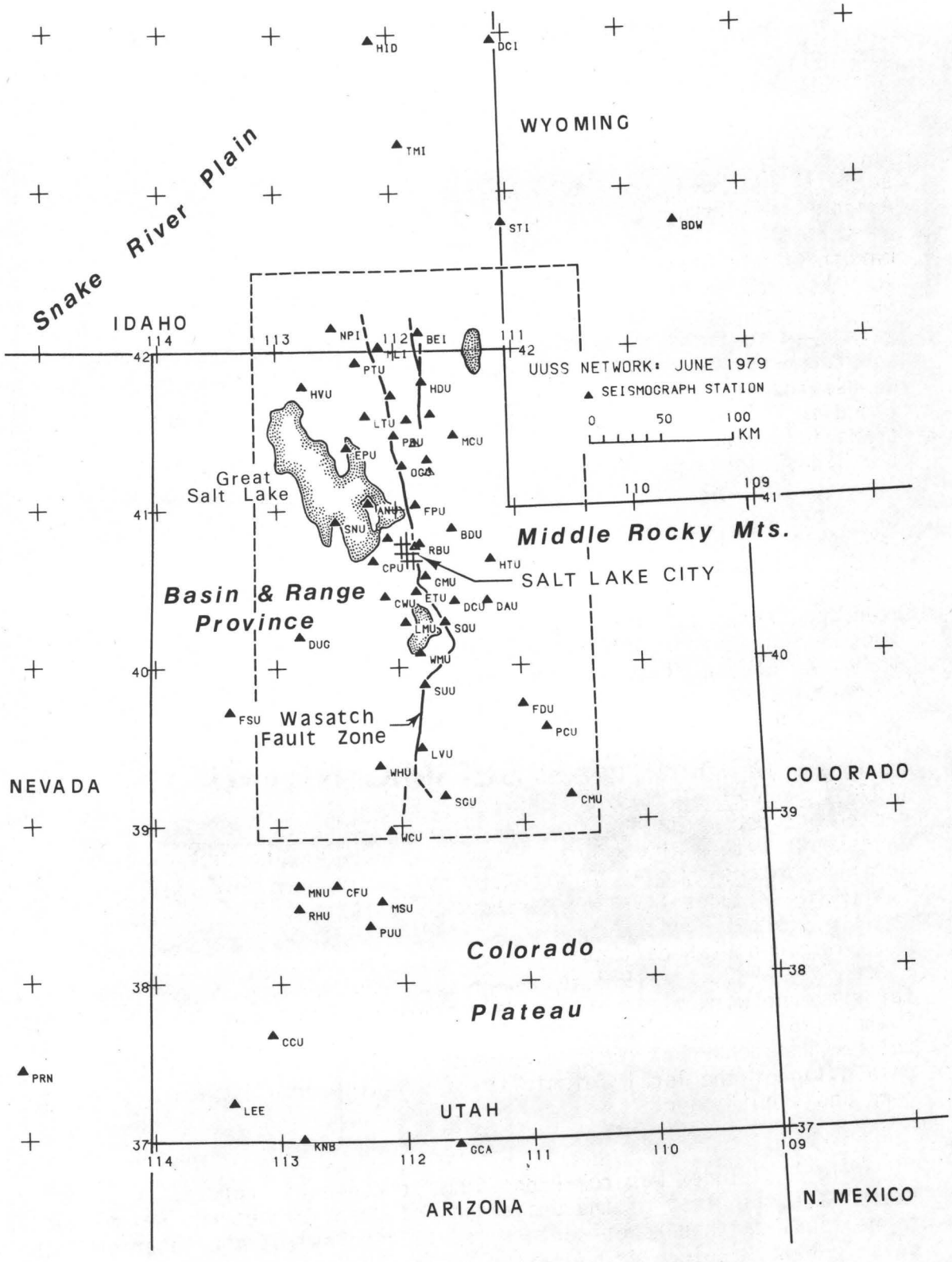

Fig. 2. Location Map of the University of Utah telemetered seismic network. Dashed line outlines Wasatch Front reference area.

Until the last few years, instrumental monitoring of seismicity within the interior of the western United States chiefly relied on near-regional seismographic coverage (i.e., with a closest station at about 100-600 km). On the basis of such regional data, Woolard (1958), Ryall et al. (1966), Sbar et al. (1972), and particularly Smith and Sbar (1974) focused attention on the Intermountain seismic belt as a coherent belt of earthquake activity extending more than 1,300 km from southern Nevada and northern Arizona to northwestern Montana (see also Smith, 1978). Within the area of this study (Figures 1 and 2), the ISB coincides with the eastern margin of the Basin and Range province and roughly centers on the 370-km-long Wasatch fault, which is continuous as a zone of complex fracturing and which represents a major normal fault zone along which young mountain blocks have been uplifted to form a prominent west-facing physiographic scarp (the Wasatch Front) from Gunnison, Utah, to Malad City, Idaho. In this paper we use the term "Wasatch Front area" as synonymous with the study area outlined in Figures 1 and 2 and generally to indicate the broad structural transition zone that separates the eastern Basin and Range province from the Middle Rocky Mountains and northern Colorado Plateau.

The Wasatch Front area is well recognized as being seismically hazardous (e.g., Smith, 1974, 1978; Cluff et al., 1975; Algermissen and Perkins, 1976), and earthquakes of M_L=7.5 have been postulated as "credible" for this area by the U.S. Geological Survey (1976). Although surface faulting has been documented for only one historical (i.e., post-1847) earthquake in the Utah region--the magnitude 6.6 (Gutenberg and Richter, 1954) Hansel Valley, Utah, earthquake of 1934, which produced a scarp 0.5 m high (Shenon, 1936)--there is clear agreement that fault features indicate extensive late Quaternary faulting (e.g., Morisawa, 1972; Cluff et al., 1970, 1973, 1974; Hamblin, 1976; Anderson, 1978). Documentation of Holocene dating for recurrent movement on the Wasatch fault has recently been given by Bucknam (1978), Swan et al. (1978), and Schwartz et al. (1979). Since 1850, when earthquake documentation for the Utah region began, at least 55 earthquake mainshocks within the Wasatch Front area have reached a maximum Modified Mercalli intensity of V or greater, the largest of which was the magnitude 6.6 (M.M. IX) Hansel Valley earthquake of 1934.

Although Utah earthquakes have been located by the University of Utah since July 1962, pre-1974 resolution was rudimentary and based on a skeletal state network of several widely-spaced seismographs (e.g., Cook and Smith, 1967). Accordingly, data from the first 45 months of operation of the new Wasatch Front earthquake network allow, for the first time, adequate resolution of the local seismicity--and key observations regarding its pattern and significance.

Wasatch Front Seismic Network

Network background and instrumentation. The 43-station Wasatch Front seismic network (Figure 2) was installed by the University of Utah beginning in mid-1974 with funding from the U.S. Geological Survey, the National Science Foundation, and the State of Utah. Effective seismic monitoring

began approximately October 1, 1974 (15 stations), with fairly complete seismic coverage of the Wasatch Front by December 1974 (26 stations). The station distribution was constrained by several factors including requirements for unobstructed radio transmission, accessibility (particularly in rugged terrain east of the Wasatch fault), exposure of solid bedrock in the Great Basin west of the Wasatch fault, and the need to cover a broad area of earthquake activity along the Wasatch Front with a relatively small number of instruments. The most dense part of the network lies north of 40°N latitude covering an area about 250 km by 100 km with an average station spacing of ∿30 km.

Data from the 43 stations are telemetered to the University of Utah campus in Salt Lake City via a combination of radio and telephone FM-transmission links. Site instrumentation generally consists of 1-Hz short-period vertical-component seismometer (Mark Products MOdel L4C or Geotech Model S-13), a VCO/preamplifier pacakage, a 100-milliwatt radio transmitter and directional antenna, and interfacing electronics powered by air-cell batteries. In addition to a vertical component seismometer, 12 sites have a single horizontal-component seismometer (Mark Products Model 14C), and 3 sites operate with matched 3-component short period systems. Central recording on the University of Utah campus is currently limited to 16-mm film Develocorders and Helicorder monitors. A three-component set of long period instruments operates at Dugway (DUG), a WWSSN station.

Prior to late 1974, reasonable instrumental monitoring of the Wasatch Front region dates back only to 1962 when the University of Utah installed the first three stations of a skeletal state-wide network. Extensive efforts have been made to systematically revise all locations and magnitudes for earthquakes in the Utah region since 1962 (see Arabasz et al., 1979)--including the integration of data from stations of the University of Utah network with data from other near-regional stations intermittently operated by other agencies in southern Utah, Nevada, western Wyoming, southeastern Idaho, and Colorado. For the revision of earthquake data within the Wasatch Front area for the period July 1962 to September 1974, station spacing ranged from approximately 75 to 150 km. Instrumentation for the Utah Stations generally consisted of a 3-component set of short-period 1-Hz seismometers photographically recorded on-site.

Data analysis. To locate earthquakes within the Wasatch Front study area, film records from telemetry stations along the Wasatch Front--as well as those from stations in south-central Utah, southeastern Idaho, and western Wyoming are routinely scanned, interpreted, and processed using the earthquake location program HYPOELLIPSE (Lahr, 1979). Two velocity models are used in order to model the transition in crustal structure across the Wasatch Front between the Basin and Range province to the west and the Middle Rocky Mountains-Colorado Plateau to the east (see Smith, 1978). The first model, informally designated the Wasatch Front model, is applied to all stations west of 111°W longitude, with the exception of GCA on the Arizona-Utah border. The model was determined by seismic refraction profiling (Keller et al., 1975) and is specified by:

Layer	Depth (km)	P-Velocity (km/sec)
1	0 to 1.4	3.4
2	1.4 to 15.5	5.9
3	15.5 to 25.4	6.4
4	25.4 to ∞	7.4

The second model, informally designated the Colorado Plateau model, is applied to all stations east of 111°W longitude plus the station GCA. This model is from Roller (1965) and is specified by:

Layer	Depth (km)	P-Velocity (km/sec)
1	0 to 1.5	3.0
2	1.5 to 27.5	6.2
3	27.5 to 40.0	6.8
4	40.0 to ∞	7.8

Reliable S-wave-arrival times are used in addition to P-wave-arrival times whenever possible, with an empirically determined ratio of 1.74 for V_p/V_s, corresponding to a Poisson's ratio of 0.25. S-wave arrivals prove particularly helpful in controlling locations near or slightly outside the boundaries of station subsets. Corrections for elevation are made to a datum level of 1250 m (above mean sea level) using the angle of incidence and the near-surface velocity of the appropriate velocity model. Some corrections are as large as 0.6 sec. Station corrections for the October 1, 1974, to June 30, 1978, data set were calculated and applied using average station travel-time residuals when at least 50 readings (P-wave-arrival times) per station were available. These corrections were generally less than ±0.1 sec. Average station travel-time residuals for the July 1, 1962, to September 30, 1974, data set were not applied because they were larger than the expected timing errors; the large station spacing (75 to 150 km) and relatively few stations recording each earthquake (usually less than 10) resulted in poor estimates of error. Focal depths were routinely restricted to a depth of 7.0 km, the average for well located earthquakes in Utah, when the epicentral distance to the closest recording station was greater than twice the focal depth, or about 15 to 20 km.

Large quarry blasts at various sites within the Wasatch Front network during the period 1974-1978 have been instrumentally located with an accuracy of ±1 km. An analysis of array resolution made by Kastrinsky (1977) yielded estimates of epicentral accuracy for well recorded earthquakes located on the Wasatch Front during 1975-1976 at ±2.0 km (using

30 stations), and ±5.0 km (using 7 stations) for the period 1962-1974. Focal-depth determinations for both time periods were judged to be reliable to within ±2.0 km only when the epicentral distance to the closest recording was approximately equal to or less than the focal depth. Confidence ellipsoids computed with HYPOELLIPSE (Lahr, 1979) indicate similar esimates of location error.

Local magnitudes (M_L) for all earthquakes located in the Utah region since 1962 have been systematically revised by either direct or indirect relation to Wood-Anderson-type seismographs at three (now five) widely spaced sites within Utah. The revisions are based on completed statistical studies of determinations of M_L from the Utah Wood-Anderson network (including a study of amplitude-versus-distance corrections) and the derivation of coda-magnitude scales--both for standard Benioff short-period vertical seismographs and for telemetered short-period, high-gain stations within the University of Utah seismic network (see Arabasz et al., 1979, pp. 433-443).

For the majority of events less than about $M_L = 2.8$, local magnitude for earthquakes during the 1962-1974 period was estimated from signal duration on paper records from Benioff short-period vertical seismographs using the empirical relation (e.g., Lee et al., 1972; Real and Teng, 1973):

$$M_L = -4.26 + 2.79 \log \bar{\tau} + 0.0026 \bar{\Delta} \qquad (1)$$

where $\bar{\tau}$ is the average total signal duration in seconds (measured from P-wave onset) from a network of four seismographs, and Δ is the average epicentral distance in kilometers. The standard error of estimation is 0.28.

For earthquakes since October 1974, M_L for events for which Wood-Anderson magnitudes cannot be determined is estimated from signal duration using 16-mm film records from the telemetry stations. A network equation for these stations is:

$$M_L = -3.13 + 2.74 \overline{\log\tau} + 0.0012 \bar{\Delta} \qquad (2)$$

where $\overline{\log\tau}$ is the average logarithm of total signal duration (measured in seconds from P-wave onset) and Δ, again, is the average epicentral distance in kilometers. The standard error of estimation is 0.27. Station corrections are applied for both network formulas (1) and (2).

It is important to note compelling evidence that coda-magnitude scales cannot justifiably be extrapolated below about $M_L = 1.5$ without special calibration (Bakun and Lindh, 1977; Suteau and Whitcomb, 1979). Thus symbols in various figures of this paper that indicate smaller magnitudes should be interpreted only as indicating relatively small size.

Seismicity of the Wasatch Front

An accurate description of the seismicity, i.e., the spatial patterns, sizes, rates of occurrence, and other characteristics of earthquakes, in the Wasatch Front area is of fundamental importance in assessing seismic risk. Available data are grouped into three time periods that will be discussed individually: 1850-June 1962, July 1962-September 1974, and October 1974-June 1978. We first consider the historical seismicity, then the best available instrumental data, for 1974 to 1978, and finally the revised instrumental data for 1962 to 1974.

Historical seismicity, 1850 to June 1962. Figure 3 shows the historical seismicity of the Wasatch Front area for the 113-yr period 1850 to 1962, giving a general overview of the pattern of earthquake activity. The 148 open circles are for the period 1850 to 1949, chiefly representing non-instrumentally located epicenters, and the 73 solid circles are for the period 1950 to June 1962, chiefly representing instrumental locations determined by the U.S. Coast and Geodetic Survey. The reader should not be confused by the patterns of concentric circles resulting from the assignment of non-instrumental epicenters to the same locality. Also note that the non-instrumental epicenters correspond to a location where felt effects were strongest--typically an established city or town. Hence the coincidence of historical epicenters with the Wasatch fault zone largely reflects the locations of settlements along the Wasatch Front--not necessarily earthquake activity on the Wasatch fault itself.

Six earthquakes in the Wasatch Front area during the time period of Figure 3 had an epicentral intensity (M.M.) of VII or greater, corresponding to a Richter magnitude of about 5-1/2 or greater. These earthquakes whose epicenters are dated in Figure 3, include: (1) a magnitude 6 earthquake in Bear Lake Valley in November 1884, (3) a magnitude 5-1/2 earthquake near Eureka in August 1900, (3) a magnitude 6 earthquake in Hansel Valley in October 1909, (4) a magnitude 5-1/2 earthquake close to Salt Lake City in May 1910, (5) a magnitude 5-1/2 earthquake close to Ogden in May 1913, and (6) a magnitude 6.6 earthquake in Hansel Valley in March 1934. Of these six largest events, the epicenter for the 1884 earthquake is the most uncertain. On the basis of damage and felt effects described by Williams and Tapper (1953) at Paris, Idaho, within Bear Lake Valley, we infer a nearby epicenter within Bear Lake Valley (arbitrarily assumed to be on the Idaho-Utah border along the major fault bounding the east side of Bear Lake)--rather than on the Crawford Mountain fault more than 50 km to the south, as interpreted by the U.S. Geological Survey (1976).

October 1, 1974, to September 30, 1978. Figure 4 shows a compilation of located earthquakes within the Wasatch Front study area for the period October 1, 1974, through June 30, 1978. The 45-month sample includes 2,482 earthquakes in the magnitude range 0.0 to 6.0, exclusive of more than 500 aftershock locations from a special study of the March 1975 Idaho-Utah border (Pocatello Valley) earthquake of magnitude (M_L) 6.0 (see Arabasz et al., 1979, pp. 339-373). For the first two months of aftershock activity,

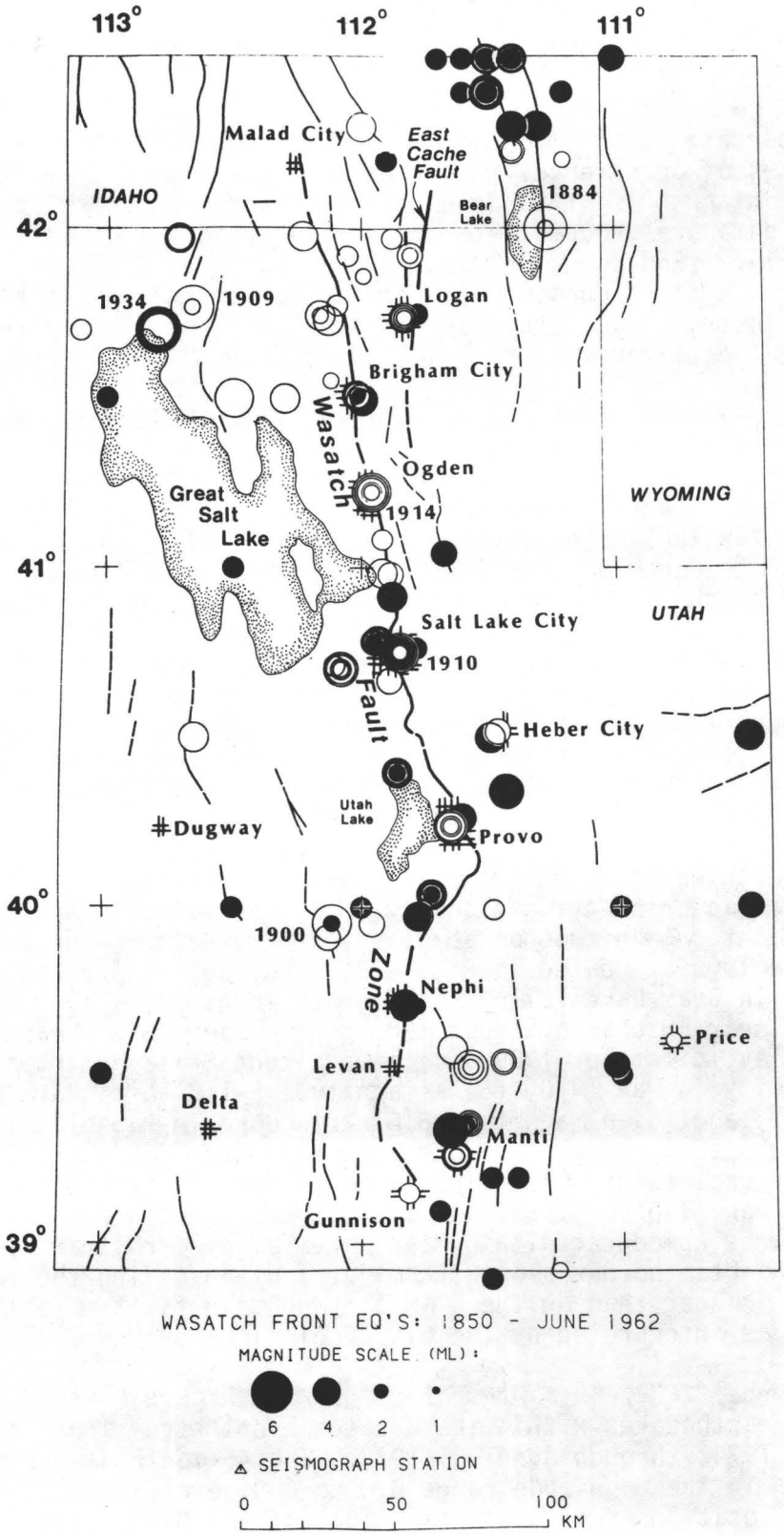

Fig. 3. Epicenters of earthquakes in the Wasatch Front area for 1850-1949 (open circles) and 1950-June 1962 (solid circles).

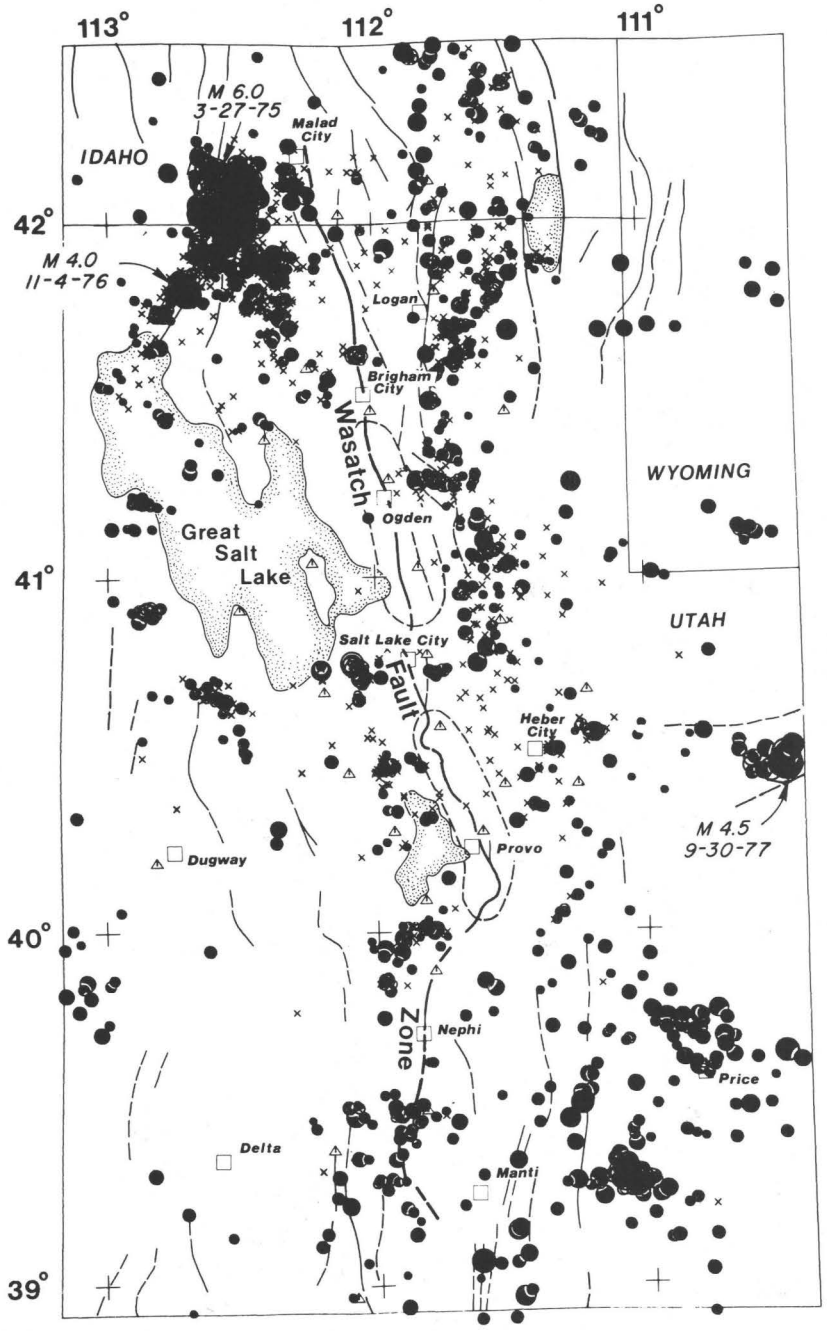
113°
112°
111°
42°
41°
40°
39°
M 6.0
3-27-75
M 4.0
11-4-76
M 4.5
9-30-77
IDAHO
WYOMING
UTAH
Malad City
Logan
Brigham City
Ogden
Great Salt Lake
Salt Lake City
Wasatch Fault Zone
Heber City
Provo
Dugway
Nephi
Price
Delta
Manti
WASATCH FRONT EQ'S: OCT 74 TO JUN 78
MAGNITUDE SCALE (ML)
6
4
2
1
< 1
SEISMOGRAPH STATION
0
50
100
KM

Fig. 4.

only events of magnitude 3.0 or greater were included. The pattern of earthquake activity illustrated in Figure 4 includes several notable features:

(1) An intense cluster of earthquake activity along the Idaho-Utah border north of the Great Salt Lake represents, for the most part, aftershock activity following the M_L = 6.0 Idaho-Utah border earthquake of March 28, 1975. This is not simply the case, however; the prominent earthquake clusters extending southwest and southeast from the state border--forming an inverted "Y" with the dense cluster north of the border--chiefly occurred more than several months after the M_L = 6.0 mainshock. The zone of earthquakes extending to the southwest encompasses the historically active Hansel Valley fault at the northern end of the Great Salt Lake.

(2) The paucity of small-magnitude earthquake activity along much of the Wasatch fault zone is a striking feature of Figure 4--and certainly is not an accident of station coverage or systematic mislocation. Indeed, persistent quiescence along major sectors of the Wasatch fault since 1962 or longer is a topic that we discuss at length below. Two notably quiet sectors of the fault are indicated by elongate dashed areas in Figure 4. Earthquakes <u>are</u> occurring along the southernmost Wasatch fault, with pronounced clustering near Levan (39.5°N). Earthquakes can also be closely correleated with the Wasatch fault north of Brigham City (41.5°N). At the latitude of Salt Lake City (40.8°N), scattered earthquakes appear to separate quiet sectors of the Wasatch fault both to the north and south of Salt Lake City. Clustered events ∿20 km west of the Wasatch fault, at the southeastern end of the Great Salt Lake area beneath the populated and industrialized northwestern part of the Salt Lake Valley--the source region of the damaging Magna earthquake (M_L = 5.2) of 1962. South of Utah Lake at 40°N, the concentration of earthquakes approximately 10 km west of the Wasatch fault has been verified by special field recording.

(3) Another prominent feature of Figure 4 is the north-south alignment of intense seismicity a few tens of kilometers to the east of the Wasatch fault. A band of epicenters extends from the northern map limit southward for at least 200 km to the latitude of Salt Lake City (40.8°N) where the axis of the east-west Uinta Mountain structural trend intersects the Wasatch fault. Within this zone, seismicity has been consistently high in the vicinity of the East Cache fault (see Figure 3), which passes east of Logan, and beneath the Bear River Range to its east. Some of this activity can be ascribed to residual aftershock activity of the M_L = 5.7 Cache Valley (Logan) earthquake of 1962. However, the extent and rates of activity indicate that the earthquakes represent continuous background seismicity where occasional larger events can be expected. In the southern half of this epicentral band, there is no through-going active fault to the east of the Wasatch fault and an explanation for the high level of seismicity in the area remains elusive. There are suggestions that it may be fundamentally influenced by pre-Cenozoic structure. The two largest reservoirs within the Wasatch Range lie within this north-south zone of earthquake activity--Pineview Reservoir (41.2°N) east of Ogden, and Deer Creek Reservoir (40.4°N) northeast of Provo.

(4) Much of the scattered activity west of the Wasatch fault is as difficult to correlate with major active faults as that to its east. There is good control--both seismographic and in terms of discriminating local blasting--to at least 50 km west of the Wasatch fault. Scattered epicenters further west are more problematical, particularly south of 41.5°N. Some of the clustered epicenters west of about 112.5°W and south of about 41.3°N--beyond our effective network coverage--almost certainly include sporadic blasts.

(5) In the east-central part of the map area, an earthquake seqeuence close to the southern flank of the Uinta Mountains occurred in September-October, 1977, including events of M_L = 4.5 (m_b = 5.0) and M_L = 4.0. A detailed aftershock study was carried out co-operatively with the U.S. Geological Survey (Carver et al., 1978).

(6) South of 40°N, pre-1978 coverage was widely spaced, but seismic activity is obviously substantial in this region. This includes earthquakes near the southern terminus of the Wasatch fault zone and particularly in the southeastern part of the map area where intensely clustered events within a 40-km range of Price at least partly represent mining-related seismicity below levels of active coal extraction (see Smith et al., 1974). Detailed field studies of the broadly active southern part of the Wasatch Front area are currently being carried out.

Revised compilation of Wasatch Front seismicity, 1962-1974. Results of the earlier-discussed project to systematically revise all earthquakes and magnitudes for the Wasatch Front area since 1962 are summarized in Figure 5. The compilation includes 581 events, predominantly larger than M_L = 2.0, with the largest event in the sample being the M_L = 5.7 Cache Valley (Logan) earthquake of August 30, 1962, located along the East Cache fault. Five other relatively large events in the sample include: (1) the M_L = 5.2 Magna earthquake of September 5, 1962, located 20 km west of the Salt Lake City at the southern end of the Great Salt Lake; (2) the M_L = 4.4 Juab Valley (Levan) earthquake of July 7, 1963, located near the southern end of the Wasatch fault; (3) the M_L = 4.6 Cache Valley earthquake of March 17, 1966, located beneath the Bear River Range east of Logan; (4) the M_L = 4.3 Heber City earthquake of October 1, 1972, located 35 km east of the Wasatch fault at 40.5°N; and (5) an earthquake of M_L = 4.4 that occurred north of the Great Salt Lake along the Idaho-Utah border on April 14, 1973.

In general, the pattern of seismicity for the 12.3 year sample in Figure 5 is remarkably similar to that documented for the independent 45-month sample located with the modern telemetry network (Figure 4). Most of the discussion related to Figure 4 applies to Figure 5 for earthquakes in the 1962-1974 sample, both west and east of the Wasatch fault. Of particular significance is the pattern of seismicity along the Wasatch fault itself. The two notably quiet sectors of the Wasatch fault to the north and south of Salt Lake City indicated in Figure 4 are also apparent in Figure 5. Also, the seismically active sectors are the same in both figures--i.e., the southernmost Wasatch fault, the northernmost Wasatch fault, and apparently a short segment close to Salt Lake City.

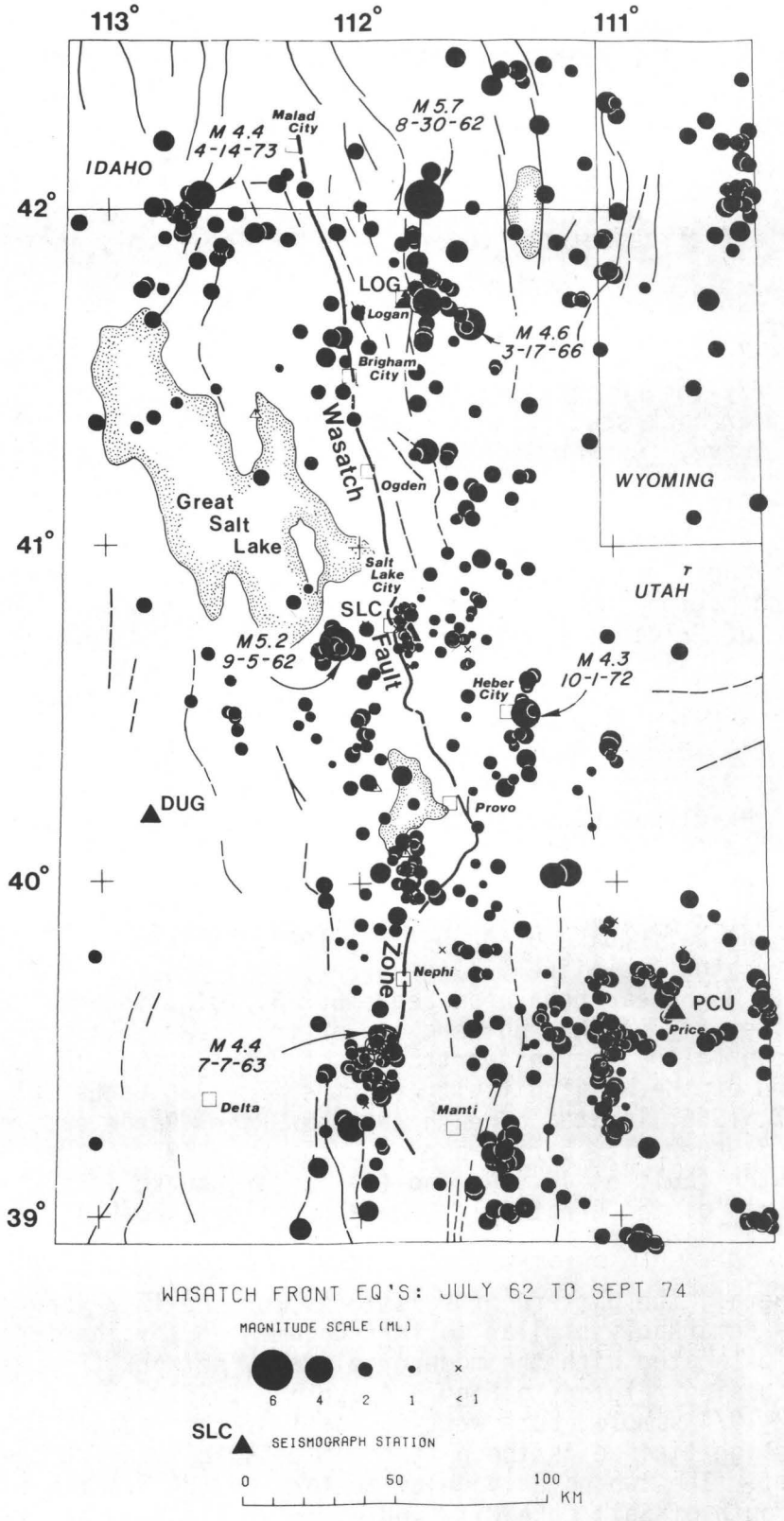
113°
112°
111°
42°
41°
40°
39°
IDAHO
WYOMING
UTAH
Malad City
M 4.4
4-14-73
M 5.7
8-30-62
LOG
Logan
M 4.6
3-17-66
Brigham City
Wasatch
Ogden
Great
Salt
Lake
Salt Lake City
SLC
M 5.2
9-5-62
Fault
M 4.3
10-1-72
Heber City
DUG
Provo
Zone
Nephi
PCU
Price
M 4.4
7-7-63
Delta
Manti
WASATCH FRONT EQ'S: JULY 62 TO SEPT 74
MAGNITUDE SCALE (ML)
6
4
2
1
< 1
SLC
SEISMOGRAPH STATION
0
50
100
KM

Fig. 5

Seismic gaps along the Wasatch fault. The segments of the Wasatch fault that have been persistently aseismic since 1962 are "seismic gaps" in a general sense and deserve special discussion (see also Smith, 1974, 1978). They currently mark areas of unusually low earthquake activity within a broadly active seismic zone and along a major geologically active structure. Evidence of recurrent Holocene faulting along these quiet segments of the Wasatch fault (e.g., Swan et al., 1978; Schwartz et al., 1979) clearly argues against long-term inactivity.

Figure 6 shows the space-time distribution of earthquakes since 1962 along nearly the entire extent of the Wasatch fault from north of the Idaho-Utah border to south of Levan. All earthquakes located within 10-km epicentral distance of the Wasatch fault from July 1, 1962, through June 30, 1978 (i.e., the combined data of Figures 4 and 5), are included. The most significant features of the space-time pattern in Figure 6 are the definition of spatial gaps both to the north and south of Salt Lake City, each approximately 70 km in length, and the definition of a 10-year time gap for the sector to the north of Brigham City. There are less reliable indications of a smaller spatial gap a few tens of kilometers long near Nephi and time gaps for activity along the sector of the fault between Nephi and Provo. The apparent segmentation of the Wasatch fault into discrete sectors several tens of kilometers long suggests that these sectors may represent individual source zones for major episodes of faulting.

The time gap for the sector of the Wasatch fault north of Brigham City (Figure 6) may be significant in view of recent findings from world-wide data (e.g., Wyss et al., 1978) that prior to large earthquakes there frequently appears to be a precursory pattern of seismic quiescence, ocassionally interrupted by a burst of seismicity followed again by quiescence. Arabasz and Griscom (1978) have identified some such patterns of precursory quiescence before historical earthquakes in the Utah region.

The seismic gaps located to the north and south of Salt Lake City are separated by a zone of persistent but moderate earthquake activity that coincides with the location of the well exposed Warm Springs sector of the Wasatch fault zone on the west side of the Salt Lake salient (see Pavlis and Smith, this volume). Holocene faulting along the Wasatch fault within both seismic gaps has recently been established by geologists of Woodward-Clyde Consultants, San Francisco. Trenching across the Wasatch fault near Kaysville 32 km north of Salt Lake City has indicated that two large scarp-forming earthquakes (probably of magnitude 7 or larger) have occurred on this segment of the fault within the past 1580 ±150 years (Swan et al., 1978). Preliminary results from trenching across the Wasatch fault 13 km southeast of Provo at Hobble Creek indicate similarly youthful faulting (and hence prehistoric large earthquakes) within the southern seismic gap (Schwartz et al., 1979). Another prominent example of young faulting within the southern seismic gap is at the mouth of Little Cottonwood Canyon southeast of Salt Lake City.

How long have the major seismic gaps north and south of Salt Lake City existed? The pre-1962 data of Figure 3 include numerous epicenters of earthquakes felt strongly between Salt Lake City and Brigham City, within

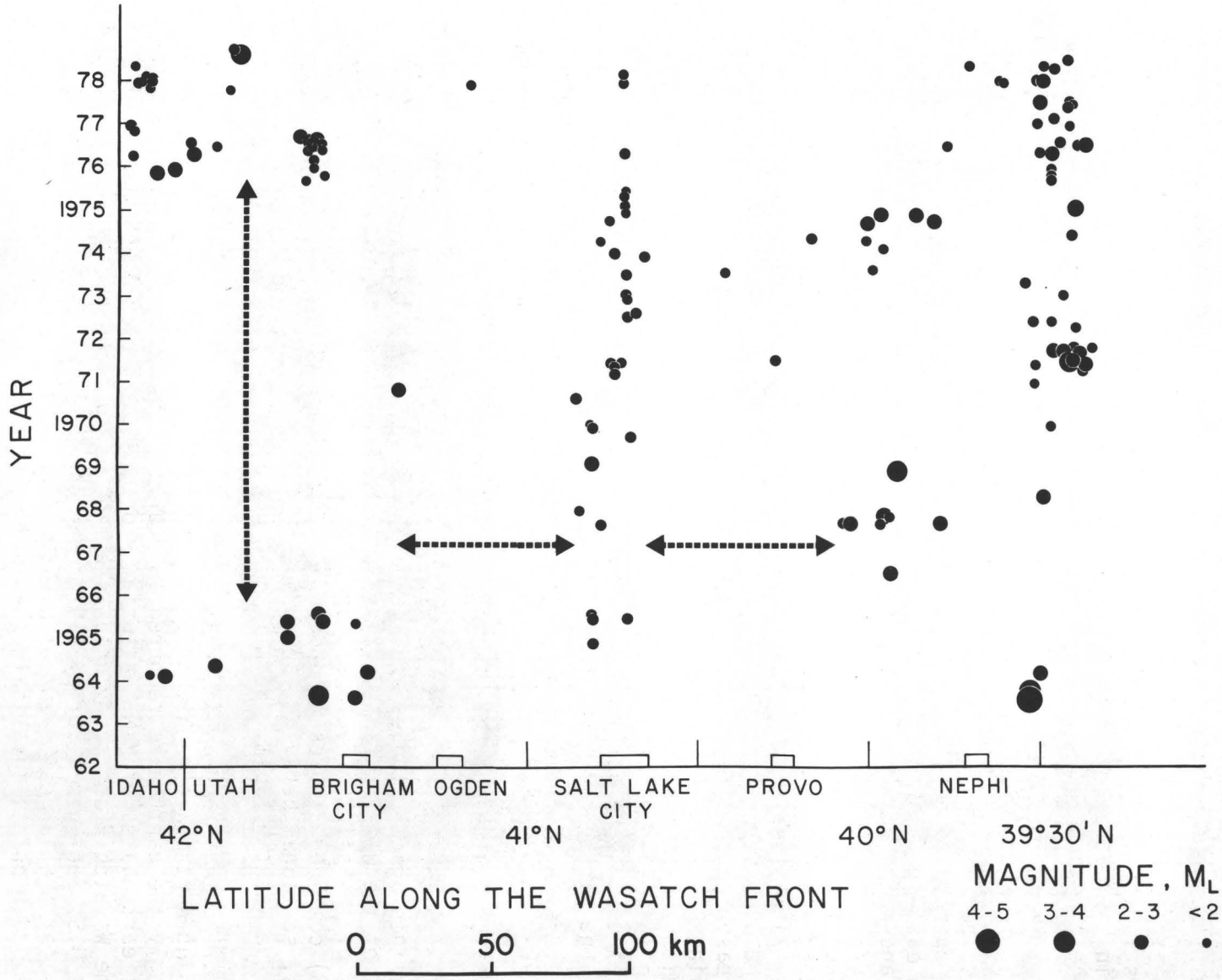

Fig. 6. Space-time distribution of earthquakes within 10-km epicentral distance of the Wasatch fault, July 1962 through June 1978. Arrows indicate time and space gaps in the seismicity referred to in the text.

15

the area of the northern gap. Similarly, numerous events were felt in the Provo area within the southern gap. Each gap also contains a non-instrumental epicenter for the 1950-1962 period: the epicenter in the gap north of Salt Lake City is for an earthquake of M.M. intensity V on May 12, 1955; the one near Provo in the southern gap is for an earthquake of M.M. intensity V on August 11, 1951. The pre-1962 data set, however, is ambiguous. One can argue from the pattern of current seismicity that pre-1962 epicenters located in the seismic gaps may actually have related to earthquakes occurring a few tens of kilometers away from the Wasatch fault. At a minimum, the gaps have existed since 1962, and probably since at least 1955.

The seismic gaps along the Wasatch fault might be variously explained (see Sbar et al., 1972; Smith, 1974) by: (1) "shadow zones" of large prehistoric earthquakes (e.g., Wesson and Ellsworth, 1973), (2) opposition to strain energy accumulation on the Wasatch fault by Lake Bonneville rebound, (3) an eastward migration of tectonic activity at the eastern margin of the Basin and Range province, (4) precursory seismic quiescence (e.g., Wyss et al., 1978), or (5) fault inactivity with no accumulation of strain energy. If indeed the Wasatch fault is the expression of a lithospheric boundary within the western North American plate (Smith and Sbar, 1974; Smith, 1978), analogy with other active plate boundaries suggests that future movement--averaged over several centuries--can be expected along the entire boundary. Such reasoning combined with new geological information from exploratory trenching points to hypotheses (1) or (4) as more likely. In other words, the quiet zones probably represent sectors of the Wasatch fault that are passing through some stage of a seismic cycle that is marked by a very low level of earthquake activity. Two such stages that we know of are (1) a post-large earthquake stage following the decrease of aftershocks (Wesson and Ellsworth, 1973; Ryall and Priestley, 1975), and (2) a pre-earthquake stage occurring at a high level of strain accumulation (e.g., Wyss et al., 1978). We do not know yet which is applicable to the quiet segments of the Wasatch fault--but the distinction is obviously crucial.

The seismic gaps along the Wasatch fault emphasize the need for: (1) further geological studies and age-dating to establish the long-term seismicity of the Wasatch fault, (2) seismological studies to identify the stages of the seismic cycle appropriate to individual sectors of the fault, and (3) combined studies to understand the segmentation, mechanics, stress levels, sectional behavior, and probably timing of future large earthquakes along the Wasatch fault. Work is just beginning on all these aspects.

Earthquake recurrence. What do the Wasatch Front earthquake data imply regarding earthquake magnitude versus frequency of occurrence, and correspondingly the earthquake recurrence interval? Analyses of the entire catalog of earthquakes of M.M. intensity V or greater from 1850 through 1978 for the Wasatch Front study area were made using techniques similar to those of the U.S. Geological Survey (1976) for the whole of Utah. Only mainshocks (or the largest event of a swarm sequence) were included in our sample in order not to invalidate the assumption of a Poisson dist-

Figure 7 shows the results of linear regression calculations of frequency of occurrence, corrected for sample incompleteness using Stepp's (1972) technique, upon Modified Mercalli epicentral intensity I_o. The historical data were found to be complete for $I_o \geq$VI for the last 40 years. Completeness for $I_o \geq$V was assumed since 1950; for $I_o \geq$VII, during the last 100 years; and for $I_o \geq$VIII, during the entire 129-yr record since 1850. Assuming the Gutenberg and Richter (1956) relationship: $M_L = 1 + 2/3\ I_o$, as justified for Utah by the U.S. Geological Survey (1976), the results of Figure 7 can be transformed to express either n, the annual frequency of occurrence of earthquakes of a given magnitude, or N_c, the annual frequency of occurrence of earthquakes equal to or greater than a given magnitude, in the common form of the frequency-magnitude relation log (number) = a - bM; accordingly:

$$\log n = 2.35 - 0.63\ M_L \qquad (3)$$

$$\log N_c = 2.98 - 0.72\ M_L \qquad (4)$$

Equation (4), for example, indicates that the annual number of earthquakes of $M_L \geq 7.5$ in the Wasatch Front reference area is 3.8×10^{-3} or one every 263 years. Using equation (3), the recurrence interval for $M_L = 7.5$ within the same area would be 237 years. Note that calculations of recurrence intervals always imply an areal flux that must be clearly specified to compare rates of recurrence intervals meaningfully.

Application of the method of extreme values (e.g., U.S. Geological Survey, 1976; Knopoff and Kagan, 1977) to the historical data set to minimize errors for sample incompleteness yields estimates of earthquake frequency that are close to those of equation (4). The extreme-value distribution of maximum intensities in each year of the historical record is estimated by:

$$F(x) = \exp\{-\exp[-(x-4.25)/1.01]\},\ -\infty < x < +\infty \qquad (5)$$

where F(x) is the probability that the largest earthquake in a year will have intensity less than or equal to x. The return period R, the interval in which an earthquake of a given intensity or greater has a 63% probability of occurrence, is estimated by (see U.S. Geological Survey, 1976):

$$R = 1/[1 - F(x)] \qquad (6)$$

The extreme probability distribution thus predicts that the return period for an earthquake of $I_o \geq$9-3/4 (i.e., $M_L \geq 7.5$) in the standard Wasatch Front area is 232 years--based on the 129-yr historical record.

In using the post-1962 instrumental seismicity data to compute earthquake recurrence for the Wasatch Front area, the following approach was

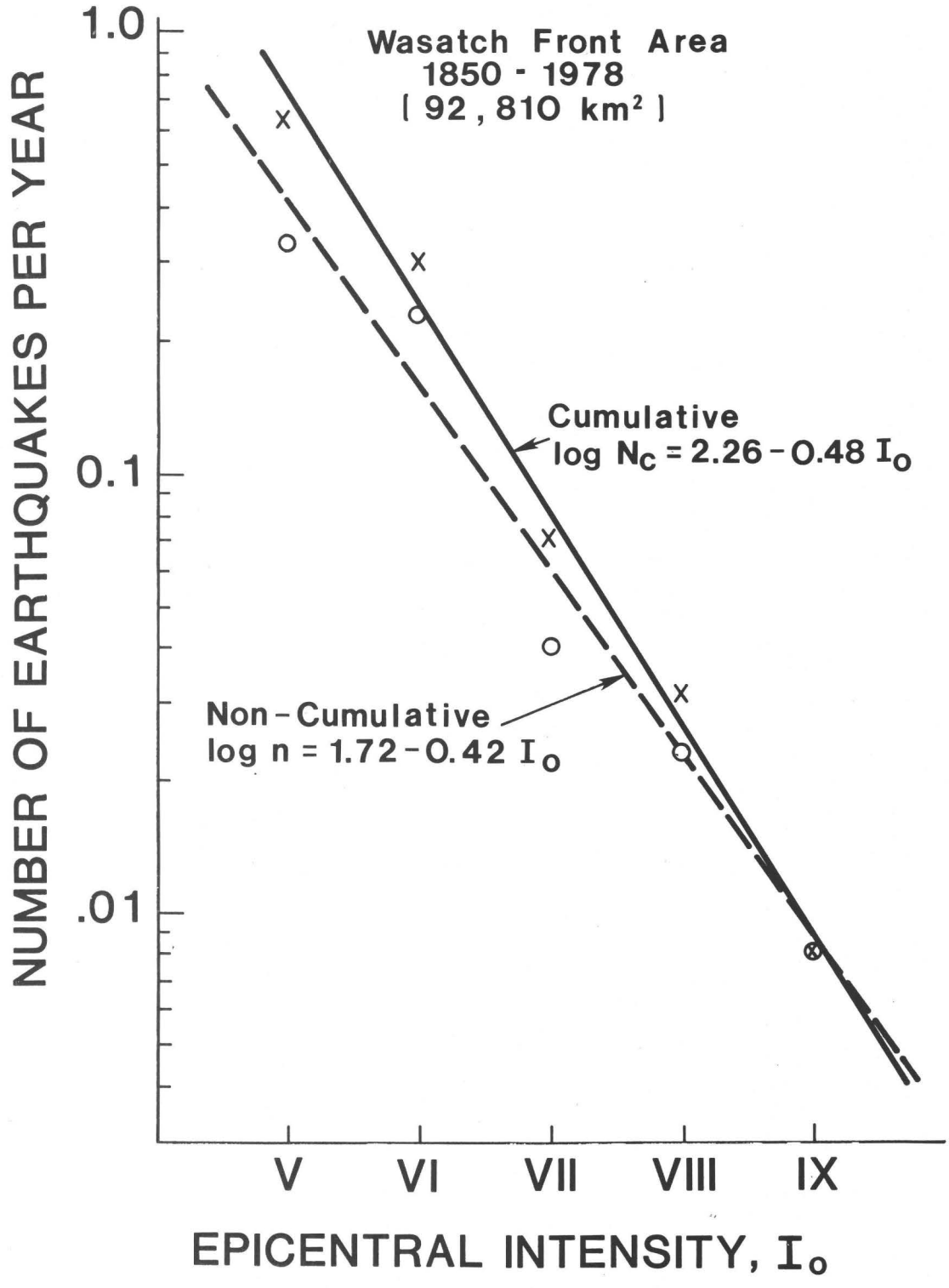

Fig. 7. Annual frequency of occurrence versus Modified Mercalli epicentral intensity for the Wasatch Front reference area based upon the 129-yr record: 1850 through 1978, corrected for sample incompleteness by Stepp's (1972) method.

taken. Only a restricted part of the Wasatch Front reference area between 111°15'W and 112°15'W longitude was considered, for two chief reasons: (1) to exclude the intense mining-related seismicity in the southeastern corner of the study area east of 111°15'W (Figures 4 and 5), and (2) to exclude abundant aftershocks and seismicity related to the March 1975 Idaho-Utah border earthquake west of 112°15' (Figure 4). The sample area thus contains the Wasatch fault zone, the feature of primary interest, and the sampled seismicity should be representative of strain-energy release in the general vicinity of the fault.

Separate analyses were made for the 12.25-yr period: July 1962-September 1974, for the 3.75-yr period: October 1974-June 1978, and for the total 16.0-yr period: July 1962-June 1978. First, the cumulative number of earthquakes was plotted for each period to determine the magnitude threshold for sample completeness. The magnitude threshold is 2.3 (N=111) for 1962-74; 2.0 (N=98) for 1974-78, and 2.3 (N=159) for the total period 1962-78. The method of maximum likelihood (Utsu, 1965; Aki, 1965)--which is preferable to least-squares techniques for an unbiased estimate of the slope coefficient b in the frequency-magnitude relation--was then applied to the three sets of earthquakes, grouped in magnitude intervals, ΔM, of 0.3, accounting for the respective magnitude thresholds. Figure 8 shows values for the coefficient b, corrected for the product $b\Delta M$ (Utsu, 1966), at 95 percent confidence limits for the three samples. Note that the recurrence curve is constrained to pass through the minimum magnitude.

An important result of Figure 8 is that values of b from the instrumental data are significantly higher than the values 0.63 and 0.72 determined from the non-instrumental historical data (equations 3 and 4). As a check, the historical intensities were converted to magnitudes using the relation: $M_L = 1 + 2/3\ I_o$, to determine a maximum-likelihood value of b for the historical data; a value of 0.60 ± 0.13 was computed. An equivalent b-value computed from the extreme-value distribution of equation (5) (see U.S. Geological Survey, 1976) for the historical data is 0.64.

Table 1 summarizes information to facilitate computations and to normalize the various recurrence relationships for comparison. Recurrence information has been added from the U.S. Geological Survey (1976) for the whole of Utah, and from Ryall *et al.* (1966) and Smith and Sbar (1974) for the Intermountain seismic belt. Recurrence rates tabulated by Smith (1972) are basically extrapolations of the data of Ryall *et al.* (1966) for the 1932-1961 period; note, however, that the recurrence data tabulated by Smith (1972) in his Table 1 imply an area only of about 6-7 x 10^3 km^2.

The data of Table 1 clearly point out that the extrapolation of recurrence for very large earthquakes in the Wasatch Front area is problematical. The extrapolations are extremely sensitive to the slope coefficient b, which can vary both in space and time, and to a lesser extent to the values of a, which are functions of the areal flux. Again, we emphasize the importance of a clear specification of area. The reader should also be aware of the importance of noting the consistency of magnitude scales when comparing different data.

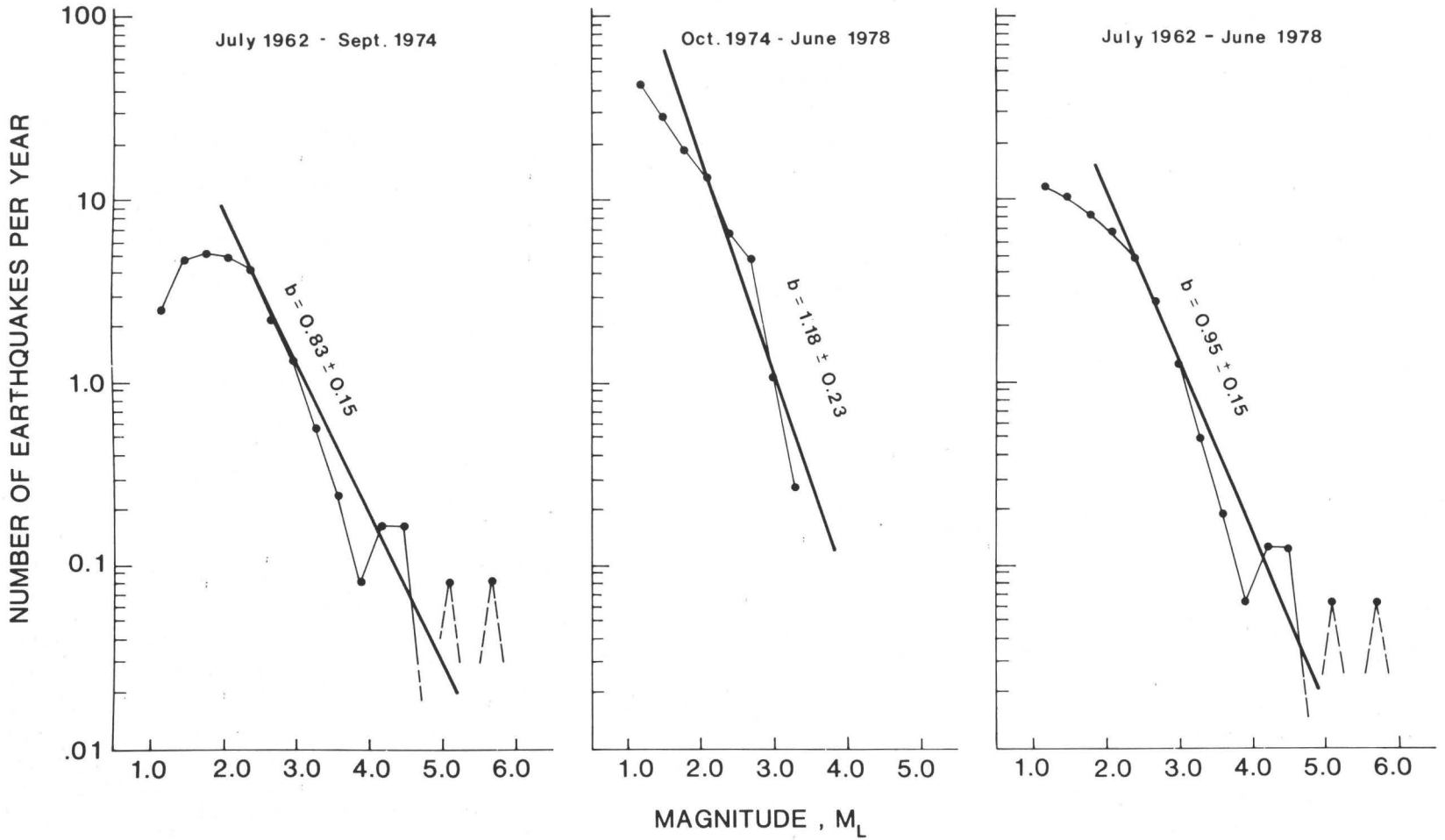

Fig. 8. Annual rate of occurrence of earthquakes of magnitude M_L for three separate time samples and for a sub-region of the Wasatch Front area (111°15'-112°15'W, 38°54'-42°30'N). Area = 92,810 km^2. Values of the slope coefficient b at the 95 percent confidence limits computed by the method of maximum likelihood (see text).

20

Table 1

Parameters of recurrence curves applicable to the Wasatch Front area. In terms of the common frequency-magnitude relation: long $N = a\text{-}bM$, $a = \hat{a}$ for $N = \hat{n}$, the number of earthquakes of a given magnitude M per year per 1,000 km^2; $a = \hat{a}_c$ for $N = \hat{N}_c$, the number of earthquakes equal to or greater than a given magnitude per year per 1,000 km^2. $(n_{3.0})_{WF}$ = the expected number of shocks of magnitude 3.0 per year throughout the Wasatch Front reference area (92,810 km^2); $(T_{7.5})_{WF}$ = the expected time for the recurrence of a magnitude 7.5 earthquake within the same area.

No.	Source	Period	Area ($km \times 10^3$)	b	$\hat{a}$	$\hat{a}_c$	$(n_{3.0})_{WF}$	$(T_{7.5})_{WF}$ (yrs)
1.	Fig. 7	1850-1978 (129.0 yrs)	92.81 Wasatch Front reference area)	0.63 (interval)	0.38	-	2.87	238
				0.72 (cumulative)	-	1.01	-	-
2.	Fig. 8	1962-1974 (12.25 yrs)	33.75 (Wasatch fault area)	0.83	1.08	1.36	3.61	1,505
3.	Fig. 8	1974-1978 (3.75 yrs)	33.75 (Wasatch fault area)	1.18	2.07	2.25	3.14	64.924
4.	Fig. 8	1962-1978 (16.0 yrs)	33.75 (Wasatch fault area)	0.95	1.43	1.67	3.53	5.338
5.	U.S. Geological Survey (1976)	1850-1974 (125.0 yrs)	220.18 (Utah)	0.76 (interval)	1.15[1]	-	6.88	382
				0.79 (cumulative)	-	1.47	-	-

21

Table 1 (continued)

No.	Source	Period	Area ($km \times 10^3$)	b	$\hat{a}$	$\hat{a}_c$	$(n_{3.0})_{WF}$	$(T_{7.5})_{WF}$ (yrs)
6.	Ryall et al. (1966)	a. pre-1932 (82 yrs)	∿71.3 ("Rocky Mt. zone")	0.52	-0.07[2]	-	2.18	101
		b. 1932-1961 (30.0 yrs)	∿220.9 ("Rocky Mt. zone")	0.61	1.52[2]	-	45.5	12
7.	Smith & Sbar (1974)	1961-1970 (10.0 yrs)	(Intermountain seismic belt)	1.06	-	-	-	-

[1]Area of the entire state of Utah used to compute areal flux; reduction of area by one-half--to correspond more closely to seismogenic area--would double $(n_{3.0})_{WF}$ and halve $(T_{7.5})_{WF}$.

[2]Computed directly from value given by Ryall et al. (1966) for the number of shocks with M = 4.0 per year per 1,000 km^2.

22

Instrumental seismicity of the Wasatch Front area for the 1962 to 1978 period indicates a significantly higher value of b, and hence a larger proportion of small to large earthquakes, than expected from the historical data. The method of analysis precludes this effect being due to increased network coverage. The persistence of major seismic gaps along the Wasatch fault during the 1962 to 1978 period emphasizes that the seismicity sample for that period is basically anomalous. From 1962 through 1978, twelve independent mainshocks of magnitude 4.0 or greater occurred within the Wasatch Front reference area. Twenty-one such shocks would have been expected from extrapolation of the historical data (No. 1, Table 1).

A fundamental assumption regarding the extrapolation of earthquake recurrence is that the data used to calculate the values of a and b accurately represent the long-term seismicity of a region. Ideally they should represent a long enough period of time that includes at least one repeat interval of the largest earthquake. The large seismic gaps along the Wasatch fault occupy a significant portion of the Wasatch Front study area and implicitly influence the calculation of seismic flux by their non-contribution. Because we assume that the faults within the gap have an equal potential of producing earthquakes as the active segments, the recurrence intervals tend to be overestimated by an undetermined amount.

In sum, rates of current earthquake recurrence in the Wasatch Front area can be estimated fairly accurately for magnitudes up to about 5.0 using the instrumental seismicity monitored since 1962. For the present, extrapolations to larger magnitudes would seem more reasonably based on the longer-term historical record until more data becomes available on the geological dating of pre-hisoric surface faulting during the past several thousand years. The historical earthquake data imply expected return periods, as specified earlier, for the Wasatch Front area (92,810 km^2), of 22 to 25 years for $M_L \geq 6.0$, 111 to 115 years for $M_L \geq 7.0$, and 232 to 263 years for $M_L \geq 7.5$. Such return periods for major earthquakes of magnitude 7 and larger in the Wasatch Front area are compatible with new measurements of pre-historic rupture intervals now being acquired on segments of the Wasatch fault (Swan et al., 1978; Schwartz et al., 1979)--assuming the episodic rupture of each of several segments of the Wasatch fault.

Focal depths. Of the 2,482 earthquakes located in the Wasatch Front area during the period October 1, 1974 to June 30, 1978 (Figure 4), unrestricted focal depths were determined for 1,160, i.e., the epicentral distance to the nearest recording station for these earthquakes was either less than the focal depth or less than 20 km--a maximum distance for which the focal depth can be confidently resolved. Histograms of focal depths for two sub-regions of the Wasatch Front area are shown in Figure 9 together with data from two special field studies.

The data of Figure 9a are for a restricted part of the Wasatch Front area to exclude the sampling of mining-related seismicity in the southeastern part of the study area as well as to separate the intense aftershock activity in the Idaho-Utah border area in the northwestern part (see Figure 5). The sample of Figure 9b consists almost entirely of earthquakes in that area.

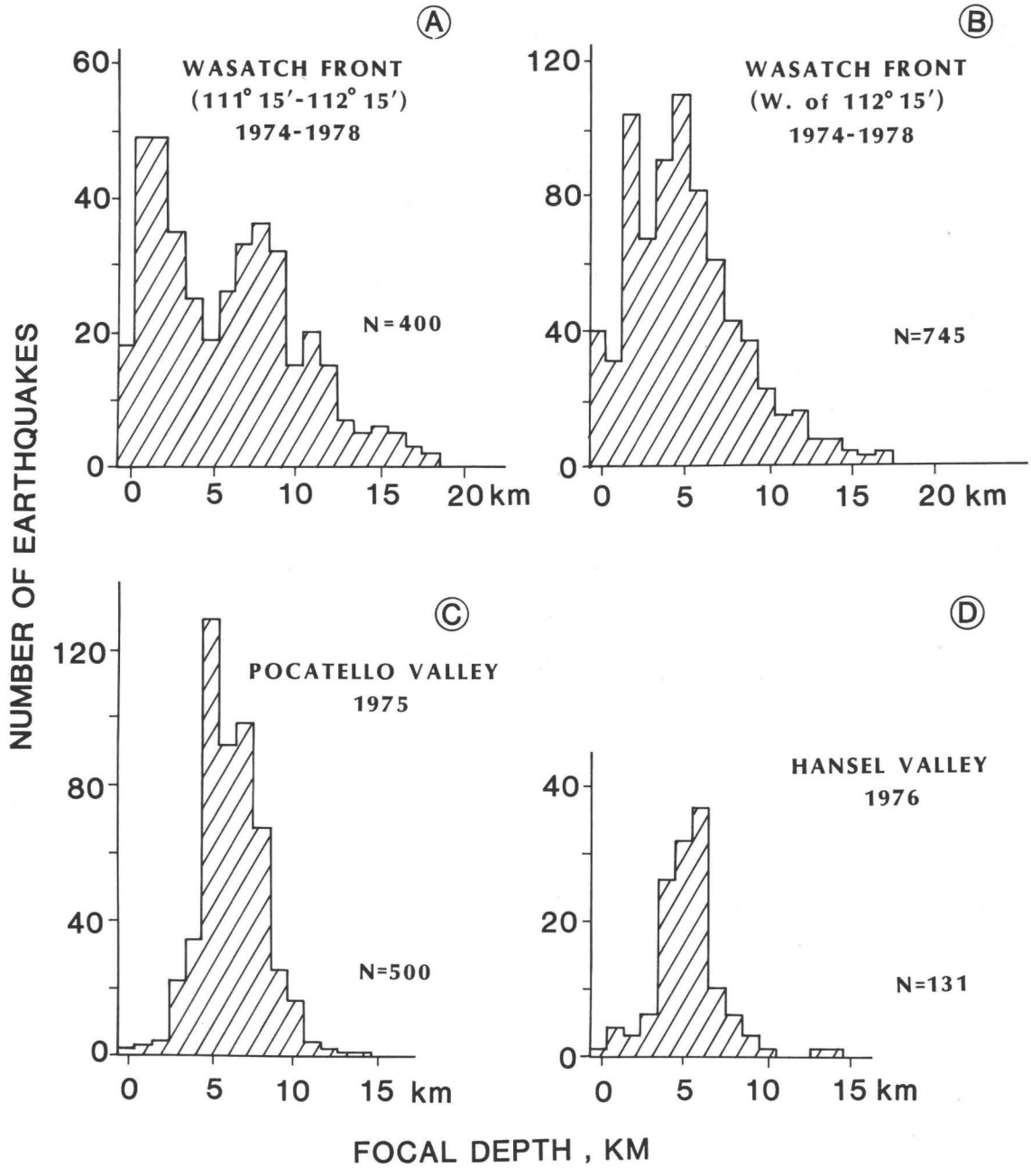

Fig. 9. Frequency histograms of accurately determined focal depths in the Wasatch Front area: (a and b) for the period: October 1, 1974 - June 30, 1978, (c) for aftershocks of the March 1975 Idaho-Utah border (Pocatello Valley) earthquake, and (d) for a 1976 earthquake seqeuence in Hansel Valley.

Almost all earthquakes in the Wasatch Front area are shallower than 20 km in depth, as is general for the Intermountain area (Smith, 1978). Mean depths for the samples in Figure 9 range from 5.3 to 6.2 km. Figure 9a shows a bimodal distribution with peaks at 1-3 km and at 7-9 km. For most of the very shallow events the epicentral distance to the nearest station in fact exceeds the focal depth, so that the very shallow depths may not be accurate. However, a systematic pattern of travel-time residuals for these events results when their focal depths are held fixed at 7.0 km--indicating that they are significantly shallower.

Focal depths for earthquakes in the Idaho-Utah border area west of 112°15' determined with the fixed network (Figure 9b) give similar focal depths as those determined in the same general area from field studies involving dense coverage with portable seismographs.

Fault-plane solutions. Focal mechanismshave been determined for widely-spaced earthquakes throughout the Wasatch Front area as well as throughout the Intermountain seismic belt (see Smith and Lindh, 1978). Five composite solutions determined with the Wasatch Front network since October 1974 are shown in Figure 10; the location of earthquakes corresponding to the focal mechanisms is indicated in Figure 11, which schematically summarizes all available data for the asatch Front area.

The composite solutions (Figure 10) each comprise first motions from several closely spaced events and display good internal consistency. Solution (a) for events along the East Cache fault indicates dip-slip, extensional faulting and is similar to solution (f) (Figure 11) determined by Smith and Sbar (1974) and discussed by them for the M_L = 5.7 Cache Valley (Logan) earthquake of 1962. The preferred interpretation for solution (a) is that of normal faulting based upon similarity with normal faulting of Holocene age along the East Cache fault. Solutions (b) and (e) are similar to the majority of focal mechanisms in the Wasatch Front area (Figure 11), present normal faulting, with sightly varying trends of extension. Solutions (c) and (d), on the other hand, point out that there are local complications, i.e., they reflect components of thrust or high-angle reverse faulting.

Although aftershocks of the M_L = 4.3 Heber City earthquake of 1972 reflect normal faulting (solution (g), Figure 11), solutions (c) and (d) for nearby clusters of earthquakes indicate significant horizontal components of compressional stress. Earthquakes in this area are near the intersection of the Wasatch Front and the major east-west trending Uinta fold axis. Solution (h) determined by Smith et al. (1974) for shallow earthquakes beneath the Sunnyside coal mining district suggests thrust faulting and is similar to solutions (c) and (d) suggesting that stress orientations in the southeastern part of the Wasatch Front area may more generally relate to the tectonics of the northwestern part of the Colorado Plateau. The contrast in stress orientation across the boundary of the Basin and Range province in this area differs from that to the north of Salt Lake City, where fault plane solutions imply that east-west extensional strain extends well east of the Wastch fault zone, but not beyond mapped zones of Cenozoic normal faulting.

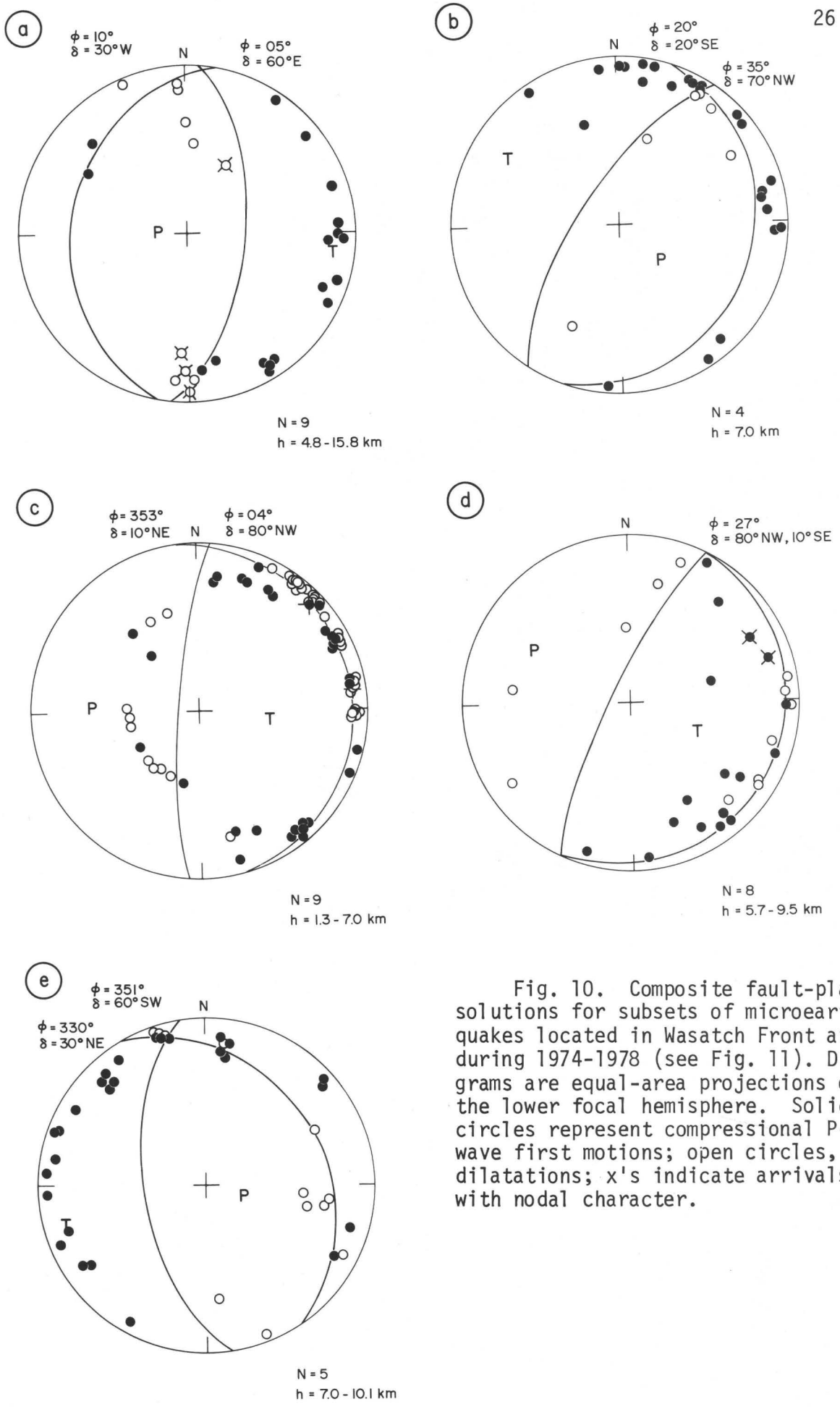

Fig. 10. Composite fault-plane solutions for subsets of microearthquakes located in Wasatch Front area during 1974-1978 (see Fig. 11). Diagrams are equal-area projections of the lower focal hemisphere. Solid circles represent compressional P-wave first motions; open circles, dilatations; x's indicate arrivals with nodal character.

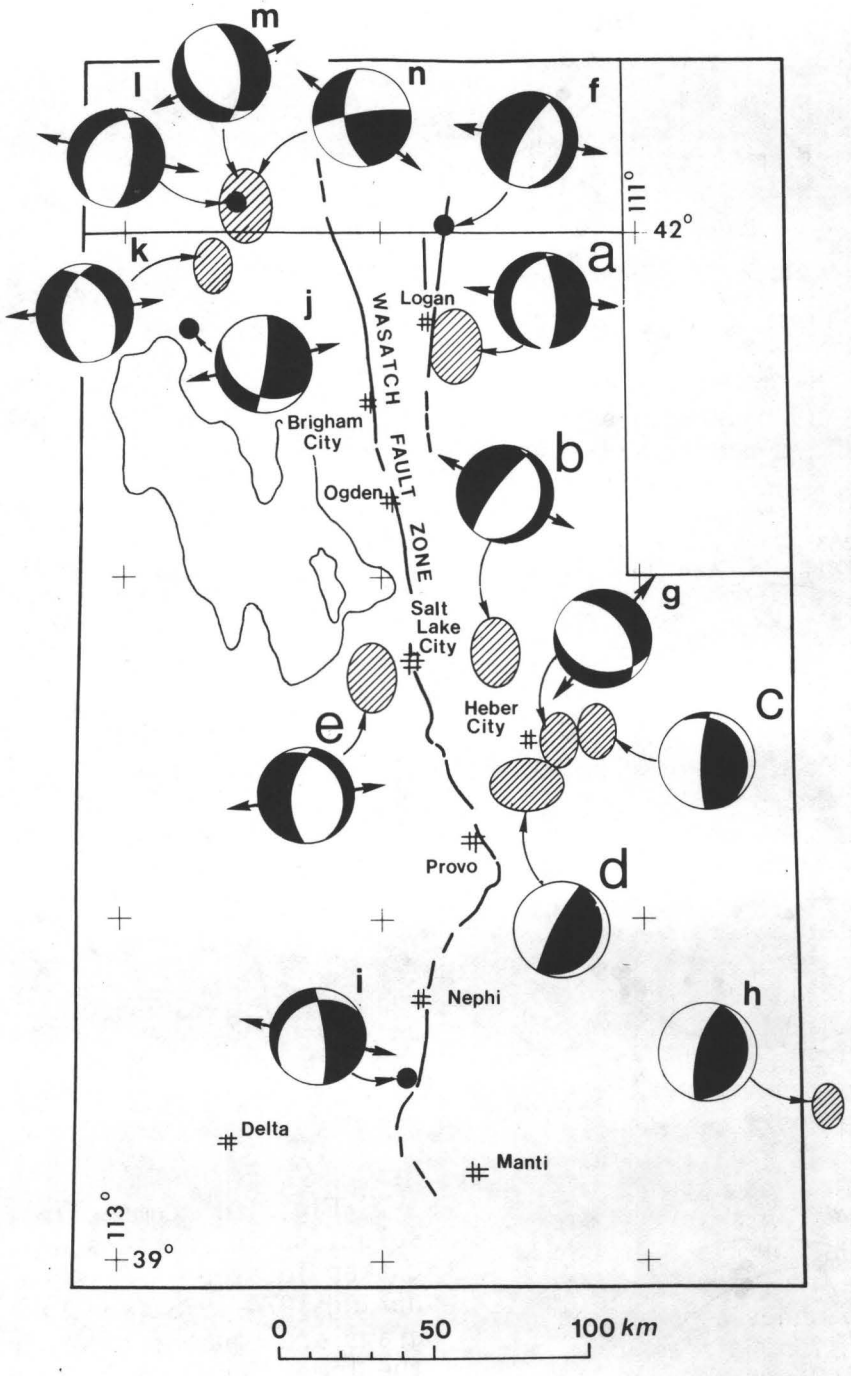

Fig. 11. Schematic summary of fault-plane solutions (lower-hemisphere projections) for the Wasatch Front area. Compressional quadrants are shaded. Trends of T-axes shown by heavy arrows. Large dots show location of single-event solutions; hachured zones show sample areas for composite solutions. Sources: (a-e), this study (keyed to Figure 10); (f and i), Smith and Sbar (1974); (h) Smith et al. (1974); (j) Dewey et al., (1973); (l) Bache et al. (1979); (g, k, m, and n) from aftershock studies included in Arabasz et al. (1979).

Another area where the focal mechanisms indicate a local complication is the Idaho-Utah border area north of the Great Salt Lake. Focal mechanisms in the Hansel Valley area (solution (j) and (k)) reflect a predominance of normal faulting with general E-W extension, as does solution (k) for the mainshock of the 1975 M_L = 6.0 Idaho-Utah border (Pocatello Valley) involving normal, oblique, and strike-slip faulting. Solutions (m) and (n) are two of eight aftershock mechanisms that illustrate some of the complexity of the aftershock seqeuence (see Arabasz et al., 1979, pp. 339-373.

Earthquake Hazards and Seismic Risk Along the Wasatch Fault

In terms of risk or the level of exposure to personal injury and property damage from earthquakes, the Wasatch Front area clearly faces a comparatively high probabilistic risk of destructive ground shaking that might reach 0.2g horizontal acceleration in a 50-yr period (Algermissen and Perkins, 1976). Risk is enhanced by the concentration of 85% of Utah's 1.3 million population, and accelerating economic development along major active faults that have ruptured repeatedly in late Quaternary and Holocene time. At least six damaging earthquakes of maximum M.M. intensity VII or greater have occurred in the Wasatch Front area since 1850, but a greater threat is posed by the susceptibility of the area to a "credible" earthquake of magnitude 7.5 (U.S. Geological Survey, 1976)--chiefly because of the Wasatch fault and its length, continuity of faulting, and evidence of repeated surface faulting in the recent pre-historic past. The sapce-time pattern of seismicity along the Wasatch fault, including the existence of major seismic gaps along it, suggests the separate activation of discrete segments of the fault several tens of kilometers long and the potential for future large earthquakes along individual sectors. Historical earthquake data and new measurements of pre-historic rupture intervals on the Wasatch fault suggest the occurrence of magnitude 7+ earthquakes every few hundred years somewhere in the Wasatch Front area--assuming the episodic rupture of each of several segments of the Wasatch fault. At the same time, the cumulative destructive effects of more frequent moderate-size earthquakes cannot be overlooked..

The primary earthquake hazards of ground shaking and displacement along surface faults in the Wasatch Front area are similar to those, for example, in California. In addition, potential earthquake hazards in the Wasatch Front area include: (1) earthquake-triggered landslides and rock and snow avalanches along the mountainous Wasatch Front (Smith, 1974); (2) soil liquefaction, differential ground settlement, and landsliding (Parry, 1974; Buck, 1976; Van Horn, 1975); (3) catastrophic flooding from impounded reservoirs in the Wasatch mountains upstream from densely populated centers--including Pineview Reservoir (110,150 acre-feet), whose dam failure could cause 8,000 fatalities in Ogden (U.S. Geological Survey, 1976), and Deer Creek Reservoir (152,600 acre-feet), whose dam failure could cause, 11,900 fatalities in Provo (U.S. Geological Survey, 1976); and (4) disruption of vulnerable life-support facilities (U.S. Geological Survey, 1976). Some secondary hazards that have been pointed out by other observers include: (1) the explosion of combustible gases both occurring naturally and in man-made storage close to the Wasatch fault (Kaliser, 1976); and (2) seasonal

hazards, such as a high fire danger during summer months when strong canyon winds are common in the morning and evening, and exposure to freezing and sub-freezing temperatures during the winter as a consequence of losing natural gas and electrical supplies (U.S. Geological Survey, 1976).

Acknowledgments

We are grateful to the numberous students and staff members at the University of Utah who participated in the acquisition and analysis of the extensive data used in this study. A.J. Kastrinsky and M. Griscom made substantial contributions to the systematic revision of historical epicenters and magnitudes, respectively. This research was supported by: the U.S. Department of the Interior, Geological Survey, Contract Nos. 14-08-0001-14585, 14-08-0001-15895 and 14-08-0001-16725; the Division of Earth Sciences, National Science Foundation, NSF Grants EAR 73-00555 A02 and EAR 77-23706; and the State of Utah.

References

Aki, K. (1965). Maximum likelihood estimate of b in the formula log N = a-bM and its confidence limits, Bull. Earthquake Res. Inst., Tokyo Univ. 43, 237-239.

Algermissen, S. T. and D. M. Perkins (1976). A probabilistic estimate of maximum acceleration in rock in the contiguous United States, U.S. Geological Survey Open-File Rept. 76-416, 45 pp.

Anderson, R. E. (1978). Quaternary tectonics along the Intermountain seismic belt south of Provo, Utah, Brigham Young University Geology Studies 25, 1-10.

Arabasz, W. J. and M. Griscom (1978). Precursory seismicity patterns in the Utah region: Can variations in the precursor time scale be large? (abstract), EOS, Trans. Am. Geophys. Union 59, 1126.

Arabasz, W. J., R. B. Smith, and W. D. Richins, editors (1979). Earthquake Studies in Utah, 1850 to 1978, University of Utah, Salt Lake City, 552 pp.

Bache, T. C., D. G. Lambert, and T. C. Barker (1979). A source model for the March 28, 1975 Pocatello Valley earthquake from time domain modeling of teleseismic P waves (preprint submitted to Bull. Seism. Soc. Am.).

Bakun, W. H. and A. G. Lindh (1977). Local maginudes, seismic moments, and coda durations for earthquakes near Oroville, California, Bull. Seism. Soc. of Am. 67, 615-629.

Buck, B. W. (1976). Physico-chemical properties of sensitive soils in the lower Jordan Valley, Utah, M.S. Thesis, University of Utah, Salt Lake City,

Bucknam. R. C. (1978). Northwestern Utah seismotectonic studies, U.S. Geol. survey, National Earthquake Hazards Reduction Program, Summeries of Tech. Repts. 7, 64

Carver, D., C. J. Langer, W. D. Richins, and R. Henrisey (1978). Aftershocks of the September 30, 1977, Uinta Basin, Utah, earthquakes (abstract), Earthquake Notes 49, 41.

Cluff, L. S., G. E. Brogan, and C. E. Glass (1970). Wasatch fault, northern portion: Earthquake fault investigation and evaluation, Report to Utah Geol. and Min. Survey, Woodward- Clyde and Associates, 27 pp.

Cluff, L. S., G. E. Brogan, and C. E. Glass (1973). Wasatch fault, southern portion: Earthquake fault investigation and evaluation, Report to U.S. Geol. Surv., Woodward-Lundgren and Associates, 79 pp.

Cluff, L. S., G. E. Brogan, and C. E. Glass (1974). Investigation and evaluation of the Wasatch fault north of Brigham City, and Cache Valley faults, Utah, and Idaho: A guide to land-use planning with recommendations for the seismic safety, Report to U.S. Geol. Surv., Woodward-Lundgren and Associates, 147 pp.

Cluff. L. S., L. F. Hintze, G. E. Brogan, and C. E. Glass (1975). Recent activity of the Wasatch fault, northwestern Utah, U.S.A., Tectonophysics 29, 161-168

Cook, K. L. and R. B. Smith (1967). Seismicity in Utah, 1850 through June 1965, Bull. Seism. Soc. Am. 57, 689-718.

Dewey. J. W., W. H. Dillinger, J. Taggert and S. T. Algermissen (1973). A technique for seismic zoning: Analysis of earthquake locations and mechanisms in nothern Utah, Wyoming, Idaho, and Montana, in Contributions to Seismic Zoning, S. L. Harding, editor, NOAA Tech. Rept. ERL 267-ESL 30, U.S. Dept. of Commerce.

Gutenberg, B. and C. F. Richter (1954). Seismictiy of the Earth, 2nd ed. Princeton Univ. Press, Princeton, N. J.

Gutenberg, B. and C. F. Richter (1956). Earthquake magnitude, intensity, energy, and acceleration, Bull. Seism. Soc. Am. 46, 105-145.

Hamblin, W. K. (1976). Patterns of displacement along the Wasatch fault, Geology 4, 619-622.

Kastrinsky, A. J. (1977). Seismicity of the Wasatch Front, Utah: Detailed epicentral patterns and anomalous activity, M.S. Thesis, University of Utah, Salt Lake City, Utah, 138 pp.

Keller, G. R., R. B Smith, and L. R. Braile (1975). Crustal structure along the Great Basin-Colorado Plateau Transition from seismic refraction profiling, J. Geophys. Res. 80, 1093-1098.

Knopoff, L. and Y. Kagan (1977). Analysis of the theory of extremes as applied to earthquake problems, J. Geophys. Res. 82, 5647-5657.

Lahr, J. C. (1979). HYPOELLIPSE: A computer program for determining local earthquake hypocentral parameters, magnitude, and first motion pattern, U.S. Geol. Surv. Open-File Rept., 79-431, 53pp.

Lee, W. H. K., R. E. Bennet, and K. L. Meahger (1972). A method of estimating magnitude of local earthquakes from signal duration, U.S. Geol. Survey, Open-File Report, 28 pp.

Morisawa, M. (1972). The Wasatch fault zone--general aspects, in Environmental Geology of the Wasatch Front, 1971, L. S. Hilpert editor, D1-D17, Utah Geol. Assoc. Publ. 1.

Parry, W. T. (1974). Earthquake hazards in sensitive clays along the central Wasatch Front, Utah, Geology 2, 559-560.

Real, C. R. and T. L. Teng (1973). Local Richter magnitude and total signal duration in southern California, Bull. Seism. Soc. Am. 63, 1809-1827.

Roller, R. C. (1965). Crustal structure in the eastern Colorado plateaus province from seismic-refraction measurements, Bull. Seism. Soc. Am. 55, 107-119.

Ryall, A., and K. Priestley, (1975). Seismicity, secular strain, and maximum magnitude in the Excelsior Mountains area, western Nevada and eastern California, Bull. Geol. Soc. Am. 86, 1585-1592.

Sbar, M. L., M.Barazangi, J. Dorman, C. H. Scholz, and R. B. Smith (1972). Tectonics of the Intermountain seismic belt, western United States: Microearthquake seismicity, and composite fault plane solutions, Bull. Geol. Soc. Am. 83, 12-28

Schwartz, D. P., F. H. Swan III, K. L. Hanson, P.L. Knuepfer, and L. S. Cluff (1979). Recurrence of surface faulting and large magnitude earthquakes along the Wasatch fault zone near Provo, Utah, (abstract), Geol. Soc. Am. Abstracts with Programs 11, 301.

Shenon, P.J. (1936). The Utah earhquake of March 12, 1934 (extracts from unpublished report), pp. 43-48 in Neumann, F., United States Earthquakes, 1943, U. S. Coast and Geodetic Survey, serial 593.

Smith, R. B. (1972). Contemporary seismicity, seismic gaps, and earthquake recurrences of the Wasatch Front, in Environmental Geology of the Wastch Front, Utah Geol. Assoc. Publ. 1, 11-19.

Smith, R. B. (1974). Seismicity and earthquake hazards of the Wasatch Front, Utah, July - August 1974, Earthquake Information Bulletin 6, 12-17.

Smith, R. B. (1978). Seismicity, crustal structure, and intraplate tectonics of the Western Cordillera, in Cenozoic Tectonics and Regional Geophysics of the Western Cordillera, R. B. Smith and G. P. Eaton, editors, Memoir 152, Geol. Soc. Am., 111-144.

Smith, R. B. and A. G. Lindh (1978). Fault-plane solutions of the Western United States: A compilation, in Cenozoic Tectonics and Regional Geophysics of the Western Cordillera, R. B. Smith and G. P. Eaton, editors, Memoir 152, Geol. Soc. Am., 107-110.

Smith, R. B. and M. L. Sbar (1974). Contemporary tectonics and seismicity of the western United States with emphasis on the Intermountain seismic belt, Bull. Geol. Soc. Am. 85, 1205-1218.

Smith, R. B., P. L. Winkler, J. G. Anerson, and C. H. Scholz (1974). Source mechanisms of microearthquakes associated with underground mines in eastern Utah, Bull. Seism. Soc. Am. 64, 1295-1317.

Stepp, J. C. (19720. Analysis of the completeness of the earthquake sample in the Puget Sound area and its effect on statistical estimates of earthquake hazards, Proc. Intern, Conf. on Microzonation for Safer Construction, Research and Application, 2, Seattle, Washington Univ., 897-909.

Suteau, A. M. and J. H. Whitcomb (1979). A local earthquake coda magnitude and its relation to duration, moment M_O, and local Richter magnitude M_L, Bull. Seism. Soc. Am. 69, 353-368.

Swan, F. H., III, S.P. Schwartz, K. L. Hanson, P. L. Kneupfer, and L. S. Cluff (1978). Recurrence of surface faulting and large magnitude earthquakes along the Wasatch fault, Utah (abstract), EOS, Trans. Am. Geophys. Union 59, 1126.

United States Geological Survey (1976). A study of Earthquake Losses in the Salt Lake City, Utah Area, Open File Report 76-89, 357 pp.

Utsu, T. (1965). A method for determining the value of b in a formula log n = a-bM showing the magnitude-frequency relation for earthquakes, Geophys. Bull., Hokkaido Univ. 13, 99-103 (in Japanese with English abstract).

Utsu, T. (1966). A statistical significance test of the difference in b-value between two earthquake groups. J. Phys. Earth 14, 37-40.

Van Horn, R. (1975). Earthquake hazard analysis--an example from the Sugar House Quadrangle, Utah, Earthquake Information Bull. 7, 12-14.

Wesson, R. L. and W. L. Ellsworth (1973). Seismicity preceding moderate earthquakes in California, J. Geophys. Res. 78, 8527-8546.

Williams, J. S. and M. L. Tapper (1953). Earthquake history of Utah, 1850-1949, Bull, Seism. Soc. Am. 43, 191-218.

Woolard, G. P. (1958). Areas of tectonic activity in the United States as indicated by earthquake epicenter, Trans. Am. Geophys. Union 39, 1135-1150.

Wyss, M., R. E. Habermann, and A. C. Johnston (1978). Long term precursory seismicity fluctuations, Pure and Applied Geophysics (in press).

Discussion

I. Regarding apparent disagreement in comparing seismic attenuation in Utah to that in California -- between Arabasz et al. (based on Wood-Anderson data) and Clow & Evernden (based on attenuation of intensity):

A. Ryall: The difference between different attenuation curves would be much more pronounced in the near field, at 10 to 50 km, than, say, at 100 to 600 km. Also, the curves given by different people, for example, Schnabel and Seed, are different for different magnitudes, so there still is the possibility that for larger events, attenuation in the near field may be different in certain areas. Murphy and Lahoud, measuring accelerations on rock for large nuclear explosions, 200 kilotons to 1 megaton, found the same type of attenuation as Evernden proposes for the Basin and Range -- and it's different than what Schnabel and Seed, for example, give the Pacific coastal zone.

W. J. Arabasz: I think we'll find at the conclusion of this conference that attenuation [in the Great Basin] is one of the main parameters for which we have pathetically little information. We all need to be aware of at the outset, the idea that the size of an earthquake in different regions may well be different, for reasons that Jack Evernden has pointed out.

II. Regarding creep and seismic gaps on the Wasatch fault:

R. E. Wallace: Along the Wasatch Front, is there any creep that's been measured, or warping in the quiet areas [along the Wasatch fault] without cracks? Is there any explanation other than that [the quiet segments] are true seismic gaps?

L. S. Cluff: We haven't been able to document creep [on the Wasatch fault] in our studies for certain. There are places along the East Bench fault scarp in Salt Lake City where one can clearly state that [apparent deformation] is attributable to gravity rather than to tectonic creep. Regarding the seismic gaps on the Wasatch fault, we find, geologically, the same gaps. They're not gaps that will continue. They are gaps that I would say will fill.

R. B. Smith: About ten year ago we observed cracks in asphalt along the trace of the Wasatch fault where it obliquely crosses Wasatch Drive near the [Woodward-Clyde] trenches. I put in a nail line, remeasured it for about two years, and saw displacements on the order of two or three millimeters per year. The road was then resurfaced, but the new asphalt broke again. An engineer from the Utah Highway Department confirmed that there was some fill beneath that segment of road, but not very much, such that in his estimation the road deformation was not

simply due to compaction of fill.

In the early sixties the National Geodetic Survey did a geodetic triangulation survey of Salt Lake County extending to Utah County on the south, and the U.S. Geological Survey did a trilateration survey from essentially Salt Lake City north to Ogden. Jim Savage and his group have reobserved the trilateration net to the north (see Jour. Geophys. Res. 84, 5423-5435) and show evidence of east-west compression in the vicinity of the northern seismic gap, as opposed to extension, expected from focal mechanisms or from the geology. By comparison, the Hebgen Lake area is in very well developed north-south extension compatible with the active seismicity.

B. N. Kaliser: The Utah Geological and Mineral Survey has been involved in mapping features such as fractures in pavement along the East Bench fault, a branch of the Wasatch fault, and elsewhere. But it's extremely difficult with the relief that exists along the fault traces, and [because] time is required to observe and reobserve the same point, there is nothing conclusive with respect to creep anywhere, to my knowledge, along any branch of the Wasatch.

[Regarding the road deformation mentioned by Bob Smith,] I have a photograph of a cavity that resulted from the Pocatello Valley earthquake .... right where the observations were. There is evidence of a very large subsurface cavern as a result of mining activity -- an old adit over a hundred years old [whose] limits are not precisely known.

R. C. Bucknam: There's another example of road deformation along the Wasatch, a little more evident than [at Wastch Drive near the Woodward-Clyde trenches]-- at Rock Creek near Provo. There the paved highway crosses the fault scarp nearly at a right angle. There's about a foot of relief right at the fault trace. Again, there's a cut-and-fill situation .... but according to Ken Hamblin this has developed over a period of twenty years, and it clearly steps. Whether it's indeed tectonic creep or compaction of fill beneath the pavement could probably be defined by a special survey.

R. B. Smith: With respect to the problem of creep along the Wasatch, there have been two geodetic surveys done in the Salt Lake Valley area. One was in the vicinity of the University of Utah in the Thirteenth East area done in the early sixties or late fifties by the Civil Engineering Department in conjunction with the National Geodetic Survey, and monuments were established. Professor C. G. Bryner [of the Civil Engineering Department] also established another triangulation net about the same time in the vicinity of Little Cottonwood Canyon where the trenches are now exposed. To my knowledge, neither of these nets have been reobserved.

B. N. Kaliser: Some of the points are no longer available according to Cliff Bryner.

R. B. Smith: A lot of the monuments have been disturbed because of subdivsion development, but according to Professor Bryner, there are still some around, so [reobservation] is possible.

G. Greene: I have some critical slides of the spot in Rock Creek that was described if [anyone is interested].

B. N. Kaliser: [Regarding the long-term deformation at that site], I would say that the classical engineering behavior of fill is not always what it would be. Settlement should occur within a couple of years, but frequently that is not the case, especially if you disturb the subsurface drainage characteristics of the material. So we [can] have fill settling for decades.

SEISMICITY RELATED TO STRUCTURE AND ACTIVE TECTONIC PROCESSES IN THE WESTERN GREAT BASIN, NEVADA AND EASTERN CALIFORNIA

By

J. D. VanWormer and Alan Ryall

Seismological Laboratory
University of Nevada
Reno, NV 89557

ABSTRACT

Precise epicentral determinations based on local network recordings are compared with mapped faults and volcanic features in the western Great Basin. This region is structurally and seismically complex, and seismogenic processes vary within it. In the area north of the rupture zone of the 1872 Owens Valley earthquake dispersed clusters of epicenters agree with a shatter zone of faults that extend the 1872 breaks to the north and northwest. An area of frequent earthquake swarms east of Mono Lake is characterized by northeast-striking faults and a crustal low-velocity zone; seismicity in this area appears to be related to volcanic processes that produced thick Pliocene basalt flows in the Adobe Hills and minor historic activity in Mono Lake. In the Garfield Hills between Walker Lake and the Excelsior Mountains, there is some clustering of epicenters along a north-trending zone that does not correlate with major Cenozoic structures. In an area west of Walker Lake low seismicity supports a previous suggestion by Gilbert and Reynolds (1973) that deformation in that area has been primarily by folding and not by faulting. To the north, clusters of earthquakes are observed at both ends of a 70-km long fault zone that forms the eastern boundary of the Sierra Nevada from Markleeville to Reno. Clusters of events also appear at both ends of the Dog Valley fault in the Sierra west of Reno, and at Virginia City to the east.

Fault-plane solutions for the belt in which major earthquakes have occured in Nevada during the historic period (from Pleasant Valley in the north to the Excelsior Mountains on the California-Nevada Border) correspond to normal-oblique slip and are similar to that found by Romney (1957) for the 1954 Fairview Peak shock. However, mechanisms of recent moderate earthquakes within the SNGBZ are related to right- or left-lateral slip, respectively on nearly vertical, northwest- or northeast-striking planes. These mechanisms are explained by a block faulting model of the SNGBZ in which the main fault segments trend north, have normal-oblique slip, and are offset or terminated by northwest-trending strike-slip faults. This is supported by the observation that seismicity during the period of observation has been concentrated at places where major faults terminate or intersect.

INTRODUCTION

The University of Nevada Seismological Laboratory has operated dense seismic networks in the Reno-Carson City-Truckee and Mono Lake-Walker Lake areas, respectively since 1972 and 1974. The network around Reno initially consisted of a few stations in the Truckee area, installed to investigate possible reservoir-induced earthquakes; it has since been expanded to the north, south and east. A 30-station network between Walker and Mono Lakes was constructed to study faults that might be used for an earthquake control experiment; it has since been reduced in size. Hypocenters within the two dense networks were determined with the USGS computer program HYPO71 (Lee and Lahr, 1972), using a crustal model consisting of a 28-km layer with P-velocity of 6.0 km/sec over a halfspace with P-velocity 7.85 km/sec. This model agrees with the results of Ryall and Jones (1964), and has been verified by analysis of P-wave residuals as a function of distance for well-located events. No compelling evidence has been found for the existence of an intermediate crustal boundary in the western Great Basin (Eaton, 1963); if such a boundary exists it may not be continuous over the entire region.

For epicenter locations in the remainder of the western Great Basin, the Seismological Laboratory operates a sparse network of stations in the area bounded by Tonopah on the southeast. Battle Mountain on the northeast, and the Sierra Nevada on the west. Epicenter locations for events recorded by the regional network for the period from 1 October 1969 to 31 December 1975 were determined with a program NEVLOC that used only phases identified by the analyst as Pg or Sg, and apparent velocities of 6.1 and 3.55 km/sec, respectively, for the two phases. For the period following 31 December 1975, a program NEVLOC2 was used, and in calculations with this program about 5% of the readings were Pn and Sn (W. Peppin, verbal communication).

In this paper, hypocentral determinations and fault-plane solutions based primarily with data collected by the dense seismic networks around Reno and Mina are compared with geologic structure and tectonic characteristics of this region. The results of this comparison serve to identify active and quiescent areas, particularly for the Sierra Nevada-Great Basin boundary zone (SNGBZ).

ANALYSIS AND RESULTS

Figure 1 shows a generalized map of major faults in the western Great Basin (Stewart, 1979), approximate rupture zones of large earthquakes during the historic period, and more than 5,000 earthquakes located by the various Nevada networks for the period 1969-1978. As noted above, network coverage for this period was not uniform, and this is reflected by epicentral distributions on Figure 1 and the figures that follow. For example, station coverage in the region north of 40 deg N latitude was sparse until 1977, and as a result small earthquakes in that region have not been detected. The same is true of the central part of the SNBGZ from about

Bridgeport to Markleeville. For the southern part of the zone, analysis of data from the dense Mina network did not begin until mid-1974, and detection of small events was generally not as good in the area south of Mono Lake as it was between Mono Lake and Walker Lake. However, based on comparisons of our data lists with those of the University of California and California Institute of Technology, our recording and analysis are generally complete for magnitude greater than 3.0 for the entire SNGBZ, and the threshold is generally around magnitude 2 for most of the region and period studied.

Figure 1 illustrates a previous observation (see Figure 3 in Ryall, 1977) that the level of current seismicity in rupture zones of major historic earthquakes in the Great Basin is inversely proportional to elapsed time since the mainshock, reaching some minimum level after about a century. Dense clusters of earthquakes within the SNGBZ also support the conclusion by Ryall and VanWormer (1980, this volume) that seismic risk is at least as high in this zone as anywhere in the western Great Basin. In the following sections, detailed hypocentral distributions and fault plane solutions are compared with mapped faults and other geologic features for various parts of the SNGBZ.

Bishop and Long Valley Areas

Seismicity in the southern part of the SNGBZ is shown on Figure 2, together with faults taken from geologic maps of California (Jennings, 1977) and Nevada (Stewart and Carlson, 1978). In the lower right corner of the figure, dense clusters of faults at the northern end of the narrow Owens Valley zone spread out along the White Mountains block to the north and the Sierra Nevada to the northwest. Seismicity in the area reflects this pattern, with epicentral lineups along NNE-trending groups of faults in the area just north of the 1872 rupture zone, and a dense cluster of epicenters extending toward Long Valley to the northwest. An earthquake on 4 October 1978 with M = 5.5 was located in the middle of this cluster. Little seismicity is observed between this group of epicenters and the prominent east-trending cluster in the area east of Mono Lake. This relatively quiescent area includes the Long Valley Caldera, where Steeples and Pitt (1976) reported that a month-long survey of microearthquakes in 1973 revealed very little activity within the caldera.

Adobe Hills Volcanic Center

The marked east-west cluster of epicenters at the east end of Mono Valley is in a zone where the rate of occurrence of microearthquakes and small earthquakes is continuously high, as opposed to sporadic bursts of activity in some other parts of the Sierra Nevada frontal fault zone. This group of epicenters runs through the Adobe Hills volcanic center, which Ekren et al. (1976) have characterized as a buried cauldron complex, and which Gilbert et al. (1968) have identified as the source of the most voluminous eruptions in the Mono region during the last four million years. The western part of the area is still active, based on a re-

port that in 1889 the waters of Mono Lake boiled and emitted puffs of steam, presumably as a result of subaqueous eruptions (Christensen and Gilbert, 1964). However, K-Ar ages of basalts in the area east of Mono Lake are 2.6 my or greater (Gilbert et al., 1968).

Earthquakes in the Adobe Hills display a distinct tendency for temporal clustering. For example, during 1978 more than a third of the events analyzed were accompanied by one or more additional events within a one-minute time frame. In a previous study, Richins (1974) suggested that temporal clustering of small earthquakes may be characteristic of areas that are geothermally active in the Great Basin, and this correlation would certainly apply to the Mono area. Another interesting, but not yet explained, observation is that earthquake swarms in the Mono area tend to occur in the late summer and fall. During five years of monitoring with a local network, almost three-fourths of the activity in this area has occurred in the months of July through October (Figure 3), and this pattern has been consistent from year to year. There has also been a tendency for swarm activity within the Adobe Hills zone to migrate toward the west and shallower focal depth. As shown by Figure 4, focal depths of earthquakes in this area are shallowest (2-7 km) under Mono Lake, and deeper (5-15 km) to the east.

To investigate the possibility that seismicity in the Adobe Hills might be related to a zone of partial melting in the crust or uppper mantle, we analyzed teleseismic P-residuals for stations in the area north and east of Mono Lake. Preliminary results of this analysis are shown on Figure 5. Following a previous study by Koizumi et al. (1973), residuals for the various stations were computed relative to observations at Tonopah (TNP). This "standard station" approach was used by Bolt and Nuttli (1966); the rationale for selecting TNP as the standard station was based on analysis which indicated that TNP arrivals were less affected by local structures than other high-quality stations in the region. Residuals (observed minus computed) were first calculated relative to the Herrin (1968) tables, and the TNP residuals were subtracted from those at the other stations. Thus a positive final value means that a particular arrival was late relative to TNP. On all records picks were made by overlaying a trace of the TNP P-wave; times were read to an accuracy of about 0.02 second. Readings were corrected for station elevation relative to TNP using a factor of 4.E-4 sec/m, determined empirically.

For teleseismic sources to the southeast (azimuth 119-155 deg.), Figure 5a shows an area of relatively late arrivals east of Mono Lake, elongated to the northeast around the southern edge of the Excelsior Mountains and the eastern side of the Garfield Hills. For sources to the northwest (azimuth 303-316 deg.), Figure 5b shows a very similar feature. The amplitude of this traveltime anomaly is about 0.5 second, which is higher than a value of 0.3 second found by Steeples and Iyer (1976) for the Long Valley caldera, equal to that reported by Iyer et al. (1979) for the Geysers geothermal area in California, and less than Iyer's (1979) value of 1.5 seconds for Yellowstone National Park. The size of this anomaly,

as well as the agreement in its location for waves propagating in opposite directions indicates that it is due to shallow (i.e.. crustal) structure. However, the plateau between the -0.1 and -0.2 second contours in the upper left part of Figure 5a, and the plateau between the 0.1 and 0.2 second contours in the lower right part of Figure 5b suggest an upper-mantle component of the anomalous zone in this area. For waves propagating toward the northwest, the steep gradient in the lower right corner of Figure 5a also suggests crustal thickening beneath the White Mountain block.

Comparison of Figures 1, 2 and 5 indicates that the level of seismicity is low in the area of largest positive anomalies, but quite high at the ends of the zone (east of Mono Lake and west of Mina). As mentioned above, the focal zone for earthquakes in the swarm area east of Mono Lake is deeper toward the east, i.e. toward the anomalous zone (Figure 4). East of the anomaly, well-determined focal depths in the Excelsior Mountains range from near-surface to almost 25 km, the latter being unusually large for the western Great Basin. North of the Excelsior Mountains focal depths are generally less than 15 km.

Taken together with the volcanic character of the Mono Lake area, and compared with similar results obtained in other regions (Steeples and Iyer, 1976; Iyer, 1979; Iyer et al.. 1979), the P-residual patterns described above would be consistent with a region of partial melting in the crust below the Adobe Hills (centered about 25 km east of Mono Lake), extending to the northeast along a zone of mapped faults (Figure 6) and connected to an upper-mantle source below the Excelsior Mountains.

Deformation by Warping West of the Wassuk Range

North of the Mono seismic zone and west of the Wassuk Range (west of Walker Lake), Figure 1 shows an area that appears to have low seismicity. This area also has low seismic station density; however, the sparsity of activity is probably real, based on comparisons with other areas that are not well covered by the Nevada network. According to Gilbert and Reynolds (1973), this is an area that prior to 7.5 my bp was characterized by faulting, but since that time has been deformed by warping with little faulting (Figure 7). They conclude that this area is bounded on the northwest by a northeast-trending lineament, defined by the en-echelon termination of major Quaternary north-trending normal faults, and on the southeast it is bounded by the northeast-trending "Mono Basin-Excelsior Mountains zone" (line labeled M-E on Figure 7), which forms a structural "knee" with the NNW-striking faults to the south (Gilbert et al.. 1968).

The focal zone east of Mono Lake has an east-west trend, and does not agree with the northeast-strike of surface faults or the Mono-Excelsior trend of Gilbert et al. However, the fault-plane solution for a small earthquake in this zone (see Figure 9 and discussion below) had one plane with N50E strike and 60NW dip, suggesting that the east-west seismic zone consists of a series of northeast-striking en-echelon fractures. Within the area where Gilbert and Reynolds hypothesize deformation by warping,

Figure 7 shows low seismicity, although groups of epicenters within the zone suggest that the stable (i.e., aseismic) block may be smaller than indicated by the stippled area on the figure.

"Seismic Gap" Between Owens Valley and Walker Lake

A map of epicenters determined using data from the dense station network in the area southeast of Walker Lake (Figure 6) shows many dense clusters of earthquakes, in an area that Ryall et al. (1966) and Wallace (1978) have identified as a "seismic gap" between the 1872 Owens Valley and 1932 Cedar Mountains/1934 Excelsior Mountains earthquakes. Ryall and Priestley (1975) discussed the dispersed character of earthquake activity in this highly seismic area, and suggested that it was an area in which a high degree of crustal fracturing might lead to release of tectonic strain by a continuing series of small- to-moderate earthquakes and fault creep. If so, they concluded, the 1934 Excelsior Mountains earthquake (M about 6.3) could represent the maximum magnitude event for this area.

In general, the distribution of earthquakes in the Garfield Hills between Walker Lake and the Excelsior Mountains (central part of Figure 6) agrees with the interpretation by Ryall and Priestley. Some clustering occurs along faults of the Walker Lane which are the most prominent mapped faults in the area (NNW-trending faults in top part of Figure 6), but in general the activity is diffuse. One possible exception is a northerly-trending zone of epicenters located about 20 km east of Walker Lake. This zone is about 50 km long, and is characterized by northwest and northeast epicenter lineups similar to those described by Ryall and Malone (1971) for the Fairview Peak aftershock zone.

Reno-Carson City-Truckee Area

Epicenters determined using data from the dense network of stations in the Reno-Carson City-Truckee area are shown in detail on Figure 8 together with faults and lineaments (Jennings, 1977; Bonham and Papke, 1969). In the area north of Truckee (T on Figure 8) current seismicity is clustered at the intersection of the northwest-striking Mohawk Valley and northeast- striking Dog Valley faults, where a magnitude 5.7 earthquake occurred in 1966 (Ryall et al., 1968). Twenty-five kilometers to the northeast, another cluster occurs where the Dog Valley fault intersects with the northwest-striking Last Chance fault, and where a magnitude 6.0 earthquake occurred in 1948 (Bell et al., 1976).

Just south of Reno is an area of frequent earthquake swarms, similar in temporal character to the activity described above for the Adobe Hills volcanic center. This swarm area is located in a shatter zone of north-trending faults, within a known geothermal resource area that is currently being explored for power generation. According to Silberman et al. (1979), ages of rhyolite domes near the thermal area are 1.2 my, and he concludes that hydrothermal activity there has continued, perhaps intermittently, for more than 2 1/2 my. This is near the north end of the

Genoa fault zone, which bounds the eastern side of the Carson Range and according to Slemmons (written communication, 1973) is represented in the downtown Reno area by scarps 15-20 feet in height. East of the Steamboat swarm area, Figure 8 shows a cluster of earthquakes that occurred in June 1976 near Virginia City (cluster located just northeast of the "V" on Figure 8).

In the area near Carson City, epicenters follow the eastern side of Carson Valley, along a zone of north-striking east-dipping faults within the Pine Nut range (Moore and Archbold, 1969). A few epicenters trend northeast along the Carson lineament (CL on Figure 7; Shawe, 1965), but this feature appears to be seismicically less significant than other east- or northeast-trending zones in the region.

Well-determined focal depths in the Reno-Carson City area range from near- surface to about 18 km, and east-west profiles show vertical groupings of foci rather than zones that would correspond to dipping planes.

Focal Mechanisms

Figure 9 shows P-wave fault-plane solutions for 12 selected events in the western Great Basin. As discussed by Ryall and Malone (1971), focal mechanisms in the Dixie Valley-Rainbow Mountain-Fairview Peak area are generally consistent with an interpretation of simple block faulting, with faults of different orientation having the same slip direction and with a consistent orientation of about N60W for the axis of minimum principal stress (T-axis). Figure 9 (points 10 and 11) indicates that this type of mechanism is characterized by right-oblique slip on a plane striking NNW and dipping east, or left-oblique slip on a northeast-striking plane that dips northwest. This pattern persists to the southwest. for earthquakes near Mono Lake and Mina (points 8 and 9 on the figure).

However, for most of the SNGBZ, fault-plane solutions on Figure 9 (points 1-5 and 7) indicate mechanisms which are predominantly strike-slip and have east-west T-axes. This agrees with the observation by Eaton et al. (1979) that northwest-striking faults are concentrated along the western margin of the Great Basin, while north-striking faults are concentrated in the central part of the province. However, it does not agree with observed surface faulting, which is primarily normal. For one of the earthquakes studied (number 6 on the figure) the mechanism corresponds to oblique slip; the T-axis for this event is east-west, in agreement with other mechanisms along the boundary zone.

DISCUSSION

Epicentral determinations and fault-plane solutions obtained with data primarily from dense local networks in the northern and southern parts of the SNGBZ have made it possible to compare details of the seismicity, geologic structure and tectonic characteristics of this zone. The results serve to identify active and stable areas along the zone, and illustrate the value of a long-term network data base.

The western margin of the Great Basin is seismically, as well as structurally complex. In the southern part of this zone, dense earthquake clusters occur in the area just north of the 1872 Owens Valley rupture zone, and earthquake lineups in this area are along the irregular Sierran front on the west and NNE-trending groups of faults on the east (Figure 2). The potential for a large earthquake on the Sierran frontal fault system north of Bishop is supported by the frequent occurrance of moderate earthquakes and earthquake swarms along this zone.

Epicenters in the Adobe Hills area east of Mono Lake form an east-west zone, but occur in an area where the strike of mapped faults is predominantly northeast (Gilbert et al.. 1968). Seismicity in this area is characterized by temporal clustering, including earthquake swarms, features that are typical of earthquakes in geothermal areas of the Great Basin (Richins, 1974). Just east of the Adobe Hills, teleseismic P-residuals indicate the presence of a broad crustal low-velocity zone, which could represent the source area for extensive late Quaternary volcanism in the Mono Lake area. If so, the Adobe Hills seismic zone, which has very shallow events under the east end of Mono Lake and greater depth in the vicinity of the crustal low-velocity zone (Figure 4), may be related primarily to volcanic processes.

In the Garfield Hills southeast of Walker Lake, the seismicity is diffuse and appears to reflect a high degree of crustal fracturing, as pointed out by Ryall and Priestley (1975). However, in the northwest part of this area there is a vague tendency for epicenters to form a northerly-trending zigzag series of northwest and northeast lineups, similar to the pattern that Ryall and Malone (1971) described for the Dixie Valley-Fairview Peak aftershock zone to the northeast. While the Garfield Hills epicentral zone is not marked by major Holocene fault scarps, the seismicity suggests that it might have the potential for a sizeable earthquake, of the type that produced relatively nondescript surface fractures in the Cedar Mountains in 1932 (Gianella and Callaghan, 1934).

The seismicity shown on Figures 1 and 8 is noteworthy relative to seismic risk in the Reno-Carson City area. As noted by Ryall and VanWormer (1980, this volume), clusters of earthquakes are observed at both the north and south ends of a 70-km long, major fault zone that bounds the eastern flank of the Carson Range. This fault which lies in an area classed as relatively low- risk on current seismic zone maps (Algermissen and Perkins, 1976; International Council of Building Officials. 1976;

Applied Technology Council, 1978), has had several major offsets during the late Quaternary (Cordova, 1969; Pease, 1979), has the potential for large earthquakes in the future, and with its proximity to population centers represents the zone of highest seismic risk in Nevada at the present time.

Just south of Reno, frequent earthquake swarms occur in the area of Steamboat Springs, and these earthquakes, like the swarm activity east of Mono Lake, are probably related to geothermal processes. Earthquakes in the Truckee area are clustered at both ends of a 25-km long fault, in places where magnitude 6.0 and 5.7 shocks occurred respectively in 1948 and 1966.

For the zone in which large earthquakes have occurred during the historic period, fault-plane solutions on Figure 9 are generally consistent with an interpretation of simple block faulting, with faults of different orientation having the same slip direction (Ryall and Malone, 1971). Thus, for the Rainbow Mountain and Fairview Peak areas, crustal blocks to the east of the fracture zone move down and southeast with respect to blocks on the west side, and faulting in the zone from Dixie Valley southwest to Mono Lake is consistent with regional extension acting in the direction N60W-S60E.

Fault-plane solutions (Figure 9) for most of the moderate earthquakes recorded in the SNGBZ from 1976 to 1979, however, correspond to right- or left-lateral slip, respectively on nearly vertical, northwest- or northeast-striking planes. The T-axis for these events is east-west, rather than the NW-SE orientation usually observed for earthquakes in central Nevada. Strike-slip motion on northwest- or northeast trending planes at depth does not agree with observed faulting on the surface: the main faults in the SNGBZ trend north, and motion on these faults is primarily normal, dip-slip. This discordance can be explained by a block-faulting mechanism similar to that proposed for the Fairview Peak zone by Ryall and Malone (1971). In the SNGBZ such a mechanism would consist of normal-oblique slip on north- trending fault segments, and right-lateral strike-slip on northwest-trending faults that terminate or offset the north-south segments. This agrees with the observation that seismicity over the period of observation has tended to concentrate at the ends of historic rupture zones or places where major fault segments intersect.

ACKNOWLEDGEMENTS

F. Ryall assisted with studies of earthquakes in the Mono Lake-Walker Lake region, and made a number of the observations discussed in this paper relative to earthquake clustering in the Adobe Hills area. G. Smith and T. Boydston assisted with analysis, respectively, of the Nevada network data and P-residuals for the Mina network. W. A. Peppin and M. R. Somerville reviewed the manuscript and made helpful suggestions. This research was partly supported by the US Geological Survey, under contract number 14-08-0001-16741.

REFERENCES

Algermissen, S. T. and D. M. Perkins (1976). A Probabilistic Estimate of Maximum Acceleration in Rock in the Contiguous United States, US Geological Survey, Open-File Rept. 76-416, 45 pp.

Applied Technology Council (1978). Tentative Provisions for the Development of Seismic Regulations for Buildings, National Bureau of Standards, 514 pp.

Bell, E. J. R. Broadbent and A. Szumigala (1976). Analysis and effects of the 1948 earthquake at Verdi, Nevada. in Geol. Soc. Am.. Abs. with Programs, 9 (4), 387.

Bolt, B. A. and O. W. Nuttli (1966). P-wave residuals as a function of azimuth, 1: Observations, J. Geophys. Res., 71, 5977-5986.

Christensen, M. N. and C. M. Gilbert (1964). Basaltic cone suggests constructional origin of some guyots, Science, 143, 240-242.

Cordova, T. (1969). Active Faults in Quaternary Alluvium, and Seismic Regionalization, in a Portion of the Mount Rose Quadrangle, Nevada, Univ. of Nevada MS Thesis, 53 pp.

Eaton, G. P.. R. R. Wahl, H. J. Prostka, D. R. Mabey and M. D. Kleinkopf (1979). Regional gravity and tectonic patterns: their relation to late Cenozoic epeirogeny and lateral spreading in the western Cordillera, Geol. Soc. Am. Memoir 152, 51-91.

Eaton, J. P. (1963). Crustal structure from San Francisco, California, to Eureka, Nevada, from seismic refraction measurements, J. Geophys. Res.. 68 (20), 5789-5806.

Ekren, E. B., R. C. Bucknam, W. J. Carr, G. L. Dixon and W. D. Quinlivan (1976). East-Trending Structural Lineaments in Central Nevada, US Geol. Survey, Prof. Paper 986, 16 pp.

Gianella, V. P. and E. Callaghan (1934). The earthquake of December 20, 1932, at Cedar Mountain, Nevada, and its bearing on the genesis of Basin Range structure J. Geol. , 42, 1-12.

Gilbert, C. M., M. N. Christensen, Y. T. Al-Rawi and K. R. Lajoie (1968). Structural and volcanic history of Mono Basin, California-Nevada, Geol. Soc. Am., Memoir 116, 275-329.

Gilbert, C. M. and M. W. Reynolds (1973). Character and chronology of basin development, western margin of the Basin and Range province, Bull. Geol. Soc. Am.. 84, 2489-2510.

Herrin, E. (Chairman; 1968). Seismological tables for P, Bull. Seism. Soc. Am., 58, 1196-1219.

International Council of Building Officials (1976). Uniform Building Code, Whittier, California, 728 pp.

Iyer, H. M. (1979). Deep structure under Yellowstone National Park, USA: a continental "hot spot", Tectonophysics, 56, 165-197.

Iyer, H. M., D. H. Oppenheimer and T. Hitchcock (1979). Abnormal P-wave delays in the Geysers-Clear Lake geothermal areas. California, Science, 204, 495-497.

Jennings, C. W. (1977). Geologic Map of California, Calif. Geol. Data Map Ser., Calif. Dept. Conserv.. Sacramento, CA.

Koizumi, C. J., A. Ryall and K. F. Priestley (1973) Evidence for a high- velocity lithospheric plate under northern Nevada, Bull. Seism. Soc. Am., 63 (6), 2135-2144.

Lee, W. H. K. and J. C. Lahr (1972). HYPO71: A Computer Program for Determining Hypocenter, Magnitude and First Motion Pattern of Local Earthquakes, US Geol. Survey, Open-File Rept.. 100 pp.

Moore, J. G. and N. L. Archbold (1969). Geology and Mineral Deposits of Lyon, Douglas and Ormsby Counties, Nevada, Nev. Bur. Mines and Geol. Bull. 75, 45 pp.

Pease, R. C. (1979). Scarp Degradation and Fault History near Carson City, Nevada, Univ. Nev. MS Thesis, 95 pp.

Richins, W. D. (1974). Earthquake Swarm Near Denio, Nevada, February to April, 1973, Univ. Nevada MS Thesis, 57 pp.

Romney, C. F. (1957). The Dixie Valley-Fairview Peak, Nevada, earthquakes of December 16, 1954: Seismic waves, Bull. Seism. Soc. Am.. 47, 301-320.

Ryall, A. and A. E. Jones (1964). Computer program for automatic processing of Basin and Range seismic data, Bull. Seism. Soc. Am., 54 (6), 2295-2310.

Ryall, A., D. B. Slemmons and L. D. Gedney (1966). Seismicity, tectonism and surface faulting in the western United States during historic time, Bull. Seism. Soc. Am., 56 (5), 1105-1135.

Ryall, Alan, J. D. VanWormer and A. E. Jones (1968). Triggering of microearthquakes by earth tides and other features of the Truckee, California, earthquake sequence of September, 1966, Bull. Seism. Soc. Am., 58, 215-248.

Ryall, A. and S. D. Malone (1971). Earthquake distribution and mechanism of faulting in the Rainbow Mountain-Dixie Valley-Fairview Peak area, central Nevada, J. Geophys. Res. 76, 7241-7248.

Ryall, A. and K. Priestley (1975). Seismicity, secular strain and maximum magnitude in the Excelsior Mountains area, Nevada and eastern California, Geol. Soc. Am. Bull., 86, 1585-1592.

Ryall, A. and J. D. VanWormer (1980). Estimation of maximum magnitude and recommendations for changes in seismic zoning in the Sierra Nevada-Great Basin boundary zone, this volume.

Ryall, A. (1977). Seismic hazard in the Nevada region, Bull. Seism. Soc. Am., 67, 517-532.

Schnabel, P. B. and H. B. Seed (1973). Accelerations in rock for earthquakes in the western United States, Bull. Seism. Soc. Am., 63 (2), 501-516.

Shawe, D. R. (1965). Strike-slip control of Basin-Range structure indicated by historical faults in western Nevada, Bull. Geol. Soc. Am., 76, 1361-1378.

Silberman, M. L., D. E. White, T. E. C. Keith and R. D. Dockter (1979). Duration of Hydrothermal Activity at Steamboat Springs, Nevada, from Ages of spatially associated volcanic rocks, US Geol. Survey, Prof. Paper 458-D, 14 pp.

Steeples, D. W. and H. M. Iyer (1976). Low-velocity zone under Long Valley as determined from teleseismic events, J. Geophys. Res. 81 (5), 849-860.

Steeples, D. W. and A. M. Pitt (1976). Microearthquakes in and near Long Valley, California, J. Geophys. Res., 81, 841-847.

Steinbrugge, K. V. and W. K. Cloud (1962). The earthquake at Hebgen Lake, Montana, on August 18, 1959: Epicentral intensities and damage, Bull. Seism. Soc. Am., 52 (2), 181-234.

Stewart, J. H. (1979). Basin-range structure in western North America: a review, Geol. Soc. Am., Memoir 152, 1-31.

Stewart, J. H. and J. E. Carlson (1978). Geologic Map of Nevada, US Geol. Survey.

Tocher, D. (1958). Earthquake energy and ground breakage, Bull. Seism. Soc. Am., 48, 147-153.

Trifunac, M. D. and A. G. Brady (1975). On the correlation of seismic intensity scales with the peaks of recorded strong motion, Bull. Seism. Soc. Am., 65 (1), 139-162.

Wallace, R. E. (1978). Patterns of faulting and seismic gaps in the Great Basin province, US Geol. Survey, Open-File Rept. 78-943, 857-868.

Wright, L. (1976). Late Cenozoic fault patterns and stress fields in the Great Basin and westward displacement of the Sierra Nevada block, Geology, 4, 489-494.

FIGURE TITLES

Figure 1. Generalized map of major faults in the western Great Basin (Stewart, 1979). Dots -- earthquake epicenters for 1969-1978 (includes all events analyzed by Univ. of Nevada for 1969-1978); stippled areas -- approximate rupture zones of major earthquakes: 1 -- 1852(?) Stillwater area; 2 -- 1872 Owens Valley, M8.0(?); 3 -- 1915 Pleasant Valley, M7.6; 4 -- 1932 Cedar Mountains, M7.2; 5 -- 1954 Fallon-Stillwater, two events with M6.6 and M6.8; 6 - 1954 Dixie Valley-Fairview Peak, two events with M6.9 and M7.1. Long rectangle is area containing events that were used in compilation of Figures 10 and 11; small rectangles, from south to north, are areas shown in Figures 2, 6 and 8.

Figure 2. Southern part of Sierra Nevada-Great Basin boundary zone, showing mapped faults (Jennnings, 1977; Stewart and Carlson, 1978). Dots - earthquakes recorded by dense seismic station network in the area between Walker Lake and Owens Valley; ML -- Mono Lake; LV -- Long Valley (caldera shown by dashed line); OV -- north end of Owens Valley.

Figure 3. Number of events in the seismic zone east of Mono Lake by months in which they occurred, for the period 1974-1978.

Figure 4. East-west profile showing focal depth for earthquakes in the Adobe Hills area east of Mono Lake. x -- distance in km west of 118.0 deg. W.

Figure 5. Maps of the area southeast of Walker Lake, showing teleseismic P-residuals relative to station TNP. Figure on left (5a) is for sources to southeast, figure on right (5b) for sources to northwest. Arrows show direction of propagation. Numbers -- P-wave residuals in hundredths of a second; WL -- Walker Lake.

Figure 6. Map showing mapped faults in the area southeast of Walker Lake (Stewart and Carlson, 1978). Dots -- epicenters of earthquakes recorded by the dense seismic station network in the area between Walker Lake and Bishop.

Figure 7. Map showing interpretation of major fault zones and lineaments near the western margin of the Great Basin (solid lines and lines with long dashes; Gilbert and Reynolds, 1973), and major east-west lineaments hypothesized by Ekren et al. (1976). Stippled area -- area of warping hypothesized by Gilbert and Reynolds; CL -- Carson lineament; PL -- Pyramid Lake fault zone; WL -- Walker Lane; FV -- Fishlake Valley fault zone; WM -- White Mountains; OV -- Owens Valley.

Figure 8. Map showing mapped faults in the Reno-Tahoe-Carson City area (Stewart and Carlson, 1978; Jennings, 1977). Dots - epicenters of earthquakes for 1976-1979. R -- Reno; V -- Virginia City; C - Carson City; LT -- Lake Tahoe; T -- Truckee.

Figure 9. Generalized map of late Cenozoic structural features of the western Great Basin and eastern Sierra Nevada provinces (Wright, 1976), together with focal mechanisms of selected earthquakes: 1 -- 20 June 1976 Susanville, Calif. M4.5; 2 -- 22 February 1979 Doyle, Calif. M5.2; 3 -- 12 September 1966 Truckee, Calif.. M5.7 (Tsai and Aki, 1970); 4 -- 1 February 1977 Zephyr Cove, Calif.. M4.0; 5 -- 4 September 1978 Diamond Valley, Calif., M5.2; 6 -- 24 September 1979 Lake Crowley, Calif.. M4.0; 7 -- 4 October 1978 Bishop, Calif. M5.5; 8 -- 10 October 1977 Mono Lake Calif., M4.0; 9 -- composite solution for the area near Mina (Ryall and Priestley, 1975); 10 -- 24 August 1954 Rainbow Mountain, Nev. M6.8 (Fara, 1964); 11 -- 16 December 1954 Fairview Peak. Nev., M7.1 (Romney, 1957); 12 -- composite solution for Dixie Valley, Nev. (Ryall and Malone, 1971). P-wave first motion plots are lower-hemisphere, equal-area projections, compression sectors shaded. Arrows show direction of minimum principal stress axis.

COMMENTS

R. SMITH: Regarding the question of P-wave delays - many people are arguing on the basis of Iyer's work that large delays are evidence for magma chambers. We just completed a first analysis of the Yellowstone refraction experiment that was shot last fall. We had six shotpoints in and around Yellowstone Park, and one thing that we can see reasonably clearly is that there are delays associated with the upper crust, with the Pg arrivals, of the order of 0.5 second or greater. These account for a large portion of the delay that would be seen for teleseismic P-waves. On the other hand, we see no evidence whatsoever for P delays in the lower portion of the crust. I want to make the comment that the use of P-wave delays has to be critically looked at in terms of where the delay is occurring; I think what we're seeing is that large delays, of the order of a half second, can occur in the upper crust, and need not imply a deeper mechanism. My question is what evidence do you have, or how does the crustal structure change in an east-west direction across your zone of seismicity? Is there any significance to the fact that you have strike-slip components at the edge of the Sierra Nevada, grading out into the Great Basin? Is there an influence of the change in crustal structure upon the focal mechanisms?

RYALL: The gravity map for the area east of Mono Lake does not reflect the sort of pattern we see on the P-residual map. Topography is flat in that area, so any significant accumulation of low-velocity material near the surface should be seen as a large gravity anomaly, and we don't see such an anomaly. In the Mono area, the focal mechanism of earthquakes is the same as central Nevada; it is not strike-slip. Neither of the planes of the focal mechanism agrees with the east-west trend of the zone of seismic activity, so the zone probably consists of an en-echelon series of short, northeast-striking fault segments. From teleseismic signals propagating toward the northwest, there appears to be a break in crustal structure under the White Mountains (lower right corner of Figure 5a), but no such feature appears in the area of the low velocity anomaly east of Mono Lake. The idea of a subsurface volcanic center in the Adobe Hills area is supported by thick basalt flows there, and by historic volcanic activity in Mono Lake itself.

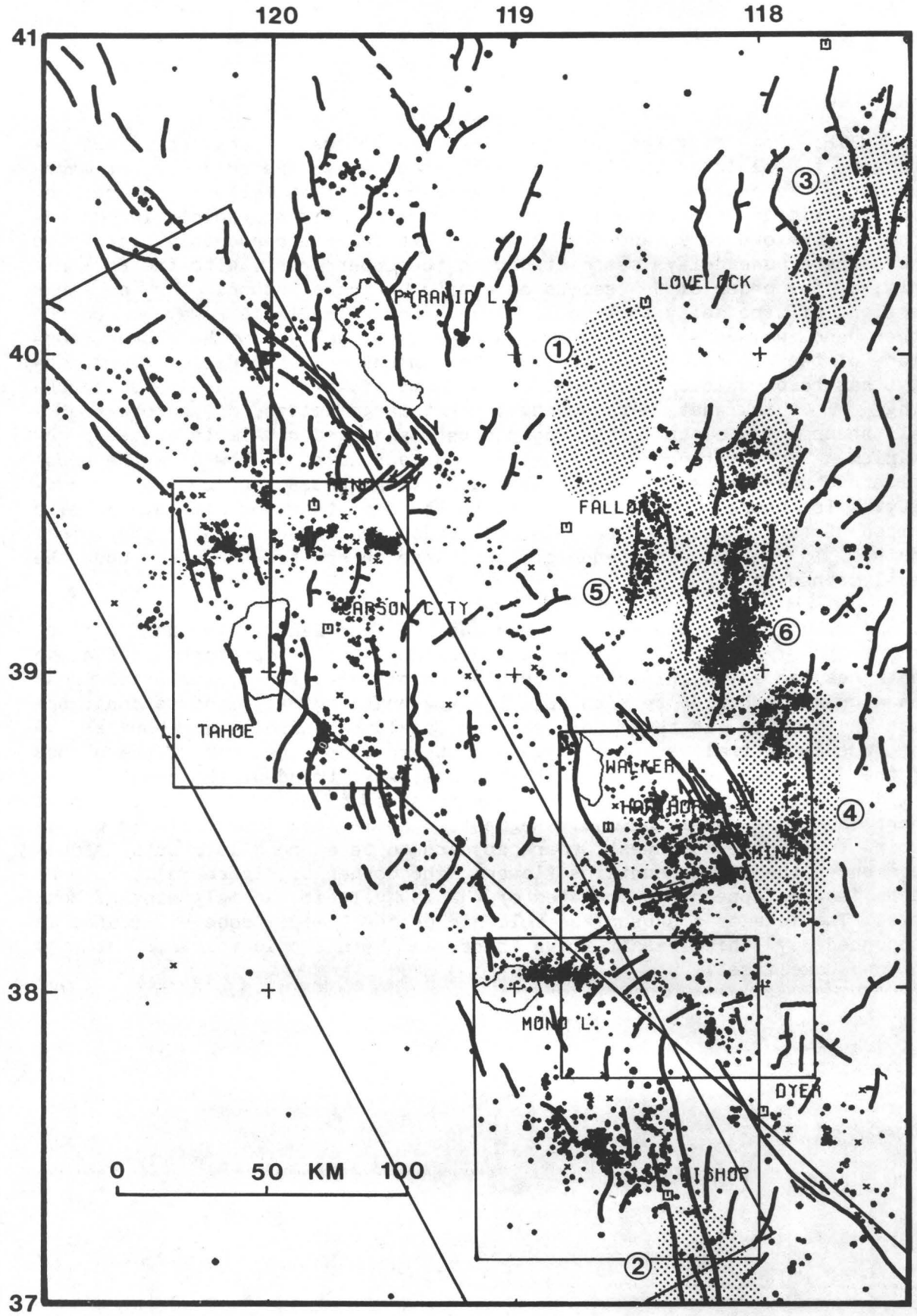
120
119
118
41
40
39
38
37
PYRAMID L.
LOVELOCK
FALLON
RENO
CARSON CITY
TAHOE
WALKER
MONO L.
DYER
BISHOP
0
50 KM
100
1
2
3
4
5
6

FIGURE 1

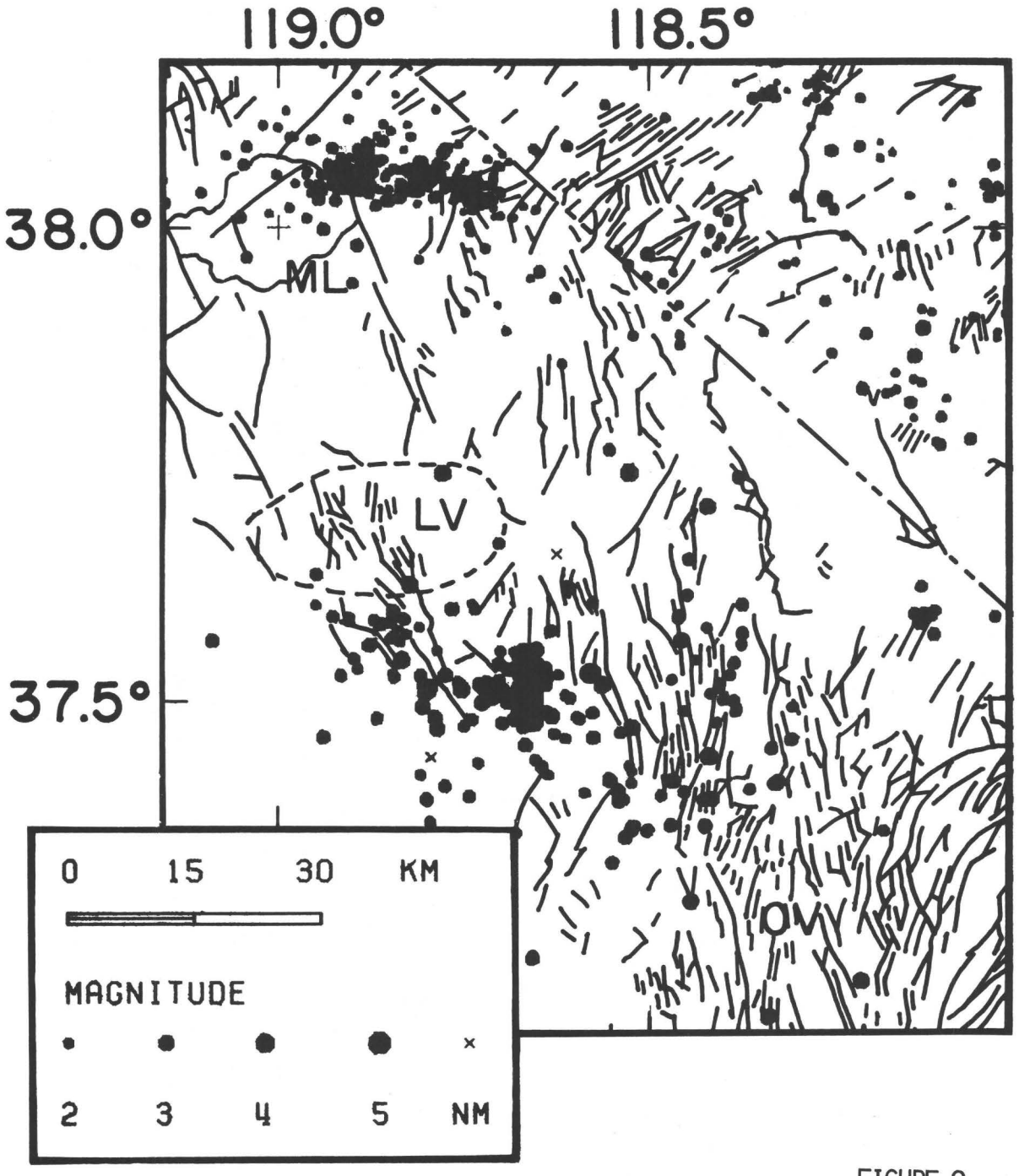

FIGURE 2

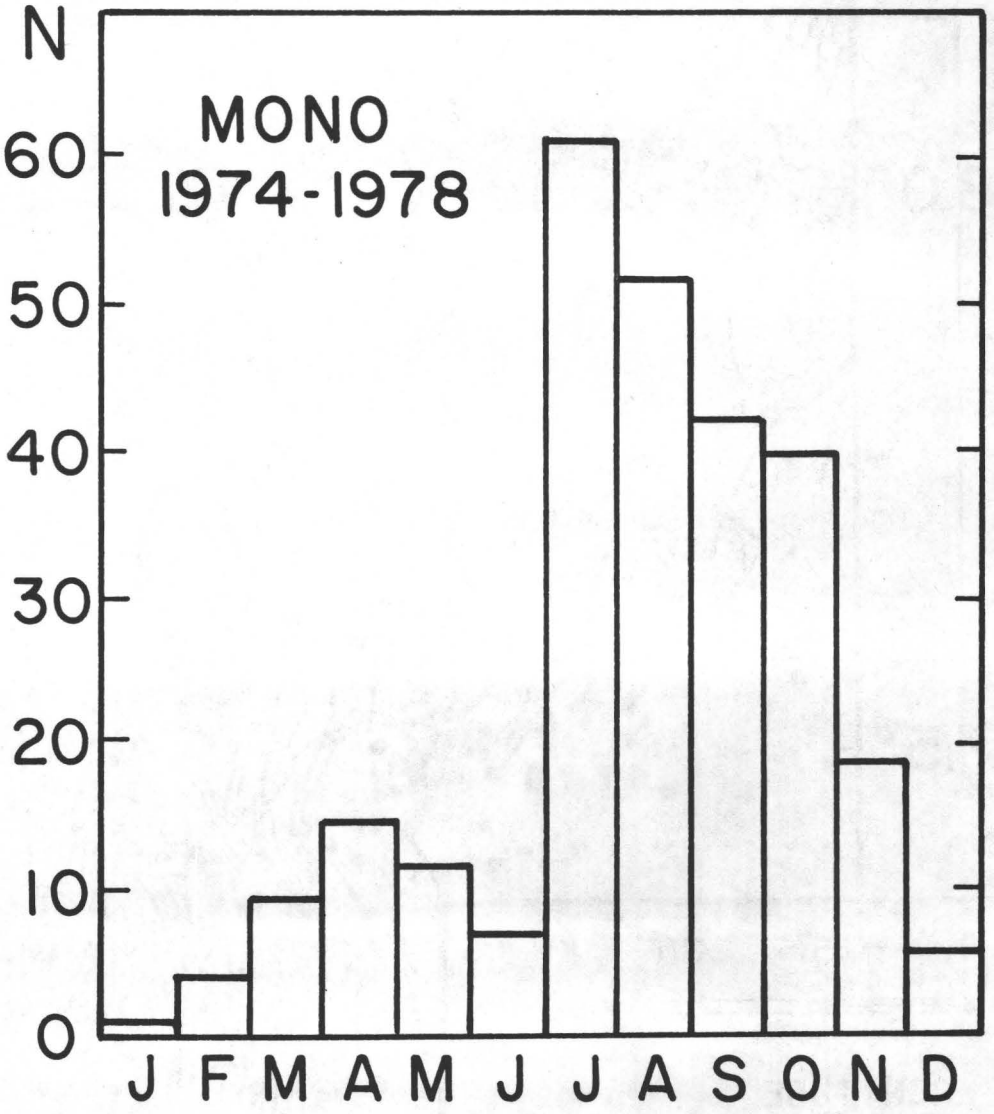

FIGURE 3

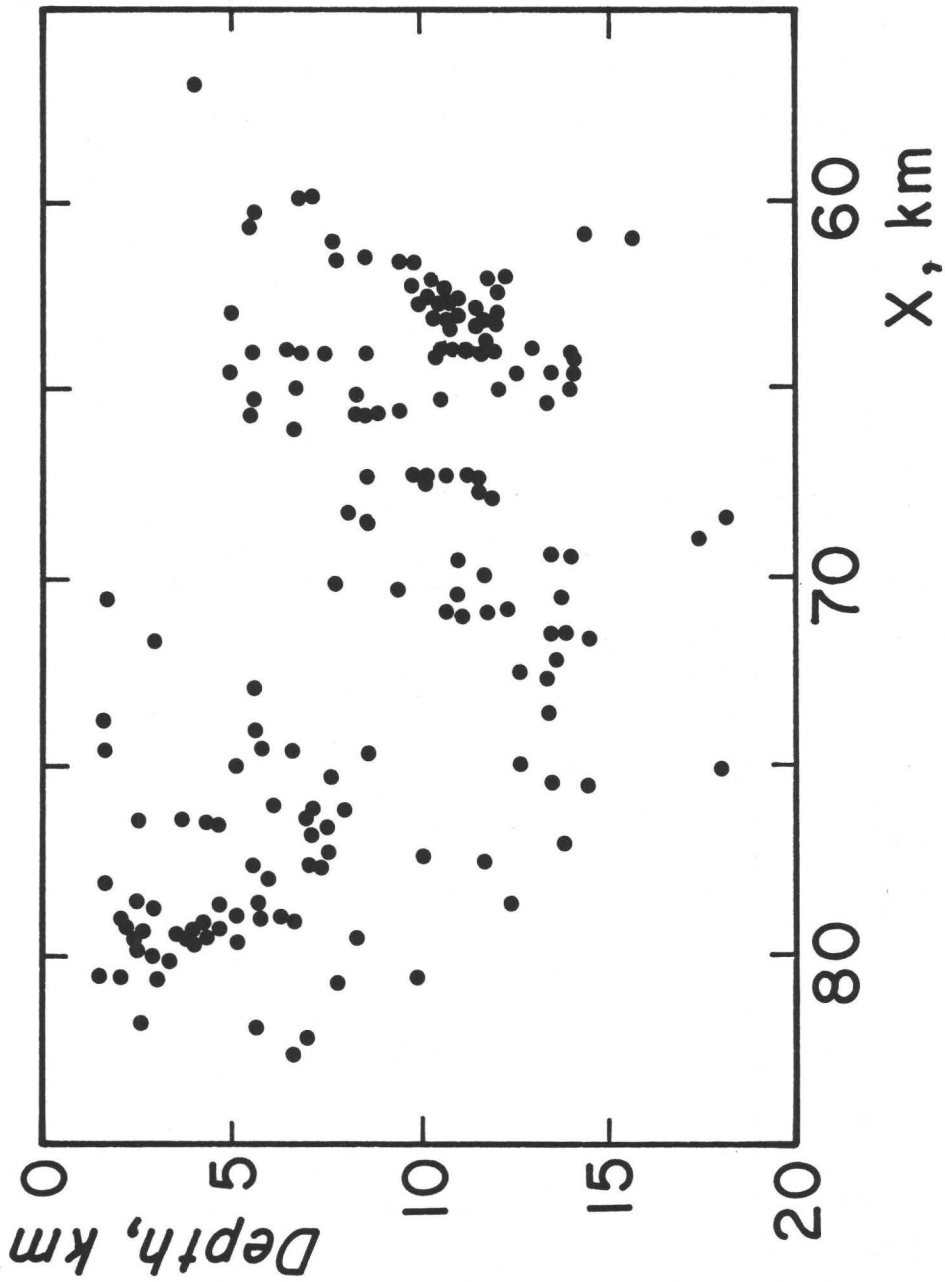

FIGURE 4

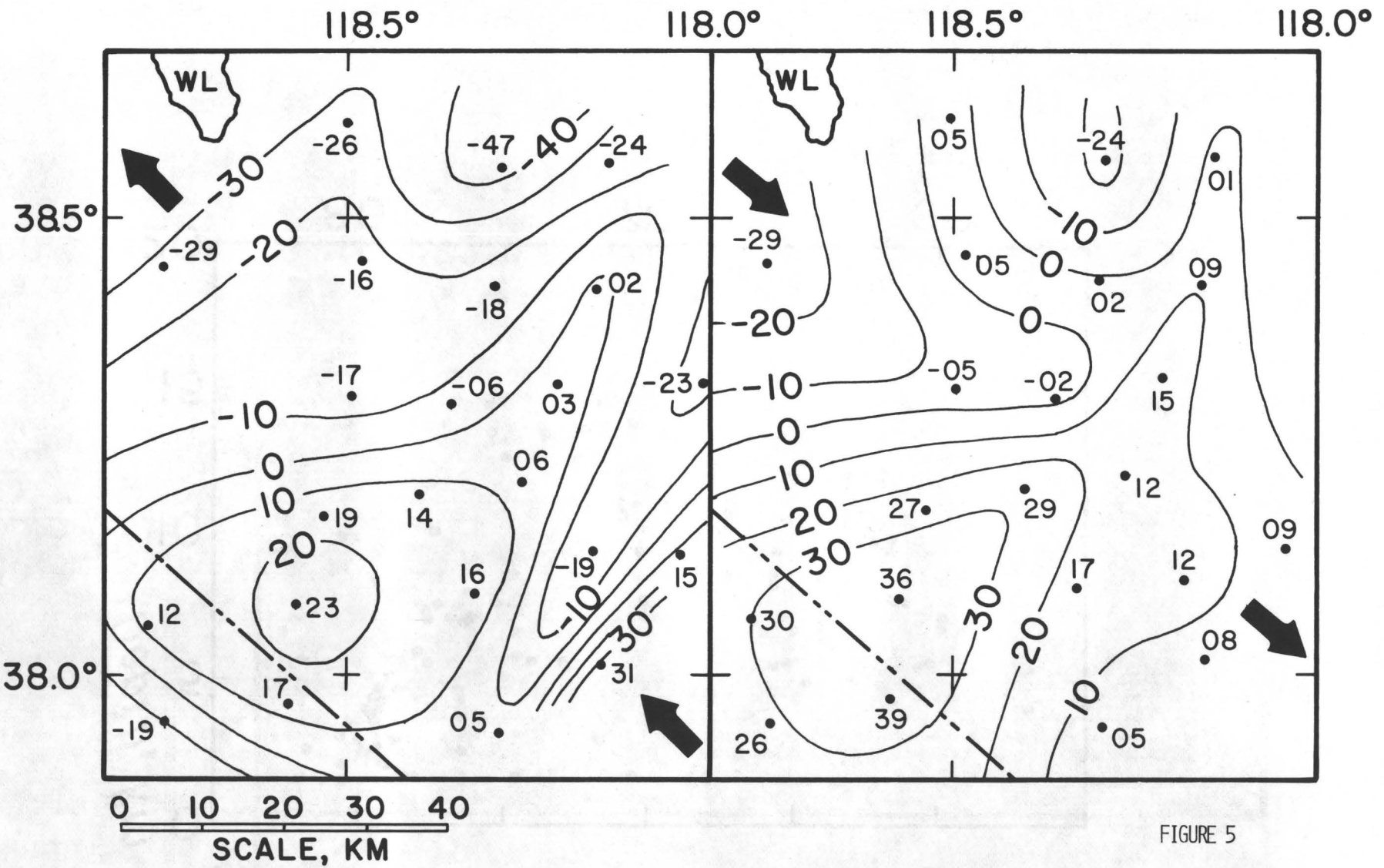
118.5°
118.0°
118.5°
118.0°
38.5°
38.0°
WL
WL
-30
-40
-20
-10
0
10
20
30
-26
-47
-24
-29
-16
-18
02
-17
-06
03
-23
06
19
14
23
16
12
17
-19
05
31
-29
-20
-10
0
10
20
30
05
-24
01
05
09
02
-05
-02
15
27
29
12
09
36
17
12
30
08
39
26
05
0
10
20
30
40
SCALE, KM

FIGURE 5

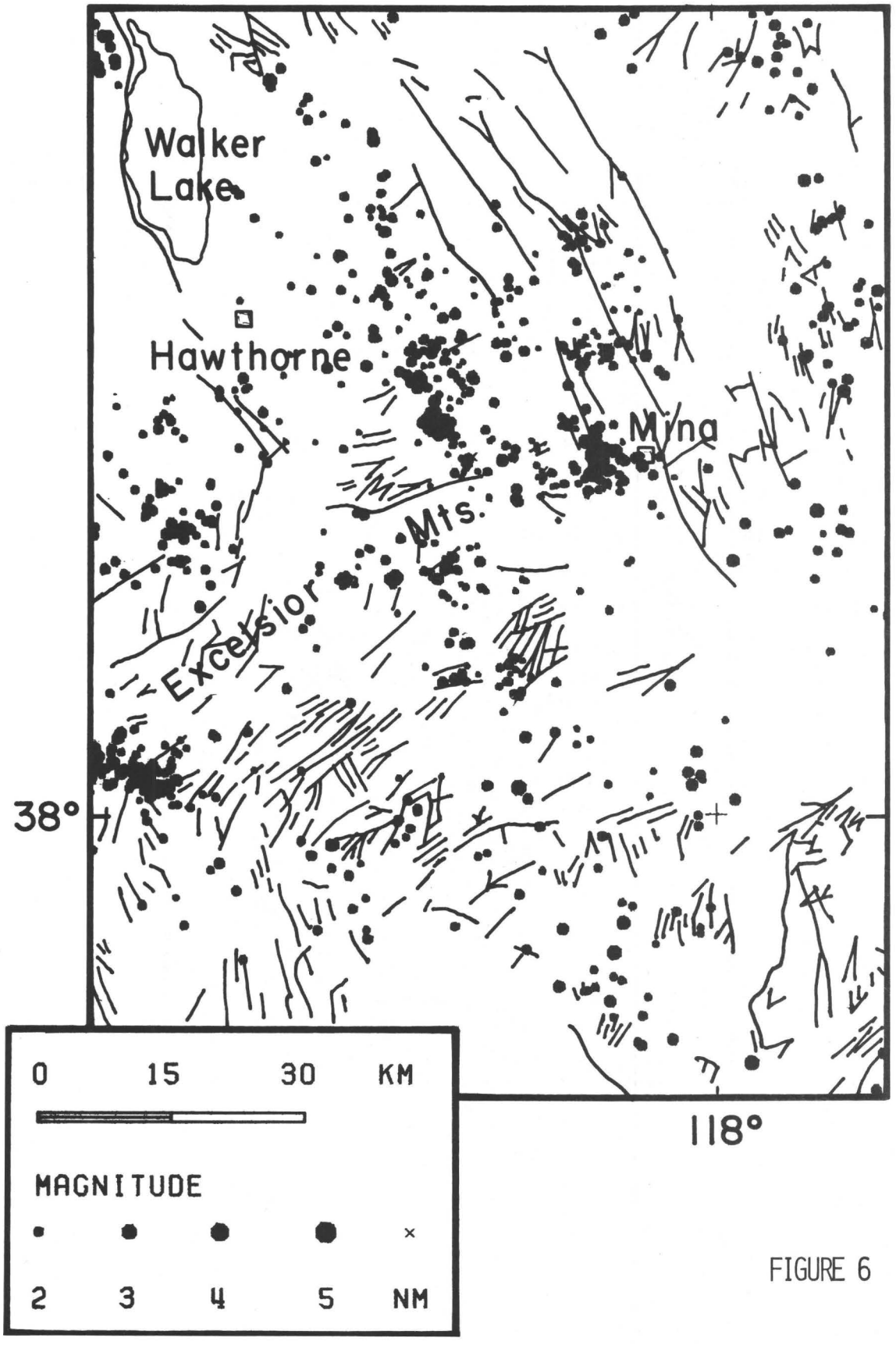
Walker Lake
Hawthorne
Mina
Mts.
Excelsior
38°
118°
0 15 30 KM
MAGNITUDE
2 3 4 5 NM

FIGURE 6

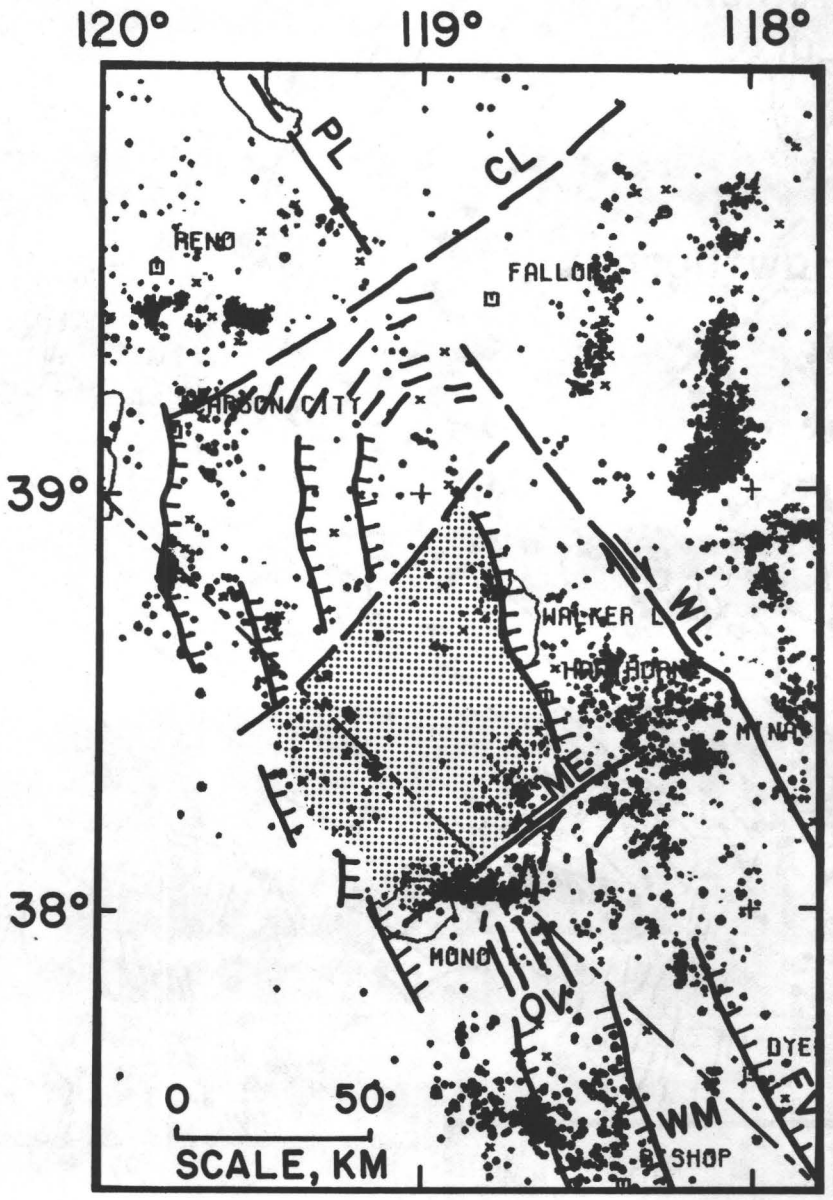
120°
119°
118°
39°
38°
PL
CL
RENO
FALLON
CARSON CITY
WL
WALKER L
HOR
MT NA
ME
E
MONO
OV
DYE
FV
WM
BISHOP
0
50
SCALE, KM

FIGURE 7

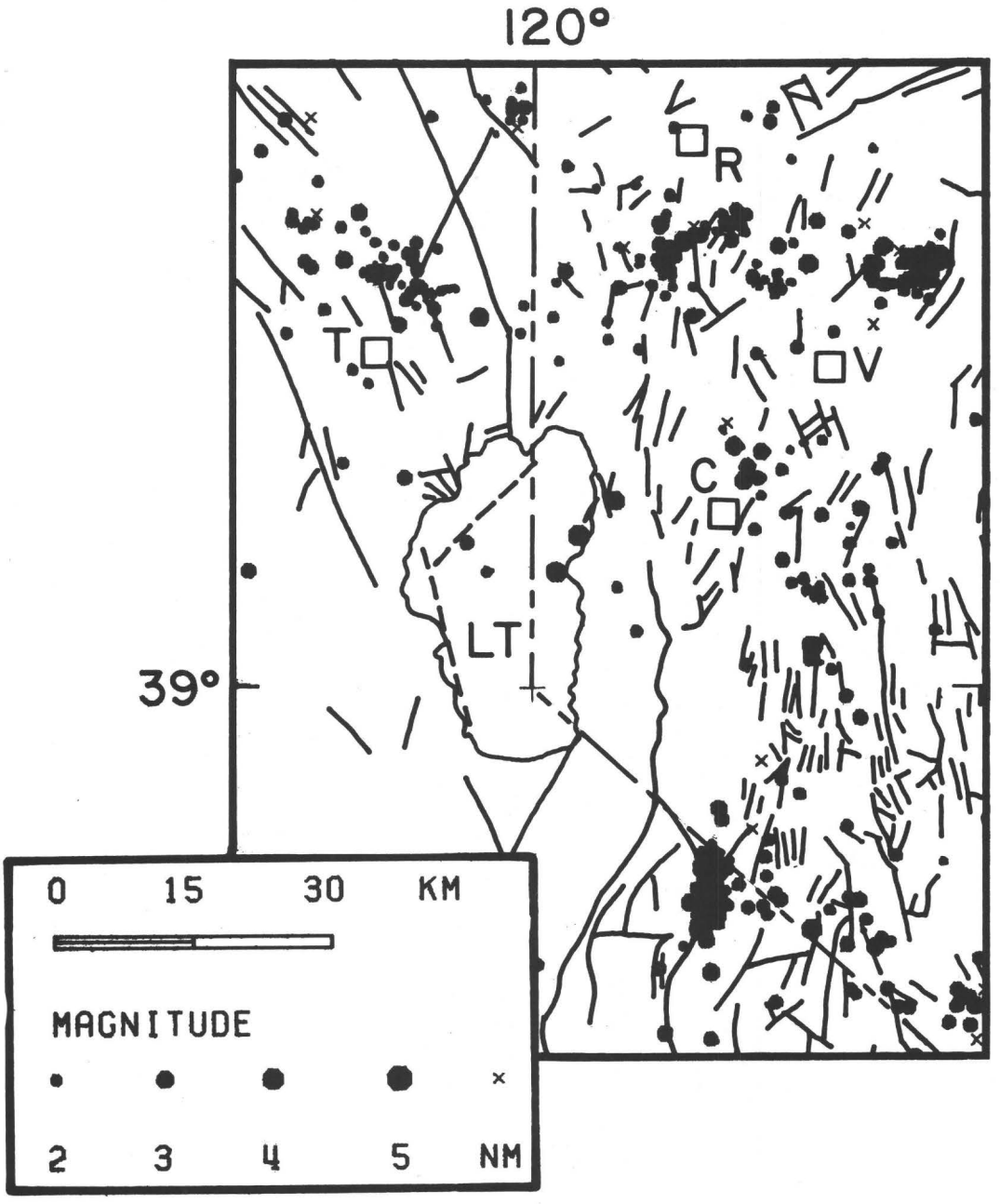

FIGURE 8

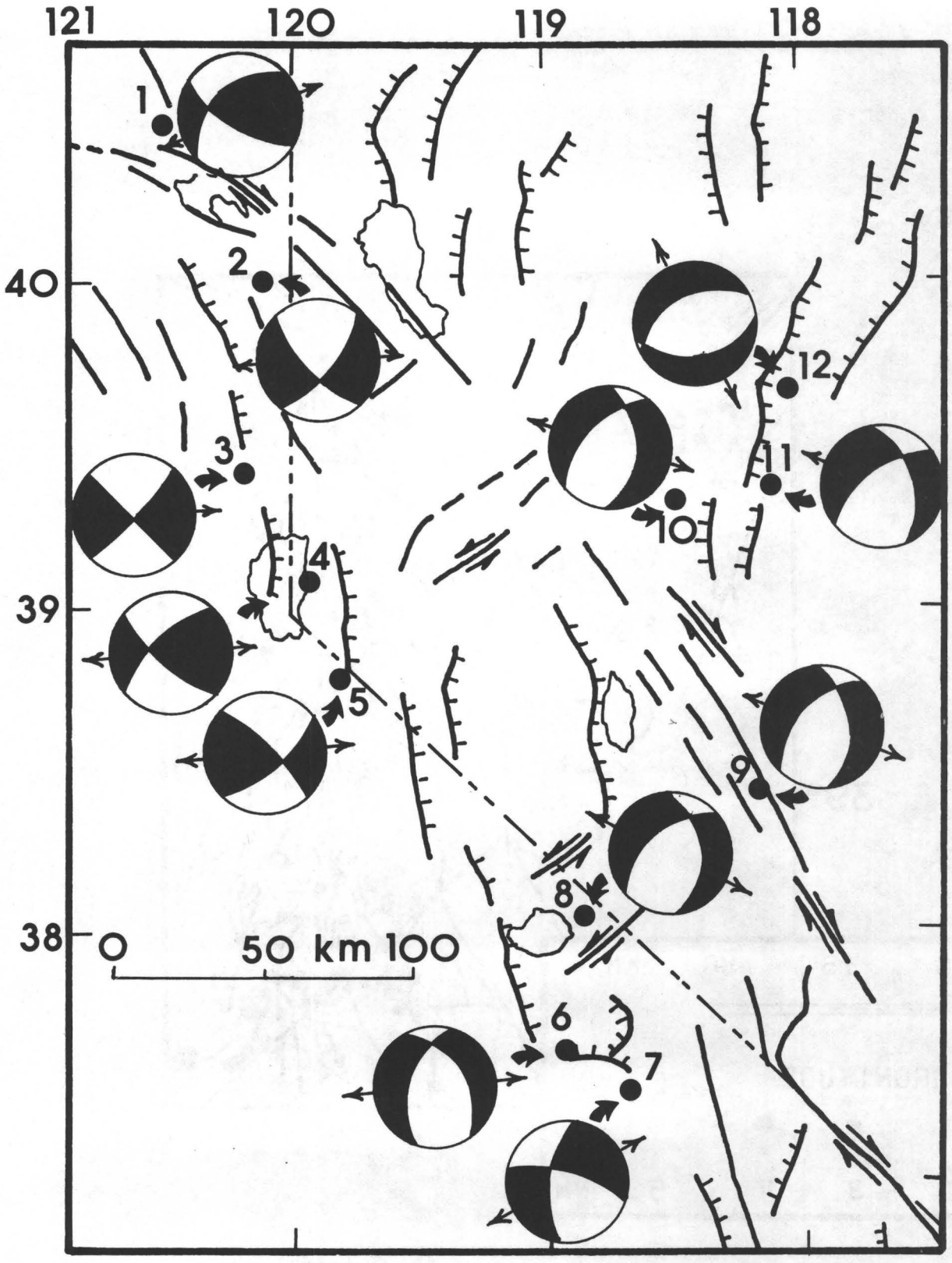

FIGURE 9

DESIGN EARTHQUAKE MAGNITUDES FOR THE WESTERN GREAT BASIN

David B. Slemmons
Department of Geological Sciences
Mackay School of Mines
University of Nevada
Reno, Nevada 89557

INTRODUCTION

Purpose and Scope of Study

The purpose of this study is to examine evidence for recently active fault zones and major subplate provinces in the western Great Basin to enable preliminary analysis of risk. Seismic risk analyses are difficult since only a few isolated fault zones have been adequately studied for evidence of maximum displacement, fault rupture lengths, recurrence intervals, fault slip rates and to determine the age of most recent surface faulting. Three regional maps of active faults with Quaternary-age displacements have been published by Slemmons (1966), Jennings (1975), and Howard and others (1978). Newer data suggest that these studies are incomplete and inadequate for the assessment of seismic potential of the western Great Basin. This report updates these earlier compilations and provides a preliminary base for estimating maximum probable earthquakes.

The use of modern seismological methods and historical records for estimation of the maximum earthquake potential of a region is limited by the short historic record, during which only a few of the main faults have experienced surface faulting with accompanying large earthquakes. The application of geologic methods enables the use of an expanded time frame, but is complicated by the following factors:

1) Active faults are difficult to detect, delineate, and define in areas of bedrock exposures, and areas of very young sedimentation.
2) The regional historic record indicates that the rupture patterns are frequently complex with anastomosing, branching, zigzag or arcuate patterns. With passing time it becomes increasingly difficult to demonstrate age-contemporaneity of related, but separate fault segments.

Terminology

The terms used in this report are defined as follows:

Earthquake Magnitude: For earthquakes of more than 7 magnitude, surface wave magnitude, M_S, is used. For earthquakes of less than 7 magnitude, the local, or Richter magnitude is used.

Maximum Credible Earthquake: The largest earthquake that can be reasonably attributed to a fault based on either its full length or longest zone of rupturing during a single earthquake. The fault length is based on rupture zones which exhibit a degree of freshness or steepness of scarp slope angle (Wallace, 1977; 1978a, and 1978b) that indicates the probability of rupturing for the observed length during one earthquake. Estimation of earthquake displacement is based on Slemmons (1977), as summarized in new tables for this report (tables 1 and 2). When differing values are obtained from the two methods (length and displacement), the average of these values is used in this report.

Maximum Probable Earthquake: The magnitude of the largest historic earthquake within the region, if available, is used, or is determined by fault half-length (table 2), or the maximum displacement (table 1).

Acknowledgments

I am grateful for the discussions and editorial assistance from Peg O'Malley, Loretta Sabini, Jean and Juri Stratford, and Bob Whitney of the University of Nevada. I also thank George Bergantz for his cartographic skills. Their assistance greatly improved the content and clarity of this report.

Table 1. Best Straight-Line Fit for Earthquake Magnitude Versus Log Length (M = A + B LOG L)

Length (km) or half-length	Earthquake Magnitude				
	Normal-slip Faults	Strike-slip Faults	Normal-oblique-slip Faults	All Fault Types North America	All Fault Types World-wide
	1	2	3	4	5
10	6.45	6.00	6.77	5.87	6.33
20	6.70	6.41	7.04	6.32	6.69
30	7.00	6.65	7.20	6.59	6.90
40	7.14	6.81	7.32	6.78	7.05
50	7.25	6.95	7.41	6.92	7.16
60	7.34	7.05	7.48	7.04	7.25
70	7.42	7.14	7.54	7.14	7.33
80	7.49	7.22	7.59	7.22	7.40
90	7.55	7.29	7.64	7.31	7.46
100	7.60	7.35	7.68	7.37	7.57
150	7.80	7.59	7.84	7.72	7.72
200	7.95	7.75	7.96	7.83	7.87

Note: For Maximum Credible Earthquake use full fault length.
For Maximum Probable Earthquake use one-half the fault length.

1. Normal-slip faults: M = 1.845 + 1.151 Log L (meters)
2. Strike-slip faults: M = 0.597 + 1.351 Log L (meters)
3. Normal-oblique-slip faults: M = 3.117 + 0.913 Log L (meters)
4. North America faults: M = -0.146 + 1.504 Log L (meters)
5. Worldwide faults: M = 1.606 + 1.182 Log L (meters)

Table 2. Best Straight-Line Fit for Earthquake Magnitude Versus Log Displacement (M = A + B LOG D)

Displace. (meters)	Earthquake Magnitude				
	Normal-slip Faults	Strike-slip Faults	Normal-oblique-slip Faults	All Fault Types North America	All Fault Types World-wide
	1	2	3	4	5
0.1	5.78	5.50	5.49	5.75	5.55
0.2	6.09	5.87	5.87	6.06	5.91
0.3	6.28	6.08	6.09	6.22	6.12
0.4	6.41	6.23	6.25	6.35	6.27
0.5	6.51	6.35	6.37	6.45	6.37
0.6	6.59	6.45	6.47	6.52	6.48
0.7	6.66	6.53	6.55	6.59	6.56
0.8	6.73	6.59	6.63	6.65	6.63
0.9	6.78	6.66	6.69	6.70	6.70
1.0	6.83	6.72	6.75	6.74	6.75
1.5	7.01	6.93	6.97	6.92	6.96
2.0	7.14	7.08	7.13	7.04	7.11
3.0	7.33	7.30	7.35	7.22	7.32
4.0	7.46	7.45	7.51	7.34	7.47
5.0	7.56	7.57	7.63	7.44	7.59
6.0	7.64	7.66	7.73	7.52	7.68
7.0	7.71	7.74	7.81	7.58	7.76
8.0	7.76	7.81	7.89	7.64	7.83
9.0	7.83	7.88	7.95	7.69	7.95
10.0	7.88	7.93	8.01	7.74	7.95

1. Normal-slip faults: M = 6.827 + 1.050 Log D (meters)
2. Strike-slip faults: M = 6.717 + 1.214 Log D (meters)
3. Normal-oblique-slip faults: M = 6.750 + 1.260 Log D (meters)
4. North American faults: M = 6.745 + 0.995 Log D (meters)
5. Worldwide faults: M = 6.750 + 1.297 Log D (meters)

DETERMINATION OF EARTHQUAKE MAGNITUDE

Historic seismicity of the western Great Basin includes ten earthquakes with magnitudes greater than 6.5, all with associated surface faulting. Thirteen seismic events involving surface faulting have occurred in this area (table 3). All have fault rupture lengths, maximum displacement, and associated magnitudes which are in agreement with the worldwide and North America datum of Slemmons (1977). The magnitude and fault rupture length relations (table 1) and the magnitude and maximum displacement relations (table 2) indicate that development of significant scarps, with fault lengths in excess of 10 km and maximum scarp heights of a half a meter or more, generally requires an earthquake of a magnitude greater than 6.5. Local, minor scarps can result from shallow focus eathquakes of lower magnitude. Wallace (1977) initially proposed that the magnitude of prehistoric earthquakes could be estimated through evaluation of fault scarp morphology and careful field observation of associated fault-related phenomena. Subsequent studies by Wallace (1978a and 1978b), Bucknam and Anderson (1979), and Pease (1979), make use of field measurements of fault displacement and rupture length coupled with thr relationships of Slemmons (1977) to predict the magnitude of the prehistoric earthquakes that accompanied scarp formation. This method is applicable for normal faults when the earthquakes are of shallow focus and sufficient size to be preserved through recent geologic time. The method is not effective when faults are strongly modified at the surface by drag, distortion, folding, warping, and detachment of the types described by Hardyman (1978), and Hardyman and others (1977).

REGIONAL SEISMIC POTENTIAL

Introduction

This discussion is based on the Sierra Nevada block and three provinces within the Great Basin: 1) the subprovince bounded on the west by the Sierra Nevada - Great Basin boundary and to the northeast by the Walker Lane; 2) the Walker Lane zone north of Tonopah; and 3) the area of the Great Basin northeast of the Walker Lane. Data

Table 3. Historic Surface Faulting in the Western Great Basin

Date	Earthquake Magnitude	Rupture Length (km)	Maximum Displacement	Faults
12-27-1869	6.7	23	3.65	Olinghouse fault, Nevada
03-26-1872	8.0	110	6.44	Mid-Valley and other faults, Owens Valley, California
1875	6.8	?	?	Wash fault, Mohawk Valley, California
1903	---	5+	1	Gold King fault, Nevada
10-02-1915	7.75	62	5.6	Several faults, Pleasant Valley, Nevada
12-20-1932	7.3	62	1.3	Several faults, Cedar Mountains, Nevada
01-30-1934	6.3	1.4-	0.12	Excelsior Mountain, Nevada
12-14-1950	5.6	8.9	0.61	Ft. Sage Mountain, California
07-06-1954	6.6	17.7	0.31-	Rainbow Mountain, Nevada
08-23-1954	6.8	30.6	0.76	Rainbow Mountain, Nevada
12-16-1954	7.1	58	5.62	Several, including Fairview Peak, Nevada
12-16-1954	6.9	61.2	3.25	Several, including Dixie Valley, Nevada
09-12-1966	6	18?	0.1?	Stampede fault, California

from faults within these sub-provinces and faults of the boundary zones are included in this study (figure 1).

Sierra Nevada Block

The Sierra Nevada is a westward tilted crustal block. Its eastern flank is bordered by a series of left-stepping en echelon frontal faults, each of the fault zones decreasing in displacement in a southerly direction. In detail, the range appears to become higher, narrower and more steeply tilted as the Mt. Whitney segment of the block is approached from the north. This is suggested by both the geologic investigations and topographic maps of the region. Slemmons and others (1979) have shown that the uplift rate for the summit of the range has been 0.14 mm/yr for the last 10 my and the present geodetic uplift rate is about 4.5 mm/yr.

The main internal faults of the northern part of the Sierra Nevada are the Bear Mountain and Melones fault systems of the Foothills region. The Melones fault zone near Sonora has a strain rate of about 0.007 mm/yr and recent studies for siting of the Auburn Dam suggest that the zone be assigned a maximum probable earthquake of about 6.5 magnitude (Cluff and others, 1977). The largest historic earthquake is near Oroville with a magnitude of almost 6. Internal deformation on northwest-trending right-slip faults and conjugate northeast-trending left-slip faults on a micro-fault scale are described by Lockwood and Moore (1979) for the eastern Sierra Nevada. The eastern zone is historically weakly seismic to aseismic (Ryall and others, 1966). Earthquakes of about 6 magnitude appear to be distributed on major faults near the eastern boundary zone or along branches of the Foothills fault system. Historic records and fault studies suggest that the maximum credible earthquake evidence derived from internal faults is about 6.5 within the Sierra Nevada block.

Sierra Nevada - Great Basin Boundary Zone

The Sierra Nevada - Great Basin zone extends as a left-stepping boundary, en echelon system of discontinuous N-S faults between the Garlock fault zone on the south to the Honey Lake depression at the northern end of the range. North of Honey Lake, the Sierra Nevada

List of Abbreviations for Figure 1, Faults, Lineaments and Subprovinces of the Western Great Basin.

A	Aubrurn
BMFZ	Bear Mountain fault zone
BRFZ	Black Rock fault zone
BVF	Bridgeport Valley fault
CLFZ	Carico Lake fault zone
CC	Carson City
CJ	Coaldale Junction
DVFZ	Death Valley fault zone
DVF	Dixie Valley faults
EMF	Excelsior Mountain fault
FPFZ	Fairview Peak fault zone
FLVFZ	Fish Lake Valley fault zone
FSMF	Fort Sage Mountain fault
FCFZ	Furnace Creek fault zone
GFZ	Garlock fault zone
GL	Goose Lake
GSVFZ	Granite Springs Valley fault zone
HL	Honey Lake
LF	Likely fault
LV	Long Valley
MP	Madeline Plains
MFS	Melones fault system
MoP	Modoc Plateau
MoV	Mohawk Valley
ML	Mono Lake
OF	Olinghouse fault
O	Oroville
OVFZ	Owens Valley fault zone
PaVFZ	Panamint Valley fault zone
RMF	Rainblow Mountain fault
R	Reno
RRV	Reese River Valley
SAVFZ	Saline Valley fault zone
SVFZ	Smith Valley fault zone
SMFZ	Smoky Valley fault zone
SON	Sonora
SFZ	Stampede fault zone
SVFZ	Surprise Valley fault zone
TON	Tonopah
TopL	Topaz Lake
TR	Truckee
WAVFZ	West Antelope Valley fault zone
WR	Weber reservoir
Y	Yerington

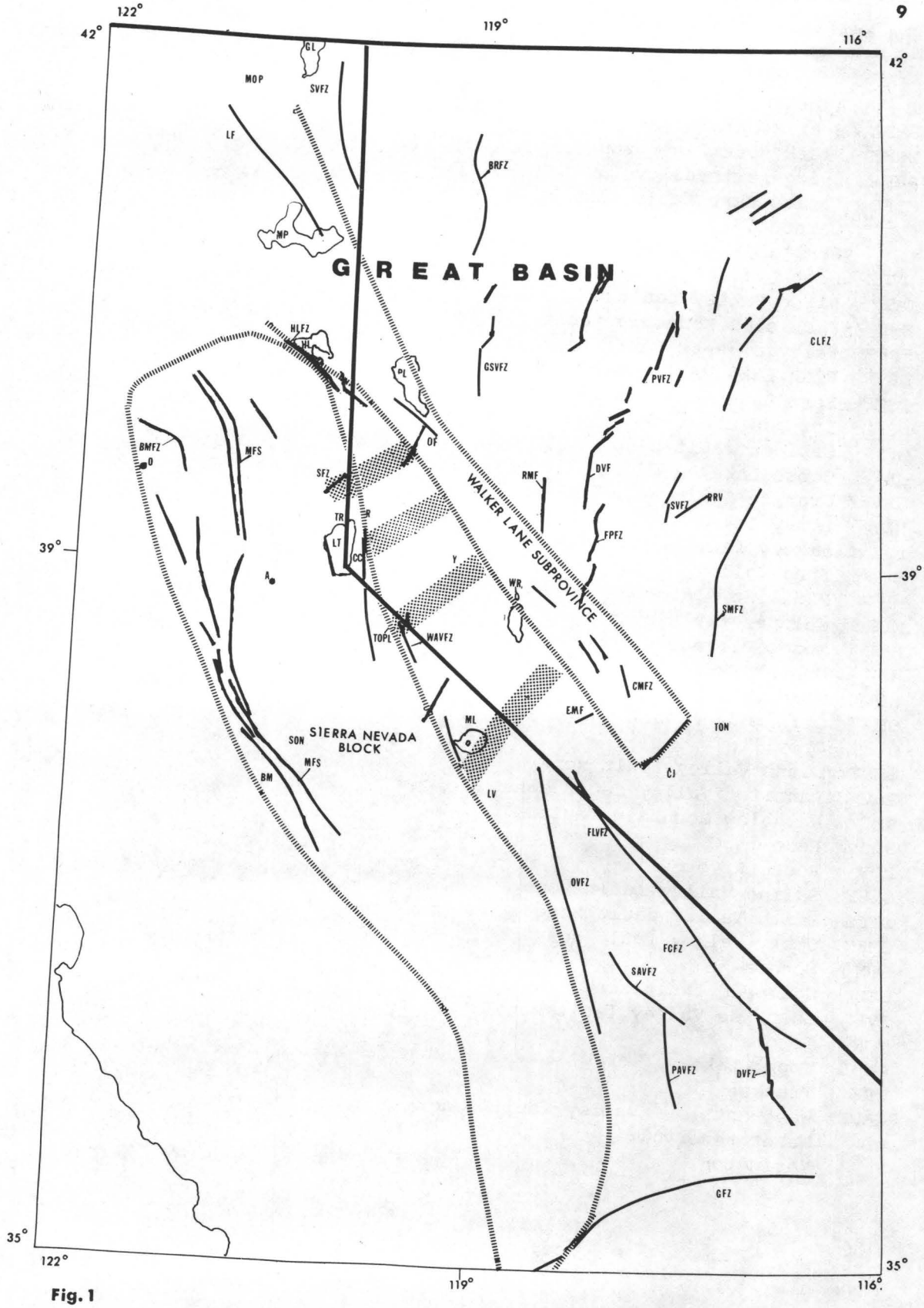
122°
119°
116°
42°
39°
35°
GL
MOP
SVFZ
LF
BRFZ
MP
GREAT BASIN
HLFZ
HL
PL
GSVFZ
PVFZ
CLFZ
OF
BMFZ
MFS
SFZ
RMF
DVF
WALKER LANE SUBPROVINCE
SVFZ
RRV
TR
R
LT
CC
Y
FPFZ
A
WR
SMFZ
TOPL
WAVFZ
CMFZ
EMF
TON
ML
SON
SIERRA NEVADA BLOCK
MFS
BM
LV
CJ
FLVFZ
OVFZ
FCFZ
SAVFZ
PAVFZ
DVFZ
GFZ

Fig. 1

basement rocks are covered by the younger andesites of the Cascade Range and the biomodal basalt-rhyolite association of the Modoc Plateau. The en echelon pattern suggests a right-slip regional strain although the faults generally exhibit dips from vertical degrees east and are of normal right-oblique-slip. The faults lie parallel to the regional compression axis and are extended by slip parallel to the N 70°W to N 90°W extension axis.

Seismic activity of this active fault zone is regulated by differential vertical separations (Slemmon and others, 1979) between the Sierra Nevada block (0.12 mm/yr uplift) and the lower Great Basin region (0.01 mm/yr uplift). The fault separations across the zone vary from about 1.2 km to 5.5 km (Owens Valley). The individual boundary fault segments generally have lengths of 60 to 200 km and have prehistoric to historic maximum displacements of up to 6 or 7 m. This yields an earthquake magnitude of 7 to 8 using the magnitude-rupture length-maximum displacement relations of Slemmons (1977).

Many, but not all, Wisconsin-age moraines, outwash surfaces, and alluvial aprons (12,000 to 60,000 years BP) have up to 5 rupture events, showing recurrence intervals of from 2400 to 14,000 years at some locations. Other major boundary faults show evidence of glacial features with ages of 40,000 to 60,000 years BP, suggesting longer recurrence intervals.

The increase in total displacement on the frontal zones of the Sierra Nevada boundary zone, the increase in freshness of scarps, and increase in length of the active scarps all combine to indicate an increasing seismic potential toward the southern part of the range. Specific suggestions for maximum credible and maximum probable earthquakes are summarized in Table 4.

Sierra Nevada Boundary Zone to Walker Lane Subprovinces

This subprovince is texturally characterized by rectilinear features with many short, conjugate NW- and NE-trending fault-bounded mountain blocks, valleys and depressions, and swarms of parallel faults. Locally, there are N-S blocks, but the conjugate NW- and NE-trending fault pattern resulting from a σ_1, as noted by Wright (1976) dominates this subprovince

Table 4. Maximum Credible and Maximum Probable Earthquakes For The Sierra Nevada Boundary Zone.

	Fault Zone	Est. L (km)	Recurrence Interval	Max. Cred.	Max. Prob.	Comments
1.	Honey Lake	80	C	7.0-7.5	6.8-7.0	
2.	Mohawk Valley	60	C	7.0-7.4	6.8-7.0	
3.	W. edge, Lake Tahoe depr.	40	C	7.0	6.6-7.0	
4.	Reno-Carson City-Genoa-Markleeville	100	B	7.3-7.6	7.0-7.25	May be segmented with lower magnitude earthquakes
5.	W. Antelope Valley	60	B	7.0-7.4	6.6-7.0	
6.	NW Bridgeport Valley	20	B	6.6-6.8	6.5-6.8	
7.	W border, Mono depr.	30	B	7.0	6.8	
8.	N Owens Valley	100	B	7.3-7.6	7.0-7.3	May be segmented, but is fairly linear
9.	South Owens Valley	100	B	7.7-7.6	7.0-7.25	
10.	Mid-Valley Fault Zone, Owens Valley	160	B	7.8-8.0	7.2-7.5	1872 earth quake of ca. 8.0 magnitude

(figure 2). The NW-trending faults which parallel the Walker Lane generally exhibit greater lengths while the NE-trending faults are shorter. The NW faults have prominent right-slip components and the NE faults have left-slip components. The NS faults are mainly normal-slip faults. Most of the faults are shorter than 30 km. All historic earthquakes in this subprovince have disturbed only a part of the total length of the related fault zone. Magnitudes vary from 5.6 for the 1950 Ft. Sage Mountain rupture to about 6.7 for the 1869 Olinghouse rupture. The longer NW-trending zones include the Honey Lake and Mohawk Valley faults of 80 and 60 km length, respectively, which form the diffuse northwestern and northeastern ends of this zone.

The maximum probable earthquakes within this zone generally range from 6.5 to 7.0 and most of the faults show only short segments exhibiting late Quaternary surface faulting. Most faults without recent activity have low scarps on surfaces with Sangamon type soils. The mature erosional character of these scarps suggests that recurrence interval for faulting is long, measured for the most part in tens of thousands of years or more. Major NE to EW cross-structures prominent within this subprovince all appear to have right-stepping en echelon patterns. Local field evidence suggests left-lateral slip. These transverse structures have a questionable fault origin at depth and are characterized by dispersed patterns of non-connecting faults and folds.

The main transverse zones are:

1) Truckee-Verdi-Reno-Olinghouse Zone. This is a NE-trending zone of en echelon, right-stepping faults that disturb the continuity of faults to the north and south. Deformation on this zone includes the Pliocene-Quaternary synclinal-like downwarp of Verdi-Reno, with an EW axis suggestive of a NS compression direction. The zone truncates both the northern end of the Truckee-Lake Tahoe depression and the northern end of the Reno-Carson City-Genoa-Silver Creek zone of active faults. The zone is seismically very active with two earthquakes accompanied by surface faulting; the 6.7 magnitude event on the Olinghouse fault zone in 1869 and the 6 magnitude Truckee earthquake of 1966 on the Stampede Dam-Hoke Valley-Dog Valley fault system. These earthquakes had left-oblique-normal-slip mechanisms. The 1869 Olinghouse earthquake

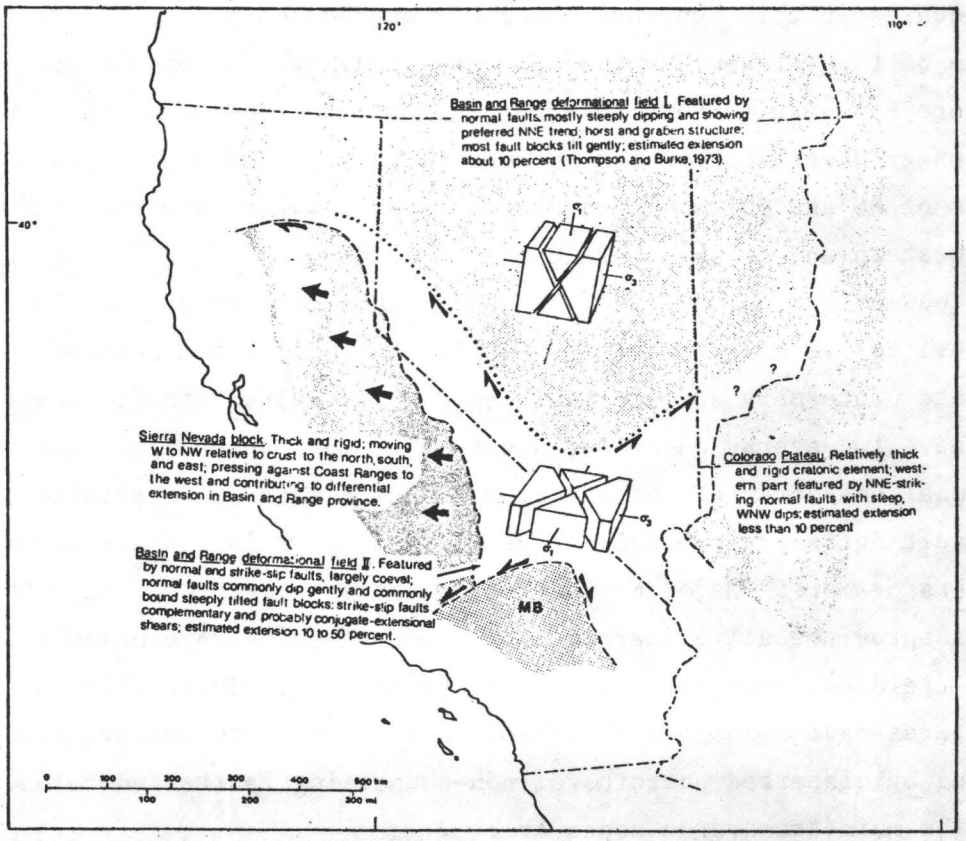

Figure 2. Tectonic model of Wright (1976) showing (1) subdivision of Great Basin into two deformation fields and (2) apparent effect of westward displacement of Sierra Nevada block and southward narrowing of Great Basin on late Cenozoic deformational features of Great Basin. Idealized block diagrams in each field show suggested principal stress orientations; σ_1, maximum principal stress σ_3, minimum principal stress; MB, Mojave block.

appears to have occurred on a branch fault having semi-circular form which bifurcates from the Walker Lane (Sanders and Slemmons, 1979; Bell and Slemmons, 1979) and which ruptured for about one-half of its total length. This part of the zone has a total length of about 40 km which suggests a maximum credible earthquake range of 6.8 to 7.1 and a maximum probable earthquake range of 6.4 to 6.7. Fresh fault scarps in Sangamon age surfaces are widely distributed but have short lengths and generally small displacements, suggesting that the recurrence intervals are long, probably in the 50,000 to 100,000 year range. The lack of narrow, and well-defined gravity and aeromagnetic anomalies, the width of the zone of faulting in the Virginia Range, and the lack of major bedrock differences across the zone suggest that the zone is complex at depth. Lack of evidence for a single simple fault at depth within this zone coupled with historic observations of seismicity suggest that evaluation of individual faults which comprise this zone will provide an adequate criterion for determination of maximum earthquake magnitudes.

2) The Carson Lineament. The Carson Lineament (Shawe, 1965) is similar to the Truckee-Verdi-Reno-Olinghouse zone described above. The lineament has a similar orientation and a length of about 75 km. This zone is also comprised of many short (up to 10 km long), active faults with Holocene and late Quaternary scarps. The NE trend suggests left-oblique-slip for many of the fault segments, although the NS en echelon pattern common to the zone may indicate NS extension in parts of the zone. The 10 km width of the fracture pattern, the gentle gravity and aeromagnetic gradients in the immediate region, and the major geological basement continuities (Stewart and Carlson, 1974; 1977; and 1978) across this zone indicate that it may represent a region of disturbance rather than a simple, major fault zone.

3) The Topaz Lake-Yerington-Weber Reservoir Zone. This zone is recognized as a major structural boundary by Gilbert and Reynolds (1973). It has a length of about 75 km that is similar to the two zones previously described and appears to be truncated by the Sierra Nevada frontal fault zone and the Walker Lane. It differs from the other two structures in that it has fewer faults aligned along the

structural trend. This zone is defined by the termination or truncation of major Quaternary faults of NS trend. It is not expressed on magnetic maps and does not appear to be a major basement marked by major lithologic or structural discontinuities. The structures that provide the highest maximum credible and maximum probable earthquakes for this zone are determined by the length of major NS-trending faults, including: 1) the active fault zone along the eastern flank of the Pine Nut Range; 2) the active fault zone at the eastern flank of Wellington Hills; and 3) the eastern frontal fault of the Wassuk Range.

4) Mono Basin-Hawthorne to Long Valley-Coaldale Jtn; This complex zone of faults and lineaments have been recognized in an area extending from the Sierra Nevada near the Mono Basin-Long Valley caldera region, to the Walker Lane (Gilbert and others, 1968; Gilbert and Reynolds, 1973, Ekren and others, 1976). This zone includes seismically and geologically active faults, including the fault of the 1934 Excelsior Mountain earthquake and major aeromagnetic, gravity and Landsat imagery lineaments. Historic activity includes earthquakes of up to 6.25 magnitude. Most of this zone is characterized by short faults with maximum lengths of 15 to 20 km. The NE trend of these segments suggests left-slip or left-oblique-slip mechanisms. A thick section of pyroclastic rocks is present in this zone. The rocks are similar to those described by Hardyman (1978) and Hardyman and others (1977). This detachment type of faulting reduces the exposed length of many of the main active traces of the Walker Lane, for example, the magnitude 7.3 Cedar Mountain earthquake, which had an aftershock zone of about 80 km length (Wilson, 1935) but only small, scattered surface fault scarps of short length and anomalously small displacements (Gianella and Callaghan, 1934). Two unresolved options appear possible for this zone. The first has a relatively low set of values; a maximum credible earthquake of about 6.5 to 6.75 and a maximum probable earthquake of about 6.25 to 6.75, based on maximum fault lengths of from 10 to 15 km. The second has relatively higher values, approximately 7.3, based on the

possibility of detachment mechanisms and long structures suggested by the aeromagnetic anomalies, Landsat lineament analysis, and the 7.3 magnitude earthquake of 1932.

Three zones of geologically recent extension and strain, described below, appear to project into the western and central Great Basin from the active plate tectonic boundary of California. All three of these zones are included in the area between the Sierra Nevada frontal faults and the Walker Lane north of Tonopah. To the east of Tonopah, the late Quaternary zones of active faulting are widely separated and do not show the NS continuity that is apparent in the western Great Basin. These three zones are defined as follows:

1) Owens Valley Zone. This zone exhibits extensional faulting on the two margins of the valley. Locally, in an inner graben, the normal movement is accompanied by a right-slip component. This zone appears to be a geologically very young expansion to the west of the Great Basin as Owens Valley had only limited expression about 3 million years ago. This extensional breakup of the Sierra Nevada block appears to have taken a N 15°W slice obliquely across the N 30°W trending southern edge of the Sierras. The activity of this zone appears to cross the Mono Basin and connect with the Sierra Nevada frontal fault system to the north as a narrow band, a few tens of kilometers in width. A major branch extends northward to the Walker Lake area.
2) Panamint Valley-Saline Valley-Eureka Valley Zone. This zone, which also appears to connect with the California active tectonic zones via the Garlock fault system, trends N 25°E and is near the original eastern frontal zone of the Sierra Nevada. The zone exhibits dominant right-slip separations, but has deep grabens and rhomb-shaped depressions that characterize the vigorous extension present to the north of the Garlock fault zone. The northern end of this active zone is truncated by a swarm of N 25°E faults, grabens and oblique structures at Deep Springs Valley - Eureka Valley. The activity of this zone appears to join the Fish Lake Valley - Northern Death Valley - Furnace Creek fault zone near Dyer, and the activity

continues northward to the Walker Lane near Mina and Teel Marsh.

3) Fish Lake Valley-Northern Death Valley-Furnace Creek Zone. This zone extends northward from the Garlock fault zone along a N 40°W-N 45°W trend coinciding with the southern Death Valley fault zone, along the predominantly normal-slip N 15°W-trending Death Valley graben to the Furnace Creek fault zone. Freshness of fault scarps increases to the north of this junction. The zone continues along the Northern Death Valley fault zone with right-slip separation (Stewart, 1967) and trends N 40°W to connect with the Fish Lake Valley fault zone. The zone is truncated at the north end of Fish Lake Valley by the EW cross structure described by Ekren and others (1976). The cross structure shows conspicuous active faults north of Lone Mountain and appears to transfer the tectonic activity of the Fish Lake Valley zone westward to three zones that extend northward from this southern end of the active Walker Lane segment. These three zones are represented by the Smith Creek-Reese River Valley zone, the upper Reese River Valley-Carico Lake zone, and the Smoky Valley-Grass Valley-Crescent Valley zone.

Walker Lane Zone

The Walker Lane north of Tonopah appears to be generally active, although a gap in apparent activity is present between Wadsworth and the region near Weber Reservoir. The fault zone changes character along its length and different segments have different projections of size for potential earthquakes. The following segments are provisionally identified:

1) Northern Walker Lane Dispersed Zone. Although the Likely fault has been termed the northern extension of the Walker Lane (Pease, 1969), the fault zone which normally has a width of about 30 km, appears to radiate as a series of spokes that trend northward from the Susanville-Pyramid Lake area. Active faults are dispersed throughout the Modoc Plateau of northeastern California. Although the region is nearly aseismic (Real and others, 1978), there are many conspicuous active faults, including those of the Tule Lake,

Honey Lake, Madeline Plains, Goose Lake and Surprise Valley areas. Active branches appear to include a northwest swarm of fault slices and tilted fault blocks, and the north-south horst and graben topography and structures to the east, near the California-Nevada state line. Unusual fault length - maximum displacement - magnitude relations are suggested by the 1978 earthquake near McCloud. An anomalously low magnitude of 4.7 and associated surface faulting with scarps up to about 0.5 meters in height may be characteristic of this region. An extremely shallow focal depth and zone of rupture may rule out the usual relationships. The horst and graben terrain to the east is assumed to have maximum credible and maximum possible earthquakes which can be evaluated by the usual methods of analysis.

2) Honey Lake-Wadsworth Segment. This segment has a width of about 30 km with activity along a western strand on the west flank of Ft. Sage Mountain to Spanish Springs, an east strand along the flank of Ft. Sage Mountain to Warm Springs Valley, and the Pyramid Lake right-slip strand (Bell and Slemmons, 1979). The Pyramid Lake strand has an observable length of 40 km, and a possible length of 80 km, suggesting a maximum credible earthquake ranging from 7.0 to 7.5, and a maximum probable earthquake in the range from 6.7 to 7.3.

3) Wadsworth-Weber Reservoir Segment. This segment of the fault shows anomalous relationships. Repeated evaluation of the available aerial photography and repeated aerial reconnaissance of this zone shows a subdued, hummocky or hilly terrain of low relief and an absence of fresh fault scarps, even in Sangamon age soils. Two alternative explanations for lack of evidence of late Quaternary faulting and generally aseismic character of this segment are:

    a) bypass of the segment by transferral of Walker Lane activity around this zone through the Carson Sink south of Weber Reservoir, or

    b) extension of detachment-type faults characteristic of the Walker Lane in the Gillis Range-Cedar Mountain region into this area, thereby effectively removing surficial evidence of active basement structures.

The latter explanation is the most plausible since the same geologic units that are present in the Gillis Range-Cedar Mountain area extend across this part of the Walker Lane. The former alternative would lead to maximum credible earthquakes ranging from 6.5 to 7 and maximum probable earthquakes of 6.0 to 6.5.

This segment extends about 60 km from Wadsworth to Weber Reservoir, but may be bisected into two 30 km segments by the Carson Lineament at Lake Lahontan. The longer segment length leads to a maximum credible earthquake of 7.0 to 7.5 and a maximum probable earthquake of 6.7 to 7.0. Using the shorter segment length yields values of 6.7 to 7.0 for the maximum credible earthquake and 6.3 to 6.5 for the maximum probable earthquake for each segment.

4) Weber Reservoir-Tonopah Segment. This segment appears to have a width of about 30 km from interpretations of lineations on the aeromagnetic maps of the region and according to published geologic mapping (Hardyman and others, 1975). Detailed structural maps show five main strands in this segment of the Walker Lane, with a cumulative right-slip of about 48 km during the last 21 million years. Hardyman (verbal communication, 1977) noted that one strand had a Holocene separation of about 3.7 meters, suggesting that the magnitude of the associated earthquake was near 7.4. This is compatible with the 7.3 magnitude for the 1932 Cedar Mountain earthquake along this same segment. The length of the segment from Weber Reservoir to Tonopah is about 150 km. For strike-slip faults the length of this segment indicates a maximum credible earthquake of about 7.6, and a maximum probable earthquake of 7.3.

The Great Basin to the East of the Walker Lane

This part of the Great Basin has several historic earthquakes of magnitudes 6.6 to 7.7, aligned along the Ventura-Winnemucca zone of Ryall and others (1966); these include the 1915, and four earthquakes of the 1954 series. The main Holocene to late Pleistocene zones of activity include the following prominent zones of discontinuous rupture: (1) the eastern side and floor of Smoke Creek Desert Holocene offsets that may extend over 30 miles, with primarily normal-slip displacement in the area from Pyramid Lake along the western border of the Fox Range, (2) the Copper Valley-Granite Springs Valley-The Lava Beds-Black Rock Fault Zone, with Holocene scarps in a zone of more than 90 miles length, (3) the lower Valley of Humboldt River, between Oreana and Mill City, with Holocene scarps in a complex zone, (4) young fault scarps described by Wallace (1978b) in Buena Vista Valley, (5) the nearly continuous zone of historic and Holocene scarps from Fairview Peak to Dixie Valley and branches into Pleasant Valley and into Buffalo Valley, (6) the zone with many normal-slip faults, at least partly of Holocene age from Ione Valley, into Smith Creek Valley, Antelope Valley and Reese River Valley, and the partly Holocene scarps of the Reese River Valley-Carico Lake, Crescent Valley zone. Another more easterly system, perhaps older in age includes the Big Smoky Valley zone of probable late Pleistocene activity.

The length of many of the linear fault segments and the historic maximum earthquakes indicate the potential for magntiudes of 7 to 7.7 for this region, with activity progressively diminishing in rate to the north.

Examples of estimated prehistoric and historic earthquake magnitudes include the following:

(1) Fox Range-Smoke Creek Desert zone: approximately 7 magnitude for the most recent event;

(2) Copper Valley-Granite Spring Valley-The Lava Beds-Black Rock fault zone: approximately 6.9 to 7.3 maximum probable Holocene earthquake (oral communication and term paper by V. Scott Moore and Joe McGinley, 1979) for the Granite Springs Valley segment, and over 7 magnitude by Rebecca Dodge and Trobridge Gross in a companion paper of this publication, for the Black Rock fault zone.

Discussion

The historic earthquake record and geologic data for fault length, maximum displacement by surface faulting, and limited earthquake recurrence data, all suggest that the regional pattern for late Quaternary active faults, and the size of maximum earthquakes is induced from, and is in part controlled by the San Andreas and Garlock fault systems to the southwest. Faults in the southern part of the Great Basin appear to be more linear and continuous and have high strain or slip rates. Faults of the southern part of the province may be characterized by larger maximum earthquakes, with a potential for surface wave magnitudes of up to about 8 for the three main fault systems--the Owens Valley zone from the Garlock to near Benton, the Panamint to Saline Valley zone of faulting, and the zone of faults that extends from the vicinity of the Garlock fault eastern termination, through Death Valley, along a segment of the Furnace Creek fault zone, to the Fish Lake Valley fault zone.

North of the latitude of Long Valley, Tonopah and Warm Springs, at the lineament previously noted by Ekren and others (1976), the branching becomes more diverse and complex, with many shorter faults of NW and NE trend in the Sierra Nevada boundary zone to Walker Lane zone, a broad zone of mainly NW right-slip faults within the Walker Lane zone, and a series of NNE-trending active structures that extend northward from the Walker Lane toward Oregon. The maximum earthquakes for these zones is determined by fault type and fault length, with maximum earthquakes of approximately 7.7, the reported M_S for the 1915 Pleasant Valley earthquake. to the north of Walker Lane.

The maximum earthquakes for the Walker Lane, if a segmented zone is postulated vary up to about 7.6 maximum credible earthquake and 7.3 for a maximum probable earthquake. If detachment faulting conceals the basement continuity between the northern and southern parts of the zone, there is a potential for maximum credible earthquakes of up to about magnitude 8.

REFERENCES

Bell, E.J., and Slemmons, D.B., 1979, Recent crustal movements in the central Sierra Nevada-Walker Lane region of California-Nevada: Part II, The Pyramid Lake right-slip fault zone segment of the Walker Lane: Tectonophysics, v. 52, p. 571-583.

Bucknam, R.C., and Anderson, R.E., 1979, Estimation of fault scarp ages from a scarp height-slope-angle relationship: Geology, v. 7, p. 11-14.

Cluff, L.S., Packer, D.R., and Moorhouse, D.C., 1977, Earthquake Evaluation Studies of the Auburn Dam Area: Woodward-Clyde Consultants, 8 volumes.

Ekren, E.B., Bucknam, R.C., Carr, W.J., Dixon, D.L., Quinlivan, D.W., 1976, East-trending structural lineaments in central Nevada, U.S. G.S. Prof. Paper 986, p. 16.

Gianella, V.P., and Callaghan, E., 1934, The earthquake of December 20, 1932, at Cedar Mountain, Nevada, and its bearing on the genesis of the Basin and Range structure, J. Geol, v. 42, p. 1-22.

Gilbert, C.M., Christensen, M.N., Al-Rawi, Y.T., and Lajoie, K.R., 1968, Structural and volcanic history of Mono Basin, California-Nevada, Geol. Soc. Am. Mem. 116, p. 275-329.

Gilber, C.M., and Reynolds, M.W., 1973, Character and chronology of Basin development, western margin of the Basin and Range Province, Bull. Geol. Soc. Amer., v. 84, p. 2489-2510.

Hardyman, R.F., 1978, Volcanic stratigraphy and structural geology of the Gillis Canyon quadrangle, northern Gillis Range, Mineral County, Nevada. Unpublished Ph.D. dissertation, University of Nevada, Reno, 248 p.

Hardyman, R.F., Ekren, E.B., and Byers, F.M., 1975, Cenozoic strike-slip, normal and detachment faults in northern part of the Walker Lane, west-central Nevada. Geol. Soc. Am. Abstr. 7 (7), P. 1100.

Howard, K.A., and others, 1978, Preliminary map of young faults in the United States as a guide to possible fault activity: U.S. Geol. Survey Misc. Field Studies Map MF-916, Scale 1:7,500,000.

Jennings, C.W., 1975, Fault map of California with locations of volcanoes, thermal springs and thermal wells: Calif. Div. Mines and Geology Data Map Series Map no. 1, scale 1:750,000.

Lockwood, J. and Moore, J., 1979, Regional deformation of the Sierra Nevada, California on conjugate microfault sets: EOS, 60, no. 25, p. 496-503.

Pease, R.C., 1979, Scarp degradation and fault history south of Carson City, Nevada: Unpublished M.S. thesis, University of Nevada, Reno, 90 p.

Pease, R.W., 1969, Normal faulting and lateral shear in northeastern California: Geol. Soc. Am. Bull., 80, p. 715-720.

Real, C.R., Toppozada, T.R., and Parke, D.L., 1978, Earthquake epicenter map of California 1900 through 1974: Calif. Div. Mines and Geol., map sheet 39, scale 1:1,000,000.

Ryall, A., Slemmons, D.B., and Gedney, L.D., 1966, Seismicity, tectonism and surface faulting in the western United States during historic time: Bull. Seism. Soc. Am., 56 (5), p. 1105-1135.

Sanders, C.O., and Slemmons, D.B., 1979, Recent crustal movements in the Central Sierra Nevada-Walker Lane region of California-Nevada: Part I111, the Olinghouse fault zone: Tectonophysics, v. 52, p. 585-597.

Shawe, D.R., 1965, Strike-slip control of Basin-Range structure indicated by historical faults in western Nevada: Geol. Soc. Am. Bull., v. 76, p. 1361-1378.

Slemmons, D.B., 1967, Pliocene and quaternary crustal movements of Basin and Range province: J. Geosci., Osaka City Univ., v. 10, art. 1-11, p. 91-103.

Slemmons, D.B., 1977, State-of-the-art for assessing earthquake hazards in the United States, faults and earthquakes magnitude: U.S. Army Engineer Waterways Expt. Station soils and pavements Lab., misc. paper 5-73-1, Rept. 6.

Slemmons, D.B., Van Wormer, D., Bell, E.J., and Silberman, M.L., 1979, Recent crustal movements in the Sierra Nevada-Walker Lane region of California-Nevada: Part 1, rate and style of deformation: Tectonophysics, v. 52, p. 561-570.

Stewart, J.H., 1967, Possible large right-lateral displacement in the Death Valley-Las Vegas area, California and Nevada: Geol. Soc. Am. Bull., v. 79, p. 131-142.

Stewart, J.H., and Carlson, J.E., 1974, Preliminary geologic map of Nevada: U.S. Geol. Surv. Misc. Field Studies Map MF-609.

Stewart, J.H., and Carlson, J.E., 1977, Cenozoic rocks of Nevada-four maps and brief description of distribution, lithology, age, and centers of volcanism: Nevada Bureau of Mines and Geology, map 57, scale, 1:100,000.

Stewart, J.H., and Carlson, J.E., 1978, Geologic map of Nevada: Nevada Bureau of Mines and Geology, Scale 1:500,000.

Wallace, R.E., 1978a, Geometry and rates of change of fault-generated range fronts, north central Nevada, Jour. Research, U.S. Geol. Survey, v. 6, no. 5, p. 637-650.

Wallace, R.E., 1978b, Patterns of faulting and seismic gaps in the Great Basin province, Proc. Conf. VI, Methodology for Identifying Seismic Gaps and Soon-to-Break Gaps: U.S. Geol. Survey Open File Report 78-983, p. 857-868.

Wilson, J.T., 1936, Foreshocks and aftershocks of the Nevada earthquake of December 20, 1932, and the Parkfield earthquake of June 7, 1934: Seismol. Soc. Am. Bull., v. 26, n. 3, p. 189-194.

Wright, L., 1976, Late cenozoic fault patterns and stress fields in the Great Basin and westward displacement of the Sierra Nevada block: Geology, v. 4, p. 489-494.

EARTHQUAKE HAZARDS MAPPING IN THE RENO-CARSON CITY AREA, NEVADA

Dennis T. Trexler
Nevada Bureau of Mines and Geology
University of Nevada, Reno
Reno, Nevada, 89557

ABSTRACT

Development of earthquake hazard maps for the Reno-Carson City area is an ongoing project of the Nevada Bureau of Mines and Geology. These programs entail a two-phased approach consisting of detailed geologic mapping at 1:24,000 scale, with emphasis on the stratigraphic relationships of unconsolidated Quaternary deposits. The second phase of the program involves collection of geotechnical data on the bulk density of the geologic units. These data are combined with SH-wave velocities to determine the "Rigidity Product" which provides an indication to the probable shaking characteristics that would be expected during an earthquake.

The structural setting along the Sierra Nevada Front in the Reno-Carson City area, as well as the entire front from the Garlock fault north, is complicated by the intersection of obliquely trending structures which are northwest trending in the south; Wilson Canyon and Mountain Springs faults, the east-west trending zone that intersects the eastern Sierra Nevada Front in the Long Valley-Mono Lake area; and the northeast trends such as the Carson Lineament and the Truckee (Olinghouse) trend in the north.

One important feature of the structural intersections is that their frequency increases northward; they tend to become closer spaced geographically and their trends rotate from northwest in the south through east-west in the central Sierra Nevada to northeast in the Carson City-Reno area.

INTRODUCTION

At the Nevada Bureau of Mines and Geology we have employed a two-phased approach in our production of earthquake hazard maps for the urban areas of western Nevada. The Reno-Carson City area and adjoining environs represent the most densely populated region in this part of Nevada and therefore has received and is continuing to receive the most intense study. The two-phased approach consists of geologic mapping at 1:24,000 scale with emphasis on the subdividing of the Quaternary deposits into as many divisions as possible based on: 1) composition, 2) stratigraphic position, 3) soil development, 4) geomorphic form, 5) degree of incision, and 6) degree of weathering. The use of relative age designations based on the above parameters is in most cases the only method available since absolute ages from C^{14} or tephrachronology are sparse, or nonexistent in a program entailing strictly geologic

mapping. The present geologic mapping program includes trenching of late Quaternary faults which may yield material suitable for absolute dating, and thus provide information on recurrence intervals.

The second phase in the production of earthquake hazard maps for the quadrangles which cover the urbanized areas, is to measure seismic velocities of the geologic units, gather data on the engineering properties and confirm suspected faults by subsurface investigations. Subsurface investigations by trenching across faults with well marked surface expression aids in determining the number of episodes of movement and the nature of the fault zone at depth. Scarps which appear to mark individual faults were shown to have multiple planes which distributed the displacement over a wide area. A more detailed discussion of the trenching performed during the most recently completed study will be presented subsequently.

Fault trends in the Reno-Carson City area, which borders the Sierra Nevada Front, are more complex than one would anticipate when mapped at 1:24,000 scale. Segments of the front are at times manifest by a prominent single fault, which may have vertical displacement of 1220 m (4000 ft) or more (Moore, 1969), while other segments exhibit a distributive surface fault pattern in which the vertical displacement is distributed across a wide zone of fracturing.

The earthquake hazard maps produced are from studies published by the Nevada Bureau of Mines and Geology in an Environmental Folio series. These maps are intended to be used by planners, developers and public officials to make prudent planning decisions. Assessment of the seismic hazards for individual sites must be based upon detailed engineering and seismic studies and should not be inferred from the 1:24,000 scale maps produced as part of this program.

PRODUCTION OF EARTHQUAKE HAZARD MAPS

BACKGROUND

It has been the intent of the Nevada Bureau of Mines and Geology to provide earthquake hazard maps depicting hazardous areas and age of last movement of faults within the Reno-Carson City area. This work has been performed by the U. S. Geological Survey (Washoe City quadrangle): supported by the U. S. Geological Survey (Reno, Carson City and New Empire quadrangles) and work underway in the Steamboat and Vista quadrangles which is supported by the U. S. Geological Survey. A geologic map and subsequent earthquake hazards maps are presently being prepared by the Nevada Bureau of Mines and Geology with funding provided by the Nevada State Disaster Preparedness Office.

APPROACH

One of the basic elements in constructing an earthquake hazard map is to group geologic units into categories based on similarities in the following parameters: 1) physical properties, such as composition, texture and degree of lithification; 2) engineering properties such as shear strength (as inferred from standard penetration test) and bulk density; and 3) shear wave velocities in the upper 10 m (30 ft) of the material.

The physical properties are inferred from field inspection during the geologic mapping phase of the program and refined, where necessary, during the more detailed work in conjunction with the earthquake hazard mapping. The engineering properties of the geologic units are acquired from consulting engineers foundation investigation reports. These data are available from many cooperating consultants and county engineering departments. These data are therefore restricted to those areas within the quadrangle under investigation where construction and development is under way or has already taken place. Limited data on the near surface bulk density of the material can be obtained by field density measurements following the methods described in ASTM D-1556 (Sand Cone), on units which do not have bulk density data. Density data from foundation investigations are preferred, but where no data exist, the sand cone method or nuclear density meter provide data on the unit's near surface density.

The techniques employed in measurement of the seismic velocities of the geologic units essentially follows the methods introduced by Kobayashi (1959) and subsequently discussed by Warrick (1974) and Power and Real (1976), for introducing predominantly transverse wave energy. Of particular interest in the near surface are the SH-waves which parallel the surface (Mooney, 1974). Procedures described by Mooney (1974) are employed to ensure the SH-wave velocities are being measured.

The method employed in this program is a modification of earlier investigators techniques. A typical sequence of measurements at any particular site using a Nimbus 12-channel enhancement seismograph consist of the following measurements. Compressional wave (P) velocities are measured by impacting an aluminum plate with a sledge hammer and recording the time to reach each geophone in the 12-phone line with 3 m (10 ft) spacing between phones. The source (plate and hammer) are moved to the opposite end of the geophone string and the compressional (P) wave travel times are measured using geophones with a vertical axis of sensitivity. Both forward and reverse P-wave data provide information on the stratification characteristics of the units and provide an indication on the configuration of the contact between units with increasing velocities as a function of depth.

Measurement of SH-waves consists of changing the geophones to horizontal component phones and inducing shear waves by striking an aluminum capped plank which is held firmly in place by the front wheels of a truck (Power and Real, 1976). In areas where optimum coupling between the plank and the ground surface is difficult to obtain, 4 steel (T-shaped) rods are driven into the ground through holes in the plank so that the transverse energy provided by hitting the end of the plank is transmitted into the ground, and slippage of the plank on the surface is minimized.

One end of the plank is struck and travel times are recorded. Depending on the type of material and the coupling characteristics between the plank and the ground additional impacts may be necessary to enhance the amplitude of the traces at distant geophones. When a satisfactory seismogram has been recorded, the opposite end of the plank is hit. This input of energy has the opposite polarity when initial arrivals are recorded at the geophones. When sufficient energy has been input and recorded, the seismograms for SH-waves are compared to ascertain if reversals are apparent and to confirm that the first arrivals being "picked" are SH-waves and not some other extraneous surface wave.

PROBLEMS ENCOUNTERED DURING SEISMIC VELOCITY MEASUREMENTS

Site selection for seismic measurements is sometimes difficult. The area must be relatively level (slope not exceeding 8%) and clear of large boulders. Accessibility to sites that provide optimum conditions is sometimes restricted by land ownership or by fences. In farming and ranching areas, irrigation ditches that parallel roads pose a problem both during the irrigation season, when filled with water, and during the winter when dry if they are deep. In addition, farming and ranching areas may limit available sites during the summer months by employing flood irrigation techniques.

In the eastern portion of the New Empire quadrangle a problem unique to most areas downwind from flood plains of the major streams draining the Sierra Nevada occurs. These areas are veneered with aeolian deposits which may range from 1-3 m (3-10 ft) in depth. This loose, unconsolidated material not only limits vehicular accessibility but significantly reduces the energy that can be input by the horizontal traction method even when employing steel rods through the plank to increase coupling.

PROBLEMS ENCOUNTERED WITH ACQUISITION OF GEOTECHNICAL DATA

As mentioned earlier most of the geotechnical data used in preparation of earthquake hazard maps are derived from construction projects that have been completed or are underway at the time of the map preparation. Many consulting engineering and geology firms are not willing to supply the needed information on bearing strength, unit density and depth to ground water for a particular site. In some cases contacts with county engineering offices have proven to be as exasperating as inquiries of individual consulting firms. The only data that are readily available from public agencies are those dealing with public buildings.

The hesitancy of county and city engineering departments to provide data from foundation investigations is disheartening and not understood. A similar lack of enthusiasm was encountered at the Department of Housing and Urban Development, Federal Housing Administration's field office in Reno. The problem becomes more exasperating because the approach we use is low keyed and the data will not be tabulated for a particular site but is combined with other similar data to represent an entire geologic unit.

Our best sources of geotechnical information are derived from consultants with whom we have developed a working relationship over the past several years. These tend to be the locally owned, well established firms as opposed to branch offices of large consulting firms whose main office is out-of-State. Possibly the hesitancy on the part of the consultants and public officials stems from the attitude that we are a State agency and have power of regulation, which is not the case. Our charter as mandated by the Nevada Legislature is one of research and public service in minerals and geology to the public of Nevada. The stigma of being regulatory is difficult to overcome and may be why our better sources of data are those firms that were built by local individuals. The fact still remains that many public agencies are not cooperative and the only reason that can be expounded to justify this attitude is either lack of knowledge of our purpose and/or the fear of a State-level agency trying to infringe in "their territory" or usurping their power.

EFFECTS OF GROUND WATER ON SEISMIC SHAKING

An important factor in determining the potential for seismic shaking is the depth to ground water. Medvedev (1965) and other investigators have shown that when the depth to ground water exceeds 10 m (30 ft) its effects on shaking characteristics including liquefaction and differential settlement are negligible. Depth to ground water is derived either from published or preliminary ground water maps where available or from boring logs of foundation investigations. When the depth to ground water is within 1 m (3 ft) of the surface and the units involved consist of fine-grained fluvial-lacustrine deposits or alluvial units with sand lenses, this combination of potentially liquefiable material and near surface ground water significantly increase the probable severity of damage.

Considerations as to the probable change in ground water conditions in the future have been addressed in the Reno quadrangle where the expropriation of agricultural lands to residential development would lead to a decrease in the near-surface perched water table due to irrigation of agricultural lands. This lowering of the water table with change in land use assumes that the high density residential development is on sewers and not individual septic systems. Moderate density (1/3 acres) sites on septic systems would tend to maintain the near-surface static water table and provide a condition of saturation.

RANKING OF GEOLOGIC UNITS INTO CATEGORIES OF SIMILAR SHAKING CHARACTERISTICS

It has been noted in the past that the degree of damage during large earthquakes (M>4) could be correlated with the type of materials underlying the site. Measurements of intensity amplifications have, however, been based primarily on empirical observation due to a lack in strong-motion instrumentation recordings. Only in recent years have strong-motion instruments been employed to quantitatively document surface accelerations. Sixteen accelergraphs and 4 seismoscopes are presently deployed in the Reno-Carson City area by the University of Nevada. Two additional U. S. Geological Survey instruments are deployed at the University of Nevada and the Veterans Administration Hospital in Reno (Alan Ryall, personal commun. 1979). No data are available from the strong-motion instruments to aid in determining differences in shaking characteristics of the geologic materials on which they are emplaced.

Although differences in intensity of shaking has been noted on deposits with differing physical properties, detailed modeling or calculations of soil amplification values are difficult to do; and without good observational or instrumental data their validity is questionable. Soil column response is dependent upon many variables, some of which are not clearly understood in terms of their influence on ground accelerations. These variables include: thickness, elastic properties, fundamental period, density, degree of saturation, and lithologic discontinuities of the soil column. These are further influenced by the frequency or period of the input seismic wave and the duration of shaking.

Past investigations (Medvedev, 1965, and Lajoie and Helley, 1975) indicate that geologic units may be grouped into broad relative response categories based on certain physical properties, namely their elastic or rigidity characteristics. If severe surficial shaking during an earthquake is assumed to be primarily due to shear-wave propagation (Seed and Schnabel, 1972; Bullen, 1963; Power and Real, 1976), the physical properties of interest are the rigidity or shear modulus (μ) and the density of the deposit. Units with significantly different rigidity and density characteristics would then be anticipated to exhibit varying degrees of shear wave amplification and different levels of shaking intensity.

Medvedev (1965) demonstrated this relationship using empirical observations of post earthquake damage for similar structures on different geologic materials. Borcherdt and others (1975) substantiated the interpretations of Lajoie and Helley (1975) in the San Francisco Bay area through strong-motion instrumental monitoring of low-strain events (nuclear detonations) and high-strain events (earthquakes). Spectral amplifications were found by Borcherdt and others (1975) to be greatest between geologic units having the greatest seismic impedance value contrast. Seismic impedance is defined by Lajoie and Helley (1975) as the product of the S-wave velocity and relative bulk density.

TECHNIQUE USED FOR GROUPING GEOLOGIC UNITS INTO SHAKING CATEGORIES

Under ideal conditions seismic zonation should be based on strong-motion instrumental monitoring of high-strain events. Since there have been no local high-strain events capable of being monitored and even if they had been, the emplacement of the previously mentioned instrumentation would not provide enough data to discriminate between gross geologic units. These strong-motion instrument arrays are emplaced to gather data mainly on the response of structures. Two instruments are located in mine shafts which would provide data on bedrock but this still does not provide data on the unconsolidated deposits which comprise the valley fill.

In the absence of both instrumental and empirical observation data, we have employed the technique of Lajoie and Helley (1975) as modified after Medvedev (1965). Lajoie and Helley (1975) categorized deposits in the San Francisco Bay area by what they termed the "seismic impedance" which was defined as the product of the transverse (S) seismic wave and the relative bulk density of the unit. Their categorization of geologic units into groups of probable response to seismic shaking was essentially validated by strong-motion instrumentation work performed by Borcherdt and others (1975).

In our work in the Reno-Carson City area potential intensity categories are outlined on the basis of the "Rigidity Product", which is the product of the near-surface shear wave (SH) velocity (Vs) and the density (ρ) of the unit. It is believed that although both P- and S-waves yield elastic moduli, the coefficient of rigidity or dynamic shear modulus, G, ($G=\rho V_S^2$) has particular importance for foundation studies and for the response of structures to dynamic foundation excitation (Mooney, 1974), and as mentioned previously shear waves are probably the principal source of severe surficial shaking.

A summary of the range of compressibility, longitudinal (P) wave, transverse (S) wave velocities, densities (expressed in g/cc) and the "Rigidity

Product" values derived from various materials in the Reno-Carson City area are presented in table 1. The groups represent average values for similar types of materials from the Reno, Carson City and New Empire 7 1/2-minute quadrangles. The general categories indicate relative or inferred response (severity of shaking) for the materials in each category. The table represents summation of 64 seismic measurement sites in the three quadrangles on 44 separate geologic units. Several of the more areally widespread, unconsolidated units which comprise the major valley fill deposits have multiple measurements.

In general the youngest fine-grained deposits have the highest potential for severe shaking during seismic loading. "Rigidity Product" (R.P.) values are less than 1000. In most cases these deposits occupy the lowest portions of the valleys or occur along the major streams. In any case they are generally saturated which further increases the severity of shaking and potential for liquefaction and/or differential compaction. The remaining unconsolidated deposits (categories II & III) decrease from high to moderately high potential based on their R.P. values (1100-1300 and 1330-1450 respectively). The deposits in category II have a high potential for shaking based solely on the R.P. values and may be affected by the presence of near surface ground water. If the material making up a geologic unit in this category is predominantly fine-grained and susceptible to liquefaction, it is given a higher category rating and included in the next higher category for map preparation.

The unconsolidated materials that make up category IV are coarser alluvial gravels and glacial outwash deposits. Other materials include weathered andesite which had a SH-wave velocity of 440 m/sec (1450 ft/sec), and decomposed granodiorite (grus) in the Carson City quadrangle that had SH-wave velocities as low as 250 m/sec (820 ft/sec). In areas where deeply weathered and weathered granodiorite could not be differentiated on the geologic map they were included into a category (for the purpose of map production) that was described as having variable severity of shaking and could have shaking characteristics across a range of intensities, figure 1. Figure 1 is a portion of the explanation for the preliminary Carson City Earthquake Hazard Map showing the use of a variable severity of shaking category which includes units that have ranges in SH-wave velocities due to degree and depth of weathering such as the granodiorite, or degree of alteration-welding and frequency of joint or fracture spacing as in ash-flow tuffs. Tabor and others (1978) were the first to employ the use of a category of shaking intensity that varied through a wide range of possible intensities because of inhomogeneity within the unit.

Category V in table 1 is a complex group of lithologies that were also included in a category of variable severity of shaking based on the degree of welding, alteration, joint spacing, and the presence of interformational gravels which in part unconformably separate the major ash-flow tuff sequences (Bingler, 1978).

The units most resistant to the effects of earthquake induced shaking are bedrock; which in this region consists of early Mesozoic(?) metamorphic rocks, Cretaceous igneous intrusives and massive Tertiary intermediate and basaltic volcanic rocks. The R.P. values for geologic units in this category (VI) have a wide range and are in excess of 3000. This category represents the most

TABLE 1. Summary of seismic velocities, densities and rigidity product values for geologic units in the Reno, Carson City and New Empire 7½-minute quadrangles, Nevada.

Category	Material	Compressibility	Vp		Vsh		Density g/cc	Rigidity product Vs (ft/sec) Xρ	Potential for seismic shaking
			ft/sec	m/sec	ft/sec	m/sec			
I	Fine-grained fluvial lacustrine deposits.	Very High	1000	300	400	120	1.4–1.8	650	Very high
II	Flood-plain and fine-grained alluvial plain deposits.	Moderately high	1115–1190	340–363	650–750	200–230	1.7–2.1	1100–1300	High
III	Older fan and terrace deposits, gypsiferous silt.	Moderately high	1220–1300	370–400	750–800	230–245	1.1–1.9	1330–1450	Moderately high
IV	Older, gravels, outwash deposits, includes weathered andesite and decomposed granodiorite.	Moderate	2500–3700	760–1130	1250–1500	380–460	1.3–2.1	2200–2700	Moderate
V	Tertiary siliceous tuff and interformational gravels and weathered granodiorite.	Moderately low	1120–4800	340–1460	800–2400	240–730	2.1–2.3	1680–5500	Moderate to low
VI	Bedrock, andesites, basalts, unweathered granodiorites and metamorphic rocks.	Low	2300–8000	701–2440	1250–4880	380–1490	2.6–2.7	3000–12,500	Low

POTENTIAL FOR GROUND SHAKING DURING EARTHQUAKES

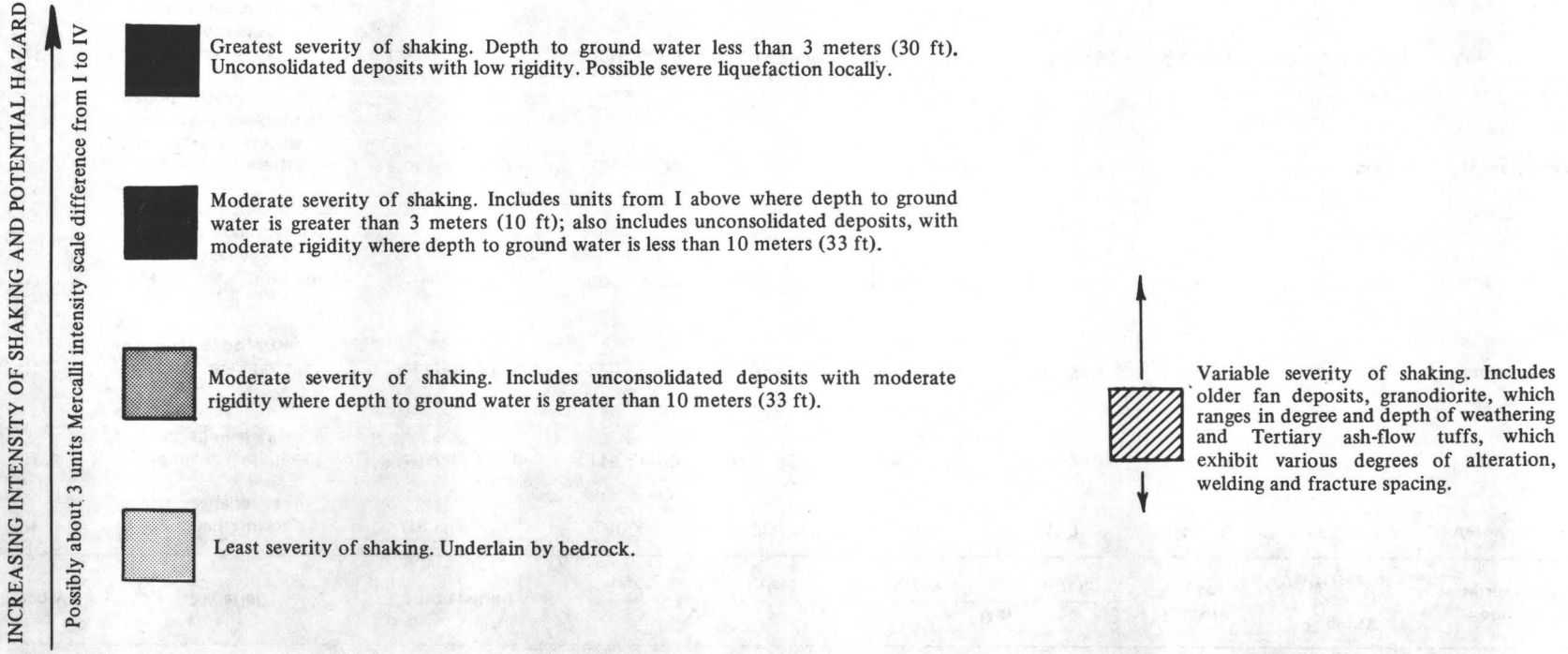

FIGURE 1. A portion of the explanation of the Carson City Earthquake Hazards Map showing the relationship of the variable category of shaking to the other categories.

stable materials that would in most probability induce the least amount of shaking during a given earthquake compared to the other categories.

ANTICIPATED RESPONSE BETWEEN CATEGORIES

The relationship between response categories based on R.P. values is difficult to ascertain. For example is the next higher category twice, three times or four times more hazardous than the lesser category? Is the entire scale from the lowest category to the highest linear? Or are the more severe categories most closely related than those lower in severity? The solution to this scalar problem in anticipated shaking characteristic was built into a computer simulated earthquake hazard model (Trexler and Bell, 1977). The present earthquake hazard maps represent the best estimate of severity of shaking in what appears on the explanation as an arithmetic succession. The hierarchy of increasing severity of shaking exists based on present data; the absolute degree of damage between each category is subjective at this point. Tabor and others (in press) state that their shaking zones on the Washoe City geologic hazards map are not intended to indicate unit differences in intensity, but they do indicate that there may be as much as 3 units in intensity difference experienced on bedrock from that observed on the least compotent material (saturated lake sediments). The computer produced earthquake hazard map allows rapid upgrading of the maps based on current data and allows for expansion of the degree of damage estimated for the categories as new information arises.

REGIONAL STRUCTURAL SETTING ALONG THE SIERRA NEVADA FRONT

Recent detailed mapping in the Reno-Carson City coupled with studies of lineaments and their relation to geothermal areas, funded by the U. S. Department of Energy under Contract No. EY-76-5-08-0671, have allowed comparisons to be made with the entire Sierra Nevada Front from the Garlock fault north. Local variations in the mode of tectonic deformation occur in the Reno-Carson City area and these variations appear to be analogous to portions of the entire front.

The intersecting structural elements with the Sierra Nevada Front tend to increase in frequency from south to north. These intersections tend to disrupt the well marked frontal fault and in general cause a westward shift in the front north of the zone of intersection. This association was first noted during a geothermal investigation for U. S. Department of Energy (Trexler and others, 1978). Figure 2 shows the fault patterns along the eastern Sierra Nevada Front (after Jennings, 1975). It is readily apparent that the two major areas of geothermal activity, Coso Hot Spring and Long Valley occur where the Sierra Nevada Front is interrupted by major northwest- or west-trending structures.

In the Coso Mountains near the southern portion of figure 2 the structure is dominated by north-south trending faults. However, northwest and northeast trending faults are present. Two northwest trending faults, the Wilson Canyon fault and the Mountain Springs fault cut the Coso Mountains. The Wilson Canyon fault forms a predominant lineament along which a chain of volcanoes has formed. West of the Coso Mountains the Sierra Nevada shift to

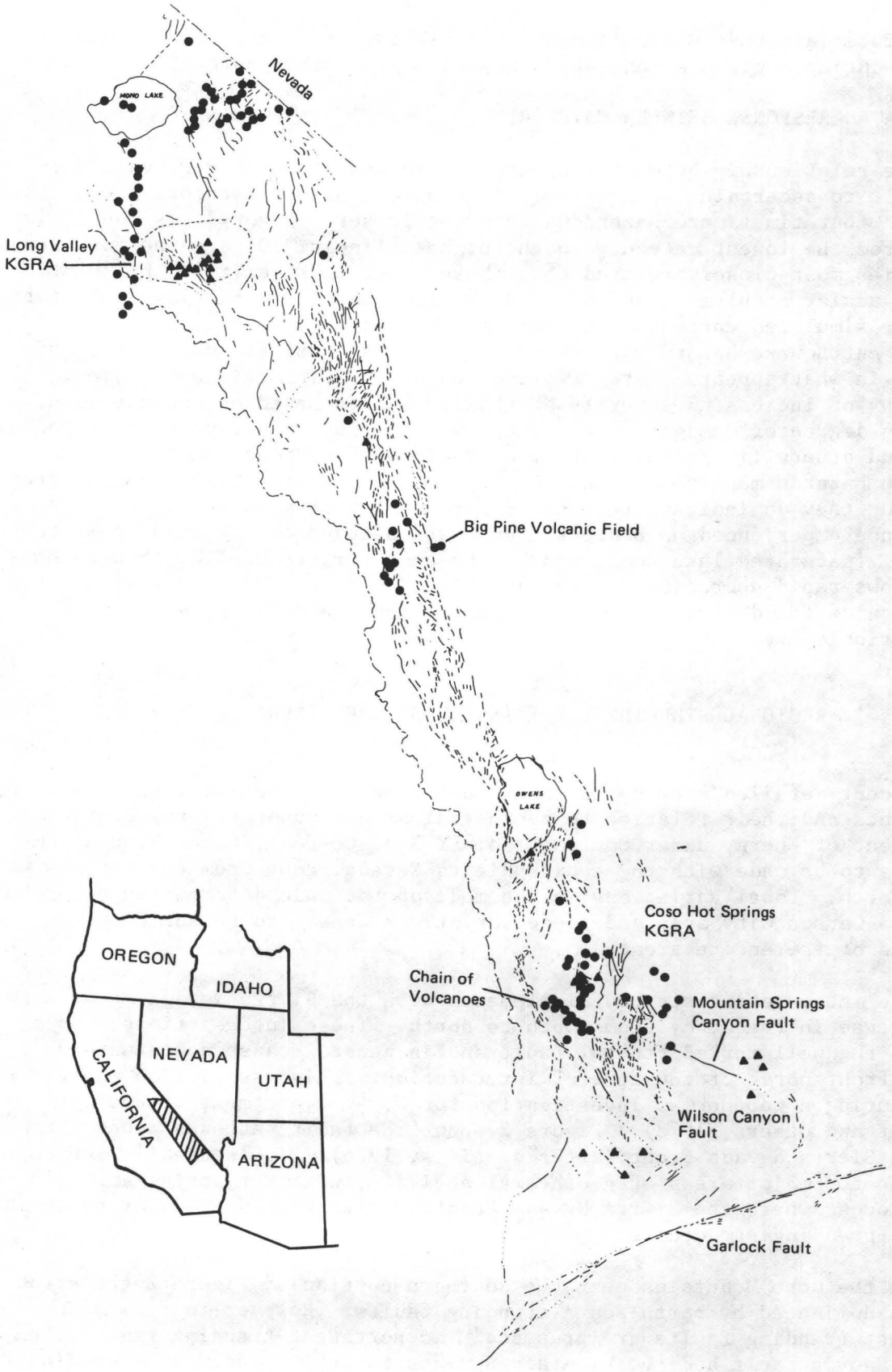

FIGURE 2. The Sierra Nevada Front from the Garlock Fault to Mono Lake showing areas of deflection to the west by intersecting structural trends. ● = hot springs, ▲ = cinder cones.

a westerly trend and abruptly shift back to the normal north-south trend. This perturbation in the trend of the Sierra Nevada Front occurs where the extension of the volcanic alignment in the Coso Mountains intersects the front.

The Big Pine volcanic field to the north is dominated by Quaternary basaltic volcanism. Orientation of faults surrounding this area is the typical north-south trend associated with the Sierra Nevada Front. However, within the Big Pine volcanic field there are northwest- and northeast-trending faults. Again the northwest-trending faults correspond in trend to the westerly shift of several miles in the Sierra Nevada Front.

Further north near the upper edge of figure 2 are the Long Valley caldera and the Mono Lake basin. Both of these areas show complex fault patterns and they are located at a position where the Sierra Nevada Front is again transposed to the west. This area of complexity may be the result of the intersection of two east-west trending lineaments that cross central Nevada (Ekren and others, 1976). Earthquake activity has been slightly higher in this area in recent years and not far to the east was the site of the 1934 Excelsior Mountain earthquake which had ground breakage along east-trending faults (Callaghan and Gianella, 1934).

LOCAL STRUCTURAL SETTING

As mentioned previously the Sierra Nevada Front has a conspicuous pattern which tends to repeat itself with greater frequency from south to north. Figure 3 shows the relation of the following three figures (figures 4, 5, and 6) to the Sierra Nevada Front. These figures will provide the basis for discussion of the local structural setting. South of latitude 39° the Sierra Nevada frontal fault is manifested by a well marked escarpment for a distance of 19 km (12 mi) to the California State line. This characteristic of the front continues northward to a point north of the small town of Genoa (figure 4), where the frontal fault becomes obscure and en echelon faults with smaller vertical offsets predominate. This splaying and departure from a well marked frontal fault continues northward into the Carson City quadrangle where it deviates from the general north-south orientation into several sets which trend more northeasterly.

The disparity of mapped faults in the bedrock portion of the Genoa and Carson City quadrangles is due to the predominance of granodiorite which limits the detection of faults based on stratigraphic offset. The majority of the faults shown in bedrock areas of figure 4 are a result of displacement in metamorphic pendants and Tertiary ash-flow tuffs; whereas tracing faults through granodiorite terrane is next to impossible unless they are pronounced on aerial photography.

One of the most striking features of figure 4 is the divergence to a northwest trend of faults with Holocene or latest Pleistocene movement beginning in the central Genoa 7 1/2-minute quadrangle and continuing through the central Carson City quadrangle and western New Empire quadrangle. The fault strands north of Carson City were reported by Rogers (1975a) as being Holocene in age and having left-lateral offset consistent with the Carson Lineament.

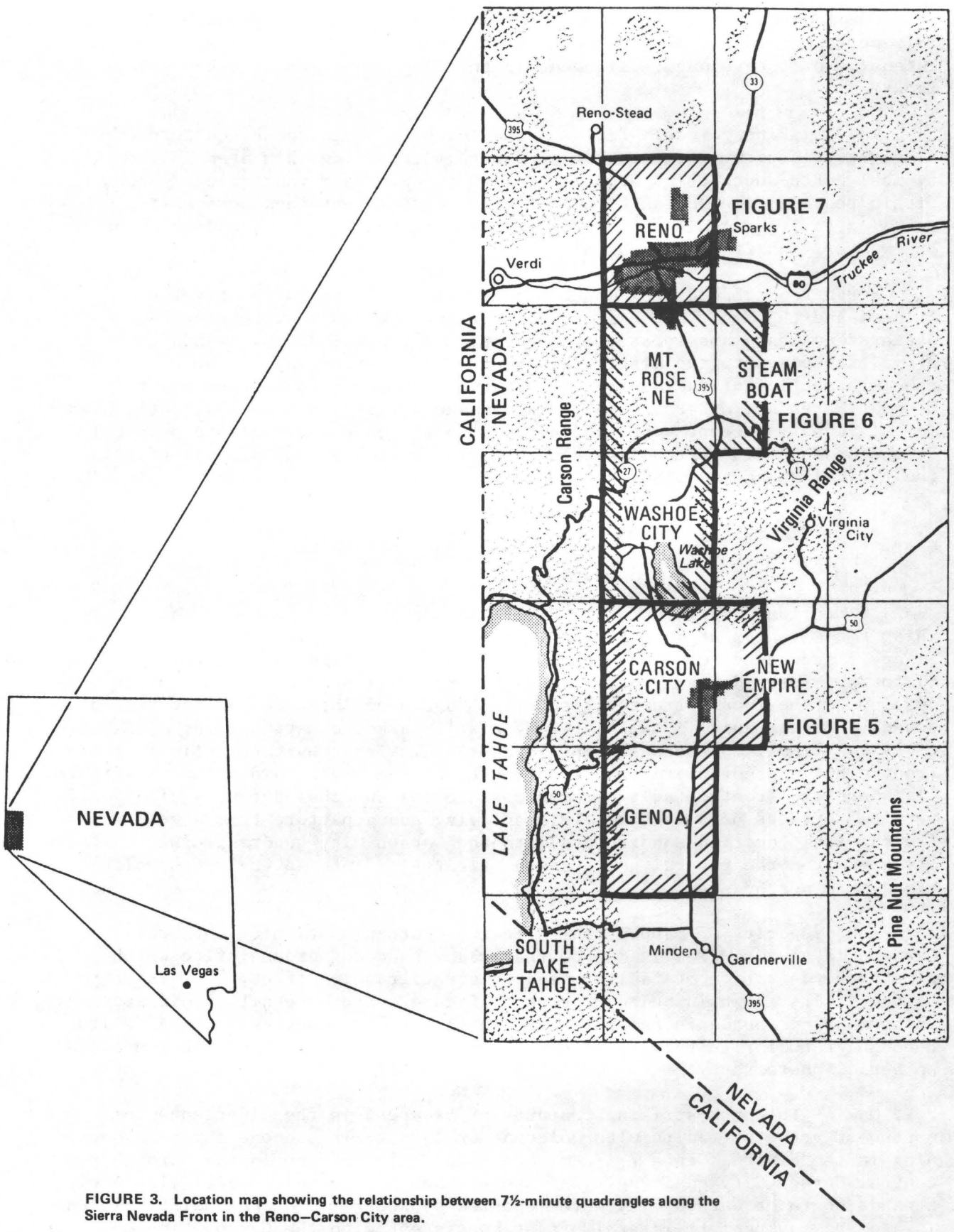

FIGURE 3. Location map showing the relationship between 7½-minute quadrangles along the Sierra Nevada Front in the Reno–Carson City area.

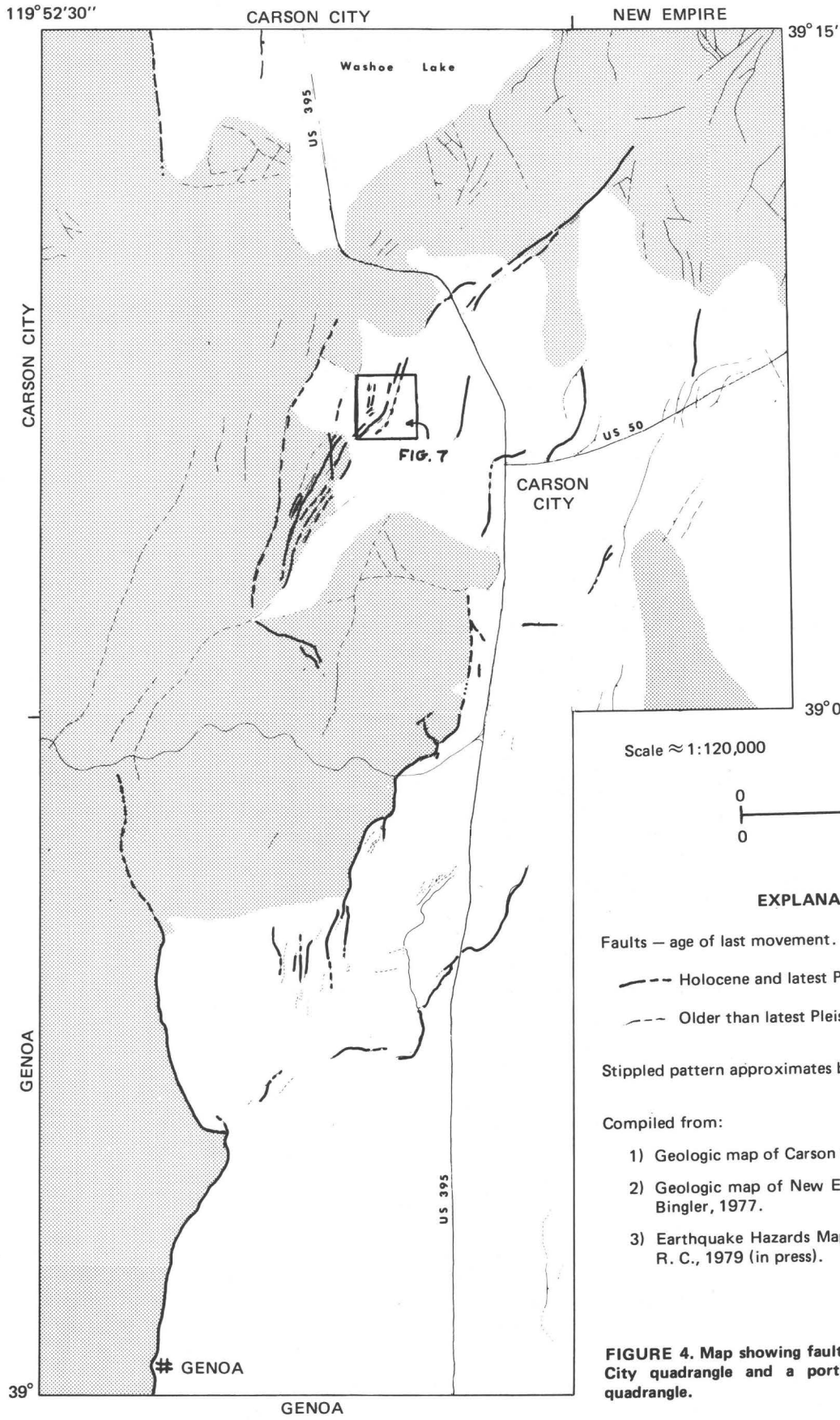

Scale ≈ 1:120,000

0 10,000 ft

0 3 km

EXPLANATION

Faults — age of last movement.

Holocene and latest Pleistocene.

Older than latest Pleistocene.

Stippled pattern approximates bedrock.

Compiled from:

1) Geologic map of Carson City, Trexler, 1977.
2) Geologic map of New Empire quadrangle, map 59, Bingler, 1977.
3) Earthquake Hazards Map Genoa quadrangle, Pease, R. C., 1979 (in press).

FIGURE 4. Map showing faults in the Genoa and Carson City quadrangle and a portion of the New Empire quadrangle.

Recent work by Bell and Pease (this volume) has confirmed a Holocene age of last movement, in fact (Bell, J. W. personal commun. 1979) the latest movement may have occurred several hundred years ago.

The extension of the northeast-trending Holocene fault in the northeast portion of figure 4 is hampered by the presence of basalt flows which have been dated at 1.36 $\pm$ .29 m.y. (Bingler, 1977). Surface manifestation of the basalt flows precludes the extension of the fault northeastward. Rogers' (1975b) studies indicated that Recent movement along faults with left-lateral offset are possibly part of the Carson Lineament.

The surficial manifestations in the vicinity, and east of the intersection of U. S. Highway 50 and U. S. Highway 395 according to Rogers (1975a) are the result of en echelon northeast-trending faulting in the basement, as interpreted from water well driller's logs.

Two faults in the northwest portion of figure 4 are considered to be younger or as young as late Pleistocene based on soil stratigraphy by Bell and Pease (this volume). This age assignment does not agree with those assigned by Tabor and others (1978) in the Washoe City quadrangle to the north (see figure 5). Tabor and others (1978) estimated the age of last movement for the faults in the alluvium as greater than 50,000-150,000 years. In figure 5 these are indicated as being Holocene (darker line) based on soil stratigraphy (Bell and Pease, this volume). The age of last movement of the range-bounding fault in the southwestern portion of figure 5 is questionable and was therefore not indicated as being Holocene or latest Pleistocene in age.

Note the similarity in structural pattern in the southern portions of figures 4 and 5. They both have singular well marked range-bounding faults that splay out into distributive faulting. This distributive faulting has been suggested by Thompson and Sandberg (1958, p. 1277) as being due to folding and warping. They suggest that the east front of the Carson Range represents an alternating series of large faults and folds.

The distributive faulting in the northern portion of the Washoe City quadrangle occurs where U. S. 395 bends easterly around the north end of Washoe Lake. Here the fault trends in the bedrock area, southwest of Steamboat Hot Springs, become northeasterly. The Holocene and latest Pliocene faults, in this zone of distributive faulting south of State Highway 27, maintain north trends. The age of the faults cutting the alluvial fan deposits in the east-central portion of the Mt. Rose NE quadrangle have not been determined by soil stratigraphy. The material which they offset is Donner Lake outwash for the most part with minor Tahoe outwash along the northern margin of the Steamboat Hills (Bingler, 1975). Based on the scarp morphology and comparison with faults at the boundary between the Mt. Rose NE quadrangle and the Washoe City quadrangle many of these faults could have ages of last movement as young as Holocene. The faults were not indicated as being latest Pleistocene or younger because all other faults so indicated in figures 4, 5, and 6 have a common basis for dating.

Again there is a difference in the density of faults in the Carson Range between the northern portion in the Mt. Rose NE quadrangle and the southern part of the Mt. Rose NE and Washoe City quadrangle. These differences are

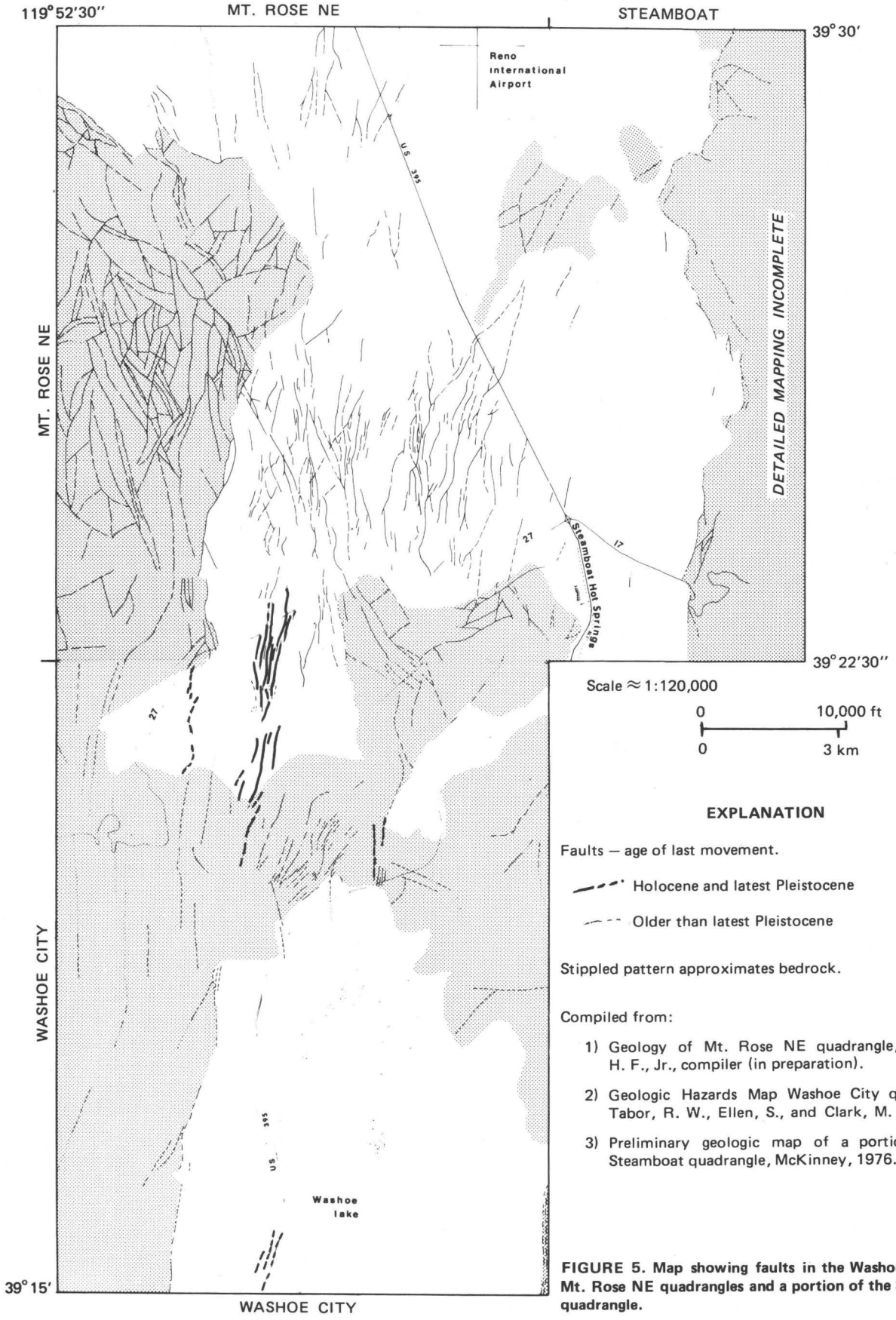

FIGURE 5. Map showing faults in the Washoe City and Mt. Rose NE quadrangles and a portion of the Steamboat quadrangle.

due to differences in rock types. The northern Carson Range is predominantly Tertiary Kate Peak Formation; flows and mudflow breccias with varying degrees of alteration and the faults are more easily mapped based on stratigraphic offsets.

Many of the faults which offset Quaternary unconsolidated deposits along the eastern margin of the Mt. Rose NE quadrangle have more northeasterly trends than those nearer the Carson Range. Faults in the bedrock area south of the Reno International Airport have similar trends.

In figure 6 (Reno 7 1/2-minute quadrangle) many of the faults which offset unconsolidated deposits also have northeast trends. The two faults indicated as being younger than latest Pleistocene have northeast trends. There has been some speculation that the more easterly of the two mapped faults is not even a fault (Bell, J. W., personal commun. 1979), but a meander scar.

In the Reno area the north-trending Sierra Nevada Front becomes obscure. Along the Truckee River Canyon west of Reno it appears to be transposed 16 km (10 mi) westward and probably proceeds northward along Long Valley and may bend as suggested by Wright (1976) into the Mt. Shasta-Lassen trend.

The significant point to be made here is that the typical Sierra Nevada Front as we have seen it from the Garlock Fault far to the south and in detail from Genoa north does not exhibit the characteristics of either folding (Thompson and Sandberg, 1958) or the spectacular single trace which has uplifted the Sierra Nevada block thousands of meters. The disruption in the style of structural development has been noted by several investigators (Shawe, 1965; Bonham, 1969; Rogers, 1975 and Sanders and Slemmons, 1979). The zones of disruptions of the Sierra Nevada Front are by northeast to east-northeast trending zones of faulting such as the faults associated with the 1948 and 1966 earthquakes near Truckee, California and the Olinghouse fault which had historical offset during the 1869 earthquake (M=6.7) east of Reno (Slemmons and others, 1979). The Carson Lineament of Shawe (1965) has been shown to have Recent movement in an area north of Carson City (Rogers, 1975a); and recent work by Trexler and Bell (1979) and Bell and Pease (this volume) indicate that the most recent movement may be as young as a few hundred years.

TRENCHING

Excavations across faults have been a recent addition to the Earthquake Hazards Reduction Program in the Reno-Carson City area. The recently completed study on earthquake hazard maps for the Carson City, New Empire and South Lake Tahoe quadrangles utilized six trenches to provide information on the number of episodes of movement and the complex nature of the fault zones at depth. The fault scarps that were trenched west of Carson City are shown on figure 7. Trench no. 1 was placed across an east-facing scarp which is 1.3 m (4 ft) in height. A portion of the detailed log of Trench no. 1 is presented in figure 8. The log indicates repeated displacement of the alluvial deposits and overlying Holocene soils. The most complex zone of disruption occurs between Sta. 15 to Sta. 45. A wide disturbed zone between

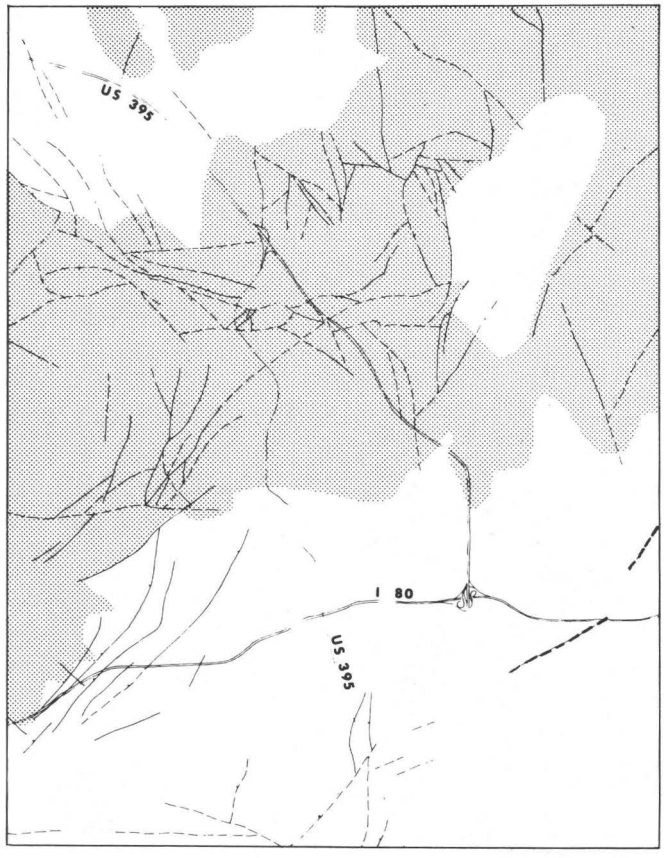

EXPLANATION

Compiled from: Earthquake Hazard Map of the Reno quadrangle, Bingler, E. C., 1974.

Faults: Holocene and latest Pleistocene

Older than latest Pleistocene

Stippled pattern approximates bedrock.

Scale ≈ 1:120,000

0 10,000 ft

0 3 km

FIGURE 6. Map showing the faults in the Reno quadrangle.

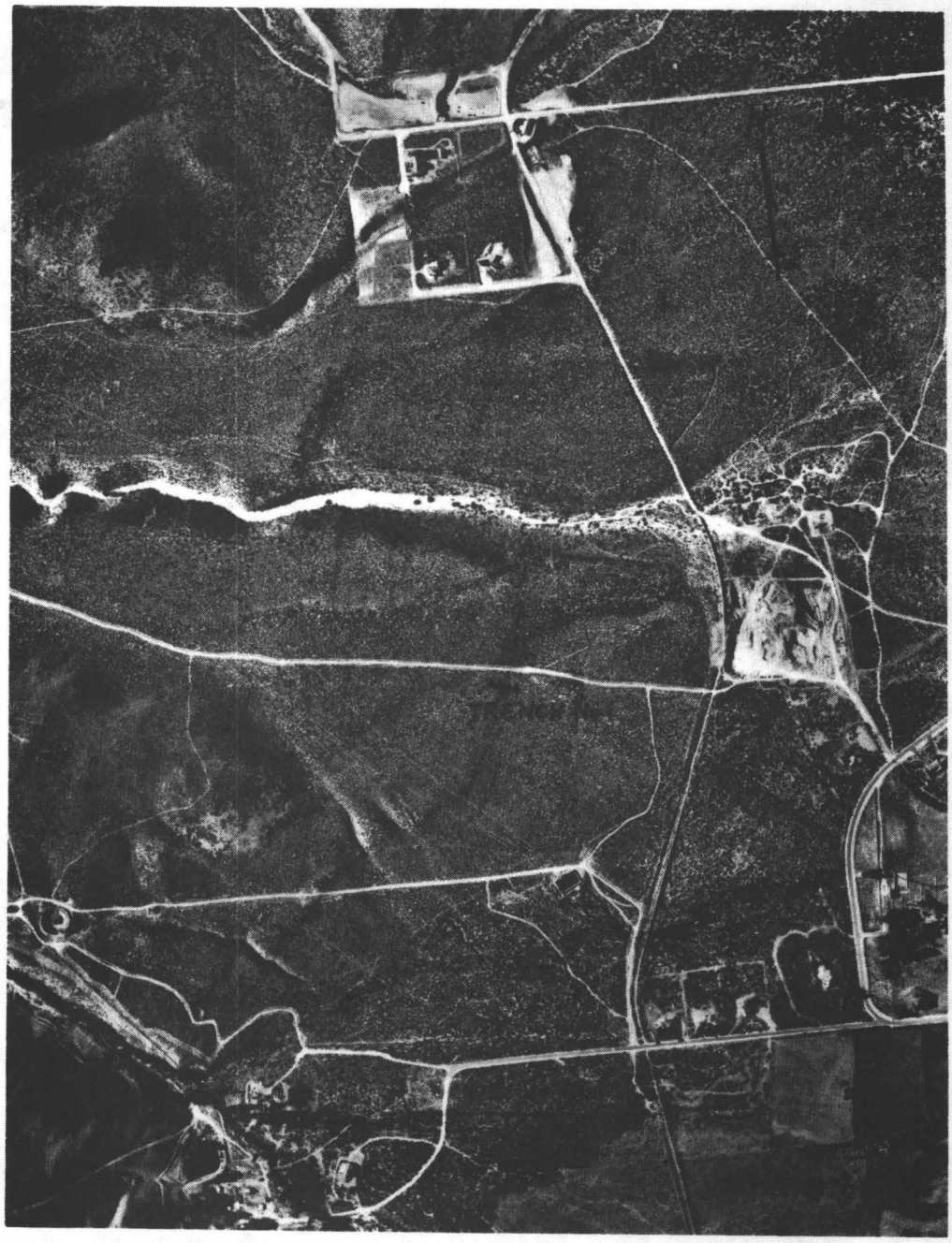

FIGURE 7. Low sun-angle photograph showing the location of Trench No. 1. For location in relation to faulting within the Carson City quadrangle, see figure 4.

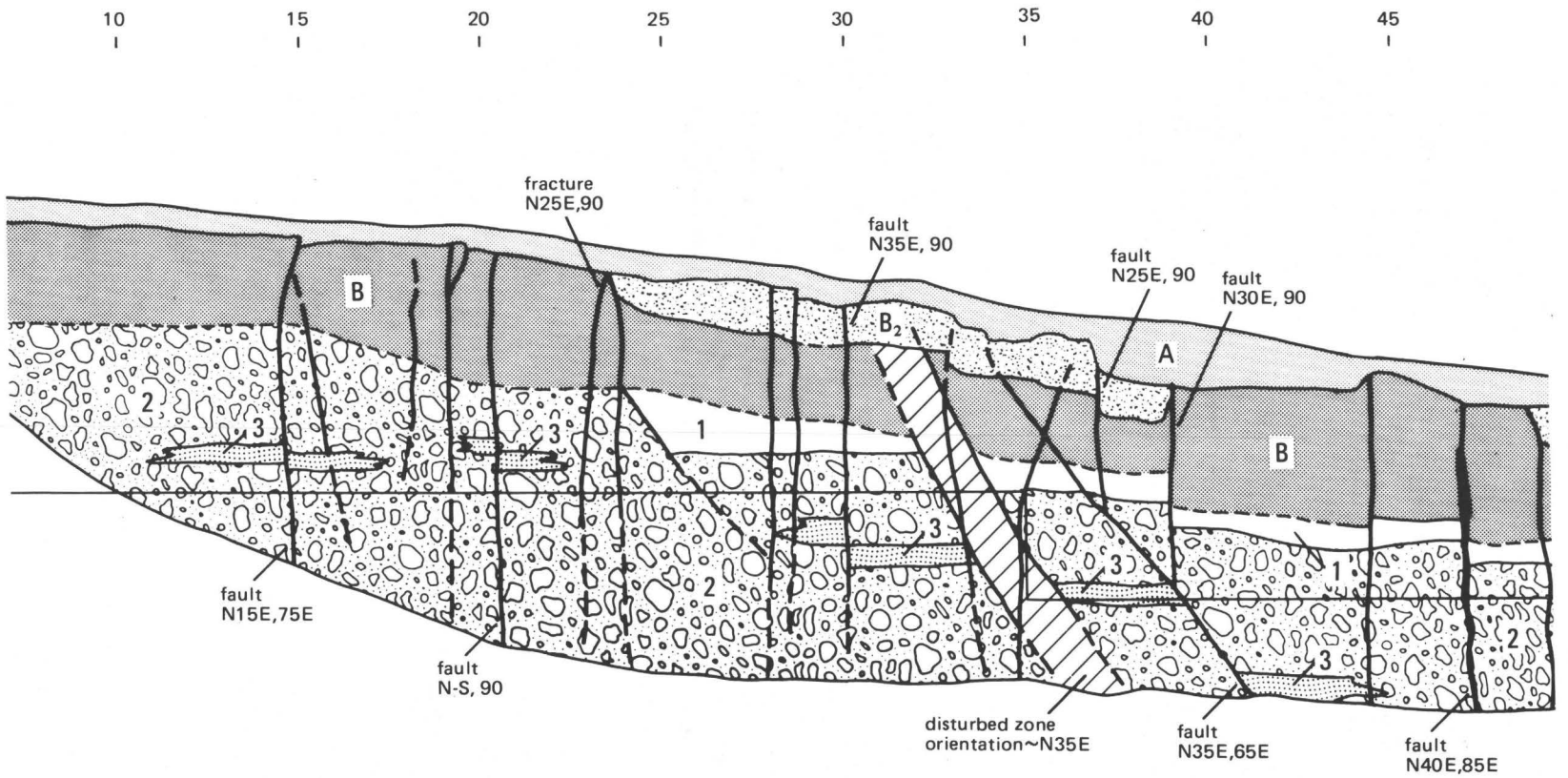

CARSON CITY TRENCH 1
NORTH WALL

N80W

VERTICAL SCALE: 1 inch = 5 feet

FIGURE 8. Portion of trench log for Trench No. 1 showing the complexity of faulting.

Sta. 30 and 40 trends N35E and dips moderately to the east. Most faults (those fractures along which movement can be substantiated) trend northeast (N25E to N40E); the predominant trends are N35E. Marker beds of clean sand (3) have been consistently offset with the east side down. A single bed of clean sand has been displaced a total of 1.7 m (5 ft) by 4 faults (including the east dipping disturbed zone). As shown in figure 8 the B soil horizon has been offset along numerous faults. In most cases small offsets at the base of the B horizon were the only indication of displacement. Open, root-filled fractures were also plotted, but adjacent horizons did not indicate displacement and they were considered to be dessication cracks.

The trenches provided information on the number of repeated movements that occurred along a particular fault and the complexity of the fault zone even though the surface manifestation indicates a single fault. The number of repeated movements is sometimes difficult to assess solely on surface morphology.

ACKNOWLEDGMENTS

The investigations described in this report were supported by several U. S. Geological Survey Earthquake Hazard Reduction Program Grants: No. 14-08-0001-G-78-73, "Earthquake hazards study in the Reno, Nevada area"; No. 14-08-0001-G-248, "Geologic mapping of the Carson City and New Empire quadrangles, Nevada"; No. 14-08-0001-G-358, "Computer-simulated earthquake hazard model for the Reno area";No. 14-08-0001-G-494, "Earthquake hazard maps for the Carson City, New Empire and South Lake Tahoe 7 1/2-minute quadrangles", Present studies include geologic mapping of the Vista and Steamboat 7 1/2-minute quadrangles under contract No. 14-08-0001-17774.

DISCUSSION

1. Question - Has the Mt. Rose Highway or any other roads in the Reno area been checked for cracks?

   Answer - To the best of my knowledge this type of investigation has not been performed in the Reno-Carson City area.

REFERENCES

Bingler, E. C. (1975) Guidebook to the Quaternary geology along the western flank of the Truckee Meadows, Washoe County, Nevada: Nevada Bur. Mines and Geology Rept. 22.

Bingler, E. C. (1977) Geologic map of the New Empire quadrangle, Nevada. Nevada Bur. Mines and Geology, Map 59.

Bingler, E. C. (1978) Abandonment of the name Hartford Hill Rhyolite Tuff and adoption of new formation names for middle Tertiary ash-flow tuffs in the Carson City-Silver City area, Nevada, U. S. Geol. Survey Bull. 1457-D.

Bolt, B. A. (1972) Seismicity: Proceedings of the International Conference on microzonation for safer construction, Research and Application, p. 13-23.

Bonham, H. F., Jr. (1969) Geology and mineral depoists of Washoe and Storey Counties, Nevada: Nevada Bur. Mines and Geology Bull. 70.

Borcherdt, R. D., Joyner, W. B., Warrick, R. E. and Gibbs, J. F. (1975) Response of local geologic units to ground shaking, in Borcherdt, R. D., ed., Studies for seismic zonation of the San Francisco Bay region: U. S. Geol. Survey Prof. Paper 941-A, p. A52-A67.

Bullen, K. E. (1963) An introduction to the theory of seismology: London, Cambridge Univ. Press., 381 p.

Callaghan, E., and Gianella, V. P. (1934) The earthquake of January 30, 1934, at Excelsior Mountains, Nevada: Bull. Seis. Soc. America, v. 25 (1935) p. 161-168.

Ekren, E. B., Bucknam, R. C., Carr, W. J., Dixon, G. L. and Quinlivan, W. D. (1976) East-trending structural lineaments in central Nevada: U. S. Geol. Survey Prof. Paper 986.

Jennings, C. W. (ed.) (1975) Fault map of California with locations of volcanoes, thermal springs and thermal wells: Cal. Div. Mines and Geology Geologic Data Map No. 1.

Lajoie, K. R. and Helley, E. J. (1975) Differentiation of sedimentary deposits for purposes of seismic zonation, in Borcherdt, R. D., ed., Studies for seismic zonation of San Francisco Bay Region: U. S. Geol. Survey Prof. Paper 941-A, p. A390A51.

Medvedev, S. V. (1965) Engineering Seismology: U. S. Department of Commerce, Nat. Tech. Info. Service, Rept. TT65-50011, 260 p.

Mooney, H. M. (1974) Seismic shear waves in engineering: Jour. Geotech. Engineering Div. ASCE v. 100 no. GT8, p. 905-923.

Moore, J. G. (1969) Geology and mineral deposits of Lyon, Douglas and Ormsby Counties, Nevada: Nevada Bur. Mines and Geology Bull. 75.

Power, J. H. and Real, C. R. (1976) Shear wave velocity, propagation and Measurement, California Geology, Feb. 1976.

Rogers, D. K. (1975a) Environmental geology of northern Carson City, Nevada: University of Nevada - Reno, M.S. Thesis, 34 p.

Rogers, D. K. (1975b) The Carson lineament: its influence on recent left-lateral faulting near Carson City, Nevada: (abs.) Geol. Soc. America Annual Mtg. Salt Lake City, Utah.

Shawe, D. R. (1965) Strike slip control of Basin and Range structure indicated by historical faults in western Nevada: Geol. Soc. America Bull., v. 76, p. 1361-1378.

Seed, H. B., and Schnabel, P. B. (1972) Soil and geologic effects on site response during earthquakes: Proceedings of the International Conference on microzonation for safer construction, Research and Application, p. 61-85.

Tabor, R. W., Ellen, S., Clark, M. M., Glancy, P. A. and Katzer, T. L. (in preparation) Environmental Folio Washoe City, Geologic Hazards Section.

Tabor, R. W., Ellen, S. and Clark, M. M. (1978) Geologic hazards map Washoe City, Environmental Folio, Nevada Bur. Mines and Geology.

Thompson, G. A. and Sandberg, C. H. (1958) Structural significance of gravity surveys in the Virginia City-Mt. Rose area, Nevada and California: Geol. Soc. America Bull., v. 69, no. 10, p. 1269-1282.

Trexler, D. T. (1977) Geologic map of the Carson City quadrangle, Nevada: Nevada Bur. Mines and Geology, Environmental Series.

Trexler, D. T., Bell, E. J. and Roquemore, G. R. (1978) Evaluation of lineament analysis as an exploration technique for geothermal energy, western and central Nevada; NVO/0671-2, N.T.I.S.

Trexler, D. T. and Bell, J. W. (1977) Computer-simulated composite earthquake hazard model for the Reno area, Final Tech. Report U. S. Geol. Survey Contract no. 14-08-0001-G-358.

Warrick, R. E. (1974) Seismic investigation of a San Francisco Bay mud site: Seis. Soc. America Bull., v. 64, p. 375-385.

Wright, Lauren, 1976, Late Cenozoic fault patterns and stress fields in the Great Basin and westward displacement of the Sierra Nevada block: Geology, v. 4, p. 489-494.

Prediction of Seismic Intensities on the Wasatch Fault

by Gary Clow and Jack Evernden
U.S. Geological Survey, Menlo Park

Introduction

A model has been developed to calculate seismic intensities for any earthquake in the conterminous United States. The model uses orientation of fault, length of break, a depth term, regional attenuation factor, and local geology to predict intensities at desired observation points. Comparisons of observational data and predictions are used to illustrate the success of the model in predicting earthquake parameters and intensities within the U.S.. Predicted intensities for fault breaks on the Wasatch Front are presented.

The Model

The model is the same as that used by Evernden (1975) and is described in Evernden, et al, 1980. Maximum ground accelerations are calculated from empirical expressions similar to those suggested by Kanai (1961). The model presently exists in two forms. The first is used for long curving fault breaks while the second is used for short straight breaks.

The starting point for both models is the seismic energy equation for Southern California:

$$E = 10^{11.8 + 1.5\, M_L} \qquad \text{(Richter, 1958)}$$

where M_L is the local southern California magnitude scale. In addition, an empirical relationship between M_L and length of break 2L appears to be valid for this region:

$$M_L = (3.2667 + \log 2L) / .711$$

Thus, seismic energy release can be expressed as a function of length of break for Southern California:

$$E = 10^{18.69 + 2.11\, (\log 2L)}$$

The approximate validity of this expression for the rest of the conterminous U.S. will be demonstrated through the use of the model.

In the first model form, a fault break is represented by a series of uniform point sources. Thus, strain energy is modeled as though stored in a set of N equally spaced points, each point having an increment of energy of

$$E_D = E/N$$

Maximum ground acceleration is calculated via the empirical formula:

$$a = A \left[E_D \sum_{i=n_1}^{n_2} (R_i + C)^{-k\gamma} \right]^{1/\gamma}$$

where:

R_i = distance from surface projection of source point i to the point of observation
C = pseudo-depth term
k = attenuation factor controlling the rate of die-off of acceleration ($a \propto \Delta^{-k}$)
γ = log [energy arriving at observation point]/a
i.e. a = [energy arriving at observation point]$^{1/\gamma}$
A = arbitrary leading coefficient
$1 \leq n_1 \leq n_2 \leq n$.

Only energies from those source points whose arrival times fall within a 10 second time window of that of the closest source point to the point of observation are allowed to contribute to maximum acceleration. A propagation velocity of 3.5 km/sec for the fault break and for shear waves is assumed.

The parameters k, γ , and A are set by calibrating the model with intensities from actual earthquakes. The attenuation factor k is regionally dependent and has been roughly determined within the conterminous U.S.(see Figure 1). For U.S. earthquakes, the depth term has negligible effect at distances greater than 60 kilometers from a fault-break. Thus, the spacing of isoseismals at distances greater than 100 km from known epicenters have been used to determine k. The best value of γ to use within the U.S. is about 4. The leading coefficient A is adjusted so that all predictions are for the ground condition of saturated alluvium. It has been calibrated by use of the data from the San Francisco 1906 earthquake. The pseudo-depth term C is used to regulate the peak intensities close to the fault break. Although C is related to depth of focus, it's exact value does not agree with the depths determined from travel-time analysis. A C value of 25 km usually gives the correct peak intensities for past California earthquakes while a value of 40 km is more appropriate for eastern U. S. earthquakes. Again, intensities at distances greater than 60 km are insensitive to C.

Rossi-Forel intensity is calculated from the equation:

$$I = 3 (\tfrac{1}{2} + \log a)$$

Corrections for local geology different from saturated alluvium are applied against this value. Conversion to the Modified Mercalli intensity scale can be done if desired (see Figure 2).

The second form of the model is identical to the first except that the discrete source points are replaced by a straight line source of length 2L. Energy per source point is replaced by energy per kilometer of break:

$$E_D = E/2L = \frac{10^{\,18.69 + 2.11\,(\log 2L)}}{2L}$$

Acceleration is calculated from

$$a = A\left[E_D \int_{L_1}^{L_2} \frac{dl}{(R^2 + C^2)^{4k/2}}\right]^{1/\gamma} \qquad -L \leq L_1 \leq L_2 \leq L$$

where use of the ten second time window places the limits on the integral, L_1 and L_2.

Computer Programs

The discrete source point model is presently programmed for use in western California (k = 1 3/4) and cannot be used directly outside a region of homogeneous k value. Predictions for a quake such as a Fort Tejon repeat presently require some level of hand calculation since regions of both k = 1½ and k = 1 3/4 will experience high intensities.

Geologic units with similar responses to high frequency seismic waves are grouped under a common ground condition unit. In this way, the surface geology for California has been digitized on a 6 minute X 6 minute grid into four ground condition units. In addition, the majority of the state has been digitized on a ½ minute X ½ minute grid into ten ground condition units. The entire U.S. has been digitized on a 25 km x 25 km grid into eight ground condition units. We assign an expected intensity to each ground condition relative to saturated alluvium, these assignments being based on empirical observations of ground motion. See Tables 1 and 2 for assignments of relative intensity vs geological unit. The program outputs a ground condition map, an intensity map in which the ground condition is assumed to be saturated alluvium, and an intensity map utilizing the digitizied ground conditions to correct for local geology. The user of the third map must be aware that the effects of thin alluvium surface layers, water table depth, and topographic focusing are not included in the present ground condition codification (although they could be in principle). Empirical data indicate that lowering of the water table by 10 meters decreases expected RF intensity by one unit. The line source model is programmed for use within the conterminous United States. Propagation of energy across zones of differing attenuation is allowed when this model is used. The same three maps are output as in the discrete source point program.

Analysis of Specific Events

As a test of the model, events with known parameters have been analyzed for consistency between observed and calculated parameters, and observed and predicted intensities. We include a few examples.

Monterey Bay Earthquake of 22 October 1926 (Rossi-Forel Intensities; Mitchell 1928)

Known Parameters:

1. k = 1 3/4 (western California)
2. C = 25 km (normal depth for California)
3. Location of fault break (from main epicenter and aftershock locations)
4. 2L = 20-40 km (aftershock zone 40 km long)

The epicenter for the Monterey Bay earthquake is well constrained to a location just offshore of Monterey. The aftershock zone, as determined from S-P times at Berkeley, extends from the epicenter of the main shock to the coastline west of Santa Cruz. The length of this zone is 40 kilometers. Intensities were predicted for fault breaks of 22 kilometers and 44 kilometers, both breaks extending northward from the main shock epicenter along the aftershock zone. Observed and predicted intensities are listed in Table 3. Stations are arranged with latitude increasing towards the bottom of the table. Note that the predicted intensities for both models agree well with observed intensities for stations to the south of the break. However, the predicted intensities for the 44km model are clearly too high to the east and north of the break while the 22km model gives reasonable agreement. The intensities listed in the table result from applying our digitized geology. In the present scheme, all Quaternary deposits are considered equivalent (i.e. thick water saturated sediments). Looking more closely at the geology of a few specific sites, it is found that Palo Alto circa 1926 was almost entirely on Older Bay Mud. This material is distinctly stronger than the younger Bay Mud for which the region is coded. Thus, predicted intensity should be dropped by ½ to 1 intensity units from those listed in the table. By 1926, the water table had been dropped to a depth of several tens of meters in the Santa Clara Valley. Thus, predicted intensities for San Jose and Morgan Hill should be dropped by at least one intensity unit. These changes would improve the agreement with observed intensities for the 2L = 22 km model. If the energy density is reduced below normal and a 44 kilometer break is used, intensities to the north are still too high. Our conclusion is that the high frequency source (i.e. those frequencies relevant to intensity calculations) for the main event was the southern half of the aftershock zone.

San Jose Earthquake of 1 July 1911
(Rossi-Forel Intensities
Templeton, 1911)

Known parameters:

1. k = 1 3/4 (western California)
2. C = 25 km (normal depth for California)
3. Location - Calaveras Fault (epicenter and aftershocks)
4. 2L = 5-11 km (aftershocks)

Wood (1911) located the epicenter and aftershock locations along a 12 km length of the Calaveras Fault. The ends of the zone were placed due south of Mt. Hamilton and due north of Gilroy. Fault breaks of 5½ kilometers and 11 kilometers were modeled, both extending northward from the southern most point of the aftershock zone. Both models give fair agreement with the observed values although the best 2L is probably closer to 5½ than 11 (see Table 4). Note that Templeton assigned San Francisco an intensity of VI-VII. This is inconsistent with the pattern established by the other observed values. A 75 km break would be required to give an intensity VII in San Francisco, a totally unacceptable value. In addition, in "Notes on California Earthquake of July 1, 1911" (BSSA 1, 110-121), it is stated "There was no damage of any consequence in San Francisco". "Few objects were overturned", etc. The assigned intensity is probably in error. Predicted values at Gilroy, Watsonville, and Santa Cruz are all a little high even for the shorter break. A saturated alluvium ground condition was assumed for these communities which may be somewhat inappropriate.

Fort Tejon Earthquake of 9 January 1857
(Modified Mercalli Intensities; Agnew and Sieh, 1978)

Known parameters:

1. k = 1 3/4 (region to be modeled is south and west of San Andreas Fault)
2. C = 25 km (normal depth for California)
3. Location of faulting - San Andreas Fault
4. 2L = 320 km (surface breakage - Cholame to Cajon Pass)

Thanks to Agnew and Sieh (1978), there is now available a compilation of numerous intensity observations for this earthquake. Table 5 lists observed and predicted intensities in Rossi-Forel units. Agreement between observation and prediction is excellent. Sacramento is in a location such that part of the propagation path is through a k=1½ region. With corrections for this mixed path, the predicted intensity agrees well with the observed value. Due to the high attenuation rates and remoteness of the San Andreas Fault from the heavily urbanized areas of southern California, a Fort Tejon repeat will not be a disaster of the magnitude sometimes cited. The San Fernando Valley will suffer less than it did from the 1971 San Fernando earthquake. Predicted intensities for San Fernando and Los Angeles assuming saturated alluvium ground condition are Rossi-Forel 8 and high 7 respectively. Since the water

table has been lowered to at least 10 meters below the surface, these predicted values should be reduced to 7 and high 6 respectively for a Fort Tejon repeat today.

Long Beach Earthquake of 10 March 1933
(Modified Mercalli Intensities; Neumann, 1935)

Known Parameters:

1. k = 1 3/4 (western California)
2. C = 25 km (normal depth for California)
3. Location of faulting - Newport-Inglewood Fault (from main epicenter and aftershocks)
4. 2L = 22-44 km (s-p times, aftershocks)

Benioff (1938) estimated 2L=27 kilometers from S-P times at southern California stations with the epicenter constrained to the Newport-Inglewood fault.

In addition to the mode of analysis used for the earthquakes described above, more refined techniques were used to estimate event parameters for this earthquake. Ignoring the effects of ground condition, a continuous range of ground accelerations, and thus intensities, should occur for any given earthquake. However, intensities are reported in discrete units. Thus intensities in the range or "band" 4.5 to 5.5 may be reported as V. Intensities in the range 3.5 to 5.5 may be reported as IV-V. Thus, the entire intensity spectrum may be considered to consist of a series of bands whose dimensions depend on the reporting units. Note that the intensity model predicts intensities in a continuous manner.

The first mode of residual analysis is to round the predicted intensites into the same discrete units in which the observations are made. Stations are grouped according to observed intensity. The number of stations with predicted intensities higher than observed intensity O_i is H_i while the number that is lower is L_i. Two residual parameters are calculated,

a) $\sum_{i=1}^{n} (H_i - L_i)$, called (H-L) in the tables

b) $\sum_{i=1}^{n} |H_i - L_i|$, called IH-LI in the tables

where n is the number of discrete observations used for the event. Parameter a) suffers from cancellation between observed intensity bands, thus allowing a family of extraneous solutions. Both parameters can be poor indicators in certain situations. Consider the hypothetical population of intensities (3.4, 4.4, 4.45, 5.3). This population would be observed as (3,4,4,5). A model with event parameters close to the real ones predicting intensities (3.6, 4.6,4.65, 5.5) would give a bad fit while the model predicting (2.6, 3.6, 3.65, 4.6) would give a perfect fit on the criteria of minimizing parameters a) and/or b). In most situations, station location will be such that a population such as the one above will not result.

The second mode of analysis is to maintain the continuous nature of the predicted intensities and assume that all the observed values from a given intensity band had the same non-rounded value before quantization. With good station coverage, the best assumed value for the "observed" intensities of a band is the mid-point for the band. However, if intensities are such that they didn't completely fill a band, it is difficult to determine what value to assign to the "observed" intensities. This is particularly true of the highest and lowest observed bands. The value for observed intensity assigned to the i th band is O_i while the predicted intensity for the j th station with observed intensity O_i is C_j. Two residual parameters are calculated,

$$c)\ \frac{1}{n} \sum_{i=1}^{m} \sum_{j=1}^{l} (O_i - C_j) \qquad \text{, called (O-C) in tables}$$

$$d)\ \frac{1}{n} \sum_{i=1}^{m} \sum_{j=1}^{l} |O_i - C_j| \qquad \text{, called |O-C| in tables}$$

where m is the number of intensity bands and l is the number of reporting stations with observed intensity O_i. Parameter c) suffers from cancellation between intensity bands as did parameter a). Even if the model parameters are chosen perfectly, a complete set of data exists, and there is no noise in the observed values, (O -C) values will have a range of values, usually -.5 to +.5 (Figure 10 shows an example of an (O-C) versus O plot for the Cache Valley Earthquake). Thus parameter d) will not minimize to zero. Perturbations of the model parameters from the best ones will change the range of (O-C) values somewhat but the result is a rather broad minimum. A wide range of solutions is usually allowed within the 95% confidence level.

The third mode of residual analysis attempts to preserve as much information from the calculated intensities as possible and yet leads to a parameter whose "best fit" value is zero. (O_i-C_j) values are regressed against O_i values to obtain a best least squares linear fit. The mean deviation of this regression line from the line $(O_i-C_j) = 0.0$ is calculated within the range of the observable intensity bands (e.g. 3.5-9.5 for this earthquake). This value is called "CP" in the tables. Minimizing CP minimizes (O_i-C_j) values in a way that utilizes the expected behavior of the residuals, and has zero as its best fit value.

In Tables 6 to 10, residual parameters are listed on a grid of 2L versus fault break location (S) relative to an arbitrary reference point on the Newport-Inglewood Fault. Tables 6 through 9 are for k = 1 3/4. All residual parameters are consistent with 2L = 22 kilometers and S = 8 km. (We had initially estimated 2L=22 km with the technique used on the Monterey Bay and San Jose earthquakes). This gives south and north termini of the break at 33° 40.1' N and 33° 49.2' N. respectively. These are to be compared with the reported epicenter at 33° 37' N with aftershocks from 33° 35-37' N to 33° 51-53' N. With the above "best" solution, there is a slight tendency for the (O_i-C_j) values for each intensity band to be dependent on O_i and thus distance. This indicates a slightly incorrect k value. The k value was changed to 1.825 and the analysis repeated. With this change, the correlation between the residuals and distance disappeared and the minimum CP value dropped from .110 to .079. The model parameters at this minimum are 2L = 34 and S = -4. The other residual parameters give minima consistent with this location. This fault break has south and north termini at 33° 39.3' N and 33° 53.4' N respectively. The k = 1.825 model is preferred to the k = 1.750 model due to the smaller CP minimum and better fit to the aftershock zone.

Lompoc Earthquake of 4 November 1972
(Rossi-Forel Intensities; Byerly, 1930)

Assumed parameters:

1. k = 1 3/4 (western California)
2. C = 25 km (normal depth)

Unkown parameters:

3. Location
4. 2L

Many different epicenters have been suggested for this earthquake. Byerly's (1930) epicenter is far offshore. Any combination of 2L and fault orientation through this epicenter badly matches the observed intensities. A 600 km break along the regional tectonic trend (parallel to the coastline) predicts intensities much too high in the Monterey region and much too low in the Point Arguello area. If the break is oriented east-west with the east end within 5 kilometers of Point Arguello (no onshore faulting was observed for this event), inland intensities fall short of those observed (see figure 4).

T. Hanks (1978) calculated the epicenter using S and P data from southern California stations. Although this epicenter is closer to shore than Byerly's, the same problems befall it (see figure 5).

W. Gawthrop (1978) suggested that the break occurred on the Hosgri Fault. We used the Hosgri Fault as a reference and repeatedly used our model, allowing the break to migrate both along the fault and along a line perpendicular to it, changing length of break while maintaining the same azimuthal orientation (figure 6). A minimum against the CP parameter was sought, while imposing the geologic constraints of not allowing the break to migrate onshore or into the Santa Barbara Channel.

Attenuations of 1.75 and 1.675 were modeled (see tables 11-13). The best solution for k = 1.75 is an 80 km break on the Hosgri Fault with southern terminus just north of Point Arguello. The best solution for k = 1.675 is a 60 km break on the Hosgri with the southern terminus near Point Arguello. Shorter fault breaks give minima onshore while larger breaks have significantly larger minimum values, indicating poor fits to the observed data. Fault breaks even 10 kilometers seaward of the Hosgri Fault are dismissed at the 95% confidence level (i.e. CP values increase by more than 2 s.d. of CP value at its minimum). We conclude that the Lompoc Earthquake occurred on the Hosgri Fault with southern terminus of the break north of Point Arguello although we are unable to distinguish between the best k = 1.675 model and the best k = 1.750 model.

Cache Valley Earthquake of 30 August 1962
Modified Mercalli Intensities
U.S. Earthquakes 1962, USCGS

Assumed Parameters:

1. k = 1½
2. C = 25 km
3. Location- USCGS epicenter

Unknown Parameter:

4. 2L

Ninety-four observations from Utah and southern Idaho are used in this analysis. Each observation is adjusted to what would be expected if saturated alluvium were present at the site (I_o). Water table depth is assumed to be at least 10 meters at most sites lying on recent alluvium. Thus for these sites that were observed at I(MM) = IV (i.e. $3.5 < I(MM) \leq 4.5$), the observations are adjusted to $I_o = 4.8$. One rossi-forel unit is equivalent to .8 modified mercalli units at I(MM) = IV. The other observations are treated similarly.

Figure 7 shows a plot of the percentage of observations within a given distance of the epicenter. Good station coverage exists from 17 km to 260 km. Changes in slope at 17, 40, and 80 km indicate relatively fewer observations in the ranges 0-17 km and 40-80 km. The $I_o = 5.9$ curve of figure 8 shows the 80 km slope change quite well. Figure 8 is a plot of the distance distributions for each of the primary observational groups. From these distributions, the distance at which 50% of the observations are nearer to the epicenter for each observational group can be found. After renormalizing the $I_o = 5.9$ and $I_o = 7.0$ curves for the relative depletion of data in the 40-80 km range, these distances are 10, 40, 90, 170 km for the $I_o = 8.0, 7.0, 5.9, 4.8$ groups respectively. These values are plotted against model predictions in figure 9. A five or six kilometer fault break is suggested by the model. Note that model predictions in this figure are appropriate for a saturated alluvium ground condition. Thus, the predicted maximum intensity I(MM) = 8.4 should be reduced to I(MM) = 7.4 since the water table presumably was not at the surface at the epicenter. Indeed, the maximum

intensity observed for this event is I(MM) = VII. According to the 2L = 6 km model, the I_o = 4.8 group should be observed out to 240 km. Thus, the cutoff in data at 260 km does not represent a significant cropping of data from this group. Similarly, the model predicts that the I_o = 7.0 group should be observed to within 28 km of the epicenter. The relative depletion of data in the 0-17 range does not represent a loss of information for this group.

Figure 10 is a plot of (observed intensity-calculated intensity) versus observed intensity for the 2L = 6 km model. Triangles indicate the group means. Group means all lie close to the zero residual line, indicating that the model parameters are providing a good fit. One interesting aspect of this plot is the large amount of scatter in each group. This scatter is greater than is typical for Californian earthquakes. Perfect data combined with a perfect model would give a maximum scatter of .5 units from the group means.

We conclude that the length of break for this event was 5-6 km. The assumed attenuation factor and depth term are consistent with the observations.

Hansel Valley Earthquake of 12 March 1934
Modified Mercalli Intensities
U.S. Earthquakes, USCGS

Assumed Parameters:

1. k = 1½
2. C = 25 km
3. Location- University of Utah epicenter

Unknown Parameter:

4. 2L

The distance distribution for the observations (figure 11) shows only one major change in slope for this event. This slope change occurs at 50 km. Good coverage exists for the range 50-270 km. Figure 12 shows the station distributions for the primary observational groups. The distributions indicate a strong mix of observations from the I_o = 4.8, 5.9, and 7.0 groups for the distance range 50-80 km. The I_o = 7.0 distribution is suspect due to cropping caused by a complete lack of data in the range 33-47 km (see figure 11). The estimated distances for which 50% of the observations are nearer to the epicenter are 23, 100, 180 km for the I_o = 8.0, 5.9, 4.8 groups respectively (after smoothing the distributions somewhat). These distances are plotted against model predictions in figure 13. The values agree well with a model with parameters 2L = 8km, C = 25 km, and k = 1½. Figure 14 is a residual plot for this event using the above model parameters. Note that the mean for the I_o = 7.0 group deviates from the zero residual line by .72 units. The 2L = 8 km model indicates that the data gap from 33 to 47 km would cause a total lack of data for the upper half of the I_o = 7.0 group. This is consistent with the lack of negative residuals for this group. I_o = 4.8 observations in the 50-80 km range cause the mean for

this group to be depressed to -.34. The complete mixing of I_o = 4.8, 5.9, and 7.0 observations in the 50-80 km range is unexplainable with this model as it is presently used.

We conclude that the length of break for this event is about 8 km. The assumed attenuation and depth term are consistent with the distance distributions outside the 50-80 km range.

Model Parameters Throughout the Conterminous U.S.

The model has been used to determine lengths of break for earthquakes throughout the conterminous U.S.. It is important to understand how these lengths are determined. Given the appropriate k value for a region, the intensity data for an earthquake are used to calculate the energy required at the focus to create the observed pattern of intensities. The length of break 2L required in the k = 1 3/4 region (the region of calibration between 2L and energy) to supply the calculated energy requirements is then found. Calculated 2L values for each attenuation region are compared with 2L values established by other means (surface breakage or analysis of seismograms) in the hope of finding scaling laws between the calculated and observed 2L values. In the k = 1 3/4 region, calculated and observed 2L's nearly agree, as they should since this is the region of calibration. Table 14 lists observed lengths of break and lengths determined by the above procedure for earthquakes in the k = 1½ region. The 2L values calculated as described above agree well with the observed 2L values in the k = 1½ region. (possible reasons for the poor agreement of two of the smaller events are discussed in Evernden, et al. 1980). This shows that a single relationship between seismic energy in the intensity pertinent frequency domain and length of break is valid for both regions.

In addition, event parameters have been determined for earthquakes in the eastern U.S.. The model is able to match the observed intensity patterns quite well. The best C value for these quakes is usually 40 kilometers, implying a slightly deeper depth of focus than for normal California earthquakes. In support of the k values shown on Figure 1, we note that Milne and Davenport (1969) found an attenuation value of k = 1.0 for much of the northeastern U.S.. Also, Peter Basham of the Dominion Observatory, Ottawa, Canada has indicated (personal communication) that the group at the observatory have confirmed the existence of the k = 1½ zone along the St. Lawrence River. For most eastern U.S. earthquakes, we do not have observed 2L values with which to compare 2L values determined from the model due to the lack of surface breakage and infrequency of events with both substantial intensity data and short period data. Due to the low attenuation rates, very short breaks adequately provide the energy to produce the observed intensities for this region.

We do have some data on one large eastern U.S. quake, these data being consistent with our calculated 2L and location. The 20 kilometer 2L calculated for the 1886 Charleston earthquake agrees well with the dimensions of the high intensity isoseismal for that quake. In addition, locations of presently occurring small earthquakes in the Charleston area cluster along a 20 kilometer zone within the same high intensity

contour (Tarr, 1979). Finally, master-event locations by J. Dewey (personal communication) of all instrumentably locatable earthquakes in the Charleston area are along this same 20 kilometer zone. Earthquakes originally placed off-shore have been shown by Dewey to have occurred along this zone. Thus, all seismic activity for the past several decades has occurred along a seismic zone that agrees in length and location with our estimates of the fault break for the 1886 Charleston earthquake.

There are no other earthquakes in the eastern United States for which demonstrations of length of break exist. The best data we have are the observations by Frank McKeown (personal communication) that there are no fault segments longer than a few kilometers in the exposed fracture zone along which the New Madrid earthquake occurred (k = 1 region). The 2L value calculated for this earthquake is 2½ - 5 kilometers (k = 1), in essential agreement with the characteristics of the fracture zone. We conclude that a single relationship between seismic energy in the high frequency domain and length of break is valid for the entire conterminous United States.

Predicted Intensities for Fault Breaks on the Wasatch Fault

The previous sections have been intended to serve as documentation of the validity of the techniques we use. Lengths of break are correctly predicted from isoseismal data over a wide range of event 'sizes'. In general, intensity patterns are correctly predicted given earthquake source parameters. The Cache Valley and Hansel Valley earthquakes in particular can be used to calibrate the model for events in Utah. An attenuation factor k = 1½ was found appropriate for those events. A depth term value C = 25 has been found appropriate for normal depth (15 km) earthquakes in California. Although most earthquakes occur at a depth of about 7 km in Utah, a depth term value c = 25 provides the best fit for the Cache Valley and Hansel Valley earthquakes. However, major earthquakes occuring at shallower depths can not be ruled out. Figures 15 and 16 give predicted intensities on recent alluvium with a water table depth of at least 10 meters. C values of 20 and 25 are used. It must be realized that the model predictions indicate the most probable intensity to occur at any given site. The large amount of scatter in observed intensities at fixed epicentral distances for the Cache Valley and Hansel Valley earthquakes will presumably occur for future events in this region. More realistic damage estimates might be obtained by convolving a 'scatter function' with present model predictions.

REFERENCES

Agnew, A. C., and K. E. Sieh, 1978, A documentary study of the felt effects of the great California earthquake of 1857, Seismol. Soc. America Bull., v. 68, p. 1717-1729.

Benioff, N., 1938, The determination of the extent of faulting with application to the Long Beach earthquake, Seismol. Soc. America Bull., v. 28, 77-84.

Borcherdt, R. D., 1970, Effects of local geology on ground motion near San Francisco Bay, Seismol. Soc. America Bull., v. 60, 29-61.

Byerly, P., 1930, The California earthquake of November 4, 1927, Seismol. Soc. America Bull., v. 20, p. 53-56.

Evernden, J. F., 1975. Seismic intensities, "size" of earthquakes, and related phenomena, Seismol. Soc. America Bull., v. 65, 1287-1315.

Evernden, J. F., 1980. et. al., in press

Gawthrop, W., 1978, The 1927 Lompoc, California earthquake, Seismol., Soc. America Bull. 68, p. 1705-1716.

Hanks, T. C., 1978, in press.

Kanai, K., 1961. An empirical formula for the spectrum of strong earthquake motions, Bull. Earthquake Res. Inst., Tokyo Univ. 39, 85-95.

Lander, J., 1964, United States Earthquakes - 1962, USCGS, Washington, D.C.

Milne and Davenport, 1969

Mitchell, G. D., 1928, The Santa Cruz earthquakes of October, 1926, Seismol. Soc. America Bull., v. 18, p. 152-213.

Neumann, F., 1935, United States Earthquakes - 1933, USCGS, Ser. 579, Washington, D. C.

Neumann, F., 1936, United States Earthquakes - 1934, USCGS, Ser. 593, Washington, D.C.

Tarr, A., 1978, personal communication, unpublished map.

Templeton, E. C., 1911, The central California earthquake of July 1, 1911, Seismol. Soc. America Bull., v. 1, p. 167-169.

Figure 1

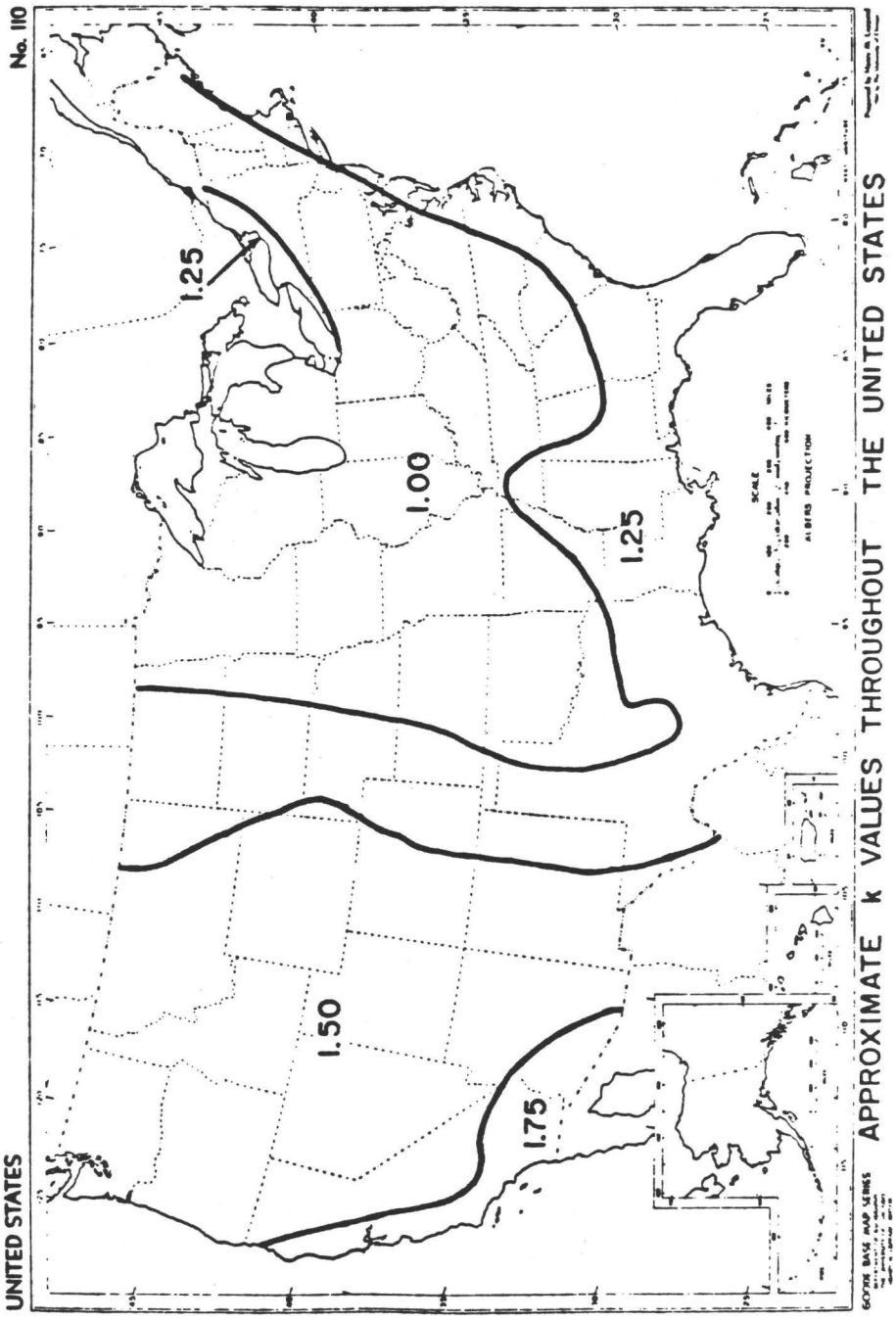
No. 110
UNITED STATES
1.25
1.00
1.25
1.50
1.75
APPROXIMATE k VALUES THROUGHOUT THE UNITED STATES

Figure 2

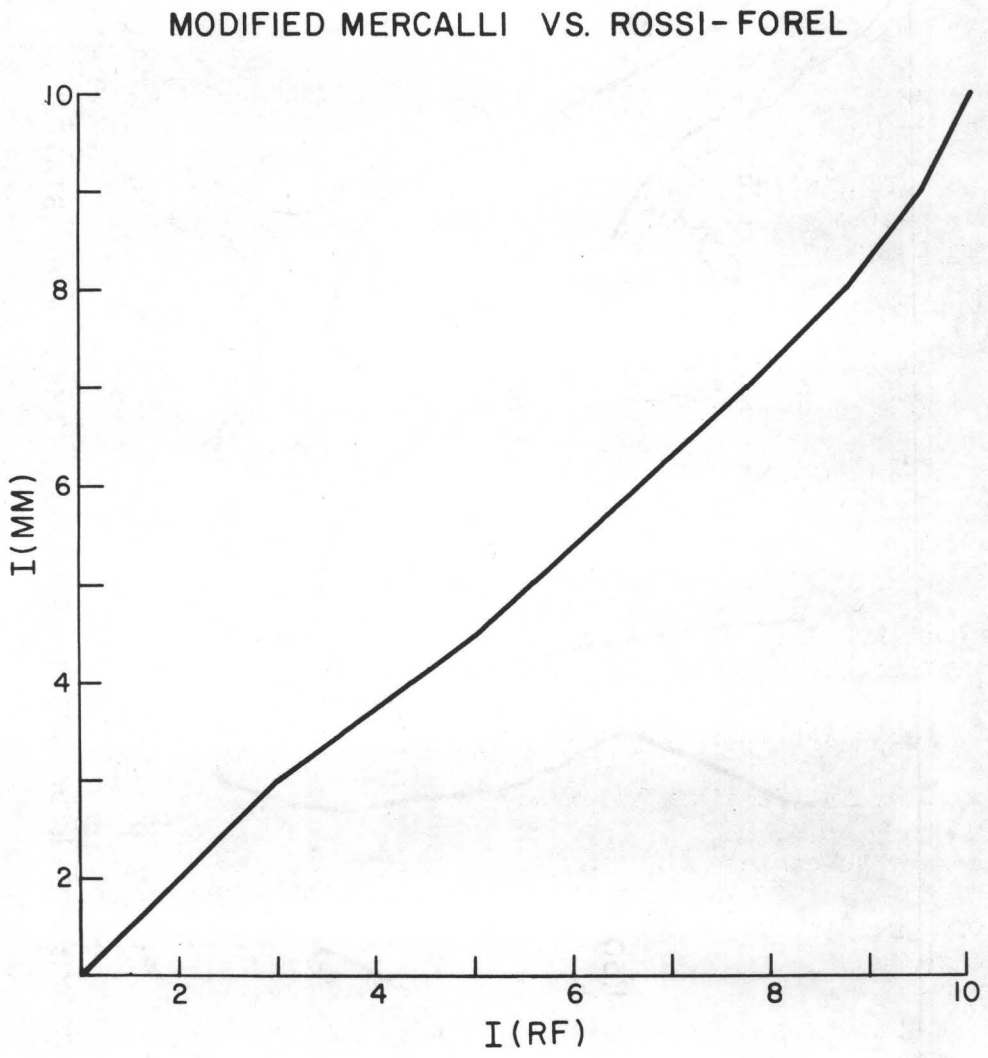

Table 1

Correlation of Geological and Ground Condition Units-California

(Source: State Geological Maps - 1/250,000)

1/2 minute x 1/2 minute Grid

Units of Geological Maps	Ground Condition Unit
Kjfv, gr, bi, ub, JT_{RV}, m, mV, PpV, PmV, Cv, Dv, pS, pSv, pCc, pCgr, pC, epC, Ti (granitic and metamorphic)	A
Ms, PP, Pm, C, CP, CM, D, S, pSs, O, E (Paleozoic Sedimentary)	B
Jk, Ju, JmE, Tr, Kjf (E. Mesozoic Sedimentary)	C
Ec, E, Epc, Ep, K, Ku, KE (Cretaceous through Eocene Sedimentary)	D
QTc, Tc, TE, Tm (undivided Tertiary Sedimentary)	E
PmEc, PmE, Mc, Muc, Mu, Mmc, Mm, ME, Øe, Ø (Oligocene through Middle Pliocene Sedimentary)	F
Qc, QP, Pc, Puc, Pu (Plio-Pleistocene Sedimentary)	G
Pv, Mv, Olv, Ev, QTv, Tv (Tertiary Volcanic)	H
Qrv, Qpv (Quaternary Volcanic)	I
Qs, QaE, Qsc, Qf, Qb, Qst, QE, Qq, Qt, Qm (Quaternary Sediments)	J

Table 1a

Correlation of Ground Condition Units of California

and Assigned Relative Intensity Values

(a)

1/2 minute x 1/2 minute Grid

Ground Condition Unit	Relative Intensity
A	-3.0
B	-2.6
C	-2.2
D	-1.8
E	-1.7
F	-1.5
G	-1.0
H	-2.7
I	-2.7
J	0.

(b)

6 minute x 6 minute Grid

	Ground Condition Unit	Relative Intensity
A.	Granite, etc.	-2.50
B.	Coast Ranges, etc.	-1.75
C.	Coastal marine sedimentary rocks	-0.80
D.	Alluvium	0

Table 2

Correlation of Geological and Ground Condition Units - USA

(Source: National Atlas of the United States)

Units of Geological Map	Ground Condition Unit
Sedimentary Rocks	
Quaternary	A
Upper Tertiary	B
Lower Tertiary	C
Cretaceous	D
Jurassic and Triassic	E
Upper Paleozoic	F
Middle Paleozoic	G
Lower Paleozoic	H
Younger Pre-Cambrian	I
Older Pre-Cambrian	J
Volcanic Rocks	
Quaternary and Tertiary Volcanic Rocks	K
Intrusive Rocks	
All Ages	L

Correlation of Ground Condition Units of USA and

Assigned Relative Intensity Values

Ground Condition Units	Relative Intensity
A	0
B	-1.00
C	-1.50
D	-2.00
E	-2.25
F	-2.50
G	-2.75
H	-2.75
I	-2.75
J	-3.00
K	-3.00
L	-3.00

Figure 3

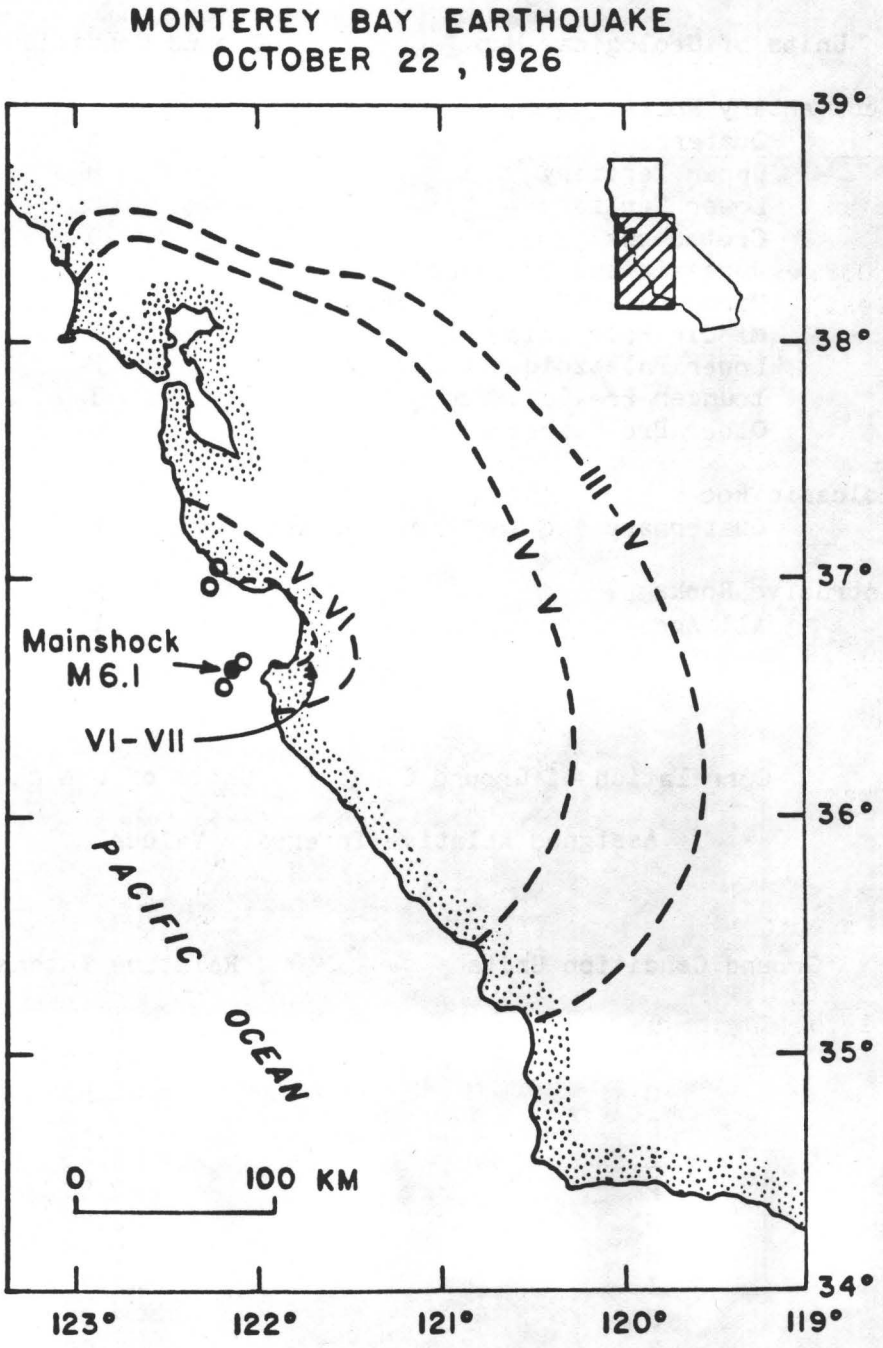
MONTEREY BAY EARTHQUAKE
OCTOBER 22 , 1926
39°
38°
37°
36°
35°
34°
123°
122°
121°
120°
119°
III-IV
IV-V
V-VI
Mainshock
M 6.1
VI-VII
PACIFIC
OCEAN
0
100 KM

Table 3

Observed and Predicted R/F Intensity Values - Monterey Bay Earthquake

Site	Observed Intensity	Predicted Intensity	
		2L=22	2L=44
Santa Maria	III	3-4	4
Lompoc	II-III	3	3
San Luis Obispo	IV	3	3
Paso Robles	IV-V	4	5
King City	V-VI	5-6	6
Carmel	VI	6	6
Monterey	VI+	6-7	6-8
Salinas	VI-VII	7	8
Hollister	IV-V	6	7
Watsonville	V-VI	7	8
Soquel	VI-VII	7	8
Santa Cruz	VII+	7-8	8
Saratoga	V	5	7
San Jose	V	6	7
Morgan Hill	V	6	6
Palo Alto	V	6	7
San Leandro	V	5	5
Berkeley	V	5	6
Walnut Creek	V	4-5	5
Novato	V	5	5
Petaluma	V	4-5	4-5
Santa Rosa	IV	4	5
Martinez-Concord	V/IV-V	5	5
Stockton	IV-V	5	5
Merced	IV	4+	5
San Francisco (downtown)		5	5

Table 4

Observed and Predicted R/F Intensities - San Jose Earthquake

Site	Observed Intensity	Predicted Intensity	
		2L=5½	2L=11
Modesto	4	5	6
Sacramento	4	4	4
Santa Rosa	4	3-4	4
Monterey	4	3-5	3-5
Berkeley	5	5	5
Hayward	5	5	5-6
Stockton	5	5	5
Watsonville	5	6-7(Al)[1]	7(Al)
Santa Cruz	6	6-7(Al)	7-8(Al)
Belmont	5	5	6
Pleasanton	5-6	5	5
Livermore	5	5	5-6
Oakland	6	5	5-6
Redwood City	6	5	6
Palo Alto	6	6	6
Calaveras Valley	6	6	6
San Martin	6	6	7
Gilroy	6	7-8(Al)	8
Boulder Creek	6	5-6	6
Pescadero	6-7	5	6
San Francisco	6-7	5(Al)	5(Al)
Morgan Hill	7	7	8
Los Gatos	7	7	7
Saratoga	7	6-7	7
Santa Clara	7	6-7	7
San Jose	7	7	7
Coyote	8+	8	8

1. (Al) signifies that predicted intensity values entered in table are based on satuarated alluvium. Discussion of the discrepancies between observation and prediction for these stations is included in the text.

Table 5

Observed and Predicted R/F Intensities - Fort Tejon Earthquake

Site	Observed Intensity	Predicted Intensity
San Diego	V-VI	5
San Bernardino	VII-VIII	8
San Gabriel Valley	VIII	8
Los Angeles (downtown)	VII+	7(high)
San Fernando Valley	VIII-	8
34.6°N 117.4°W	VIII-	8
34.1°N 119.0°W	VIII-	7
Ventura	VIII+	8
Santa Barbara	VII	7
San Andreas Fault	≥IX	≥9
Fort Tejon	VIII-IX	9
34.0°N 118.7°W	VIII+	9
35.4°N 119.0°W	VIII+	8
35.9°N 119.3°W	VI-VII	7
36.2°N 119.3°W	VII+	7
Visalia	VI-VII	6
36.7°N 121.3°W	VII	6
Monterey	IV-V+	4-6
Santa Cruz	III-V+	3-5
San Francisco	V+	4
Stockton	IV	5
Sacramento	V+	4 (all path k=1 3/4 5-6 (part of path k=1 1/2)

Table 6

Earthquake: Long Beach

Reference Fault: Inglewood-Newport Reference Coords: 33°48.0' N 118° 10.7' W

k = 1.750 T = 0 C = 25

Bands Used: VIII, VII, VI, V, IV, III

Upper Values: (H - L) Lower Values: |H - L|

S \ 2L	12	16	20	24	28	32
8	-14 16	-7 17	-1 17	2 16	6 16	9 19
4	-16 16	-7 17	-1 13	3 15	7 17	10 16
0	-20 20	-8 16	-1 13	3 16	7 15	10 15
-4	-22 22	-11 15	-2 14	4 14	9 11	13 13
-8	-21 21	-14 18	-6 16	2 12	8 10	12 12
-12	-22 22	-15 19	-11 15	-2 12	6 10	11 11
-16	-22 24	-15 17	-12 16	-7 15	1 13	7 13

2L = 22, S = -8: (H - L) = 0, H - L = 12

Table 7

Earthquake: Long Beach

Reference Fault: Inglewood-Newport **Reference Coords:** 33°48.0' N 118° 10.7' W

$k = 1.750$ $T = 0$ $C = 25$

Bands Used: VIII, VII, VI, V, IV, III

Upper Values: (O - C) **Lower Values:** $s.d._{(O - C)}$

S \ 2L	12	16	20	24	28	32
8	.402	.209	.067 (.100)	-.068	-.176	-.275
4	.400	.206	.062 (.092)	-.073 (.092)	-.178	-.276
0	.410	.216	.069 (.085)	-.066 (.085)	-.173	-.272
-4	.432	.238	.090 (.080)	-.047 (.080)	-.154	-.253
-8	.468	.272	.124 (.076)	-.015 (.077)	-.127	-.225
-12	.512	.316	.167	.028	-.087	-.187
-16	.565	.370	.219	.079	-.033	-.139

$2L = 23$, $S = -8$: $(O - C) = 0$, $s.d._{(O - C)} = .076$

Table 8

Earthquake: Long Beach

Reference Fault: Inglewood-Newport Reference Coords: 33°48.0' N 118° 10.7' W

k = 1.750 T = 0 C = 25

Bands Used: VIII, VII, VI, V, IV, III

Upper Values: $|O - C|$ Lower Values: s.d.$_{|O - C|}$

S \ 2L	12	16	20	24	28	32
8	.644	.578	.549	.537	.547	.574
4	.602	.542	.513	.503	.512	.536
0	.570	.509	.483	.472	.481	.505
-4	.550	.478	.456	.452	.455	.473
-8	.549	.463	.432	.430	.442	.460
-12	.566	.462	.422 (.048)	.415 (.043)	.435	.459
-16	.609	.483	.433	.417	.428	.461

2L = 22, S = -12: $O - C = .412$, s.d.$_{O - C} = .041$

Table 9

Earthquake: Long Beach

Reference Fault: Inglewood-Newport Reference Coords: 33°48.0' N 118° 10.7' W

k = 1.750 T = 0 C = 25

Bands Used: VIII, VII, VI, V, IV, III

Upper Values: CP Lower Values: s.d.$_{CP}$

S \ 2L	12	16	20	24	28	32
8	.292	.180 (.041)	.154 (.013)	.191 (.048)	.264	.355
4	.298	.163 (.046)	.130 (.012)	.167 (.052)	.252	.343
0	.317	.161 (.051)	.118 (.013)	.148 (.049)	.237	.329
-4	.340	.173	.114 (.017)	.130	.216	.308
-8	.373	.197	.121	.124	.191	.283
-12	.405	.228	.145	.126	.170	.256
-16	.439	.267	.180	.149	.167	.226

2L = 22, S = -4: CP = .110, s.d.$_{CP}$ = .013

Table 10

Earthquake: Long Beach

Reference Fault: Long Beach Reference Center: 33°48.0'N 118°10.7'W

k = 1.825 T = 0 C = 25

Bands Used: VIII, VII, VI, V, IV, III

Upper Values: CP Lower Values: $s.d._{CP}$

2L / S	20	24	28	32	36	40
8	.312	.214	163	143	147	175
4	.327	.200	.124	.093 (.020)	.104	.156
0	.345	.217	.124	.085 (.031)	.091 (.024)	.146
-4	.370	.240	.139	.085 (.024)	.083 (.016)	.130
-8	.399	.268	.162	.099 (.039)	.086 (.010)	.118 (.044)
-12	.430	.299	.192	.125 (.042)	.099 (.016)	.115 (.026)

2L = 34, S = -4: CP = .079, $s.d._{CP}$ = .012

LOMPOC EARTHQUAKE
NOVEMBER 4 , 1927

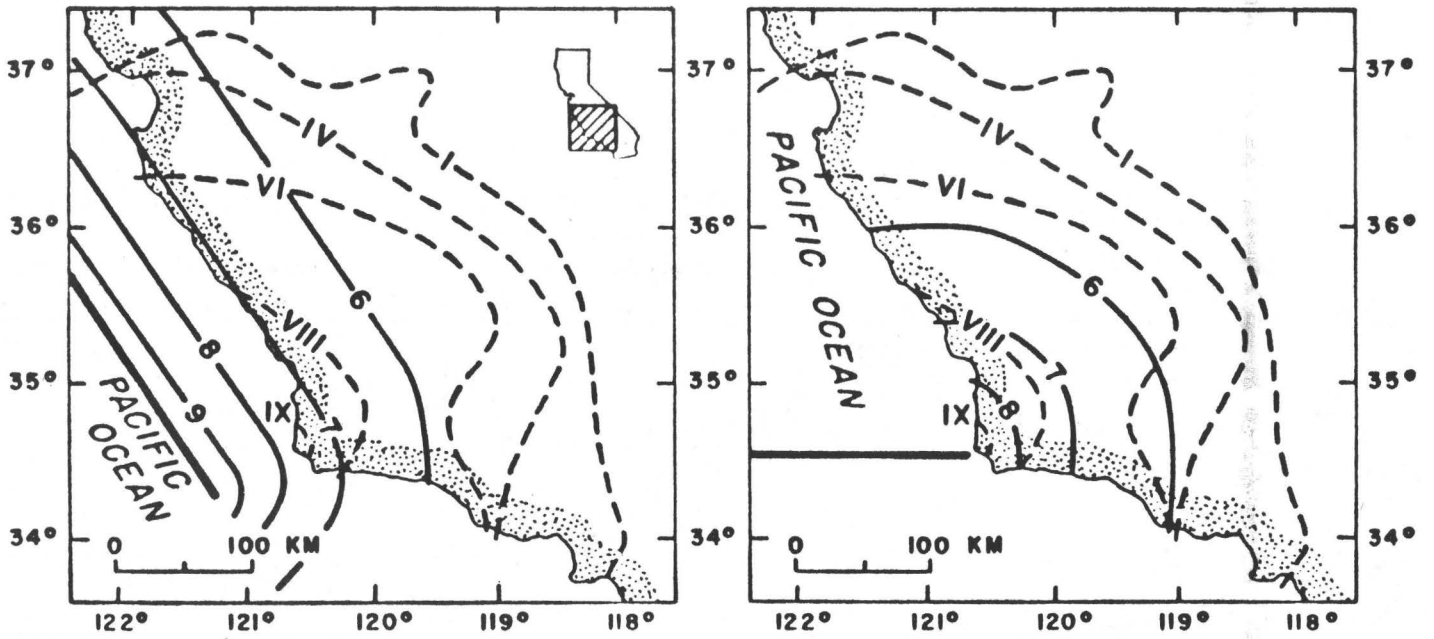

2L = 600 KM , C = 25 , k = 1.75

Byerly's epicenter

Strike of fault : Parallel to regional structure

2L = 600 KM , C = 25 , k = 1.75

Byerly's epicenter

Strike of fault : East – West , East end of break very near shore

Figure 4

Figure 5

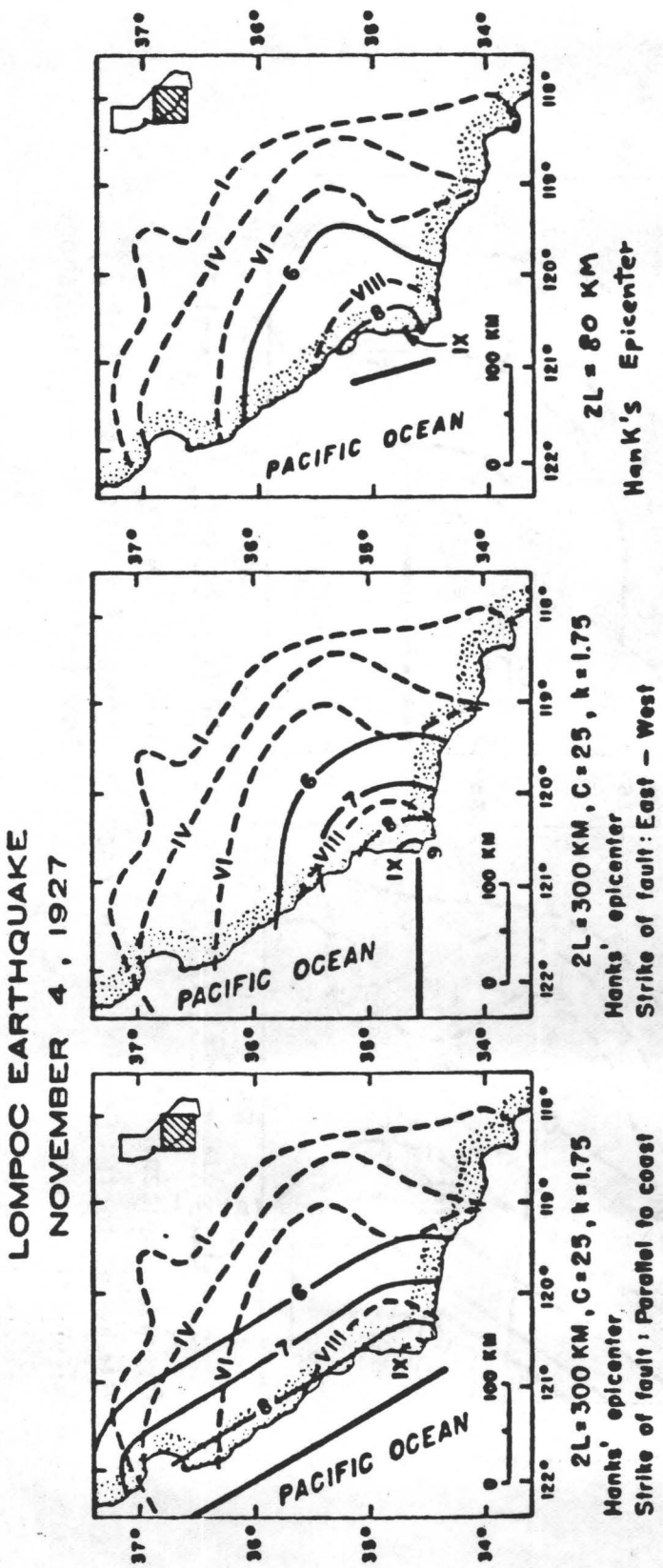
LOMPOC EARTHQUAKE
NOVEMBER 4, 1927
PACIFIC OCEAN
2L = 300 KM, C = 25, k = 1.75
Hanks' epicenter
Strike of fault: Parallel to coast
2L = 300 KM, C = 25, k = 1.75
Hanks' epicenter
Strike of fault: East – West
2L = 80 KM
Hank's Epicenter
100 KM

Figure 6

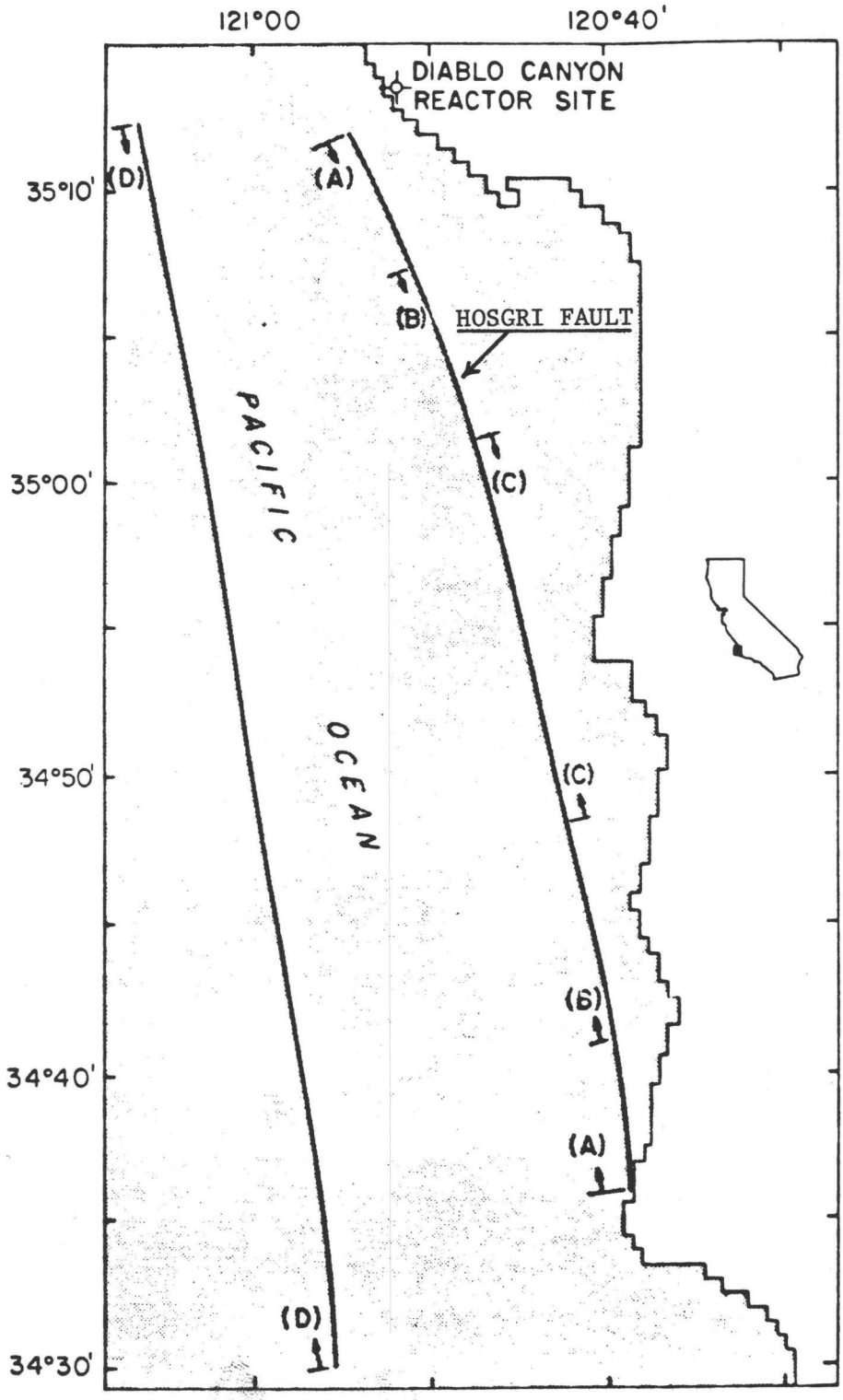
121°00
120°40'
DIABLO CANYON
REACTOR SITE
35°10'
35°00'
34°50'
34°40'
34°30'
(A)
(B)
(C)
(D)
HOSGRI FAULT
PACIFIC
OCEAN

Table 11

Earthquake: Lompoc

Reference fault: Hosgri Reference Center: 34°55.0'N 120°44.3'W

k = 1.750 2L = 80 C = 25

Bands Used: IX, VIII, VII-VI, V-IV (MODIFIED)

Upper Values: CP Lower Values: $s.d._{CP}$

S \ T	-30	-20	-10	0	10	20	30
30	.791	-	.379 (.069)	.211 (.043)	.153 (.020)	.212 (.068)	
20	.744	-	.298 (.074)	.113 (.035)	.137 (.107)	.251	
10	.725	-	.256 (.090)	.043 (.036)	.173 (.102)	.290 (.107)	
0	.733	-	.261	.026 (.099)	.173 (.103)	.294 (.108)	
-10	.763	-	.297	.063 (.103)	.138 (.094)	.263 (.112)	
-20	.812	-	.356	.127 (.110)	.100 (.057)	.201 (.119)	
-30	.877	-	.435	.213 (.117)	.075 (.013)	.110 (.114)	

Hatched region indicates the domain of geologically impossible solutions

Table 12

Earthquake: Lompoc

Reference Fault: Hosgri Reference Center: 34°55.0'N 120°44.3'W

k = 1.750 2L = 100 C = 25

Bands Used: IX, VIII, VII-VI, V-IV (MODIFIED)

Upper Values: CP Lower Values: s.d.$_{CP}$

S \ T	-30	-20	-10	0	10	20	30
30	.654	.455	.275 (.034)	.186 (.026)	.307 (.109)		
20	.608	.396 (.058)	.203 (.030)	.167 (.082)	.371		
10	.584	.362 (.061)	.158 (.030)	.186 (.097)	.399		
0	.582	.354 (.068)	.136 (.038)	.173 (.096)	.388		
-10	.601	.371 (.079)	.138 (.058)	.130 (.099)	.342		
-20	.642	.413 (.094)	.091 (.091)	.067 (.104)	.273 (.107)		
-30	.700	.478	.244 (.105)	.014 (.068)	.187 (.115)		

Hatched region indicates the domain of geologically impossible solutions

Table 13

Earthquake: Lompoc

Reference Fault: Hosgri Reference Center: 34°55.0'N 120°44.3'W

k = 1.675 2L = 60 C = 25

Bands Used: IX, VIII, VII-VI, V-IV

Upper Values: CP Lower Values: s.d.$_{CP}$

S \ T	-30	-20	-10	0	10	20	30
30							
20	.695	.567 (.022)	.457 (.012)	.395 (.017)	.409	.477	
10	.643	.504 (.023)	.385 (.011)	.327 (.024)	.371	.462	
0	.613	.464 (.026)	.334 (.012)	.274 (.031)	.353 (.091)	.458	
-10	.605	.450	.309 (.016)	.237 (.030)	.324	.434	
-20	.620	.461 (.037)	.312 (.023)	.217 (.019)	.267 (.095)	.384	
-30							

Hatched region indicates the domain of geologically impossible solutions

Figure 7

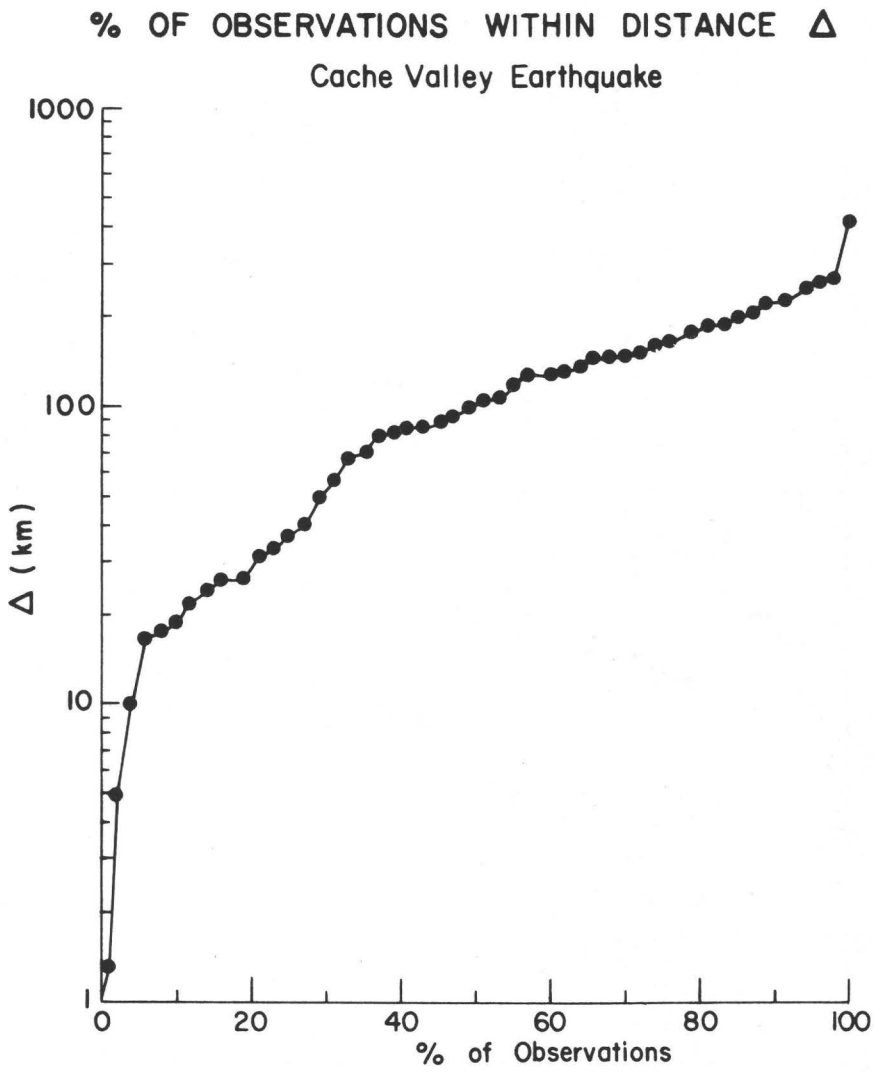
% OF OBSERVATIONS WITHIN DISTANCE Δ
Cache Valley Earthquake
1000
100
10
1
Δ (km)
0
20
40
60
80
100
% of Observations

Figure 8

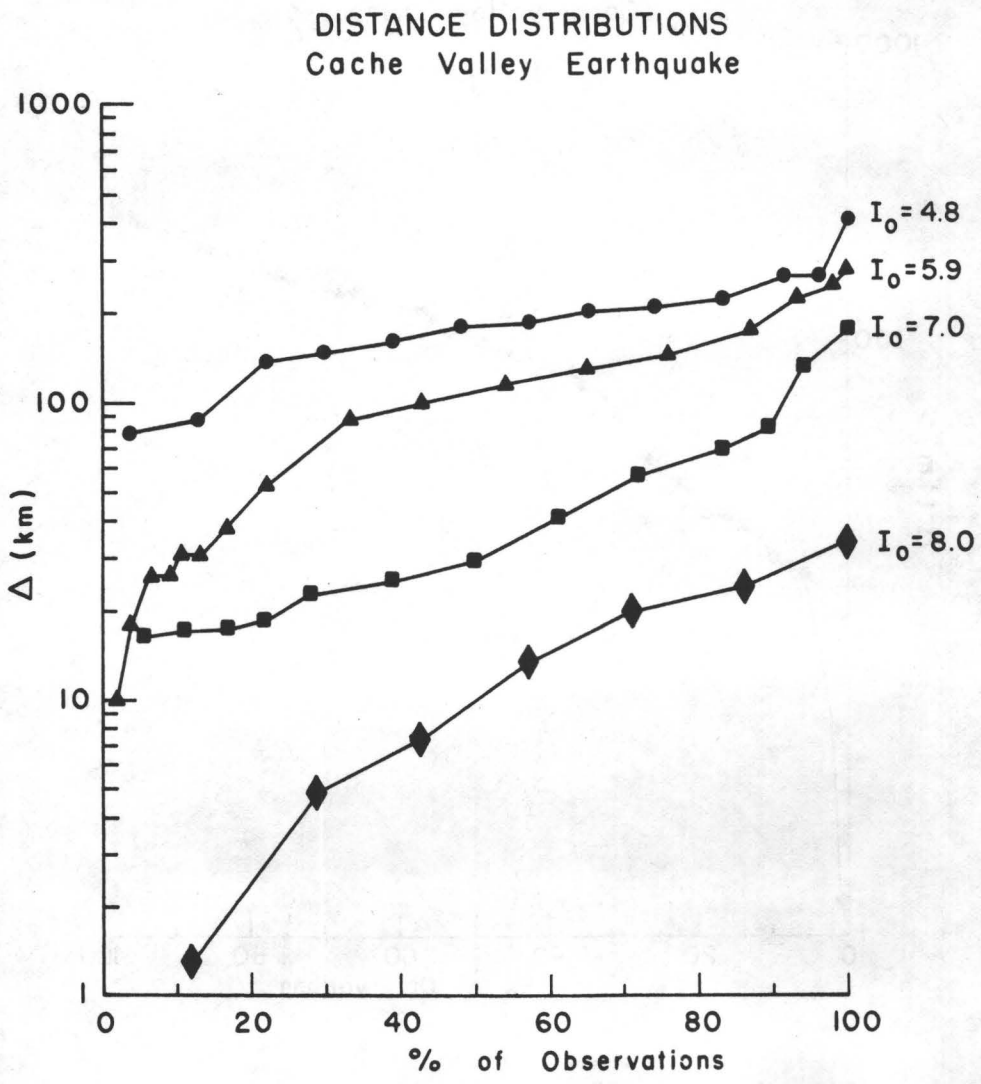
DISTANCE DISTRIBUTIONS
Cache Valley Earthquake
1000
100
10
1
Δ (km)
0
20
40
60
80
100
% of Observations
I_0= 4.8
I_0= 5.9
I_0= 7.0
I_0= 8.0

Figure 9

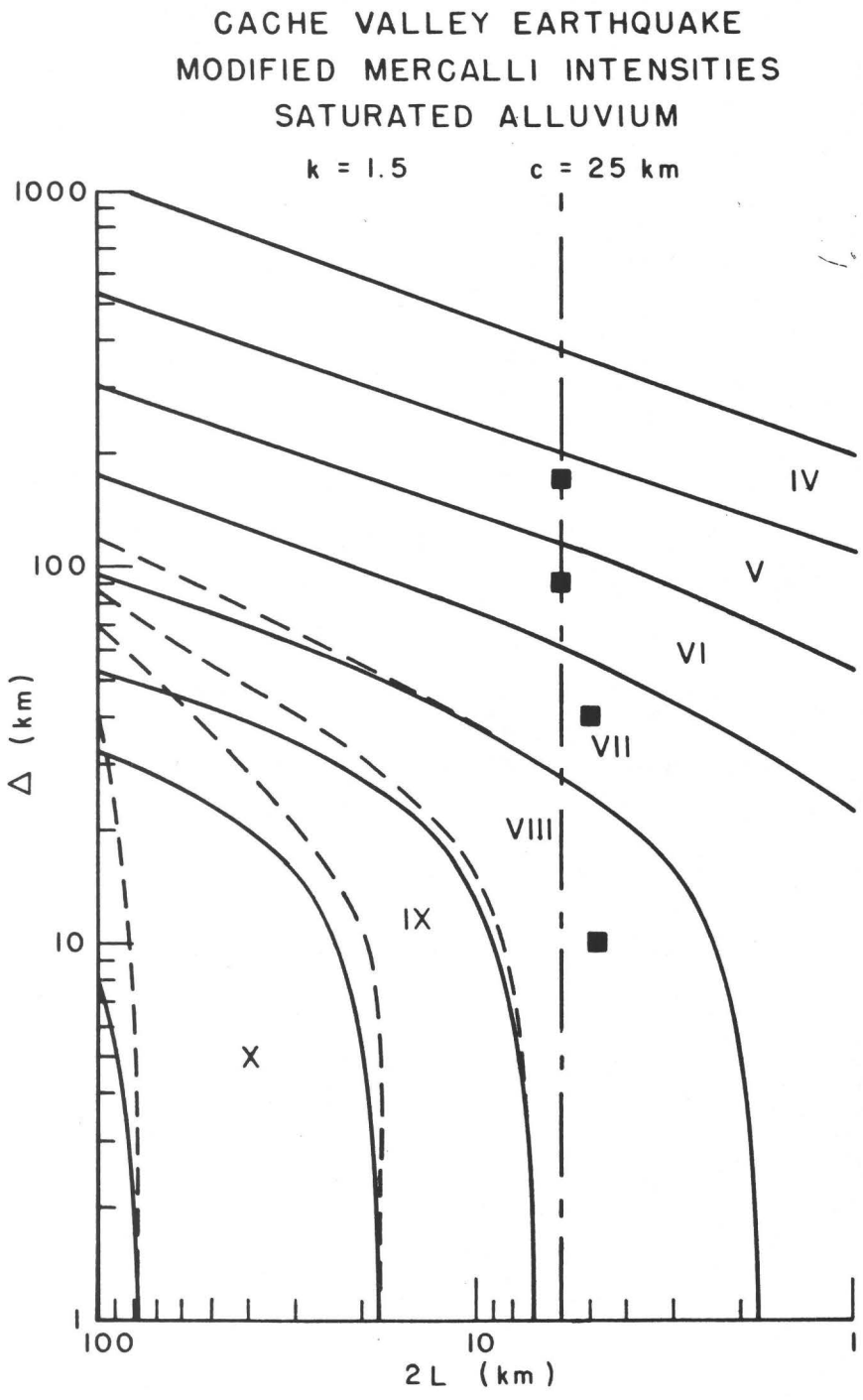
CACHE VALLEY EARTHQUAKE
MODIFIED MERCALLI INTENSITIES
SATURATED ALLUVIUM
k = 1.5
c = 25 km
1000
100
10
1
Δ (km)
IV
V
VI
VII
VIII
IX
X
100
10
1
2L (km)

Figure 10

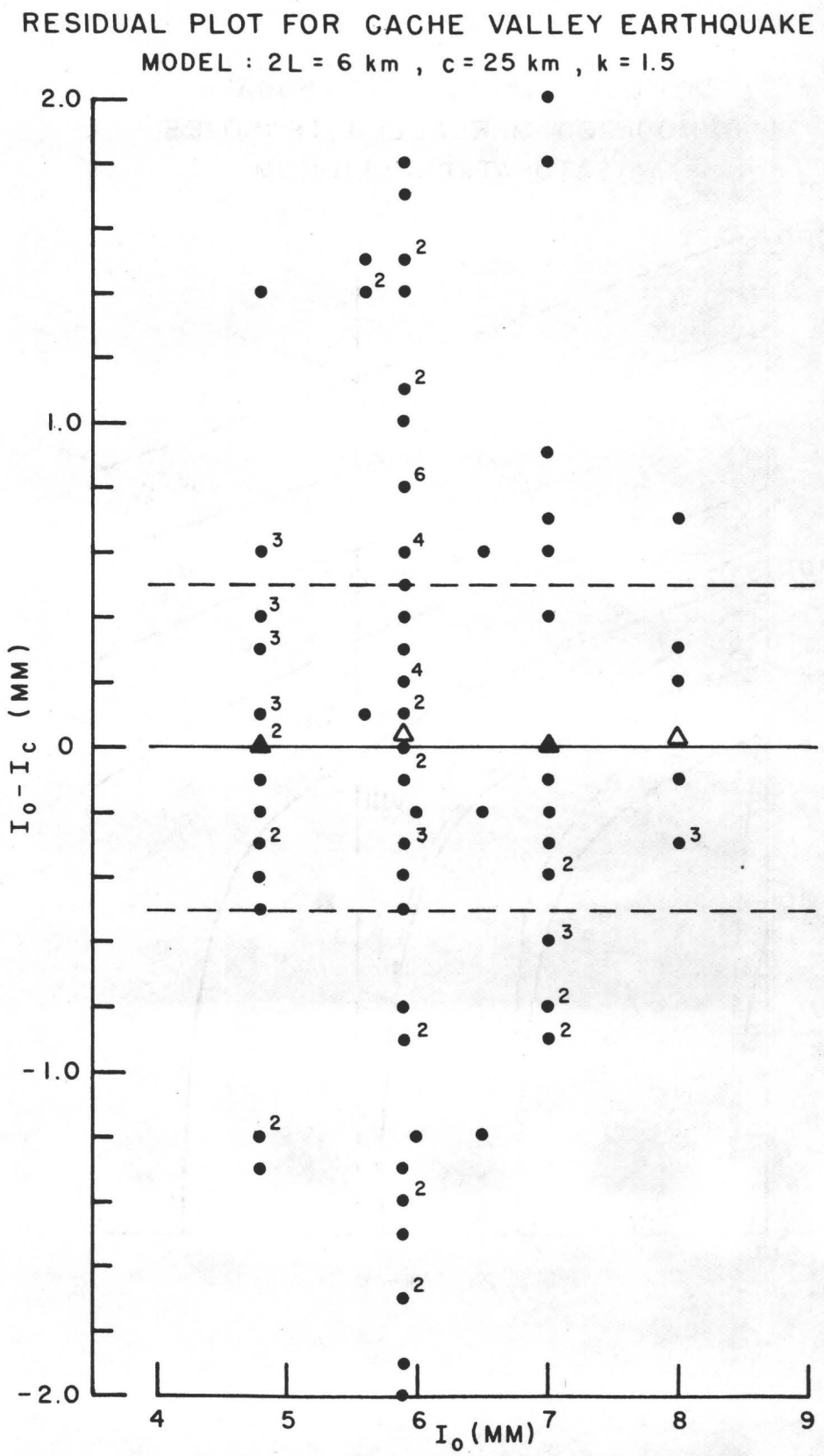
RESIDUAL PLOT FOR CACHE VALLEY EARTHQUAKE
MODEL : 2L = 6 km , c = 25 km , k = 1.5
2.0
1.0
0
-1.0
-2.0
$I_o - I_c$ (MM)
4
5
6
7
8
9
I_o (MM)

Figure 11

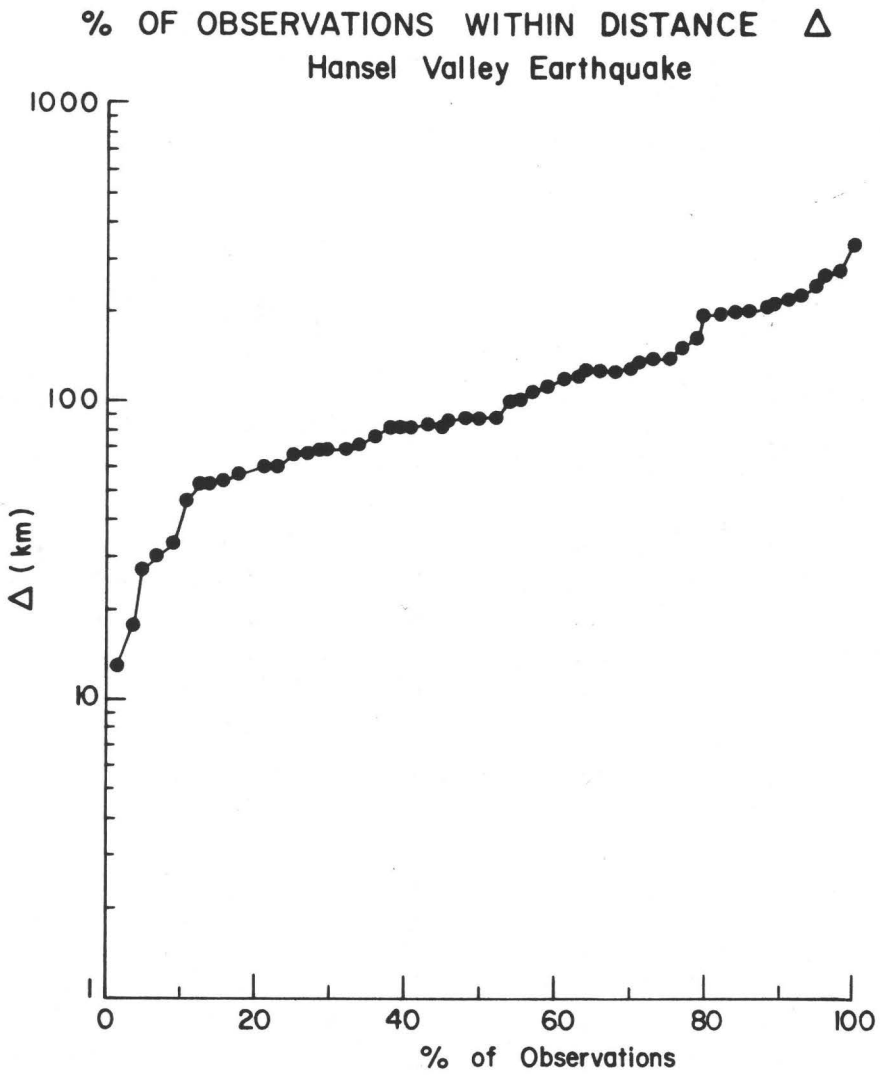
% OF OBSERVATIONS WITHIN DISTANCE Δ
Hansel Valley Earthquake
1000
100
10
1
Δ (km)
0
20
40
60
80
100
% of Observations

Figure 12

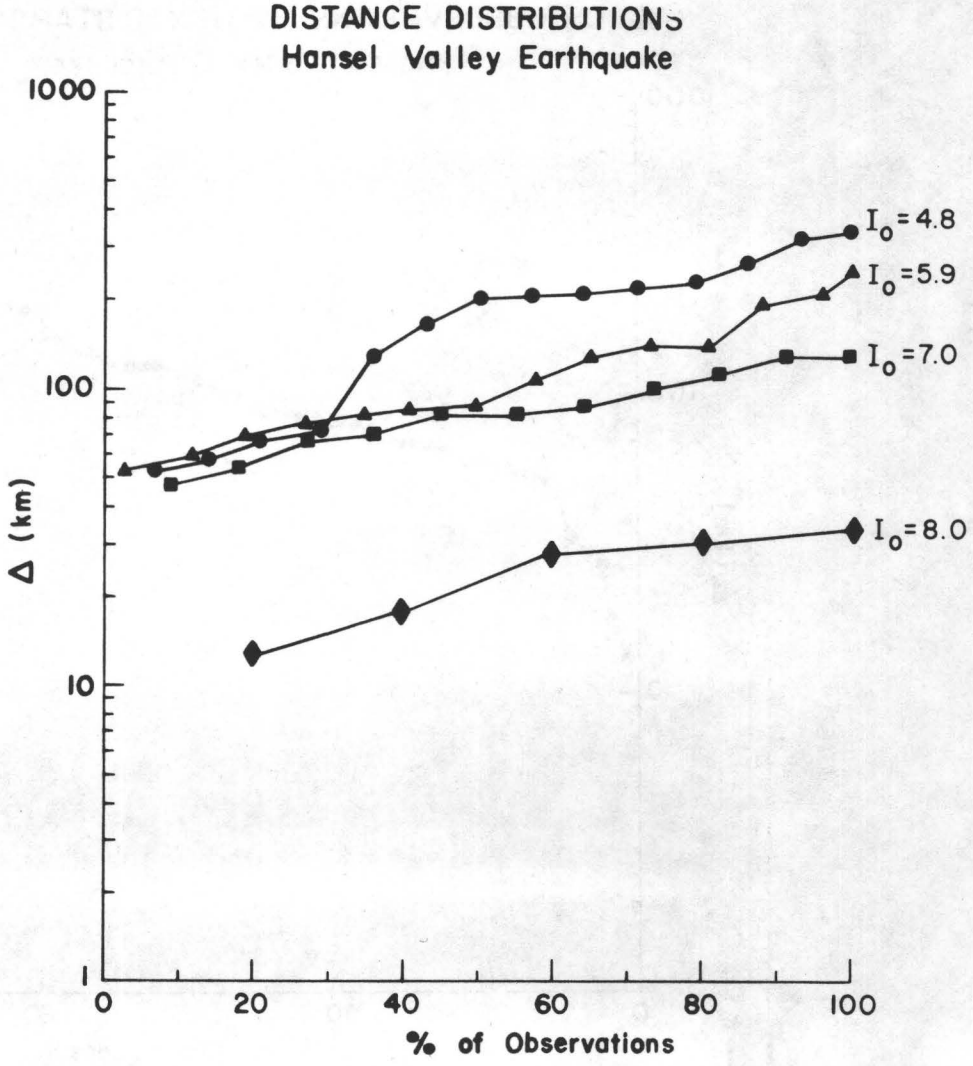
DISTANCE DISTRIBUTIONS
Hansel Valley Earthquake
1000
100
10
1
Δ (km)
0
20
40
60
80
100
% of Observations
I_o=4.8
I_o=5.9
I_o=7.0
I_o=8.0

Figure 13

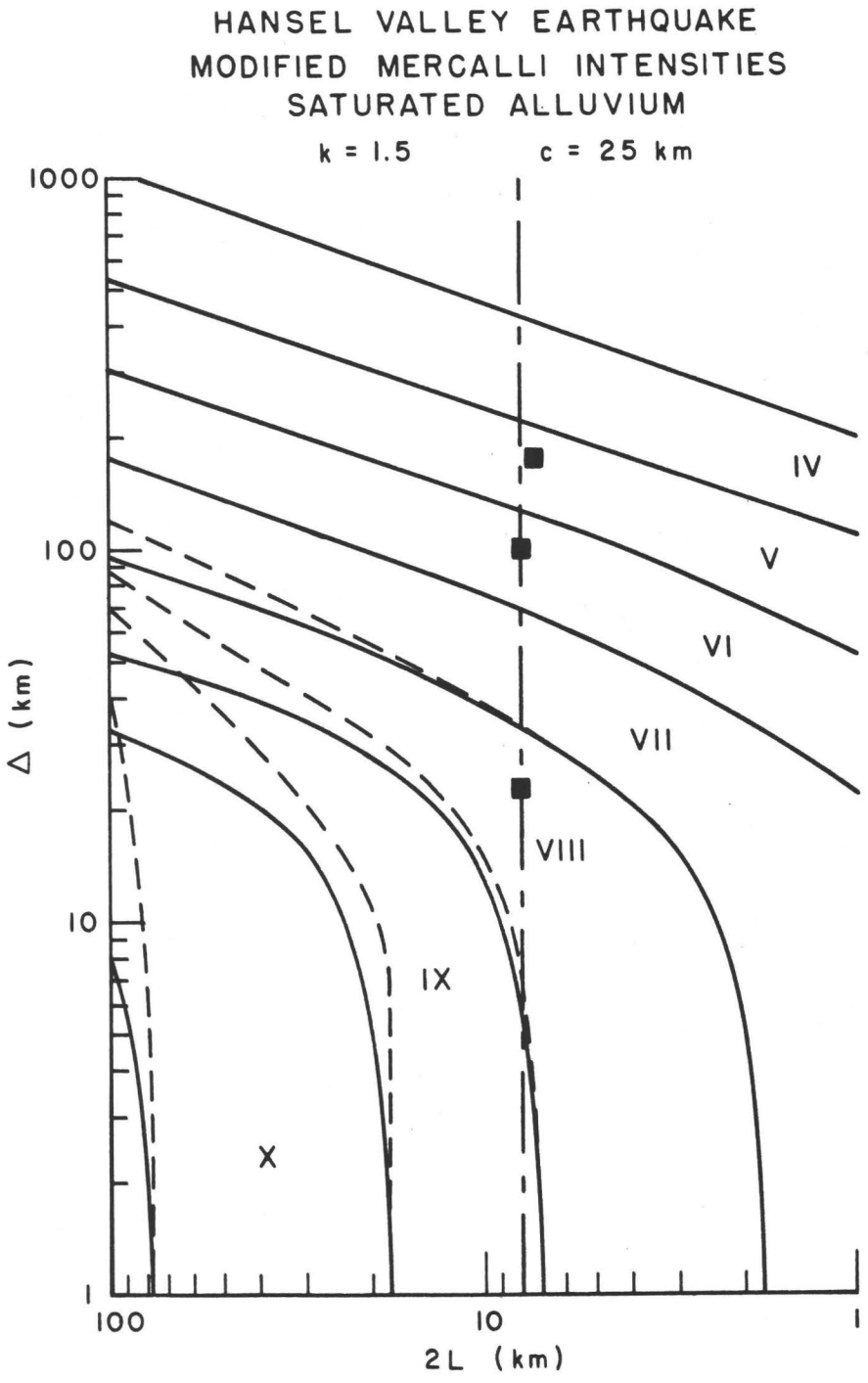
HANSEL VALLEY EARTHQUAKE
MODIFIED MERCALLI INTENSITIES
SATURATED ALLUVIUM
k = 1.5
c = 25 km
1000
100
10
1
Δ (km)
IV
V
VI
VII
VIII
IX
X
100
10
1
2L (km)

Figure 14

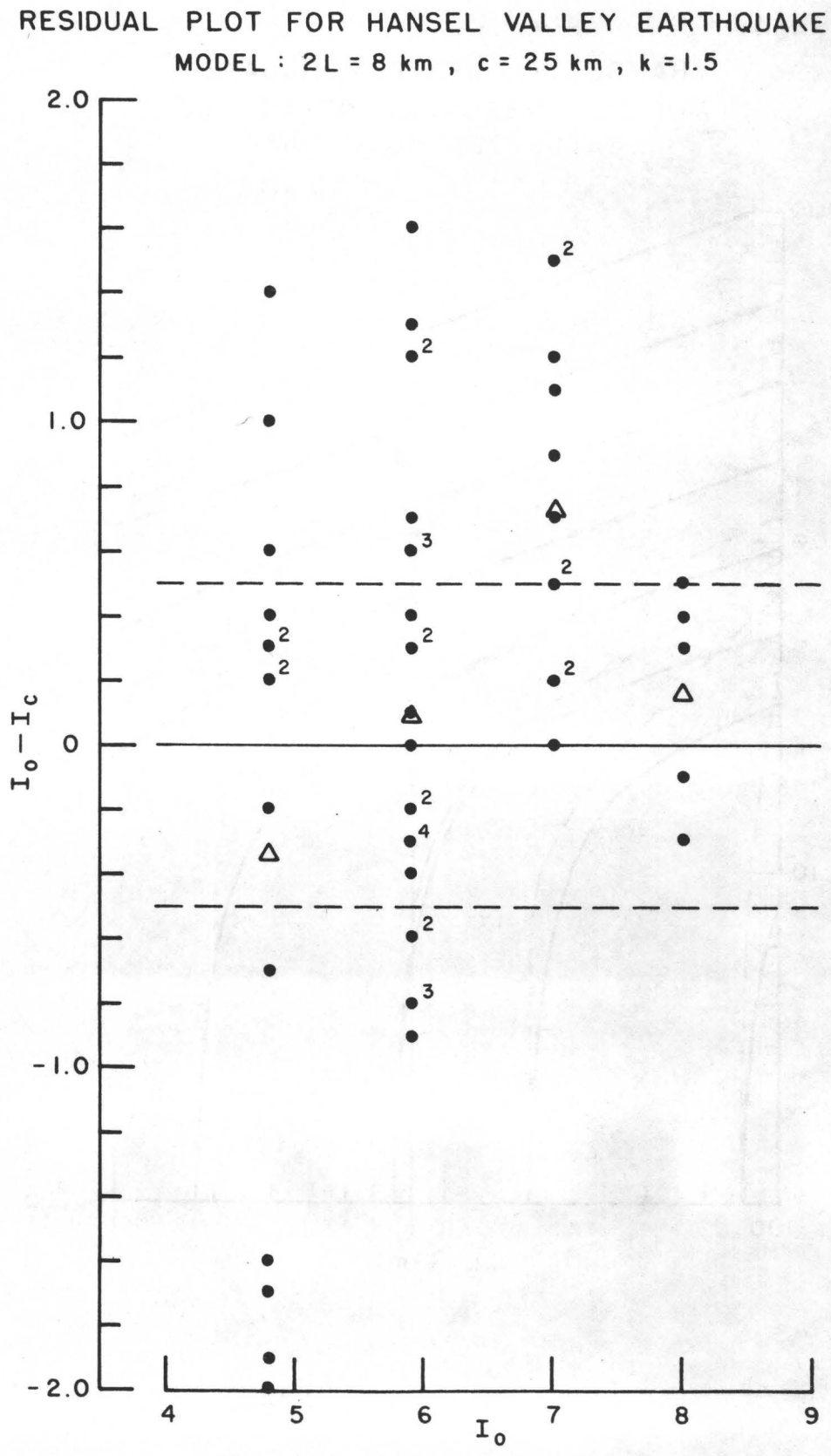
RESIDUAL PLOT FOR HANSEL VALLEY EARTHQUAKE
MODEL : 2L = 8 km , c = 25 km , k = 1.5
2.0
1.0
0
-1.0
-2.0
$I_o - I_c$
4
5
6
7
8
9
I_o

Table 14

Earthquake	YR	MO	DY	LAT(N)	LONG(W)	M(OB)	2L(OB)	2L(PRED)
Cedar Mountain, Nev.	32	12	20	38.8	118.0	7.2	61	66
Excelsior Mountain, Nev.	41	01	30	38.0	118.5	6.3	1.4	3.5
Hansel Valley, Utah	34	03	12	41.5	112.5	6.6	8	8
Manix, Calif.	47	04	10	35.0	116.6	6.4	4	10
Fort Sage Mts.,Calif.	50	12	14	40.1	120.1	5.6	8.8	1
Kern County, Calif.	52	07	21	35.0	119.0	7.7	60*	60
Rainbow Mountain, Nev.	54	07	06	39.4	118.5	6.6	18	18
Rainbow Mountain, Nev.	54	08	23	39.6	118.4	6.8	31	36
Fairview Peak, Nev.	54	12	16	39.3	118.2	7.1	48	40
Hebgen Lake, Mont.	59	08	17	44.8	111.1	7.1	24	28**
Galway Lake, Calif.	75	05	31	34.5	116.5	5.2	7	1
Pocatello Valley, Idaho	75	03	28	42.1	112.6	6.0	3***	3
Oroville, Calif.	75	08	01	39.4	121.5	5.7	4(1.5***)	1.5

* 33 kilometers of fracture in bedrock. However, epicenter was about 30 kilometers away under Quaternary deposits.
** By use of data to south of epicenter.
*** 2L values as determined from short period seismograms.

Figure 15

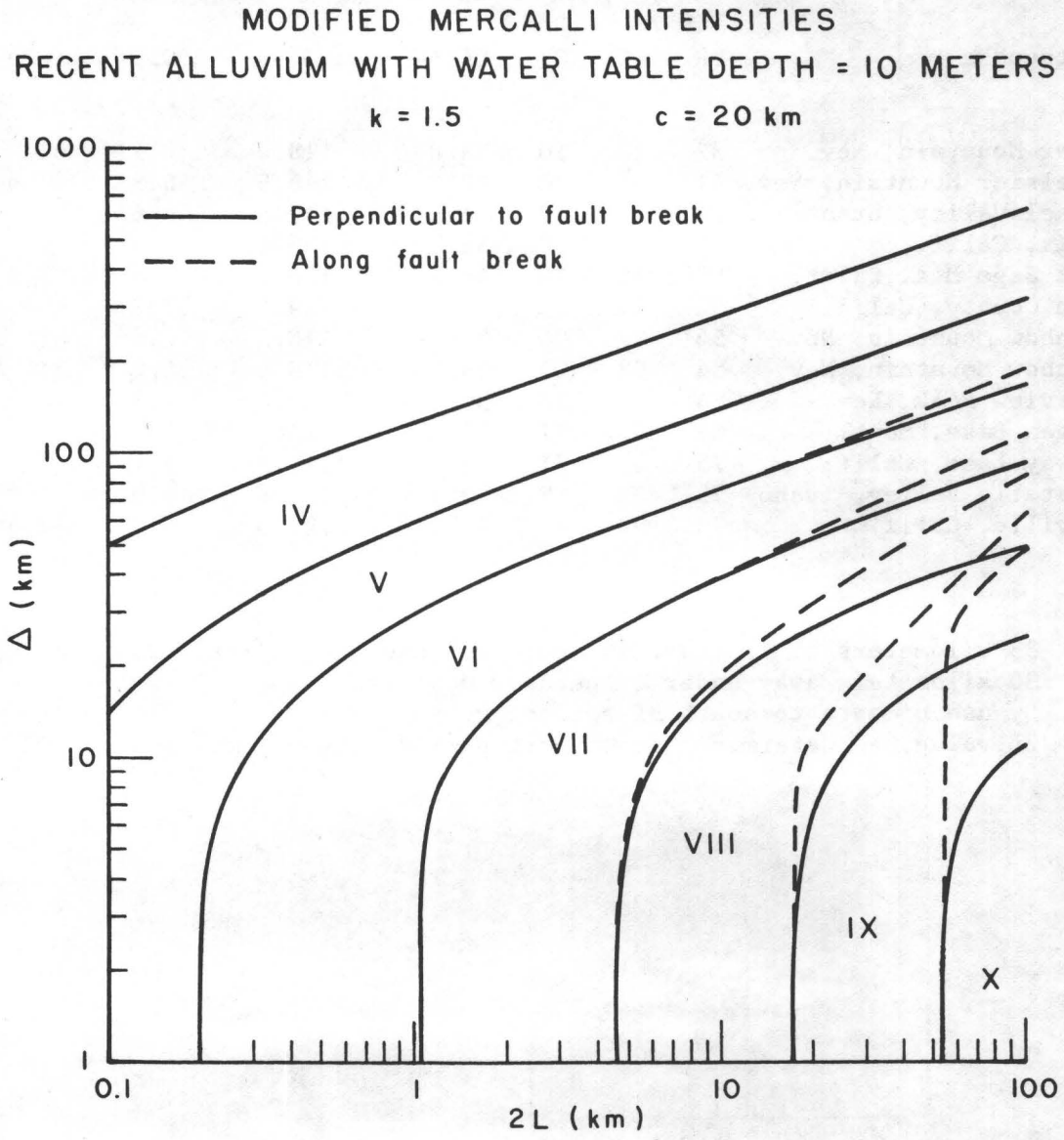
MODIFIED MERCALLI INTENSITIES
RECENT ALLUVIUM WITH WATER TABLE DEPTH = 10 METERS
k = 1.5
c = 20 km
Perpendicular to fault break
Along fault break
IV
V
VI
VII
VIII
IX
X
Δ (km)
1000
100
10
1
0.1
1
10
100
2L (km)

Figure 16

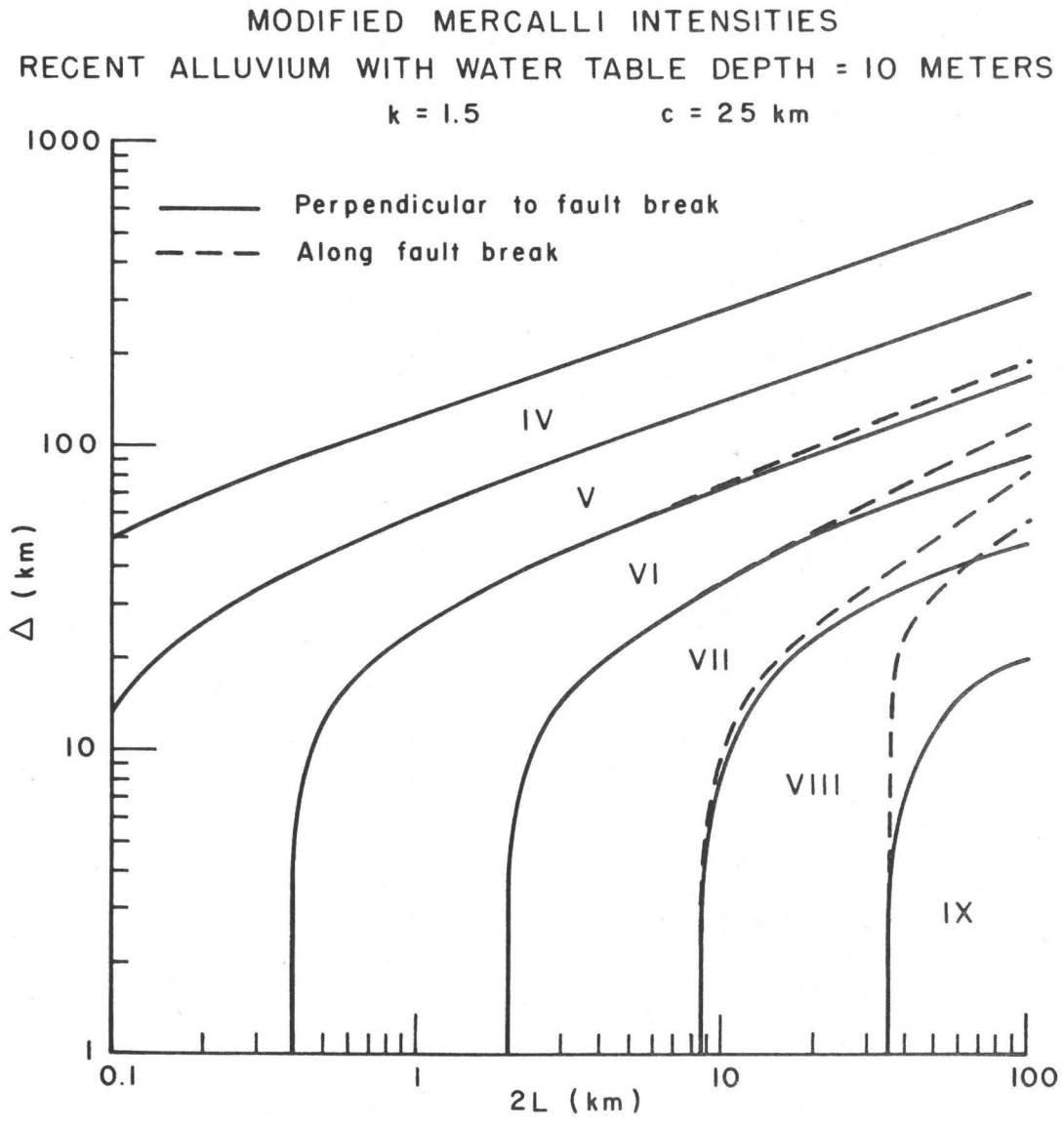
MODIFIED MERCALLI INTENSITIES
RECENT ALLUVIUM WITH WATER TABLE DEPTH = 10 METERS
k = 1.5
c = 25 km
Perpendicular to fault break
Along fault break
IV
V
VI
VII
VIII
IX
Δ (km)
1000
100
10
1
0.1
1
10
100
2L (km)

LIQUEFACTION POTENTIAL MAPS FOR LAND USE PLANNING IN UTAH

by

Loren R. Anderson[1], Jeffrey R. Keaton[2]
and William J. Gordon[2]

INTRODUCTION

Many places throughout the world have sustained extensive damage resulting from ground failure associated with earthquake-induced soil liquefaction. Liquefaction potential must be considered as part of a thorough assessment of geoseismic hazards.

The seismic history of the Wasatch front area in North-central Utah is such that the occurrence of ground motion of sufficient intensity and duration induce liquefaction of susceptible soils is very likely. Deposits of loose fine sand, highly susceptible to liquefaction, are known to exist along the Wasatch front (McGregor and others, 1974). Areas of shallow ground water are also widespread (Hely and others, 1971, Fig. 80). In addition, evidence of liquefaction was observed following the 1934 Hansel Valley earthquake in Box Elder County, Utah (Coffman and von Hake, 1973, p. 71).

The seismic history, subsurface soil and ground water conditions, and evidence of liquefaction in Utah indicate that liquefaction is a significant hazard and should be assessed as an important element in seismic hazard reduction planning. Seismic hazard maps provide an important basis for land use planning activities and aid planners in determining the level of detail appropriate for site-specific seismic hazard investigations for various developments.

---

[1]Department of Civil Engineering, Utah State University, Logan, Utah
[2]Dames & Moore Consulting Engineers, Salt Lake City, Utah

For engineering and land use planning purposes liquefaction is of consequence only if flow or ground failure is induced. In this paper, liquefaction potential is synonymous with liquefaction-induced ground failure potential. Youd and Perkins (1978) suggest a method to develop liquefaction Potential maps. The technique requires development of two maps (opportunity and susceptibility) which combine to form a liquefaction potential map. Probability concepts are used to relate data on location and frequency of earthquake occurrence in the study area to earthquake magnitude-source distance data at locations of known liquefaction-induced ground failures. By considering seismic source locations and assuming uniform distribution and attenuation of seismic energy, a liquefaction opportunity map can be prepared. The opportunity map is in terms of recurrence intervals of ground shaking of sufficient intensity and duration to induce liquefaction of susceptible soils.

Liquefaction susceptibility refers to the likelihood that subsurface soils would liquefy if given the opportunity. By considering the nature and age of deposition, depth to water table, grain-size distribution, relative density, and topographic aspects, a liquefaction susceptibility map can be prepared. The susceptibility map is basically an engineering geology map. Qualitative terms are used to classify the liquefaction susceptibility of the soil deposits. Helley and Lajoie (1979, p. 61) suggest the following classifications. Sediments considered likely to liquefy during a moderate earthquake could be classified as highly susceptible; unconsolidated sediments considered unlikely to liquefy during a large earthquake could be classified as slightly susceptible. Consolidated sediments and bedrock could be classified as non-susceptible to liquefaction.

LIQUEFACTION

Cause of Liquefaction

When a loose, saturated, fine sand deposit (with less than about 15% clay size particles) is subjected to vibratory motion, the sand can liquefy and thus, loose essentially all of its shear strength. Relatively large land masses with ground surface slopes as slight as two or three percent have liquefied and flowed laterally for great distances (San Fernando California event of 1971). This phenomenon has received much attention recently due to several rather spectacular failures such as the building foundation failures in Niigata, Japan (Seed and Idriss, 1967, 1968); the Turnagain Heights landslide in Anchorage, Alaska, the landslide in Valdez, Alaska (Seed, 1974); the Juvenile Hall mass movement in southern California (Nichols and Buchanan, 1974); and the failure of the lower San Fernando Dam (Seed et al. 1975).

Sand particles when in a loose dry condition will decrease in volume when disturbed. If the voids (pore space) within the sand mass are filled with water, the volume cannot immediately decrease upon disturbance and the load is transferred to the pore water and there is an abrupt increase in the pore water pressures and decrease in the intergranular stress. During earthquake shaking, the sand is repeatedly disturbed. Each disturbance tends to cause a decrease in void volume as described above, but since a decrease in volume cannot occur immediately, there is a transfer of load from the sand grains to the pore water. The pressure induced in the pore water in this manner is an excess hydrostatic pressure. If the disturbance persists, the pore pressure continues to increase until the intergranular stress in the sand is reduced to zero. This is termed as a condition of "initial liquefaction" (Seed, 1976). For loose sands this initial liquefaction is usually accompanied by large strains.

Factors Affecting Liquefaction Potential

Helley and Lajoie (1979, p. 61) summarize factors and condition controlling liquefaction (See Table I). These factors and conditions include soil properties, initial stresses, and the characteristics of the earthquake motion. Aside from a saturated condition, the following factors are listed as most important:

Soil type

Relative density

Initial confining pressure

Intensity of ground shaking

Duration of ground shaking

Only certain types of soil are susceptible to liquefaction. Uncemented, unconsolidated deposits of fine to medium grained sand with a rather uniform grain size have been found to be most susceptible. If the soil contains significant amounts of clay size material (more than about 15%) liquefaction will probably not occur. The relative density of the sand is very significant. Very loose sand is highly susceptible to liquefaction while dense sand has a very low liquefaction susceptibility. Investigations have shown that the stress required to initiate a liquefaction condition increases with the initial confining pressure. This effect has been shown in field cases such as at Niigata where soil under nine feet of embankment fill remained stable, while similar soils surrounding the embankment liquefied (Seed, Lee, and Idriss, 1967).

The intensity of the ground motion caused by an earthquake is also a very important factor. The opportunity for a soil to liquefy under a given confining pressure and relative density is related to the magnitude of shear forces induced by the earthquake. This effect can again be illustrated by the 1964 Niigata earthquake which had a Richter magnitude of 7.3. Records of the previous 370 years indicate only slight liquefaction problems at Niigata. During this period, 22 of the major earthquakes affecting the city produced calculated values of ground surface acceleration of 0.12 g or less. Of these,

Factor	Condition conducive to liquefaction	Conditions not conducive to liquefaction
Grain size of sediment	Coarse silt and fine sand	Clay, coarse sand, gravel
Sorting (Variability in grain size)	Well sorted Uniform grain size Clay free (less than 3 percent)	Poorly sorted Nonuniform grain size High clay content (more than 3 percent)
Cementation[1]	Uncemented Loose	Cemented Hard
Consolidation (Compaction)	Unconsolidated Noncompacted Loose Low shear strength	Semiconsolidated to consolidated Moderately to high compacted High shear strength
Relative density[2]	Low relative density Less than 65 percent for small earthquakes	High relative density More than 90 percent for largest earthquake
Standard penetration[3]	Low	High
Geologic age[4]	Generally young Holocene Late Pleistocene	Generally older Pleistocene and older
Water saturation	Saturated Pore spaces filled High ground-water table Bay deposits, flood basins, lower parts of alluvial fans	Partly unsaturated to dry Pore spaces not filled Low ground-water table Higher parts of alluvial fans
Pore-water pressure	High Greater than lithostatic load	Low Less than lithostatic load
Depth	Within 100 feet (30 m) of surface Low lithostatic load	Greater than 100 feet (30 m) depth Less than lithostatic load
Seismic activity	High seismic activity High probability of moderate to great earthquakes	Low seismic activity Low probability of moderate to large earthquakes

[1] Particles may be cemented together by calcite, silica, iron oxides, or other materials.
[2] Relative density primarily reflects the degree of compaction in a sediment. 100 percent relative density means a sediment is at its maximum compaction; all the pore space is filled. 0 percent relative density means a sediment is at its minimum compaction; it is in its loosest condition and pore space is at a maximum.
[3] Standard penetration generally reflects degree of induration, which is a combination of compaction and cementation. Low standard penetration values indicate a sediment that is not compacted and is not cemented.
[4] In a general way, the age of a deposit is reflected in certain physical properties such as induration. Older alluvial deposits are generally more highly indurated than younger deposits.

Table I. Factors and conditions controlling liquefaction. (Helley and Lajoie, 1979, p. 61).

only two earthquakes caused observable liquefaction near Niigata. These two earthquakes are believed to have caused ground surface accelerations of about 0.13 g. It wasn't until 1964, when maximum recorded accelerations of 0.16 g occurred, that extensive liquefaction in Niigata was observed. Thus, even though a long history of seismic stresses had occurred at the site, a critical condition was not observed until the 1964 earthquake (Seed, Lee, Idriss, 1967).

Duration of strong shaking and, consequently, the number of significant stress cycles to which the soil is subjected influences the extent of the build-up of excess hydrostatic pore pressures. Even though this process begins at the onset of the ground motion, instability will not result until a state of "initial liquefaction" is reached at which point the intergranular strength becomes less than the lithostatic load acting on the soil.

Another condition affecting the liquefaction potential of sand is that of the influence of the seismic history of the sand deposit. Experiments by Seed, Mori, and Chan (1975) showed that disturbed sand specimens with a given density liquefied much sooner when subjected to cyclic stresses, than similar undisturbed sand subjected to repeated minor seismic events prior to failure. Therefore, accurate assessment of the susceptibility of a sand deposit to liquefaction on the basis of laboratory tests on reconstituted samples is questionable.

Liquefaction-Induced Ground Failure

Youd and others (1975, p. A72 and A73) list three types of ground failure commonly associated with liquefaction:

(1) Flow landslides that generally occur on moderate to steep slopes underlain by loose granular deposits.

(2) Lateral-spreading landslides that occur on gentle to nearly horizontal slopes underlain by loose to moderately dense granular deposits.

(3) Quick-condition failures (loss of bearing capacity) that occur in flat areas with a high groundwater table and loose to moderately dense granular materials extending from near the surface to substantial depths.

The most common type of liquefaction-induced ground failure may be associated with lateral-spreading landslides. However, the topographic and geologic conditions of the Wasatch front area make all three types of ground failure possible.

Liquefaction Analysis

Two methods of evaluating liquefaction are commonly used. One of these methods involves the use of a chart (Fig. 1) developed by Seed, Mori, and Chan (1975) which is based on data from performance observations of many sites during past earthquakes. This chart allows the comparison of the ratio of shear stress and effective overburden pressure to the standard penetration resistance for any site under consideration.

The second method requires an evaluation of the level of stress which will be induced in the soil by an earthquake. This stress level must be compared with the level of stress in the soil necessary to cause liquefaction. The zone where these two curves overlap, as shown in Figure 2 is the zone where liquefaction may occur (Seed and Idriss, 1975).

Even though the method of comparing induced stresses with stresses required to cause liquefaction appears to be the most rational method of evaluating liquefaction susceptibility, it has a major shortcoming in that it is very difficult to determine the stress level required to induce liquefaction. The major problem being that tests on reconstituted samples do not reflect the effect that seismic history has on liquefaction. In spite of its shortcomings, for performing a site-specific evaluation of liquefaction potential, this method clearly points out that liquefaction potential is a function of

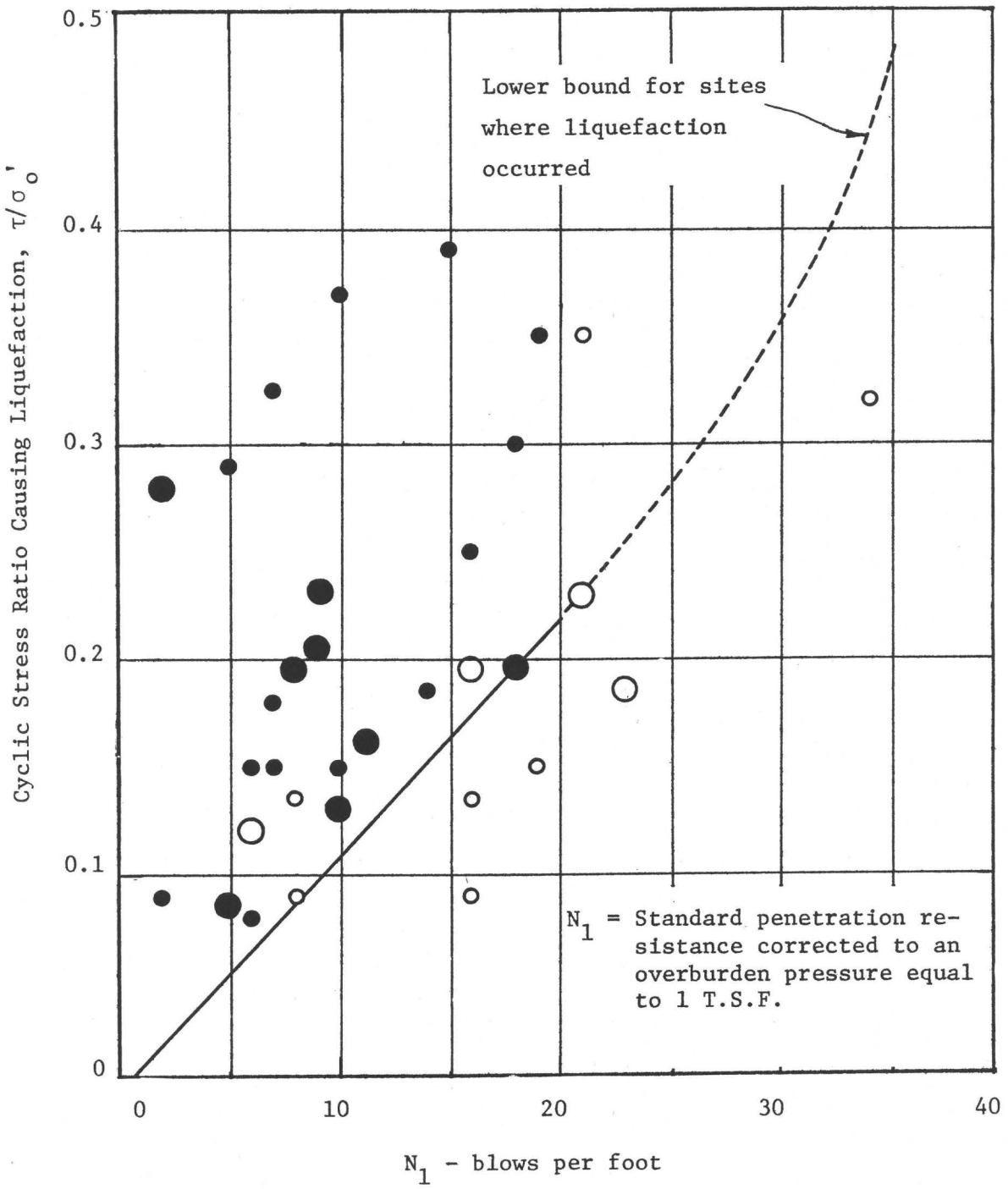

Figure 1. Correlation between stress ratio causing liquefaction in the field and penetration resistance of sand (after Seed, Mori, and Chan, 1977).

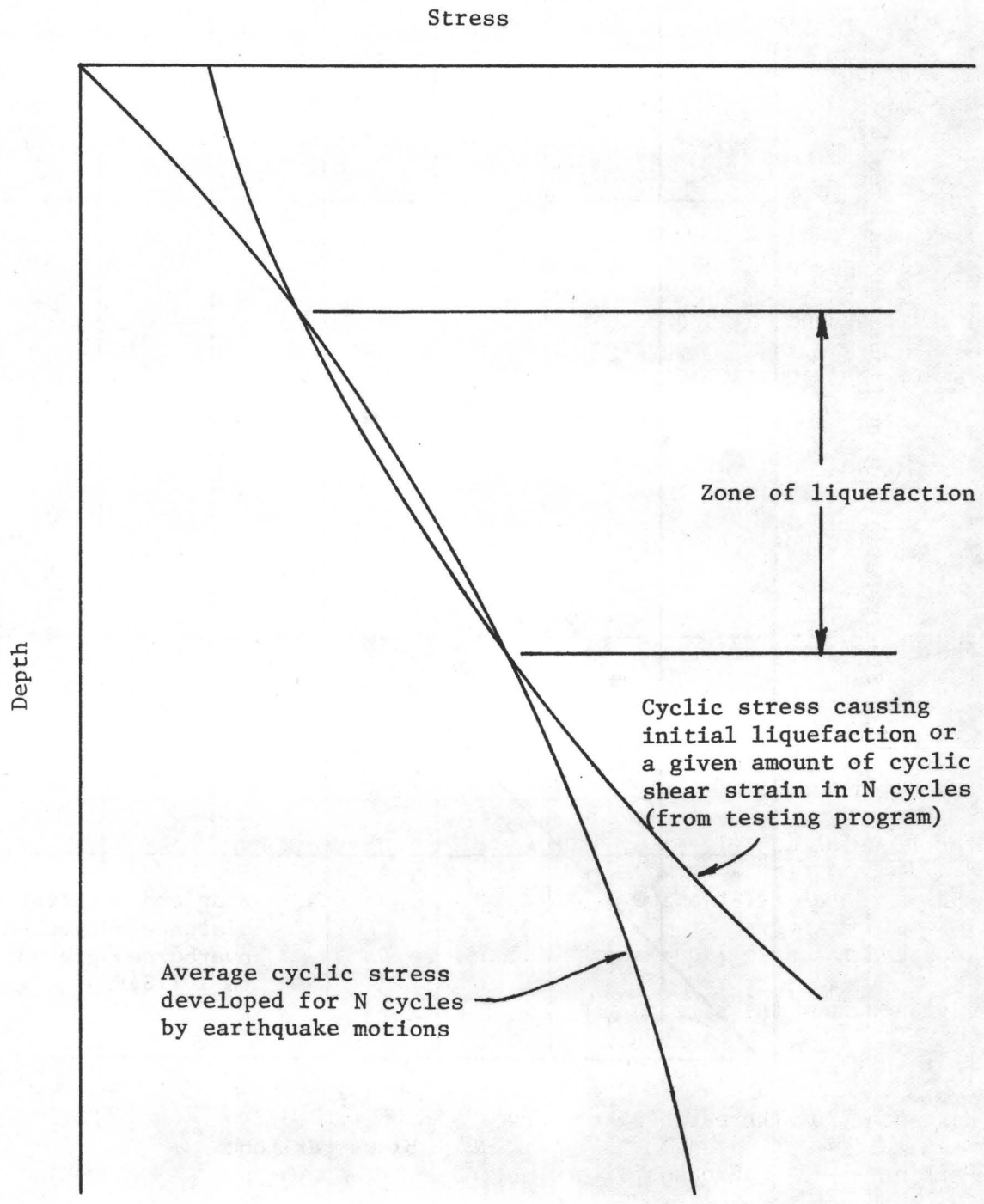

Figure 2. Method of evaluating liquefaction potential (after Seed and Idriss, 1971).

(1) Level of ground shaking

(2) Nature of the soil deposit

An evaluation of liquefaction must, therefore, consider these two elements.

DEVELOPMENT OF LIQUEFACTION POTENTIAL MAPS

In generating a map to indicate areas of various levels of liquefaction-induced ground failure potential, consideration must be given to the (1) opportunity for liquefaction (probability of sufficient ground shaking to cause liquefaction of soils that have the capability to liquefy) and (2) susceptibility to liquefaction (whether a soil will liquefy if given the opportunity by a sufficient level of ground shaking). Youd and Perkins (1978) have presented a method of mapping liquefaction potential that considers both of these elements.

Liquefaction Opportunity Maps

Youd and Perkins (1978) examined the factors that effect the opportunity for liquefaction (level of induced stress and duration of shaking) and showed that a linear relationship should exist between the magnitude of an earthquake required to cause liquefaction-induced ground failure and the logarithm of the distance from the site to the seismic source. Figure 3 shows such a relationship that was developed on observed data of earthquake magnitude and the maximum distance from the earthquake source to points of known liquefaction (Youd and Perkins, 1978). Ground failure opportunity is then calculated using procedures similar to those used in calculating seismic risk (Algermissen and Perkins, 1972) and described by Youd and Perkins (1978). The product of this phase of the analysis is a ground failure opportunity map, similar to that shown on Figure 4, that consists of return period contours of ground failure opportunity. McGuire and others (1979, p. 798) suggest that Fig. 3 may be overly conservative for preliminary seismic zoning, but they agree with the concept of such a relation-

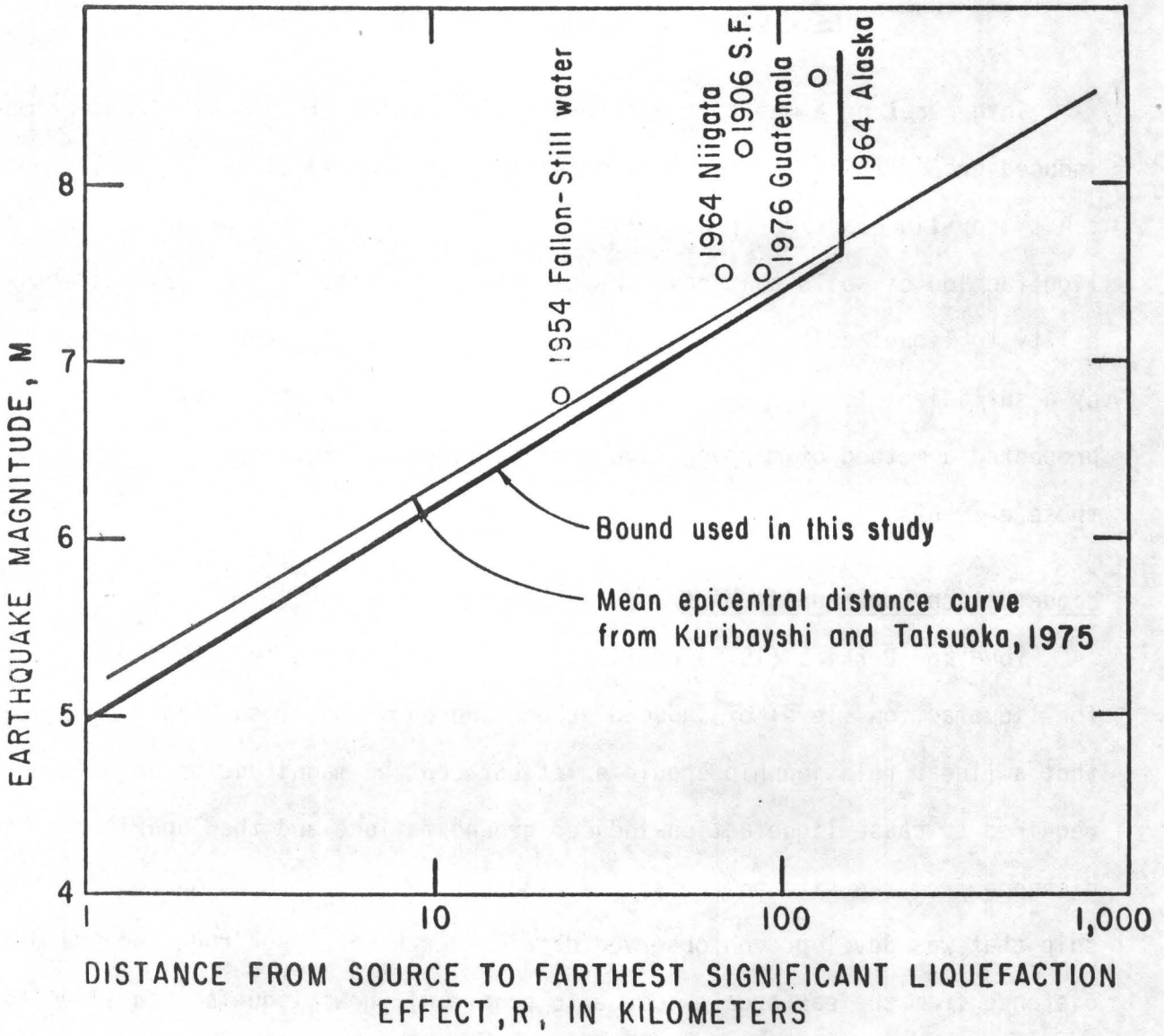

Figure 3. Earthquake magnitude versus maximum distance to significant liquefaction-induced ground failures (After Youd and Perkins, 1978, p. 437).

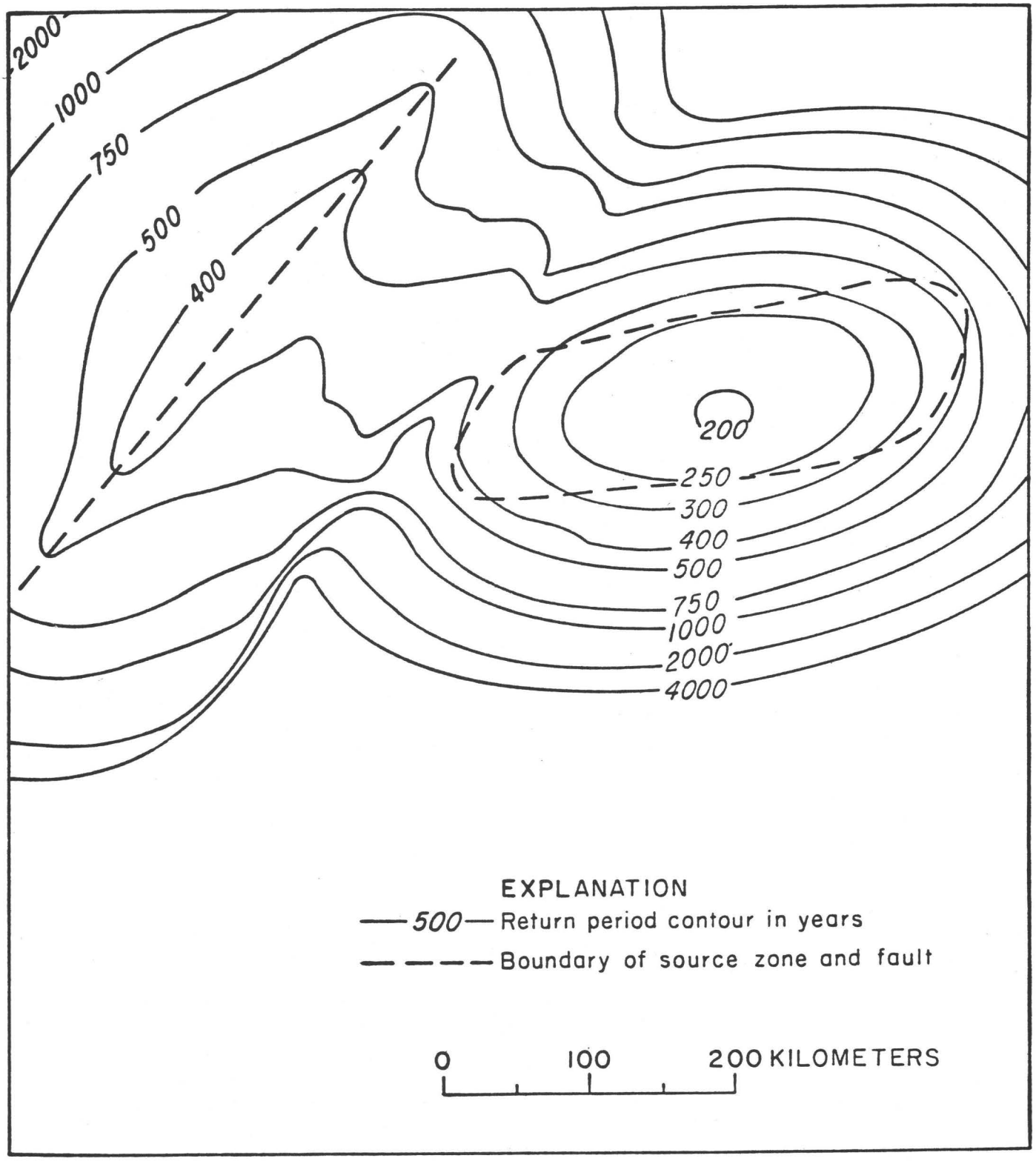

Fig. 4. **--Map of ground failure opportunity return period for hypothetical area** (After Youd and Perkins, 1978, p. 440).

ship.

Liquefaction susceptibility refers to the ease with which a deposit will liquefy if subjected to sufficient shaking. This, of course, depends on the type of soil, the relative density of the soil and the depth to the water table. Youd and Perkins (1978, p. 442) suggest that for many areas a rather gross preliminary evaluation of liquefaction susceptibility can be made on the basis of information compiled on detailed geologic maps of Quaternary units. Youd and others (1975, p. A72) compiled standard penetration data for Quaternary materials and found that younger deposits consistently had lower relative densities than older deposits. However, zones of low relative densities were also found in late Pleistocene deposits.

The accuracy of the susceptability map depends on the availabiltiy and detail of the information on the soils in the area being studied.

Liquefaction Potential Map

By superimposing the susceptibility map on the opportunity map, a map of liquefaction-induced ground failure potential can be developed. Such a map not only shows where liquefaction induced ground failure is most likely to occur, but also how frequently ground failure is likely to occur.

LIQUEFACTION POTENTIAL IN UTAH

Liquefaction Opportunity in Utah

The State of Utah is bisected by the Intermountain seismic belt. This zone of seismic activity extends in a north-south pattern from Arizona, through Utah, eastern Idaho, and western Wyoming, and terminates in north-western Montana. This belt is more than 800 miles long and up to 60 miles in width.

Many known and suspected quaternary faults have been mapped in Utah. However, there is no doubt that there are many faults that have not yet been

discovered, particularly under valley floors in the Basin and Range Province (Anderson and Miller, 1979b). The Northern Wasatch Fault is a north-south trending fault zone located along the western base of the Wasatch Mountain Range. It extends from near Gunnison, Utah to Malad, Idaho a length of about 215 miles. Its width varies from several hundred feet to perhaps several miles.

The seismic history of Utah has been documented since 1850. The most complete study of Utah Earthquakes prior to 1950 is a comprehensive report by Williams and Tapper (1953). Their report was based on earthquake data taken from the earliest Utah newspapers and scientific journals, and they assigned modified Mercalli intensities to each event. Since 1950, as better equipment was developed and seismograph stations were installed, much more reliable earthquake data has become available. Data since 1950 has been reported by several authors, Arabasz, Smith, and Richins (1979b), Cook and Smith (1967), Coffman and Von Hake (1973), Smith (1975) and U. S. Geological Survey (1976).

Currently a network of seismograph stations throughout the region provides accurate location of all seismic events. The University of Utah has recently completed work which updated and refined (in terms of magnitude and epicenter location) much of the past earthquake data for Utah.

Swan and others (1979) have released preliminary results of their study on recurrence of surface faulting and moderate to large magnitude earthquakes (U.S.G.S. contract 14-08-001-16827). Their study involved examining geologic evidence of faulting in trenches and calculating recurrence intervals. The results of their study should greatly aid the interpretation of probalistic seismic activity data.

Liquefaction Susceptibility in Utah

Because of the nature of many of the soil deposits (loose sandy soils with a shallow ground water table) in the lake bed valleys of Utah their susceptibility to liquefaction is high. Dames & Moore (1979) performed a foundation investigation for a proposed commercial facility west of the Jordan

River at a site where saturated loose silty fine sand was encountered. The owner followed Dames & Moore's recommendation and artifically densified the site prior to construction. Loose sandy soils have been encountered in many subsurface investigations in the Salt Lake City, Ogden and Logan areas.

Hill (1979) compiled a liquefaction potential map for Cache Valley, Utah. In evaluating the susceptibility of the soil deposits he considered soil type, age of deposit and depth to groundwater. Based on a geologic map compiled by Williams (1962), Hill (1979) found that most of the liquefaction susceptible soils lie along the banks and flood-plains of the major rivers that flow through the valley. These soils were transported to their present locations by rivers cutting through the deltas that were formed during Lake Bonneville time.

Evidence of Liquefaction in Utah

There is evidence that liquefaction has occurred in Utah during past earthquakes. Evidence of liquefaction-induced ground failure was observed following the 1934 Hansel Valley earthquake (Coffman and von Hake, 1973). Hill (1979) interviewed two people that observed liquefaction during the 1962 Cache Valley Earthquake. Ground surface cracking and extrusion of sand and water from the cracks were found in the north end of Cache Valley, Utah near the community of Trenton. Sand boils were also observed in this area.

Kaliser (1979) reported an exposure at a site in a rapidly developing commercial neighborhood in west Salt Lake City where age-dateable Holocene deposits were clearly penetrated by a sand dike. Some of the large topographic features north-west of Farmington, Utah are believed to be related to liquefaction during prehistoric earthquakes. VanHorn (1975) has identified two large landslides near Farmington, Utah, in Davis County, as being of the type known as failure by lateral spreading. VanHorn indicates that these are the biggest known landslides of this type in the United States. It is possible that these landslides were caused by earthquake-induced liquefaction. A number of smaller

landslides near Layton, Utah could also have been caused by earthquake-induced liquefaction.

CONCLUSIONS

The close proximity of the majority of the population of Utah to major active fault zones with documented historical seismic activity, and the nature of the soils in the lake bed valleys makes liquefaction potential an important consideration for seismic hazard reduction programs. Liquefaction has occurred in the past and it's likely to occur in the future. The writers are starting a program (April 1, 1980) sponsored by the U. S. G. S. Earthquake Hazards Reduction program to develop a liquefaction susceptibility map for Davis County, Utah.

REFERENCES

Algermissen, S.T., and Perkins, D.M., 1972, A technique for seismic zoning: general considerations and parameters: Proc. Internat. Conference on Microzonation, Seattle, Wa. p. 865-878.

Anderson, L.W., and Miller, D.G., 1979b, Quaternary fault map of Utah: Fugro, Inc. Long Beach, Ca. 30 p.

Arabasz, W.J., Smith, R.B., and Richins, W.D., 1979b, Earthquake studies along the Wasatch front, Utah: Network monitoring, seismicity, and seismic hazards: in Arabasz, Smith and Richins, eds., Earthquake studies in Utah 1850 to 1978. University of Utah, Seismograph Stations, p. 253-285.

Coffman, J.L., and von Hake, C.A., 1973, Earthquake history of the United States: National Oceanic and Atmospheric Administration, publication 41-1.

Cook, K.L., and Smith, R.B., 1967, Seismicity in Utah 1850 through June 1965; Seis. Soc. Am., Bull., Vol. 57, No. 4, p. 689-718.

Dames & Moore, 1979, Report, Soils, Foundation and Ground Water Study, Proposed Telcom products manufacturing plant, north of 1820 South Street at 3850 west, Salt Lake County, Utah for GTE Products Corp.: unpublished report dated January 18, 1979, 23p.

Helley, E.J., and Lajoie, K.R., 1979, Flatland deposits of the San Francisco Bay Region - their geology and engineering properties and their importance to comprehensive planning: U.S. Geol. Surv. Professional Paper 943, 88p.

Hely, A.G., Mower, R.W., and Harr, C.A., 1971, Water resources of Salt Lake County, Utah: Utah Department of Natural Resources Technical Publication No. 31, 244p.

Hill, Randle J., 1979, A Liquefaction Potential Map for Cache Valley, Utah: Thesis submitted in partial fulfillment of the requirements for the degree of MASTER OF SCIENCE in Engineering, Department of Civil Engineering, Utah State University, Logan, Utah.

Kaliser, B.N., 1979, Engineering geologic aspects of earthquake hazard reduction along Utah's Wasatch front: unpublished manuscript distributed at U.S. Geol. Surv. Conference on earthquake hazards along the Wasatch front and in the Reno-Carson City area, July 30, 31 and August 1, 1979, Alta, Utah, 4p.

McGregor, E.E., Van Horn, Richard, and Arnow, Ted, 1974, Map showing the thickness of loosely packed sediments and the depth to bedrock in the Sugar House Quadrangle, Salt Lake County, Utah: U.S. Geol. Surv. map I-766-M.

McGuire, R.K., Tatsuoka, F., Iwasaki, T., and Tokida, K., 1979, Assessment of the probability of liquefaction of water-saturated reclaimed land: Proc. Third International Conference on Application of Statistics and probability in soil and structural engineering, Vol. II, Sydney, Australia, January, 1979, p. 786-801.

Nichols, D.R., and Buchanan-Banks, J.M., 1974, Seismic hazards and land-use planning: U.S. Geol. Surv., Circular 690.

Seed, H.B., 1976, Evaluation of soil liquefaction effects on level ground during earthquakes: ASCE Annual convention and Exposition, State-of-the art paper preprint 2752, Philadelphia, Pa, Sept. 27 to Oct. 1, 1976.

Seed, H.B., 1974, Landslides during earthquakes due to soil liquefaction: ASCE, Terzaghi lectures, p. 191-260.

Seed, H.B., and Idriss, I.M., 1968, Analysis of soil liquefaction: Niigata earthquake: ASCE, Soil Mechanics and Foundation Div. Journal, Vol. 94, No. SM6, p. 1367-1371.

Seed, H.B., Idriss, I.M., Lee, K.L., and Makdisi, F.I., 1975, Dynamic analysis of the slide in the lower San Fernando Dam during the earthquake of February 9, 1971: ASCE, Geotechnical Engineering Div., Journal, Vol. 101, No. GT9, p. 889-911.

Seed, H.B., Lee, K.L., and Idriss, I.M., 1967, Analysis of soil liquefaction: Niigata earthquake: ASCE, Soil mechanics and foundation Div. Journal, Vol. 93, No. SM3, p. 83-108.

Seed, H.B., Mori, K. and Chan, C.K., 1975, Influence of seismic history on liquefaction characteristics of sands: EERC, College of Engineering, University of California, Berkeley, Report no. EERC 75-25.

Smith, R.B., 1975, Seismicity and earthquake hazards of the Wasatch front, Utah: University of Utah, interim report.

Swan, F.H., Schwartz, D.P., and Cluff, L.S., 1979, Recurrence of surface faulting and moderate to large magnitude earthquakes on the Wasatch fault zone at the Kaysville and Hobble Creek sites, Utah: unpublished manuscript distributed at U.S. Geol. Surv. Conference on earthquake hazards along the Wasatch front and in the Reno-Carson City area, July 30, 31 and August 1, Alta, Utah, 62p.

U.S. Geological Survey, 1976, A study of the earthquake losses in the Salt Lake City, Utah area: U.S. Geol. Surv. open-file report 76-89, 357p.

U.S. Senate, 1975, Earthquake research and Knowledge: Hearing before the committee on Aeronautical and Space Sciences, 94th Congress, 1st session, April 26, 1975, Senator Frank E. Moss, chairman.

Van Horn, Richard, 1975, Largest known landslide of its type in the United States - a failure by lateral spreading in Davis County, Utah: Utah Geological and Mineral Survey, Utah Geology, Vol. 2, No. 1, p. 83-88.

Williams, J.S., and Tapper, M.L., 1953, Earthquake history of Utah 1850-1949: Seis. Soc. Am., Bull, Vol. 43, No. 3, p. 191-218.

Youd, T.L., Nichols, D.R., Helley, E.J., and Lajoie, K.R., 1975, Liquefaction potential: in Borcherdt, R.D., ed, Studies for seismic zonation of the San Francisco Bay Region, U.S. Geol. Surv. Professional Paper 941-A, p. A68-A74.

Youd, T.L., and Perkins, D.M., 1978, Mapping liquefaction-induced ground failure potential: ASCE, Geotechnical engineering Div. Journal, Vol. 104, No. GT4, p. 433-446.

RESEARCH TO DEFINE THE GROUND SHAKING HAZARD ALONG THE WASATCH FAULT ZONE, UTAH

by

W. W. Hays
R. D. Miller and K. W. King
U.S. Geological Survey
Denver, Colorado 80225

INTRODUCTION

Evaluation of the ground-shaking hazard in the Salt Lake City-Ogden-Provo urban corridor is one of the current research goals of USGS. These three cities, which had a population of approximately 900,000 in 1975, are built on unconsolidated deposits of the Pleistocene age Lake Bonneville and are situated on or adjacent to the Wasatch fault zone. The Wasatch fault zone is a 370-km-long north-south trending zone of young, active, normal faulting. Although this fault zone has not generated an earthquake as large as magnitude 6 since 1850, the geologic and geomorphic records contain clear evidence that individual faults in this zone have been active for millions of years and may have the potential for generating a large earthquake (Hamblin, 1976).

THE RESEARCH PROGRAM

The research problem is how to quantify the ground-shaking hazard along the Wasatch fault zone and to depict it in a map format that is useful for guiding engineering, social, or political decisions. From a scientific viewpoint, evaluation of the ground-shaking hazard in the event of a large (e.g., magnitude 7.5) earthquake on the Wasatch fault zone is a complex research task. Its solution requires information about: (1) the regional and local geology, (2) seismicity, (3) the spatial distribution and mean physical properties (e.g., density, shear-wave velocity, thickness, lithology, and water content by weight) of the unconsolidated and consolidated material in the area, and (4) the relative response of the unconsolidated and consolidated material to ground motion. The map must correspond to a small enough geographic area that earthquake source and path effects are negligible and the relative ground responses are essentially repeatable from earthquake to earthquake. The research questions include:

(1) Do the various types of consolidated and unconsolidated material in an area respond to ground motion in a distinct manner?

(2) Are ground-motion data from nuclear explosions adequate for defining the relative response of geologic units to earthquake ground shaking?

(3) Over what range of ground-motion levels and strain does relative ground response behave linearly?

(4) What physical parameters control the horizontal spatial variation of ground response in a geographic area?

(5) Can the technology for constructing ground-shaking hazard maps be transferred to other urban areas?

CURRENT RESEARCH ALONG THE WASATCH FAULT ZONE AND RESULTS

At the present time, only one strong ground-motion record exists in Utah; it was obtained at Logan from the 1962 Cache Valley earthquake. No records have been obtained from past earthquakes in the Wasatch fault zone; therefore, nuclear-explosion ground-motion data were used to estimate the characteristics of ground response in Salt Lake City, Ogden, and Provo. Ground-motion measurements have been made, using broadband L-7 velocity seismographs, at 27 locations in Salt Lake City, 19 locations in Ogden, and 11 locations in Provo. The recording sites were underlain by rock (limestone, shale, sandstone, and quartz monzonite) and unconsolidated material of varying thickness, grain size, water content by weight, and depositional environment.

A representive example of an instrumentation plan is shown in Figure 1 for the Salt Lake City area. The city is built on several different deposits of unconsolidated material that correspond to offshore, nearshore, and onshore depositional environments of Lake Bonneville. The unconsolidated material varies in thickness from about 100 to 900 m, has shear-wave velocities* that typically average about 200 m/s, and exhibits an average natural moisture content by weight of about 43 percent.

Although considerably less information is available to quantify the physical properties of the unconsolidated material in the Provo and Ogden areas, the best available data suggest that the physical properties there are similar to those for Salt Lake City. A bore hole in the Provo area indicates a shear-wave velocity* of about 155 m/s, which can be compared to the range of 55-310 m/s for the soil types in the San Francisco Bay region (Gibbs and others, 1976).

The preliminary results of the research performed to date using nuclear-explosion ground-motion data indicate that a significant ground shaking hazard exists along the Wasatch fault zone. In the event of a

*Data from C. H. Miller, U.S. Geological Survey, Denver, Colorado

moderate earthquake, significant damage would probably occur from ground shaking in this urban corridor and vary as a function of the local ground conditions.

In the Salt Lake City area, the horizontal ground response (defined in terms of the average ratio of 5-percent damped horizontal response spectra for adjacent sites underlain by unconsolidated material and rock) varies as a function of the types and physical properties of the material underlying the site (Hays and others, 1978). The greatest horizontal ground response in the period band 0.1-0.7 second correlates primarily with the occurrence of thick, water saturated, fine grained unconsolidated material (Figure 2). The horizontal ground response for this period band (Figure 3) varies markedly over 15 to 20 km as a function of the laterally varying thickness and acoustic impedance contrast of the unconsolidated material and rock.

The horizontal ground response in the Provo area exhibits different characteristics over the period band 0.1-6.0 seconds than indicated for comparable sites in Salt Lake City. In Provo, the response of the unconsolidated material tends to decrease more rapidly over the period band 0.1-0.8 second (Figure 4) than in Salt Lake City, indicating a difference in the dissipative properties of the unconsolidated material.

CONCLUSIONS

The results of current research on ground response, both along the Wasatch fault zone and in other geographic areas, suggest preliminary answers to the research questions posed earlier. These answers, although based on limited data and somewhat site dependent, suggest the following:

(1) The types of consolidated and unconsolidated material in a geographic area have distinctly different response characteristics to ground shaking. The response of geologic units (including rock) exhibits some variability, but is distinctive enough to identify seismically distinct units (Hays, 1978; Borcherdt and others, 1978).

(2) Nuclear-explosion ground-motion data are useful for estimating the relative response of geologic units to earthquake ground motion. Transfer functions derived from earthquake-and nuclear explosion-ground motion recorded at pairs of sites are usually quite similar (Borcherdt, 1975; Rogers and Hays, 1978).

(3) Relative ground response for some soil types is essentially independent of shear-strain in the 10^{-5} to 10^{-3} strain range (Rogers and Hays, 1978). Above 10^{-3}, deamplification and nonlinear effects can occur (Joyner, 1975).

(4) The horizontal spatial variation of ground response in an area is complex. It can vary by a factor of 10 in some period bands

as a consequence of the laterally varying physical properties of the soil and rock (Murphy and Hewlett, 1975; Rogers and others, 1979).

At the present time, additional research is needed before the technology for constructing ground shaking hazard maps is adequate for earthquake zoning in Utah or in any other area. Progress is being made, however, and such a goal appears to be realizable in the near future for some areas.

RECOMMENDATIONS

The following actions would improve the capability to define the ground-shaking hazard along the Wasatch fault zone:

(1) Installation of strong-motion arrays along the Wasatch fault zone to record future earthquakes. At the present time, only four strong-motion instruments are in Utah.

(2) Measurement of future earthquake ground motions at sites in the Salt Lake City-Ogden-Provo area which have also recorded nuclear-explosion ground motions.

(3) Measurement of future earthquake ground motions near the fault rupture.

(4) Measurement of nuclear-explosion ground motion in an alluvium-filled valley near the source (for example, Yucca Flat, Nevada).

(5) Measurement of nuclear-explosion ground motions at the site in Logan which recorded the August 30, 1962, Cache Valley, Utah, earthquake and at nearby sites underlain by rock and unconsolidated materials of varying thickness and physical properties to define site transfer functions and scaling relations. The Logan accelerogram, the only strong-motion accelerogram recorded in Utah, has recently been processed to derive time histories and spectra. Geotechnical data are also available at the accelerograph site in Logan.

A great deal of research is also needed to develop methodology for depicting the ground-shaking hazard in map formats.

ACKNOWLEDGEMENTS

The Nevada Operations Office of the Department of Energy loaned us their L-7 seismographs which were utilized in this study. Their assistance was invaluable and is gratefully acknowledged. The support of Perry Halstead is especially appreciated.

REFERENCES

Borcherdt, R. D., (Editor) 1975, Studies for seismic zonation of the San Francisco Bay region: U.S. Geological Survey Professional Paper 941-A, 102 p.

Borcherdt, R. D., Gibbs, J. F., and Fumal, T. E., 1978, Progress on ground motion predictions for the San Francisco Bay region, Calif., Proceedings of 2nd International Conference on Microzonation, San Francisco, Calif., v. 1, p. 241-254.

Gibbs, J. F., Fumal, T. E., and Borcherdt, R. D., 1976, In-situ measurements of seismic velocities in the San Francisco Bay region, Part III, U.S. Geological Survey Open-File Report 76-731, 145 p.

Hamblin, W. K., 1976, Patterns of displacement along the Wasatch fault, Geology v. 4, p. 619-622.

Hays, W. W., 1978, Ground response maps for Tonopah, Nevada: Seimol. Soc. America Bull., v. 68, p. 451-467.

Hays, W. W., Algermissen, S. T., Miller, R. D., and King, K. W., 1978, Preliminary ground response maps for the Salt Lake City area: Proceedings of 2nd International Conference on Microzonation, San Francisco, Calif., v. 1, p. 497-508.

Joyner, W. B., 1975, A method for calculating nonlinear seismic response in two dimensions: Seismol. Soc. America Bull., v. 65, p. 1337-1358.

Murphy, J. R., and Hewlett, R. A., 1975, Analysis of seismic response in the City of Las Vegas, Nevada; a preliminary microzonation: Seismol. Soc. America Bull., v. 65, p. 1575-1698.

Rogers, A. M., and Hays, W. W., 1978, Preliminary evaluation of site transfer functions developed from nuclear explosions and earthquakes: Proceedings of 2nd International Conference on Microzonation, San Francisco, Calif., v. 2, p. 753-764.

Rogers, A. M., Tinsley, J. C., Hays, W. W., and King, K. W., 1979, Evaluation of the relationship between near-surface geologic units and ground response in the vicinity of Long Beach, Calif.: Seismol. Soc. America Bull. (in press).

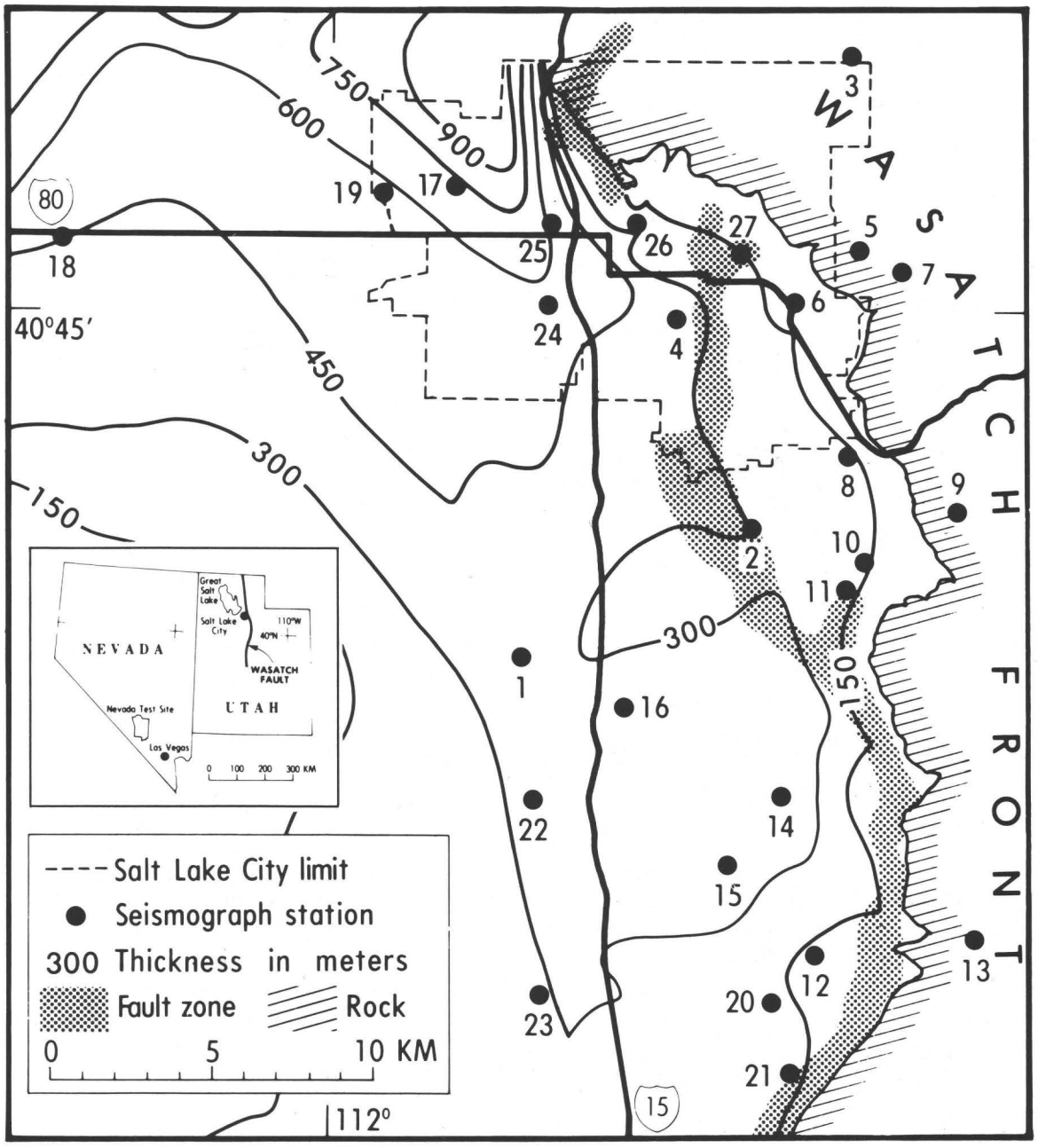

Figure 1. Map showing location of portable L-7 seismographs, thickness of unconsolidated material, and Wasatch fault zone in the Salt Lake City region.

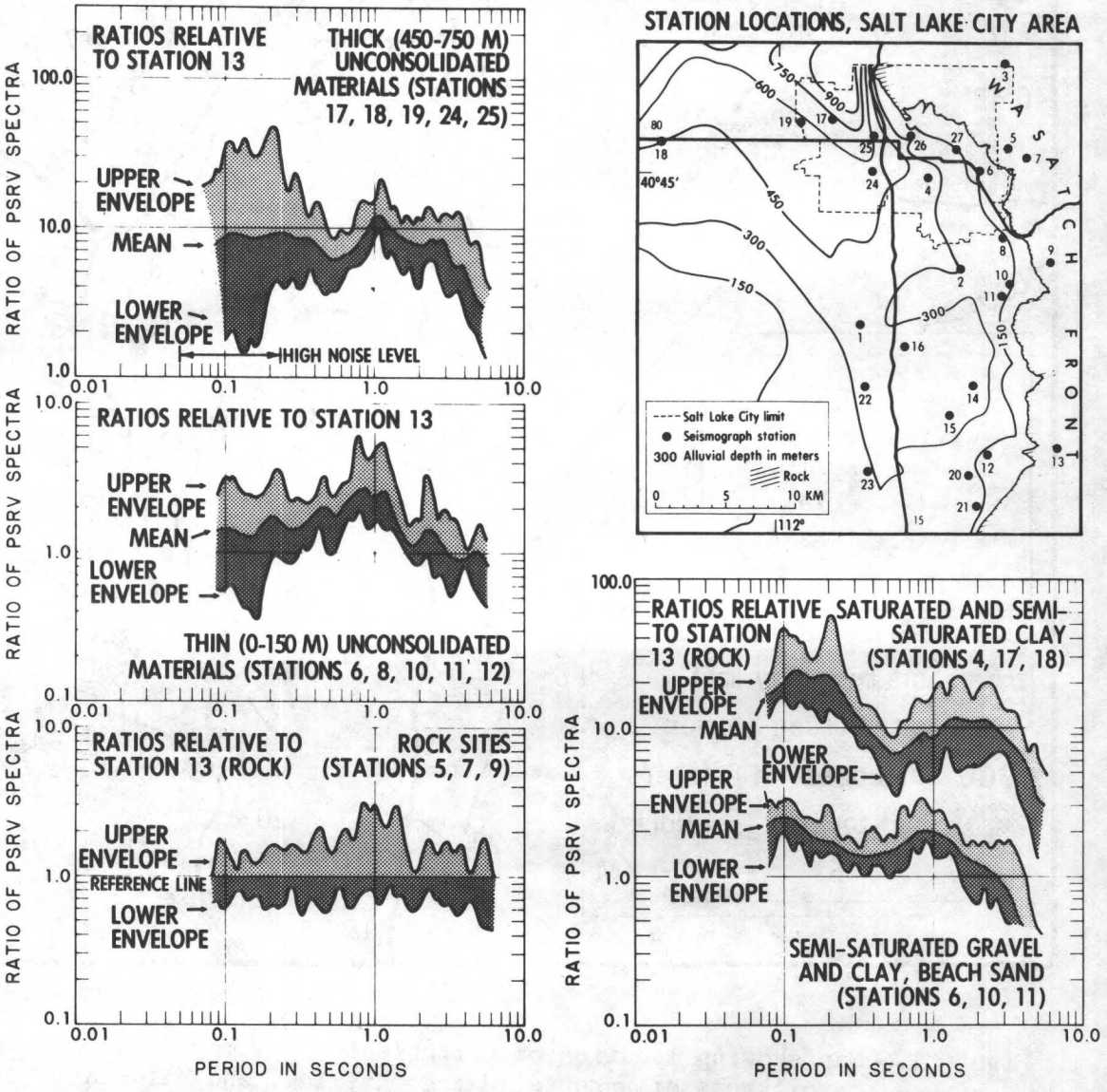

Figure 2. Graphs showing range of relative ground response in terms of thickness and relative water content of the unconsolidated material. The ratios should be treated with caution for periods less than 0.2 second due to high noise level.

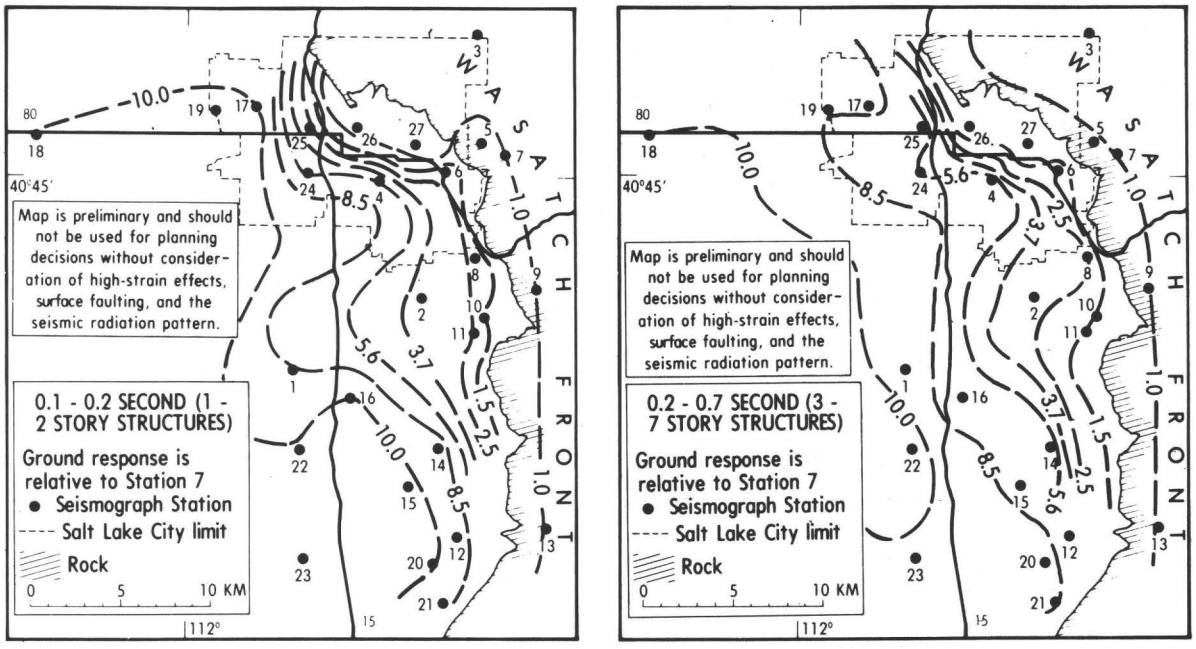

Figure 3. Preliminary maps of the ground shaking hazard, Salt Lake City region. Contours depict the ground response in the 0.1-0.2 and 0.2-0.7 period bands. Values of ground response were determined from transfer functions and are relative to station 7 located on the Wasatch front.

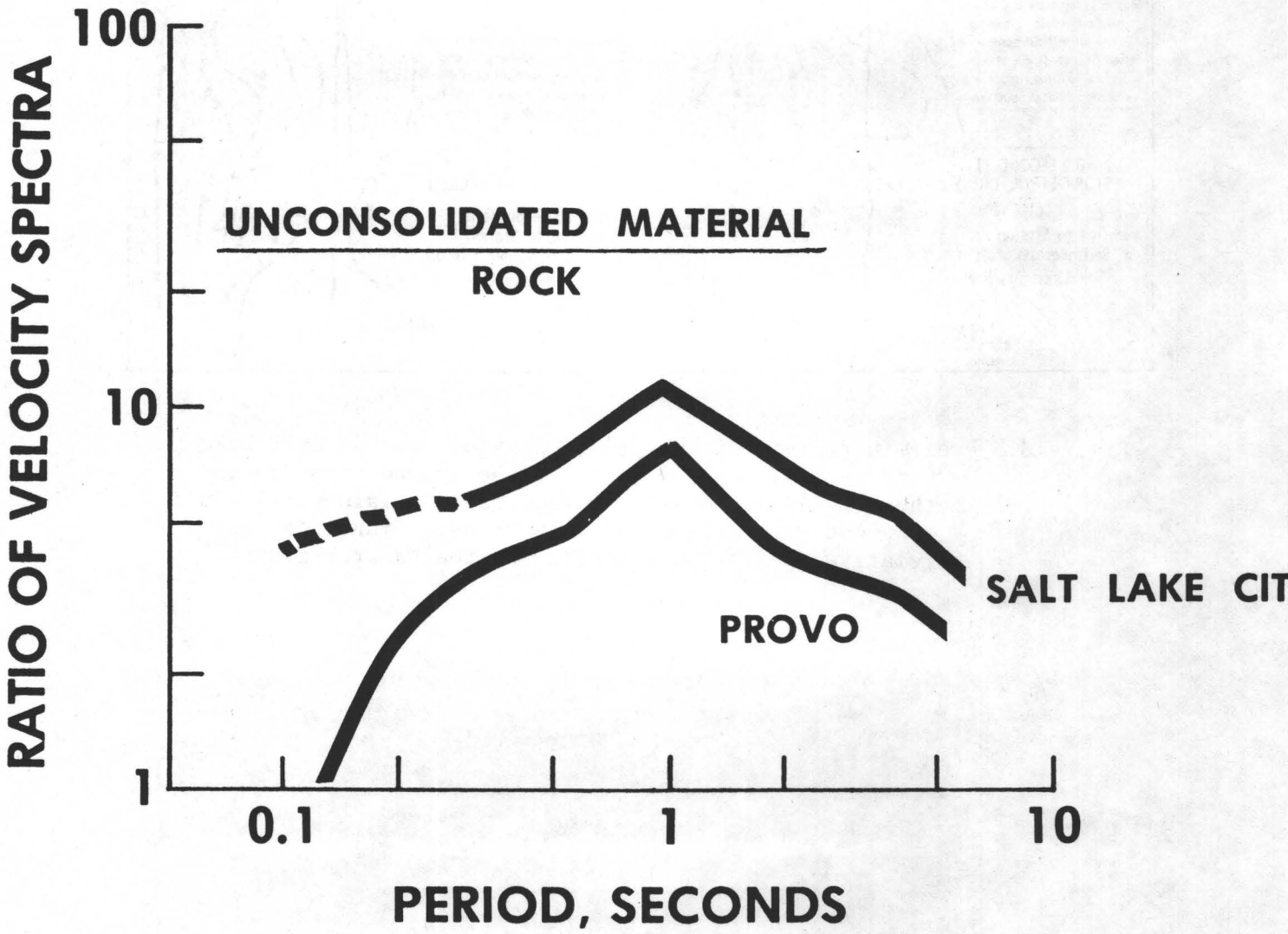

Figure 4. Comparison of mean transfer functions showing the ground response of unconsolidated material representing near-shore depositional environment in the Salt Lake City and Provo areas.

ESTIMATION OF MAXIMUM MAGNITUDE AND RECOMMENDED SEISMIC ZONE CHANGES IN THE WESTERN GREAT BASIN

By
Alan Ryall and J. D. VanWormer

Seismological Laboratory
University of Nevada
Reno, NV 89557

ABSTRACT

Recent seismic zone maps show large values of maximum expected ground motion for the zone of large historic earthquakes in central Nevada, but low values along a zone of major faults in the Sierra Nevada-Great Basin boundary zone (SNGBZ). Estimates of maximum magnitude for this zone, based on a comparison of mapped faults with seismicity, range from 8.0 or greater in the area south of Bishop to 7.5-7.8 in the area between Bishop and Susanville. With population concentrations in the Reno-Carson City-Tahoe area, the northern SNGBZ represents the most serious seismic risk for the Nevada-eastern California region, and seismic zone maps should be changed to reflect this risk. In compiling these maps, magnitude-acceleration relationships should be used that are appropriate to source types and propagation paths in the Great Basin. Relationships between maximum acceleration and magnitude based on source- receiver paths along the California coast (i.e., Schnabel and Seed, 1973) appear to overestimate near-source acceleration in the Great Basin by a factor of 2-4.

INTRODUCTION

The Uniform Building Code (UBC; International Council of Building Officials, 1976) contains a "Seismic Zone Map of the US" derived from a more detailed map presented by Algermissen and Perkins (1976). In the latter study, probabilistic estimates of maximum acceleration in rock are calculated by a method that involves three main steps: (1) delineation of seismic source areas; (2) analysis of the statistical characteristics of historic earthquakes in each seismic source area; and (3) calculation and mapping of the extreme probability Fmax,t(a), of acceleration for some time t. "Source areas" included zones where shocks of MM intensity V or greater have occurred during the historic period, plus areas adjacent to these zones where evidence of Holocene faulting is present. Quaternary or older faults not associated with historic earthquakes were not considered to be source areas.

Results of this analysis for the California-Nevada region are illustrated by a map showing horizontal acceleration (percent of gravity) that has a "90 percent probability of not being exceeded in a 50-year period" (Figure 1). Following directly from the assumptions stated above, the zone of highest probable acceleration is the one in which four major ($M > 7$) earthquakes have occurred in Nevada and eastern California during the his-

toric period (1872 Owens Valley; 1915 Pleasant Valley; 1932 Cedar Mountains; 1954 Dixie Valley-Fairview Peak). Within this zone the maximum probable acceleration is 0.4-0.6 g, while for the remainder of Nevada and eastern California it ranges from 0.04 to 0.2 g. On a similar map, the UBC stipulates that structures within the zone of major historic shocks must be designed for base shear that is one-third higher than the rest of the region.

In a report by the Applied Technology Council (ATC; 1978), seismic zones are proposed that have the same boundaries as political subdivisions (i.e., counties). The report contains proposed maps of "effective peak acceleration" (EPA), and most of Nevada, in contrast to the Algermissen-Perkins map, is assigned the maximum EPA of 0.4 g. However, Ormsby and Storey Counties in western Nevada have EPA of 0.3 g, and Douglas County, Nevada, as well as most the Sierra Nevada in eastern California have values of 0.15-0.2 g. In discussing the philosophy behind these maps the report notes that "the most widely used procedures assume that large earthquakes occur randomly in time, so that the fact that a large earthquake has just occurred in an area does not make it less likely that a large earthquake will occur next year."

SEISMIC CYCLE IN THE WESTERN GREAT BASIN

Work by several authors suggests that these maps present an incorrect assessment of seismic hazard in the western Great Basin. An early study (Ryall et al., 1966) concluded that the tectonic processes causing earthquakes and faulting in the western United States are distributed over broad regions, and that gaps in the seismicity pattern tend to be filled by successive large earthquakes. Later, Ryall (1977) found that the "seismic cycle" -- corresponding to the re-rupture time for major faults -- is of the order of thousands of years long in the Great Basin. A typical large ($M > 7$) earthquake is followed by a decaying aftershock sequence that lasts for about a century, and seismicity in the rupture zone then stabilizes at some minimum level for a long period of time. Foreshock activity, consisting of a moderate level of seismicity, has been observed in the impending rupture zone of two historic earthquakes -- the 1915 Pleasant Valley and 1954 Dixie Valley-Fairview Peak zones -- during a period of at least several decades prior to the mainshock.

Geologic Evidence

Recent studies by Wallace (1977, 1978) support the idea of long re-rupture times in the Great Basin. From analysis of fault-scarp morphology, Wallace estimated the most recent age of displacement for 19 clusters of faults in an area of 17,000 sq km in north-central Nevada. He concluded that no more than seven major events had occurred in this area during Holocene time, leading to an average recurrence rate of 3.4E-5 events per year per 1,000 sq km. Of importance to the question of seismic zoning he observed that fault-scarp morphology in the rupture zones of major historic earthquakes does not suggest faulting at a greater rate than in surrounding areas.

Wallace also reports rates of uplift of range blocks: 0.8 m per 1,000 years for the White Mountains, and 0.5 m per 1,000 years for the Stillwater Range. Based on the assumption that an event with M = 7 would involve an area of approximately 1,000 sq km and an uplift of 3 meters, these values lead to recurrence rates of (1.6-2.7)E-4 such events per year per 1,000 sq km.

In the northern part of the zone, Pease (1979) has studied fault-scarp morphology at several places along the Genoa fault south of Carson City. He found two distinct movements on this fault in the last 4,000 years and 3-4 movements during Holocene time.

Comparison with Rates Determined from Instrumental Data

The results of Wallace and Pease provide an opportunity to compare recurrence rates determined from fault scarp morphology and uplift of mountain blocks with those obtained from lists of instrumentally recorded earthquakes. In the study by Ryall et al. (1966), recurrence rates for the Nevada region were based on an 84,000 sq km area defined by the distribution of historic seismicity. However, studies by Slemmons (1967) and Wallace (1978) indicate that major earthquakes could occur within most of the region containing Holocene faulting, i.e. an area of 225,000 sq km. If we assume that the level of seismicity within this region remains at a constant level but moves from one rupture zone to another as stress is built up and released by large earthquakes, then to calculate the return period for major shocks the recurrence statistics should be applied to the entire 225,000 sq km region of Holocene faulting. Douglas and Ryall (1975) extended the earlier study and found that the recurrence relationship for all western Nevada earthquakes recorded during the 1932-1969 period was

$$\log N = 6.48 - 0.91 M,$$

where N = the cumulative number of earthquakes recorded during the 38-year period with magnitude equal to or greater than M. This corresponds to a return period of about 45 years for events in the western Great Basin with $M > 7.2$, and if we use 225,000 sq km as the area to which this statistic applies, the rate of occurrence of major shocks is about 1.0E-4 per year per 1,000 sq km.

Ryall (1977) gives a recurrence rate, based on approximately 2,000 earthquakes recorded in the Nevada region from 1970 to 1974, of

$$\log N = 4.847 - 0.784 M,$$

which leads to a return period of 31 years for earthquakes with $M > 7.2$, and to a rate of 1.4E-4 per year per 1,000 sq km for such events.

Table 1 summarizes the recurrence rates discussed above, and also gives re-rupture times for faults in areas that have been studied by the various authors. For the instrumentally-determined recurrence rates, re-rupture times were estimated by assuming that a typical rupture zone has

area of about 1,000 sq km, and that such rupture zones comprise the entire area of 225,000 sq km in which Holocene faulting has occurred. Similarly, re-rupture times estimated from fault-scarp morphology or uplift of mountain blocks were converted to recurrence rates by assuming 1.000 sq km for the average rupture zone. Caution should be used in comparing the values in Table 1, since they would be affected in different ways if the assumed rupture zone area were incorrect. With allowance for large errors, the Table indicates general agreement between recurrence rates determined from instrumental and field-geologic data. It also suggests that re-rupture times are relatively longer for faults in north-central Nevada than they area for the SNGBZ.

Over a ten-year period (1969-1978) the University of Nevada Seismological Laboratory has recorded and analyzed more than 5,000 small earthquakes in the western Great Basin (Figure 2) -- generally within the area that contains Holocene faulting (Wallace, 1978). Of approximately 90 events that occurred within Wallace's 17,000 sq km fault-scarp study area in north-central Nevada, more than a third were within or adjacent to the rupture zone of the 1915 Pleasant Valley earthquake. The remainder are scattered about the area, and appear to represent a background level of seismicity that is observed over most of the western Great Basin. Thus, with the possible exception of an extension of the 1915 zone toward the north, present seismicity does not suggest an impending earthquake in any of the zones of faulting studied by Wallace.

ESTIMATION OF MAXIMUM MAGNITUDES

To estimate maximum magnitude for various fault segments in the western Great Basin, we determined the magnitude-fault length relationship

$$\log L \text{ (km)} = -1.388 + 0.4329\ M, \qquad (1)$$

by a least-squares calculation using published instrumental magnitude and length of surface ruptures for eight historic earthquakes in the western Great Basin (Gianella, 1957; Tocher, 1958; Richter, 1958; Kachadoorian et al., 1967). Magnitude for these events ranged from 5.6 to 7.6, and length of surface ruptures was 9-65 km. Standard error of the estimate was 0.127. A ninth event (1934 Excelsior Mountains earthquake, M = 6.3, L = 1.5 km) did not fit the curve and was dropped from the least-squares calculation. Data for the nine events are listed in Table 2.

In the region north of Owens Valley, interpretive maps by various authors (Stewart, 1979; Wright, 1976; Gilbert and Reynolds, 1973; see Figure 2 of this paper and Figures 1 and 7 in VanWormer and Ryall, 1980) show north-trending fault segments 30-70 km long; based on equation (1), this would correspond to magnitudes of 6.6-7.5. In the area north of Reno, northwest-trending fault segments of the Honey Lake and Pyramid Lake zones may be as long as 100 km, corresponding to M = 7.8. From this we conclude that maximum magnitudes in the SNGBZ north of Bishop are in the range 7.5-7.8. South of Bishop, earthquakes in Owens Valley, Fishlake Valley and Death

Valley could have maximum magnitude of 8.0 or greater based on length of faulting.

Figure 2 of this paper and Figures 1, 2, 6, 7 and 8 in VanWormer and Ryall (1980) can also be used to estimate maximum magnitude for specific fault zones, using equation (1). For example, in the area just north of the 1872 Owens Valley rupture zone, earthquake lineups extend to the northwest along an en-echelon series of fault segments that continue to Bridgeport (40 km NW of Mono Lake). If an earthquake involved the entire 120-km length of this zone, it could have magnitude of 8.0. Earthquake lineups also occur along NNE-trending faults in the area north of Bishop (Figure 2 in VanWormer and Ryall), but the length of potential rupture zones in this area is limited to about 60 km (M = 7.3) by the "structural knee" east of Mono Lake (Gilbert et al., 1968). In the Garfield Hills southeast of Walker Lake (Figure 6 in VanWormer and Ryall) a north-trending group of epicenters forms a zone about 50 km long, corresponding to M = 7.1. From a cluster of epicenters near Markleeville (Figure 8 in VanWormer and Ryall) earthquakes are distributed along a group of east-dipping faults on the east side of Carson Valley, perhaps extending to an earthquake swarm at Steamboat Hot Springs (10 km south of Reno). The length of this zone is about 70 km, corresponding to M = 7.5. In the Truckee area west of Reno, clusters at both ends of a 25-km long fault in Dog Valley (Figure 8 in VanWormer and Ryall) indicate a potential magnitude of 6.4. For the area between Mono Lake and Markleeville, and the Pyramid Lake and Honey Lake areas north of Reno, network coverage has been inadequate for a detailed discussion of maximum magnitudes.

DISCUSSION

Evidence from studies of fault scarp morphology, rate of uplift of mountain blocks and instrumental seismology strongly supports the sequence of strain accumulation and release by earthquakes in the western Great Basin suggested previously by Ryall (1977). A typical large (M > 7) earthquake is followed by a decaying aftershock sequence that lasts for about a century, and activity then stabilizes at a low level for centuries or even thousands of years. Foreshock activity in this region appears to consist of a moderate increase in seismicity within with impending rupture zone or in the vicinity of the impending mainshock, continuing over a period of at least several decades prior to the major event. This does not agree at all with the idea of random occurrence of large earthquakes (Applied Technology Council, 1978), nor does it agree with a philosophy of assigning maximum probable acceleration to rupture zones that have had the most recent large earthquakes (Algermissen and Perkins, 1976). Contrary to present zoning dogma, rupture zones of the most recent large earthquakes could actually be the seismically "safest" areas in the Great Basin, since major earthquakes would not be expected to recur in these particular zones for perhaps thousands of years.

This poses a dilemma for agencies charged with seismic zoning in this region. Until methods are found to discriminate foreshock activity from other types of moderate seismicity (Ryall and Ryall, 1980), recurrence estimates based on historic or current earthquake distributions are not directly applicable to the problem of identifying the most likely locations of future large earthquakes. Eventually, seismic zoning of the Great Basin should be based on a model of the type proposed by Patwardhan et al. (1978) and applied to the Wasatch fault zone by Cluff et al. (1980). In such a model the probability that the next significant earthquake will have a given magnitude depends on the magnitude of the previous earthquake; the model also provides for the distribution of a "holding time" between successive earthquakes, which is also a function of magnitude. Unfortunately, the technique requires knowledge of elapsed time since the last earthquake in each rupture zone, as well as its magnitude. While both of these parameters can be estimated from detailed studies of fault scarp morphology, they are not now available for most faults in the western Great Basin.

Pending the accumulation of more complete data on fault scarp morphology, seismic zonation of the western Great Basin should be modified to show high values of maximum acceleration in fault zones that meet the following criteria: (1) capability for large earthquakes evidenced by previous offsets during late Quaternary time; (2) moderate level of seismicity based upon an extensive sample of small earthquake and microearthquake data; and (3) no major offsets during the historic and very recent prehistoric period. Lower values of acceleration should be assigned to rupture zones of very recent earthquakes and moderate values to areas that have capable faults which are relatively aseismic at the present time.

With regard to estimating acceleration as a function of magnitude for the Great Basin, it should be noted that source and propagation effects in this region appear to result in lower peak accelerations than would be observed for earthquakes of the same magnitude in California coastal areas. As noted by Evernden (1975), large felt areas for Nevada earthquakes are attributable in part to favorable propagation, rather than energy released at the source. His analysis of isoseismal patterns for large earthquakes indicated that acceleration attenuates with distance D as D**(-1.5) in the Great Basin and as D**(-1.75) for earthquakes along the California coast. He then proposed a revised magnitude formula that corrects for regional attenuation differences to produce estimates that are consistent in terms of energy released at the earthquake source. In general, Evernden's conclusions about attenuation differences are supported by observations of Murphy and Lahoud (1969) for the large explosions recorded on hard rock in the Great Basin, and by the results of Schnabel and Seed (1973) for large earthquakes along the California coast at distance ranges of 5-50 km. Using Evernden's attenuation factors and assuming that Richter magnitude ML for a large shock is determined from data collected at least several hundred kilometers from the causative fault, a simple calculation indicates that acceleration in the epicentral area would be 2-4 times lower for an earthquake in the Great Basin than for one with identical ML near the coast.

Two cases illustrate this point. First, of the major earthquakes that have produced surface faulting in the western Great Basin during historic time, the 1872 Owens Valley shock had the longest rupture zone and the largest felt area. According to Oakeshott et al. (1972), "faulting and rupturing took place along a portion of the Sierra Nevada fault zone for a distance of nearly 100 miles." From equation (1) with L = 160 km, this would correspond to M = 8.3, which is the same value Oakeshott et al. obtained from a comparison of the 1872 felt area with those of the 1906 San Francisco and 1954 Fairview Peak shocks. Evernden discusses this earthquake and concludes that the isoseismal pattern is explainable in terms of energy release by an an earthquake fifty times smaller than the San Francisco earthquake. His revised "magnitude" for the 1872 event is 7.2, using a formula that relates acceleration to magnitude, distance from the causative fault, local attenuation, fault length and a parameter related to depth of focus.

Maximum vibratory intensities of VII-VIII for an earthquakes with Richter magnitude 7.1 at Hebgen Lake, Montana (see discussion on p. 231 of Steinbrugge and Cloud, 1962) provide another example of relatively lower peak acceleration as a function of Richter magnitude for areas with normal faulting and favorable propagation. According to Trifunac and Brady (1976) intensities of VII-VIII would be associated with peak acceleration of 0.07-0.17 g, which is at least a factor of 4 less than the value (0.7 g) from curves of Schnabel and Seed (1973) for points less than a mile from the causative fault of an earthquake with M = 7.1.

A detailed study aimed at improving magnitude estimates for earthquakes in the western Great Basin is now in progress (M. R. Somerville, verbal communication), but results are not yet available. Consequently, we have used equation (1) in this paper to estimate magnitudes ML or MS (Richter, 1958) rather than values that depend on regional attenuation factors. However, the reader should keep in mind that although our maximum magnitude values can be used to predict felt area of potential earthquakes within the SNGBZ, attenuation relationships appropriate to the western Great Basin must be used to convert them to an estimation of strong ground motion. Based on the above discussion, for example, peak accelerations determined using our maximum magnitude values and the curves of Schnabel and Seed (1973) could be overestimated by at least a factor of two.

ACKNOWLEDGEMENTS

W. A. Peppin and M. R. Somerville reviewed the manuscript and made helpful suggestions. This research was partly supported by the US Geological Survey, under contract number 14-08-0001-16741.

REFERENCES

Algermissen, S. T. and D. M. Perkins (1976). A Probabilistic Estimate of Maximum Acceleration in Rock in the Contiguous United States, US Geological Survey, Open-File Rept. 76-416. 45 pp.

Applied Technology Council (1978). Tentative Provisions for the Development of Seismic Regulations for Buildings, National Bureau of Standards, 514 pp.

Cluff, L. S., A. S. Patwardhan and K. J. Coppersmith (1979). Estimating the probability of occurrence of surface faulting earthquakes on the Wasatch fault zone, Utah, this volume.

Douglas Bruce and Alan Ryall (1975). Return periods for rock acceleration in western Nevada, Bull. Seism. Soc. Am. 65 (6), 1599-1611.

Evernden, J. F. (1975) Seismic intensities, "size" of earthquakes and related matters, Bull. Seism. Soc. Am., 65 (5), 1287-1313.

Gianella, V. P. (1957). Earthquake and faulting, Fort Sage Mountains, California, 1950. Bull. Seism. Soc. Am., 47 (3), 173-177.

Gilbert, C. M., M. N. Christensen, Y. T. Al-Rawi and K. R. Lajoie (1968). Structural and volcanic history of Mono Basin, California-Nevada, Geol. Soc. Am.. Memoir 116, 275-329.

Gilbert, C. M. and M. W. Reynolds (1973). Character and chronology of basin development, western margin of the Basin and Range province, Bull. Geol. Soc. Am., 84, 2489-2510.

International Council of Building Officials (1976). Uniform Building Code, Whittier, California, 728 pp.

Kachadoorian, R., R. Yerkes and A. Waananen (1967). Effects of the Truckee, California, Earthquake of September 12. 1966, US Geol. Survey Circular 537.

Murphy, J. R. and J. A. Lahoud (1969). Analysis of seismic peak amplitudes from underground nuclear explosions, Bull. Seism. Soc. Am., 59 (6), 2325-2342.

Oakeshott. G. B., R. W. Greensfelder and J. E. Kahle (1972). The Owens Valley earthquake of 1872: one hundred years later, Calif. Geology, 25, 55-62.

Patwardhan, A. S., R. B. Kulkarni and Don Tocher (1978). A semi-Markov model for characterizing recurrence of great earthquakes, US Geol. Survey, Open- File Report 78-943, 635-685.

Pease, R. C. (1979). Scarp Degradation and Fault History near Carson City, Nevada, Univ. Nev. MS Thesis, 95 pp.

Richter, C. F. (1958). Elementary Seismology, W. H. Freeman Co., 768 pp.

Ryall, A., D. B. Slemmons and L. D. Gedney (1966). Seismicity, tectonism and surface faulting in the western United States during historic time, Bull. Seism. Soc. Am., 56 (5), 1105-1135.

Ryall, A. (1977). Seismic hazard in the Nevada region, Bull. Seism. Soc. Am., 67, 517-532.

Ryall, A. and F. D. Ryall (1980). Anomalous patterns of earthquake occurrence in the Sierra Nevada-Great Basin boundary zone, this volume.

Schnabel, P. B. and H. B. Seed (1973). Accelerations in rock for earthquakes in the western United States, Bull. Seism. Soc. Am., 63 (2),

Slemmons, D. B. (1967). Pliocene and Quaternary crustal movements of the Basin and Range province, USA. Jour. Geoscience, 10, 91-103, Osaka City Univ.

Steinbrugge, K. V. and W. K. Cloud (1962). The earthquake at Hebgen Lake, Montana, on August 18, 1959: Epicentral intensities and damage, Bull. Seism. Soc. Am., 52 (2), 181-234.

Stewart, J. H. (1979). Basin-range structure in western North America: a review, Geol. Soc. Am. Memoir 152, 1-31.

Tocher, D. (1958). Earthquake energy and ground breakage, Bull. Seism. Soc. Am., 48, 147-153.

Trifunac, M. D. and A. G. Brady (1975). On the correlation of seismic intensity scales with the peaks of recorded strong motion, Bull. Seism. Soc. Am., 65 (1), 139-162.

VanWormer, J. D. and Alan Ryall (1980). Seismicity related to structure and active tectonic processes in the western Great Basin, Nevada and eastern California, this volume.

Wallace, R. E. (1977). Profiles and ages of young fault scarps, north-central Nevada, Bull. Geol. Soc. Am., 88 (9), 1267-1281.

Wallace, R. E. (1978). Patterns of faulting and seismic gaps in the Great Basin province, US Geol. Survey, Open-File Rept. 78-943, 857-868.

Wright, L. (1976). Late Cenozoic fault patterns and stress fields in the Great Basin and westward displacement of the Sierra Nevada block, Geology, 4, 489-494.

Table 1. Re-rupture times for faults in the Great Basin. Values with asterisks were calculated on the assumption that a typical rupture zone has area of 1,000 sq km, and that such rupture zones comprise the entire 225,000 sq km region containing Holocene scarps in the western Great Basin.

Reference	Area	Recurrence time for ML > 7.0, per year per 1,000 sq km	Re-rupture time, years
Wallace (1978):			
	North-central Nevada	3.4E-5	29,000*
	Stillwater front	1.6E-4*	6,300
	White Mountains	2.7E-4*	3,700
Pease (1979):			
	Northern Sierra-Nevada	(2-5)E-4*	2,000-5,000
This paper from instrumental data for 1932-1969 and 1970-1974:			
	Western Great Basin	(1.0-1.4)E-4	7,000-10,000*

Table 3. Magnitude and length of surface ruptures for historic earthquakes in the western Great Basin. Data from Gianella (1957), Tocher (1958), Richter (1958), Kachadoorian et al. (1967).

Date	Location	M	L, km
10/2/1915	Pleasant Valley	7.6	65
12/21/1932	Cedar Mountains	7.2	61
1/30/1934	Excelsior Mountains	6.3	1.5
12/14/1950	Fort Sage Mountain	5.6	9
7/6/1954	Rainbow Mountain	6.6	18
8/23/1954	Stillwater	6.8	30
12/16/1954	Fairview Peak	7.1	59
12/16/1954	Dixie Valley	6.9	62
9/12/1966	Truckee	5.7	16

FIGURE TITLES

Figure 1. Preliminary map of horizontal acceleration (expressed as percent of gravity) in rock with 90 percent probability of not being exceeded in 50 years (Algermissen and Perkins, 1976).

Figure 2. Generalized map of late Cenozoic structural features of the western Great Basin (Wright, 1976), together with epicenters of small earthquakes for 1969-1978 (dots) and approximate rupture zones of major historic earthquakes (stippled areas, with year of main shock). Note: seismic network coverage was not uniform for the period of observation; best coverage was in areas around Reno and between Walker Lake and Mono Lake.

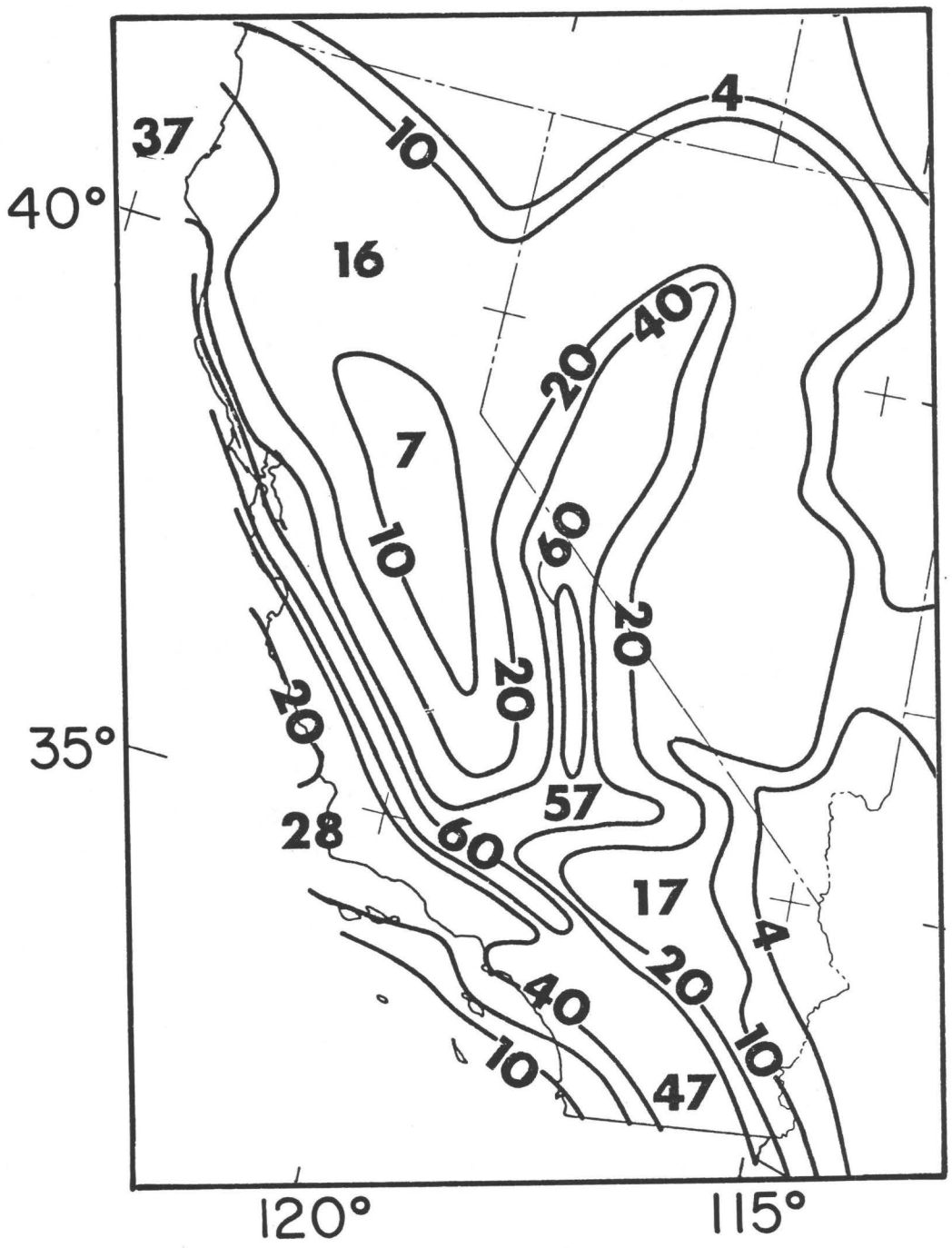
40°
35°
120°
115°
37
10
4
16
40
20
7
10
60
20
20
20
57
28
60
17
4
20
40
10
10
47

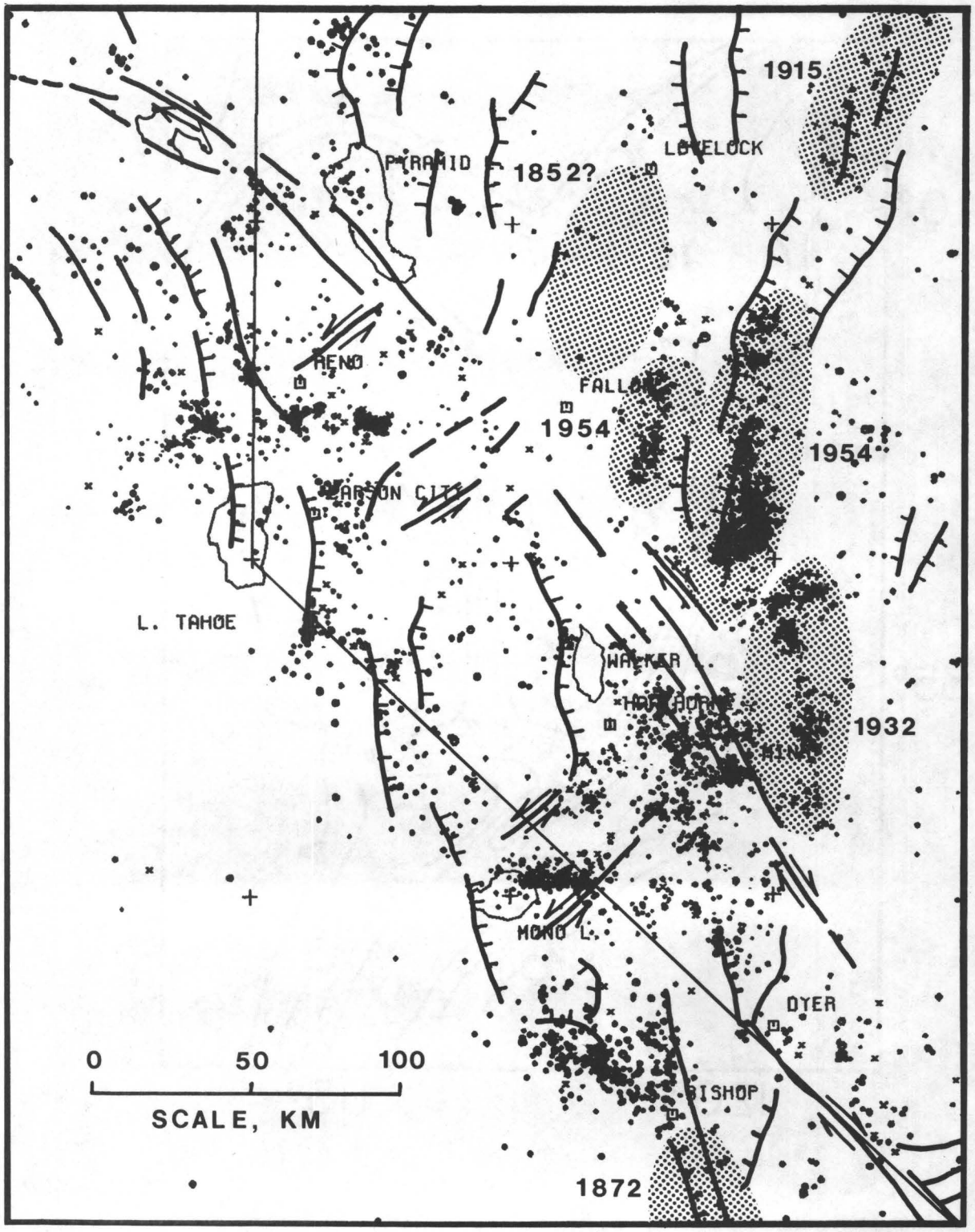
1915
LOVELOCK
PYRAMID
1852?
RENO
FALLON
1954
1954
CARSON CITY
L. TAHOE
WALKER
1932
MONO L.
DYER
0
50
100
SCALE, KM
BISHOP
1872

QUATERNARY FAULTING IN UTAH

By

Larry W. Anderson and Darryl G. Miller
Fugro, Inc., Consulting Engineers and Geologists
3777 Long Beach Boulevard
Long Beach, California 90807

INTRODUCTION

In the western United States, maps showing potentially hazardous faulting have been produced for California, Idaho, Montana, Wyoming, and Colorado (Jennings, 1975; Witkind, 1975a, 1975b, 1975c; Kirkham and Rogers, 1978). These maps have proven to be particularly useful to geologists, seismologists, engineers, and planners for conducting preliminary siting studies, fault hazard assessments, and basic overview studies.

Because such a map was needed for the state of Utah, the accompanying map (Fig. 1) was compiled showing known and suspected Quaternary faults in the state. The compilation is based on published literature and ongoing unpublished research. This map, a larger scale, "Preliminary Quaternary Fault Map of Utah" (Anderson and Miller, in press), and accompanying data (Appendices A, B, and C) present the current state of knowledge concerning Quaternary faulting in Utah. The maps and tabular data are not intended to substitute for detailed site investigations because many Quaternary faults, or faults capable of future movement, may exist that have not yet been identified. Our intent with this paper is to compile the available information in hope that it will stimulate additional investigations of the age and extent of Quaternary faulting within the state.

GEOLOGIC AND TECTONIC SETTING

The state of Utah includes portions of the Basin and Range, Colorado Plateau, and Middle Rocky Mountains physiographic provinces. The structural boundary between the Basin and Range and Colorado Plateau-Rocky Mountains is transitional; however, the physiographic boundaries of Fenneman (1931) have been adopted for our descriptions of Quaternary fault activity.

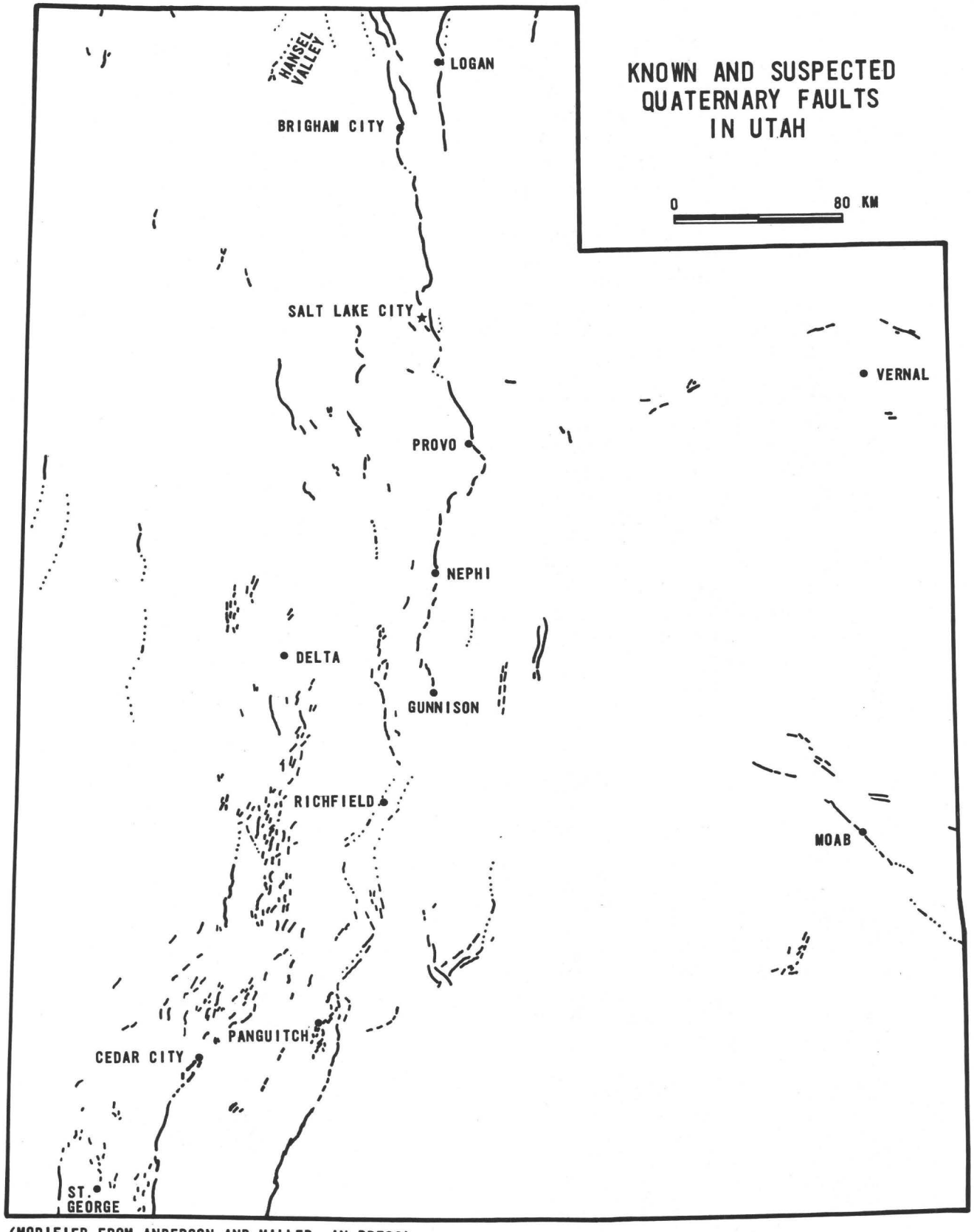

(MODIFIED FROM ANDERSON AND MILLER, IN PRESS)

FIGURE 1

Perhaps one of the most direct manifestations of neotectonic activity is ongoing seismicity. Most of Utah's historic damaging earthquakes have occurred near the boundary between the Basin and Range and Colorado Plateau-Rocky Mountains provinces (Cook and Smith, 1967; Smith and Sbar, 1974; Smith, 1978). This zone of distinctively higher ongoing seismicity has been termed the Intermountain seismic belt (Smith and Sbar, 1974). However, evidence of Quaternary faulting also is widespread along this boundary (Fig. 1), and geologic evidence suggests that most of these faults have experienced recurrent movement throughout the Quaternary. Major faults associated with the boundary include the Wasatch and Cache Valley faults, the Tushar-Elsinore fault, and the Sevier and Hurricane faults.

There are three dominant structural trends in Utah: north-south in the Basin and Range, east-west in the Uinta Mountains, and northwest-southeast in the Colorado Plateau. Most late Cenozoic faults in Utah strike roughly north-south, reflecting the east-west extension that began in middle Miocene time and has continued into the present. The east-west to northeast-southwest striking faults of the Uinta Mountains area may reflect older Laramide tectonics. The northwest-southeast and randomly oriented faults in southeastern Utah are of questionable tectonic origin; instead, they may be the result of salt migration beneath the overlying bedrock (Kelley and Clinton, 1960; Howard and others, 1978).

FAULT CLASSIFICATION

Three categories of faults were identified during this study. They are:

Holocene Faults - Faults which have experienced known or show strong evidence of probable movement during the Holocene (0 to about 10,000 B.P.). Evidence for this designation consists of steep, relatively unmodified scarps in alluvium (see Bucknam and Anderson, 1979a), or offset Holocene or latest Pleistocene alluvial, glacial, or volcanic deposits.

Late Pleistocene Faults - Faults which have had known or show evidence of probable late Pleistocene movement (10,000 to about 500,000 B.P.). Evidence for this designation consists of scarps in unconsolidated alluvial or lacustrine deposits, or displacement of alluvial, lacustrine, glacial, or volcanic rocks dated at less than approximately 500,000 B.P. Subsequent studies may show that some of these faults have also moved during the Holocene.

Suspected Quaternary Faults - Faults of suspected Quaternary age (0 to about 2 or 3 m.y. B.P.). These are generally inferred or concealed faults that have been identified because of their probable association with known late Quaternary faults. Faults which displace deposits of late Pliocene or early to middle Pleistocene age, or faults which displace deposits of uncertain but probable Pleistocene age, are also shown as suspected Quaternary faults.

Nearly all age dates used in compiling the fault data are approximate. Absolute dates on the age of last movement on specific fault segments are lacking in nearly all cases. As dating techniques improve and as more detailed fault studies are completed, refinements in the age assignments can and will be made.

The areas covered by the references used in compilation are shown in Figure 2. Differences in the quality and quantity of data available have resulted in some subjective interpretations to produce the final map and accompanying data. These interpretations remain the responsibility of the authors.

DATING CRITERIA

Various criteria have been used to assign ages to the faults of Utah. For faults displacing dated volcanic rocks, the age of the rocks is used as the maximum age of faulting. As an example, faults displacing basalts believed to be 10,000 to 20,000 B.P. are assumed to be of probable Holocene age. Faults displacing rocks of about 500,000 B.P. or less are assumed to be of late Pleistocene age although they could be younger. Faults displacing rocks with dates of approximately 500,000 B.P. to 3 m.y. B.P., as well as undated volcanic rocks believed to be of Quaternary age, are mapped as suspected Quaternary faults. The possibility exists that such faults could have late Pleistocene or even Holocene movement.

The following criteria have been used for faults mapped as displacing surficial Quaternary deposits. First, if the fault has been identified and dated in the literature, that age is used in our assignment. Secondly, faults mapped and identified as scarps in alluvium have been assigned a late Pleistocene age. We feel this assumption is justified based on scarp degradation rates (Wallace, 1977; Buckman and Anderson, 1979a). Also, faults shown displacing "younger" alluvium are assigned a late Pleistocene age. Finally, faults offsetting deposits of questionable Quaternary age, faults displacing "older" alluvial deposits, faults with geomorphic evidence of Quaternary activity but which displace pre-Quaternary units, and faults whose

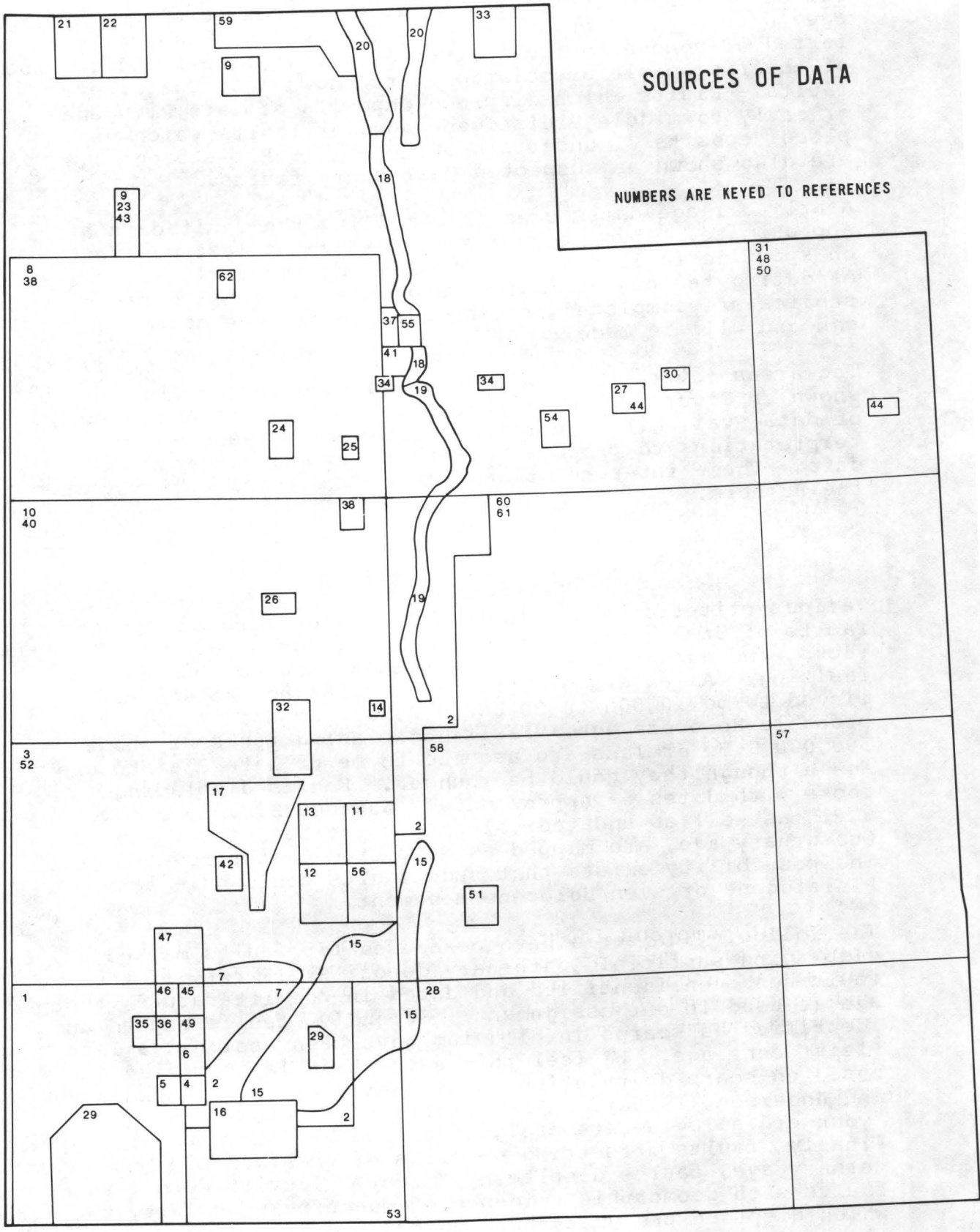
SOURCES OF DATA
NUMBERS ARE KEYED TO REFERENCES
21
22
59
9
20
20
33
18
9
23
43
8
38
62
37
55
41
18
34
19
34
27
44
30
31
48
50
44
54
24
25
10
40
38
60
61
26
19
32
14
2
3
52
58
57
17
13
11
2
42
12
56
15
51
47
15
7
1
46
45
7
28
35
36
49
15
29
6
5
4
2
15
16
2
29
53

FIGURE

existence and/or age has been questioned by different investigators are all shown as suspected Quaternary faults. Only those faults of certain Holocene age or those for which there is compelling evidence of Holocene activity (such as the Wasatch fault) have been shown as Holocene.

BASIN AND RANGE PROVINCE

Extensional block faulting began nearly simultaneously throughout the Basin and Range approximately 17 million years ago (Stewart, 1978). In western Utah, faulting was accompanied by fundamentally basaltic volcanism and deposition of alluvial basin-fill deposits. Faulting and volcanism have continued into the Quaternary. During the Quaternary, most of the basins of the region were filled by pluvial lakes. The largest of these lakes was Lake Bonneville, which covered up to 51,900 km^2 during the late Pleistocene. Spits, bars, and deltaic deposits are common along the margins of the former lake, and fine-grained, deep-water deposits are found in the center of the basins. Alluvial fans have been deposited along the margins of the basins throughout the Quaternary.

Although Quaternary alluvial deposits are extensive in western Utah, the deposits are not well dated. Most geologic maps differentiate only a "Quaternary alluvium" or at most, "older" and "younger" Quaternary deposits. Even the traditional Lake Bonneville chronology of Morrison (1965a, 1965b, 1966) is strongly debated (Scott, 1979a, 1979b, this volume). Thus, the poor dating control for the alluvial and lacustrine deposits has led to the use of fault scarp morphology to determine the approximate age of faulting (Wallace, 1977; Bucknam and Anderson, 1979a).

Geophysical data suggest the presence of many late Cenozoic faults in the Basin and Range of Utah (Cook and Berg, 1961; Cook and others, 1964, 1966; Cook and Hardman, 1967). Direct evidence of Quaternary faulting is lacking in some areas but numerous faults have been identified (Fig. 1, Appendix A). Much of our information on faulting in western Utah comes from the work of Bucknam (1977), Bucknam and Anderson (1979a, 1979b), Anderson and Bucknam (1979), and their unpublished work.

Major Faults

North-central Utah is one of the most seismically active areas of the state (Cook and Smith, 1967; Smith, 1978). The only historic earthquake in Utah known to be associated with surface rupture occurred in this area in Hansel Valley, at the north end of the Great Salt Lake on March 12, 1934. This 6.6-magnitude earthquake produced a series of scarps

up to 50 cm in height in an area of older Holocene scarps (Neumann, 1936; R. C. Bucknam, 1979, personal commun.). Much of the ground surface in the area was affected by liquefaction, and numerous springs developed in the area immediately after the event. Excellent descriptions of the effects of the earthquake are given by Walter (1934) and Neumann (1936).

Approximately 90 percent of Utah's population lives along the Wasatch fault zone which extends for over 300 km from Gunnison, Utah, to Malad, Idaho. This fault is usually considered the boundary between the Basin and Range and Middle Rocky Mountains. Although no large ($M \geq 7.0$) earthquakes have occurred along the fault since pioneer settlement, evidence of youthful fault activity is common. Absolute dates on the age of last movement of specific fault segments are available for only a few locations. Studies are presently under way to date the most recent movements and establish earthquake recurrence intervals (Swan and others, 1979, this volume; Schwartz and others, 1979).

From the Utah-Idaho border to Brigham City, the Wasatch fault zone has a more subdued appearance than it does from Brigham City to Nephi (Cluff and others, 1974), suggesting that the northern portion of the fault has not been as active in recent time as has the southern portion. Because there is a lack of youthful scarps north of Brigham City, we consider most of the recent movements on the northern portion of the fault to be of probable late Pleistocene age.

Further south, Brigham City to Nephi, geomorphic evidence of young fault activity is widespread (Cluff and others, 1970, 1973). Recent investigations near Kaysville, 30 km north of Salt Lake City, and Springville, 46 km southeast of Salt Lake City, indicate repeated fault movements during Holocene time (Swan and others, this volume). In addition, the geomorphic evidence of youthful, probable Holocene displacements in eastern Salt Lake City (Van Horn, 1972), at the mouth of Little Cottonwood Canyon (Morrison, 1965a), at Rock Creek Canyon near Provo (Hintze, 1971), and along the base of Mt. Nebo (R. C. Bucknam, 1979, personal commun.) suggests the entire fault system from Nephi to Brigham City should be suspected of having Holocene age movement.

From Nephi to Gunnison (the southern portion of the Wasatch fault zone), fault scarps are often discontinuous (Cluff and others, 1973; Anderson and others, 1978). The scarps are tentatively mapped as Holocene age based on the descriptions of the scarps given in Cluff and others (1973) and Anderson and others (1978).

In west-central Utah, Quaternary volcanics of various ages are displaced by over 350 predominantly normal faults.

Basalts dated at 0.88 m.y. B.P. (Peterson and others, 1978) are offset by a series of roughly north-south trending faults at Fumarole Butte (Morris, 1978; Bucknam and Anderson, 1979b). Hoover (1974) has mapped a series of Quaternary faults in the Black Rock Desert, and Clark (1977) has identified faults in the Cove Fort area. The faults shown as Holocene by Hoover (1974) displace basalts believed by him to be about 24,000 to 10,000 B.P. and less than 4,000 B.P. The age of the faults shown as late Pleistocene and suspected Quaternary are also based on the age of basalt that is displaced. The faults mapped by Clark (1977) displace lavas ranging in age from approximately 30,000 to 3.0 m.y. B.P. The late Pleistocene and suspected Quaternary ages given the faults in the Cove Fort and Black Rock Desert areas probably represent maximum ages for the faults; they could be younger.

The main late Cenozoic tectonic features of southwestern Utah are the Grand Wash, Hurricane, and Sevier fault systems. Movement along the Grand Wash fault may be of early Quaternary age because late Tertiary basalts (6 m.y. B.P.) are displaced over 200 m in northern Arizona (Hamblin, 1970). Additional suspected Quaternary faults have been identified by W. K. Hamblin (1978, unpub. data) north of St. George. Along the Hurricane fault, approximately 600 m of probable Quaternary displacement has occurred (Anderson and Mehnert, 1979, Anderson, this volume). Basalt flows of probable Quaternary age are offset about 60 m near the town of Hurricane (Hamblin, 1970). From the available evidence, the Hurricane fault has been recurrently active during the Quaternary (Best and Hamblin, 1978) and is considered to be of late Pleistocene age. Faults west of the main Hurricane fault zone displace Quaternary basalts and alluvial deposits (W. K. Hamblin, 1978, personal commun.; R. E. Anderson, 1979, personal commun.), and are also of probable late Pleistocene age.

MIDDLE ROCKY MOUNTAINS PROVINCE

The Wasatch and Uinta Mountains are the major ranges of the Rocky Mountains in Utah. The Wasatch Mountains are geologically similar to the ranges of the Basin and Range. The boundary between the Basin and Range and Rocky Mountains is usually shown at the western flank of the Wasatch Mountains (Fenneman, 1931), although north-south trending normal faults are found considerably east of the Wasatch fault.

Uplift of the Wasatch Mountains probably began less than 20 m.y. ago (Hintze, 1971). This uplift apparently was related to the inception of Basin and Range faulting in the region. The Uinta Mountains are the largest Laramide structure in Utah. Major uplift of that range began in late Cretaceous and continued at least into the Eocene (Hintze, 1973).

Alluvial, lacustrine, and glacial deposits are fairly widespread throughout the region. Few of the deposits are well-dated, and most studies of these deposits have been of a reconnaissance nature. For example, Atwood (1909) studied the glacial geology of the Wasatch and Uinta Mountains and Williams (1962) studied Lake Bonneville deposits in southern Cache Valley. Cluff and others (1974) investigated recent fault activity in the Cache Valley area by the use of low-sun-angle photography. To date, this has been the only systematic study of Quaternary faulting in the Rocky Mountains region of Utah.

Earthquakes in the magnitude 4.0 to 5.7 range are numerous in the region (Cook and Smith, 1967; Smith, 1978), but none has been associated with surface rupture. Appendix B lists the Quaternary faults identified in Figure 1.

Major Faults

Cache Valley is an asymmetrical graben approximately 13 to 30 km in width, located approximately 10 km east of the Wasatch Front. Quaternary faults that bound the valley have been investigated by Cluff and others (1974).

The West Cache Valley fault system parallels the east side of the Wellsville Mountains and Malad Range. Based on the description of Cluff and others (1974), most of the fault zone is probably of late Pleistocene age. Near Cache Butte, Lake Bonneville deposits of probable late Wisconsin (Provo) age are apparently displaced. This fault segment is probably of Holocene age.

The East Cache Valley fault zone parallels the west side of the Bear River Range. It also has been studied by Cluff and others (1974). The only area which appears to have young, possibly Holocene displacement is immediately east of Logan. There, late Wisconsin (Provo age) Lake Bonneville deposits are offset about 2 m. Most of the fault zone appears to be of late Pleistocene age.

Ritzma (1974) identified the Towonta Lineament in northern Utah. A few faults with evidence of Quaternary activity have been identified along the trend of the lineament south of the Uinta Mountains. Garvin (1969) has mapped the east-west-trending Little Valley fault about 3 km north of Tabiona, believed to be late Pleistocene (H. R. Ritzma, 1978, personal commun.). Ritzma (1978, personal commun.) has also mapped a northeast striking late Pleistocene fault 5 km east of Tabiona. Along the same trend and north of Duchesne, numerous late Pleistocene faults offset glacial outwash of early Wisconsin (Bull Lake) age (Hansen, 1969).

COLORADO PLATEAU PROVINCE

The Colorado Plateau is a region of Precambrian through early Cenozoic rocks that has been broadly uplifted. There is little evidence of late Cenozoic faulting in the eastern Colorado Plateau (Fig. 1). The western Colorado Plateau is structurally transitional with the Basin and Range because north-south trending, Basin and Range type faults are common there. During the late Cenozoic, uplift, east-west extensional faulting and fundamentally basaltic volcanism have migrated eastward and slightly northward from the Basin and Range into the Colorado Plateau (Best and Hamblin, 1978). Faulting along the major faults of the Plateau, Hurricane, Sevier, and associated faults, has continued during the Quaternary (Appendix C). However, it appears that major faults are not as numerous as in the Basin and Range and, in general, do not show as much total displacement. The western margin of the Plateau has been one of the more seismically active areas in the western United States. The largest recorded or estimated earthquakes in this area have been in the magnitude 5.0 to 6.0+ range (Cook and Smith, 1967; Smith, 1978).

Quaternary surficial deposits in the Colorado Plateau region are primarily thin veneers of eolian sand, with alluvium in the major drainages. During the Quaternary, some of the higher mountains and plateaus were glaciated. The general lack of Quaternary deposits makes it difficult to determine the age of last movement on many faults.

Major Faults

Numerous north-south trending normal faults have been mapped in the Wasatch Plateau region (Witkind and others, 1978; I. J. Witkind, 1979, personal commun.). Evidence of youthful faulting is apparent in Joes Valley, where a large graben occurs in the Price River and North Horn Formations. In Joes Valley, reconnaissance studies indicate that apparently late Wisconsin glacial outwash, landslides, and alluvial fans are displaced by normal faulting. Some of the fault activity may be Holocene in age, but faults are shown as late Pleistocene until more definitive information becomes available.

Faults have also been mapped near the crest of the Wasatch Plateau (Witkind and others, 1978) which appear quite young and apparently displace cirques high in the plateau (I. J. Witkind, 1979, personal commun.). Many other faults in the Wasatch Plateau area may be related to the faults in the Joes Valley and plateau crest areas (see Witkind, 1978). There is no strong evidence that these faults are of Quaternary age, but the nature of the faults and their association with known or suspected Quaternary faults suggest that some could be of Quaternary age.

The Sevier fault is one of the major late Cenozoic structural features of southwestern Utah. The Sevier fault system (including the Toroweap fault of the western Grand Canyon) is over 340 km in length. The northern portion of the fault extends from the Panguitch area north to near Richfield, along the west side of Sevier Plateau. Late Quaternary fault scarps have been mapped by Anderson and Bucknam (1979). Callaghan and Parker (1961, 1962a, 1962b), Willard and Callaghan (1962), and Steven and others (1978) have identified suspected Quaternary fault traces that locally displace the late Pliocene to early Pleistocene Sevier River Formation.

Near Red Canyon (southeast of Panguitch), approximately 500,000-year-old basalt flows (Anderson and others, 1978) are displaced about 200 m by the Sevier fault giving a late Pleistocene age to this segment of the fault. The age of last movement on the fault system from south of Red Canyon to the Utah-Arizona border is unknown. At Black Mountain, basalts of suspected Quaternary age are displaced (Cashion, 1961). As their actual age is unknown, the entire fault south of Red Canyon is considered to be of suspected Quaternary age.

Suspected Quaternary faults have been identified in the Paradox Basin area of southeastern Utah (Moab-Colorado River area). Normal faults bound many of the valleys in this region (Williams, 1964; Williams and Hackman, 1971). The area has very low seismicity and the faults are not believed to be the result of tectonic processes but rather the result of salt flowage beneath the overlying bedrock (Kelley and Clinton, 1960; Howard and others, 1978).

DISCUSSION

Our present knowledge of Quaternary faulting in Utah is governed by two factors. First, rapid erosion and thick alluvial deposits in areas such as the Basin and Range, or the lack of Quaternary cover in areas such as the Colorado Plateau, makes an evaluation of Quaternary fault activity extremely difficult. Secondly, detailed studies of Quaternary faulting have not been conducted in many areas of the state, and many studies are not finished. Undoubtedly, many more Quaternary faults may exist in Utah that have not as yet been identified.

Even in areas where Quaternary faults have been identified and where extensive Quaternary cover exists, the age of faulting is poorly documented. This is because only a few detailed studies of the Quaternary geology of Utah have been conducted and because of the general difficulty in dating

the deposits. The use of fault-scarp morphology to determine relative ages of fault activity (Wallace, 1977; Bucknam and Anderson, 1979a) is obviously a step toward resolving some of the problems concerning the dating of recent faults.

CONCLUSIONS

Quaternary faults are widely scattered over the state, but the majority of late Quaternary faulting is concentrated along the Wasatch, Cache Valley, Hurricane, Sevier, and associated fault zones. The abundance of faults in these areas suggests these faults have had recurrent movement throughout the Quaternary. The more random and widely scattered distribution of Quaternary faults in the western portion of the state suggests that fault movements have longer recurrence intervals in that area and thus thick Quaternary deposits have obliterated much of the evidence of faulting.

Both geologic evidence and historic seismicity suggests that the Basin and Range-Colorado Plateau boundary zone is experiencing the highest rate of ongoing tectonic activity in the state. Faults within this zone should be considered the most potentially hazardous, and large magnitude earthquakes may be expected to occur there in the future. However, studies of the region are not sufficiently advanced to characterize the relative hazard for most of the state, with a satisfactory degree of certainty needed for engineering uses.

Two areas of Utah that particularly require further study are the Uinta Mountains and the Aquarius Plateau to Cache Valley region. A few Quaternary faults have been identified along the south flank of the Uinta Mountains and some small earthquakes have occurred there. Recent studies in Colorado that have identified Quaternary faults along the margins of some of the ranges of the Rocky Mountains (see Kirkham and Rodgers, 1978) suggest that Quaternary faults should be suspected along the margins of the Uinta Mountains.

The area between the Aquarius Plateau on the south and the Bear Lake-Cache Valley area to the north has a few Quaternary faults, but the presence of extensive north-south trending normal faults in the area (Stokes and others, 1963) suggests that many more Quaternary faults may exist there. The area is moderately seismic (Smith, 1978), and if the apparent relative eastward migration of uplift and extensional faulting continues, one could expect to find more Quaternary faults in this region. We might also expect large magnitude earthquakes to occur on faults in this region in the future.

Surficial evidence of Quaternary faulting is often difficult to document and, as mentioned, most areas of the state require further study. However, this study has probably identified those faults that have been the most recently active and thus pose the greatest potential hazard to life and property. These data are best applied as a guide for siting studies and hazard assessments, and we hope they will aid and stimulate future geologic investigations in Utah.

ACKNOWLEDGMENTS

This work has benefited greatly from comments and new data generously provided by the following individuals:

R. E. Anderson, R. C. Bucknam, W. R. Hansen, R. D. Miller, P. D. Rowley, W. E. Scott, and I. J. Witkind of the U.S. Geological Survey; J. Campbell, B. Everett, B. N. Kaliser, and H. R. Ritzma of the Utah Geological and Mineral Survey; W. J. Arabasz, R. B. Smith, and R. Van Arsdale of the University of Utah; C. T. Hardy of Utah State University; and L. F. Hintze and W. K. Hamblin of Brigham Young University.

Support for this project has been provided by research and development funds from Fugro, Inc., project number 78-202. Discussions with J. C. Stepp, J. S. Scott, B. A. Schell, and G. DeVries of Fugro were of considerable help in preparation of this report. J. C. Stepp and B. A. Schell reviewed earlier drafts of the manuscript.

APPENDIX A

QUATERNARY FAULTS IN BASIN AND RANGE PROVINCE

FAULT	LOCATION	YOUNGEST DEPOSIT DISPLACED	CLASSIFICATION	SOURCE	COMMENTS
-	Grouse Creek and Raft River Mts.	Quaternary alluvium	Late Pleistocene	Compton, 1972, 1975	Scarps in alluvium.
-	West side of Hansel Mts.	Quaternary (?) alluvium	Suspected Quaternary	Witkind, 1975a	Quaternary activity on fault in Idaho.
Hansel Valley	SW side of Hansel Valley	Holocene alluvium	Holocene (Historic)	Walter, 1934 Neuman, 1936 Bucknam, 1979	Location of 1934 earthquake of M=6.6. Produced a series of scarps up to 50 cm in height in area of older Holocene fault scarps.
-	West side of West Hills	Quaternary (?) alluvium	Suspected Quaternary	Witkind, 1975a	Possible Holocene activity on fault in Idaho.
-	East side of West Hills	Quaternary (?) alluvium	Suspected Quaternary	Witkind, 1975a	Possible late Pleistocene activity on fault in Idaho.
-	East side of Newfoundland Mts.	Quaternary (?) alluvium	Suspected Quaternary	Paddock, 1956	Existance doubted by Bucknam (1979).
-	Puddle Valley (41^0N, 113^0W)	Quaternary alluvium	Holocene	Bucknam, 1977, 1979	Fault scarps.
-	East side of Lakeside Mts.	Pre-Lake Bonneville alluvium	Suspected Quaternary	Young, 1955	
-	West side of Stansbury Mts.	Quaternary alluvium	Late Pleistocene	Bucknam, 1977	Fault scarps.

-	NW and NE side of Onoqui Mts.	Quaternary (?) alluvium	Suspected Quaternary	Moore and Sorensen, 1978 Croft, 1956	
-	Rush Valley	Quaternary alluvium	Late Pleistocene	Bucknam, 1977	Fault scarps.
-	West side of Oquirrh Mts.	Quaternary alluvium	Late Pleistocene	Bucknam, 1977	Fault scarps.
-	West side of Thorpe Hills ($40^0$15'N., $112^0$10'W)	Quaternary alluvium	Late Pleistocene Suspected Quaternary	Bucknam, 1977 Everitt, 1979	Fault scarps.
Wasatch (northern)	Brigham City to Malad, Idaho	Pleistocene alluvial fans and Lake Bonneville deposits	Late Pleistocene	Cluff and others, 1974	Geomorphically appears older than central Wasatch. Fault scarps modified by Lake Bonneville.
Wasatch (central)	Nephi to Brigham City	Late Pleistocene Lake Bonneville deposits, glacial moraines, Holocene alluvium	Holocene	Bucknam, 1979 Cluff and others, 1970, 1973 Hintze, 1971 Morrison, 1965a Schwartz and others, 1979 Swan and others, 1979, Van Horn, 1972	Abundant evidence of Holocene activity.
Wasatch (southern)	Nephi to Gunnison	Quaternary alluvium	Holocene(?)	Anderson and others, 1978 Cluff and others, 1973	Probable Holocene activity.

-	Near Bluffdale, south end Salt Lake Valley (40°23'N., 111°58'W)	Lake Bonneville (?) deposits	Suspected Quaternary	Kaliser, 1979	Personal communication, unmapped.
-	Near Granger, west side Salt Lake Valley (40°40'N., 111°55'W)	Lake Bonneville deposits	Holocene	Marine and Price, 1964	Post-Lake Bonneville fault scarps.
-	Near Vernon (40°06'N., 112°20'W)	Quaternary alluvium	Late Pleistocene	Bucknam, 1977	Scarps.
-	East side of Sheeprock Mt.	Quaternary alluvium	Late Pleistocene	Bucknam, 1977	Scarps along range front.
-	South end of Cedar Valley (40°02'N., 112°05'W)	Quaternary (?) alluvium	Late Pleistocene	Everitt, 1979	
-	East and West sides of Deep Creek Mts.	Quaternary alluvium	Late Pleistocene	Bucknam, 1977 Bucknam and Anderson, 1979b	Scarps along range front.
Fish Springs	East side of Fish Springs Range	Holocene alluvial fans	Holocene	Bucknam and Anderson, 1979a, 1979b	Prominant scarps along base of range.
-	West side of House Range	Lake Bonneville deposits	Holocene	Bucknam and Anderson, 1979b	Scarp along base of range.
Drum Mt.	East side of Drum Mts.	Lake Bonneville deposits	Holocene	Bucknam and Anderson, 1979a, 1979b	Numerous scarps.
-	Fumarole Batte	Quaternary basalts	Suspected Quaternary	Peterson and others, 1978 Morris, 1978 Bucknam and Anderson, 1979b	Faults displace basalts dated at 0.88 m.y.B.P.

-	15 km North of Delta	Lake Bonneville deposites	Late Pleistocene	Fugro, 1978	
-	North end of Tintic Valley	Pleistocene (?) fanglomerate	Suspected Quaternary	Morris, 1964	
-	East side of Tintic Valley	Quaternary (?) alluvium	Late Pleistocene (?)	Bucknam and Anderson, 1979b	Highly dissected scarps.
-	South end of Tintic Valley	Quaternary (?) alluvium	Suspected Quaternary	Morris, 1978	
-	About 10 km SW of Deseret	Quaternary basalts	Suspected Quaternary	Morris, 1978 Bucknam and Anderson, 1979b	
-	North end of Cricket Mts.	Quaternary alluvium	Late Pleistocene	Bucknam and Anderson, 1979b	Scarps older than Lake Bonneville
Clear Lake	About 20 km south of Deseret	Late Quaternary lacustrine and eolian deposits	Holocene	Bucknam and Anderson, 1979b Hoover, 1974	
Black Rock-Pavant Butte Fault zone	20 km West of Fillmore	Holocene (?) and Pleistocene volcanics	Holocene Late Pleistocene, Suspected Quaternary	Hoover, 1974 **Anderson and Bucknam, 1979**	Series of faults displacing volcanics of various ages.
-	Northeast flank Pavant Range ($38^0$55'N., $112^0$05'W)	Quaternary alluvium	**Holocene**	Anderson and Bucknam, 1979	Scarps along base of range.
Cove Fort Fault zone	West of Cove Fort	Quaternary volcanics	Late Pleistocene, Suspected Quaternary	Clark, 1977	Faults displace volcanics dated at 3 m.y.B.P. to 30,000 B.P.

-	Near West Hills ($39^0$40'N., $111^0$55'W)	Quaternary (?) colluvium	Suspected Quaternary	Witkind and others, 1978	
-	Near Sage Valley Pass ($39^0$35'N., $111^0$58'W)	Quaternary (?) colluvium	Suspected Quaternary	Witkind and others, 1978	
-	Japanese Valley ($39^0$12'N., 112^0W)	Quaternary alluvium	Late (?) Pleistocene Suspected Quaternary	Anderson and others, 1978 Morris, 1978	Small scarps?
-	Little Valley	Quaternary alluvium	Late Pleistocene	Bucknam and Anderson, 1979b	Series of scarps, older than high stand of Lake Bonneville.
-	Scipio Valley	Quaternary alluvium	Holocene Late Pleistocene	Bucknam and Anderson, 1979b	Series of scarps with two ages of movement.
-	NE flank of Pavant Range	Quaternary colluvium	Holocene (?)	Bucknam and Anderson, 1979b	Scarps along base of range.
-	Maple Grove ($39^0$15'N., $112^0$05'W)	Quaternary alluvium	Late Pleistocene	Bucknam and Anderson, 1979b	Series of scarps.
-	West side of Mineral Mts.	Quaternary alluvium	Late Pleistocene	Neilson and others, 1978	Scarps.
-	Minersville	Quaternary alluvium	Late Pleistocene	Anderson and Bucknam, 1979	Scarps.
-	Black Mt., northern Escalante Desert	Quaternary alluvium and Quaternary (?) basalt	Late Pleistocene, Suspected Quaternary	Rowley, 1977	Series of faults.

Beaver Fault zone	Beaver Valley ($38^0$15'N., $112^0$45'W)	Quaternary alluvium and terrace deposits	Late Pleistocene (?)	Anderson and Bucknam, 1979 Stevan and others, 1978	Some faults may be older than 500,000 B.P.
-	Parowan and Buckskin Valley	Quaternary alluvium	Late Pleistocene(?), Suspected Quaternary	Anderson and Bucknam, 1979 Bjorkland and others, 1978	
-	Northern Cedar Valley	Quaternary alluvium and Quaternary (?) basalt	Late Pleisto-cene, Suspected Quaternary	Anderson and others, 1978 Bjorkland and others, 1978 Rowley, 1975 Macken and Rowley, 1976 Rowley and Treet, 1976	Inferred faults mapped by Thomas and Tayler (1946) have not been shown.
-	Eastern Escalante Desert	Quaternary alluvium	Late Pleisto-cene, Suspected Quaternary	Anderson, 1979 Mackin and Rowley, 1975 Rowley, 1976	
-	Southern Escalante Desert near Enterprise	Quaternary alluvium	Late Pleistocene	Anderson, 1979	
-	Braffits Creek, 10 km NE of Cedar City	Quaternary alluvium and colluvium	Suspected Quaternary	Anderson and others, 1978 Anderson, 1979	May not be of tectonic origin.
Hurricane and assoc. faults	Cedar City area	Quaternary alluvium and Quaternary (?) basalts	Suspected Quaternary and Late Pleisto-cene	Anderson and others, 1978 Averitt, 1967 Averitt and Treet, 1973 Averitt, 1962	

-	Pine Valley Mts. north of St. George	Quaternary (?) alluvium and basalts	Suspected Quaternary	Hamblin, 1978	
Grand Wash	Western Grand Canyon, Arizona to Gunlock, Utah	Tertiary basalts Quaternary (?) alluvium	Suspected Quaternary	Hamblin, 1978	
Hurricane and assoc. faults	Western Grand Canyon to Cedar City	Quaternary basalts and Quaternary alluvium	Late Pleistocene	Hamblin, 1978 Anderson, 1979	Up to 600 m of Quaternary displacement.
-	West side Cricket Mts.	Quaternary alluvium	Late Pleistocene	Anderson and Bucknam, 1979	Scarps
-	West side San Francisco Mts.	Quaternary alluvium	Late Pleistocene (?)	Anderson and Bucknam, 1979	Scarps
-	SE end of Wah Wah Mts.	Quaternary alluvium	Late Pleistocene	Anderson and Bucknam, 1979	Scarps

APPENDIX B

QUATERNARY FAULTS IN ROCKY MOUNTAINS PROVINCE

FAULT	LOCATION	YOUNGEST DEPOSIT DISPLACED	CLASSIFICATION	SOURCE	COMMENTS
West Cache Fault	West side of Cache Valley	Late Wisconsin (Provo) age Lake Bonneville deposits	Holocene, Late Pleistocene	Cluff and others, 1974	Short probable Holocene break near Cache Butte, remainder of fault zone appears to be Late Pleistocene.
East Cache Fault	East side of Cache Valley	Late Wisconsin (Provo) age Lake Bonnevill deposits at Logan	Holocene, Late Pleistocene	Cluff and others, 1974	Short Holocene break at Logan, remainder of fault zone appears to be Late Pleistocene.
East Bear Lake Fault	East side of Bear Lake	Late Quaternary alluvial fans	Holocene	Kaliser, 1972	
West Bear Lake Fault	West side of Bear Lake	Quaternary (?) alluvium	Suspected Quaternary	Kaliser, 1972	
-	South side of Heber Valley	Quaternary (?) alluvium	Suspected Quaternary	Kaliser, 1979	Unmapped.
-	NE side of Strawberry Reservoir	Tertiary and Quaternary sediments	Late Pleistocene	R. Van Arsdale, 1978	Scarps.
-	3 km north of Tabiona	Quaternary alluvium	Late Pleistocene	Garvin, 1969 Ritzma, 1978	
-	10 km east of Tabiona	Quaternary alluvium	Late Pleistocene	Ritzma, 1978	
-	Towonta Flat	Bull Lake age glacial outwash	Late Pleistocene	Hansen, 1969	Numerous fault scarps.

-	North and East of Icy Cave Peak, 30 km NW of Vernal	Miocene-Pliocene (?) Browns Park Fm.	Suspected Quaternary	Rowley and others, 1978 Rowley, 1979 Hansen, 1978	Has surface expression, has not been found to offset Quaternary alluvium.
-	Diamond Mt. 30 km NE of Vernal	Miocene-Pliocene (?) Browns Park Fm.	Suspected Quaternary	Rowley and others, 1978 Rowley, 1979 Hansen, 1978	Has surface expression, has not been found to offset Quaternary alluvium.

APPENDIX C

QUATERNARY FAULTS IN COLORADO PLATEAU PROVINCE

FAULT	LOCATION	YOUNGEST DEPOSIT DISPLACED	CLASSIFICATION	SOURCE	COMMENTS
Spring Hollow Fault	22 km SE of Vernal	Quaternary alluvium	Holocene	Ritzma, 1978	
Tank Spring Fault	23 km SE of Vernal	Quaternary alluvium	Late Pleistocene	Ritzma, 1978	
-	West side Sanpete Valley, near Wales ($39^0$30'N., $111^0$40'W)	Quaternary alluvium	Late Pleistocene	Witkind and others, 1978 Witkind, 1979	
-	15 km east of Manti, along crest of Wasatch Plateau	Tertiary Flagstaff limestone	Suspected Quaternary	Witkind and others, 1978 Witkind, 1979	Faults displace cirques high in Plateau.
Joes Valley	30 km east of Manti	Late Quaternary alluvium, landslide debris and glacial deposits	Late Pleistocene	Witkind and others, 1978 Witkind, 1979	Some faults could be Holocene.
Sevier (northern portion)	Glenwood to Junction along west side of Sevier Plateau	Pliocene-Pleistocene sediments (Sevier River Fm) and Quaternary alluvial fans	Suspected Quaternary, late Pleistocene	Anderson and others, 1978 Callaghan and Parker, 1961, 1962a, 1962b Willard and Callaghan, 1962	Little evidence of late Quaternary activity.

Tushar-Elsinor	North of Richfield to Circleville, along east side of Pavant Range and Tushar Mts.	Pliocene-Pleistocene Sevier River Fm. and Quaternary alluvial fans	Suspected Quaternary and Late Pleistocene	Anderson and Bucknam, 1979 Callaghan and Parker, 1961, 1962a, 1962b Steven and others, 1978	Little evidence of late Quaternary activity.
Sevier (central)	Junction to near Panguitch, along west side of Sevier Plateau	Pliocene-Pleistocene sediments (?)	Suspected Quaternary	Carpenter and others, 1967 Stokes and others, 1963	
-	NE and SE of Panguitch	Quaternary alluvium and basalts	Late Pleistocene	Anderson and others, 1978 Hamblin, 1978	Numerous scarps, some may be as old as 500,000 years.
-	Bear Valley, 20 km NW of Panguitch ($37^0$55'N., $112^0$35'W)	Quaternary alluvium	Late Pleistocene Suspected Quaternary	Anderson and others, 1978 Carpenter and others,1967	
-	Panguitch Lake	Quaternary (?) basalt	Suspected Quaternary	Carpenter and others, 1967	
-	5 km NE of Navajo Lake	Quaternary (?) basalt	Suspected Quaternary	Carpenter and others, 1967	
-	Black Mt.	Quaternary (?) basalt	Suspected Quaternary	Hamblin, 1978	
-	The Plains, 10 km SW of Navajo Lake	Quaternary (?) basalt	Suspected Quaternary	Cashion, 1961	
Sevier	Red Canyon area	Late Quaternary basalt	Late Pleistocene	Hamblin, 1978 Anderson and others, 1978	500,000 B.P. basalt flows displaced 200 m.

Sevier (southern)	Red Canyon to Utah-Arizona border and Western Grand Canyon	Quaternary (?) basalt	Suspected Quaternary	Cashion, 1961 Stokes and others, 1963	
-	Johns Valley	Quaternary (?) alluvium	Suspected Quaternary	Carpenter and others, 1967	From mapping it is unclear if Quaternary deposits are acturally displaced.
-	North side Aquarius Plateau	Tertiary-Quaternary (?) basalts	Suspected Quaternary	Williams and Hackman, 1971 Hackman and Wyant, 1973	
Thousand Lake	West side of Aquarius Plateau and Thousand Lake Mt.	Late Pleistocene (Bull Lake age) glacial outwash	Late Pleistocene, Suspected Quaternary	Smith and others, 1963	Only known to displace Quaternary deposits near Bicknell
-	Paradox Basin-Moab area	Quaternary (?) alluvium	Suspected Quaternary	Williams, 1964 Williams and Hackman, 1971	Faults believed to be the result of salt flowage beneath underlying bedrock. (Kelly and Clinton, 1960; Howard and others, 1978).
-	The Graben area ($38^{0}05'$N., $109^{0}55'$W)	Quaternary (?) alluvium	Suspected Quaternary	Williams, 1964 Williams and Hackman, 1971	Faults believed to be the result of salt flowage beneath underlying bedrock. (Kelly and Clinton, 1960; Howard and others, 1978).

REFERENCES*

Anderson, L. W., and Miller, D. G., Preliminary Quaternary fault map of Utah (in press).

1. Anderson, R. E., 1979, personal communication.

2. Anderson, R. E., Bucknam, R. C., and Hamblin, W. K., 1978, Road log to the Quaternary tectonics of the Intermountain seismic belt between Provo and Cedar City, Utah: Geol. Soc. Amer., Rocky Mtn. Sec. Ann. Meeting, Provo, Utah.

3. Anderson, R. E., Buckman, R. C., 1979, Map of fault scarps in unconsolidated sediments, Richfield 1" x 2" quadrangle, Utah: U.S. Geol. Survey open-file report OF-79-1236.

Anderson, R. E., and Mehnert, Harold, 1979, The Hurricane fault in Utah as a predominantly Quaternary structure: Geol. Soc. America Abs. with Programs, v. 11, no. 3, p. 66.

Atwood, W. W., 1909, Glaciation of the Uinta and Wasatch Mountains: U.S. Geol. Survey Prof. Paper 61, 96 p.

4. Averitt, Paul, 1962, Geology and coal resources of the Cedar Mountain quadrangle, Iron County, Utah: U.S. Geol. Survey Prof. Paper 389, 72 p.

5. _____, 1967, Geologic map of the Kanarraville quadrangle Utah: U.S. Geol. Survey Geol. Quad. Map GQ-694.

6. Averitt, Paul, and Threet, R. L., 1973, Geologic map of the Cedar City quadrangle, Iron County, Utah: U.S. Geol. Survey Geol. Quad. Map GQ-1120.

Best, M. G., and Hamblin, W. K., 1978, Origin of the northern Basin and Range province: Implications from the geology of its eastern boundary, in Smith, R. B., and Eaton, G. P., eds., Cenozoic tectonics and regional geophysics of the western Cordillera: Geol. Soc. America Mem. 152, p. 313-340.

*Numbers refer to sources of data used in map compilation shown on Figure 2.

7. Bjorklund, L. J., Sumsion, C. T., and Sanberg, G. W., 1978, Ground-water resources of the Parowan-Cedar City drainage basin, Iron County, Utah: Utah Dept. of Natural Res. Tech. Pub. no. 60, 93 p.

8. Bucknam, R. C., 1977, Map of suspected fault scarps in unconsolidated deposits, Tooele 2° sheet, Utah: U.S. Geol. Survey open-file report OF-77-495.

9. _____, 1979, personal communication.

Bucknam, R. C., and Anderson, R. E., 1979a, Estimation of fault-scarp ages from a scarp-height-slope-angle relationship: Geology, v. 7, p. 11-14.

10. _____, 1979b, Map of fault scarps on unconsolidated sediments, Delta 1° x 2° quadrangle, Utah: U.S. Geol. Survey open-file report OF-79-366.

11. Callaghan, Eugene, and Parker, R. L., 1961, Geology of the Monroe quadrangle, Utah: U.S. Geol. Survey Geol. Quad. Map GQ-155.

12. _____, 1962a, Geology of the Delano Peak quadrangle, Utah: U.S. Geol. Survey Geol. Quad Map GQ-153.

13. _____, 1962b, Geology of the Sevier quadrangle, Utah: U.S. Geol. Survey Geol. Quad. Map GQ-156.

14. Campbell, J., 1979, personal communication.

15. Carpenter, C. H., Robinson, G. B., and Bjorklund, L. J., 1967, Ground-water conditions and geologic reconnaissance of the upper Sevier River Basin, Utah: U.S. Geol. Survey Water-Supply Paper 1836.

16. Cashion, W. B., 1961, Geology and fuels resources of the Orderville-Glendale area, Kane County, Utah: U.S. Geol. Survey Coal Inv. Map C-49.

17. Clark, E. E., 1977, Late Cenozoic volcanic and tectonic activity along the eastern margin of the Great Basin, in the proximity of Cove Fort, Utah: Brigham Young Univ. Geol. Studies, v. 24, Part 1, p. 87-113.

18. Cluff, L. S., Brogan, G. E., and Glass, C. E., 1970, Wasatch fault, northern portion: Earthquake fault investigation and evaluation: Woodward-Clyde and Associates, report for Utah Geol. and Mineral Survey.

19. _____, 1973, Wasatch fault, southern portion: Earthquake fault investigation and evaluation: Woodward-Lundgren and Associates, report for Utah Geol. and Mineral Survey.

20. Cluff, L. S., Glass, C. E., and Brogan, G. E., 1974, Investigation and evaluation of the Wasatch fault north of Brigham City and Cache Valley faults, Utah and Idaho: Woodward-Lundgren and Associates, report for U.S. Geol. Survey.

21. Compton, R. R., 1972, Geologic map of the Yost quadrangle, Box Elder County, Utah, and Cassia County, Idaho: U.S. Geol. Survey Misc. Inv. Map I-672.

22. _____, 1975, Geologic map of the Park Valley quadrangle, Box Elder County, Utah, and Cassia County, Idaho: U.S. Geol. Survey Misc. Inv. Map I-783.

Cook, K. L., and Berg, J. W., Jr., 1961, Regional gravity survey along the central and southern Wasatch front, Utah: U.S. Geol. Survey Prof. Paper 316-E, p. 75-89.

23. Cook, K. L., Halverson, M. O., Stepp, J. C., Jr., and Berg, J. W., 1964, Regional gravity survey of the northern Great Salt Lake Desert and adjacent areas in Utah, Nevada, and Idaho: Geol. Soc. America Bull., v. 75, p. 715-740.

Cook, K. L., Berg, J. W., Jr., Johnson, W. W., and Novotny, R. T., 1966, Some Cenozoic structural basins in the Great Salt Lake area, Utah, indicated by regional gravity surveys: Utah Geol. Soc. Guidebook 20, p. 57-75.

Cook, K. L., and Hardman, Elwood, 1967, Regional gravity survey of the Hurricane fault area and Iron Springs District, Utah: Geol. Soc. America Bull., v. 78, p. 1063-1076.

Cook, K. L., and Smith, R. B., 1967, Seismicity in Utah, 1950 through June 1965: Bull. Seis. Soc. America, v. 57, no. 4, p. 689-718.

24. Croft, M. G., 1956, Geology of the northern Onaqui Mountains, Tooele County, Utah: Brigham Young Univ. Geol. Studies, v. 3, no. 3, 45 p.

25. Everitt, Ben, 1979, personal communication.

Fenneman, N. M., 1931, Physiography of Western United States: New York, McGraw-Hill Book Co., 534 p.

26. Fugro, 1978, unpublished data.

27. Garvin, R. G., 1969, Stratigraphy and economic significance, Currant Creek Formation, northwest Uinta Basin, Utah: Utah Geol. and Mineral Survey Spec. Studies 27, 62 p.

28. Hackman, R. J., and Wyant, D. G., 1973, Geology, structure, and uranium deposits of the Escalante quadrangle, Utah and Arizona: U.S. Geol. Survey Misc. Inv. Map I-744.

Hamblin, W. K., 1970, Structure of the western Grand Canyon region, in Hamblin, W. K., and Best, M. G., eds., Guidebook to the geology of Utah: Utah Geol. Soc., no. 23, p. 3-20.

29. _____, 1978, unpub. data, compiled from 1:20,000 black and white aerial photos.

30. Hansen, W. R., 1969, The geologic story of the Uinta Mountains: U.S. Geol. Survey Bull. 1291, 144 p.

31. _____, 1978, personal communication.

Hintze, L. F., 1971, Wasatch fault zone east of Provo, Utah, in Environmental geology of the Wasatch Front: Utah Geol. Assoc. Pub. No. 1, p. F1-F10.

_____, 1973, Geologic history of Utah: Brigham Young Univ. Geol. Studies, v. 20, pt. 3, 181 p.

32. Hoover, J. D., 1974, Periodic Quaternary volcanism in the Black Rock Desert, Utah: Brigham Young Univ. Geol. Studies, v. 21, pt. 1, p. 3-72.

Howard, K. A., Aaron, J. M., Brabb, E. E., Brock, M. R., Gower, H. D., Hunt, S. J., Milton, D. J., Muehlberger, W. R., Nakata, J. K., Plafker, G., Prowell, D. C., Wallace, R. E., and Witkind, I. J., 1978, Preliminary map of young faults in the United States as a guide to possible fault activity: U.S. Geol. Survey Misc. Field Studies Map MF-916.

Jennings, C. W., 1975, Fault map of California, with locations of volcanoes, thermal springs and thermal wells: Calif. Div. Mines and Geology, Calif. Geol. Data Map Series, Map No. 1.

33. Kaliser, B. N., 1972, Environmental geology of Bear Lake area, Rich County, Utah: Utah Geol. and Mineral Survey Bull. 96, 32 p.

34. _____, 1979, personal communication.

Kelley, V. C., and Clinton, N. J., 1960, Fracture systems and tectonic elements of the Colorado Plateau: Univ. of New Mexico Pub. in Geol., no. 6, 104 p.

Kirkham, R. M., and Rogers, W. P., 1978, Earthquake potential in Colorado: Colorado Geol. Survey open-file report 78-3.

35. Mackin, J. H., and Rowley, P. D., 1975, Geologic map of the Avon SE quadrangle, Iron County, Utah: U.S. Geol. Survey Geol. Quad. Map GQ-1294.

36. _____, 1976, Geologic map of the Three Peaks quadrangle, Iron County, Utah: U.S. Geol. Survey Geol. Quad Map GQ-1297.

37. Marine, I. W., and Price, Don, 1964, Geology and ground-water resources of the Jordan Valley, Utah: Utah Geol. and Mineral Survey Water-Res. Bull. 7, 66 p.

38. Moore, W. J., and Sorensen, M. L., 1978, Preliminary geologic map of Tooele 2° quadrangle, Utah: U.S. Geol. Survey open-file map OF-78-257.

39. Morris, H. T., 1964, Geology of the Tintic Junction quadrangle, Tooele, Juab, and Utah counties, Utah: U.S. Geol. Survey Bull. 1142-L, 23 p.

40. _____, 1978, Preliminary geologic map of Delta 2° quadrangle, west-central Utah: U.S. Geol. Survey open-file map OF-78-705.

41. Morrison, R. B., 1965a, Lake Bonneville: Quaternary stratigraphy of eastern Jordan Valley, south of Salt Lake City, Utah: U.S. Geol. Survey Prof. Paper 477, 80 p.

_____, 1965b, Quaternary geology of the Great Basin, in Wright, H. E., and Frey, D. G., eds., The Quaternary of the United States: Princeton, N. J., Princeton University Press, p. 265-285.

_____, 1966, Predecessors of Great Salt Lake, in Stokes, W. L., ed., The Great Salt Lake: Guidebook to the geology of Utah, v. 20, Utah Geol. Soc., p. 77-104.

Neumann, Frank, 1936, United States Earthquakes, 1934: U.S. Dept. of Commerce, p. 13-17 and 43-48.

42. Nielson, D. L., Sibbett, B. S., McKinney, D. B., Hulen, J. B., Moore, J. N., and Samberg, S. M., 1978, Geology of Roosevelt Hot Springs KGRA, Beaver County, Utah: Earth Sci. Lab., Univ. of Utah Res. Inst., Salt Lake City, Utah, 120 p.

43. Paddock, R. E., 1956, Geologic map of the Newfoundland Mountains, Box Elder County, Utah: unpub. M.S. thesis, Univ. of Utah.

Peterson, James, Turley, Charles, Nash, W. P., and Brown, F. H., 1978, Late Cenozoic basalt-rhyolite volcanism in west-central Utah: Geol. Soc. America Abs. with Programs, v. 10, no. 5, p. 236.

Ritzma, H. R., 1974, Towanta lineament, northern Utah, in Hodgson, R. A., Gay, S. P., Jr., and Benjamins, J. Y., eds., Proceedings of the first international conference on the new basement tectonics: Utah Geol. Assoc. Pub. No. 5, p. 118-125.

44. _____, 1978, personal communication.

45. Rowley, P. D., 1975, Geologic map of the Enoch NE quadrangle, Iron County, Utah: U.S. Geol. Survey Geol. Quad Map GQ-1301.

46. _____, 1976, Geologic map of the Enoch NW quadrangle, Iron County, Utah: U.S. Geol. Survey Geol. Quad Map GQ-1302.

47. _____, 1977, Preliminary geologic map of the Thermo 15-minute quadrangle, Beaver and Iron Counties, Utah: U.S. Geol. Survey open-file map OF-77-508.

48. _____, 1979, personal communication.

49. Rowley, P. D., and Treet, R. L., 1976, Geologic map of the Enoch quadrangle, Iron County, Utah: U.S. Geol. Survey Geol. Quad. Map GQ-1296.

50. Rowley, P. D., Tweto, Ogden, and Hanson, W. R., 1978, Preliminary geologic map of the Vernal 1° x 2° quadrangle, Colorado, Utah, and Wyoming: U.S. Geol. Survey open-file map OF-78-573.

Schwartz, D. P., Swan, F. H., III, Hanson, K. L., Knuepfer, P. L., and Cluff, L. S., 1979, Recurrence of surface faulting and large magnitude earthquakes along the Wasatch fault zone near Provo, Utah: Geol. Soc. America Abs. with Programs, v. 11, no. 6, p. 301.

Scott, W. E., 1979a, Evaluation of evidence for controversial rise of Lake Bonneville about 10,000 years ago: Geol. Soc. America Abs. with Programs, v. 11, no. 6, p. 301-302.

_____, 1979b, Stratigraphic problems in the usage of Apine and Bonneville Formations in the Bonneville Basin, Utah: Geol. Soc. America Abs. with Programs, v. 11, no. 6, p. 302.

51. Smith, J. F., Jr., Hugg, L. C., Hinrichs, E. N., and Luedke, R. G., 1963, Geology of the Capitol Reef area, Wayne and Garfield Counties, Utah: U.S. Geol. Survey Prof. Paper 363.

Smith, R. B., 1978, Seismicity, crustal structure, and intraplate tectonics of the interior of the western Cordillera, in Smith, R. B., and Eaton, G. P., eds., Cenozoic tectonics and regional geophysics of the western Cordillera: Geol. Soc. America Mem. 152, p. 111-144.

Smith, R. B., and Sbar, M. L., 1974, Contemporary tectonics and seismicity of the western United States with emphasis on the Intermountain seismic belt: Geol. Soc., America Bull., v. 85, p. 1205-1218.

52. Steven, T. A., Rowley, P. D., Hintze, L. F., Best, M. G., Nelson, M. G., and Cunningham, C. G., 1978, Preliminary geologic map of the Richfield 1° x 2° quadrangle, Utah: U.S. Geol. Survey open-file map OF-78-602.

Stewart, J. H., 1978, Basin - Range structure in western North America: A review, in Smith, R. B., and Eaton, G. P., eds., Cenozoic tectonics and regional geophysics of the western Cordillera: Geol. Soc. America Mem. 152, p. 1-31.

53. Stokes, W. L., Hintze, L. F., and Madson, J. H. (compilers), 1963, Geologic map of Utah: Utah State Land Board and Utah Geological and Mineral Survey.

Swan, F. H., III, Schwartz, D. P., Hanson, K. L., Kneupfer, P. L., and Cluff, L. S., 1979, Recurrence of surface faulting and large magnitude earthquakes along the Wasatch fault zone, Utah: Geol. Soc. America Abs. with Programs, v. 11, no. 3, p. 131.

Thomas, E. H., and Taylor, G. H., 1946, Geology and ground-water resources of Cedar City and Parowan Valleys, Iron Counties, Utah: U.S. Geol. Survey Water-Supply Paper 993.

54. Van Arsdale, Roy, 1978, personal communication.

55. Van Horn, Richard, 1972, Map showing relative ages of faults in the Sugar House quadrangle, Salt Lake County, Utah: U.S. Geol. Survey Misc. Inv. Map I-766-B.

Wallace, R. E., 1977, Profiles and ages of young fault scarps, north-central Nevada: Geol. Soc. America Bull., v. 88, p. 1267-1281.

Walter, H. G., 1934, Hansel Valley, Utah, earthquake: Compass of Sigma Gamma Epsilon, v. 14, no. 4, p. 178-181.

56. Willard, M. E., and Callaghan, Eugene, 1962; Geology of the Marysvale quadrangle, Utah: U.S. Geol. Survey Geol. Quad Map GQ-154.

Williams, J. S., 1962, Lake Bonneville: Geology of southern Cache Valley, Utah: U.S. Geol. Survey Prof. Paper 257-C, p. 131-152.

57. Williams, P. L., 1964, Geology, structure, and uranium deposits of the Moab quadrangle, Colorado and Utah: U.S. Geol. Survey Misc. Inv. Map I-360.

58. Williams, P. L., and Hackman, R. J., 1971, Geology, structure, and uranium deposits of the Salina quadrangle, Utah: U.S. Geol. Survey Misc. Inv. Map I-571.

59. Witkind, I. J., 1975a, Preliminary map showing known and suspected active faults in Idaho: U.S. Geol. Survey open-file report OF-75-278.

_____, 1975b, Preliminary map showing known and suspected active faults in Wyoming: U.S. Geol. Survey open-file report OF-75-279.

_____, 1975c, Preliminary map showing known and suspected active faults in western Montana: U.S. Geol. Survey open-file report OF-75-285.

60. _____, 1979, personal communication.

61. Witkind, I. J., Lidke, D. J., and McBroome, L. A., 1978, Preliminary geologic map of the Price 1° x 2° quadrangle, Utah: U.S. Geol. Survey open-file report OF-78-465.

62. Young, J. C., 1955, Geology of the southern Lakeside Mountains, Utah: Utah Geol. Mineral Survey Bull. 56, 108 p.

RECURRENCE OF SURFACE FAULTING AND MODERATE TO LARGE MAGNITUDE EARTHQUAKES ON THE WASATCH FAULT ZONE AT THE KAYSVILLE AND HOBBLE CREEK SITES, UTAH

By
F. H. SWAN, III, DAVID P. SCHWARTZ, and LLOYD S. CLUFF

Woodward-Clyde Consultants
Three Embarcadero Center, Suite 700
San Francisco, California 94111

ABSTRACT

No historical earthquakes associated with surface faulting are known to have occurred along the Wasatch fault during at least the past 132 years. However, there is abundant geologic and geomorphic evidence of Late Quaternary faulting along almost the entire length of the 370 kilometer-long fault. Detailed mapping, topographic profiling, and trenching at two sites along the Wasatch fault provide new data on the recurrence of moderate to large magnitude earthquakes produced by surface faulting during the late Pleistocene and Holocene. During the past 6000 years, at least three surface faulting events have produced 10 to 11 m of cumulative net vertical tectonic displacement at the Kaysville site. The vertical tectonic displacement per event is between 1.7 and 3.7 m and the interval between the two most recent events was probably more than 500 years and less than 1000 years. The late Holocene slip rate is 1.7 to 1.8 mm per year and the average recurrence interval at the Kaysville site is probably closer to 1000 years. During the past 12,000 years at least six and possibly seven surface faulting events have produced 11.5 to 13.5 m of cumulative net vertical tectonic displacement at the Hobble Creek site. The average vertical tectonic displacement per event is between 0.8 and 2.8 m. The Holocene slip rate is 1.1 mm per year and the average recurrence interval is between 1500 and 2400 years. The displacement data indicate that magnitude 6 1/2 to 7 1/2 earthquakes have occurred repeatedly along these segments of the fault zone. If the recurrence intervals at the Kaysville and Hobble Creek site are typical of the other segments of the fault zone, the recurrence of moderate to large magnitude earthquakes on the entire Wasatch fault zone may be between 50 and 400 years.

INTRODUCTION

No earthquakes associated with surface fault rupture are known to have occurred along the Wasatch fault zone during historical time (Cook, 1972; Cook and Smith, 1967; Smith and others, 1978). However, abundant geomorphic and geologic evidence indicates that large earthquakes have occurred repeatedly along this fault zone throughout the late Pleistocene and Holocene (Gilbert, 1980; Cluff and others, 1970, 1973, 1974, 1975). Detailed geologic mapping, topographic profiling, and trenching were conducted at

two sites along the Wasatch fault zone, the Kaysville and the Hobble Creek sites (Figure 1), to measure the cumulative fault displacements in Quaternary strata of various ages and to obtain data regarding the amount of displacement per surface faulting event and the number and recurrence of faulting events that produced the cumulative displacement. Where datable material was found, the ages of the displaced units were determined by C-14. Where the deposits could not be dated directly, their ages were assessed by correlating them to deposits that have been dated elsewhere. The regional correlations used in assigning ages to these displaced units are summarized on Table 1. The displacement and recurrence data from the segments of the fault at Kaysville and Hobble Creek are used to estimate the magnitude and frequency of recurrence of earthquakes associated with surface faulting along the entire Wasatch fault zone.

GEOLOGY OF THE KAYSVILLE SITE

LOCATION AND SETTING

The Kaysville site is located along the Wasatch fault zone between Baer Creek and Shepard Creek, approximately 3 km east-southeast of the town of Kaysville, Davis County, Utah (Section 1, T3N, R1W, Kaysville 7 1/2 minute quadrangle). A series of small graben occurs along this segment of the Wasatch fault (Figure 2a). These graben are bounded by prominent west-facing fault scarps on the east (Figure 2b) and by a series of en echelon antithetic fault scarps on the west. The height of the main fault scarp decreases from 22 m in the central part of the site area to less than 10 m to the north where it has been partly buried by alluvium from Baer Creek. The antithetic fault scarps vary in height from less than 1 m to 2.5 m.

Seven trenches and five test pits were excavated across the southern end of a closed depression that occurs in the graben in the central part of the site area (Plate 1). The depression is closed to the south by a small alluvial fan and to the north by alluvial fan deposits derived from Baer Creek and two unnamed ephemeral streams. The closed depression is intermittently occupied by a small pond that is fed by two springs located along the base of the main fault scarp.

The Kaysville site is at an elevation of 1410 m. It is below the Bonneville and Provo shorelines (Figure 2 and Plate 1). Lacustrine sediments deposited during high stands of Lake Bonneville are exposed in the fault scarp and in outcrops along entrenched stream valleys. These sediments are unconformably overlain by coarser post-Provo alluvial fan deposits. Faulting has displaced the fan surfaces down to the west across the main fault scarp and graben.

Other linear breaks in the post-Provo alluvial fan surfaces both east and west of the main fault scarp and graben (Plate 1) are of

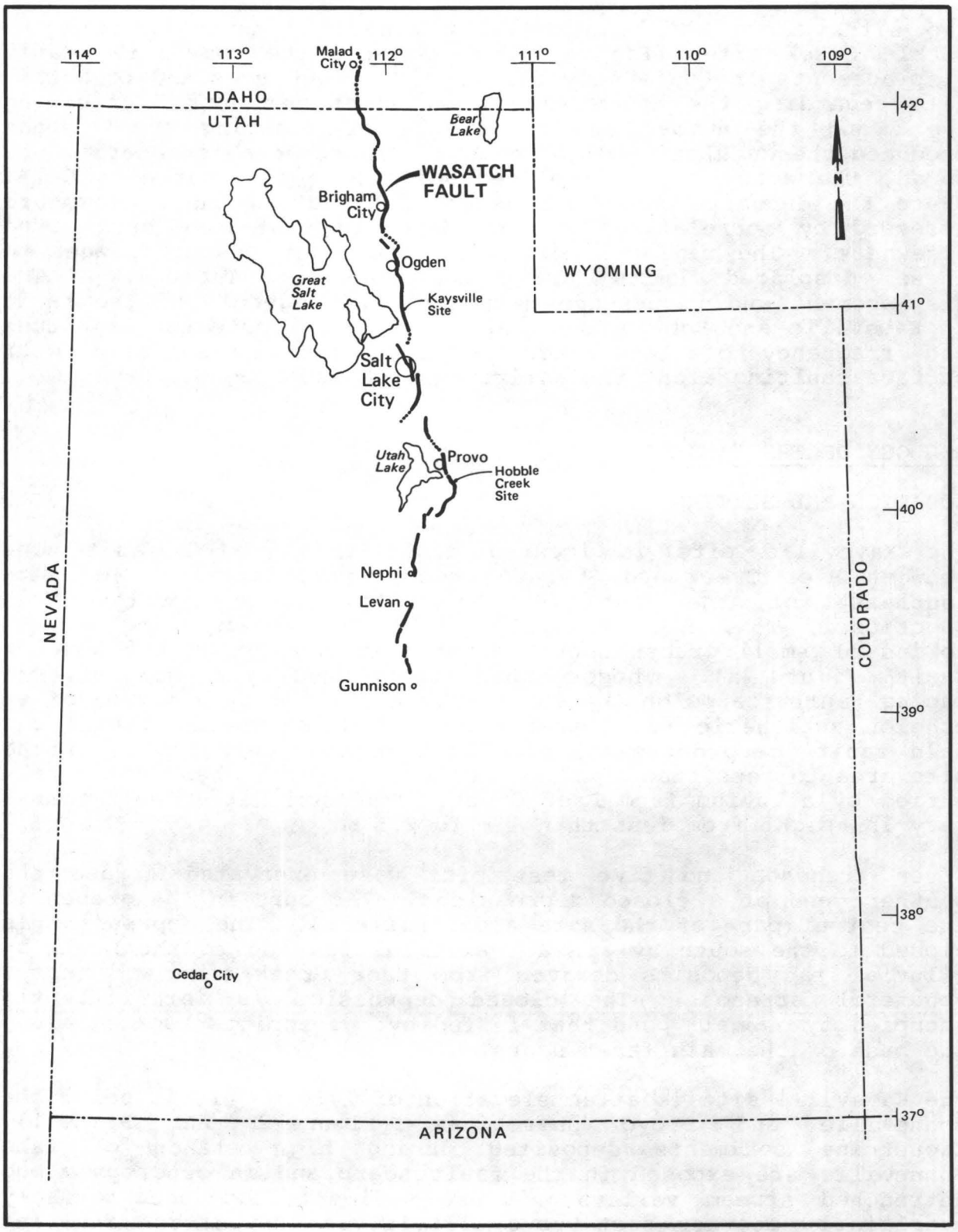

Figure 1 - REGIONAL LOCATION MAP

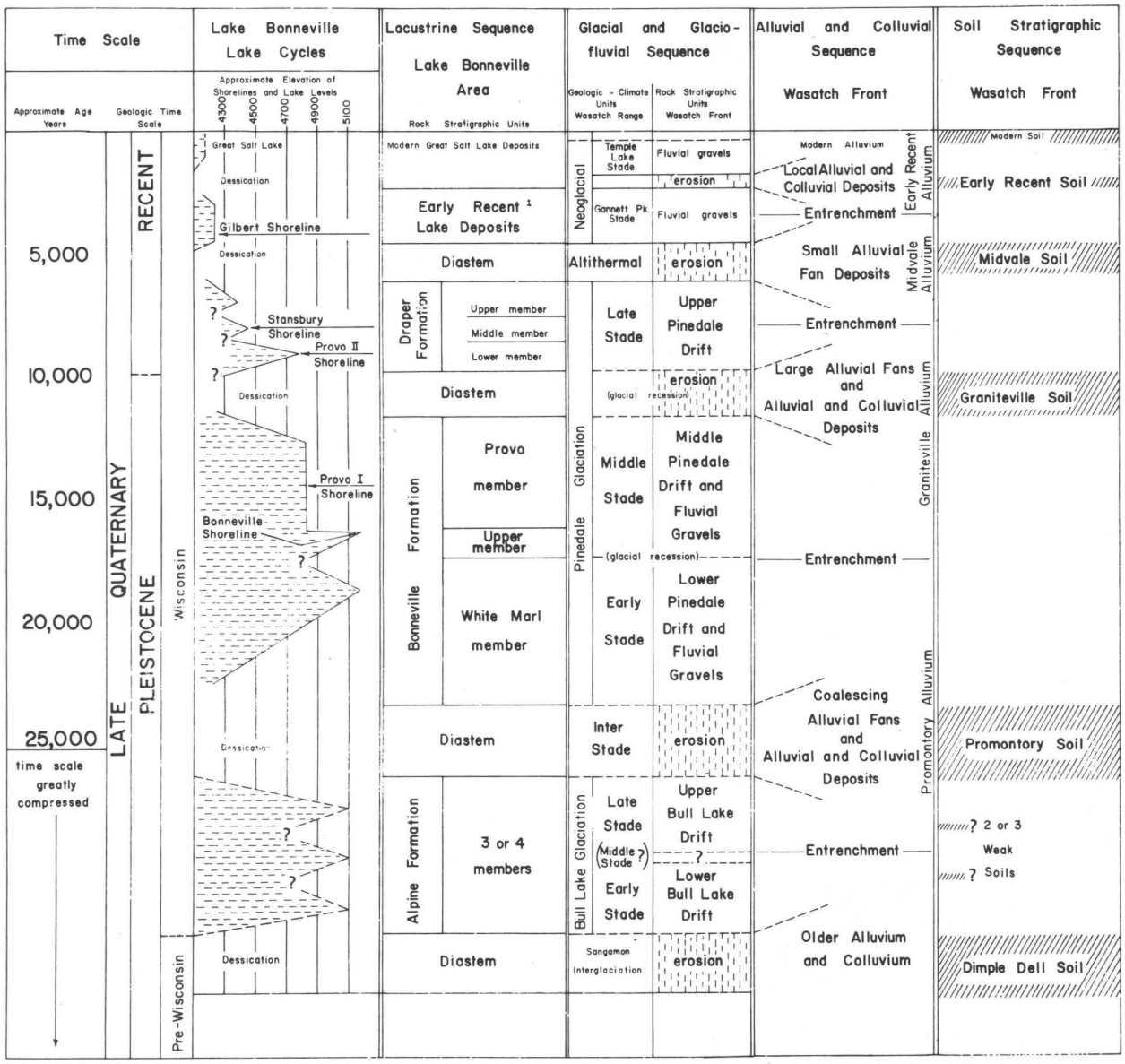

Source: Woodward-Clyde Consultants, 1975
(Modified from Bissel, 1963; Morrison, 1965; and Richmond, 1964)

TABLE 1 - STRATIGRAPHIC CORRELATIONS FOR WASATCH FAULT SYSTEM

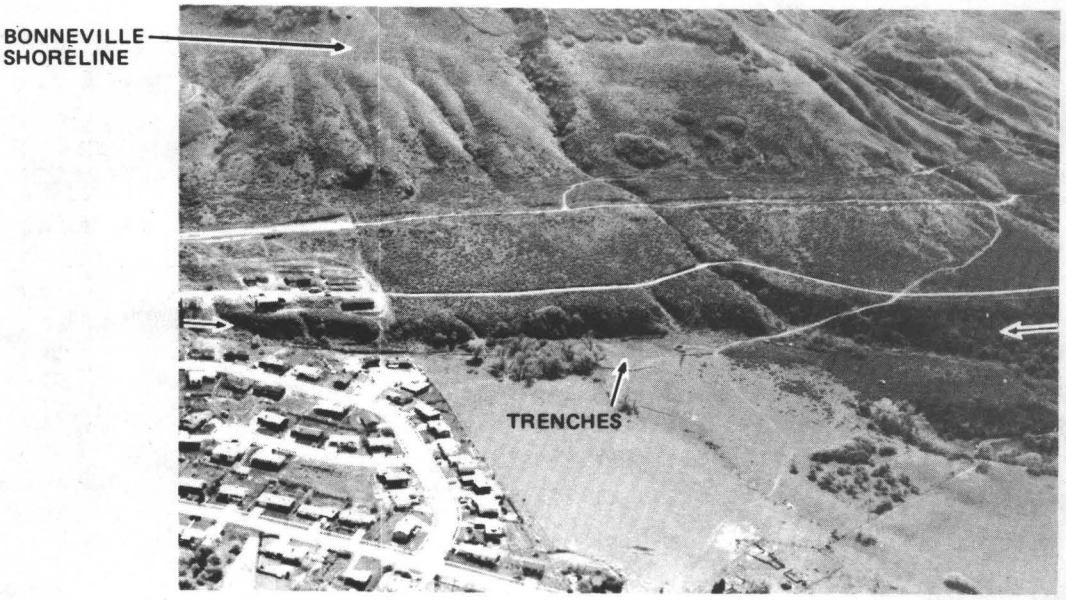

(a) Aerial view of main fault scarp, (arrows), and associated graben at Kaysville Site.

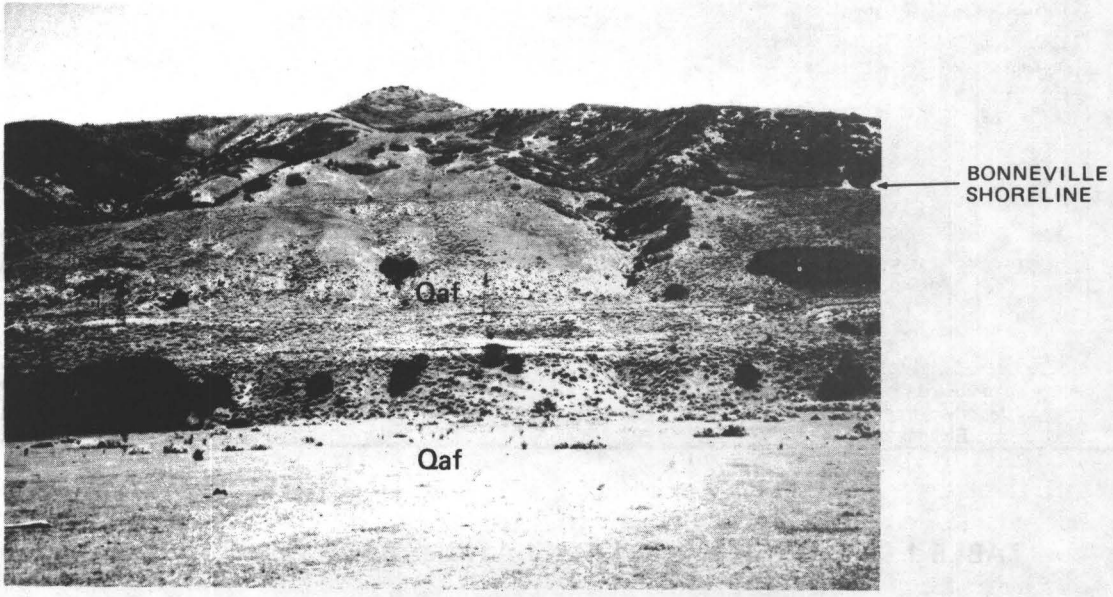

(b) View east across graben and main fault scarp showing displaced alluvial fan surface (Qaf).

Figure 2 - PHOTOGRAPHS SHOWING RECENT FAULT SCARP AT KAYSVILLE

uncertain origin and may represent additional fault traces. Modification of the major break in slope east of the main fault scarp by road and powerline construction makes it difficult to determine if it is a fault or a recessional shoreline.

The Kaysville site was selected for detailed investigation for the following reasons. First, the most recent faulting at this location occurred along a single prominent fault scarp; in most other places, the Wasatch fault zone contains multiple traces that occur in zones up to several kilometers wide. Second, there is abundant geomorphic evidence for repeated late Quaternary displacement along this segment of the fault. Finally, the closed depression formed by the graben on the downthrown side of the fault has acted as a sediment trap and is a favorable environment for preserving organic material that can be dated by the C-14 method. These sediments are likely to preserve the most recent fault displacements.

QUATERNARY STRATIGRAPHY

The Quaternary deposits exposed in the trenches at the Kaysville site consist of lake sediments, alluvial fan and stream deposits, and sag fill and associated colluvium that occur in an area of subsidence adjacent to and at the toe of the main fault scarp. The soils that have developed on the fan surface adjacent to the graben and those buried beneath historical deposits in the graben are weakly developed, attesting to their young age. The stratigraphic and structural relationships between these deposits and soils are shown on the log of trench A across the main fault and graben (Plate 2) and on the geologic cross section shown on Figure 3. The major stratigraphic units identified in the trenches at the Kaysville site are described below. The identification number following the unit name corresponds to those shown on the trench log (Plate 2).

Lithologic Units

Alpine-Bonneville lake deposits (undifferentiated) (unit 1). The oldest deposits exposed in the trenches and test pits are lake sediments deposited during Pleistocene high stands of Lake Bonneville. These deposits consist of thinly bedded silt and very fine to fine sand; the interbedded silts and fine sands alternate with coarser sequences of well stratified medium to coarse sand and fine gravel.

These lake sediments were probably deposited when the lake level was at the Bonneville and/or Provo shorelines. They could be as old as the Alpine Formation or as young as the Bonneville Formation (Table 1). In either case, the lake sediments at the site undoubtedly predate recession of Lake Bonneville from the Provo shoreline to an elevation below 1430 m. The lake deposits at the site are therefore older than approximately 12,000 years.

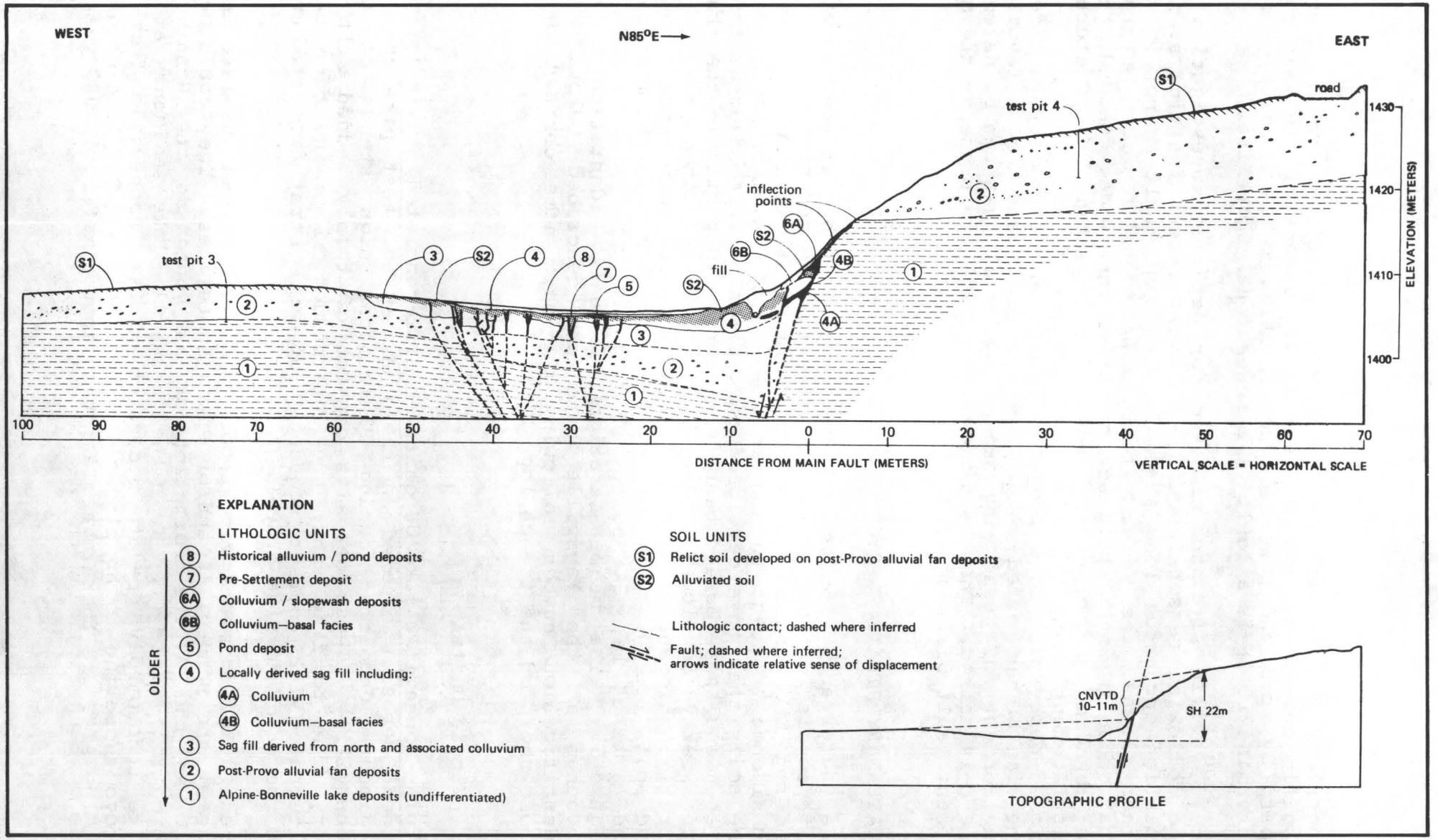

Figure 3 - GEOLOGIC CROSS SECTION OF GRABEN AT THE KAYSVILLE SITE

Post-Provo alluvial fan deposits (unit 2). Deposits that consist primarily of poorly sorted and stratified gravelly sand and cobble and boulder gravel unconformably overlie undifferentiated Alpine-Bonneville lake deposits (Figure 3). The most recent displacements along this segment of the Wasatch fault are represented by a prominent fault scarp that traverses the surface of the post-Provo fan (Figure 2).

In general, bedding within the alluvial fan deposits dips 3 to 10 degrees to the west (steepest dips are in the eastern part of the fan). Across the antithetic scarp and in the graben, the fan deposits have been back-tilted and bedding generally dips 3 to 5 degrees to the east; eastward dips to 21 degrees were measured locally. Although erosion and deposition still occur locally along the intermittent distributary channels that are incised into the fan surface, a weakly developed soil profile (unit S1) has formed on the fan surface between these intermittent streams.

The post-Provo alluvial fan deposits postdate the underlying erosional unconformity, which could be as old as 12,000 years (recession of Provo shoreline). The deposits predate the formation of the soil developed on the fan surface (unit S1), which probably began about middle Holocene time (see discussion of unit S1 below).

Baer Creek alluvial fan deposits. An alluvial fan formed primarily by Baer Creek lies north of the Kaysville trench site. This fan postdates the post-Provo alluvial fan deposits. The streams that deposited the fan sediments have breached the main fault scarp and the fan deposits partially bury the scarp, resulting in a decrease in scarp height from 22 m at the trench site to less than 10 m towards the apex of the fan. Subsequent faulting of the fan is evidenced by pronounced graben on the south flank and at the apex of the fan.

Drainage channels visible on 1958 aerial photographs suggest that Baer Creek may have been diverted southward along the base of the main fault scarp and flowed down the valley that lies immediately south of the trench locality. Some of the sag fill exposed in the trenches probably originated from Baer Creek.

Sag fill derived from the north and associated colluvium (unit 3). The sag formed by the back-tilted post-Provo alluvial fan deposits on the downthrown side of the fault is filled by at least three distinct units. These units consist of colluvium that grades laterally into alluvium and/or pond deposits (Plate 3).

The oldest of these units exposed in the trenches consists of colluvium (unit 3A), derived from the fault scarp, that grades laterally into and partly overlies sag fill deposits (units 3C and 3B). The sag fill onlaps and unconformably overlies the east-dipping (back-tilted) post-Provo alluvial fan deposits at the western margin of the sag (Plate 2). The lower part of these

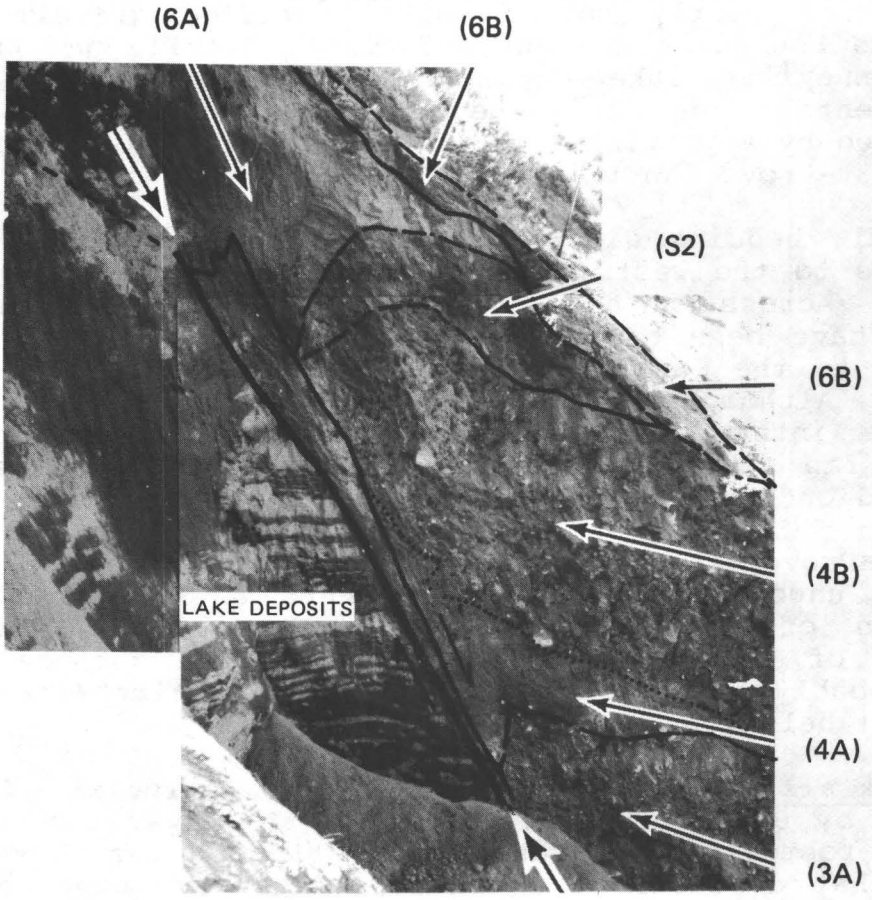

Main fault, (arrows), exposed in the south wall of Trench A, Kaysville site. The two lower colluvial units, (3A and 4A-B), and a soil (S2), are in fault contact with well bedded lake deposits. The upper colluvial unit, (6A), which formed subsequent to the most recent displacement, is in depositional contact with the fault scarp. See Plates 1 and 2 for descriptions of these units.

Figure 4 - PHOTOGRAPH SHOWING MAIN FAULT EXPOSED AT KAYSVILLE SITE

sediments. This unit was deposited immediately after the most recent surface faulting event along this trace of the fault. Unit 6B consists of slopewash and colluvium that is actively accumulating. These colluvial deposits are not as thick as the colluvial facies of units 3 and 4.

Pre-settlement pond deposit/soil (unit 7). The oldest depositional unit exposed in the trenches that is not displaced by faults is a clayey silt pond deposit that conformably overlies units 5 and S2. The pond deposit is mottled by dark organic material that represents the incipient development of a gley soil. These deposits occupy the central portion of the graben. They are the deposits that existed at the ground surface when the area was first settled in 1847. This unit has subsequently been buried by deposits that are historical in age.

Historical deposits (unit 8). Following settlement of this area in 1847, water from the two springs at the base of the main fault scarp was artificially impounded in the graben (R. Harvey, personal communication). This ponding is represented by massive fine silt (unit 8A). A flash flood during the fall of 1919 (R. Harvey, personal communication) added significant amounts of material (unit 8B) to the small alluvial fan located immediately south of the trench sites. Intermittent ponding of the graben subsequent to this flooding event has deposited additional silty pond sediments (unit 8C).

Soil Units

Soil developed on post-Provo alluvial fan deposits (unit S1). A weak-to-moderately well developed relict soil occurs on the post-Provo alluvial fan deposits. This soil exhibits an incipient textural B horizon characterized by a few, thin clay films along pebble and pore surfaces. The soil profile consists of a 40 cm thick A horizon overlying a 20 cm thick A/B horizon that grades downwards into unweathered parent alluvial fan sediments.

Soil S1 began to form after the deposition of the post-Provo alluvial fan deposits, and the soil forming processes have continued to the present. Based on the degree of soil profile development, this soil is tentatively correlated with the Midvale soil (Table 1) (R. B. Morrison, oral communication), which began to form approximately 6,000 years ago.

Alluviated soil (unit S2). A weakly developed soil characterized by an accumulation of carbonaceous material has formed on gravelly colluvium (unit 4B) and finer-grained sag deposits (unit 3B). Although much of the organic material in this soil is illuvial in origin, some of the carbonaceous material appears to be alluviated material incorporated into the sediments during deposition. High ground-water conditions in the fault sag favor preservation of this organic material. Formation of this soil

unit occurred during a period represented by the deposition of the sag fill deposits (correlation chart, Plate 2).

Topsoil (unit S3). A thin (5 to 10 cm) topsoil unit consisting of micaceous silt loam is developed at the surface of the youngest deposits within the graben. In places, this soil unit has been disturbed by plowing, particularly in the southern part of the graben.

FAULTING AND DEFORMATION AT THE KAYSVILLE SITE

Faulting Associated with the Main Scarp

Faulting associated with the main scarp occurs across a zone at least 5.5 m wide as: a) a zone of deformation that defines the main fault, b) minor displacements in lakebeds east of the main fault, and c) a narrow fault zone in colluvium 3.5 m west of the main fault. These faults are shown on Plate 2 and are described below.

The main fault, which is shown in Figure 4, juxtaposes undifferentiated Alpine-Bonneville lake sediments (unit 1) against a sequence of scarp-derived colluvial deposits (units 3, 4, and 6). Cumulative stratigraphic separation across the main fault is greater than the height of the exposures in trench excavations (greater than 11 m). The fault is a zone that strikes N2E and varies in dip from 74 to 55 degrees west. The zone widens from 10 cm near the base of the trench to 40 cm near the surface. The fault zone is bounded on the east by a well defined plane. The eastern part of the zone (4 to 30 cm wide) consists of poorly sorted, fine to coarse, pebbly sand. The long axes of the pebbles generally parallel the dip of the fault. The western part of the fault is a zone (2 to 8 cm wide) of reddish yellow silty sand bounded by a shear plane. The western boundary of the fault zone is clearly defined in the lower part of the trench; it becomes more irregular and less clearly defined towards the ground surface. Several other well defined shears, which are traceable for distances varying between 0.1 and 3 m, occur within the fault zone.

Numerous faults having minor displacements occur across a zone at least 1.5 m wide in the well stratified undifferentiated Alpine-Bonneville lake sediments exposed in the footwall. These faults strike parallel and subparallel to the main fault and dip from 50 degrees west to 85 degrees east. Displacements range from less than 1 cm to an observed maximum of 25 cm. Displacements are predominantly normal down to the west, but high-angle, west-dipping reverse faults also occur. Several faults having minor displacements (less than 2 cm) that appear to decrease downwards are also observed. These minor faults within the lake sediments are defined by displaced bedding that occurs along paper-thin planes that lack distinctive gouge.

A fault oriented N5E, 78W occurs 3.5 m west of the main fault zone in the trench (Plate 2). On the south wall, the fault displaces colluvial units (units 3A, 4A, and 4B). Between stations 5 and 6 a reddish brown basal colluvial sand (unit 4A) is displaced approximately 60 cm down to the west. The fault does not exhibit strong expression in the upper coarse colluvium (unit 4B) and is primarily defined by a soft zone within the colluvium. On the north wall of the trench the fault is marked by an iron-oxide-stained contact between coarse, bouldery colluvium (unit 3A) and a down-faulted block of undifferentiated Alpine-Bonneville lake sediments. This fault may be coincident with the small, west-facing break in slope and small topographic bench that extends approximately 70 m north from trench A and occurs just west of the base of the main fault scarp.

Faulting Associated with the Antithetic Scarps

A zone of faulting containing approximately 100 individual fault planes extends 26 m from the center of the graben across the antithetic scarp (station 24 to station 48; Plate 2). Most of the faults strike north, parallel to the strike of the antithetic scarp, but strikes of up to N12E were observed locally. Faults within the zone are defined by single straight to curvilinear planes and by clusters of planes that anastomose and branch upwards to produce a complex series of horsts and graben. Most of the faults are near-vertical, although dips as low as 55 degrees to both the east and west were observed, especially where faults branch, refract through different layers or, rarely, appear to deflect along bedding planes (station 45.5). The main fault zones associated with the antithetic scarp (stations 42.5 and 45) have an average dip of 70 degrees east; these are coincident with the major breaks in slope of the antithetic scarp. Cumulative vertical displacement across these two zones is 210 cm.

Many faults in the western part of the graben (Plate 2) appear to die out upwards. Whereas some faults may not extend through the section, others do, although they are poorly exposed in the coarser colluvium (units 3B and 4B) and in the soil (unit S2) that is developed on the colluvial deposits. This may be clearly seen between stations 25 and 32, where faults cannot be traced much above the S2 soil contact; however, the base of unit 5 is displaced along the upward projection of each of these faults.

In the bedded deposits the faults associated with the antithetic scarps are planes or paper-thin zones that lack gouge. However, discontinuous zones of fine silt up to 1.5 cm wide occur for short distances along some of the fault planes. These silt zones appear to be most common where single faults splay to form small graben and horsts, and especially where they emerge from gravel unit 2 into sandy silt and sand of unit 3C. At several locations in the trench (stations 24.5, 26.5, 27.7, 31, 33, 26, 39, 45), both V-shaped and irregularly fault-bounded wedges containing

organic-rich material were observed within the sag fill deposits. These wedges of organic-rich material along fault traces occur both as infillings of fissures by the overlying alluviated soil (unit S2) and, in places, as alluvial organic material deposited by surface water percolating down along faults and fractures.

Careful observations were made for any systematic changes in displacement along individual fault planes. In the three trenches that cross the antithetic scarps consistent amounts of displacement of successively younger strata are observed across individual faults. The lack of recurrent displacement on faults associated with the antithetic scarp indicates that these faults and the graben formed during one surface faulting event. Evidence of liquefaction was not observed in any of the trenches.

Back-tilting

Eastward dips measured on units 2, 3C, and 4C indicate that the downthrown block was tilted back towards the main fault during at least two surface faulting events. Between stations 50 and 58 (Plate 3) post-Provo alluvial fan deposits have a measured dip of 3 to 5 degrees east; the fan deposits originally dipped approximately 5 degrees west. This suggests that, within 58 m of the main scarp, these deposits have been rotated as much as 8 to 10 degrees to the east. The initial dips of units 3B, 3C, and 4C were horizontal. These units have been tilted 5 to 6 degrees to the east across a zone that extends 38 m from the main scarp. Younger deposits (units 4E, 5, 7, and 8) overlying these units do not appear to be tilted, suggesting that this 5 to 6 degrees of back-tilting occurred during the second most recent faulting event. West of station 38, the bedded deposits (unit 3C) that onlap the east-dipping post-Provo alluvial fan deposits are horizontal. This change in the attitude of unit 3C may define the hinge line for the tilt of these deposits or it may represent a rotation of the tilted beds back to horizontal during formation of the antithetic scarp.

SEQUENCE OF DEPOSITION AND FAULTING AT THE KAYSVILLE SITE

The following sequence of events is inferred from the structural and stratigraphic relationships at the Kaysville site.

1. Post-Provo alluvial fans (unit 2) were unconformably deposited on Alpine-Bonneville lake deposits (unit 1). The unconformity between these units was displaced by faulting and the fan deposits on the downthrown block were tilted back toward the main scarp, producing a fault sag.

2. The fault sag was filled with a bedded sequence of sand, silt, and gravel (units 3B and 3C) derived from the north, and with associated scarp-derived colluvium (unit 3A). Detrital charcoal from unit 3C has yielded a radiocarbon date

of 1580 ± 150 years B.P. The time interval between the intital back-tilting of the post-Provo alluvial fans and deposition of unit 3C is uncertain. It is possible that more than one surface faulting event occurred during this time interval.

3. The main fault scarp was breached at the southern end of the fault sag. This resulted in formation of a small alluvial fan that blocked through-flowing drainage. A small pond, represented by unit 4C, and cut-and-fill channels (unit 4D) developed within the sag.

4. Surface faulting occurred. This event resulted in tilting of the sag fill (units 3B and 3C) and pond deposits (unit 4C) toward the main fault scarp. Uplift of the scarp during this event exposed Alpine-Bonneville lake deposits.

5. Erosion of the lake deposits exposed in the fault scarp produced a basal facies colluvium (unit 4A) which filled a fissure that formed at the base of the scarp. As erosion of the scarp continued, post-Provo alluvial fan deposits became the dominant source for scarp-derived colluvium (unit 4B). At the same time, the main part of the sag continued to fill with sediments derived from the alluvial fan to the south. An alluviated soil (unit S2) formed during, and subsequent to, deposition of these units.

6. Surface faulting occurred. This faulting produced a graben and renewed uplift along the main fault scarp. The graben to the north in the Baer Creek area and to the south around Shepard Creek also formed during this event. No detectable back-tilting of the downthrown block occurred during this event. Extension across the graben led to formation of numerous small faults in a 25-m-wide zone associated with the antithetic scarp. Infilling of fissures with organic-rich gravel derived from the S2 soil occurred at this time.

7. Erosion of the main fault scarp following this surface faulting event led to deposition of a sequence of scarp-derived colluvium consisting of a basal facies derived primarily from lake sediments (unit 6A) overlain by coarser colluvium (unit 6B) that incorporated material derived from the post-Provo alluvial fans. This colluvial sequence is similar to the colluvial sequence (units 4A and 4B) derived from the scarp subsequent to the previous surface faulting event.

8. Deposition within the graben since the most recent surface faulting has continued. This is represented by pre-settlement silt (unit 7) and historical flood and pond deposits (unit 8).

SLIP RATE, AMOUNT OF DISPLACEMENT PER EVENT, AND RECURRENCE OF SURFACE FAULTING AT THE KAYSVILLE SITE

Slip rate, the amount of displacement per event, and the recurrence interval between surface faulting events are all factors that can be used to assess the potential for earthquake hazards. These factors are discussed below.

Slip Rate

The late Holocene slip rate for the segment of the fault at Kaysville can be estimated by dividing the cumulative vertical tectonic displacement (10 to 11 m) by the minimum age of the offset fan surface (approximately 6000 years B.P.). These values give an average slip rate of 1.7 to 1.8 mm per year.

Amount of Displacement Per Event

The cumulative vertical tectonic displacement of the unconformity between Alpine-Bonneville sediments and post-Provo alluvial fan deposits across the main fault and graben is 10 to 11 m down to the west; this value is approximately equal to the cumulative displacement of the alluvial fan surface. The amount of displacement across the main fault scarp is significantly greater (approximately two times greater) than cumulative vertical tectonic displacement across the zone. This difference is the result of graben formation and back-tilting at this locality. In Figure 3, the unconformity has been projected toward the main fault using dips observed in the post-Provo alluvial fan deposits. If this projection is correct, it indicates displacement of the unconformity across the main fault of about 25 m, which is approximately equal to the present height of the scarp.

Back-tilting, graben formation, lack of distinctive stratigraphic horizons across the fault, and modification of the base of the scarp by erosion and deposition are factors that complicate estimates of amount of displacement per event. One approach to evaluating displacement per event is to divide the cumulative tectonic displacement by the three events interpreted as having occurred at this site. This yields average values of 3.3 to 3.7 m per event. The actual values will be different if more than three events have occurred at the site and/or if the amount of displacement was not the same for each event.

Estimates of the amount of displacement per event can be based on the geometry of the main fault, the scarp morphology, and the thicknesses of the scarp-derived colluvial units. Geometrical relationships suggest that tectonic displacement during the most recent surface faulting event may have been approximately 2 m. In trench A, the point of intersection of the projection of the main fault plane with the ground surface is coincident with the

lower inflection point on the scarp profile (Figure 3). This inflection point is interpreted to be the top of the free face developed on the scarp during the most recent faulting event. The distance between this inflection point and the base of the colluvium derived from the fault scarp is approximately 3.5 m. One-half meter of displacement also occurred across the west-dipping fault at station 4.5 (Plate 2), producing a total down-to-the-west displacement of at least 4 m. Total displacement across the antithetic faults was 2.2 m down to the east during this event. Models of graben formation discussed by Slemmons (1957) suggest the true tectonic displacement across the zone (slip on main fault minus height of graben) is at least 1.8 m.

Analysis of the colluvial stratigraphy adjacent to the main scarp suggests that slip along the main fault during the second most recent faulting event was a minimum of 3.4 m. This is based on the assumption that colluvial unit 3A was in equilibrium with the scarp (not actively aggrading) prior to the second most recent event and on the measured thickness of colluvium derived from the fault scarp produced as a result of this event (unit 4). Back-tilting of deposits in the sag during this event contributed an unknown amount of slip along the main fault. As noted above, the amount of displacement across the main fault may be as much as two times the tectonic displacement. This suggests that the tectonic displacement during the second most recent faulting event was a minimum of 1.7 m.

Assessment of amount of displacement per event for the oldest event(s) recognized at the Kaysville site is more difficult because critical stratigraphic relationships are below depths that were exposed by the trenches. If the two most recent faulting events accommodated approximately one-third to one-half the 10 to 11 m of tectonic displacement, tectonic displacement associated with the oldest event recognized at the site would have to be 5 to 8 m. Stratigraphic relationships allow the possibility that more than one event could have occurred prior to the second most recent event. This would reduce the amount of displacement per event. The available data suggest a range in values of between 1.7 m and 3.7 m of tectonic displacement per surface faulting event along this segment of the Wasatch fault.

Recurrence of Surface Faulting

At least three surface faulting events have produced a cumulative vertical tectonic displacement of 10 to 11 m of the erosional unconformity between post-Provo alluvial fan deposits and Alpine-Bonneville lake sediments. The maximum age of this unconformity is estimated to be 12,000 years B.P. The post-Provo alluvial fan surface is displaced approximately the same amount. This surface is younger than soil S1; formation of this soil is estimated to have begun approximately 6000 years ago. These observations indicate that the 10 to 11 m of vertical tectonic displacement probably occurred within the past 6000 years.

A radiocarbon age of 1580 ± 150 years B.P. was obtained on charcoal from a silt layer in unit 3C. At least one surface faulting event occurred between formation of the unconformity and deposition of unit 3C; the time interval between faulting of the fan deposits and deposition of unit 3C is uncertain.

Two surface faulting events have occurred since deposition of the charcoal-bearing layer. At least 1.6 m of sediment was deposited after the charcoal-bearing layer and prior to the second most recent faulting event. Therefore, the date of this event is 1580 ± 150 years, less the time it took to deposit at least 1.6 m of sediment. The exact rate of sediment accumulation in the sag is not known. The youngest unit displaced during the most recent faulting event is a thinly laminated organic silt (unit 5). The silt is overlain by a 25- to 30-cm-thick pond deposit (unit 7) and 35 to 40 cm of historical (1847 and younger) flood and pond deposits. These stratigraphic relationships suggest that the age of unit 5 is probably several hundred years (perhaps 500 years). The available data suggest that the interval between the two most recent events is unlikely to be greater than 1000 years or less than 500 years.

If it is assumed that the time interval between the two most recent surface faulting events is typical of past events, there would have been six to twelve events during the past 6000 years. If the displacement during the most recent event is typical of past events, it would take five to six events to produce the observed 10 to 11 m of cumulative tectonic displacement. This suggests the intervals between past events was probably closer to 1000 years than to 500 years. However, sufficient data are not yet available to determine whether or not the intervals between these events have been uniform through time.

GEOLOGY OF THE HOBBLE CREEK SITE

LOCATION AND SETTING

The Hobble Creek site is 4.8 km east of the town of Springville in Utah County, Utah (Sections 2, 1, and 12; T85; R3E; Springville 7 1/2 minute quadrangle) (Figure 1). The site is located on the eastern margin of Utah Valley where the west-flowing Hobble Creek leaves the Wasatch Range. In this area, the Wasatch fault zone is characterized by a prominent fault scarp associated with the main trace of the fault, several small graben, and wide zones of back-tilting of the downthrown block towards the main fault scarp (Plate 3).

Sediments deposited during high stands of Pleistocene Lake Bonneville are exposed in the fault scarp and terrace escarpments. Geomorphic surfaces associated with these deposits are displaced down to the west across the fault zone; cumulative tectonic displacements of these surfaces and deposits are progressively greater with increasing age (Figure 5b). Complex

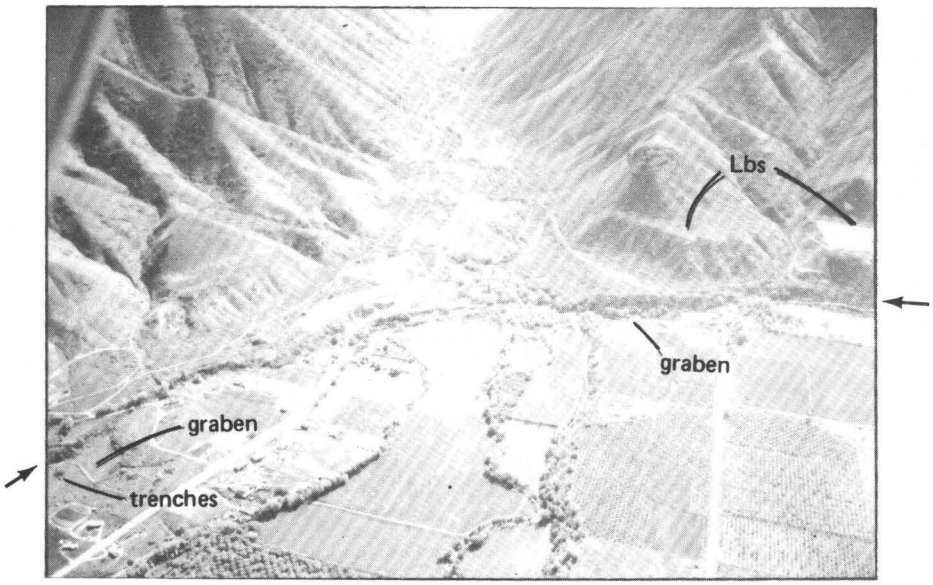

(a) View is east towards mouth of Hobble Creek Canyon showing main fault scarp (arrows), grabens, shoreline of Lake Bonneville (Lbs), and trenches.

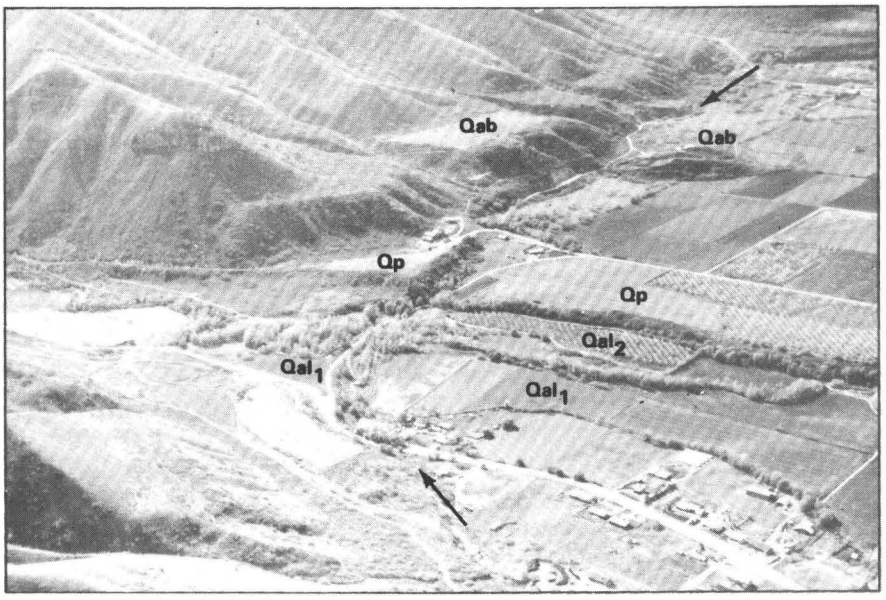

(b) View is towards the southeast along the main fault scarp (arrows) and shows the progressively lower scraps associated with the successively younger Quarternary deposits. From oldest to youngest, the deposits and related scrap scarp heights are: Alpine-Bonneville lake deposits, (**Qab**), 60 m; Provo fan-delta deposits (**Qp**), 28.5 m; post-Provo-pre-Utah Lake deposits (Qal_1), 12.5 m; and the modern flood plain deposits (Qal_2), which show no detectable displacement.

Figure 5 - OBLIQUE AERIAL PHOTOGRAPHS OF HOBBLE CREEK SITE

alluvial fans that consist of several fan segments occur in several places along the range front. The segmentation of these fans is the result of repeated slip along the Wasatch fault.

Three trenches were excavated across the main fault trace and an associated graben 0.96 km northwest of the mouth of Hobble Creek (Plate 3 and Figure 5a). The graben at this location is 50 to 65 m wide. It is bounded on the northeast by the main fault scarp and on the southwest by a series of antithetic fault scarps. The graben cuts deposits of a large alluvial fan complex at the mouth of Deadmans Hollow. The main fault scarp has been partly buried by younger fan deposits, and the height of the scarp decreases southeastward from 15 m to 11.8 m near the apex of the young fan segment. The main antithetic fault scarp at this location is approximately 140 m long and progressively decreases in height from a maximum of 1.5 m to less than 0.5 m before it dies out to the southeast.

QUATERNARY STRATIGRAPHY

The Quaternary deposits mapped at the Hobble Creek site consist of lake deposits, fan-delta and stream sediments, alluvial fan deposits, and colluvium. The areal distribution of these deposits is shown on the photogeologic map of the Hobble Creek site (Plate 3). The major stratigraphic units mapped at the Hobble Creek site and observed in the trenches are discussed below. Figure 6 shows the correlation between the units shown on the photogeologic map (Plate 3) and the units shown on the log of trench HC-1 (Plate 4).

Lithologic Units on Photogeologic Map

Alpine-Bonneville lake deposits (undifferentiated) (Qab) and Bonneville lake deposits (Qb). The oldest Quaternary deposits mapped at the Hobble Creek site consist of lake sediments deposited during the last major Pleistocene high stand of Lake Bonneville. These deposits extend to a maximum elevation of approximately 1555 m, which marks the high stand of the Alpine-age lake according to Bissell (1963). The prominent bench that forms the Bonneville shoreline (Figure 5) is interpreted by Bissell (1968) to have been formed during the Alpine lake cycle and was occupied only briefly during the later Bonneville lake cycle. This bench is generally underlain by cobble and boulder gravel that is coarser and less well sorted than the underlying lake deposits. These gravel deposits are generally thin (less than 11 m) and occur as discontinuous remnants along the Bonneville shoreline at an elevation of approximately 1566 m. Bissell (1963) maps the well sorted lake deposits as Alpine Formation and these coarser gravels as Bonneville Formation.

Bissell (1963) states that, locally, the Alpine and Bonneville Formations are separated by a disconformity, subaerial deposits,

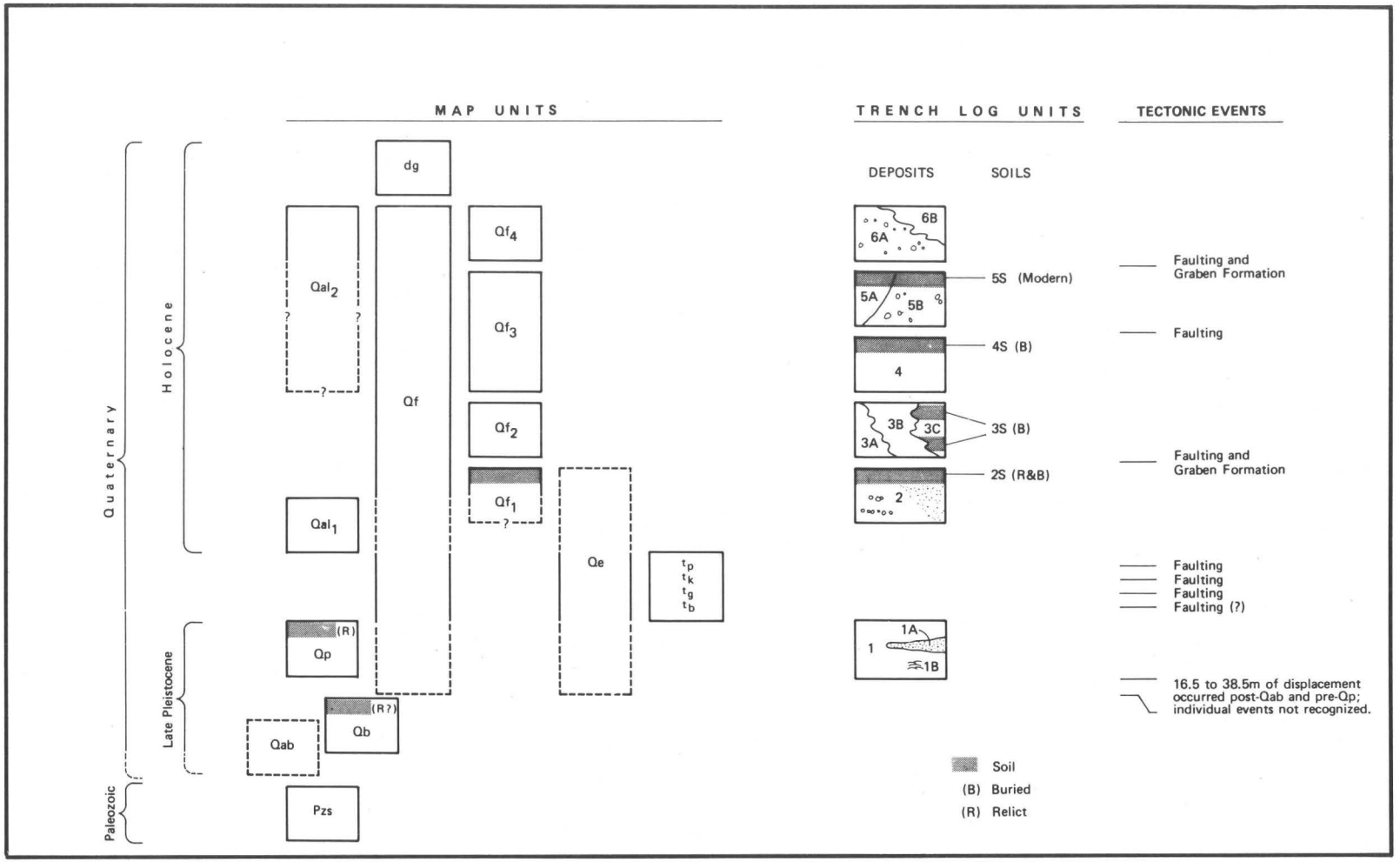

Figure 6 - CORRELATION CHART SHOWING THE CORRELATION BETWEEN THE UNITS ON THE PHOTOGEOLOGIC MAP (PLATE 3) AND THE LITHOLOGIC AND SOIL UNITS EXPOSED IN TRENCH HC-1 (PLATE 4) AND THEIR RELATIONSHIP TO SURFACE FAULTING EVENTS ALONG THE WASATCH FAULT AT THE HOBBLE CREEK SITE.

and a submature soil. Stratigraphic relationships between these deposits are well exposed in the sides of gullies that are eroded into the Alpine-Bonneville bench between Hobble Creek and Maple Canyon. Evidence for a major disconformity between the Alpine sediments and Bonneville gravel is not apparent in these exposures. It might be argued, therefore, that rather than representing separate lake cycles, the Bonneville and Alpine Formations may be deep water (Alpine) and shallow water (Bonneville) facies of a single lake cycle. Scott (1979) suggests that this situation may exist at many places along the Wasatch Front.

These different interpretations affect the ages that can be assigned to these deposits. Therefore, an informal nomenclature has been adopted for this report: the thick sequence of well sorted lake deposits that predate Provo-age deposits are referred to as Alpine-Bonneville lake deposits (undifferentiated) (Qab on Plate 3), which reflects the uncertainty in their age, and the coarser poorly sorted gravels that overlie these lake deposits and underlie the Bonneville bench are referred to as Bonneville gravel (Qb on Plate 3).

Provo fan-delta deposits (Qp). Gravel deposits of Provo age crop out in places along the main fault scarp and along terrace escarpments that parallel Hobble Creek. The Provo gravel deposits are mapped by Bissell (1963) as a composite delta built by Hobble Creek, Spring Creek, and nearby smaller streams. Between the mouth of Hobble Creek Canyon and the trench site, steep foreset bedding characteristic of deltaic deposits are not observed. The structure of these gravel beds is more typical of alluvial terrace deposits, and it appears that the increased sediment load of Hobble Creek was deposited in an alluvial fan-delta complex rather than a typical deltaic environment. Recession of Lake Bonneville from the Provo level occurred prior to approximately 12,000 years B.P. A moderately developed relict paleosol (A/B/Cca profile) has formed on the Provo fan-delta surface.

Strath terraces (t_b; t_g; t_k; t_p). There is a sequence of three paired strath terraces and one unpaired terrace that is eroded into the Provo fan-delta deposits near the mouth of Hobble Creek Canyon east of the main trace of the Wasatch fault (Plate 3). The terraces are below the Provo terrace, which is 25 to 28 m above Hobble Creek, and above a terrace underlain by post-Provo pre-Utah Lake alluvium (Qal_1), which is 4.5 to 5.5 m above Hobble Creek. Two transverse valley profiles that show these terraces are presented in Figure 7.

From highest to lowest, these strath terraces are t_b, t_g, t_k, and t_p. Terrace t_b occurs on the south side of Hobble Creek 17.5 to 19 m above the thalweg of the creek. It is the only unpaired terrace in this sequence. Terrace t_g is 13.6 m above the creek. It is mapped only on the south side of Hobble Creek (Plate 3) because it is buried by alluvial fan deposits (Qf_1) on the north

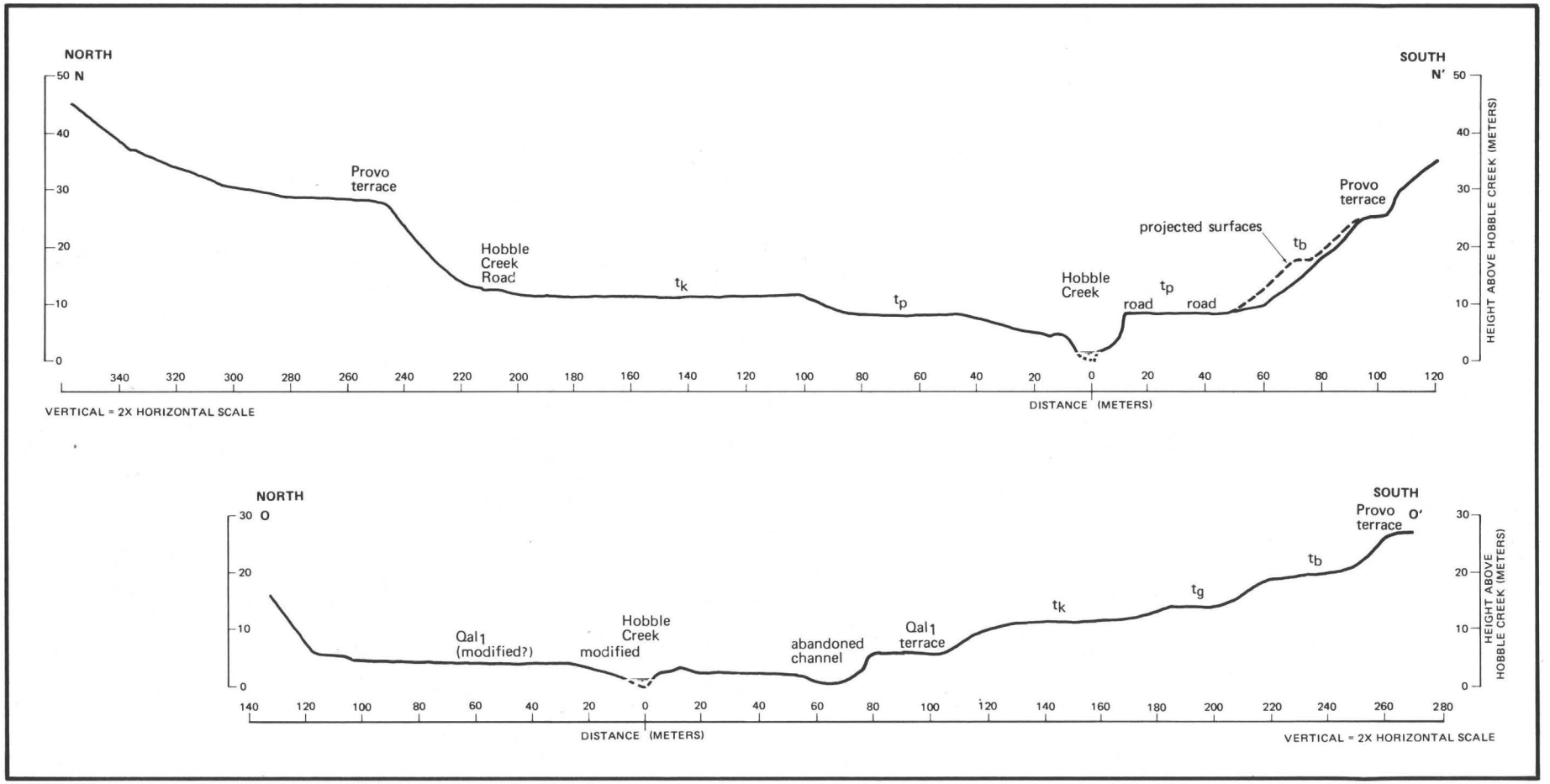

Figure 7 - TOPOGRAPHIC PROFILES SHOWING TERRACES ALONG HOBBLE CREEK

side of the creek. Terraces t_k and t_p are 10.5 to 11.5 m and 8 to 8.5 m above the thalweg of Hobble Creek, respectively.

The paired terraces, and possibly even the unpaired terrace, are believed to be of tectonic origin. They only occur on the upthrown side of the fault. Each terrace probably represents incision of Hobble Creek into the upthrown block following a faulting event. The sequence of terraces is post-Provo and pre-Qal_1 in age (post about 12,000 years B.P. and pre-middle Holocene or about 6000 years B.P.).

Post-Provo Pre-Utah Lake deposits (Qal_1). Recession of Lake Bonneville below the Provo stage resulted in incision of the Provo fan-delta surface by Hobble Cleek. The eroded material was subsequently redeposited as an alluvial fill and large alluvial fan (Qal_1) on which Springville is located. The post-Provo pre-Utah Lake alluvium is probably correlative with deposits that are mapped as Draper Formation by Morrison in Salt Lake Valley, which he estimated to have been deposited between 10,000 and 6000 years ago (Morrison, 1965, figure 2).

Flood-plain deposits (Qal_2). Alluvium that consists of poorly sorted, lenticular bedded gravel and sand, with some silt and clay, occurs along the present flood plain of Hobble Creek, which grades to Utah Lake. The flood plain and, locally, the post-Provo pre-Utah Lake terrace surface (Qal_1) are veneered with sediment from a major flood that occurred in 1952. The channel of Hobble Creek, particularly on the upthrown block, has been extensively modified as a result of this flood and subsequent flood control measures.

Fan deposits (Qf). Numerous small fans that consist primarily of poorly sorted debris-flow deposits occur at the mouths of intermittent streams and gullies along the mountain front. A few small fans grade to the Bonneville bench on the upthrown block east of the main fault. Most of the fans, however, are inset below the Alpine-Bonneville deposits and unconformably overlie Provo-age and younger deposits on both the upthrown and downthrown sides of the fault.

Slip along the Wasatch fault has repeatedly beheaded many of these fans, producing fan segments of different ages. Remnants of displaced fan segments are preserved on the upthrown block south of Hobble Creek at the mouths of Ether Hollow and the next major intermittent stream to the south, and north of Hobble Creek at the mouth of Deadmans Hollow. In many places, the fault scarp is breached by younger fan segments that do not appear to be faulted. Individual fan segments are not differentiated on Plate 3, except for the fan complex at the mouth of Deadmans Hollow.

The Deadmans Hollow fan complex is composed of four segments. The oldest segment, Qf_1 (equivalent to unit 2, trench HC-1), buries Provo-age gravel and grades to a terrace underlain by

post-Provo pre-Utah Lake alluvium. At the trenching site, these fan deposits are inset at least 5 m below the Provo fan-delta deposits in the upthrown block east of the main fault. A relict soil occurs on the Qf_1 fan surface, which is tentatively correlated with Morrison's (1965) Midvale soil. This soil is buried by the younger fan deposits (Qf_2 and Qf_3). Based on its geomorphic position, this soil is believed to be younger than the post-Provo pre-Utah Lake alluvium (post about 6000 years B.P.).

Fan segment Qf_2 (equivalent to unit 3C, trench HC-1) consists of debris flow deposits that partly fill the graben on the northwest flank of the fan complex. Fan segment Qf_3 occupies the area at the apex of the fan complex. Qf_3 deposits partly bury the main fault scarp, which decreases in height towards the apex of the fan. A lobe of this fan segment extends into the graben. The most recent faulting has beheaded this fan along the main trace of the fault; a remnant of the fan segment is preserved on the upthrown block. Qf_4, which is located on the east flank of the fan complex, is the youngest fan segment. Qf_4 deposits postdate the most recent faulting event.

Eolian deposits (Qe). Windblown deposits of silt and fine sand (Qe) mantle Bonneville gravel on the Bonneville bench and Alpine deposits at Murdock mountain. The deposits occur above the Provo shoreline in places and could represent eolian deposition during and shortly following late Bonneville time; however, most of the eolian deposits are probably post-Provo in age.

Lithologic and Soil Units Exposed in Trench HC-1

Trench HC-1 was excavated across the graben on the northwest flank of the Deadmans Hollow fan complex and exposed the stratigraphic and structural relationships between Provo-age gravels and the deposits related to the individual fan segments. These relationships are shown on the log of trench HC-1 (Plate 4). The lithologic and soil units exposed in this trench are described below.

Provo fan-delta deposits (unit 1). The oldest deposits exposed in the trenches at the Hobble Creek site are Provo fan-delta deposits. These deposits were exposed in the footwall on the upthrown side of the fault and are juxtaposed against a sequence of scarp-derived colluvium across the main fault.

Alluvial fan and loess deposits (unit 2). Adjacent to the steep mountain front, the alluvial fan (Qf_1), which grades to the post-Provo pre-Utah Lake surface (Qal_1), consists primarily of coarse poorly sorted mudflow debris. Locally, the individual mudflow units are separated by weakly developed soils characterized by slightly darker zones of accumulating organic matter. With increasing distance from the mountain front, the fan deposits contain greater amounts of reworked loess and may contain some primary loess.

Post-unit 2 soil (unit 2S). A moderately developed soil having a weak textural B horizon and stage I carbonate accumulation has formed on these fan deposits. This soil is tentatively correlated with the Midvale soil (Table 1). It is displaced across the antithetic main fault and buried by younger mudflow deposits (unit 3C).

Fan deposits and associated colluvium (unit 3). Deposits of a lobe of fan segment Qf_2 observed in trench HC-1 consist primarily of a sequence of individual mudflow units (unit 3C) separated by weakly developed soils (unit 3S) characterized by A/C profiles that formed on the individual mudflow units. These deposits were observed only in the graben and appear to have been deposited against a preexisting antithetic fault scarp. These deposits are presently in fault contact with loess and alluvial fan deposits (unit 2) across the largest antithetic fault scarp, and are displaced across numerous minor faults within the graben.

The sequence of mudflow deposits (unit 3C) grades laterally into an alluvial facies (unit 3B) at the northeastern margin of the graben, which in turn grades into a colluvial facies (unit 3A) adjacent to the main fault scarp.

Colluvium (unit 4). Reddish yellow colluvium that infills a wedge-shaped depression at the toe of the fault scarp is in fault contact with the Provo fan-delta deposits. This wedge-shaped feature is interpreted to be an infilling of a fissure that formed at the top of the debris slope near the base of the fault scarp during a surface faulting event. The colluvium contains abundant rounded to well rounded clasts derived primarily from Provo fan-delta gravel deposits in the upthrown block.

Channel and fan deposits (unit 5). Alluvial deposits (unit 5A) consisting of stratified, poorly sorted to moderately well sorted sand, gravelly sand, and minor amounts of fine gravel occupy a buried channel at the base of the main fault scarp. The channel deposits are overlain by poorly sorted, sandy gravel debris flow deposits (unit 5B). The topsoil developed on the debris flow deposits at the ground surface is an entisol that exhibits only minor accumulation of organic matter.

Young scarp colluvium and associated channel deposit (unit 6). The youngest colluvial unit on the main fault scarp, unit 6A, consists of pebbly silty sand that grades laterally into a silty coarse sand alluvium that fills a channel at the base of the fault scarp. This unit overlies the main fault and is in depositional, rather than fault, contact with the underlying Provo fan-delta deposits (unit 1) and older fault scarp derived colluvium (unit 4). This unit was deposited immediately after the most recent surface faulting event. Unlike the older colluvium derived from the fault scarp (unit 4), this unit does not occupy a wedge-shaped fissure at the base of the scarp. The colluvium is buried by loose debris resulting from the construction of a farm access road higher up on the fault scarp.

FAULTING AND DEFORMATION AT THE HOBBLE CREEK SITE

Faulting and Deformation Observed in Exploratory Trenches

Faulting associated with the main scarp. The faulting exposed in trench HC-1 on the upthrown block occurs completely within Provo-age gravel and sand, and has produced horsts and graben across a zone extending 3 1/2 m northeast of the main fault plane (Plate 4). Trench HC-1 extended an additional 10 m to the northeast (not shown on Plate 4); no other faults are observed in this segment. Faults strike between N20W and N40W, generally parallel the main fault, and dip steeply east or west. Displacements vary from as little as 0.5 cm on faults in sand and silt immediately northeast of the main fault, to as much as 54 cm on the northeasternmost fault in the zone.

The main fault is oriented N36W, 58W. It juxtaposes Provo-age gravel and sand in the footwall against colluvium derived from the fault scarp. Cumulative stratigraphic separation across the main fault is greater than the height of exposures in the trench (approximately 15 m).

Antithetic faulting and back-tilting. The fan deposits in the graben at the trench site are faulted and tilted back towards the main fault scarp. The zone of faulting within the graben exposed in trench HC-1 contains at least 16 faults. The faults vary in strike from N29W to N66W; most strike between N40W and N58W. The faults dip steeply to the northeast or southwest as much as 72 degrees, producing series of horsts and graben (Plate 4). Most of the faults are straight to curvilinear planes or thin zones, but some splay or anastomose upwards to produce a series of small steps or minor horsts and graben (station 33). At stations 36, 39, 46.5, and 52, irregularly shaped fault-bounded zones containing softer unbedded sediment and a higher concentration of organic material than the surrounding sediment may be observed; these may represent infillings of fissures by the overlying soil or illuvial organic material deposited by surface water percolating down along faults and fractures.

Displacements on individual faults within the graben range from 3 to 36 cm. Most of the faults appear to extend into, and displace the base of, unit 5B. Displacements on many of these faults are the same on successively younger stratigraphic units, indicating that they formed during the most recent surface faulting event. However, some faults appear to die out before extending into unit 5B. At station 22.5, the contact between units 2 and 3C is displaced 16 cm down to the northeast by a northeast-dipping fault. The fault splays upward and displaces a gravel layer within 3C by the same amount, but no displacement of the contact between units 3C and 5B was observed. At station 26, an east-dipping fault displaces the contact between units 2 and 3B and a soil horizon within unit 3B 16 cm down to the northeast; the contact betwen units 3C and 5B is not clearly displaced, but appears to be warped across the fault. At station 47, a

sand-gravel contact within unit 2 is displaced 20 cm down to the northeast by a fault; this fault cannot be traced above, and does not appear to displace, the contact between units 2 and 3C.

The cumulative vertical displacement of soil unit 2S across the largest antithetic fault in the central part of the graben is approximately 2 1/2 m. About 100 m the southeast, the displacement of unit 2 across this fault is 1.3 m.

The fan deposits on the downthrown side of the main fault are tilted towards the main fault over a wide zone that extends for approximately 120 m from the main fault scarp. The tilt of the beds is greatest adjacent to the main fault and rapidly decreases away from the fault. The actual amount of rotation of these fan deposits is difficult to determine because the initial dips of these units are not known. The effects of back-tilting on the assessment of the net tectonic displacement are discussed in the following sections.

Cumulative Displacements Based on Scarp Profiles

Surface faulting throughout Late Quaternary time is indicated by the progressively smaller cumulative displacements that are observed in the successively younger datums measured. Back-tilting and antithetic faulting significantly increase the apparent cumulative vertical separation across the main fault (scarp height) relative to the true tectonic displacement across the entire deformed zone. If this factor is considered, corrected values of the cumulative net tectonic displacement can be calculated. Measurements of scarp heights, the amount of back-tilting, and the cumulative net vertical tectonic displacements of different age deposits are discussed below.

Scarp heights and vertical stratigraphic separation. The heights of the fault scarps in Bonneville-Alpine lake deposits, Provo fan-delta deposits, and post-Provo pre-Utah Lake alluvium are 60 m, 28.5 m, and 12.5 m, respectively (Figures 5 and 8). These heights include the effects of back-tilting and graben formation. The fault scarp in the Alpine-Bonneville lake deposits has been significantly modified by erosion and by deposition of younger eolian deposits; consequently, the scarp height (60 m) may not accurately reflect the post Alpine-Bonneville displacement on the main fault. The top of a gravel unit in these lake deposits is exposed in the sides of gullies eroded into the upthrown block east of the main fault and in the west end of a canal cut through Murdock mountain on the downthrown block west of the fault (Figure 8). The vertical stratigraphic separation of this gravel marker is 56 m.

Back-tilting. Topographic profiling of the post-Provo pre-Utah Lake terrace and the Provo terrace show measurable tilting of each terrace surface back toward the main fault scarp (Figure 8). West of the deformed zone, the post-Provo pre-Utah Lake terrace

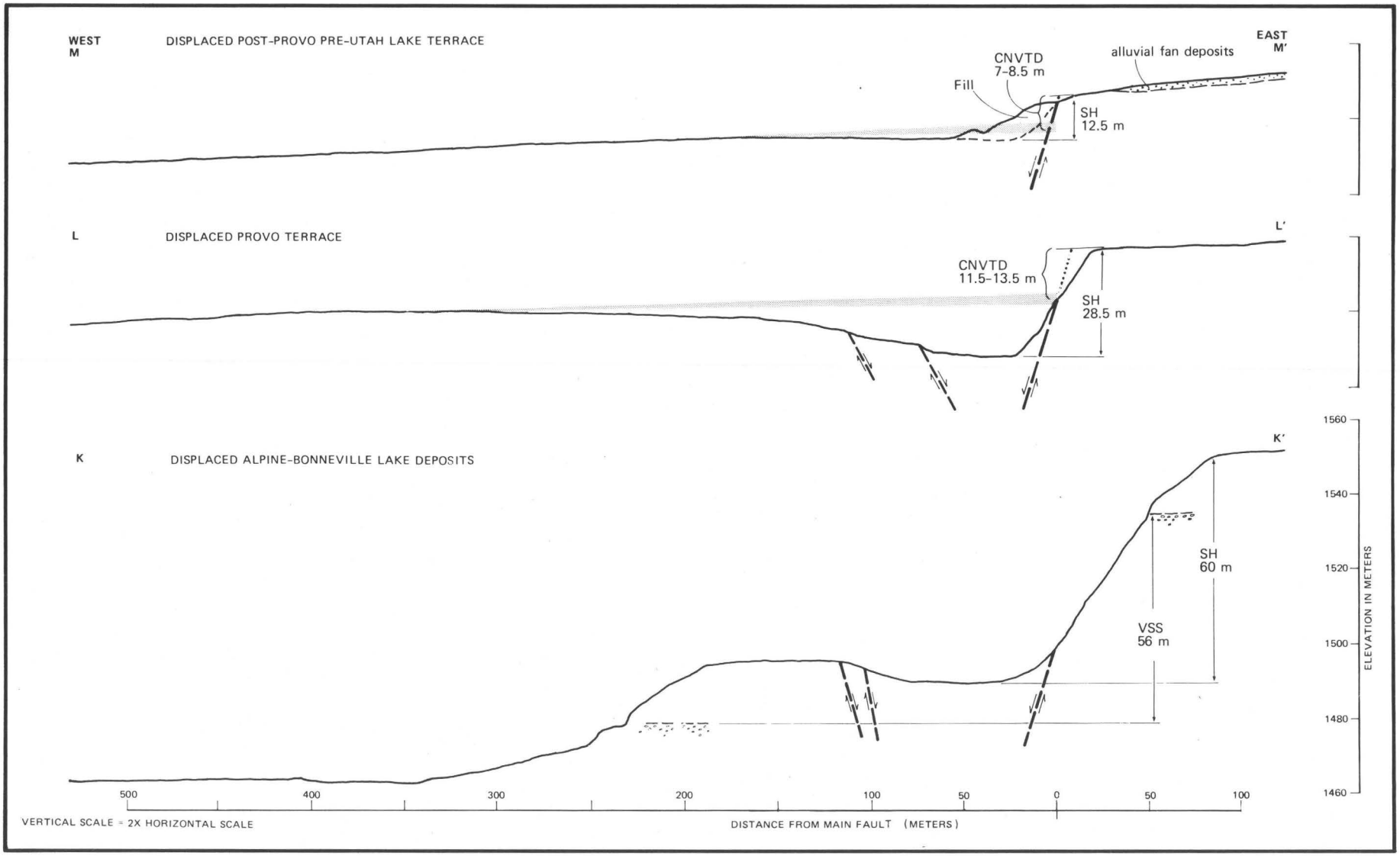

Figure 8 - LONGITUDINAL PROFILES SHOWING FAULTED TERRACES AND LAKE DEPOSITS HOBBLE CREEK SITE

surface dips 1/2 degree to the west. This surface rotated an average of 1/2 degree toward the main scarp across a zone that extends 200 m from the scarp. The initial dip of the Provo terrace surface is approximately 1 degree toward the west. This surface has subsequently been rotated an average of 1 1/2 degrees eastward across a zone extending 385 m from the main scarp. Near the main fault this surface dips as much as 3 degrees to the east.

Due to erosion and subsequent deposition, the amount of rotation associated with the Alpine-Bonneville lake deposits cannot be measured. Presumably, these deposits are affected to the same degree as, or possibly to an even greater degree, than the Provo-age deposits.

Cumulative net vertical tectonic displacement. Back-tilting and formation of antithetic faults affect the fault scarp height and increase the vertical stratigraphic separation across the main fault relative to the true tectonic displacement (the cumulative net vertical displacement across the deformed zone). The cumulative net vertical tectonic displacement is calculated by projecting the measured datum (terrace surface or stratigraphic horizon) on both sides of the fault plane from outside the deformed zone to the projected trace of the fault (Figure 8). The vertical distance between the intersections of the projected datum with the projected trace of the fault is the cumulative net vertical tectonic displacement. Small errors in the angle of the projection of the surfaces across the wide zones of deformation can produce significant differences in the calculated values for the net vertical tectonic displacement. Consequently, these calculated displacements are more accurately expressed as a range of values. The cumulative vertical tectonic displacements of the Provo terrace and the post-Provo pre-Utah Lake terrace are 11.5 to 13.5 m and 7 to 8.5 m, respectively (Figure 8).

The cumulative net vertical tectonic displacement on the Alpine-Bonneville marker horizon is uncertain because the effect of back-tilting on the deposits is not known. A maximum value can be estimated by subtracting the amount of post-Provo subsidence due to back-tilting from the measured vertical stratigraphic separation. The Provo surface along profile L-L' (Figure 8) has subsided about 6 m at a distance of 220 m from the fault scarp, which is the approximate distance from the fault scarp to the exposure of the Alpine-Bonneville marker horizon on the downthrown side of the fault. This suggests a maximum tectonic displacement of 50 m. A minimum value for the cumulative net vertical tectonic displacement can be estimated by assuming an average rotation of 3 degrees (two times the post-Provo rotation) on the Alpine-Bonneville marker horizon over a distance of 500 m. If these assumptions are valid, the marker horizon could have subsided as much as 26 m due to back-tilting, and the cumulative net vertical displacement could be as little as 30 m or one-half the scarp height. This seems to be a reasonable value because a 1:2 ratio between true tectonic displacement and scarp height

occurs to the north on this segment of the fault (profile L-L' in Figure 8) and also along the segment of the Wasatch fault at the Kaysville site. The cumulative net vertical tectonic displacements for the different age deposits at Hobble Creek are summarized on Table 2.

SEQUENCE OF DEPOSITION AND FAULTING AT THE HOBBLE CREEK SITE

The following sequence of events is inferred from the stratigraphic and structural relationships observed during mapping and exploratory trenching at the Hobble Creek site:

1. During late Pleistocene time, the Hobble Creek site was inundated by Lake Bonneville. The earliest evidence of this lake at the Hobble Creek site is a thick sequence of relatively fine grained lacustrine deposits capped by nearshore gravels that were deposited as the lake surface was attaining an elevation of approximately 1566 m. The deep water lacustrine deposits are interpreted by Bissell (1963) to have been deposited during the Alpine stage of Lake Bonneville, which suggests they are a few to several tens of thousands of years old. However, no major unconformity is observed at the Hobble Creek site between the deep water lacustrine sediments and the nearshore gravel deposits, and it is possible that both were deposited during the Bonneville stage, which ended approximately 15,000 years ago.

2. During the late Pleistocene, repeated surface faulting events along this trace of the Wasatch fault produced 16.5 to 38.5 m of net vertical tectonic displacement of the Alpine-Bonneville lake deposits. The number of events and the duration of the intervals between these events are not known.

3. Approximately 15,000 years ago, Lake Bonneville spilled over into Red Rock Pass, and incision of the spillway lowered Lake Bonneville until it stabilized at the Provo stage. A large fan-delta complex was built out from the mouth of Hobble Creek Canyon as the lake slowly receded. Lacustrine deposits interbedded with topset alluvial gravels indicate that the lake level fluctuated during the Provo stage. The lake receded from the Provo level about 12,000 years ago.

4. Following recession of the Provo-age lake, the Provo delta-fan surface was incised by Hobble Creek. On the upthrown block east of the fault, one unpaired and three paired strath terraces were eroded into the Provo gravels beneath the Provo terrace and above the post-Provo pre-Utah Lake terrace. The proximity of these terraces to the fault scarp and the fact that similar terraces are not present on the downthrown block west of the fault suggest that they are tectonic in origin. The terraces probably represent at

DATUM	APPROXIMATE AGE (yrs. B.P.)	CUMULATIVE VERTICAL TECTONIC DISPLACEMENT POST DATUM (m)	CUMULATIVE VERTICAL TECTONIC DISPLACEMENT DURING INTERVAL (m)	NUMBER OF EVENTS DURING INTERVAL	AVERAGE DISPLACEMENT PER SURFACE FAULTING EVENT (m)	AVERAGE RECURRANCE INTERVAL FOR SURFACE FAULTING EVENTS (yrs.)
ALPINE-BONNEVILLE LAKE DEPOSITS	>15,000 to <35,000	30 – 50	—	—	—	
	—	—	16.5 – 38.5	?	?	
PROVO TERRACE	12,000	11.5 – 13.5	—	—	—	
	—	—	3 – 6.5	3 – 4	0.8 – 2.2	1500 – 2400
MIDDLE HOLOCENE TERRACE	6,000	7 – 8.5	—	—	—	
	—	—	7 – 8.5	3	2.3 – 2.8	
PRESENT FLOOD PLAIN	0	0	—	—	—	

Table 2 - SUMMARY OF DATA ON FAULT DISPLACEMENTS AT THE HOBBLE CREEK SITE

least three, and possibly four, faulting events that produced a cumulative net vertical tectonic displacement of 3 to 6.5 m between about 12,000 and 6000 years B.P.

5. Continued downcutting followed by alluviation along Hobble Creek during middle-Holocene time is represented by the post-Provo pre-Utah Lake alluvium (Qal_1), which underlies a low terrace above Hobble Creek. The main fault scarp was incised at least 5 m by an intermittent stream that flowed from Deadmans Hollow and built a large alluvial fan (Qf_1) that grades to the pre-Utah Lake alluvium (Qal_1). A soil (unit 2S on Plate 4) that is estimated to be about 6000 years old began to form on this fan surface.

6. Surface faulting occurred. This event produced a graben at the trench site and created a fault scarp across the apex of fan Qf_1.

7. The fault scarp crossing Qf_1 was breached by erosion, and the graben was partly filled by a sequence of mudflows and colluvium from the main fault scarp (Qf_2 on Plate 3; unit 3 on Plate 4).

8. Surface faulting occurred. This resulted in rejuvenation of the main fault scarp across the Deadmans Hollow fan complex, and produced a fissure at the top of the debris slope that had formed at the base of the old scarp. Colluvium was deposited at the base of the fault scarp and filled the fissure (unit 4).

9. The fault scarp was subsequently breached and fan Qf_3 formed, partly burying older fan segments Qf_1 and Qf_2. A thin veneer of channel and mudflow deposits (unit 5) was deposited in the graben.

10. Surface faulting occurred. Renewed uplift on the main fault was accompanied by renewed displacement on the main antithetic fault and development of new faults within the graben. Fan segment Qf_3 was beheaded as a result of this faulting. Erosion of the main fault scarp following this surface faulting event resulted in the deposition of a scarp-derived colluvium (unit 6A) that grades into alluvial sediments deposited in a small channel at the base of the scarp.

11. Subsequent to this most recent faulting event, the main fault scarp was breached again and fan segment Qf_4 was formed.

SLIP RATE, AMOUNT OF DISPLACEMENT PER EVENT, AND RECURRENCE OF SURFACE FAULTING AT THE HOBBLE CREEK SITE

Slip Rate

Figure 9 is a graph showing the relationship between cumulative net vertical tectonic displacement (ordinate) and age of the displaced datum (abscissa). Uncertainties in the calculated values for the tectonic displacement and in the ages assigned to the displaced datum are shown by the boxes. Because of these uncertainties, a range of values for the slip rate (slope of line between two points on the graph) is represented by the shaded area on Figure 9.

The data for Holocene (post-Provo) displacements are reasonably well constrained. The best-fit line for these data (solid line on Figure 9) indicates that the average Holocene slip rate is 1.1 mm per year. The late Pleistocene slip rate is not as well constrained because of the uncertainties in the amount of displacement and age of the Alpine-Bonneville lake deposits. Using the range of values for displacements and ages of the Provo terrace and Alpine-Bonneville lake deposits shown on Table 2, the late Pleistocene slip rate is between 0.7 and 12.8 mm per year. The available stratigraphic evidence suggests the faulted lake deposits at Murdock mountain are Bonneville and not Alpine in age. Also, the cumulative net vertical tectonic displacement of the lake deposits is probably closer to 30 m than to the maximum value of 50 m. If these interpretations are correct, the late Pleistocene slip rate is between 2 and 6 mm per year. These data suggest that there was a decrease in the slip rate along this segment of the fault between the late Pleistocene and the Holocene, and that the Holocene slip rate has been uniform.

Amount of Displacement Per Event

Amounts of displacement for individual surface faulting events are not clearly defined at the Hobble Creek site. Therefore, an average displacement per event has been calculated. The average displacement per event is equal to the cumulative displacement divided by the number of surface faulting events. Table 2 summarizes the data for cumulative vertical tectonic displacement, number of faulting events, and calculated average net tectonic displacement per event during different intervals. Values for the average vertical displacement per event range from 0.8 m to 2.8 m per event during the Holocene.

Recurrence of Surface Faulting

The recurrence interval is a function of the number of events that have occurred and their distribution in time. The structural and stratigaphic relationships indicate that at least six, and possibly seven, surface faulting events have occurred in

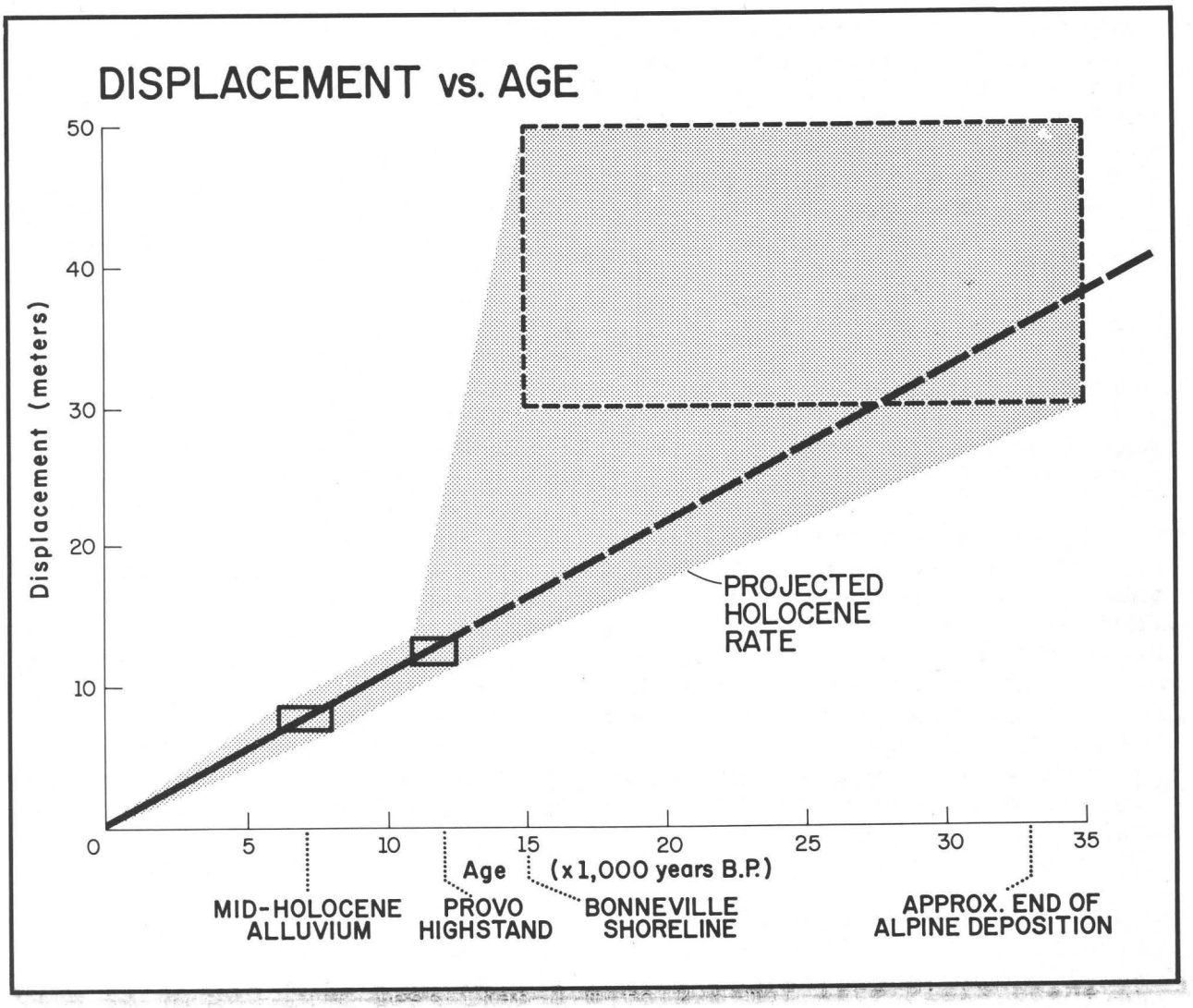

Figure 9 - GRAPH SHOWING RELATIONSHIP BETWEEN CUMULATIVE TECTONIC DISPLACEMENT AND TIME

post-Provo time along the segment of the fault at Hobble Creek. Three, and possibly four, of these events occurred during early Holocene time and are indicated by pre-middle Holocene strath terraces that are eroded into Provo gravels on the upthrown side of the fault. Three additional events during late Holocene time are indicated by the segmented alluvial fan and the faulted fan deposits observed in the trenches at the mouth of Deadmans Hollow. The available data do not permit absolute dating of individual events and calculation of the actual intervals between successive events. However, the average recurrence interval between these events can be calculated.

Figure 10 summarizes possible average recurrence intervals for six and seven surface faulting events during the past 12,000 years. The recurrence interval depends, in part, on when the first and last events occurred during the 12,000 year interval. If the first identified event occurred immediately after formation of the Provo terrace (case 1 in Figure 10), the average recurrence interval would be 2400 years. If a period less than the recurrence interval elapsed before the first identified faulting event (case 2), the average recurrence interval would be 2000 years. If a surface faulting event occurred immediately before the formation of the Provo terrace and a period equal to the recurrence interval elapsed before the first identified event, the average recurrence interval would be a minimum of 1700 years for six events. Similarly, given seven surface faulting events in the past 12,000 years, the average recurrence interval would be between 1500 and 2000 years (cases 4, 5, and 6, Figure 10).

The average recurrence interval between surface faulting events at the Hobble Creek site is between 1500 and 2400 years. The actual intervals between successive events may have varied from these mean values.

EARTHQUAKE MAGNITUDE AND RECURRENCE OF SURFACE FAULTING ON THE WASATCH FAULT ZONE

EARTHQUAKE MAGNITUDE

The empirical relationship between the logarithm of maximum displacement and earthquake magnitude can be used to estimate the size of earthquakes (Slemmons, 1977). Estimates of the net tectonic displacement for individual surface faulting events at the Kaysville site range from 1.7 to 3.7 m, based on the colluvial stratigraphy and structural relationships observed in trenches. According to Slemmons' curve for normal-slip faults, displacements of 1.7 to 3.7 m are associated with magnitude 7.0 to 7.3 earthquakes. Slemmons' curves, however, are based on the maximum resultant displacement observed during historical surface faulting events, and the reported values include both fault slip (net tectonic displacement) and distortion (such as exaggerated scarp height due to back-tilting and graben formation).

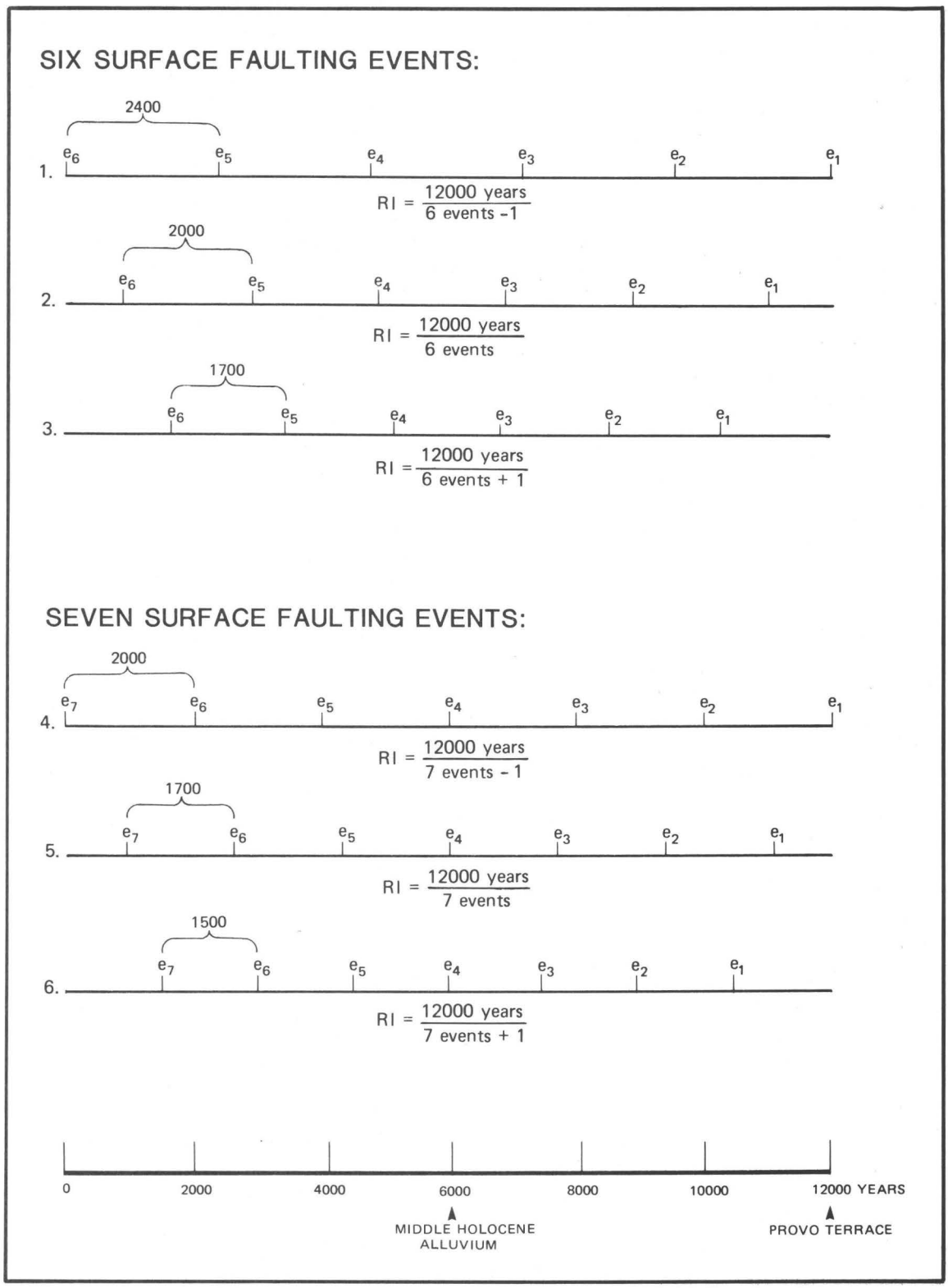

Figure 10 - AVERAGE RECURRENCE INTERVALS (R-1)
FOR SURFACE FAULTING EVENTS (e)
HOBBLE CREEK SITE

Back-tilting and graben formation may increase the net tectonic displacement by as much as a factor of two along the segment of the Wasatch fault at the Kaysville site. If this factor is taken into account, the displacement for a single event may have been as high as 7.4 m, which gives a magnitude of 7.6 on Slemmons' curve.

The amount of displacement that occurred during individual surface faulting events at the Hobble Creek site could not be measured. The average displacement per event for different intervals, which was calculated by dividing the cumulative displacement by the number of surface faulting events, is summarized on Table 2. Values for the average vertical tectonic displacement per event range from 0.8 to 2.8 m per event during the Holocene. Displacements of 0.8 m to 2.8 m produce earthquakes having magnitudes of 6.7 to 7.2, according to Slemmons' curve. As at the Kaysville site, the scarp height at the Hobble Creek site is approximately twice the cumulative net tectonic displacement in the Provo deposits. If this factor is taken into account, the average resultant displacement per event could be as high as 5.6 m, which gives a magnitude of 7.5 on Slemmons' curve.

Estimates of earthquake magnitude should be based on as many parameters as possible. Average displacement data will not necessarily define the maximum earthquake that has occurred. More rigorous analysis is required to assess the maximum earthquake that can occur. Nonetheless, the available data indicate that surface faulting events associated with earthquakes in the magnitude range of 6 1/2 to 7 1/2 have occurred repeatedly along the fault segments at the Kaysville and Hobble Creek sites.

RECURRENCE OF SURFACE FAULTING EARTHQUAKES

Data on the recurrence of surface faulting events at the Kaysville and Hobble Creek sites are in the preceding sections. Factors that affect these recurrence intervals and those on the entire Wasatch fault zone are discussed below, and questions are posed regarding fault behavior and the mechanics of faulting and earthquake generation.

Based on the geologic evidence of past surface fault displacements during the late Pleistocene and Holocene, the recurrence interval of moderate to large magnitude earthquakes associated with surface fault rupture along the segment of the Wasatch fault zone at the Kaysville site is estimated to be between 500 and 1000 years. The longer interval is believed to be closer to the average late Holocene value. Similarly, the average recurrence interval for the segment of the fault at the Hobble Creek site is estimated to be between 1500 and 2400 years. The Wasatch fault zone contains several other segments and the recurrence interval of surface faulting events on the entire zone is undoubtedly shorter than the recurrence interval on any one segment.

Based on the geomorphic expression of the fault zone and on rupture lengths associated with historical moderate to large magnitude earthquakes along other normal-slip faults, there may be from six to ten separate segments. If the recurrence intervals along the Kaysville and Hobble Creek segments of the fault (minimum of 500 years and maximum of 2400 years per event) are representative of the recurrence intervals along the other segments, the recurrence interval for the entire zone may be one-sixth to one-tenth that of the individual segments, that is, between 50 and 400 years per event. No surface faulting events have occurred along the Wasatch fault zone during at least the past 132 years; this suggests a moderate to large magnitude surface faulting event is either due or past due. However, there are many factors that affect the actual values for the recurrence interval on the entire zone.

Factors that affect estimates of the recurrence interval on the entire fault zone include: 1) the geologic interpretations that affect the ages assigned to the faulted Quaternary deposits and number of faulting events; 2) the behavior of individual fault segments; 3) the number of individual segments; and 4) the relationship between different segments of the fault.

The accuracy of recurrence intervals based on geologic evidence of past surface faulting events depends on the accuracy of the ages assigned to the displaced stratigraphic horizons and geomorphic surfaces, and on being able to determine the number of events that have occurred. Despite the numerous studies of the Late Quaternary geologic history of the Bonneville basin that have been made during the past 25 years, there are still many unresolved controversies regarding stratigraphic interpretations and ages assigned to the Quaternary deposits and paleosols. Fortunately, research in this area is continuing which will facilitate future studies of earthquake recurrence intervals along the Wasatch Front (see paper by Scott; this volume). The ages assigned to the faulted Quaternary units described in this report are based on generally accepted regional correlations and available radiometric dates. The recurrence intervals at the Kaysville and Hobble Creek sites are based primarily on displacements of Holocene deposits and the ages asigned to these units probably will not change significantly as new data become available.

The number of faulting events interpreted to have occurred during a geologic interval is a function of how well geologic evidence of these events is preserved, and on the resolution with respect to the minimum size event that can be recognized. Evidence of past events may be buried too deep to be exposed in trenches, or it may have been removed by erosion. Also, it may be very difficult to recognize surface faulting events that produced very small displacements. If surface faulting events occurred that are not identified, the calculated recurrence interval between successive events will be longer than the actual recurrence interval. Therefore, the average recurrence intervals for

surface faulting events at the Kaysville and Hobble Creek sites could be even shorter than the values cited above.

The distribution of large earthquakes depends upon: 1) the rate of strain accumulation, and 2) the amount of strain release (magnitude of earthquake) during an event. In nature, both these factors may, and probably do, vary. Although it is mathematically appealing and sometimes a prerequisite of statistical models of earthquake behavior to assume that large magnitude earthquakes have a linear or other mathematically uniform distribution with respect to time, it may not be a correct assumption. Historical seismicity data indicate that earthquakes along a given fault may be clustered and not uniform in their temporal distribution. Much more needs to be learned about the actual behavior (temporal distribution and magnitudes) of past earthquakes occurring on individual faults. Because the interval between successive large earthquakes is long (hundreds to thousands of years) compared to the historical record, studies of fault behavior must be based on the history of past events in the Quaternary geologic record.

The recurrence interval of surface faulting events for the entire Wasatch fault zone depends on: 1) the recurrence interval on the individual segments, 2) the number of segments, and 3) the relationship between the individual segments. The recurrence interval along two of the segments has been discussed above. The data indicate that the Kaysville and Hobble Creek segments have different Holocene slip rates and different recurrence intervals. Therefore, to accurately assess the recurrence interval for the entire fault zone, the recurrence interval should be known for each of the segments.

Presumably, the more active segments there are within the fault zone, the shorter the recurrence interval will be on the entire zone. Except for historical cases where the length of surface fault rupture can be measured directly, it is extremely difficult to determine the length of the fault that actually ruptured during individual past events. Consequently, it is very difficult to define fault segments that are likely to rupture during future events and to determine the number of individual segments. Also, it is not known whether the same segment will rupture along its entire length during successive events or whether longer and/or shorter lengths may rupture during subsequent earthquakes. This is further complicated by the fact that more than one segment, or parts of more than one segment, may rupture during a single event. Additional research is needed to characterize fault segments and to understand their behavior.

The assumption that individual fault segments behave independently is inherent in most statistical models of fault behavior. However, the occurence of a large magnitude earthquake along one segment of the fault zone may actually change the likelihood of an event on an adjacent segment by causing a readjustment of the regional stresses. Can a large magnitude earthquake along one

segment of the fault induce an event (energy release) along other segments of the fault zone that otherwise would not have had slipped until more time had elapsed allowing more stress to build up? More information is needed regarding the past behavior of the various fault segments and on the mechanics of fault slip and earthquake generation to answer these questions.

Despite the uncertainties regarding factors that may affect the recurrence of surface faulting events, assumptions can be made that allow quantitative assessments of the probability of future events along the Wasatch fault zone. A companion paper by Cluff and others (this volume) presents a model for fault behavior and discusses probability of future occurrence of moderate to large magnitude earthquakes on the Wasatch fault zone based on the recurrence data obtained at the Kaysville and Hobble Creek sites.

ACKNOWLEDGMENTS

This work was supported by the U.S. Geological Survey's National Earthquake Hazards Reduction Program (contract no. 14-08-0001-16827) and by Woodward-Clyde Consultants' Professional Development Committee. Kathryn L. Hanson and Peter L. Knuepfer assisted with the geologic investigations. Ray Harvey, Mary Phelps, and Ralph Ladle gave permission for excavating soil test pits and trenches on their properties in the Kaysville (Fruit Heights) and Hobble Creek areas.

REFERENCES CITED

Bissell, H. J., 1963, Lake Bonneville -- Geology of southern Utah Valley, Utah: U.S. Geological Survey, Professional Paper 257-B, p. 101-130.

Bissell, H. J., 1968, Bonneville -- An ice age lake: Brigham Young University Geology Studies, v. 15, pt. 4, 66 p.

Cluff, L. S., Brogan, G. E., and Glass, C. E., 1970, Wasatch fault, northern portion, earthquake fault investigation and evaluation: a guide to land-use planning prepared for the Utah Geological and Mineralogical Survey, Woodward-Lundgren & Associates, Oakland, California.

Cluff, L. S., Brogan, G. E., and Glass, C. E., 1973, Wasatch fault, southern portion, earthquake fault investigation and evaluation: a guide to land-use planning prepared for the Utah Geological and Mineralogical Survey, Woodward-Lundgren & Associates, Oakland, California.

Cluff, L. S., Glass, C. E., and Brogan, G. E., 1974, Investigation and evaluation of the Wasatch fault north of Brigham City and Cache Valley faults, Utah and Idaho: a guide to land-use planning with recommendations for seismic safety prepared for the U.S. Geological Survey, Woodward-Lundgren & Associates, Oakland, California.

Cluff, L. S., Hintze, L. F., Brogan, G. E., and Glass, C. E., 1975, Recent activity of the Wasatch fault, northwestern Utah, U.S.A.: Tectonophysics, v. 29, p. 161-168.

Cook, K. L., 1972, Earthquakes along the Wasatch Front, Utah--the record and the outlook, in Environmental Geology of the Wasatch Front, 1971: Utah Geological Association Publication 1, p. H1-H29.

Cook, K. L., and Smith, R. B., 1967, Seismicity in Utah, 1850 through June 1965: Seismological Society of America Bulletin, v. 57, no. 4, p. 689-718.

Gilbert, G. K., 1890, Lake Bonneville: Monographs of the U.S. Geological Survey, v. I, 438 p.

Morrison, R. B., 1965, New evidence on Lake Bonneville stratigraphy and history from southern Promontory Point, Utah, in Geological Survey Research, 1965: U.S. Geological Survey, Professional Paper 525-C, p. C110-C119.

Scott, W. E., 1979, Stratigraphic problems in the usage of Alpine and Bonneville Formations in the Bonneville Basin, Utah: Geological Society of America Abstracts with Programs, v. 11, no. 6, p. 302.

Slemmons, D. B., 1957, Geologial effects of the Dixie Valley-Fairview Peak, Nevada, earthquakes of December 16, 1954: Seismological Society of America Bulletin, v. 47, no. 4, p. 353-375.

Slemmons, D. B., 1977, State-of-the-art for assessing earthquake hazards in the United States, Report 6, Faults and Earthquake Magnitude: U.S. Army Corps of Engineers, Miscellaneous Paper S-73-1.

Smith, R. B., Arabasz, W. J., Cook, K. L., and Ward, S. H., 1978, Earthquake research on the Wasatch Front, Utah: U.S. Geological Survey, National Earthquake Hazards Reduction Program, Summaries of Technical Reports, v. 5, p. 303-305.

Wallace, R. E., 1977, Profiles and ages of young fault scarps, north-central Nevada: Geological Society of America Bulletin, v. 88, p. 1267-1281.

Woodward-Clyde Consultants, 1975, Study of earthquake recurrence intervals on the Wasatch fault, Utah; final technical report, 1975: prepared for the U.S. Geological Survey under Contract No. 14-08-001-14567 by Woodward-Clyde Consultants, San Francisco, California, 37 p.

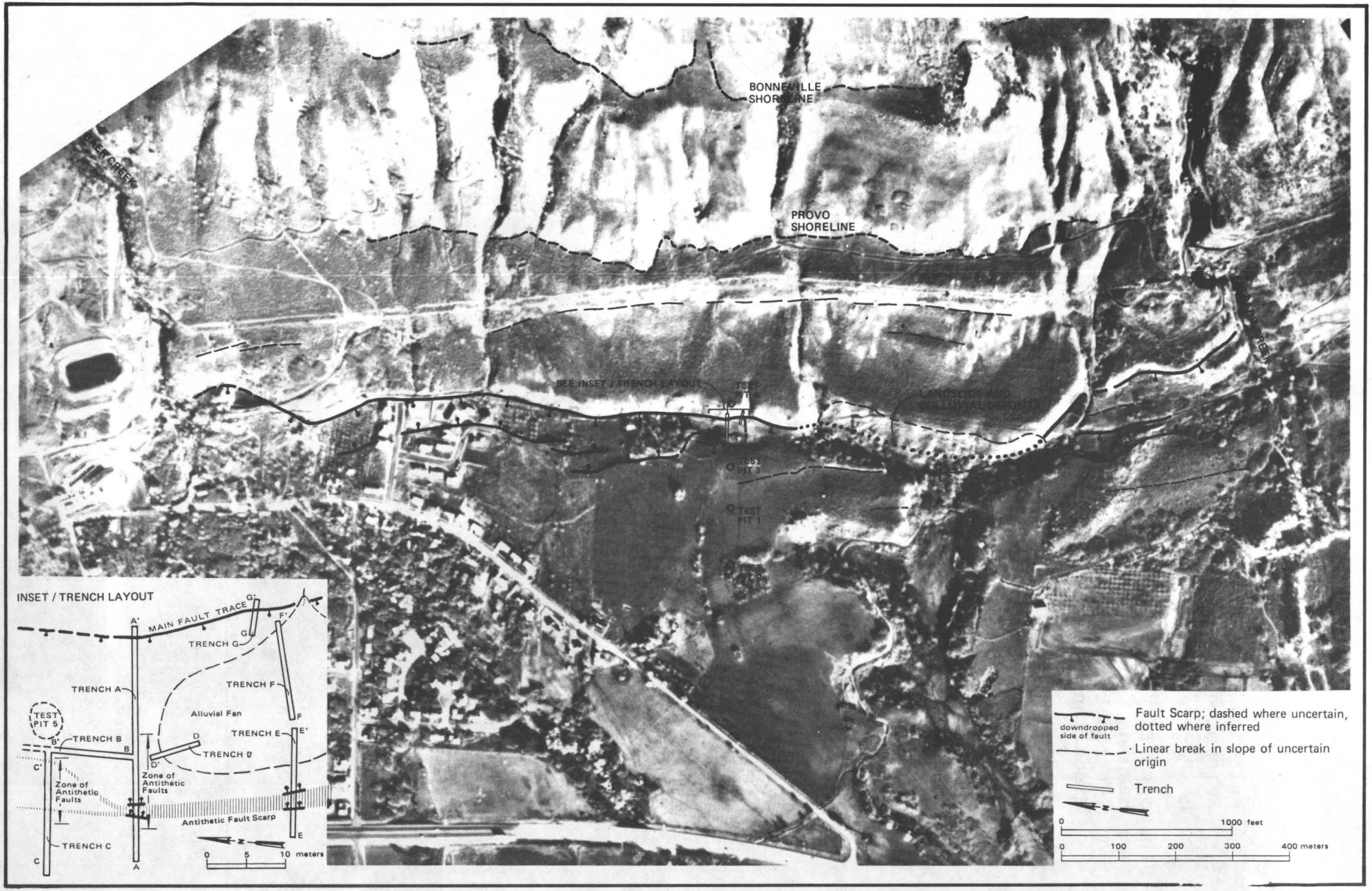

PLATE 1 - PHOTOGEOLOGIC MAP KAYSVILLE SITE

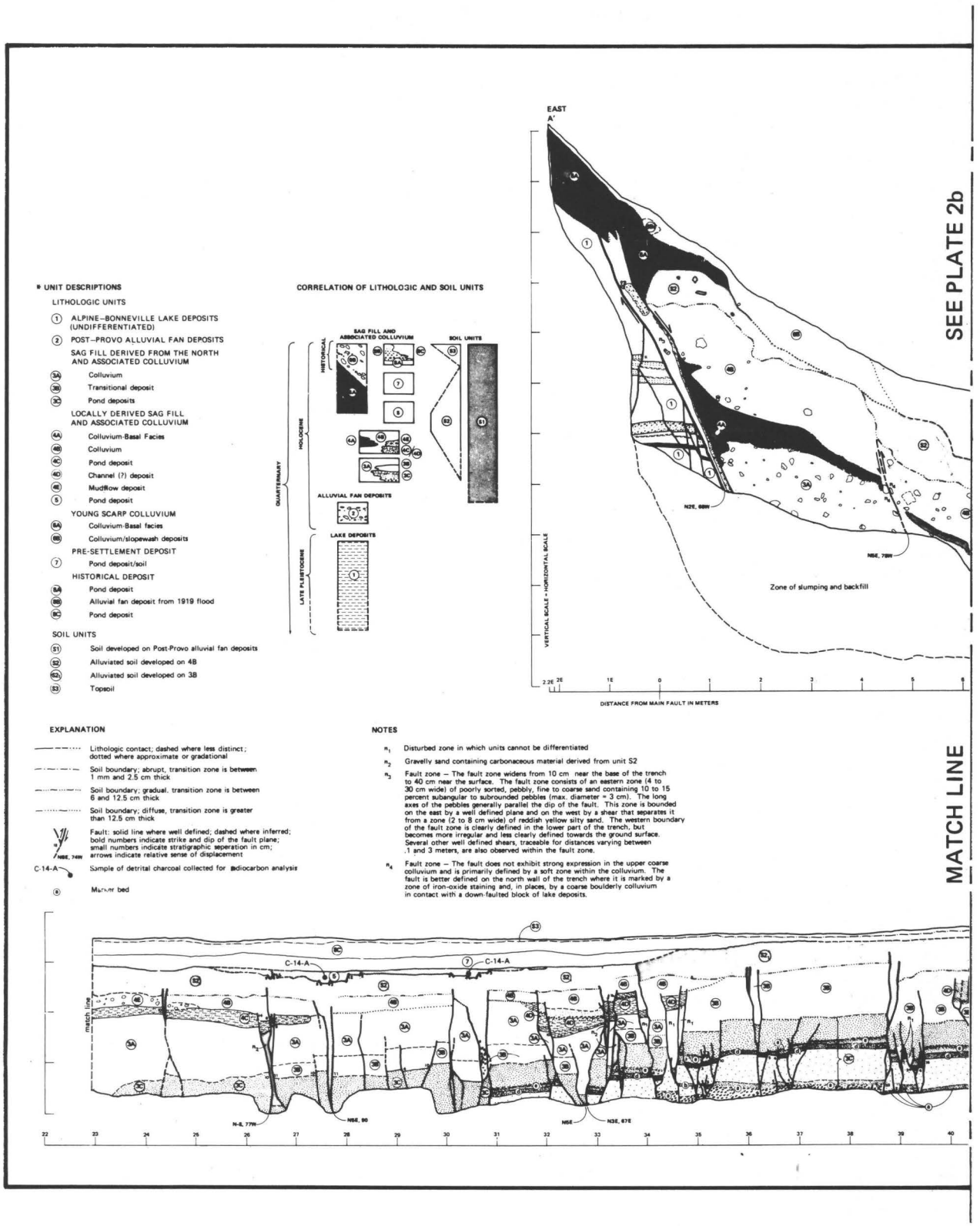

PLATE 2a - LOG OF TRENCH A KAYSVILLE SITE

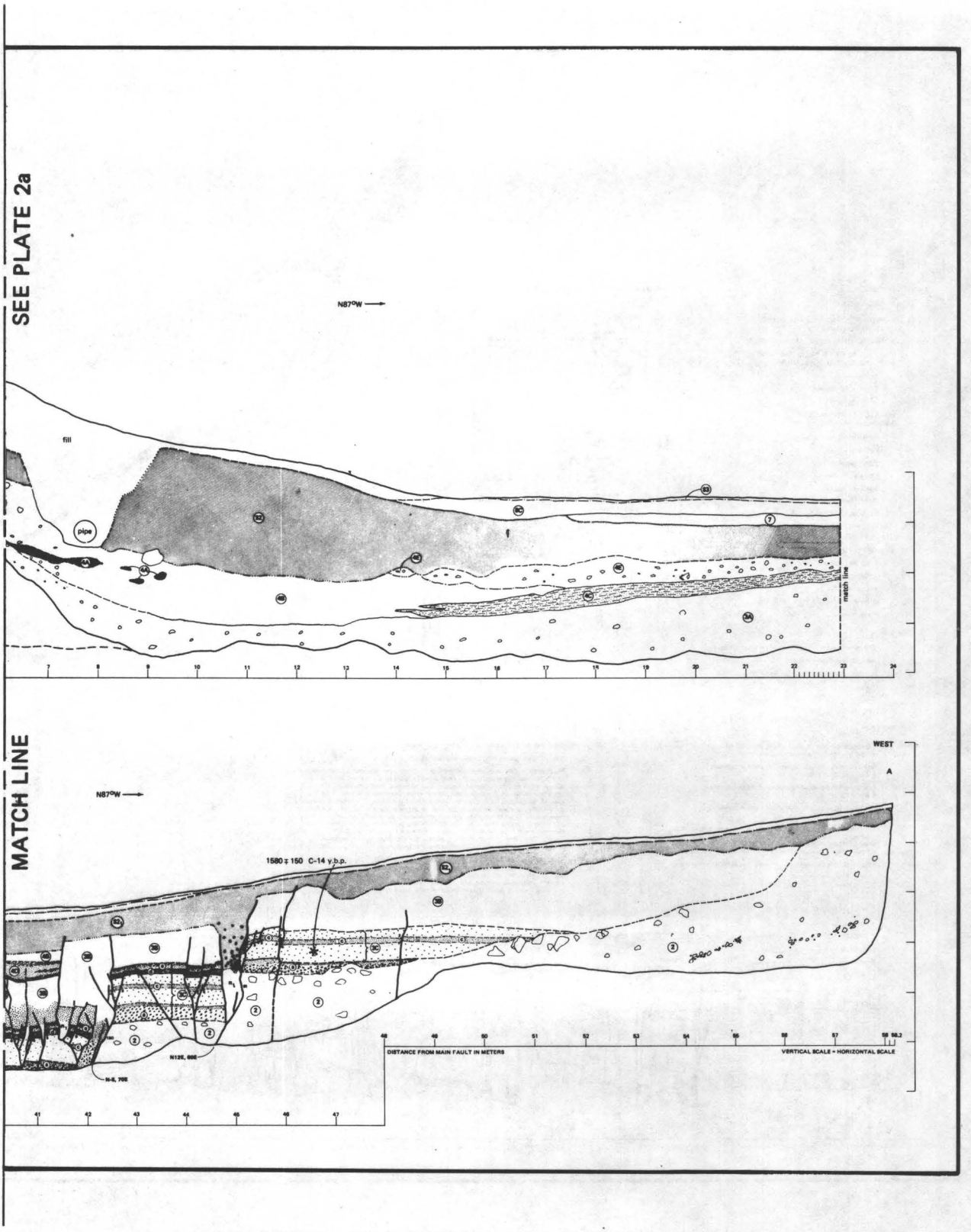

PLATE 2b - LOG OF TRENCH A KAYSVILLE SITE

CORRELATION OF MAP UNITS

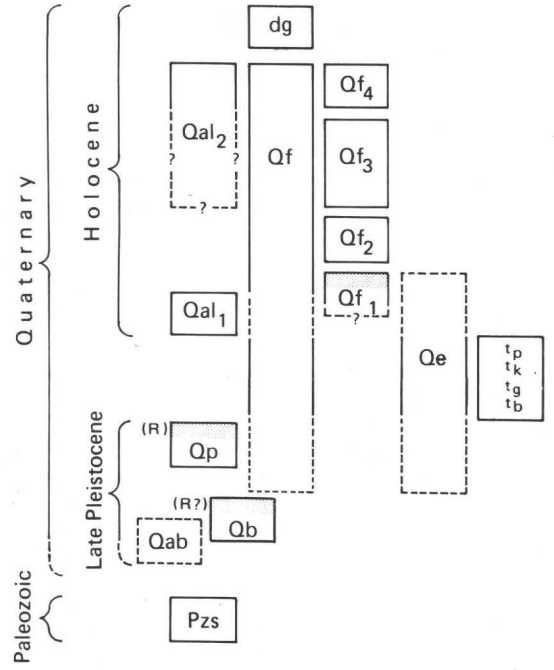

MAP SYMBOLS:

- Lithologic contact
- Gradational lithologic contact
- Lithologic contact approximately located
- Terrace scarp
- Fault; dashed where less well defined; dotted where buried; balls on downthrown side.
- Linear break in slope; possibly of tectonic origin; circles on lower side.

LITHOLOGIC UNITS:

MAN- MADE DEPOSITS

- dg — Disturbed ground

FAN DEPOSITS

- Qf — Fan deposits (Undifferentiated)

Deadmans Hollow fan complex:

- Qf_4 — Fan segment 4 (youngest)
- Qf_3 — Fan segment 3
- Qf_2 — Fan segment 2
- Qf_1 — Fan segment 1 (oldest)

HOLOCENE ALLUVIUM

- Qal_2 — Utah Lake age alluvium
- Qal_1 — Post-Provo Pre-Utah Lake alluvium

EOLIAN DEPOSITS

- Qe — Eolian fine sand and silt

STRATH TERRACES

- t_p t_k t_g t_b — lowest … highest — Strath terraces

BONNEVILLE GROUP

- Qp — Provo fan-delta deposits
- Qb — Bonneville gravel
- Qab — Alpine-Bonneville lake deposits (Undifferentiated)

BEDROCK

- Pzs — Paleozoic sedimentary rocks

PLATE 3a - PHOTOGEOLOGIC MAP EXPLANATION HOBBLE CREEK SITE

NOTE: map explanation is given on Figure 3a

PLATE 3b - PHOTOGEOLOGIC MAP HOBBLE CREEK SITE

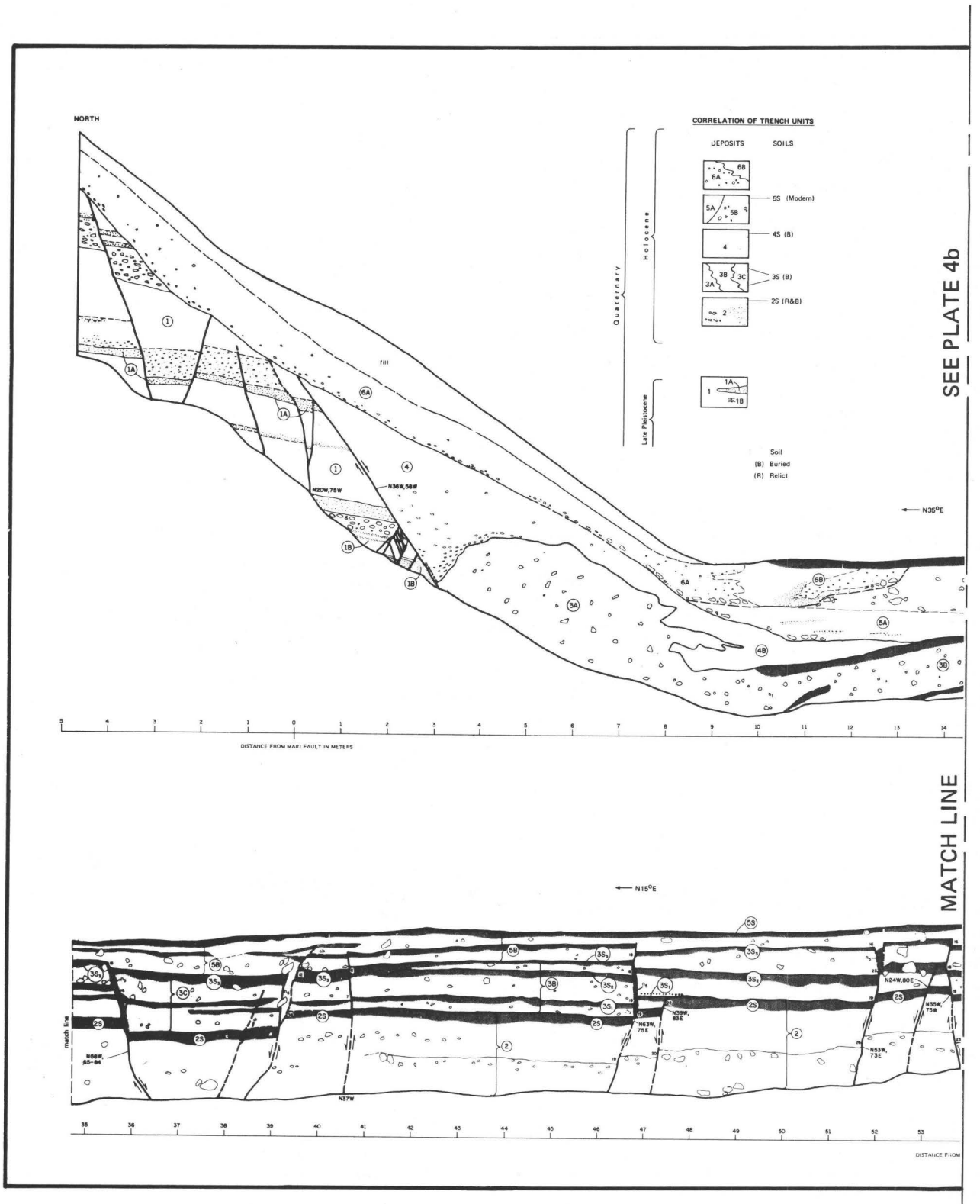

PLATE 4a - LOG OF TRENCH HC-1 HOBBLE CREEK SITE

SEE PLATE 4a

MATCH LINE

EXPLANATION:

Lithologic contacts; dashed where less distinct; dotted where approximate or gradational; heavier contacts are between major lithologic units; fine contacts are between different lithologies within a unit.

A soil horizons

FAULT; solid line where well defined; dashed where inferred; bold numbers indicate strike and dip of fault plane; small numbers indicate stratigraphic separation in cm; arrows indicate relative sense of displacement.

N30W, 78W

UNIT DESCRIPTIONS:

Fill

UNIT8: YOUNG SCARP COLLUVIUM AND ASSOCIATED CHANNEL DEPOSITS
- (8A) Colluvium
- (8B) Channel deposits

UNIT 5: CHANNEL AND FAN DEPOSITS
- (5S) Topsoil and buried soils between mudflows
- (5A) Channel facies
- (5B) Mudflow facies

UNIT 4: COLLUVIUM
- (4S) Buried soil on scarp colluvium
- (4) Colluvium

UNIT 3: FAN DEPOSITS AND ASSOCIATED COLLUVIUM
- (3S) Buried A soil horizons
- (3A) Colluvial facies
- (3B) Alluvial facies
- (3C) Mudflow facies

UNIT 2: ALLUVIAL FAN AND LOESS DEPOSITS
- (2S) Post unit 2 soil
- (2) Fan and loess deposits

UNIT 1: PROVO FAN-DELTA DEPOSITS
- (1) Gravel
- (1A) Fine sand and silt lake deposits
- (1B) Cross-bedded sand

NOTES:

n_1 Gradual facies change between colluvial (3A) and alluvial (3B) deposits.

n_2 Gradual facies change between alluvial (3B) and mudflow (3C) deposits.

n_3 Upper contact of mudflow strikes N15W and dips 4NE.

n_4 Upper contact of mudflow unit 2 strikes N4W and dips 12NE.

n_5 Zone of disturbance; darker in color, softer, contacts disrupted.

n_6 Zone of disturbance; contacts uncertain, numerous roots in upper part.

n_7 Upper contact of unit 2 strikes N70E and dips 2 to 4 NW.

n_8 Bedding in unit 2 strikes N53W and dips 4 to 5 NE.

n_9 Upper contact of unit 2 strikes N15W and dips 2NE.

n_{10} Disturbed zone; northern boundary is indistinct.

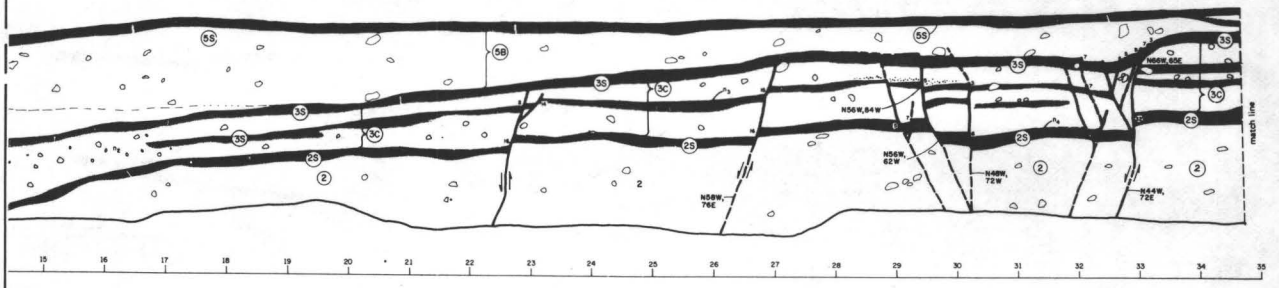

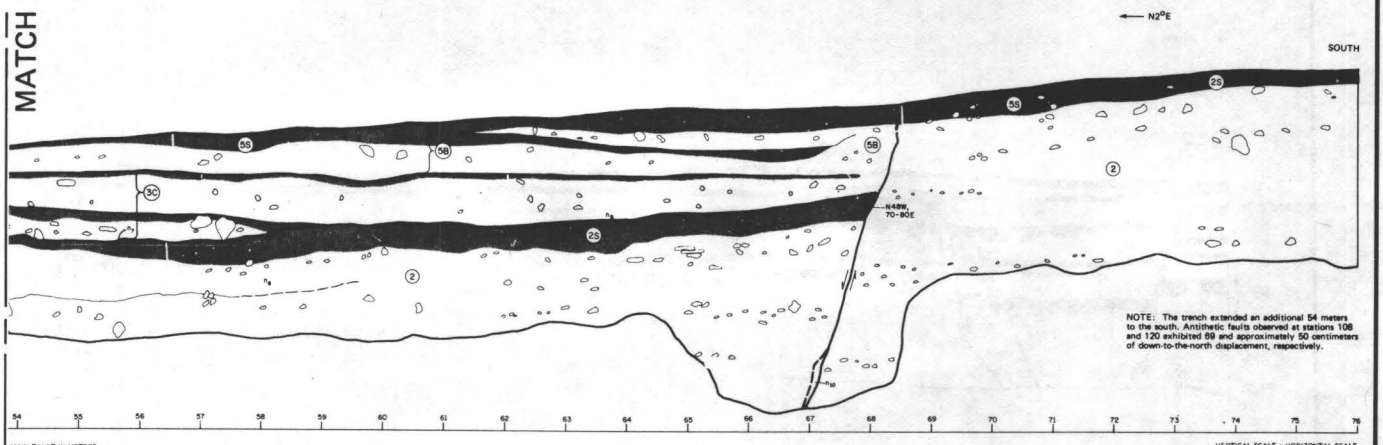

PLATE 4b - LOG OF TRENCH HC-1 HOBBLE CREEK SITE

ESTIMATING THE PROBABILITY OF OCCURRENCE OF SURFACE FAULTING EARTHQUAKES ON THE WASATCH FAULT ZONE, UTAH

By

LLOYD S. CLUFF, ASHOK S. PATWARDHAN, and KEVIN J. COPPERSMITH

Woodward-Clyde Consultants
Three Embarcadero Center, Suite 700
San Francisco, California 94111

INTRODUCTION

The Wasatch fault zone is an active intraplate fault zone of the Intermountain Seismic Belt. It extends more than 370 km from Malad City, Idaho to Gunnison, Utah (Cluff and others, 1975) (Figure 1). Along its length, the Wasatch fault zone displays impressive geomorphic evidence of late Quaternary surface displacement; however, it has not been associated with earthquakes of magnitudes larger than about 5 1/2 in the past 132 years. The time elapsed since the most recent surface faulting earthquake[1] on the Wasatch fault zone may be several hundred years; hence, the potential appears to be high for the occurrence of such an event in the near future. The Wasatch Front is occupied by approximately 80 percent of Utah's total population, all of which is located within 20 km of the Wasatch fault zone, and substantial future urban and industrial growth is projected for this area. Therefore, there is a need to assess the probabilities of moderate to large earthquakes occurring anywhere on the fault, as well as at specific locations along the fault.

Many highly active plate-boundary faults, such as those within subduction zones, have very high slip rates and relatively short periods between major earthquakes. For many of these faults, the record of historical seismicity may be sufficient to estimate recurrence intervals between small to moderate earthquakes and, possibly, large earthquakes. In the case of non-plate-boundary faults, such as the Wasatch, that have a somewhat lesser degree of activity, characterizing future earthquake occurrence is more complicated for the following reasons:

1. The historical seismicity record is usually inadequate. In the western United States, the historical record is generally no longer than approximately 150 years. The recurrence interval of earthquakes on a fault is generally longer than the time period for which a data base can be established.

---

[1]Surface faulting on the Wasatch fault zone is judged to be associated with moderate to large earthquakes, that is, earthquakes of magnitude 6 1/2 or larger.

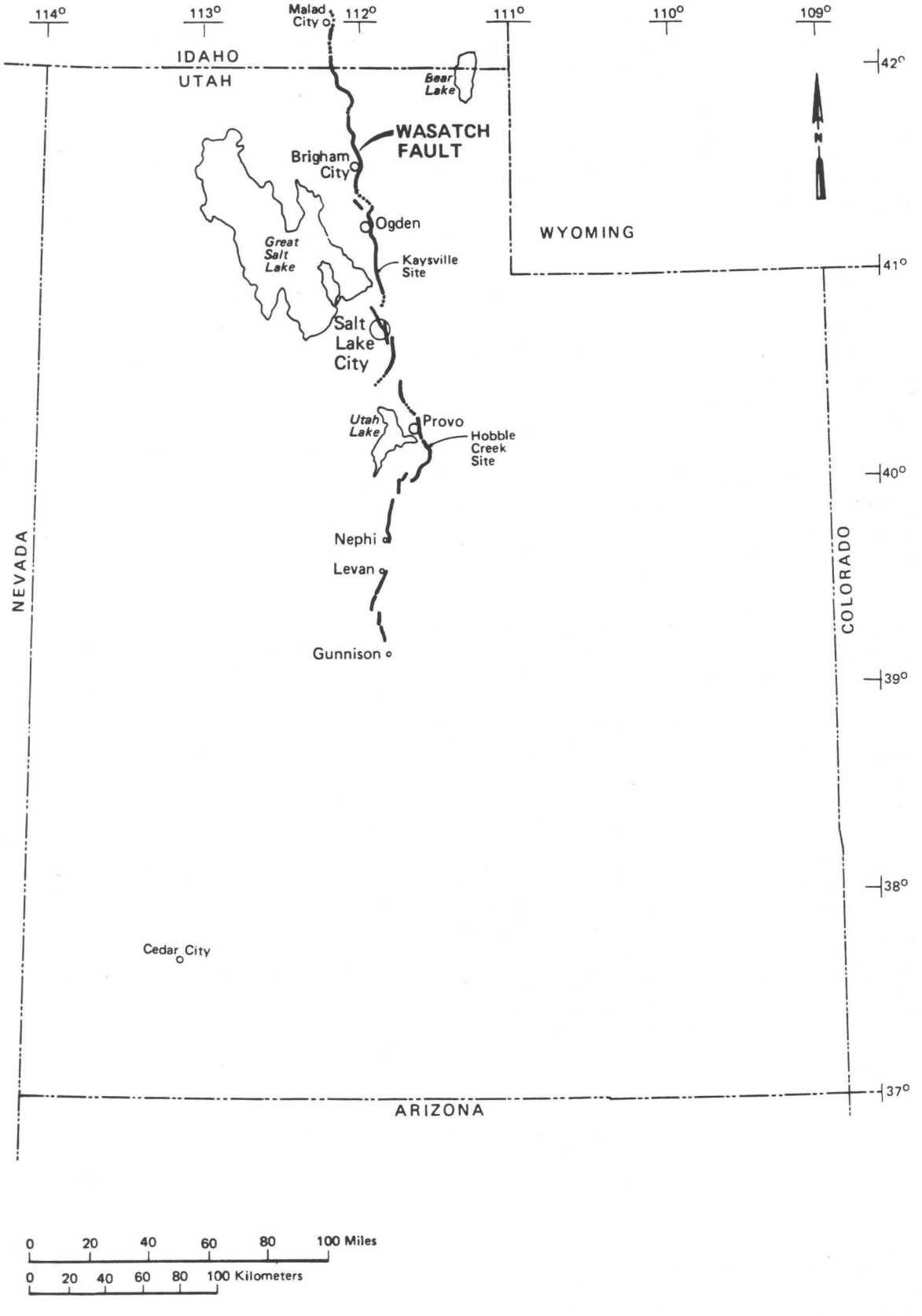

Fig. 1 - REGIONAL LOCATION MAP

2. The available data on fault behavior are not adequate to formulate or test models for estimating future fault behavior.

3. The potential for the occurrence of damaging earthquakes varies from fault to fault and along the same fault at different locations.

4. Location-specific data are seldom available on a given fault, hence, time and magnitude relationships between successive events cannot be assessed for a given location.

Too often, estimates of future earthquake activity are made using only historical seismicity data, resulting in misleading conclusions. Although these data may provide reasonable estimates of earthquake activity for small to moderate earthquakes (magnitude 6 or less) in highly active environments, only in rare cases are they adequate for obtaining reasonable estimates for moderate to large earthquakes[2]. As shown in Figure 2, the frequency of earthquakes of magnitudes greater than about 6 can be estimated through extrapolation of relationships established for smaller magnitudes. However, as also shown on Figure 2, combining the historical seismicity record with the Quaternary geologic record of siesmic activity and applying professional judgment may result in more realistic estimates of future damaging earthquakes. In addition, due to the uncertainties that exist regarding the earthquake generation process of strain accumulation and release, these estimates are best expressed probabilistically.

The purpose of this paper is to discuss how historical seismicity data for the Wasatch fault zone can be supplemented by geologic data to expand the available data base, and how the data can be used in conjunction with a probabilistic model of the physical earthquake generation process to estimate the probability of future moderate to large earthquakes on an individual segment, as well as on the entire Wasatch fault zone. The procedure for calculating the probabilities of occurrence of different magnitude ranges is also presented.

---

[2]In this discussion, a "moderate to large" earthquake is defined for the Wasatch fault zone as an event that is accompanied by enough surface fault displacement to be recognizable in an exploratory trench. The magnitude of such an earthquake is estimated to be about 6 1/2 or greater.

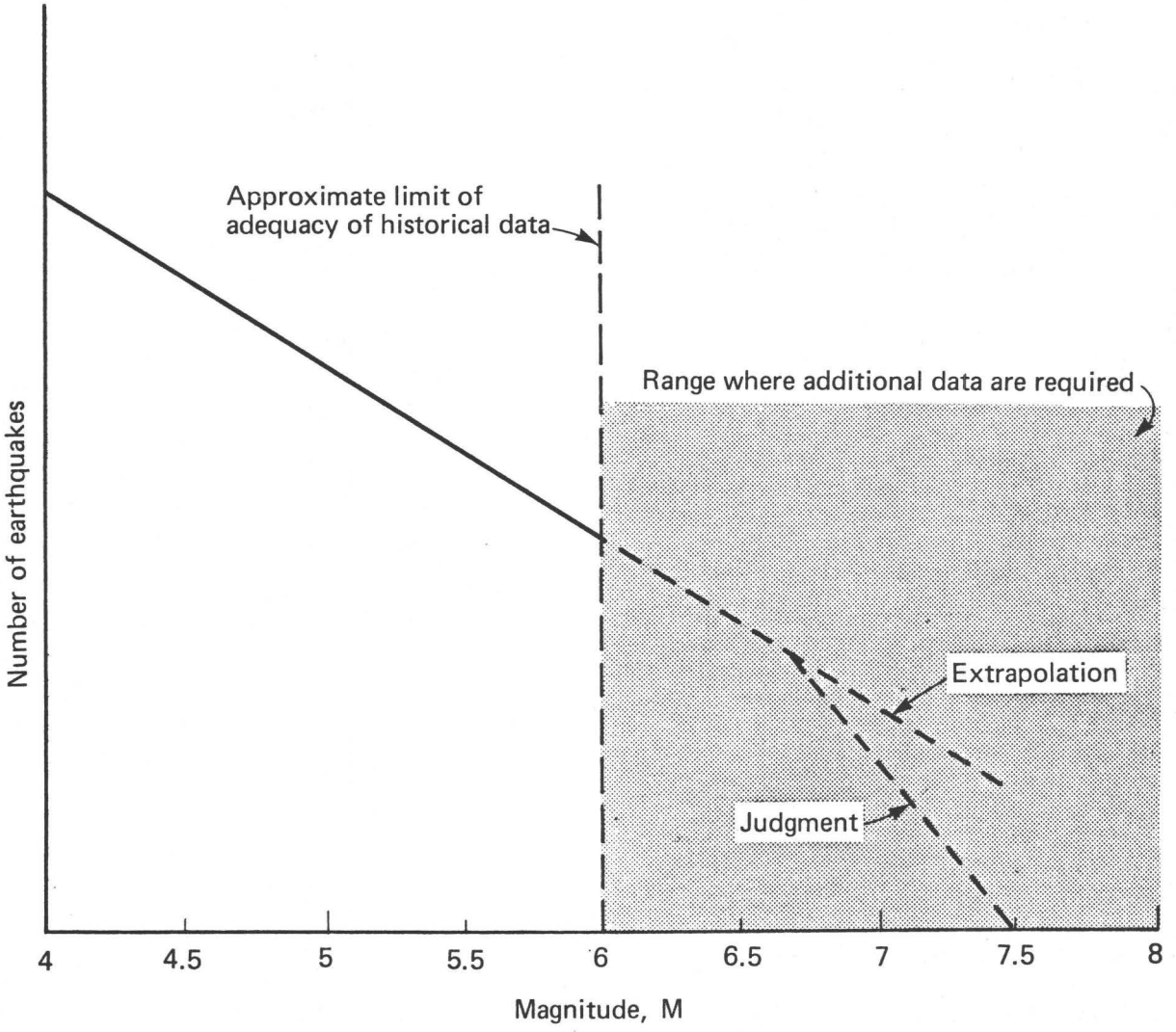

Fig. 2 - SCHEMATIC RELATIONSHIP OF EARTHQUAKE AND MAGNITUDE

SEISMIC GEOLOGY ALONG THE WASATCH FAULT ZONE

Abundant geomorphic evidence of late Quaternary faulting exists along the 370-km-long Wasatch fault zone. Recent investigations (Schwartz and others, 1979; Swan and others, 1979b) have shown that surface faulting has occurred repeatedly during Holocene time along at least several segments of the zone. Although portions of the fault are associated with microseismicity (Arabasz and others, 1978), the available historical record does not indicate the occurrence of moderate to large earthquakes in the past 132 years on the Wasatch fault zone.

The Wasatch fault zone is a discontinuous en echelon and segmented zone comprised of westward-dipping normal faults. The number and extent of individual segments of the fault are uncertain and are the subject of further investigations. The available data suggest that there are six to ten segments that range in length from about 30 to 60 km. It is assumed that individual segments of the fault behave similarly but somewhat independently of one another. The Kaysville and Hobble Creek sites (Figure 1) are situated on segments estimated for this analysis to be about 60 and 40 km long, respectively. The morphology and fault displacements observed at both sites are believed to be representative of each individual segment. Both sites have been subjected to detailed geologic investigation to assess late Quaternary slip rates and recurrence intervals between surface faulting earthquakes. Data summarized in this section are from ongoing geologic investigations of the displacement history of the Wasatch fault zone and the reader is directed to a companion paper by Swan and others (1979a) for a detailed discussion of these data.

Both the Kaysville and Hobble Creek segments display convincing evidence of multiple Holocene surface faulting events. At the Kaysville site, at least two earthquakes associated with surface faulting have occurred in the past 1580 $\pm$ 150 years, and stratigraphic relationships suggest a recurrence interval of 500 to 1000 years. Net tectonic displacement during each event is estimated to have been between 1.7 and 3.7 m. During late Holocene time, the rate of slip on this segment has averaged 1.7 mm/year. At the Hobble Creek site, at least six or seven surface faulting events have occurred in the past 12,000 years; three of these have occurred in the past 6000 years. Surface faulting produced an average of 0.8 to 2.8 m of net tectonic displacement per event and the average recurrence interval between events is estimated to be 1500 to 2400 years along this segment of the fault. The average Holocene slip rate on the Hobble Creek segment is estimated to be 1.1 mm/year.

For both segments, recurrence intervals and slip rates were determined independently. At Kaysville, the recurrence interval was estimated by bracketing the time period between two surface faulting events using an absolute age and stratigraphic relationships. At Hobble Creek, the recurrence interval was

calculated by dividing a geologically recognized time period by the number of events judged to have occurred within that period. Slip rates, on the other hand, were calculated by dividing the observed amount of displacement of a geologic unit or geomorphic surface by its age.

Because of the nature of the geologic record, rarely can the interval between individual surface faulting events be precisely measured. More commonly, one or more events can be shown to have occurred within a time window the size of which is a function of the completeness of the stratigraphic record and availability of datable materials within a geologic exposure. The assumption is usually made that individual faulting events are more or less evenly distributed in time throughout the bracketed time interval, although the interval between any two particular events may differ from the average. This assumption is consistent with a physical model of gradual strain accumulation and intermittent release along the fault. For example, exploratory trenching at the Hobble Creek site revealed at least three episodes of surface displacement since mid-Holocene time (6000 years ago). Therefore, the average recurrence interval between events is about 1500 to 2400 (Swan and others, 1979a).

No surface faulting events have occurred anywhere along the Wasatch fault zone during historical time (the past 132 years). At the Kaysville site, at least 300 years, and perhaps as many as 500 years, are judged to have elapsed, based on post-faulting sediment deposition. A minimum elapsed time of about 300 years is also likely at the Hobble Creek site and may be as long as 1000 years.

EARTHQUAKE RECURRENCE MODELS FOR THE WASATCH FAULT ZONE

Several analytical models have been proposed to represent the process of earthquake occurrence. Generally, these models are used in the broad context of estimating earthquake occurrence over relatively large tectonic regions. The most common is the Poisson model, which assumes spatial and temporal independence of all earthquakes, including the maximum earthquake associated with a fault or within a region. In this model, it is assumed that the occurrence of one earthquake does not affect the likelihood of a similar earthquake at the same location in the next unit of time. Other models, such as those proposed by Esteva (1976) and Shlien and Toksoz (1970), consider the clustering of earthquakes in time. Within a region, Knopoff and Kagan (1977) have used a stochastic branching process that considers a stationary rate of occurrence of main shocks and a distribution function for the space-time location of foreshocks and aftershocks.

Other probabilistic models have been used to represent earthquake sequences as strain energy release mechanisms. Hagiwara (1975) has proposed a Markov model to describe an earthquake mechanism simulated by a belt-conveyor model. A Weibull distribution is assumed by Rikitake (1975) for the ultimate strain of the earth's

crust to estimate the probabilities of earthquake occurrences. Earthquake magnitudes, however, are not represented in this model.

The above models are not adequate to characterize the occurrences of moderate to strong earthquakes on a fault at specific locations. A Poisson process provides estimates of the probability of occurrence of earthquakes of any size up to the designated maximum size that is characteristic of a whole region, but the estimates are independent of the size and time elapsed since the most recent major earthquake. Also, the estimates are invariant in time and insensitive to location within the region.

It has been noted that the occurrence of moderate to large earthquakes on a fault is nonrandom in space and time (see, for example, Sykes (1971) for earthquakes in subduction zones). A model that considers the nonrandom character of earthquake size and occurrence time is the semi-Markov model proposed by Patwardhan and others (1978). A general concept of earthquake generation on a fault can be described as the process of gradual, continuous accumulation of strain energy in the earth's crust, which is interrupted intermittently by episodes of sudden strain release along specific faults (Figure 3). Since the buildup of strain energy sufficient to generate a moderate to large earthquake takes some time, the occurrence of such an earthquake at a given location is not very likely within relatively short periods following an earthquake of similar size at the same location. As the time elapsed without the occurrence of a similar magnitude earthquake increases, the amount of accumulated energy increases, thereby increasing the potential for earthquakes above a given size. It is reasonable to assume that both the size and waiting time until the next earthquake is influenced by the amount of strain energy released in the previous earthquake (related to the magnitude of that earthquake) and the length of time over which strain has been accumulating without any significant release. For instance, the strain buildup required to generate a magnitude 7.5 earthquake is likely to take longer than the strain buildup to generate a magnitude 6 earthquake at the same location.

Available data suggest that the occurrence of major earthquakes on faults is consistent with the above process. The occurrence of earthquakes of magnitudes greater than a certain magnitude will be influenced by the occurrence of similar magnitude earthquakes at the same location. The occurrence of earthquakes of smaller magnitudes may not significantly affect the holding time or size of the next major earthquake. The size of a major earthquake is not constant and will vary from fault to fault, depending upon factors such as the relative dimensions of the rupture surfaces and the total available fault surface, slip rate, stress conditions, and shearing resistance.

As described previously, the Wasatch fault may be divided into six to ten segments (seven are assumed for the purposes of this

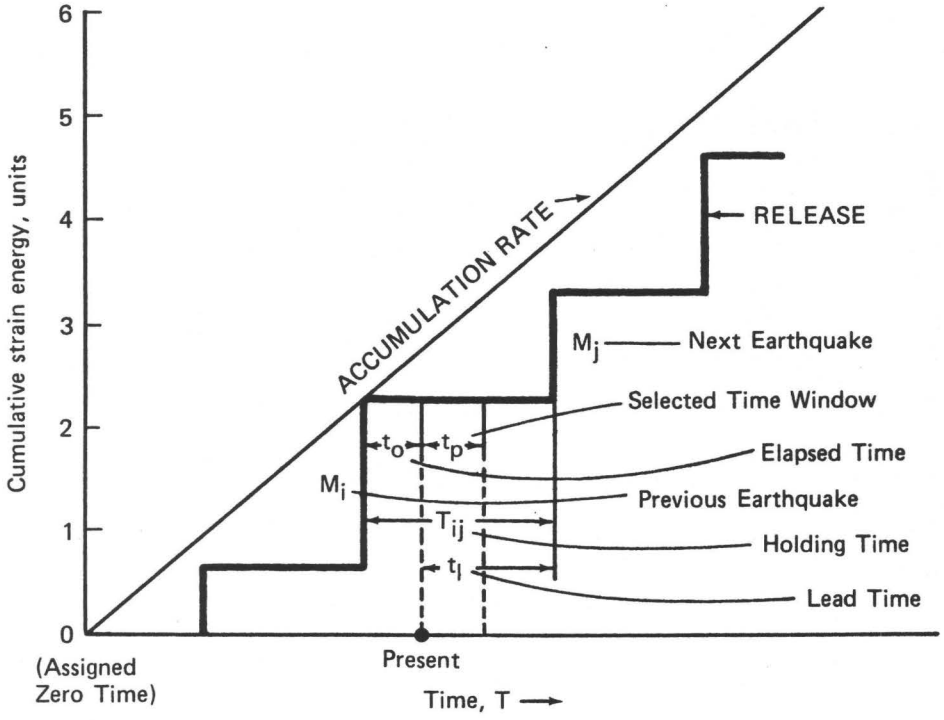

Fig. 3 - SCHEMATIC DIAGRAM OF THE EARTHQUAKE GENERATION PROCESS ON A FAULT

analysis) having lengths varying from 40 to 60 km. For the Wasatch fault, the interdependencies may be assumed to apply for shallow earthquakes of magnitudes greater than 6 to 6.5 for which the average rupture surfaces will be equal to approximately 20 to 35 percent of the estimated fault surface area of a segment. Earthquakes of these sizes also represent an approximate threshold for the occurrence of geologically recognizable surface fault displacement. Therefore, the following discussion is directed toward the evaluation of recurrence of earthquakes of magnitude 6.5 or larger.

A semi-Markov process models the occurrence of such earthquakes in a satisfactory manner (Patwardhan and others, 1978). The basic components of this model are shown in Figure 3 and are described below. A typical trajectory is shown in Figure 4.

1. Initial Seismicity Conditions - The initial seismicity conditions define the characteristics of the most recent earthquake of a size in the range included in the model. Two parameters are required: the magnitude of the most recent earthquake, M_i, and the elapsed time (t_o) since the occurrence at that earthquake.

2. Transition Probabilities (P_{ij}) - The likelihood that an earthquake of size M_i will be followed by an earthquake of size M_j defines the transition probability, P_{ij}.

3. Probability Distribution of Holding Times, H_{ij} (.) - The time between the occurrence of two successive major earthquakes, the first of size M_i and the next of size M_j, is termed the holding time, T_{ij}. The amount of holding time would depend both on M_i and M_j for a given region. The likelihood that T_{ij} equals M for all possible values of M defines the probability distribution, H_{ij} (.) of the holding time.

   The assessment of P_{ij} and H_{ij} (.) is made based on the analysis of all available information including historical seismicity data, geologically derived recurrence intervals, and an evaluation of the tectonic environment of the region.

4. Period of Interest - This is the period (for example, design life of a structure), t_p, during which probabilities of occurrences of different size earthquakes are required. These probabilities are a function of real time; that is, for the same time period, t_p, the probabilities depend on the starting time of the analysis.

The primary result of the semi-Markov model is specified in terms of the joint probability distribution as l/i (K_1, K_2, ..., K_n|T), which gives K_1 earthquakes of size M_1 and K_2 earthquakes of size M_2, ..., and K_n earthquakes of size M_n during the period of interest, T. All possible combinations of K_1, K_2, ..., and K_n are considered in specifying the joint probability distribution.

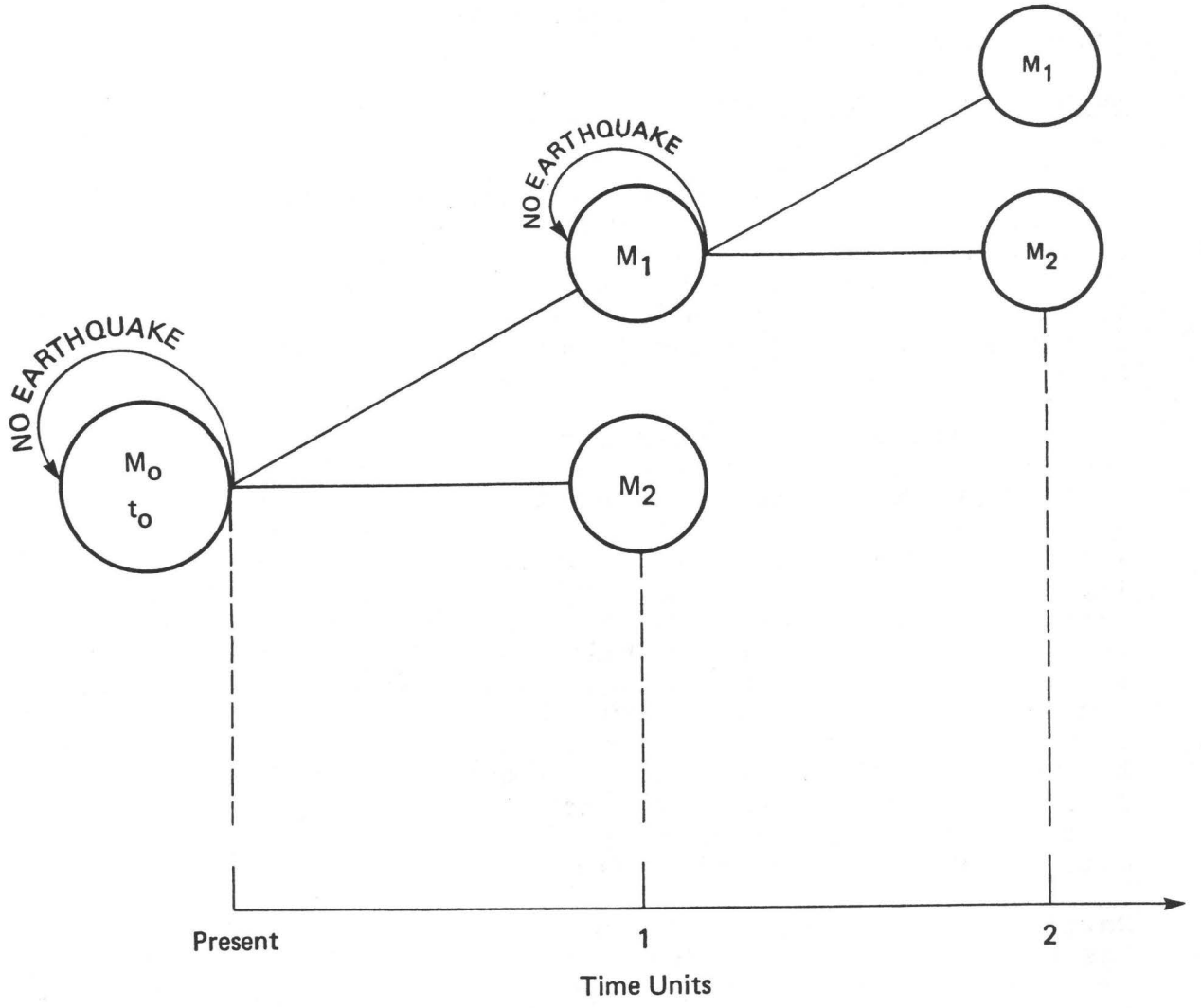

Fig. 4 - SCHEMATIC REPRESENTATION OF THE TRAJECTORY OF A SEMI-MARKOV PROCESS

ESTIMATION OF EARTHQUAKE RECURRENCE INTERVALS

As illustrated by Figure 2, geologic information is needed to supplement the seismicity record for moderate to large earthquakes. Models, such as that represented by a semi-Markov process, may serve to further refine estimates of recurrence intervals in the larger magnitude range.

Recurrence Interval Estimates From Historical Seismicity

Historical seismicity data can be represented by a frequency-magnitude N(M) curve that reflects a Poisson distribution of earthquake occurrence. Arabasz and others (1979) summarize earthquake data for the 92,815-sq-km Wasatch Front area that includes the Wasatch fault zone (38° 54' to 42° 30'N, 110° 25' to 113° 10'W) for the period 1850 to 1978. Preinstrumental intensities were converted to magnitudes using the Gutenberg and Richter relation (1956): $M = 1 + 2/3\ I_o$.

The cumulative relationship between earthquake magnitude and the number of events per year of a given or higher magnitude has the form (curve A, Figure 5) (Arabasz and others, 1979a):

$$\log N = 2.98 - 0.72\ M_L$$

The solid portion of the curves shown in Figure 5 ends at the largest magnitude in their respective data sets; dashed lines are extrapolations. Curves A, B, and C have been normalized to an area of 265 sq km, or one kilometer length of the Wasatch Front area. This allows comparisons with earthquake frequency relations on the Hobble Creek and Kaysville segments per kilometer length. The data set represented by curve A is for a 92,815-sq-km region having approximate dimensions of 265 km by 350 km. Included in the region are several earthquakes not associated with the Wasatch fault zone and large areas distant from any active faults and devoid of seismic activity.

Narrowing the width of the study region by one-third toward the Wasatch fault (from 265 to 175 km, area: 61,250 sq km) effectively removes from the data set large aseismic areas and several earthquakes that are not associated with the Wasatch fault zone. The total number of earthquakes is reduced by about one-quarter by spatial reduction. Assuming no change in b value, the N(M) relation has the form (curve B, Figure 5):

$$\log N = 3.03 - 0.72\ M_L$$

The net effect of the reduction is an increase in the areal flux or the mean number of events per year per unit area. Calculated probabilities of earthquake occurrence over a 50-year period for 40- and 60-km segments based on the historical seismicity record (curve B, Figure 5) are given below:

Magnitude	40 km	60 km
6.5	0.12	0.17
7.0	0.05	0.08
7.5	0.02	0.04

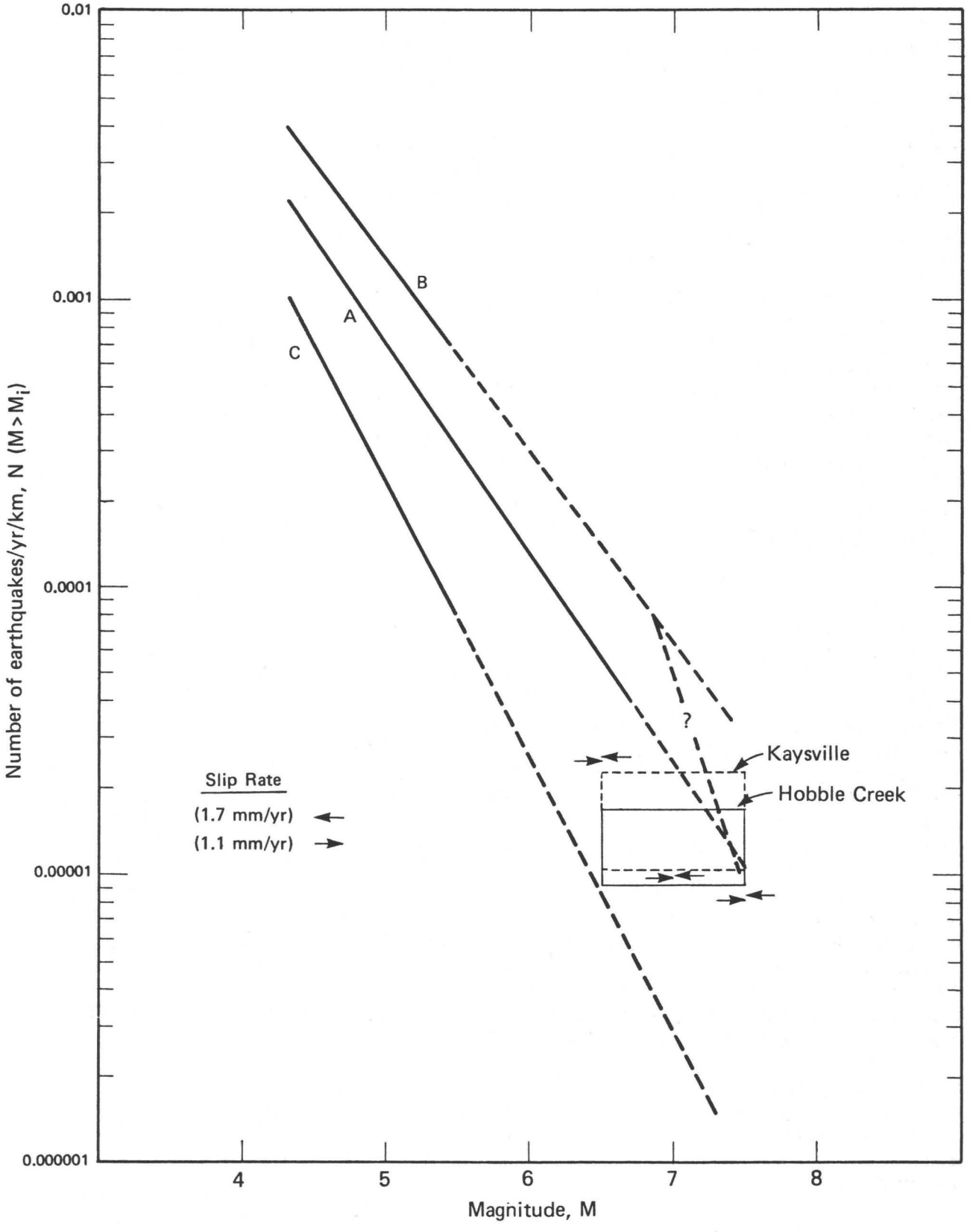

Fig. 5 - FREQUENCY-MAGNITUDE BASED ON HISTORICAL SEISMICITY AND GEOLOGIC DATA

These probabilities are somewhat high when compared with results given later in this section derived from the semi-Markov model and using geologic data from the Hobble Creek and Kaysville segments.

Arabasz and others (1979) have examined separately the instrumental (1962 to 1978) seismicity data for a 33,750-sq-km area that includes the Wasatch fault zone. These data show a significantly higher value of b than the total historical data set. The normalized curve is C in Figure 5. Arabasz and others (1979) state that the seismicity during the 1962 to 1978 period was anomalous, as shown by the persistence of at least two seismic gaps.

Recurrence Interval Estimates From Geologic Data

Surface faulting recurrence intervals and slip rates for the Hobble Creek and Kaysville segments, summarized earlier, are based on geologic investigations discussed in Swan and others (1979a). The recurrence interval data are represented in Figure 5 by the mean rate of occurrence of moderate to strong earthquakes (magnitude 6.5 or larger), normalized per kilometer length of segment. The vertical bars represent the range of error in estimating recurrence intervals for each segment and the horizontal bars represent the judged range in magnitude (6.5 to 7.5) of surface faulting earthquakes on the Wasatch fault zone.

To use geologic information on fault slip rates, estimates were made to calculate the average waiting period for a surface faulting earthquake based on average slip rates for the two segments. Assuming an average magnitude/moment relationship suggested by Kanamori and Anderson (1975), moments corresponding to magnitudes of 6.5, 7.0 and 7.5 were estimated. Utilizing slip rates of 1.1 and 1.7 mm/year, for Hobble Creek and Kaysville, respectively, the average waiting time to accumulate moments for a given magnitude earthquake were calculated. These average waiting times are summarized in the table below.

	Average Waiting Time (yrs)	
Magnitude	Hobble Creek (assuming 1.1 mm/yr)	Kaysville (assuming 1.7 mm/yr)
6.5	1000	647
7.0	2450	1590
7.5	3000	1940

Utilizing the values given above, the mean number of earthquakes per year per kilometer of segment may be calculated. These values are indicated in Figure 5 by the arrows. Note that the mean rate of occurrence of moderate to strong earthquakes based on average slip rates is in reasonable agreement with that based on average recurrence intervals.

As has been stated previously, the historical seismicity record does not seem to adequately represent the rate of occurrence of moderate to large earthquakes. Particularly for the reduced area (curve B in Figure 5), which is more specific to the Wasatch fault, the extrapolated N(M) relationship overestimates the frequency of occurrence of surface faulting events. This may be due to the fact that the Gutenberg and Richter relationship was derived primarily for smaller magnitude earthquakes and may, in fact, have a bilinear character for larger magnitude earthquakes (see queried portion of curve B, Figure 5.). The paucity of moderate to large earthquakes in the 1962 to 1978 period causes an underestimate of their frequency of occurrence relative to geologically based estimates (curve C, Figure 5).

Probabilities of Occurrence Calculated Using A Semi-Markov Model

Probabilities of occurrence were calculated using a semi-Markov model for the following cases:

a) The probability of occurrence of at least one earthquake of magnitude 6.5 or larger on each of two segments of the Wasatch fault zone (Kaysville and Hobble Creek).

b) The probability of occurrence of at least one earthquake of magnitude 6.5 or larger for the entire Wasatch fault zone.

c) The probability of occurrence of earthquakes in the magnitude ranges 6.5 to 7.0 and 7.1 to 7.5 for one segment of the Wasatch fault zone (Kaysville).

Case a: Probability of Occurrence of at Least One Earthquake of Magnitude 6.5 or Larger on Two Segments -

As a first step, the basic components of the semi-Markov model, described previously and shown in Figure 3, are established. For earthquakes of magnitude 6.5 or larger, it is reasonable to assume that the probability of occurrence of successive earthquakes within a small-unit time interval is very small. For purposes of this analysis, a unit time interval of 50 years is reasonable. In the present case, the trajectory in Figure 4 has only one transition state, magnitude 6.5 or larger. The given segment would, therefore, either hold in the present state (no earthquake would occur), or make a transition to a state of the occurrence of an earthquake of magnitude 6.5 or larger.

Parameters of the probability distribution of holding times were assessed based on geologic data on earthquake recurrence (Swan and others, 1979a). These data were supplemented by subjective judgment using the fractile method suggested by Raiffa (1968). Probability fractiles for the Kaysville and Hobble Creek segments are summarized in Table 1. Because the holding times used in analysis were obtained by combining a prior distribution based on subjective judgments with available data, the sensitivity of the model to the holding time distribution was assessed. Summarized

in Table 1 are four possible distributions used in sensitivity analysis for the range of holding times indicated by geologic data at the Kaysville site. Computations show that the calculated probabilites of earthquake occurrence are not significantly different, especially with greater elapsed times.

TABLE 1

SUMMARY OF HOLDING TIMES USED FOR ONE-STATE ANALYSIS

Initial State Mi	Following State Mj	Fractiles (yrs) 0.25	0.50	0.75	1.00
Kaysville 6.5+	6.5+	700	1100	1600	2200
Hobble Creek 6.5+	6.5+	1400	2100	2700	3200

Sensitivity Analysis

Mi	Mj	Distribution	Fractiles (yrs) 0.25	0.50	0.75	1.00
6.5+	6.5+	A	700	1100	1600	2200
		B	400	650	900	2200
		C	900	1100	1300	2200
		D	1600	1850	2000	2200

The calculated values of probabilities of occurrence of earthquakes of magnitude 6.5 or larger for various elapsed times are shown graphically in Figure 6. For example, Figure 6 shows that if the elapsed time after a magnitude 6.5 or larger earthquake on the Kaysville segment is 600 years, the probability of experiencing at least one magnitude 6.5 or larger earthquake in the next 50 years on that segment is approximately 0.05. This result is reasonable considering the holding time distribution given in Table 1 and the relatively short period of interest (50 years).

Case b: Probability of Occurrence of at Least One Earthquake of Magnitude 6.5 or Larger on the Entire Fault Zone -

As discussed earlier, the Wasatch fault may consist of about six to ten segments and is assumed in this analysis to be composed of seven segments. To estimate the probability of occurrence of at least one earthquake of magnitude 6.5 or larger on the entire fault zone in the next 50 years, it is necessary to estimate the probability of occurrence of earthquakes on each of the seven segments. Suppose the segments are numbered as 1, 2, 3,...7 and the corresponding probabilities of not experiencing an earthquake in the next 50 years on each individual segment are designated as p_1, p_2, p_3,...p_7. Then the probability of having no earthquake

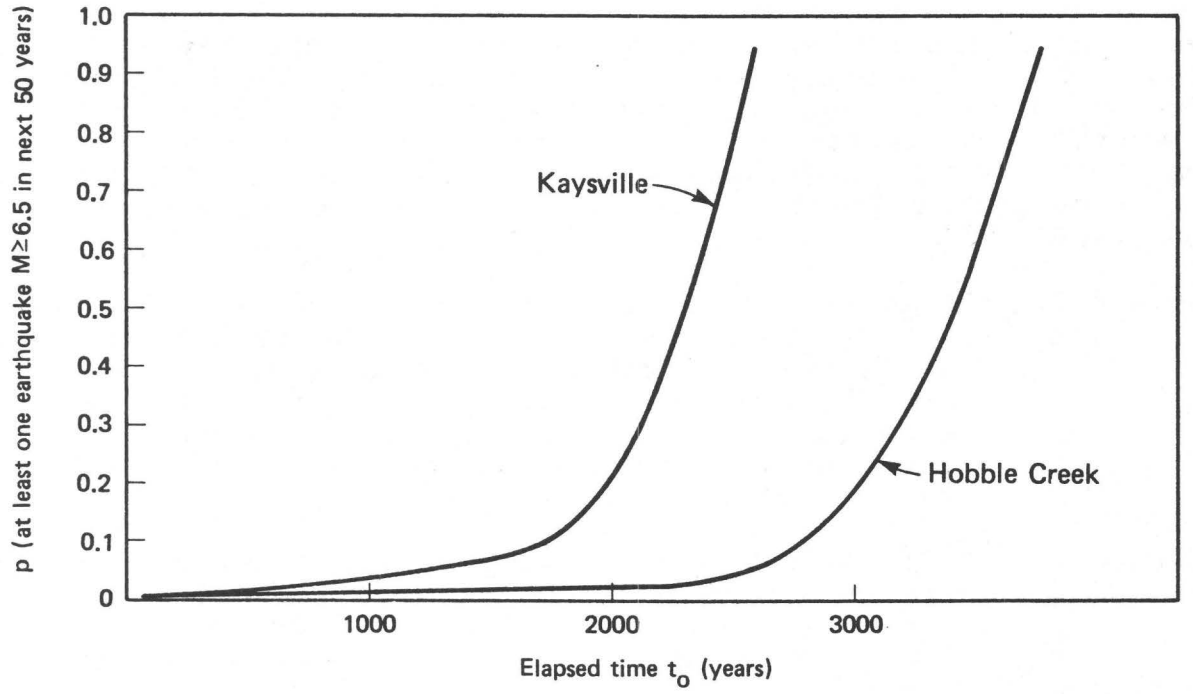

Fig. 6 - PROBABILITY VERSUS ELAPSED TIME ASSUMING ONE TRANSITION STATE

of magnitude 6.5 or larger on the entire fault zone is based on the joint probability distribution for the segments:

$$p_c = p_1 \times p_2 \cdot \cdot \cdot p_7$$

and the probability of occurrence of at least one earthquake of magnitude 6.5 or larger is given by

$$p \text{ (at least one earthquake } M \geq 6.5) = 1 - p_c$$

To estimate values of p_1, p_2, etc., it is necessary to derive relationships similar to those given in Table 1 for all segments and to estimate elapsed times for each segment. Additional geologic investigations similar to that for the Kaysville and Hobble Creek segments are required to obtain the necessary accurate data on recurrence intervals and elapsed times on other segments. To obtain a preliminary estimate of the range of probabilities of occurrence of at least one earthquake of magnitude 6.5 or larger on the entire fault, three subcases are considered:

Subcase 1: All seven segments are assumed to have an elapsed time (t_o) versus probability (p) of occurrence of at least one earthquake of magnitude 6.5 or larger relationship similar to that for the Kaysville segment in Figure 6. The average elapsed times for all segments are similar and equal to about 500 years.

Subcase 2: All seven segments have $(p)/(t_o)$ characteristics similar to those described in Subcase 1. Six segments have an elapsed time of 500 years and the remaining segment has an elapsed time of 2000 years.

Subcase 3: All seven segments have $(p)/(t_o)$ characteristics similar to those described in Subcase 1. Five segments have an elapsed time of 500 years and the remaining two segments have an elapsed time of 2000 years.

For purposes of illustration, the conditions assumed in the subcases above are geologically reasonable for the Wasatch fault zone, and the calculated probabilities provide useful insights into the influence of variation in elapsed times on the probability of experiencing a future earthquake of magnitude 6.5 or larger in the next 50 years. The calculated probabilities are:

Subcase	p_c (at least one earthquake $M \geq 6.5$ anywhere on the entire fault zone in the next 50 years)
1	0.19
2	0.58
3	0.79

The values tabulated above show that the nature of the $(p)/(t_o)$ relationship and the elapsed time has a significant effect on the estimated probabilities of occurrence of a major earthquake somewhere on the Wasatch fault zone. The presence of only one segment with an elapsed time comparable to the p = 0.75 to 1 holding times in Table 1 (for example, 1600 to 2200 years) significantly influences the probability p_c. Although the values in the above table may not be representative of the Wasatch fault, they serve to underscore the need for geologic studies along other portions of the zone and the importance of assessing both recurrence intervals and elapsed times in these investigations.

Case c: Probabilities of Occurrence of Earthquakes of Different Magnitude Ranges on Individual Segments -

The discussion of probabilities in Cases (a) and (b) pertain to the occurrence of earthquakes of magnitude 6.5 or greater without differentiation of magnitudes. It is estimated that the maximum magnitude associated with an individual segment of the Wasatch fault zone is about 7.5. Therefore, the range of magnitudes of interest is 6.5 to 7.5. This range of magnitudes represents mean fault rupture surface areas varying from 200 to 1000 sq km and mean seismic moments varying from 10^{25} to 10^{27} dyne-cm. In terms of consequences, the areas within which significant shaking effects may be experienced (peak ground acceleration 0.1 g or greater) will also differ by one to two orders of magnitude. Therefore, to refine estimates of seismic exposure and seismic risk it is desirable to obtain probabilities for ranges of magnitudes. For purposes of discussion, two ranges are assumed for the Wasatch fault zone: Range i, 6.5 to 7.0 and range ii, 7.1 to 7.5.

State-of-the-art geologic investigations do not yet provide sufficient information to confidently assess magnitude ranges for past surface faulting events. In the absence of these data, inputs to the semi-Markov model, including holding times, must be transition probabilities (P_{ij}), and the magnitude of the most recent earthquake, based on judgments. The inputs used in this analysis are summarized in Table 2. The distributions are based on the same schematic physical model as in Figure 3. Thus, it is assumed that the holding times to accumulate enough strain energy for a magnitude 6.5 to 7.0 earthquake will be smaller than the holding time for magnitude 7.1 to 7.5. The magnitude of the most recent event was assumed to have been 6.5 to 7.0.

TABLE 2

SUMMARY OF HOLDING TIME DISTRIBUTIONS AND TRANSITION PROBABILITIES USED FOR TWO-STATE ANALYSIS

Holding Times

Initial State Mi	Following State Mj	Fractiles (yrs) 0.75	0.5	0.75	1.0
6.5-7.0	6.5-7.0	550	700	900	1000
6.5-7.0	7.1-7.5	600	850	1100	1300
7.1-7.5	6.5-7.0	650	1000	1250	1450
7.1-7.5	7.1-7.5	700	1100	1600	2200

Transition Probabilities

Initial State Mi	Following State Mj	Probability
6.5-7.0	6.5-7.0	0.6
6.5-7.0	7.1-7.5	0.4
7.1-7.5	6.5-7.0	0.6
7.1-7.5	7.1-7.5	0.4

Results of the calculation of probabilities for the distribution shown in Table 2 are given in Figure 7. A qualitative comparison with the results of a single transition state magnitude 6.5 for the Kaysville segment given in Figure 6 is informative, although a quantitative comparison is not warranted because of the uncertainties in the input parameters. Clearly, for faults such as the Wasatch which have not had repeated historical moderate to large earthquakes, additional data are required before more definitive magnitude/recurrence relationships can be established.

SUMMARY

Various investigators in the last decade have recognized the Wasatch fault zone to be active and with this recognition has come the need to estimate the fault's potential for surface rupture and associated damaging earthquakes. Estimates of future earthquake activity should incorporate the widest possible range of available seismic and geologic data. Uncertainties in the data should be accounted for by utilizing a probabilistic framework. Some of the conclusions of this study are:

1. Historical seismicity data are not adequate for realistically estimating the recurrence of earthquakes of magnitude 6.5 or larger on the Wasatch fault zone. They need to be supplemented by geologic data and by probabilistic models.

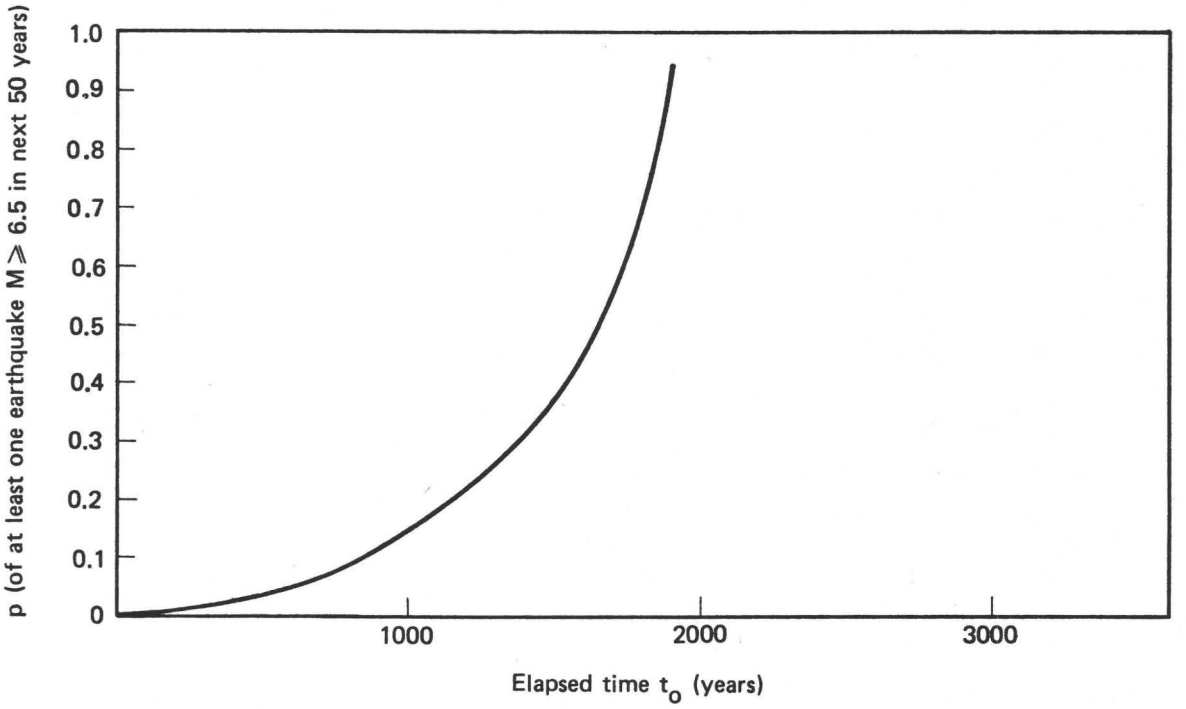

Fig. 7 - PROBABILITY VERSUS ELAPSED TIME ASSUMING TWO TRANSITION STATES KAYSVILLE SITE

2. Estimates of earthquake activity for earthquakes of magnitude 6.5 or larger that are based on historical seismicity records (1850-1978) overestimate the frequency of occurrence of such earthquakes compared to estimates based on average fault slip rates and surface faulting recurrence intervals.

3. Because available models do not take into account the dependencies of future earthquakes on the size of previous earthquakes and the time elapsed since they occurred, a semi-Markov process has been applied to characterize location-specific patterns of earthquake recurrence based on a physical model of strain accumulation and intermittent release.

4. Using geologic data, recurrence estimates can be obtained for earthquakes of magnitude 6.5 or larger based on a semi-Markov model for individual segments of the Wasatch fault zone. The probability of occurrence of at least one earthquake along a single segment depends upon the elapsed time since the most recent similar magnitude earthquake on each segment.

5. The probability of experiencing at least one earthquake of magnitude 6.5 or larger on the entire fault zone can be significantly influenced by the elapsed time since such an earthquake on any individual segment. To obtain realistic estimates for the entire zone, site geologic investigations of individual segments must assess both surface faulting recurrence intervals and elapsed time since the most recent event.

6. For the purposes of seismic exposure and seismic risk assessments, it is desirable to estimate the probability of occurrence of at least one earthquake for magnitude ranges (for example, magnitude 6.5 to 7.0 and 7.1 to 7.5). Adequate data for estimating these probabilities for the Wasatch fault zone are not available at present and, therefore, estimates must be based on judgment.

ACKNOWLEDGMENTS

This work is part of an ongoing study supported by the Professional Development Program of Woodward-Clyde Consultants. The authors gratefully acknowledge the assistance of Ram Kulkarni and Ezio Alviti in computer analysis. Michael Scott, Dennis Fischer, and Christine Daniel provided technical assistance. The manuscript was greatly improved by discussions with Peter L. Knuepfer and review by David P. Schwartz, F.H. Swan, III, and Janet L. Cluff. We also appreciate the cooperation of Robert B. Smith and Walter J. Arabasz at the University of Utah.

REFERENCES

Arabasz, W.J., Smith, R.B., Richins, W.D., 1979, Earthquake studies along the Wasatch Front, Utah, network monitoring, seismicity, and seismic hazards: Proceedings of the Conference on Earthquake Hazards along the Wasatch Front and in the Reno-Carson City area, National Earthquake Hazards Reduction Program, U.S. Geological Survey open-file report, in press.

Arabasz, W.J., Smith, R.B., Richins, W.D., and Kastrinsky, A.J., 1978, Seismicity and seismic network coverage of the Wasatch Front, Utah, (abs.): Geological Society of America Abstracts with Programs, v. 10, p. 209-210.

Cluff, L.S., Hintze, L.F., Brogan, G.E., and Glass, C.E., 1975, Recent activity of the Wasatch fault, northwestern Utah, U.S.A.: Tectonophysics, v. 29, p. 161-168.

Esteva, L., 1976, in Seismic Risk and Engineering Decisions; Developments in Geotechnical Engineering 15: Elsevier Scientific Publishing Company, New York.

Gutenberg, B., and Richter, C.F., 1956, Earthquake magnitude, intensity, energy, and acceleration: Seismological Society of America Bulletin, v. 46, p. 105-145.

Hagiwara, Y., 1975, A stochastic model of earthquake occurrence and the accompanying horizontal land deformations: Tectonophysics, v. 26, no. 1/2, March, p. 91-101.

Kanamori, H., and Anderson, D.L., 1975, Theoretical basis of some empirical relations in seismology: Seismological Society of America Bulletin, v. 65, p. 1073-1095.

Knopoff, L., and Kagan, Y., 1977, Analysis of theory of extremes as applied to earthquake problems: Journal of Geophysical Research, v. 82, no. 36.

Patwardhan, A.S., Kulkarni, R.B., and Tocher, D., 1978, A semi-Markov model for characterizing recurrence of great earthquakes: Proceedings of Conference VI, Methodology for Identifying Seismic Gaps and Soon-to-Break Gaps; National Earthquake Hazards Reduction Program, U.S. Geological Survey open-file report 78-943, p. 635-685.

Raiffa, H., 1968, Decision analysis: Addison-Wesley, Reading, Massachusetts.

Rikitake, T., 1975, Statistics of ultimate strain of the earth's crust and probability of earthquake occurrence: Tectonophysics, v. 26, no. 1/2, March, p. 1-21.

Schwartz, D.P., Swan, F.H., III, Knuepfer, P.L., Hanson, K.L., and Cluff, L.S., 1979, Surface deformation along the Wasatch fault, Utah, (abs.): Geological Society of America Abstracts with Programs, v. 11, no. 3, p. 127.

Shlien, S., and Toksoz, M., 1970, A clustering model for earthquake occurrences: Seismological Society of America Bulletin, v. 60, no. 6, p. 1765-1787.

Swan, F.H., III, Schwartz, D.P., and Cluff, L.S., 1979a, Recurrence of surface faulting and moderate to large magnitude earthquakes on the Wasatch fault zone at the Kaysville and Hobble Creek sites: Proceedings of the Conference on Earthquake Hazards along the Wasatch Front and in the Reno-Carson City area, National Earthquake Hazards Reduction Program, U.S. Geological Survey open-file report, in press.

Swan, F.H., III, Schwartz, D.P., Hanson, K.L., Knuepfer, P.L., Cluff, L.S., 1979b, Recurrence of surface faulting and large magnitude earthquakes along the Wasatch fault zone, Utah (abs.): Geological Society of America Abstracts with Programs, v. 11, no. 3, p. 131.

Sykes, L.R., 1971, Aftershock zones of great earthquakes, seismicity gaps, and earthquake prediction for Alaska and the Aleutians: Journal of Geophysical Research, v. 76, p. 8021.

PATTERNS OF LATE QUATERNARY FAULTING IN WESTERN UTAH AND AN APPLICATION IN EARTHQUAKE HAZARD EVALUATION

by

R. C. Bucknam, S. T. Algermissen, and R. E. Anderson
U.S. Geological Survey, Denver, Colorado

INTRODUCTION

In 1972, S. T. Algermissen and D. M. Perkins presented a technique for seismic zoning and made a probabilistic evaluation of expected ground motion in Utah and Arizona. Using the techniques described in that paper they prepared (1976) a map of probabilistic estimates of maximum accelerations in rock expected for the contiguous United States. Their studies were based primarily on the historic seismic record which was generalized to define seismic source zones and the temporal characteristics of seismic activity in the source zones.

As part of geologic studies related to earthquake hazards in Utah, we are making a photogeologic compilation of fault scarps formed on unconsolidated sediments in western Utah and are making quantitative field studies of their morphology to determine their distribution and age. Features of the faulting allow characterization of large seismic source regions that are distinctive on the basis of ages of most recent movements on the faults within the region and the frequency of movement within late Quaternary time.

In this paper we tentatively redefine the seismic source zones in western Utah on the basis of geologic data. In particular, we assess the implications of long-term characteristics of large magnitude earthquake activity (as indicated by the geologic data) on the use of short-term historic data for seismic hazard evaluation. The new source zones are used in a probabilistic analysis to provide an improved estimate of maximum accelerations expected along the Wasatch Front in the vicinity of Salt Lake City, Utah.

GEOLOGIC STUDIES

As part of regional geologic studies related to developing an understanding of the seismicity of Utah we are preparing a map of fault scarps in the region. A preliminary generalized version of that map is shown in figure 1. It is based on published work for three 1° x 2° quadrangles (Bucknam, 1977; Bucknam and Anderson, 1979; Anderson and Bucknam, 1979), on a strip of large scale maps along the Wasatch fault (Cluff and others, 1970, 1973, 1974), and on our partially completed unpublished work in the remainder of the area. As discussed in more detail in a following section, the scarps are believed to provide a record of high-energy late Quaternary seismic events.

The map shows the locations of fault scarps developed on deposits of unconsolidated to weakly consolidated alluvium. It is not a comprehensive map of Cenozoic or even Quaternary faults and thus does not show all faults that

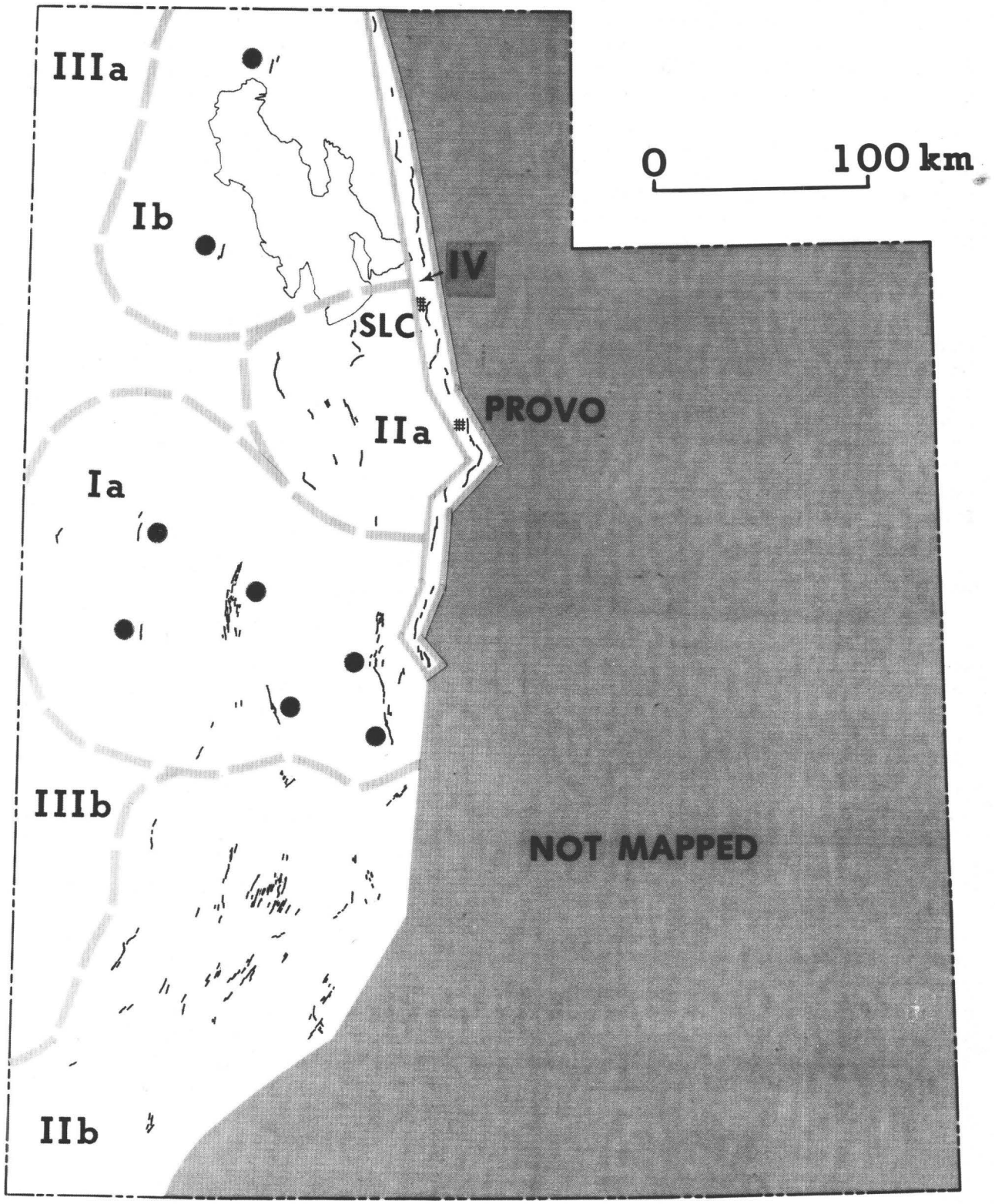

Figure 1.--Map showing late Quaternary fault scarps (fine lines), Holocene fault scarps (fine lines with adjacent dot), and source regions I, II, III, IV (heavy dashed lines).

might produce earthquakes. Such a map would include all Quaternary faults in bedrock and at bedrock-alluvium contacts. The objective sought in compiling the map is to determine regional characteristics of seismic activity as averaged over thousands of years rather than to delineate all possible individual faults that might give rise to earthquakes.

For the mapping, aerial photographs at the scale 1:60,000 were systematically scanned for all possible fault-related offsets of geomorphic surfaces developed on surficial materials. The photo-reconnaissance was followed by compilation of the traces of all identified surface discontinuities at a scale of 1:250,000. This preliminary compilation has served as a guide for the field studies that have followed.

Field studies have three objectives: (1) fault traces are mapped or deleted from the preliminary compilation of features if they are judged not to be fault scarps or show no surface offset (lineaments); (2) stratigraphic indicators of amount and (or) age of displacements are sought; and (3) surface profiles normal to the scarp trace are measured according to the procedures described in Bucknam and Anderson (1979). Profiles are measured only at places where scarps are sufficiently continuous and unmodified by deposition and erosional channels at their base to be diagnostic of surface offset. Profiles were not measured on all scarps.

A major goal of the study is to rank the fault scarps according to their relative age, as well as to determine their approximate numerical age. In general, the slope of a scarp would be expected to decrease with increasing age, but in addition Bucknam and Anderson (1979) found that the slope of the scarp is strongly dependent on its height as well as its age. In order to make direct comparisons between maximum slope angles measured on different scarps it is necessary to eliminate the effect of this dependence on scarp height. If profiles for each scarp or group of scarps are measured over a sufficiently broad range of scarp heights, the data can be normalized to an arbitrary scarp height for comparisons of relative ages. The data indicate that within the area studied the method allows fairly reliable discrimination of Holocene from pre-Holocene scarps.

Between the upper convex and lower concave parts of a fault scarp, the profiles of some fault scarps consist of two distinct slope segments. The steeper of the two segments probably represents renewed movement on the fault and the more gentle part represents one or more earlier displacement events. We interpret such two-stage or multi-stage scarps as resulting from earthquakes and not from creep because the creep rates would have to vary dramatically over the displacement history in order to produce the observed scarp morphology. In addition, historic earthquakes have produced fault scarps at 11 locations in the Basin and Range province while no scarps in the province associated with range frontal faults are known to have developed in historic time in a manner that would suggest fault creep.

Many scarps in western Utah, some of which are as much as 25 m high, show no evidence of compound slopes. These scarps, when compared to those produced by large, historic earthquakes, seem too high to have formed in a single event. We infer that most, or possibly all, of these very high scarps with smooth profiles were produced by several displacement events despite the fact that direct evidence for multiple events is lacking. This lack of direct

evidence indicates that the time elapsed since the last event has been sufficiently long for erosional processes to produce a smooth profile. A high scarp with a youthful-looking steep scarp segment at its base represents at least two periods of activity. The number of individual displacement events directly indicated by the morphology of a scarp is clearly a minimum.

MAGNITUDES REPRESENTED BY SCARPS

An important part of our evaluation involves the assumption that the mapped fault scarps provide a useful estimate of the number of earthquakes of a given magnitude range that have occurred in a given span of time. For the reasons given below we believe that within the area studied the mapped fault scarps represent a nearly complete record of earthquakes in the magnitude range 7 to 7 1/2 that have occurred there during Holocene time. To the extent that the record is incomplete, rates of seismicity determined from Holocene fault scarp data would be expected to err by underestimating the frequency of large earthquakes.

Data on historic surface faulting (Slemmons, 1977) provide a guide to interpretation of the sizes of earthquakes represented by the fault scarp data. We have selected those data derived from the Basin and Range province (table 1). Displacements there are primarily the result of normal faulting and although some of the earthquakes also had a strike-slip component, it is probably the most representative information available for estimating the sizes of fault scarps expected for earthquakes in western Utah.

Eleven earthquakes in the Basin and Range province have produced surface faulting in historic time. All of those less than magnitude 6.8 resulted in less than one meter of maximum displacement. The one historic earthquake in Utah with observed surface faulting (Hansel Valley, 1934) was of magnitude 6.6; surface fractures had a maximum of 0.5 m of dip-slip displacement. There is a strong tendency for earthquakes above magnitude 7 to be associated with a maximum displacement of at least several meters. Because all scarps mapped by us are the result of at least 1 meter of vertical displacement we infer that they were produced by earthquakes of about magnitude 7 or larger.

Scarps associated with the shoreline of the high stand of Lake Bonneville, which occurred about 12,000 to 15,000 years ago (Bucknam and Anderson, 1979), are widespread in the mapped area, and in many respects closely resemble fault scarps. Their expression thus offers a guide to the degree of preservation expected for fault scarps of similar or younger age and the extent of our ability to recognize them.

Erosion and deposition have made the shoreline scarp locally discontinuous. However, segments of the scarp 200 m long and equivalent to a 1 m fault offset cut on alluvial fan gravels are clearly recognizable on the 1:60,000 scale aerial photographs that we used for the mapping. In general, dissection of the scarps or burial by alluviation is not sufficient to be expected to totally obliterate all evidence of their existence over tens of kilometers. The data of table 1 indicate that a magnitude 7 earthquake would produce a surface rupture tens of kilometers long and with a meter or more of maximum displacement. The shoreline observations suggest that it is highly unlikely that all evidence of such scarps would be eliminated during Holocene time.

Table 1.--Historic surface faulting in the Basin and Range Province

	Date	M_L[1]	Location	Maximum[2] Displacement (m)	Length (km)[2]
1	26 March 1872	8.0	Owens Valley, California	6.4	110
2	3 May 1887		Sonora, Mexico	4	50
3	3 October 1915	7.8	Pleasant Valley, Nevada	5.6	62
4	21 December 1932	7.2	Cedar Mountain, Nevada	0.9[3]	61
5	30 January 1934	6.3	Excelsior Mountain, Nevada	0.1	1.5
6	12 March 1934	6.6	Hansel Valley, Utah	0.5	11.5
7	14 December 1950	5.6	Ft. Sage Mts., California	0.2	8.8
8	6 July 1954	6.8	Fallon-Stillwater, Nevada	0.3	17.7
9	24 August 1954	6.8	Fallon-Stillwater, Nevada	0.8	31
10	16 December 1954	7.2	Fairview Peak, Nevada	5.6	58
11	16 December 1954	7.1	Dixie Valley, Nevada	3.2	61

[1]From Meyers and von Hake (1976).
[2]From Slemmons (1977), except as noted.
[3]From Paul P. Orkild, personal commun., 1979.

A comparison of the data on surface faulting and on historic earthquakes (Myers and von Hake) shows that all historic earthquakes in the Great Basin larger than M.L = 6.3 (7 earthquakes) have produced surface ruptures. We believe that it is reasonable to assume that during late Quaternary time large earthquakes ($M_L \geq 7$) characteristically produced similar fault scarps.

SOURCE REGIONS

In an effort to generalize the patterns of faulting we have taken a largely heuristic approach in defining seismic source regions, modified locally where suggested by our understanding of geologic structure and history. Characteristics of the faulting within the mapped area allow delimitation of large regions (fig. 1) that are distinctive on the basis of ages of most recent movement on the faults within the region and the frequency of movement on the faults in late Quaternary time. Regions defined in this way do not carry direct implications as to the potential of any given fault within the region to undergo movement (in other words, generate an earthquake). Nor, as mentioned earlier, is it implied that all faults capable of generating earthquakes within each region are shown.

The areas thus shown define large regions within which the long-term average seismic activity has certain distinctive characteristics. The new source regions and their associated seismic characteristics form the basis for evaluating, in a probabilistic manner, seismic accelerations expected in the Salt Lake City area. These seismic source regions will also provide a basis for making a seismic acceleration map of the type prepared by Algermissen and Perkins (1976). The regions shown on figure 1 do not consider similar characteristics in areas outside the mapped area. Reconnaissance observations indicate that there may be some modification of source regions within Utah near the boundaries of the area that has been mapped thus far.

Source regions (fig 1):

1. The occurrence of faulting of Holocene age characterizes two large regions in western Utah (Ia,Ib). The largest (25,000 km^2, Ia) in west central Utah, contains 6 zones of Holocene faulting. The zones of faulting in this region are fairly regularly spaced about 50 km apart. Because of the relatively low rate of occurrence of large events the limit of the tectonic area characterized by this type of activity may be somewhat larger than the area shown by existing Holocene fault scarps. To allow for this we have arbitrarily drawn the source region boundary generally at a distance from the zones of faulting equal to their average spacing.

   The second region which contains two zones of Holocene faulting (Ib) is defined in north-central Utah. The most northerly of these includes the zone of faulting associated with the 1934 Hansel Valley earthquake. That faulting occurred along a preexisting Holocene fault scarp.

2. Two other large regions (IIa, IIb) are defined on the basis of the occurrence of late Quaternary fault scarps and the absence of Holocene fault scarps. Because of the longer period of activity involved (about 100,000 to 500,000 years) the areal extent of such scarps should more closely depict the actual tectonic unit involved than in the case of

Holocene faulting. The boundary has thus been drawn close to the outermost extent of fault scarps in the region.

An occurrence of fault offset of Holocene age within region IIb at Braffits Creek 17 km northeast of Cedar City, Utah, is described by Anderson (this volume). The relationship of that faulting, which occurs within a range block, to tectonic processes is problematical, but it is most likely associated with an aseismic style of deformation different from that producing fault scarps in most of the area.

3. Two regions (IIIa, IIIb) are defined on the basis of the absence of fault scarps in unconsolidated deposits. The time interval during which faulting has not occurred is difficult to define; geomorphic studies and better knowledge of the late Quaternary history of alluvial fan sediment will make it possible to better estimate ages of unfaulted surfaces in those regions.

4. A region restricted to a narrow band along a single fault zone (IV) is defined along the Wasatch fault zone. The region has been drawn about 10 km wide to enclose the traces of fault scarps in alluvium with straight line segments to facilitate computer modeling.

Until recently, there have been no direct determinations on the ages of the youthful appearing fault scarps along the Wasatch fault zone. However, recent work by Swan and others (1979) near Kaysville, Utah, 30 km north of Salt Lake City indicates 3 surface faulting events at the site totaling 11 m of displacement in the past 9,000 to 12,000 years. Based on radiocarbon age determinations on charcoal from sediments at the site they determined that the last two of these events occurred within the past 1,580 $\pm$ 150 years. Schwartz and others (1979) report three surface faulting events since middle Holocene time from a site at Hobble Creek near Provo.

Further to the south along the Wasatch fault zone near Mona, about 50 km south of Provo, charcoal from faulted alluvial gravels (see appendix 1) at the mouth of North Creek has been dated as 4,580 $\pm$ 250 years B.P. (U.S. Geological Survey Lab No. W-4057). The date provides a maximum age for the faulting event at the site which resulted in about 8 m of offset.

Details of the late Quaternary fault history throughout the zone are not yet known, but are the focus of research by several investigators. However, the evidence for the occurrence of Holocene faulting and locally recurrent movement in Holocene time is clear. Taken together, the continuity of the zone of fault scarps, the common occurrence of Holocene faulting, and the local evidence for recurrent movement in Holocene time serve as a basis for defining the Wasatch fault zone as a distinct seismic source region.

SEISMICITY

Evaluation of the characteristics of historic seismicity utilizes a catalog of historic data published by Hays and others (1975) that includes earthquakes occurring in Utah between 1853 and 1974. We have used that data

to prepare a seismic energy release map of western Utah (fig. 2) showing contours of numbers of equivalent magnitude 4 earthquakes. Such a map can be used to characterize the general regional pattern of historic seismic activity, but a major question in evaluating earthquake hazards expected tens or hundreds of years into the future is to what extent the observed seismicity is representative of the long-term activity of the region. An important aspect of the geologic data is that they provide a long-term basis for judging the significance of historic seismicity and the kinds of extrapolations that may be appropriate in the various seismic source regions.

For example, region IIb (figs. 1, 2) has a relatively high rate of historic seismic energy release yet lacks Holocene fault scarps. The region is characterized by numerous pre-Holocene, late Quaternary fault scarps, which shows that fault scarps can be recognized in the area and that surface faulting has characterized the tectonic style there in the past. However, there is the question of whether or not the absence of Holocene scarps indicates a long-term change in the tectonic regime and a decrease in the rate of occurrence of large magnitude events.

The fault scarp data in region IIb provide evidence for about 15 to 20 large events in an area of 24,000 km^2 in a span of time that we estimate to be about 100,000 years, equivalent to an average rate of occurrence of about one magnitude 7.0 to 7.6 earthquake per 5,000 years or about 2 events in Holocene time. The probability that 0 events would occur in Holocene time where 2 are expected is given by the Poisson probability

$$P(0/\gamma=x) = e^{-x};$$ (D. M. Perkins, oral commun., 1979).

For this case, $P(0/\gamma=2) = e^{-2} = 13.5\%$. That is, there is about a 13 percent chance of 0 scarps occurring when 2 are expected if the rate that we have determined is correct, the underlying process is constant, and the events are random in time. Note that few statisticians accept significance levels greater than 10 percent and most prefer 5 percent. We thus do not suggest that the Holocene history implies a change in the rate of occurrence of large earthquakes when compared with the late Quaternary record. We believe that the observed historic seismicity of the region IIb is consistent with strain release primarily by numerous relatively small earthquakes and comparatively infrequent large events (M = 7.0 to 7.6).

This is in contrast to region IV along the Wasatch fault zone which is poorly defined by seismic energy release (figs. 1, 2), and for which Smith and Sbar (1974) have noted a distinctly low rate of seismicity along the central Wasatch Front extending 75 km south from Salt Lake City. The character of this region appears consistent with a relatively low rate of occurrence of small earthquakes and with a dominant mode of strain release by large magnitude events.

CALCULATION OF HAZARD ON THE WASATCH FAULT

Accelerations expected from earthquakes in an area are sensitive to the seismic source regions used in most methods of calculation. Because Salt Lake City lies along the Wasatch fault zone and the source regions defined by this study differ greatly from those used for the United States hazard map of Algermissen and Perkins (1976), we have calculated accelerations expected in

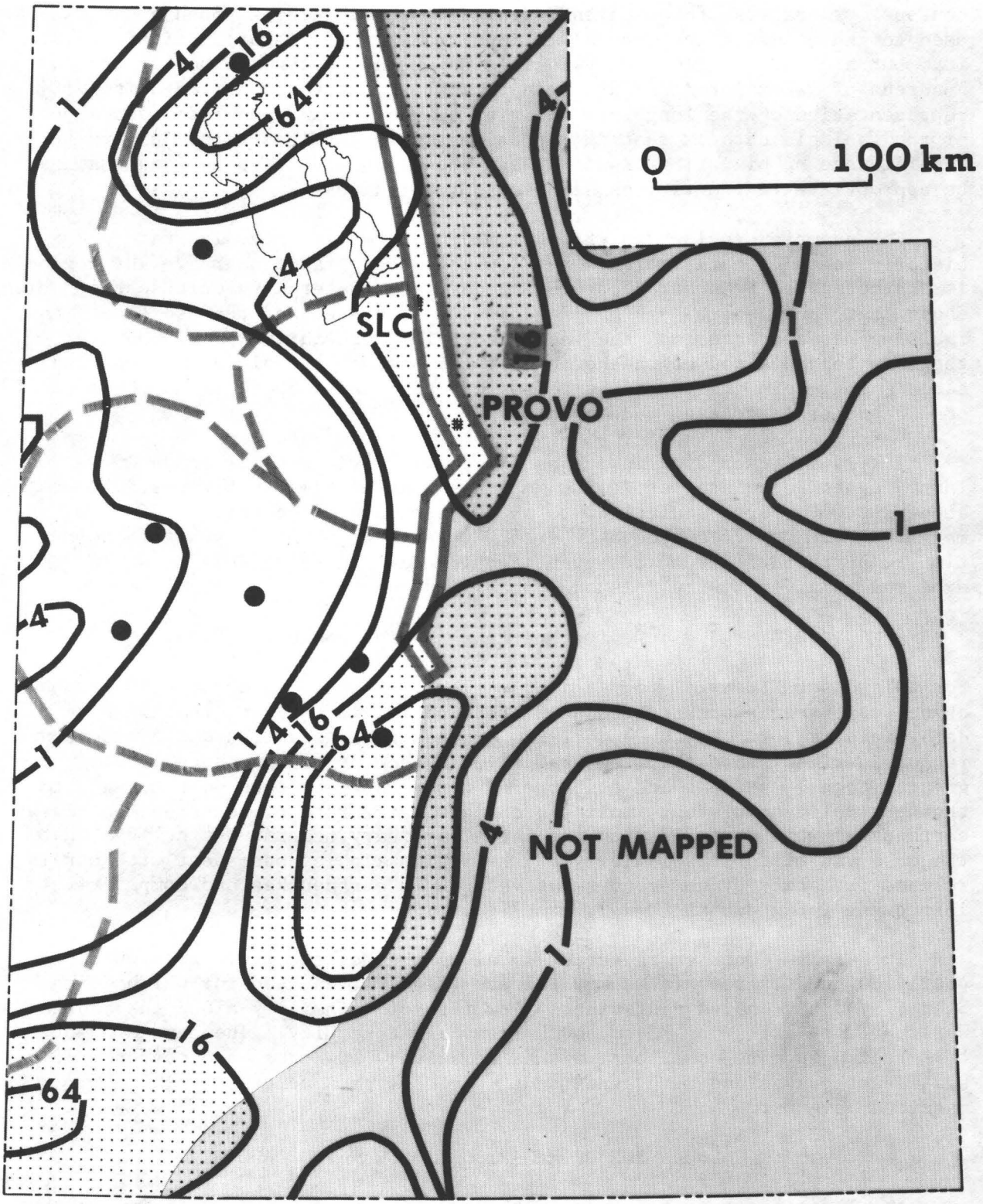

Figure 2.--Map showing contours of equivalent numbers of magnitude 4 earthquakes (heavy lines) based on historical earthquakes occurring between 1853 and 1974.

the Salt Lake area using the newly defined region IV. Note that the contributions of earthquakes in adjacent source regions have not been considered although their effect would be relatively small.

The calculation is a standard probabilistic estimate (Cornell, 1968) of maximum acceleration in rock (10 percent probability of exceedance in 50 years) along a line perpendicular to the Wasatch fault zone through Salt Lake City. A computer program developed by McGuire (1978) was used in the calculation. The input parameters were as follows:

1. The slope of the cumulative frequency curve (-.80) was derived from earlier studies (Algermissen, 1969; Algermissen and Perkins, 1976) using regional values for earthquake activity in Idaho, Utah, and Arizona. That value and consideration of earthquakes with maximum intensities from I_o = IV to I_o = VIII that have occurred since 1853 in a zone 50 km wide centered on the Wasatch fault zone define the relationship log $N_c = 3.168 - .80M$; N_c is the number of earthquakes per year of magnitude equal to or greater than M. The values imply the occurrence of a magnitude 7.0 or larger earthquake every 270 years on the average.

2. A maximum magnitude of 7.6 was assumed for the Wasatch fault zone.

3. The Wasatch fault was considered to be a line source 330 km long that breaks in segments whose lengths are determined by the relations given by Mark (1977):

   $$\log L = -1.085 + .389\ M$$
   where L = fault length in kilometers
   M = magnitude.

   Fault rupture length was used in the calculation first as mean values and, secondly, they were considered to be lognormally distributed with a standard deviation (σ) of 0.52.

4. Attenuation curves for acceleration developed by Schnabel and Seed (1973) were used in the calculations. Two cases were considered. First, the attenuation curves were used as mean curves (as published) without consideration of variability. Second, the attenuation curves were considered to be lognormally distributed with a standard deviation (σ) of 0.62. Schnabel and Seed did not publish standard deviations for their attenuation curves but we consider the standard deviation used reasonable for data of this type.

Figure 3 shows the results of the calculations. Using mean curves for attenuation and rupture length, the maximum accelerations near the fault are about 0.6 g. With parameter variability in attenuation and fault length introduced, the maximum acceleration is about 1.0. Figure 4 shows the effect on estimated acceleration of variation in the input parameters, rate and b (slope of the frequency-magnitude curve), used in McGuire's (1978) program.

The maximum accelerations estimated near the Wasatch fault are about three times those obtained by Algermissen and Perkins (1976) in the calculation of their hazard map of the United States. They modeled the seismic activity of central Utah as a relatively broad zone rather than as a single

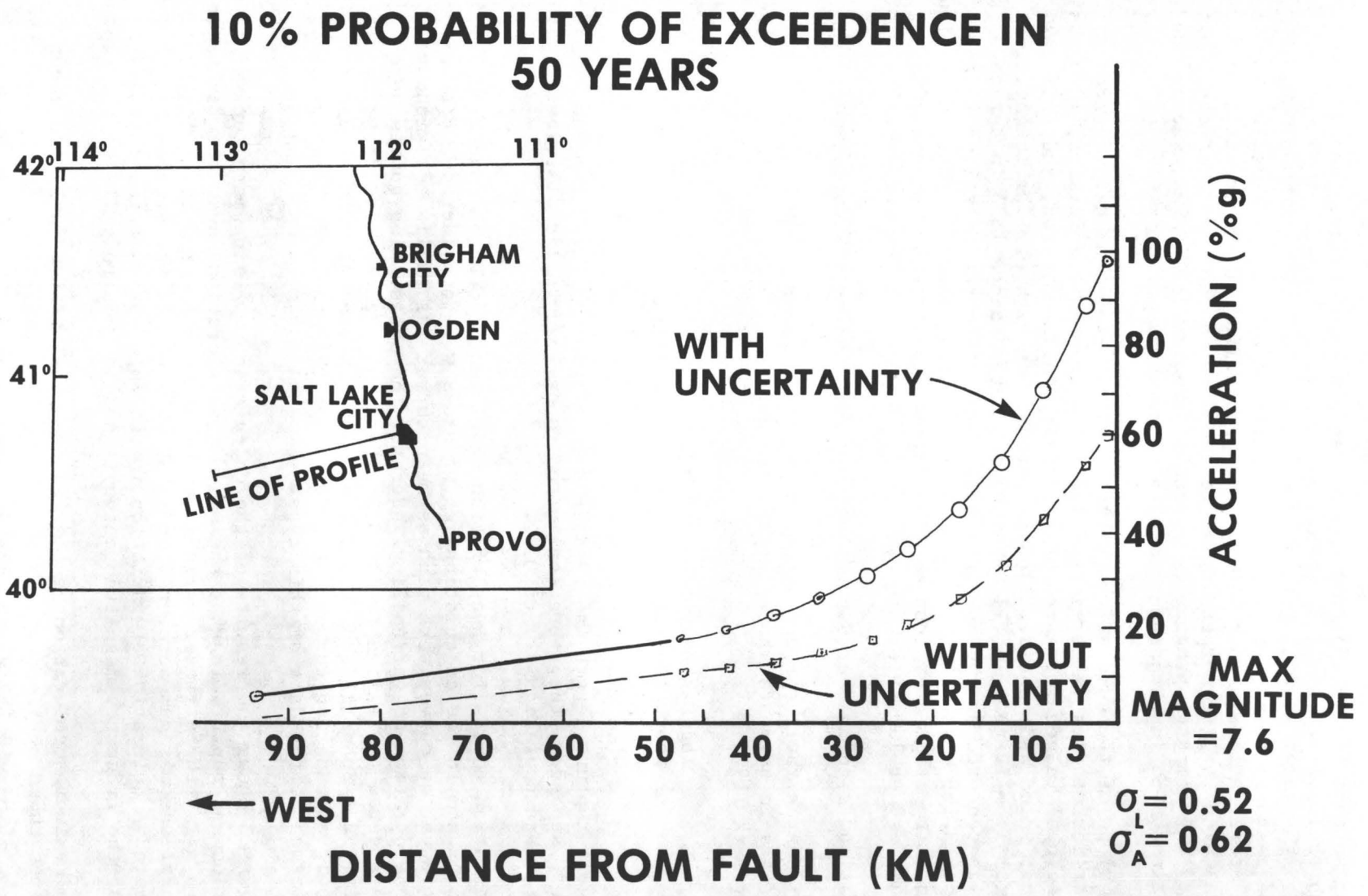

Figure 3.--Probabalistic estimates of maximum accelerations in rock with a 10 percent probability of exceedance in 50 years. σA = assumed standard deviation of attenuation date; σL = standard deviation of fault length data.

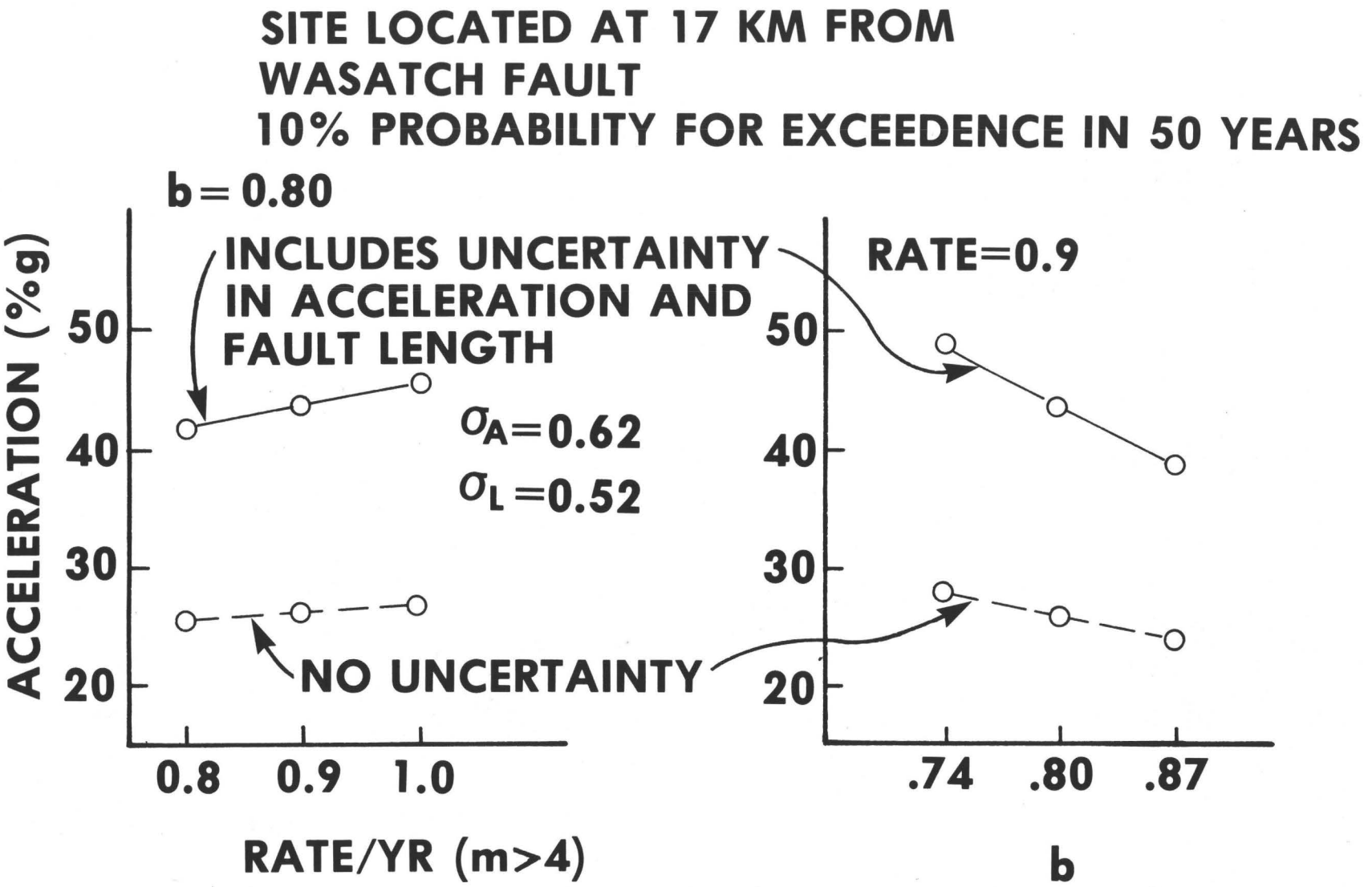

Figure 4.--Plots showing effect on estimated acceleration due to changing input values of rate and b (slope of frequency-magnitude curve).

fault or series of faults. The seismicity was thus distributed over a broader area, resulting in lower seismic activity per unit area and, consequently, smaller ground motion. It should be noted, however, that modeling of the seismicity of central Utah by concentrating the seismicity along one or, at most, a few faults would result in some areas of Utah having lower estimated ground motion and some areas having higher ground motion than those shown on the Algermissen-Perkins map. The general effect of the inclusion of parameter variability in the calculation is to raise the levels of ground motion. It should also be pointed out that the use of other proposed acceleration relationships (for example, Donovan, 1978, and McGuire, 1978) together with parameter variability in these hazard calculations results in even higher estimates of ground acceleration (2.0 to 3.0 g) close to the Wasatch fault.

REFERENCES CITED

Algermissen, S. T., 1969, Seismic risk studies in the United States: World Conference on Earthquake Engineering, 4th, Chilean Association for Seismology and Earthquake Engineering, Santiago, Chile, 1969, Proceedings; and also reprinted by U.S. Department of Commerce, ESSA, Coast and Geodetic Survey, 20 p.

Algermissen, S. T., and Perkins, D. M., 1976, A probabilistic estimate of maximum acceleration in rock in the contiguous United States: U.S. Geological Survey Open-File Report 76-416, 45 p.

Anderson, R. E., and Bucknam, R. C., 1979, Map of fault scarps on unconsolidated sediments, Richfield 1° x 2° quadrangle, Utah: U.S. Geological Survey Open-File Report 79-1236, 15 p.

Bucknam, R. C., 1977, Map of suspected fault scarps in unconsolidated deposits, Tooele 2° sheet, Utah: U.S. Geological Survey Open-File Report OF77-495.

Bucknam, R. C., and Anderson, R. E., 1979, Map of fault scarps on unconsolidated sediments, Delta 1° x 2° quadrangle, Utah: U.S. Geological Survey Open-File Report 79-366, 21 p.

Cluff, L. S., Brogan, G. E., and Glass, C. E., 1973, Wasatch fault, southern portion, earthquake fault investigation and evaluation: Woodward-Lundgren and Associates,

Cluff, L. S., Glass, C. E., and Brogan, G. E., 1974, Investigation and evaluation of the Wasatch fault north of Brigham City and Cache Valley faults, Utah and Idaho; a guide to land-use planning with recommendations for seismic safety: Woodward-Lundgren and Associates.

Cornell, C. A., 1968, Engineering seismic risk analysis: Seismological Society of America Bulletin, v. 58, no. 5, p. 1583-1606.

Donovan, N. C., and Bornstein, A. E., 1978, The problems of uncertainties in the use of seismic risk procedures: Journal of the Geotechnical Engineering Division, American Society of Civil Engineers, v. 104, no. GT7, Proceedings Paper 13896, July, p. 869-887.

Hays, W. W., Algermissen, S. T., Espinosa, A. F., Perkins, D. M., and Rinehart, W. A., 1975, Guidelines for developing design earthquake response spectra: U.S. Army Construction Engineering Research Laboratory, Technical Report M-114, 349 p.; Appendix A, Catalog of Historical U.S. Earthquakes, p. 155-314.

Mark, R. N., 1977, Application of linear statistical models of earthquake magnitude versus fault length in estimating maximum expectable earthquakes: Geology, v. 5, p. 464-466.

McGuire, R. K., 1978, FRISK: computer program for seismic risk analysis using faults as earthquake sources: U.S. Geological Survey Open-File Report 78-1007, 70 p.

Meyers, Herbert, and von Hake, C. A., 1976, Earthquake data file summary: Key to Geophysical Records Documentation No. 5, National Oceanic and Atmospheric Administration, Environmental Data Service.

Schnabel, P. B., and Seed, H. B., 1973, Accelerations in rock for earthquakes in the Western United States: Seismological Society of America Bulletin, v. 63, p. 501-516.

Schwartz, D. P., Swan, F. H., III, Hanson, K. L., Knuepfer, P. L., and Cluff, L. S., 1979, Recurrence of surface faulting and large magnitude earthquakes along the Wasatch fault zone near Provo, Utah: Geological Society of America Abstracts with Programs, v. 11, no. 6, p. 301.

Slemmons, D. B., 1977, State-of-the-art for assessing earthquake hazards in the United States; Report 6, faults and earthquake magnitude: U.S. Army Waterways Experiment Station, Miscellaneous Paper S-73-1.

Smith, R. B., and Sbar, M. L., 1974, Contemporary tectonics and seismicity of the Western United States with emphasis on the Intermountain seismic belt: Geological Society of America Bulletin, v. 85, p. 1205-1218.

Swan, F. H., III, Schwartz, D. P., Hanson, K. L., Knuepfer, P. L., and Cluff, L. S., 1979, Recurrence of surface faulting and large magnitude earthquakes along the Wasatch fault zone, Utah: Geological Society of America Abstracts with Programs, v. 11, no. 3, p. 131.

APPENDIX I

Sample information for radiocarbon dated charcoal,
U.S. Geological Survey Lab No. W-4057.

Age: 4,580 ± 250 years B.P.

Location: 6 km northeast of Mona, Juab Co., Utah at the mouth of the canyon of North Creek. (39°51.4'N., 111°48.2'W.)

Geologic environment: The site is in the face of a fault scarp that offsets alluvial gravels at the mouth of the canyon of North Creek. The layer from which the dated charcoal was taken is exposed in a nearly vertical face excavated into the fault scarp at the concrete headgate for an irrigation ditch.

The sample occurs as comminuted fragments of charcoal up to about 1 cm in diameter in a 20 cm thick lenticular layer of clay, silt gravel. The layer occurs in a sequence of fluvial gravels containing clasts to 50 cm in diameter. Boulders to 2 m in diameter associated with debris flows occur in the faulted gravels nearby.

A Feasibility Study of Earthquake Prediction Using Temporal Variations in Seismic Velocity Along the Wasatch Front from Quarry-Blast Monitoring

R. B. Smith
G. Zandt
J. E. Gaiser

Department of Geology and Geophysics
University of Utah
Salt Lake City, Utah 84112

Abstract

From October 1974 through June 1978, P-wave arrival times were measured from large quarry blasts at Kennecott's Bingham Canyon copper mine as a means of investigating possible temporal variations of seismic velocity measured across the Wasatch Front, Utah. A new technique was devised that eliminated the need for origin times and allowed accurate measurements of the velocity with an average standard deviation of ±0.10 sec on 24 stations. The velocity data revealed remarkable stability for the observation period. However, during the study no earthquakes of magnitude greater than 3.6 occurred near any ray path. Velocity anomalies at 14 stations were identified for the study, but none could be correlated with earthquake activity. An earthquake swarm near Magna, Utah, (maximum magnitude 3.3) revealed no significant anomaly. Also aftershocks (as large as magnitude 3.6) of the 1975, M=6 Pocatello Valley earthquake also produced no velocity perturbations. These results suggest that velocity variations before small earthquakes provide inadequate precursory information. However, because no large shocks greater than magnitude 3.6 occurred during the study, we cannot assess the effectiveness of the method for larger more damaging earthquakes.

Introduction

The expanded University of Utah seismograph network has operated since October, 1974, as part of a program to evaluate earthquake hazards along the Wasatch Front (see Arabasz et al., 1979a). Another objective of this program has been the identification and evaluation of possible precursory phenomena associated with earthquakes in this region. Of the many precursory phenomena identified by investigators in the United States and other countries none have been found to be universally applicable, although some prediction techniques appear to work for a restricted subset of earthquakes in certain regions (Semenov, 1969; Aggarwal, et al., 1973, 1975). One of the most widely investigated precursory phenomena is the variation of seismic velocity in the focal zone of an impending earthquake. In this paper we present results of velocity monitoring of quarry blasts as a means

of detecting temporal variations in seismic velocities along the Wasatch Front.

Large blasts from Kennecott's Bingham Canyon copper mine, located 25 km southwest of Salt Lake City, Utah, have been recorded almost daily since late 1974 on the Wasatch Front array. These data provide an opportunity to monitor on a daily to weekly basis the apparent P-wave velocities across the University of Utah, Wasatch Front seismograph network. With the application of new data reduction technique, described here, the resulting stability and resolution of the seismic velocity measurements allows the comparison of apparent velocities for almost four years.

Temporal Velocity Variations. Systematic measurements of temporal variations in seismic velocities in the Garm region of the USSR (Semenov, 1969) provided the first indications of a correlation with earthquake occurrences. Soviet seismologists measured arrival times of compressional and shear waves from clustered, small earthquakes and discovered that the ratio of the compressional to shear wave velocities, V_p/V_s, changed regularly before moderate sized earthquakes of magnitude 3 to 5. The ratio decreased about 6% to a minimum value and then returned to its normal value just about the time of the main shock.

The Soviet studies motivated similar research in other countries, especially the U.S. and Japan. Aggarwal et al. (1973, 1975) reported precursory decreases in V_p/V_s of up to 13% for earthquakes of magnitude 1 to 3 in upstate New York. At nearly the same time Whitcomb et al. (1973) reported a V_p/V_s ratio decrease before the 1971, magnitude 6.4 San Fernando earthquake and showed that the 10% reduction could be accounted for by changes in P-wave velocity.

Workers in the field of rock mechanics had been investigating the behavior of rocks under stress that might be used to model the velocity variations. The study by Brace et al. (1966) of dilatancy in crystalline rocks--"The increase of volume relative to elastic changes, caused by deformation"--focused the attention of seismologists on this effect as a possible mechanism of the observed velocity variations. Nur (1972) proposed a model to explain the velocity variations in terms of dilatancy in low-porosity rocks and fluid flow. In his model an initially saturated region dilates (fractures) prior to rupture, decreasing the degree of saturation. In the undersaturated state the rock voids fill with vapour--the total effect is to decrease V_p and hence V_p/V_s. Then pore water from the surrounding region slowly diffuses into the dilatant zone, increasing the fluid pressure and triggering the earthquake. The influx of pore water corresponds to the return of V_p/V_s to its normal value and hence was one explanation of the occurrence of an earthquake about that time.

Scholz et al. (1973) and Whitcomb et al. (1973) advanced somewhat more detailed models, but these differed only in detail from Nur's model. These authors, however, presented important empirical releationships between anomaly duration prior to the event and some indication of the size of the dilatant volume. Although the amplitude of the anomaly appears to be independent of the magnitude, the logarithm of the duration of the anomaly

scales directly with magnitude. For example, Whitcomb et al. (1973) gave an empirical relationship between magnitude (M) and anomaly time τ: $\log \tau = 0.80M - 1.92$; where τ is in days. This formula predicts anomaly durations of:

Magnitude	τ(duration)
8	80 years
7	10 years
6	2 years
5	4 months
4	20 days
3	1 day

Both studies concluded that the dilatant volume had a characteristic dimension of several times the characteristic fault dimension.

The diffusionless-dilatancy models such as proposed by Stuart (1974), Brady (1975) and Mjachkin and others (1975) do not require the flow of pore fluid into a pre-cracked dilatant region. Rather, these models call upon a sequence of opening and closing of microfractures, where the impending earthquake is postulated to occur during a period of decreasing stress and the velocity recovery is due to crack closure as the stress relaxes. Both diffusion and non-diffusion models predict velocity decreases prior to the impending shock and the models are difficult to differentiate on the basis of velocity anomalies alone. In this report we do not attempt to distinguish between either model since the precursory parameter that we seek to evaluate is the change in seismic velocity.

The successful experiments in the Garm region, New York State, and California, as well as the theoretical studies, stimulated numerous similar studies elsewhere in the U.S. and the world. Other techniques were developed to monitor temporal variations of seismic velocities. Among these were quarry-blast monitoring and teleseismic residual analysis. Although some successes were reported, many careful experiments had negative results. In particular the quarry blast experiments, which were probably the best controlled and thus the highest precision experiments, consistently resulted in negative findings.

Allen and Helmberger (1973) measured apparent P-wave velocities from large explosions at the Corona quarry and at the Eagle Mountain iron mine in southern California. They reported temporal P-wave velocity variations of less than 3.5 percent and attributed the velocity variations to instrumental and reading inaccuracies and not to changes in locations at the blast sites that varied in location from one to a few km within the quarries. McEvilly and Johnson (1974) measured P- and S-wave travel times from quarry

blasts in central California. Blast locations in their study varied about 1 km within the quarries and the authors attributed changes in observed travel times of 2.3% to reading errors and uncertainties in source times and locations. Kanamori and Hadley (1975) also used quarry blasts to measure temporal variations in average velocities in southern California. They reported that the blast location varied as much as 0.8 km within each quarry of their survey and suggested, however, that the effect of variable source location on average velocities was smaller than the observed systematic temporal velocity changes of 3%. Boore et al. (1975) reported on a study of quarry-blast monitoring for a seven-month period prior to the M_L 5.5, 1966 Parkfield earthquake. For P-waves recorded at Gold Hill, only 0.5 km from ground breakage, there were no apparent time changes.

With this history of success and failure, we thought it important to evaluate this potential prediction tool on the Wasatch Front. Fortunately, both a seismic array and frequent blasts of large size were available for the experiment.

Area of study. The quarry blasts used in this study were recorded on the Wasatch Front seismograph array (Figure 1) consisting of a 40-station telemetered, short-period network that was installed by the University of Utah beginning in mid-1974 with support from the U.S. Geological Survey, the National Science Foundation, and the State of Utah. The network has a north-south extent of 300 km, an east-west extent of 130 km, and an average station spacing of 30 km. The array is centered at Salt Lake City and covers the populated Wasatch Front as well as the Wasatch fault zone. Data are detected on 1 Hz vertical seismometers and then telemetered by radio and telephone links to the University of Utah for recording on Develocorder film. Details of the instrumentation and array parameters are given in Richins, (1979).

A general assessment of the seismicity and earthquake hazards of the Wasatch Front was given by Smith (1974) for the period 1962-1974. Arabasz et al. (1979a) provides a detailed assessment of seismicity and hazards using the new Wasatch Front array data. We summarize here the pertinent details of the seismicity as it relates to the objectives of this paper. Figure 2 shows the epicenter map of the Wasatch Front from July 1962 through June 1978. The general pattern of epicenters outlines a 200-km wide zone of earthquake activity centered on the Wasatch fault zone. Most historic activity has occurred in areas 10 km to 20 km east and west of the northern Wasatch fault, with events as large as M_L 5.2 in September, 1962, on the west side of Salt Lake City. A M_L 6.0 earthquake occurred in March 1975 at the Utah-Idaho border, and a M_L 5.7, September 1962 tremor occurred north of Logan. Prior to instrumental monitoring one M6.6 earthquake occurred in 1934 at Hansel Valley, north of the Great Salt Lake.

A rather perplexing distribution of earthquakes is evident from Figure 2 along the Wasatch Front, i.e., pronounced zones of seismic quiescence or seismic gaps extend in two zones north and south of Salt Lake City. These areas of seismic quiescence include zones of well developed

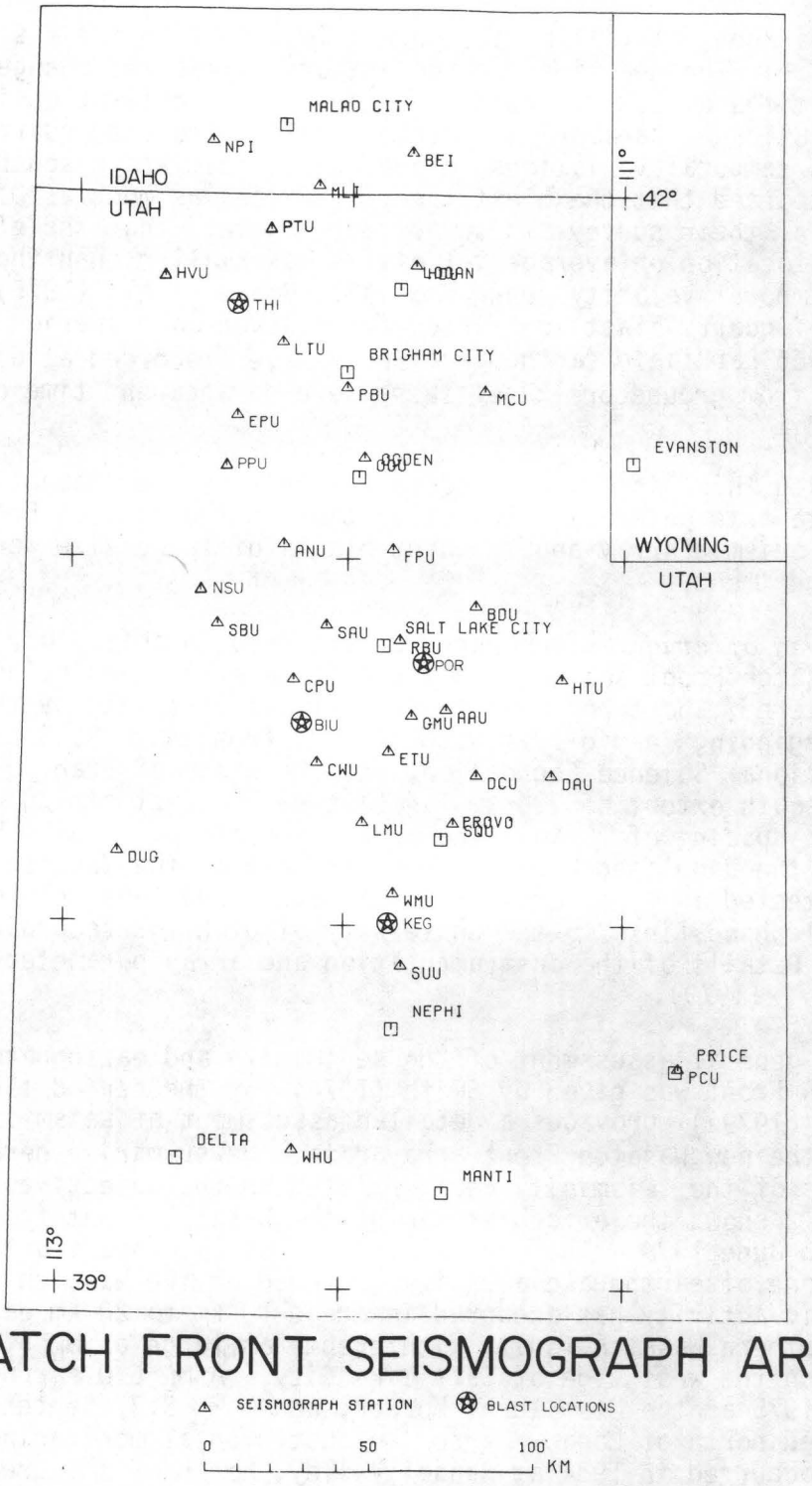

Fig. 1. Map of University of Utah Seismograph Network along the Wasatch Front showing locations of seismograph stations (triangles) and blast locations (stars). Bingham Canyon copper mine blast site is identified as BIU.

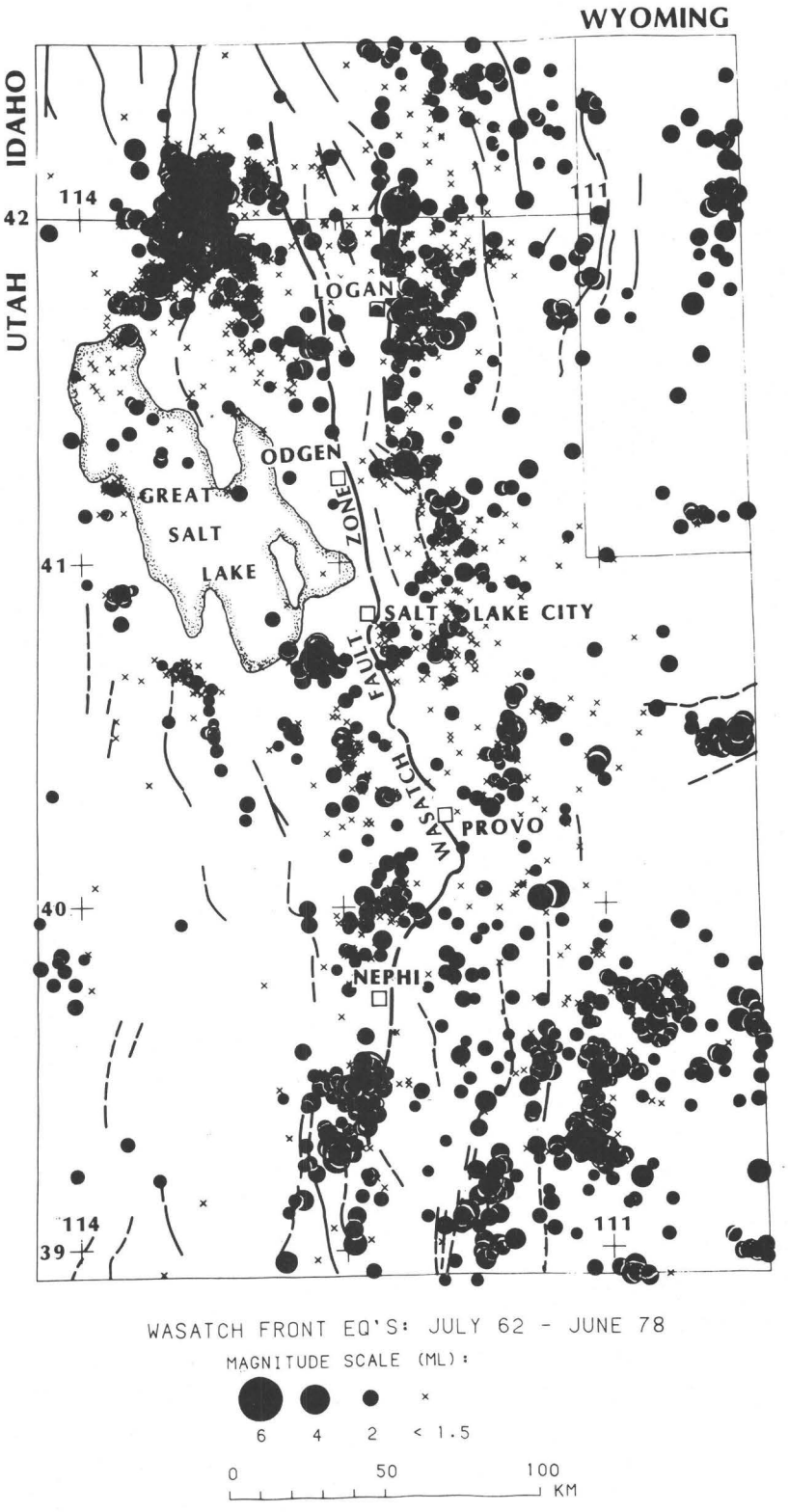

Fig. 2. Earthquake epicenter map of Wasatch Front, Utah for period 1962-June, 1978.

Quaternary faulting (Cluff et al., 1970, 1973; Swan et al., 1978) and suggest the potential for future large earthquakes. Earthquake activity persists near Salt Lake City and on the northernmost and southernmost segments of the Wasatch fault. We consider it important to evaluate crustal velocities for temporal variations in both the seismically active areas as well as within the seismic gaps as a means of evaluating the feasibility of earthquake prediction that could be implemented on the Wasatch Front.

Bingham quarry blasts. The principal source of data reported here were from large detonations of ammonium nitrate and explosive slurry (30,000 lbs to 100,000 lbs) that are detonated daily in Kennecott Copper Corporation's open-pit Bingham Canyon copper mine. These quarry blasts are used to fracture rocks for over-burden removal. Blasts are fired in several 60-foot bore holes aligned in rows parallel to bench faces. Blast delays of up to 25 millisec were sometimes used but the first P-wave arrivals, used for this study, were not adversely affected by the delays.

Seismic arrivals from the blasts were recorded on 16mm Develocorder film, recorded at 1 cm/sec that allowed timing accuracy to ±0.05 sec. Origin times were recorded at the blast site by University of Utah personnel from one to three times per week during the early stages of the project. Origin times, accurate to ±0.002 sec, were taken from primacord detonation.

The quarry blasts produced P-wave arrivals that were well recorded to distances of 300 km. The blasts have also been used as sources to calibrate epicenter determinations and for crust-mantle refraction profiles that were recorded to distances of 350 km in northern and central Utah (Braile et al., 1974; Keller et al., 1976).

Because of the large size of the Bingham Canyon mine, the blast site varied laterally within the pit as much as 3.4 km, producing variations in the travel times as much as 0.6 sec. To use these blasts for studies of temporal velocity variations, corrections were required to account for the variability in blast location.

During the early stages of the research, March 1975 through March 1976, apparent velocities were determined from inter-station travel-time differences (Estill, 1976). Stations were selected to be nearly co-linear with the azimuth of the ray path from the source along four profiles that extended radially from the Bingham Canyon mine across the Wasatch Front. However, because of variability in blast locations, the azimuths of the rays between the station locations also varied. To correct for this effect, least-squares estimates of the azimuths from various blast locations were used for each station-pair. Statistical estimates from these data showed a ±0.18 sec standard deviation unaccounted for after the variances due to the picking accuracy, and origin times were subtracted from the total variance (Estill, 1976). The unexplained variance was assumed to have been produced by variations in station-pair azimuths produced by shot-point location variations. This deviation was considered too large to confidently apply the station-pair velocity technique. Thus another technique was sought that eliminated the dependence on blast location.

Blast location correction. To demonstrate the effect in travel-times produced by variations in blast locations at the Bingham Canyon mine, a plot of maximum travel-time differences, Δt, against blast separation distance, Δx, is shown for several blasts (Figure 3). The maximum travel-time difference is 0.53 sec corresponding to a maximum blast-pair separation distance of 3.4 km and demonstrates the necessity for correcting for blast site variations.

Corrections for travel-time changes due to variations in mine blast locations were made by a method that solves for a harmonic function of travel-time change versus azimuth of a line connecting the seismograph station and the midpoint between a standard mine blast and a sample mine blast. Our definition of a standard blast was that of a large blast for which we knew the location and origin time and that produced impulsive arrivals that were recorded across the entire network. As more stations were added to the array new standard blasts were used to update the data. A sample blast is any other blast for which we want to correct the travel times to the standard blast location.

If we assume laterally homogeneous layers for the velocity model, the travel-time difference, Δt_i, between a "standard" blast and a sample blast recorded at the ith seismograph station can be derived in the following way. The arrival time of a refracted P-wave at the ith station, from the sample blast is:

$$T_{SAM} = OT_{SAM} + \frac{2z_o \cos i_o}{V_o} + \frac{X_{SAM}}{V_1} + \frac{\Delta z_s \cos i_o}{V_o} \qquad (1)$$

where T_{SAM} = travel-time of sample blast; OT_{SAM} = origin time of sample blast; T_{STD} = travel time of standard blast; and OT_{STD} = origin time of standard blast. See Figure 4 for ray path diagram. The P-wave arrival time from the standard blast is:

$$T_{STD} = OT_{STD} + \frac{2z_o \cos i_o}{V_o} + \frac{\Delta z \cos i_o}{V_o} + \frac{X_{SAM}+\Delta X}{V_1} + \frac{\Delta z_s \cos i_o}{V_o} \qquad (2)$$

Then the travel-time difference for the ith station, $\Delta t_i = T_{STD} - T_{SAM}$, is:

$$\Delta t_i = OT_{STD} - OT_{SAM} + \frac{\Delta z \cos i_o}{V_o} + \frac{\Delta X}{V_o} \qquad (3)$$

Assuming that the blast-station distance is large compared to the distance between the standard and the sample blasts (Figures 4, 5), that is, if

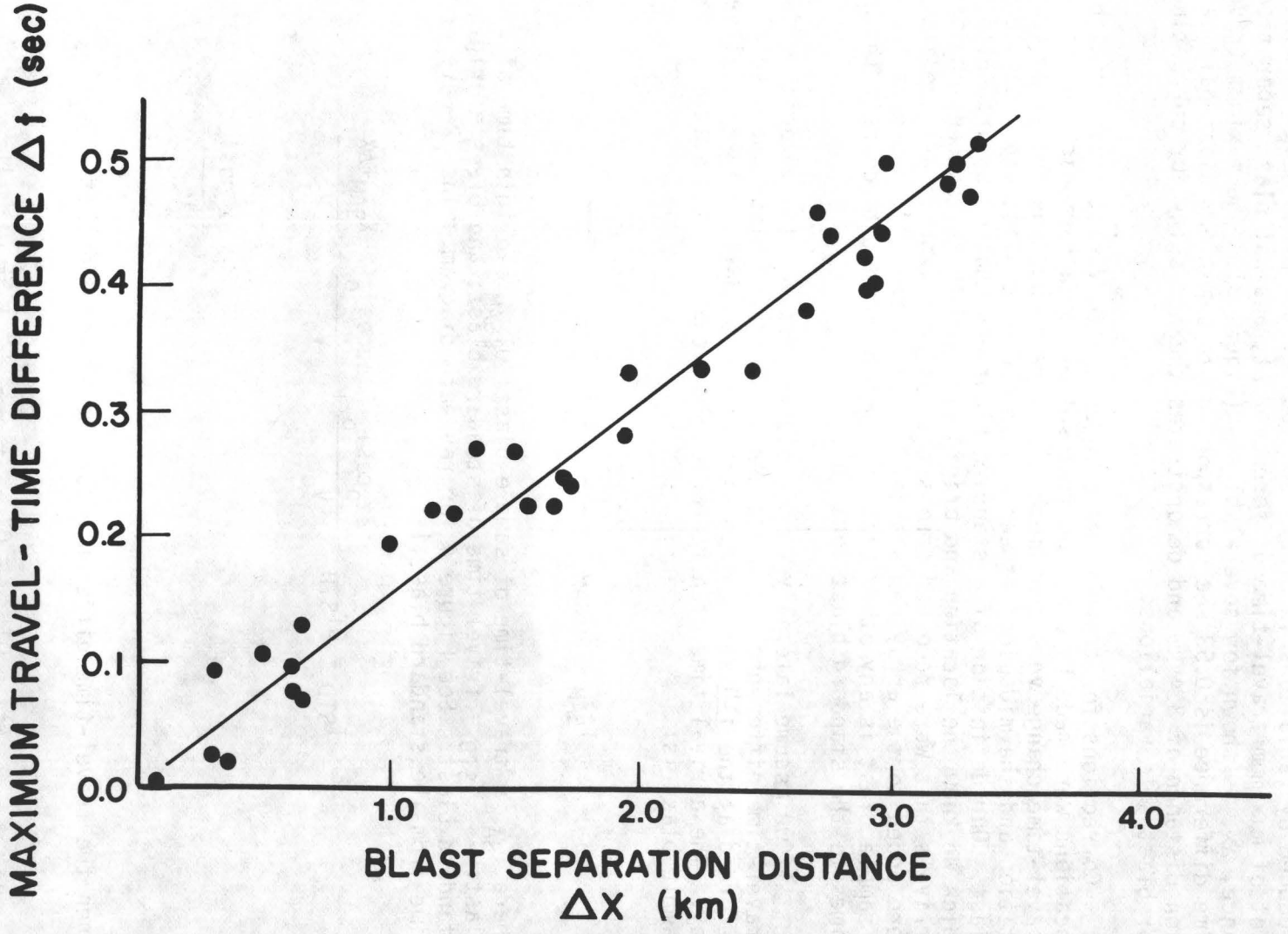

Fig. 3. Maximum travel-time differences versus blast separation distance for several blast pairs.

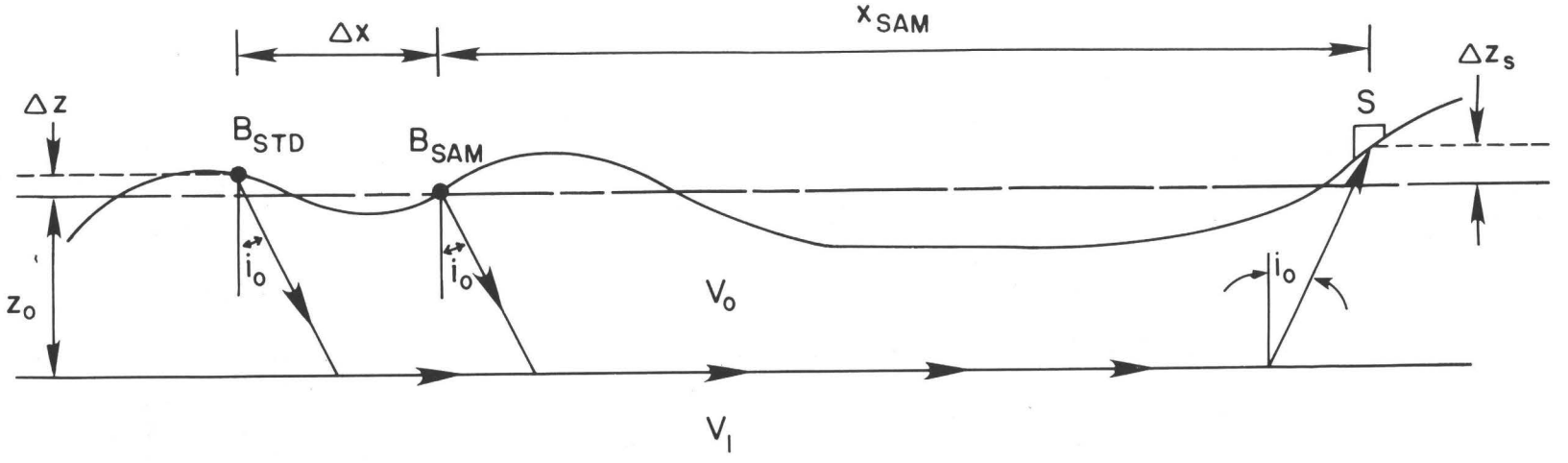

Fig. 4. Schematic diagram of ray path between Bingham Canyon copper mine, B, and seismograph stations, S, for a standard and sample blast site.

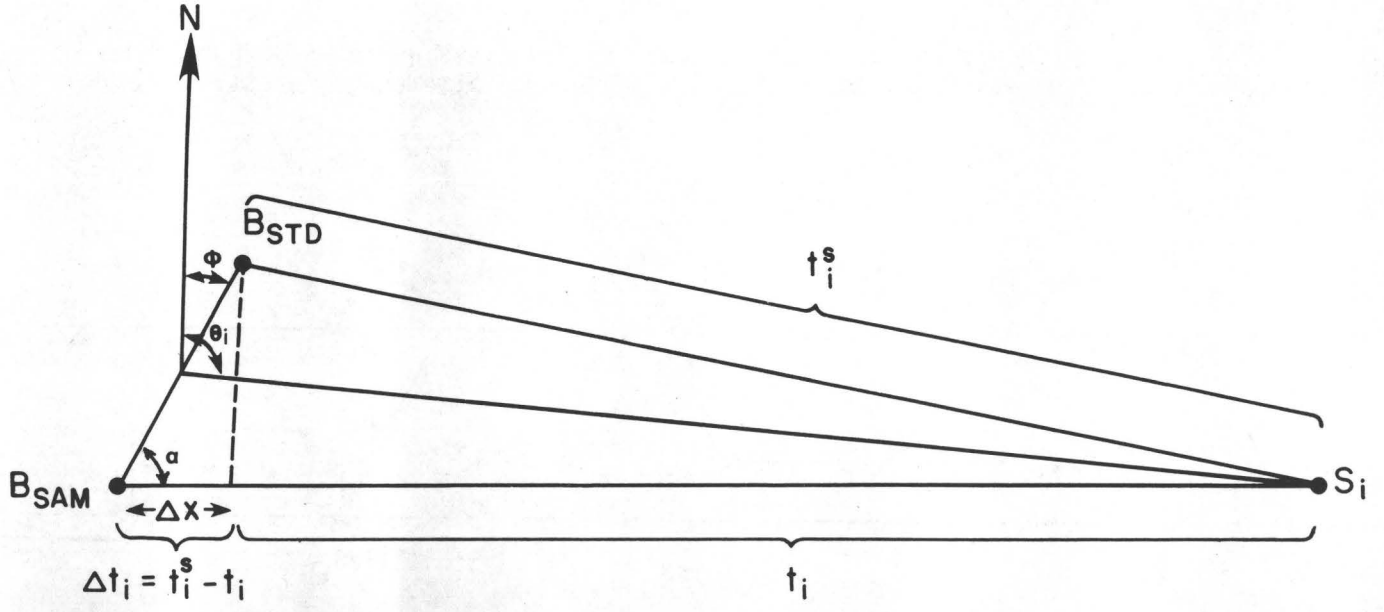

Fig. 5. Diagram illustrating the travel-time difference between a standard and sample Bingham blast for the ith station. B_{STD} = location of standard blast; B_{SAM} = location of sample blast. Other symbols defined in test.

$X_1 >> \Delta X$ then $\alpha \doteq (\theta_i - \phi)$ where ϕ is the azimuth between the standard and sample blasts. If ΔD is the distance between the standard and sample blasts (Figure 5):

$$\Delta X = \Delta D(\cos\theta_i \cos\phi + \sin\theta_i \sin\phi) \tag{4}$$

Substituting ΔX into equation (3) gives:

$$\Delta t_i = OT_{STD} - OT_{SAM} + \frac{\Delta z \cos i_o}{V_o} + \frac{\Delta D}{V_1} \cos\phi\cos\theta_i + \frac{\Delta D}{V_1} \sin\phi\sin\theta_i \tag{5}$$

Letting:

$$a_o = OT_{STD} - OT_{SAM} + \frac{\Delta z \cos i_o}{V_o} \tag{6a}$$

$$a_1 = \frac{\Delta D}{V_1} \cos\phi \tag{6b}$$

$$b_1 = \frac{\Delta D}{V_1} \sin\phi \tag{6c}$$

yields the first three terms of a Fourier series:

$$\Delta t_i = a_o + a_1 \cos\theta_i + b_1 \sin\theta_i \tag{7}$$

This expression is a harmonic function of azimuth, θ_i, and from a number of measurements of Δt_i at various azimuths, θ_i, the coefficients can be determined by the least-squares method.

When the origin time and location of sample blasts are unknown a small error remains in the azimuth determination for each station. To minimize this error the assumed location of these blasts was chosen at the center of Bingham Canyon mine. The station azimuth was specified from the midpoint of the line connecting the blast pair (Figure 5). This point is fixed for all blasts with unknown location and lies between the center of the mine and the standard blast. However, since the mine is approximately a circle, with a diameter of 3.4 km, the maximum distance the fixed point deviated from the actual point is 1/4 of the diameter or 0.85 km. For the extreme case of a sample blast located at the edge of the Bingham Canyon mine, the maximum error in the travel time due to the azimuth error is 0.05 sec for a station at 9 km from the shot, but is reduced to 0.002 sec for stations beyond 25 km.

The coefficients of equation (7) were calculated from a least-squares fit to the data. Observed travel-time differences that deviated by more than the range in picking-error, ±0.1 sec, were eliminated from the data used to solve the equations. As a result, errors in phase timing, variations due to lateral inhomogeneities, variations due to arrival of different branches, and possible premonitory travel-time variations greater than ±0.1 sec were eliminated from the standard curve fit. Thus, only systematic travel-time variations that exceeded ±0.1 sec were considered significant or anomalous in the later interpretation.

As an example, Figure 6 shows a plot of a typical station travel-time difference versus azimuth for a blast pair with known locations. Equation (7) was evaluated for this pair to give:

$$\Delta t = -0.06 + 0.52 \cos\theta - 0.01 \sin\theta. \qquad (8)$$

The dashed curve in Figure 6 corresponds to Equation (8). The vertical distances between the data points and the curve are the observed travel-time differences, Δt_i, to various seismograph stations.

Examination of Figure 6 shows that stations north of the Bingham Canyon mine have an increase in the travel-time difference of up to 0.4 seconds. Stations to the east, at 90° azimuth, indicate a near zero travel-time change and to the south, at 180° azimuth, a decrease of about -0.6 seconds. A DC-shift of -0.06 sec is primarily due to the elevation difference of 0.18 km between the two blast sites. From the other two coefficients we can calculate the angle ϕ between the two blasts and the distance factor $\frac{\Delta X}{V_1}$ from the relationships:

$$\phi = \tan^{-1}\left(\frac{b_1}{a_1}\right) \qquad (9)$$

$$\frac{\Delta X}{V_1} = a_1^2 + b_1^2 \qquad (10)$$

Using the values given above for a_1 and b_1, the angle ϕ is equal to -1.1° and $\frac{\Delta X}{V_1}$ is equal to 0.52 sec. Using V_1 = 6.3 km/sec gives a value for ΔX = 3.3 km. The actual values for this blast pair are ϕ = 6° and ΔX = 3.4 km. The resulting error in location of approximately ±0.2 km contributes to the scatter of an apparent velocity time plot but that scatter is now reduced four times compared to the uncorrected data.

Once the coefficients in Equation (7) are determined, the travel times from any given sample blast are corrected to the location of a standard blast. Figure 6 illustrates how the corrections are determined from the ith seismograph station. If t_i is the travel time of the sample blast and t_i^s is the travel time of the standard blast (Figure 6), then the observed travel time difference, Δt_i, is:

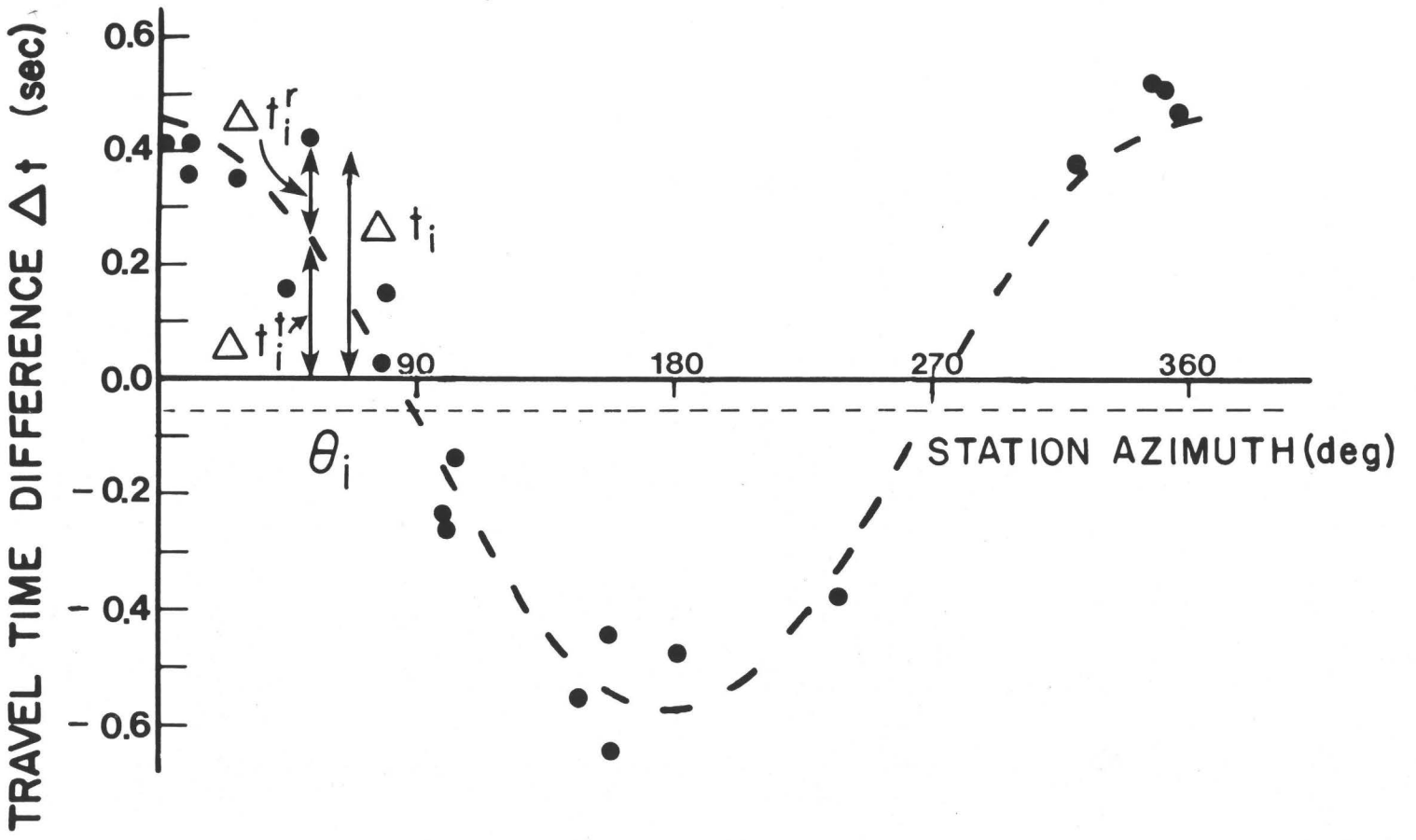

Fig. 6. Plot of travel-time differences versus station azimuth for blasts recorded on September 23 and 29, 1976. Symbols are explained in text.

$$\Delta t_i = t_i^s - t_i \tag{11}$$

The theoretical travel-time difference, Δt_i^t, at the ith seismograph station is the value defined by the harmonic function at θ_i. The corrected travel time, t_i^c, is then:

$$t_i^c = t_i + \Delta t_i^t \tag{12}$$

$$t_i^c = t_i^s - \Delta t_i + \Delta t_i^t \tag{13}$$

$$= t_i^s - \Delta t_i^r \tag{14}$$

where, $\Delta t_i^r = \Delta t_i + \Delta t_i^t$, is the travel time perturbation between the standard and sample blast with the effect of blast location removed. Note that the term Δt_i^r is independent of the mean level, a_o, of the harmonic function. Also note that the residual term is independent of the origin times and the elevation difference of the standard and sample blasts. Thus, the calculation of the corrected travel time requires no knowledge of the origin time or exact location of the sample blast.

Given a number of sample blasts, we can accumulate a suite of corrected travel times, t_{ij}^c, where the j subscript refers to the jth sample blast. For the ith station the standard travel time, t_i^s, is subtracted from the data to give the travel time perturbation:

$$-\Delta t_{ij}^r = t_{ij}^c - t_i^s \tag{15}$$

$$= \Delta t_{ij}^t = \Delta t_{ij} \tag{16}$$

This parameter is plotted for blasts, j = 1, 2, ..., N, as a function of time. This calculation, Equation (16), is the basis of our travel-time-difference monitoring, and significant time variations in this parameter, $-\Delta t_{ij}^r$, reflect temporal variations in velocity along the ray path between Bingham mine and the ith seismograph station.

The travel time data can also be converted to apparent velocities by:

$$V_{ij}^c = \frac{X_i^s}{t_{ij}^c} \tag{17}$$

Apparent velocity perturbations, ΔV_{ij}^r, are obtained by subtracting the time average of a sequence of apparent velocities:

$$\Delta V^{r}_{ij} = V^{c}_{ij} - \overline{V}_{i} \tag{18}$$

where

$$\overline{V}_{i} = \frac{1}{N}\sum_{j=1}^{N} V^{c}_{ij} \tag{19}$$

Equation (18) gives the apparent velocity perturbation that is also plotted as a function of time.

There are important advantages in using the location-corrected method described above instead of the absolute travel time or the inter-station travel time method. Most important, it significanly reduces the standard error of calculated travel-time from the mine blasts. The standard deviations of absolute travel times is ±0.2 sec. For travel-time differences between station pairs it is ±0.13 sec; whereas the standard deviation of the corrected travel time is ±0.07 sec. Another advantage of the method is that it enables us to greatly increase the number of blast recordings without on-site recording of the origin time and location of their respective blasts.

A few disadvantages are associated with this method. An array-wide anomalous velocity cannot be detected because it would be absorbed in the a_0 coefficient of the harmonic function. But because the Wasatch Front array is so large, an anomaly of that size is considered very unlikely. Also, the method requires a relatively even azimuthal distribution of stations. Although weighted to the eastern azimuths, our station-azimuth distribution from the Bingham Mine is adequate to obtain good fits to the harmonic function.

Before proceeding with the presentation of the results, the basic assumptions of the location-correction method used to reduce the data are summarized: (1) lateral heterogeneity does not contribute significantly to the scatter in the travel time data, (2) the same refracted arrivals (P_g) are used to find the coefficients of the harmonic function, and (3) the results are independent of the choice of a specific standard blast.

Results

The results presented here are derived from systematic blast monitoring and analyses from October 30, 1974, to June 30, 1978. The data for the period October 1974 to March 1976 were collected by Estill (1976); those from April 1976 to March 1977 by Gaiser (1977). Three standard blasts were used to reprocess the entire data set with the blast-location-correction method outlined above.

Standard Blasts

Date	Origin time (GMT)	Lat.	Long.	Pounds of explosive
9 Dec. 1977	21:51:29.870	40°30.75'	112°08.75'	75,000
29 June 1978	20:50:06.643	40°30.65'	112°09.30'	120,000
16 Aug. 1978	21:15:31.153	40°31.70'	112°08.10'	65,000

Corrected travel times and apparent velocities were computed for 24 stations of the Wasatch Front array (see Figure 1). For each station the average travel time and apparent velocity, and the standard deviation for these parameters are listed in Table 1. All data are from profiles between the Bingham Canyon mine (BIU) and the respective seismograph stations.

The most notable feature of the data is the remarkable stability of the measurements over the entire period of observation. The average standard deviation of the travel times is 0.10 sec with extremes of 0.06 sec at PTU and 0.31 sec at MCU. Station MCU had the only travel-time standard deviation significantly larger than the timing precision; the next largest standard deviation was only 0.14 sec at LTU and RBU. Time plots of both the travel times and apparent velocities have been produced for all 24 stations; only six stations were selected for presentation. These plots for profiles shown in Figure 7 are reproduced as Figures 8, 9, and 10. The temporal stability of these parameters is evident except for the occasional one-point excursion explained by random picking errors.

Systematic trends are present on the plots of some stations. For example, the travel times to station SQU exhibit periods of stability, alternating with periods of relatively large scatter. This effect is probably due to fluctuations in station performance. Factors such as weather, telemetry problems, and electronic failures can cause the noise level of a particular station to increase appreciably. During these times, the timing of the first arrival becomes increasingly difficult resulting in greater scatter in the data.

Plots for some stations (MCU, LTU, and RBU) had more scatter than most stations during the entire period. Stations MCU and LTU are located near the crossover distance for the P_g, P_n branches. Consequently the timing of the first arrival is very sensitive to changes in noise level. Other stations such as RBU are located in areas of high background noise resulting in degraded timing precision.

Characterization of anomalies. Initially we examined the travel time and apparent velocity plots to identify "anomalous" periods without regard to any specific causal mechanisms such as earthquakes. We use the term "anomaly" to signify a period during which a parameter behaves differently from the average. This can include changes in the mean, or variations in the data scatter. To characterize an "anomalous" period of duration τ, the following criteria were considered:

TABLE 1

STATION	TIME PERIOD (Dates in Julian Days)	NOBS*	TT ± SD† (secs)	AV ± SD†† (km/secs)
		n	$\sum_{i=1}^{n} TT_i/n \pm \sigma_i$	
1. ANU	75-326 to 78-180	134	10.44 ± .13	5.66 ± .07
2. BDU	74-343 to 78-180	180	12.53 ± .13	5.28 ± .05
3. BEI	74-303 to 78-180	214	30.12 ± .09	6.01 ± .02
4. CPU	74-332 to 78-180	237	3.72 ± .09	4.92 ± .13
5. CWU	74-303 to 78-180	197	2.24 ± .10	4.28 ± .16
6. DAU	74-330 to 78-170	222	14.19 ± .13	5.32 ± .05
7. DCU	74-330 to 78-180	236	9.94 ± .08	5.34 ± .04
8. ETU	74-304 to 78-170	215	5.57 ± .06	4.53 ± .05
9. FPU	75-165 to 78-180	326	11.43 ± .08	5.53 ± .04
10. GMU	74-303 to 78-180	223	6.54 ± .09	5.19 ± .07
11. HDU	75-055 to 78-180	180	25.46 ± .12	5.78 ± .03
12. HTU	75-009 to 78-165	167	15.09 ± .08	5.38 ± .03
13. LMU	74-306 to 78-115	217	6.29 ± .07	4.93 ± .06
14. LTU	74-305 to 78-180	237	20.98 ± .14	5.73 ± .04
15. MCU	75-017 to 78-180	181	21.05 ± .31	5.64 ± .08
16. MLI	74-315 to 78-180	277	27.86 ± .07	6.04 ± .02
17. NPI	75-121 to 78-180	231	29.90 ± .10	6.16 ± .02
18. PBU	75-269 to 78-180	88	18.74 ± .09	5.71 ± .03
19. PTU	76-353 to 78-180	79	26.49 ± .06	5.97 ± .01
20. RBU	74-330 to 78-180	156	8.04 ± .14	5.21 ± .09
21. SAU	75-040 to 78-180	155	6.79 ± .07	5.15 ± .06
22. SQU	74-347 to 78-170	181	9.63 ± .08	5.42 ± .05
23. SUU	74-306 to 78-180	235	13.71 ± .09	5.51 ± .04
24. WMU	74-303 to 77-347	147	10.27 ± .08	5.31 ± .04

*NOBS = No. of observations
†TT±SD = travel time ± standard deviation
††AV ± SD = apparent velocity ± standard deviation

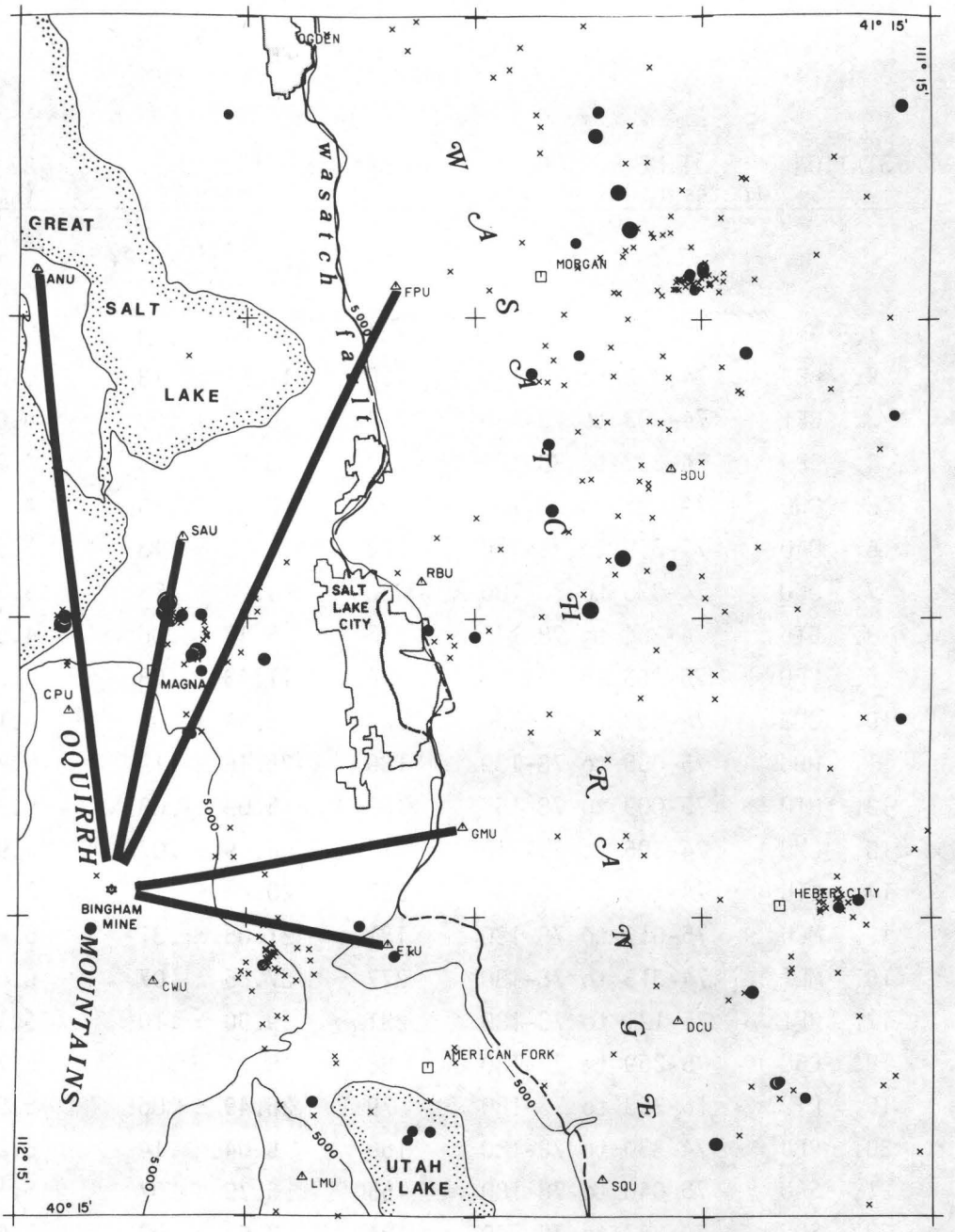

Fig. 7. Detailed epicenter map of central Wasatch Front showing locations of profiles (dark lines) and stations used for travel-time and velocity calculations.

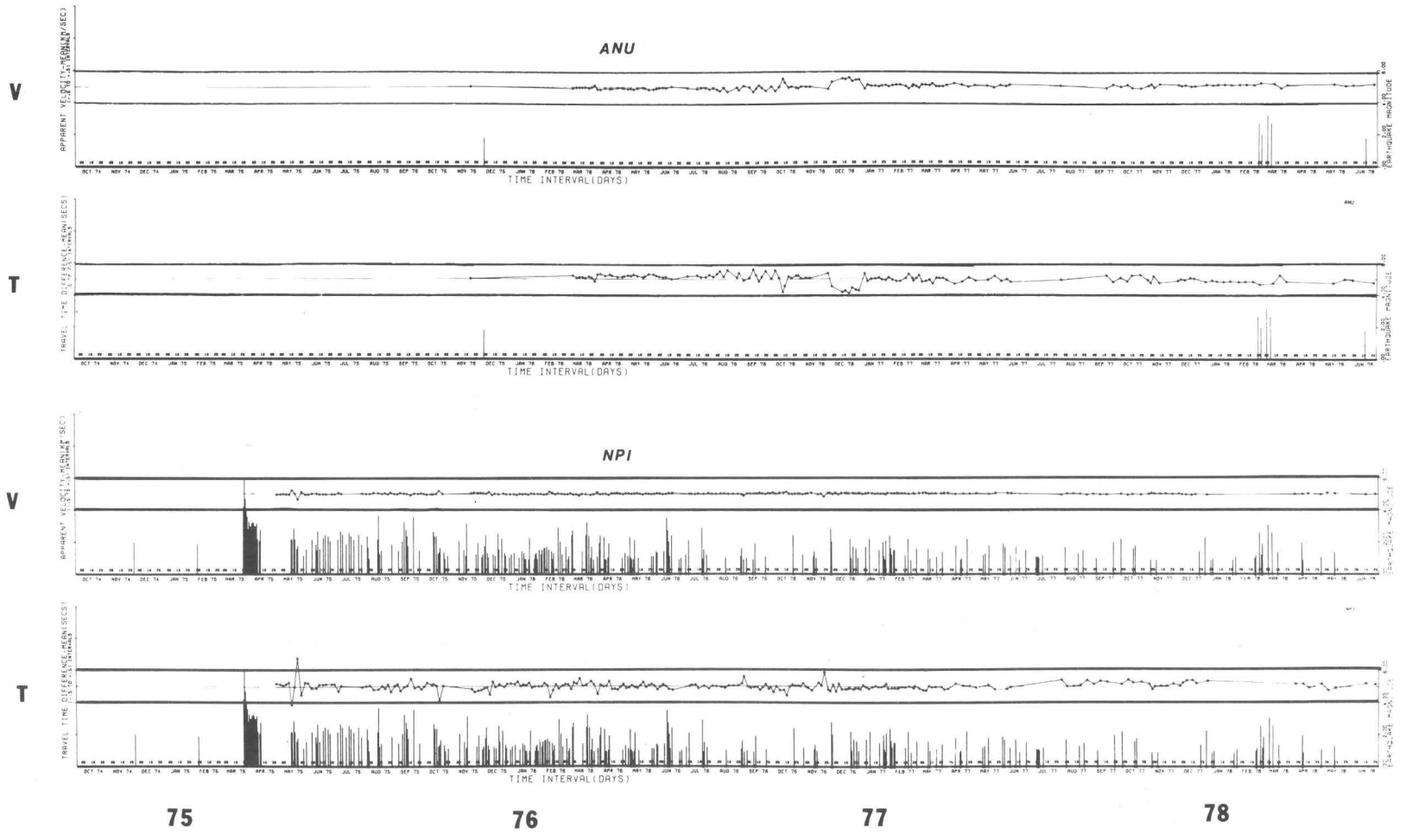

Fig. 8. Plot of apparent velocity, $\overline{V}$, and travel time differences, Δt_r, versus time for profiles from Bingham Canyon mine to stations ANU and NPI. Earthquakes that occurred within 10 km of the profile are shown by vertical bars corresponding to M_L.

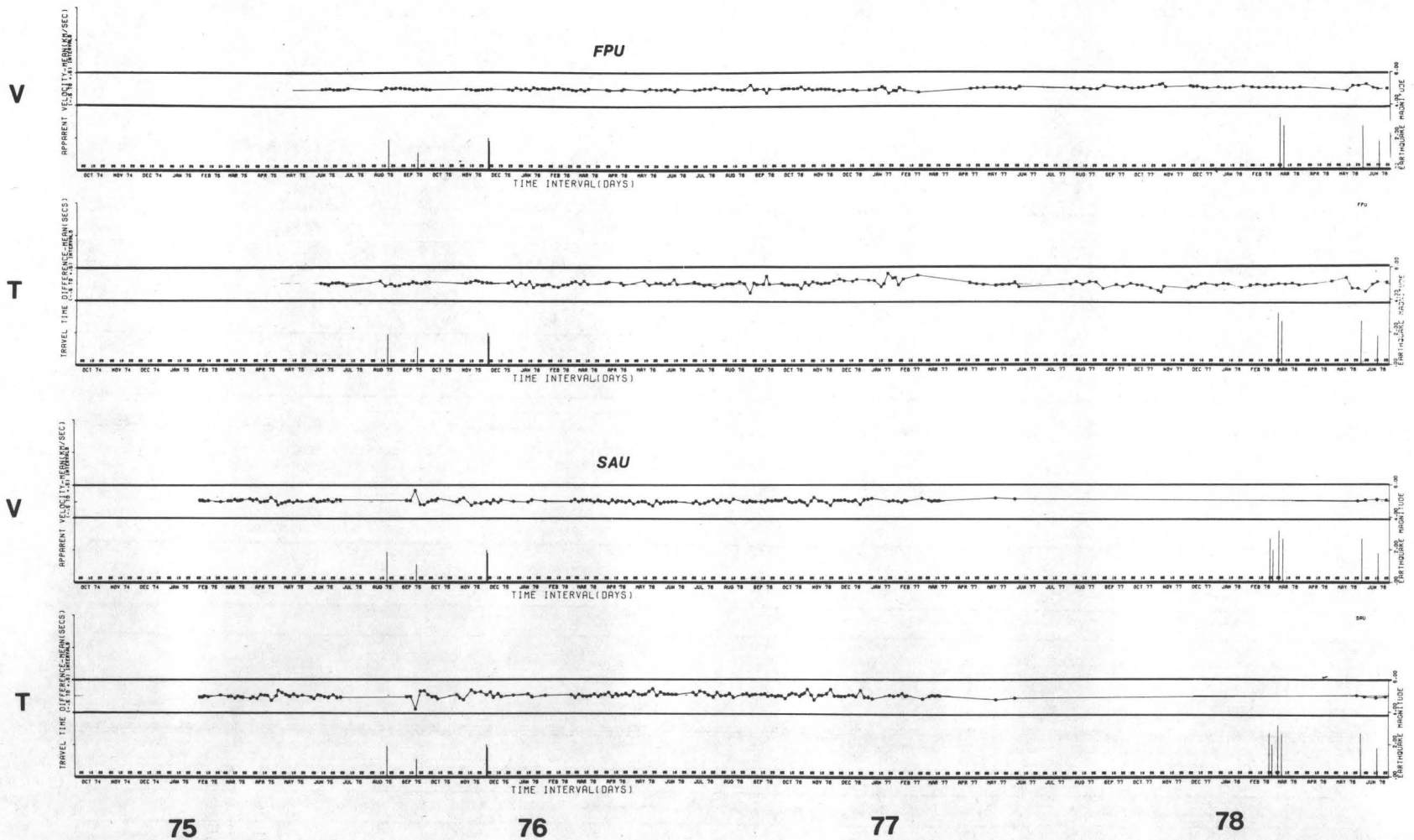

Fig. 9. Plot of apparent velocity, $\overline{V}$, and travel time differences, Δt_r, versus time for profiles from Bingham Canyon mine to stations FPU and SAU. Earthquakes that occurred within 10 km of the profile are shown by vertical bars corresponding to M_L.

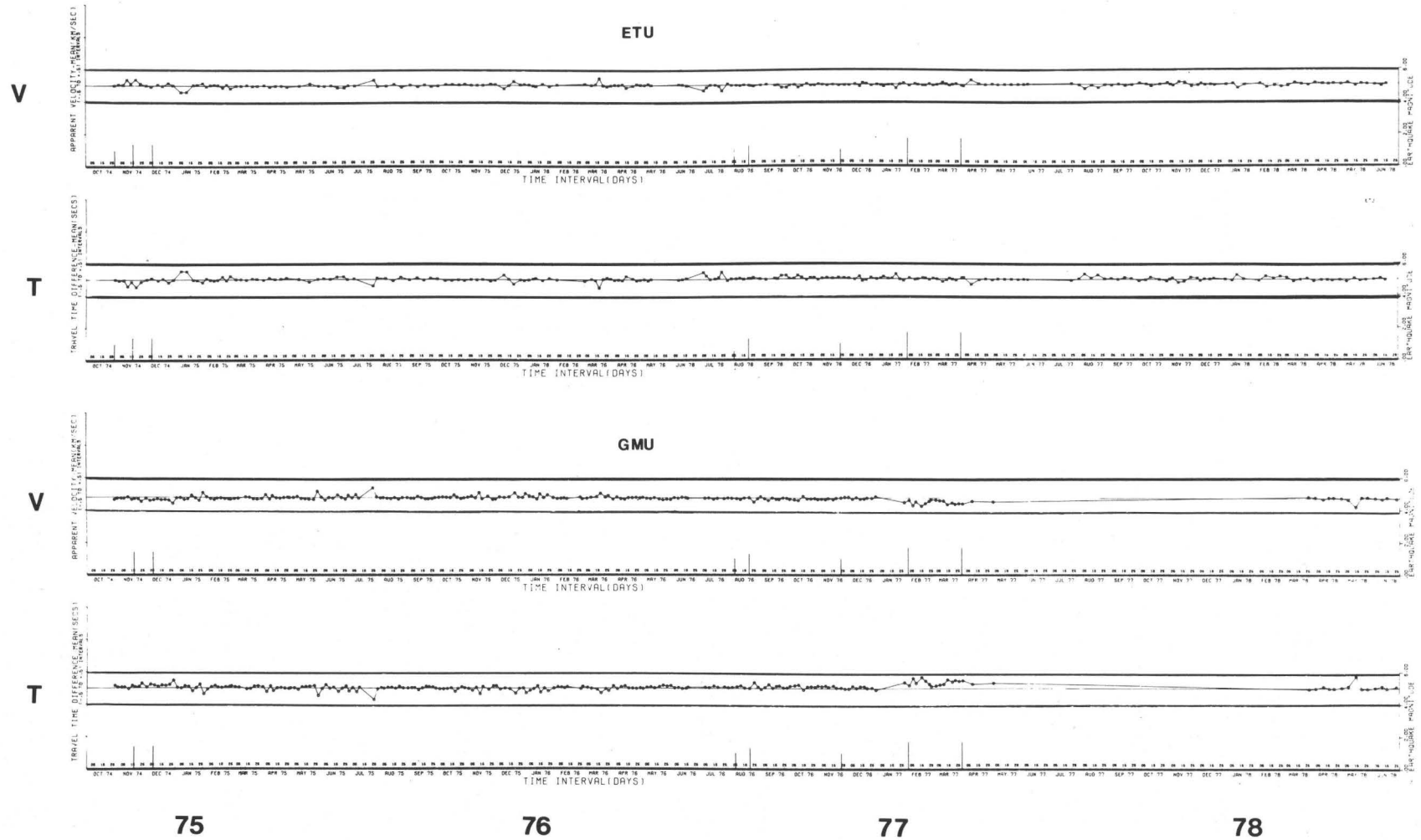

Fig. 10. Plot of apparent velocity, $\overline{V}$, and travel time differences, Δt_r, versus time for profiles from Bingham Canyon mine to stations ETU and GMU. Earthquakes that occurred within 10 km of the profile are shown by vertical vars corresponding to M_L.

1) data variance, σ^2, that defines the minimum amplitude of a detectable anomaly;

2) interval of data sampling which limits the minimum length of a detectable anomaly;

3) the number of data within the anomalous period, $N(\tau)$, that is a measure of confidence in the reality of an anomaly;

4) the amplitude of the anomaly, $A(\tau)$, that is a measure of confidence;

5) the smoothness of an anomaly measured by the variance of the data within the anomalous period, $S(\tau)$, that is an additional confidence factor; and

6) all possible artificial causes.

For all the data (24 stations), the average variance is 0.01 sec^2. Factors contributing to this value include timing errors, blast location correction errors, and temporal variations in velocity, if present. Therefore, in our usage, an anomaly must have a significantly greater amplitude, greater than or equal to 2σ or 0.2 sec to be recognized. However, the data variance changes with time in response to fluctuations of station performance. Hence, the minimum detectable anomaly amplitude is in reality a time-varying function of all the factors contributing to the noise level of the data.

The interval of data sampling is another time-varying parameter. In the early stages of the project, arrival times were picked once every day to every other day. Origin times and blast locations were recorded for many of these blasts while the development and testing of the blast location correction technique was in progress. Analysis of the early data by Estill (1976) and Gaiser (1977) revealed no significant anomalies correlated with earthquakes with magnitude up to 3.5.

In 1977, the blast analysis was reduced to about once a week. For uniformity the early data were windowed to attain approximately the same sampling interval throughout the entire set. Then the two data sets were combined and used to compile the statistics in Table 1 and the plots in Figures 8, 9, and 10. Thus, the average minimum length of an anomaly detectable with the data set described here is about 5 to 10 days.

The above two considerations established amplitude and duration limits on the minimum resolvable anomaly. With these minimum considerations alone, however, many perturbations in the data could qualify as anomalies. A combination of three additional parameters aids in further constraining the sub-set of plausible anomalies. The confidence level increases with both greater number of data, $N(\tau)$, within the anomaly, and with greater amplitude, $A(\tau)$, of the anomaly. On the other hand, a large scatter in the data (within the anomaly) as measured by $S(\tau)$ decreases the confidence level. The latter relationship is based on the assumption that any

velocity changes associated with a natural phenomena, such as an earthquake, will occur in a smoothly varying manner. Finally, even those anomalies with a high confidence level must be evaluated for evidence of any possible artificial causes. These include effects such as changes in station performance, changes in instrument magnification, and inter-station cross-talk. Examples of the application of these criteria to the Bingham blast data are discussed next.

Anomalies. An initial examination of the travel time and apparent velocity plots has revealed "anomalies" for 14 of the 24 stations (see Table 2). These anomalies consisted primarily of two types: bay-shaped excursions of relatively short duration (10-60 days); and long-term (3-12 months) small-amplitude changes in the mean. No large-amplitude, long-duration anomalies were recognized.

Analysis of the anomalies using the format discussed above revealed few anomalies with a high confidence level. Most of the short-duration changes were defined by only two or three observations and had amplitudes of only one standard deviation from the mean. The random occurrences and small amplitudes of these "anomalies" suggest picking errors as their primary source. A few of these anomalies, however, have amplitudes significantly larger than the standard deviation and are discussed later. The long-term changes in mean are defined by many data points, but low amplitudes can reduce the confidence level. If these long-term changes are due to artificial causes there must be a systematic effect, such as long term variations in station performance.

The largest anomaly revealed in this study occurred during the period December 16, 1976, to January 3, 1977, on station ANU (Figure 8). The bay-like negative travel-time anomaly lasted approximately 18 days during which the travel time was 0.45s ±.09 less than the mean--a 4.5% decrease. The data for the previous month, November 1976, had a standard deviation of ±0.11 sec, and for the following month, January 1977, the standard deviation was ±0.07 sec. Thus the anomaly amplitude was 4 to 7 times greater than the data scatter. The plots for station ANU also exhibited long-term variations. For example, during a 7-month period in late 1975 and early 1976 the travel time average was 10.50 ±0.07 sec; during the following 4 months the average did not change but the scatter increased greatly (mean = 10.51 ±0.18 sec). In 1977 the mean changed to 10.42 ±0.08 sec and in 5 months of 1978 the average decreased further to 10.36 ±0.06 sec.

These and other significant anomalies found for stations FPU and GMU are summarized in Table 2. The anomaly for station GMU began with an abrupt increase in the travel time average of 0.10 sec on January 2, 1977. In the previous three months the mean travel time was 6.55 ±0.05 sec, hence the 1.5% increase is equivalent to about two standard deviations. The increased mean was maintained for three months until the station failed at the end of March 1977. We interpret this anomaly as due to an artificial cause. In January 1977 there was a significant decrease in the magnification of the recorded signal at GMU. Hence, the amplitude of the first P-arrival from Bingham blasts decreased to the noise level which led to consistently late picks.

TABLE 2

Table of Anomalies
(referred to travel times)

1. ANU

   i) 16 Dec. 76 - 03 Jan. 77:
   τ~18d; A(τ)~-.45s; N(τ) = 10; S(τ)~.09s.
   Preceded by large scatter; followed by small scatter.

   ii) Long-term variations in mean (m) travel time.
   22 Nov. 75 - 11 June 76 : N = 65 m = 10.50 ± .07s
   12 June 76 - 23 Oct. 76 : N = 41 m = 10.51 ± .18s
   24 Feb. 77 - 16 Nov. 77 : N = 49 m = 10.42 ± .08s
   4 Jan. 78 - 30 May 78 : N = 19 m = 10.36 ± .06s

2. BDU

   i) Long-term variations in mean.
   Aug. 76 - Apr. 77 : ~ within std. dev. below mean.
   May 77 - June 78 : ~ within std. dev. above mean.

3. BEI

   - No Anomalies.

4. CPU

   i) 1975 : Series of 4 dips of -2, -3 std. dev. with 2, 3 pts. each; short durations.

5. CWU

   i) May 75:
   τ~10d; A(τ)~-.2s; N(τ) = 3.

   ii) Aug. 75:
   τ~10d; A(τ)~ .2s; N(τ) = 3.

6. DAU

   i) Long-term variations:
   Aug. 76 - Feb. 77 : within std. dev. but predominantly below mean.

7. DCU

   - No Anomalies

TABLE 2 (continued)

8. ETU

   - No Anomalies.

9. FPU

   i) Nov. 76 - Jan. 77:
   τ~2 mos.; A(τ)~.1s; N(τ) - 7.

   ii) Jan. 77 - Feb. 77:
   τ~15d; A(τ)~.2-.3s; N(τ) = 3.

   iii) Oct. 77 - Dec. 77:
   τ~2 mos.; A(τ)~-.1s; N(τ) = 7.

   iv) June 78:
   τ~1-1½ mos.; A(τ)~-.3s; N(τ) = 4.

10. GMU

   i) 02 Jan. 77 - 30 Mar. 77:
   τ~3 mos.; A(τ)~.1s; N(τ) = 37, S(τ) = .08s.
   followed by a long down period.

11. HDU

   i) Nov. 76 - Dec. 76:
   τ~20d; A(τ)~-.1s; N(τ) = 5.

   ii) May 78 - June 78:
   τ~10d; A(τ)~.1s; N(τ) = 3.

12. HTU

   i) Sept. 77 - June 78: within std. dev. below mean.

13. LMU

   i) Sept. 75 - Mar. 76: cyclic variations
   τ~15-20d; A(τ)~.1s; N(τ) = 47.

14. LTU

   - Large scatter; No anomalies.

15. MCU

   i) Nov. 76 - Mar. 77:
   All points above mean and scatter much reduced from normal.

TABLE 2 (continued)

16. MLI

- No Anomalies.

17. NPI

i) Aug. 77 - Oct. 77:
τ~2 mos.; A(τ)~.1, .2s; N(τ) = 8.

18. PBU

i) July 76:
τ = 20d; A(τ)~.3, .4s
isolated between two long down periods.

19. PTU

- No Anomalies.

20. RBU

- Large scatter; No Anomalies.

21. SAU

- No Anomalies.

22. SQU

- No Anomalies.

23. SUU

i) Apr. 76:
τ~1 mo.; A(τ)~-.1s, -.2s; N(τ) = 5.

24. WMU

- No Anomalies.

Correlation with earthquakes. The principal objective of this project has been the evaluation of temporal velocity variations with earthquake occurrence as a feasibility study of monitoring possible earthquake precursors. For this purpose Figures 8, 9, and 10 include a time plot of earthquake occurrences that occurred within 10 km either side of the ray path from Bingham Mine to the particular seismograph station. The height of the vertical bar representing the earthquake is proportional to the magnitude of the event.

The spatial pattern of the seismicity of the central Wasatch Front, for the period 1974-1978, is depicted in Figure 7. Also shown in the figure are five of the six profiles corresponding to the data in Figures 8, 9, and 10. The pattern of seismicity along the Wasatch Front is discussed in detail in other papers (Arabasz et al., 1979a, and Smith et al., 1979). However we describe here two earthquake sequences of special significance to this study. One was the swarm-like activity near Magna in the northwestern Salt Lake Valley in February, March, and June of 1978 (Figure 7). This is an area of recurrent activity including a M_L 5.2 earthquake in 1962. The recent swarm sequence involved small earthquakes with a maximum M_L 3.3 event; however, the shocks were of interest because of their location in a heavily industrialized area and within one of the most densely instrumented portions of the seismograph network. The other earthquake sequence was the aftershock activity of the March 28, 1975, M_L 6.0, Idaho-Utah border earthquake (described in detail by Arabasz et al., 1979b). Although located near the edge of the network, the Idaho-Utah border earthquake is of special interest because it was the largest in the region during the four-year period of this study.

The Magna swarm area was monitored by stations ANU, SAU, and FPU. The largest short-term anomaly was found for station ANU during December 1976-January 1977; however, inspection of Figure 9 indicates no correlation with earthquakes. Also, during the periods of the swarms, no significant anomalies were detected at ANU. An absence of anomalies during the swarms also characterizes the travel times to SAU; although the station was inoperative during part of the swarm of February-March 1978. Only station FPU had a positive correlation of anomaly and earthquake occurrence. An apparent-velocity increase of 1.8% coincides in time with two Magna earthquakes in June 1978. The mean apparent-velocity for the Bingham Mine-FPU profile, in the twelve months preceding the anomaly, was 5.49 km/sec with a standard deviation of 0.03 km/sec (~1/2%). During the one-month anomalous period the apparent velocity increased to a mean of 5.59 km/sec, an increase of greater than three standard deviations. In terms of travel time, the anomalous arrivals are 0.34 second earlier than the average travel time. The anomaly, however, is defined by only three data points, considerably lowering the confidence level.

On June 3, 1978, a M_L 2.7 earthquake occurred during the middle of the anomalous period and was located within 3 km of the Bingham mine-FPU ray path. The June 20, 1978, M_L 1.8 earthquake occurred after the end of the anomaly but was about 5 km from the FPU profile. The Magna swarm of February and March, 1978 was centered about 7 km from the line, however no

anomalies were detected for that period on the FPU profile. The M_L 2.7 and M_L 1.8 tremors were located, respectively, about 5 km and 3 km from the SAU profile, but no anomalies were detected at that station.

After identification of the anomaly at FPU we repicked the anomalous FPU arrival times as well as several picks prior to and after the anomaly. All arrivals were picked to within 0.05 sec of the original picks except the middle anomalous pick which was unreliable due to a noisy record. Thus, we do not have much confidence in the reality of this anomaly; however, if it is real, the implication is that the detection of the earthquakes of $M_L <$ 3-1/2 requires a ray path within several kilometers of the impending hypocenter.

The Idaho-Utah border earthquake sequence would have been ideal to test for premonitory velocity variations except that it was located at the edge of the array, about 180 km north of the Bingham mine. Station NPI was installed within the epicentral area shortly after the main event and was within the aftershock zone. As indicated in Figure 8,a large number of aftershocks, some as large as M_L 3.6 have occurred near NPI, yet no significant anomaly was detected. The only hint of an anomalous period was in September - October 1977 during which travel times were consistently late by about 0.10 sec. This was probably due to picking errors during a period of increased background noise.

Discussion

A major accomplishment of this study was the establishment of a four-year baseline of P-wave travel-times for future analyses. Because the Bingham mine is expected to continue its frequent blasting program we have the capability to make detailed temporal velocity measurements at any of the network stations as changing seismicity might warrant.

A number of observations were made during this study and their implications to earthquake prediction by travel time measurements along the Wasatch Front are summarized here:

1) Travel times, corrected for blast location are generally very stable ($\pm$0.10 sec). Thus if large velocity changes ($\geq$10%) accompany earthquakes in this region, this is a viable technique to search for them.

2) Variable station performance, due to several factors, produces the most false alarms. For example, as noise-to-signal ratio increases, arrivals are often picked late, resulting in a false anomaly. Such anomalies tend to be small in amplitude and erratic in behavior when noise conditions are changing.

3) One anomaly at station ANU could not be explained by site conditions as described above, yet it was not associated with an earthquake. Whether the anomaly is due to a "real" velocity change associated with some

aseismic effect is irrelevant to this point--if such an anomaly is detected on a real time basis and cannot be easily explained as an artifact, it will be thought to be real.

4) During the four-year study, including the detailed work of Gaiser (1977), enough earthquakes of $M_L \leq 3.5$ occurred within the network to substantiate that we cannot predict the occurrence, with any confidence, of earthquakes of $M_L \leq 3.5$ based on the blast-recording technique. A few small anomalies (recorded at FPU) might have been associated with M_L 3 events (of the Magna swarm) but the data were poor. This observation imples that the effect is either nonexistent or of such small magnitude as to be undetectable using the present data. If the latter situation is the case, the anomalous zone must be less than or at most equal to a source dimension, up to several kilometers for earthquakes up to magnitude 3; or the velocity perturbation must be less than several percent. Another possibility for the lack of observing systematic travel time changes is that the rays are refracted around the dilatant zone. In that case the velocity decrease must be quite large in magnitude in order to induce the refraction and restricted in volume not to cause a significant delay in travel time.

Aggarwal et al.(1975) suggested that dilatancy will induce seismic anisotropy in the crust with the velocity in the direction of least compressive stress being affected the greatest. The direction of least compressive stress for the Wasatch Front is approximately east-west (Arabasz et al., 1979a). Because the Bingham mine is located near the center of the north-south trending Wasatch Front, most of the raypaths are in north or south directions to the stations. Hence, the absence of detectable velocity perturbations in our data may be attributed to the orientation of the stress field.

5) No large-amplitude, long-term variations in travel time were observed. However, no events of magnitude greater than about 3.5 occurred in an advantageous location with respect to raypaths. The March 28, 1975, Idaho-Utah border earthquake had a magnitude of M_L 6.0. The closest station, MLI, was 33 km east of the epicenter, and travel times to MLI had no significant fluctuations during that period. The source dimension of the earthquake based on aftershocks is estimated to be about 10 to 20 km (Arabasz et al., 1979b). Hence the only constraint imposed by the MLI data is that the dilatant zone, if one existed, be somewhat less than several source dimensions.

"Great" Wasatch Front earthquakes presumably will recur on or near the Wasatch fault. Assuming such earthquakes will be preceded by large velocity changes in the hypocentral area, stations east and west of the Wasatch fault can monitor for stress buildup on the fault. Bingham blast raypaths to MLI transect the northernmost section of the fault near Malad, Idaho; raypaths to BEI and HDU intersect the fault near Ogden, Utah; and nine stations provide relatively dense coverage of the Wasatch fault east of the Salt Lake Valley from Farmington to Provo. None of the data for these stations exhibited any significant long term apparent velocity variations. We emphasize, however, that because of the lack of a sufficient test of

this technique for $M_L \geq 3.5$ earthquakes, we cannot say earthquake-generating stresses are not building up along the Wasatch fault.

Based on the experience gained in this study we have a few general conclusions regarding blast monitoring as an earthquake prediction tool. Although these conclusions refer specifically to the Wasatch Front area, the results might apply as well in other regions of extensional tectonics.

We have established that, with the present data, velocity percursors to small magnitude earthquakes ($M_L < 3.5$) in our area have not been detected. Even though the duration and magnitude of an anomaly is expected to be larger for higher magnitude earthquakes, the probability of such an event occurring on one of the monitored raypaths gets progressively smaller. Thus the probability of predicting small earthquakes by blast monitoring in this region with the present network appears to be limited. But we must carefully note that during the time of this study no earthquakes of $M_L > 3.6$ occurred near a raypath of the Wasatch Front seismic network. Thus a meaningful test of the premonitory prediction technique applied to the Wasatch Front has not yet been accomplished. Most velocity monitoring projects have involved the use of microearthquake data to measure variations in V_p/V_s. One can make a conjecture that observed travel time changes may well be due to source effects, such as systematic hypocentral migration, rather than to changes in rock properties along the seismic ray paths.

Although the results of this study were inconclusive for the small shocks, we plan to continue the velocity monitoring for the following reasons: 1) the important test of the technique for larger earthquakes was not possible--leaving open the possibility of predicting larger earthquakes, 2) the blasts are continuously and routinely recorded, and 3) data analysis is not too costly or time consuming. In regard to the last point, we plan to maintain the velocity analysis on a weekly to bi-monthly basis--sufficient to detect predicted anomalies for $M_L \geq 4.5$ tremors.

Acknowledgments

R. E. Estill helped initiate the blast monitoring and contributed significantly to this project in its early stages and B. W. Hawley did much of the data analysis in the later stages. Dr. W. J. Arabasz, T. Meyer, W. D. Richins, R. S. Bellon, J. Hanson, T. May, J. Milano and D. T. Whipp assisted in data acquisition. We are especially indebted to the Kennecott Copper Corporation's, Utah Division, management for permission and assistance in recording the mine blasts. N. Stallivieve and T. Pollock of Kennecott Copper Corporation, Bingham Canyon Mine Drilling and Blasting Division, were particularly helpful in the blast recording. This research was supported by the U.S. Geological Survey, Office of Earthquake Studies, Contract Nos. 14-08-0001-14585, 14-08-0001-15895, and 14-08-0001-16725.

References

Aggarwal, Y. P., L. R. Sykes, J. Armbruster, and M. I. Sbar (1973). Premonitory changes in seismic velocities and prediction of earthquakes, Nature 241, 632-635.

Aggarwal, Y. P., L. R. Sykes, D. W. Simpson and P. G. Richards (1975). Spatial and temporal variations in t_S/t_P and in P-wave residuals at Blue Mountain Lake, New York; Application to earthquake prediction, J. Geophys. Res. 80, 718-732.

Allen, C. R. and D. V. Helmberger (1973). Search for temporal changes in seismic velocities using large explosions in southern California, in Proceedings of the conference on tectonic problems of the San Andreas fault system, Stanford Univ. Publ. Geol. Sci. 13, 436-445.

Arabasz, W. J., Smith, R. B., Richins, W. D. (1979a) Earthquake Studies Along the Wasatch Front, Utah: Network Monitoring, Seismicity, and Seismic Hazards, in Utah Earthquakes, Arabasz, W. J., Smith, R. B., Richins, W. D. eds. published by Univ. Utah.

Arabasz, W. J., W. D. Richins, C. J. Langer (1979b) Earthquake Studies Along the Wasatch Front, Utah: The Idaho-Utah Border (Pocatello Valley) Earthquake Sequence of March-April 1975, in Utah Earthquakes, Arabasz, W. J., Smith, R. B., Richins, W. D., eds. published by Univ. Utah.

Boore, E. M., T. V. McEvilly, and A. Lindh (1975). Quarry blast sources and earthquake prediction: the Parkfield, California earthquake of June 28, 1966. Pure and Applied Geophysics 113, 293-296.

Brace, W. F., B. W. Paulding, and C. H. Scholz (1966). Dilatancy in the fracture of crystalline rock, J. Geophys. Res. 71, 3939-3953.

Brady, B. T. (1975). Theory of earthquakes: II. Inclusion theory of crustal earthquakes, Pure and Applied Geophysics 113, 149-168.

Braile, L. W., R. B. Smith, G. R. Keller and R. M. Welch (1974). Crustal structure across the Wasatch Front from detailed seismic refraction studies, J. Geophys. Res. 79, 2669-2677.

Cluff, L. S., G. E. Brogan and C. E. Glass (1970). Wasatch fault, northern portion: earthquake fault investigation and evaluation, Report to Utah Geol. and Min. Survey, Woodward-Clyde and Associates, 27 p.

Cluff, L. S., G. E. Brogan, and C. E. Glass (1973). Wasatch fault, southern portion: earthquake fault investigation and evaluation, Report to Utah Geol. and Min. Survey, Woodward-Lundgren and Associates, 79 p.

Estill, R. E. (1976). Temporal variations of P-wave travel times and lateral velocity structure across the Wasatch Front, Utah, M.S. thesis, University of Utah.

Gaiser, J. E. (1977). Origin-time corrected variations measured across the Wasatch Front, M.S. thesis, University of Utah.

Kanamori, H. and D. Hadley (1975). Crustal structure and temporal velocity change in southern California, Pure and Appl. Geophys. 113, 257-280.

Keller, G. R., R. B. Smith, and L. W. Braile (1975). Crustal structure along the Great Basin-Colorado Plateau transition from seismic refraction studies, J. Geophys. Res. 80, 1093-1098.

McEvilly, T. V. and L. R. Johnson (1974). Stability of P and S velocities from central California quarry blasts, Bull. Seism. Soc. Am. 64, 343-353.

Mjachkin, V. I., W. F. Brace, G. A. Sobolev, and J. H. Dieterich (1975). Two models for earthquake forerunners, Pure and Appl. Geophys. 113, 169-182.

Nur, A. (1972). Dilatancy, pore fluids, and premonitory variations of t_s/t_p travel times, Bull. Seism. Soc. Am. 62, 1217-1222.

Richins, W. D. (1979). Station data and instrumentation, in Earthquake Studies in Utah 1850 to 1978, Arabasz, W. J., Smith, R. B., Richins, W. D. eds. published by Univ. Utah.

Scholz, C. H., L. R. Sykes, Y. P. Aggarwal (1973). Rock dilatancy and water diffusion may explain a large class of phenomena precursory to earthquakes, Science 181, 803-810.

Semenov, A. M. (1969). Variations in the travel time of transverse and longitudinal waves before violent earthquakes, IZV., Earth Phys. No. 4, 72-77.

Smith, R. B. (1974). Seismicity and earthquake hazards of the Wasatch Front, Utah. Earthquake Information Bull. 6, 12-17.

Smith, R. B. and W. J. Arabasz (1979) Earthquake Studies Along the Wasatch Front, Utah: Seismicity, tectonics, and crustal structure in Utah: important aspects from new data, in Utah Earthquakes, Arabasz, W. J., Smith, R. B., Richins, W. D., eds. published by Univ. Utah.

Stuart, W. D. (1974). Diffusionless dilatancy model for earthquake precursors, J. Geophys. Res. 1, 261-264.

Swan, F. H., III., D. P. Schwartz, K. L. Harison, P. L. Knuepfer, and L. S. Cluff (1978). Study of earthquake recurrence intervals on the Wasatch fault Utah, Semi-Annual Technical Report, September, 1978, to the Office of Earthquake Studies, U.S. Geological Survey, 31 p.

Whitcomb, J. H., J. D. Garmany, and D. L. Anderson (1973). Earthquake prediction: Variation of seismic velocities before the San Fernando earthquake, Science 180, 632-635.

ANOMALOUS PATTERNS OF EARTHQUAKE OCCURRENCE IN THE SIERRA NEVADA-GREAT BASIN BOUNDARY ZONE

By

Alan Ryall and Floriana Ryall

Seismological Laboratory
University of Nevada
Reno, NV 89557

ABSTRACT

Anomalous temporal variations, consisting of a general decrease in seismicity in the southern part of the Sierra Nevada-Great Basin boundary zone (SNGBZ) from October 1977 to September 1978, followed by a burst of moderate earthquakes that has continued for more than a year, is suggestive of a pattern that several authors have identified as precursory to strong earthquakes. The 1977-1979 variations are particularly noteworthy because they occurred over the entire SNGBZ, indicating a regional, rather than local, cause for the observed changes. A search for changes in P-wave velocity changes within the SNGBZ, based on recordings of Nevada Test Site explosions at pairs of stations, has so far produced negative results.

INTRODUCTION

Attempts to define the character of seismicity preceding major earthquakes are now converging on anomalous patterns of earthquake occurrence, either within the impending rupture zone or in the immediate vicinity of the impending mainshock; however, published results are not entirely consistent from region to region. Early work on this problem was by Fedotov (1968, 1969), who found an increase in background seismicity about 15 years before most, but not all, large shocks in the Kurile-Kamchatka region. Nersesov et al. (1974) found a tendency for moderate shocks in the Garm region of Central Asia to be located in areas of relative quiescence but to occur at a time when activity in the region surrounding the focal zone was at a limiting high value. Kelleher and Savino (1975) concluded that major earthquakes around the northern and eastern Pacific were generally preceded by several decades of quiescence in the main rupture zone, although increased seismicity might occur in the vicinity of the impending mainshock. Jones and Molnar (1978) found foreshock activity preceding a large fraction of the world's major earthquakes, with a suggestion that seismicity in the vicinity of the impending mainshock increases to about twice the previous level three months before a large event. According to Keilis-Borok et al. (1978), anomalous clustering of earthquakes in time and space is a characteristic pattern of seismicity that precedes strong earthquakes.

In the western United States, Tocher (1958) concluded that large earthquakes in central California in 1868 and 1906 were preceded by a regional increase in seismicity, and a later study suggested that seismicity

before the 1906 San Francisco earthquake was within the main rupture zone (see Figure 8 in Ryall et al., 1966). Kanamori (1978) reported that the 1971 San Fernando, California, earthquake was preceded by four years of relative quiescence, followed by about two years of increased activity in the vicinity of the impending mainshock. He also reported a similar pattern for the 1952 Kern County, California, event. However, over longer periods of two to three decades before both of these earthquakes, periods of alternating quiescence and increased activity occurred that were not followed by large events. For the Nevada region Ryall (1977) observed that a moderate level of seismicity, including felt earthquakes, occurred over periods of at least several decades in or near the rupture zones of two major historic earthquakes (1915 Pleasant Valley and 1954 Dixie Valley- Fairview Peak). A follow-on study is in progress to identify the spatial- temporal character of seismicity before the 1954 events.

In companion papers, VanWormer and Ryall (1980) and Ryall and VanWormer (1980) present a comparison of seismicity, structure and tectonic processes; estimation of maximum magnitudes; and recommendations for changes in seismic zoning for the Sierra Nevada-Great Basin boundary zone (SNGBZ). In this paper we describe anomalous temporal variations in earthquake occurrence and a search for P-wave velocity changes within this zone.

OBSERVED TEMPORAL VARIATIONS

The spatial-temporal character of seismicity in the SNGBZ is illustrated by Figure 1, which shows earthquake occurrence as a function of time and latitude, for events recorded by the dense Mina and Reno seimic networks for 1 January 1974-30 April 1979. As noted by VanWormer and Ryall (1980), uneven network coverage for the period shown on the figure has affected the detection and analysis of events with M.LT.3.0 in some areas. This is reflected in some places on the figure (i.e., "gap" in late 1975 and early 1976 at Truckee, due to lack of data); however, fluctuations in network detection capability have been taken into account in the discussion that follows.

The most dramatic feature on the figure is a general decrease in activity in the southern part of the zone from the fall of 1977 to summer 1978, followed by a burst of sizeable earthquakes, aftershocks and swarms in all parts of the zone in late 1978 and 1979. Table 1, chronologically listing events in the zone for the period June, 1976 to June, 1979, illustrates this change in activity, and Figure 9 in VanWormer and Ryall (1980; points 1, 2, 4, 5, 6, 7 and 8) shows the location of most of the events listed in the table. It is interesting to note that in addition to the six events listed for 1978-1979, a magnitude 4.3 earthquake also occurred on 14 June 1979 at Inyokern, in the southern Owens Valley. Thus over a thirteen-month period, moderate earthquakes have occurred in the Sierran frontal fault zone, for more than 300 km in the region shown on Figure 9 and perhaps an additional 200 km to the south. Comparison of our data list with those of the University of California and California Institute of Technology indicates that this activity is quite unusual: of 21 events with M.GE.4.0 in the SNGBZ from 1969 to 1979, 14 have occurred in five dif-

ferent locations since 4 September 1978.

Figure 2 is a three-dimensional plot showing earthquake energy release as a function of time and latitude within the SNGBZ. For the five-year period shown, the level of activity in the entire zone is shown by this figure to increase with time, with peaks in activity during late 1978 and 1979.

To determine whether regional velocity changes might be associated with the observed changes in seismicity, we analyzed P-wave arrival times for underground nuclear explosions at the Nevada Test Site. In this analysis, arrival-time differences were determined for pairs of stations that had almost identical azimuths (within a few degrees) to NTS, in order to eliminate effects due to differences in depth of burst and near-source structure. Stations that met this requirement are shown in the lower left corner of Figure 3; shot-receiver distances were all greater than 180 km, so the phase measured was in all cases Pn. The original tape recordings were played out on strip-chart recordings at a time scale of 25 mm/second of real time, and arrival times measured from these records were accurate to within 0.02 second. The results of this analysis, shown on Figure 3, were negative: no systematic changes in velocity were detected, and the scatter was generally less than +/- 1%.

DISCUSSION

Previous studies suggest that seismicity preceding large earthquakes in this region might be expected to display one or more of the following characteristics: (1) moderate level of seismicity continuing for several decades before the mainshock (Ryall, 1977); (2) anomalous clustering of activity in time and space (Keilis-Borok et al., 1978); (3) alternating periods of quiescence followed by increased activity in the vicinity of the impending mainshock (Kanamori, 1978); and/or (4) significant increase in seismicity three months before the mainshock (Jones and Molnar, 1978).

In general, clustering of earthquakes is characteristic of the entire SNGBZ, so it is difficult to associate clustering in this zone with precursory effects observed in other regions. In some areas clusters represent a persistent high level of seismicity associated with active volcanic processes, while in other areas they occur where major faults terminate or intersect. In general, the recent temporal behavior illustrated by Figures 10 and 11 for the SNGBZ is unique in the authors' experience over the last fifteen years. The temporal character of the activity -- a period of quiescence followed by an unusually high level of seismicity -- agrees with the pattern that preceded large earthquakes in southern California (Kanamori, 1978) and with the anomalous clustering of earthquakes that Keylis-Borok et al. (1978) have identified as a typical precursory phenomenon.

It is significant that the flurry of moderate earthquakes starting in the fall of 1978 has affected the entire boundary zone, from Doyle in the north to Inyokern at the southern end of Owens Valley. At the same time,

according to a News item in EOS (1979, Vol. 60, No. 43), there has been a noticeable increase in emission of radon in some water wells in southern California, and laser-ranging measurements in that region have shown a change, from primarily north-south compression to primarily east-west extension.

These observations suggest that precursory phenomena reported in the literature may have been the result of regional, rather than local stress changes. If so, such changes could create favorable conditions for large shocks to occur anywhere within a sizeable region, rather than in the immediate vicinity of the anomalous observations. Interpretation of observed temporal variations in earthquake occurrence along the SNGBZ in terms of an impending major earthquake is in any case ambiguous, because of the long period of time during which seismicity alternately increased and decreased before the 1952 Kern County and 1971 San Fernando earthquakes (Kanamori, 1978).

ACKNOWLEDGEMENTS

W. A. Peppin and M. R. Somerville reviewed the manuscript and made helpful suggestions. This research was partly supported by the US Geological Survey, under contract number 14-08-0001-16741.

REFERENCES

Fedotov, S. A. (1968). On the seismic cycle, possibility of collective seismic regionalization and long-term seismic forecasting, in Seismic Regionalization of the USSR, "Nauka", Moscow, 121-150 (in Russian).

Fedotov, S. A. (1969). Seismicity in the south of the Kurile Island Arc. The disastrous Etorofu earthquake of 6 November 1958 and the seismic regime of the southern Kurile zone before and after it, in Earthquakes and the Deep Structure of the South Kurile Island Arc, "Nauka", Moscow, 58-121.

Jones, L. M. and P. Molnar (1978). Some characteristics of foreshocks, US Geol. Survey, Open-File Rept. 78-943. 211-233.

Kanamori, H. (1978). Nature of seismic gaps and foreshocks, US Geol. Survey, Open-File Rept. 78-943, 319-334.

Keilis-Borok, V. I. L. Knopoff, I. M. Rotvain and T. M. Sidorenko (1978). Bursts of seismicity as long-term precursors of strong earthquakes, US Geol. Survey, Open-File Rept. 78-943, 351-386.

Kelleher, J. and J. Savino (1975). Distribution of seismiciy before large strike-slip and thrust type earthquakes, J. Geophys. Res., 80, 260-271.

Nersesov, I. L., V. S. Ponomarev and V. K. Kuchai (1974). Characteristics of the spatial distribution of seismic background, Search for Earthquake Forerunners in Prediction Test Areas, "Nauka", Moscow, 119-131 (in Russian).

Richter, C. F. (1958). Elementary Seismology, W. H. Freeman, 768 pp.

Ryall, A., D. B. Slemmons and L. D. Gedney (1966). Seismicity, tectonism and surface faulting in the western United States during historic time, Bull. Seism. Soc. Am. 56 (5), 1105-1135.

Ryall, A. and J. D. VanWormer (1980). Estimation of maximum magnitude and recommended seismic zone changes in the western Great Basin, this volume.

Ryall, A. (1977). Seismic hazard in the Nevada region, Bull. Seism. Soc. Am., 67, 517-532.

Tocher, D. (1958). Earthquake energy and ground breakage, Bull. Seism. Soc. Am., 48, 147-153.

VanWormer, J. D. and Alan Ryall (1980). Seismicity related to structure and active tectonic processes in the western Great Basin, Nevada and eastern California, this volume.

Table 1. Earthquakes with M.GT.3.5 in the Sierra Nevada-Great Basin Boundary zone.

Date	Latitude, Deg. N	Longitude, Deg. W	Depth, km.	M	Description
6/20/1976	40.41	120.35	--	4.5	Susanville, CA
6/24/1976	39.42	119.65	2.8	3.5	Virginia City, NV
2/1/1977	39.15	119.94	14.8	4.0	Zephyr Cove, NV
2/22/1977	38.48	119.28	8.6	4.8	Bridgeport, CA
10/10/1977	38.04	118.82	12.3	4.0	Mono Lake, CA
9/4/1978	38.82	119.77	5.8	5.2	Markleeville, CA
10/4/1978	37.50	118.67	5.9	5.5	Bishop, CA
10/20/1978	38.05	118.92	--	3.8	Swarm, Mono L., CA
2/22/1979	40.00	120.12	10.9	5.2	Doyle, CA
9/24/1979	37.63	118.90	--	4.0	Crowley Lake, CA
10/7/1979	38.21	119.35	--	4.9	Bridgeport, CA

Figure 1. Earthquake occurrence in the Sierra Nevada-Great Basin boundary zone as a function of time and latitude. Size of symbols is proportional to magnitude, location of zone shown on Figure 2.

Figure 2. Energy released by earthquakes in the Sierra Nevada-Great Basin boundary zone as a function of time and distance toward the northwest along the zone. A(2.0) -- logarithm of the number of M2.0 earthquakes that would be equivalent to total energy released by earthquakes within grid square. Number of earthquakes were smoothed with a triangular filter before log N(2.0) was calculated. Energy was determined for each earthquake using log E = 11.8 + 1.5 M (Richter, 1958).

Figure 3. Plot of Pn slowness (sec/km) for Nevada Test Site explosions recorded at station pairs in the western Great Basin. Inset map shows station locations. Dots -- Yucca Valley shots; squares -- Pahute Mesa shots; open symbols -- data read from 10 mm/sec playbacks; closed symbols -- data read from 25 mm/sec playbacks.

COMMENTS

W. ARABASZ: This is a loaded question: Apart from earthquake prediction, what part is to be played in the earthquake hazards program by the people who put dots on maps of the Great Basin? Smith and Ryall showed results of a type that seismologists established decades ago in the California region. On each side of the Great Basin two or three people have to run as fast as they can to study an enormous area with a sparse network of seismic stations. If people in California were interested in the same sort of information, they'd add an extra 150 stations in a much smaller area. My question to the group, to put things in perspective, is the following: Seismologists are playing catch-up ball in this region just to carry out the type of research that was done a long time ago in California, and at the same time are required to cover the instrumental monitoring. They probably have scientific interests other than putting dots on maps, and I would like to hear comments as to what their continued role is now, in terms of earthquake hazards?

R. E. ANDERSON: In many ways, even though the geophysical data base may not be adequate, it is more adequate than the geologic data base. So there are a few geologists running around as well, and they too have a long way to go.

RYALL: We have heard of concern within higher echelons in the Survey because of the amount of effort that has gone into operating dense networks of stations. However, I think the work presented at this meeting illustrates the value of operating such networks for at least a sufficient period of time to identify patterns of seismicity and determine their relation to geologic structure and tectonic processes. Even without uniform coverage, we are seeing patterns that would not have been possible with the sparse network we operated previously: identification of major rupture zones and related estimation of maximum magnitude, delineation of active zones and stable blocks, and so on. We are also developing the data base with which to show changes in the temporal and spatial distribution of earthquakes. It seems to me that the Great Basin is an ideal region in which to test various prediction techniques: it has low background noise, high seismicity, and deserted areas in which we can operate sensitive equipment without being concerned about interference or vandalism. Later on, we want to replace large numbers of narrow-band analog seismic stations with a few high-quality, broadband, digital stations, probably installed in mine tunnels to minimize background noise. We are testing a prototype digital telemetering station now, and starting to develop master-event routines and digital analysis techniques such as moment tensor analysis that will enable us to obtain more information from a few digital stations than we now get from the dense analog network. This conversion will require considerable time and effort. however, and in the meantime we still have plenty of work to do with the data on hand.

D. PERKINS: The Survey is obligated to put out another national hazard map within the next fiscal year, and one of the things we have come up against in mapping the outer continental shelf and coastal areas is the dis-

parity in possible models -- the extent to which the models are based on geology as opposed to historical seismicity. One of the things emerging from this conference is that there is not a great discrepency between indicated historical rates and indicated geological rates. To the extent that this is true, it means that the models will be relatively simple to develop, because we will be using a combination of both sets of information. To the extent that it is not true, we can come up with what I can see as three different likely models, and we will have to decide among the people who are doing the work as to what is the proper way to weight these models for the national map. In California we can zone on the basis of geology and just sort of let the seismicity catch up; here. we do not know enough to zone on the basis of geology, and the relevance of the seismic history has to be determined.

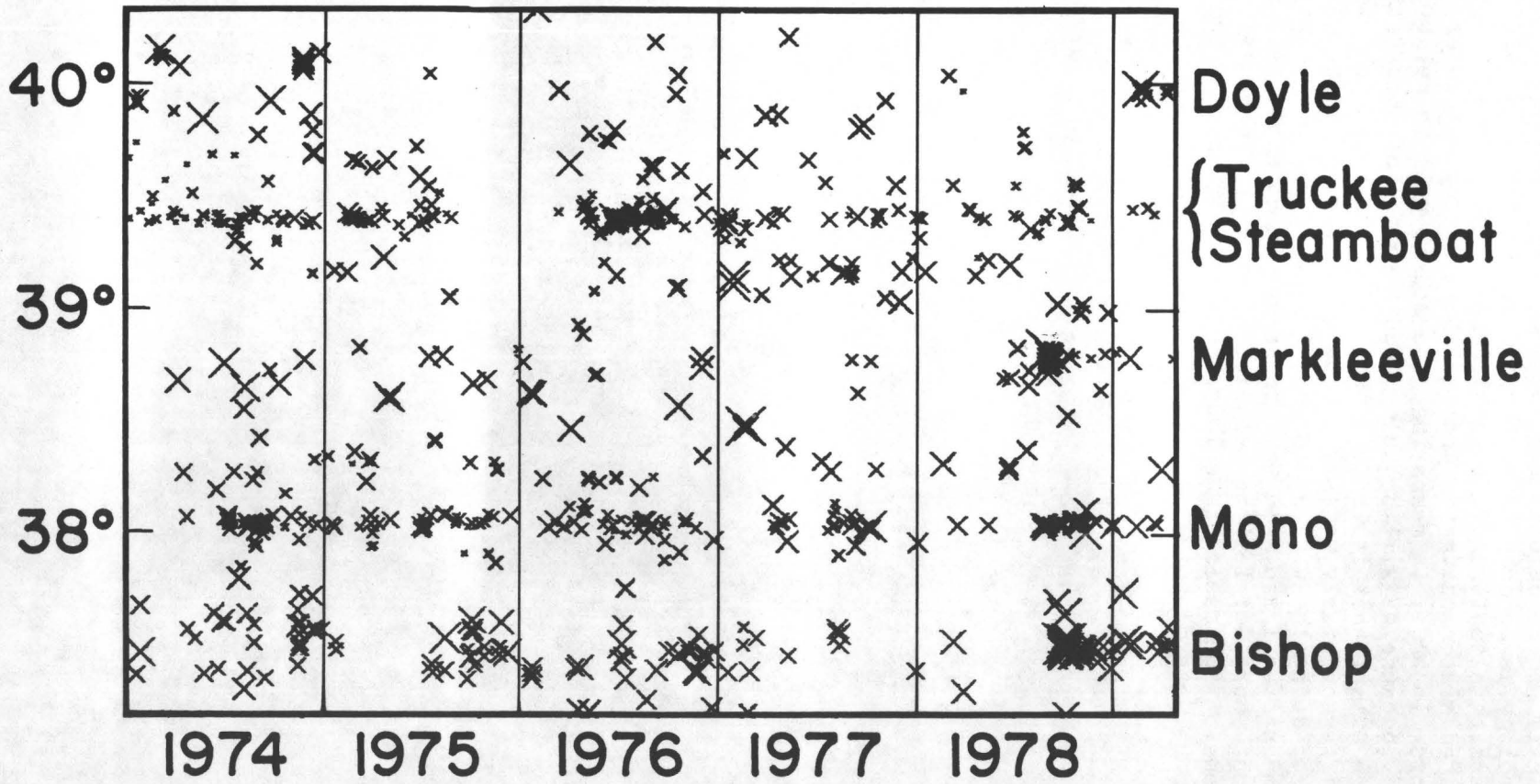
40°
39°
38°
1974
1975
1976
1977
1978
Doyle
Truckee
Steamboat
Markleeville
Mono
Bishop

FIGURE 1

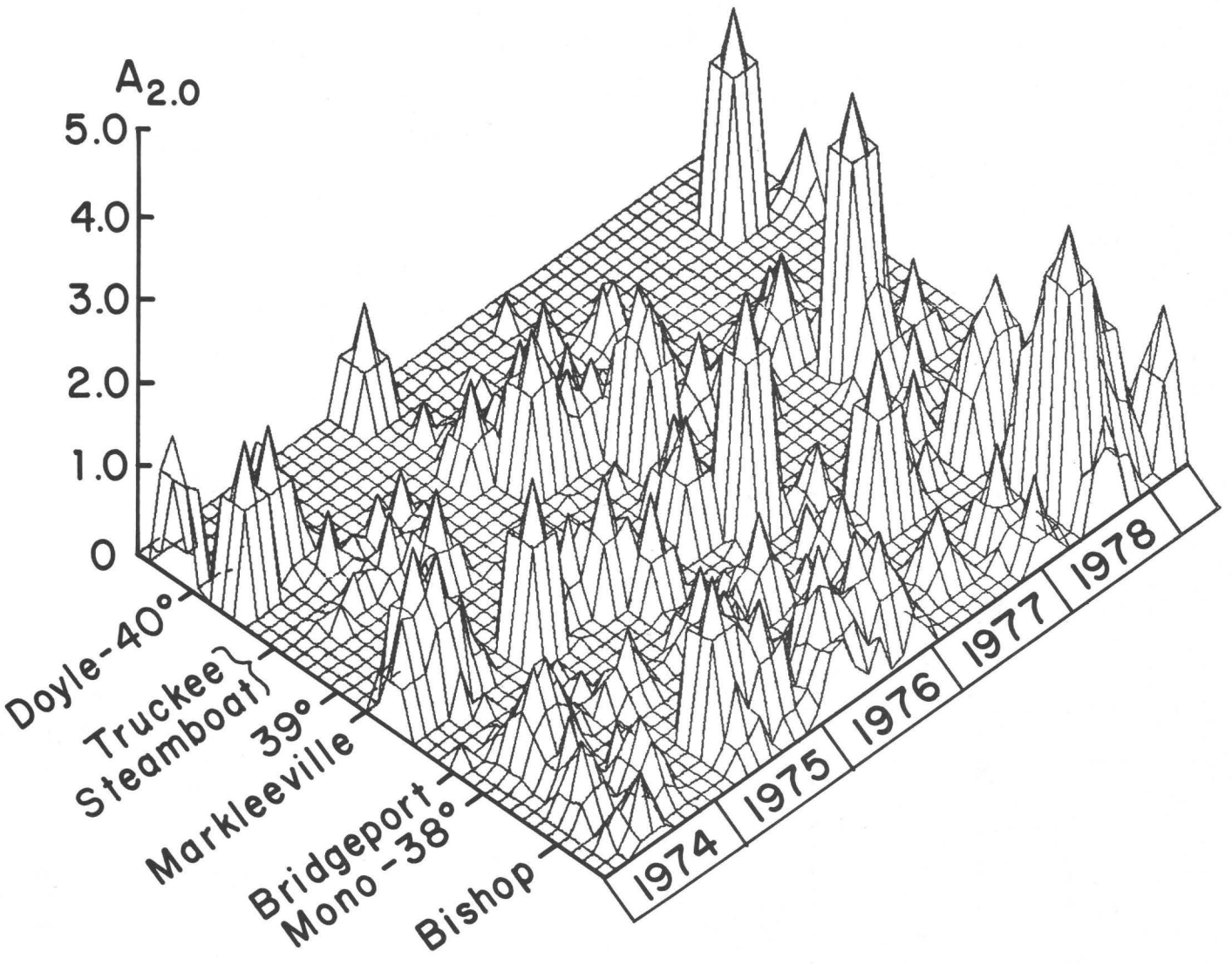
$A_{2.0}$
5.0
4.0
3.0
2.0
1.0
0
Doyle-40°
Truckee
Steamboat
39°
Markleeville
Bridgeport
Mono-38°
Bishop
1974
1975
1976
1977
1978

FIGURE 2

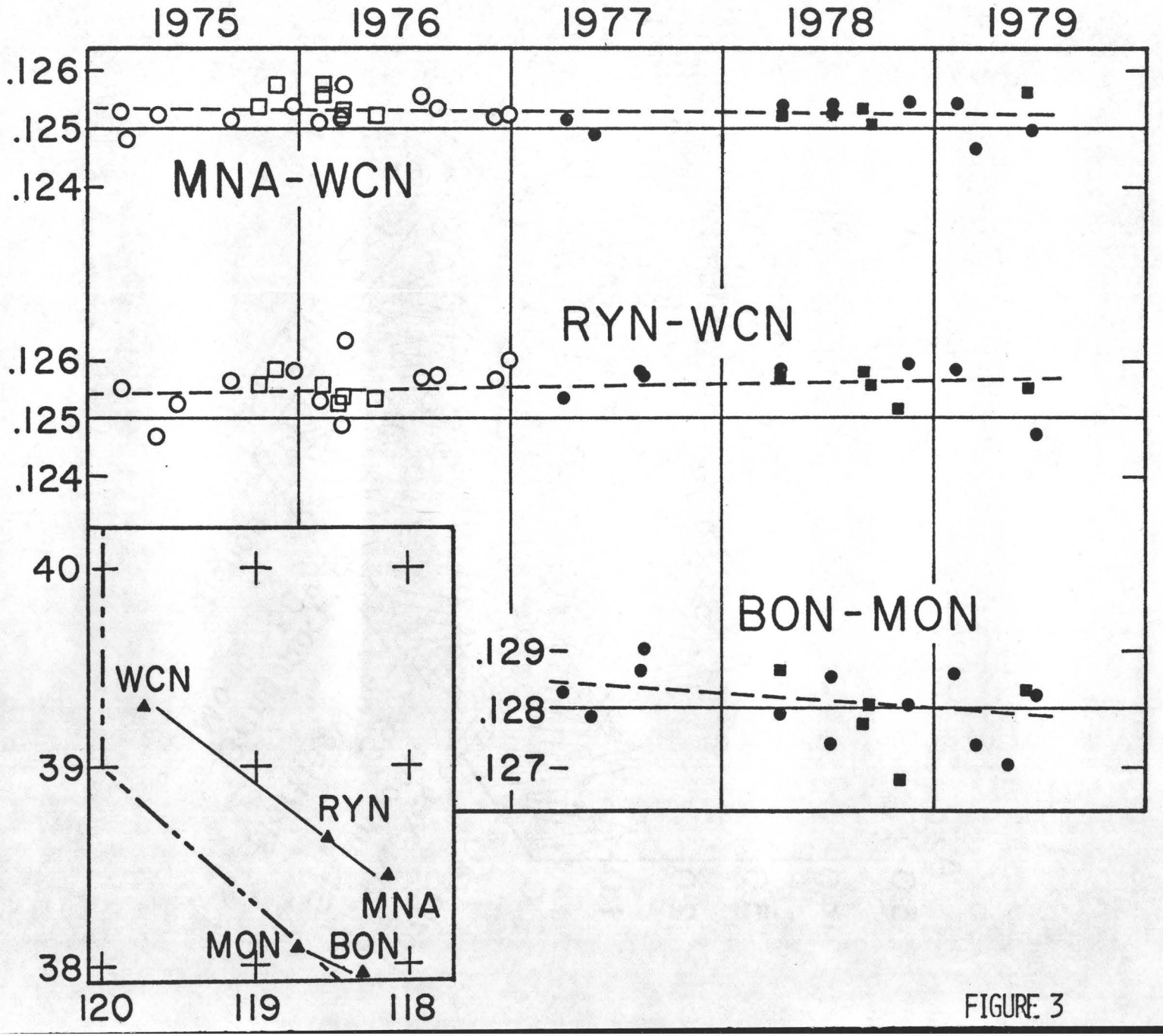
1975
1976
1977
1978
1979
.126
.125
.124
MNA-WCN
RYN-WCN
.126
.125
.124
40
39
38
120
119
118
WCN
RYN
MNA
MON
BON
BON-MON
.129
.128
.127

FIGURE 3

STATE OF STRESS IN THE WESTERN UNITED STATES[1]

Mary Lou Zoback

Mark Zoback

U. S. Geological Survey
Menlo Park, California

ABSTRACT

By inferring principal stress orientations from geologic data, focal mechanisms and in-situ stress measurements we have prepared a map of least principal horizontal stress orientations for the coterminous United States. The map indicates that the state of intraplate stress is not uniform. On the basis of orientation and relative magnitudes of principal stresses the country was subdivided into stress provinces. In the western United States, a region of active tectonism characterized by high levels of seismicity and generally high heat flow, the stress pattern is complex and numerous stress provinces can be well-delineated. Despite relative tectonic quiescence in the eastern and central United States several major variations in principal stress orientation are apparent.

Within a given province, stress orientations appear quite uniform ($\sim \pm 15^{o}$, within the estimated range of accuracy of the different methods used) over broad regions up to 2000 km in extent. However, regions of only 150-200 km wide have been found to be characterized by a distinct stress field relative to surrounding areas. Available data on the transition in orientation between the different stress provinces indicate that these transitions can be abrupt, occurring over less than 75 km in places.

Most of the eastern United States is marked by predominantly compressional tectonics (combined thrust and strike-slip faulting) while much of the region west of the Great Plains is characterized by predominantly extensional tectonics (combined normal and strike-slip faulting). However, along the San Andreas and in part of the Sierra Nevada deformation is nearly pure strike-slip. Exceptions to this general pattern include areas of compressional tectonics in the western United States (the Pacific Northwest, the Colorado Plateau interior, and the big bend region of the San Andreas) and the normal faulting along the Gulf Coastal Plain.

---

1 This paper is excerpted from "Interpretative Stress Map of the Coterminous United States" by Zoback and Zoback which appears in its entirety in Proceedings of Conference on Magnitude of Deviatoric Stresses in the Earth's Crust and Upper Mantle, U.S. Geological Survey Open-File Report 79- .

The suggested possible sources of tectonic stresses in the crust are: plate interactions along the Pacific coast, asthenospheric resistance to plate motion, ridge-push forces acting at passive continental margins, density differences in regions of abrupt changes in lithosphere/asthenosphere structure, and sediment loading.

INTRODUCTION

Detailed knowledge of the pattern of intraplate stress provides important constraints on models of global scale tectonic processes and the mechanism of plate motions. The pattern of stress and variations in this pattern must also be known to properly understand intraplate volcanism and tectonism. In addition, in regions of relative tectonic quiesence, knowledge of the in-situ stress field allows prediction of possible seismic hazards associated with favorably-oriented, pre-existing zones of weakness in the crust.

Our paper represents an attempt to map the modern stress field in the coterminous United States. Principal stress orientations have been determined from geologic observations, earthquake focal mechanisms, and in-situ stress measurements. An attempt has also been made to categorize broad regions not only by the orientation of the principal stress directions but also by their relative magnitudes as inferred from currently active tectonism.

The major contribution of the present study is the inclusion of the geologic data, largely in the western United States. In addition, we have attempted to go back to original references and check the reliability of previously compiled data, particularly for focal mechanisms. We have excluded poorly constrained points and have relied, whenever possible, on averages of a number of solutions at a given locale. The quality criterion we used are elaborated in detail below.

PRINCIPAL STRESS ORIENTATION INDICATORS

Some discussion is warranted of the different techniques used for determining principal stress orientations. Our purpose is to outline the major assumptions associated with each technique as well as the inherent difficulties and uncertainities. These detailed descriptions of the techniques are presented to give an idea of the types of measurements and/or observations that could routinely be made and reported as part of a scientific investigation and which would contribute to our knowledge of the state of stress in the earth's crust. Incorporation of the geologic stress indicators is our main contribution to previous compilations of stress data.

Geologic Data

Geologic information on principal stress orientations can be subdivided into two main categories: observations of fault slip and the alignment of volcanic feeders. In the western United States, much of this data comes from Zoback (1979), Thompson and Zoback (1979) and Zoback and Zoback (in press).

Detailed information on fault slip can be used to determine the net horizontal component of motion on oblique-slip normal and thrust faults. Measurements of fault slip yield the net direction of horizontal shortening in the case of oblique-slip thrust faults and the net horizontal extension direction on oblique-slip normal faults. The occurence of oblique slip suggests slip on favorably-oriented, pre-existing planes of weakness (faults). The assumption here is that the actual horizontal slip direction is indicative of the regional stress field. Hence, in a normal faulting regime such as the Basin and Range and the Gulf Coast provinces, the horizontal component of slip (or opening) is inferred to be regionally in the direction of the least principal stress. Similarly, in a thrust faulting regime the net horizontal slip should be in the direction of the greatest principal stress.

There are two methods of determining fault slip geologically: (1) measured historic offsets and (2) measurements of grooves and slickensides on exposed fault scarps. Of the two methods the first is often the most difficult to obtain and the least reliable. Surface scarps of earthquakes are rarely a single trace but rather a zone of breaks and a complete picture of slip requires knowledge of the total dip-slip and strike-slip components of motion for all the breaks. Particularly, if a major break can be identified, the maximum vertical and strike-slip offsets (along the same segment of the break) can be used to determine the net horizontal components of slip. Historic corehole offset by fault motion is considered to be a reliable stress indicator when 1) fault motion occurs years after excavation and 2) the sense of motion is not caused by the creation of a stress-free surface and hence, gravitationally controlled. An excellent data set of Shafer (1979) in the Appalachian Fold Belt of the eastern United States fit these criteria.

Large scale grooves and parallel slickensides on an exposed fault surface indicate the direction of motion of two crustal blocks past one another. Unfortunately well preserved fault scarps in competent rocks are rarely exposed. In the Basin and Range province, a site of abundant Quaternary faulting, most young scarps occur in alluvium, basin-ward of the main ranges. However, scattered surface exposures are known and often several kilometers (sometimes tens of kilometers) of fault surface along strike are exposed. Measurement of grooves and slickensides at a number of sites along the fault provide a mean horizontal direction of slip for a major crustal block. Consistency of the horizontal component of slip despite changes in strike of as much as 90° (Smith and Pavlis, in press and M. L. Zoback, 1978) indicate that these grooves and slickensides accurately record the major block motion. A source of error in this kind of study is the possibility of a local downdip component of motion of gravitationally unstable blocks that slip down into the

valley. This could result in measured slip directions which are spuriously rotated toward the valley.

Some of the geologic slip data reported is derived from detailed studies involving a number of localities on a given fault surface while other points represent only a single measurement (see Table 1 for details). The standard deviation of the mean horizontal component of slip in the detailed studies is ± 10-15o, which is probably a reasonable estimate of the accuracy of all the fault slip points despite the fact that individual measurements generally have a precision of ± 2o.

When detailed information on the direction of slip is not available an approximate method for determining stress orientation relies on the trend of young faults and only the sense of the predominant type of offset. Such data have been used in the Atlantic Coastal Plain and Gulf Coast areas. The assumption of pure dip-slip faulting in the case of the active Gulf Coast normal faults is probably valid. In the Atlantic Caostal Plain this type of data is used because it is the only data available to us.

The second type of geologic indicator of principal stress orientation is linear volcanic feeders such as dikes and cinder cone alignments (where the cinder cone alignment is presumably reflecting the geometry of an underlying "fissure" or dike). Anderson (1951) and Odé (1956) have concluded, on theoretical grounds, that dike intrusion should follow planes perpendicular to the axis of least principal stress within a rock mass. Clearly there can be no static shear stress across a magma-filled crack. The question of whether dikes really sense the regional stress field or if they merely fill pre-existing fractures is still often disputed. One of the most impressive field examples which clearly disputes the passive filling of pre-existing fractures is a NNW-trending, 15 m.y. diabase dike swarm exposed in the Roberts Mountains, Nevada (Christiansen and McKee, 1978, p. 294). Despite the abundant pre-existing fractures and faults within the range, the dike swarm maintains a constant trend, cross-cutting the earlier structure.

Koons (1945) in a careful study of late Quaternary basalt fields north of the Grand Canyon saw through the possible confusion of parallel cinder cone alignments and nearby faults:

> "Detailed examination of exposed bedrock near these aligned groups shows that though the lines of cones parallel faults trends, the cones do not lie on observed fault lines. Cones tend to occur in distinct lines, parallel to, but not associated with surface fractures. This parallelism may have resulted from stresses in existence at the time of deformation".

More recently Nakamura (1977) and Nakamura et al (1978) have convincingly demonstrated the correspondence between linear volcanic feeders and regional stress as determined from studies of active faults, earthquake focal mechanisms, and the direction of convergence along major plate boundaries.

Thus, in regions of active volcanism, linear volcanic feeders can be used to determine principal stress orientations. It has also been suggested that the axis of maximum elongation of calderas should correspond to the regional least principal stress direction (Lachenbruch and Sass, 1979). In the present study, however, we have used only dike trends and cinder cone alignments which can be determined with more precision. It is worth pointing out that this technique is the only one that can yield quick and accurate information on past stress fields.

Stress directions inferred from cinder cone alignments are generally based on linear alignments of 4 or more vents. Some of these linear zones are quite impressive, extending for nearly 20 km and containing as many as 16 individual eruptive centers (for example, the Don Carlos Hills in northeastern New Mexico, data point NM 22). Dike trends are based on a visual regional average with the longest and most continuous dikes generally given the greatest weight. Again, as in the case of the fault slip data, individual measurements may be made with an accuracy of $\pm$ 1-2°. However, variations in any given area suggest that a more reasonable assessment of the accuracy of the stress orientation determination is $\pm$ 5-10°.

Finally, some discussion is warranted regarding the age of the geologic stress field indicators included in our study. In the western United States, only features less than 5 million years old and generally less than 3 million years old were included (the ages of specific points are indicated in a table of the data). Considerable stress field uniformity is found over this period in several areas. In the eastern United States two groups of data were used. The points in New England represent post glacial and Recent faulting. The tectonism in the Atlantic coastal plain, however, can only be shown to be of late Tertiary or Quaternary age. These points are individually discussed below.

Focal Mechanisms

Pressure (P-) and tension (T-) axes derived from earthquake focal mechanisms are the most commonly used indicator of tectonic stress. Unfortunately principal stress orientations obtained from fault plane solutions are inherently the least reliable indicators of stress orientation because the P- and T- axes cannot be equated with certainty to the greatest and least principal stress directions. McKenzie (1969) demonstrated that for the general case of triaxial stress, the only restriction on the greatest principal stress imposed by the fault plane solution is that this stress direction must lie in the quadrant containing the P-axis, but could in fact, be nearly at right angles to the P-direction. McKenzie's objections were based largely on the fact that most shallow, crustal earthquakes occur on pre-existing faults (rather than by the fracturing of intact homogeneous material) and that shear stresses at these shallow levels are much too small to produce failure. Raleigh et al (1972), however, pointed out that the strength of intact homogeneous rock is such that new faults will be generated

even if faults exist at unfavorable orientations. Using experimentally derived faulting relationships, Raleigh et al concluded that the P-axis (taken as 45° from the fault plane) could be in error by no more than 40° when sliding on a pre-existing fault produces the earthquake. Furthermore, they suggested that if the nodal plane corresponding to the fault is known, the P-axis (corresponding to the greatest principal stress) should be plotted at 60° to the normal of the fault plane and at 30° to the slip direction. In this case the orientation of the greatest principal stress would be in error by no more than 20°.

Unfortunately, selection of the actual fault plane is often difficult and the P- and T- axes standardly reported are at 45° to the nodal planes. Thus, it appears that the best method of analyzing focal mechanism data is to consider a number of earthquakes occurring on different faults in a particular area and then rely on average P- and T-directions. In this way, the errors due to slip on pre-existing planes of various trends will hopefully tend to cancel, giving the correct average P- and T-direction. There is evidence in the northern Basin and Range that this may in fact be the case. Zoback and Zoback (1979) presented a comparison of extension directions on major faults determined using fault slip data and of T-axes of focal mechanisms. Despite large scatter in the focal mechanism data (standard deviation = $\pm$ 25°, the mean directions and the geologically determined extension directions are probably within 3° of one another suggesting that the T-axes are fairly reliable indicators of least principal stress directions. Both Smith (1977) and Eaton (1979b) have also noted the regionally good correlation between earthquake P- and T- axes and nearby in-situ stress data throughout the United States. In the present study we have considered stress directions derived from individual focal mechanisms to have an accuracy of about $\pm$ 20°. We have attempted to rely, whenever possible, on averages of a number of solutions in any given area.

The best seismic coverage is in California where there are a number of detailed studies of focal mechanisms along segments of the San Andreas fault. From these studies the mean P- and T-axes were considered for the present compilation. Elsewhere in the United States coverage is largely from single event solutions and more rarely, from microearthquake composite solutions. However, in the central and eastern United States, the majority of the focal mechanisms used are from Herrmann (1979) and are constrained by both body wave and surface wave solutions.

For the purposes of this study we have assumed that two of the principal stress directions lie in a horizontal plane and the third is vertical. Thus, only horizontal stress axes inferred from the fault plane solutions which have plunges of less than 20° were considered. A few rare exceptions of T-axes with plunges up to 30° were included where the consistency of the stress orientation with surrounding data justify their inclusion. The information on the plunges of the P- and T-axes are included in the data table.

Compilations of fault plane solutions in the western United States by Smith and Lindh (1978), in the Rio Grande rift by Sanford et al (1979) and in the eastern United States by Sbar and Sykes (1977) and Herrmann (1979) were the primary data sources for the present study. However, we have attempted, whenever possible, to go back to original references and reject poorly constrained mechanisms and data which are internally inconsistent over small regions. Further details of particular focal mechanisms will be discussed in the sections on individual stress subprovinces.

In-Situ Stress Measurements

The third stress indicator used in this study is direct determinations of both the orientation and magnitude of the tectonic stress at depth. We have primarily considered measurements made with the hydraulic fracturing technique, currently the only method capable of measuring stress at large distances from free surfaces. The technique consists of hydraulically isolating a section of a well or borehole (by means of inflatable rubber packers), and pressurizing the isolated section until inducing a tensile fracture at the well bore. If the borehole is parallel to one principal stress (usually the lithostat), a vertical fracture forms at the azimuth of the greatest horizontal principal stress. This direction can usually be determined to better than $\pm$ 10°. However, repeated measurements at different depth intervals within a given borehole generally have a range of $\pm$ 15°. This is probably a more accurate estimate of the reliability of the method.

From the pressure-time history of hydraulic fracture formation and extension, the magnitude of both horizontal principal stresses can be computed. Assessing the accuracy of stress magnitudes yielded by any given measurement can be quite difficult and requires detailed knowledge of the pressure-time data and well conditions. Typically, the least horizontal principal stress can be determined with greater accuracy than the maximum, as the latter requires the assumption of linear elasticity around the well bore. The hydrofrac technique has been described in detail by Haimson and Fairhurst (1970) and others. McGarr and Gay (1978), Zoback et al (1977) and Zoback et al (1979) discuss interpretation of hydrofrac data at length. The compilations of hydrofrac stress measurements by Haimson (1977) and McGarr and Gay (1978) were used extensively in our study.

A number of other widely used stress measurement methods can be broadly categorized as stress relief techniques. These methods are all basically passive and involve measurement of the strain or displacement that occurs when the ambient stress field is relieved by techniques such as overcoring. The most significant drawback of stress relief techniques are that they typically cannot be used more than several tens of meters from free surfaces, and that the techniques seem to be extremely sensitive to local inhomogeneity in the rock. McGarr and Gay (1978) give an excellent review of these techniques and discuss many of the inherent difficulties.

Stress measurements made within several tens of meters of the surface have not been included in this study. Such measurements are susceptible to the pronounced effects of weathering, erosion, and deglaciation. Also, near surface fractures and joints can apparently act to decouple surface rocks from the tectonic stress field (see Haimson, 1978 and Zoback et al, 1979).

STRESS MAP OF THE COTERMINOUS UNITED STATES

Utilizing the three types of principal stress indicators discussed above we have assembled a map of least compressive principal horizontal stress for the coterminous United States. The data are numbered by states and presented on a map of physiographic province of the United States as Plate I. The legend defines the type of stress indicator used for each determination. Points in which more than one type of stress indicator were used are designated by multiple symbols. A description of each point is given in Table 1. We have assumed that regionally the horizontal components of the in-situ stress field represent principal stresses and that one principal stress is vertical. Evidence supporting this assumption includes observations of the nearly vertical attitude of dikes exposed over significant depths at a given locality (see Johnson, 1961) as well as the general paucity of exposed dikes which do not appear to have been emplaced vertically (D. Pollard, pers. comm.). In addition, measurements of the complete stress tensor in deep mines (McGarr and Gay, 1978) and the near horizontal orientations of the great majority of stress axes inferred from earthquake focal mechanisms also indicate that regionally the principal stresses are horizontal and vertical.

We chose to present one map showing a single stress axis, the least principal horizontal stress. The selection of the least principal stress direction (S_3) rather than the greatest principal stress direction (S_1) was biased by our observation of the consistency of this principal axis throughout a large portion of the western United States including the Basin and Range province, the Sierra Nevada, and along the San Andreas. In regions of active thrust or reverse faulting the least principal horizontal stress shown is actually S_2, the intermediate stress; thus, when using thrust focal mechanism data, the null axis was determined and plotted. However, in all other stress regimes the map indicates the least principal stress direction, S_3.

General Observations

The United States can be broken up into provinces according to the orientation and relative magnitudes of the principal stresses. These stress provinces seem to correspond, in a general way, with the physiographic provinces. The individual subprovinces will be discussed in detail as to the principal stress orientation and style of tectonism in the following section. At this point, however, there are a few important general observations that can be made from the map:

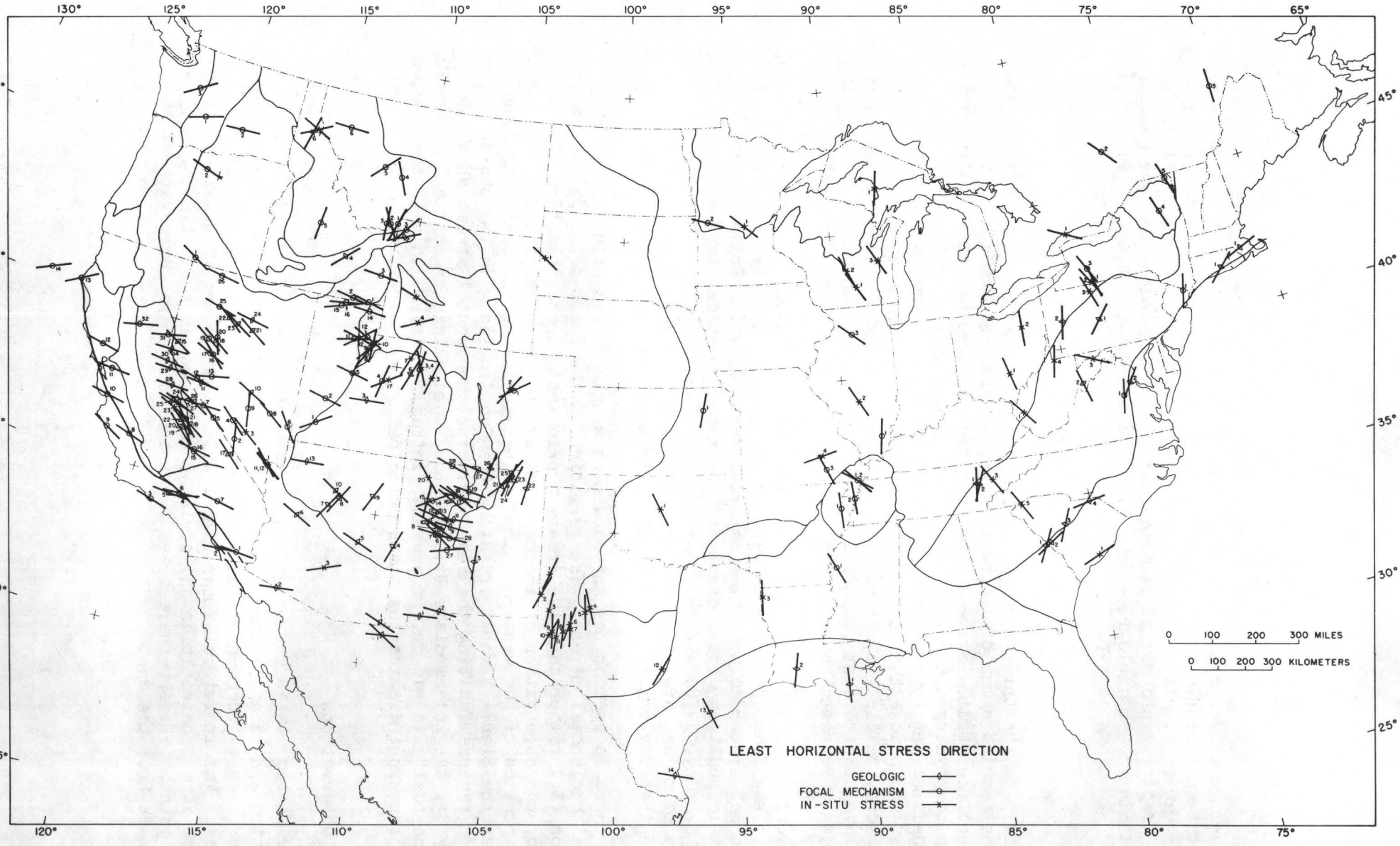
130°
125°
120°
115°
110°
105°
100°
95°
90°
85°
80°
75°
70°
65°
45°
40°
35°
30°
25°
0 100 200 300 MILES
0 100 200 300 KILOMETERS
LEAST HORIZONTAL STRESS DIRECTION
GEOLOGIC
FOCAL MECHANISM
IN-SITU STRESS

PLATE 1

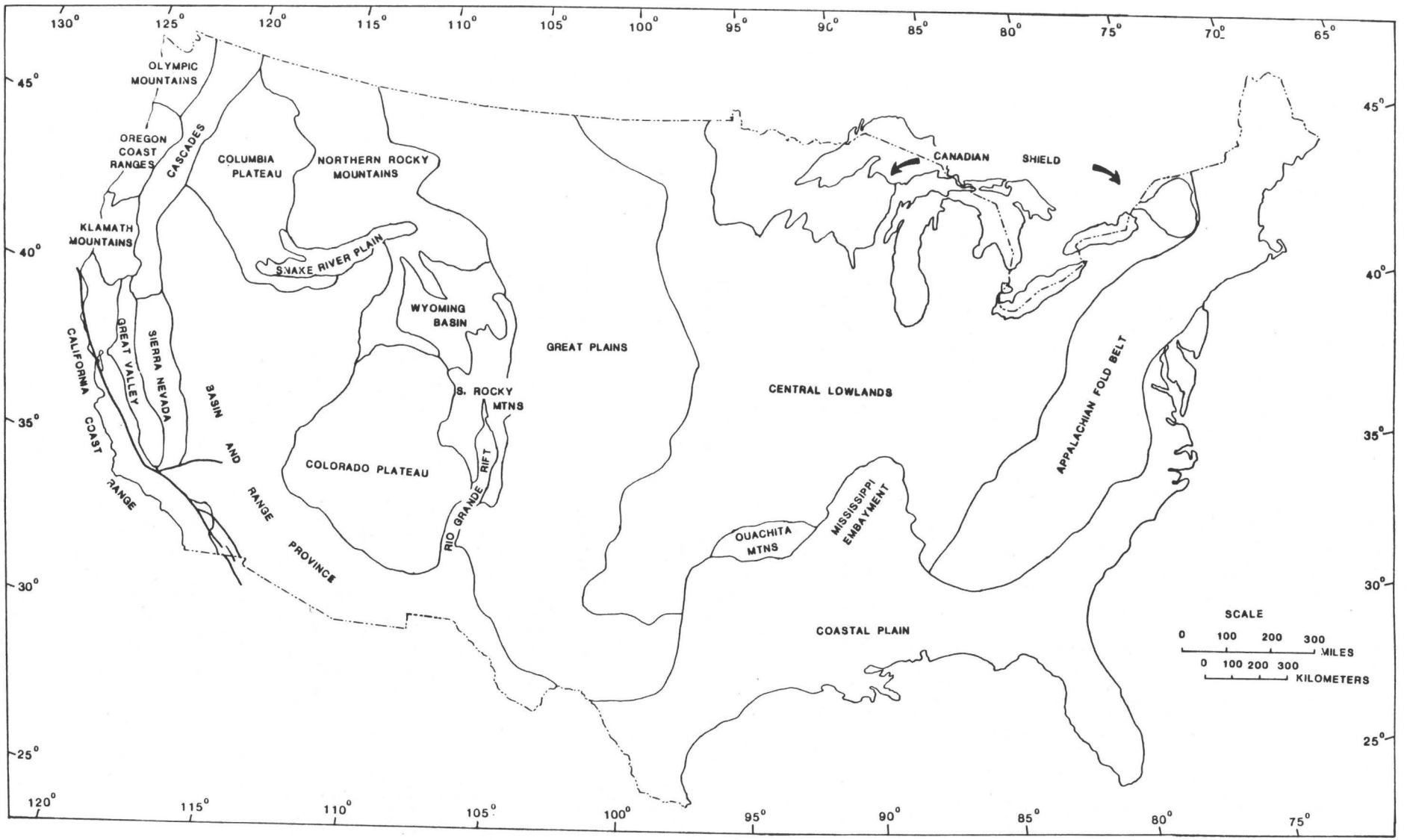

Plate 1a. Index map giving names of physiographic provinces indicated on Stress Map.

(1) In regions where more than one type of stress indicator is available there is a good correspondence between the results of the different methods, generally well within the estimated accuracy of the individual determinations.

(2) The intraplate stress field for the portion of the North American plate represented by the conterminous United States is not uniform. The western United States, a site of active tectonism characterized by a high level of seismicity and generally high heat flow, is marked by major variations in relative magnitude and orientation of the principal stresses. These variations have wavelengths which range from 150 to 2000 km. Even in the eastern United States, despite its relative tectonic quiescence, there appear to be several major variations in principal stress orientations.

(3) Broad regions of the crust (regions with linear dimensions as large as 2000 km in the eastern/central United States) can be characterized by a relatively uniform stress field (within ± 10-20°).

(4) Large changes in orientation of the principal stress field (up to 90°) can occur laterally over very short distances (less than about 75 km). These changes may result from an actual rotation of the principal stress field or a rapid change in the relative magnitudes of the principal stresses.

STRESS PROVINCES - WESTERN UNITED STATES

The western United States represents a broad zone of active tectonism as evidenced by the high level of seismicity (Figure 1), and generally high heat flow (Figure 7). As might be anticipated, the pattern of principal stress orientations in this region is complex. Figure 2 shows the western half of Plate I and indicates our interpretation of the different stress provinces of this region. Where data coverage is somewhat sparse we have also relied on the seismicity map (Figure 1), and Howard et al's (1978) map of young faults in the United States along with their accompanying discussion of regions of characteristic faulting to delineate the stress provinces. In regions of good data coverage, there appears to be a good general correspondence between the provinces Howard et al define on the basis of patterns and styles of faulting, and the provinces defined by stress magnitudes and orientations.

Pacific Northwest

This province is the only active volcanic arc and back-arc region within the coterminous United States; it includes the Pacific coastal ranges in Washington and Oregon, the Cascade andesitic volcanic chain, the Columbia

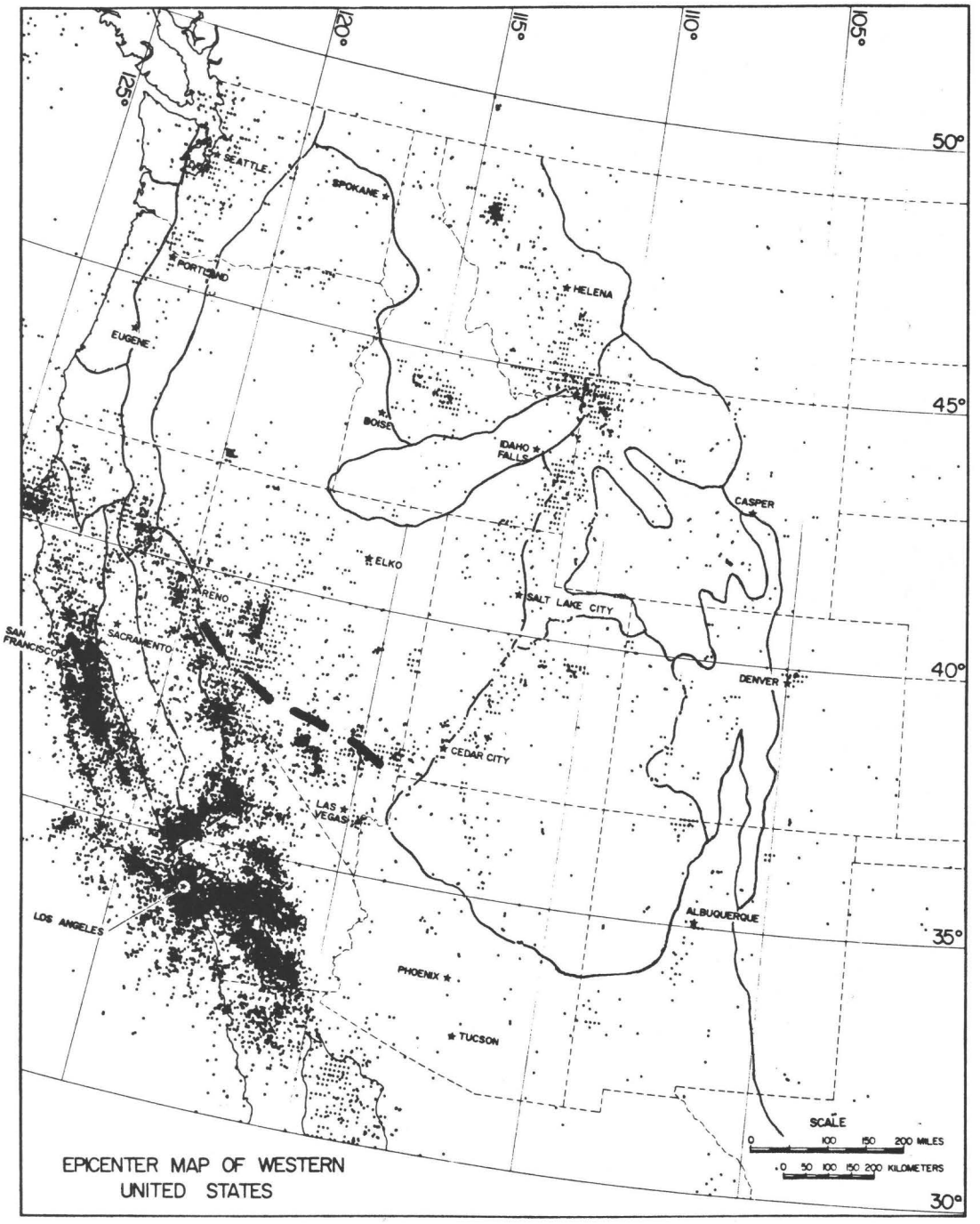

Figure 1. Seismicity map of the western United States (from Smith, 1978, used with permission). Data set includes primarily instrumentally located earthquakes from 1950 to 1972, but some older earthquakes are also incorporated. Events are not differentiated by magnitude. In California, minimum magnitude earthquakes plotted are M $\sim$ 1, for the rest of the western United States, M $\sim$ 3. Outlines of physiographic provinces have been added. Heavy dashed line in the southern part of the northern Basin and Range marks the approximate eastward extent of pure strike-slip fault plane solutions in this province.

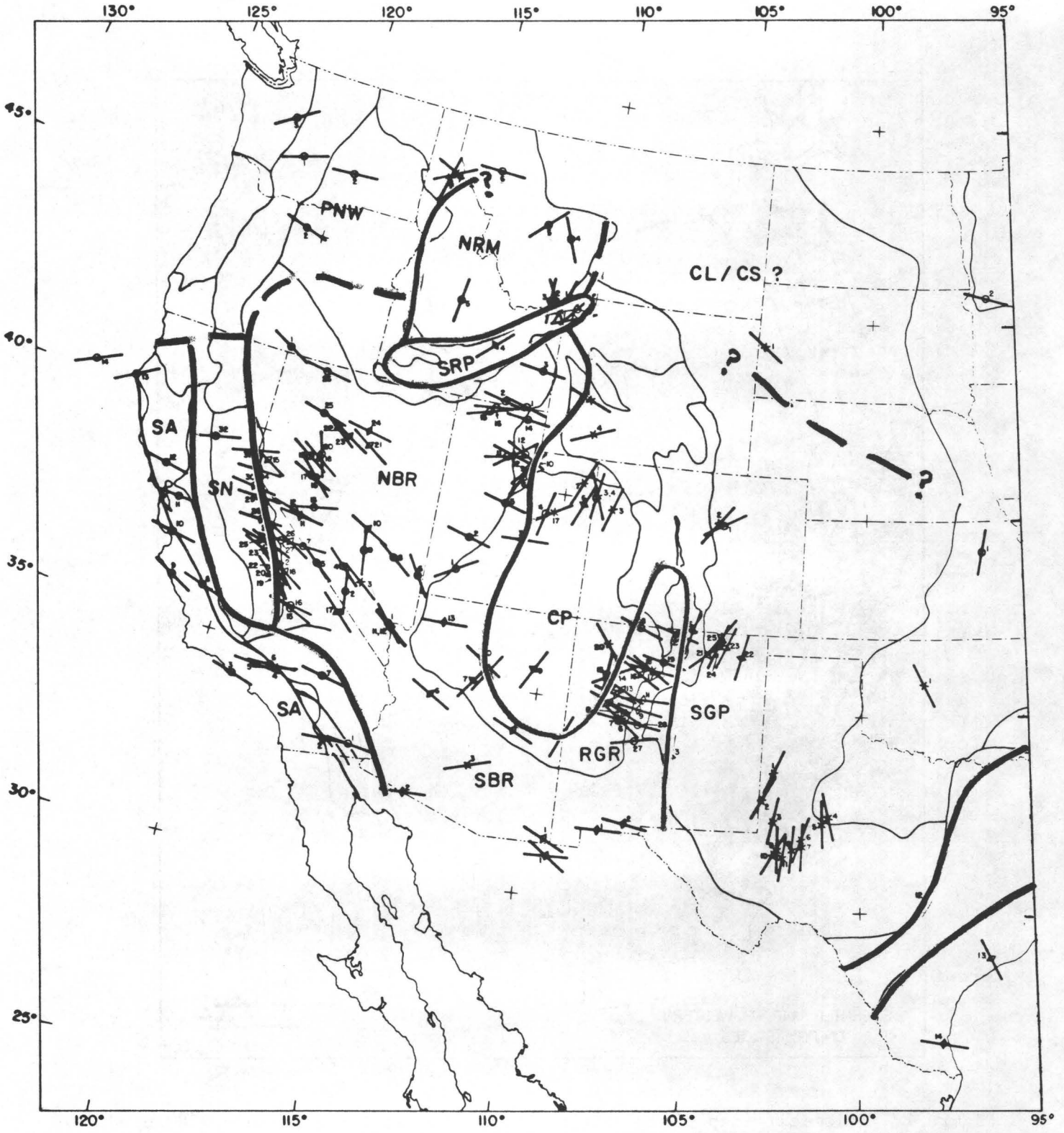

Figure 2. Map of western United States least principal horizontal stress directions with stress provinces discussed in the text indicated by thick, shaded lines. Names of the provinces are as follows: PNW-Pacific Northwest; SA-San Andreas; SN-Sierra Nevada; NBR-northern Basin and Range; SBR-southern Basin and Range; and RGR-Rio Grande rift--all part of the Basin and Range/Rio Grande rift stress province: SRP-Snake River Plain/Yellowstone NRM-Northern Rocky Mountains; CP-Colorado Plateau interior; GP-southern Great Plains; and CL/CS-Central Lowlands/Canadian Shield.

Plateau, and a portion of the northern Rocky Mountains. The following discussion draws heavily from excellent summaries of the regional stresses and tectonic setting of the Pacific Northwest by Davis (1977) and by Smith (1977, 1978).

The least principal horizontal stress throughout this region averages about east-west. However, the consistent stress axis appears to be the greatest principal stress (S_1), a N-S compression. Focal mechanisms indicate both strike-slip and thrust faulting, suggesting the least principal stress (S_3) can be either vertical or horizontal (E-W). This implies that regionally the intermediate stress (S_2) is approximately equal in magnitude to S_3. The relative magnitudes of the principal stress can be represented in the following manner:

$$S_1 > S_2 \simeq S_3 \quad \text{or}$$

$$S_{N-S} > S_{Vert} \simeq S_{E-W}$$

The predominance of strike-slip focal mechanisms suggests that the vertical stress may be, in general, the intermediate stress.

Two distinct regions of relatively active tectonism within the Pacific Northwest demonstrate contrasting styles of deformation resulting from the N-S compression. The Puget Sound-Olympic Peninsula is the site of several large historic earthquakes and also numerous Quaternary scarps with strike-slip and reverse movement. Further to the east in the central Columbia Plateau, a largely aseismic region, folding along east-west axes which began in Late Tertiary time have continued throughout the Quaternary (see Davis, 1977 for references).

The predominance of N-S compression within the Pacific Northwest distinguishes this region from the Basin and Range stress province to the south as the latter is characterized by WNW-ESE directed extensional tectonics. An approximately east-west zone at about 44.5°N latitude (roughly the northernmost extent of Basin and Range style normal faulting) separates these two regions. Smith (1978) identified this east-west zone as a relatively aseismic intraplate boundary that may extend eastward to either the edge of the aseismic Snake River Plain or to a NW-trending zone of earthquakes through the Idaho batholith (Figure 1). Blackwell (1978) has shown that an east-west thermal energy boundary coincides with this stress boundary.

The general N-S compression in the Pacific northwest is not consistent with estimates of northeast-southwest convergence between the Juan de Fuca and North American plate and suggests decoupling between the subducting Juan de Fuca plate and the over-riding North American plate (Davis, 1977). Such a decoupling may be consistent with estimates of a relatively slow rate of convergence and the absence of an inclined seismic Benioff zone beneath western Washington and Oregon. If this decoupling is the case, then the stress field may be more controlled by the larger scale transform motion between the Pacific and North American plates.

An alternate hypothesis to explain the N-S crustal shortening in the Pacific Northwest has been proposed by Smith (1977). Within the context of a subplate model of the entire western Cordillera he suggests that the N-S shortening in the Pacific Northwest may result from compression between the N-S extending Northern Rocky Mountain subplate (with a NW-trending western boundary) and the Juan de Fuca plate. The available stress data, however, while admittedly sparse, do not indicate a NW-trending western boundary for the Northern Rocky Mountain province.

San Andreas

The most seismically active region within the United States is the California coastal area which includes the San Andreas fault system. The San Andreas and many smaller parallel faults mark a major right-lateral transform plate boundary between the Pacific and North American plates.

Least principal horizontal stresses are relatively uniform throughout the region, trending E-W to WNW-ESE. The general strike-slip style of deformation indicates that this horizontal stress direction does in fact correspond to S_3. The relative magnitudes of the stresses are thus:

$$S_1 > S_2 > S_3 \qquad \text{or}$$

$$S_{\sim N-S} > S_{Vert} > S_{\sim E-W}$$

Exceptions to this general style of strike-slip deformation occur throughout the province on faults whose strikes are at large angles to the NW-SE San Andreas trend. Motion on these faults appears consistent with the regional stress field, i.e. thrust or reverse motion on E-W trending faults and normal displacements on N-S fault. The consistency of the P- and T-axes for slip on these faults of widely varying trends reinforces the use of average P- and T- directions as reliable indicators of the principal stress directions.

The most obvious example of a change in deformational style along the San Andreas occurs where the fault markedly changes trend in the big bend region in southern California. The post Miocene to present development of the Transverse Ranges is dramatic evidence of crustal shortening in this region (Jahns, 1973). Here, the fault system trends nearly east-west and the primary mode of deformation is folding and thrust or reverse faulting. This large scale thrust and reverse faulting requires a vertical least principal stress as opposed to the regional horizontal orientation of S_3. This apparent exchange (or rotation) of the principal stresses can be easily explained if in this region the least horizontal stress and the vertical stress are approximately equal in magnitude.

Crustal shortening in the big bend area can be thought of as resulting from the large left-stepping shift of the San Andreas. Similarly, in the

vicinity of en-echelon offsets between active strands of the fault, a change in deformational style can be expected. The geometry of these offsets require local crustal shortening in the case of left-stepping offsets and local crustal extension in the case of right-stepping offsets. Weaver and Hill (1979) have developed a model to explain the style of deformation and extension within the right-stepping offsets. This model was tested with data from two localities along the San Andreas fault. Active extension at one of these localities (Salton Trough) is strongly suggested by normal fault scarps (Sharp, 1976), high heat flow, and a few normal fault microearthquake focal mechanisms within the zone of offset. Weaver and Hill also report that the T-axes for fault plane solutions from earthquakes along the offset fault strands and within the offset volume are nearly invariant. This suggests that the direction of S_3 is not significantly perturbed from its regional orientation in the vicinity of the offsets.

The occurrence of normal faulting however, suggests that locally S is vertical rather than horizontal; this is the opposite of the big bend area where the thrusting indicates a vertical direction for S_3. Thus locally in the vicinity of the right-stepping offsets, the expected state of stress should be:

$$S_1 \simeq S_2 >> S_3 \qquad \text{or}$$

$$S_{Vert} \simeq S_{\sim N\text{-}S} >> S_{\sim E\text{-}W}$$

It should be pointed out that these right-stepping offsets are local and small scale features relative to the major left-stepping shift of the fault in the big bend area.

Also included in the San Andreas subprovince is the Garlock fault and the Mojave block. In middle to late Miocene time the Mojave block was deformed primarily by normal faulting along NW-trending faults (Dibblee, 1967). Current tectonism in this region as evidenced by recent seismicity, faulting, geodetic data, and generally subdued topography indicates primarily right-lateral strike-slip motion on these NW-trending faults and justify its inclusion as part of the general San Andreas system.

The Mojave block is separated from the Sierra Nevada and southwestern Great Basin to the north by the ENE-trending Garlock fault. The Garlock fault has been described as a major left-lateral fault conjugate to the San Andreas system (Hill and Dibblee, 1953) and also as a major continental transform which accomodates extension in the Basin and Range to the north relative to the Mojave block (Davis and Burchfiel, 1973). Westward shifting of the block to the north of the Garlock due to this extension has probably contributed to the westward bending or deflection of the San Andreas fault where the two faults meet (Davis and Burchfiel, 1973). Increasing fault offsets on the Garlock to the west support the transform fault interpretation. However, limited information on extension directions on normal faults north of the Mojave block indicate that the horizontal displacement may not parallel the Garlock fault as would be required for true transform-style faulting.

Sierra Nevada

The Sierra Nevada marks the transition from the primarily strike-slip deformation along the San Andreas to the extensional tectonics of the Basin and Range province. Accordingly, various lines of evidence on active tectonics of the Sierras indicate both strike-slip and normal faulting. Geologic investigations have revealed examples of pure shear deformation including the identification of the Kern Canyon fault, a major N-S trending right lateral fault ($\sim$80 km in length) which was active throughout late Tertiary time (Moore and duBray, 1978). However, the extensional tectonics of the Basin and Range province, including normal faulting and high heat flow, extend 50-100 km into the eastern Sierras. Lake Tahoe, for example, is a downdropped basin like those to the east in Nevada. Also, major earthquakes with both strike-slip (Truckee earthquake, 1966, CA-31) and normal (Oroville earthquake, 1975, CA-32) faulting mechanisms have been recorded in the northern Sierras.

Least principal horizontal stress directions trend WNW-ESE to E-W in the northern Sierras and appear to gradually rotate, trending approximately NW-SE in the southern Sierras. There is fairly good agreement within the Sierran block between stress orientations from different types of indicators. In addition, there is also good agreement with least horizontal stress directions in the surrounding San Andreas and Basin and Range province. A possible mechanism to explain the apparent clockwise rotation of the stress field from north to south is discussed in the Basin and Range/Rio Grande rift section.

The existence of contemporaneous strike-slip and normal faulting in the Sierras indicates that the vertical and greatest horizontal stress are nearly equal and can readily exchange relative magnitudes. The principal stress field is probably of the form:

$$S_1 \simeq S_2 >> S_3 \qquad \text{or}$$

$$S_{NNE} \simeq S_{Vert} >> S_{WNW}$$

Thus, local variations in the relative magnitudes of S_{NNE} and S_{Vert} determine whether strike-slip or normal faulting occurs.

A large number of the least principal stress directions in the Sierran block (CA 19-22, 24-25, and 28-30, Table 1) come from a unique study by Lockwood and Moore (1979) of offsets on near-vertical microfaults. These microfaults are oriented in conjugate sets, a north to northeast-striking set that shows right-lateral offset, and an east to northeast striking set which shows left-lateral offset. The maximum horizontal extensional strain (assumed to be regionally in the least principal stress direction) was taken as the bisector of the obtuse angle of the average microfault trends. A pure shear, constant volume analysis based on a detailed study of microfault offsets at one locality indicates that the true maximum extensional strain direction differed by only 6° from the bisector. Thus, use of the bisector of the average fault trends appears valid if the estimated accuracy of this geologic

stress indicator is taken as $\pm$ 10o. The age of this microfaulting is not well established; it developed after consolidation of the youngest plutons in the Sierras ($\sim$ 79 m.y.B.P.) and is known to cut a late Miocene volcanic dike in one area. Parallelism between the least principal stress orientations inferred from these microfaults with those in the surrounding San Andreas and Basin and Range province suggest that these faults are a young feature recording deformation in a stress field similar to the modern one.

Basin and Range/Rio Grande Rift

The Basin and Range province is a region of active crustal spreading characterized by high regional elevation, a thin crust, and high heat flow. The Basin and Range/Rio Grande rift stress province discussed here extends from the Sierra Nevada eastward to well within the Colorado Plateau physiographic province and extends around the southern margin of the Plateau and up into the Rio Grande rift proper in New Mexico. The Rio Grande rift is often referred to as a distinct continental rift; however, similarities in geophysical characteristics and tectonic style warrant its inclusion in the same stress province as the Basin and Range.

A broad zone of seismicity characterizes this province (see Figure 1). Modern seismicity, however, appears most concentrated along the margins of the northern Basin and Range (in the N-S trending Nevada seismic zone on the west and the intermountain seismic belt on the east). A roughly N-S trending belt of historic earthquakes of greater than about magnitude 7 occurs within the Nevada seismic belt. However, as Slemmons (1971) has pointed out, this pattern of modern seismicity is not a good indicator of tectonic activity in the recent past as Quaternary scarps are widespread throughout the northern Basin and Range.

Least principal stress indicators trend generally WNW-ESE throughout the Basin and Range/Rio Grande Rift province. Exceptions to this general pattern occur in southern Nevada (where the data are somewhat scattered but seem to indicate a more NW-SE directed least principal stress direction) and along the Wasatch fault where modern crustal extension appears to be more in an E-W direction. Possible explanations of these regional variations are discussed later in the section.

The primary mode of deformation within the Basin and Range/Rio Grande Rift is normal faulting with a consistent WNW direction of opening indicating a stress field of the form:

$$S_1 > S_2 >> S_3$$

$$S_{Vert} > S_{NNE} >> S_{WNW}$$

A detailed discussion of the relative magnitudes of these principal stresses constrained by an analysis of slip directions and pattern of faulting in northern Nevada has recently been presented by Zoback and Zoback, 1979.

A consistent direction of extension throughout much of the Basin and Range/Rio Grande Rift province arises from the relatively uniform pattern of horizontal displacements despite the complex geometry of the fault blocks. A necessary result of this uniform extension is oblique-slip normal faulting (that is, with both strike-slip and dip-slip components of motion) on faults which are not perpendicular to the least principal stress direction.

Examples of this oblique-slip style of faulting are abundant throughout the province. The geometry of the pattern of displacements requires pure dip-slip motion on approximately NNE-trending faults, a component of right-lateral slip on faults trending N to NW and a component of left-lateral slip on faults trending NE to ENE. Thus, modern components of right-lateral strike-slip should be expected on the generally NW-trending faults in the southern Basin and Range (in contrast to nearly pure dip-slip motion expected on the NNE-striking faults characterizing much of the northern Basin and Range). Scanty data on fault slip in the southern Basin and Range (AZ-7; MX-1; NM-6, 16, 27, Table 1) indicate that this is, in fact, the case.

It is important to point out that these oblique-slip faults are basically normal faults, not strike-slip faults. The oblique-slip arises as the major crustal blocks to attempt to extend in the least principal stress direction regardless of the trend of the fault.

While the majority of the Basin and Range province is characterized by normal faulting, the stress transition (from strike-slip deformation along the San Andreas) evident in the Sierra Nevada, extends into the westernmost Basin and Range (the Walker Lane-Las Vegas shear zone region). In this region, examples of pure, normal, strike-slip, and oblique-slip faults can be found.

Earthquake focal mechanisms indicate consistent T-axes regardless of the style of faulting (see Hamilton and Healy, 1969, for example). This zone of stress transition, as inferred from the distribution of pure strike-slip fault plane solutions, extends roughly 200-250 km eastward into the Basin and Range (see Figure 1). The relative magnitudes of the principal stresses within this region, as inferred from the co-existence of normal and strike-slip faulting are:

$$S_1 \simeq S_2 >> S_3$$

$$S_{Vert} \simeq S_{NNE} >> S_{WNW}$$

Thus, while locally the relative magnitudes of S_{Vert} and S_{NNE} can interchange, the S_3 (WNW) direction remains invariant.

As noted above, the general trend of ranges in the northern Basin and Range is NNE, roughly perpendicular to the modern least principal stress direction, suggesting development of this region in a stress field similar to the modern one. This NNE trending pattern of faulting is in marked contrast to the general NW-trending structural grain of the southern Basin and Range.

The Rio Grande Rift itself and the ranges within it trend roughly N-S and are generally believed to be following a zone of weakness resulting from superimposed earlier deformations (see Chapin and Seager, 1975, for example).

A low level of modern seismicity as well as geomorphic evidence (including the paucity of Quaternary scarps) argues that much of the deformation in the southern Basin and Range occurred earlier than in the northern Basin and Range. Detailed geologic investigations are beginning to verify this (see Eaton, 1979b for references). The general NW-trending structural grain of the southern Basin and Range suggests that the region developed largely under a stress field oriented differently than the modern one. Dated geologic indicators of stress orientation can be used to test this hypothesis. Miocene age dikes in Arizona and New Mexico have been found to trend NW-SE to NNW-SSE, approximately parallel to the trend of the ranges (Rehrig and Heidrick, 1976 and Zoback, 1979 and in prep.). The implied least principal stress direction (perpendicular to the dike trends) is SW-NE to WSW-ENE, roughly a 45o difference from the modern WNW-ESE least principal stress direction. This result agrees with evidence in the northern Basin and Range and Columbia Plateau reported by Zoback and Thompson (1978) for a similar 45o clockwise change in the least principal stress direction since mid-Miocene time. Structural relationships in one area in northern Nevada constrain this change in the least principal stress orientation to have occurred between 15 and 6 m.y.B.P. Changes in the trend of dikes and the style of deformation in the Castaneda Hills in northwestern Arizona suggest that in this region the clockwise change in least principal stress direction occurred some time between 12-7 m.y.B.P. (I. Lucchita, pers. comm.). A possible explanation of this phenomenon suggested by Zoback and Thompson (1978) is that early rifting in the Basin and Range was related to back-arc style deformation with the subsequent 45o clockwise change in least principal stress direction resulting from the superposition of right-lateral shear along the continental margin related to the development of the San Andreas transform.

Distributed right-lateral shear related to the San Andreas transform superimposed upon fundamental extension within the Basin and Range (probably initiated as a form of back-arc extension) has been proposed to explain the modern state of stress in this region (see for example Smith, 1977 and 1978; Eaton, 1979a,b and Eaton et al, 1978; Stewart 1978; and Zoback and Thompson, 1978). This distributed shear due to the relative plate motions fades away eastward as evidenced by the regional variation from WNW to NW directed extension on normal, oblique-slip, and strike-slip faults in the western Great Basin (northern Basin and Range) to approximately E-W directed, pure extension in the eastern Great Basin (Best and Hamblin, 1978; Eaton, 1979b and Eaton et al, 1978; and Smith 1977 and 1978).

A second major regional variation in least principal stress orientation within the Basin and Range (and possibly the Sierra Nevada) occurs in a broad E-W band transecting the southern Great Basin. Here, as mentioned previously, the least principal stress directions trend more northwesterly, representing a

clockwise rotation relative to the well-established WNW to E-W directed extension in the region to the north. This E-W band that crosses southern Nevada and Utah coincides with an E-W zone of seismicity and a major decrease in elevation from the Great Basin (mean elevation $\sim$1700 m) to the Arizona-New Mexico (southern) Basin and Range (mean elevation $\sim$750 m) accompanied by a nearly 100 mgal increase in gravity of crustal origin (Eaton et al, 1978). Presumably this E-W zone acts as the boundary between the actively extending region to the north and the currently tectonically quiescent southern Basin and Range. In this sense the zone can be viewed as a broad band of left-lateral, transform-style shearing consistent with focal mechanisms and geologic evidence (Stewart, 1978) in this region. Locally this left-lateral shearing (or drag resistance to this shearing) could cause a clockwise rotation of the stress field compatible with the more northwesterly trend of the least principal stress orientation observed in this region.

The available data indicate a rather abrupt transition in stress orientation from the Basin and Range/Rio Grande rift province into the Colorado Plateau and along the Great Plains/Rio Grande rift boundary. The extension of the Basin and Range/Rio Grande rift stress field well into the physiographic Colorado Plateau is consistent with high heat flow, faulting, and recent volcanism along the Plateau margins. These stress transitions will be discussed in more detail in the sections on the Colorado Plateau interior and the Great Plains.

Colorado Plateau

The Colorado Plateau stress province is distinctly smaller than the Colorado Plateau physiographic province (see Figure 2). The state of stress within the Plateau interior is discussed in detail by Thompson and Zoback (1979); their discussion is summarized below.

The Colorado Plateau interior is characterized by roughly NNE-SSW least principal horizontal stress orientation. This direction is perpendicular to the general WNW-ESE least principal stress direction in the surrounding Basin and Range and Rio Grande rift. The Basin and Range/Rio Grande rift stress field, however, appears to extend 100-200 km into the Plateau proper, with the actual stress transition possibly being rather abrupt occurring over distances of 75-100 km. Available data on the character of the marginal or "transition" regions of the Plateau (including thermal, structural, and seismic data - see Thompson and Zoback, 1979 for references) appears consonant with the extension of the Basin and Range/Rio Grande rift stress field into the Plateau.

The occurrence of both strike-slip and thrust focal mechanisms indicate a compressional stress regime in the Plateau interior; thus, the Plateau appears to be a region of compression between two zones of horizontal extension (Smith et al, 1974 and Smith and Sbar, 1974). This implies a different shear stress at the base of the lithosphere and seems inconsistent with the idea that the Plateau is merely an inherited, more coherent subplate subjected to the same stresses as its surroundings.

The lack of major faulting and/or seismicity within the Plateau interior indicates low differential stresses. Consistent with this regional observation, in-situ stress measurements (at $\sim$.5 km depth) in the Piceance Basin (CO-3) in NW Colorado indicated all three principal stresses were approximately equal to the lithostat (Bredehoeft et al, 1972). The occurrence of both strike slip and thrust focal mechanisms mentioned above further supports the existence of high horizontal stresses (locally exceeding the lithostat).

In the Basin and Range/Rio Grande rift province the least principal horizontal stress S_3 (WNW-ESE) must be sufficiently lower than the greatest principal stress S_1 (vertical) to allow failure. The consistent pattern of slip on Basin and Range faults suggests that

$$S_1 > S_2 >> S_3 \qquad \text{or}$$

$$S_{Vert} \gtrsim S_{NNE} >> S_{WNW}$$

whereas on the Plateau:

$$S_1 \gtrsim S_2 \simeq S_3 \qquad \text{or}$$

$$S_{WNW} \gtrsim S_{Vert} \simeq S_{NNE}$$

Thus, to convert the Basin and Range stress field to the Plateau field, S_{WNW} must be elevated to a value slightly larger than the other horizontal stress, S_{NNE}, and the vertical stress, S_{Vert}.

One possible mechanism capable of producing the compressional stress field on the Colorado Plateau may be related to density differences within the lithosphere/asthenosphere structure of the Basin and Range and the Colorado Plateau (Figure 3a). A static model of deviatoric stresses within the Colorado Plateau lithosphere arising from these density differences is shown in Figure 3b). Isostatic equilibrium is assumed for both the Colorado Plateau and the Basin and Range province and the depth of compensation (constant pressure) is the base of the Plateau lithosphere, approximately 80 km. The predicted state of stress at shallow lithospheric levels is deviatoric tension due largely to the lower density crust in the Basin and Range and also to the excess topography of the Plateau. The thick keel of mantle lithosphere under the Plateau, however is subjected to deviatoric compression arising from a "ridge push" force by the shallow Basin and Range and Rio Grande rift asthenosphere.

Physically, it seems plausible that the unsupported margins of the Plateau would be subjected to the deviatoric tension created by the crustal-level density contrasts; however, well within a flat plate (represented by the Plateau with a width to thickness ratio about 7.5) one might expect the deep stress effects to predominate resulting in compression within the plate interior. Qualitatively this model is consistent with the

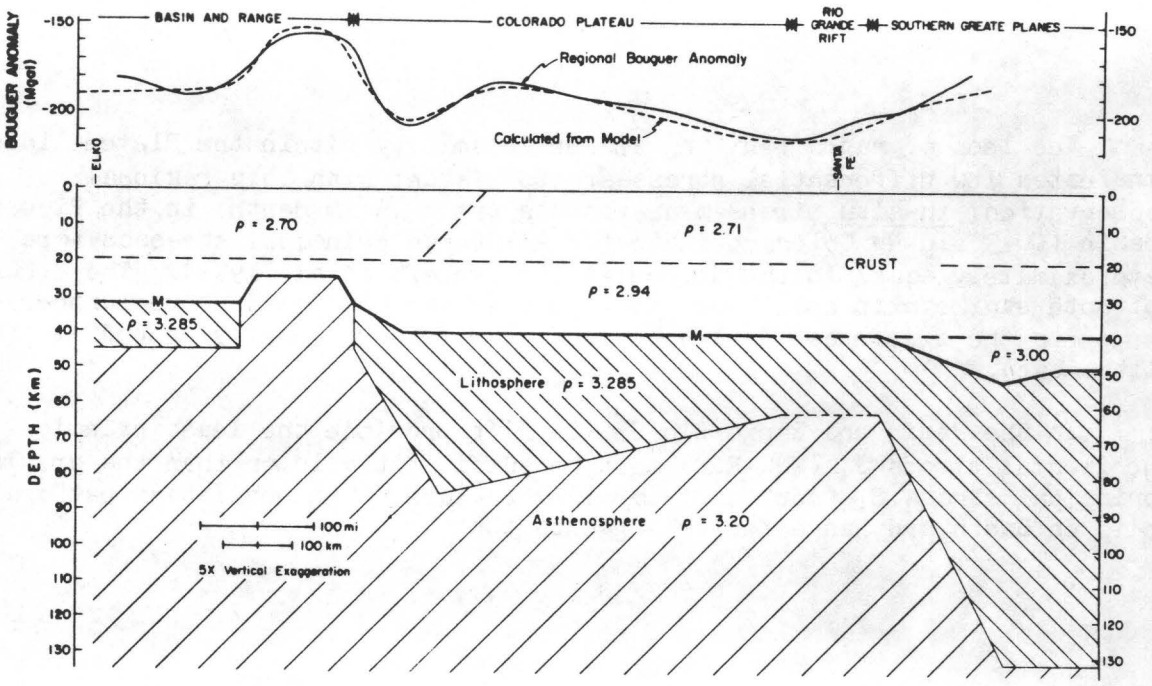

Figure 3(a). Gravity model of lithosphere/asthenosphere structure along a NW-SE trending section line running from Elko, Nevada through Santa Fe, New Mexico. Crustal structure constrained by seismic refraction data; lithosphere structure constrained by seismic and deep electrical data. From Thompson and Zoback, 1979.

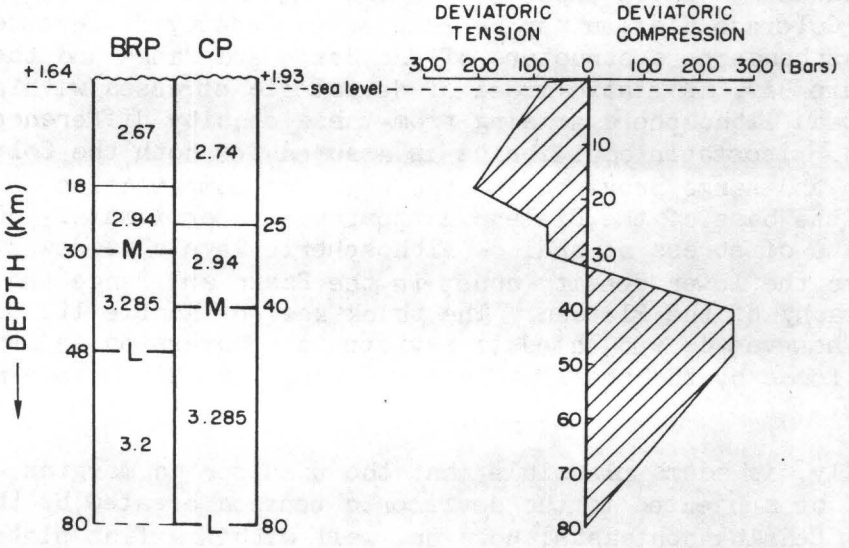

Figure 3(b). Shown on the left are comparative average density columns for the Basin and Range province and Colorado Plateau. On the right are shown computed static stresses acting on the Colorado Plateau at different levels derived from these density contrasts. Pressures (stresses) are assumed equal at the depth of isostatic compensation, taken as the base of the Plateau lithosphere, ∿80 km. From Thompson and Zoback, 1979

observation of normal faulting along the margins of the Plateau and compression within the Plateau interior.

The static model discussed above generates nearly uniform horizontal compressive stresses in the interior part of the Plateau block due to the roughly circular shape of the Colorado Plateau. To increase the magnitude of S_{WNW} above S_{NNE} an additional stress such as basal shear traction in the direction of regional spreading is required. Therefore it is interesting to examine available evidence on motions on the lithospheric plates relative to the deeper mantle.

Absolute motion of the Colorado Plateau relative to the deep mantle is generally in a southwesterly direction (approximately the direction of absolute motion of the North American plate as determined by Minster and Jordan, 1978--small additional motion due to the opening of the Rio Grande rift is nearly an order of magnitude lower and can be ignored for this discussion). Obviously, the orientation of principal stresses in the Plateau interior cannot be due simply to asthenospheric resistance to motion of the thick keel of mantle lithosphere underlying the Plateau; such a resistance would tend to increase compression in the direction of absolute motion of the Colorado Plateau block. This direction (NE-SW), however, is approximately the direction of <u>least</u> horizontal principal stress on the Plateau.

The actual extension direction of the BRP and RGR is roughly 45° oblique to the absolute motion of the North American plate; thus, the dynamic problem is quite complex. Certainly a ridge push force derived from the pressure disequilibrium due to the thick Plateau lithosphere must exist, but dynamic forces associated with regional extension in a roughly WNW-ESE direction are required to explain the 90° rotation of least principal stress from the Plateau interior to the Basin and Range/Rio Grande rift province. Smith (1977) has proposed that the roughly E-W compression within the Colorado Plateau occurs because of the buttress effect between the western deforming Cordillera and the eastward stable interior. Such an interpretation is valid only if there is a <u>fixed</u> boundary for the western deforming zone; if, however, this boundary is considered free, then extension in both the Rio Grande and Basin and Range province need not necessarily affect the Plateau stress field.

Snake River Plain/Yellowstone

The Snake River Plain is a downwarped volcanic plain formed in the last 17 m.y. by a steady northeast migration of silicic volcanism and subsequent semicontinuous outpourings of basalt along its older (western) reaches (Armstrong et al, 1975). The site of modern silicic volcanism on the plain is the Yellowstone caldera. The Snake River Plain/Yellowstone trend has been considered by some to be a propagating lithospheric crack (possibly aligned with pre-existing zone of weakness) and is thought by others, to mark an active hot spot trace. A least squares analysis of global relative plate motions indicate that the absolute motion of the North American plate for the

last 10 m.y. is well represented by the Snake River Plain/Yellowstone trend (Minster and Jordan, 1978). Rather than argue the relative merits of these two hypotheses, we present data on the present stress field within the Plain which may help constrain these and other models.

The Snake River Plain is largely aseismic with the exception of some shallow (< 6 km) earthquakes at Yellowstone. Thus, the only data available on principal stress orientations are geologic and come from numerous young (less than 1 m.y.B.P.) feeder vents which cut across the plain. As Weaver et al (1979) noted, these indicators suggest a roughly NW-SE least principal stress direction, parallel to the axis of the Snake River Plain, not perpendicular as originally suggested by Hamilton and Myers (1966). This extension along the axis of the Plain requires a transform-style of faulting along the margins of the Plain, particularly to the north.

The region immediately surrounding Yellowstone is marked by a high level of seismicity (see Figure 1). Detailed focal mechanism studies in this area by Trimble and Smith (1975), Smith et al (1977), and Pitt et al (1979) further document an approximately 90o rotation of the least principal horizontal stress direction moving onto the Snake River Plain from the northern Rocky Mountains first noted by Friedline et al (1976). This rotation occurs over a lateral distance of only 100 km.

The enormous volume of volcanism on the Snake River Plain and related normal faulting indicate extensional style tectonics. Thus, the stress field on the Snake River Plain can be characterized by

$$S_1 > S_2 > S_3$$

$$S_{Vert} > S_{NW} > S_{NE}$$

The orientation of the least principal stress on the Snake River Plain appears somewhat oblique to that in the Basin and Range province directly to the south, where the least principal stress direction trends WNW-ESE to E-W. This distinction in trend is the justification for making the Snake River Plain a separate stress province; it is possible, however, that it should be included as part of the Basin and Range province.

Northern Rocky Mountains

Available data in the northern Rocky Mountains suggest a distinct stress field relative to regions to the south and west. Stress indicators, though somewhat sparse, seem to indicate a least principal horizontal stress oriented approximately N-S. Locally, in the Yellowstone region, there is nearly a 90o difference in the least principal stress directions occurring over a lateral distance of less than 100 km as discussed earlier in the Snake River Plain/Yellowstone section.

The occurrence of both normal and strike-slip focal mechanisms in the Northern Rocky Mountains suggest a stress field of the form:

$$S_1 \simeq S_2 >> S_3$$

$$S_{\sim E\text{-}W} \simeq S_{Vert} >> S_{\sim N\text{-}S}$$

The tectonic style of this province also distinguishes it from the Pacific Northwest province where the predominant mode of deformation is compressional, with both thrust and strike-slip faulting.

It may be possible to include the Northern Rocky Mountains in a single stress province with the Colorado Plateau and Great Plains areas. However, the few scattered data points in South Dakota and eastern Colorado suggest additional complexity which appears to preclude delineation of a single continuous stress field through that region.

Southern Great Plains

The southern Great Plains area (with the exception of the point in Oklahoma) is characterized by a very uniform state of stress with the least principal horizontal stress oriented NNE-SSW. The data come from two primary sources: (1) alignment of volcanic feeders in the Raton-Clayton volcanic field in northern New Mexico, and (2) fracture orientations obtained from hydraulically fractured wells in the Permian Basin of west Texas (Zemanek et al, 1970). Data in eastern Colorado trend more NE to ENE. However, the poor data coverage regionally make it difficult to establish the validity and/or extent of this apparent rotation. On the basis of a single point to the north, near the Wyoming/South Dakota border, there appears to be a stress province boundary between the stress field of the southern Great Plains characterized by a NNE least principal horizontal stress direction and the western continuation of the Central Lowlands/Canadian Shield stress field characterized by a NW-trending least principal horizontal stress direction.

The only information on relative magnitudes of principal stresses comes from a single focal mechanism in eastern Kansas which indicates thrust faulting (D. W. Steeples, personal communication). The thrust motion implies a true least principal stress direction oriented vertically with the least principal horizontal stress actually representing the intermediate stress, S_2.

Two important characteristics of the southern Great Plains stress fields are: (1) its uniformity ($\sim \pm 15^o$ which is within the range of estimated accuracy of the different stress indicators) over a broad region of 800-1200 km on a side; and (2) a very abrupt transition in stress orientation relative to the Rio Grande rift which occurs over a lateral distance of less than 50 km. This approximately 90° change in least principal horizontal stress orientation along the Rio Grande rift-Great Plains boundary corresponds to a decrease in heat flow and a crustal and lithospheric thickening under the Great Plains relative to the Rio Grande rift (see Figure 4a and Thompson and Zoback, 1979).

STRESS PROVINCES - EASTERN UNITED STATES

Detailed discussion of the state of stress in the eastern United States is not included in this manuscript. Accompanying Figures 4 and 5 are also deleted. A complete discussion of the state of stress in the coterminous United States can be found in "Interpretative Stress Map of the Coterminous United States" by M. L. Zoback and M. D. Zoback referenced at the beginning of this paper.

DISCUSSION AND CONCLUSIONS

Stress Field Indicators

The generally good correspondence of the different methods used to determine stress orientations suggest that the criteria defined for the methods are basically sound. At the Nevada Test Site (NV-3), for example, all three of the methods have been utilized. Both hydraulic fracturing and overcoring at depth, geologic indicators, and strike-slip and normal faulting, as well as oblique-slip earthquake focal mechanisms yield very consistent results.

The least reliable stress indicator seems to be the overcoring measurements made in mines. For example, markedly different stress directions (and magnitudes) are observed for two measurements made in mines less than 3 km apart at nearly the same depth at Coeur d'Alene district in Idaho (ID-7) and the overcoring measurement in southern Missouri (MO-4) is completely inconsistent with surrounding earthquake and hydrofrac data. It is not clear if these methods are unreliable at times because of perturbations of the stress field due to the mining operations, or because of the fact that mines are typically located in areas of particularly complex geologic structure and history.

Hydraulic fracturing seems to be a reliable stress measurement technique when done at depths sufficient to avoid the effects of topography (see Haimson, 1979) and near surface fracturing (Zoback and Roller, 1979). For example, the eleven sets of hydrofrac measurements in west Texas (Zemanek et al, 1970) are all quite consistent.

Despite fairly large uncertainties inherent in using focal plane mechanisms for determining stress directions, the criteria previously mentioned generally results in good agreement between focal mechanisms and the other techniques. Focal mechanism data are probably most reliable when there are earthquakes occurring on fault planes of varying trend in a given area and the average of P- and/or T- directions can be used (see Zoback and Zoback, 1979). When small earthquakes occur in areas of sparse network coverage large errors can potentially occur. For example, this occurred in the case of earthquakes occurring near the Ramapo fault system; focal mechanisms initially thought to indicate steep normal faulting (Sbar et al, 1970) are now believed

to indicate steep thrust faulting (Aggarwal and Sykes, 1978). When possible, the use of surface waves to constrain focal mechanisms seems to be advantageous. An earthquake in the Attica, New York area (NY-3) is a good example. The stress direction resulting from the surface wave mechanism of Herrmann (1979) is more consistent with nearby stress measurements than that constrained by body waves alone (Fletcher and Sykes, 1977).

The geologic stress indicators considered here are also have difficulties. Dike trends and cinder cone alignments are not always linear and can be influenced by favorably oriented pre-existing fracture and joint sets. To use fault slip data correctly, major block movement should be considered. Anomalous small scale movements may occur between major blocks and thus yield erroneous results. The use of offset corehole data, such as that of Schafer (1979), can be questioned because the magnitudes and rates of movement are so large (centimeters of motion occurring in several years) as to seem possibly non-tectonic in origin.

Stress Provinces

On the basis of orientations and relative magnitudes of the principal stresses (determined from the current style of tectonism) the country has been subdivided into stress provinces. Figure 6 shows a generalized version of the stress map with the stress provinces indicated; a summary of the principal stress orientations and current style of tectonism for each of the different stress provinces is given in Table 2. It should be emphasized that these stress provinces, particularly in the East, will no doubt be refined or redefined as new data accumulates. The present boundaries appear to represent the most general interpretation of the stress data consistent with available geologic and geophysical information. More complex patterns could be drawn; however, present data coverage does not appear to warrant them.

In general, in the tectonically active western United States the stress pattern is complex and numerous distinct stress provinces can be well-delineated. In the central and eastern United States, it is apparent even from the relatively sparse data coverage that the state of intraplate stress is not uniform despite the relative tectonic quiescence of this area. The available data appear to define several major regions of consistent principal stress orientation. Also note that the stress provinces generally show a good correlation with the physiographic provinces, particularly in the western United States.

Within the stress provinces defined in this study, the orientation of the least principal horizontal stress field is generally uniform (to about $\pm$ 15°, within the estimated accuracy of the different methods used to determine stress orientations). In the case of the southern Great Plains and the Central Lowlands/Canadian Shield provinces, the orientation and possibly also the relative magnitudes of the principal stresses appear uniform over areas with linear dimensions up to 2000 km. At the other end of the spectrum, the

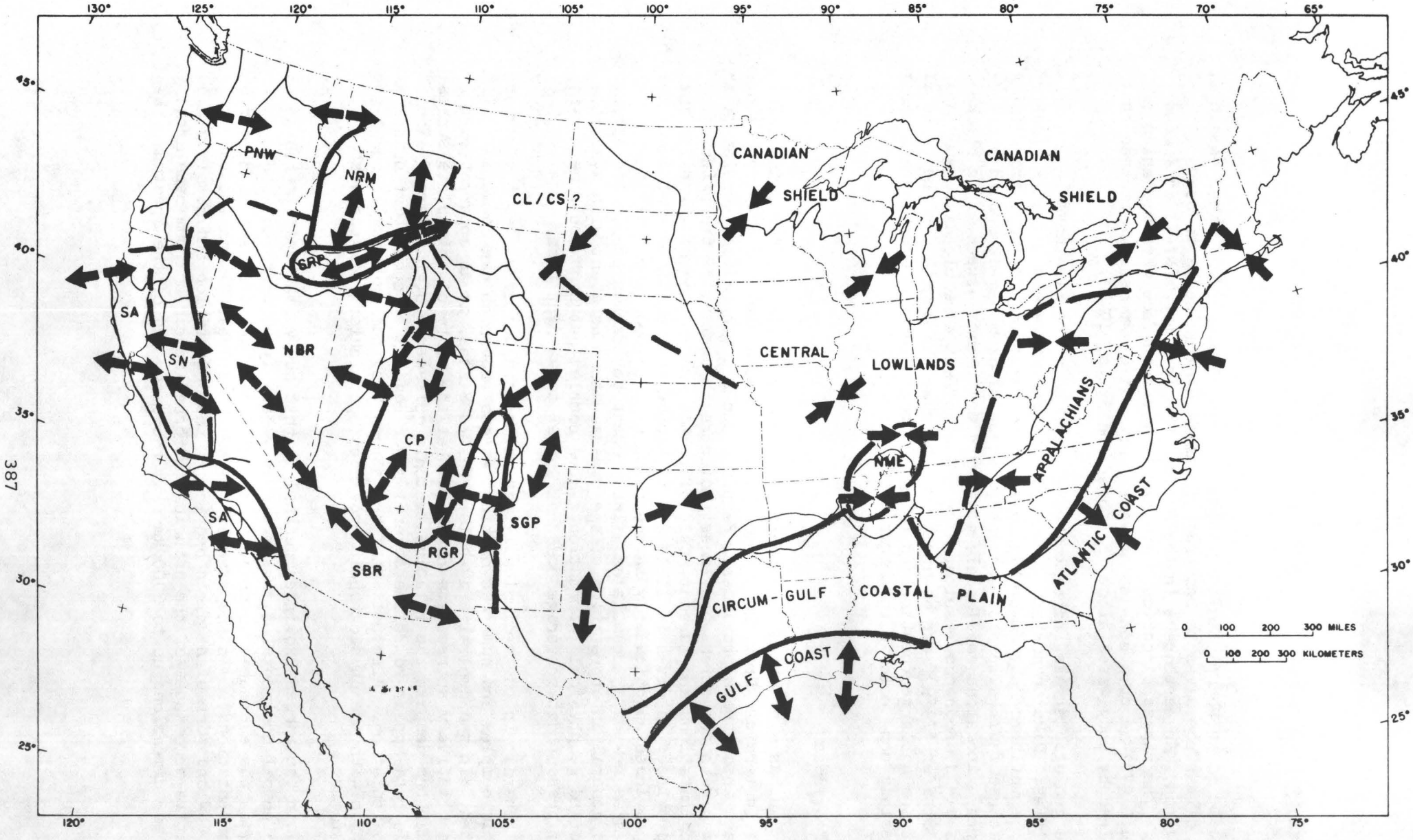

Figure 6. Generalized stress map of the coterminous United States. Stress provinces (indicated by thick lines) are discussed in the text and are the same as shown in Figures 2 and 4. Arrows represent direction of either least (outward-directed) or greatest (inward-directed) principal horizontal compression.

TABLE 2

Province	Primary Mode(s) of Faulting (Secondary Mode)[1]	Least Principal Horizontal Stress Direction	Comments
Pacific Northwest	T + SS	E - W	Both thrust and strike-slip focal mechanisms, Late Tertiary to Quaternary folding in eastern part of province.
San Andreas	SS (T)	WNW - ESE to E - W	Predominantly strike-slip deformation except in big bend region where is a large component of thrust and reverse faulting. Local normal faulting between right-stepping en-echelon offsets of the fault.
Sierra Nevada	N + SS	WNW - ESE to NW - SE	Region of stress transition from the San Andreas to the Basin and Range.
Basin and Range/ Rio Grande Rift	N (SS)	WNW - ESE locally E - W and NW - SE	Region of active crustal spreading by distributed normal and oblique-slip normal faulting. Westernmost part of region exhibits both pure strike-slip and pure normal faulting.
Colorado Plateau interior	SS + T	NNE - SSW	Very low level of tectonic activity, near hydrostatic stress?
Snake River Plain/ Yellowstone	N ?	NE - SW to ENE - WSW	Smallest distinct stress province, characterized by a least principal stress direction parallel to the axis of the Plain, not perpendicular to it.
Northern Rocky Mountains	N + SS	N - S	Abundant Late Tertiary normal faulting, moderate level of modern seismic activity. Abrupt stress transition (over less than 100 km) to Snake River Plain.
Southern Great Plains	T ?	NNE - SSW	Very uniform stress field over broad region (800-1200? km), abrupt stress transition to Rio Grande rift (less than 50 km).
Central Lowlands/ Canadian Shield	T + SS	NW - SE	Stable interior of the United States, broad region of uniform northeast-southwest compressive stress field. Few earthquakes in region show components of thrust and strike-slip motion.
Atlantic Coast	T ?	NE - SW	Earthquakes associated with Ramapo fault and geologic evidence indicates thrust faulting resulting from compression generally perpendicular to the continent. Faulting in Charleston, South Carolina, area may be more complex.
Appalachians	?	∿N - S locally NE - SW, NW - SE	This province is defined to represent a stress field intermediate between that of the AC and CL/CS stress provinces. Although approximately east-west compression is observed, local variations, especially near the western boundary, are observed.
Northern Mississippi Embayment	SS + T	N - S locally NW - SE	Site of great New Madrid earthquakes of 1811-1812 and of continuing high level of intraplate activity. Focal mechanism data suggest local reorientation of stress field in the vicinity of New Madrid.
Gulf Coast	N	N - S to WNW - ESE	Active listric normal faulting resulting from sediment loading defines this province. Faults strike sub-parallel to continental margin.
Circum-Gulf Coastal Plain	-	-	Only two measurements in this province inadequately describe the stress field. The active listric normal faulting of the Gulf Coast is defined to be southward of this now quiescent province.

smallest regions characterized by a distinct stress field are found in the western United States. Both the Rio Grande rift and the Snake River Plain stress provinces have widths on the order of 150-200 km and exhibit differently-oriented stress fields and different styles of tectonism relative to surrounding areas.

In addition, there exist broad regions, up to 1000 km wide, crossing stress province boundaries which are characterized by a relatively uniform least principal stress direction. In these areas, the distinction of the different provinces is based solely on the relative magnitudes of the principal stresses and the style of deformation. The most obvious example of this is in the western United States where the least principal stress direction in the San Andreas, Sierra Nevada, and Basin and Range/Rio Grande rift provinces is fairly uniformly WNW-ESE. If this distinction is broadened to include regions with similarly-oriented principal stress axes (NNE, WNW, and vertical) but with different relative magnitudes for the horizontal stresses, then both the Colorado Plateau interior and the southern Great Plains can also be included. Principal stress axes for regions in the Pacific Northwest, however, appear somewhat oblique to those to the south.

Available data on the transition in orientation between different stress provinces indicate that these transitions can be abrupt, occurring over less than 75 km in the case of the Rio Grande rift-southern Great Plains transition. Data around the Colorado Plateau margins suggest the existence of a zone 50-100 km wide where the two horizontal principal stresses are approximately equal in magnitude and the direction of the least horizontal stress alternates between the two. There appears to be two ways in which the stress transition can occur: either by actual rotation of the stress field as reported in the Northern Rocky Mountains-Snake River Plain/Yellowstone transition (Friedline et al, 1976; Smith et al, 1977; and Pitt et al, 1979), or by a switch of relative magnitudes of the principal stresses as appears to be the case for the Basin and Range/Rio Grande rift-Colorado Plateau interior and the Rio Grande rift/southern Great Plains transition.

In contrast to these sharp stress transitions in the tectonically active western United States, in the eastern United States a broad zone of stress transition (about 500 km wide) appears to separate a region of predominantly northwest compression along the Atlantic Coast from the predominantly northeast compression characterizing the Central Lowlands/ Canadian Shield region. Within this broad zone of transition, stress orientations are generally intermediate in direction between those in the two surrounding regions (that is, the maximum principal horizontal stress orientation is approximately E-W). However, examples of both northwest and northeast compression can be found within this transitional province indicating that its boundaries are diffuse and ill-defined.

On the basis of the stress orientation data described above, the eastern United States (exclusive of the Gulf Coastal Plain and the northern Mississippi Embayment) was subdivided into three major provinces with

northeast trending boundaries. These provinces are strikingly similar to the central, eastern, and western provinces in the east defined by Diment et al (1972) on the basis of the general level of gravity anomalies, crustal thickness, seismic velocity and attenuation, and heat flow. Most of these geophysical characteristics appear related to the modern structure and/or composition of the crust which is, of course, the product of past geologic processes. The variation in physical properties of the crust may, however, have an important effect on the stress field. One mechanism for producing compression perpendicular to a passive continental margin (as seems to be the case for the Atlantic Coast province and other passive margins around the world - see Yang and Aggarwal, 1979) arises from density contrasts in the crust and uppermost mantle between the thin oceanic crust and the adjacent continental crust (see for example, Theilen and Meissner, 1979).

Constraints were placed on the relative magnitude of the principal stresses using information from the measured magnitudes of in-situ stress and, largely, on the current style of deformation within each region. In the western United States the high level of seismicity and broad zone of active faulting indicates generally large stress differences. In the eastern United States the seismicity is concentrated and it is unknown whether the regions of high seismicity occur within localized zones of weakness or if they result from some mechanism which is producing local stress concentration.

Styles of deformation can be broadly categorized into two main groups based on the relative magnitudes of the principal stresses: a predominantly extensional mode in which the least principal stress is near horizontal and remains invariant, and a predominantly compressional mode in which the greatest principal stress is horizontal and remains invariant. Obviously, one end member of the extensional mode is pure normal faulting whereas, pure thrust faulting is the corresponding end member of the compressional mode. Pure strike-slip faulting, such as occurs along much of the San Andreas, with the exception of the big bend area, represents the other end member in both modes.

Pure extensional tectonics are exhibited in the eastern Basin and Range, along the Gulf Coastal Plain, and probably also in the Rio Grande rift and the Snake River Plain. Regions of pure compressional tectonics, if they exist within the coterminous United States, are not well documented.

Much of the remainder of the United States exhibits a mixed style of faulting (Table 2). Regions characterized by predominantly extensional tectonics (normal and strike-slip faulting) are found in the western United States and include: the Sierra Nevada, the westernmost region of the Basin and Range province, the northern Rocky Mountains, and local regions along the San Andreas in the vicinity of right-stepping en-echelon offsets. Regions of predominantly compressional tectonics (strike-slip and thrust faulting) are located in the eastern and central United States and also within the western United States. These regions include: the Pacific Northwest, the big bend region of the San Andreas, the Colorado Plateau interior, the Atlantic Coast

province, the northern Mississippi Embayment, the Appalachian province, and the Central Lowlands/Canadian Shield area. The general aseismic character and lack of recent faulting in the southern Great Plains (and also the Central Lowlands/Canadian Shield region) make it difficult to categorize such regions in terms of relative magnitudes of principal stresses.

Comparison with Heat Flow Data

A map of least principal horizontal stress orientations presented in this study is shown overlain on the heat flow map of the United States of Lachenbruch and Sass (1977) in Figure 7. As can be seen in this figure, the general level of heat flow is much higher in the west than in the east. Also, in the west the pattern of heat flow is much more complex, marked by large regional variations (areas of both the highest and lowest heat flow in the United States are found in the west) and sometimes abrupt transitions between the major heat flow provinces (see Lachenbruch and Sass, 1977 and 1978; and Blackwell, 1978 for discussion of the heat flow provinces in the western United States). As mentioned earlier similar features (a complex pattern, major regional variations and abrupt transitions) also characterize the modern stress field of the western United States. In particular, there is a generally good correlation between the stress data and heat flow data in the actively extending Basin and Range/Rio Grande rift region and along its margins. This broad region of crustal rifting is characterized by a mean heat flow of about 2.1 HFU ($\mu cal/cm^2 sec$), well above the continental mean of about 1.5 HFU (Lachenbruch and Sass, 1978).

There is a fairly good correlation between the regions of high heat flow and the lateral extent of rifting. This is most notable on the Colorado Plateau where the high heat flow and associated young faulting and Quaternary volcanism extends well inward of the Plateau physiographic boundary (Thompson and Zoback, 1979). A Colorado Plateau interior of relatively uniform average heat flow ($\sim$1.5-1.6 HFU) can be defined which is similar to the Plateau interior defined on the basis of the stress data (Thompson and Zoback, 1979, and Reiter et al, 1979). The worst correlation occurs along the Rio Grande rift/southern Great Plains boundary in northern New Mexico. Here the stress transition is well controlled by data from young volcanic fields in both the Rio Grande rift and the southern Great Plains. As might be expected because of the young volcanism on the Great Plains, the high heat flow extends through this region and the actual heat flow transition lies to the east.

New data on heat flow in the Mojave block (San Andreas stress province) are quite uniform and reveal a mean heat flow of about 1.6 HFU (Lachenbruch et al, 1978). The heat flow rises sharply to the east along a north-northwest-trending boundary that coincides with the eastern limit of active seismicity and a change from predominantly strike-slip to normal faulting within the Basin and Range province.

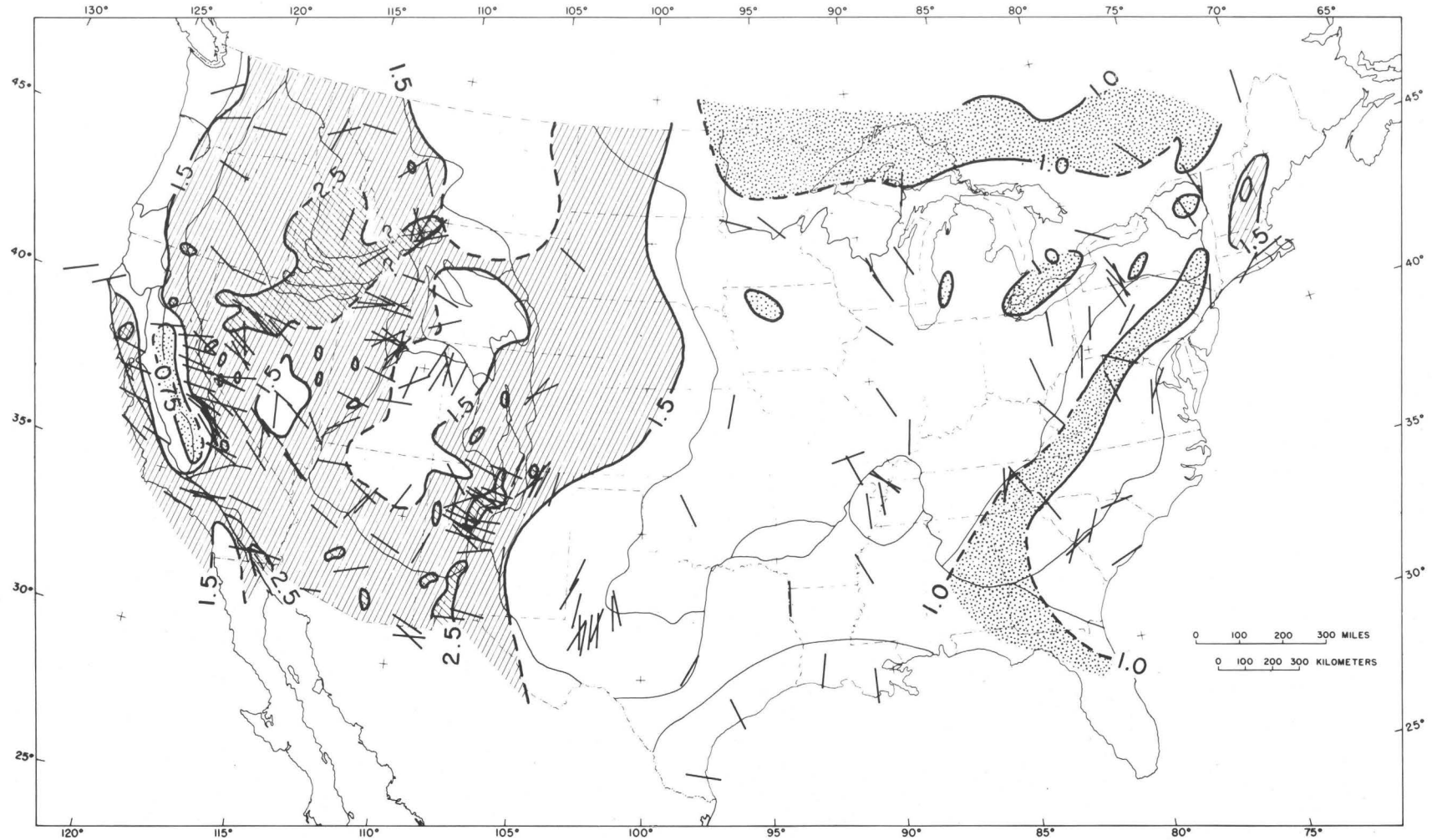

Figure 7. Comparison of least principal horizontal stress orientation with heat flow. Heat flow data are from Lachenbruch and Sass (1977). In the western United States the cross-hatched area is >2.5 HFU, hachured area is 1.5 to 2.5 HFU, unshaded area is 0.75 to 1.5 HFU, and stippled area is <0.75 HFU. In the east the hachured area is >1.5 HFU, unshaded area is 1.0 to 1.5 HFU, and stippled area is <1.0 HFU.

Lachenbruch and Sass (1978) have developed thermo-mechanical models compatible with observed extension rates to explain the high surface heat flow in the Basin and Range province. These models require convection (either solid state or by magmatic intrusion) in the crust and uppermost mantle. Such models are consistent with gravity data which require that an influx of mass must accompany the horizontal extension in this province (Thompson and Burke, 1974).

Such shallow level thermal sources are consistent with abrupt heat flow transitions along the margins of the Basin and Range/Rio Grande rift province. The Sierra Nevada/Basin and Range heat flow transition has been found to occur over less than 20 km in places (Sass et al, 1971, and A. H. Lachenbruch, pers. comm.). Data on the eastern Basin and Range/Colorado Plateau heat flow transition are sparse; however, available data limit this transition to less than 75 km (Chapman et al, 1979). The Colorado Plateau/Rio Grande rift heat flow transition is also abrupt, occurring over less than about 50 km (Reiter et al, 1975, and Thompson and Zoback, 1979).

These abrupt heat flow transitions are consistent with the abrupt stress transition found along the margins of the actively extending regions and indicate shallow level sources (crust or uppermost mantle) for both the extensional stresses and the heat. The excellent correlation both in the pattern and the transition between provinces of the heat flow and stress data suggest that the stresses responsible for rifting are intimately linked to the thermal processes.

Regional variations in heat flow in the eastern United States are generally small and believed to be non-tectonic in origin, arising from variations in radioactive heat generation (Diment et al, 1972). However, one possible thermal anomaly of tectonic origin in the east has been identified by Swanberg et al (1979) in the New Madrid (northern Mississippi Embayment) region using heat flow data and several hundred bottom hole temperature measurements. They report that the bottom hole temperature data revealed a small, but well defined, thermal anomaly associated with the most seismically active area and that the heat flow values within the seismic zone were slightly high relative to the rest of the stable interior. The absolute values of the heat flow (1.3-1.6 HFU) are not, however, sufficiently above the midcontinent mean to verify the existence of a major heat flow anomaly. Swanberg et al favor the interpretation of a small convective heat flow component resulting from deep groundwater circulation along upper crustal fractures associated with the active faulting in this region to explain the local thermal anomaly. Silica geothermometry data suggest a possible thermal anomaly in the Charleston region (Swanberg and Morgan, 1978); however, heat flow measured in a 790 m deep well near the site or the 1886 Charleston earthquake was 1.3 HFU (Sass and Ziago, 1977), similar to measurements made in surrounding regions.

Sources of Stress

In this section we briefly discuss sources of lithospheric stress, the manner in which the stress field changes at province boundaries, and the ephemeral nature of stress fields in tectonically active areas.

Possible sources of lithospheric stress active within the coterminous United States are:

1. Plate interactions along the Pacific coast -- The strike-slip deformation within the San Andreas-Sierra Nevada-westernmost Basin and Range province is a direct manifestation of the right-lateral motion between the North American and Pacific plates. Distributed shear related to this transform boundary appears to be superimposed on spreading in the Basin and Range province which was initiated in a back-arc setting in Miocene time (in response to earlier plate interactions along the Pacific coast) (see for example Zoback and Thompson, 1977; Smith, 1977, 1978; and Eaton, 1979a). An approximately 45° clockwise change of the least principal stress orientation in the Basin and Range province since mid-Miocene time is postulated to have occurred in response to the superposition of right-lateral shear corresponding to the development of the San Andreas (Zoback and Thompson, 1977).

Principal stress orientations in the Pacific Northwest do not appear related to the direction of convergence determined for the subduction of the Juan de Fuca plate under this region. The stress orientations however, are consonant with the larger scale transform motion between the Pacific and North American plates (Davis, 1977).

2. Asthenospheric resistance to plate motion -- Absolute plate motion models ascribe a roughly SW direction of motion for the stable part of the U. S. relative to the deep mantle (Minster and Jordan, 1978). Lithospheric thicknening under the eastern and central U. S. (relative to the western U. S.) has resulted in a thick keel of mantle lithosphere underlying this region. Asthenospheric resistance to motion of this keel may explain the general pattern of NE-SW compression in the central Lowlands/Canadian Shield area. Richardson et al, (1979) have found that models of global stresses resulting from plate interaction are best matched to intraplate stress data when asthenospheric viscous forces resist rather than drive plate motions.

3. Ridge-push forces acting at passive continental margins -- Yang and Aggarwal (1979) have recently suggested that compression perpendicular to passive continental margins may be a general characteristic of these margins originating from ridge push forces transmitted to the continent through the oceanic crust. Stress data along the eastern seaboard do appear to indicate, in general, compression perpendicular to the continental margin.

4. Density differences in regions of abrupt changes in lithosphere/ asthenosphere structure -- A mechanism for producing shear tractions on the base of the lithosphere which are analogous to ridge push forces has been proposed by Thompson and Zoback (1979) to explain in part, both the general state of compression and the 90o rotation of the least principal horizontal stress direction in the Colorado Plateau interior. Static stresses are speculated to arise from pressure differences created when a thick keel of mantle lithosphere (under the Plateau) is surrounded by shallow, less dense, asthenospheric mantle. Similarly this mechanism may apply to crust and uppermost mantle thickness changes along passive continental margins and result in compression perpen- dicular to the coast (Theilen and Meissner, 1979).

5. Sediment loading -- Stresses arising from sediment loading are generally believed responsible for the normal ("growth") faulting along the Gulf Coastal Plain.

6. Boundary drag resistance -- A second order effect, drag resistance to the relative motions of subplates, appears to be capable of locally rotating the regional stress field. An example of such an effect may be the rotation of the least principal stress orientation in southern Nevada and Utah. This rotation occurs along a broad "transform" zone which separates the actively extending Great Basin (northern Basin and Range) from the presently more quiescent southern Basin and Range. Numerical studies by Fujita and Sleep (1979) predict such a rotation of the regional stress along ocean-ridge transform faults.

The abrupt transitions observed in the orientation and/or magnitude of the in-situ stresses in the western United States implies a shallow (crustal or uppermost mantle) source of these stresses. These abrupt transitions are found only in areas of active extensional tectonics (Basin and Range, Rio Grande rift, Snake River Plain). The accompanying high heat flow in these regions also show abrupt transitions and thus similarly imply sources in the crust or uppermost mantle level sources. As mentioned previously, the excellent correlation of these two phenomena indicate that the stresses responsible for rifting are intimately linked to the thermal processes; whereas in the relatively quiescent eastern United States, the apparently broad (approximately 500 km wide) region of stress transition (the Appalachian province) suggests stresses derived from broad/deep sources. Both asthenospheric resistance to plate motion (to produce the northeast-southwest compression in the CL/CS province) and transmitted ridge push (to produce compression perpendicular to the continental margin in the Atlantic Coast province) represent such broad/deep sources. In terms of broad/deep sources of stress, the apparently complex nature of the stress field in the transition zone is not unexpected; it may result from differences in structural or geologic provinces.

A final note should be added on the apparent ephemeral nature of regional stress fields in areas of active tectonism. In the Basin and Range province there is evidence of an approximately 45o clockwise change of the least principal orientation since mid-Miocene time (Zoback and Thompson, 1977). Detailed data in one area suggest that this change occurred between 15-6 m.y.B.P. The general trend of ranges in the northern Basin and Range, roughly perpendicular to the modern least principal stress direction, suggests that this change may have occurred very rapidly (< 5 m.y. ?). Data are now accumulating which strongly suggest a markedly different orientation of the least principal stress in this region during Oligocene-early Miocene time ($\sim$30-25 m.y.B.P.) (Rehrig and Heidrick, 1976; and Zoback, M. L., in prep.). Thus, stress fields in tectonically active regions can be relatively short-lived (< 10-15 m.y. ?). Unfortunately, data on the maximum length of time that a given stress regime may be maintained in a stable cratonal region is much more difficult to obtain.

REFERENCES

Abou-Sayed, A. S., C. E. Brechtel, and R. J. Clifton, In-situ stress determination by hydraulic fracturing: a fracture mechanics approach, J. Geophys. Res., 83(B6), 2851-2862, 1978.

Aggarwal, Y. P., and L. R. Sykes, Earthquakes, faults, and nuclear power plants in southern New York, Science, 200, 425-429, 1978.

Aggarwal, Y. P., J. P. Yang, and E. Cranswick, Seismological investigation in the Adirondacks and environs (abstract), Geol. Soc. Amer. Abstr. Program, 9, 234, 1977.

Aggson, J., Report on in situ determination of stresses, Mather Mine, Ishpeming, Michigan, U.S. Bur. Mines Prog. Rep., DMRC 10006, 1972.

Aggson, J. R., and V. E. Hooker, In-situ rock stress determination: techniques and applications, Underground Mining Handbook, Soc. of Mining Eng. of AIME, in press, 1979.

Akers, J. P., J. C. Shorty, and P. R. Stevens, Hydrogeology of the Cenozoic igneous rocks, Navajo and Hopi Indian Reservation, Arizona, New Mexico, and Utah, U.S. Geol. Surv. Prof. Paper 521-D, 18 pp., 1971.

Algermissen, S. T., and S. T. Harding, The Puget Sound, Washington, earthquake of April 29, 1965, Preliminary seismological report, U.S. Coast and Geodetic Survey, Rockville, Maryland, 1965.

Anderson, C. A., E. A. Scholz, and J. D. Strobell Jr., Geology and ore deposits of the Bagdad area, Yavapai County, Arizona, U.S. Geol. Surv. Prof. Paper 278, 103 pp., 1955.

Anderson, E. M., The Dynamics of Faulting and Dyke Formation with Applications to Britain, 2nd edition, Oliver and Boyd, Edinburgh, 1951.

Arabasz, W. J., R. B. Smith, and W. B. Richins, Earthquake studies along the Wasatch Front, Utah: network monitoring, seismicity, and seismic hazards, in Earthquake Studies in Utah, 1850 to 1978, W. J. Arabasz, R. B. Smith, and W. D. Richins, eds., Univ. of Utah, Salt Lake City, 253-286, 1979.

Armstrong, R. L., W. P. Leeman, and H. E. Malde, K-Ar dating, Quaternary and Neogene volcanic rocks of the Snake River Plain, Idaho, Amer. J. Sci., 275, 225-251, 1975.

Babenroth, D. L., and A. N. Strahler, Geomorphology and structure of the East Kaibab monocline, Arizona and Utah, Geol. Soc. Amer. Bull., 56, 107-150, 1945.

Bache, T. C., and D. G. Lambert, Earthquake ground motion from the 1975 Pocatello Valley earthquake, Systems, Science and Software, Rep. SSS-R-78-3507, La Jolla, California, 43 pp., 1977.

Bailey, J. P., Seismicity and contemporary tectonics of the Hegben Lake-Centennial Valley, Montana area, M.S. thesis, Univ. Utah, Salt Lake City, 1976.

Baldwin, B., and W. R. Muehlberger, Geologic studies of Union County, New Mexico, New Mexico Bur. Mines and Min. Resour. Bull., 63, 171 pp., 1959.

Balk, R., Geologic map and sections of Tres Hermanas Mountains, New Mexico Bur. Mines and Min. Resour. Geol. Map 16, 1962.

Bateman, P. C., Willard D. Johnson and the strike-slip component of fault movement in the Owens Valley, California, earthquake of 1872, Seis. Soc. Amer. Bull., 51, 483-493, 1971.

Best, M. G., and W. K. Hamblin, Origin of the northern Basin and Range province: implications from the geology of its eastern boundary, GSA Memoir 152, 313-340, 1978.

Bickel, D. L., and D. R. Dolinar, In situ determination of stresses, Lakeshore Mine, Casa Grande, Arizona, U.S. Bur. Mines Prog. Rep., DMRC 10018, 1976.

Blackwell, D. D., Heat flow and energy loss in the western United States, GSA Memoir 152, 175-207, 1978.

Block, J. W., R. C. Clement, L. R. Lew, and J. de Boer, Recent thrust faulting in southeastern Connecticut, Geology, 7, 79-82, 1979.

Bolt, B., C. Lomnitz, and T. V. McEvilly, Seismological evidence on the tectonics of central and northern California and the Mendocino escarpments, Seis. Soc. Amer. Bull., 58, 1725-1767, 1968.

Bredehoeft, J. D., R. G. Wolff, W. S. Keys, and E. Shuter, Hydraulic fracturing to determine the regional in situ stress field, Piceance Basin, Colorado, Geol. Soc. Amer. Bull., 87, 250-258, 1976.

Byerly, P., The Montana earthquake of June 28, 1925, GMT, Seis. Soc. Amer. Bull., 16, 209-263, 1926.

Carr, W. J., Summary of tectonic and structural evidence for stress orientation at the Nevada Test Site, U.S. Geol. Surv. Open File Rep. 74-126, 53 pp., 1974.

Cash, D. J., The Dulce, New Mexico, earthquake of January 23, 1966: location, focal mechanism, magnitude and source parameters, Ph.D. dissertation, New Mexico Inst. of Mining and Technology, Socorro, 1971.

Cash, D. J., The focal mechanism of the Dulce, New Mexico, earthquake of January 23, 1966, Eos Trans. AGU, 56, 1022, 1975.

Chan, S. S. M., and T. J. Crocker, A case study of in situ rock deformation behavior in the Silver Summit Mine, Coeur D'Alene Mining district, in Proceedings of the 7th Canadian Rock Mechanics Symposium, Edmonton, 1971, 135-160, Mines Branch, Dept. of Energy, Mines and Res., Ottowa, 1972.

Chapin, C. E., and W. R. Seager, Evolution of the Rio Grande Rift in the Socorro and Las Cruces area, New Mexico Geol. Soc. Guidebook, 26th Field Conference, Las Cruces County, 297-321, 1975.

Chapman, D. S., K. P. Furlong, R. B. Smith, and D. J. Wechsler, Geophysical characteristics of the Colorado Plateau and its transition to the basin and range province in Utah, Tectonophysics, in press, 1979.

Christiansen, R. L., and E. H. McKee, Late Cenozoic volcanic and tectonic evolution of the Great Basin and Columbia Intermontane regions, GSA Memoir 152, 283-311, 1978.

Cotton, H. S., The basaltic cinder cones and lava flows of the San Francisco Mountain volcanic field, Flagstaff, Arizona, Museum of Northern Arizona, 58 pp., 1967.

Cooper, J. B., and E. C. John, Geology and ground water occurrence in southeastern McKinlay County, New Mexico, New Mexico State Engineer Tech. Rep., 35, 108 pp., 1968.

Couch, R., G. Thrasher, and K. Keeling, The Deschutes Valley earthquake of April 12, 1976, The Ore Bin, 38, 151-161, 1976.

Crosson, R. S., and J.-W. Lin, A note on the Mt. Rainier earthquake of April 20, 1974, Seis. Soc. Amer. Bull., 65, 549-556, 1975.

Dames and Moore, Summary report on the in-progress seismic monitoring program at the North Anna Site, January 21, 1974 through May 1, 1976, 1976.

Davis, G. A., Tectonic evolution of the Pacific Northwest: Precambrian to present, Subappendix 2R C, Preliminary Safety Analysis Report, Amendment 23, Nuclear Project No. 1, Washington Public Power Supply System, p. i-2Rc-46, 1977.

Davis, G. A., and B. C. Burchfiel, Garlock fault: an intracontinental transform structure, southern California, Geol. Soc. Amer. Bull, 84, 1407-1422, 1973.

Dibblee, T. W., Jr., Areal geology of the western Mojave Desert, California, U.S. Geol. Surv. Prof. Paper 522, 153 pp., 1967.

Diment, W. H., T. C. Urban, and F. A. Revetta, Some geophysical anomalies in the eastern United States, in The Nature of the Solid Earth, F. C. Robertson, ed., McGraw-Hill, New York, 544-572, 1972.

Donnelly, M. F., Geology of the Sierra del Pinacate volcanic field, northern Sonora, Mexico, and southern Arizona, U.S.A., Ph.D. thesis, Stanford Univ., Stanford, Calif., 722 pp., 1974.

Duffield, W. A., Late Cenozoic ring faulting and volcanism in the Coso Range area of California, Geology, 3, 335-338, 1975.

Eaton, G. P., A plate-tectonic model for late Cenozoic crustal spreading in the western United States, in Rio Grande Rift: Tectonics and Magmatism, R. E. Riecker, ed., AGU, Washington, D.C., 7-32, 1979a.

Eaton, G. P., Geophysical and geological characteristics of the crust of the Basin and Range province, in Continental Structure and Evolution, National Research Council Studies in Geophysics, B. C. Burchfiel, L. T. Silver, and J. E. Oliver, eds., National Academy of Sciences, Washington, D.C., in press, 1979b.

Eaton, G. P., R. R. Wahl, H. J. Prostka, D. R. Mabey, and M. D. Kleinhopf, Regional gravity and tectonic patterns: their relation to late Cenozoic epeirogeny and lateral spreading in the western Cordillera, GSA Memoir 152, 51-92, 1978.

Finnell, T. L., Geologic map of the Chediski Peak quadrangle, Navajo County, Arizona, U.S. Geol. Surv. Quad. Map GQ-544, 1966.

Fischer, F. G., P. J. Papanek, and R. M. Hamilton, The Massachusetts Mountain earthquake of 5 August 1971 and its aftershocks, Nevada Test Site, U.S. Geol. Surv. Rep., USGS-474-149, 16 pp., 1972 (available only from U.S. Dept. Commerce, National Tech. Inf. Service, Springfield, VA 22151).

Fletcher, J. B., and L. R. Sykes, Earthquakes related to hydraulic mining and natural seismic activity in western New York State, J. Geophys. Res., 82, 3767-3780, 1977.

Friedline, R. A., R. B. Smith, and D. D. Blackwell, Seismicity and contemporary tectonics of the Helena, Montana, area, Seis. Soc. Amer. Bull., 66, 81-95, 1976.

Fujita, K., and N. H. Sleep, Membrane stresses near mid-ocean ridge-transform intersections, Tectonophysics, 50, 207-221, 1979.

Gawthrop, W. H., Seismicity and tectonics of the central California coastal region, M.S. thesis, Univ. of Colorado, Boulder, 76 pp., 1977.

Gianella, V. P., Faulting in northeastern Sonora, Mexico, in 1887 (abstract), Geol. Soc. Amer. Bull., 71, 2061, 1960.

Griggs, R. L., Geology and ground-water resources of the eastern part of Colfax County, New Mexico, New Mexico Bur. Mines and Min. Resour. Ground-Water Rep. 1, 180 pp., 1948.

Grose, L. T., Late Quaternary tectonic controls of occurrence of geothermal systems in Gerlach-Hualapai Flat area, northwestern Nevada, Colorado School Mines Quart., 73(3), 11-14, 1978.

Gumper, F. J., and C. Scholz, Microseismicity and tectonics of Nevada seismic zone, Seis. Soc. Amer. Bull., 61, 1413-1432, 1971.

Hack, J. C., Sedimentation and volcanism in the Hopi Buttes, Arizona, Geol. Soc. Amer. Bull., 53, 335-372, 1942.

Hadley, J. B., and J. F. Devine, Seismo-tectonic map of the eastern United States, Map MF 620, U.S. Geol. Survey, Reston, Virginia, 1974.

Haimson, B. C., Earthquake related stresses at Rangely, Colorado, in New Horizons in Rock Mechanics, H. Hardy and R. Stefanko, eds., Amer. Soc. of Civil Eng., 689-708, 1973.

Haimson, B. C., A simple method for estimating in situ stresses at great depths, Field Testing and Instrumentation of Rock, ASTM Spec. Tech. Publ. 554, 156-182, 1974a.

Haimson, B. C., Stress measurements in faults and their vicinities, U.S. Geol. Surv. Semiannual Rep., Grant 14-08-0001-6118, 1974b.

Haimson, B. C., Preexcavation deep-hole stress measurements for design of underground chambers - case histories, in Proceedings of the 1976 Rapid Excavation and Tunneling Conference, R. J. Robins, and R. J. Conlon, eds., Soc. Min. Eng., New York, 699-714, 1976b.

Haimson, B. C., A stress measurement in West Virginia and the state of the stress in southern Appalachians (abstract), Eos Trans. AGU, 58, 493, 1977a.

Haimson, B. C., Crustal stress in the continental United States as derived from hydrofracturing tests, in The Earth's Crust, Geophys. Monogr. 20, J. C. Heacock, ed., AGU, 576-592, 1977b.

Haimson, B. C., Near surface and deeper hydrofracturing stress measurements in the Waterloo quartzite, Eos Trans. AGU, 59, 327-328, 1978a.

Haimson, B. C., Additional stress measurements in the Michigan Basin, Eos Trans. AGU, 59(12), 1209, 1978b.

Haimson, B. C., New hydrofracturing measurements in the Sierra Nevada Mountains and the relationship between shallow stresses and surface topography, 20th U.S. Symposium on Rock Mechanics, 675-682, 1979.

Haimson, B. C., and C. Fairhurst, In situ stress determination at great depth by means of hydraulic fracturing, in Rock Mechanics - Theory and Practice, Proceeding of the 11th Symposium on Rock Mechanics, W. Somerton, ed., AIME, New York, 559-584, 1970.

Haimson, B. C., J. Lacomb, A. H. Jones, and S. J. Green, Deep stress measurements in tuff at the Nevada Test Site, Advances in Rock Mechanics, IIa, National Academy of Sciences, Washington, D.C., 557-561, 1974.

Haimson, B.C., and C. F. Lee, Stress measurements in underground nuclear slant design, in Proceedings of 1979 Rapid Excavation and Tunneling Conference, Atlanta, Georgia, Soc. Min. Eng. of AIME, Littleton, Colorado, 1979.

Hamilton, R. M., Aftershocks of the Borrego Mt. earthquake from April 12 to June 12, 1968, U.S. Geol. Surv. Prof. Paper 787, 31-54, 1972.

Hamilton, R. M., and J. H. Healy, Aftershocks of the Benham nuclear explosion, Seis. Soc. Amer. Bull., 59, 2271-2281, 1969.

Hamilton, W., and W. B. Myers, Cenozoic tectonics of the western U.S., Rev. Geophys., 4, 509-549, 1966.

Healy, J. H., D. T. Griggs, W. W. Rubey, and C. B. Raleigh, The Denver earthquakes, Science, 161, 1301-1310, 1968.

Herrmann, R. B., Surface wave focal mechanisms for eastern north America earthquakes with tectonic implications, J. Geophys. Res., 84(B7), 3543-3552, 1979.

Herrmann, R. B., and J. A. Canas, Focal mechanism studies in the New Madrid seismic zone, Seis. Soc. Amer. Bull., 68, 641-652, 1978.

Hildenbrand, T. G., M. F. Kane, and W. Stauder, Magnetic and gravity anomalies in the northern Mississippi embayment and their special relation to seismicity, U.S. Geol. Surv. Misc. Field Studies, Map MF-914, 1978.

Hill, D. P., A model for earthquake swarms, J. Geophys. Res., 82, 1347-1352, 1977.

Hill, R. L., and D. J. Beeby, Surface faulting associated with the 5.2 magnitude Galway Lake earthquake of May 31, 1975, Mojave Desert, Bernadino County, Calif., Geol. Soc. Amer. Bull., 88, 1378-1384, 1977.

Hill, M. L., and T. W. Dibblee, Jr., San Andreas, Garlock and Big Pine faults, California - a study of the character, history, and tectonic significance of their displacements, Geol. Soc. Amer. Bull., 64, 443-458, 1953.

Hoffer, J. M., The Potrillo basalt field, south-central New Mexico, in Cenozoic volcanism in southwestern New Mexico, W. E. Elston and S. A. Northrop, eds., New Mexico Geol. Soc. Spec. Publ., 5, 89-92, 1976.

Hooker, V. E., J. R. Aggson, and D. L. Bickel, Improvements in the three-component borehole deformation gage and overcoring techniques, U.S. Bur. Mines Rep. Invest. 7894, 29 pp., 1974.

Hooker, V. E., and C. F. Johnson, Near-surface horizontal stresses including the effects of rock anisotropy, U.S. Bur. Mines Rep. Invest 7224, 29 pp., 1969.

Horino, F. G., and J. R. Aggson, Pillar failure analysis and in situ stress determination at the Fletcher Mine, Bon Tene, Missouri, U.S. Bur. Mines Prog. Rep., DMRC 10019, 1976.

Horner, R. B., A. E. Stevens, H. S. Hasegawa, and G. LeBlanc, The Maniwaki, Quebec, earthquake of July 12, 1975 (abstract), Earthquake Notes, 46, 48, 1975.

Howard, K. A., J. M. Aaron, E. E. Brabb, M. R. Brock, H. D. Gower, S. J. Hunt, D. J. Milton, W. R. Muehlberger, J. K. Nakata, G. Plafker, D. C. Prowell, R. E. Wallace, and I. J. Witkind, Preliminary map of young faults in the United States, U.S. Geol. Surv. Misc. Field Studies, Map MF-916, 1978.

Howell, D. E., and A. J. W. Zupan, Evidence for post-Cretaceous tectonic activity in the Westfield Creek area north of Cherow, South Carolina, Geologic Notes, South Carolina Development Board, Columbia, 18(4) 98-105, 1974.

Hubbert, M. K., and D. G. Willis, Mechanics of hydraulic fracturing, AIME Trans., 210, 153-168, 1957.

Huff, L. C., E. Santos, and R. G. Raabe, Mineral resources of the Sycamore Canyon primitive area, Arizona, U.S. Geol. Surv. Bull., 1230-F, 19 pp., 1966.

Hunt, C. B., Igneous geology and structure of the Mount Taylor volcanic field, New Mexico, U.S. Geol. Surv. Prof. Paper 189-B, 1938.

Inden, R. F., and A. J. W. Zupan, Normal faulting of upper coastal plain sediments, Ideal Kaolin Mine, Langley, South Carolina, Geologic Notes, South Carolina Development Board, Columbia, 19(4), 160-165, 1975.

Jahns, R. H., Tectonic evolution of the Transverse Ranges province as related to the San Andreas fault system, in Proc. Conf. on Tectonic Problems of the San Andreas Fault System, R. L. Kovach, and A. Nur, eds., Stanford Univ. Publ., Stanford, Calif., 494 pp., 1973.

Jicha, H. L., Jr., Geology and mineral resources of Mesa del Oro quadrangle, Socorro and Valencia Counties, New Mexico, New Mexico Bur. Mines and Min. Resour. Bull., 56, 67 pp., 1958.

Johnson, C. E., and D. M. Hadley, Tectonic implications of the Brawley earthquake swarm, Imperial Valley, California, January 1975, Seis. Soc. Amer. Bull., 66, 1133-1144, 1976.

Johnson, R. B., Patterns and origin of radial dike swarms associated with West Spanish Peak and Dike Mountain, south-central Colorado, Geol. Soc. Amer. Bull., 72, 579-590, 197_.

Kanamori, H., and G. Fuis, Variation of P-wave velocity before and after the Galway Lake earthquake (M = 5.2) and the Goat Mountain earthquakes (M = 4.7, 4.7), 1975, in the Mojave Desert, California, Seis. Soc. Amer. Bull., 66, 2017-2037, 1976.

Kelley, V. C., Albuquerque - its mountains, valley, water, and volcanoes, New Mexico Bur. Mines and Min. Resour., Scenic Trips to the Geol. Past, 9, 101 pp., 1969.

Keys, W. S., R. G. Wolff, J. D. Bredehoeft, E. S. Shuter, and J. H. Healy, In-situ stress measurements near the San Andreas fault in central California, J. Geophys. Res., 84(B4), 1583-1591, 1979.

King, P. B., The Tectonics of Middle North America, Princeton Univ. Press, Princeton, New Jersey, 203 pp., 1951.

Koons, E. D., Geology of the Unikaret Plateau, northern Arizona, Geol. Soc. Amer. Bull., 56, 151-180, 1945.

Kumamoto, L., Microearthquake survey in the Gerlach-Fly Ranch area of northwestern Nevada, Colorado School Mines Quart., 73(3), 45-64, 1978.

Kuntz, M. A., Geologic map of the Arco-Big Southern Butte area, Butte, Blaine, and Bingham Counties, Idaho, U.S. Geol. Surv. Open File Rep. 78-302, 1978.

Lachenbruch, A. H., and J. H. Sass, Thermo-mechanical aspects of the San Andreas fault system, in Proc. Conf. on Tectonic Problems of the San Andreas Fault System, R. L. Kovach, and A. Nur, eds., Stanford Univ. Publ., Stanford, Calif., 494 pp., 1973.

Lachenbruch, A. H., and J. H. Sass, Heat flow in the United States and the thermal regime of the crust, AGU Geophys. Mon. 20, 626-675, 1977.

Lachenbruch, A. H., and J. H. Sass, Models of an extending lithosphere and heat flow in the Basin and Range Province, GSA Memoir 152, 209-250, 1978.

Lachenbruch, A. H., and J. H. Sass, Frictional resistance and heat flow on the San Andreas fault, in Proc. Conf. on Magnitude Deviatoric Stress, J. H. Evernden, ed., this volume, 1979.

Lachenbruch, A. H., J. H. Sass, and S. P. Galanis, Jr., New heat flow results from southern California (abstract), Eos Trans. AGU, 59, 1051, 1978.

Lambert, W., Notes on the Late Cenozoic geology of the Taos-Questa area, New Mexico, New Mexico Geol. Soc. Guidebook, 17th Field Conf., 43-50, 1966.

Langer, C. J., G. R. Keller, and R. B. Smith, A study of the aftershocks of the October 1, 1972 M = 4.7, Heber City, Utah, earthquake, in Earthquake Studies in Utah, 1850-1978, W. J. Arabasz, R. B. Smith, and W. D. Richins, eds., Univ. of Utah, Salt Lake City, 383-394, 1979.

Langston, C. A., and R. Butler, Focal mechanism of the August 1, 1975, Oroville, earthquake, Seis. Soc. Amer. Bull., 66, 1111-1120, 1976.

LeBlanc, G., and G. Buchbinder, Second microearthquake survey of the St. Lawrence Valley near La Malboie, Quebec, Canada, J. Earth Sci., 14, 2778-2789, 1977.

Lee, W. H. K., R. F. Yerkes, and M. Simerenko, Recent earthquake activity and focal mechanisms in the western Transverse Ranges, California, U.S. Geol. Surv. Circular 799-A, 37 pp., 1979.

Lee, W. H. K., C. E. Johnson, T. L. Henyey, and R. F. Yerkes, A preliminary study of the Santa Barbara, California, earthquake of August 13, 1978 and its aftershocks, U.S. Geol. Surv. Circular 797, 11 pp., 1978.

Lockwood, J. P., and J. G. Moore, Regional extension of the Sierra Nevada, California, on conjugate microfault sets, J. Geophys. Res., in press, 1979.

Luedke, R. G., and R. L., Smith, Map showing distribution, composition, and age of late Cenozoic volcanic centers in Arizona and New Mexico, U.S. Geol. Surv. Misc. Inv., Map I-1091, 1978.

Mabey, D. R., I. Zietz, G. P. Eaton, and M. D. Kleinkopf, Regional magnetic patterns in part of the Cordillera in the western United States, GSA Memoir 152, 93-106, 1978.

Malone, S. D., G. H. Rothe, and S. W. Smith, Details of microearthquake swarms in the Columbia Basin, Washington, Seis. Soc. Amer. Bull., 65, 855-864, 1975.

McEvilly, T. V., Preliminary seismic data, June-July, 1966 (Parkfield), Seis. Soc. Amer. Bull., 56, 967, 1966.

McGarr, A., and N. C. Gay, State of stress in the earth's crust, Ann. Rev. Earth Planet. Sci., 6, 405-436, 1978.

McKenzie, D. P., The relationship between fault plane solutions for earthquakes and the directions of the principal stresses, Seis. Soc. Amer. Bull., 59, 591-601, 1969.

McKinlay, P. F., Geology of Costilla and Latir Peak quadrangles, Taos County, New Mexico, New Mexico Bur. Mines and Min. Resour. Bull., 42, 32 pp., 1956.

Merrill, R. H., In situ determination of stress by relief techniques, in State of Stress in the Earth's Crust, W. R. Judd, ed., Elsevier, New York, 343-369, 1964.

Merrill, R. K., and T. L. Péwé, Late Cenozoic geology of the White Mountains, Arizona, Arizona Bur. of Geol. and Min. Tech. Spec. Paper No. 1, 65 pp., 1977.

Minster, J. B., and T. H. Jordan, Present day plate motions, J. Geophys. Res., 83, 5331-5354, 1978.

Mixon, R. B., and W. L. Newell, Stafford fault system: structures documenting Cretaceous and Tertiary deformation along the Fall Line in northeastern Virginia, Geology, 5, 437-440, 1977.

Moench, R. H., and J. S. Schlee, Geology and uranium deposits of the Laguna District, New Mexico, U.S. Geol. Surv. Prof. Paper 519, 117 pp., 1967.

Moore, J. G., and E. DuBray, Mapped offset on the right-lateral Kern Canyon fault, southern Sierra Nevada, California, Geology, 6, 205-208, 1978.

Moore, R. B., and E. W. Wolfe, Geologic map of the eastern San Francisco volcanic field, Arizona, U.S. Geol. Surv. Misc. Inv. Ser., Map I-953, 1976.

Muffler, L. J. P., Geology of the Frenchie Creek quadrangle, north-central Nevada, U.S. Geol. Surv. Bull., 1179, 99 pp., 1964.

Nakamura, K., Volcanoes as possible indicators of tectonic stress orientation - principle and proposal, J. Volcanology and Geothermal Res., 2, 1-16, 1977.

Nakamura, K., K. H. Jacob, and J. N. Davies, Volcanoes as possible indicators of tectonic stress orientation - Aleutians and Alaska, Pure Appl. Geophys., 115, 87-112, 1978.

Obert, L., In-situ determination of stress in rock, Min. Eng., 14, 51-58, 1962.

O'Connell, D., C. Bufe, and M. D. Zoback, Microearthquakes near Reelfoot Lake, Tennessee, U.S. Geol. Surv. Prof. Paper, in press, 1980.

Odé, H., A note concerning the mechanism of artificial and natural hydraulic fracture systems, Colorado School Mines Quart., 51, 19-29, 1956.

Oliver, J., T. Johnson, and J. Dorman, Postglacial faulting and seismicity in New York and Quebec, Can. J. Earth Sci., 7, 579-590, 1970.

Overbey, W. K., Jr., and R. L. Rough, Surface studies predict orientation of induced formation fractures, Producers Monthly, June 1968, 16-19, 1968.

Overbey, W. K., Jr., and R. L. Rough, Prediction of oil and gas bearing rock fracture from surface structural features, U.S. Bur. Mines Rep. Invest., 1971.

Parsons, R. C., and H. D. Dahl, A study of the causes of rock instability in the Pittsburgh coal seam, in The 7th Canadian Symposium on Rock Mechanics, Edmonton, Alberta, Mines Branch, Dept. of Energy, Mines and Resour., Ottawa, 1972.

Pavlis, T. L., and R. B. Smith, Slip vectors on faults near Salt Lake City, Utah, from Quaternary displacements and seismicity, Seis. Soc. Amer. Bull., in press, 1979.

Pechmann, J. C., Tectonic implications of small earthquakes in the central Transverse Ranges, California, U.S. Geol. Surv. Prof. Paper, in press, 1979.

Pitt, A. M., and D. W. Steeples, Microearthquakes in the Mono Lake-northern Owens Valley, California, region from September 28, to October 18, 1970, Seis. Soc. Amer. Bull., 65, 835-844, 1975.

Pitt, A. M., C. S. Weaver, and W. Spence, The Yellowstone Park earthquake of June 30, 1975, Seis. Soc. Amer. Bull., 69, 187-205, 1979.

Power, D. V., C. L. Schuster, R. Hay, and J. Twombly, Detection of hydraulic fracture orientation and dimensions in cased wells, J. Petrol. Tech., 28, 1116-1124, 1976.

Prowell, D. C., B. J. O'Connor, and M. Rubin, Preliminary evidence for Holocene movement along the Belair fault zone near Augusta, Georgia, U.S. Geol. Surv. Open-File Rep. 75-680, 1975.

Raleigh, C. B., J. H. Healy, and J. D. Bredehoeft, Faulting and crustal stress at Rangely, Colorado, in Flow and Fracture of Rocks, AGU Monogr. 16, 275-284, 1972.

Rehrig, W. A., and T. L. Heidrick, Regional tectonic stress during the Laramide and late Tertiary intrusive periods, Basin and Range province, Arizona, Arizona Geol. Soc. Digest, X, 205-228, 1976.

Reiter, M., C. L. Edwards, H. Hartman, and C. Weideman, Terrestrial heat flow along the Rio Grande Rift, New Mexico and southern Colorado, Geol. Soc. Amer. Bull., 86, 811-818, 1975.

Reiter, M., A. J. Mansure, and C. Shearer, Geothermal characteristics of the Colorado Plateau, Tectonophysics, in press, 1979.

Richardson, R. M., S. C. Solomon, and N. H. Sleep, Tectonic stress in the plates, Rev. Geophys. Space Phys., in press, 1979.

Richins, W. D., Earthquake swarm near Denio, Nevada, February to April, 1973, ARPA Tech. Rep., Univ. of Nevada, Reno, 1974.

Richins, W. D., The Hansel Valley, Utah, earthquake sequence of November, 1976, in Earthquake Studies in Utah, 1850 to 1978, W. J. Arabasz, R. B. Smith, and W. D. Richins, eds., Univ. of Utah, Salt Lake City, 409-421, 1979.

Roegiers, J., The development and evaluation of a field method for in situ stress determination using hydraulic fracturing, Ph.D. thesis, Univ. of Minnesota, Minneapolis, 1974.

Rogers, A. M., and W. H. K. Lee, Seismic study of earthquakes in the Lake Mead, Nevada-Arizona region, Seis. Soc. Amer. Bull., 66, 1657-1681, 1976.

Rogers, G. C., The Vancouver Island earthquake of 5 July 1972, Can. J. Earth Sci., 13, 92-101, 1976.

Rogers, G. C., Two recent Georgia Strait earthquakes (abstract), Geol. Assoc. Can., Ann. Mtg. Program with Abstr., 2, 45, 1977.

Romney, C., The Dixie Valley-Fairview, Peak, Nevada, earthquakes of December 16, 1954: seismic waves, Seis. Soc. Amer. Bull., 47, 301-320, 1957.

Russell, B. J., A structural break and kinematics of faulting in the White Mountains, California, Geol. Soc. Amer. Abstr. with Program, 9, 491, 1977.

Ryall, A., The Hebgen Lake, Montana, earthquake of April 18, 1959: P-waves, Seis. Soc. Amer. Bull., 52, 235-271, 1962.

Ryall, A., and S. D. Malone, Earthquake distribution and mechanism of faulting in the Rainbow Mountain-Dixie Valley-Fairview Peak area, central Nevada, J. Geophys. Res., 76, 7241-7248, 1971.

Ryall, A., and K. Priestley, Seismicity, secular strain, and maximum magnitude in the Excelsior Mountains area, western Nevada and eastern California, Geol. Soc. Amer. Bull., 86, 1585-1592, 1975.

Sanford, A. R., K. H. Olsen, and L. H. Jaksha, Seismicity of the Rio Grande Rift: Rio Grande Rift: Tectonics and Magmatism, R. E. Riecker, ed., AGU, Washington, D.C., 145-168, 1979.

Sass, J. H., A. H. Lachenbruch, R. J. Munroe, G. W. Greene, and T. H. Moses, Jr., Heat flow in the western United States, J. Geophys. Res., 76, 6376-6413, 1971.

Sass, J. H., and J. P. Ziagos, Heat flow from a corehole near Charleston, South Carolina, U.S. Geol. Surv. Prof. Paper 1028, 115-118, 1977.

Sbar, M. L., J. Armbruster, and Y. P. Aggarwal, The Adirondack, New York, earthquake swarm of 1971 and tectonic implications, Seis. Soc. Amer. Bull., 62, 1303-1317, 1972a.

Sbar, M. L., M. Barazangi, J. Dorman, C. Scholz, and R. B. Smith, Tectonics of the Intermountain seismic belt, western U.S.: microearthquake seismicity and composite fault plane solutions, Geol. Soc. Amer. Bull., 83, 13-20, 1972b.

Sbar, M. L., J. M. W. Rynn, F. J. Gumper, and J. C. Lahr, An earthquake sequence and focal mechanism solution, Lake Hopateong, northern New Jersey, Seis. Soc. Amer. Bull., 60, 1231-1243, 1970.

Sbar, M. L., and L. R. Sykes, Contemporary compressive stress and seismicity in eastern North America: an example of intraplate tectonics, Geol. Soc. Amer. Bull., 84, 1861-1882, 1973.

Sbar, M. L., and L. R. Sykes, Seismicity and lithospheric stress in New York and adjacent areas, J. Geophys. Res., 82, 5771-5786, 1977.

Schafer, K., Recent thrusting in the Appalachians, Nature, 280, 223-226, 1979.

Schaff, C. S., The 1968 Adel, Oregon, earthquake swarm, unpub. thesis, Univ. of Nevada, Reno, 1976.

Scott, D. H., and N. J. Trask, Geology of the lunar crater volcanic field, Nye County, Nevada, U.S. Geol. Surv. Prof. Paper 599-I, 22 pp., 1971.

Sharp, R. V., Surface rupturing in Imperial Valley during the earthquake swarm of January-February, 1975, Seis. Soc. Amer. Bull., 66, 1145-1154, 1976.

Shoemaker, E. M., R. L. Squires, and M. I. Abrams, Bright Angel and Mesa Butte fault systems of northern Arizona, GSA Memoir 152, 341-368, 1978.

Slemmons, D. B., Pliocene and Quaternary crustal movements of the Basin-and-Range Province, USA, J. Geosci., Osaka City Univ., 10, 91-101, 1967.

Smith, C. T., Geology of the Little Black Peak quadrangle, Socorro and Lincoln Counties, New Mexico, New Mexico Geol. Soc. Guidebook, 15th Field Conf., 92-99, 1964.

Smith, R. B., Intraplate tectonics of the western North-American plate, Tectonophysics, 37, 323-336, 1977.

Smith, R. B., Seismicity, crustal structure, and intraplate tectonics of the interior of the western Cordillera, GSA Memoir 152, 111-144, 1978.

Smith, R. B., and A. G. Lindh, A compilation of fault plane solutions of the western United States, in Cenozoic Tectonics and Regional Geophysics of the Western U.S., R. B. Smith and G. P. Eaton, eds., GSA Memoir 152, 107-109, 1978.

Smith, R. B., and M. L. Sbar, Contemporary tectonics and seismicity of the western United States with emphasis on the intermountain seismic belt, Geol. Soc. Amer. Bull., 85, 1205-1218, 1974.

Smith, R. B., R. T. Shuey, J. R. Pelton, and J. P. Bailey, Yellowstone hot spot: contemporary tectonics and crustal properties from earthquake and aeromagnetic data, J. Geophys. Res., 82, 3665-3676, 1977.

Smith, R. B., P. Winkler, J. Anderson, and C. H. Scholz, Source mechanisms of microearthquakes associated with underground mines in Utah, Seis. Soc. Amer. Bull., 64, 1295-1317, 1974.

Smith, R. L., R. A. Bailey, and C. S. Ross, Geologic map of the Jemez Mountains, New Mexico, U.S. Geol. Surv. Misc. Geol. Inv., Map I-571, 1970.

Smith, S. W., Skagit Valley earthquakes of 1974-1975 (abstract), Eos Trans. AGU, 57, 90, 1976.

Speed, R. C., and A. H. Cogbill, Candelaria and other left-oblique slip faults of the Candelaria region, Nevada, Geol. Soc. Amer. Bull., 90, 149-163, 1979.

Stauder, W., and O. W. Nuttli, Seismic studies: south central Illinois earthquake of November 9, 1968, Seis. Soc. Amer. Bull., 60(3), 973-981, 1970.

Stevenson, P. R., Microearthquakes of Flathead Lake, Montana: a study using automatic earthquake processing, Seis. Soc. Amer. Bull., 66, 61-80, 1976.

Stewart, J. H., Basin-range structure in western North America: a review, GSA Memoir 152, 1-32, 1978.

Stierman, D. J., and W. C. Ellsworth, Aftershocks of the February 21, 1973 Point Mugu, California, earthquake, Seis. Soc. Amer. Bull., 66(6), 1931-1952, 1976.

Stokes, W. L., and J. H. Malsen, Jr., Geologic map of Utah, northeast quarter, Univeristy of Utah, Salt Lake City, 1961.

Strubhar, M. K., J. L. Fitch, and E. E. Glenn, Jr., Multiple vertical fractures from an inclined wellbore - a field experiment, J. Pet. Tech., 27, 641-647, 1975.

Sumner, J. R., The Sonoran earthquake of 1887, Seis. Soc. Amer. Bull., 67, 1219-1223, 1977.

Sutton, R. L., The geology of Hopi Buttes, Arizona, in Geol. Soc. Amer. Guidebook 27, Rocky Mtn. Section Mtg., Flagstaff, Arizona, 647-671, 1974.

Swanberg, C. A., and P. Morgan, The linear relation between temperatures based on the silica content of groundwater and regional heat flow: a new heat flow map of the United States, Pure Appl. Geophys., 117, 227-241, 1978.

Swanberg, C. A., B. J. Mitchell, R. L. Lohse, and D. D. Blackwell, Heat flow in the upper Mississippi embayment, Eos Trans. AGU, 60, 310, 1979.

Tarr, A. C., Recent seismicity near Charleston, South Carolina, and its relationship to the August 31, 1886, earthquake, U.S. Geol. Surv. Prof. Paper 1028, 43-58, 1977.

Thaden, R. E., S. Merrin, and O. B. Raup, Geologic map of the Grants SE quadrangle, Valencia County, New Mexico, U.S Geol. Surv. Geol. Quad Map GQ-682, 1967.

Theilen, Fr., and R. Meissner, A comparison of crustal and upper mantle features in Fennoscandia and the Rhenish Shield, two areas of recent uplift, Tectonophysics, in press, 1979.

Thompson, G. A., and D. B. Burke, Rate and direction of spreading in Dixie Valley, Basin and Range province, Nevada, Geol. Soc. Amer. Bull., 84, 627-632, 1973.

Thompson, G. A., and D. B. Burke, Regional geophysics of the Basin and Range province, Ann. Rev. Earth and Planet. Sci., 2, 213-228, 1974.

Thompson, G. A., and M. L. Zoback, Regional geophysics of the Colorado Plateau, Tectonophysics, in press, 1979.

Tobin, D. G., and L. R. Sykes, Seismicity and tectonics of the northeastern Pacific Ocean, J. Geophys. Res., 73, 3821-3845, 1968.

Trexler, D. T., E. J. Bell, and G. R. Roguemore, Evaluation of lineament analysis as an exploration technique for geothermal energy, western and central Nevada, Final Rep., Contract EY-76-S-08-067, U.S. Dept. Energy, 1978.

Trimble, A. B., and R. B. Smith, Seismicity and contemporary tectonics of the Hegben Lake-Yellowstone Park region, J. Geophys. Res., 80, 733-741, 1975.

Tsai, Y.-B., and K. Aki, Source mechanism of the Truckee, California, earthquake of September 12, 1966, Seis. Soc. Amer. Bull., 60, 1199-1208, 1966.

Untermann, G. E., and B. R. Untermann, Geology of Uintah County, Utah Geol. and Min. Surv. Bull., 72, 112 pp., 1964.

von Schonfeldt, H. A., An experimental study of open-hole hydraulic fracturing as a stress measurement method with particular emphasis on field tests, Ph.D. thesis, Univ. of Minn., Minneapolis, 1970.

von Schonfeldt, H. A., R. O. Kehle, and K. E. Gray, Mapping of stress field in the upper earth's crust of the U.S., U.S. Geol. Surv. Final Tech. Rep., Grant 14-08-0001-1222, 78 pp., 1973.

Wanek, A. A., Reconnaissance geologic map of parts of Harding, San Miguel, and Mora Counties, New Mexico, U.S. Geol. Surv. Oil and Gas Inv. Map OM-208, 1962.

Wallace, R. E., Strain pattern represented by scarps formed during the earthquakes of October 2, 1915, Pleasant Valley, Nevada, Tectonophysics, 52, 599, 1979.

Weaver, C. S., and D. P. Hill, Earthquake swarms and local crustal spreading along major strike-slip faults in California, Pure Appl. Geophys., 117, 51-64, 1978.

Weaver, C. S., A. M. Pitt, and D. P. Hill, Crustal spreading direction of the Snake River Plain-Yellowstone system, AGU Fall Meeting, San Francisco, Calif., Dec. 1979, in press.

Weber, R. H., Geology of the Carrizozo quadrangle, New Mexico, New Mexico Geol. Soc. Guidebook, 15th Field Conf., 100-109, 1964.

Wetmiller, R. J., The Quebec-Maine border earthquake, 15 June 1973, Can. J. Earth. Sci., 12, 1917-1928, 1975.

Whitcomb, J. H., C. R. Allen, J. D. Garmany, and J. A. Hileman, San Fernando earthquake series, 1971: focal mechanisms and tectonics, Rev. Geophys. Space Phys., 11(3), 369-730, 1973.

Winchester, D. E., Geology of Alamosa Creek Valley, Socorro County, New Mexico, U.S. Geol. Surv. Bull. 716-A, 1-15, 1920.

Wood, G. H., Jr., S. A. Northrup, and R. L. Griggs, Geology and stratigraphy of Koehler and Mount Laughlin quadrangles and parts of Abbott and Springer quadrangles, eastern Colfax County, New Mexico, U.S. Geol. Surv. Oil and Gas Inv. Map OM-141, 1953.

Woodward, L. A., Rate of crustal extension across the Rio Grande Rift near Albuquerque, New Mexico, Geology, 5, 269-272, 1977.
Woodworth, J. B., Postglacial faults of eastern New York, New York State Museum Bulletin 102, Geology, 12, 5-28, 1907.
Wright, H. E., Jr., Tertiary and Quaternary geology of the Lower Rio Puerco area, New Mexico, Geol. Soc. Amer. Bull., 57, 383-456, 1946.
Wright, L. A., J. K. Otton, and B. W. Troxel, Turtleback surfaces of Death Valley viewed as phenomena of extensional tectonics, Geology, 2, 53-54, 1974.
Yang, J. P., Y. P. Aggarwal, E. Cranswick, S. Nishenko, and J. Beavan, An earthquake swarm sequence in northern New Jersey, Eos Trans. AGU, 59(4), 317, 1978.
Yang, J. P., and Y. P. Aggarwal, Intraplate stresses near Atlantic type passive continental margins, Eos Trans. AGU, 60(18), 309, 1979.
Zemanek, J., E. E. Glenn, L. J. Norton, and R. L. Caldwell, Formation evaluation by inspection with the borehole televiwer, Geophysics, 35(2), 254-269, 1970.
Zoback, M. D., Measurement of in situ stress, natural fracture distribution, and fracture permeability in a well near Palmdale, California, in Proc. Workshop on Measurement of Stress and Strain Phenomena Related to Earthquake Prediction, J. F. Evernden, ed., 1978.
Zoback, M. D., R. M. Hamilton, A. J. Crone, D. P. Russ, F. A. McKeown, and S. R. Brockman, Recurrent intraplate tectonism in the New Madrid seismic zone, submitted to Science, 1980.
Zoback, M. D., J. H. Healy, and J. C. Roller, Preliminary stress measurements in central California using the hydraulic fracturing technique, Pure Appl. Geophys., 115, 135-152, 1977.
Zoback, M. D., J. H. Healy, J. C. Roller, G. S. Gohn, and B. B. Higgins, Normal faulting and in situ stress in the South Carolina coastal plain near Charleston, Geology, 6, 147-152, 1978.
Zoback, M. D., and J. C. Roller, Magnitude of shear stress on the San Andreas fault: implications from a stress measurement profile at shallow depth, Science, in press, 1979.
Zoback, M. D., J. C. Roller, D. Seeburger, and J. Svitek, Hydraulic fracturing stress measurements and natural fracture studies near the San Andreas fault in southern California, this issue, 1979.
Zoback, M. L., Mid-Miocene rifting in north-central Nevada: a detailed study of late Cenozoic deformation in the northern Basin and Range, Ph.D. thesis, Stanford Univ., Stanford, Calif., 247 pp., 1978.
Zoback, M. L., State of stress in the southern Basin and Range province and Colorado Plateau, Eos Trans. AGU, 60, 311, 1979.
Zoback, M. L., Upper crustal model of a mid-Miocene rift in northern Nevada, in prep.
Zoback, M. L., and G. A. Thompson, Physical characteristics of a mid-Miocene rift, Eos Trans. AGU, 58, 1125, 1977.
Zoback, M. L., and M. D. Zoback, Faulting patterns in north-central Nevada and strength of the crust, J. Geophys. Res., in press, 1979.
Zupan, A. J. W., and W. H. Abbot, Clastic dikes: evidence for post-Eocene(?) tectonics in the upper coastal plain of South Carolina, Geologic Notes, South Carolina Development Board, Columbia, 19(1), 14-23, 1975.

TABLE 1

Stress data arranged by state (within each state data are generally numbered from south to north). Stress regimes indicated are:

N - normal faulting (S_1 vertical)

SS - strike-slip faulting (S_2 vertical)

T - thrust or reverse faulting (S_3 vertical).

For a mixed mode of deformation or for data where one of the stress magnitudes is unknown, a slash separates the two possible stress states. The type of indicators are:

Geologic

G-CC	Cinder cone alignment
G-D	Dike trends
G-FS	Fault slip based on trend of fault and primary type of offset
G-FS(G)	Fault slip indicated by grooves and slickensides
G-FS(H)	Fault slip based on measured offsets in historic earthquakes
G-FS(C)	Fault slip determined from offset coreholes

Focal Mechanisms

FM(S)	Single event mechanism
FM(C)	Composite mechanism
FM(A)	Average stress direction from a number of mechanisms

In-situ Stress

HF	Hydrofrac
OC	Overcore

ARIZONA

NUMBER	LOCATION	LEAST HORIZONTAL PRINCIPAL STRESS ORIENTATION	STRESS REGIME	TYPE OF INDICATOR	COMMENTS	REFERENCES
AZ-1	San Bernadino volcanic field 31.45°, 109.30°	N62°W	N	G-CC	Basaltic cindercones 3 m.y. to 200,000 yrs. old. Best alignment on youngest cones.	Luedke and Smith, 1978
AZ-2	Pinacate volcanic field 32.12°, 113.50°	∿E-W	N/SS?	G-CC	Alignment of three major centers of eruption, less than 100,000 yrs. old.	Donnelly, 1974
AZ-3	Lakeshore Mine ∿33°, 111.7°	N73°E	N	OC	Depth = 480 m. Magnitude of S_{Hmin} is approx. half the magnitude of S_{vert}.	Bickel and Dolinar, 1970
AZ-4	White Mtns. volcanic field ∿34°, 109.5°	N25°E	N?	G-CC	Alignment of basaltic cindercones, 2-3 m.y. old.	Luedke and Smith, 1978 Merrill and Péwé, 1977
AZ-5	Chediski Quadrangle 34.02°, 110.60°	∿N63°W	N?	G-CC	Basalt overlies gravel which overlies rim gravel. Less than 5 m.y., probably less than 3 m.y. Shaky, based on two cones.	Finnell, 1966
AZ-6	Bagdad 34.58°, 113.21°	N58°W	N	G-FS(G)	Right-lateral oblique slip on Hawkeye fault which cuts Plio-Pleistocene (?) Gila conglomerate.	Anderson et al., 1955
AZ-7	Sycamore Canyon Primitive Area 35.08°, 111.96°	∿N35°E	N?	G-D,CC	Avg. trend, actual range in strike N45°W-N73°W. Based on a spatter cone alignment and numerous dikes exposed in canyon.	Huff et al., 1966
AZ-8	San Francisco volc. field (SE) ∿35.25°, 111.42°	N30°E	N	G-D,CC	Basaltic cindercones all less than 1 m.y. in age, includes Sunset Crater rift zone (∿1000 A.D.).	Moore and Wolfe, 1976 Cotton, 1967
AZ-9	Hopi Buttes 35.42°, 110.17°	N30°W	?	G-CC,D	Numerous dike and cindercones, monchiquite volcanism primarily 4-6 m.y. in age.	Akers et al., 1971 Hack, 1942
AZ-10	San Francisco volc. field (N) 35.55°, 11.42°	N55°W	N	G-CC	Basaltic cindercones less than 1 m.y. old (Dog Knobs) aligned parallel to Mesa Butte fault/graben system.	Babenroth and Strahler, 1945 Shoemaker et al., 1978
AZ-11	Lake Mead 36.0°, 114.7°	N46°W	SS	FM(C)	T-axis plunges 20°SE, P-axis trends N43°E plunges 2°SW.	Smith and Lindh, 1978
AZ-12	Boulder Dam 36.03°N, 114.73°W	N54°W	N/SS	OC	Overcore at 107 m depth, $S_{Hmax} = S_{vert} >> S_{Hmin}$.	Merrill, 1964
AZ-13	North Rim Grand Canyon 36.42°, 113.17°	∿E-W	N	G-CC	Basaltic cones between 0.1 and 1.0 m.y. in age.	Koons, 1945

ARKANSAS

NUMBER	LOCATION	LEAST HORIZONTAL PRINCIPAL STRESS ORIENTATION	STRESS REGIME	TYPE OF INDICATOR	COMMENTS	REFERENCES
AR-1	New Madrid (SW) 35.6o, 90.5o	N30W	SS/T	FM(A)	Avg. of two avents with similar solutions, both have thrust and strike-slip components.	Herrmann and Canas, 1978 Herrmann, 1979
AR-2	New Madrid (NE) 35.9o, 89.9o	N40W	SS	FM(S)	Primarily strike-slip event based on both body wave and surface wave solutions. T-axis plunges 32oS; P-axis azimuth = N88oW, plunge = 9oW	Herrmann and Canas, 1978 Herrmann, 1979

CALIFORNIA

NUMBER	LOCATION	LEAST HORIZONTAL PRINCIPAL STRESS ORIENTATION	STRESS REGIME	TYPE OF INDICATOR	COMMENTS	REFERENCES
CA-1	Brawley 32.92o, 115.5o	N81oW	SS	FM(A)	Avg. stress directions taken from primarily strike-slip earthquakes occurring in a left-stepping offset of the San Andreas Fault.	Hill, 1977
CA-2	Borrego Mtn. 33o, 116o	~E-W	SS	FM(A)	Avg. trend of stress orientations based on 72 composite focal mechanisms of aftershocks of the Borrego Mtn earthquake 1968. Predominantly strike-slip, a few thrust mechanisms.	Hamilton, 1972
CA-3	Point Mugu 34.13o, 119.04o	N72oW	T/SS	FM(A)	Point Mugu earthquake 1973. Avg. orientation based on main shock (thrust) and numerous aftershocks (thrust & strike-slip.	Stierman and Ellsworth, 1976
CA-4	Palmdale 34.45o, 117.87o	N80oE	T	HF	Results from ~200 m depth in two wells adjacent to the San Andreas. Estimated precision of stress orientations ±5o.	M. D. Zoback, 1978
CA-5	San Fernando 34.41o, 118.40o	N85oE	T/SS	FM(A)	Avg. of both main shocks and aftershocks of San Fernando 1971 earthquake. Includes strike-slip and thrust events.	Whitcomb et al., 1973
CA-6	Central Transverse Ranges 34.5o, 118o	E-W	T/SS	FM(A)	Avg. stress orientation from 22 mechanism for small events. Predominantly thrusting on E-W planes, some strike-slip on NE and NW planes.	Pechmann, in press
CA-7	Galway Lake 34.52o, 116.48o	N75oW	SS	FM,G-FS	Right-lateral slip on vertical fault striking N-S to N25oW, based on first motion data, distribution of aftershocks and ground breakage.	Hill and Beeby, 1977 Kanamori and Fuis, 1977

NUMBER	LOCATION	LEAST HORIZONTAL PRINCIPAL STRESS ORIENTATION	STRESS REGIME	TYPE OF INDICATOR	COMMENTS	REFERENCES
CA-8	Parkfield 35.92°, 120.42°	N70°W	SS	FM(S)	Parkfield earthquake 1966, nearly pure strike-slip. T-axis plunges 13°E, P-axis N13°E, plunge = 14°S.	McEvilly, 1966
CA-9	Central coastal Calif. ~36°, 121.5°	~N60°W	SS/T	FM(A)	Avg. of 30 events, approx. equal number of strike-slip and thrust events. Range P-axes N10°W-N60°E.	Gawthrop, 1977
CA-10	S.F. Bay Area/Central San Andreas. 37°, 121.5°	~N80°W	SS	FM(A)	Avg. of 40 events, predominantly strike-slip and some thrust. Range T-axes N67°E - N133°E, Std. Dev. ±33°.	Ellsworth, written commun.
CA-11	Danville 37.87°, 121.94°	N85°W	SS	FM(A)	Avg. T direction from strike-slip swarm. Focal depths 5-10 km.	Weaver and Hill, 1978
CA-12	Santa Rosa 38.48°, 122.68°	N77°W	SS	FM(A)	Avg. composite solution for aftershocks of the 1969 Santa Rosa earthquake. T-axis plunge 2°W, P-axis N77°W plunge = 11°N.	Smith and Lindh, 1978
CA-13	Cape Mendocino 40.30°, 124.50°.	N59°E	SS	FM(S)	Pure strike-slip event in 1962.	Bolt et al., 1968.
CA-14	Offshore Cape Mendocino 40.34°, 125.84°	N63°E	SS	FM(S)	Pure strike-slip event on Mendocino fracture zone.	Tobin and Sykes, 1968.
CA-15	East end of Garlock Fault 35.92°, 117.80°	N66°W	SS	FM(S)	Pure strike-slip solution.	Smith and Lindh, 1978
CA-16	Coso Hot Springs 36.0°, 117.83°	N80°W	N/SS	FM(A) G-CC,D	Both strike-slip and normal fault events with consistent T-axis, consistent with volcanic feeder trends.	Weaver and Hill, 1978 Duffield, 1975
CA-17	Death Valley 36.1°, 116.8°	NW-SE	N	G-FS(G)	Trend of striated surfaced on "turtlebacks."	Wright et al., 1974.
CA-18	Owens Valley 36.75°, 118.2°	N57°W	N	G-FS(H)	Owens Valley earthquake 1872, oblique slip on NNW-trending fault. Used maximum vertical and right-lateral offsets (which occurred very close to one another) and avg. fault trend.	Bateman, 1971
CA-19	Mt. Whitney Quad. ~36.625°, 118.275°	N34°W	SS	G-FS(G)	Strain pattern deduced from near conjugate sets of micro-faults, stress direction taken as the appropriate bisector of the angle between intersecting trends of right-lateral and left-lateral faults.	Lockwood and Moore, 1979
CA-20	Triple Divide Peak Quad ~36.625°, 118.625°	N46°W	SS	G-FS(G)	SEE CA-19	Lockwood and Moore, 1979

NUMBER	LOCATION	LEAST HORIZONTAL PRINCIPAL STRESS ORIENTATION	STRESS REGIME	TYPE OF INDICATOR	COMMENTS	REFERENCES
CA-21	Mt. Pinchot Quad ~36.875°, 118.375°	N43°W	SS	G-FS(G)	SEE CA-19	Lockwood and Moore, 1979
CA-22	Marion Peak Quad ~36.875°, 118.625°	N49°W	SS	G-FS(G)	SEE CA-19	Lockwood and Moore, 1979
CA-23	Dinkey Creek ~37.15°, 119°	N65°W	SS	HF	Hydrofrac at 160 and 320 m. At deeper interval S_{Hmax} Svert S_{Hmin}..	Haimson, 1976b
CA-24	Mt. Abbott Quad ~37.375°, 118.875°	N68°W	SS	G-FS(G)	SEE CA-19	Lockwood and Moore,
CA-25	Kaiser Peak Quad ~37.375°, 119.125°	N74°W	SS	G-FS(G)	SEE CA-19	Lockwood and Moore, 1979
CA-26	White Mountains 37.5°, 118.3°	N60°W	N	G-FS(G)	Grooves and slickensides on fault bounding White Mountains.	Russell, 1977
CA-27	Mono Lake area 37.5°, 118.5°	~E-W	SS	FM(C)	Composite focal mechanism for strike-slip events in Mono Lake-northern Owens Valley area.	Pitt and Steeples, 1975
CA-28	Tuolumne Meadows Quad ~37.875°, 119.375°	N87°W	SS	G-FS(G)	SEE CA-19	Lockwood and Moore, 1979
CA-29	Sonora Pass Quad ~38.375°, 119.625°	N88°W	SS	G-FS(G)	SEE CA-19	Lockwood and Moore, 1979
CA-30	Markleeville Quad ~38.625°. 119.875°	N81°W	SS	G-FS(G)	SEE CA-19	Lockwood and Moore, 1979
CA-31	Truckee 39.43°, 120.17°	N78°E	SS	FM(S)	1956 Truckee earthquake; T-axis plunges 6°E, P-axis trends N20°W plunge = 7°N.	Tsai and Aki, 1966
CA-32	Oroville 39.5°, 121.5°	N77°E	N/SS	FM(S)	1975 Oroville earthquake; predominantly normal faulting with T-axis plunge = 16°SW and P-axis N53°W, plunge = 64°SE.	Langston and Butler, 1976

CANADA

NUMBER	LOCATION	LEAST HORIZONTAL PRINCIPAL STRESS ORIENTATION	STRESS REGIME	TYPE OF INDICATOR	COMMENTS	REFERENCES
CN-1	Oshawa 43.88°, 78.85°	N65°W	T	HF	Depth 230-300 m.	Haimson and Lee, 1979
CN-2	Maniwaki 46.3°, 76.22°	N40°W	T/SS	FM(S)	Predominantly thrust w/component of strike-slip. P-axis trends N50°E, plunge 19°NE	Horner et al. (1975) Sbar and Sykes (1977)
CN-3	St. Lawrence 47.5°, 70.2°	N-S	T/SS	FM(A)	Six events have avg. compression in E-W direction and T-axis switch between horizontal and vertical.	Le Blanc and Buchbinder, 1977

COLORADO

NUMBER	LOCATION	LEAST HORIZONTAL PRINCIPAL STRESS ORIENTATION	STRESS REGIME	TYPE OF INDICATOR	COMMENTS	REFERENCES
CO-1	Rocky Mtn Arsenal (Denver) 39.7°, 104.7°	N70°E	SS	FM(A)	Earthquakes induced by fluid injection at Rocky Mtn arsenal. Avg. of 36 predominantly strike-slip events.	Healy et al, 1968
CO-2	Henderson Project 39.77°, 105.83°	N38°E	N?	OC	Overcores at different depths at at 3 localities. Only shallowest (624 m) had vertical and horizontal stress orientations. Deeper two had principal stress axes with large plunge so horizontal azimuths not meaningfull. Shallow measurement $S_1 = S_{vert.}$, in deeper measurements the axis with the steepest plunge is S_3.	Hooker et al., 1972
CO-3	Piceance Basin 39.83°, 108.38°	N20°E	SS?	HF	Avg. S_3 direction from 6 wells. At 0.5 km depth $S_1 = S_v$ in one hole, $S_2 = S_v$ in 3 holes and S_3 S_v in all holes.	Bredehoeft et al., 1976
CO-4	Rangely 40.10°, 108.88°	N20°W N12°E	SS SS	HF FM(C)	One hydrofract. measurement at depth of earthquake foci. (~1.8 km). Focal mechanism consistent with slip on pre-existing fault. Surface overcore measurements somewhat scattered, least principal horizontal stress directions range between N27°W - N10°E.	Raleigh et al, 1972 Haimson, 1973

CONNECTICUT

NUMBER	LOCATION	LEAST HORIZONTAL PRINCIPAL STRESS ORIENTATION	STRESS REGIME	TYPE OF INDICATOR	COMMENTS	REFERENCES
CT-1	Colchester 41.5°, 72.25°	N32°E	T	G-FS	Offset coreholes indicate modern thrust motion on pre-existing fault. Grooves and slickenslides were measured on slip surfaces.	Block et al, 1979

GEORGIA

NUMBER	LOCATION	LEAST HORIZONTAL PRINCIPAL STRESS ORIENTATION	STRESS REGIME	TYPE OF INDICATOR	COMMENTS	REFERENCES
GA-1	Augusta 33.5°, 82.22°	N25°E	T	G-FS	Late Cenozoic/possibly Holocene age beds offset by high angle reverse fault, Belair fault system.	Prowell et al., 1975

IDAHO

NUMBER	LOCATION	LEAST HORIZONTAL PRINCIPAL STRESS ORIENTATION	STRESS REGIME	TYPE OF INDICATOR	COMMENTS	REFERENCES
ID-1	Cache Valley 42.05°, 111.8°	N77°W	N	FM(S)	Cache Valley earthquake, 1962. Nearly pure normal fault, T-axis plunges 13°W, P-axis azimuth = N51°W, plunge = 76°SE.	Smith and Sbar, 1974
ID-2	Pocatello 42.2°, 112.5°	N76°W	N	FM(S)	Pocatello Valley earthquake, 1975, nearly pure normal fault.	Bache and Lambert, 1977 Arabasz et al, 1979
ID-3	Caribou Range 43.0°, 111.4°	N81°W	N	FM(C)	Predominantly normal faulting, small strike-slip component T-axis plunges 10°W; P-axis azimuth = N10°W, plunge = 75°S.	Sbar et al, 1972b
ID-4	Central Snake River Plain ~43.42°, 113.21°	~N48°E	N	G-CC	Rift zone crossing Plain marked by normal faults, open fissures, and cinder cones. Age of associated basaltic volcanism is Upper Pleistocene (12,000-100,000 yrs. ago).	Kuntz, 1978

NUMBER	LOCATION	LEAST HORIZONTAL PRINCIPAL STRESS ORIENTATION	STRESS REGIME	TYPE OF INDICATOR	COMMENTS	REFERENCES
ID-5	Salmon River Mountains 44.3o, 114.7o	N9oE	N	FM(S)	Virtually a pure normal fault. T-axis plunge 1oN, P-axis azimuth = N85oW, plunge = 83o.	Smith and Sbar, 1974.
ID-6	Kellogg 47.33o, 116.06o	N15oE	N	HF	Hydrofrac at 2285 m depth, S_3/S_1 = 0.42.	Haimson, 1977b
ID-7	Coeur d'Alene district 47.47o, 116.0o	N65oW N63oE	SS T	OC OC	Depth = 1670 m $S_{Hmax} >> S_{vert} > S_{Hmin}$ Depth = 1616 m, all streses approx. equal in magnitude. Measurements made in separate mines only 3 km apart.	Chan and Crocker, 1972 Skinner et al., 1974

ILLINOIS

NUMBER	LOCATION	LEAST HORIZONTAL PRINCIPAL STRESS ORIENTATION	STRESS REGIME	TYPE OF INDICATOR	COMMENTS	REFERENCES
IL-1	Southern 37.95o, 88.48o	N70oE	T	FM(S)	Well constrained single event solution. P-axis azimuth = N83oW, plunge = 1oE.	Stauder and Nuttli, 1970.
IL-2	Central 39.3o, 89.35o	N30oW	SS/T	HF	Depth = 100 m. $S_1 > S_{vert} = S_3$.	Haimson, 1974a
IL-3	Northern 41.6o, 89.4o	N51°W	SS	FM(S)	Based on both surface wave and body wave solutions. T-axis plunge = 28oSE; P-axis azimuth = N38oE, plunge = 1oNE.	Herrmann, 1979.

KANSAS

NUMBER	LOCATION	LEAST HORIZONTAL PRINCIPAL STRESS ORIENTATION	STRESS REGIME	TYPE OF INDICATOR	COMMENTS	REFERENCES
KS-1	Northeast 39.14o, 96.30o	N10oE	T	FM(S)	Microearthquake solution, P- and T-axes constrained to ±10o.	D. W. Steeples, pers. comm.,

LOUISIANA

NUMBER	LOCATION	LEAST HORIZONTAL PRINCIPAL STRESS ORIENTATION	STRESS REGIME	TYPE OF INDICATOR	COMMENTS	REFERENCES
LA-1	Southeastern 29.6o, 90.75o	N-S	N	G-FS	Active growth faults, general regional trend.	Howard et al, 1978
LA-2	Southern 30.2o, 92.8o	N80E	N	G-FS	Active growth faults, general regional trend.	Howard et al, 1978
LA-3	Caddo-Pine Island 32.67o, 94o	N-S	N/SS? SS	HF	Depth 425 m. Maximum horizontal stress not measured, $S_{vert} > S_3$.	Strubhar et al, 1975.

MASSACHUSETTS

NUMBER	LOCATION	LEAST HORIZONTAL PRINCIPAL STRESS ORIENTATION	STRESS REGIME	TYPE OF INDICATOR	COMMENTS	REFERENCES
MS-1	Attleboro 41.94o, 71.32o	N67oE	T	G-FS(G)	Post-glacial offsets on high angle NE-striking reverse faults.	Woodworth, 1907 Oliver et al., 1970

MEXICO

NUMBER	LOCATION	LEAST HORIZONTAL PRINCIPAL STRESS ORIENTATION	STRESS REGIME	TYPE OF INDICATOR	COMMENTS	REFERENCES
MX-1	Northern Sonora 31.08o, 109.17o	N50oW to E-W	N	G-FS(H)	Sonoran earthquake M $\sim$ 7.8. Generally a N-S fault with controversy over the amount of offset. Gianella reported 6 m dip-slip and 6 m strike-slip offset. Sumner, looking at a different part of the scarp, reported only 4 m of dip-slip movement and felt the strike-slip component was small (<1 m) or non-existent.	Gianella, 1960 Sumner, 1977 Sumner, pers. comm. 1978

MICHIGAN

NUMBER	LOCATION	LEAST HORIZONTAL PRINCIPAL STRESS ORIENTATION	STRESS REGIME	TYPE OF INDICATOR	COMMENTS	REFERENCES
MC-1	Ishpenning 46.5°, 87.6°	N8°E	SS	OC	Depth = 976 m.	Aggson, 1972

MINNESOTA

NUMBER	LOCATION	LEAST HORIZONTAL PRINCIPAL STRESS ORIENTATION	STRESS REGIME	TYPE OF INDICATOR	COMMENTS	REFERENCES
MN-1	St. Cloud 45.5°, 94.2°	N50°W N40°W	T ?	HF OC	Depth only 15 m. S_1 S_2 Svert Surface measurement in quarry.	Von Schonfeldt, 1970 Hooker et al, 1974
MN-2	West-central 45.7°, 96.0°	N77°W	SS	FM(S)	Strike-slip event with thrust component. Based on surface wave and body wave data. T-axis plunges 14°W, P-axis azimuth = N17°E; plunge = 14°N.	Herrmann, 1979

MISSISSIPPI

NUMBER	LOCATION	LEAST HORIZONTAL PRINCIPAL STRESS ORIENTATION	STRESS REGIME	TYPE OF INDICATOR	COMMENTS	REFERENCES
MI-1	West-central 33.6°, 90.9°	N25°W	SS	FM(S)	Primarily strike-slip event, based on both surface wave and body-wave data. T-axis plunges 21°SE, P-axis plunges 7°NW.	Herrmann, 1979

MISSOURI

NUMBER	LOCATION	LEAST HORIZONTAL PRINCIPAL STRESS ORIENTATION	STRESS REGIME	TYPE OF INDICATOR	COMMENTS	REFERENCES
MO-1	New Madrid area 36.5°. 89.7°	N47°W	SS	FM(S)	Primarily strike-slip, with normal component. Based on surface wave and body wave solutions. T-axis plunges 8°NW; P-axis azimuth - N49°E, plunge = 34°NE.	Herrmann, 1979

MISSOURI (continued)

NUMBER	LOCATION	LEAST HORIZONTAL PRINCIPAL STRESS ORIENTATION	STRESS REGIME	TYPE OF INDICATOR	COMMENTS	REFERENCES
MO-2	New Madrid area 36.5°, 89.6°	N59°W	SS/T	FM(S)	Primarily strike-slip, with thrust component. Based on surface wave and body wave solutions. T-axis plunges 28°NW; P-axis azimuth = N43°E, plunge = 19°NE.	Herrmann, 1979
MO-3	Ozark uplift 37.5°, 91.0°	N24°W	N	FM(S)	Primarily normal fault. Based on surface wave and body wave solutions. T-axis plunges 7°SE; P-axis azimuth = N87°W, plunge = 7°W.	Herrmann, 1979
MO-4	Bunker 37.45°, 91.22°	N73°E	T	OC	Depth = 305 m. S_{Hmax} S_{Hmin} $S_{vert.}$.	Horino and Aggson, 1976

MONTANA

NUMBER	LOCATION	LEAST HORIZONTAL PRINCIPAL STRESS ORIENTATION	STRESS REGIME	TYPE OF INDICATOR	COMMENTS	REFERENCES
MT-1	Hegben Lake 44.75°, 111.18°	N18°E	N	FM(S+A)	1959 Hegben Lake earthquake, primarily normal faulting. T-axis plunge = 19°S; P-axis azimuth = N3°E, plunge = 70°N. Consistent stress orientation obtained from a number of recent microearthquakes in the region.	Ryall, 1962 Bailey, 1976
MT-2	Southeastern Madison Valley 44.8°, 111.43°	N26°W	N	FM(C)	Nearly pure normal faulting. T-axis plunge = 8°N; P-axis azimuth = N24°E, plunge = 82°S.	Trimble and Smith, 1975
MT-3	Madison Valley 44.8°, 111.6°	N2°E	SS	FM(S)	Predominantly strike-slip event. T-axis plunge = 30°N; P-axis azimuth = N88°E, plunge = 7°W.	Smith and Sbar, 1974
MT-4	Southeast of Helena 46.4°, 111.3°	N21°W	SS	FM(S)	1925 Montana earthquake (M = 6.7). Poorly constrained, from one of Byerly's first determinations of first motion patterns.	Byerly, 1926 Smith and Sbar, 1974
MT-5	Helena ~46.67°, 112.17°	N45°E	N/SS	FM(A)	Avg. of composite solutions for 3 swarms. Two of the solutions were primarily normal faulting one mostly strike-slip, all have comparable T-axes (±10°).	Friedline et al, 1976
MT-6	Flathead Lake 47.8°, 114.3°	N86°W	N/SS	FM(A)	Avg. of two composite focal mechanisms, one strike-slip and one normal with T-axes trending ~N85°W and ~N87°W respectively.	Sbar et al, 1972b Stevenson, 1976

NUMBER	LOCATION	LEAST HORIZONTAL PRINCIPAL STRESS ORIENTATION	STRESS REGIME	TYPE OF INDICATOR	COMMENTS	REFERENCES
NV-1	Lake Mead area 36.08°, 114.74°	N38°W	N/SS	FM(A)	Avg. of two composite mechanisms with similar T-axes. One is a strike-slip and one is a normal event.	Rogers and Lee, 1976.
NV-2	Northwest of Las Vegas 36.60°, 116.27°	N60°W	N	FM(S)	Predominantly normal event with a small strike-slip component. T-axis plunge = 3°N; P-axis azimuth = N77°E, plunge = 66°SE.	Smith and Lindh, 1978
NV-3	Nevada Test Site (NTS) 37°, 116°	N50°W	N/SS	G, HF, FM	Based on trends of Quaternary faulting, strain measurements, tectonic cracking, focal mechanisms including both strike-slip and normal events, and hydrofracts.	Carr, 1974 Fischer et al, 1972 Haimson et al, 1974
NV-4	Northwest of NTS 37.2°, 116.5°	N45°W	N/SS	FM(A)	Consistent T-axis orientation from two composite events: one pure strike-slip, the other a normal fault event.	Hamilton and Healy, 1969
NV-5	Near California border 37.13°, 117.32°	N50°W	N	FM(S)	Predominantly normal event with strike-slip component, T-axis plunges 30°NW; P-axis azimuth = N85°W, plunge = 45°E.	Smith and Lindn, 1978
NV-6	Near southern Utah border 37.4°, 114.2°	N30°W	SS	FM(S)	Nearly pure strike-slip mechanism. T-axis plunges 16°SE; P-axis azimuth = N59°E, plunge = 0°.	Smith and Sbar, 1974
NV-7	Silver Peak Range 37.47°, 117.87°	N88°W	N	FM(S)	Predominantly normal event with small strike-slip component. T-axis plunge = 3°W; P-axis azimuth = N15°E, plunge = 63°N.	Smith and Lindh, 1978
NV-8	Northern Pahroc Range 37.73°, 115.05°	N51°W	N	FM(S)	Predominantly normal event with strike-slip component. T-axis plunge = 30°SE; P-axis azimuth = N160°W, plunge = 81°N.	Smith and Lindh, 1978
NV-9	Southern Quinn Canyon Range 37.75°, 116.0°	N60°W	SS	FM(C)	Predominantly strike-slip. T-axis plunge = 15°S; P-axis azimuth = N87°E, plunge = 2°W.	Smith and Lindh, 1979
NV-10	Lunar Crater volcanic field 38.25°. 116.0°	N60°W	N	G-CC	Avg. trend of alignments of basaltic craters, cones, mounds and fissure vents. Basalts tentatively Quaternary, possibly Holocene.	Scott and Trask, 1971
NV-11	Candelaria Hills 38.2°, 118.15°	N82°W	N/SS	G-FS(G)	Large component of left-lateral slip on an ∿E-W trending fault.	Speed and Cogbill, 1979
NV-12	Excelsior Mtns 38.3°, 118.4°	N75°W	N	FM(C)	Predominantly normal event with strike-slip component. T-axis plunge ≈0°; P-axis azimuth ≈N10°E, plunge ≈60°S.	Ryall and Priestley, 1975

NEVADA (continued)

NUMBER	LOCATION	LEAST HORIZONTAL PRINCIPAL STRESS ORIENTATION	STRESS REGIME	TYPE OF INDICATOR	COMMENTS	REFERENCES
NV-13	Cedar Valley 38.5°, 117.8°	~N80°E	N	FM(C)	Predominantly normal event with strike-slip component. T-axis plunge = 21°W; P-axis azimuth N33°E, plunge = 59°N.	Gumper and Scholz, 1971
NV-14	Genoa 390.00, 119.8°	~E-W	N	G-FS(G)	Well exposed bedrock scarp.	Thompson and Burke, 1973
NV-15	Comstock/Virginia City 39.3°, 119.6°	N60°W	N	G-FS(G)	Based on surface and below surface observations.	Thompson and Burke, 1973
NV-16	Fairview Peak, south zone 39.2°, 118.00	~N44°W	N	FM(C)	Pure normal faulting. T-axis plunges 5°NW; P-axis azimuth = N44°W, plunge = 85°SE.	Ryall and Malone, 1971
NV-17	Fairview Peak, central zone 39.2°, 118.1°	N65°W	N/SS	FM(A)	Avg. of similar composite mechanisms and single mechanism for 1954 earthquake, combination normal and strike-slip component. T-axes plunge 2-3°, P-axes plunge 40-45°.	Romney, 1957 Ryall and Malone, 1971
NV-18	Dixie Valley 39.7°, 118.00	N55°W	N	G-FS(G)	Mean extension direction based on 55 measurements along fault zone on west side of Dixie Valley.	Thompson and Burke, 1973
NV-19	Rainbow Mtn. 39.7°, 118.4°	N56°W	N	FM(C)	Pure normal faulting. T-axis plunge = 5°NW; P-axis azimuth = N56°W, plunge = 85°SE.	Ryall and Malone, 1971
NV-20	Fairview Peak, north zone 39.8°, 118.00	~N14°W	N	FM(C)	Predominantly normal with strike-slip component. T-axis plunges 1°N; P-axis azimuth = N53°E, plunge = 59°SW.	Ryall and Malone, 1971
NV-21	Cortez 40.2°, 116.5°	N55°W	N	G-FS(G)	Well exposed Holocene bedrock scarp. Mean extension direction based on 56 measurements along 8 km length of fault.	Zoback, 1978, and in press Muffler, 1964
NV-22	Pleasant Valley 40.3°, 117.6°	N50-70°W	N	G-FS(H)	Based on offsets on scarps formed during the 1915 Pleasant Valley earthquakes.	Wallace, 1979
NV-23	Buffalo Valley 40.37°, 117.33°	N60°W	N	G-CC	Trend of zone of basaltic cindercones 1.35 ± 0.15 m.y. in age.	Trexler et al, 1978
NV-24	Argenta Rim 40.6°, 116.75°	N77°W	N	G-FS(G)	Avg. of 5 directions measured at one locality.	M. L. Zoback, 1978 and in press
NV-25	Black Rock Desert 40.75°, 119.25°	N75°W	N	FM(A), G-FS	Avg. of several microearthquake focal mechanisms, also based trends of "tectonic" cracks and Quaternary faulting.	Grose, 1978 Kumamoto, 1978

NEVADA (continued)

NUMBER	LOCATION	LEAST HORIZONTAL PRINCIPAL STRESS ORIENTATION	STRESS REGIME	TYPE OF INDICATOR	COMMENTS	REFERENCES
NV-26	Denio 41.83°, 118.48°	∿N80°W	N	FM(C)	Normal faulting event with strike-slip component. T-axis plunge = 0°; P-axis azimuth = ∿N45°E, plunge ≅ 45°SW.	Richins 1974 Smith and Lindh, 1978

NEW JERSEY

NUMBER	LOCATION	LEAST HORIZONTAL PRINCIPAL STRESS ORIENTATION	STRESS REGIME	TYPE OF INDICATOR	COMMENTS	REFERENCES
NJ-1	Ramapo Fault 41.00, 74.25°	∿N10°E	T	FM(A)	Modern slip on reactivated Triassic normal fault (Ramapo fault). Predominantly thrust events, some strike-slip. Avg. P-axis N80° ± 20°.	Aggarwal and Sykes, 1978

NEW MEXICO

NUMBER	LOCATION	LEAST HORIZONTAL PRINCIPAL STRESS ORIENTATION	STRESS REGIME	TYPE OF INDICATOR	COMMENTS	REFERENCES
NM-1	Tres Hermanas Mtns 31.83°, 107.80°	∿E-W	N	G-D,CC	Basaltic volcanism, latest Tertiary - Quaternary in age.	Balk, 1962
NM-2	Potrillo volcanic field ∿32°, 107°	∿N80°W	N	G-CC	Basaltic volcanism about 100,000 yrs old.	Luedke and Smith, 1978 Hoffer, 1976
NM-3	North of Carrizozo 33.81°, 105.83°	∿N5°E	N?	G-D,CC	Broken Back crater and Little Black Peak, Quaternary to recent in age.	Smith, 1964 Weber, 1964
NM-4	Socorro 34.12°, 106.92°	N80°E	N	FM(A)	Avg. T-direction taken from 3 composite solutions; all normal events.	Sanford et al, 1979
NM-5	Belen 34.5°, 106.85°	N81°W	N/SS	FM(A)	Avg. T-direction taken from 4 composite solutions, two events nearly pure normal faulting and two strike-slip	Sanford et al, 1979

NEW MEXICO (continued)

NUMBER	LOCATION	LEAST HORIZONTAL PRINCIPAL STRESS ORIENTATION	STRESS REGIME	TYPE OF INDICATOR	COMMENTS	REFERENCES
NM-6	Northern Socorro County 34.55°, 107.33°	~N50°W	N	G-FS(G)	Normal faults striking N10°W with consistent right-lateral components of motion.	Jicha, 1958
NM-7	Valencia, Socorro, & Catron Co. 34.62°, 107.53°	N80°W	N	G-CC	Basaltic volcanism in the age range of 1-5 m.y.	Luedke and Smith, 1978 Winchester, 1920
NM-8	West of Los Lunas 34.80°, 107.35°	N61°W	N	G-D	Trend of single basaltic dike, Quaternary in age.	Wright, 1946
NM-9	Cat Hills 34.88°, 106.87°	N79°W	N	G-CC	Basaltic volcanism 140,000 yrs in age.	Luedke and Smith, 1978
NM-10	Grants 35°, 48.81°	N67°W	N	G-D	Basaltic dike (latest Pliocene-Quaternary in age) parallel to the Mal Pais volcanic field which is marked by a prominent NNE-trending gravity high.	Thaden et al, 1967
NM-11	Albuquerque 35.15°, 106.77°	N87°W	N	G-CC	Spectacular alignment of 18 basaltic cones, 190,000 yrs old.	Kelley, 1969
NM-12	Mount Taylor volcanic field 35.33°, 107.63°	N70-75°W	N	G-CC,D	Basaltic volcanism Pliocene to Holocene in age.	Hunt, 1938 Moench and Schlee, 1967
NM-13	Southeast McKinley Co. 35.37°, 107.48°	N60°W	N	G-CC	Based on several cindercone alignments and trends of numerous parallel faults, 2-3 m.y. in age.	Cooper and John, 1968.
NM-14	Northwest of Mt. Taylor 35.7°, 107.73°	N63°E	SS	FM(S)	Predominantly strike-slip event, no information on plunge of P- and T-axes given.	Sanford et al, 1979
NM-15	Northwest of Mt. Taylor 35.7°, 107.98°	N7°E	SS	FM(S)	Predominantly strike-slip event, no information on plunge of P- and T-axes given.	Sanford et al, 1979
NM-16	Bernillo 35.83°, 106.83°	N55°W	N	G-FS(G)	Normal fault striking N5°W with a component of right-lateral slip in addition to dip-slip.	Woodward, 1977
NM-17	Jemez Mtns 35.92°, 106.83°	N55°W N80°W	N N?	HF G-D,CC	Hydrofrac to depths of 2.93 km. Avg. trend of Quaternary dikes and cindercones, also Vallez caldera elongation.	Haimson, 1977b Smith, et al, 1970
NM-18	Naciemento Uplift 36.0°, 106.88°	N62°W	N	FM(C)	Predominantly normal with strike-slip component. No information given on plunge of P- or T-axes.	Sanford et al, 1979

NUMBER	LOCATION	LEAST HORIZONTAL PRINCIPAL STRESS ORIENTATION	STRESS REGIME	TYPE OF INDICATOR	COMMENTS	REFERENCES
NM-19	Espanola 36.14°, 106.27°	N75°W	N	FM(C)	Predominantly normal event. No information on plunge of P- or T-axes.	Sanford et al, 1979
NM-20	Farmington 36.45°, 108°	N35°W	N/SS	HF	Massive hydrafracting at 2150 m. $S_{vert} \simeq S_{Hmax} >> S_{Hmin}$..	McGarr and Gay, 1978
NM-21	Western Raton volcanic field 36.42°, 104.92°	N48°E	N?	G-D	Basaltic dikes generally 3-5 km long, late Tertiary - Quaternary in age.	Griggs, 1948
NM-22	Southeast of Raton 36.53°, 103.25°	N14°E	N?	G-CC	Based on several basaltic cindercone alignments, Quaternary in age. Longest alignment, Don Carlos Hills, contains 16 cones in 22 km.	Baldwin and Muehlberger, 1959
NM-23	Raton volcanic field 36.62°, 104.33°	N23°E	N?	G-D	Well exposed basaltic dike swarm with avg. trend N67°W. Probably 2-3 m.y. old based on nearby flows.	Wood et al, 1953
NM-24	Raton volcanic field 36.67°, 104.57°	N20°E	N?	G-D	Several well exposed basaltic dike swarms with avg. trend ~N70°W. Late Tertiary - Quaternary in age.	Griggs, 1948
NM-25	Mora Co. 36.87°, 104.5°	N36°E	N?	G-D	Basaltic dike about 8 km long. Probably 3-4 m.y. old based on nearby flows.	Wanek, 1962
NM-26	N. end Sangre de Christo Mtns. 36.98°, 105.40°	N74°W	N?	G-D	Basaltic dike which intrudes Quaternary fan gravels.	McKinlay, 1956
NM-27	Taos Plateau 36.84°, 105.95°	N73°W	N	G-CC,FS	Basaltic volcanism 3-4 m.y. old. Lambert mentions transform-style, near vertical faults that trend nearly E-W and have horizontal slickensides.	Luedke and Smith, 1978 Lambert, 1966
NM-28	Dulce 36.9°, 106.9°	N68°W	N/SS	FM(S)	1966 Dulce earthquake. Probably strike-slip, however also possible to fit data with normal fault mechanism with considerably less confidence. In either case T-axis remains same and is well determined.	Cash, 1971 Cash, 1975

NEW YORK

NUMBER	LOCATION	LEAST HORIZONTAL PRINCIPAL STRESS ORIENTATION	STRESS REGIME	TYPE OF INDICATOR	COMMENTS	REFERENCES
NY-1	Alma Township 42.08o, 78o	N15oW	SS/N	HF	Depth = 510 m. $S_{Hmax} > S_{vert} = S_{Hmin}$.	Haimson, 1974a
NY-2	Allegany Co. 42.08o, 78o	N30oW	?	HF	Only orientation given, no information on magnitudes or depth.	Overbey and Rough, 1968
NY-3	Attica 42.8o, 78.2o	N29oW	SS/T	FM(S)	Based on surface wave and body wave solutions. T-axis plunges 28oW. P-axis azimuth = N62oE, plunge = 1oNE.	Herrmann, 1979
NY-4	Blue Mtn Lake 43.88o, 74.33o	N19oW	T	FM(A)	Avg. of numerous thrust events.	Sbar et al, 1972
NY-5	Altona 44.90o, 73.67o	N17oW	T	FM(S)	P-axis azimuth = N73oE, plunge = 8oT, T-axis plunge = 84o	Aggarwal, 1977

OHIO

NUMBER	LOCATION	LEAST HORIZONTAL PRINCIPAL STRESS ORIENTATION	STRESS REGIME	TYPE OF INDICATOR	COMMENTS	REFERENCES
OH-1	Hocking Co./Falls Township 39.5o, 82.5o	N25oW	SS	HF	Depth = 810 m.	Haimson, 1974a
OH-2	Barberton 41.01o, 81.64o	N-S	SS/N	OC	Depth = 701 m. $S_{Hmax} >> S_{vert} \approx S_{Hmin}$.	Obert, 1962

OKLAHOMA

NUMBER	LOCATION	LEAST HORIZONTAL PRINCIPAL STRESS ORIENTATION	STRESS REGIME	TYPE OF INDICATOR	COMMENTS	REFERENCES
OK-1	Kingsfisher County 35.9o, 97.9o	N25oE	?	HF	Depth and magnitudes of stresses not given.	von Schonfeldt et al, 1973

OREGON

NUMBER	LOCATION	LEAST HORIZONTAL PRINCIPAL STRESS ORIENTATION	STRESS REGIME	TYPE OF INDICATOR	COMMENTS	REFERENCES
OR-1	Adel 42.17°, 119.92°	N60°W	N/SS	FM(S)	1968 Adel (Warner Valley) earthquake. P-axis azimuth = N65°E, plunge = 35°NE, T-axis plunge = 13°SE.	Schaff, 1976
OR-2	Deschutes Valley 45.15°, 120.86°	N72°W	T	FM(C)	1976 Deschutes Valley earthquake. Composite mechanism using foreshocks, mainshock; and aftershocks. P-axis azimuth = N18°E, plunge = 13°S; T-axis plunge = 77°.	Couch et al, 1976

PENNSYLVANIA

NUMBER	LOCATION	LEAST HORIZONTAL PRINCIPAL STRESS ORIENTATION	STRESS REGIME	TYPE OF INDICATOR	COMMENTS	REFERENCES
PA-1	Port Matilda 40.78°, 78.07°	N50°E	T	G-FS(C)	Modern offset of coreholes exposed in road-cut, motion on pre-existing reverse fault.	Schafer, 1979
PA-2	Millerstown 40.95°, 79.75°	N10°E	T	G-FS(C)	Modern offset of coreholes exposed in road-cut, motion on pre-existing reverse fault.	Schafer, 1979
PA-3	McKean County 41.8°, 78.6°	N20°W	?	HF	Depth and stress magnitudes not reported.	Overbey and Rough, 1968

SOUTH CAROLINA

NUMBER	LOCATION	LEAST HORIZONTAL PRINCIPAL STRESS ORIENTATION	STRESS REGIME	TYPE OF INDICATOR	COMMENTS	REFERENCES
SC-1	Summerville 32.60°, 80.32°	N65°E	N?	HF	Avg. of 2 impression orientations in depth range 100-340 m. Estimate accuracy of orientation ±10°.	Zupan and Abbot, 1975
SC-2	Langley 33.53°, 81.85°	N55°E	N	G-FS	Post-Eocene motion on normal faults with an avg. trend of N35°W ± 5°	Inden and Zupan, 1975
SC-3	West of Columbia 34.00°, 81.00°	N23°E	N?	G-D	Orientation of post-Eocene (?) clastic dikes.	Zupan and Abbot, 1975
SC-4	Cheraw 34.75°, 80.0°	N78°E	T	G-FS	Post-Eocene motion on reverse faults with an avg. trend of N78°E.	Howell and Zupan, 1974

SOUTH CAROLINA (continued)

NUMBER	LOCATION	LEAST HORIZONTAL PRINCIPAL STRESS ORIENTATION	STRESS REGIME	TYPE OF INDICATOR	COMMENTS	REFERENCES
SC-5	Lake Jocassee 35.0°, 82.87°	N30°W	T	HF	Depth = 185-255 m. Stress orientation sub-parallel to topography; S_{Hmax} SHmin Svert.	Haimson, 1976b

SOUTH DAKOTA

NUMBER	LOCATION	LEAST HORIZONTAL PRINCIPAL STRESS ORIENTATION	STRESS REGIME	TYPE OF INDICATOR	COMMENTS	REFERENCES
SD-1	Lead 44.35°, 103.80°	N40°W	N	OC	Depth = 1890 m, S_{vert} S_{Hmax} S_{Hmin}.	Aggson and Hooker, in press

TENNESSEE

NUMBER	LOCATION	LEAST HORIZONTAL PRINCIPAL STRESS ORIENTATION	STRESS REGIME	TYPE OF INDICATOR	COMMENTS	REFERENCES
TN-1	Rockwood-Harriman 35.90°, 84.67°	N10°E	T	G-FS(C)	Modern offset of coreholes exposed in road-cut, motion on pre-existing reverse fault.	Schafer, 1979
TN-2	Rockwood-Harriman 35.9°, 84.53°	N20°E	T	G-FS(C)	Avg. horizontal component of shortening N70°W, range in values E-W to N50°W.	Schafer, 1979

TEXAS

NUMBER	LOCATION	LEAST HORIZONTAL PRINCIPAL STRESS ORIENTATION	STRESS REGIME	TYPE OF INDICATOR	COMMENTS	REFERENCES
TX-1	Morton 33.65°, 102.7°	N24°E	?	HF	Avg. of fracture orientations in 3 wells, 5° range in values. Depth range = 1.52-1.55 km. No information on relative magnitudes of stresses.	Zemanek et al., 1970

NUMBER	LOCATION	LEAST HORIZONTAL PRINCIPAL STRESS ORIENTATION	STRESS REGIME	TYPE OF INDICATOR	COMMENTS	REFERENCES
TX-2	Denver City 32.92°, 103.05°	N29°E	?	HF	Avg. of fracture orientations in 3 wells, 4° range in values. Depth 2.32 km. No information on relative on relative magnitudes of stresses.	Zemanek et al., 1970
TX-3	Andrews 32.3°, 102.75°	N6°E	?	HF	Avg. of fracture orientations in 4 wells, 33° range in values. Depth range = 1.3-1.4 km. No information on relative magnitudes of stresses.	Zemanek et al., 1970
TX-4	West of Snyder 32.5°, 101.12°	N12°W	?	HF	Avg. of fracture orientations in 2 wells, 18° range in values. Depth 915 m. No information on relative magnitudes of stresses.	Zemanek et al., 1970
TX-5	Big Spring 32.3°, 101.2°	N6°W	?	HF	Avg. of fracture orientations in 3 wells, 22° range in values. Depth range 820-915 m. No information on relative magnitudes of stresses.	Zemanek et al., 1970
TX-6	Southeast of Midland 31.87°, 101.85°	N17°E	?	HF	One well, depth = 2.13 km. No information on relative magnitudes of stresses.	Zemanek et al., 1970
TX-7	Southeast of Midland 31.7°, 101.9°	N3°E	?	HF	One well, depth = 2.59 km. No information on relative magnitudes of stresses.	Zemanek et al., 1970
TX-8	Southwest of Odessa 31.62°, 102.15°	N4°E	?	HF	Avg. of fracture orientations in 2 wells, 3° range in values. Depth 2.38 km. No information on relative magnitude of stresses.	Zemanek et al., 1970
TX-9	Monahans 31.62°, 102.6°	N5°E	?	HF	Avg. of fracture orientations in 4 wells, 29° range in values. Depth 1.04 km. No information on relative magnitudes of stresses.	Zemanek et al., 1970
TX-10	South of Monahans 31.5°, 102.67°	N29°E	?	HF	One well, depth = 1.43 km. No information on relative magnitudes of stresses.	Zemanek et al., 1970
TX-11	Southeast of Monahans 31.42°, 102.45°	N9°E	?	HF	One well, depth = 975 m. No information on relative magnitudes of stresses.	Zemanek et al., 1970
TX-12	Marble Falls 30.57°, 98.27°	N30°E	N	HF	Depth = 255 m. S_{Hmax} S_{vert} S_{Hmin}.	Roegiers, 1974
TX-13	Southeast 28.9°, 96.30°	N26°W	N	G-FS	Active growth faults, general regional trend.	Howard et al., 1978

TEXAS (continued)

NUMBER	LOCATION	LEAST HORIZONTAL PRINCIPAL STRESS ORIENTATION	STRESS REGIME	TYPE OF INDICATOR	COMMENTS	REFERENCES
TX-14	Southern 26.75°, 97.72°	N81°W	N	G-FS	Active growth faults, general regional trend.	Howard et al., 1978

UTAH

NUMBER	LOCATION	LEAST HORIZONTAL PRINCIPAL STRESS ORIENTATION	STRESS REGIME	TYPE OF INDICATOR	COMMENTS	REFERENCES
UT-1	Cedar City 37.8°, 113.03°	N60°E	N	FM(S)	Normal fault event, T-axis plunge = 10°E, P-axis plunge = 76°.	Smith and Sbar, 1974
UT-2	Cove Fort 38.58°, 112.83°	N75°W	N	FM(C)	Predominantly normal with strike-slip component. T-axis plunge = 34°W; P-axis azimuth = N54°W, plunge = 54°SE.	Smith and Lindh, 1978
UT-3	West of San Rafael Swell 38.75°, 111.0°	E-W	N?	G-D	Basaltic dikes, latest Pliocene in age.	P. Delaney, pers. comm.
UT-4	Price 39.5°, 110.5°	N15°E	T	FM(C)	Predominantly thrust event, T-axis plunge = 65°, P-axis azimuth = N75°W plunge = 25°.	Smith et al., 1974
UT-5	Nephi 39.6°, 111.9°	N74°W	N/SS	FM(S)	Approx. equal components of strike-slip and normal faulting. T-axis plunge = 20°E, P-axis azimuth = N40°E, plunge = 48°S.	Smith and Sbar, 1974
UT-6	Uinta Basin 39.83°, 109.25°	N25°E	?	G-D	Gilsonite dikes, Post-Eocene in age. Mapped as cutting Quaternary alluvium.	Untermann and Untermann, 1964
UT-7	Vernal 40.33°, 109.42°	N25°E	N	HF	Depth = 2.75 km. $S_{vert} > S_{Hmax} \approx S_{Hmin}$.	McGarr and Gay, 1978
UT-8	Heber City (south) 40.4°, 111.4°	N27°E	T	FM(C)	Motion on very high angle reverse fault (dip = 80°) or low angle thrust. T-axis plunge = 55°, least horizontal stress taken as null axis: N27°E, plunge = 0°.	Arabasz et al., 1979.
UT-9	Heber City (central) 40.52°, 111.31°	N41°E	N	FM(C)	Predominantly normal event. T-axis plunge = 17°NE; P-axis plunge = 67°.	Langer et al., 1979
UT-10	Heber City (north) 40.6°, 111.2°	N3°E	T	FM(C)	Motion on very high angle reverse fault (dip = 80°) or low angle thrust (dip = 10°). T-axis plunge = 55°, least horizontal stress direction taken as null axis: N3°E, plunge = 2°N.	Arabasz et al., 1979

NUMBER	LOCATION	LEAST HORIZONTAL PRINCIPAL STRESS ORIENTATION	STRESS REGIME	TYPE OF INDICATOR	COMMENTS	REFERENCES
UT-11	Salt Lake City 40.72°, 112.04°	N98°W	N	FM(C)	Predominantly normal fault event. T-axis plunge = 14°SW, P-axis plunge = 72°.	Arabasz et al., 1979
UT-12	Salt Lake City 40.78°, 111.88°	N72°W & N125°W	N	G-FS(G)	Two consistent groove sets found on two faults whose strike varied by nearly 90°.	Pavlis and Smith, 1979
UT-13	East of Salt Lake City 40.8°, 111.5°	N60°W	N	FM(C)	Predominantly normal fault event. T-axis plunge = 25°NW, P-axis plunge = 64°.	Arabasz et al., 1979
UT-14	Logan 41.7°, 111.7°	N84°W	N	FM(C)	Nearly pure normal fault event. T-axis plunge = 15°E, P-axis plunge = 75°.	Arabasz et al., 1979
UT-15	Near Idaho border 41.8°, 112.9°	N105°W	N	FM(S)	Predominantly normal event. T-axis plunge = 30°NE, P-axis azimuth = N60°W, plunge = 50°W. Hansel Valley earthquake 1934.	Dewey et al., 1972
UT-16	Idaho border 41.9°, 112.66°	N103°W	N	FM(C)	Predominantly normal with strike-slip component. T-axis plunge = 2°W, P-axis azimuth = N19°W, plunge = 57°S.	Richins, 1979
UT-17	Sunnyside 39.57°, 110.40°	N59°E	T	OC	Depth = 323 m., $S_{Hmax} > S_{Hmin} \gg S_{vert}$.	Aggson and Hooker, in press

VIRGINIA

NUMBER	LOCATION	LEAST HORIZONTAL PRINCIPAL STRESS ORIENTATION	REGIME	INDICATOR	COMMENTS	REFERENCES
VA-1	North Anna 38.03°, 77.73°	N10°E	T	FM(A)	Avg. of composite, predominantly thrust mechanisms. P-axes range from N80°E to N 120°E.	Dames and Morre, 1976
VA-2	Stafford Fault Zone 38.40°, 77.37°	N33°E	T	G-FS	Latest Tertiary possible Quaternary reverse slip on fault trending N33°E.	Nixon and Newell, 1977

WASHINGTON

NUMBER	LOCATION	LEAST HORIZONTAL PRINCIPAL STRESS ORIENTATION	STRESS REGIME	TYPE OF INDICATOR	COMMENTS	REFERENCES
WA-1	Mount Rainier National Park 46.76°, 121.52°	N70°E	SS	FM(S)	Nearly pure strike-slip event.	Crosson and Lin, 1975
WA-2	Columbia River Basin 46.75°, 119.58°	N85°E	T	FM(A)	Based on composites from 3 separate swarm events and from a nearby single event solution. Predominantly thrust mechanisms with T-axes scattered about vertical.	Malone and others, 1975 Smith and Lindh, 1978
WA-3	Puget Sound 47.4°, 122.3°	N55°E	N	FM(S)	Puget Sound earthquake 1965. Predominantly normal fault with strike slip component. Plunge of T-axis = 8°SE, P-axis azimuth = N46°W, plunge 58°W.	Algermissen and Hardy, 1965

WEST VIRGINIA

NUMBER	LOCATION	LEAST HORIZONTAL PRINCIPAL STRESS ORIENTATION	STRESS REGIME	TYPE OF INDICATOR	COMMENTS	REFERENCES
WV-1	Wayne 38.14°, 82.27°	N30°W	SS	HF	Depth = 835 m. $S_{Hmax} \gg S_{vert} \geq S_{Hmin}$.	Haimson, 1977a
WV-2	Franklin 38.65°, 79.35°	N15°W	T	G-FS(C)	Modern offset of coreholes exposed in road-cut, motion on pre-existing reverse faults.	Schafer, 1979
WV-3	Berkeley County 39.55°, 78.75°	N65°W	T	HF	Depth = 25 m and 135 m. $S_{Hmax} \gg S_{Hmin} \approx S_{vert}$. Depth of orientation measurement not given.	Haimson, 1977b
WV-4	Northwestern 39.75°, 80.42°	N6°E	T	HF	Avg. stress orientation from four locations, several miles apart.	Parsons and Dahl, 1972

WISCONSIN

NUMBER	LOCATION	LEAST HORIZONTAL PRINCIPAL STRESS ORIENTATION	STRESS REGIME	TYPE OF INDICATOR	COMMENTS	REFERENCES
WS-1	Waterloo 43.18°, 89.00°	N33°W	T	HF	Avg. of deeper measurements in two wells. Measurements at 17-238 min one well and 2-74 m in another well. Found decoupling between surface stresses and tectonic stresses at depth. Accuracy of orientations ±15°.	Haimson, 1978a
WS-2	Montello 43.78°, 89.33°	N25°W	SS	HF	Measurements at 75 m and 190 m. $S_{Hmax} > S_{vert} \gg S_{Hmin}$ at 190 m.	Haimson, 1976b
WS-3	Valders 44.07°, 87.85°	N30°W	T	HF	Depth = 300 m. Stress orientations consistent with depth, vertical stress is minimum stress at all depths.	Haimson, 1978b

WYOMING

NUMBER	LOCATION	LEAST HORIZONTAL PRINCIPAL STRESS ORIENTATION	STRESS REGIME	TYPE OF INDICATOR	COMMENTS	REFERENCES
WY-1	Greeen River Basin 42.5°, 109°	N65°W	SS	HF	Depth = 2775 m.	Power et al., 1976
WY-2	Yellowstone caldera 44.47°, 110.65°	WSW-ENE	N?	G-D	Based on alignment of rhyolite domes, thermal zones, and the trend of young faults.	Christiansen, in prep.
WY-3	North rim Yellowstone caldera 44.68°, 110.62°	N40°E	N/SS	FM(A)	Avg. of several single event solutions and foreshock-main event composites. Predominantly normal faulting, some strike-slip events.	Pitt et al., 1979
WY-4	Green River 41.55°, 109.45°	N60°E	SS	OC	Avg. of two overcore measurementa at separate localities both in Green River. One measurement depth - 259 m., S_{Hmin} = N52°E; the other depth = 488 m, S_{Hmin} = N67°E.	Aggson and Hooker, in press

SEISMOTECTONIC REGIONALIZATION OF THE GREAT BASIN, AND COMPARISON OF MOMENT RATES COMPUTED FROM HOLOCENE STRAIN AND HISTORIC SEISMICITY

by

Roger W. Greensfelder, Department of Geophysics,
Stanford University, Stanford, California 94305

Frederic C. Kintzer, URS/John A. Blume & Associates, Engineers,
130 Jessie Street, San Francisco, California 94105

Malcolm R. Somerville, Seismological Laboratory,
Mackay School of Mines, University of Nevada, Reno, Nevada 89557

ABSTRACT

A seismotectonic regionalization of the Great Basin and adjacent parts of the Basin-Range province, forming six zones, is developed on the basis of late Cenozoic patterns of deformation, relative Holocene strain rates, and historic seismicity. Belts of strike-slip movement are found to be significant in that they separate zones of differing strain rate, style of deformation, and historic seismicity. Within these zones, however, the distribution of historic seismicity may not represent that of Holocene or Quaternary time. Moment rates are computed from both Holocene strain rates and magnitude-frequency parameters of historic seismicity for each of the zones. Although the correlation of these moment rates is quite good, the average ratio of Holocene to historic moment rates may be about two. If Holocene aseismic stress release is insignificant, then we might conclude that seismicity in Holocene time is roughly double that of historic time, averaged over the entire Great Basin. Alternately, it is possible that nearly one-half of Holocene strain has been aseismic.

Our two major objectives in this paper are (1) a zonation of the Great Basin into six seismotectonic subprovinces, based on Late Cenzoic faulting and historic seismicity, and (2) analysis of an apparent correlation between inferred late Quaternary crustal strain rates and historic seismicity among the six subprovinces. This work is thought to be significant for the inference of magnitude-frequency parameters of secular seismicity, which are desirable in the prediction of seismic hazard. The present study grew out of an assessment of ground motion probabilities in Las Vegas, Nevada, and, therefore, data selected for analysis come primarily from the southern Great Basin.

In this paper, the designation "Great Basin" refers to that part of the Basin and Range province north of latitude 34° N. This includes areas south of the region customarily termed Great Basin, lying entirely north of latitude 35-1/2° N.

In order to establish a framework for Quaternary deformation, Mesozoic and Cenozoic tectonics are reviewed briefly. The Quaternary tectonic pattern appears to have been largely established during late Miocene time, although older structures and tectonic styles may be related to contemporary activity in the westernmost Great Basin. Late Quaternary crustal strain rates are inferred from fault displacement and geodetic data, as well as from the relative spatial density of normal-fault scarps. Patterns of late Quaternary faulting and of historic seismicity are used qualitatively to establish six seismotectonic subprovinces in the Great Basin.

Estimated crustal strain rates and levels of historic seismicity, based on the instrumental record (from 1932 to 1973), are compared, both directly and in terms of moment rate. Published studies making such comparisons are few, probably because of the general lack of data on strain rates. Anderson (1979) has analyzed the relationship between "geologic seismicity," inferred from fault slip rates or regional strain rates, and historic seismicity in both southern California and the Great Basin. Wallace (1977a, 1978) has compared paleoseismicity, inferred from Late Quaternary faulting, with historic seismicity in north-central Nevada; Bucknam et al., (1979) made a similar study in western Utah. The findings of these workers are compared with our own.

Pre-Cenozoic History

The Great Basin is a region of highly complex geologic structure, having been affected by a succession of tectonic events with contrasting deformational styles since Precambrian time. Briefly, these events may be classed as compressional tectonic events during two Paleozoic orogenies; uplift and east- to southeast-oriented crustal shortening, which produced geosyncline-marginal thrusting during late Mesozoic and earliest Cenozoic time; and east-west-oriented crustal extension during late Cenozoic time and persisting to the present.

It is noteworthy that a general north-south orientation of the continental margin has persisted since Precambrian time as recorded in the bedding planes of geosynclinal rocks and trends of Paleozoic orogenic belts. Wright (1976) stated that planes of weakness along these trends have undoubtedly influenced the orientation of Cenozoic faulting throughout the Great Basin. Thus, an understanding of ancient structures of the Great Basin may help to explain the present pattern of seismicity and active faulting.

Roberts (1972) summarized current knowledge of the Paleozoic Antler and Sonoma orogenies. Each of these events produced a north-to-northeast trending belt of thrusting and a parallel foldbelt across the northwestern part of the Great Basin. Evidence for the presumed plate margin interactions that produced east-west compression lies to the west, partially obliterated by the subsequent tectonic events that accompanied subduction of the Farralones Plate.

Neither of these Paleozoic orogenies interrupted miogeosynclinal deposition in the southern portion of the Great Basin. However, the Mesozoic era brought uplifting and change toward continental styles of deposition. Throughout the Great Basin, outcrops of Mesozoic rocks are scattered and demonstrate a history of progressive uplifting and isolation of Paleozoic depositional basins.

Mesozoic compressional tectonic events caused the superposition of a subparallel series of northeast-trending thrust systems upon the generally north-south grain of the Precambrian and Paleozoic basement structure. Within the Great Basin there are at least three such major belts of thrusting that affected pre-Mesozoic rocks during the Sevier-Nevadan orogeny.

The Nevadan orogeny resulted in the initial elevation of the Sierra Nevada and was contemporaneous with the Sevier orogeny of the Great Basin. Stewart, Ross, Nelson, and Burchfiel (1966) noted the close association between Mesozoic thrusting and plutonism east of the Sierra Nevada. The range of age estimates based on stratigraphic and radiometric evidence (Fleck, 1970a, and Burchfiel et al., 1974) indicates that deformation took place in several pulses throughout the period from Late Triassic to Late Cretaceous time.

The southernmost Mesozoic thrust belt, termed the Sevier orogenic belt (Armstrong, 1968), is approximately 50 km wide and trends north to northeastward across southern Nevada and into western Utah. Several imbricate thrust plates within this belt show a similar style of contemporaneous folding and thrusting towards the southeast.

Estimates of crustal foreshortening across the Sevier belt vary from about 33 to 75 km (Fleck, 1970b, and Burchfiel et al., 1974). At least two other major belts of thrust faulting are known farther west, in the Nevada Test Site region (Barnes and Poole, 1968) and north of Death Valley in the Inyo Mountains, California (Stewart et al., 1966). Crustal shortening across the former system has been estimated at about 58 km and, assuming a comparable figure for the latter system, the total northwest-southeast crustal shortening produced by Mesozoic thrusting across the Great Basin could be approximately 150 to 190 km.

Late Cenozoic Evolution

Since early Miocene time the lithosphere of the Basin and Range province has undergone major east-west oriented extension, on the order of 5% to 20%. Various tectonic theories have been advanced to explain the still poorly known mechanics of deformation. Here, we emphasize regional kinematic pattern and sketch two important, complementary theories.

Total east-west extension in the northern Great Basin portion of the Basin and Range province in late Cenozoic time has been variously estimated to be from 50 to 100 km by Hamilton and Myers (1966), about 72 km by Stewart (1971), and about 100 km by Thompson and Burke (1974). Thus, the rate of extension may have been between 0.3 and 0.6 cm per year over the last 17 million years, for a strain rate of the order of 10^{-8}/yr. Based on ideas developed by Thompson (1965) among others, Stewart (1971) suggested that this ongoing deformation is a response of the relatively brittle and thin crustal rocks to movement of a plastically extending substratum below the Great Basin.

The relationship between regional east-west extension and plate-tectonic theory has not yet been fully clarified, but many workers have contributed to a plausible explanation. Atwater (1970) proposed the concept of a "soft" continental margin, a broad zone of deformation extending far inland and responding to the stress system that causes the transcurrent motions along the San Andreas fault. The stress system called upon for this model would account for the presence of right-lateral faulting at the western margin of the Great Basin, for example the Death Valley - Furnace Creek fault system and the now-inactive Walker Lane and Las Vegas shear zone. This model sees the Great Basin as tectonically passive.

In contrast, Scholz, Barazangi, and Sbar (1971), proposed that cessation of subduction has allowed basaltic melt to rise from the mantle and spread outward beneath the center of the Great Basin to produce extensional faulting in the overlying continental crust. This volcano-tectonic activity probably began in a back-arc setting (Zoback and Thompson, 1978), but northwestward development

of the transform boundary has gradually altered this setting since about 15 m.y.b.p. Lachenbruch and Sass (1978) showed mathematically that the anomalous heat flux in the Great Basin is thermodynamically consistent with convection of basaltic melt from the aesthenosphere upward to the base of or into lithosphere extending at the approximate observed rate of 10^{-8} per year.

Whatever the underlying cause, it is now believed that Basin-and-Range style normal faulting in the Great Basin was initiated about 17 million years ago, and somewhat earlier in Mexico and southern Arizona (Christiansen and McKee, 1978). Andesitic volcanism virtually ceased in the Great Basin and after a short period of quiescence from 19 to 17 million years ago, volcanism resumed with a predominantly basaltic composition (McKee, 1971). Late Cenozoic seismicity and volcanism have been concentrated at the margins of the Great Basin where, presumably, tensional stresses have been greatest.

Throughout the Great Basin, probably since about 6 million years ago, the orientation of maximum extension has ranged from westerly to westnorthwesterly, depending on location. However, earthquake focal mechanism studies show T-axes ranging in orientation from westerly to northerly in western and southern Nevada (Zoback, 1978). Thus, one might conclude that principal stress orientations may vary considerably over periods much less than a million years at a given location. Together, the historic seismic record and Pliocene-to-present faulting data suggest an average orientation of approximately N 70° W for maximum extension.

Strike-slip motion has been an important factor in deformation of the Great Basin. Right-slip is prominent in its western and northern parts, and left-slip in its southern part. Zones of strike-slip appear to separate regions having different style and magnitude of faulting, and they are, therefore, important to our seismotectonic regionalization.

The concept of differential extension across strike-slip features has been called on to explain tectonic features in the northern and southern parts of the Great Basin (Wright, 1976; Lawrence, 1976). Lawrence (1976) described large fracture zones trending northwestward across Oregon, and hypothesized right-lateral deformation decreasing in magnitude northward across successive faults in order to explain the northern termination of the Basin and Range province. Davis and Burchfiel (1973) suggested a similar role for the Garlock fault, taking up differential extension in a left-lateral sense at the southwestern margin of the Great Basin. Left-lateral fault zones in southern Nevada may play a role in distributing westward extension relative to the west edge of the Colorado Plateau. Below, we summarize major strike-slip features which are significant in our zonation procedure. Tectonic features discussed below may be seen in Figure 2.

Right-Lateral Deformation. Since middle Miocene time, right-lateral deformation has been important in the westernmost part of the Great Basin, in a zone extending eastward from the Sierra Nevada front to the Walker Lane and the Las Vegas shear zone. Most of the movement probably has occurred since the middle Miocene, although some may have taken place earlier in Tertiary time. Historic surface-faulting characteristics and earthquake mechanism solutions show that right-lateral movement still continues in this region, but probably does not occur as far east as the Las Vegas shear zone.

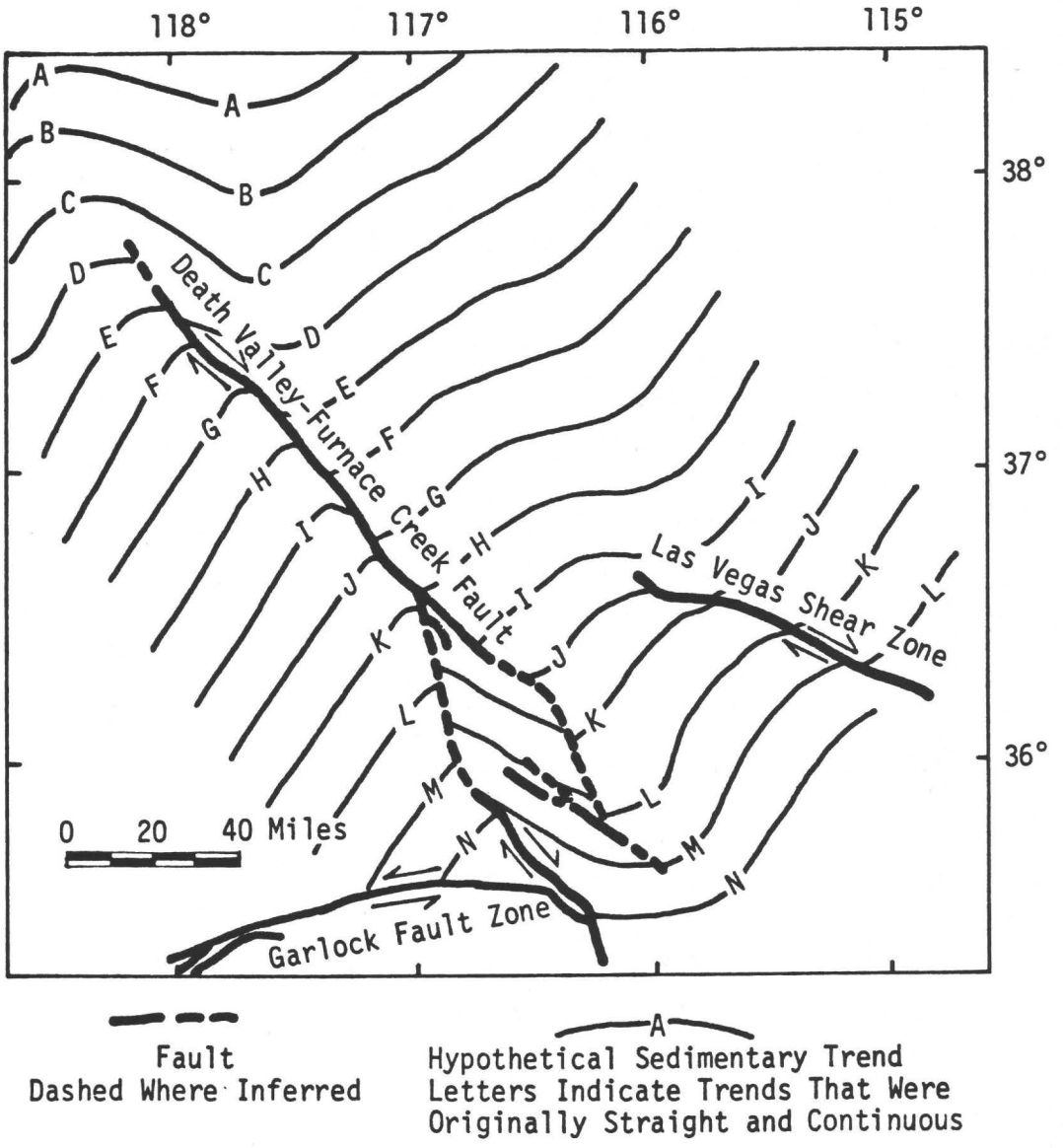

FIGURE 1 INTERPRETATION OF RIGHT-LATERAL FAULT DISPLACEMENTS IN THE SOUTHWESTERN GREAT BASIN (FROM STEWART, 1967)

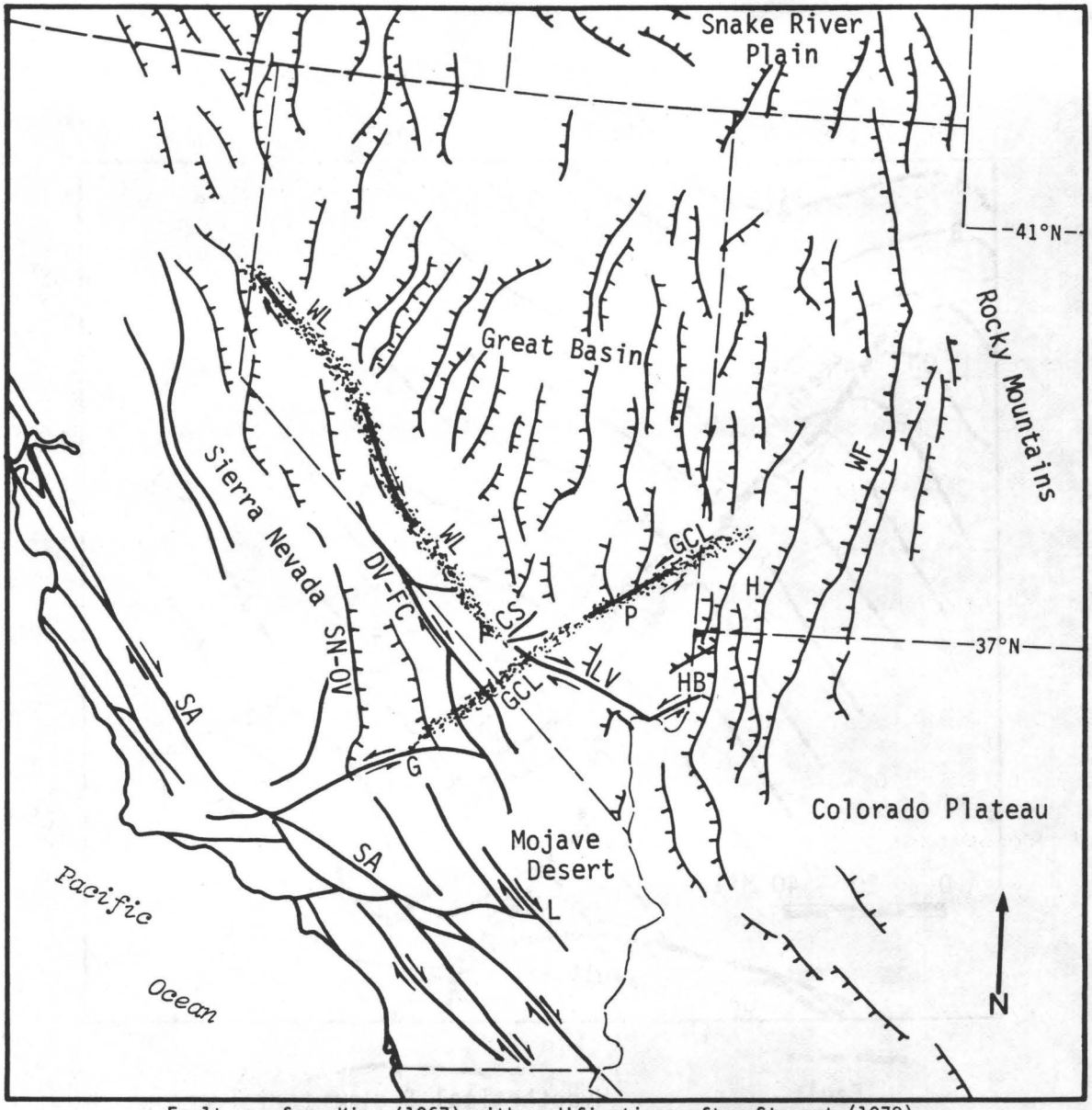

Fault map from King (1967) with modifications after Stewart (1978).

Major basin and range fault hatchures on downthrown side

Strike-slip fault - arrows indicate relative movement

Garlock-Caliente lineament and Walker Lane observed on ERTS-1 Satellite imagery, scale 1:5,000,000 (USDA Soil Conservation Service, 1974)

NOTE
CS = Cane Spring fault and related faults
DV-FC = Death Valley - Furnace Creek fault zone
G = Garlock fault
HB = Hamblin Bay fault
H = Hurricane fault
L = Ludlow Fault
LV = Las Vegas shear zone
P = Pahranagat shear zone
SA = San Andreas fault
SN-OV Sierra Nevada - Owens Valley frontal fault
WF = Wasatch frontal faults
WL = Walker Lane (stippled)
GCL = Garlock-Caliente Lineament (stippled)

Scale
0 100 200 mi
0 100 200 300 400 km

FIGURE 2 LATE CENOZOIC TECTONIC FEATURES OF THE GREAT BASIN AND ADJACENT REGIONS

Albers (1967) described a belt of sigmoidal bending, which occupies the region between the Sierra Nevada front and the Walker Lane. Within this belt, range-trends and structures in rocks as young as early Miocene display S-shaped arcs. These he called "oroflexes," which are the result of oroclinal bending of the earth's crust (i.e., folding about vertical axes). They may be the result of regionally distributed right-lateral shear, oriented along northwest-trending planes. Deformation may have begun as early as late Early Jurassic, and has apparently continued to the present in the western part of the belt. Bending must have ceased by middle Miocene time, and more recent movements have been restricted to faulting.

The Walker Lane is a belt of topographic lows, extending southeastward from near Honey Lake, California, to near Mercury, Nevada. Ranges north of it trend predominantly north to north-northeast, while those south of it trend generally northwest. The zone was recognized in the 1930s, and was named by Locke, Billingsley, and Mayo (1940). They, and a number of other writers, have postulated major right-lateral offset along the belt. However, right-lateral faults are documented in only two areas, one near Soda Springs Valley southeast of Walker Lake, and the other at the border of northwestern Nevada near Honey Lake. Nielsen (1965) presented strong evidence for some 20 km of offset in Soda Springs Valley, in rocks of Permian to Miocene age. Most of the offset appears to have taken place since Miocene time, and physiographic features suggest significant Quaternary movement. Distribution of Quaternary faulting and historic seismicity suggest that the post Miocene offset in the vicinity of Soda Springs Valley could be more directly related to the historically active Excelsior Mountain-to-Pleasant Valley seismic belt, than to the Walker Lane. It is probable that the Walker Lane is a now inactive feature whose structure is largely obscured by late Cenozoic structures and Quaternary alluvium.

Stewart's (1967) interpretation, included here as Figure 1, also demonstrates a regional system of late Cenozoic right-lateral faulting south of the Walker Lane. His detailed isopach studies of upper Precambrian and Lower Cambrian strata indicate 130 to 200 km of right-lateral offset from Death Valley to Las Vegas. Most of this offset is accounted for by displacements on the Las Vegas shear zone and on the recently active Death Valley - Furnace Creek fault zone. The remaining offset may have been accomodated by broad regional folds. Since late Miocene time, about 11 million years ago, when motion on the Las Vegas shear zone ceased (Longwell, 1974), right-lateral deformation has been restricted primarily to faulting in the region west of and including the Death Valley - Furnace Creek fault zones, and related trends farther south in the Mojave Desert (Jennings, 1975).

As previously noted, Mesozoic structural trends associated with the Sevier orogenic belt are oriented north to northeast across southern Nevada. This structural grain makes a sharp, right-angle bend at Las Vegas Valley, a fact that led Longwell (1960) to hypothesize the existence of a buried fault along the length of Las Vegas Valley. Geological structures adjacent to the valley appear to have been consistently drag-folded by post-Sevier right-lateral faulting. No fault trace definitely belonging to the Las Vegas shear zone has been discovered; however, possible subsidiary traces have been found.

Longwell (1974) deduced a total right-lateral offset of about 65 km across Las Vegas Valley, based primarily on reconstructions of offset and distorted thrust plates. Formerly it was speculated that deformation on the Las Vegas shear zone had begun perhaps as early as Mesozoic time. However, Longwell's data support the hypothesis that most right-lateral displacement occurred within late Miocene time, over the interval 17 to 11 million years before present. Ekren et al. (1968), Fleck (1970a), and Anderson et al. (1972), arrived at similar age estimates.

As shown on Figure 2, the Las Vegas shear zone is thought to extend about 125 km northwestward from Lake Mead past the city of Las Vegas. The extent of the shear zone northwestward and southeastward beyond the ends of Las Vegas Valley has long been a matter of speculation. It seemed natural to

connect the shear zone with active faults in west-central Nevada via the Walker Lane. However, little evidence has arisen to support the existence of a continuous right-lateral shear zone as suggested by Shawe (1965).

The Specter Range lies athwart the northwestward extension of the Las Vegas shear zone. Burchfiel (1965) and Moench (1965) have mapped the complex structural geology of this area without finding any clear indications of a large right-lateral shear zone. Both authors interpreted the structural grain in the Specter Range as probably continuous in an east-west direction, cutting across the north to northwesterly trend of the shear zone and the mountain ranges immediately to the south. Burchfiel suggested that the Las Vegas shear zone either is bent westward through the Specter Range and into the Amargosa Desert, or merges into a broad fold. Another possibility, which we favor, is that the east-to-northeast-trending structures in the vicinity of the Specter Range are part of a younger left-oblique-slip fault system that has offset the shear zone toward the east and erased its former connection with the Walker Lane.

Late Cenozoic right lateral deformation along the western margin of the Great Basin apparently continues southward from the Death Valley - Furnace Creek fault zone into the Mojave Desert area. The western Mojave block, lying between the San Andreas and Ludlow faults, is traversed by several northwest-trending faults along which offset has been mainly right-lateral, with a small component of dip slip (Dibblee, 1961). The amount and age of fault displacements is poorly known. Dibblee (1961, 1967) reported that strike-slip displacements are small, but gave specific data only for the Helendale fault, which has offset Tertiary metavolcanics several miles. Garfunkel (1974) believes that late Tertiary volcanics (older Neogene and late Miocene to Pliocene) are offset as much as 40 km on each of the five major faults. He developed a tectonic model in which west-trending left shear, as exhibited on the Garlock fault and in the Transverse Ranges, has rotated the western Mojave block counterclockwise by about 30°. Constraining the north edge of the block to remain fixed, and allowing the west edge to deform to make the bend in the San Andreas fault, requires right-lateral slip on the major Mojave faults, as indicated above.

We are of the opinion that Garfunkel's model results in a "maximum credible" right-lateral strain. Based on inspection of relations on Rogers' (1967) map of the San Bernardino area, we estimate that 10 km may represent a maximum offset on any of these faults.

North of the Furnace Creek fault, the eastern limit of major right slip appears to step easterly into the Walker Lane north of latitude 38° N, in the vicinity of Soda Springs Valley. This trend extends northwesterly through and beyond the vicinity of Pyramid Lake, Nevada.

Left-Lateral Faulting. Northeasterly trending left-lateral faults have been mapped in three areas within the southern Great Basin. These are located as follows: along the north side of Lake Mead, in the southern part of the Nevada Test Site, and in south-central Lincoln County 70 miles due north of Las Vegas. In the first of these areas, immediately north of Lake Mead, Anderson (1978) has mapped a series of left-lateral oblique faults parallel to the Hamblin Bay fault. His interpretation projects this southwesterly trend across the southeastern end of the Las Vegas shear zone. The shear zone apparently does not continue into the Black Mountains, which lie on the Arizona side of Lake Mead between the two basins of the reservoir (Longwell, 1963). A system of generally north-trending normal faults approaches the Lake Mead area from the south. Prominent among these are the Eldorado and the Boulder Wash faults. This system appears to be truncated by the left-lateral faults, although interpretation is difficult because they are widely covered by Pliocene and younger volcanic rocks and alluvium. Anderson (1973) believed that many of the normal faults dip at unusually low angles and are genetically related to the left-lateral system. Based on potassium-argon ages, he inferred more than 20 km of left-lateral slip on the Hamblin Bay fault

system between 12.7 and 11.1 million years ago. The entire zone of parallel left-lateral faults may represent a larger total deformation over a somewhat longer period of time.

Other northeasterly left-lateral trends have been mapped in the Nevada Test Site. The complex structural relationships in this area have not been completely resolved. However, some of the left-lateral features, such as the Cane Spring fault near Frenchman Flat, appear to offset all structures except the most recent northerly trending normal faults. These relationships are seen on maps by Ekren and Sargent (1965) and Poole, Elston, and Carr (1965). The east- to northeast-trending left-oblique faults described by Burchfiel (1965) in the Specter Range may be a westward continuation of this system. The amount of left-lateral offset in this area is unknown. Most movement on the Cane Springs fault probably took place before 11 million years ago, although some probably occurred after 7 million years ago. No left-lateral displacements in Quaternary alluvium have been observed (Ekren, 1972).

Another belt of east-to northeast-trending faults, apparently left-lateral, is centered in southern Lincoln County, east of the Nevada Test Site and has been described by Tschanz and Pampeyan (1970). Named the Pahranagat shear system, the belt comprises three left-lateral faults and has a length of 40 km. Total apparent post-Miocene displacement across the sytem is some 10 to 16 km. Volcanic units of probable Pliocene age are only slightly offset, suggesting that the system is less active now than in Pliocene time.

Of the three faults, the Arrowhead Mine fault is the most speculative. Tschanz and Pampeyan (1970) suggested that Laramide motion on this fault may have been some 50 km in a right-lateral sense, based upon apparent offset of structures in Paleozoic rocks. They speculated that the entire belt originated in Laramide time as a right-lateral shear zone.

The Arrowhead Mine fault cannot actually be mapped within individual range-blocks. However, it, as well as the mapped left-lateral faults immediately south, appears to be almost colinear with part of a major northeast-trending lineament shown on Figure 2. The lineament may be seen on 1:5,000,000 scale ERTS satellite photography (USDA Soil Conservation Service, 1974), and

appears to be tangent to the Garlock fault and to strike N 50° E, extending across southern Nevada and into the southern Escalante Desert, near Modena, Utah. It may separate regions having different magnitudes of crustal extension, i.e. generally greater to the north; if so, then left-lateral shear is required all along the lineament. This feature and its probable left-lateral character have been mentioned frequently in the literature (Slemmons, 1967; Suppe et al., 1975; Wright, 1976; Christiansen and McKee, 1978; Eaton et al., 1978); we shall call it the Garlock-Caliente lineament. It is interesting to consider that left-lateral motion on the lineament may have separated the Walker Lane and Las Vegas shear zone in the vicinity of the Specter Range.

In the foregoing discussion of the Great Basin, we have shown that both the style and magnitude of faulting vary considerably from region to region, despite the near-uniformity of orientation of maximum extension. We wish to point out that, on the basis of both style and magnitude together, Great Basin faulting may be regionalized into the following subprovinces: (1) the northern Great Basin, that lies north of the Garlock-Caliente lineament and east of the Walker Lane, and is characterized by almost pure normal faulting of moderate intensity; (2) the Western Great Basin bounded by the Sierra Nevada frontal fault, the Garlock fault, and Death Valley - Furnace Creek fault zone and related trends to the north, and exhibiting intense right-lateral-oblique faulting with comparable strike-slip and dip-slip components; (3) the southeastern Great Basin, that lies south of the Garlock-Caliente lineament and east of the Death Valley and Ludlow faults, and features both normal and left-slip faulting of low intensity; and (4) the western Mojave block, characterized essentially by right lateral strike-slip faulting of low-moderate intensity.

Certainly the largest of these regions, the northern Great Basin, could be further subdivided in a similar manner, however, we have not done so; the classifications would be more subtle, and therefore debatable.

In the following discussion, we will examine the most recent activity of these regions, and compare quantitative estimates of strain rate and seismicity in each.

REGIONALIZATION AND RATES OF LATE QUATERNARY STRAIN

We have just distinguished four regions of the Great Basin on the basis of the style, orientation, and magnitude of late Cenozoic faulting. In this section, we shall further characterize and subdivide these regions, based upon data presented above as well as Holocene strain rates and historic seismicity. The Salton Trough is also discussed as it is included in the correlation of strain rate and seismicity discussed in the last section.

Figure 3 outlines six seismotectonic zones. The first five of these (numbers 1 through 5) have boundaries based chiefly upon the above discussion and strain rates described below; zone number 6, the Rocky Mountain marginal zone, is based on strain-rate and seismicity data.

The spatial distribution of historic seismicity (Figure 5) was important in drawing attention to zones 1, 4, and 6, but was used to draw only one boundary -- the west side of zone 6. Ryall et al. (1966) described an alinement of large (M > 6-1/2) earthquakes and associated faulting, which they termed the "Ventura-Winemucca belt," that cuts across the boundary between our zones 1 and 3. The "Ventura-Winnemucca belt" has a 100-km gap just south of its intersection with our boundary, near Excelsior Mountain, Nevada, and we believe it is a fortuitous alinement.

Methods of Analysis and Data Sources

We seek to characterize Holocene fault activity in terms of hypothetical homogeneous strain rates. Broadly speaking, each of several regions of the Great Basin is featured by a quasi-uniform style and intensity of faulting (see Figures 2 and 4). Therefore, it seems reasonable to quantify deformation in each such region in terms of data available for one, presumably representative portion thereof, e.g., a single basin and its two adjoining ranges; lacking detailed data for most areas, this sort of generalization is often necessary to our analysis. In this manner, a known displacement rate across a particular basin or area may be converted to a strain rate which is then presumed to characterize the entire region or subprovince containing it.

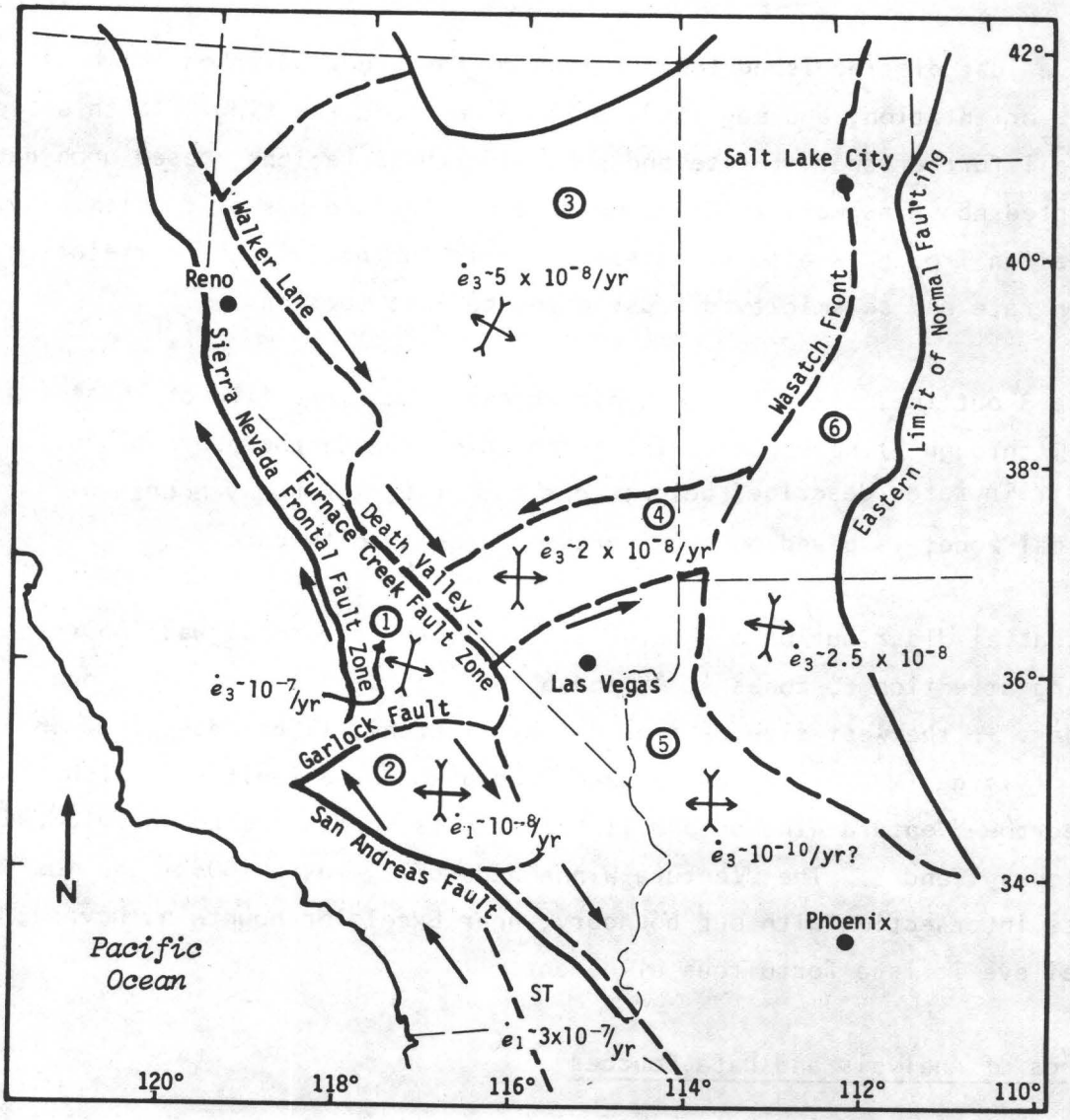

EXPLANATION

- Boundary of northern Basin and Range province
- Boundary of seismotectonic subprovinces
- ② Number of subprovince of Great Basin (extended), used in text
- Principal strain axes
- Sense of strike-slip motion, shown where such motion is significant
- $\dot{e}_1$ Principal compressional strain rate
- $\dot{e}_3$ Principal extensional strain rate

Scale

0 50 100 mi

0 100 200 km

FIGURE 3 SEISMOTECTONIC REGIONALIZATION OF THE GREAT BASIN AND ADJACENT REGIONS

Regional compilations of Quaternary fault-age data have been found to be more or less imprecise, as they are based upon either published geologic mapping or geomorphologic analysis. In general, only painstaking study of excavations across faults and radiocarbon dating of offset deposits can provide full details of fault-movement history. Cost prohibits carrying out such studies for many faults.

In the Great Basin, published geologic mapping has identified many faults that break Quaternary deposits. However, geologists often have not mapped faults that break only Quaternary deposits. Geomorphic analysis is a valuable and practical means of identification and relative age classification of late Quaternary basin-range faults.

Slemmons (1967) made the only known photogeomorphic study of late Quaternary faulting which covers most of the Great Basin; only the eastern California portion is incomplete; in Nevada, three age divisions were established. Wallace (1977b) has made a more detailed field investigation in north-central Nevada, covering some 17,000 km^2, using quantitative methods to analyze scarp morphology in order to establish approximate ages of fault displacements. Bucknam et al. (1979) have studied late Quaternary faults in western Utah, by means of photogeologic compilation of scarps and quantitative field studies of scarp morphology. However, their work is not published in sufficient detail (no maps are given) to be useful here.

For California, Jennings (1975) has compiled all Quaternary faults from the geologic literature, and, on the basis of geomorphic and geophysical characteristics, he has distinguished those that are probably active. No map-compilation of Quaternary fault data has been published for Arizona, although some Basin and Range faults in that state almost certainly have Quaternary displacement.

Strain Rates of the Seismotectonic Zones

Subprovince 1. Subprovince 1 is bounded by the Sierra Nevada frontal fault system on the west; the Garlock fault on the south; the Death Valley - Furnace Creek fault zone on the southeast, and the Walker Lane on the northeast (from Cedar Mountain north). As noted earlier, this region was subjected to

major oroclinal bending, due to distributed right-lateral shear on northwest-trending planes, in pre-middle-Miocene time; the Walker Lane southeast of Cedar Mountain is itself a defunct right-lateral shear zone. However, since Miocene time, right-lateral deformation appears to have become a second-order response, along established planes of weakness, to northwesterly oriented extension. This hypothesis is strongly supported by evidence that oroclinal bending ceased in the Miocene and by the apparently predominant dip-slip nature of Quaternary faulting (note extreme topographic relief of order 3 km).

Quantitative study of deformation of the latest Quaternary deposits in Death Valley (Hooke, 1972) indicates northwest-oriented extension on the Death Valley fault at a rate of about 1 to 2 cm/yr. He observed tilting that appears to have a rate of 0.3 microradian/yr and suggested 7 mm/yr dip-slip movement on the Death Valley fault. Also, Hooke found northeast-oriented grabens that indicate 2-4 cm/yr extension, which he interpreted to be the result of right slip on the Death Valley fault. Together, the data indicate a strain rate between 10^{-6}/yr and 10^{-7}/yr.

In Owens Valley, geodetic measurements indicate about 4 mm/yr of right-lateral deformation parallel to the Owens Valley fault and extension normal to it at about 1 mm/yr (Savage et al., 1975). In addition, down-to-the-east tilt of the block east of the fault is 0.2 microradian/yr. Together, these data indicate northwest-oriented extensional strain at a rate of about 10^{-7}/yr across Owens Valley. These data are in substantial agreement with fault motions observed for the 1872 Owens Valley earthquake (M ~ 7-1/2), although dip slip and right slip had comparable magnitudes (~ 5 m).

On the Garlock fault, left-lateral offset in Holocene time has been estimated at about 7 mm/yr at Koehn Lake (Clark and Lajoie, 1974). It is thought that this figure represents extension parallel to the Garlock fault within the region immediately north of it.

Displacement rates in other parts of the region have not been measured but are probably comparable to those listed above. Holocene faulting occurs in Saline, Panamint, Coso, and northern Death valleys.

Extensional strain rate across the subprovince may be estimated with reference to its southeast corner, the junction of the Garlock and Death Valley faults. Net displacement is 2 cm/yr oriented to the northwest; this amounts to a strain rate of about 1×10^{-7}/yr.

Subprovince 2. This is the western Mojave Desert block, bounded by the San Andreas, Garlock, and Ludlow faults on the west, north, and east respectively, and by the Transverse Ranges on the south. The right-lateral style of deformation in this block, and the major uncertainty about magnitudes and ages of fault displacements, were discussed in the first section of this paper. From an examination of the San Bernardino sheet of the California State Geologic Map (Rogers, 1967), we conclude that right-lateral offsets on the five major faults of this block range from about 4 to 10 km, probably dating since about 17 m.y.b.p. Hence, it is estimated that the late Cenozoic shear strain rate across the block is of the order of 2×10^{-8}/yr. This implies a principal compressional strain rate of about 10^{-8}/yr, subject to an uncertainty of perhaps a factor of five. No definitive data could be found concerning Holocene displacements.

Subprovinces 3, 4, and 5. Together, these three regions comprise most of the Great Basin, and, tectonically, all are characterized by northerly trending normal faults. However, subprovince 4 is distinguished by left-lateral faulting that trends east-northeast, perhaps associated with differential east-west extension, as described in the previous section of this paper. As shown below, late Quaternary strain rate appears to vary markedly among the three regions.

In Nevada, Slemmons (1967) has mapped and classified according to relative age, faults that offset late Quaternary sediments. Typically, the offset materials are alluvial fans at range fronts; less commonly they are playa deposits formed in Pluvial-period lakes (e.g., lakes Lahontan and Bonneville). The age classification scheme is as follows: historic offsets, less than 100 years old; pre-historic offsets, estimated to be from 100 to several thousand years old (i.e., Holocene); pre-Holocene faulting, from 10,000 to 100,000 years old. Figure 4 shows the distribution of faults in these age ranges in the state of Nevada.

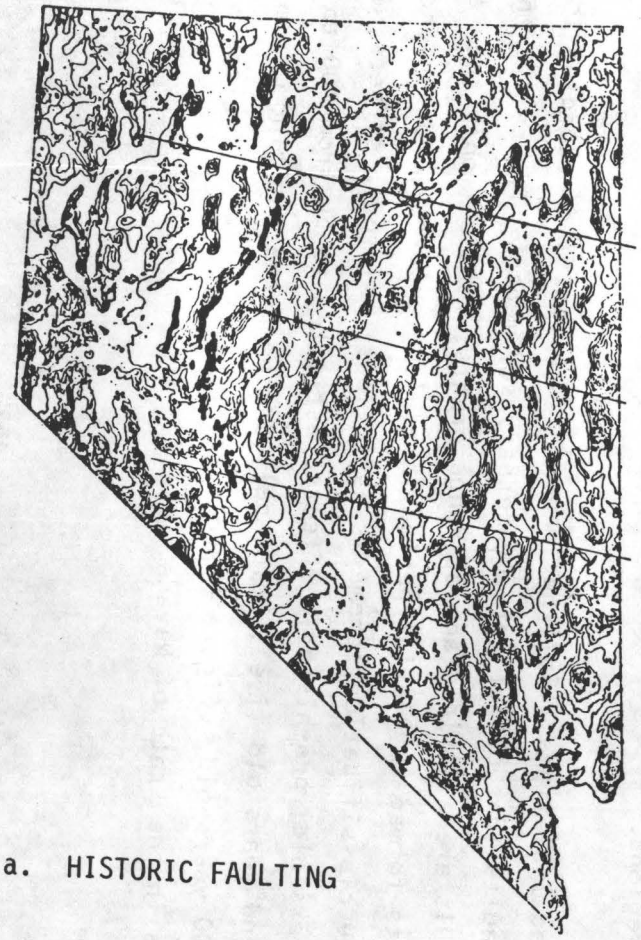

a. HISTORIC FAULTING

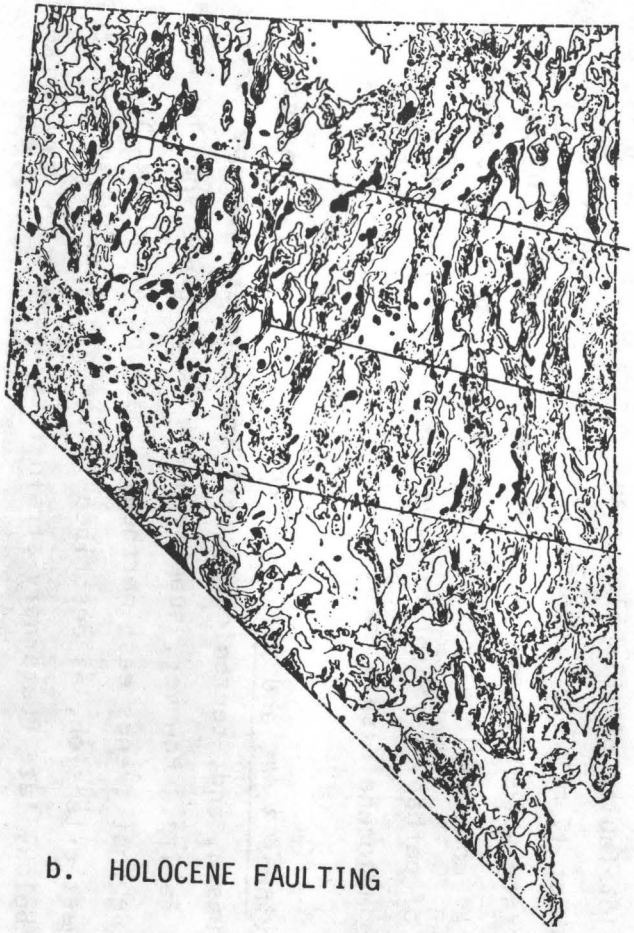

b. HOLOCENE FAULTING

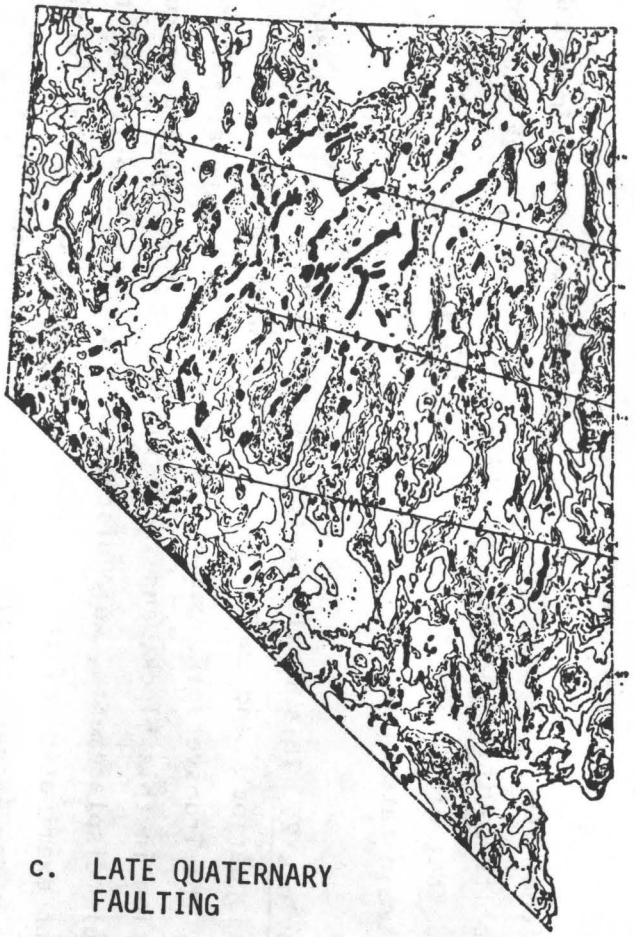

c. LATE QUATERNARY FAULTING

FIGURE 4 HISTORIC, HOLOCENE, AND LATE QUATERNARY FAULTS IN NEVADA (FROM SLEMMONS, 1967)

Historic faults form a closely connected chain (Figure 4A) that extends northward from Cedar Mountain to Pleasant Valley. The faulting accompanied eight earthquakes, with magnitudes ranging from 6-1/4 to 7-1/2, between 1903 and 1954. This belt of intense activity is seen in the seismicity distribution of Nevada (Figure 5); a number of the smaller earthquakes ($4 < M < 6$) in the belt are aftershocks of those that were accompanied by surface faulting.

Holocene scarps appear in Figure 4B. They are spread out rather evenly across northern and central Nevada, in tectonic subprovince 3. Note, however, the sparseness of their occurrence south of latitude 38° N (in subprovinces 4 and 5). Pre-Holocene scarps appear in Figure 4C. They also are more concentrated in the northern and central parts of the state and are generally sparse south of the 38th parallel, except for a diffuse northeast-trending belt of scarps in subprovince 4. Both Holocene and pre-Holocene scarps tend to be of shorter length in eastern Nevada.

After comparing the distributions of faulting in the three age-groups, Slemmons (1967) concluded that the historic faulting and earthquake activity are not representative of the long-term (i.e., last 100,000 years) distribution of seismotectonic activity and that future activity may be expected to shift to zones that have been historically dormant; the historic pattern suggests that for short time intervals there may be a tendency for concentrated activity along belts parallel to the tectonic grain. In accordance with this notion, Wallace (1977) observed that Holocene scarps tend to cluster along some range-fronts but are absent along others, in north-central Nevada.

Strain rate in subprovince 3 (northern Great Basin) may be estimated using Holocene fault displacement data from Dixie Valley, probably the best-known basin in terms of Quaternary tectonics. Thompson and Burke (1974) estimated that the Holocene extension rate there is about 1 mm/yr, trending N 55° W. This implies a strain rate of 5×10^{-8} per year across Dixie Valley, and we shall assume this represents all of the northern Great Basin.

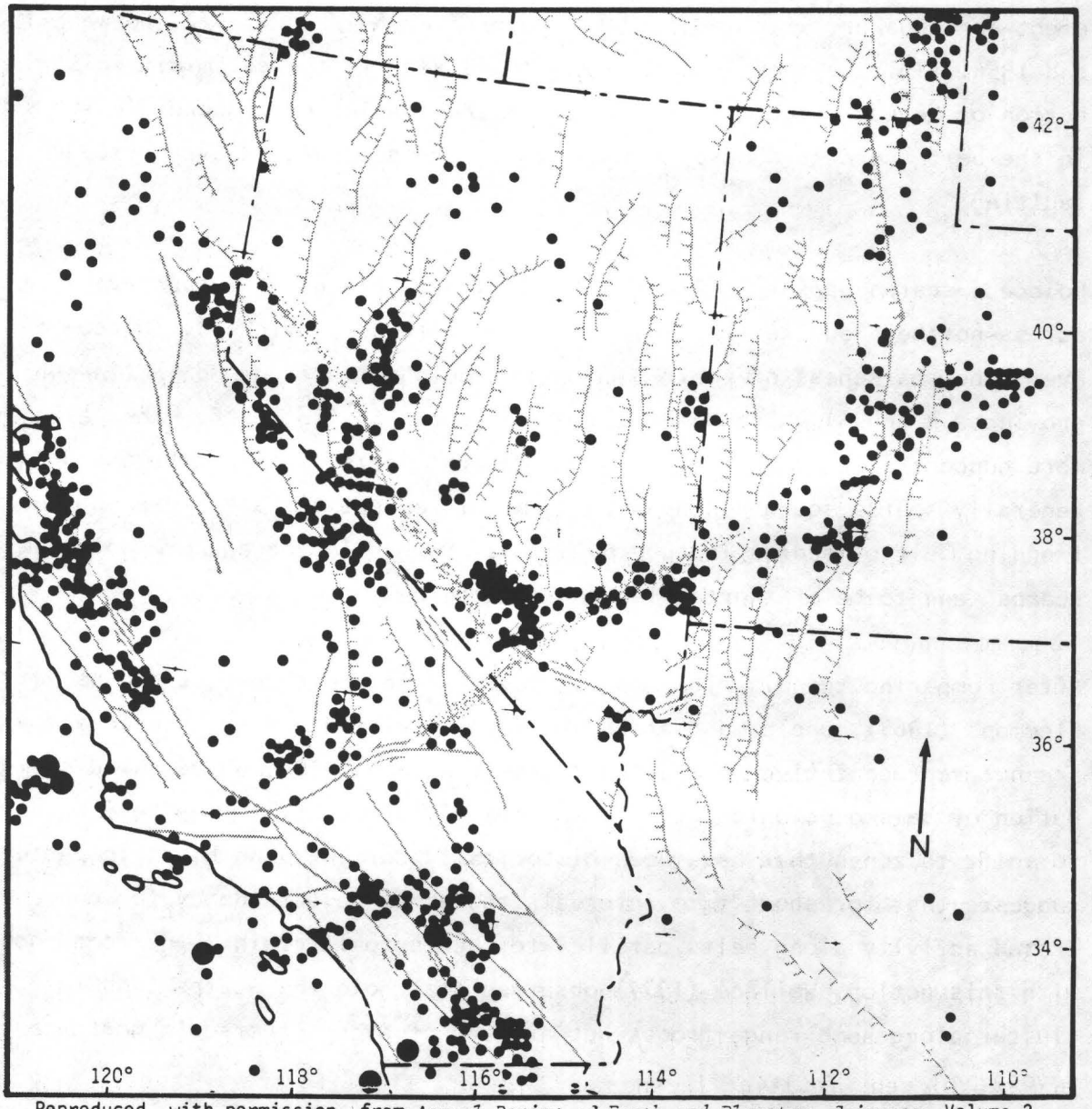

Reproduced, with permission, from *Annual Review of Earth and Planetary Sciences*, Volume 2,
© 1974 Annual Reviews, Inc.

Scale

0 100 200 mi

0 100 200 300 km

FIGURE 5 SEISMICITY MAP OF THE WESTERN UNITED STATES, 1961-1970, AND LATE CENOZOIC TECTONIC FEATURES

Subprovince 4 is characterized by normal faults that trend more northerly than in the region to the north and by left-lateral faults. The abundance of late Quaternary faults indicates significant tectonism, but the scarcity and shortness of Holocene faults indicates that tectonic activity is much less than in subprovince 3. The spatial frequency of occurrence of Holocene faults is about 10% to 20% of that of subprovince 3. On this basis, the extensional strain rate in this region is estimated to be between 5×10^{-9}/yr and 10^{-8}/yr. This region is also the locus of a rather sparse belt of historic seismicity, as seen in Figure 5.

At this point, we should note that Wallace (1978) distinguishes eastern Nevada and westernmost Utah from adjacent regions, because this region appears to lack late Quaternary (last 1/2 m.y.) scarps long enough to be associated with major ($M \geq 7$) earthquakes. Nevertheless, numerous young scarps are present (Figure 4), and, disregarding the historically active belt of western Nevada, the spatial frequency of scarps and of historic earthquakes does not seem to undergo a marked change from west to east. Thus, for earthquakes with $M < 7$, our zonation may well be valid despite Wallace's observation.

Subprovince 5 (southeastern Great Basin and southern Basin and Range province) in Nevada appears entirely devoid of Holocene and latest Quaternary faulting. Also, it is an area of extremely low seismicity. Hence it is thought to have extensional strain rate of less than 10^{-9}/yr -- perhaps as low as 10^{-10}/yr.

In the Mojave and Colorado deserts of California, east of the 116th meridian, documented Quaternary faulting is practically nonexistent (Jennings, 1975), and no Holocene faulting is known. However, the literature reveals little concerning this geologic aspect of the region.

Quaternary and Holocene faulting is unknown in the Basin and Range province of northwestern Arizona. But, as in adjacent California, it has not been looked for carefully. Published regional maps (Arizona Bureau of Mines) show no range-bounding faults. Dr. I. Lucchitta (personal communication, 1977), who has worked extensively in the Colorado River country, feels that the ranges may be exhumed pre-Quaternary structures. Certainly they have much

lower relief than those in the northern Basin and Range province. Seismicity in this region is extremely low.

From the above, it can be concluded tentatively that extensional strain rate in this entire subprovince is as already estimated from Nevada data: between 10^{-9}/yr and 10^{-10}yr.

Subprovince 6. The Colorado Plateau- Rocky Mountain marginal zone displays north-trending normal faults, many of which exhibit Quaternary or Holocene offsets. Details of recent faulting are not published for most of this region. Displacement rates across the Wasatch fault are available at two points, in Jordan Valley and near Kaysville, located south and north of Salt Lake City, respectively. In Jordan Valley, Suppe et al. (1975) estimated 1 mm/yr; near Kaysville, Swan et al. (1978) presented data indicating 0.5 mm/yr, assuming a dip of 60° for the fault.

It is unclear what zone-width should be assigned this extension. Taking the width of Jordan Valley as a lower bound, a rate of 2.5 to 5 x 10^{-8}/yr is implied; taking that of the entire tectonic belt as an upper bound, then about 1 x 10^{-8}/yr is suggested. Probably the true value is bracketed by these estimates.

Salton Trough. This zone extends from the Elsinore fault on the west to the San Andreas on the east, and is characterized by almost pure right-lateral slip on these and several intervening faults. Geodetic data for the period 1973-1977 (Savage et al., 1979) indicate principal compressional strain as about 3 x 10^{-7}/yr. Right-lateral shear strain is about 4 x 10^{-7}/yr across this zone, corresponding to distributed right-lateral slip totalling about 50 mm/yr (Savage et al., 1979). This figure is nearly the 56 mm/yr relative displacement rate for the North American and Pacific Plates found by Minster and Jordan (1978) for the past 5 to 10 m.y. This suggests that the strain rate observed during 1973-1977 is probably close to the long-term average.

HISTORIC SEISMICITY

Our objective in this part of the paper is to derive what we believe are best estimates of magnitude-frequency relations for the seismotectonic provinces defined above.

Figure 5 shows the seismicity of the western United States for the period 1961 to 1970, which adequately represents major zones of high seismic energy release for the last two centuries. Within the Basin and Range province, major historic seismicity has been confined to two belts of surface faulting, one in Owens Valley and another extending from Cedar Mountain to Pleasant Valley, Nevada. Two other important seismicity zones are seen, one in southern Nevada and the other along the margin of the Colorado Plateau. These historic seismic zones correlate partly with the seismotectonic subprovinces shown in Figure 3, which represent a time span from 100 to 500 times longer. However, it is important to observe that historic seismicity of the Basin and Range province is restricted largely to the western portions of Great Basin subprovinces 1 and 3.

Ryall et al. (1966) derived magnitude-frequency parameters ($N_{4.0}$ and b in the relation $\log N = A - bM$, with $\log N_{4.0} = A - 4b$) of the western United States, for pre-instrumental times (1769-1931) and for the instrumental period 1932-1961. Values of $N_{4.0}$ and b are consistently lower for the pre-1932 period as compared to that following 1932, and b-values for 1932-1961 seem anomalously low in at least three of the six regions studied. Ryall et al., concluded that poor detection and reporting of smaller shocks is the probable cause of the low b-values, and that the problem is more serious during pre-instrumental time. We concur, and would add that the same thing may be said about a-values for the time before 1932.

The record of pre-instrumental seismicity is based entirely on felt and damage reports, which depend on the population density in any given region. Our study region has been very sparsely populated, and therefore the pre-1932 record is considered quite unreliable, in light of Ryall et al's (1966) findings. Futhermore, magnitudes estimated from Mercalli intensities are not reliable. Hence, we chose not to use the pre-1932 record.

Data Sources

For the years 1932 to 1962, the best seismographic record of the study area is assembled from two sources: the California Institute of Technology (CIT) and the University of Nevada, Reno (UNR) earthquake catalogs (Hileman et al., 1973; Slemmons et al., 1965). Combined, these are considered nearly complete above magnitude ~ 4 in Nevada and California. For the years 1963 to present, the catalog of the Environmental Data Service, National Oceanic and Atmospheric Administration (NOAA) is essentially complete for $M \geq 4$; this source is relied upon for the years 1963 to 1973. Also included are microearthquakes recorded and located by the Nevada Special Projects Party (USGS/NOAA) during 1971 to 1973 (Bayer, Mallis, and King, 1972; Bayer, 1973a, 1973b, and 1974). Magnitude data were not available for the microearthquakes.

Figure 6 is an index map showing the geographic areas for which original seismicity data compilations were made for this study; data sources and references to figure numbers of epicenter maps (Figures 7 through 10) are given.

Since 1932, the Seismological Laboratory of the California Institute of Technology has provided apparently complete reporting of southern California earthquakes of magnitude 4± and larger (south of 38° N, east of 119° W). With the addition of a number of new seismograph stations during the 1950s and 1960s, the magnitude threshold of detection in southeastern California dropped from 4± to 3± (Willis et al., 1974). The CIT laboratory has also reported many shocks in southern Nevada (south of 38° N), but probably with less reliability than in California (Hileman et al., 1973). CIT has consistently reported local magnitude, but only to the nearest 1/2-unit until 1943.

Two agencies in the Department of Commerce have maintained earthquake history files for the U.S. since 1928. Until the early 1960s, the U.S. Coast and Geodetic Survey (USCGS) reported intensities routinely, but magnitudes were reported only occasionally, depending on proximity to population centers. Magnitude threshold ranged from as low as 3 to more than 5. Since

1963, NOAA (briefly ESSA) has routinely reported magnitudes (usually M_L) for earthquakes, and it has apparently reported all shocks of $M \geq 4$ and many of $3 < M < 4$.

Coverage of earthquakes in western Utah and northwestern Arizona is afforded only by the NOAA/USCGS files. Apparently, seismicity data in that sparsely populated region are incomplete for the period 1932 to 1962; shocks with $M < 5\text{-}1/2 \pm 1/2$ were not consistently reported. The lack of magnitude data for this period is a serious handicap for interpretation.

The University of Nevada (Slemmons et al., 1965) has compiled a catalog of Nevada earthquakes for the period 1852 to 1960; all available data were compiled. For southern Nevada, instrumental data comprised essentially just the CIT data. Felt reports were compiled from newspaper articles, as well as from published USCGS lists (*U.S. Earthquakes*, annual series). Because of the sparse population of this area, felt reports are very incomplete for shocks with $M < 5$, except for those occurring within a few miles of Las Vegas, Boulder City, or a few small towns to the north. With the exception of felt reports of more than 200 small shocks ($M \leq 4\pm$) in the vicinity of Lake Mead, the UNR catalog adds little to the CIT catalog of earthquakes in the southern Nevada area.

Before 1961, no seismograph stations operated in southern Nevada or in adjacent parts of Utah and Arizona. Thus, only rather large shocks were reliably reported in this region prior to 1961. Beginning in 1961, the Atomic Energy Commission (AEC) contracted for the operation of high-gain stations in the area between Las Vegas and Tonopah. Willis et al. (1974) stated that the threshold of reliable detection for this region ranged in magnitude from 4.6 to 5.2 during 1943-1952, from 3.6 to 5.2 during 1953-1962, and from about 2.6 to 3.2 since 1963. However, magnitude-frequency plots (Figures 14 and 15) suggest that published catalogs are nearly complete for $M > 4$ but are incomplete for $M < 4$, even since 1963. Therefore, it appears that the AEC contract stations either did not record local earthquakes (as they may not have run continuously) or did not report them to NOAA.

It can be concluded, therefore, that earthquake detection and reporting in the study region have varied significantly in both time and space. The

minimum magnitude threshold of reliable reporting (M_{min}), has decreased with time, but has always increased from southwest to northeast; the function M_{min} (X, Y, t) is not linear, but varies stepwise in time and in space. No attempt has been made to exactly specify this function, although it has been estimated in the above discussion and has been used in isolating relatively complete sets of seismicity data for analysis. For a given sample space, such sets contain only $M \geq M_C$, where M_C is the maximum value of M_{min} in that space. Some data sets presented here contain $M < M_C$, but M_C is generally known, so the smaller events may be simply ignored. These data sets are indexed in Figure 6.

Special problems of data quality, particularly for the Rocky Mountain marginal zone (subprovince 6), are discussed in the following data analysis.

Identified nuclear detonations and their afterevents (collapses and aftershocks) were removed from the catalog lists and epicenter plots. Identification relied upon published lists. Unidentified events that were not thought to be true earthquakes were also removed.

Geographic Distribution. Figures 7 through 9 present all published epicenter data for the regions and time periods covered (see index map, Figure 6) for $M \geq 4$ (CIT and UNR) and $M \geq 3$ (NOAA); Figure 10 shows all microearthquake epicenters. Earthquakes of $M \geq 3$ are largely confined to seismotectonic subprovinces 1, 2, 4, and 6. Almost none of subprovince 3 is included within the area of the epicenter plots. Other than the diffuse NNE-trending belt in subprovince 4, no obvious alignments of epicenters are evident. Rather, they are scattered through the region outside subprovince 5. In subprovince 5, which includes Las Vegas, the few events plotted are all very near Lake Mead and are believed to be the result of pore-pressure increases induced beneath the lake.

Numerous microearthquakes (Figure 10) are scattered across the entire region, and their distribution shows little relationship to mapped faults. Clustering of events is most pronounced in the Nevada Test Site (NTS), where many are probably unverified afterevents of nuclear detonations. Three earthquake sequences have been identified at the north and east margins of

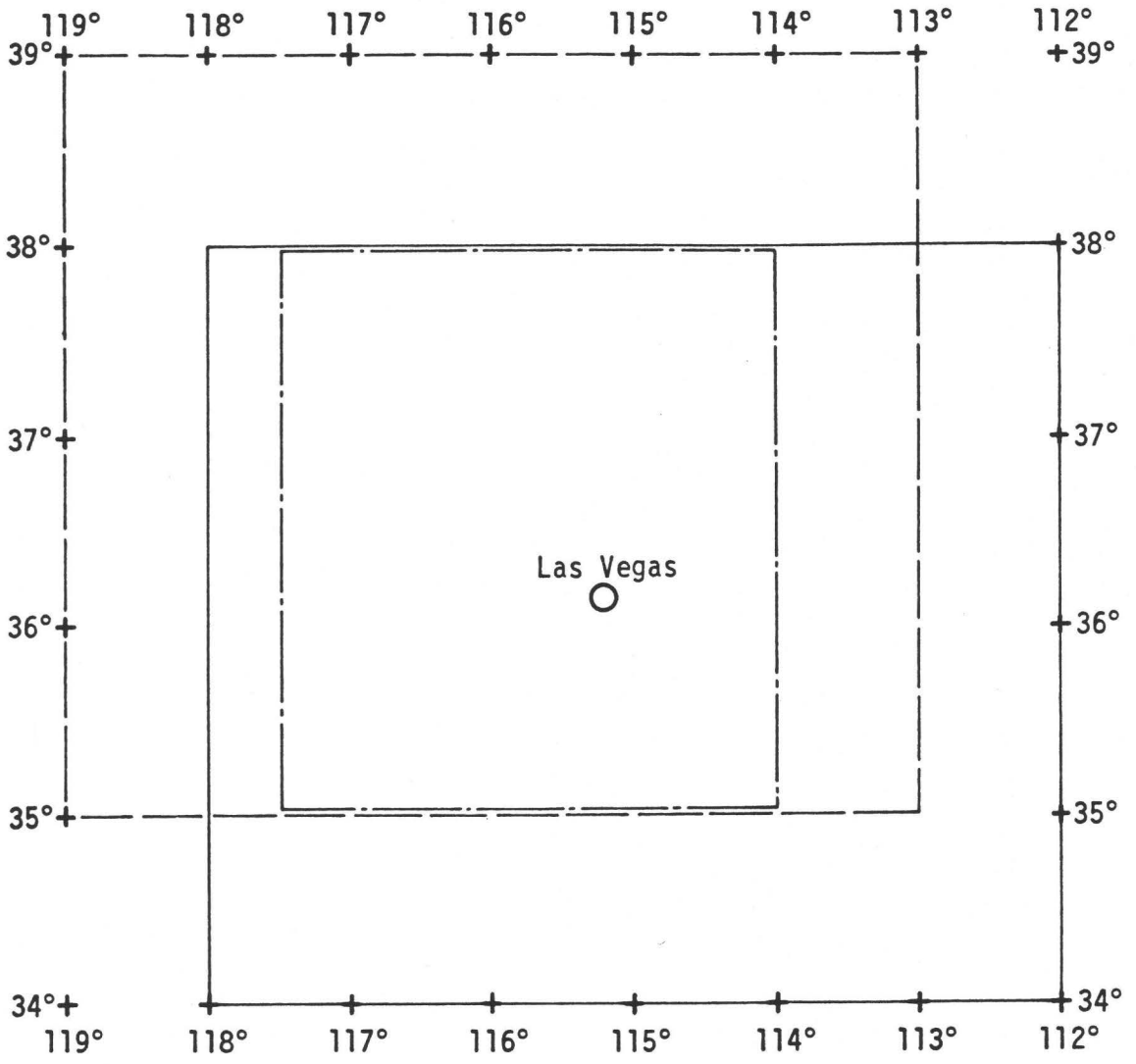

NOAA Data, $M \geq 3$, 1963-1973 (Figure 7)

CIT & UNR Data, $M \geq 4$, 1932-1962 (Figure 8)

NOAA, CIT, & UNR, $M \geq 5$, 1932-1973 (Figure 9)

NSPP (Microearthquakes), $M > 1\pm$, 1971-1973 (Figure 10)

FIGURE 6 INDEX MAP FOR EPICENTER PLOTS OF FIGURES 7 THROUGH 10

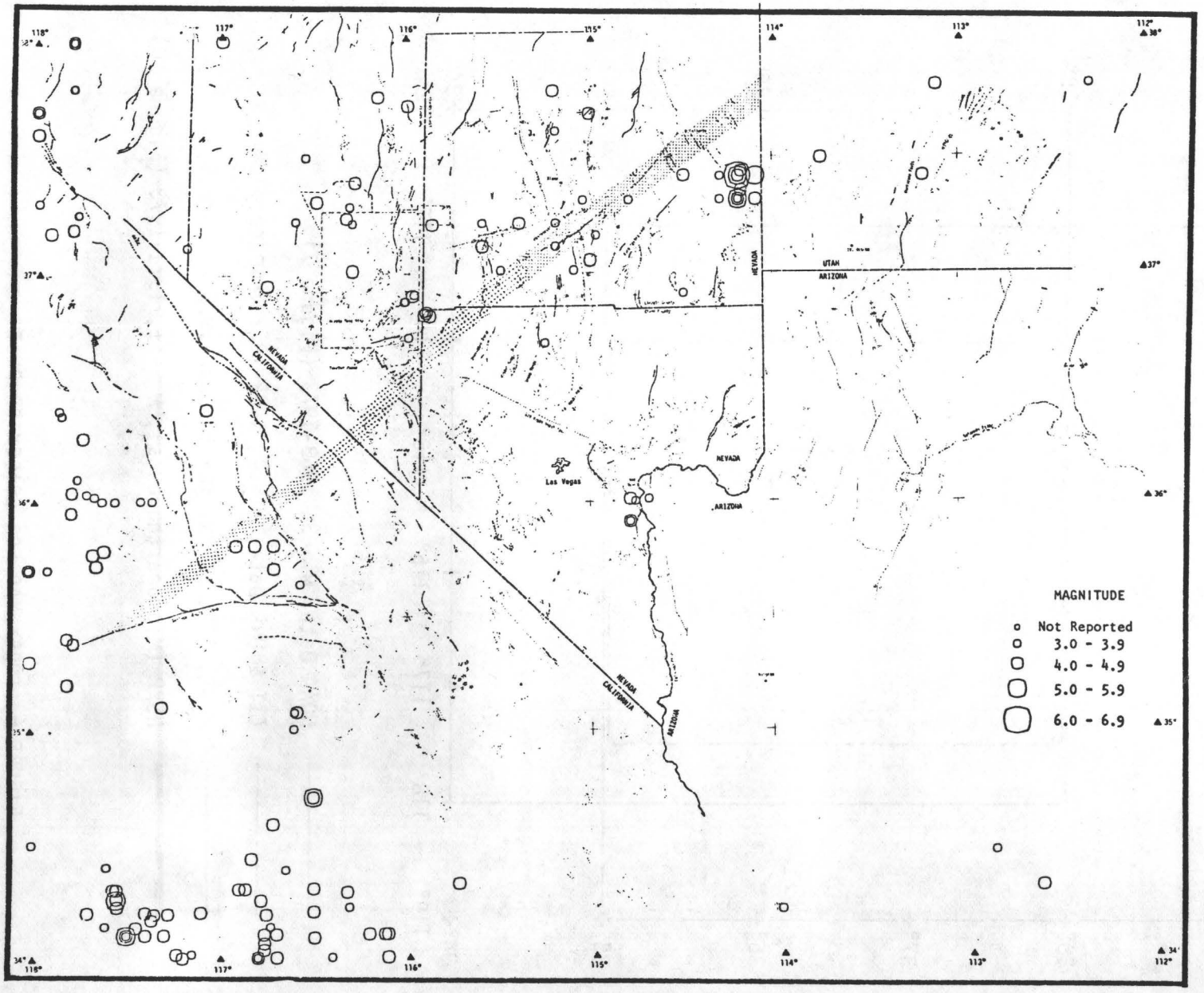

FIGURE 7 EPICENTERS, M ≥ 3, 1963-1973 (NOAA CATALOG)

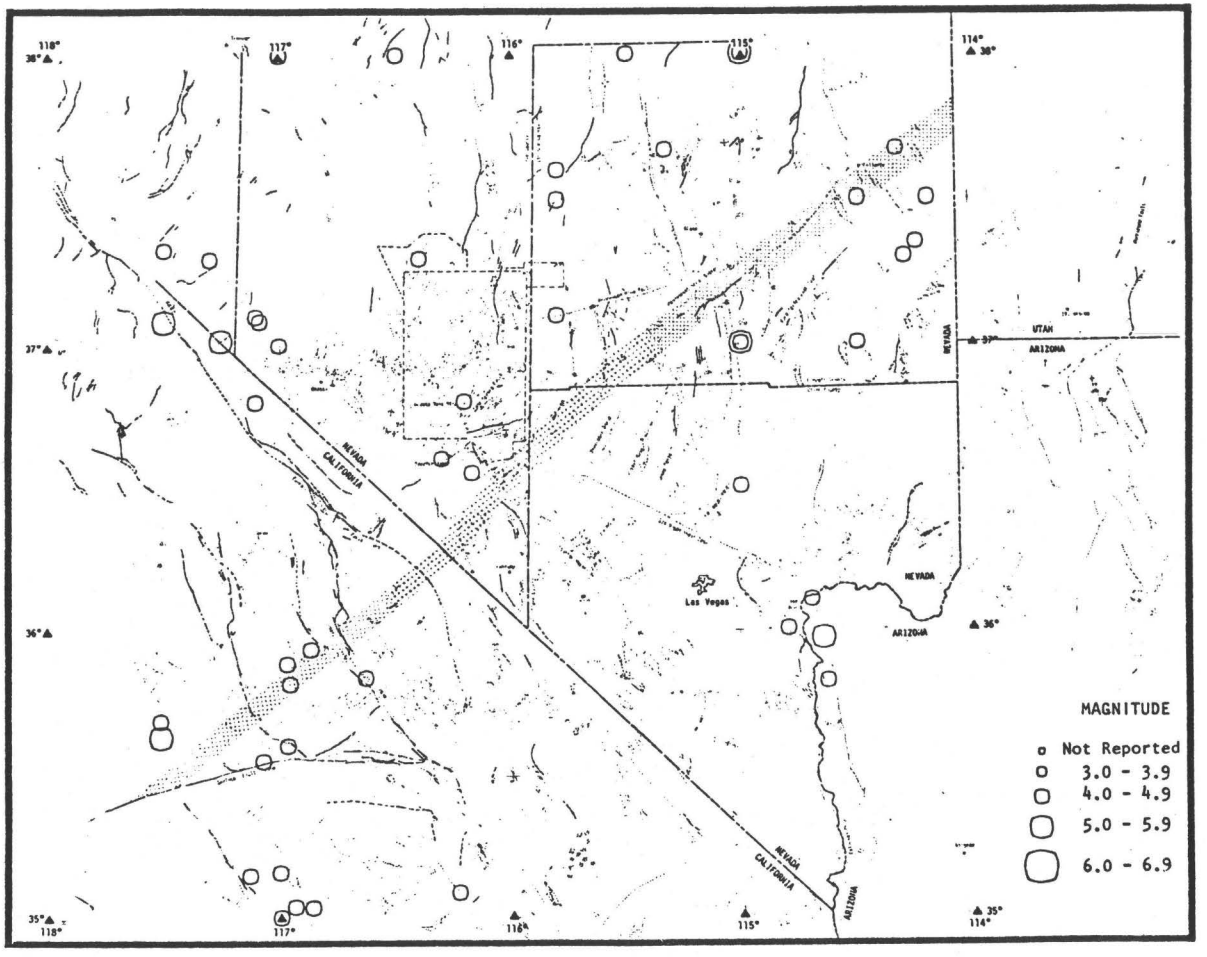

FIGURE 8 EPICENTERS, M ≥ 4, 1932-1962 (CIT & UNR CATALOGS, MERGED AND EDITED)

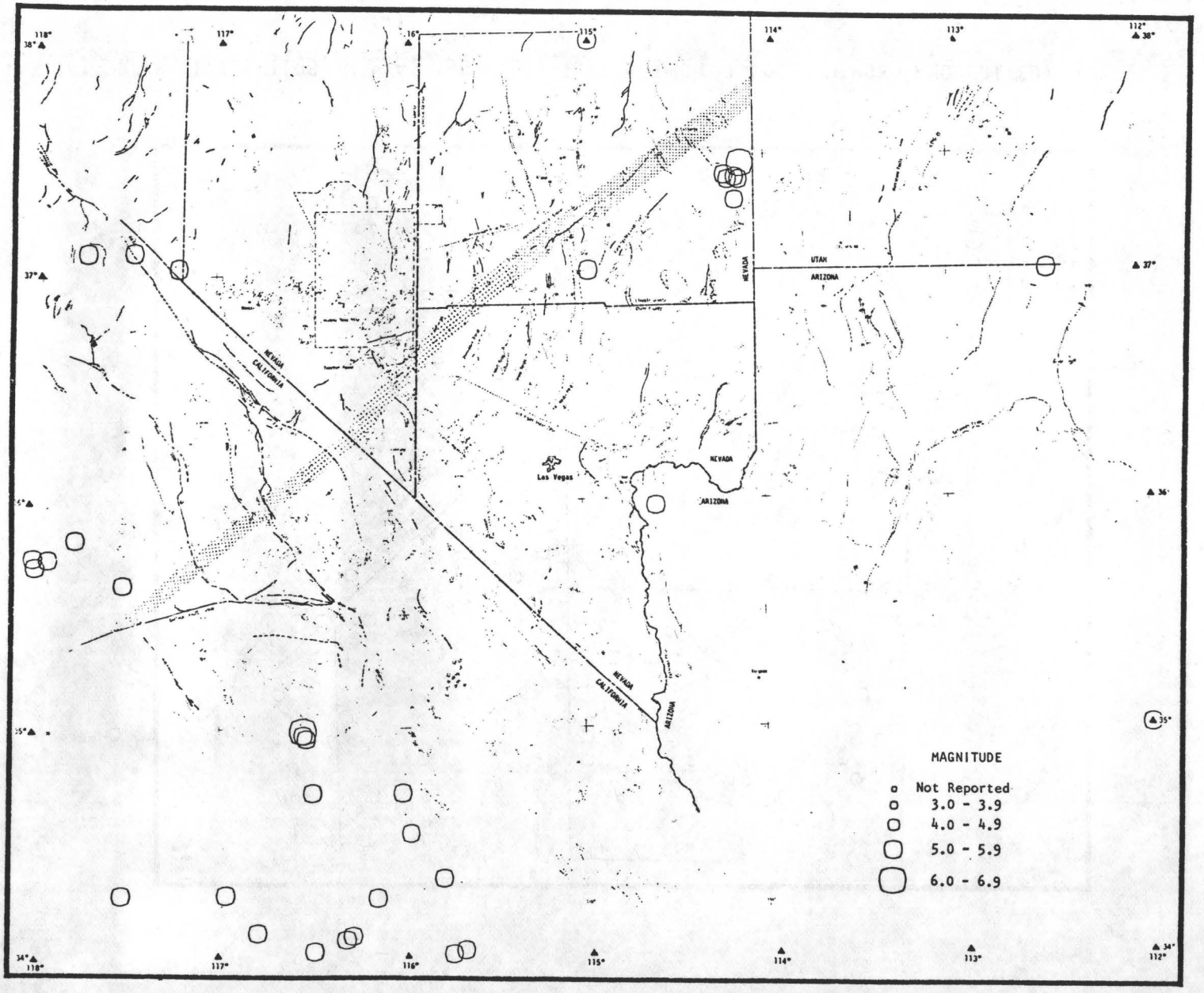

FIGURE 9 EPICENTERS, M ≥ 5, 1932-1973 (NOAA, CIT, UNR CATALOGS, MERGED AND EDITED)

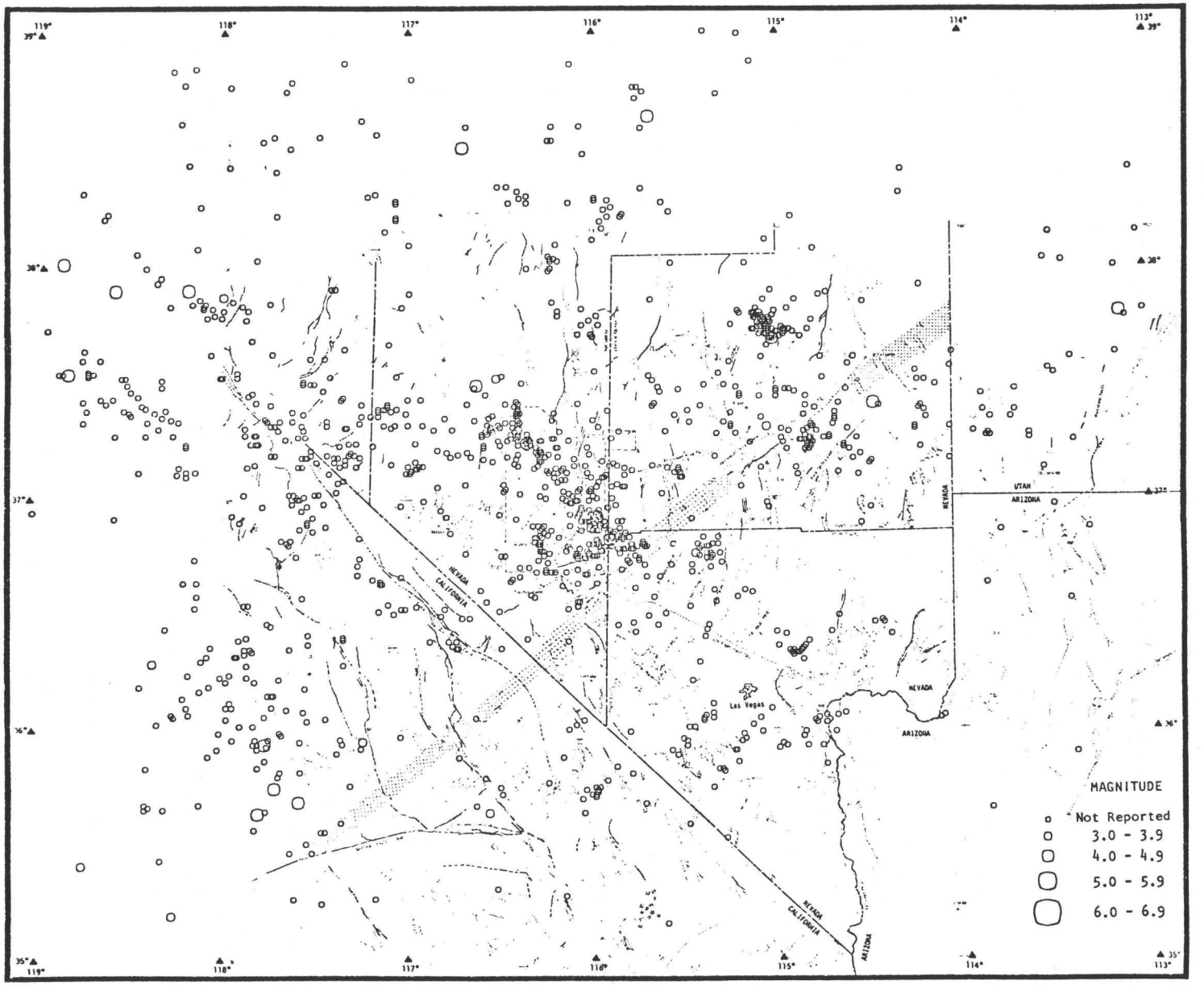

FIGURE 10 MICROEARTHQUAKE EPICENTERS, M ≥ 1±, 1971-1973 (USGS, NEVADA SPECIAL PROJECTS PARTY)

NTS. Most interesting of these is the Silent Canyon sequence (March 1972), which appears as a narrow, north-trending alignment that closely parallels several faults on Pahute Mesa. Two others, Massachusetts Mountain (August to November 1971, maximum magnitude 4.3) and Ranger Mountain (February and March 1973) occurred east of Yucca Flat. They had a swarm-like character and no alignments: all events with $M < 2.9$ were deleted, and as a result only several out of more than 200 located events were plotted. Near Hiko, far to the east of NTS, a diffuse sequence with maximum magnitude 4.8 occurred in December 1971.

Many alignments may be seen, but very few are correlated with mapped fault trends. Near Las Vegas, four northeast-trending alignments of epicenters are seen. Three long ones are located south of Las Vegas and cut across mapped faults trending north to northwest. The shortest is located 30 km northeast of Las Vegas and coincides with a cluster of minor, pre-late-Quaternary faults.

Farther west, in subprovince 1, there is weak clustering of events about the Furnace Creek and Garlock faults. Microearthquake monitoring by the USGS in Death Valley (Papanek and Hamilton, 1972) revealed many events along the Furnace Creek fault zone during a 10-month period.

Magnitude-Frequency Relations. Magnitude-frequency data were compiled and plotted for the six seismotectonic subprovinces of the Great Basin and the Salton Trough. Plots are shown in Figures 11 to 16, and parameters are summarized in Table 1. Data for subprovinces 2, 4, and 5 come entirely from the original compilation prepared for this study; those for subprovinces 3 and 6 are from published analyses of seismicity (Ryall et al., 1966; Sbar and Smith, 1974). Data for subprovince 1 and the Salton Trough are from a published analysis (Hileman et al., 1973) and from the present compilation.

Determination of b-values in the empirical relation

$$\log N = A - bM$$

is a problem for small data samples, in which stable relative frequencies of events as a function of magnitude may not appear. When the total number of

events is sufficiently large (say several hundred), log N is nearly linear in M for $M > M_c$ (M_c is the threshold of complete reporting) with standard deviation less than 0.1 (or ± 25% in N). And for larger regions, such as all of southern California, b-values typically are in the range 0.95 ± 0.05. In zones 1 through 5, $M_c \simeq 4.0$ because values of log N for $M < 4$ are consistently below the linear relation observed for $M \geq 4$; in zone 6, $M_c \simeq 5\frac{1}{2}$.

In the areas analyzed in this study, the conditions for well-determined b-values are not generally satisfied: N is usually small for $M \geq M_c$ and magnitudes for the pre-1963 period are not always of the best quality. Before 1943, CIT reported magnitude only to the nearest half-unit, which distorts data for the eastern-California, southern-Nevada area. In subprovince 6, magnitudes for the period 1932 to 1960 were generally estimated from maximum reported Mercalli intensities or felt area (Ryall et al., 1966), and the b-slope indicated by these data (about 0.6) is probably incorrect.

In order to establish optimal A-values from the historic (1932-1973) data, it was assumed that all b-values had to be in the range 0.9 to 1.0, which characterizes the larger and more complete data sets of the western U.S. Where not adopted from the three literature references mentioned above, b-values were estimated using the maximum likelihood method (Aki, 1965), which is considered better than a least-squares approximation for small data sets. When estimated b-values were outside the range 0.95 ± 0.05, a value of 1.0 was arbitrarily assigned. Sources of all adopted b-values are given in Figures 11 to 16 and in Table 1.

In the following section, the parameter $N_{4.0}$ is treated as a measure of overall regional seismicity, given that b-values vary only slightly. $N_{4.0}$ is the number of shocks per 1,000 km^2 per year with $M \geq 4.0$, and is related to A by log $N_{4.0} = A - 4b$. Major differences in $N_{4.0}$-values from different data sets are observed for seismotectonic subprovinces 1 and 4. These differences seem to be related mainly to the time interval analysed.

In subprovince 1 (Figure 11), the 1932-1962 values are three and a half times greater than the 1963-1973 values. Furthermore, regions around the

ends of the 1872 fault rupture zone appear to be some one and a half times as active per unit area as the whole subprovince. A log-mean (geometric-mean) $N_{4.0}$-value is felt to be representative of the entire region.

In subprovince 4 (Figure 12), the 1963-1973 value of $N_{4.0}$ is about seven times greater than the 1932-1962 value. Much of the difference may be explained by the occurrence in 1966 of a large (M = 6) earthquake and its many aftershocks (27 with $M \geq 4$). This sort of earthquake series did not occur during the 1932-1962 period. Deleting this event and its aftershocks would lower $N_{4.0}$ for 1963-1973 by 50% to a value only three and a half times that for 1932-1962. The value so obtained is the same as the log-mean of the two observed $N_{4.0}$ values and is considered a good estimate for the entire 1932-1973 period.

Magnitude-frequency data for subprovince 6 (Figure 16) are from published analyses (Ryall et al., 1966; Sbar and Smith, 1974). The highly nonlinear appearance of the 1932-1961 data is probably caused by inconsistent reporting of events and by incorrect magnitudes derived from intensity data. The 1963-1973 data are more linear, but still deviate somewhat from a linear fit. A best-fit curve was found by constructing upper-bound and lower-bound curves (using b = 0.96) and then taking the logarithmic mean of these curves.

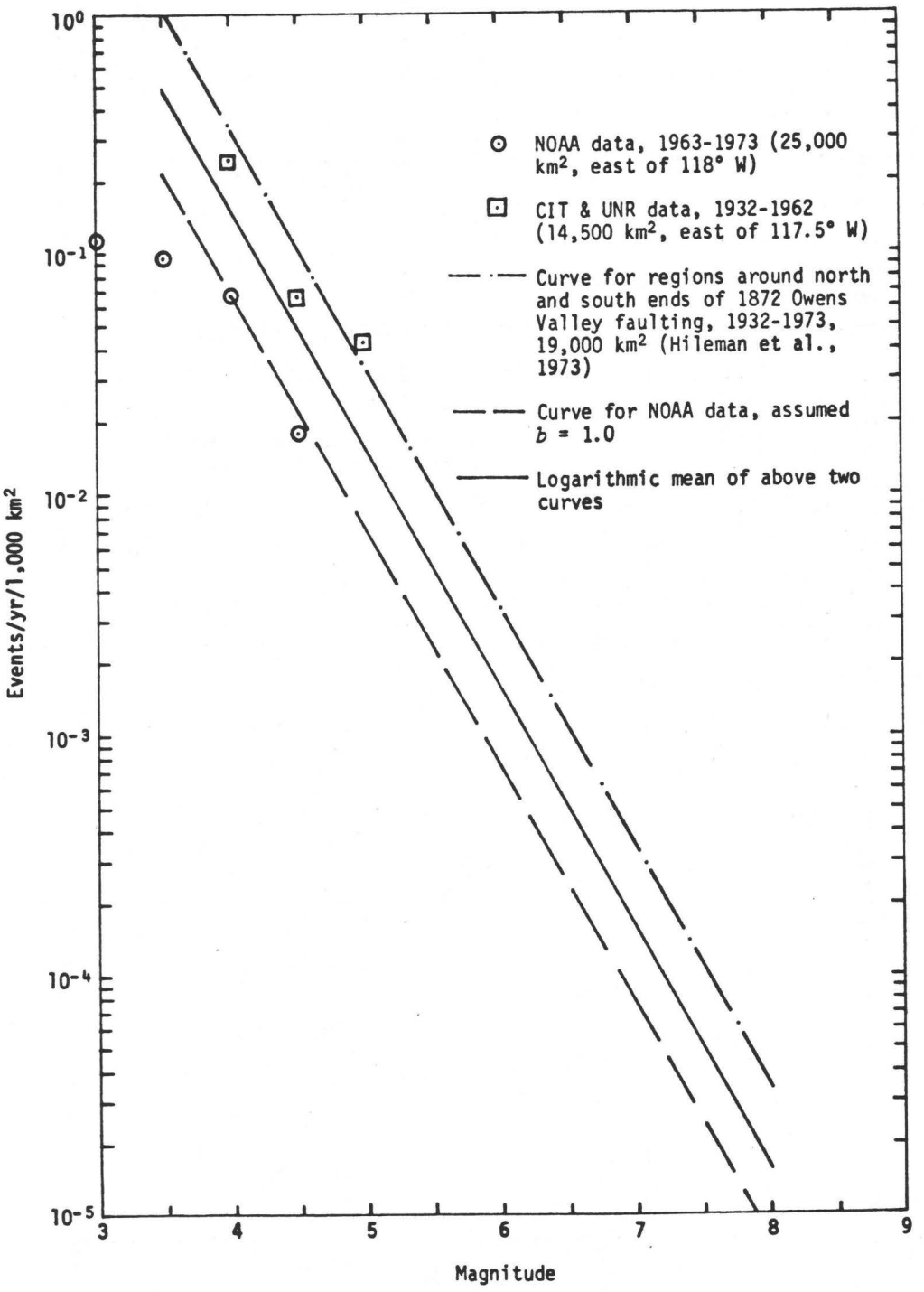

FIGURE 11 MAGNITUDE-FREQUENCY RELATIONS, SEISMOTECTONIC SUBPROVINCE 1 (OWENS VALLEY - DEATH VALLEY REGION), 1932 TO 1973

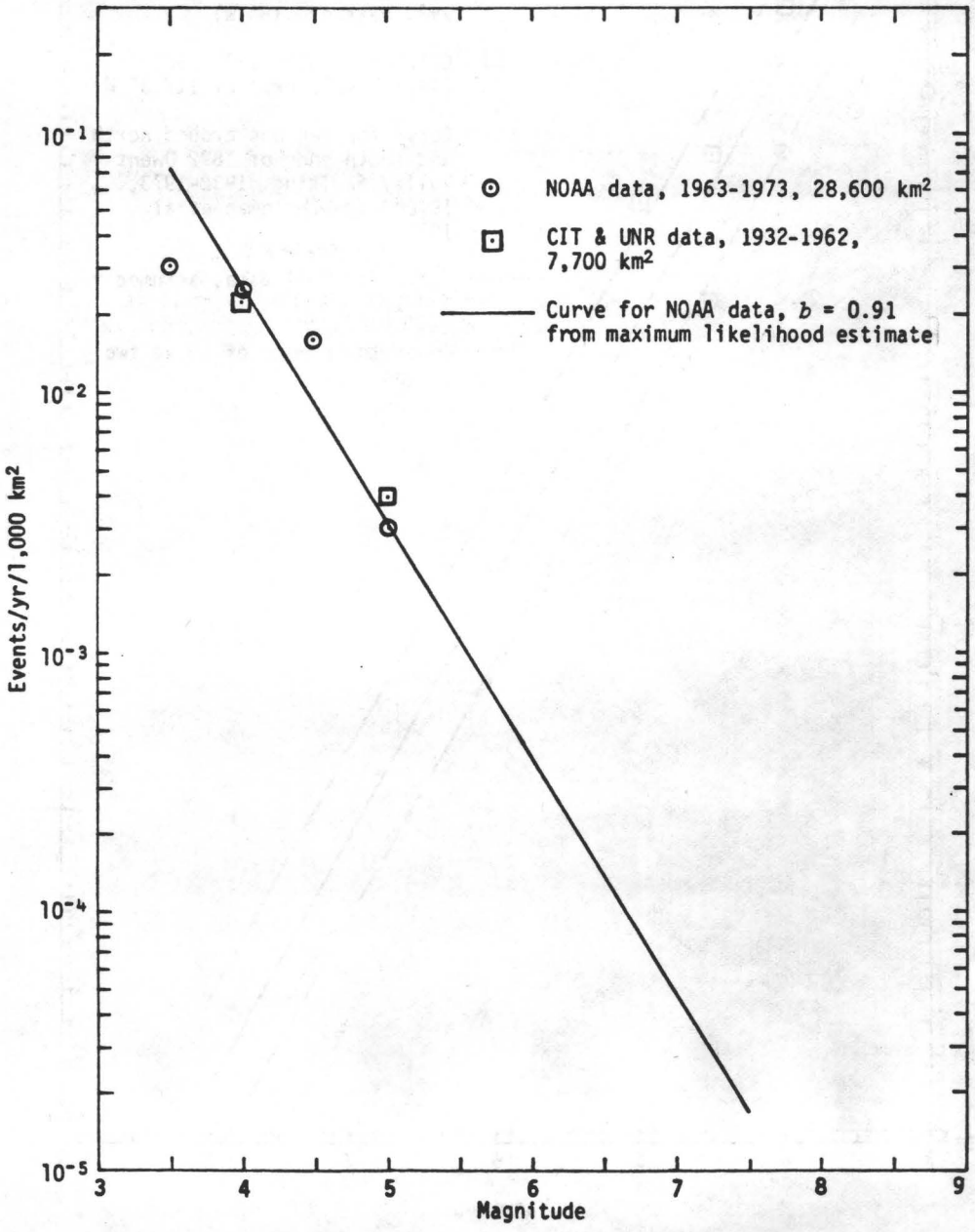

FIGURE 12 MAGNITUDE-FREQUENCY RELATIONS, SEISMOTECTONIC SUBPROVINCE 2 (WESTERN MOJAVE DESERT), 1932 TO 1973

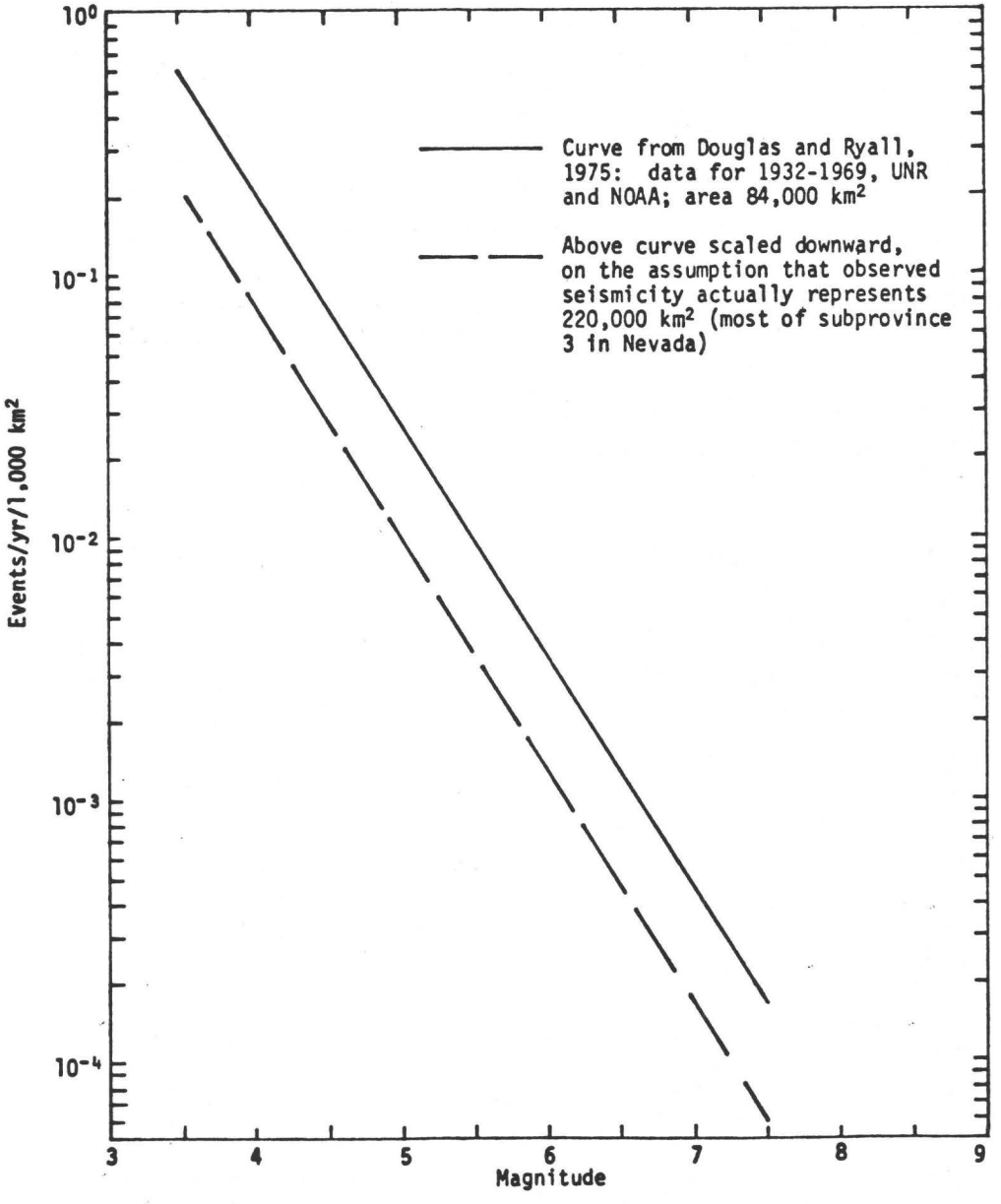

FIGURE 13 MAGNITUDE-FREQUENCY RELATIONS, SEISMOTECTONIC SUBPROVINCE 3 (NORTHERN NEVADA), 1932 TO 1973

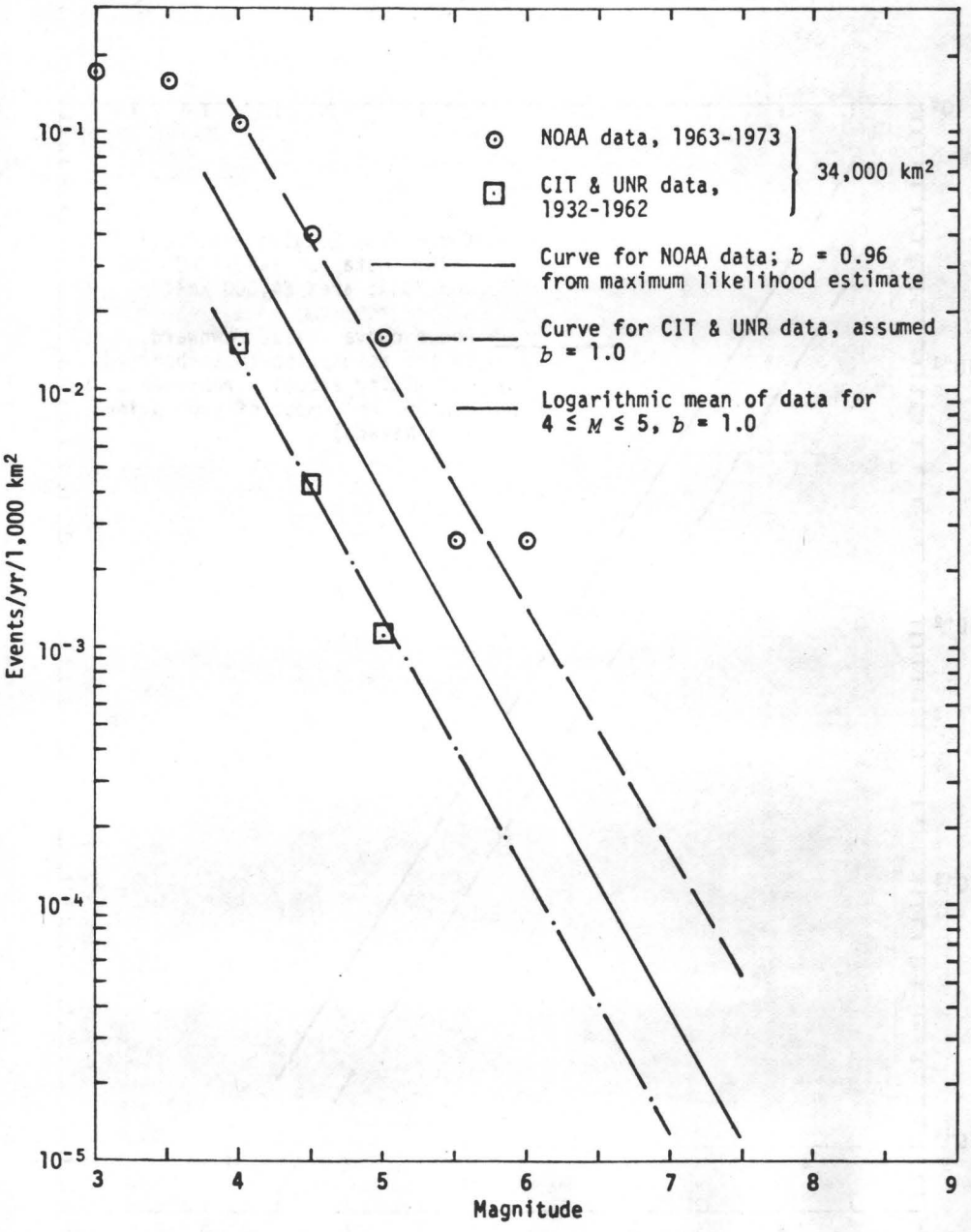

FIGURE 14 MAGNITUDE-FREQUENCY RELATIONS, SEISMOTECTONIC SUBPROVINCE 4 (SOUTHERN NEVADA SEISMIC BELT), 1932 TO 1973

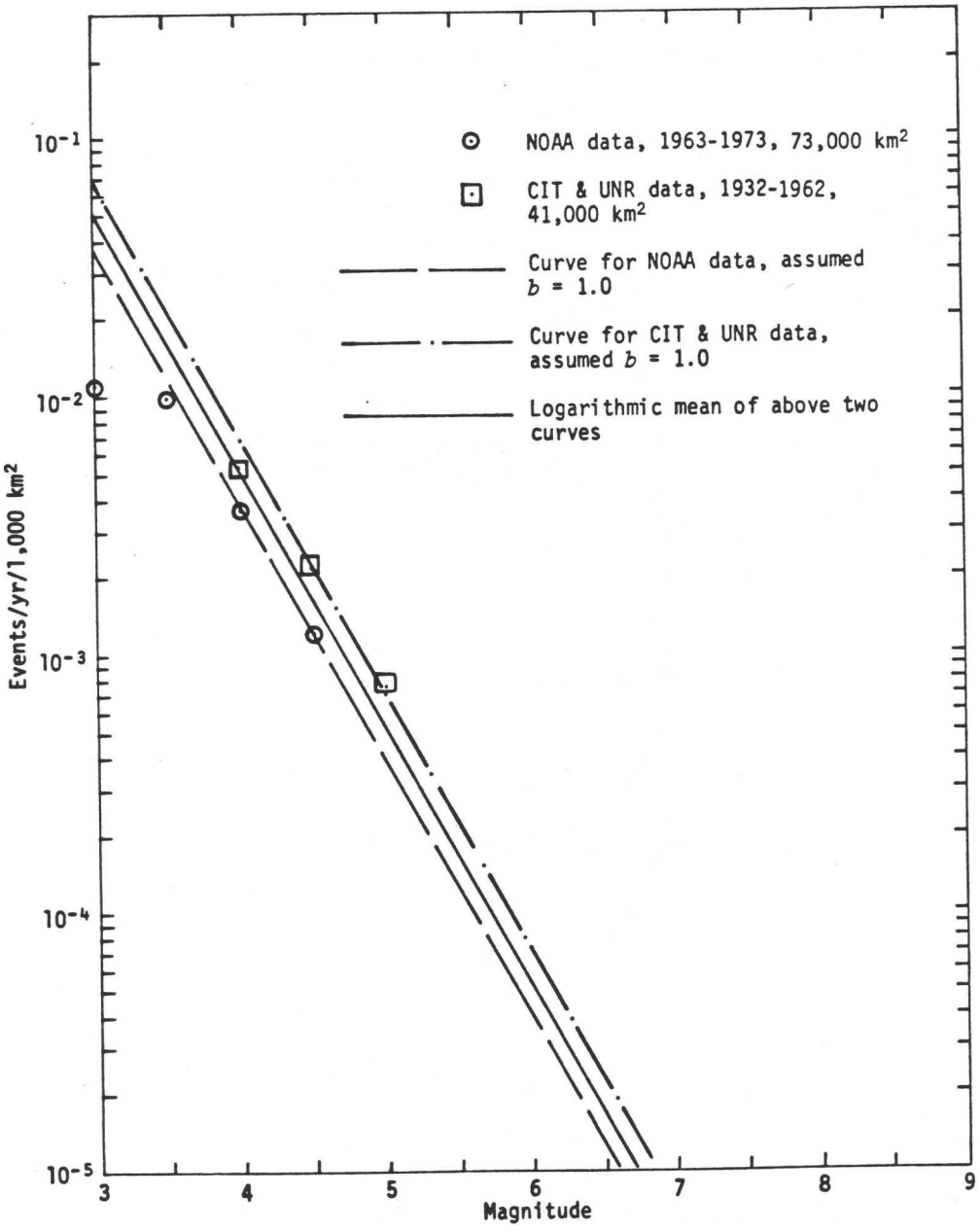

FIGURE 15 MAGNITUDE-FREQUENCY RELATIONS, SEISMOTECTONIC SUBPROVINCE 5 (SOUTHERN BASIN AND RANGE PROVINCE), 1932 TO 1973

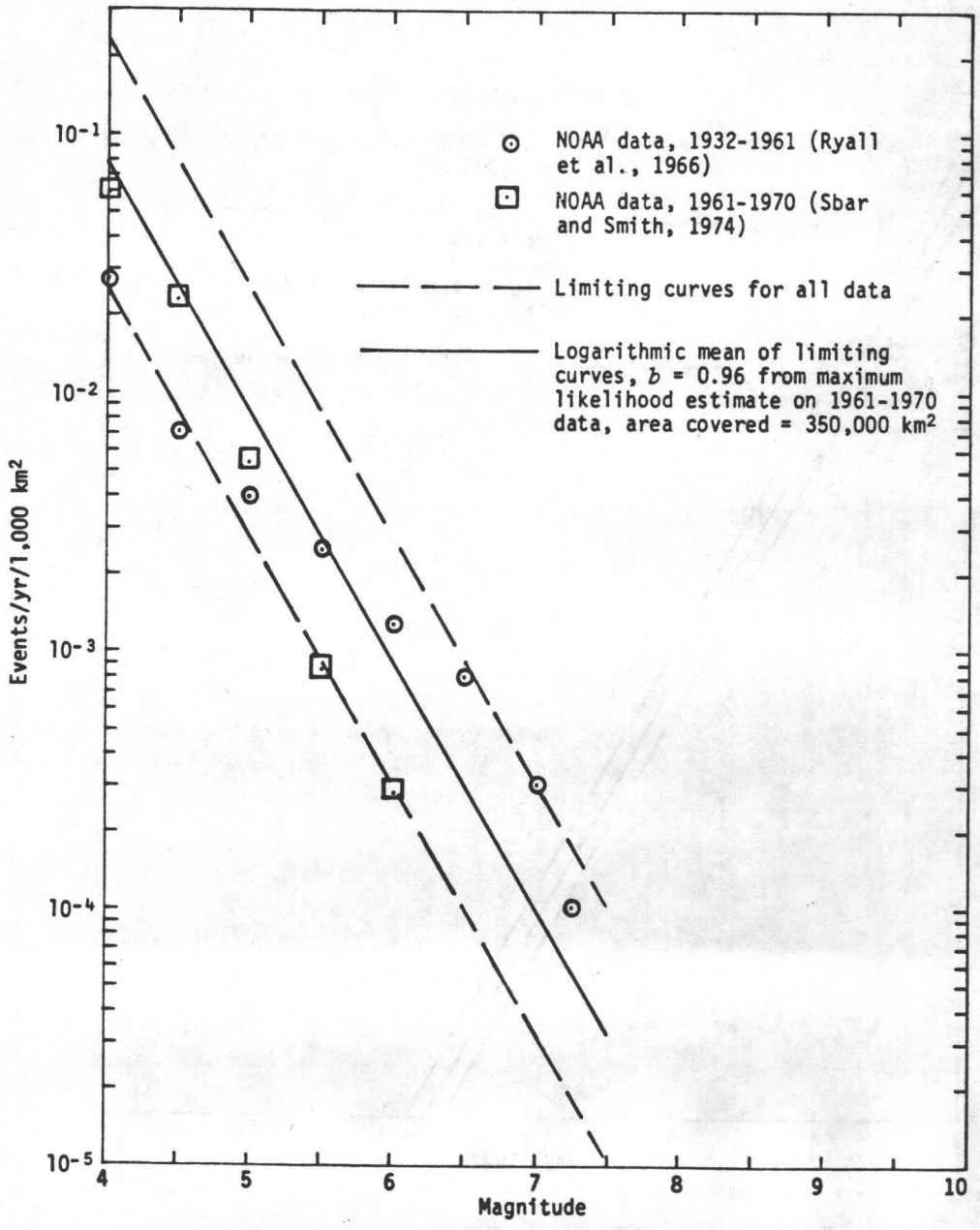

FIGURE 16 MAGNITUDE-FREQUENCY RELATIONS, SEISMOTECTONIC SUBPROVINCE 6, 1932 TO 1973

TABLE 1

SUMMARY OF SEISMICITY DATA FOR SIX SEISMOTECTONIC SUBPROVINCES OF THE GREAT BASIN AND FOR THE SALTON TROUGH

Seismotectonic Subprovince Portion	Area (km^2)	Period	$N_{4.0}$*	b**	$T_{7.0}$***	Data Sources/Comments ****
1/east of 117.5°W	14,500	1932-1962	0.25	--	--	CIT + UNR
1/east of 118°W	25,000	1963-1973	0.068	1.0†	13,000	NOAA
1/near ends of 1872 faulting	19,000	1932-1972	0.34	1.0	3,000	CIT; N and b from Hileman et al., 1973
1/south of 38°N	32,000	1932-1973	0.15‡	1.0‡	6,700‡	Log mean of above data
2/all	28,000	1963-1973	0.025	0.91†	22,000	NOAA
2/northern strip	7,700	1932-1962	0.024	--	--	CIT
3/western Nevada	84,000	1932-1969	0.22	0.91	2,200	UNR + NOAA; N and b from Douglas and Ryall, 1975
3/entire Nevada portion	222,000±	1932-1969	0.08‡	0.91‡	6,000‡	Assumes that observed data actually represent activity of entire subprovince
4/all	34,000	1963-1973	0.11	0.96†	6,000	NOAA
4/all	34,000	1932-1962	0.015	1.0‡	77,000	CIT + UNR
4/all	34,000	1932-1973	0.04	1.0‡	25,000‡	Log mean of above data
5/north of 34°N	73,000	1963-1973	0.0037	1.08†	270,000	NOAA
5/north of 35°N, west of 114°W	41,000	1932-1962	0.0070	1.0‡	140,000	CIT + UNR
5/north of 34°N	73,000	1932-1973	0.0052‡	1.0‡	190,000‡	Log mean of above data
6/all	350,000	1961-1970	0.06	0.96†	12,500	NOAA (Sbar and Smith, 1974)
	350,000	1932-1961	0.025 to 0.25	0.96‡	3,000 to 30,000	NOAA (Ryall et al., 1966)
	350,000	1932-1970	0.075‡	0.96‡	10,000	Log mean of above data
Salton Trough	15,102	1932-1971	0.50	0.85	700	CIT

Explanation

* number of events $M \geq 4$ per year per 1,000 km^2

** b-slope, in relation $\log N = A - bM$; note that $A = \log N_{4.0} + 4b$

*** modal recurrence time for $M > 7$ earthquakes per 1,000 km^2

**** CIT = Hileman et al. (1973)

UNR = Slemmons et al. (1965)

NOAA = Earthquake Data File, National Oceanic and Atmospheric Administration

† b computed using maximum likelihood method

‡ b-value assumed ; N-value estimated as geometric (logarithmic) mean of observed data

COMPARISON OF STRAIN RATE AND SEISMICITY

We have examined the empirical correlation of historical (1932-1973) seismicity with crustal strain rates estimated from late Quaternary faulting and geodetic data, as described above. Figure 17 shows a straight-line fit of the logarithms of principal strain rates ($\dot{e}$) and $N_{4.0}$ for the Great Basin subprovinces 1, 3, 4, 6. It can be seen that the correlation is good ($r = .965$), and the regression line has a slope of $2.04 \pm .30$, indicating $\dot{e} \propto N_{4.0}^{[2.04 \pm .30]}$. Also, subprovinces 2 and 5 agree with this relation to within a factor of two. This result is interesting, and suggests to us that the 40-year sample of seismicity could estimate long-term seismicity ($> 10^4$ yrs) to within a factor of 2, for regions as small as 30,000 km^2. As we had expected a linear relation, the appearance of an exponential relation caused us to seek some basis in theory.

A quasi-theoretical relation between strain-rate and seismicity, in terms of moment rate, has been presented by Anderson (1979). Moment rate may be expressed as

$$\dot{M}_0 = \left| \frac{2\mu}{0.75} v\dot{e} \right| , \tag{1}$$

where μ is the shear modulus, v the volume, and $\dot{e}$ the strain rate of a brittle crustal block undergoing deformation; $\dot{e}$ is measured parallel to the direction of relative plate motion (e.g., direction of extension in the Basin-Range). The constant 0.75 is an empirical estimate of the ratio of the absolute principal values of the moment tensor to the total moment, M_0. The rigidity (μ) is taken to be 3×10^{11} dynes/cm^2, a value that is typical in the literature on earthquake source mechanisms (e.g., Thatcher et al., 1975). The volume (v) is the area of the region considered times the maximum depth of focus, about 15 km in the study region.

Anderson (1979) also developed the relationship between moment rate and seismicity, beginning with the exact expression

$$\dot{M}_o = \int_{-\infty}^{\infty} 10^{\gamma} n(\gamma) d\gamma , \tag{2}$$

TABLE 2

LATE QUATERNARY STRAIN RATES AND SEISMICITY IN THE SEISMOTECTONIC ZONES

Province	$\dot{e}_{(yr^{-1})}$*	EEF($\dot{e}$)†	$N_{4.0}$	EEF($N_{4.0}$)†	Source of Strain Data
Basin and Range:					
subprovince 1	10^{-7}	2	0.15	2	Geodetic and Holocene fault displacement
subprovince 2	10^{-8}?	?	0.025	1.5	Late Cenozoic fault displacement
subprovince 3	5×10^{-8}	2	0.08	2	Holocene fault displacement
subprovince 4	7×10^{-9}	2	0.04	3	Spatial frequency of Holocene faulting relative to subprovince 3
subprovince 5	10^{-10}?	?	0.005	2	
subprovince 6	2.3×10^{-8}	2	0.075	3	Holocene fault displacement
Salton Trough	3×10^{-7}	1.5	0.50	<1.5	Geodetic (trilateration)

*principal strain rate: extensional, except in subprovince 2 and Salton Trough, where compressional

†estimated error factor = $\log^{-1} 2\sqrt{s}$, where s is estimated variance of sample logarithms

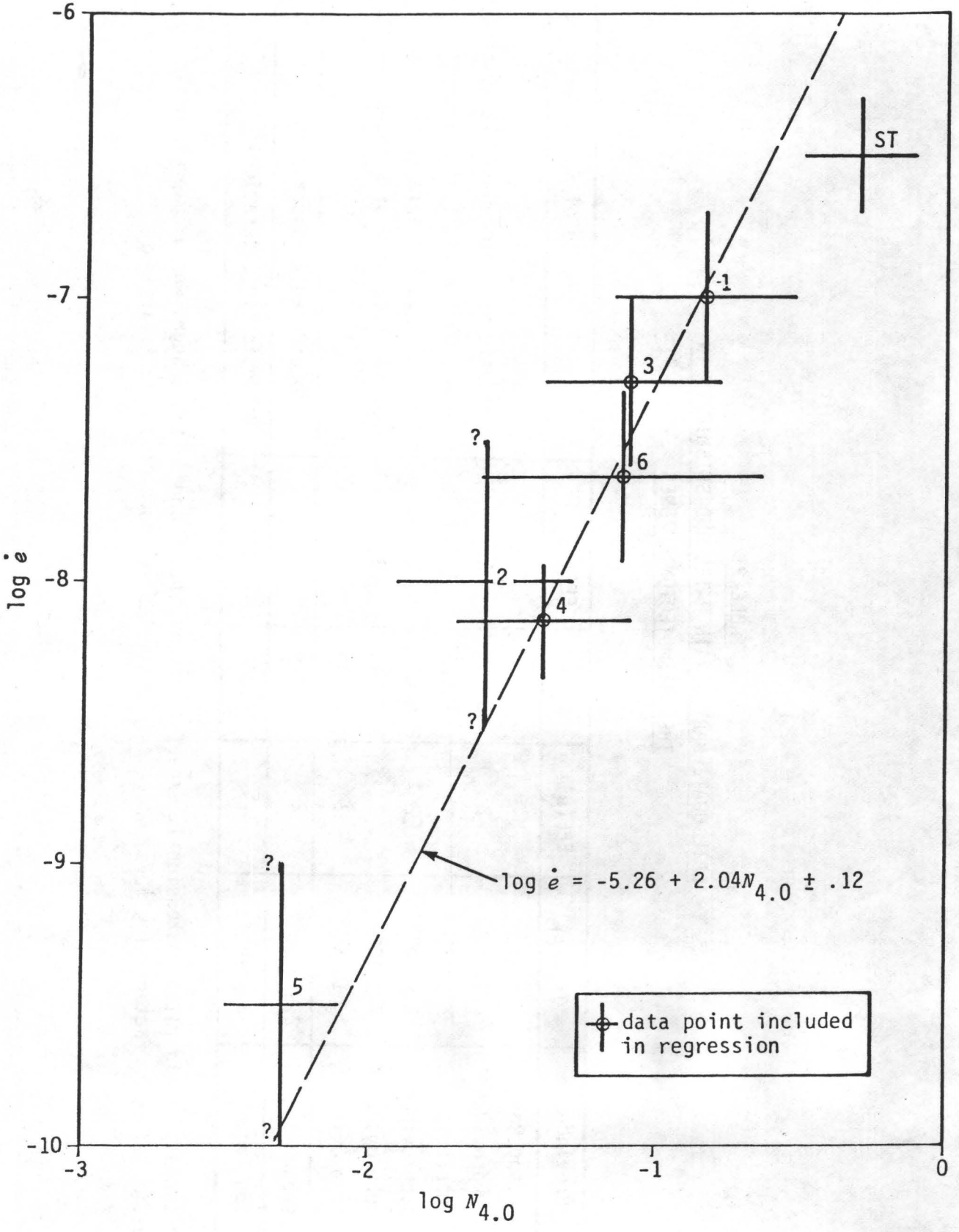

FIGURE 17 CORRELATION OF LATE QUATERNARY STRAIN RATES AND HISTORIC SEISMICITY IN THE SIX SEISMOTECTONIC SUBPROVINCES OF THE BASIN AND RANGE

where $\gamma = \log M_o$ and $n(\gamma)$ is the frequency density of shocks as a function of γ. Using the empirical magnitude-frequency and magnitude-moment (Thatcher and Hanks, 1973) relations

$$\log n(M) = a - bM \tag{3a}$$

and

$$\gamma = 16 + \frac{3}{2}M \ , \tag{3b}$$

one finds the frequency distribution

$$n(\gamma) = 10^{c} - d\gamma \tag{3c}$$

From these equations, Anderson obtained

$$\dot{M}_o = \frac{10^c}{(1 - d)\ \ln 10}\, 10^{(1 - d)\ \gamma_{max}} \tag{4a}$$

where

$$d = \frac{2}{3}b \tag{4b}$$

$$c = a + 16d - \log \frac{3}{2} \ . \tag{4c}$$

Note that

$$a = A + \log(b\ \ln 10) \tag{4d}$$

where A is the intercept in the usual cumulative magnitude-frequency relation

$$\log N(M) = A - bM \tag{4e}$$

and γ_{max} is the upper bound to γ in a region with $(1-d) > 0$, i.e., $b < \frac{3}{2}$ (usually $b \simeq 1$).

Comparing equations (1) and (4), it is evident that $\dot{e}$ and $N_{4.0}$ should be directly proportional. However, if we make the assumption that γ_{max} and

$\dot{M}_0$ are linearly correlated as

$$\gamma_{max} = C + \beta \log \dot{M}_o \tag{5}$$

with C an arbitrary constant, then we find that

$$\dot{e} \propto N_{4.0}^{\frac{1}{1 - \beta + d}} \tag{6}$$

Based upon the observation that regions of higher overall seismicity tend to have had larger historic earthquakes and longer late Quaternary faults, equation (5) is a reasonable postulate; however, the value of β is really unknown. Still, with a nominal value of $b = 1$, assuming $\beta = 1$, gives an exponent of 1.5 in (6).

Finally, we computed moment rates independently from seismicity and strain rates, using equations (1) and (4). These are compared in Table 3 and Figure 18. The parameter γ_{max} estimated from maximum Quaternary fault lengths using empirical magnitude-fault length relations (Slemmons, 1977) and equation (3b); estimated maximum magnitudes range from 7.0 in the Basin Range of Arizona to 8.0 in the Salton Trough. It may be noted that although the data are fairly well correlated, $\dot{M}_0$ ($\dot{e}$) are all larger, by an average factor of about 2, than $\dot{M}_0$ from seismicity. Among the better-known areas of the Great Basin (subprovinces 1, 3, 4, 6) this factor is 3.2.

Discussion

The tendency for $\dot{M}_0$ ($\dot{e}$) to exceed $\dot{M}_0$ (seismicity) may be explained by a combination of the following: (1) some strain release is aseismic; (2) maximum moment (γ_{max}) has been consistently underestimated; (3) rigidity has been over-estimated; (4) historic seismicity is actually less than late Quaternary seismicity. In Southern California, Anderson (1979) obtained

TABLE 3

MOMENT RATES FROM HISTORIC SEISMICITY

AND LATE QUATERNARY STRAIN RATES

Subprovince	$N_{4.0}$	b	γ_{max}	log $\dot{M}_0$ (seismic)	$\dot{e}$(1)	log $\dot{M}_0(\dot{e})$
1	.15	1.0	27.6	23.344	10^{-7}	24.079
2	.025	0.91	27.4	22.710	10^{-8}	23.079
3	.080	0.91	27.4	23.215	5×10^{-8}	23.778
4	.040	1.0	26.8	22.503	7×10^{-9}	22.924
5	.005	1.0	26.5	21.500	10^{-10}	21.079
6	.075	0.96	27.6	23.141	2.3×10^{-8}	23.441
Salton Trough	.50	0.85	28.0	24.410	3×10^{-7}	24.556

(1) $\dot{e}$ is principal extensional strain rate, except in the Salton Trough and subprovince 2 where it is principal compression

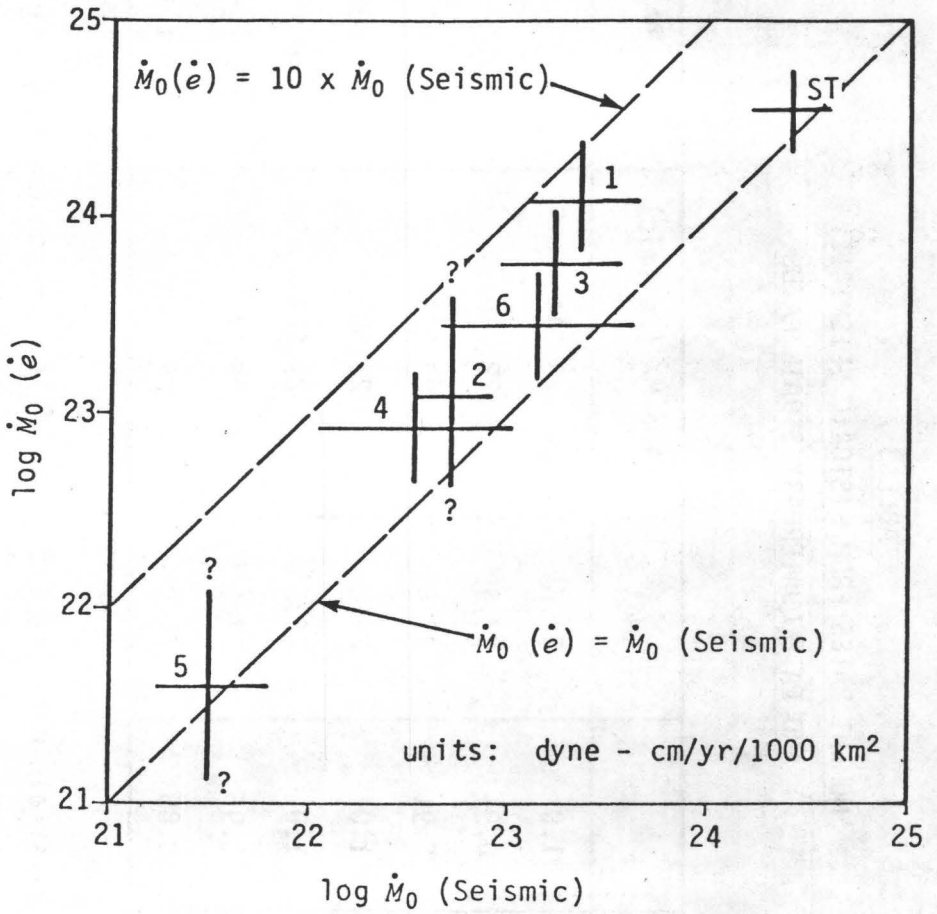

FIGURE 18 COMPARISON OF MOMENT RATES COMPUTED FROM LATE QUATERNARY STRAIN RATES AND HISTORIC SEISMICITY

excellent agreement (within 10%) of moment rates computed from Holocene fault slip and from historic seismicity; here, we find agreement within 25% for the Salton Trough. If crustal rheology in the Great Basin is much like that of southern California, then one should give little weight to alternatives (1) and (3) above. However, aseismic strain is known to be important in many tectonically active parts of the world, and it might be significant in the Great Basin.

Nevertheless, we give greatest weight to alternative (4), less to (2) and (3), and least to (1).

In our calculations, the average upper-bound moment $\langle \gamma_{max} \rangle$ is 27.3, corresponding to $M = 7.5$. Raising this to 28.0 ($M = 8.0$) would increase $\langle \dot{M}_0 \text{ (seismic)} \rangle$ by a factor of 1.7. Such an increase would produce virtual agreement of $\langle \dot{M}_0 \text{ (seismic)} \rangle$ with $\langle \dot{M}_0 (\dot{e}) \rangle$ over all seven regions treated; considering only Great Basin subprovinces 1, 3, 4, and 6, the increase in $\langle \gamma_{max} \rangle$ would make $\langle \dot{M}_0 (\dot{e}) \rangle \approx 2 \langle \dot{M}_0 \text{ (seismic)} \rangle$. Therefore, if the assumed rigidity of 3×10^{11} is not seriously in error, we have yet to explain an apparent factor-of-two to three difference between historic <u>seismic</u> moment rate and late Quaternary <u>total</u> (seismic and aseismic) moment rate.

We consider the possibility that late Quaternary seismicity actually exceeds historic seismicity by a factor of nearly 2. Wallace's (1977) findings bear directly on the paleoseismicity of north-central Nevada, in our subprovince 3. His detailed studies of fault scarp morphology, covering an area of 17,000 km^2, indicate that seven earthquakes with magnitude 7 to 8 have occurred in the past 12,000 years. This represents a rate of some 3×10^{-5} per year per 1,000 km^2, for a mean recurrence period ($T_{7.0}$) of 33,000 years.

This is about 15 times the 2,200 years for $T_{7.0}$ based directly on observed seismicity in the western part of subprovince 3 (Douglas and Ryall, 1975), covering some 84,000 km^2. If it is assumed that the total observed seismicity of western Nevada (84,000 km^2) actually represents all of subprovince 3, an area of about 222,000 km^2, then $T_{7.0}$ from seismicity becomes about 6,000 years. This assumption is based on the notion (described previously) that seismicity in northern Nevada is characteristically confined to rather narrow, northerly trending zones at any given time. Even under this assumption, $T_{7.0}$ from scarp data would be about 5 times that from historic seismicity. Moment rate calculations (Table 3) suggest that paleoseismicity in this region could be 3-1/2 times greater than historic, reckoned under the above assumption concerning sample area. Hence, we are led to the conclusion that our estimated strain rate and Wallace's scarp data imply levels of paleoseismicity which differ by a factor of 18. And so, one might reasonably conclude that available data concerning paleoseismicity in northern Nevada, that is from scarps and displacement rate, stand in no clear relation to historic seismicity.

In western Utah, however, Bucknam et al. (1979), concluded that there is broad regional agreement between paleoseismicity inferred from Holocene scarps and historic seismicity. Their finding is based on quantitative analysis of the ages and distribution of scarps with dimensions corresponding to events of magnitude 7.0 to 7.6.

CONCLUSION

Based upon a qualitative assessment of late Cenozoic tectonic styles and a rough quantitative analysis of relative rates of late Quaternary deformation and historic seismicity, we have developed a seismotectonic regionalization of the Great Basin, dividing it into six subprovinces. Although data concerning rates of deformation are very sparse, they appear to be consistent with rates of historic seismicity among the subprovinces to within a factor of two, in a relative sense. In an absolute sense, however, the agreement is poor: moment rates computed from late Quaternary strain rates consistently exceed those from historic seismicity by a factor estimated to lie between two and three. On the other hand, studies of late Quaternary faulting in north-central Nevada (Wallace, 1977) and in western Utah (Bucknam et al., 1979) suggest that Holocene seismicity is nearly an order of magnitude less than historic seismicity in the first area, but that they are comparable in the second.

The disagreement of absolute moment rates estimated from historic seismicity and Holocene strain rate suggests either that a large fraction (perhaps $\frac{1}{2}$) of the latter is aseismic, or that there is a real difference in seismicity during the two periods. Although we prefer the latter, perhaps both of these hypotheses are true to some extent. In any case, available data concerning fault displacement rates are extremely limited, and are inadequate to determine absolute levels of paleoseismicity over most of the Great Basin.

It is hoped that, as further investigations of faulting such as those conducted by Wallace (1977) and Bucknam et al. (1979) are published, the relationship between historic and long-term seismicity in the Great Basin may be better understood.

ACKNOWLEDGMENTS

This work was supported by the Department of Energy, Nevada Operations Office, through a contract (DE-AC08-76DP 99.) with URS/John A. Blume & Associates, Engineers, as part of an ongoing study of structural response to seismic ground motion in southern Nevada. We wish to thank Roger E. Skjei and Andrew B. Cunningham of URS/Blume, and George Thompson of the Stanford University Geophysics Department, who critically reviewed the manuscript. Richard Wundermann (URS/Blume) assisted in compilation of geologic data.

REFERENCES CITED

Aki, K., 1965, Maximum likelihood estimate of b in the formula log $N = a-bM$ and its confidence limits: Tokyo University Earthquake Research Institute Bulletin, v. 43, p. 237-239.

Albers, J.P., 1967, Belt of sigmoidal bending and right-lateral faulting in the western Great Basin: Geological Society of America Bulletin, v. 78, p. 143-156.

Anderson, J.G., 1979, Estimating the seismicity from geological structure for seismic risk studies: Seismological Society of America Bulletin, v. 69, p. 135-158.

Anderson, R.E., 1973, Large-magnitude late tertiary strike-slip faulting north of Lake Mead, Nevada: U.S. Geological Survey Professional Paper 794.

Anderson, R.E., Longwell, C.R., Armstrong, R.L., and Marvin, R.F., 1972, Significance of K-Ar ages of tertiary rocks from the Lake Mead region, Nevada-Arizona: Geological Society of America Bulletin, v. 83, p. 273-288.

Armstrong, R.L., 1968, Sevier orogenic belt in Nevada and Utah: Geological Society of America Bulletin, v. 79, p. 429-458.

Atwater, T., 1970, Implications of plate tectonics for the Cenozoic tectonic evolution of western North America: Geological Society of America Bulletin, v. 81, p. 3513-3516.

Barnes, H., and Poole, F.G., 1968, Regional thrust-fault system in Nevada Test Site and vicinity, *in* Nevada Test Site: Geological Society of America Memoir 110, p. 233-238.

Bayer, K.C., 1973a, Seismic data report, southern Nevada region, December 22, 1971 to December 31, 1972: NVO-746-10, U.S. Department of Commerce, National Oceanic and Atmospheric Administration, Earth Sciences Laboratories.

Bayer, K.C., 1973b, A preliminary seismicity study of the southern Nevada region, quarterly report, January-March 1973: NOV-746-12, U.S. Department of Commerce, National Oceanic and Atmospheric Administration, Earth Sciences Laboratories.

Bayer, K.C., 1974, A preliminary seismicity study of the southern Nevada region, quarterly report, April-June 1973: NVO-474-1.

Bayer, K.C., Mallis, R.R., and King K.W., 1972, Earthquakes recorded by a seismograph network located in the southern Nevada region, January 1 to December 22, 1971: NVO-746-TM3, U.S. Department of Commerce, National Oceanic and Atmospheric Administration, Earth Sciences Laboratories.

Bucknam, R.C., Algermisson, S.T., and Anderson, R.E., 1979, Late Quaternary faulting in western Utah and its implications in earthquake hazard evaluation: Geological Society of America Abstracts with Programs, v. 11, no. 3, p. 71-72.

Burchfiel, B.C., 1965, Structural geology of the Specter Range Quadrangle, Nevada, and its regional significance: Geological Society of America Bulletin, v. 76, p. 175-192.

Burchfiel, B.C., Fleck, R.J., Secor, D.T., Vincelette, R.R., and Davis, G.A., 1974, Geology of the Spring Mountains, Nevada: Geological Society of America Bulletin, v. 85, p. 1013-1022.

Christiansen, R.L., and Lipman, P.W., 1972, Cenozoic volcanism and plate-tectonic evolution of the western nited States: II, late Cenozoic: Royal Society of London, Philosophical Transactions, ser. A, v. 271, p. 249-284.

Christiansen, R.L., and McKee, E.H., 1978, Late Cenozoic volcanic and tectonic evolution of the Great Basin and Columbia Intermountain regions, *in* Smith, R.B., and Eaton, G.P., eds., Cenozoic tectonics and regional geophysics of the western Cordillera: Geological Society of America Memoir 152, p. 283-311.

Clark, M.M., and Lajoie, K.R., 1974, Holocene behavior of the Garlock Fault: Abstract, Geological Society of America Abstracts with Programs, v. 6, p. 156.

Davis, G.A., and Burchfiel, B.C., 1973, Garlock Fault: An intracontinental transform structure, Southern California: Geological Society of America Bulletin, v. 84, p. 1407-1422.

Dibblee, T.H., 1961, Evidence of strike-slip movement on northwest-trending faults in the Mojave Desert, California: U.S. Geological Survey Professional Paper 424B, p. 197-199.

Dibblee, T.H., 1967, Aerial geology of the western Mojave Desert, California: U.S. Geological Survey Professional Paper 522.

Eaton, G.P., Wahl, R.R., Prostka, H.J., Mabey, D.R., and Kleinkopf, M.D., 1978, Regional gravity and tectonic patterns: Their relation to late Cenozoic epeirogeny and lateral spreading in the western Cordillera, *in* Smith, R.B., and Eaton, G.P., eds., Cenozoic tectonics and regional geophysics of the western Cordillera: Geological Society of America Memoir 152, p. 51-91.

Ekren, E.B., 1972, Geologic examination of Super Kukla reactor site, Nevada Test Site: U.S. Geological Survey Report 474-161 to Nevada Operations Office, U.S. Energy Research and Development Administration.

Ekren, E.B., and Sargent, K.A., 1965, Geologic map of the Skull Mountain Quadrangle, Nye County, Nevada: U.S. Geological Survey Geologic Quadrangle Map GQ-387.

Ekren, E.B., Rogers, C.L., Anderson, R.E., and Orkild, P.P., 1968, Age of basin and range normal faults in Nevada Test Site and Nellis Air Force Range, Nevada, *in* Nevada Test Site: Geological Society of America Memoir 110, p. 247-250.

Fleck, R.J., 1970a, Age and possible origin of the Las Vegas Valley shear zone, Clark and Nye Counties, Nevada: Geological Society of America Abstracts with Programs (Rocky Mountain Section), v. 2, no. 5, p. 333.

Fleck, R.J., 1970b, Tectonic style, magnitude, and age of deformation in the Sevier orogenic belt of southern Nevada and eastern California: Geologic Society of America Bulletin, v. 81, p. 1705-1720.

Garfunkel, Z., 1974, Model for the late Cenozoic tectonic history of the Mojave Desert, California, and for its relation to adjacent regions: Geologic Society of America Bulletin, v. 85, p. 1931-1944.

Hamilton, W., and Myers, W.B., 1966, Cenozoic tectonics of the western United States: Reviews of Geophysics, v. 4, p. 509-549.

Hileman, J.A., Allen, C.R., and Nordquist, J.M., 1973, Seismicity of the southern California region, 1 January 1932 to 31 December 1932: Seismology Laboratory, California Institute of Technology, Pasadena.

Hooke, R.L., 1972, Geomorphic evidence for Holocene and late Wisconsin tectonic deformation, Death Valley, California: Geological Society of America Bulletin, v. 83, p. 2073-2090.

Jennings, C.W., 1975, Fault map of California with locations of volcanoes, thermal springs, and thermal wells: Geologic Data Map Series, Map. No. 1, California Division of Mines and Geology.

Lachenbruch, A.H., and Sass, J.H., 1978, Models of an extending lithosphere and head flow in the Basin and Range province, *in* Smith, R.B., and Eaton, G.P., eds., Cenozoic tectonics and regional geophysics of the western Cordillera: Geological Society of America Memoir 152, p. 209-250.

Lawrence, R.D., 1976, Strike-slip faulting terminates the Basin and Range province in Oregon: Geological Society of America Bulletin, v. 87, p. 846-950.

Locke, A., Billingsley, P., and Mayo, E.B., 1940, Sierra Nevada tectonic pattern: Geological Society of America Bulletin, v. 51, p. 513-599.

Longwell, C.R., 1960, Possible explanation of diverse structural patterns in southern Nevada: American Journal of Science, v. 258-A (Bradley Volume), p. 192-203.

Longwell, C.R., 1963, Reconnaissance geology between Lake Mead and Davis Dam, Arizona-Nevada: U.S. Geological Survey Professional Paper 374E.

Longwell, C.R., 1974, Measure and date of movement on Las Vegas Valley shear zone, Clark County, Nevada: Geological Society of America Bulletin, v. 85, p. 985-990.

McKee, E.H., 1971, Tertiary igneous chronology of the Great Basin of western United States - implications for tectonic models: Geological Society of America Bulletin, v. 82, p. 3497-3502.

Minster , J.B., and Jordan, T.H., 1978, Present-day plate motions: Journal of Geophysical Research, v. 83, p. 5331-5354.

Moench, R.H., 1965, Structural geology of the southern part of the Amargosa Desert and vicinity: U.S. Geological Survey, Technical Letter NTS-106 for U.S. Atomic Energy Commission.

Nielsen, R.L., 1965, Right-lateral strike-slip faulting in the Walker Lane, west-central Nevada: Geological Society of America Bulletin, v. 76, p. 1301-1308.

Papanek, P.J. and Hamilton, R.M., 1972, A seismicity study along the northern Death Valley - Furnace Creek fault zone, California-Nevada boundary: U.S. Geological Survey, Special Studies - 90 (USGS 474-141)

Poole, F.G., Elston, D.P., and Carr, W.J., 1965, Geologic map of the Cane Spring Quadrangle, Nye County, Nevada: U.S. Geological Survey Geologic Quadrangle Map GQ-455.

Roberts, R.J., 1972, Evolution of the Cordilleran fold belt: Geological Society of America Bulletin, v. 83, p. 1989-2004.

Rogers, T.H., 1967, San Bernardino sheet, geologic map of California: California Division of Mines and Geology.

Ryall, A., Slemmons, D.B., and Gedney, L.D., 1966, Seismicity, tectonism, and surface faulting in the western United States during historic time: Bulletin of the Seismological Society of America, v. 56, p. 1105-1135.

Savage, J.C., Church, J.P., and Prescott, W.H., 1975, Geodetic measurement of deformation in Owens Valley, California: Bulletin of the Seismological Society of America, v. 65, p. 865-874.

Savage, J.C., Prescott, W.H., Lisowski, M., and King, N., 1978, Deformation across the Salton Trough, California, 1973-1977: Journal of Geophysical Research, v. 84, p. 3069-3080.

Sbar, M.L., and Smith, R.M., 1974, Contemporary tectonics and seismicity of the western United States with emphasis on the intermountain seismic belt: Geological Society of America Bulletin, v. 85, p. 1205-1218.

Scholz, C.H., Barazangi, M., and Sbar, M.L., 1971, Late Cenozoic evolution of the Great Basin, western United States, as an ensialic interarc basin: Geological Society of America Bulletin, v. 82, p. 2979-2990.

Shawe, D.R., 1965, Strike-slip control of basin-range structure indicated by historical faults in western Nevada: Geological Society of America Bulletin: v. 76, p. 1361-1378.

Slemmons, D.B., 1967, Pliocene and Quaternary crustal movements of the Basin and Range province, USA: Journal of Geoscience, Osaka University, v. 10, p. 91-103.

Slemmons, D.B., 1977, Faults and earthquake magnitude: U.S. Army Waterways Experiment Station, State-of-the-Art for Assessing Earthquake Hazards in the United States, Report 6, Miscellaneous Paper S-73-1.

Slemmons, D.B., Jones, A.E., and Gimlett, J.I., 1965, Catalog of Nevada earthquakes, 1852-1960: Bulletin of the Seismological Society of America, v. 55, p. 537-583.

Stewart, J.H., 1967, Possible large right-lateral displacement along fault and shear zones in the Death Valley - Las Vegas area, California and Nevada: Geological Society of America Bulletin, v. 78, p. 131-142.

Stewart, J.H., 1971, Basin and Range structure: A system of horsts and grabens produced by deep-seated extension: Geological Society of America Bulletin, v. 82, p. 1019-1044.

Stewart, J.H., Ross, D.C., Nelson, C.A., and Burchfiel, B.C., 1966, Last Chance thrust - a major fault in the eastern part of Inyo County, California: U.S. Geological Survey Professional Paper 550-d, p. 23-24.

Suppe, J., Powell, C., and Berry, R., 1975, Regional topography, seismicity, Quaternary volcanism, and present-day tectonism of the western United States: American Journal of Science, v. 275-A, p. 397-436.

Swan, F.H. III, Schwartz, D.P., Hanson, K.L., Knuepfer, P.L., and Cluff, L.S., 1978, Recurrence of surface faulting and large magnitude earthquakes along the Wasatch fault, Utah: Trans. American Geophysical Union, v. 59, no. 12, p. 1126 (abs.).

Thatcher, W., and Hanks, T.C., 1973, Source parameters of southern California earthquakes: Journal of Geophysical Research, v. 78, p. 8547-8576.

Thatcher, W., Hileman, J.A., and Hanks, T.C., 1975, Seismic slip distribution along the San Jacinto fault zone, southern California, and its implications: Geological Society of America Bulletin, v. 86, p. 1140-1146.

Thompson, G.A., 1965, The rift system of the western United States, *in* The World Rift System: Report of the International Upper Mantle Committee: Geological Survey of Canada Paper 66-14, p. 280-290, Ottawa.

Thompson, G.A., and Burke, D.B., 1974, Regional geophysics of the Basin and Range province: Annual Review of Earth and Planetary Science, v. 2, p. 213-238.

Tschanz, C.M., and Pampeyan, E.H., 1970, Geology and mineral deposits of Lincoln County, Nevada: Nevada Bureau of Mines Bulletin 73.

USDA Soil Conservation Service, 1974, Mosaic of imagery from the earth resources technology satellite-1 of the prepared for NASA Goddard Space Flight Center, Satellite Image Mosaic, Band 7--Summer.

Wallace, R.E., 1977a, Time-history analysis of fault scarps and fault traces -- a longer view of seismicity: Sixth World Conference on Earthquake Engineering, p. 2-409 - 2-411.

Wallace, R.E., 1977b, Profiles and ages of young fault scarps, north-central Nevada: Geological Society of America Bulletin, v. 88, p. 1267-1281.

Wallace, R.E., 1978, Patterns of faulting and seismic gaps in the Great Basin province, *in* Proceedings of Conference VI, Methodology for Identifying Seismic Gaps and Soon-to-Break Gaps: U.S. Geological Survey Open File Report 78-943, p. 858-868.

Willis, D.E., Principal invest., Taylor, R. W., Torfin, R. D., Tatar, P. J., Revock, K. L., Poetzl, R. G., Goerge, G. D., Bufe, C. G., 1974, Explosion-induced ground motion, tidal and tectonic forces and their relationship to natural seismicity: Department of Geological Sciences, University of Wisconsin, Madison.

Wright, L., 1976, Late Cenozoic fault patterns and stress fields in the Great Basin and Westward displacement of the Sierra Nevada block: Geology, v. 4, p. 489-494.

Zoback, M. L., 1978, Mid-Miocene rifting in north-central Nevada: A detailed study of late Cenozoic deformation in the northern Basin and Range: PhD Thesis, Stanford University.

Zoback, M.L., and Thompson, G.A., 1978, Basin and Range rifting in northern Nevada: Clues from a mid-Micone rift and its subsequent offsets: Geology, v. 6, p. 111-116.

TECTONIC AND GEOMORPHIC EVOLUTION OF THE BLACK ROCK FAULT, NORTHWESTERN NEVADA

by

R. L. Dodge and L. T. Grose
Colorado School of Mines
Golden, Colorado 80401
June, 1979

The absolute age, recurrence, and magnitude of late Pleistocene and Holocene faulting is often difficult to determine, because of the absence of datable horizons. Accurate relative dating techniques are necessary for a realistic evaluation of seismic risk. For example, the geomorphic form of fault scarps is used as a relative dating technique; scarp-slope angle decreases with increasing age. The purpose of our study, with the Black Rock Fault (BRF) of northwestern Nevada as our subject, is to: 1) define the recurrence of faulting, 2) postulate the magnitude of earthquake associated with faulting, 3) determine the relationship between scarp morphology and age, and 4) evaluate the control of material faulted on the rate of scarp degradation.

The BRF is located northwest of the Nevada Seismic Zone, defined by eight historic earthquakes ranging in magnitude from 5.6 to 7.6 (fig. 1). The BRF is a typical Basin and Range normal fault, remarkable for its length (60 km), its excellently preserved scarps, and the variety of materials offset by faulting. It is known to displace Holocene and late Pleistocene age deposits; therefore, it is particularly well suited for this study.

Investigations

Initial research consisted of literature search and photogeologic interpretation of 1:24,000-scale low sun-angle photographs (LSAP). The LSAP interpretation revealed a variety of evidence for late Quaternary faulting, including fault scarps, linear vegetation anomalies, sand dune alignments, and abrupt linear changes in drainage density.

Field geologic mapping, in preparation for detailed trenching, occupied May-July of 1978. Twenty-seven parallel and en echelon breaks, ranging in length from less than one km to over 15 km, were mapped (fig. 2 shows the larger breaks). Well preserved scarps from tens of cm to over 9 m high form a westerly concave arc over 60 km long. All of the offset appears to be dip-slip--no evidence of a strike-slip component was found. Two ages of Holocene fault scarps (those that offset Lahonton wave-cut features) were separated on the basis of morphology and preservation.

Miocene to Holocene age units are offset by the BRF, but of particular interest to this study are Holocene alluvial and eolian deposits, late Pleistocene Lake Lahonton deposits containing fossils and tephra beds, and a late Pleistocene (pre-Lahontan) pediment surface and pediment gravels. Figure 3 shows the late Pleistocene and Holocene stratigraphy of the Lahontan Basin (after Davis, 1978) along with the important age reference datums identified in the Black Rock Desert area. The older Holocene fault scarps identified during

geologic mapping were formed after the retreat of the lake from the 1,329 m high stand (which began about 11,500 years B.P.). The most recent scarps were formed by faulting after about 1,100 years B.P. The 1,100 years B.P. is a C-14 date from an archeological site at Trego (fig. 2), collected near the top of the youngest unit offset by the BRF (J. O. Davis, personal communication, 1978).

Prior to the inundation of the Black Rock Desert by Lake Lahontan during the Late Pleistocene, a pediment one to two kilometers wide formed along the western margin of the Black Rock Range. This fault-bounded pediment is particularly well-preserved east of the northern one-third of the BRF. Wallace (1978) has stated that a few million years are required to develop a pediment a few kilometers wide. The presence of this pediment suggests a long period of slow or absent tectonic uplift, during which time the range front retreated from the range-bounding fault. This appears to be at odds with the relatively short average recurrence interval of about 5,500 years estimated for the Holocene based on two earthquakes within the last 11,500 years. It probably indicates that the present period of active uplift, characterized by short recurrence intervals, was preceded by an episode of relative quiescence during which the pediment formed. This interpretation agrees with that advanced by Wallace (1978) to explain pediment surfaces bounded by faults along the east sides of the Humboldt and Tobin Ranges in north-central Nevada.

Over ninety profiles were measured along individual fault breaks on the BRF zone, in conjunction with geologic mapping. Profiles were measured perpendicular to the scarp face, and included upper and lower original surfaces, as well as the deformed zone. This profiling technique, and the definitions of scarp slope angle and scarp height, were first described by Bucknum and Anderson (1979).

Initially, profiling revealed several types of deformation other than simple scarp formation. Large (km-size) blocks of alluvial fans, pediments, and playa lake surfaces on both sides of the west-dipping fault zone are tilted eastward, up to 2.5°. Narrow (5-10 m) subsidence zones parallel the fault on the downthrown side for one-third of its length. Most of the numerous hot springs along the BRF zone occur in these graben-like features. Where a plastic lake clay is faulted, small-scale rotational slumping has taken place in the upthrown block. Also, unusually high (8.5 m) scarps, with step-like profiles, were identified. These probably represent renewed faulting and scarp formation, superimposed on an older eroded scarp. Profiling also delineated scarp-slope angle and scarp height.

Detailed statistical study of scarp profiles shows the strong dependence of scarp-slope angle on scarp height, and also confirmed our initial impression that material faulted strongly affects scarp degradation rates. The data also suggest that scarp-slope rounding, which has long been used as a general indication of the age of a scarp, can be quantified and used as a relative dating tool.

Figure 4 shows lines of best fit, determined by linear regression, for scarp-slope angle versus the log of scarp height, for 3 types of material offset by the BRF. Table 1 shows the equations and R^2 values for the data. For comparison with Bucknum and Anderson's data, the best-fit line and equation for their Fish Spring scarp (approximately 1,000 years old) are also shown on figure 4 and Table 1.

The different lines for different materials show that for scarps of the same age and height, scarp-slope angle decreases as grain size decreases. The lines also have a lower slope with decreasing grain size. Both trends indicate that geomorphic degradation takes place more quickly on scarps sustained in finer-grained materials, making them appear older than scarps sustained in coarse grained material. Figure 5 shows lines of best fit for two other material types, angular pediment gravels, and sand. These materials are also included in Table 1, but because of the small number of observations, it is difficult to evaluate the data.

Table 1. Scarp slope Y vs log of scarp height (X), for scarps less than 1,100 years old.

Material	Best fit line (linear regression)	Coefficient of determination (r^2)	Number of Observations
Pediment gravels	y=7.88 + 26.09 (x)	53%	6
Angular alluvial gravel	y=15.29 + 29.73 (x)	80%	18
Sandy gravel	y=10.70 + 24.48 (x)	83%	12
Sand	y=4.13 + 39.76 (x)	85%	6
Clay	y=9.36 + 24.11 (x)	88%	11
Fish Springs alluvial fan deposits	y=17.01 + 23.60 (x)	82%	38

Referring to figure 4, it can be seen that for a scarp of a given age and height of 3.5 meters, you could expect a scarp-slope angle of 31° in angular alluvial gravels, 24° in rounded, sandy gravels, and 19° in clays. Actual profiles from scarps less than 1,400 years old, shown in figure 6, illustrate this trend.

The profiles in figure 6 also show the increase in rounding of the scarp crest as grain size decreases. In an attempt to quantify scarp rounding as a measure of scarp degradation, the angle omega (Ω), the "scarp rounding angle", shown in figure 6 was defined. Perpendicular lines were drawn on the scarp profile at two inflection points, one at the break in slope between the upper original slope and the rounded segment, and the other at the first 5° or greater break in slope between the steeply sloping scarp face and the rounded segment. The angle defined by the intersection of the two lines is smaller in the more degraded scarps. Figure 7 shows lines of best fit for scarp rounding angle versus log of scarp height. Table 2 shows the equations of the lines and the R^2 values. Since the scarp in sandy gravel appears older than that in angular alluvial gravel, we suggest that this measure of scarp degradation, the scarp rounding angle, can also be used quantatively to differentiate scarps of different ages. Similarly to the scarp-slope angle, scarp rounding angle is strongly dependent on scarp height, and both decrease with increasing degradation.

Geologic mapping and profiling suggested at least two earthquakes along the BRF zone, one after 1,100 years B.P., and an earlier movement of late Pleistocene or possibly Holocene age (post 11,500 years B.P.). Since several age reference horizons had been identified during geologic mapping, trenches for detailed

Table 2. Scarp rounding angle Y vs log of scarp height (X), for scarps less than 1,100 years old.

Material	Best fit line (linear regression)	Coefficient of determination (r^2)	Number of Observations
Angular alluvial grains	y=13.22 + 31.05 (x)	83%	16
Sandy gravel	y=5.48 + 25.08 (x)	86%	9

study of earthquake magnitude and recurrence was located where age references were found. Seven back-hoe trenches, from ten to thirty m long and up to 3 m deep, were dug perpendicular to the BRF. Detailed logs, at a scale of 1" = 1 m to 1" = 50 cm., were drawn of 5 trenches. Heavy rains filled one trench after a preliminary log was drawn, and collapsed a second trench before it could be logged.

Trench number one, shown in simplified form in figure 8, was particularly valuable in defining repeated fault movements. Two unconformities and two dated tephra units were offset in this trench alone. The first faulting occurred after deposition of the 25,000 year old Wono ash, and before deposition of the 23,000 year old Trego Hot Springs ash. A second earthquake faulted the Trego ash, and the associated scarp was subsequently eroded. A Holocene soil, possibly the 5,000 year old Toyeh soil, formed on this erosional surface; it is also offset by faulting. The scarp associated with the third episode of faulting is completely eroded and buried by alluvial and eolian deposits.

The modern, well preserved scarps marking the BRF zone today were formed during a fourth earthquake, after about 1,100 years B.P. Therefore, at least 4 earthquakes have taken place along the BRF in the last 25,000 years, which suggests an average recurrence interval on the order of 6,000 years. This agrees closely with the average recurrence of about 5,500 years estimated from the 2 Holocene events identified during geologic mapping.

The magnitude of the earlier three earthquakes could not be determined, because correlable units were eroded on the upthrown side, or beyond the reach of the back-hoe and soil augers on the downthrown side. The magnitude of the most recent earthquake could be determined, using maximum offset/magnitude and total length/magnitude relationships.

Trench 2A (fig. 9) shows the total offset of the Wono ash along one segment of the BRF, during the $<$ 1,100 year old event, to be 2.3 m. The scarp height (2.2 m) is a good measure of this total offset, indicating that height has not been reduced significantly during scarp degradation. The maximum displacement along major breaks of the BRF zone ranges from 3 to 7 m, suggesting an earthquake of magnitude of at least 7 produced the most recent scarps. This is supported by the combined length (over 50 km) of the recent breaks, which suggest a magnitude greater than 7.

Conclusions

1. An earthquake of magnitude 7 or greater produced the youngest scarps along the BRF zone.

2. A minimum of four earthquakes have occurred along the BRF in the past 25,000 years, suggesting a maximum average recurrence interval of about 6,000 years.

3. The development of a one to two-kilometer-wide pediment along the Black Rock Range prior to the late Pleistocene suggests a long period of little or no uplift during which range front retreat and pediment formation occurred. The relative duration of periods of short recurrence versus long recurrence is uncertain.

4. For scarps of a given age and height:

   a. Scarp-slope angle decreases as grain size decreases. Therefore scarps in finer grained materials appear older relative to scarps of the same age and height sustained in coarser materials.

   b. Scarp rounding angle (Ω) decreases as grain size decreases. This suggests the Ω may be a useful measure in relative dating of scarps of different ages.

   c. Scarp-slope angle and scarp rounding angle are strongly dependent on scarp height.

References Cited

Bucknum, R. C., and R. E. Anderson, 1979, Estimation of fault-scarp ages from a scarp-height-slope-angle relationship: Geology, v. 7, p. 11-14.

Davis, J. O., 1978, Quaternary tephrochronology of the Lake Lahontan area, Nevada and California: Nevada Archeological Survey Research Paper no. 7, University of Nevada, Reno, Nevada.

Wallace, R. E., 1977, Profiles and ages of young fault scarps, north-central Nevada: Geological Society of America Bulletin, v. 88, p. 1267-1281.

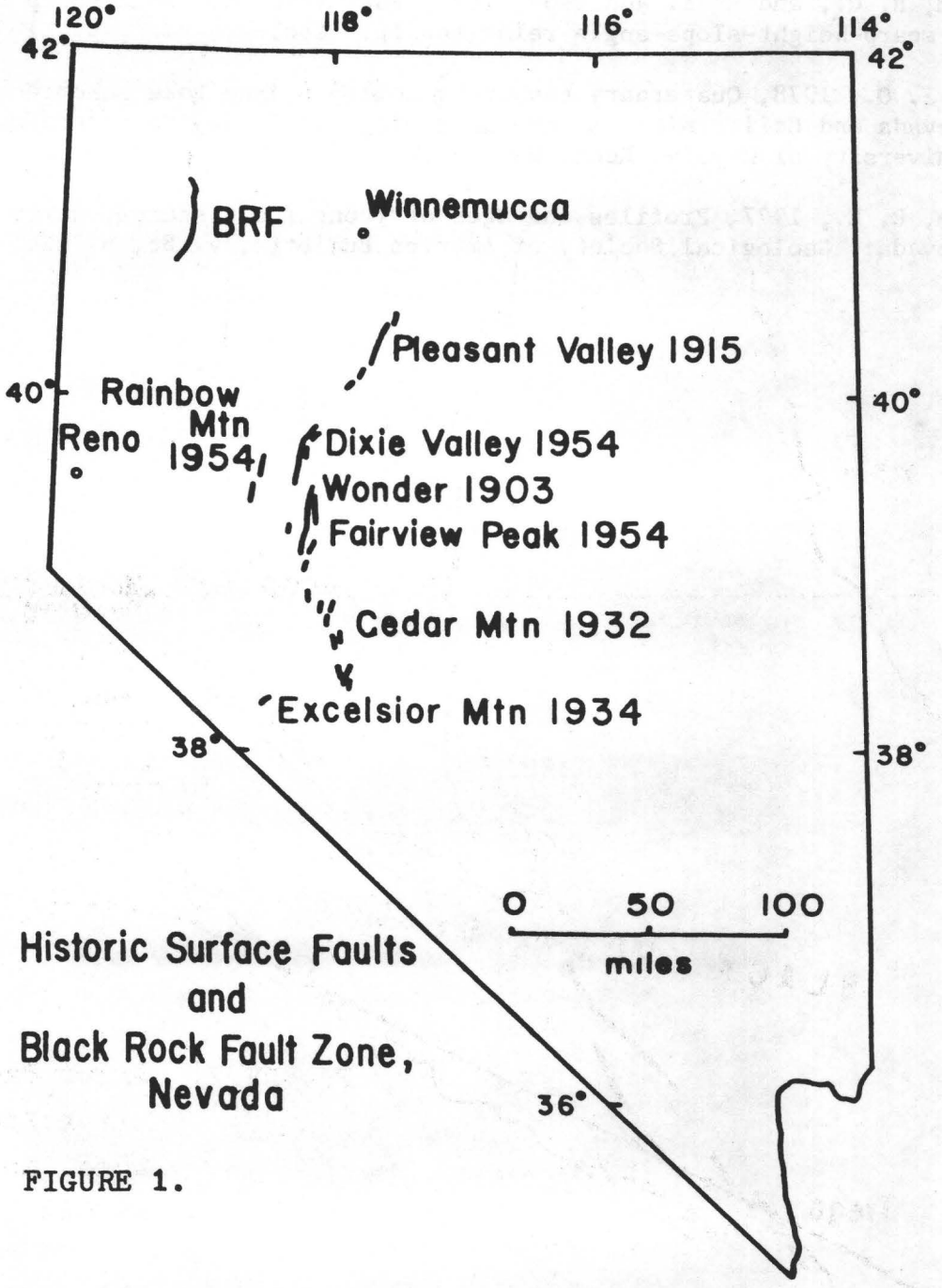
120°
118°
116°
114°
42°
42°
BRF
Winnemucca
Pleasant Valley 1915
40°
Rainbow Mtn 1954
Reno
Dixie Valley 1954
Wonder 1903
Fairview Peak 1954
40°
Cedar Mtn 1932
Excelsior Mtn 1934
38°
38°
0 50 100
miles
Historic Surface Faults and Black Rock Fault Zone, Nevada
36°

FIGURE 1.

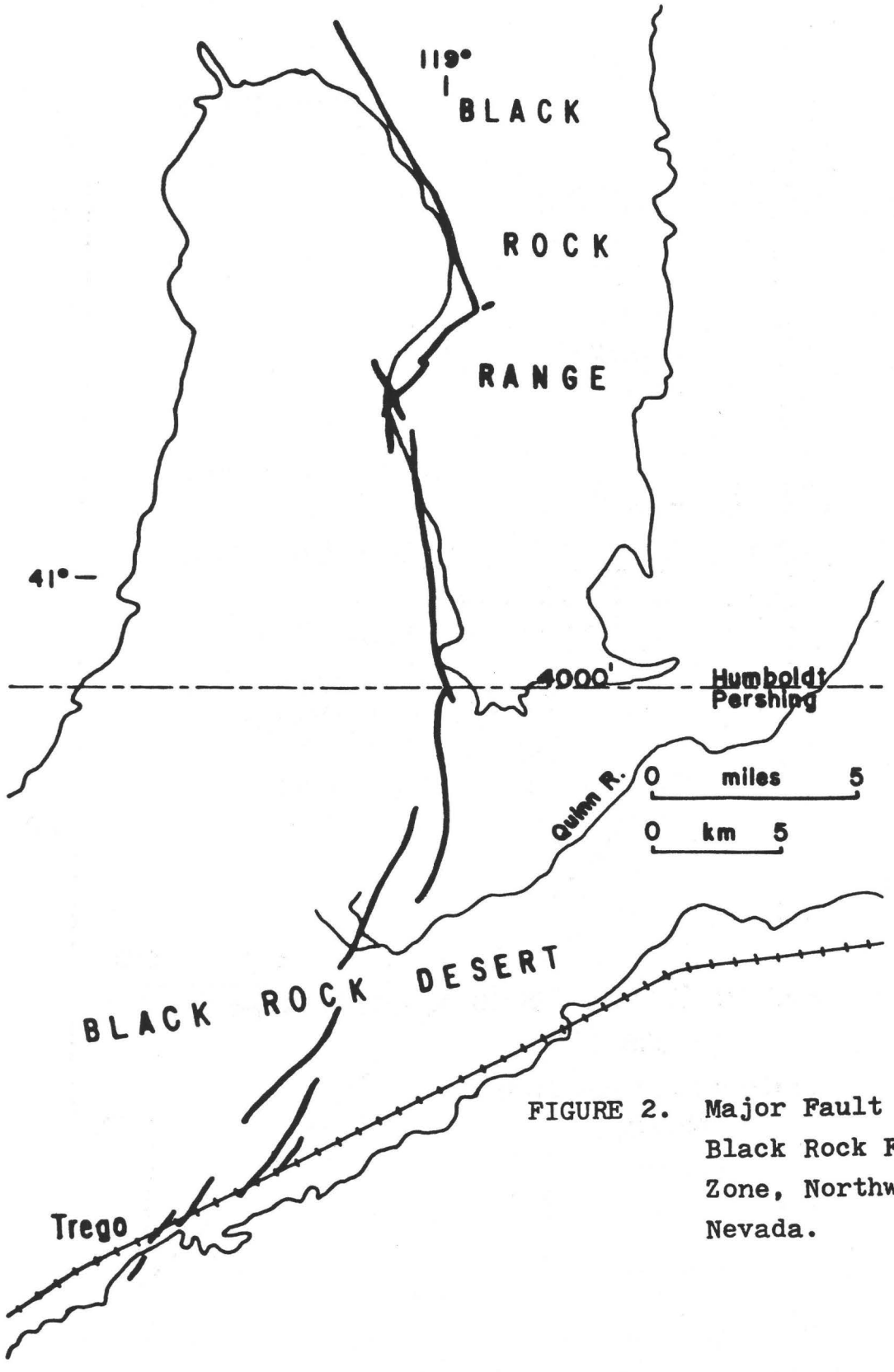

FIGURE 2. Major Fault Breaks Black Rock Fault Zone, Northwestern Nevada.

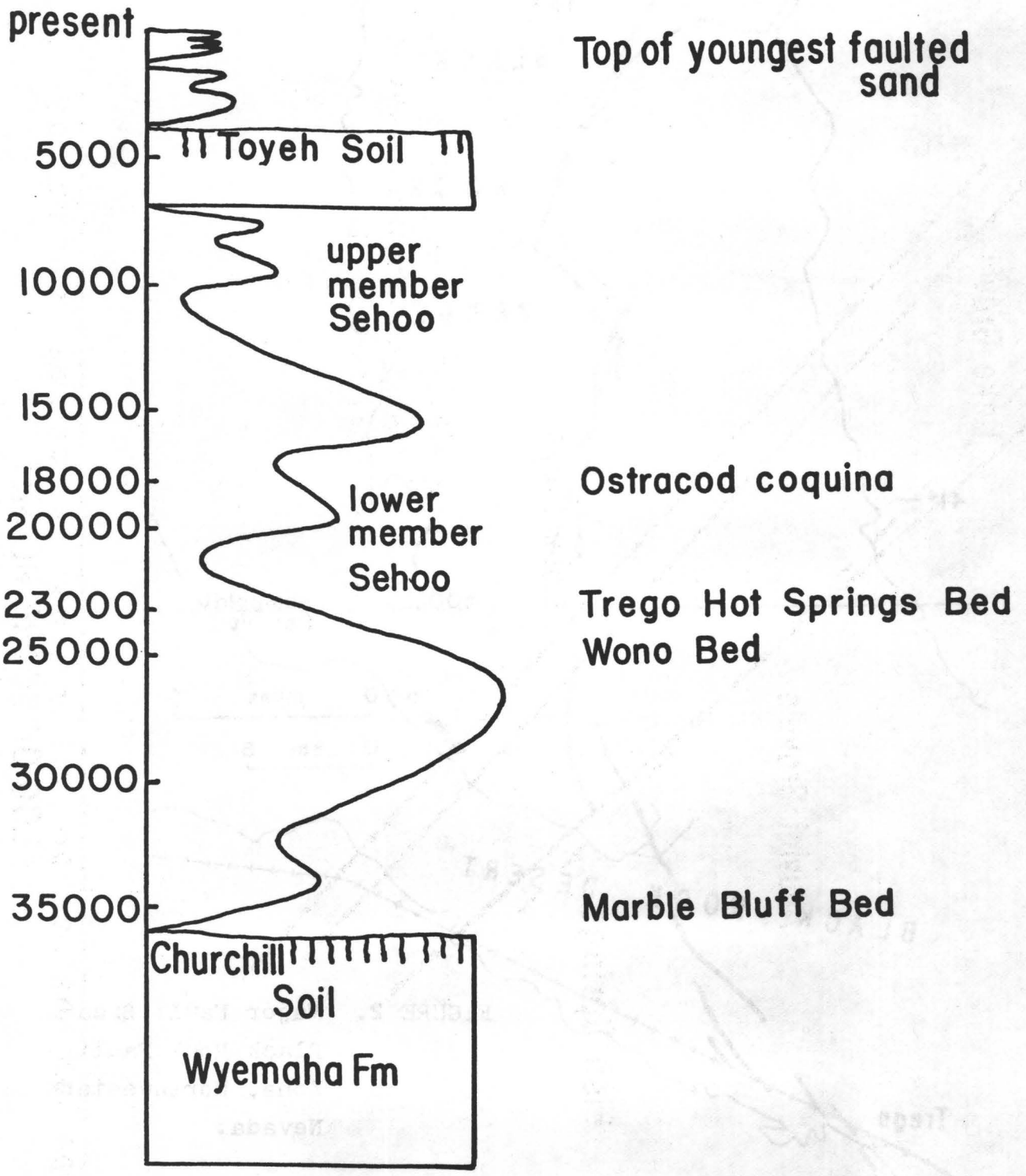

Figure 3. Late Pleistocene and Holocene stratigraphy of of the Lahontan Basin (after Davis, 1978) and Age Reference Datums for the Black Rock Desert.

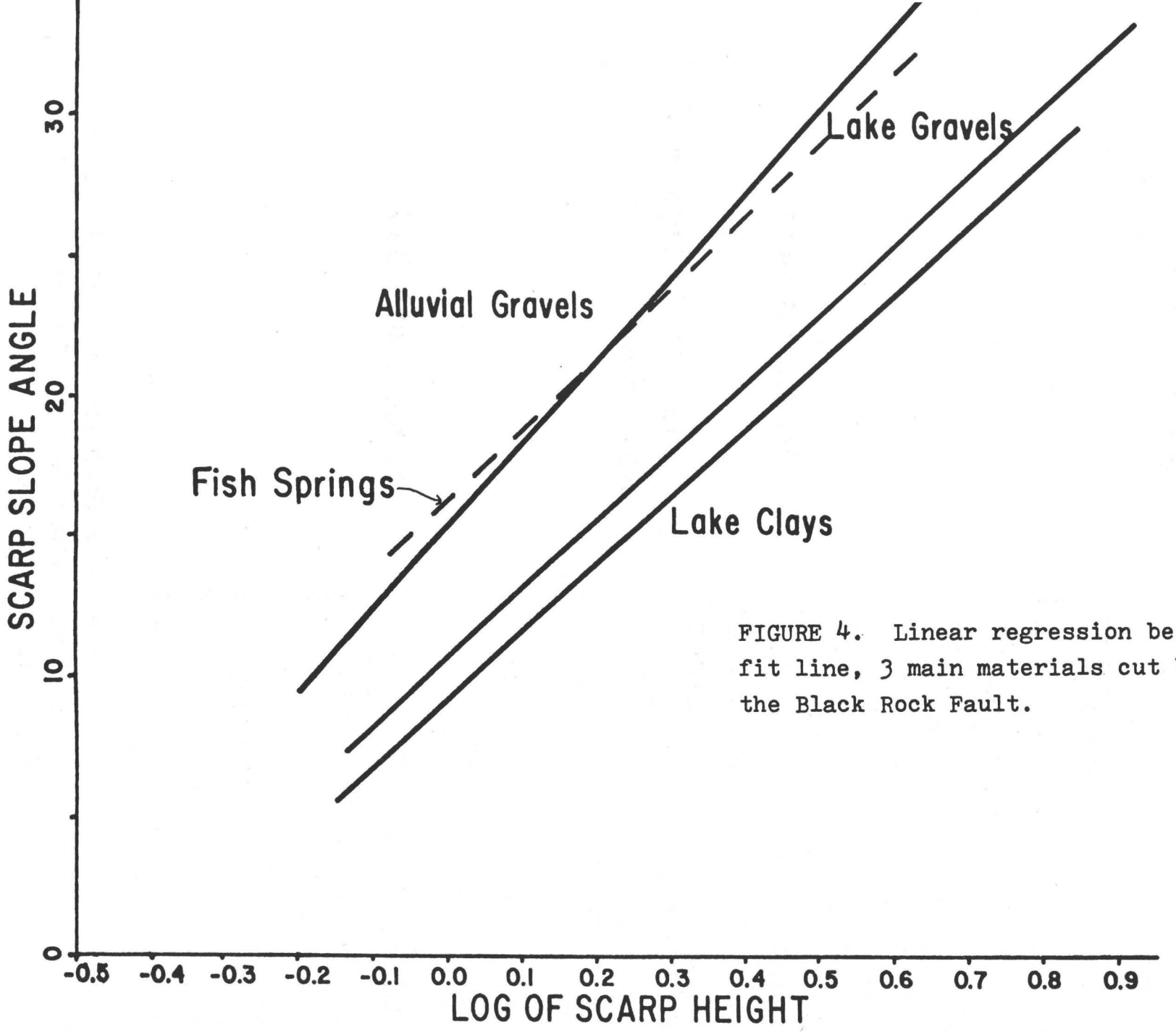

FIGURE 4. Linear regression best-fit line, 3 main materials cut by the Black Rock Fault.

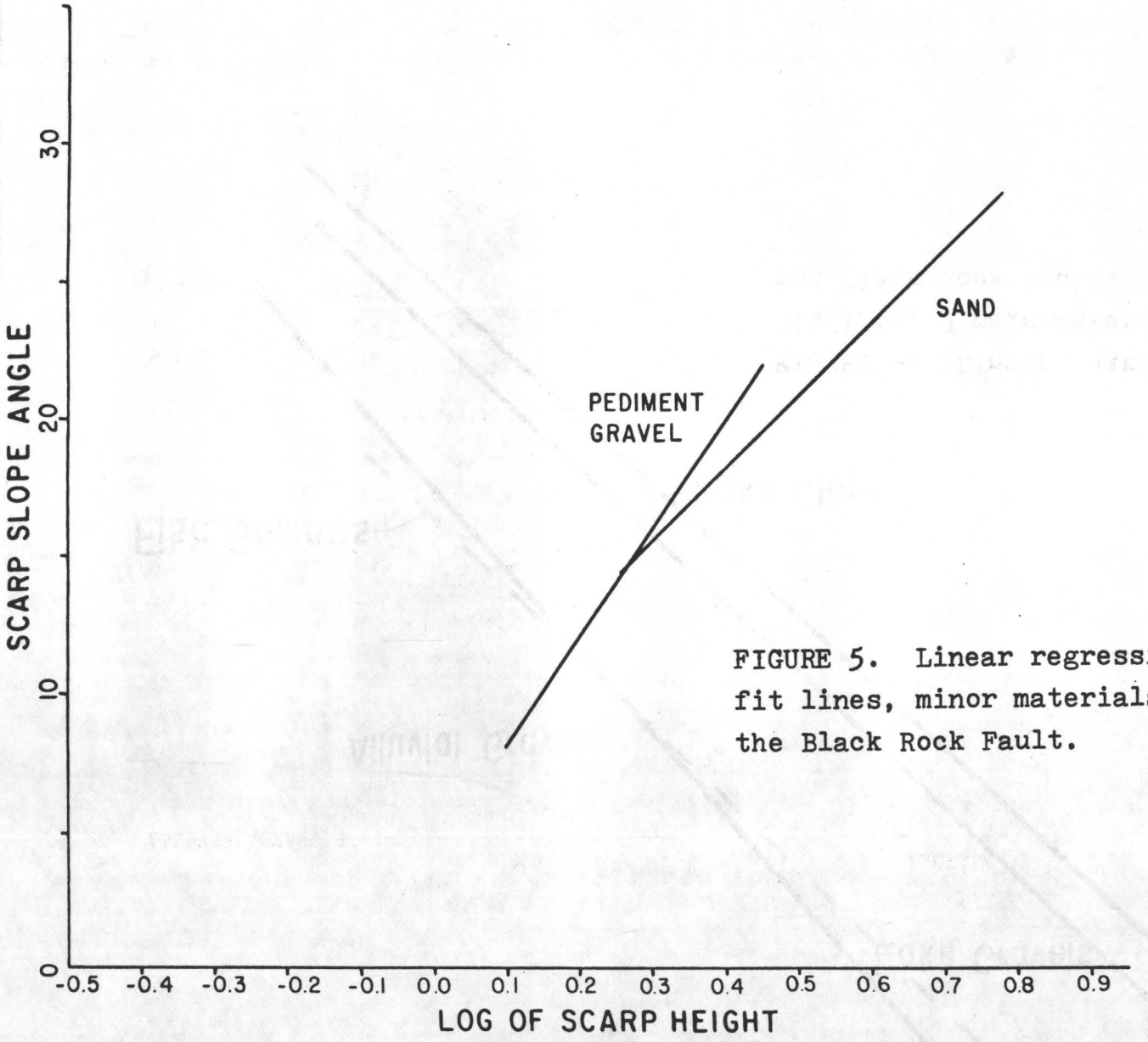

FIGURE 5. Linear regression best-fit lines, minor materials cut by the Black Rock Fault.

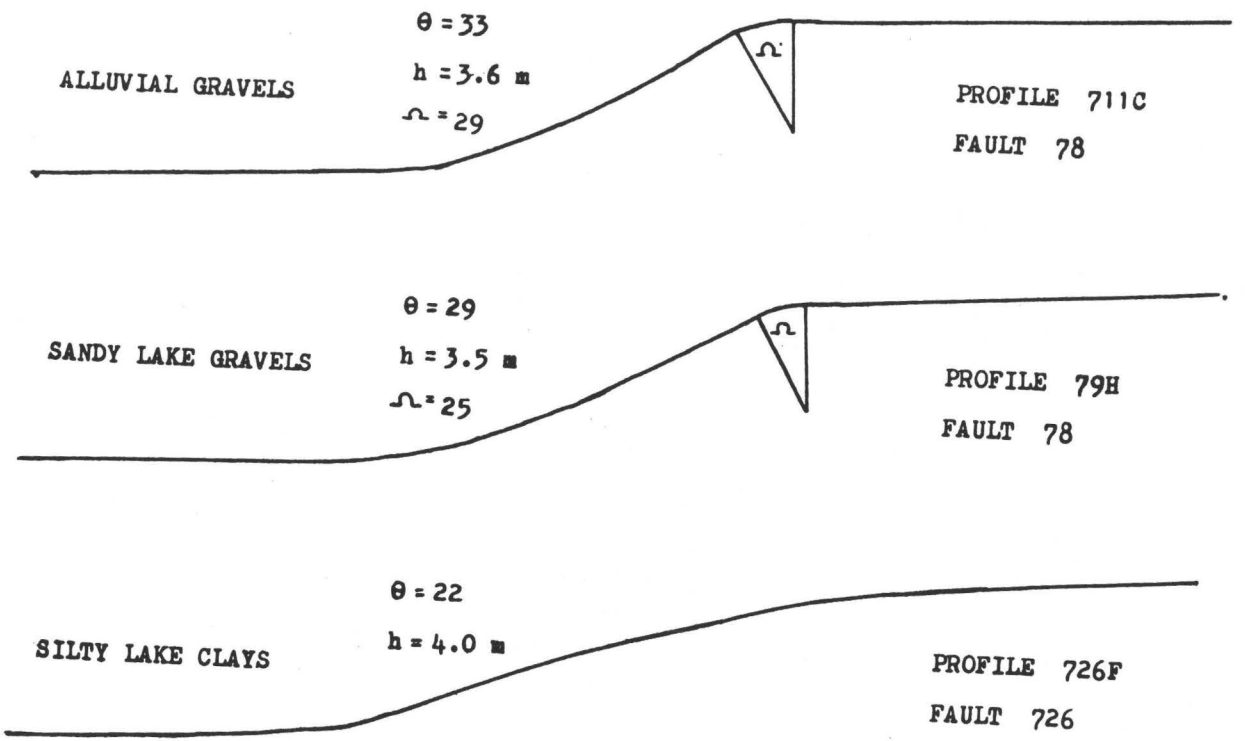

Figure 6. Scarp profiles in 3 main materials cut by the Black Rock Fault.

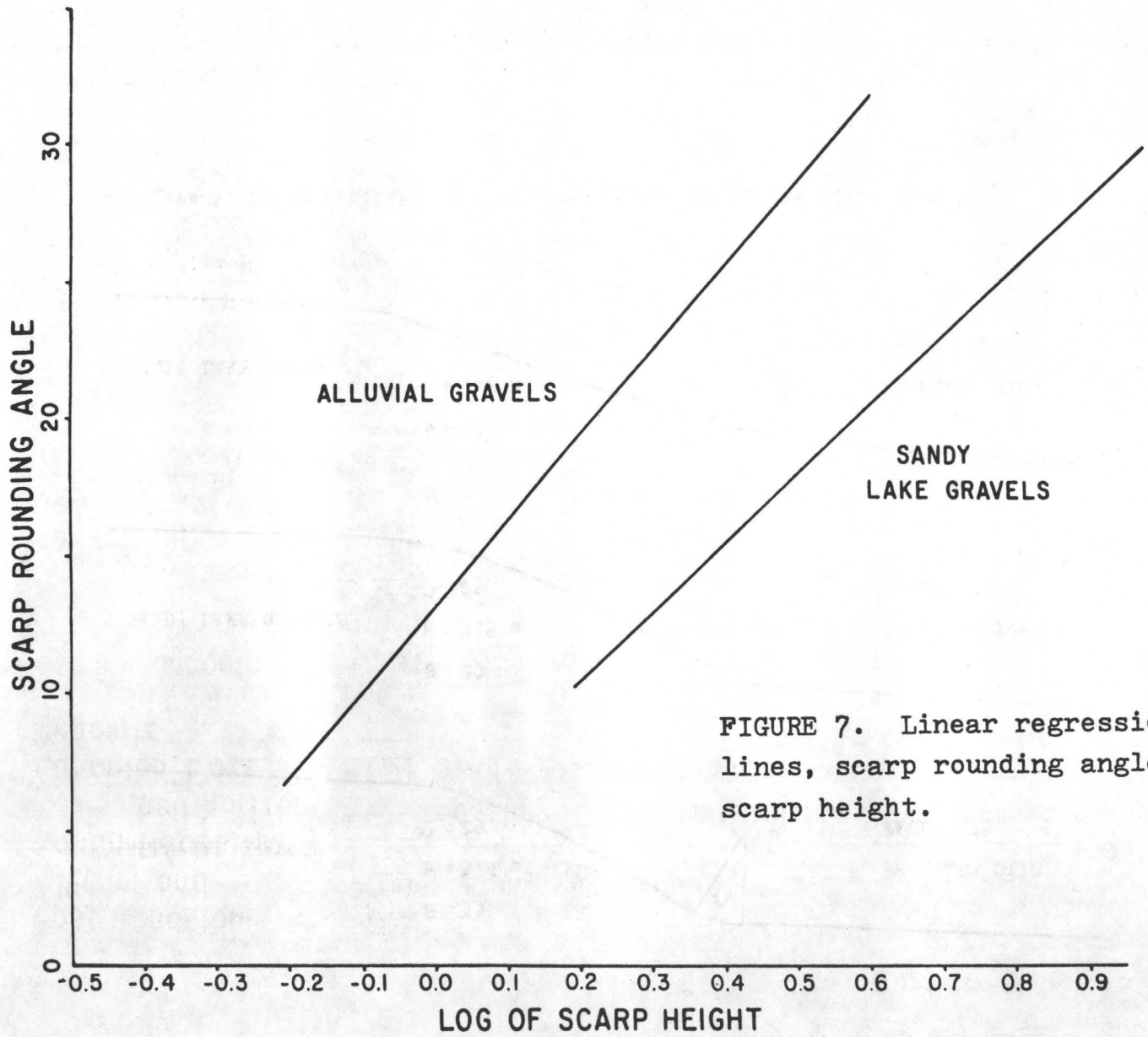

FIGURE 7. Linear regression best fit lines, scarp rounding angle vs log of scarp height.

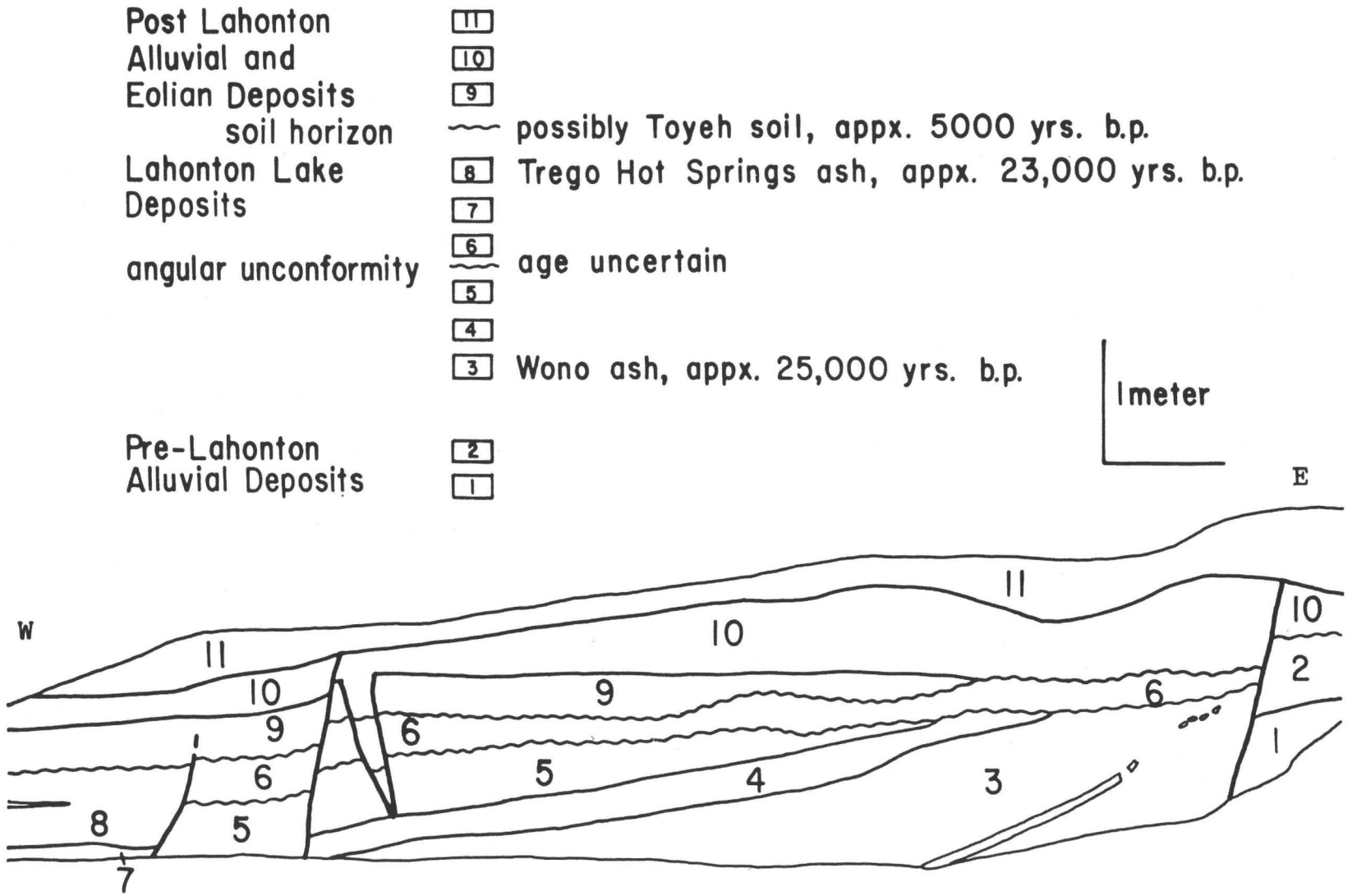

FIGURE 8. Trench 1, multiple offsets on the Black Rock Fault.

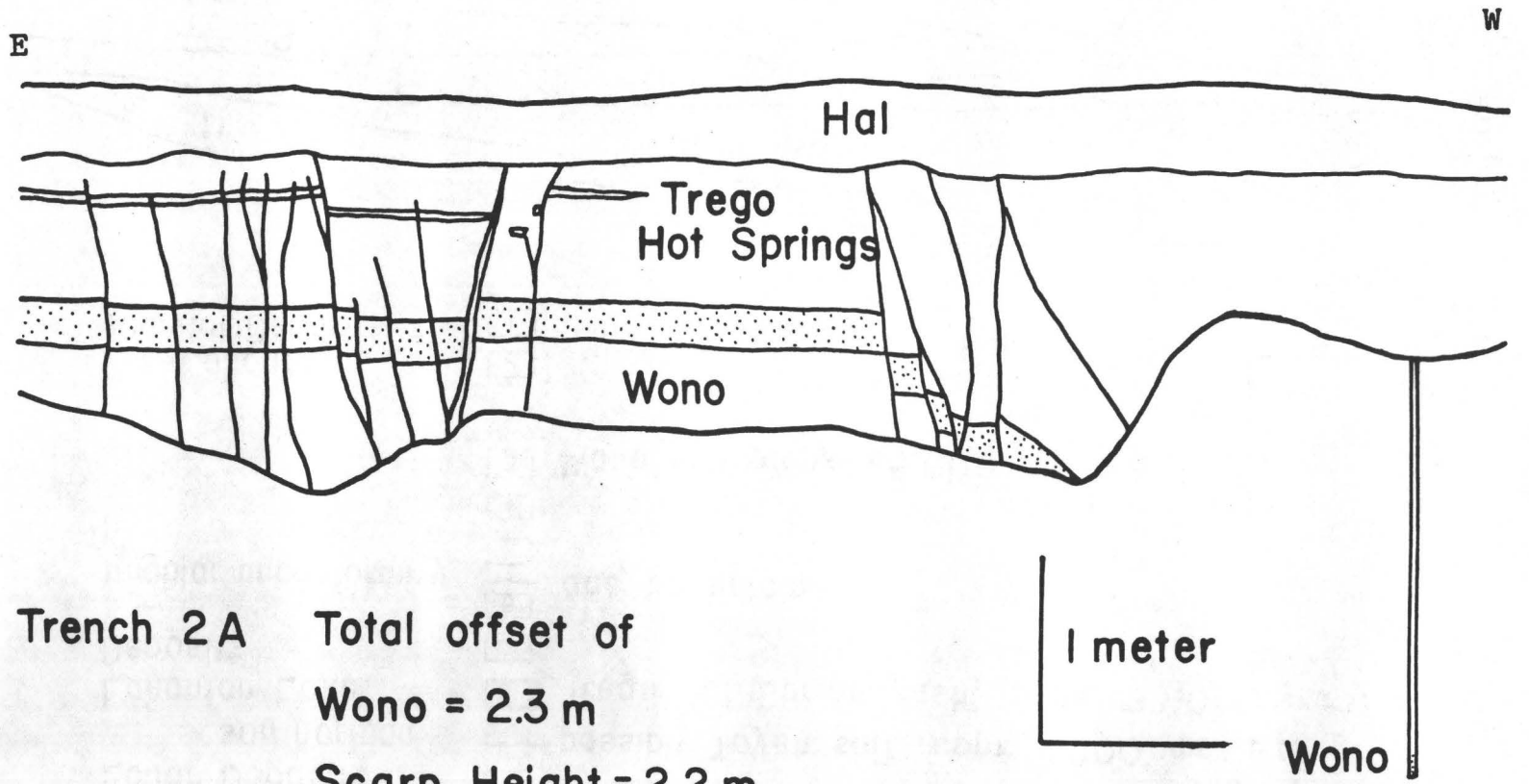
E
W
Hal
Trego
Hot Springs
Wono
Trench 2A
Total offset of
Wono = 2.3 m
Scarp Height = 2.2 m
1 meter
Wono

FIGURE 9.

PROBLEMS IN LAKE BONNEVILLE STRATIGRAPHIC RELATIONSHIPS IN THE NORTHERN SEVIER BASIN REVEALED BY EXPLORATORY TRENCHING

by

Alan P. Krusi and
Roy H. Patterson

Dames & Moore
Los Angeles, California

INTRODUCTION

During 1978 and 1979, extensive investigations were performed in the northern Sevier Basin, Utah, as part of a siting investigation. Subsurface investigations conducted approximately 18 km north of Delta, Utah revealed new evidence relating to the stratigraphy of the Lake Bonneville Group in this area.

A 6,000-foot-long exploratory trench (Trench Delta-1) excavated during January 1979 revealed a complex Quaternary sedimentary sequence comprising lacustral, deltaic, and fluvial (?) materials. These deposits are lithologically diverse and display significant lateral and vertical heterogeneity. The materials exposed range in texture from clay to cobble gravel: the observed lithologic variations provide a basis for distinguishing over 100 individual lithologic units. Detailed mapping and stratigraphic analysis allowed grouping of individual units into larger depositional packages or suites. A relative chronology was established based on analysis of the spatial relationships between these suites and the nature of intersuite contacts. Absolute age dates obtained for several of the depositional units were then applied to the chronology. This paper summarizes some of the problems encountered when the "classical" Lake Bonneville Pleistocene stratigraphy and chronology is applied to the Trench Delta-1 sedimentary sequence.

GEOLOGIC SETTING

Hintze and Baer (1979) summarized the geologic history of the area now occupied by the Sevier Desert. Rocks exposed in and surrounding the Sevier Desert range in age from Precambrian to Recent (Mower and Feltis, 1968; Morris, 1978). The basin fill deposits within the Sevier Basin are volcanic and sedimentary rocks of Tertiary to late Quaternary age which are overlain by lacustrine sediments deposited in ancient Lake Bonneville and its predecessors. The following summary of the Lake Bonneville lacustral stratigraphy is presented to provide a framework within which surface and near-surface materials exposed in the exploratory trenches may be correlated.

Presently, the most widely acknowledged references on the Pleistocene chronology and stratigraphy of the ancestral Lake Bonneville are Morrison (1965a, 1965b, 1975) and Morrison and Frye (1965). The following discussion has been primarily abstracted from these sources. The maximum recorded elevations of sedimentary deposits associated with various late Pleistocene lacustrine intervals are included to provide reference to the study area elevation (4,600 to 4,700 feet).

In the Sevier Basin, pre-Lake Bonneville lacustrine sediments of Pleistocene age are reported only from the subsurface, where they range in thickness from 0 to 2,000 feet (Mower and Feltis, 1968). These materials are overlain by sedimentary deposits associated with the Lake Bonneville Group which are exposed extensively in the cut-banks of the Sevier River and are thought to blanket the basin (R. Van Horn and D. J. Varnes, 1978, personal communications).

A strongly developed soil (Dimple Dell soil) separates the pre-Lake Bonneville sediments from lacustrine deposits assigned to the Lake Bonneville Group (Figure 1). The Lake Bonneville Group contains three, the Alpine, Bonneville, and Draper Formations which are respectively separated by the Promontory and Graniteville soils (Morrison, 1965; Figure 1). Lacustrine sediments associated with these formations were deposited during cyclical episodes of lake advance, while soils formed during periods of lake retreat and subaerial exposure. These coincided with glacial advances and retreats during the late Pleistocene to early Holocene (approximately 70,000+ to about 8,000 years before present) (Morrison and Frye, 1965; Morrison, 1965).

The Alpine Formation, deposited between approximately 70,000+ and 32,000 years b.p., is the most extensive of the formations attributed to Lake Bonneville and generally contains more than three-fourths of the Lake Bonneville deposits (Varnes and Van Horn, 1961). Four lake cycles, separated by local diastems (periods of nondeposition), are recorded within the Alpine Formation. From oldest to youngest, these four wedges of lacustrine sediments have been located at maximum elevations at Promontory Point of 5,050+, 5,150+, 5,150+ to 5,280?, and 4,800 feet (Morrison, 1965).

The strongly developed Promontory soil locally separates the Alpine and Bonneville Formations. The Bonneville Formation, ranging in age from 20,700 to approximately 12,000 years b.p., has two members, a lower (older) white marl member and the upper (younger) member (Morrison and Frye, 1965; Anderson, 1978). The maximum elevation of the white marl member at Promontory Point is 5,220+ feet (Morrison, 1965). The upper member of the Bonneville Formation was deposited at elevations approaching the highest level reached by Lake Bonneville. This is the Bonneville shoreline which has been variously reported at 5,250 feet at Little Valley by Morrison (1965), 5,140 feet for the Provo area by Anderson (1978), and from 5,110 feet in Leamington Canyon to 5,200 feet across the Sevier Desert along the eastern edge of the Drum Mountains by Mower and Feltis (1968). The lake maximum which produced the Bonneville shoreline occurred between 15,000 and 12,000 years b.p. (Morrison, 1965).

During the last three cycles of Lake Bonneville the Draper Formation was deposited; it is locally separated from the Bonneville Formation by

the Graniteville soil. Radiocarbon dates on land-snails found in alluvium separating Bonneville and Draper foundations yielded ages of 11,600 and 11,900 years b.p. (Morrison and Frye, 1965). It is therefore inferred that, the Draper Formation was deposited after 11,600 years b.p. These three latest cycles attained relatively low shoreline elevations and were of relatively brief duration (Morrison, 1965). The maximum elevation of the Provo II shoreline, which marks the maximum advance of the lower member, is reported as 4,800 feet at Promontory Point (Morrison and Frye, 1965), 4,800 to 4,900 feet along the upper reaches of the Sevier River Delta (Mower and Feltis, 1968), and at 4,810 to 4,820 feet at the base of the Drum Mountains on the western margin of Sevier Basin (R. C. Bucknam, 1978, personal communication). The lacustrine transgressions associated with the middle and upper members of the Draper Formation attained elevations of 4,470 and 4,410 feet, respectively, in the Jordan Valley (Morrison and Frye, 1965).

Comparison of the elevation of the study area (4,600 to 4,700 feet) with maximum elevations of the various wedges of lacustrine sediments associated with Lake Bonneville and its predecessors indicates that all but the two most recent lake cycles (represented by the middle and upper members of the Draper Formation) attained elevations greater than that at the study area. Thus, any of the deposits associated with the pre-Lake Bonneville lacustrine intervals, the Alpine and Bonneville Formations and the lower member of the Draper Formation could conceivably occur at the surface or in the shallow subsurface of the study area.

TRENCH DELTA - 1

Trench Delta-1 was oriented east-west and located in the northeast corner of Section 24, Township 15S, Range 5W. The trench provided a continuous 6,000-foot lateral exposure of interbedded sedimentary deposits to a depth of 5-1/2 to about 12 feet. A single stratum or stratigraphic boundary could not be traced along the entire length of the trench; however, contacts between interfingering stratigraphic units and intra-unit stratification within this sequence provided visible means of establishing stratigraphic continuity along the length of the trench. These exposed deposits are lithologically diverse and display significant lateral and vertical heterogeneity. The materials exposed range in texture from clay to cobble gravel. The observed lithologic variations (primarily grain size, color, and internal structure) provided a basis for dinstinguishing individual lithologic units. Over 100 units were identified and logged in the trench exposure.

The mapped units were grouped into eight depositional suites on the basis of lithologic similarities and/or the occurrence of erosional intervals or unconformities in the sequence. These eight suites are shown schematically in Figure 2. The suite boundaries are generally distinguished by contrasting lithotypes or variations in stratification of the deposits. Table I presents a brief lithologic description of the suites.

Grouping of individual units into larger depositional packages or suites provided a means by which the complex stratigraphic relationships could be more effectively analyzed. After analysis of the intersuite relationships, a sequence of deposition was established, and thus absolute age dates obtained from localized units could be relatively applied to the remaining units.

TABLE I

Summary of Lithologic Suites of Deposits Exposed in Trench Delta-1

Suite	Stations Spanned	Nature of Suite Boundaries	Brief Lithologic Description
1	00-6000	Unconformable lower boundary	Massive to locally poorly stratified gravelly sand to silty fine sand, and soil
2	4400-6000	Concordant western boundary	Massive and cross-stratified sand, gravelly sand, and matrix- to clast-supported gravel
3	3880-4760	Unconformable western boundary	Massive to locally horizontally stratified silty fine sand, silty clay, and clay
4	2590-3170 3300-3450	Unconformable boundaries	Massive and cross-stratified channel fill gravel, gravelly sand, and sand
5	3170-3300 3450-3880	Unconformable boundaries	Horizontally stratified to locally massive sand, silty sand, and clay with minor gravel and clayey silt
6	1740-2590	Conformable (intercalated) western boundary	Massive to locally horizontally stratified clay, silt, and silty fine sand
7	1220-1740	Unconformable western boundary	Cross-stratified sand and silty sand with minor silt and clay
8	00-1220		Massive silty clay and cross-stratified gravelly sand, sand, and silty sand. Contains rhyolitic ash unit at base

*Station numbers refer to surveyed locations (in feet) commencing at the western end of the trench (Station 00) and ending at the eastern end of the trench (Station 6,000).

Deposits assigned to Suite 1 (Figure 2, Table I) blanket the entire trench exposure. The base of these deposits truncates the gentle eastward inclination of underlying deposits (units). This generally uniform eastward inclination of the majority of the deposits exposed in the trench is reflected by the eastward onlapping relationships between the various suites. These relationships indicate that, with the exception of one suite which represents episodes of channel cut-and-fill, the depositional suites young to the east. This eastward inclination, in conjunction with the spatial position of each suite, was used to deduce relative ages of the exposed materials.

With the possible exception of Suite 4, Suites 1 through 8 are listed in Table I in order of increasing age. The channel cut-and-fill sequence of Suite 4 is incised into Suites 5 and 6 and is overlain by Suite 1. Therefore, Suite 4 is younger than Suites 5 and 6 and older than Suite 1. Due to their spatial relationships, the relative age of Suite 4, with respect to Suites 2 and 3, is not known.

AGE DATING

In order to assess the age of materials exposed in the trenches, an age dating program was initiated. This program consisted of radiocarbon dating (C^{14}), volcanic ash correlation and fission track dating, and soil-stratigraphic age estimation.

Radiocarbon Dating

Four samples of gastropods were collected from the base of Suite 1 at the eastern end of Trench Delta-1 and were submitted to a commercial laboratory for radio carbon dating. In addition, a fifth sample was submitted for dating as a check on the analytical error inherent in the dating process. Sample locations and C ages for the five samples are shown in Table II.

Radiocarbon dating of fresh water gastropods from the Bonneville Group has typically yielded problematic results (Morrison and Frye, 1965; M. Rubin, personal communication, 1979; and W. Scott, personal communication, 1979). Morrison (1965) reports radiocarbon dates in the range of 25,000 to 28,000 years for the same samples which yielded $Th^{230} - U^{234}$ age determinations in the range of 90,000 to 200,000+ years. Varnes and Van Horn (unpublished data) report similar discrepancies in dates on gastropods from the Delta-Oak area. These widely divergent results are due principally to sample contamination by young carbon. This contamination may occur either by replacement and recrystallization of the original shell material or by secondary calcite ($CaCO_3$) mineralization on the outside of the original shell.

In an effort to evaluate the possibility of contamination by recent carbon, microscopic analyses of the samples were conducted. The gastropod samples were examined under both light and petrographic microscopes and it was determined that the original aragonitic composition of the shells has been completely altered to calcite. However, the original shell micro-structure is intact, indicating that no large-scale recrystallization has occurred. While there exists evidence of substantial secondary mineralization, it appeared that the gastropod samples should yield reliable radiocarbon age dates with proper treatment.

TABLE II

SUMMARY OF RADIOCARBON DATING RESULTS

Sample	Mean Depth Below Ground Surface (inches)	C^{14} Age
Delta-1	34	12,215±300 years b.p.
Delta-2	39	11,555±240 years b.p.
Delta-3	25	12,695±360 years b.p.
Delta-4	30	11,630±280 years b.p.
Delta-5	(Replicate of Delta 4)	12,350±285 years b.p.

(All samples were collected from the base of Suite 1 within an 800-foot interval)

Volcanic Ash Correlation

A white rhyolitic ash unit occurs at the base of the Suite 8 deposits. This unit is the oldest unit exposed in the trench. Samples of the ash were collected from the western end of Suite 8 for ash correlation analysis and fission track dating. These analyses were conducted by Dr. Glen Izett and Dr. Charles Naeser, respectively, of the U.S. Geological Survey, Denver.

Ash correlation analyses conducted by Dr. Izett include x-ray fluorescence chemical analysis of volcanic glass shards, petrographic determination of index of refraction of the glass phase and determination of major mineral constituents, and microprobe chemical analysis of glass and several phenocryst phases. The major element chemical conposition of both glass and phenocryst phases are typical of the Bishop Ash. In addition, the major mineral constituents and the index of refraction of the glass shards are "Bishop-like." Based on the density of fission tracks in zircons and uranium content determined as part of the fission track dating, the ash has a very high radioactivity level compared to other late Pleistocene ashes. The Bishop Ash is the only late Pleistocene ash known in the western United States with a high uranium content. Based on all of these analyses, Dr. Izett feels quite confident that the ash from Trench Delta-1 is the Bishop Ash.

Zircons separated from the ash were dated by the fission track technique by Dr. Naeser. The analysis yielded a date of 730,000 ± 10 percent for the ash. This date is well within the range of values reported for the Bishop Ash. Thus, the results of all analyses conducted to data indicate that the ash collected from Trench Delta-1 is probably the Bishop Ash, which originated from an eruption at Round Valley Caldera near Lake Crowley, California, approximately 730,000 years ago.

DISCUSSION

Freshwater gastropods collected from the base of Suite 1 near the eastern end of the trench yielded radiocarbon ages ranging from 11,555 to 12,695 C years before present. Thus, materials comprising Suite 1 could conceivably be correlative with either the lower member of the Draper Formation (Holocene) or the upper member of the Bonneville Formation (latest Pleistocene). Since the consensus of opinion among a number of qualified researchers is that freshwater gastropods from deposits associated with Lake Bonneville typically yield young radiocarbon ages, it is concluded that the Suite 1 deposits are likely correlative with the upper member of the Bonneville Formation. Two explanations are offered to explain the absence of the Draper Formation in the exposed sedimentary section: 1) the Draper Formation was never deposited in this portion of the Sevier Basin; or 2) the Draper Formation was deposited but has been subsequently removed by erosion.

The stratigraphic order of the various suites which underlie Suite 1, and the slight angular discordance between Suite 1 and the underlying materials requires that Suites 2 through 8 be greater than about 12,000 years in age. Thus, the eastward onlapping deposits which comprise Suites 2 through 8 may be correlative with either the Bonneville or Alpine Formations or pre-Lake Bonneville lacustrine units.

Results of ash correlation analyses indicate that the ash collected from the base of the western end of the trench is probably correlative with the Bishop Tuff. Fission track dating on zircons separated from the ash yielded an age of 730,000 years supporting the Bishop Tuff correlation. The relatively shallow occurrence of the Bishop Tuff at a depth of 3m is somewhat enigmatic when compared with its reported depth of occurrence elsewhere in the Bonneville Basin; i.e., at 96m below the surface in the Burmester Core (Eardley and others, 1973).

The age of the sedimentary materials immediately overlying the ash is not known. The ash is discontinuous in nature and is separated from the superjacent deposits by an unconformity. The temporal significance of this unconformity is not known, and it is not possible to estimate the amount of missing sedimentary section it represents. The presence of the ash is significant in that it indicates that near-surface sediments in this part of the Sevier Basin may be, at least in part, significantly older than what might be expected based on the classical concepts of Lake Bonneville stratigraphy and evidence from other parts of the Bonneville Basin.

The near surface occurrence of the ash and the inferred absence of the Draper Formation strongly support current ideas by some researchers that a reexamination of the classical Lake Bonneville stratigraphy is in order (see Scott, this volume). In addition, the stratigraphic correlation problems revealed by our studies in the Sevier Basin suggests that extreme care should be exercised when applying classical Lake Bonneville stratigraphic concepts to the assessment of recency of faulting in this and other parts of the Bonneville Basin.

REFERENCES

Anderson, R. E., 1978, Quaternary tectonics along the intermountain seismic belt south of Provo, Utah: Brigham Young University Geology Studies, V. 25, Part 1, p. 1-10.

Eardley, A. J., R. T. Shuey, V. Gvosdetsky, W. P. Nash, M. D. Picard, D. C. Grey, and G. J. Kukla, 1973, Lake cycles in the Bonneville basin, Utah: Geol. Soc. America Bull., V. 84, p. 211-216.

Hintze, L. F., and J. L. Baer, 1979, Regional geological setting of the Sevier Desert for Intermountain Power Project, January (unpublished report).

Morris, H. T., 1978, Preliminary geologic map of the Delta 2° quadrangle, west-central Utah: U.S. Geological Survey Open-File Report 78-705.

Morrison, R. B., 1965a, Lake Bonneville: Quaternary stratigraphy of the eastern Jordan Valley south of Salt Lake City, Utah: U.S. Geol. Survey Prof. Paper 477, 80p.

Morrison, R. B., 1965b, New evidence on Lake Bonneville stratigraphy and history from southern Promontory Point, Utah: U.S. Geol. Survey Prof. Paper 525-C, p. C110-C119.

Morrison, R. B., and J. C. Frye, 1965, Correlation of the middle and late Quaternary successions of the Lake Lahontan, Lake Bonneville, Rocky Mountain (Wasatch Range), southern Great Plains, and eastern midwest areas: Nevada Bureau of Mines Report 9, p. 1-45.

Mower, R. W., and R. D. Feltis, 1968, Ground-water hydrology of the Sevier Desert, Utah: U.S. Geological Survey Water Supply Paper 1854, 75 p.

Varnes, D. J., and Richard Van Horn, 1961, A reinterpretation of two of G. K. Gilbert's Lake Bonneville sections, Utah, in Geological Survey Research, 1961: U.S. Geological Survey Professional Paper 424-C, p. C98-C99.

REVISIONS BY ____ DATE ____

FILE TASK 3212-93

BY DSL DATE 4-22-93

CHECKED BY ____

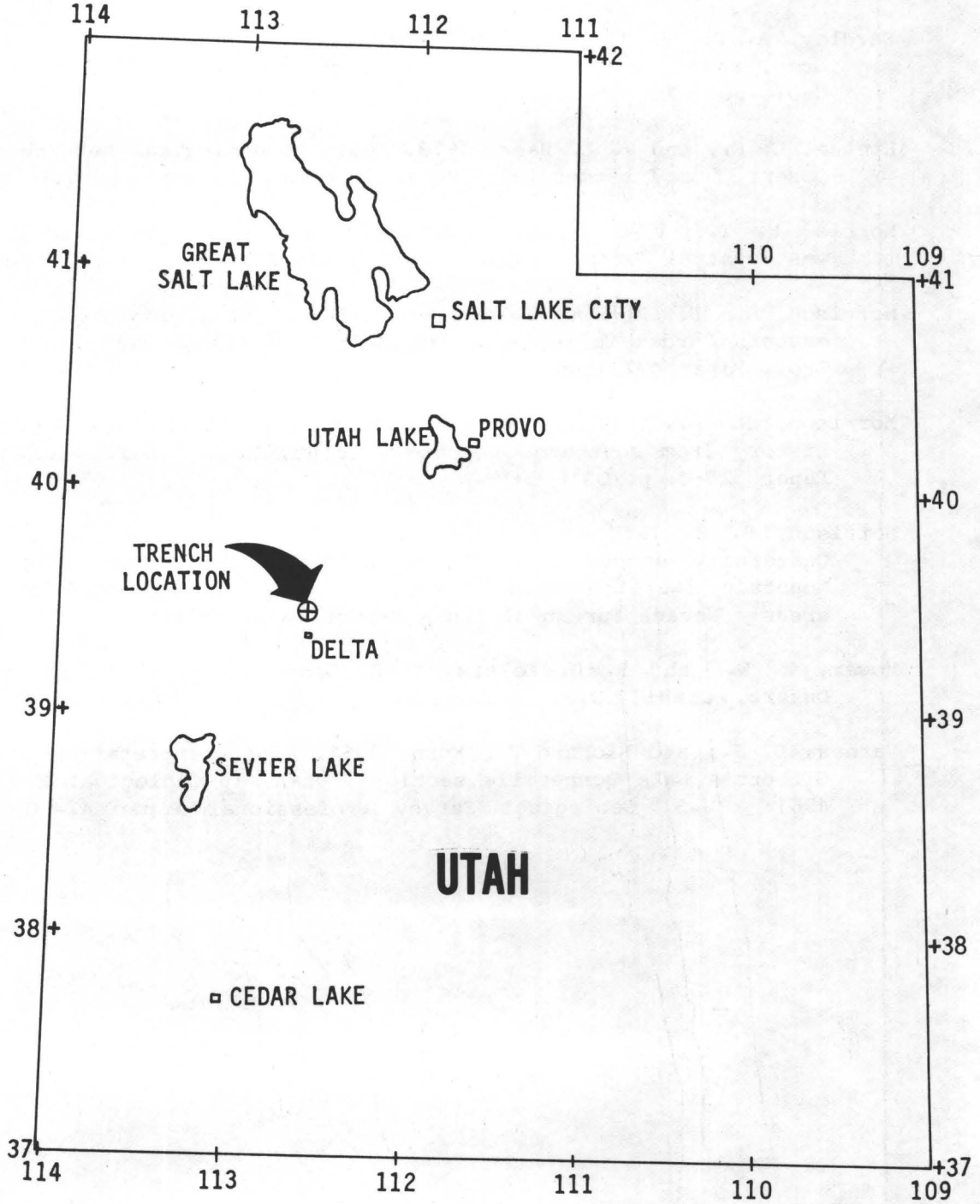

LOCATION MAP

0 50 100KM

SCALE

PLATE 1

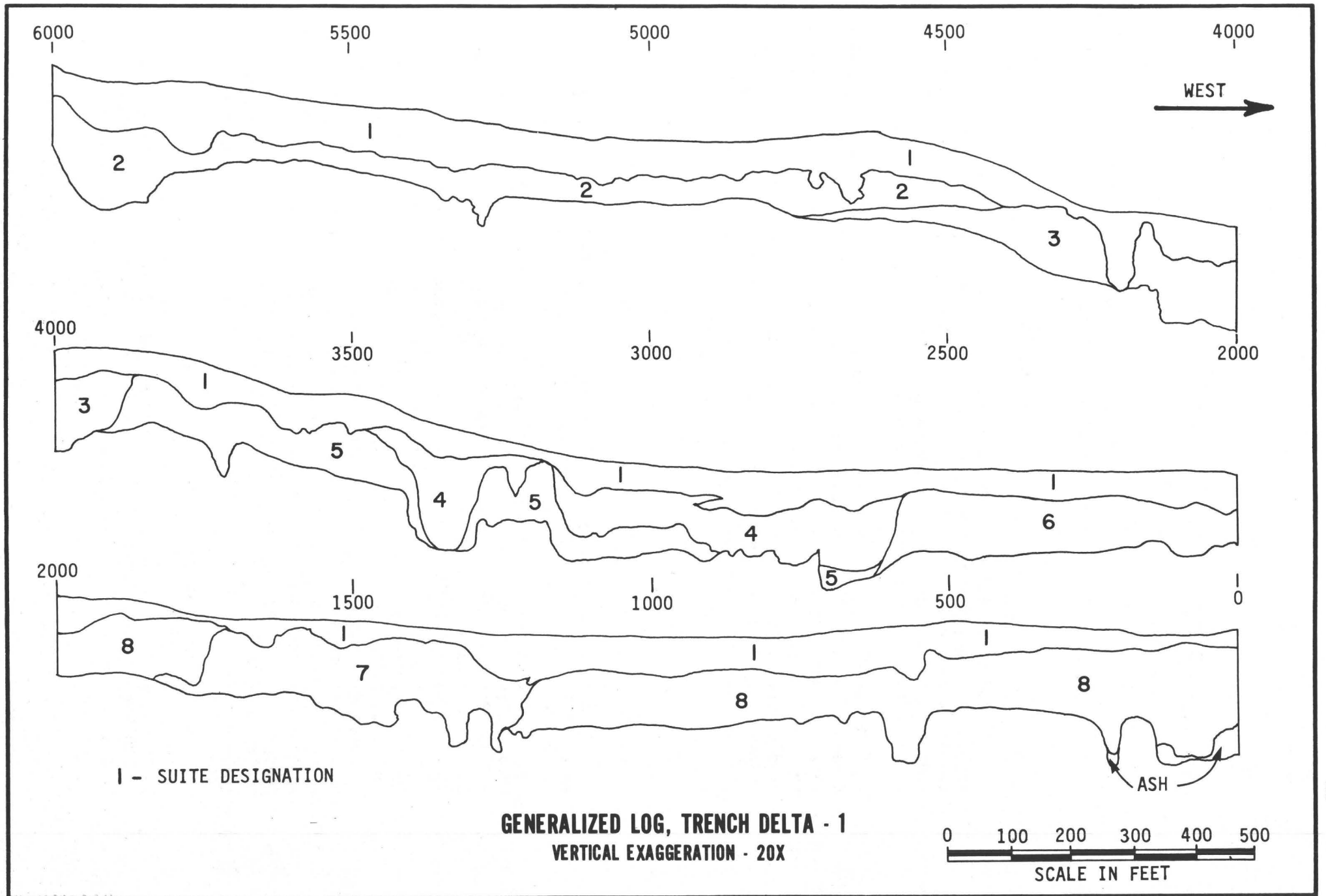

GENERALIZED LOG, TRENCH DELTA - 1

VERTICAL EXAGGERATION - 20X

PLATE 2

518

10

THE STATUS OF SEISMOTECTONIC STUDIES OF SOUTHWESTERN UTAH

by

R. Ernest Anderson
U.S. Geological Survey, Denver

INTRODUCTION

A project entitled "Southwestern Utah seismotectonic studies" has been active since September 1975. Its two chief goals have been: (1) to define the distribution in space and time of Quaternary faulting and deformation in southwestern Utah and (2) to provide an improved understanding of the late Cenozoic tectonic history and framework of the area.

The purpose of the present report is to summarize the results of highly diverse studies made under this project. Because the studies include a broad range of topics studied in widely scattered areas they do not lend themselves to a well-integrated summary format. To present this potpourri of results the studies are grouped according to (1) Quaternary studies and (2) tectonic framework studies--a grouping that roughly parallels the chief project goals. Localities and geologic features referred to are shown in figure 1.

QUATERNARY STUDIES

Fault maps and scarp profiles

As a joint effort with R. C. Bucknam, who has worked on a project of parallel scope in northwestern Utah, maps showing the distribution of late Quaternary fault scarps in alluvium have been prepared at 1:250,000 scale and some have been released as open-file reports covering individual 1° x 2° quadrangles (Bucknam, 1977, Bucknam and Anderson, 1979, Anderson and Bucknam, 1979). Field studies associated with the compilation of these maps have focused on the measurement of profiles of the fault scarps and of wave-cut scarps produced at the highest stand of Lake Bonneville (the Bonneville shoreline). These studies have resulted in development of a method of assigning fault scarps to relative age categories on the basis of scarp morphology (Bucknam and Anderson, 1979a). The profile data on fault scarps have been compared directly with profile data on the Bonneville erosional scarp. Because the erosional scarps represent a temporal datum the direct comparison allows for partitioning of fault scarps into groups that appear to be older or younger than the Bonneville scarps. For fault scarps that cut high-stand or younger deposits or surfaces, or on which high-stand surfaces or deposits are superposed, the validity of the age partitioning can be checked directly. In all areas where such checks have been made the age partitioning appears valid.

The age of formation of the Bonneville shoreline is estimated on the basis of radiocarbon determinations to be between 15,400 and 11,800 B.P. (Morrison and Frye, 1965). This age is sufficiently close to the approximately 10,000 B.P. age of the boundary between the two epochs of the Quaternary Period, the Pleistocene and Holocene Epochs, (Hopkins, 1975) that fault scarps

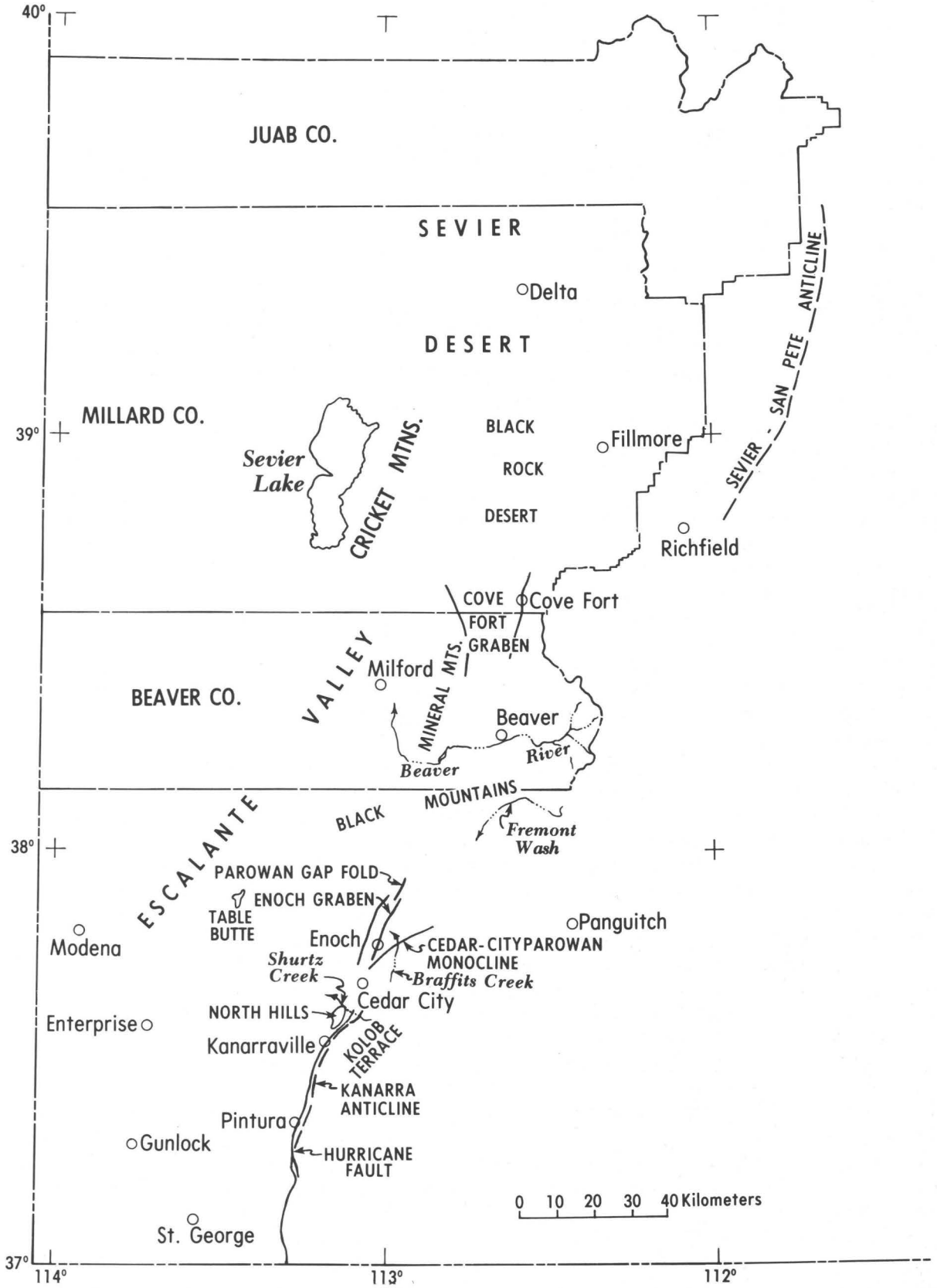

Figure 1.--Index map of southwestern Utah showing localities and geologic features mentioned in text.

can be assigned to Holocene and pre-Holocene categories with reasonable certainty.

The ability to make such assignments over a large region has led to the preparation of a preliminary map of western Utah showing areas of Holocene scarps vs. areas of late Pleistocene scarps (fig. 2). The map also shows areas where we have not identified any late Quaternary scarps as well as a unique area along the Wasatch fault which, on the basis of evidence gathered in recent trenching experiments by Woodward-Clyde Associates (Schwartz and others, 1979; Swan and others, 1979), is a structure that has had recurrent movement during the Holocene. Such a map can serve as a basis for defining seismic source zones in western Utah (Bucknam and others, 1979, and this volume) which is a primary goal of this project.

Acquisition of profile data will continue in southwestern Utah and adjacent Nevada and Arizona in the hope of providing a basis for refining the source-zone map of western Utah. Also, present plans call for compilation of the fault data at 1:500,000 and preparation of an interpretative companion text.

Beaver and Panguitch areas

For faults less than about 20,000 years old, the age of last movement can be estimated from scarp profile data by comparison with profile data for the Bonneville shoreline and with the rate of degradation of scarps produced by surface faulting. Estimates can probably be made with an accuracy of about 30 to 40 percent of the age (R. C. Bucknam, oral commun., 1978). For older scarps there is no basis for direct comparison, and estimates of actual age are either not feasible or must be based on indirect geologic reasoning. There is a critical need to determine quantitatively the age of old late Quaternary scarps in alluvium so that scarp-profile data collected from them can be used as a basis for direct comparison to data from other old late Quaternary scarps. Profile data from two areas in southwestern Utah, Beaver and Panguitch, yield meaningful regression lines of scarp-slope angle on the logarithm of scarp height for old scarps of probable late Quaternary age (Bucknam and Anderson, 1979a; Anderson and Bucknam, 1979). In both areas recurrent fault movement has produced contrasting amounts of offset of alluvial surfaces of contrasting age. Soils developed on the offset surfaces provide potential for bracketing the age of faulting by comparing the faulted soils with soil chronosequences. The possibility also exists that fault events can be dated directly by uranium-series or thermoluminescense analysis of carbonate materials from fault zones.

The Beaver valley was a structural basin with interior drainage during Pliocene and early Pleistocene time. Tephra within the sediments range from 2.4-2.0 m.y. At some time during the middle Pleistocene the southwestern valley wall was breached in topographically low areas between the Black and Mineral Mountains and drainage was integrated with Escalante Valley and the Sevier Desert by the establishment of Beaver River as a through-going stream. Sediments deposited during the interior drainage phase have been incised by the downcutting of streams of the Beaver River system. Downcutting produced the initial gravel-mantled pediment and subsequent stream terraces throughout the Beaver valley, and many of the surfaces have fault scarps formed on them. Faulted surfaces of 4 or 5 different ages may be present and, in general, old surfaces show greater offset than young surfaces.

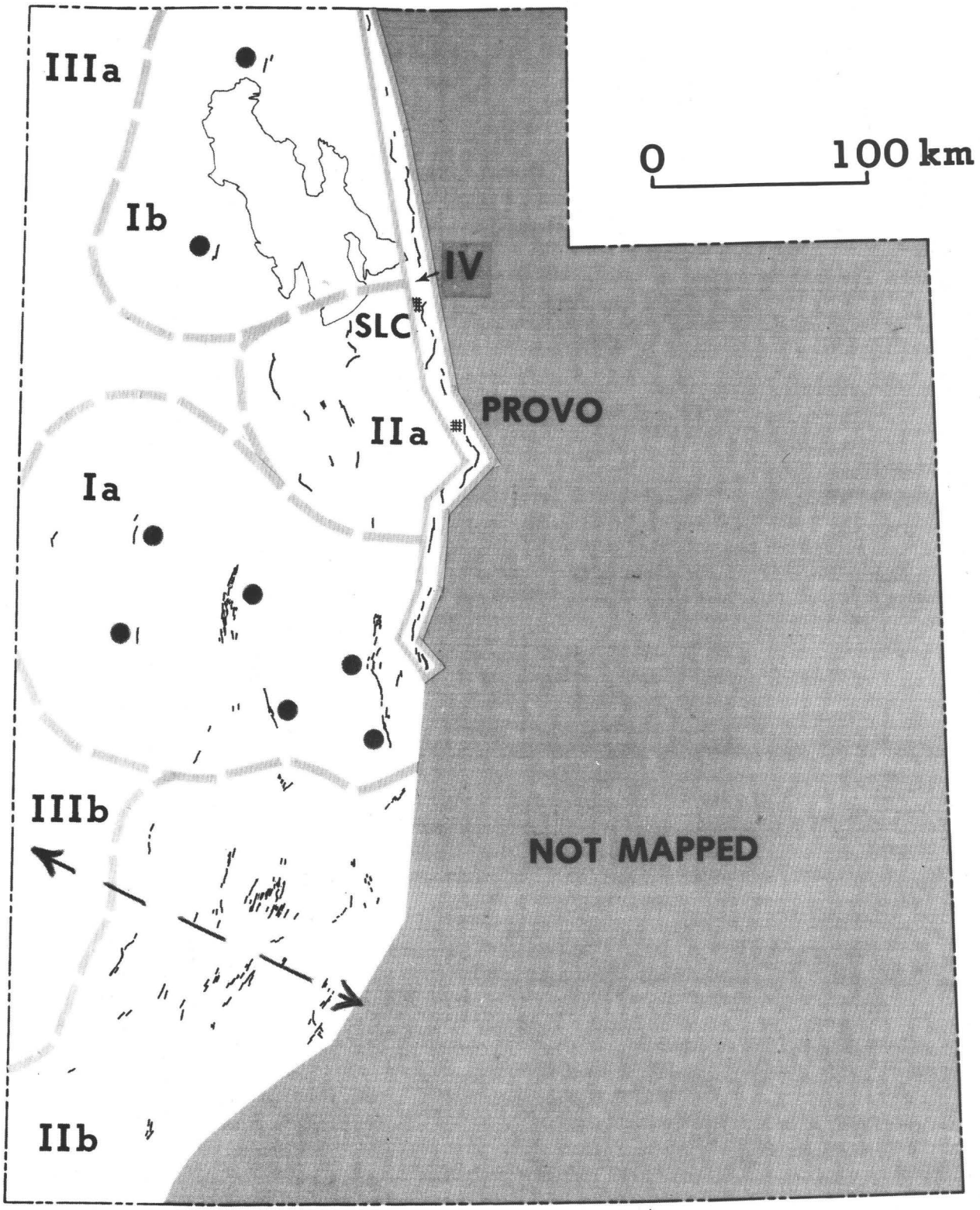

Figure 2.--Map of western Utah showing late Quaternary fault scarps (light lines), Holocene fault scarps (light lines with dot and lines within zone IV), and source zones I, Ia, and so forth (see Bucknam and others, this volume). Dashed line with arrows indicates approximate direction of least principal stress inferred from fault orientations.

Studies of the geomorphology and pedology of the Beaver valley are underway by Michael Machette of the U.S. Geological Survey and by a group from the University of Colorado, Boulder. Samples for quantitative age data are being collected but the data are not yet available. On the basis of qualitative comparison of the extent of soil development in the Beaver valley to other areas in the southwestern United States and age control from a local tephra unit, Machette estimates that the oldest faulted erosion surface is about 500,000 $\pm$ 100,000 years old and the youngest faulted surface is a few tens of thousand years old. Profile data from fault scarps on the oldest and youngest surfaces show good separation on a plot of slope angle against scarp height, but indicate that scarps with a height of 3 m differ in maximum slope angle by less than 3 degrees (Anderson and Bucknam, 1979). If the scarps differ in age by almost an order of magnitude or more, the small difference in maximum slope angle is discouraging because it suggests that the wide variety of geologic, pedologic, geomorphic, and climatic processes that act to modify scarps make it improbable that accurate estimates of age of old scarps can result from profile data alone. Of special significance are the widespread calcic soils on old alluvial surfaces in southwestern Utah. These soils tend to cement the surficial gravels and thereby retard the normal process of scarp modification as seen on unconsolidated sediments. Though pedogenic cements probably retard scarp retreat, they do not have an effect similar to that of a caprock as is indicated by extensive profiling of scarp crests that yield generally smooth curves.

Cricket Mountains and Escalante Valley

One of the goals of OES-sponsored research along the Wasatch front is to establish displacement rates and recurrence times for structures in the Wasatch fault zone. The stratigraphic and geomorphic record of Lake Bonneville should provide much of the chronologic reference data needed to achieve these goals as well as to achieve the goal of determining the regional distribution in space and time of late Quaternary deformation in and adjacent to the Bonneville basin. The success clearly depends on the accuracy with which the chronology of Pleistocene and Holocene lacustrine events is known. A reading of Bill Scott's contribution to this volume underscores the uncertainty regarding published stratigraphic divisions, correlations, and age determinations of the eastern Bonneville basin. Recent studies in the Cricket Mountains also serve to underscore problems encountered with the validity of published interpretations.

The Cricket Mountains are located west of Fillmore, 40-50 km west of the boundary between the Colorado Plateaus and Basin and Range provinces (fig. 1). Four factors contribute to making the Cricket Mountains an ideal setting for the study of the history of Lake Bonneville.

1. The range has a relief of only about 400 m and therefore processes of erosion and sedimentation on its flanks are moderate to minimal compared to those processes along the Wasatch Front or along other major range fronts.

2. The range, which consists of northerly trending tilted fault blocks of lower Paleozoic strata, is drained by several strike valleys with substantial catchment area and by a series of transverse valleys of much more limited catchment area, thus providing an opportunity to compare

interrelated fluvial and lacustrine erosion and sedimentation over a range of drainage size.

3. Bedrock in some drainage basins is exclusively quartzite; in some it is exclusively carbonate rock and in others it is a mixture thus providing an opportunity to assess the effect of clast type on alluvial, lacustrine, and soil-forming processes.

4. There has been an episode of youthful base-level decline (possibly by deflation and downwarping of the basin containing Sevier Lake west of the Cricket Mountains) that has resulted in erosion which, in turn, has provided good exposures of stratigraphic relationships on the flanks of the range.

Recent geologic studies on the east and west flanks of the Cricket Mountains in the interval between the Bonneville and Provo shorelines have shown that lacustrine sediments that are predominantly pale greenish gray clay, silt, and sand with minor gravel but also include reddish-colored strata of similar texture are overlain by deposits of fanglomerate. The highest elevation at which the pre-fanglomerate lacustrine sediments have been found is 1,562 m (5,110 ft). The fanglomerate deposits tend to form evenly graded well-formed fans. At numerous localities above the Bonneville shoreline the surficial fan gravels are cemented or partially cemented by carbonate that represents remnants of a once-continuous relatively mature carbonate-dominant soil profile that developed on stabilized portions of the fans. Cursory examination indicates that the extent of carbonate accumulation is independent of whether the parent material is quartzite or carbonate rock.

Of special significance to the history of Lake Bonneville is the fact that the final lake transgression to the Bonneville shoreline (about 1,575 m (5,150 ft) in this area) was a simple event that progressed quasicontinuously and was followed by an episode of rapid regression to about the Provo level (about 1,470 m (4,800 ft) in this area). This rise and fall of the lake postdates formation of the fans and the relatively mature calcic soil that had formed on the fans. The erosional scarp is cut into the soil at some localities and at others gravel bars at the Bonneville level are deposited on the soil. Evidence that the transgression was a simple quasicontinuous event is found lakeward from the mouths of small transverse drainage basins on the west flank of the range. Between elevations of about 1,470 m (4,800 ft) and the Bonneville level sets of lobate deltas composed of coarse to very coarse bouldry detritus are arranged in belts situated parallel to and adjacent to several of the small modern ephemeral streams that issue from the small transverse drainage basins. Each lobate delta probably represents rapid deposition of storm-generated debris-flow material carried to an ancient lake margin by ancestral versions of the modern ephemeral streams during brief periods of stillstand that punctuated the lake rise. In each belt the frontal scarps of the lobes are convex lakeward (westward) and the lobate deltas are arranged in an eastward-rising stairstep pattern. The frontal portion of each successively higher (easterly) delta is constructed on the back portion of the next lower delta proving that the deltas formed during a period of rising lake level. Along no stream course is there more than one band of these stairstep lobate deltas, indicating that there has only been one post-fanglomerate lake transgression between the 1,470 m elevation and the Bonneville level.

Areas adjacent to the bands of lobate deltas display remarkably well-preserved parallel beach terraces that produce a conspicuous banded pattern on aerial photographs. These terraces are much more closely spaced and therefore have lower amplitude rises than the adjacent lobate deltas. The terraces were formed on the ancient fan surfaces by strand-line erosional processes. In the higher parts of some fans the detailed form of the original fan surface can be traced from elevations above the Bonneville level across the Bonneville shoreline into the area of the ancient lake indicating very minimal modification during lake occupation. At one locality the height of the erosional scarp that formed on fan gravels at the Bonneville level is only 70 cm. As the beach terraces were etched onto the subaerially formed fan surfaces, there was in most areas a slight decrease in the average elevation of these surfaces. Of considerable importance is the fact that for the fans formed by the small ancient ephemeral streams there was no major erosional change in shape of the fans during occupation of the area by the late lake cycle. For those areas the chief alteration of landscape is directly related to localized deposition on the ancient fan surface of coarse clastic debris in belts of lobate deltas as described above.

There is no obvious record of retreat of the ancient lake shore across the area between the Bonneville level and 1,470 m. If the interpretation of a single episode of lake transgression is correct, it is clear that Lake Bonneville rose through the 1,470-1,575 m interval at a very much slower rate than it fell through that interval. In fact, it appears that lake retreat was a catastrophic event.

The chief conclusion that can be drawn from these observations is that a long period of dessication ensued between an early lake and the final lake cycle--the Bonneville lake cycle. This period had to be long enough to construct beautifully graded large fans at the mouths of small drainages and to form a mature carbonate-dominant soil on the fan surfaces. This time interval is estimated to be at least 100,000 years and may be much longer. Morrison (1965) suggests a complex late lake history that includes five lake transgressions to levels considerably higher than 1,470 m during the Wisconsinan stage. There is clearly no such complex lacustrine record in the Cricket Mountains. The observations and conclusions made from the recent studies in the Cricket Mountains strongly support the conclusions drawn by Gilbert (1890), who, on the basis of the first comprehensive study of the history of Lake Bonneville, proposed two high stands of the lake separated by an interval of nearly complete evaporation that lasted five times longer than the post-Bonneville interval. These observations and conclusions are also consistent with the results of recent studies of Lake Bonneville stratigraphy of Bill Scott (this volume). They have great importance with regard to interpreting the history of faulting along the Wasatch Front. They are also very important to the interpretation of the late Quaternary record of regional deformation because over broad areas of western Utah that lie distant from major mountain fronts, the data argue strongly for a landscape that has been modified very little during or after the Bonneville Lake cycle. On this basis, it is reasonable to infer that the record of faulting seen in the form of displaced surfaces is many times longer than the post Lake Bonneville interval even in many areas inundated during the Bonneville cycle.

The importance of the results of studies in the Cricket Mountains can be seen in the need that they imply for a reinterpretation of studies made in the

southern part of Escalante Valley--the southernmost extent of ancient Lake Bonneville. Conspicuous features that mark the Bonneville shoreline in the Cricket Mountains can be traced southward for 40 km to the vicinity of Milford, but south of there along Escalante Valley they become progressively less conspicuous. This has led to long-standing uncertainty as to location of the southernmost extent of Lake Bonneville. Anderson and Bucknam (1979a) attempted to clarify the matter by reporting the location and elevation of inconspicuous shoreline features in Escalante Valley (fig. 3) and inferring that they correlate with the Bonneville shoreline. The inference added about 800 km^2 to the previously determined southern extent of the lake (Anderson and Bucknam, 1979a). Elevation data on the inconspicuous shorelines show that they are presently as much as 31 m higher than they should be if they represent the Bonneville shoreline; and this led Anderson and Bucknam to postulate Holocene uplift of about that amount.

That a lake existed in this southern area is proven by the presence of well exposed undated lacustrine sediments near Table Butte (fig. 3). Though Anderson and Bucknam inferred a correlation of the sediments with the Alpine Formation of Wisconsinan age, the sediments are likely to be pre-Wisconsinan on the basis of the recent findings in the Cricket Mountains and those reported by Scott (this volume) from his studies along the Wasatch front.

Near Table Butte the sediments are at about the same elevation as subdued sinuous to sublinear ridges that were interpreted by Anderson and Bucknam (1979a) as looped and intersecting offshore bars of Bonneville age. If an uplift rate analogous to that implied for the bar-like features at Table Butte were projected back in time to include the age of deposition of the sediments, the sediments should be at least 175 m higher than they are. That the sediments and bar-like features are at the same elevation places limits on the range of reasonable interpretations. Uplift either did not occur prior to the Lake Bonneville cycle (20,000-12,000 B.P.) and has been very active since, or the bar-like features and inconspicuous shoreline features in southern Escalante Valley are not of Bonneville age and the uplift, which is probably as much as 57 m at Enterprise (fig. 3 and Anderson and Bucknam, 1979), has occurred gradually over a period that is more than 125,000 years in length. At present, I favor the latter interpretation.

Present plans call for additional stratigraphic studies in the Cricket Mountains including sampling and analysis of carbonate soils hopefully leading to a reliable estimate of their age, and sampling and analysis of fossils from back-bar silts and sands deposited during the final rise of Lake Bonneville, hopefully leading to reliable estimates of the timing and duration of that event. No additional studies are planned for southern Escalante Valley.

Whether or not an area of active uplift exists in the Beryl-Enterprise portion of Escalante Valley could be evaluated if a first-order level line that was established along the Union Pacific Railroad in 1908 were resurveyed. The line has not been resurveyed since it was established. A systematic search for the 1908 monuments revealed that they remain at only eight localities along the 75 km of railroad northeast of Modena (fig. 3).

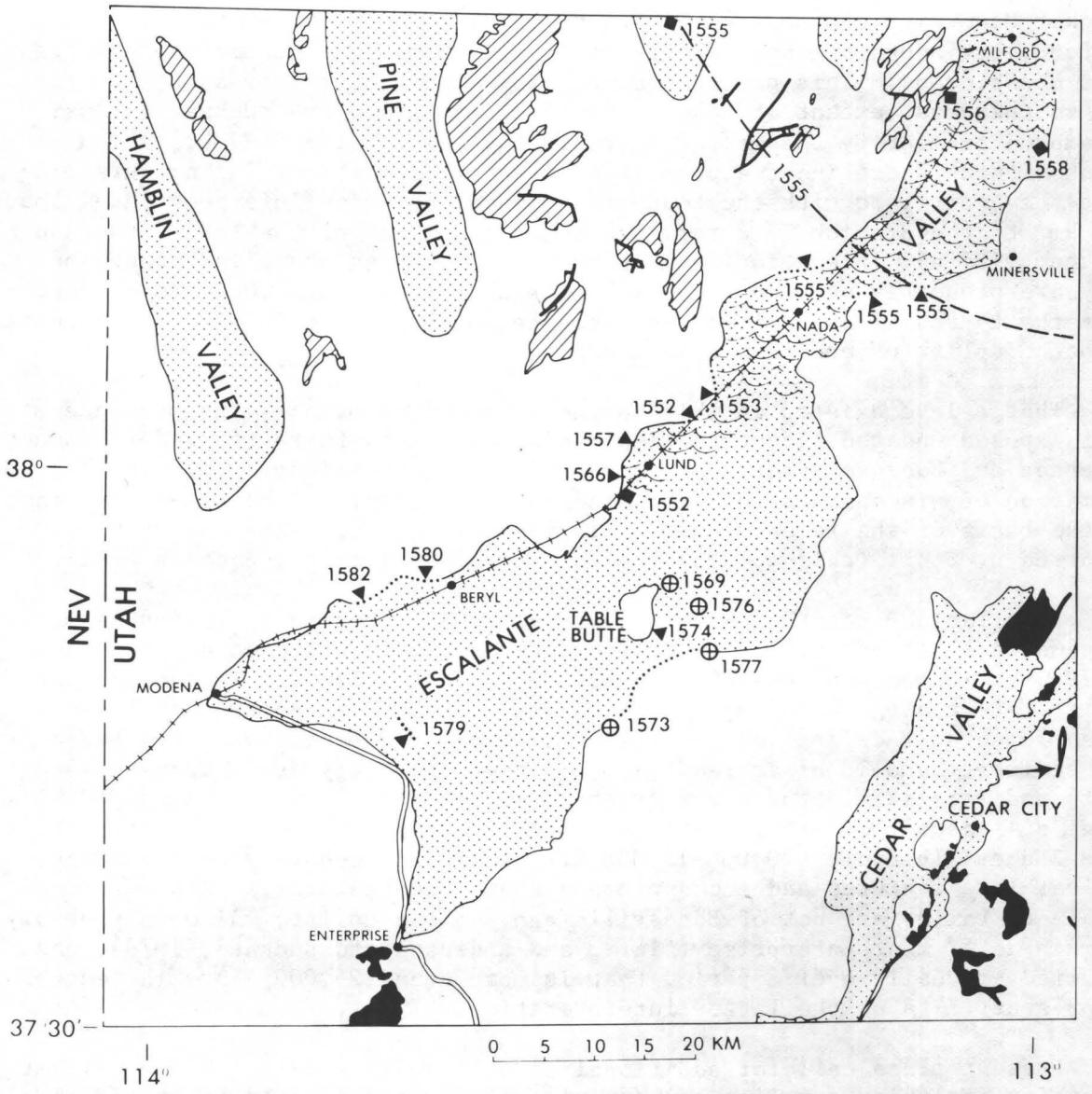

Figure 3.--Map of Escalante Valley and environs showing the location of the major valleys (stippled) relative to outcrops of Paleozoic rocks (rules) and Quaternary basalt (black); the unpatterned areas are underlain mostly by rocks of Mesozoic and Tertiary age. Heavy solid lines are faults; heavy dashed line is a portion of the southernmost isobase showing elevation (1,555 m) of maximum high stand of ancient Lake Bonneville (from Crittenden, 1963); dotted lines mark locations where continuous or quasi-continuous shoreline features can be seen on aerial photographs; hachured line is Union Pacific Railroad. Solid squares mark localities at which Crittenden (1963) measured maximum elevations of Bonneville shorelines; solid triangles mark localities where we determined shoreline elevations, using an altimeter; open circles with cross where we determined the elevations from 7 1/2-min topographic maps; all elevations are in meters. Wave pattern indicates extent of ancient Lake Bonneville as reported by Crittenden (1963). Heavy arrow points to faults along the West Fork of Braffits Creek where we recognize evidence of Holocene displacement. From Anderson and Bucknam, 1979a.

Radiocarbon dating

Early in the history of the project it was hoped that radiocarbon dating of materials collected from deformed strata or from strata that post-date deformation would provide a basis for "absolute" age control on widespread specific fault events. Hope dimmed as work progressed because carbon-bearing strata were not found at critical localities or in critical stratigraphic positions. At present, radiocarbon data have been acquired from 5 localities (table 1). At two of the localities (Panguitch and Fremont Wash) early interpretations of the structural significance of the dated beds were found, as a result of continued study, to be in error, thus minimizing the structural significance of the data.

Braffits Creek--only at the Braffits Creek locality (figs. 1, 3), which is in the drainage basin of one of several structurally controlled north-flowing creeks that drain the western Markagunt Plateau, is there clear evidence that strata dated by the radiocarbon technique are faulted (fig. 4). Study of the surrounding areas of the Markagunt Plateau has revealed widespread geomorphic evidence of youthful deformation in the form of closed basins and unfilled trenches along fault lines, but at no locality was evidence found of deformation as young as that at Braffits Creek. Although the ages indicated by the radiocarbon analyses are discordant to the stratigraphic position of the samples (the oldest material yielded the youngest apparent age, 810 $\pm$ 200), the data suggest Holocene displacement. The magnitude of displacement is uncertain. If it is pure dip slip the apparent stratigraphic separation is 6 m. This documentation of young displacement is consistent with abundant geomorphic evidence of very young deformation in a narrow graben along Braffits Creek (Anderson and Bucknam, 1979a). The graben probably reflects tensional collapse along the flanks of a rising and spreading monoclinal flexure at the boundary between the Basin and Range and Colorado Plateaus provinces. The fault illustrated in figure 4 is not one of the main graben faults, but geomorphic evidence suggests that these faults also have been active during Holocene time. To what extent the faulting was accompanied by seismicity is not known. Many surficial features along Braffits Creek such as open fissures and toppled trees are clearly historic and indicate active instability. Because there has been no known historic earthquake in the area with an intensity large enough to produce surface rupture, some deformation in the area is clearly aseismic. The uncertainty as to whether the fault illustrated in figure 4 and the main graben-forming faulting are accompanied by strong seismicity has led to the omission of this as an area of Holocene faulting in regional compilations (fig. 2).

In order to provide a base for monitoring strain in the area, monuments that form sets of bridged quadrilaterals were installed across the province boundary and surveyed with a laser Ranger III by the Topographic Division, U.S. Geological Survey, in October 1977.

Enoch--Strata dated by the radiocarbon technique at Enoch are probably faulted, but the relationships are equivocal. North-northeast-trending horst and graben structures are well-defined in the area north and northeast of Cedar City (Thomas and Taylor, 1946). One of the structures, the Enoch Graben, is about 15 km long. It is expressed in its northern part as bold inward-facing escarpments formed on basalt that has been dated by the K-Ar

Table 1.--Radiocarbon ages indicated for samples from southwestern Utah.

Analyses by Meyer Rubin, USGS

Sample No.	Lab. No.	Material	Locality	Location	Age (referenced to A.D. 1950)
C-346-67C	W3791	charcoal-bearing pebbly alluvium	Braffits Cr. (Cedar Breaks 15' quad.)	112°58'05" W., 37°44'32" N.	1150 ± 200
C-346-67	W3784	---do----------	---do----------	---do----------	1240 ± 200
C-346-67B	W3781	---do----------	---do----------	---do----------	810 ± 200
C-345-5	W3530	organic sandy clay	Enoch (Enoch 7.5' quad.)	113°01'23" W., 37°46'05" N.	9500 ± 300
C-345-21	W3531	charcoal from silty alluvium	N. of Enoch (Enoch 7.5' quad.)	113°00'37" W., 37°48'45" N.	5400 ± 200
C-2068-13B	W3733	charcoal from buried soil on fanglomerate	Panguitch (Casto Canyon 7.5' quad.)	112°20'55" W., 37°48'22" N.	4300 ± 400
C-2068-16	W3738	detrital charcoal from buried soil	---do----------	112°20'48" W., 37°47'40" N.	7000 ± 250
R-439-3	W3628	detrital charcoal concentrated from sandy alluvium	Fremont Wash (Kane Canyon 7.5' quad.)	112°35'15" W., 38°07"48" N.	3800 ± 800
R-439-3A	W3636	charcoal-bearing sandy alluvium	---do----------	---do----------	3700 ± 400
C-1385-6	W3633	charcoal concentrated from clayey and silty sand	Enterprise (Enterprise 7.5' quad.)	113°41'30" W., 37°33'55" N.	4930 ± 400

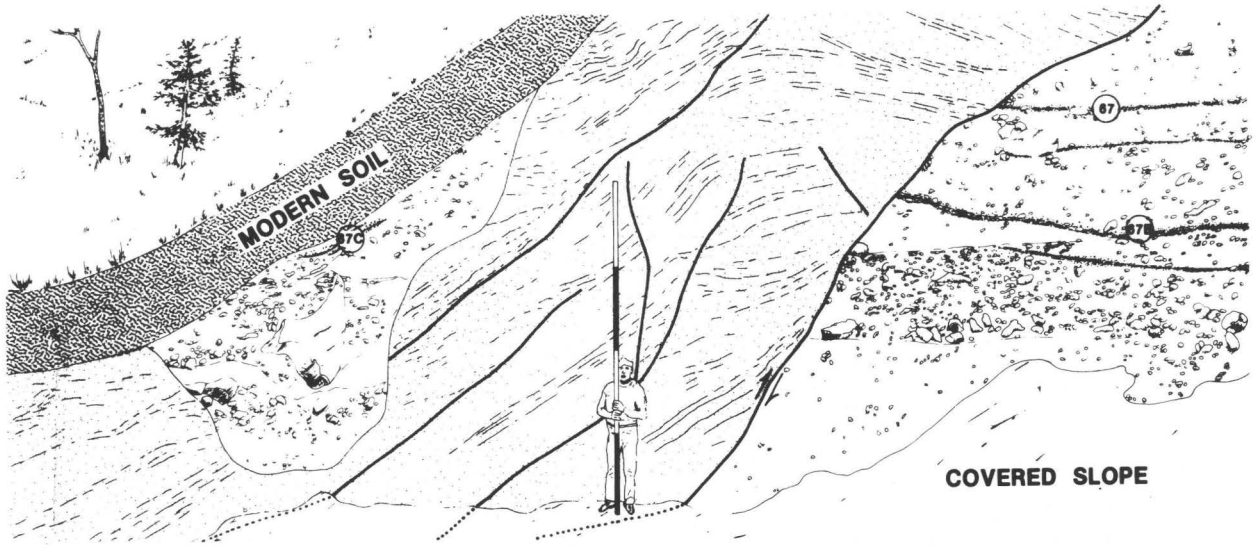

Figure 4.--Sketch looking southeast at exposure along Braffits Creek, 10 km northeast of Cedar City. Patterned area consists of well-bedded pale-red silt, sand, and gravel that has an average attitude of N. 20° E. 55° SE. (trace of bedding indicated by form lines). These sediments consist of a relatively homogeneous clast assemblage derived from lower Tertiary sedimentary rocks. They are sheared and brecciated and are in high-angle reverse-fault contact (N. 20° E. 75° SE.) with flat-lying heterogeneous alluvium to the right of man and are channeled and filled by coarse alluvial debris to the left of man. Numbers refer to localities represented by radiocarbon ages shown in table 1.

method at about 1 m.y. (Anderson and Mehnert, 1979) and in its southern part by subdued scarps formed on unconsolidated alluvium. In the southern part near Enoch the upthrown block of the eastern graben fault has been trenched in several places by local residents in efforts to stimulate flow from springs that issued from the fault line. The fault is exposed in the northernmost trench, but materials datable by the radiocarbon technique were not found there. The southern trenches expose several layers of brown to dark brown humic sandy clay, but the exposures are not adequate to show if these strata are faulted. A sketch of the north wall of a trench from which a sample of humic sandy clay yielded a radiocarbon age of 9,500 $\pm$ 300 is shown in figure 5. The graben fault is probably buried beneath alluvial materials west of the trenched scarp. An effort to excavate the fault and locate the dated strata on the downthrown block failed (fig. 5).

The dated layer of dark humic clay separates indistinctly bedded pebble- and cobble-bearing alluvium below from well-bedded sandy clay above. The well-bedded clay shows no evidence of thinning or pinching out toward the fault trace. This suggests that the beds probably extended westward to the fault and have been downdropped into the graben. The dated dark layer forms a gentle sag or depression that is filled by and buried beneath parallel-bedded sandy clay that exhibits distinct color banding caused by variations in content of humus (fig. 5). A younger flexure and small sag is seen in the beds of sandy clay. To what extent these flexural features are related to displacements on the graben fault is not known.

A radiocarbon age of 5,450 $\pm$ 200 was obtained on detrital charcoal collected from silty alluvium in an arroyo wall located along the trace of the eastern graben fault 4.5 km north of Enoch (table 1). The silty sediments were deposited in a channel cut across the eastern graben fault and they are not faulted. Therefore, available data suggest, but do not prove, that a displacement event occurred on the eastern graben fault in the vicinity of Enoch between about 9,500 and 5,450 radiocarbon years. On the basis of the morphology of the scarp, the last displacement event appears to be much older than that which can be inferred from available isotopic and geologic data. Perhaps the inconsistency could be resolved if a trench were excavated into the downthrown block so that stratigraphic displacement could be evaluated. As with the Braffits Creek area, the fault at Enoch is not included in regional compilations as one that has had displacement during Holocene time.

Panguitch--Alluvial deposits of probable Quaternary age are extensively faulted and gently tilted near Panguitch. Northeast of Panguitch the morphology of the fault scarps suggests recurrent movement on some faults. The scarps and the tilted blocks are breached in that area by several west-flowing streams that drain from the Sevier Plateau into the Sevier River. Each of these streams had an early syn- and post-faulting history of extensive downcutting during which major landscape changes were produced in the adjacent lowlands and during which an extensive mature calcic soil formed on the graded surfaces. These early events occupy most of the time lapsed since faulting--probably more than 100,000 years. They were followed during Holocene time by an episode of aggradation during which the early-formed post faulting stream channels and well-developed soils were partially buried by sediments that are unfaulted. This depositional episode was followed, in turn, by extensive downcutting to form the modern arroyos--an event that provided several good exposures of buried soils.

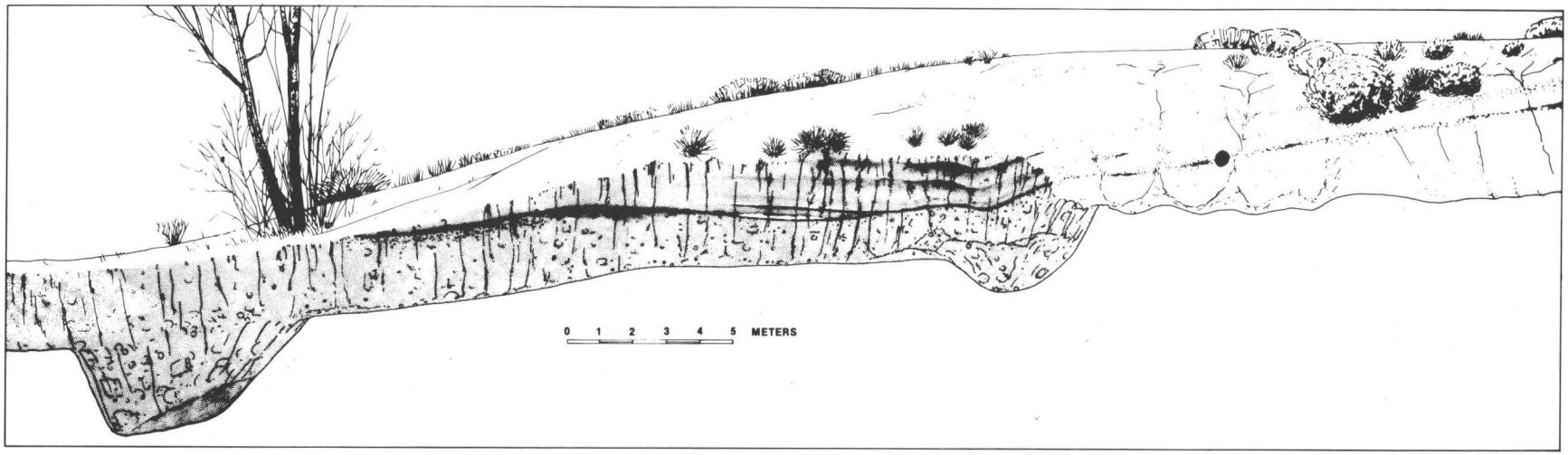

Figure 5.--Sketch looking north at north wall of old trench cut into fault scarp at Enoch. Patterned area shows portion of preexisting trench wall that was reexcavated as well as position of shallow pits excavated in floor of old trench. Dot shows approximate location of sample collection for radiocarbon analysis that yielded age of 9,500 ± 300 B.P. Shaded bands depict color contrasts in silty and sandy clays resulting from concentration of humus. A fault is not recognized in the trench. Lightly patterned area at west end of excavation depicts concentration of secondary carbonate possibly related to deposition from ground water in a fault zone. A lack of bedding in that area precludes recognition of a fault if one exists. Illustration by Bryan Gough.

The older of two radiocarbon ages on charcoal (7,000 ± 200) indicates the age of parent material on which the humic upper horizon of a buried soil profile was formed and the younger of the ages (4,370 ± 400) indicates the time lapsed since the soil was buried by Holocene alluvial deposits. Both values are much younger than the last fault event that produced scarps in alluvium.

Fremont Wash and Enterprise--At Fremont Wash and Enterprise strata that yielded ages of about 3,700 and 4,930 radiocarbon years respectively (table 1) postdate the last movement on faults that project toward the sample sites. The indicated ages only provide minimum estimates of the time lapsed since the last displacement event.

General note--Although radiocarbon dating has not provided much data useful for defining the age of fault events, the available data may be of value in assessing Holocene climatic changes in southwestern Utah. Deposits of relatively fine-grained sediments in stream channels along which conspicuously coarser detritus had been transported during earlier downcutting are common to many areas in southwestern Utah that lie in the elevation range between 1,200 and 2,300 m. At Enoch, Fremont Wash, and Enterprise stream channels that had been eroded in late Pleistocene time were sites of extensive deposition of predominantly silty and sandy sediments by about 5,450, 3,000, and 4,930 B.P. respectively, and at Panguitch a similar depositional event appears to have begun about 4,370 B.P. as described above. The common occurrence of detrital carbon in the young sediments at Enoch, Fremont Wash, and Enterprise as well as at several undated localities suggests derivation of the relatively fine detritus from adjacent highlands that were wooded and soil-covered prior to or during sedimentation. At Panguitch detrital caliche of presumed pedogenic origin is a common constituent in the Holocene sediments suggesting their derivation, in part, from soil-covered terrain. The suggested widespread loss of soil from bedrock highlands during middle to late Holocene time and their redeposition in stream channels flowing across adjacent piedmont terrains is an event that probably records a decrease in precipitation and a significant warming such as are inferred for the Altithermal phase of Holocene climate in the Great Basin.

The Hurricane fault

Published estimates of normal stratigraphic separation on the Hurricane fault in Utah range over almost an order of magnitude from 430 to 4,000 m (fig. 6). The great discrepancy arises, in large part, from the failure of several investigators to subtract from the total apparent stratigraphic separation at the fault the portion of the separation that is related to pre-fault folding of possible Laramide age. Kurie (1966) made the subtraction which led him to estimate that the normal component of displacement on a 32-km segment of the fault south of Kanarraville ranges from 430-1,200 m. Anderson and Mehnert (1979) estimate the vertical stratigraphic separation on the fault to be 600-850 m on the basis of comparisons between the structural level of the Jurassic Navajo Sandstone at distances of 8 to 10 km east and west of the fault. Comparisons made at those distances tend to eliminate the complicating effects of prefault structures and fault-related drag structures near the fault, and provide an estimate of what Anderson and Mehnert (1979) have called major-block displacement.

Dutton 1880	3,700 - 4,000
Gardner 1941	>3,100
Thomas and Taylor 1946	no more than 2,450
Averitt 1962	at least 2,450
Hamblin 1970	3,100
Kurie 1966	430 - 1,200
Anderson and Mehnert 1979	600 - 850

Figure 6.--List of selected published estimates of normal stratigraphic offset on the Hurricane fault in Utah.

Area	Rate m/m.y.	Basis	Reference
Northern Hurricane fault	310±80	6 K-Ar and 1 thermolumi-nescence determinations	R. D. Holmes, M. G. Best and W. K. Hamblin, B.Y.U., written commun., 1978
Pintura (Hurricane fault)	470	Unpublished K-Ar age of about	M. G. Best, B.Y.U., oral commun., 1979
North Hills (Hurricane fault)	400	K-Ar ages of 1.09±0.34 and 1.06±0.28 on offset basalt	Anderson and Mehnert, 1979
Farmington (Wasatch fault)	400	40 fission-track ages on apatite	Naeser and others, this volume

Figure 7.--List of displacement rates estimated for the Hurricane fault on the basis of stratigraphic offset of basaltic flows and for the Wasatch fault on the basis of fission-track ages from the Precambrian Farmington Canyon complex of the Wasatch Mountains.

Basaltic flows with isotopic ages of about 1 m.y. and younger are widespread along the Utah segment of the Hurricane fault and its coextensive structure to the northeast--the Cedar City-Parowan monocline. At some localities individual flows or series of flows can be found on both sides of the main structures, thus providing an ideal situation for estimating vertical stratigraphic offset. A summary of available data is given in figure 7. From these data it appears as though the Hurricane fault has had a vertical component of separation ranging from 310 to 470 m in the last million years. If, as is suggested above, the total vertical separation that must be accounted for is 600-850 m (Anderson and Mehnert, 1979) or 430-1,200 m (Kurie, 1966), and if a constant displacement rate is assumed, the Hurricane fault is probably no older than Pliocene and could be a predominantly Quaternary structure.

Rowley and others (1978) reviewed published postulations of an early Tertiary (Laramide) age for the Hurricane fault and found them to be without substantiating evidence. Anderson and Mehnert (1979) reviewed the interpretations of Oligocene and Miocene displacements in the Hurricane fault and found that there is no conclusive evidence for such early displacements. In particular, they found that the distribution patterns of Oligocene-early Miocene ash-flow tuffs erupted from centers in the Basin and Range provide no conclusive evidence of topographic restrictions related to early displacements on the Hurricane fault or its coextensive and coeval structures to the northeast. On the contrary, they cite stratigraphic evidence that such restrictions did not exist. Anderson and Mehnert (1979) also found that some of the geologic relationships referred to in published reports as evidence for Miocene displacement actually argue against Miocene displacement. In particular, the distribution and provenance of coarse clastic debris preclude the presence of a topographic barrier along the northern trace of the Hurricane fault during at least part of Miocene time. Anderson and Mehnert (1979) also considered, on the basis of isotopic, geologic, and gravity data, the relationship of the Hurricane fault to the age of formation and distribution of sediment-filled basins in the region and found that the Hurricane fault does not form the boundary of a significant sediment-filled basin and therefore bears no first-order relationship to such structures. In summary, a thorough review and evaluation of published reports, supported by considerable new field and laboratory data, failed to disclose evidence that is in conflict with the suggestions made above that the Hurricane fault is probably no older than Pliocene and could be a predominantly Quaternary structure.

An understanding of the seismotectonics of the Hurricane fault is important to the evaluation of seismic hazards in the relatively small but growing population centers such as Cedar City and St. George. Averitt (1962) described and illustrated a conspicuous scarp at the mouth of Shurtz Creek about 8 km south-southwest of Cedar City. The scarp is at least 20 m high, is formed on very coarse bouldery alluvium, has a slope angle of 29°, and is deeply incised by active streams. On the basis of its profile, the scarp appears to be pre-Holocene, but its age is probably close to the Pleistocene-Holocene boundary. The surface that is displaced at this scarp was referred to by Averitt (1962) as the Shurtz Creek pediment. Recent studies have shown that the Quaternary gravels that mantle the pediment serve as parent material for a soil that is definitely pre-Holocene and is probably more than 50,000 years old.

Stereographic studies of aerial photos together with field studies have failed to disclose geomorphic evidence for Holocene displacement on the Hurricane fault. Long-term vertical displacement rates on the Hurricane fault calculated from vertical offset of dated basalt are comparable to those determined by Naeser (this volume) for the Bountiful-Ogden segment of the Wasatch fault calculated from fission-track analyses of apatite (fig. 7). Continuous youthful-looking scarps in alluvium such as those that are common along major segments of the Wasatch fault are not found along the Hurricane fault. Alluvial fan surfaces adjacent to the bedrock base of the Hurricane Cliffs appear unbroken. Most of the fans are small and are probably of Holocene age.

The absence of a record of Holocene displacement on the Hurricane fault suggests several possibilities:

1. Large displacements have occurred during Holocene but have not left an obvious geomorphic record,

2. The fault is inactive or is in a cycle of relative dormancy,

3. The fault is incapable of storing large stresses, and it moves in very small increments that do not result in conspicuous scarps,

4. Stress has been stored on the fault at a rate consistent with the long-term average, but the return period for stress release is long--similar in length to the Holocene Epoch.

There does not appear to be any process active along the Hurricane Cliffs that would serve to systematically remove evidence of large Holocene faulting. Rates of sedimentation and erosion cannot be inferred to be especially high as compared, for example, to those along the Wasatch front. The first possibility does not seem reasonable. The ability to locate earthquake epicenters accurately enough to assign them to specific structures has not existed in the region of the Hurricane fault. The second possibility could probably be evaluated with improved network capabilities. The third possibility seems unreasonable in light of the 20 m-high scarp at the mouth of Shurtz Creek. The fourth possibility is preferred. For a cursory evaluation of seismic flux and return periods in the southwestern Utah region see Bucknam and others, this volume.

The suggestion that the northern Hurricane fault is a structure that may have stored strain energy over a long period would seem to provide adequate justification for improving seismic monitoring capabilities to the point where the seismic flux of the structure could be monitored.

TECTONIC FRAMEWORK STUDIES

Tectonic framework studies fall into two main categories--those focused on the recognition of patterns in the distribution or trends of available data and those focused on geologic mapping of bedrock. Two examples of each are outlined, though none of the examples represent completed studies. Geologic mapping of bedrock at varied scales has focused sharply on scattered areas that have been determined to be critical to deciphering late Cenozoic tectonic

history and mechanics of deformation. The areas studied are located within and beyond the limits of the main zone of seismicity in southwestern Utah.

Landscape patterns

On the basis of historic seismicity southwestern Utah can be divided into a broad northeast-trending region within which the seismic flux is relatively high (includes part of the southern intermountain seismic belt of Smith, 1978) and an aseismic region (or a region of much lower seismic flux) to the northwest. These two regions correspond respectively to regions within which there are fault scarps in alluvium and within which such scarps are not found (fig. 2). Mountain masses in the aseismic region tend to be flanked by broad areas of pedimentation or are deeply penetrated by the apical portions of alluvial fans whereas mountain masses in the seismic region tend to be sharply bounded by faults that displace alluvium against bedrock or bedrock against bedrock. Stereographic study of landscapes developed on bedrock terrains as seen on 1:60,000-scale aerial photos reveals that relatively youthful physiographic features such as small closed basins and troughs with minimal sediment fill are widespread within the seismic belt and are absent or sparse in the aseismic region. Taken together, these landscape patterns suggest that the general area of tectonism in southwestern Utah has remained relatively stationary during late Quaternary time and is fairly well-represented by the distribution of historic seismicity.

Fault patterns

Late Quaternary fault scarps in southwestern Utah show a strong preference for northeasterly strikes--especially for scarps located west of the Colorado Plateau (fig. 2). If pure normal slip is inferred for these faults the indicated average extension direction is about N. 65° W. This direction is in good agreement with directions inferred from abundant faults in Quaternary igneous rocks in the southern Black Rock Desert west of Fillmore (Hoover, 1974) and in the vicinity of Cove Fort (Clark, 1977) as well as with directions inferred from the alinement of cinder cones and faults in the Enoch graben north of Cedar City and from cinder cones on the Kolob Terrace south of Cedar City. Despite the good agreement of these geologic indicators of stress they do not establish an extension direction of N. 65° W. for the neotectonic regime. Several factors that contribute to the uncertainty with which this inferred extension direction should be regarded are discussed in the paragraphs that follow.

First, slip vectors have not been determined at localities where faults displace Quaternary rocks or deposits. The late Quaternary fault scarps in southwestern Utah are mostly so old and modified by erosion that details of transverse topographic features formed on the offset surfaces that might otherwise serve as kinematic indicators have been destroyed. Therefore, the assumption of pure normal slip has not been tested.

Second, in some areas the indicated N. 65° W. direction is probably influenced by pre-Quaternary structures and is therefore not a reliable indicator of stress conditions. Examples of parallelism between Quaternary faults and lineaments and late Cretaceous or early Tertiary structures are: (1) The faults southeast of Richfield (fig. 2) which are at the southern end of and parallel to the Sevier-San Pete anticline (fig. 1 and Gilliland, 1963);

(2) the faults and aligned volcanic vents in the Enoch area which parallel the Parowan Gap fold (Threet, 1963); and (3) the volcanic vents on the Kolob Terrace which lie on a trend that parallels the adjacent Kanarra fold (Averitt, 1962, 1967; Hintze, 1963) and the Hurricane fault, which, in its Pintura-Cedar City segment, follows the axis of the Kanarra fold. Examples of parallelism between Quaternary structures and mid- to late-Tertiary structures are found at Cove Fort and in the North Hills near Cedar City. A north-trending normal fault that is well-exposed in an excavation south of Cove Fort forms the east boundary of the Cove Fort graben. The fault has an estimated minimum late Quaternary stratigraphic offset of 18-20 m (fig. 8). The fault parallels the strike of Tertiary strata that are highly deformed in an overturned fold seen beneath an unconformity on the upthrown block. The overturned fold and minor fault and drag structures within it resemble the Kanarra fold and its minor structures although there is more than an order of magnitude difference between the scale of the two fold structures. The fold near Cove Fort is probably post early Oligocene in age, and it probably had an important influence on the location and strike of the east boundary of the Cove Fort graben just as the early Tertiary Kanarra fold probably had an influence on the location and strike of the Cedar City-Pintura segment of the Hurricane fault. Recent mapping in the North Hills southwest of Cedar City (Anderson and Mehnert, 1979) has shown that stratal tilting in Quaternary basalt dated at about 1 m.y. describes an open northerly trending anticlinal structure that is cut by several faults having displacements that are down toward the axis of the anticline. Dips on the flanks of the anticline are probably associated with rotations on faults and average about 20°. This Quaternary structure is coaxial with a late Tertiary faulted anticline characterized by greater stratal rotations and larger fault offsets than in the Quaternary structure. The coaxial arrangement suggests an influence by the older structure. The suggested influence has special significance with regard to stress directions inferred from trends of geologic structures because the adjacent Kanarra fold has apparently influenced Quaternary development of the Hurricane fault on trends that differ in strike from that of the Quaternary anticline by as much as 60° (Anderson and Mehnert, 1979).

Third, limited data suggest that in some areas Quaternary faults with inferred normal displacement are either not normal faults or their trends have been influenced by earlier faults with major components of strike-slip motion. Examples are found near Cove Fort, east of Beaver, northwest of Milford, at Parowan Gap, and south of Gunlock. About 5 km northwest of Cove Fort Tertiary strata are cut by steep N. 25° E. faults on which a major component of the youngest movement was strike-slip as indicated by striations and stratigraphic offsets. These faults are located to the north of and along strike of faults with the same trend on which normal displacement of Quaternary strata is inferred. Pure strike slip is indicated by corrugations on a steep N. 20° E. fault that cuts late Tertiary volcanic rock in the highlands east of Beaver. This fault parallels numerous late Quaternary normal faults in Beaver Valley as noted under an earlier heading. In Tertiary and pre-Tertiary rocks in the northern Beaver Lake Mountains northwest of Milford numerous northerly trending faults, some marked by conspicuous recemented breccia zones, have glazed and polished surfaces containing horizontal to gently plunging lineations indicating a major component of lateral slip associated with the youngest displacements. The strike is parallel to the ranges and basins in that region. In Tertiary strata at Parowan Gap horizontal striations are well developed on a N. 25° E. 80 E.

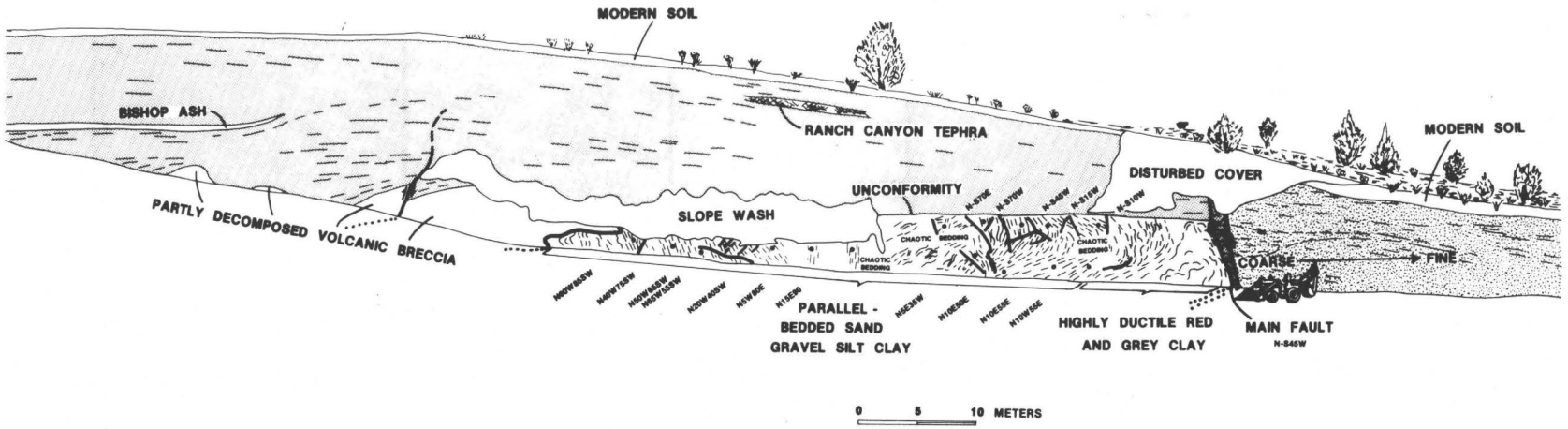

Figure 8.--Generalized sketch looking southeast at margin of large borrow pit south of Cove Fort. The excavation trends about N. 35° E. The subdued scarp on which the modern soil is formed is related to displacement on a north-trending fault (labeled main fault) that forms the east boundry of the Cove Fort graben--a structure within which Quaternary mafic lava flows were extruded over an area of about 518 km^2 and were cut by nearly 300 normal faults (Clark, 1977). The subdued scarp is highly dissected indicating structural quiescence during Holocene time. Patterned area on upthrown block and in the narrow horse block at the main fault consists mostly of coarse fanglomerate but includes beds of sand, silt, and clay and two beds of volcanic sediment of mid-Pleistocene age (Bishop ash and Ranch Canyon tephra, G. Izett, oral commun., 1978). Patterned area on downthrown block consists of indistinctly bedded sandy alluvium in which angular boulders and cobbles that are abundant near the fault are sparse 30 m from the fault. These beds are not found on the upthrown block, and are assumed to have been deposited in the Cove Fort graben as it subsided. A minimum of 18-20 m of late Pleistocene normal stratigraphic offset is indicated. Strata beneath the unconformity are clastic and are derived from the erosion of andesitic rocks of pre-late Oligocene age. Heavy lines are faults, light lines indicate approximate trace of bedding, dots mark localities referred to by adjacent in-line bedding attitudes. All attitudes with a westerly component of dip are on overturned strata. These highly deformed strata are of possible late Eocene or early Oligocene age.

fault of small displacement indicating pure strike-slip movement. This fault shares its attitude with several nearby faults of inferred normal displacement of basalt that is about 1 m.y. old. South of Gunlock a N. 5° E. fault with apparent normal displacement of Quaternary basalt can be traced southward where drag structures in pre-Tertiary rocks strongly suggest earlier motion that had an important strike-slip component.

Stress indicators inferred for southwestern Utah from fault-plane solutions are too few to serve as a basis for comparison to that inferred from geologic evidence, and I am not aware of published in situ stress measurements. Until the modern stress field is adequately sampled or geologic studies provide a better basis for kinematic analysis, the neotectonic least principal stress direction will remain highly uncertain. There are numerous localities along the Hurricane fault where slip surfaces record the youngest displacement direction in the form of striations or corrugations. To date, no systematic study has been made. Because the fault has a dog-leg trace it should provide a good opportunity for a detailed analysis of slip.

Bedrock studies in the Cedar City area

The reinterpretation of the Hurricane fault as a Plio-Pleistocene structure, as outlined under a previous heading, is the result of bedrock studies in the Cedar City area. Following is a summary of additional important results of studies in the Cedar City area.

1. An episode of relatively ductile deformation that resulted in highly faulted and steeply tilted strata with highly variable trends affected a broad corridor extending west-southwest from Cedar City into Nevada--essentially coincident with the zone of current seismicity that sweeps across southern Nevada into Utah (Smith, 1978). The deformation was most intense near the Oligocene-Miocene boundary when numerous plutons were emplaced (Mackin, 1947, 1960; Cook, 1957), but continued into the Miocene Epoch when high mountain masses, most of which were centered on plutons, were formed. Some of the high mountains located in the area now occupied by the Basin and Range served as source terrains for coarse clastic debris that flowed into areas now occupied by the Colorado Plateau. The episode of relatively ductile deformation is probably related to thermal softening of the crust during the widespread late Oligocene igneous activity in the region. It preceded basin development by block faulting.

2. On the basis of newly acquired K-Ar ages basin development associated with block faulting in the region west, northwest, and north of Cedar City began 8-10 m.y. ago (Anderson and Mehnert, 1979, and additional data).

3. On the basis of published and newly acquired K-Ar ages basaltic lavas erupted profusely about 1 m.y. ago from numerous vents along the Hurricane fault and coextensive structures to the north and northeast such as the Enoch Graben and Cedar City-Parowan monocline. Eruptions were followed by large-magnitude faulting and monoclinal flexuring. This suggests a deep-seated causal relationship between faulting and basaltic magma production and eruption.

4. The Hurricane fault is strikingly different from the Wasatch fault. It is predominantly a Quaternary structure and as such may reflect a youthful eastward migration of normal faulting into the Colorado Plateau province. It probably does not mark the location of a tectonic province boundary now and certainly did not during pre-Quaternary time. Its surface trace, like the surface traces of other normal faults in the Utah-Arizona border region of the western Colorado Plateau province, separates bedrock from bedrock with local thin patches of surficial debris. It is closely associated with Quaternary basaltic volcanism. The Wasatch fault zone, by contrast, marks a major province boundary. It is bounded on the west by a 290-km-long belt of deep grabens filled with as much as 3 km of Tertiary and Quaternary sediments that are probably as old as the Eocene (Cook and Berg, 1961; Peterson, 1974; McDonald, 1976). Associated basaltic volcanism is not reported.

Bedrock studies in western Millard County-- a comment on the adequacy of geologic mapping for earthquake hazards evaluations

The general correlation between distribution of seismicity and landforms indicative of young deformation in southwestern Utah was recognized early in the project history. A search was made of available geologic maps for evidence of how far back in time the contrast in tectonic behavior of the two subregions could be traced and for other structural patterns that might aid in determining why the current seismicity is where it is. A 14,000 km^2 area within the aseismic subregion was compared with a 5,000 km^2 area within the seismic subregion. Escalante Valley was chosen as the buffer zone between the two subregions as illustrated schematically in figure 9. Faults otherthan thrusts shown on available geologic maps ranging in scale from 1:250,000 to 1:24,000 within each area were inventoried for the following.

1. The percentage of faulted vs. the percentage of depositional contacts between Tertiary and pre-Tertiary rocks.

2. For faults that strike toward the mapped depositional contacts from the pre-Tertiary side, the percentage of those that cross the contact vs. the percentage of those that do not.

3. The number of faults shown on the Tertiary side of the contact vs. the number shown on the pre-Tertiary side (a band of variable width was chosen such that areas of equivalent size were inventoried on each side of the contact).

The findings are remarkable and unexpected, and they serve to point up limitations in the usefulness of the geologic data base for pattern recognition that might be applied to earthquake hazards research.

Regardless of scale the maps suggest that there is a major difference between the age of faults in the area north of Escalante Valley versus the area south of Escalante Valley (fig. 9). Data presented on the Geologic Map of Southwestern Utah indicate that in the 14,000 km^2 northern area only 6 percent of the total length (425 km) of mapped contact between Oligocene and pre-Oligocene rocks is occupied by faults. The remaining 94 percent is mapped as a depositional contact. In that same area there are about 13 times more

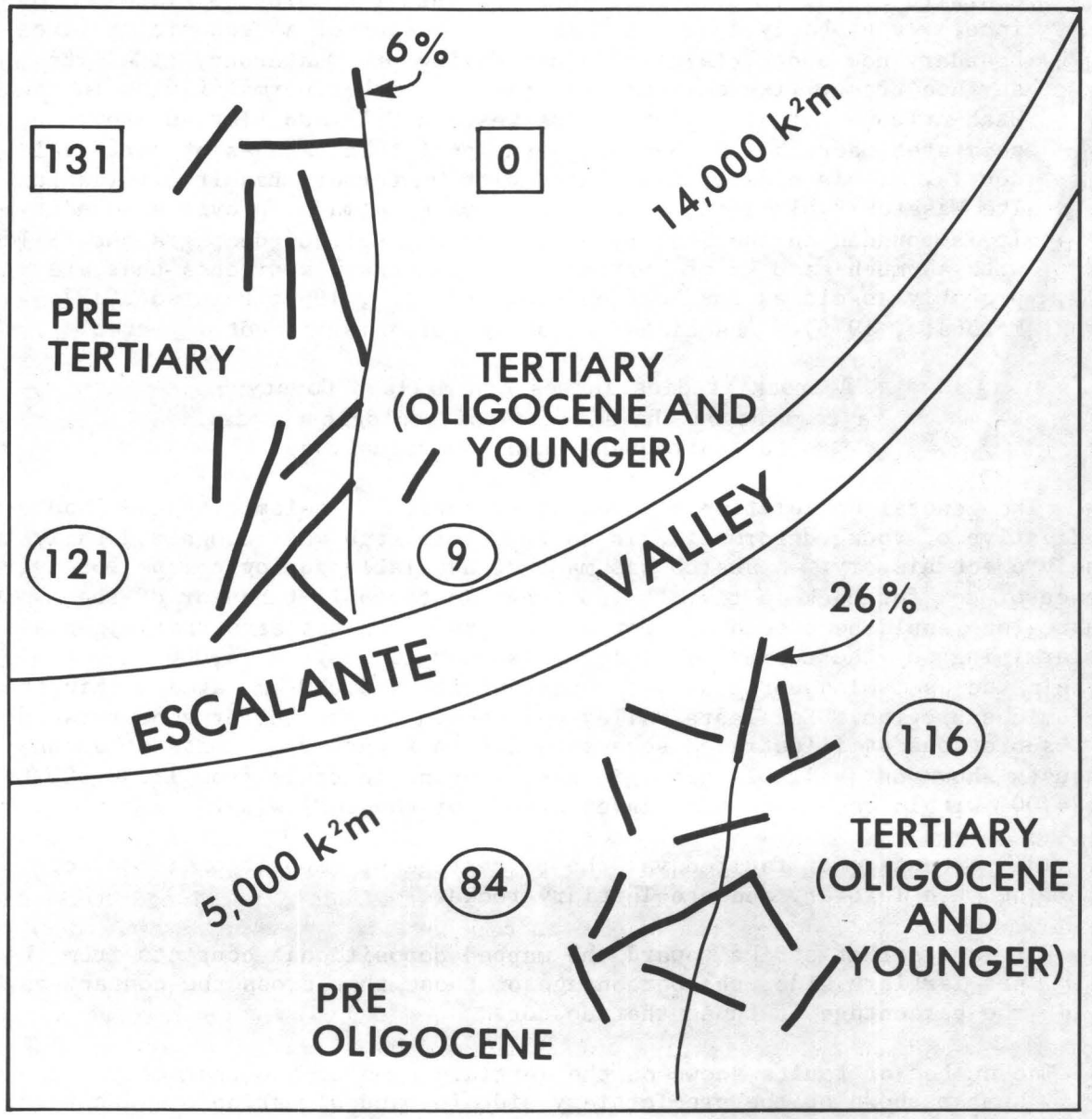

Figure 9.--Schematic diagram of southwestern Utah showing approximate proportion of contact between Oligocene and pre-Oligocene rocks mapped as a fault (heavy lines) versus that mapped as depositional (light lines), and distribution of faults relative to contact. Numbers enclosed by rectangles are summations of fault abundances from quadrangles mapped by Hose and others (see summary in Hose, 1977); those enclosed by circles are summations from the 1:250,000 state geologic map.

faults shown on the pre-Oligocene side of the contacts than on the side with Oligocene and younger rocks, and almost all faults that strike into the contact terminate at the contact and do not cut the Oligocene and younger rocks. An inventory of faults on larger scale maps covering 11 quadrangles yields similar results. Mapping by Dick Hose and others in seven 7.5' quadrangles (see summary in Hose, 1977) shows no faults on the side of the contact where Oligocene and younger rocks are exposed and 130 faults in an area of equal size on the pre-Oligocene side. Mapping by Lehi Hintze in four 15' quadrangles shows that the Oligocene-pre-Oligocene contact is occupied by faults along only 1 percent of its length and faults are 23 times more abundant in the area of pre-Oligocene rocks along the contact than in the areas of Oligocene and younger rocks. The conclusion to be drawn from a careful reading of many of these maps is that most of the mountain ranges in western Millard and Juab Counties predate eruption of Oligocene volcanic rocks.

In contrast to the area north of Escalante Valley, the fault relationships in the 5,000 km^2 southern area are very different. Data presented on the Geologic Map of Southwestern Utah indicate that 26 percent of the total length (270 km) of contact between Oligocene and pre-Oligocene rocks is occupied by faults. Of greater significance is the fact that the abundance of faults is somewhat similar on either side of the contact (84 on the pre-Oligocene side and 116 on the other side), and faults that strike into the contact generally cut rocks on both sides of it with similar magnitudes of offset. An inventory of faults on four recently published 7.5' quadrangles shows normal fault abundances and distribution patterns that are very similar to those found on the smaller scale state map.

These differences suggest that the area north of Escalante Valley was the site of extensive faulting prior to the main episodes of Cenozoic volcanic activity in the Oligocene and Miocene and has not been faulted much since then whereas faulting, mostly normal faulting, south of Escalante Valley is mostly and perhaps completely younger than the Oligocene and Miocene rocks. This suggested long-term tectonic contrast, if correct, would provide a basis for understanding the contrast in neotectonic behavior. An alternative interpretation, which I favor on the basis of extensive photogeologic and limited field studies, holds that the differences result from inadequate mapping of Cenozoic rocks north of Escalante Valley and are therefore not real. A notable exception is a recently published quadrangle map of a part of the Needles Range on which Best (1976) shows continuity of normal faults and similar fault densities between areas of Cenozoic and pre-Cenozoic rocks. In other areas of western Juab, Millard, and Beaver counties where I have mapped, the Oligocene and post-Oligocene rocks are cut by many normal faults that do not appear on most of the available geologic maps. There is widespread evidence of major episodes of Cenozoic faulting that predate the episode that blocked out the present system of basins and ranges. It is not possible to relate the contrast in late Quaternary structural behavior and historic seismicity of the two subregions of southwestern Utah to contrasts in late Cenozoic faulting because the latter contrasts do not seem to exist.

REFERENCES CITED

Anderson, R. E., and Bucknam, R. C., 1979, Map of fault scarps on unconsolidated sediments, Richfield 1° x 2° quadrangle, Utah: U.S. Geological Survey Open-File Report 79-1239, p.

_____1979a, Two areas of probable Holocene deformation in southwestern Utah: Tectonophysics, v. 52, p. 417-430.

Anderson, R. E., and Mehnert, Harald, 1979, Reinterpretation of the history of the Hurricane fault in Utah: Rocky Mountain Association of Geologists 1979 Guidebook. [In press].

Averitt, Paul, 1962, Geology and coal resources of the Cedar Mountain quadrangle, Iron County, Utah: U.S. Geological Survey Professional Paper 389, 72 p.

_____1967, Geologic map of the Kanarraville quadrangle, Iron County, Utah: U.S. Geological Survey Geologic Quadrangle Map GQ-694, scale 1:24,000.

Best, M. G., 1976, Geologic map of the Lopers Spring Quadrangle, Beaver County, Utah: U.S. Geological Survey Miscellaneous Field Studies Map MF-739.

Bucknam, R. C., 1977, Map of suspected fault scarps in unconsolidated deposits, Tooele 2° sheet, Utah: U.S. Geological Survey Open-File Report 77-495.

Bucknam, R. C., Algermissen, S. T., and Anderson, R. E., 1979, Late Quaternary faulting in western Utah and its implications in earthquake hazard evaluation: Geological Society of America Abstracts with Programs, v. 11, no. 3, p. 71-72.

Bucknam, R. C., and Anderson, R. E., 1979, Map of fault scarps on unconsolidated sediments, Delta 1° x 2° quadrangle, Utah: U.S. Geological Survey Open-File Report 79-366, 21 p.

_____1979a, Estimation of fault-scarp ages from a scarp height-slope angle relationship: Geology, v. 7, p. 11-14.

Clark, E. E., 1977, Late Cenozoic volcanic and tectonic activity along the eastern margin of the Great Basin, in the proximity of Cove Fort, Utah: Brigham Young University Geology Studies, v. 24, pt. 1, p. 87-114.

Cook, E. F., 2957, Geology of the Pine Valley Mountains, Utah: Utah Geological and Mineralogical Survey Bulletin 58, 111 p.

Cook, K. L., and Berg, J. W., Jr., 1961, Regional gravity survey along the central and southern Wasatch front, Utah: U.S. Geological Survey Professional Paper 316-E, 88 p.

Dutton, C. E., 1880, Report on the geology of the high plateaus of Utah with atlas: U.S. Geographical and Geological Survey, Rocky Mountain Region, 307 p.

Gardner, L. S., 1941, The Hurricane fault in southwestern Utah and northwestern Arizona: American Journal of Science, v. 239, p. 241-260.

Gilbert, G. K., 1890, Lake Bonneville: U.S. Geological Survey Monograph 1, 438 p.

Gilliland, W. N., 1963, Sanpete-Sevier Valley anticline of central Utah: Geological Society of America Bulletin, v. 74, p. 15-124.

Hamblin, W. K., 1970, Structure of the western Grand Canyon region, in The western Grand Canyon district, 1970: Utah Geological Society Guidebook to the Geology of Utah, no. 23, p. 3-20.

Hintze, L. F., compiler, 1963, Geologic map of southwestern Utah, in Geology of southwestern Utah, 1963: Intermountain Association of Petroleum Geologists Guidebook, Annual Field Conference, 12th, Utah Geological and Mineralogical Survey, 232 p.

Hoover, J. D., 1974, Periodic Quaternary volcanism in the Black Rock Desert, Utah: Brigham Young University Geology Studies, v. 21, pt. 1, p. 3-72.

Hopkins, D. M., 1975, Time-stratigraphic nomenclature for the Holocene Epoch: Geology, v. 3, p. 10.

Hose, R. K., 1977, Structural geology of the Confusion Range, west-central Utah: U.S. Geological Survey Professional Paper 971, 9 p.

Kurie, A. E., 1966, Recurrent structural disturbance of Colorado Plateau margin near Zion National Park, Utah: Geological Society of America Bulletin, v. 77, p. 867-872.

Mackin, J. H., 1947, Some structural features of the intrusions in the Iron Springs district: Utah Geological Society Guidebook to the Geology of Utah, no. 2, 62 p.

_____1960, Structural significance of Tertiary volcanic rocks in southwestern Utah: American Journal of Science, v. 258, p. 81-131.

McDonald, R. E., 1976, Tertiary tectonics and sedimentary rocks along the transition--Basin and Range province to Plateau and Thrust Belt province, Utah: in Hill, J. G., ed., Geology of the Cordilleran Hingeline: Denver, Rocky Mountain Association of Geologists, p. 281-317.

Morrison, R. B., 1965, Quaternary geology of the Great Basin, in Wright, H. E., and Frey, D. G., eds., The Quaternary of the United States: Princeton, N.J., Princeton University Press, p. 265-285.

Morrison, R. B., and Frye, J. C., 1965, Correlation of the middle and late-Quaternary successions of the Lake Lahontan, Lake Bonneville, Rocky Mountain (Wasatch Range), southern Great Plains, and eastern Midwest areas: Nevada Bureau of Mines Report 9, 45 p.

Morrison, R. B., and Frye, J. C., 1965, Correlation of the middle and late-Bonneville basin, Utah and Idaho: U.S. Geological Survey Miscellaneous Field Studies Map MF-627, scale 1:250,000.

Rowley, P. D., Anderson, J. J., Williams, P. L., and Fleck, R. J., 1978, Age of structural differentiation between the Colorado Plateaus and Basin and Range provinces in southwestern Utah; reply: Geology, v. 6, no. 9, p. 572-575.

Schwartz, D. P., Swan, F. H., III, Hanson, K. L., Knuepfer, P. L., and Cluff, L. S., 1979, Recurrence of surface faulting and large magnitude earthquakes along the Wasatch fault zone near Provo, Utah: Geological Society of America Abstracts with Programs, v. 11, no. 6, p. 301.

Smith, R. B., 1978, Seismicity, crustal structure, and intraplate tectonics of the interior of the western Cordillera, in Smith, R. B., and Eaton, G. P., eds., Cenozoic tectonics and regional geophysics of the western Cordillera: Geological Society of America Memoir 152, 388 p.

Swan, F. H., III, Schwartz, D. P., Hanson, K. L., Knuepfer, P. L., and Cluff, L. S., 1979, Recurrence of surface faulting and large magnitude earthquakes along the Wasatch fault zone, Utah: Geological Society of America Abstracts with Programs, v. 11, no. 3, p. 131.

Thomas, H. E., and Taylor, G. H., 1946, Geology and ground-water resources of Cedar City and Parowan Valleys, Iron County, Utah: U.S. Geological Survey Water-Supply Paper 993, 210 p.

Threet, R. L., 1963, Structure of the Colorado Plateau margin near Cedar City, Utah, in Geology of southwestern Utah, 1963: Intermountain Association of Petroleum Geologists Guidebook, Annual Field Conference, 12th, Utah Geological and Mineralogical Survey, p. 104-117.

New Interpretations of Lake Bonneville Stratigraphy and Their Significance for Studies of Earthquake-Hazard Assessment along the Wasatch Front

Manuscript submitted for Conference on Earthquake Hazards along the Wasatch Front and in the Reno-Carson City Area
July 30 - August 1, 1979; Alta, Utah

William E. Scott
U.S. Geological Survey M.S. 913
Federal Center Box 25046
Denver, Colorado
80225

ABSTRACT

Initial investigations of problems of Lake Bonneville stratigraphy and history suggest that some previous observations and interpretations are in need of revision.

Previous workers' evidence for a low regression of Lake Bonneville 11 to 12,000 ya followed by a rise to or nearly to the Provo shoreline at about 10,000 ya (highest rise of the Draper lake cycle or Provo II cycle) is not compelling. Data from Red Rock Pass and Danger Cave indicate that the lake probably fell below the Provo shoreline sometime before 12,000 ya and regressed to a level below about 40 m of present Great Salt Lake by about 10,000 to 11,000 ya and has never been higher since.

Sediments of lake cycles older than the Bonneville cycle are little exposed and difficult to identify unless related to unconformities characterized by 1) soil or soil complex generally better developed than soils on Bonneville-cycle deposits, 2) major disconformity, expecially along mountain fronts, and 3) deposits of alluvium, colluvium, eolian sand, or loess. In applying these criteria to previously mapped areas, I feel that much of the Alpine Formation of previous workers was deposited during the Bonneville lake cycle as major unconformities are not present. The highest lake deposits demonstrably older than the Bonneville cycle occur at altitudes about 80 m below the level of the Bonneville shoreline. At present I find no irrefutable evidence for lake fluctuations older than the last that rose close to the level of the Bonneville shoreline.

Significance of these interpretatins for studies of earthquake-hazard assessment along the Wasatch Front relate to the use of Lake Bonneville and related deposits and landforms as indicators of past tectonic rates and earthquake recurrence. Current interpretations suggest 1) an older age (few thousand years) than previously thought for the last regression of Lake Bonneville below the Provo shoreline, 2) that much of the faulted lake deposits close to the Wasatch Front previously mapped as Alpine Formation are probably of the Bonneville cycle and thus as much as 3 to 10 times (15,000 yr vs. 50,000 or 150,000 yr) younger in age, than previously thought and 3) the chances of using lake deposits on the order of 150,000 yr old to assess longer term rates of tectonism may not be possible because the deposits are often concealed and may be absent high on piedmont areas where faults generally lie.

Introduction

In this paper, I will discuss some new interpretations of Lake Bonneville stratigraphy, primarily from recent work along the Wasatch Front (fig. 1). As this work has been in progress for only about two years, much of the material presented here is preliminary and may be revised after future studies. The purpose here is to present these new interpretations of Lake Bonneville history, to discuss their significance for stratigraphic and earthquake-related studies of recurrence intervals of faulting and rates of tectonism along the Wasatch Front, and also to discuss recognized problems that are the subject of present investigations.

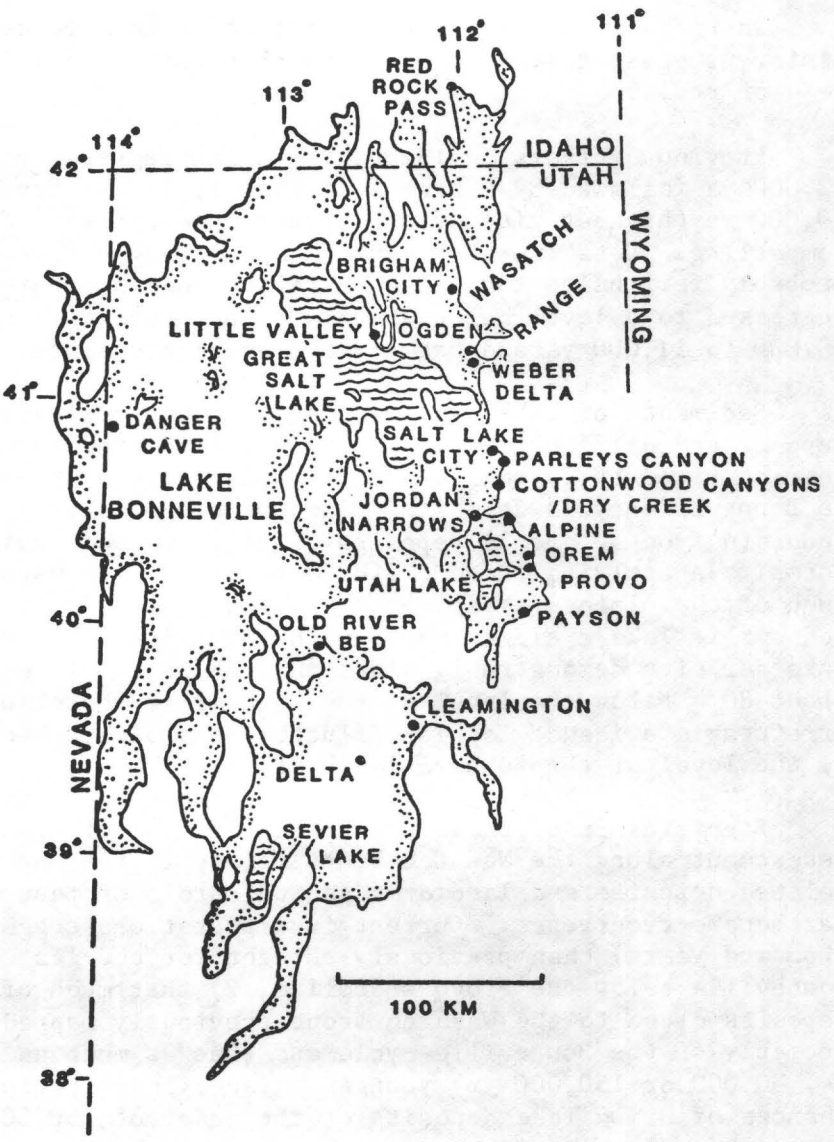

Figure 1.--Index map to localities discussed in text. Outline of maximum extent of Lake Bonneville (stippled area) from Morrison (1965d).

Previous Concepts

Because much of the following discussion necessarily refers to the concepts of Lake Bonneville stratigrapy and history that were developed by previous workers, a brief summary of previous concepts follows.

Stratigraphic studies and regional correlations by Morrison (1965a, 1965b, 1975) and Morrison and Frye (1965), and dating investigations by Broecker and Kaufman (1965) are presently the most widely cited sources on Lake Bonneville stratigraphy and chronology. These investigators present a complex history of lake fluctuations extending back to ca. 800,000 ya (years ago) (fig. 2) based on studies of pluvial[1] and interpluvial deposits and soils along the Wasatch Front, in the Delta-Oak City area, and at Little Valley near Promontory Point (fig. 1), and a large number of radiocarbon and uranium-series dates, many of which are inconsistent. Deposits of earlier (pre-Alpine) lake fluctuations have been recognized at Little Valley (Morrison, 1965b) and from cores (Eardley and Gvosdetsky, 1960; Eardley and others, 1973) where they are associated with Pearlette type-O (600,000 yr old) and Bishop (730,000 yr old) ashes. Because deposits of these earlier lake cycles have not been recognized along the Wasatch Front, they will not be discussed further.

The following aspects of this chronology (fig. 2) are of special interest here. 1) The several fluctuations of the Alpine lake cycle that were thought to have attained levels close to the altitude of the Bonneville shoreline. 2) A major soil (Promontory Soil) that formed during the interpluvial following deposition of the Alpine deposits. 3) The two-fold Bonneville cycle, during which the lake presumably rose twice to the Bonneville shoreline with an intervening regression to a very low level. During the second rise the lake overflowed at Red Rock Pass and fell quickly to the Provo shoreline before falling more gradually to a very low level between 11,000 and 12,000 ya. 4) The rise to near the Provo level about 10,000 ya during the Draper lake cycle. 5.) The drop to near the present level of Great Salt Lake by about 7,000 ya.

---

[1]Pluvial, as used in this paper, refers to times when there was significantly more water on the landscape than at present -- effective precipitation was greater, lake levels in desert basins were high, and streams had greater discharges than at present. In mid-latitudes pluvials and interpluvials were probably broadly synchronous with glacials and interglacials.

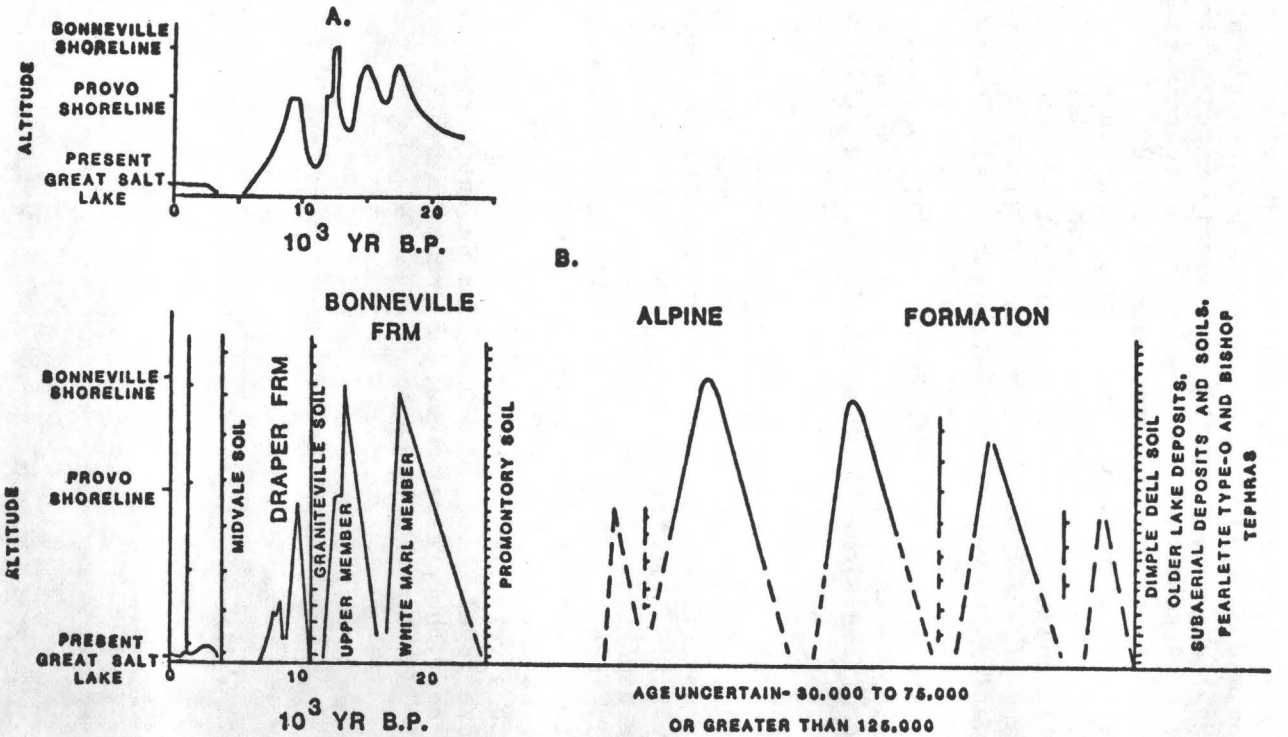

Figure 2. Chronologies of inferred fluctuations of Lake Bonneville modified from, A., Broecker and Kaufman (1965) and B., Morrison (1965b; 1975) and Morrison and Frye (1965). Because of differential isostatic uplift of the basin, altitudes of lake maxima are shown in relation to altitude of Bonneville and Provo shorelines. No adjustments of older lake minima due to less basin fill have been made. Hachured solid and dashed lines without names represent minor soils.

New Interpretations[2]

The validity of this reconstruction (fig. 2) rests on the interpretation of many stratigraphic sections; the recognition, tracing, and correlation of unconformities and buried soils; and the accuracy of numerous radiometric dates. Many of these basic observations and interpretations are now being

---

[2]The stratigraphic usage in this report is different from that of previous workers, most of whom have used Hunt's (1953) or Morrison's (Morrison and Frye, 1965) classifications:

Hunt (1953)	Morrison and Frye (1965)
Provo Formation	Draper Formation
Bonneville Formation	Bonneville Formation
Alpine Formation	Alpine Formation
Pre-Lake Bonneville deposits and soil	Pre-Lake Bonneville deposits, lacustrine deposits, and soils

In this report I generally use the same names as previous workers did when referring to their observations or interpretations. However, because of 1) confusion over the validity of these units as rock-stratigraphic units and 2) my disagreement with these authors concerning the differentiation and correlation of Lake Bonneville deposits, I use the following classification scheme for my observations and interpretations.

Lake Bonneville refers to the Pleistocene lake that periodically flooded the Bonneville basin. In this use cycles of Lake Bonneville extend through most of the Pleistocene.

The Bonneville lake cycle was the last major cycle of Lake Bonneville, generally correlated with the late Wisconsin. Deposits of the Bonneville lake cycle are lacustrine sediments deposited during this lake cycle.

The next-to-the-last lake cycle predates the last interpluvial which occured prior to the Bonneville lake cycle. Deposits of the next-to-the-last lake cycle are, in concept, the Alpine Formation of previous workers, although not necessarily as mapped by them.

Deposits of lake cycles older than the Bonneville cycle are generally referred to as pre-Bonneville-cycle deposits.

scrutinized and are in need of revision. I will present several interpretations consistent with my recent observations.

The work of Morrison (1965a, 1967, 1978), including his work in the Bonneville basin, has been instrumental in the development of the concepts of soil stratigraphy. Much of the utility of soil stratigraphy relies on the assumptions that, 1) soils formed intermittently and at rapid rates during the Quaternary, 2) these soils possess distinct properties that allow their recognition in the field, and 3) the relative degree of development of the various soils in a stratigraphic sequence is important in long-distance correlation with other sequences. Birkeland and Shroba (1974) have presented evidence that refutes the basis of assumption 1, and have argued that rates of soil formation have changed, but not to the extreme degree envisioned by Morrison (1967). Contrary to assumption 2, the characteristics of the various older buried soils in the Lake Bonneville sequence are not diagnostic and, in themselves, do not offer very effective means of correlation between widely separated exposures. For instance the type Dimple Dell Soil (Morrison, 1965a) and the type Promontory Soil (Morrison, 1965b) (fig. 2) display somewhat different characteristics. However, if the following new interpretations of Lake Bonneville stratigraphy (fig. 9) are correct, the soils may well represent the same interpluvial. Considering the cyclic changes of climate during the Quaternary as depicted in the marine record (Shackelton and Opdyke, 1973), it is also difficult to imagine that the soil assemblage on landscapes of various interpluvials differed significantly, as duration and intensity of the major cycles are probably not greatly dissimilar. R. R. Shroba of the U.S. Geological Survey is now conducting detailed studies of soils in the eastern Bonneville basin to help solve some of these problems.

At present, there are two major parts of the published Lake Bonneville chronology (fig. 2) that are in need of revision (Scott, 1979a, 1979b), 1) the inferred lake rise to or close to the altitude of the Provo shoreline about 10,000 ya and 2) broad problems in the definition, identification, and correlation of Alpine and Bonneville Formations.

Inferred Lake Rise at about 10,000 Years Ago

Morrison (1965a) and Broecker and Kaufman (1965) presented evidence for a rise of Lake Bonneville to or nearly to the Provo shoreline (altitude about 1,455 m along the Wasatch Front) at or slightly after 10,000 ya following a brief low stage between 11,000 and 12,000 ya (fig. 2). Deposits of this lake rise are included in the lower member of the Draper Formation of Morrison (1965a). The name Provo II was applied by Bissell (1963) and Eardley and others (1957) for the younger deposits of their two-fold Provo Formation which were assumed equivalent to the lower member of the Draper Formation by Morrison (1965a). The evidence for this low regression and lake rise came from several widely spaced areas (fig. 1) including several localities near Salt Lake City (Eardley and others, 1957) that are either no longer exposed or were discussed and modified by Morrison (1965a), three areas in the southern Utah Valley (Bissell, 1963), the delta of Weber River southeast of Ogden (Broecker and Kaufamn, 1965), and Dry Creek in the eastern Jordan Valley (Morrison,

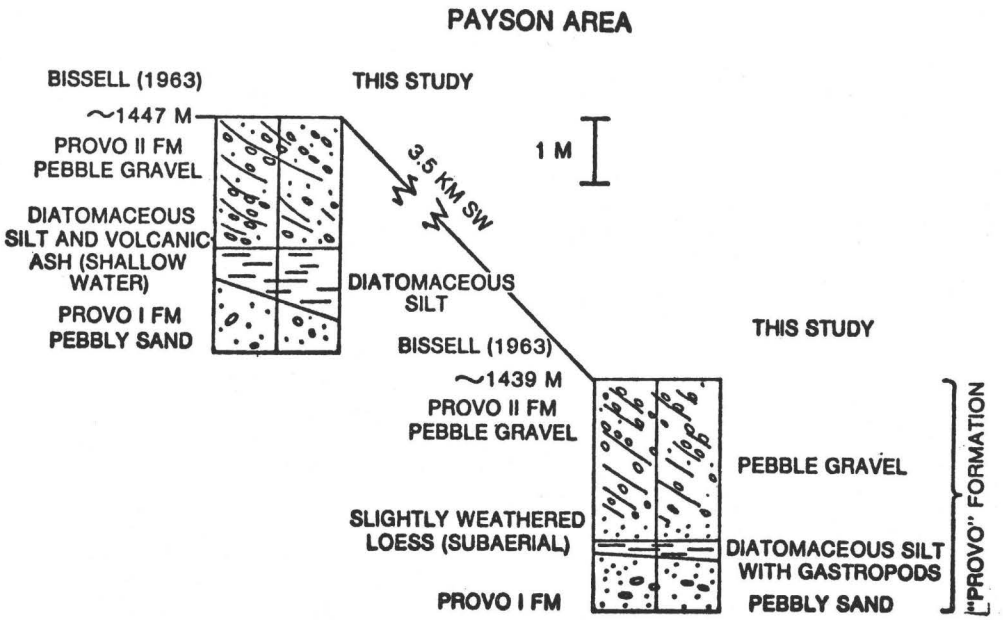

Figure 3. Bissell's (1963) stratigraphic sections near Payson presumably showing evidence of Provo I/ Provo II fluctuations. In this study, the deposits of silt are considered to be of lacustrine origin and no evidence of an unconformity is present.

1965a). Thus far in my investigations, in none of these areas or elsewhere have I found any convincing evidence for this lake fluctuation.

In the southern Utah Valley, Bissell (1963) presented evidence that suggested to him that the lake had dropped at least 24 m below the Provo shoreline and had then risen to within about 12 m of the level of the Provo shoreline -- a minor fluctuation compared to the fall of almost 300 m inferred by Morrison (1965a) and Broecker and Kaufman (1965) (fig. 2). Bissell's evidence came from three stratigraphic sections, of which two near Payson are still exposed (figs. 1 and 3). At both localities, thin (generally less than 40 cm), fine-grained deposits, lie between lacustrine pebbly sand and pebble gravel of the Provo I and II Formations respectively. These fine-grained deposits have been variously described as diatomaceous and bentonitic silt, volcanic ash, and slightly weathered loess all indicating shallow water or subaerial exposure. Because the localities are geographically separated and are not radiometrically dated, at present, only the similarity of the sequences suggests that they are of equivalent age.

My examination of these deposits revealed no evidence of weathering or of subaerial deposits. Oxidation in the fine-grained units is confined to along contacts with the enclosing deposits and is more likely of ground-water than pedogenic origin. Samples of these fine-grained units were examined by J. P. Bradbury and R. M. Forester of the U.S. Geological Survey (pers. commun., 1979) and found to contain numerous ostracodes, diatoms, charophytes, sponge spicules, gastropods, and bivalves that all indicate depostion in a lacustrine environment. The diatom and ostracode assemblages from the lower locality (right side of fig. 3) indicate shallow-water conditions (less than a few meters) with abundant aquatic vegetation. All three units at the lower locality are part of a spit complex at and below the Provo shoreline trending south from the delta of Peteetneet Creek. The diatomaceous silt was probably deposited in a shallow lagoon within this spit complex and later covered by prograding spit gravel. The depth of water in which the upper gravel was deposited is not known, but the pebble-size clasts suggests shallow water also. Thus there is no compelling evidence for a significant lake fluctuation, and, indeed, there may be no evidence for any fluctuation at all. There is certainly no evidence to support a fluctuation of the magnitude envisioned by Morrison (1965a) and Broecker and Kaufman (1965).

Broecker and Kaufman (1965) dated marl and disseminated organic material from deposits mapped as Alpine Formation by Feth and others (1966) and obtained dates indicating that 20 m of clay, silt, and fine sand were deposited on the Weber delta after about 10,000 ya when the lake stood above 1,426 m (figs. 1 and 4). There are two problems in interpreting these dates and deposits -- first with the validity of the dates and second with the stratigraphy itself.

There are inconsistencies in the radiocarbon dates (fig. 4). The dates by both laboratories on disseminated organic matter within the sediments and L-dates on marl were nearly equivalent. However dates on marl by Rubin and Alexander (1958) were 3,000 to 3,500 years older than the other dates eventhough marls are subject to contamination by exchange with young carbon in ground water. Possibly the lake water, from which the carbonates were precipitated, had a great enough ^{14}C deficiency to give an apparent age several thousand years too old, but this seems unlikely (Broecker and Walton,

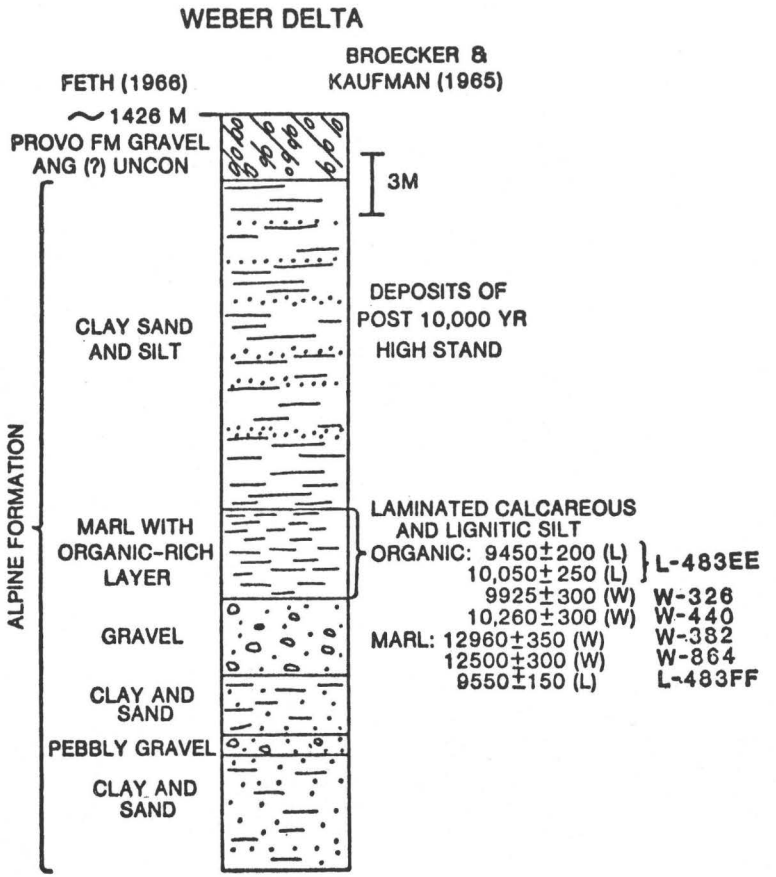

Figure 4. Section north of Weber River described by Feth and others (1966) with dates and interpretations of Broecker and Kaufman (1965) (L-dates) and dates of Rubin and Alexander (1958) (W-dates).

1959). It's more likely that the dates on organic matter and the young date on marl are contaminated and that the older carbonate ages are less contaminated and closer to the true age, which may be significantly older still.

Another problem is that the deposits in this section are disrupted by repeated landsliding and their original order is not reliably known. There is no way to confidently interpret this section. In fact, it is possible that landsliding, following dissection of the deltic deposits during the last regression of the lake, not only initiated the landsliding of the sediments, but also provided the mechanism, through infiltration of roots and ground and surface water, for contamination of the dated materials. In addition, there is no evidence in this section from below the dated sediments for the major lake regression that presumably occured prior to the 10,000 yr old rise.

Examination by me and others of Morrison's (1965a) type area of the lower member of the Draper Formation along Dry Creek (figs. 1 and 5) did not find evidence to support his interpretation of a lake rise to 1,450 m following near dessication of the lake and formation of the Graniteville Soil after deposition of Provo deposits (fig. 2). The sequence is well described (Morrison, 1965a, p. 37-39) -- my argument is with the lacustrine origin of the lower Draper deposits. The sediments dip gently toward the axis of the valley of Dry Creek indicating that they were derived from the slopes of the valley, and can not possibly be deltaic (Morrison, 1965c) with a source up valley. The deposits are also very poorly sorted and crudely bedded. They have none of the sedimentary characteristics of typical lacustrine sediments; in fact, they are of colluvial and alluvial origin. Many of the features of sorting and bedding characteristic of the lower Draper are produced in small modern fans at the mouths of gullies eroded into the lower Draper. The deposits also contain at least one soil with a weak cambic B horizon and several zones with insect burrows and root tubes indicating subaerial exposure.

These lower Draper deposits in Dry Creek are also probably younger than previously interpreted. Broecker and Kaufman (1965) report a date of 9,800 $\pm$ 300 ^{14}C yr B.P. (L-680B) on charcoal from the alluvium beneath the Graniteville Soil. Allowing at least 2,000-3,000 yr for the formation of the cambic B horizon of the soil makes the base of the lower Draper about 6,800-7,800 yr old -- well within the Holocene and a time that most workers agree pluvial lakes in the southwestern United States were at low levels.

In addition to the absense of any definitive evidence to support the lake rise at 10,000 ya, there is other evidence that strongly suggests that lake levels were low at this time (Mehringer, 1977). The best evidence comes from Danger Cave (altitude 1,314 m, about 40 m above the level of present Great Salt Lake) near Wendover on the Utah-Nevada border (figs. 1 and 6). Here, more than twenty years ago, Jesse D. Jennings (1957) presented stratigraphic and dating evidence for low lake levels from shortly before 10,000 to 11,000 ya to the present. Hunt and Morrison (1957) found no evidence of inundation of the cave by lake water after the initiation of deposition of cave sediments sometime before 10,000 to 11,000 ya. In the 1960's, many of the materials first dated by the old solid-carbon techniques used in the 1950's by the Michigan and Chicago laboratories were redated at Texas using modern methods and comparable dates were obtained (Tamers and others, 1964). Significant to

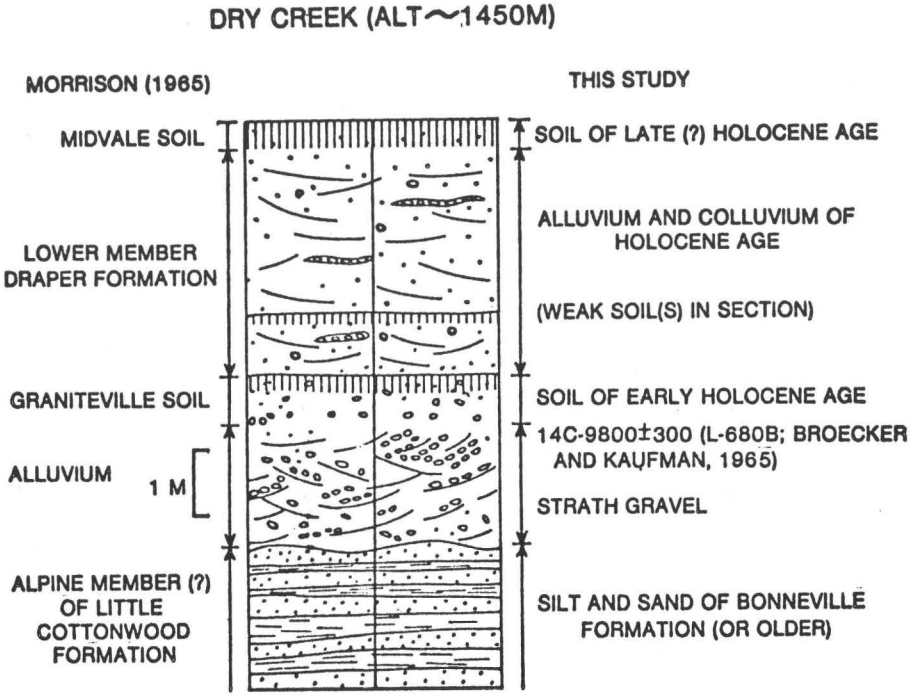

Figure 5. Section along Dry Creek at Morrison's (1965a) type area of the lower member of the Draper Formation (originally referred to as the lower tongue of the Draper Formation). In this study, the lower Draper is considered to be of alluvial and colluvial origin, whereas Morrison considered it to be lacustrine.

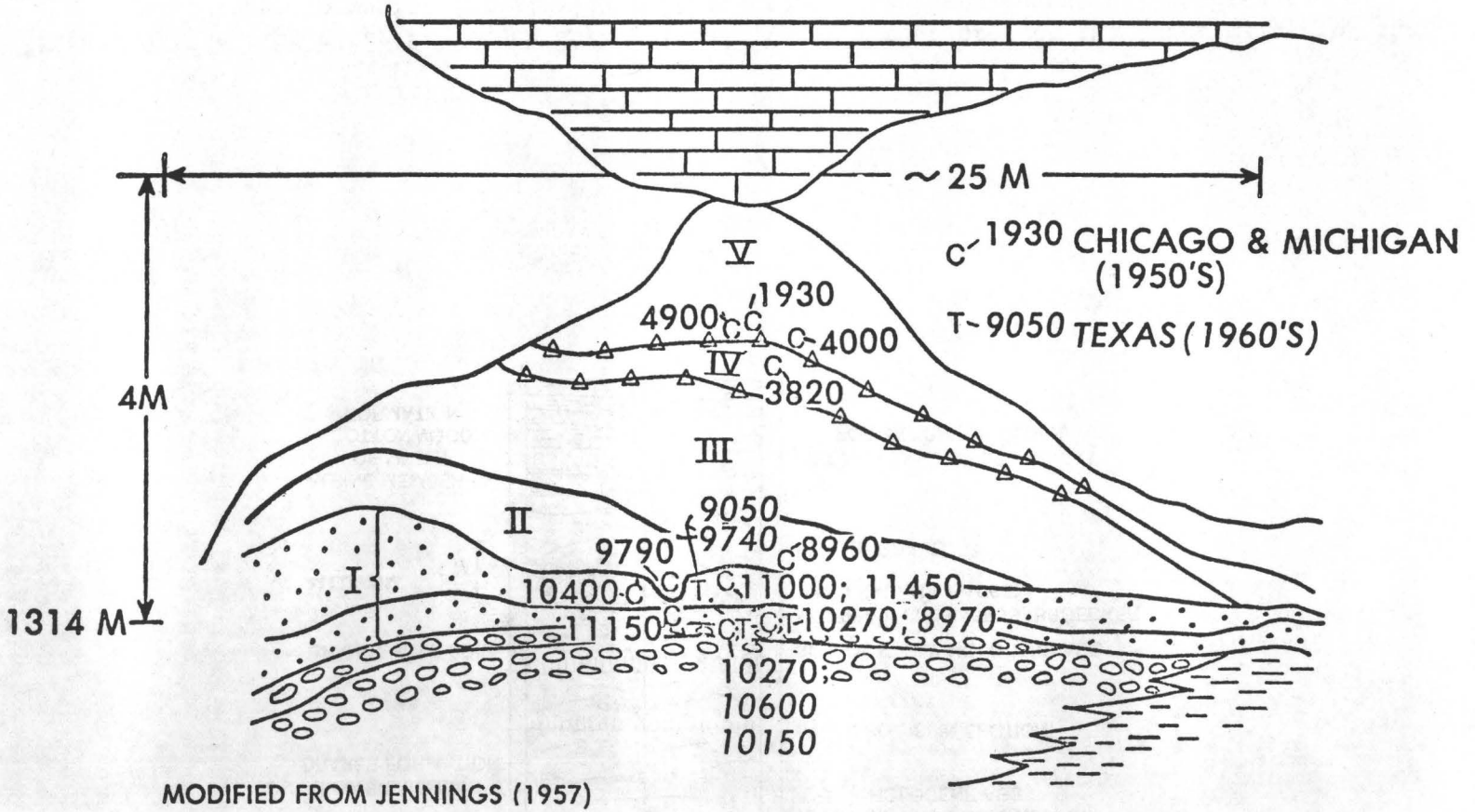

Figure 6. Stratigraphy and dates from Danger Cave after Jenning (1957) and Tamers and others (1964). Pebble pattern = lake gravel; dashed pattern = lacustrine silt and clay; dot pattern of Unit I = sand (lower part of unit is lacustrine sand; upper part of unit is eolian sand); triangles = roof-fall deposits; Units II to V are cave deposits.

the interpretation is that many of the dates are on dung. According to T. VanDevender (pers. commun., 1978) the dung would probably not have been preserved had the cave ever been wet -- which it surely would have been had it been under more than 130 m of water during the proposed lake rise at 10,000 ya.

At present, no available data closely date the regression of Lake Bonneville from its late Wisconsin high during the Bonneville cycle. Bright (1966) presents evidence from Red Rock Pass indicating that overflow through the pass ceased prior to 12,090 ± 300 ^{14}C yr B.P. (W-1338) as the lake fell below the Provo shoreline. The information from Danger Cave suggests that by sometime before 10,000 to 11,000 ya the lake stood below 40 m of the level of present Great Salt Lake, or perhaps somewhat more than 40 m if isostatic effects are considered. A date from the Hooper Drain near Ogden on rooted plant remains in sands having characteristics of shallow-water deposition suggests a low lake level (perhaps not greatly more than 10 m above the level of present Great Salt Lake) about 9,730 ± 350 ^{14}C yr B.P. (W-386) (Feth, 1955, p. 48; Rubin and Alexander, 1958). Recently R. D. Miller (pers. commun.), 1979) obtained a date on gastropods from sediments 9 m above the level of Great Salt Lake at the north end of Bear River Bay lying below deposits related to the Gilbert shoreline. The date (W-4395) of 10,920 ± 150 ^{14}C yr B.P. strongly suggests that after 11,000 ya lake fluctuations were small. This is in accord with other climate-related evidence from the area. Bright's (1966) pollen diagram from Swan Lake at Red Rock Pass indicates that the major vegetation change at the end of the last glacial/pluvial had occured by about 10,000 ya, suggesting that environmental conditions more like the present than full glacial/pluvial conditions existed at that time. Mehringer, Nash, and Fuller (1971) date deglaciation of the Raft River Mountains at about 12,000 ya. Madsen and Currey (1979) have shown that by 10,000 to 12,000 ya glaciers in the Wasatch Range had retreated far up into valleys presumably reflecting that a change to more interglacial conditions had occured prior to 10,000 ya. A pattern of lake regression, with low lakes after 10,000 to 11,000 ya, is also consistent with data from Lake Lahontan (Benson, 1978) and Searles Lake (Smith, 1979). A major expansion of Lake Bonneville at this time to about one-half of its maximum volume during the Bonneville cycle seems unlikely.

Problems of Bonneville and Alpine Formations

The problems of Bonneville and Alpine Formations involve their definition usage, age, and correlation, therefore a brief history of their use follows.

Bonneville Formation contains deposits of the last major lake cycle of Lake Bonneville; Alpine sediments were deposited during the next to the last major lake cycle or group of cycles (fig. 2) (Hunt, 1953; Varnes and Van Horn, 1961; Bissell, 1963; Morrison, 1965a, 1965b; Feth and others, 1966; and Van Horn, 1972). Explicit in this concept is that between these major pluvial cycles an interpluvial occurred -- a time of incision of lacustrine deposits, formation of soils, and deposition of alluvial, colluvial, and eolian deposits in areas that during pluvials were inundated by Lake Bonneville. However, in none of the mapping along the Wasatch Front by Hunt (1953), Bissell (1963), Morrison (1965a), Feth and others (1966), and Van Horn (1972), was convincing evidence presented for a major break between the deposits mapped as Bonneville and Alpine particularly at altitudes above about 1,455 m (approximately the

altitude of the Provo shoreline). In fact, Morrison (1965a) mapped Bonneville and Alpine Members of the Little Cottonwood Formation because he could find no major break. Feth and others (1966) mapped much "Bonneville-Alpine Formations, undifferentiated" and Williams (1962, p. 137) did likewise, noting that the break used by others was more likely a facies change than a major unconformity. Bright (1963) discussed the problem of identifying Alpine deposits unless clear evidence of an unconformity is present. He described sediments of possible Alpine age in northern Cache Valley that occur below disconformities with associated buried soils.

Morrison (1965b), working in the large gravel pits at Little Valley near Promontory Point, locally mapped Alpine Formation as being separated from deposits of the Bonneville lake cycle by a buried soil (Promontory Soil) and subaerial deposits (figs. 2, 9, and 10). The lack of such evidence between deposits mapped as Bonneville and Alpine along the Wasatch Front has been ascribed to the effectiveness of erosion on the exposed shores there during lake transgressions.

Throughout the 1960's, the consensus, based largely on the inferred age of the moraines at the mouths of Little Cottonwood and Bells Canyons (Richmond, 1964) (revised in recent work by McCoy (1977) and Madsen and Currey (1979)) and their relationship to deposits of Lake Bonneville (Morrison, 1965a) and on correlations with the midwestern glacial sequence through the use of soil stratigraphy (Morrison and Frye, 1965), was that the Bonneville Formation was of late Wisconsin age (22,000 to 12,000 yr old) and that the Alpine was of early Wisconsin age (75,000 to 30,000 yr old). In 1975, based on a reevaluation of the Bonneville sequence in light of recent evidence from marine oxygen-isotope studies and dating of glacial deposits in the Rocky Mountains, Morrison (1975) revised his previous work and suggested correlation of the Alpine with isotope stage 6 of the marine record, indicating an inferred age of 135,000 to 150,000 yr.

The basic problem in the use of Alpine and Bonneville Formations is shown in Figure 7. As mapped locally at Little Valley by Morrison (1965b) and at a few localities along the Wasatch Front by other workers (fig. 9) (in almost all cases at altitudes below the Provo shoreline), Bonneville and Alpine Formations are separated by an unconformity displaying one or more of the following characteristics: 1) a soil or soil complex, 2) subaerial deposits, and 3) a disconformity with relief of from several meters to as much as several tens of meters formed by landscape incision following the base-level fall caused by the regression of a deep lake. However, everywhere I have observed the previously mapped contact between Bonneville and Alpine Formations in the high-shore zone (the zone within about 80 m vertically of the Bonneville shoreline) I could find no evidence of a major disconformity. In most places the contact seems better explained as a facies change, or as a minor disconformity with little relief, perhaps only representing minor scouring by lake currents. Many of the presumed coarse-grained subaerial deposits are coarse-grained subaqueous debris-flow deposits. No where is there a soil, subaerial deposits, or a significant disconformity; the sediments of both formations seem to have been deposited during the same lake cycle. In high-shore zones where exposures are deep, a soil or unconformity at the base of the Bonneville and Alpine sediments is invariably formed on subaerial deposits or bedrock--older lacustrine sediments are not present. This soil and associated unconformity beneath deposits mapped as Alpine appear

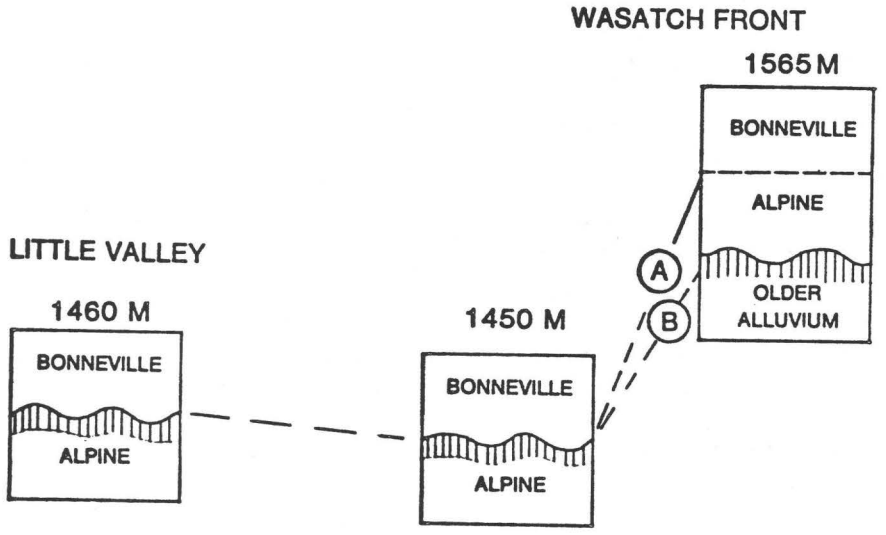

Figure 7. Relationship of Alpine and Bonneville Formations at Little Valley and along the Wasatch Front. Wavy lines are disconformities; hachures represent soils or soil complexes and/or subaerial deposits. A is correlation of previous workers; B is suggested correlation discussed in this paper. Vertical dimensions of sections are not to scale.

likely to correlate with the Alpine-Bonneville unconformity at the localities from lower altitudes shown in figure 9 (B in fig. 7). Such confusion in the use of Alpine Formation and the realization that the type deposits (Hunt, 1953) were probably deposited during the Bonneville lake cycle suggest to me that the term Alpine Formation needs to be redefined or perhaps abandoned.

The character of the unconformity below deposits of the Bonneville cycle in a high-shore zone, having the expected characteristics mentioned earlier, is well displayed in large gravel pits north of the mouth of Big Cottonwood Canyon (figs. 1 and 8). Here lake sediments of the Bonneville cycle, including marly sandy silt, sand, gravel, clayey silt, and bouldery subaqueous debris-flow deposits, and related outwash of Pinedale age, bury a topography with relief of at least 20 m and probably as much as 80 to 100 m -- similar in relief to the topography eroded into Bonneville deposits along the mountain front during the Holocene. A soil or soil complex, better developed than soils formed on Bonneville deposits during the Holocene, are widely present below the unconformity, on here what was a point projecting into the lake and greatly exposed to wave attack. Debris-flow deposits, loess (?), and other subaerial deposits also mark the unconformity. The dominant pre-Bonneville-cycle deposit here is alluvium, similar in lithology to the outwash of Pinedale age, but having a somewhat siltier matrix and more boulders. This older deposit is probably also outwash from Big Cottonwood Creek. In a gravel pit to the north of the pit shown in figure 8, once deeply concealed older lacustrine gravels have now been exposed that interfinger and grade upwards into the older outwash. The highest altitude reached by the lake sediments is 1,520 m, about 65 m below the Bonneville shoreline. Here these deposits are greatly disrupted by faulting and may now be at a higher altitude than when deposited.

In contrast to previous interpretations of one or several pre-Bonneville-cycle fluctuations that reached close to the Bonneville shoreline (Hunt, 1953; Bissell, 1963; Morrison, 1965a and 1965b; Van Horn, 1972), I feel that there is no unequivocal evidence of deposits of lake cycles older than the last that occur within about 70 m of the level of the Bonneville shoreline. One problem in identifying these older sediments along the Wasatch Front is that they have generally been deeply buried by Bonneville-cycle and related deposits. Significantly the two highest exposures of pre-Bonneville-cycle sediments that I have studied, including the one described in the previous paragraph, consist of shore facies and may well mark the highest rise of the next-to-the-last lake cycle. The deposits at the second locality, which is at Point-of-the-Mountain near Jordan Narrows, are probably less deformed by faulting than the sequence in the Big Cottonwood area. Here the highest pre-Bonneville-cycle lake gravels are exposed at an altitude of about 1,494 m, about 90 m below the Bonneville shoreline. If this significant difference between Bonneville and pre-Bonneville-cycle levels is real, its cause is not clear at present and further work is necessary before an explanation can be offered. Possibilities include the diversion of Bear River into the Bonneville basin (Bright, 1963) or differences in the character of the last two pluvials.

Many exposures occur at altitudes below high-shore zones where lacustrine deposits of the Bonneville cycle are separated from lake deposits of the previous (?) cycle by major unconformities bearing soils and subaerial deposits (fig. 9). For most of these sections, except for the notoriously

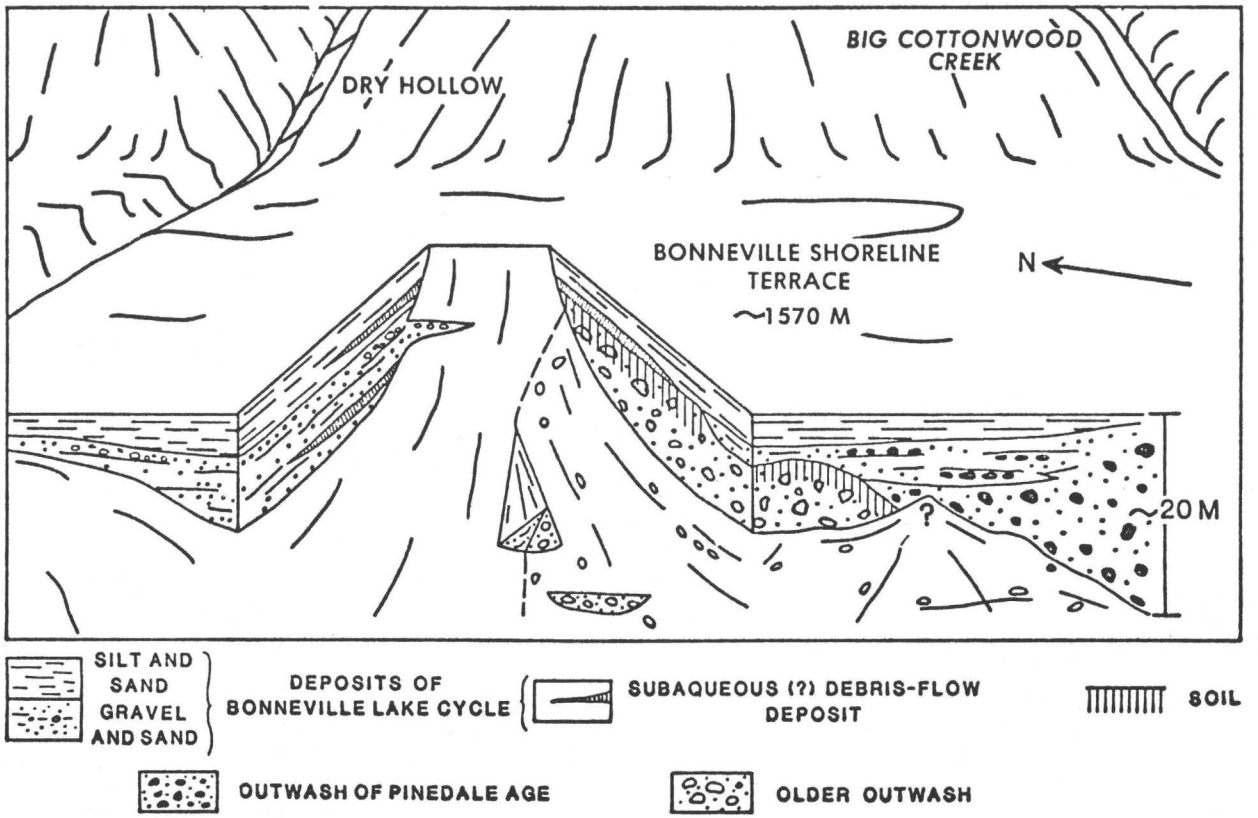

Figure 8. Relations in gravel pit north of the mouth of Big Cottonwood Canyon showing disconformity and soil and subaerial deposits on older outwash of Big Cottonwood Creek and overlying deposits of the Bonneville lake cycle and Pinedale Glaciation.

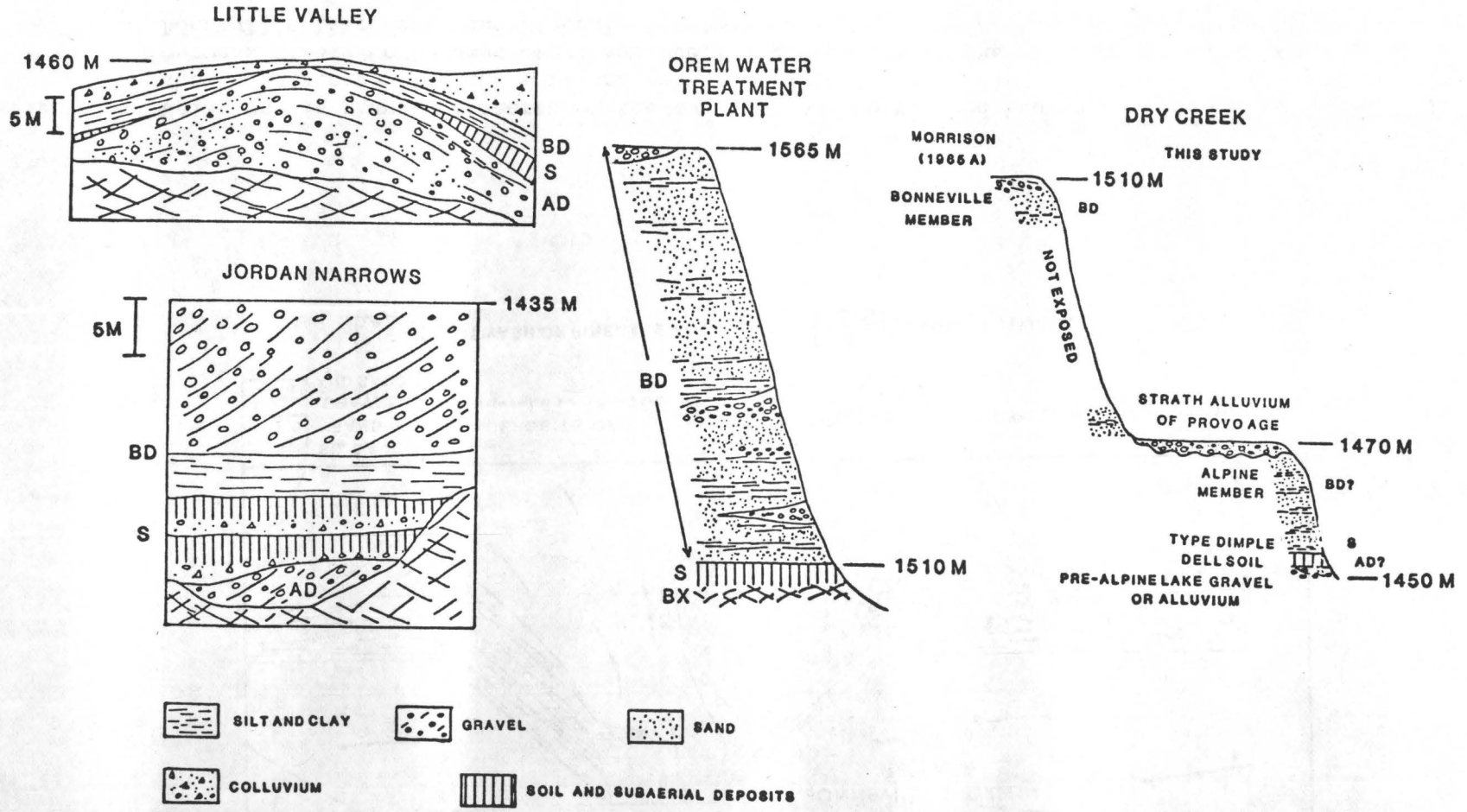

Figure 9. Diagrammatic stratigraphic sections from localities in the eastern Bonneville basin showing relationship between deposits of the Bonneville lake cycle (BD), unconformity and associated soil or soil complexes (hachured) and subaerial deposits (S), and deposits of the "Alpine" cr next-to-the-last lake cycle (AD). Bx = bedrock. Section at Little Valley is adjacent to Morrison's (1965b) type locality of the Promontory Soil. Section from strath gravel to valley bottom is at type Dimple Dell Soil (Morrison, 1965a).

uncertain technique of counting in sequence, there is no reliable method for correlating the older lake deposits in these widely spaced localities. Current studies by W. D. McCoy, University of Colorado, of amino-acid stereochemistry of calcareous fossils from these deposits will hopefully provide such a reliable correlation tool.

A further stratigraphic consequence of this evaluation of previous mapping in high-shore zones is the inaccuracy of the long-held paradigm that the Bonneville Formation is thin and represents a relatively brief lake cycle compared with the long cycle or series of cycles during which the thick Alpine Formation was deposited (Hunt, 1953; Bissell, 1963; Morrison, 1965b). As sediments previously mapped separately as Alpine and Bonneville Formations, especially in high-shore zones, appear to have been deposited during the same lake cycle, the deposits of the Bonneville lake cycle are thick, especially in high-sedimentation-rate areas along the Wasatch Front such as at the mouths of Big and Little Cottonwood, Dry (both), Hobble, and Maple Creeks, and Weber, Ogden, and Provo Rivers, and American and Spanish Forks -- generally drainages that contained glaciers. Furthermore the thickness of the sediments of the Bonneville cycle as measured from the top of the first buried soil in the Burmester core (10 m) (Eardley and others, 1973) is comparable in thickness to deposits of the older lake cycles present in the core. This suggests that the deposits of the the various lake cycles did not differ greatly in thickness, nor did the lake cycles apparently vary greatly in duration.

Observations at numerous localities in the eastern Bonneville basin attest to the large thickness of the sediments of the Bonneville cycle that were deposited during the transgression to and the stand at the Bonneville shoreline. Delta and bar complexes with associated alluvial and lagoonal deposits occur at several levels between the Provo and Bonneville shorelines -- the Intermediate shorelines of Gilbert (1890) -- and also below the Provo shoreline (fig. 8 and 10). As seen where stratigraphic relations are well exposed, successively higher deposits overlap lower deposits. Thus the sediments become progressively younger toward the Bonneville shoreline. In many areas, these shore deposits at intermediate altitudes are overlain by a sequence of fine-grained beds deposited while the lake stood nearer to or at the Bonneville shoreline. No convincing evidence of major fluctuations in lake level during the Bonneville cycle has been seen (see next paragraph). These relations and the lack of regressional deposits between Bonneville and Provo levels agree with Gilbert's (1890) conclusions that the lake transgressed to the Bonneville shoreline with several intermediate stillstands and then fell rapidly from the Bonneville shoreline to the Provo shoreline during the Bonneville Flood. Pending ^{14}C dates on wood and gyttja and amino-acid measurements on mollusk shells from within these transgressional deposits should yield valuable information on their age and on the history and character of the Bonneville transgression.

These observations relate to another stratigraphic problem concerning the nature of the Bonneville cycle. From his work in Little Valley, Morrison (1965b) proposed that the lake had risen to or close to the Bonneville shoreline twice during the Bonneville cycle, separated by a low transgression to within at least 35 m of the present level of Great Salt Lake (fig. 2). In light of the previous discussion of the character of unconformities formed during major lake regressions, the unconformity between the mapped members of the Bonneville Formation is not convincing in supporting this interpretation.

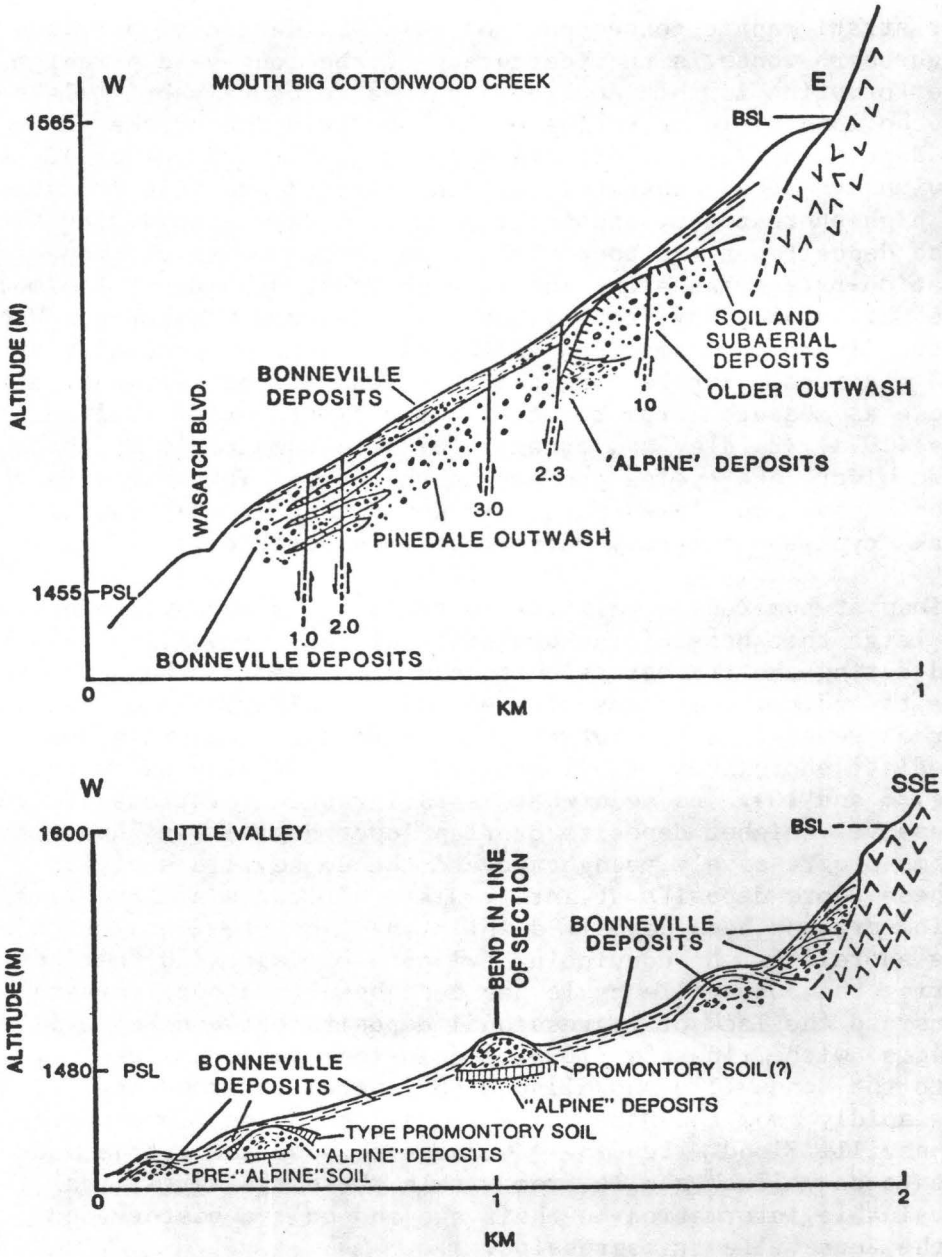

Figure 10. Diagrammatic longitudinal sections through deposits of the Bonneville lake cycle and older deposits and soils between the altitudes of the Bonneville (BSL) and Provo (PSL) shorelines. Hachured zones represent soils and subaerial deposits. Dashed units are fine-grained deposits of the Bonneville cycle, which in many places are marly. Dots and solid circles are lacustrine sand and gravel; dots and open circles are outwash. In previous investigations (Morrison 1965b, 1965d) at Little Valley; Van Horn (1972) in the Big Cottonwood area) much of the gravel mapped here as Bonneville was mapped as Alpine Formation. On Big Cottonwood section, numbers on faults are offsets in meters.

Very little disconformity occurs even though the lower member (white marl member) mantles the valley sides and the fine-grained marl would have been highly susceptible to gullying if exposed on these steep slopes. Thin, coarse-grained deposits of angular to subangular gravel occur locally between the members, but always below steep slopes where rubble could have been transported the short distance to deep water, perhaps as rockfall or as subaqueous debris flows or rafted by shore ice. In other places at Little Valley, the contact is marked by a few centimeters or less of sand and pebbles that locally contain gastropods. This thin unit may also be of lacustrine origin. As sand and pebbles occur scattered throughout both members, which are generally marly, the thin zone of sand and pebbles may relate more to a minor shoaling of the lake or cessation of marl deposition than to a major lake regression. Elsewhere, including the Wasatch Front, no evidence has been reported to support this proposed two-fold Bonneville cycle. More work is necessary to better understand the relationship between the members at Little Valley, but the above observations suggest that the two-fold Bonneville cycle may not be valid. Furthermore, the major regression between deposition of the members would have occurred at a time (13,000 to 18,000 ya) of major glaciation in mid-latitudes -- an unlikely time for a major drop in lake level.

Another problem related to the Bonneville cycle concerns the lake history during earlier times of the Wisconsin -- isotope stages 3 and 4 of the marine oxygen-isotope record (Shackleton and Opdyke, 1973). Climate-related indicators such as the marine record show clearly that in mid-latitudes the Wisconsin Glaciation began about 75,000 ya, fluctuated in intensity, and ended about 12,000 to 10,000 ya. By radiometric dating, many deposits of the Bonneville cycle are known to be equivalent in age to isotope stage 2, the classical late Wisconsin. Certainly an important problem remaining is how synchronous and similar in magnitude were Lake Bonneville fluctuations to glacial oscillations inferred from the marine record. Also, did some of the deposits of the various stillstands during the transgression to the Bonneville shoreline occur during isotope stages 4 and/or 3, or did they all occur during stage 2? What was the lake history during these earlier times of the Wisconsin?

The answers to these and many of the stratigraphic problems discussed earlier must await the outcome of current stratigraphic and dating studies, both along the Wasatch Front and in other areas in the eastern Bonneville basin. Especially important will be the results of amino-acid studies of fossils from the Lake Bonneville deposits. Although in a developmental stage, preliminary results look promising (Miller, Nelson, McCoy, and Metcalf, 1979). Problems in taxa-dependent factors, reaction kinetics, and temperature history are currently being investigated. Hopefully the technique will become a significant correlation tool and perhaps a reliable dating method as well.

Summary

Figure 11 summarizes my current view of the status of Lake Bonneville chronology. The diagram stresses events that I feel are relatively well supported as well as major gaps in our knowledge. There were multiple fluctuations of Lake Bonneville throughout the Quaternary. In basin-floor cores, some of the deposits of early Quaternary age are well dated by associated volcanic ashes and paleomagnetic reversals (Eardley and others,

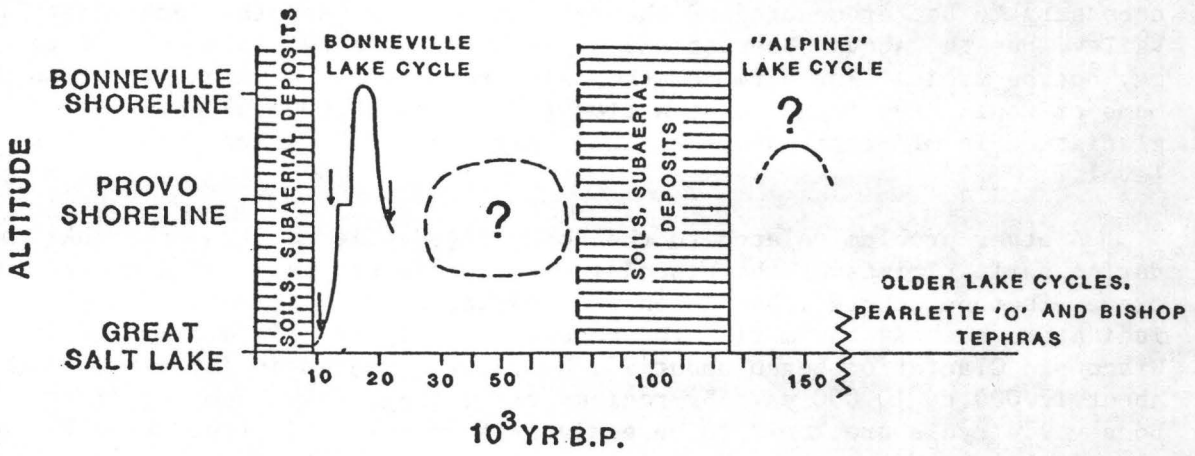

Figure 11. Summary diagram showing, for the last 150,000 yr, well supported events in Lake Bonneville history and problem areas (?) discussed in text. Older lake fluctuations, soils, and tephras are not shown in detail. Evidence of these fluctuations occurs below 1400 m in altitude. Arrows indicate limiting radiocarbon dates on wood or plant material on the chronology of the Bonneville lake cycle.

1973). Equivalent deposits are only positively known in the shore record from Little Valley, where they occur at low altitudes -- below about 1,400 m (Morrison, 1965b). In other areas, especially along the Wasatch Front, high sedimentation rates and active tectonism make exposure of these deposits unlikely.

The following parts of the younger record (last 150,000 yr or so) are of major importance to Wasatch Front studies.

1) Presently no convincing evidence proves that fluctuations of pre-Bonneville-cycle lakes reached above about 1,495 m along the Wasatch Front; more than 80 m below the level of the Bonneville shoreline.

2) A major disconformity with associated soil and subaerial deposits occurs between deposits of the last and the next-to-the-last major lake cycles. The characteristics of the soil formed on the older lake sediments and buried by deposits of the Bonneville lake cycle suggests that the older deposits are probably correlative with isotope stage 6 (130,000 to 150,000 yr) of the marine record.

3) Nothing is yet known from shore areas of lake history during the early Wisconsin (30,000 to 75,000 ya) -- isotope stages 3 and 4 of the marine record.

4) Radiocarbon dates on wood indicate that by 21,000 to 20,000 ya the level of the Bonneville-cycle lake was approaching about 1,400 m (Morrison, 1965b).

5) The general transgression to the Bonneville shoreline included several apparent stillstands during which bar complexes with associated lagoonal sediments were locally deposited (fig. 10). However, there is no good evidence of major regressions within the Bonneville-cycle deposits.

6) The lake level dropped quickly from the Bonneville shoreline to the Provo shoreline during the Bonneville Flood as evidenced by the lack of regressional deposits between these shorelines (Gilbert, 1890).

7) Sometime before 12,000 ya overflow through Red Rock Pass ceased and the lake level fell below the Provo shoreline (Bright, 1966). By 10,000 to 11,000 ya the lake level had dropped below about 1,314 m as indicated by the Danger Cave data and has not been higher since (Jennings, 1957; Hunt and Morrison, 1957). Holocene fluctuations are poorly understood, but are currently being studied by D. R. Currey and his students at the University of Utah.

Significance of New Stratigraphic Interpretations to Earthquake-Hazard Studies

The evaluation of previous stratigraphic concepts and new interpretations of Lake Bonneville history just presented are important to investigations of earthquake-hazard assessment including studies of fault-scarp morphology as a method of dating surface faults, studies of fault age using the relationship of faults to landforms and deposits of known age such as Lake Bonneville shore features and pre- and post-Lake Bonneville alluvial fans, and estimating recurrence intervals of faulting and rates of tectonism using deposits and landforms of known age as datums.

Methods of estimating the age of fault scarps that rely on fault-scarp morphology (Wallace, 1978: Bucknam and Anderson, 1979) require that scarps of known age be used to calibrate their models of fault-scarp modification. Thus

far in the eastern Great Basin, dated fault scarps are not abundant. The shorelines of Lake Bonneville, where eroded into older deposits, are valuable fault-scarp analogues (Bucknam and Anderson, 1979). The shorelines and their associated deposits are also valuable datums for providing limiting ages of faults, evidence of recurrent movement on faults, and estimation of rates of tectonism when age and offset of the datum is known. Unfortunately none of the major shorelines are yet well dated .

The age range of the Bonneville shoreline -- 20,000 to 12,000 yr old -- can presently only be estimated from limiting dates from deposits at altitudes generally more than 100 m below the shoreline (Morrison, 1965b; Broecker and Kaufman, 1965). Most of the radiometric ages are on carbonates and inspire little confidence in their reliability. Present stratigraphic studies in several Wasatch Front areas are providing potentially closer limiting ages from altitudes much closer to the level of the shoreline. Charcoal and disseminated organic matter (A horizons) associated with soils buried by transgressive Bonneville deposits within 30 m of the level of the Bonneville shoreline are now being prepared for radiocarbon dating and hopefully will provide reliable dates. Radiocarbon dating and amino-acid determinations from materials that were collected from transgressive deposits at lower altitudes will also provide closer limiting ages than are currently available.

A related problem that could potentially introduce error in these fault-related studies involves the possibility that shorelines of "Alpine" age are locally the highest shorelines along some ranges in the center of the basin (Morrison, 1965b, p. C114), due to greater isostatic rebound of the older shorelines as a result of a longer lake cycle that would provide a longer time for the crust to attain equilibrium with its load (Crittenden, 1963a; 1963b). Considering from the preceeding discussion of Alpine and Bonneville Formations that no convincing evidence of pre-Bonneville-lake-cycle deposits within about 80 m of the Bonneville shoreline has been found, the possibility of older shorelines occurring above the Bonneville shoreline appears remote.

The age of the Provo shoreline is more closely known -- 13,000 to 9,000 yr. However, as discussed earlier, the possibility of its having been occupied twice (Provo II) seems unlikely and at present an age of 12,000 to 14,000 yr seems more likely. A significant lower limiting age on the occupation of the Provo shoreline is a basal date of 12,090 $\pm$ 300 (W-1338) from Swan Lake in Red Rock Pass. Apparently by that time lake overflow at the Provo level through Red Rock Pass had ceased and fans from local drainages had dammed Swan Lake (Bright, 1966).

The ages of shorelines at lower altitudes (Stansbury and Gilbert) are also poorly known. However they are generally depositional shorelines rather than erosional (in sediments) and of little use as fault-scarp analogues. Also they tend to lie on lower basin slopes that are generally not faulted. A point of debate is whether or not the Gilbert shoreline is of pre-Altithermal (>7,000 yr old) (Currey and Madsen, 1974) or post-Altithermal (<4,000 yr old) age (Van Horn, 1979).

Recent detailed investigations of late Quaternary behavior of the Wasatch Fault south of Provo (Schwartz and others, 1979) show well the potential for using stratigraphic units of late Quaternary age to determine recurrence of faulting. However, uncertainities in the age of critical, faulted deposits in

the high-shore zone need to be resolved before a reliable estimate of longer term recurrence can be made. These deposits were mapped by Bissell (1963) as thin gravelly Bonneville Formation ovelying thick, generally fine-grained Alpine Formation -- the unit for which an estimate of fault displacement is obtainable. According to published mapping and correlations, the Alpine could be from 30,000 to 75,000 or 135,000 to more than 150,000 yr old -- too broad a range to be of much use in estimating recurrence of faulting. However, as seen elsewhere in high-shore zones, the stratigraphic sequence (similar although finer grained than the section near Orem in figure 9) does not contain a major unconformity between mapped Alpine and Bonneville deposits. The faulted deposits therefore may be of Bonneville age, 13,000 to 21,000 yr, or possibly equivalent to sediments of earlier Wisconsin age. Further stratigraphic investigations supplemented with amino-acid studies should allow better dating of these deposits.

The difficulty of using datums in the 10^5 - yr- old range, such as deposits of the next-to-the-last major lake cycle, for evaluating fault activity is now known to be great, particularly in high-sedimentation-rate areas -- much of the Wasatch Front. The deposits are little exposed and then typically in section, not as relict surfaces. However, large gravel pits, such as those in the Big Cottonwood area, are creating deep and large enough exposures that it is possible locally to trace stratigraphic units and measure their fault offset. Locally, faulted relict surfaces of alluvial fans above the Bonneville shoreline, which are broadly datable by their associated soils, may also prove useful in these investigations.

At present there are important stratigraphic, correlation, and dating problems that need to be addressed before deposits of Lake Bonneville can be reliably used in fault studies. The published mapping, stratigraphic framework, and chronology (fig. 2) are in need of revision. Some aspects are clear, but many unknowns exist (fig. 11) for current and future investigations.

Acknowledgements

I greatly appreciate the valuable interaction I have had with many colleagues -- especially the fruitful field excursions and/or office discussions with R. B. Morrison, R. Van Horn, R. D. Miller, D. J. Varnes, D. R. Currey, W. D. McCoy C. G. Oviatt, R. R. Shroba, R. E. Anderson, Heber Lessig, R. C. Bucknam, and K. L. Pierce. D. W. Moore and R. D. Miller offered suggestions that greatly improved the manuscript.

References

Benson, L. V., 1978, Fluctuations in the level of pluvial Lake Lahontan during the last 40,000 years: Quaternary Research, v. 9, p. 300-318.

Birkeland, P. W., and Shroba, R. R., 1974, The status of the concept of Quaternary soil-forming intervals in the Western United States, in Mahaney, W. C., ed., Quaternary environments: Proceedings of a Symposium: First York University Symposium on Quaternary Research, Geographic Monographs, no. 5, p. 241-276.

Bissell, H. J., 1963, Lake Bonneville: Geology of southern Utah Valley: U.S. Geological Survey Professional Paper 257-B, p. 101-130.

Bright, R. C., 1963, Pleistocene Lakes Thatcher and Bonneville, southeastern Idaho: unpublished Ph.D. dissertation, University of Minnesota, 292 p.

_____1966, Pollen and seed stratigraphy of Swan Lake, southeastern Idaho: Its relation to regional vegetational history and to Lake Bonneville history: Tebiwa, v. 9, no. 2, p, 1-47.

Broecker, W. S., and Kaufman, Aaron, 1965, Radiocarbon chronology of Lake Lahontan and Lake Bonneville II, Great Basin: Geological Society of America Bulletin, v. 76, p. 537-566.

Broecker, W. S., and Walton, A., 1959, The geochemistry of C^{14} in fresh-water systems: Geochim. et Cosmochim. Acta, v. 16, p. 15-38.

Bucknam, R. C., and Anderson, R. E., 1979, Estimation of fault-scarp ages from a scarp-height - slope-angle relationship: Geology, v. 7, p. 11-14.

Crittenden, M. D., Jr., 1963a, New data on the isostatic deformation of Lake Bonneville: U.S. Geological Survey Professional Paper 454-E, p. E1-E31.

_____1963b, Effective viscosity of the earth derived from isostatic loading of Pleistocene Lake Bonneville: Journal of Geophysical Research, v. 68, no. 19, p. 5517-5530.

Currey, D. R., and Madsen, D. B., 1974, Holocene fluctuations of Great Salt Lake: Abstracts of the Third Biennial Meeting of the American Quaternary Association, p. 74.

Eardley, A. J., and Gvosdetsky, Vasyl, 1960, Analysis of a Pleistocene core from Great Salt Lake, Utah: Geological Society of America Bulletin, v. 71, p. 1323-1344.

Eardley, A. J., Gvosdetsky, Vasyl, and Marsell, R. E., 1957, Hydrology of Lake Bonneville and sediments and soils of its basin: Geological Society of America Bulletin, v. 68, p. 1141-1202.

Eardley, A. J., Shuey, R. T., Gvosdetsky, Vasyl, Nash, W. P., Picard, M. D., Grey, D. C., and Kukla, G. J., 1973, Lake cycles in the Bonneville basin, Utah: Geological Society of America Bulleltin, v. 84, p. 211-216.

Feth, J. H., 1955, Sedimentary features in the Lake Bonneville Group in the east shore area near Ogden, Utah: Utah Geological Society Guidebook no. 10, p. 45-69.

Feth, J. H., Barker, D. A., Moore, L. G., Brown, R. J., and Veirs, C. E., 1966, Lake Bonneville: Geology and hydrology of the Weber Delta district, including Ogden, Utah: U.S. Geological Survey Professional Paper 518, 76 p.

Gilbert, G. K., 1890, Lake Bonneville: U.S. Geological Survey Monograph 1, 438 p.

Hunt, C. B., 1953, General Geology, in, Hunt, C. B., Varnes, H. D., and Thomas, H. E., Lake Bonneville: Geology of the northern Utah Valley, Utah: U.S. Geological Survey Professional Paper 257-A, p. 11-45.

Hunt, C. B., and Morrison, R. B., 1957, Appendix A: Geology of Danger and Juke Box Cavesn near Wendover, Utah, in, Jennings, J. D., Danger Cave: Utah University Antropology Papers, no. 27, p. 298-301.

Jennings, J. D., 1957, Danger Cave: Utah University Antropology Papers, no. 27.

Madsen, D. B., and Currey, D. R., 1979, Late Quaternary glacial and vegetation changes, Little Cottonwood Canyon area, Wasatch Mountains, Utah: Quaternary Research, v. 12, p. 254-270.

Mehringer, P. J., Jr., Nash, W. P., and Fuller, R. H., 1971, A Holocene volcanic ash from northwestern Utah: Utah Academy Science, Arts, and LeHers, v. 48, pt. 1, p. 46-51.

McCoy, W. D., 1977, A reinterpretation of certain aspects of the late Quaternary glacial history of Little Cottonwood Canyon, Wasatch Mountain, Utah: unpublished M.A. thesis, University of Utah, 84 p.

Mehringer, P. J., Jr., 1977, Great Basin late Quaternary environments and chronology, in, Fowler, D. D., ed., Models and Great Basin prehistory: A symposium: University of Nevada Desert Research Institute Publications in the Social Sciences, no. 12, p. 113-167.

Miller, G. H., Nelson, A. R., McCoy, W. D., and Metcalf, A. L., 1979, Amino acid geochronology utilizing terrestrial gastropods from western U.S.: Geological Society of America Abstracts with Programs, v. 11, no. 6, p. 280 and 297.

Morrison, R. B., 1965a, Lake Bonneville: Quaternary stratigraphy of the eastern Jordan Valley south of Salt Lake City, Utah: U.S. Geological Survey Professsional Paper 477, 80 p.

_____1965b, New evidence on Lake Bonneville stratigraphy and history from southern Promontory Point, Utah: U.S. Geological Survey Professional Paper 525-C, p. C110-C119.

_____1965c, Day 3- Salt Lake City area, in, Wahrhaftig, C., Morrison, R. B., and Birkeland, P. W., eds., Guidebook to northern Great Basin and California: INQUA Guidebook I, Nebraska Academy of Science, p. 6-14.

_____1965d, Part H: Lake Bonneville, in, Schultz, C. B., and Smith, H.T.U., eds., VII INQUA Congress, Guidebook of field conference E: Northern and Middle Rocky Mountains: Lincoln, Nebraska, Nebraska Academy of Science p. 104-112.

_____1967, Means of time-stratigraphic division and long-distance correlation of Quaternary successions, in, Morrison, R. B., and Wright, H. E., Jr., Means of correlation of Quaternary successions: Proc. VII INQUA Cong., v. 8, Utah University Press, p. 1-113.

_____1975, Predecessors of Great Salt Lake: Geological Society of America Abstracts with Programs, v. 7, no. 7, p. 1206.

_____1978, Quaternary soils: Third York Quaternary Symposium, Geological Abstracts, Norwich, England, p. 77-108.

Morrison, R. B., and Frye, J. C., 1965, Correlation of the middle and late Quaternary successions of Lake Lahontan, Lake Bonneville, Rocky Mountain (Wasatch Range), southern Great Plains, and eastern Midwest areas: Nevada Bureau of Mines Report 9, 45 p.

Richmond, G. M., 1964, Glaciation of Little Cottonwood and Bells Canyons, Utah: U.S. Geological Survey Professional Paper 454-D, 41 p.

Rubin, Meyer, and Alexander, Corinne, 1958, U.S. Geological Survey radiocarbon dates, Part IV: Science, v. 127, p. 1476-1487.

Schwartz, D. P., Swan, F. H., III, Hanson, K. L., Kneupfer, P. L., and Cluff, L. S., 1979, Recurrence of surface faulting and large magnitude earthquakes along the Wasatch Front near Provo, Utah: Geological Society of America, Abstracts with Programs, v. 11, no. 6, p. 301.

Scott, W. E., 1979a, Evaluation of evidence for controversial rise of Lake Bonneville about 10,000 years ago: Geological Society of America Abstracts with Programs, v. 11, no. 6, p. 301-302.

_____1979b, Stratigraphic problems in the usage of Alpine and Bonneville Formations in the Bonneville basin, Utah: Geological Society America Abstracts with Programs, v. 11, no. 6, p. 302.

Shackelton, N. J., and Opdyke, N. D., 1973, Oxygen isotope and paleomagnetic stratigraphy of equatorial Pacific core V-28-238: Oxygen isotope temperatures and ice volumes on a 10^5 and 10^6 year scale: Quaternary Research, v. 3, p. 39-55.

Smith, G. I., 1979, Subsurface stratigraphy and geochemistry of late Quaternary evaporites, Searles Lake, California: U.S. Geological Survey Professional Paper 1043, 130 p.

Tamers, M. A., Pearson, F. J., Jr., and Davis, E. M., 1964, Univeristy of Texas radiocarbon dates II: Radiocarbon, v. 6, p. 138-159.

Van Horn, Richard, 1972, Surficial geology of the Sugar House quadrangle, Salt Lake County, Utah: U.S. Geological Survey Miscellaneous Geologic Investigations Map I-766A.

_____1979, The Holocene Ridgeland Formation and associated Decker Soil (new names) near Great Salt Lake, Utah: U.S. Geological Survey Bulletin, 1457-C, p. C1-C11.

Varnes, D. J., and Van Horn, Richard, 1961, A reinterpretation of two of G. K. Gilbert's Lake Bonneville sections, Utah: U.S. Geological Survey Professional Paper 424-C. p. C98-C99.

Wallace, R. E., 1977, Profiles and ages of young fault scarps, north-central Nevada: Geological Society of America Bulletin, v. 88, p. 1267-1281.

Williams, J. S., 1962, Lake Bonneville: Geology of the southern Cache Valley, Utah: U.S. Geological Survey Professional Paper 257-C, p. 131-152.

SOIL STRATIGRAPHY AS A TECHNIQUE FOR FAULT ACTIVITY ASSESSMENT IN THE CARSON CITY AREA, NEVADA

John W. Bell and Robert C. Pease

Nevada Bureau of Mines and Geology
Mackay School of Mines
University of Nevada-Reno
Reno, Nevada 89557

ABSTRACT

A relatively clear-cut stratigraphic record for the eastern flank of the Sierra Nevada and western part of the Basin and Range allows the use of soil stratigraphy for approximately defining the age and recency of movement of faults in the Carson City area, Nevada. Based primarily on the work of Birkeland (1968) and Morrison (1964), four major soil-stratigraphic units can be recognized: Toyeh-interval (post-Tioga) Soil; Churchill-interval (post-Tahoe) Soil; Cocoon-interval (post-Donner Lake) Soil; and Humboldt Valley-interval (post-Hobart) Soil. These soils are approximately dated at 5000-12,000, 35,000, 100,000 and 200,000 years, respectively. In addition, previous work has shown that there has been no appreciable argillic B horizon development in soils younger than the last high stand of Lake Lahontan about 12,000 years ago, and soils with little or no diagnostic horizon development are less than a few thousand years old.

By examining the soils mantling the faulted alluvial surfaces and the fault scarp, age and recency of fault movement can be estimated for earthquake hazard planning purposes. In and south of Carson City, field mapping and trenching have shown that, based on soil-stratigraphic relationships, multiple movements have occurred periodically along the same fault traces within the Sierra Nevada Fault Zone. Although movements have occurred throughout Quaternary time, two movements have taken place in the last 12,000 years suggesting a re-rupture interval for recent faults of thousands (as opposed to hundreds) of years for this portion of the fault zone.

INTRODUCTION

The Carson City area is situated along the western margin of the Basin and Range Province on the eastern flank of the Sierra Nevada structural block (fig. 1). The area exhibits a composite network of young faults derived from a merging of several separate structural trends (see Trexler, this volume). Evidence for early- through late-Quaternary faulting is abundant in nearly all areas of the Sierra Nevada Fault Zone, and, as will be discussed in this paper, very young (possibly historic) surface ruptures occur in and south of Carson City.

The Reno-Carson City area displays a relatively clear-cut alluvial and soil-stratigraphic record that allows greater definition of fault activity than most areas of the Basin and Range Province. The glacial outwash stratigraphy along the Truckee River (Birkeland, 1968; Bonham and Bingler, 1973) and the pluvial sequence of Lake Lahontan slightly east of Reno and Carson City (Morrison, 1964) provide a reasonable data base from which soils can be inferred as time-stratigraphic horizons to most geomorphic surfaces in the area, and allow, within certain limits, a reasonable assessment of young fault activity for earthquake hazard planning purposes. It is the purpose of this paper to outline this approach by discussing the origin and age of the soil-stratigraphic record, and by describing the application of this tool to the assessment of fault movements in the Carson City area.

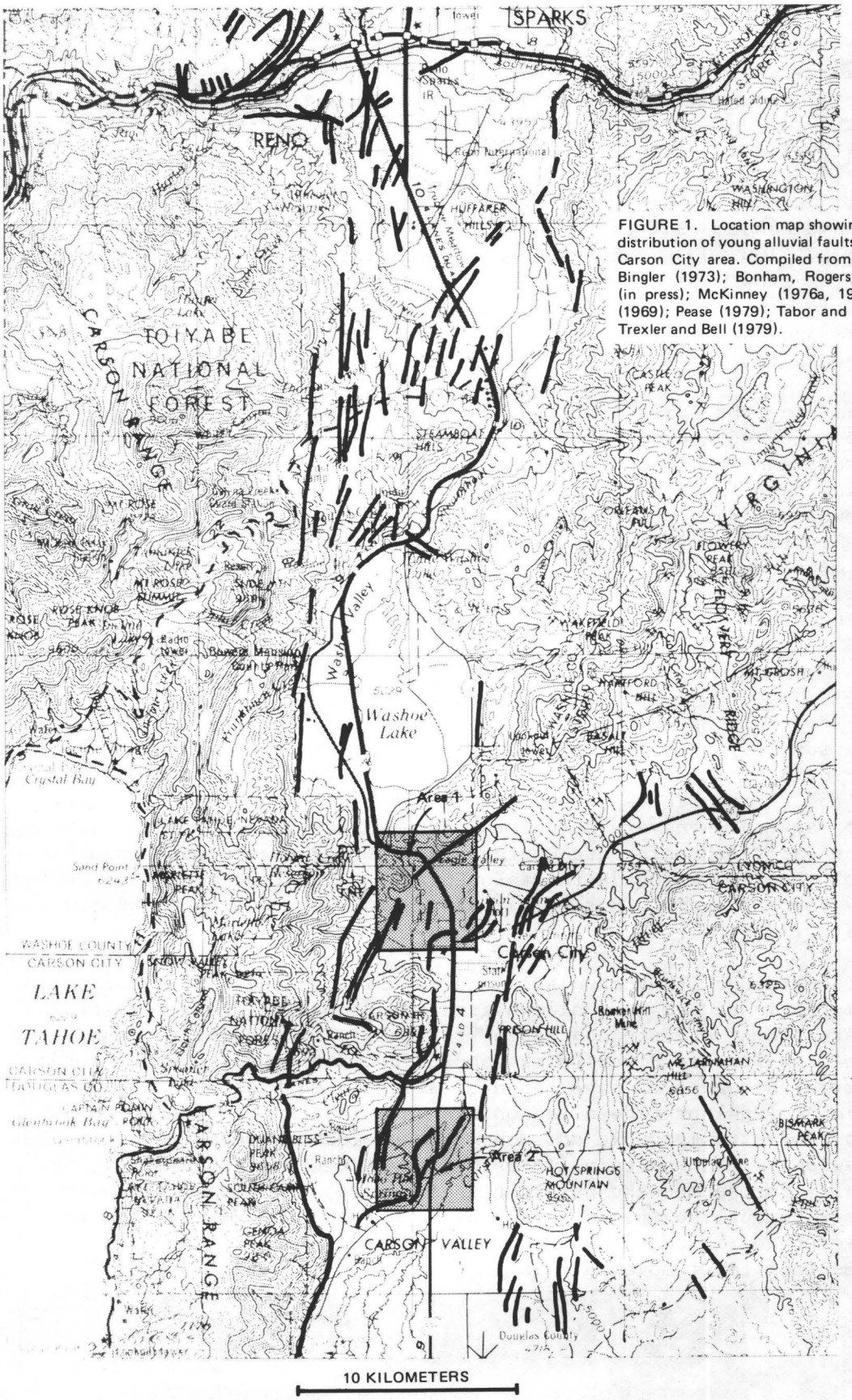

FIGURE 1. Location map showing generalized distribution of young alluvial faults in the Reno-Carson City area. Compiled from Bonham and Bingler (1973); Bonham, Rogers, and Trexler (in press); McKinney (1976a, 1976b); Moore (1969); Pease (1979); Tabor and Ellen (1975); Trexler and Bell (1979).

Soil-stratigraphic units, as used in this paper, are those defined by the American Commission on Stratigraphic Nomenclature (1970):

> A soil-stratigraphic unit is a soil with physical features and stratigraphic relationships that permit its consistent recognition and mapping as a stratigraphic unit. Soil-stratigraphic units are distinct from both rock-stratigraphic and pedologic units.

It should be noted that the basic rank of a soil-stratigraphic unit is the "soil", and that this soil may contain -- although it does not necessarily have to -- more than one pedologic soil type. This terminology is frequently confusing to both geologists and pedologists, and Morrison (1967) therefore suggests that the term "geosol" be used to distinguish soil-stratigraphic meaning from pedologic meaning. This informal convention will be used in this paper, with the term "soil" restricted to the pedologic meaning except where reference is made to a soil-stratigraphic name.

GENERAL STRATIGRAPHIC SETTING

The general use of soil stratigraphy for interpreting geologic age relationships is straightforward; it is summarized in numerous references (e.g., Birkeland, 1974; Morrison and Wright, 1967, 1968) and will not be discussed in detail here.

In the western Basin and Range, previous investigators have suggested that individually recognizable geosols formed during each of the interglacials/interpluvials, and that these geosols represent relatively discrete time-stratigraphic horizons that can be age-bracketed by glacial, interglacial, pluvial, and interpluvial deposits of approximately known age. The work of Morrison (1964) is the most extensive of these studies, in that he has mapped and defined several key geosols of the western Basin and Range through detailed studies of the Lake Lahontan sequence. Morrison identified four major geosols: Toyeh, Churchill, Cocoon, and Humboldt Valley Soils (tables 1 and 2).

Complementing Morrison's work is that of Birkeland (1968) who described glacial-related deposits and geosols of the Sierra Nevada and its eastern flank, and suggested that the units are regionally time-equivalent to those of Morrison (table 2). Geosols displaying characteristic morphologies were found by Birkeland to have developed on glacial outwash deposits along the Truckee River following each of the glacial periods and thus were identified as the post-Tioga, post-Tahoe, post-Donner Lake and post-Hobart Soils. By describing and correlating geosols of the Carson Range area with those described by Morrison, Birkeland (1967, 1968, 1974) helped establish the time-stratigraphic equivalence of the major geosols of western Nevada.

Elevations of lake-cycle maxima and minima are from the Truckee River badlands below Wadsworth unless indicated by^{F}, which are from southern Carson Desert (Fallon) area, and by^{R}, which are from Rye Patch Dam area.

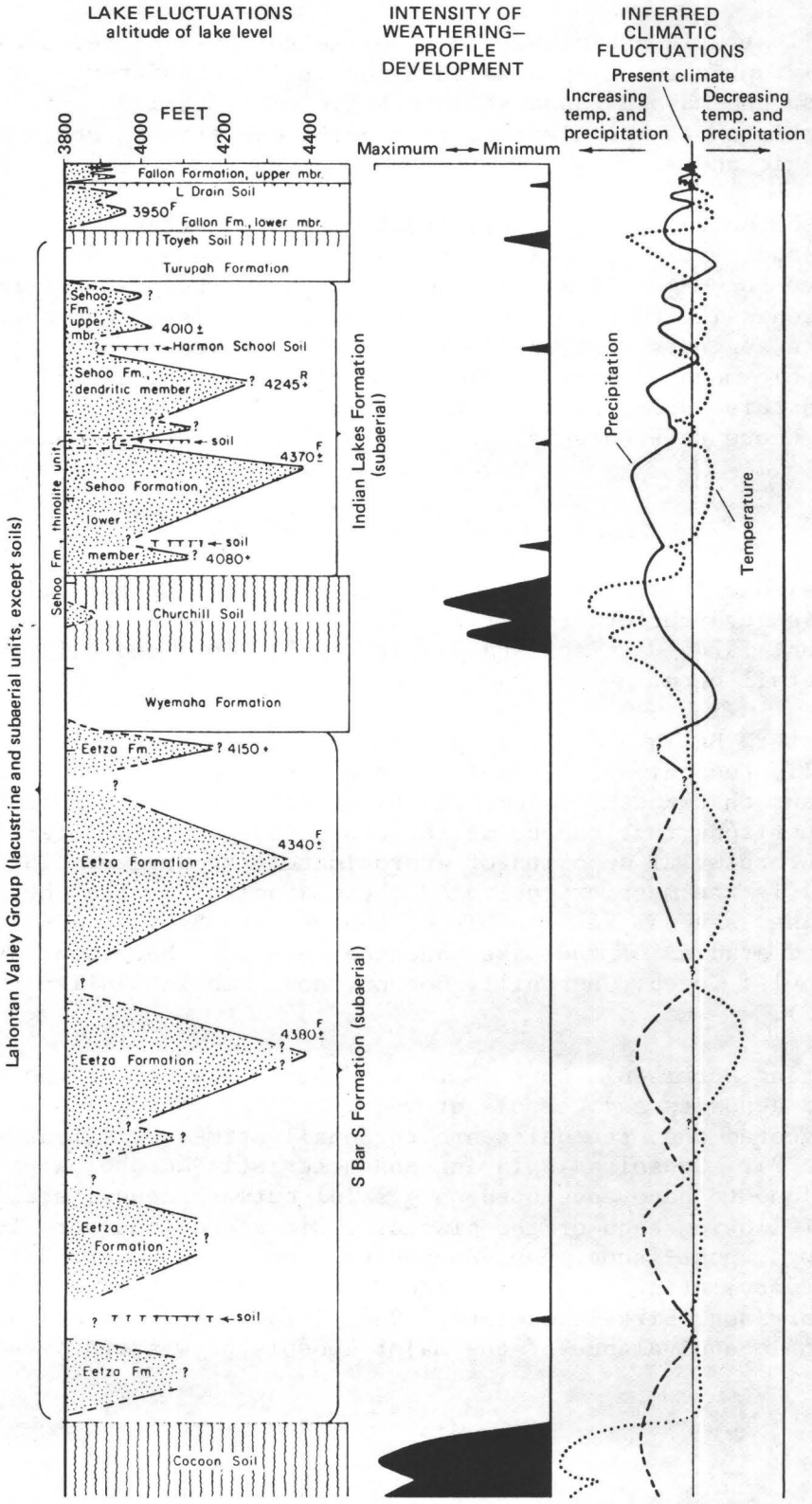

TABLE 1. Stratigraphic, weathering and climatic relations in the Lake Lahontan area (Morrison and Frye, 1965)

TABLE 2. Tentative Correlation of Quaternary Stratigraphy and Geologic Events Along the Truckee River (Birkeland, 1968).

Carson Range—Verdi Basin— Northern Truckee Meadows	Lake Lahontan Area
River alluvium Post-Tioga Soil	Fallon Fm. Toyeh Soil Turupah Fm.
Tioga Outwash	Sehoo Fm.
Most of Post-Tahoe Soil	Churchill Soil Wyemaha Fm.
Tahoe Outwash	Eetza Fm.
Most of Post-Donner Lake Soil	Cocoon Soil
Donner Lake Outwash	Paiute and Rye Patch Fms.
Post-Hobart Soil(s)	Humboldt Valley Soil
Hobart Outwash	Lovelock Fm.

All of the geosols that Birkeland worked with and many of those that Morrison studied are relict. Both investigators suggest that many geosols are products of major soil-forming intervals, and therefore are similar in degree of development in both buried and relict occurrences. This interpretation is supported by data presented by Birkeland (1974) where he shows that the Churchill Soil exhibits similar profile morphology and clay mineralogy in both buried and relict occurrences. Although the general concept of the intense weathering (soil-forming) interval in the western U. S. is now being questioned by Birkeland and Shroba (1974), these authors do cite (p. 245) the Churchill Soil as being one of the best field examples of a soil-forming interval.

For this study, the major geosols of western Nevada are considered, in the absence of any compelling evidence to the contrary, to represent distinct weathering episodes, and are referred to here as the Toyeh-, Churchill-, Cocoon-, and Humboldt Valley-interval Soils.

- Pedologic Soil Types -

A comparison of the geologic maps for the Reno-Carson City corridor (e.g., Bonham and Bingler, 1973; Bonham and others, in press; Tabor and Ellen, 1975) with the corresponding soils maps (Soil Conservation Service, 1974, 1977a, b) shows that, in general, the geologic units of known age (glacial outwash and correlative deposits) are mantled by individually characteristic groups of soils. Although each geomorphic surface may be underlain by several Soil Series, it is evident that surfaces of the same geologic age contain relatively consistent Great Groups or Subgroups (and in some cases, Soil Series) as defined by the Soil Survey Staff (1975).

In the Reno-Carson City area (table 3) the relict Toyeh-interval Soil typically displays a non-clayey B horizon about 30 cm thick (Camborthids or Haploxerolls); the relict Churchill-interval Soil typically displays a textural clay B horizon about 30 cm thick (Haplargids or Argixerolls); the relict Cocoon-interval Soil typically exhibits a thick (30-100 cm) textural clay B horizon commonly underlain by a siliceous duripan or a calcic or petrocalcic horizon (Argixerolls, duric Argixerolls, Haplargids, duric Paleargids, and Durargids); and the relict Humboldt Valley-interval Soil typically exhibits Great Groups and Subgroups similar to those of the Cocoon-interval except that they are generally thicker and better differentiated. For example, on some pre-Illinoian surfaces argillic B horizons and duripans, each in excess of 2 m thick, may be encountered.

- Ages of Pedologic Soils and Geosols -

Pluvial Lake Lahontan (Wisconsinan age) provides a key datum for defining Holocene and pre-Holocene soils. Regional pedologic studies in the western Nevada region (Nettleton and others, 1975; Alexander and Nettleton, 1977, Nettleton and Peterson, in press; Peterson and Bell, unpub. data)

TABLE 3. Key Soil-Stratigraphic Units
Reno-Carson City area

Soil-Stratigraphic Unit	Characteristic Relict Pedologic Type (Great Group or Order)	Approximate Age (yrs.)
Little or no soil (A-C) Profile	Entisol	<2000–3000
Toyeh-interval Soil	Camborthid; Haploxeroll	5000–12,000
Churchill-interval Soil	Haplargid; Argixeroll	35,000
Cocoon-interval Soil	Haplargid; Durargid; Paleargid; Durixeroll	100,000
Humboldt Valley-interval Soil	Durargid; Paleargid; Durixeroll (better developed than Cocoon Soil)	200,000

have demonstrated that there has been no appreciable argillic[1)] horizon development since the last high stand of Lake Lahontan about 12,000 years ago. For example, in the chronosequence investigated by Nettleton and others (1975; fig. 2) near Fernley (40 km east of Reno) and Dayton (15 km east of Carson City, it was found that no appreciable illuvial clay occurred in post-Lahontan sediments, and that both the volume of clay increase and the depth to maximum clay appear to increase with greater age beyond the 12,000 year time line.

All soils that stratigraphically overlie the last high stand of the lake are either Entisols or cambic soils (exceptions are natric soils; see following discussion). Cambic soils occur either as Mollisols or Aridisols and include Haploxerolls, Cryoborolls, Haplaquolls, and Camborthids. South of Carson City (fig. 4) a ^{14}C date of 7140±400 years (Tx-3504) was obtained below a Haploxeroll during this study, supporting the Holocene-age interpretation, and at Reno, a ^{14}C age of 2130±165 years was obtained by Bingler and Bonham (1976) on floodplain and lake deposits underlying a Fluvaquentic Haplaquoll.

Cumulative age data suggest that Entisols are less than 2000-3000 years old. The 2130 year age date cited above is from beneath a soil that is only slightly beyond an Entisol stage of development. The Fallon Formation (table 2) is dated by Morrison and Frye (1965) at less than 4000 years old, and the pedons that occur on and within the formation are Entisols. This suggests that more than a few thousand years are required to progress from an A-C, or Entisol, stage to a cambic stage. This agrees with the observations of Nettleton and Peterson (in press), Gile (1975), and Gile and Hawley (1968) for soils in the New Mexico area. In the Washoe Lake area (fig. 1), an A-C soil overlies a deposit dated at 360 years by Tabor and Ellen (1975), and in the Genoa area, an Entisol overlies a carbon-dated hearth 460 years old (Elston, 1971).

The distribution of these pedologic types (Entisols and cambic soils) allows a key "rule of thumb" to be developed: if these soil types are present, the surface on which they occur is most probably Holocene age. The soils in the western Nevada region will, therefore, provide a relatively useful Pleistocene/Holocene boundary for earthquake hazard purposes if the boundary is placed at 12,000 years.

---

1) Argillic soils are defined (Soil Survey Staff, 1975) as having an illuvial (B) horizon with at least 3% more clay than the eluvial (A) horizon if the eluvial horizon has less than 15% total clay. If the argillic horizon is loamy or clayey, it should be at least 7.5 cm thick.

Entisols are defined as having little or no diagnostic pedogenic horizon development, and they typically display A-C profiles.

Cambic soils are defined as having an altered B horizon that shows movement or aggregation of soil particles (generally reduction or removal of iron oxides and leaching of carbonates). The base of the horizon must be at least 25 cm below the surface.

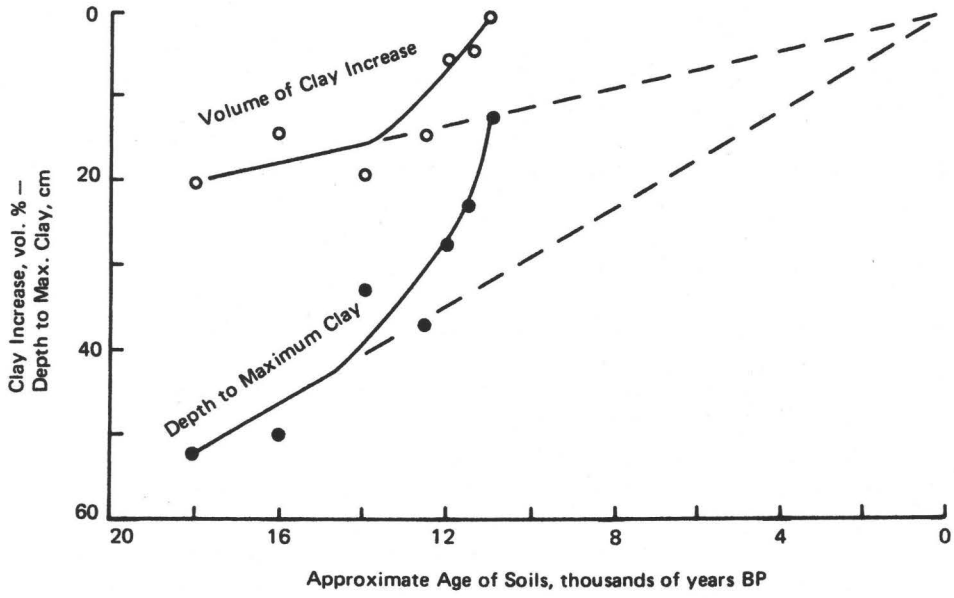

FIGURE 2. Relation between volume of clay increase, depth to maximum clay in the B, and age of soils in the chronosequences near Fernley and Dayton, Nevada (Nettleton and others, 1975).

On pre-Holocene surfaces, soils exhibiting illuvial clay horizons predominantly occur. Therefore, if a surface is underlain by an argillic horizon, it is of late Wisconsinan age or older. An exception to this is the occurrence of sodium-rich soils (Natrargids; Alexander and Nettleton, 1977) which is discussed in a following section. Also, some pre-Holocene soils lack argillic B horizons, which may lead to erroneous age interpretations in the absence of supplementary evidence. The presence of $CaCO_3$ (for example, in alluvial deposits composed largely of carbonate clasts) can inhibit clay dispersion and eluviation, resulting in the formation of only a cambic horizon (Nettleton and Peterson, in press). Such soils frequently contain duripans (siliceous hard-pans) beneath the cambic B horizon (Durorthids) which provide supplementary evidence of Pleistocene age.

In addition to the age relationships determined through the use of pedologic soil types, soil-stratigraphic units provide approximate age control. If it is assumed that the bulk of the major pre-Holocene soil-stratigraphic units (table 3) formed during weathering intervals having greater effective moisture (as discussed earlier), geosols provide relatively concise time-stratigraphic horizons. Approximate ages of the geosols have been determined by dating the geologic units stratigraphically above and below, and by correlating the weathering intervals with other similar intervals of known age (tables 2 and 3). The Toyeh Soil underlies the Fallon Formation (4000 years old) and overlies the Sehoo Formation, which ranges in age from about 6000 to 35,000 years old (Davis, 1978). Thus, the Toyeh Soil could be as young as 5000-6000 years old, but is regarded here as also possibly being earliest Holocene age, i.e. 5000-12,000 years old.

The Churchill Soil underlies the Sehoo Formation and overlies the interpluvial Wyemaha Formation. Radiocarbon ages from the Wyemaha Formation range from 25,500 to 33,500 years, and a single date on pedogenic carbonate from the soil yielded an age of 26,300 years (Morrison and Frye, 1965). These dates lead Morrison and Frye to conclude that the Churchill Soil was formed between 25,000 to 30,000 years ago. Tephrochronologic and ^{14}C studies by Davis (1978), however, place the beginning of Sehoo time at about 35,000 years, and suggest the Eetza Formation (underlying the Wyemaha Formation) may be as young as 35,000 years. Thus, the Churchill Soil is best dated at about 35,000 years old.

The Cocoon and Humboldt Valley Soils represent major interpluvial/interlacustral intervals that can be correlated to continental (or worldwide) interglacial stages (Morrison and Frye, 1965). The Cocoon Soil is of Sangamon age; it underlies the Eetza Formation which is Tahoe age (35,000-75,000 years). The Humboldt Valley Soil underlies the Rye Patch Formation of Illinoian age (125,000-150,000 years) and represents the Yarmouth interglacial stage. If worldwide sea-level data are utilized (for example, Hopkins, 1973), the Sangamon and Yarmouth stages are approximately dated at 100,000 and 200,000 years, respectively.

PROCEDURE FOR USING SOILS IN ASSESSING FAULT ACTIVITY

Evaluation of fault activity can be initiated through several levels of investigation. The most basic level merely requires the plotting of fault traces on soil survey maps (at least 2nd- or 3rd-order surveys) and is essentially an office procedure (figs. 3, 4). Such composite maps readily allow the delineation of Holocene-age faults where Holocene soils are transected. For example, figure 3 shows multiple fault traces cutting non-argillic soils: Haploxerolls and Camborthids. Similarly, figure 4 shows non-argillic soils in fault contact with older argillic soils, and further delineates faulted areas within Entisols.

The second level of investigation requires surficial field examination of alluvial and soil-stratigraphic units so that a structural history can be constructed. Soils on the upthrown and downthrown alluvial surface and those on the fault scarp are examined by soil pit and auger, and identified. The soil which has formed on the fault scarp is possibly the most important tool in interpreting the age of last movement. The morphology of the scarp must, however, be carefully evaluated before selecting a soil-profile site; multiple scarp bevels, if not recognized, could produce erroneous data.

It should be mentioned at this point that the presence of a soil -- particularly an old one -- on a scarp is not totally compatible with the currently accepted theory of scarp decline. This theory, as discussed by Wallace (1977), Bucknam and Anderson (1979), and Bucknam and others (this volume), is based upon the interpretation that for alluvial scarps of a given height, the scarp slope angle consistently decreases as a logarithmic function of the scarp age. The fact that older scarps of a given height have gentler slope angles is not in question, but the existence of a well-differentiated soil on the slope suggests that the scarp has been stable for a significantly long period of time. Soil formation and scarp decline appear to involve mutually exclusive processes, unless some form of dynamic equilibrium can be shown to exist, and this contradiction cannot at present be explained.

A third level of investigation can be implemented through trenching of selected faults. Trenching of both the faulted alluvial surface and the escarpment can clearly document the soil-fault relationship and determine the existence, if any, of small displacements along pre-existing scarps.

RECENCY OF MOVEMENT

Utilizing the soil-stratigraphic relationships outlined here, recency of fault movement categories can be constructed (table 4). These categories are defined solely on the basis of the youngest soils and geosols observed to be displaced, and on the character of the soil found on the fault scarp. The ages of the youngest displacement will, in most instances, be apparent rather than absolute based on the limiting factors of the technique. This approach to dating movement is not intended to supplant alluvial-stratigraphic techniques or other sources of dating faults. It is suggested that the soil-stratigraphic technique is best utilized in combination with other types of

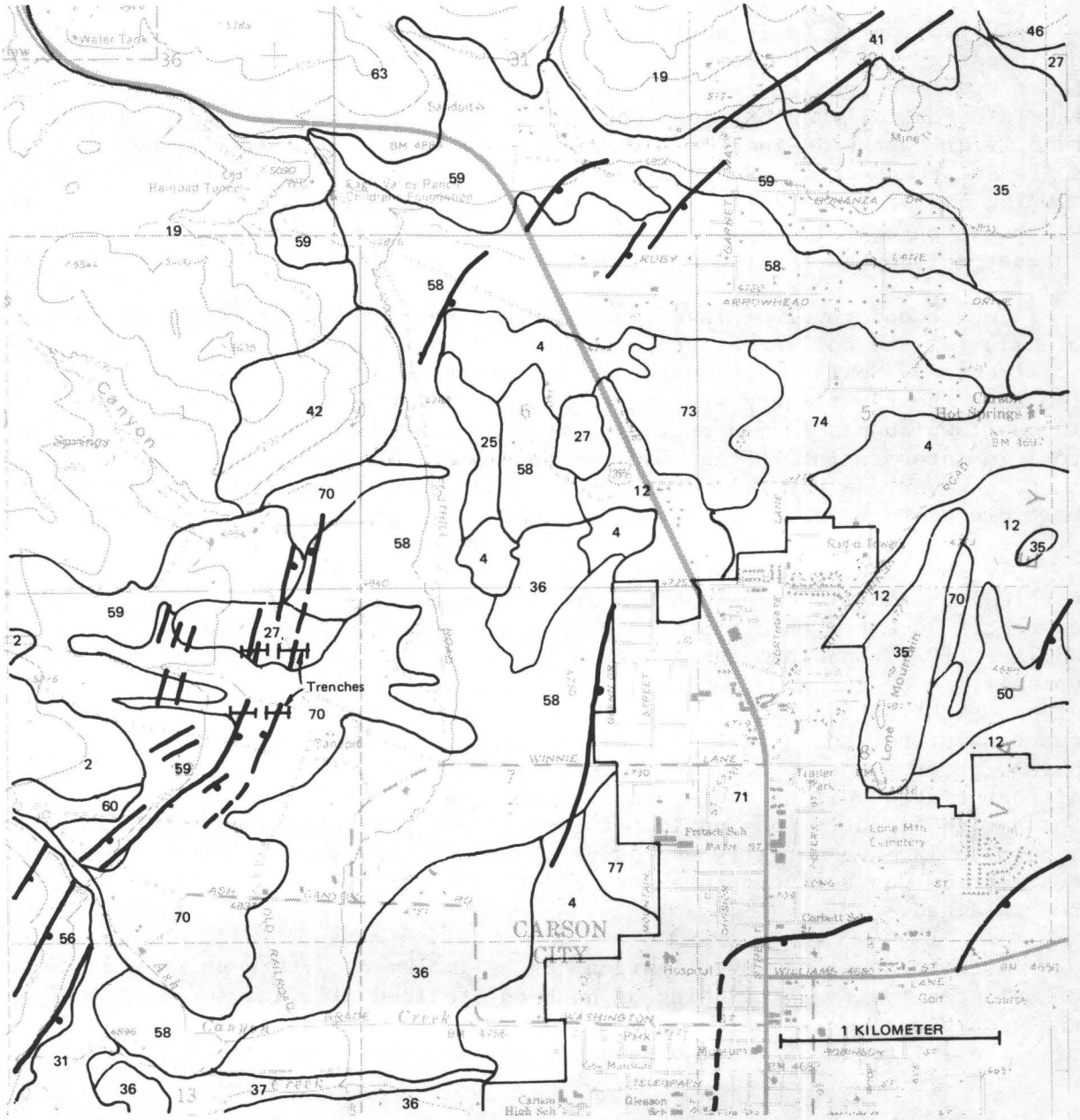

FIGURE 3. Faults in area 1 superimposed on soils map of Soil Conservation Service (1975).

2 – Aldax Variant-Rock outcrop complex (Haploxeroll and rock)
4 – Bishop loam (Haplaquoll)
12 – Dalzell fine sandy loam (Nadurargid)
19 – Glenbrook-Rock outcrop complex (Entisol and rock)
25, 27 – Haybourne sandy loam, gravelly sandy loam (Camborthid)
31 – Holbrook gravelly fine sandy loam (Haploxeroll)
35 – Indiano Variant gravelly fine sandy loam (Haplargid)
36, 37 – Jubilee coarse sandy loam, sandy loam (Haplaquoll)
41, 42 – Koontz-Sutro complex, Koontz-Sutro Variant association (Argixeroll, Haploxeroll)
46 – Old Camp-Holbrook Variant association (Haplargid, Haploxeroll)
50 – Orizaba loam (Halaquept)
56 – Rock outcrop-Variant complex (rock and Haploxeroll)
58, 59, 60 – Surprise coarse sandy loam, sandy loam (Haploxeroll)
63 – Tarloc-Glenbrook association (Haplargid and Entisol)
70 – Toll gravelly loamy sand (Entisol)
71 – Urban land
73, 74 – Vamp fine sandy loam (Durorthid)
77 – Voltaire silty clay loam (Haplaquoll)

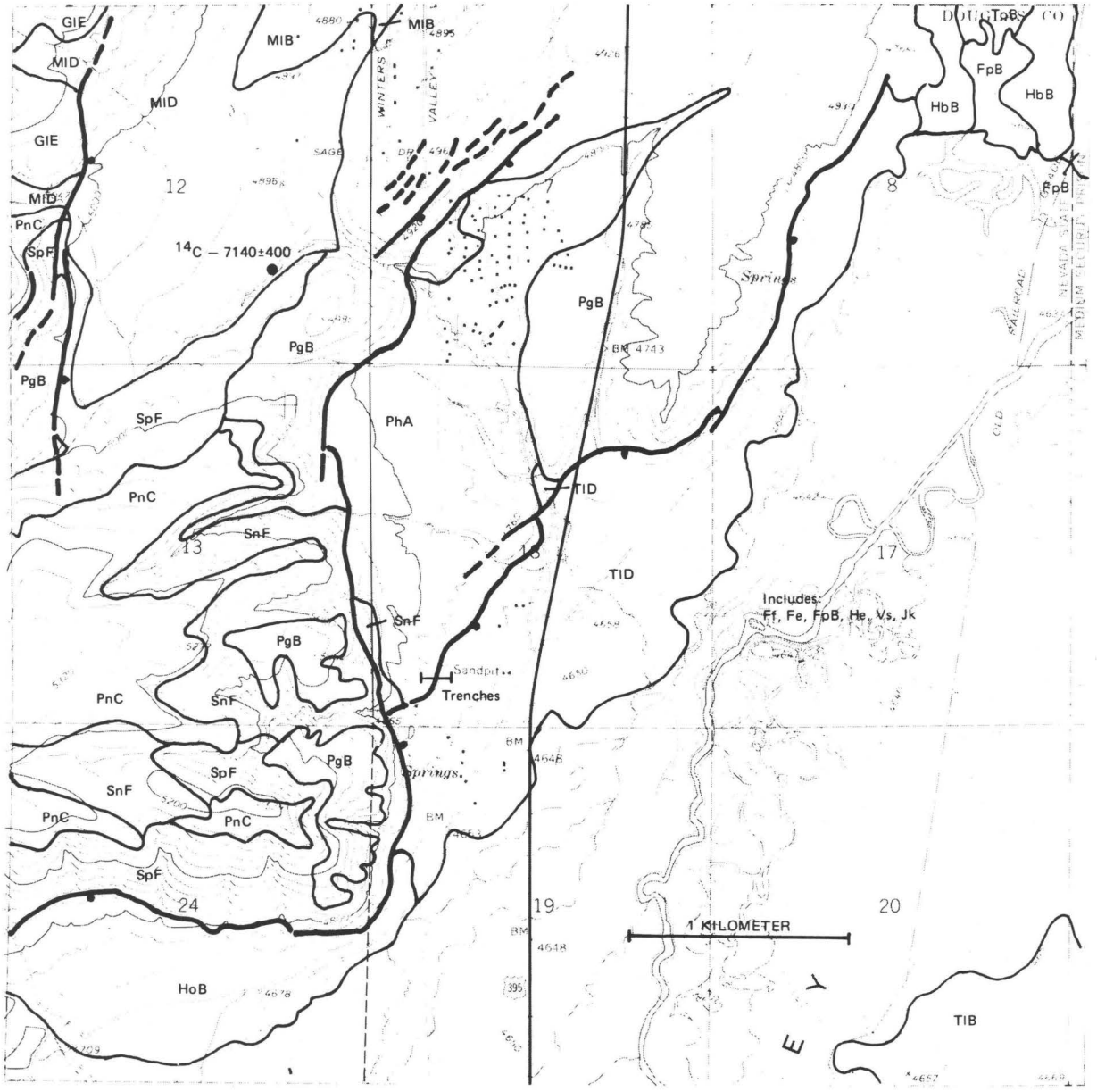

FIGURE 4. Faults in area 2 superimposed on soils map of Soil Conservation Service (1971).

Ff, Fe, FpB – Fettic clay loam, very fine sandy loam (Natrixeroll)
GIE – Glenbrook sand (Entisol)
He – Heidtman loam (Haploxeroll)
HbB – Haybourne sand (Camborthid)
HoB – Holbrook gravelly fine sandy loam (Haploxeroll)
Jk – Job loam (Entisol)
MIB, MID – Mottsville loamy coarse sand (Haploxeroll)
PgB, PhA, PnC – Prey gravelly loamy sand, loamy sand, stony loam (Durargid)
SnF, SpF – Springmeyer stony fine sandy loam, very stony fine sandy loam (Argixeroll)
TIB, TID – Toll sand (Entisol)
ToB – Toll sandy loam (Entisol)
Vs – Voltaire silty clay loam (Haplaquoll)

TABLE 4. Recency of fault movement categories
Carson City area

Age of youngest displacement (yrs.)	Soil-Stratigraphic Evidence
<2000-3000	Entisol displaced
<5000-12,000	Toyeh-interval Soil displaced
12,000-35,000	Churchill-interval Soil displaced; scarp overlain by Holocene (Toyeh-interval) Soil
35,000-100,000	Cocoon-interval Soil displaced; scarp overlain by Churchill-interval Soil
100,000-500,000	Humboldt Valley-interval Soil (or older soils) displaced; scarp overlain by Cocoon-interval Soil

relative age control, but that in the absence of such additional control the soil technique can provide a relatively reasonable estimation of the age of faulting for hazard planning purposes.

CARSON CITY AREA FAULT ASSESSMENT

- Age Assessments -

Young faults in and south of Carson City were evaluated using the soil-stratigraphic technique, and the ages of most recent movement were estimated and probable maximum re-rupture intervals were calculated. All faults were assessed using first and second levels of investigation, and selected faults were further assessed by trenching (Pease, 1979, in press; Trexler and Bell, 1979).

In area 1 (fig. 3) numerous north-northeast-trending faults can be seen cutting Holocene-age soils (Haploxerolls, Camborthids) on plan view. Most of the faults are extensions of bedrock structures, and as such serve to document a relatively broad regional picture. Since the faulted soil types represent the Toyeh-interval Soil, the faults represent, based on map interpretations alone, regional structural displacements within the last 12,000 years.

Soil pits and auger holes on displaced alluvial surfaces and on fault scarps show similar Haploxeroll soils, suggesting that both the alluvial surfaces and fault scarps are relatively close in age. Trenching of four of the faults, however, (fig. 3) further indicates that, although the escarpments are underlain by a Haploxeroll soil, small, surficially undetectable breaks also have displaced the soil. Shown schematically in figure 5 are the soil-stratigraphic relationships found through trenching of the four faults. The Haploxeroll (Toyeh-interval) soil mantles both the alluvial surface and the scarp, and it clearly truncates the faults underlying a portion of the scarp. In addition, at least one of the fault planes has ruptured the soil with a displacement of about 15 cm, and it is marked by an in-filling of A-horizon material. On the opposite side of the graben at the toe of the main scarp, a small (30 cm) west-facing escarpment similarly cuts the soil. Because of the poorly indurated character of the parent material (>95% decomposed granite fragments) it is believed that such a small scarp would be destroyed through normal erosion processes in probably no more than a few hundred years. Consequently, this youngest break could, for all practical purposes, be considered an historic rupture. Several kilometers northeast of area 1, the same north-northeast fault traces are overlain by a Haplargid (Churchill-interval) soil and show a similarly young 30 cm rupture at the surface.

These recent ruptures, as well as some of the most recent breaks described in the following paragraphs for area 2, could conceivably be related to the 1887 Carson City earthquake. Slemmons and others (1965) describe this earthquake as having a Modified Mercalli intensity of VII (maximum observed) and report that shaking was very severe in Carson City with a noise like thunder before the shock. An intensity of VII would be

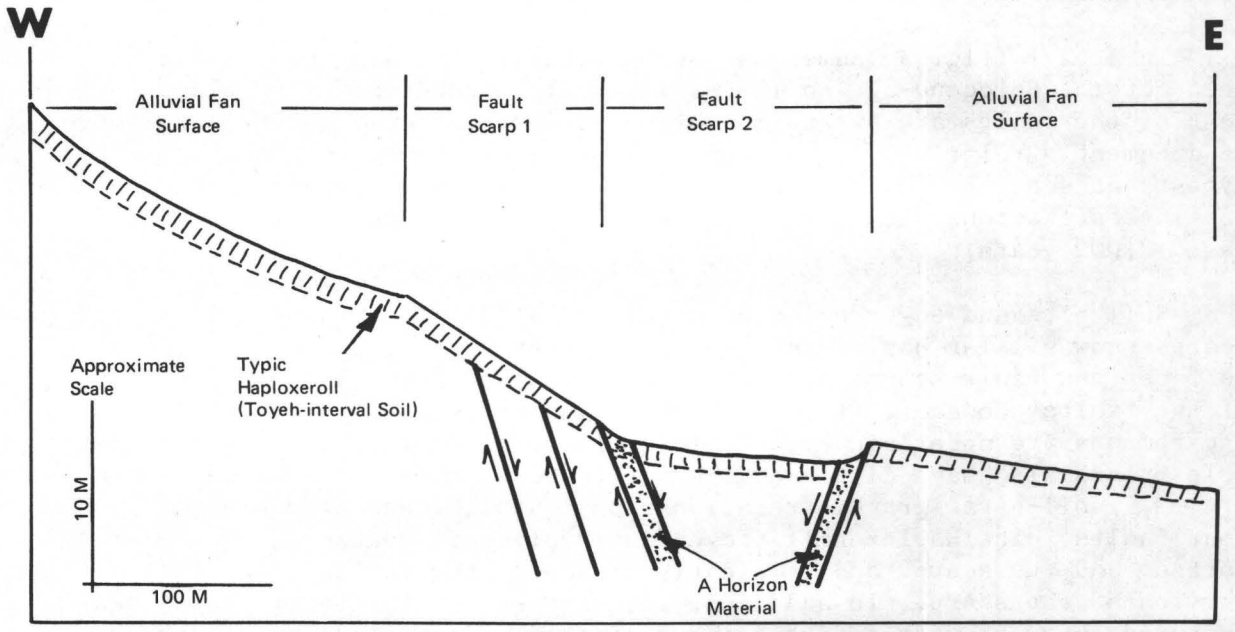

FIGURE 5. Schematic cross-section showing fault scarp and soil relationships exposed through trenching in area 1.

approximately equivalent to a Richter magnitude of 5-6 (Slemmons and others, 1965), and such magnitudes have been associated with similar small surface ruptures, such as during the 1950 Fort Sage earthquake (Gianella, 1957).

South of Carson City in area 2 (fig. 4) the technique indicates that: 1) faulting has occurred repeatedly throughout Pleistocene time; 2) at least two periods of fault activity have taken place in the past 12,000 years; and 3) one of the periods of activity occurred within the last 2000-3000 years. The oldest Quaternary deposits are of late Pliocene-early Pleistocene age and contain Durargid soils that have siliceous duripans ranging from 0.5 to more than 2 m thick. Along the southernmost east-trending fault in figure 4, these old soils have been displaced more than 120 m since early Quaternary time. The most recent activity has offset the alluvial fans, which contain Entisols, and thus took place within the last 2000-3000 years.

Shown schematically on figure 6, fault scarp B cuts the oldest Quaternary deposits (A). A Durargid soil has formed on the scarp and geomorphic features (debris-slope bevels) suggest several movements. At the base of fault C, slightly younger alluvium (early- to mid-Pleistocene) has been deposited that also has a Durargid soil (Humboldt Valley-interval Soil?) on the surface (D), although this soil is much thinner than that on the oldest alluvium. These early- to mid-Pleistocene deposits have also been faulted, and the soil on fault scarp E is a Haplargid (lacks a duripan). It is equivalent in age to the Churchill-interval Soil (about 35,000 years old). At least two episodes of faulting apparently occurred on this trace prior to the development of the Haplargid based on trenching results and debris-slope bevels. Trenching also exposed the Haplargid across fault G where it has been displaced and buried by Holocene alluvium (H) which has also been displaced twice.

Evidence suggests that the central segment of the eastern fault on figure 4 has not moved during Holocene time since the scarp is mantled by a Haplargid soil. Other segments of the same trace are, however, Holocene-age, and the relationships indicate that care must be exercised in the selection of representative soil sites in order to accurately estimate the age of last movement.

Several of the faults shown on figure 4 displace Entisols, and all of these faults have about the same amount of offset. It is therefore probable that they all ruptured during the same event.

From an examination of two faults within area 2, a periodic nature of movement becomes apparent. Fault C underwent several episodes of movement during early Pleistocene time and has since become dormant. Fault G had periods of movement between about 35,000-100,000 years age; it became dormant until about middle Holocene time and then displayed renewed movement. This suggests that Quaternary faults within this area may become dormant for long intervals but should not be considered dead.

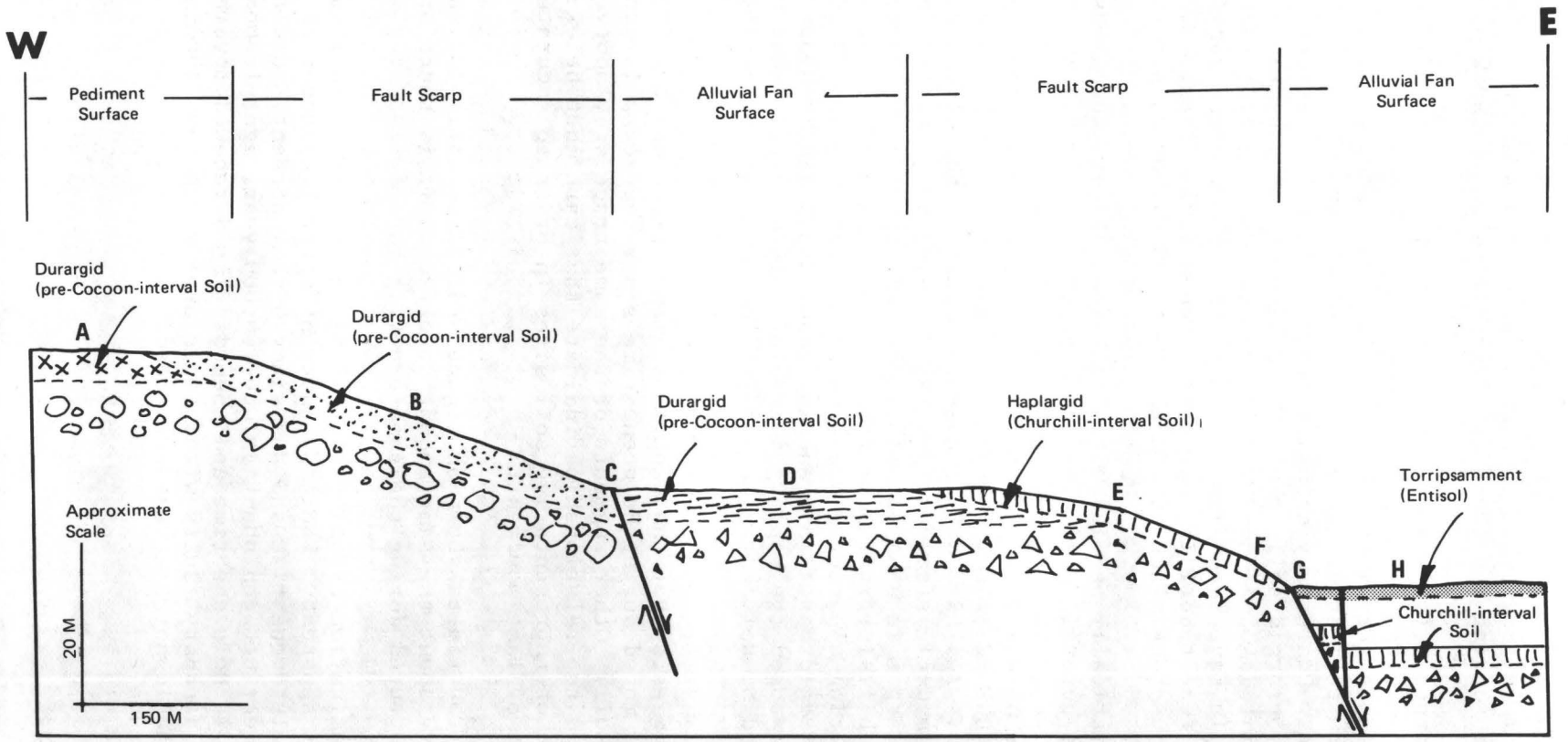

FIGURE 6. Schematic cross-section showing fault scarp and soil relationships exposed through trenching in area 2.

RE-RUPTURE INTERVALS

Studies in both areas 1 and 2 illustrate that multiple movements have occurred along all or portions of the same major fault traces, thus allowing an estimation of maximum re-rupture intervals to be made. In as much as single fault traces may not be representative of the fault zone as a whole, a combination of data from the two areas yields corroborating evidence. Re-rupture estimates are restricted to Holocene-age activity because of the superior age control and because of the restrictions imposed by the periodic nature of the active and dormant states.

In area 1, the same fault trace has broken at least twice in the last 12,000 years, with one break occurring 5000-12,000 years ago and the other probably less than a few hundred years ago. Similarly, in area 2 at least two different faulting events have occurred along the same trace during the last 12,000 years. The most recent movement displaces an Entisol and therefore is less than a few thousand years old. Two movements within 12,000 years interpolates to a 6000 year maximum re-rupture rate.

These data suggest that order of magnitude values for re-rupture times in the Carson City portion of the Sierra Nevada Fault Zone are thousands of years for young faults. This is in general agreement with other independently derived recurrence data. Ryall (1977) demonstrated that the seismic cycle for large (M>7) earthquakes in Nevada is on the order of thousands (rather than hundreds) of years based on seismicity for 1970-74 in the zones of large historic earthquakes in central Nevada. Douglas and Ryall (1975) used instrumentally monitored earthquake data for 1932-1969 to calculate that the expected return period for rock accelerations greater than 0.5g due to earthquakes of M>7 is on the order of 2000 years. As Ryall (1977) points out, however, this time would be increased by a factor of 3 if current seismicity represents the entire area exhibiting Quaternary faulting rather than the area used which contains only historic data.

LIMITATIONS TO THE SOIL-STRATIGRAPHIC TECHNIQUE

As with any stratigraphic technique, soil stratigraphy contains certain inherent limitations that must be recognized and accounted for in making earthquake hazard assessments. Climate is one of the most important parameters influencing rate and degree of soil development, and if climatic zonations are not recognized, results of soil interpretations may be erroneous. The Carson City area is situated in a transitional zone between semi-arid and arid conditions receiving about 30 cm of average annual precipitation (U. S. Weather Bureau). The Reno area receives about 18 cm of average annual precipitation, and the areas east of Reno and Carson City (including Morrison's study area) receive slightly lesser amounts: 10-20 cm (Houghton and others, 1975). It could be argued that with variations of as much as a factor of 2 between precipitation zones, that rates of soil formation could be significantly different with a critical influence, for example, in the rate of argillic horizon development. This is indeed the case for the high Sierra Nevada area immediately west of the Carson City study area, which receives 76-114 cm of annual precipitation and displays much more strongly differentiated soils, but presently avail-

able soil-age relationships found in the study area and in the western Basin and Range, as a whole, support the general soil-stratigraphic relationships described here. In viewing paleoclimatic fluctuations, it is assumed that all such changes were regional in nature.

Sodium-rich (natric) soils, as previously mentioned, can produce erroneous age interpretations if unrecognized. Soils containing large (>15%) amounts of exchangeable Na can develop argillic horizons in less than 6600 years (Alexander and Nettleton, 1977) because the presence of exchangeable Na tends to accelerate the mobilization of illuvial clay. In most cases, however, natric soils are shown on standard soils maps, but they may also be inferred in the field through pH tests.

The level of investigation undertaken can lead to significant differences in recency of faulting interpretations, especially if subtle soil and structure relationships appear only through trenching. For example, the trenches emplaced in the Carson City area (fig. 3) exposed very small offsets superimposed on a larger escarpment which would have otherwise gone undetected.

ACKNOWLEDGMENTS

The authors would like to express appreciation to Fred F. Peterson, who provided much assistance in the interpretation of some of the soil relations and review of this paper.

Portions of this study were funded through U. S. Geological Survey Earthquake Hazards Reduction Grant no. 14-08-0001-G-494.

DISCUSSION

Q. Have you done scarp slope/scarp height profiling, and, if so, how does the data compare with the soils data?

A. Scarp slope and height measurements have been taken on every scarp in which the soils have been identified. I have not compiled or analyzed the data yet mainly because I don't feel that I have a broad enough data base. I will say that in general the scarps displaying the older soils appear to have the gentler slope angles. However, the point here is that the presence of a soil, especially an old one, indicates to me that the scarp has not been reclining for a long time. My present feeling is that there is some sort of threshold involved. The scarp lays back very rapidly, and the scarp angle/age curve flattens out very quickly.

Q. But that's what we've been saying all along.

A. No, I think my point is that there is a problem in relating 1000, 10,000 and 100,000 year old scarp angles to a consistent continual decline. It appears that you can find similar scarp slope/height relationships on scarps of greatly varying age.

REFERENCES CITED

Alexander, E. B., and Nettleton, W. D., 1977, Post-Mazama natrargids in Dixie Valley, Nevada: Soil Sci. Soc. America Jour., v. 41, p. 1210-1212.

American Commission on Stratigraphic Nomenclature, 1970, Code of stratigraphic nomenclature: Tulsa, Okla., Am. Assoc. Petroleum Geologists, 17 p.

Birkeland, P. W., 1967, Correlation of soils of stratigraphic importance in western Nevada and California, and their relative rates of profile development, in Morrison, R. B., and Wright, H. E., eds., Quaternary soils: Proceedings, VII INQUA Congress, v. 9, Desert Research Institute, University of Nevada-Reno, p. 71-91.

_____1968, Correlation of Quaternary stratigraphy of the Sierra Nevada with that of Lake Lahontan area, in Morrison, R. B., and Wright, H. E., eds., Means of correlation of Quaternary successions: Proceedings, VII INQUA Congress, v. 8, p. 469-500.

_____1974, Pedology, weathering and geomorphological research: Oxford Univ. Press, New York, 283 p.

Birkeland, P. W., and Shroba, R. R., 1974, The status of the concept of Quaternary soil-forming intervals in the western United States, in Mahaney, W. C., ed., Quaternary environments: Proceedings of a symposium: First York University Symposium on Quaternary Research, Geographical Monographs, no. 5, p. 244-275.

Bingler, E. C., and Bonham, H. F., Jr., 1976, Geologic map, in Reno folio: Nev. Bur. Mines and Geol. Environ. Folio Series, p. 24-33.

Bonham, H. F., Jr., and Bingler, E. C., 1973, Geologic map, Reno 7½-minute quadrangle: Nev. Bur. Mines and Geol. Environ. Map 4Ag.

Bonham, H. F., Jr., Rogers, D. K., and Trexler, D. T., in press, Geologic map, Mt. Rose NE 7½-minute quadrangle: Nev. Bur. Mines and Geol. Map.

Bucknam, R. C., and Anderson, R. E., 1979, Estimation of fault-scarp ages from a scarp-height -- slope-angle relationship: Geology, v. 7, p. 11-14.

Davis, J. O., 1978, Quaternary tephrochronology of the Lake Lahontan area, Nevada and California: Nev. Arch. Survey Res. Paper No. 7, 137 p.

Douglas, B. M., and Ryall, Alan, 1975, Return periods for rock acceleration in western Nevada: Bull. Seis. Soc. America, v. 65, no. 6, p. 1599-1611.

Elston, R. C., 1971, A contribution to Washo archeology: Nev. Arch. Survey Res. Paper No. 2, 144 p.

Gianella, V. P., 1957, Earthquake and faulting, Fort Sage Mountains, California, December, 1950: Bull. Seis. Soc. America, v. 47, no. 3, p. 173-177.

Gile, L. H., 1975, Holocene soils and soil-geomorphic relations in an arid region of southern New Mexico: Quat. Res., v. 5, p. 321-360.

Gile, L. H., and Hawley, J. W., 1968, Age and comparative development of desert soils at the Gardner Spring Radiocarbon Site, New Mexico: Soil Sci. Soc. America Proc., v. 30, p. 261-268.

Hopkins, D. M., 1973, Sea level history in Beringia during the past 250,000 years: Quat. Res., v. 3, p. 520-540.

Houghton, J. G., Sakamoto, C. M., and Gifford, R. O., 1975, Nevada's weather and climate: Nev. Bur. Mines and Geol. Spec. Pub. 2, 78 p.

McKinney, R. F., 1976a, Preliminary geologic map of a portion of the Vista 7½-minute quadrangle: Nev. Bur. Mines and Geol. open-file map.

_____1976b, Preliminary geologic map of a portion of the Steamboat 7½-minute quadrangle: Nev. Bur. Mines and Geol. open-file map.

Mock, R. G., 1972, Correlation of land surfaces in the Truckee River Valley between Reno and Verdi, Nevada: Univ. of Nevada, Reno, unpub. M.S. thesis, 91 p.

Moore, J. G., 1969, Geology and mineral deposits of Lyon, Douglas, and Ormsby Counties, Nevada: Nev. Bur. Mines and Geol. Bull. 75, 45 p.

Morrison, R. B., 1964, Lake Lahontan: geology of the southern Carson Desert, Nevada: U. S. Geol. Survey Prof. Paper 401, 156 p.

_____1967, Principles of Quaternary soil stratigraphy, in Morrison, R. B., and Wright, H. E., eds., Quaternary Soils: Proceedings, VII INQUA Congress, v. 9, Desert Research Institute, University of Nevada-Reno, p. 1-70.

Morrison, R. B., and Frye, J. C. 1965, Correlation of the middle and late Quaternary successions of the Lake Lahontan, Lake Bonneville, Rocky Mountain (Wasatch Range), southern Great Plains, and eastern Midwest areas: Nev. Bur. Mines and Geol. Rept. 9, 45 p.

Morrison, R. B., and Wright, H. E., eds., 1967, Quaternary Soils: Proceedings, VII INQUA Congress, v. 9, Desert Research Institute, University of Nevada-Reno, 338 p.

_____1968, Means of correlation of Quaternary successions: Proceedings, VII INQUA Congress, v. 8, 631 p.

Nettleton, W. D., and Peterson, F. F., in press, Aridisols: soil genesis and morphology, chapter 14: Elsevier Pub., 26 p.

Nettleton, W. D., Witty, J. E., Nelson, R. E., and Hawley, J. W., 1975, Genesis of argillic soils of desert areas of the southwestern United States: Soil Sci. Soc. America Proc., v. 39, p. 919-926.

Pease, R. C., 1979, Scarp degradation and fault history south of Carson City, Nevada: Univ. of Nevada, Reno, unpub. M.S. thesis, 90 p.

_____ in press, Geologic map, Genoa 7½-minute quadrangle: Nev. Bur. Mines and Geol. Map.

Ryall, Alan, 1977, Earthquake hazard in the Nevada region: Bull. Seis. Soc. America, v. 67, no. 2, p. 517-532.

Slemmons, D. B., Jones, A. E., and Gimlett, J. I., 1965, Catalog of Nevada earthquakes, 1852-1960: Bull. Seis. Soc. America, v. 55, no. 2, p. 537-583.

Soil Conservation Service, 1971, Soil survey, Carson Valley Area, Nevada-California: U. S. Dept. of Argiculture, 129 p.

_____1974, Soil map, Reno 7½-minute quadrangle: Nev. Bur. Mines and Geol. Map 4Ad.

_____1975, Soil survey, Carson City Area, Nevada: U. S. Dept. Agriculture open-file map.

_____1977a, Soil map, Mt. Rose NE 7½-minute quadrangle: Nev. Bur. Mines and Geol. Map 4Bd.

_____1977b, Soil map, Washoe City 7½-minute quadrangle: Nev. Bur. Mines and Geol. Map 5Ad.

Soil Survey Staff, 1975, Soil taxonomy: U. S. Dept. Agriculture Handbook No. 436, 754 p.

Tabor, R. W., and Ellen, S., 1975, Geologic map, Washoe City 7½-minute quadrangle: Nev. Bur. Mines and Geol. Map 5Ag.

Trexler, D. T., and Bell, J. W., 1979, Earthquake hazard maps of Carson City, New Empire,and South Lake Tahoe quadrangles: Final Tech. Rept., U. S. Geol. Survey Earthquake Hazard Reduction Grant 14-08-0001-G-494, 43 p.

Wallace, R. E., 1977, Profiles and ages of young fault scarps, north-central Nevada: Geol. Soc. America Bull., v. 88, p. 1267-1281.

Patterns and Rates of Recurrent Movement Along the Wasatch-Hurricane-Sevier Fault Zone, Utah During Late Cenozoic Time

by

W. K. Hamblin and M. G. Best
Brigham Young University
Provo, Utah
(801) 374-1211

Introduction

The Wasatch Hurricane fault system is a major structural feature in the western United States as it is the eastern boundary of the Great Basin. Recurrent movement along this fault zone has probably occurred since mid-Tertiary time and recent displacement can be seen in displaced Pleistocene Lake Bonneville shoreline features, moraines, alluvial fans and basaltic lava flows. This fault zone lies along the Intermountain Seismic Belt which cuts through the most populous part of the state of Utah. Many serious earthquakes have occurred since man has occupied the state and studies in progress by K. L. Cook, R. B. Smith, and others at the University of Utah are delineating the nature of current seismicity--the frequency, location, magnitude, and sense of ground motion.

Although modern seismological investigations are capable of defining current earthquake activity, the limited time period (< 100 years BP) over which the phenomena have been monitored hampers a thorough analysis of the whole problem. Indeed, the intensity, frequency, and location of activity at present as monitored by seismology, may bear no necessary relation to activity in prehistoric time, nor necessarily be the best basis for predicting future activity. Clarence Allen (1975, p. 1041)

> ". . . argues that the geologic record, and the late Quaternary history in particular, is a far more valuable tool in estimating seismicity and associated seismic hazard than has generally been appreciated . . . earthquakes in these regions (the Orient, Middle East) show surprisingly large long-term temporal and spatial variations. The very short historic record in North America should, therefore, be used with extreme caution in estimating possible future seismic activity. The geologic history of late Quaternary faulting is the most promising source of statistics on frequencies and locations of large shocks. The most important contribution to the understanding of long term seismicity, which is critical to the siting and design of safe structures and to the establishment of realistic building codes, is to learn more--region by region--of the late Quaternary history of deformation.

As a specific example of the sort of temporal and spatial variations that can occur in earthquake fault activity, the area near Cove Fort in central Utah may be cited. In a detailed survey of Quaternary faulting, E. Clark (1977) has found that areas of highly concentrated faulting activity during the Quaternary do not correspond with the area of seismic activity monitored during the summer of 1975 (Olsen, 1975, personal communication).

In order to understand the dynamics of the Wasatch-Hurricane fault zones in Utah, we must first understand the history of movement during the late Cenozoic and attempt to formulate a working model of recurrence rates and magnitudes of strain.

The purpose of this project is to attempt to determine the history of recurrent movement along the Wasatch-Hurricane fault zone during late

Cenozoic time by studying morphology of the mountain front. Preliminary studies (Hamblin, 1976) suggests that a significant history of fault movement is preserved in the morphology of the upthrown block, and that periods of active movement, separated by periods of stability along the fault zone can be identified. Our objective in studying scarp morphology is to understand the patterns of fault dynamics, i.e., recognize the patterns in which active displacement and periods of quiescence have alternated during late Cenozoic time.

In the southern part of the fault zone from Filmore, Utah to the Grand Canyon, a number of late Cenozoic basalt flows have been extruded along the fault zone. The flows have been uplifted and faulted by recurrent movement along the fault zone and provide a means of establishing a time framework with which other geologic observations can be set. Utilizing the radiometric and thermoluminescence dates on the basalts which have been offset by faulting, we have attempted to establish rates of displacement and a time framework for the history of activity along the fault zone. It is hoped that this information will provide a better understanding of the history of the fault zone which should help to provide a sound geologic basis for the interpretation of seismic data currently being obtained in the region.

Rationale

W. M. Davis (1903) recognized that the face of a mountain range carved in a fault block should preserve certain features reflecting its origin. He considered that the scarp along the Wasatch front was developed by continuous displacement along the Wasatch fault at a slow, relatively uniform rate and that the faceted spurs were formed as the scarp was dissected by stream erosion. Davis believed that the small basal facets along the fault line near Spanish Fork, Utah, resulted from dissection of larger facets by small ravines.

Remnants of narrow erosional surfaces are preserved at the apices of many faceted spurs and suggest that movement along the fault was not continuous, but that periods of movement were separated by definite periods of tectonic stability during which essentially no displacement occurred. During these periods of quiescence, erosion caused the scarp to recede from the fault line to produce a small narrow incipient pediment at the base of the mountain front.

The origin and evolution of the geomorphology of a mountain range carved on a fault block is not simple, but depends upon the balance of a number of surficial processes, all operating contemporaneously upon a fault block which is experiencing recurrent uplift. Some of the more important processes would include: (1) development of the fault scarp, (2) development of faceted spurs by stream erosion, (3) development of pediments during periods of tectonic stability, and (4) structural and stratigraphic controls of geomorphic feature.

Development of the fault scarp. If the amount of displacement along faults that cut alluvial fans, lake sediments, and moraines in the Basin and Range province is typical of the type of movement that occurred in the past, then displacement to produce large fault scarps occurred in increments of a few meters each, separated by periods of stability of hundreds or thousands of years during which additional displacement would possibly continue as tectonic creep. Although weathering and erosion would begin to act upon the scarp as soon as differential relief was produced, the length of time between each period of displacement would be insufficient to allow significant modification of the fault scarp formed on resistant bedrock.

Development of faceted spurs. The characteristics of the drainage system that existed prior to uplift would have a significant effect upon the development of the morphology of the fault scarp. Antecedent streams cutting across the fault line would immediately dissect the scarp into a series of triangular faceted spurs (Fig. 1) as slope retreat would enlarge the stream valleys at the expense of the scarp and faceted spurs (Fig. 2).

New consequent streams formed on the facets and fault scarp would modify the larger facets in a manner noted by Davis (1909, p. 746):

> The moderate dissection of the large facet by small ravines results in the development of several little basal facets along the fault line, where they form the truncating terminals of several little spurs.

Davis considered this effect to be the sole origin of compound faceted spurs as he did not recognize the effects of recurrent uplift on facets (although he did recognize that recurrent uplift is likely). Inasmuch as these consequent streams, like the antecedent ones, are unevenly distributed, the small basal facets so produced will be of varying sizes. An important point to note concerning these secondary facets developed from erosion by consequent streams is that there would be no remnant of a pediment at their apices. Each facet would develop at the end of a sloping ridge.

Development of pediment surfaces. As noted by King (1953), pediment formation appears to be a universal process, occurring in all climates and is the end product of slope retreat. If a prolonged period of tectonic stability occurred on a fault scarp during which little if any displacement developed, slope retreat would cause the scarp (series of faceted spurs) to recede back from the fault line with the development of a narrow pediment along the mountain front. The surface of the facets would be reduced to a stable slope and would not represent the actual fault surface which, whenever observed, is more than 80°.

Recurrent uplift along the fault would produce a new generation of faceted spurs and the pediment surface produced by the period of tectonic stability would be largely destroyed by downcutting and slope retreat by the drainage of the mountain front. Remnants of the pediment would be preserved as a horizontal or slightly inclined ridge at the apex of the newly formed facets (Figure 3). The length of the ridge (pediment remnant) would be an expression of the duration of the period of tectonic stability.

The uplifted pediment remnants would suffer further modification with time. It is believed that these horizontal ridge segments would be carried back with the general slope retreat of the mountain front and although the original pediment surface would be destroyed, the horizontal ridge segment would not be lost in backwearing. With time, however, the pediment remnant would ultimately be obscured or lost.

Structural and stratigraphic controls. Where alternating resistant and non-resistant rocks occur in the uplifted block, the morphology of the mountain front may be dominated by cliffs and slopes not related to pediments or fault scarps. This type of structural and stratigraphic controls of the landform, however, can usually be identified because the resistant rock units generally produce good outcrops so the relation between cliff and slope topography to rock type is readily apparent.

Model of the geomorphic evolution of a fault block mountain. Considering the various processes described above, we have constructed a simplified graphic model of how a fault block mountain would evolve (Fig. 4). Diagram A shows the beginning of uplift with the development of a fault scarp. Downcutting by the antecedent drainage is concurrent with uplift and the triangular facets produced during this stage are not all the same size as a result of the uneven spacing of the streams. Diagram B shows the morphology developed or mountain front if uplift is continuous. With no significant periods of tectonic stability, the scarp simply grows without interruption. Consequent streams develop upon the major faceted spurs and develop secondary facets at the base of the mountain front. The apex of each facet connects with the undissected surface with a smooth sloping ridge line rather than meeting it directly.

If, however, a prolonged period of tectonic stability occurred (Diagram C), the faceted spurs would recede back from the fault line by slope retreat which would cause a narrow pediment to form along the mountain front. As the scarp receded, the slope angle would also gradually decrease.

Diagram D shows a period of renewed movement along the fault which would produce a new scarp and series of faceted spurs dissected by the

pre-existing drainage, that is, the major crosscutting streams which formed the original faceted spurs shown in B, and by the consequent streams formed on the face of the faceted spurs shown in E. The original spur face would be modified by erosion, but its outline would be preserved. Remnants of the small pediment developed in C would be preserved at the apices of the new generation of faceted spurs, and secondary faceted spurs would develop as a result of dissection by the major crosscutting streams and the consequent streams. A third period of stability (F) followed by recurrent movement (G) would produce another generation of faceted spurs with pediment remnants at their apices (H). The slope profile of each generation of facets would progressively flatten with age.

The important element in recognizing the history fault displacement is the presence of pediment remnants. They are best preserved on the younger facets, but can be seen by distinct breaks in the ridge crest in the higher and older facets.

If the model of physiographic evolution of a fault scarp represented in Figure 4 is correct, then the episodes and magnitude of movement along a fault are indicated by the number, size, and spacing of the pediment remnants that form crests of faceted spurs.

Pediment Remnants and Faceted Spurs Along the Wasatch Front

The results of our study of the faceted spurs and pediment remnants along the Wasatch Mountains are shown in the series of cross-sections (Figure 5). Some erosional surfaces are recognized throughout most of the length of the Wasatch Ranges but others are preserved only in local areas and correlation of these is quite subjective. The major erosional surfaces which can be correlated for an appreciable distance are labeled alphabetically from the lowest to the highest.

The lower pediments and faceted spurs (Levels A, B, and C). The lowest and youngest pediments are carved on the mountain front at elevations ranging up to 1,000 feet above the shoreline of Lake Bonneville. It is possible that other facets and pediments were formed at lower elevations but have since been buried by lake deposits and alluvium. In general, the lower pediment remnants are approximately 300 to 600 feet wide and in most areas at least three levels can be seen. Most of the surfaces are nearly horizontal but some are inclined up to 10° to the west and locally some pediments are tilted to the east. This suggests an eastward tilting of the fault block accompanying the displacement.

The faceted spurs associated with the lower pediments are fresh and relatively unaltered in most areas and consequent streams are not firmly established on the facet. Locally, erosion is quite advanced, however, and the fault scarp is carved into classical compound faceted spurs.

The intermediate pediment surface (Level D). Along most of the Wasatch front, a prominent erosional surface exists above the lower compound facets and marks what is perhaps the most significant pediment to form during the displacement along the Wasatch fault. The pediment remnants occur from 2,000' to 2,500' above the shoreline of Lake Bonneville and are mostly isolated horizontal ridge crests although some flat relatively wide surfaces are preserved. These erosional surfaces are usually 400-500 feet wide but in the Salt Lake City area, the surface is as much as 21,000 feet wide. The exceptionally wide surface is expressed as the nearly horizontal ridge crests on both sides of City Creek Canyon, Red Butte Canyon, and

Emigration Canyon. Several individual pediment surfaces are undoubtedly represented in the intermediate level, but they have been modified by erosion to such an extent that they cannot be correlated with confidence. The intermediate level thus probably represents several separate erosional events which occurred in the same general time period throughout the fault zone.

The faceted spurs below the intermediate levels, of course, include the lower facets which combine with the intermediate facet to form a large well-defined compound facet. Consequent streams are well established on the upper surface of the facets and have eroded wide valleys which are narrow near the base of the mountain to form the well-known "wine-glass" valley form.

The high pediment surfaces . Above the intermediate pediment surface are vestiges of older and higher erosional surfaces. They generally occur at elevations above 8,000 feet and cannot be correlated with confidence over a large area. In places, these surfaces appear to merge with that of the intermediate level but elsewhere, remnants of the high pediment surfaces appear to have simply been destroyed by erosion.

Methods

The faceted spurs and remnants of incipient pediments were mapped on topographic quadrangles at a scale of 1:24,000. This was done by utilizing standard stereoscopic aerial photographs and special oblique aerial photos flown specifically for this study. Flights were made during both early morning and late afternoon which provided optimum lighting for the entire area regardless of the orientation of the mountain front. The faceted spurs and pediment surfaces were identified and outlined on the photographs and then plotted on topographic maps. These features were usually expressed well enough by topographic contours so that there was little difficulty locating their position and elevations to the nearest contour.

A series of cross-sections across the mountain front were then constructed from the data on the topographic maps. These profiles show the overall character of the morphology of the mountain front and not a precise cross-section along a specific line. Important erosional surfaces which did not fall on the line of profile were projected to it and the width of pediment surfaces were exaggerated in order to emphasize their relationships to other morphologic features.

After the profiles across the scarp were constructed, the pediment remnants were correlated visually, using size, elevation, trends and sequences as keys to identification. A cross-section showing the pediment surfaces in the plane of the fault parallel to the mountain front was then constructed (Figure 5). These data then served as the basis for interpretation.

The Northern End of the Wasatch Fault (Figure 6)

The Wasatch fault terminates to the north in the vicinity of Tremonton, Utah, where the mountain range gradually descends to the level of Lake Bonneville. The fault system, however, continues northward, probably in an en echelon pattern, into the vicinity of Malad, Idaho.

This area is important because it shows the three major erosional surfaces converging northward and merging where the range dies out. The general nature of displacement on all levels shows scissor-type displacement.

Southward, the lower levels (A, B, and C) diverge until they reach elevations of 5,800', 6,000' and 6,300' respectively and then continue southward as well defined pediment remnants and associated faceted spurs which rise and fall in culminations and depressions. The topography of the range becomes quite rugged with numerous outcrops of resistant lower Paleozoic limestone and quartzite so that there is significant structural control to the details of the morphology of the mountain front. Compound faceted spurs are nevertheless well developed.

The intermediate level (D) is perhaps the most pronounced erosional surface in this area and east of Honeyville, it forms a prominent break in slope up to 1,000' wide at an elevation of 7,000'. The rocks in this area are steeply dipping resistant lower Paleozoic quartzite and limestones, but the pediment surface cuts across resistant and non-resistant units alike. A smaller, but similar, surface is preserved at 6,100' to 6,230'. The lowest erosional surface is between 5,400' and 5,600'. The associated faceted spurs terminate northward around the small reentrant just north of Honeyville where the main fault is offset to the east in an en echelon pattern. Two important relations are shown here: (1) the fault has an en echelon pattern which produces reentrants in the trend of the range, and (2) all erosional levels show pronounced scissor movement. This is, of course, best developed in the lowest A and B levels which rise and fall and in places pinch out completely near the south end of the Honeyville quadrangle.

Suggestions of high level pediments at elevations of 7,500', 7,800' and 8,600' are found along this segment of the range, but these cannot be correlated over long distances.

Brigham City Area (Figure 7)

The outcrops of resistant Paleozoic limestone and quartzite continue to dominate the geomorphology of the mountain front for several miles south of Honeyville, but there is still a strong tendency for erosion to develop the typical compound faceted spurs. The height of the Wasatch mountains decreases to a minimum near Brigham City where the crest is at an elevation of only 6,500'. This depression in topography could represent a major structural depression with the uppermost erosional surfaces converging down to the intermediate (D) level. If this is the case, then the area around Brigham City did not experience uplift during the early stages of the development of the Wasatch fault but remained stable until after the intermediate erosional surface was developed. Since then, uplift along the fault in the Brigham City area has been similar to that in other parts of the Wasatch Range.

The intermediate level is at approximately 6,500' and forms a wide flat surface about 1/4 mile wide at the crest of the range.

The record of movement along the fault in this area appears to be quite simple. Little or no displacement is recorded during the earlier history of the fault when uplift occurred both to the north and to the south. After the period of regional stability along the fault, which is recorded by the intermediate level, this area was then uplifted in much the same manner as the rest of the fault.

Brigham City to Ogden (Figure 8)

Southward from Brigham City, the crest of the Wasatch Range gradually rises to an elevation of 9,712' at Ben Lomand Peak. The structure is complex with large areas of Precambrian metamorphic rocks complicated by thrust faulting. Immediately south of Brigham City, the compound faceted spurs below the intermediate level are well defined and deeply dissected. The lower levels A, B, and C show culminations and depression indicating scissor movement during the more recent history of displacement.

The salient just north of Ogden exhibits some of the most rugged topography of the Wasatch front. Here, the thick Brigham Quartzite forms a steep rugged cliff below which is a ragged terrain formed on the Precambrian metamorphic rocks. The Brigham Quartzite inhibits development of pediment surfaces and faceted spurs but the metamorphic rocks below are carved into compound faceted spurs and intermediate (D level) pediment surfaces are apparent midway up the mountain face. A, B, and C levels are also developed.

In the Ogden reentrant, structural and stratigraphic complexities are so pronounced that most faults and pediment surfaces did not develop. There appears to be another area of depression in the vicinity of North Ogden which is best expressed in the A and C levels.

On the face of Mt. Ogden, the intermediate is well developed and can be traced with considerable confidence southward to Utah County.

Ogden to Bountiful (Figure 8)

From Weber Canyon to Bountiful, the morphology of the Wasatch front becomes progressively dominated by a series of long simple spurs which terminate in compound facets near the base of the mountain. The importance of this morphologic development is that it represents a different history than that recorded in most other regions. Both the erosional surfaces, the slope of the spur face, and the shape of the ridge crust (shape of intervening valleys) indicate that: (1) total displacement was less, (2) recurrence rate during tectonism was more gradual, and (3) stability between active periods was probably longer.

An interesting observation in this area is that there are a series of sharp bends in the major drainage patterns which occur along linear trends in the Kaysville area over a distance of several miles. Only those streams antecedent to the spurs are offset; those consequent on the spur surface show no irregularities in their course. These have been interpreted by Eardley (1939) as being fault controlled. They appear, however, to correspond with the apex of various spurs and probably represent adjustment of the streams course along the mountain front when the various levels were localized along the fault line.

In the vicinity of Kaysville, the general morphology of the mountain front when viewed from the valley floor appears to be a series of long simple spurs descending from the crest of the range down to the base of the mountain front where they terminate in a single facet. It is apparent from the topographic maps of the area, however, that this portion of the Wasatch Mountains is not unlike that in the Spanish Fork region, but is much more subdued. Most elements of it simply show a much more advanced stage of development. The mountain front is more subdued, the

stream profiles are flatter, and the valley walls are cut by secondary tributaries. The ridge map of Kaysville area has many characteristics similar to those of Lofer Mountain.

The spur consists of a long sloping ridge with a major compound facet at the apex of the D level. The compound facet is highly dissected and faceted spurs below the C and B levels are well defined. The facets below the A level, however, are only locally developed. The long simple ridge above the D level extends upslope to the crest of the range. Remnants of higher erosional surfaces can be seen on the ridge crest and in some areas tilt eastward suggesting an eastward tilt to the fault block.

The central theme that each section in this area repeats is that there is a long record of displacement along the fault prior to the formation of the D facets and that during this period, the uplift was separated by longer periods of stability than is recorded both to the north and south of Salt Lake City.

One of the most significant features along the Wasatch Mountains between Ogden and Bountiful is the gradual descent of the crest of the mountain range to a low depression at North Salt Lake. The intermediate level descends from a general elevation of 7,600' near Ogden to a level of about 6,200' at North Salt Lake. The lower levels, A, B, and C also descend in a comparable fashion. The profile of the mountain front becomes progressively more subdued southward and the intermediate and high erosional surfaces broaden to become 4,000 to 5,000' wide along the crest of the spurs at North Salt Lake. This is the most significant structural depression along the Wasatch fault and is also the area where the intermediate and high erosional surfaces are widest.

Salt Lake City Area (Figure 9)

The morphology of the Wasatch Mountains in the Salt Lake City area has a number of unique features which provide important data concerning the nature and history of fault displacement. Throughout most of its length, the crest of the Wasatch Range is only a mile or two east of the fault line, and the mountain front is characteristically steep, typical of that produced by uplift of a fault block. In the Salt Lake City area, in contrast, the crest of the Wasatch has been eroded back 7-10 miles from the fault line and the mountain front is deeply dissected by large consequent streams such as City Creek, Red Butte Creek, Emigration Canyon, and Parley's Canyon. This has produced a series of long, gently-sloping spurs extending from the crest of the range to the fault line where they terminate in a series of compound facets.

The longest ridge is just north of City Creek Canyon and extends from Grandview Peak to Meridian Peak along the Salt Lake-Davis County line. The ridge has two long sections which are nearly horizontal: one at an elevation of 6200' which is believed to be made by the convergence of the C and D levels and one at 7000'; a well-preserved remnant of an upper (E) level surface. Both are over a mile wide and are easily recognized on the topographic map. Vestages of higher upper-level surface (F, G, and H) are preserved at elevations of 8200', 8600' and 9200'. The D and E surfaces can be recognized along most of the spurs from Bountiful to Parleys Canyon at remnants of the widest erosional surfaces along the Wasatch front.

A second significant fact is that these surfaces are 1000' to 1500' lower in the Salt Lake area than the adjacent regions to the north and south. This indicates that the Salt Lake area was an area of prolonged tectonic quiescence during the early and intermediate periods of displacement above the fault. Furthermore, when movement did occur during this period, displacement was significantly less in the Salt Lake region than in the areas to the north and south.

The elongate spurs in the Salt Lake area all terminate at the fault line in compound faceted spurs with the major apex located at the intermediate level (D) at elevations from 6200' near Bountiful to 7100' in the vicinity of Parleys Canyon. The major apex of the spur is between 1 and 1 1/2 miles back from the fault line and the various facets are dissected to a much greater degree than similar facets to the north and south. Remnants of well-defined erosional surfaces of the A, B, and C levels are preserved on every compound facet. The A level is distinct, but is generally less than 100' wide. The B level ranges in width to nearly 1/2 mile wide and the C level is in places over 1/2 mile wide.

The high degree of dissection on the compound facets plus the wide remnants of erosional surfaces at each level indicate that a significantly longer period of tectonic quiescence occurred between the major periods of displacement in the Salt Lake City area than elsewhere. The total amount of displacement during the A, B, and C periods, however, is approximately the same as other areas along the Wasatch fault.

South of Parleys Canyon, the general character of the mountain front grades rapidly into that typical of the rest of the Wasatch Range. The crest of the range swings back to within 2-3 miles of the fault line and the mountain front becomes steeper. The intermediate and high erosional surfaces become progressively narrower southward and at Mount Olympus they attain the width of 400-600 feet, typical of those in other parts of the range. The intermediate level rises from its low position of 6200' north of City Creek Canyon to 7400' at Mount Olympus and Lone Peak. The lower levels (A, B, and C) rise and fall in small culminations and depressions typical of other parts of the range but maintain their general elevation of 5400', 5700', and 6100' respectively.

The rocks exposed on the face of Mount Olympus consist of alternating resistant and non-resistant strata dipping steeply to the south. Details of the morphology of the mountain front reflect considerable lithologic control but remnants of the A and D surfaces are remarkably well-developed. The D level occurs at an elevation of 7400' and is approximately 2 miles long. Possible remnants of high level surfaces occur on the flat spurs ridge at 8400'.

The low level surfaces are also well-defined but only 100-200' long. Just north of Little Cottonwood Canyon, the lower levels and facets are among the most obvious features along the lower mountain front. The lower levels are easily correlated in this area and show pronounced scissor movement.

Lone Peak at the southern end of Salt Lake Valley provides additional independent evidence of periods of tectonic activity along the Wasatch Fault alternating with periods of tectonic stability. On the south side of Lone Peak are four streams which do not flow down the slope of the mountain face, but are entrenched into the mountain block and flow almost parallel to the regional contours of the mountain slope. These were noted by Gilbert (1928) and by Bullock (1958) and were interpreted by Gilbert to be former segments of Corner Creek which were entrenched into the mountain

block and uplifted by recurrent movement. This interpretation is significant in that it implies quiescence during which time the streams were allowed to cut a deep channel. Recurrent movement along the fault then elevated the channels to their present position.

American Fork Canyon to Provo Canyon

Mt. Timpanogos exhibits a wealth of potential remnant pediments but strong structural control for terrace development exists as several surfaces and structural terraces are formed where the Manning Canyon Shale has been stripped off the resistant Great Blue Limestone. The D level is again very prominent and coincides with the wide ridge behind Big Baldy and with the summit of Mahogany Mountain. While classic faceted spurs are scarce, the A level is well represented. Whether or not uplifted pediment remnants are preserved on the face of Mt. Timpanogos above the D level is somewhat speculative, but the data appears to strongly support the higher level as shown and the others may be valid as well.

Provo Canyon to Springville (Figure 10)

This segment begins as an area of potentially greater structural control due to the complex stratigraphy. Many more data points are present in this area, probably not because of better preservation, but due to greater frequency of nonpediment-related surfaces such as structural benches. Nevertheless, good correlations are found. The D level is especially apparent on the face of Buckley Mountain, at Maple Flat, and behind Squaw Peak. Maple Flat is critical, as it is a broad surface carved on the resistant Humbug Formation. The C and D levels are all well expressed. Lower level surfaces are particularly well preserved at the mouth of Provo Canyon.

Springville to Spanish Fork Canyon

This area has been called by Davis (1909) the type area for faceted spurs. It undoubtedly has the best compound facets of any area and the record here is clearly one of relatively uniform cumulative uplift composed of individual scissors or hinge movements separated by distinct periods of quiescence. The basal facets and associated A level are well preserved, and the D level is quite well developed on the face of Spanish Fork Peak, at the summit of Ether Peak and at the summit of Powerhouse Mountain. Several of the pediment remnants just north of Hobble Creek Canyon indicate by their attitude a possible eastward tilt of the fault block. A section of A level continues in from the south.

Spanish Fork Canyon to Payson Canyon

This segment of the Wasatch Fault is the eastern portion of an echelon pattern which presumably dies out southward and picks up again offset to the west. The D level is well developed, and is seen as a broad upland above the prominent scarp. The E level is also present at the apices of two prominent facets perched quite high, and this development is quite similar to that seen elsewhere to the north. While the A and B levels are missing, or pinched out at the extreme southern end, they appear and are well preserved on the west face of Loafer Mountain. Northward from there, the A level remnants disappear for a stretch as the fault trace bends eastward but are preserved closer to the mouth of Spanish Fork Canyon.

Payson to Nephi

The mountain front from Payson to Nephi is a unique area along the Wasatch Front. In this area, large alluvial fans have been built up along the base of the mountain range and shoreline features which characterize the other parts of the mountain front are lightly etched into alluvium in the central part of the basin far beyond the mountain front. This area, therefore, provides a model of the geomorphic processes active along the Wasatch Mountains before the basins were occupied by Pleistocene lakes.

The major geomorphic features are large alluvial fans and debris flows of various ages. These have been cut by recurrent movement along the fault and provide an excellent record of displacement along this segment of the fault not preserved in other areas.

In this segment of the Wasatch Fault, the morphology of the mountain range front is complex and undoubtedly represents a complex history of movement. There are as many as twelve erosional surfaces preserved along certain segments of the mountain front, but others have only six. Correlation in this area becomes a problem and it appears that the minor surfaces die out along strike, much like the recent scarps in alluvium, but on a much larger scale.

One larger erosional surface can be correlated from Nephi to Payson and provides important insight into the history and evolution of the Wasatch Fault. This surface is approximately 9000 feet high near Nephi but descends rapidly to 6300 feet in the central part of the area and to 5700 feet just south of Payson. The slope of this surface is reflected in the total height of the mountain range and strongly suggests that the total scissor-type movement is directly reflected in the present topography.

Rates of Displacement

At present, there are no effective methods of determining rates of displacement along the Wasatch Fault but to the south, along the Hurricane and Toroweap fault zones, a series of late Cenozoic basalt flows have crossed the fault line at various times and have been subsequently displaced. Absolute dates have been determined for a number of these flows and provide some insight into rates of movement along the border faults of the Basin and the Range. Many lava flows were dated using K-Ar methods, but we also utilized the thermoluminescence method.

The thermoluminescence (TL) method of age dating has been used for over 15 years to date archaeological materials which contain inclusions of quartz or feldspar. By comparing TL ratios to age for samples previously dated by the K-Ar or ^{14}C methods, it is possible to accurately date oceanic basalt from 5,000 to 200,000 years old. Similar techniques were developed in this study for application to the TL age dating of continental basalt (Holmes, in press). Samples of known age (from 3,000 to 440,000 years old) were used to construct the TL calibration curves shown in Figure 11. The TL calibration for continental basalts was shown to be significantly affected by variations in bulk rock composition. Accordingly, the samples were divided into three petrochemical groups--alkali olivine basalts and basanites (Type II), Fe-rich olivine tholeiite basalt (Type I), and basaltic andesites (Type III). The calibration curves for each sample type are shown in Figure 11. Only a portion of the Type II samples are considered in this report.

The quantitative data presented below suggest that such a pattern of alternating periods of tectonic activity and inactivity indicated by geomorphic features along the Wasatch Fault may also be typical of segments of the Hurricane and Toroweap faults some 400 km to the south.

The theoretical limitations of calculating absolute strain rates from the fault displacements of lavas of known age can be seen by a careful examination of Figure 12. In contrast to the semi-continuous record of displacement preserved by the geomorphic development of major fault scarps, a measured displacement and age give only the <u>average rate</u> of fault displacement since that time; no specific information is gained regarding the detailed history and sequence of that displacement (Figure 12). Moreover, the analytical uncertainties in the age determinations may make it impossible to determine details of the displacement history even when several data points are available (see, for example, Point C in Figure 12).

Nonetheless, even when the average strain rate is the only available evidence, as is the case in this study, it may still be possible to draw some generalizations regarding the gross patterns of displacement history. Recent strain rates, which are markedly different from the average rates of displacement since some older event, may allow some boundary conditions to be set on the recent patterns and history of fault displacement. For example, the strain rates recorded by lavas erupted across a fault exhibiting recurrent movement (Figure 12) may be greater than, less than or indistinguishable from, the average rates of displacement since some older event (e.g. the inception of faulting). These data, respectively, might indicate or delimit periods of active tectonism, of relative quiescence, or of "normal" fault activity.

Dated lavas from three distinct fault segments were available for analysis in this study. The dated basalts range in age from 0.09 to 1.05 m.y. The three fault segments studied are shown in Figure 55; they are the northern Hurricane fault (in southern Utah), the southern Hurricane fault (in Whitmore Wash, Arizona) and the Toroweap fault (in Toroweap Valley, Arizona). The total displacements of these faults throughout geologic time, as given by Hamblin (1970), are 2400 m (8000'), 460 m (1500'), and 240 m (800'), respectively.

The fault displacements for each of the flows dated by the TL method, together with their TL age dates and calculated rates of displacement are listed in Table 1. Also listed in Table 1 are the ages, displacements and strain rates of several older basalts from this area which have been dated by the K-Ar method.

For the dated flows available, the average rates of displacement are 320 $\pm$ 80 m/m.y. for the northern Hurricane fault, 170 $\pm$ 30 m/m.y. for the southern Hurricane fault, and 70 $\pm$ 15 m/m.y. for the Toroweap fault. The significantly lower strain rate recorded by sample Zion-68 may be due to an error in the TL age date. Its proximity to samples Zion-20, Zion-57, and SG-81, which are only slightly greater age and which cluster near the average strain rate of 320 m/m.y., suggests that the value of 77 m/m.y. is anomalous and does not actually record a period of tectonic quiescence.

Further calculations suggest that two of these average rates of recent displacement are significantly higher than the corresponding presume average rates of fault displacement over the last 10 m.y. McKee and McKee (1972) estimate that most of the uplift of the Grand Canyon region has taken place within the last 5-10 m.y. By assigning an arbitrary age of 6 m.y. to the inception of faulting at the three studied locations, it is possible to project these most recent strain rates back over the postulated lifetime of these faults and to calculate the total displacement that would occur. The projected displacement of the northern Hurricane fault is 1900 $\pm$ 500 m, slightly lower than but not significantly different than the observed total displacement of 2400 m. In contrast, the projected displacement of the southern Hurricane fault segment is 1000 $\pm$ 200 m, more than twice the observed displacement of 460 m; the calculated displacement of the Toroweap fault, 420 $\pm$ 80 m, is also nearly twice the observed total displacement (240 m). These calculations appear even more significant in consideration of the fact that the arbitrarily assigned age of 6 m.y. is considerably younger than either the inception of Basin and Range faulting 16-19 m.y. ago or the 10 m.y. upper limit set by McKee and McKee (1972) for the beginning of major uplift in this area. These data show that recent displacement (<0.5 m.y.) along the southern Hurricane and Toroweap faults have taken place at rates significantly higher than those typical of the preceding 5-10 m.y.

We suggest, therefore, that the southern Hurricane and Toroweap fault segments are currently undergoing a period of active tectonic displacement and that these lavas record the type of recent tectonic activity modeled by Event A in Figure 12. The northern Hurricane fault, in contrast, appears to have undergone recent displacement at rates not markedly different from its presumed average rate of displacement since the beginning of Pliocene time and records the type of displacement history modeled by Event C in Figure 12. These data suggest that a "stop-and-go" pattern of alternating periods of recurrent fault movement and of tectonic quiescence may have typified the displacement history of these fault segments.

Summary of a Conceptual Model of Displacement in Normal Faults

From the data collected in this study, it is possible to construct a conceptual model of the nature of displacement along the Wasatch Fault and the evolution of the fault resulting from a series of recurrent displacements. The main idea developed is summarized graphically in a series of diagrams drawn in the plane of the fault (Figure 13).

A single tectonic event would produce a local scarp up to 4-5 meters high. The scarp would extend for possibly several kilometers and would represent scissor or ramp type displacement. In most cases, the upthrown block would be the active block moving up beyond the essentially stationary or passive downthrown block. Antithetic faults producing local grabens, of course, would be an exception. A series of tectonic events along the length of the fault line would produce a series of small discontinuous scarps like those shown in Figure 13.

Continual recurrent movement would produce larger compound scarps of greater areal extent separated by areas of tectonic stability (Figure 13). The fault scarps in the shorelines of Lake Bonneville would be an example of the style of development during this stage.

Prolonged recurrent movement would cause many of the first and second order scarps to merge and produce a continuous compound scarp with large culminations in areas of previous displacement, and depressions in areas of previous tectonic stability (Figure 13).

At some stage, stress along essentially the entire fault could be relaxed and tectonic stability would occur long enough to produce significant slope retreat and an incipient pediment at the base of the fault scarp. As stress built up, resurgence of tectonic activity would occur along the fault zone. Many small and local culminations and depressions resulting from first and second order scissor-type displacement would be removed by displacement in the formerly inactive areas, so that the rising scarp would become a continuous cliff (Figure 13).

Subsequent cycles of recurrent displacement separated by periods of tectonic stability would produce a series of erosional surfaces preserved at the top of compound faceted spurs.

History of Displacement Along the Wasatch Fault

Little is known about the topography of the Basin and Range province and Colorado Plateau prior to the initiation of Basin and Range faulting. During early Tertiary time, the area was the site of erosion of the Sevier orogenic belt and deposition of the debris as wedges of coarse alluvium. Remnants of the conglomerate are still preserved in many areas of the Wasatch Mountains. Later Oligocene-Miocene ash flow tuffs were extruded and covered large areas of the Basin and Range and western Colorado Plateaus in central Utah. Prior to faulting, the area of western Utah could be envisioned as a surface of relatively low relief (several hundred feet) consisting of erosional remnants of the Sevier topography and adjacent alluvial surfaces partly dissected into well-rounded low hills. The history of faulting can be outlined as follows:

1. Faulting was initiated during the uparching of the Basin and Range province. The initial series of displacements produced a series of discontinuous mountain ranges along what is now the Wasatch Front. Ranges occurred from Tremonton to Brigham City, Brigham City to Bountiful, and Salt Lake City to Nephi, each segment separated by a lowland. Minor periods of tectonic stability occurred locally within each range during this time. The first generations of consequent streams formed during this time and later evolved to become the large drainage systems along the Wasatch Front whose headwaters extend to the crest of the range.

2. A general period of tectonic stability occurred along the entire Wasatch Front and persisted long enough to develop what is now the high level erosional surfaces shown in Figure 14. This period of stability was longest in the Bountiful-northern Salt Lake City region where remnants of the erosional surface are several miles wide.

3. A second period of tectonism occurred and developed in a continuous scarp along the entire Wasatch Front with depressions in the vicinity of Brigham City and Bountiful (Figure 14). A second generation of consequent streams formed on the lower scarp.

4. Tectonic stability followed permitting significant slope retreat along the scarp and the D erosional surface at the base of the mountain front.

5. Recurrent tectonism followed developing a fresh scarp along the entire mountain range and elevating the two previously formed erosional surfaces.

6. Tectonic stability followed with associated slope retreat forming the series of level surfaces now preserved above the faceted spurs at elevations between 4500' and 6400'.

7. Resurgent tectonism along the entire fault zone developing a fresh scarp at the base of the mountain front which is now eroded into the faceted spurs 200-400 feet above the level of Lake Bonneville.

The widespread occurrence of fault scarps along the Wasatch Front in Lake Bonneville sediments together with the freshness of the most recent faceted spurs suggests that we are still in the later stages of the last period of active tectonism, which can be expected to continue intermittently for some time to come.

BIBLIOGRAPHY

Anderson, T. C., 1977, Compound faceted spurs and recurrent movement in the Wasatch fault zone, north central Utah: Brigham Young Univ. Geology Studies, v. 24, pt. 2, p. 83-101.

Bullock, R. L., 1958, Geology of the Lehi quadrangle: Master's thesis, Brigham Young Univ., Provo, Utah, 59 p.

Clark, E. E., 1977, Late Cenozoic volcanic and tectonic activity along the eastern margin of the Great Basin in the Proximity of Cove Fort, Utah. BYU Geol. Studies, v. 24, pt. 1, p. 87-114.

Davis, W. M., 1903, The Basin Ranges of Utah and Nevada: Jour. Geol. v. 11, p. 120-121.

_____, 1909, Mountain ranges of the Great Basin: Geographical essays: Boston, Ginn, p. 725-72.

_____, 1939, Structure of the Wasatch-Great Basin region: Geol. Soc. Amer. Bull., v. 50, p. 1277-1310.

Gilbert, G. K., 1928, Studies of Basin and Range structure: U.S. Geol. Surv. Prof. Paper 153, 92 p.

Hamblin, W. K., 1976, Patterns of displacement along the Wasatch fault: Geology, v. 4, p. 619-22.

Holmes, R. D., Thermoluminescence dating of Quaternary basalts: Continental basalts from the eastern margin of the Basin and Range province, Utah and northern Arizona: Brigham Young Univ. Geology Studies (in press).

King, L. C., 1953, Canons of landscape evolution: Geol. Soc. Amer. Bull., v. 64, no. 7, p. 721-51.

McKee, E. D., and McKee, E. H., 1972, Pliocene uplift of the Grand Canyon region-time of drainage adjustment: Geol. Soc. America Bull., v. 83, p. 1923-1932.

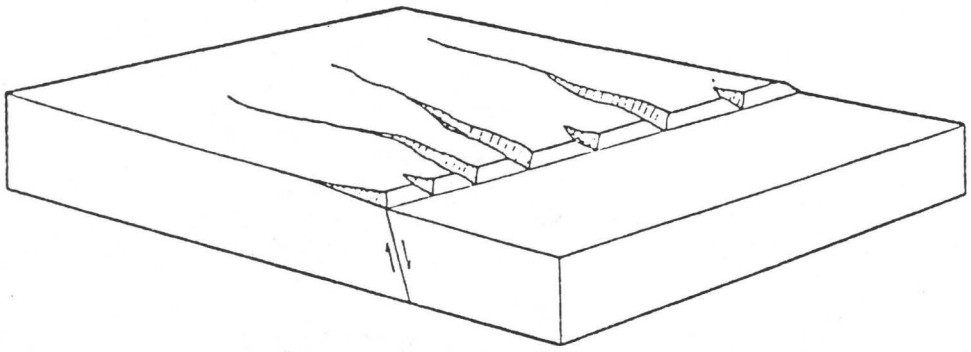

Fig. 1 - Dissection of a fault scarp by antecedent streams to produce simple faceted spurs.

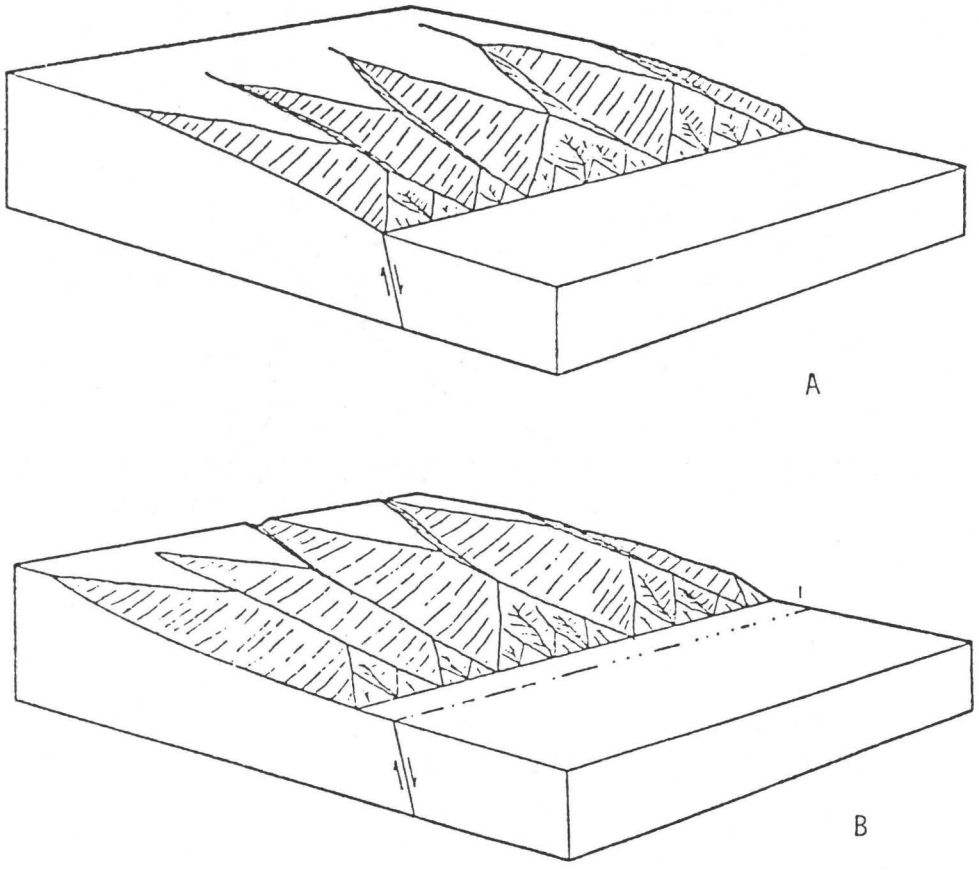

Fig. 2 - Growth of spur ridge by slope retreat of valley walls.

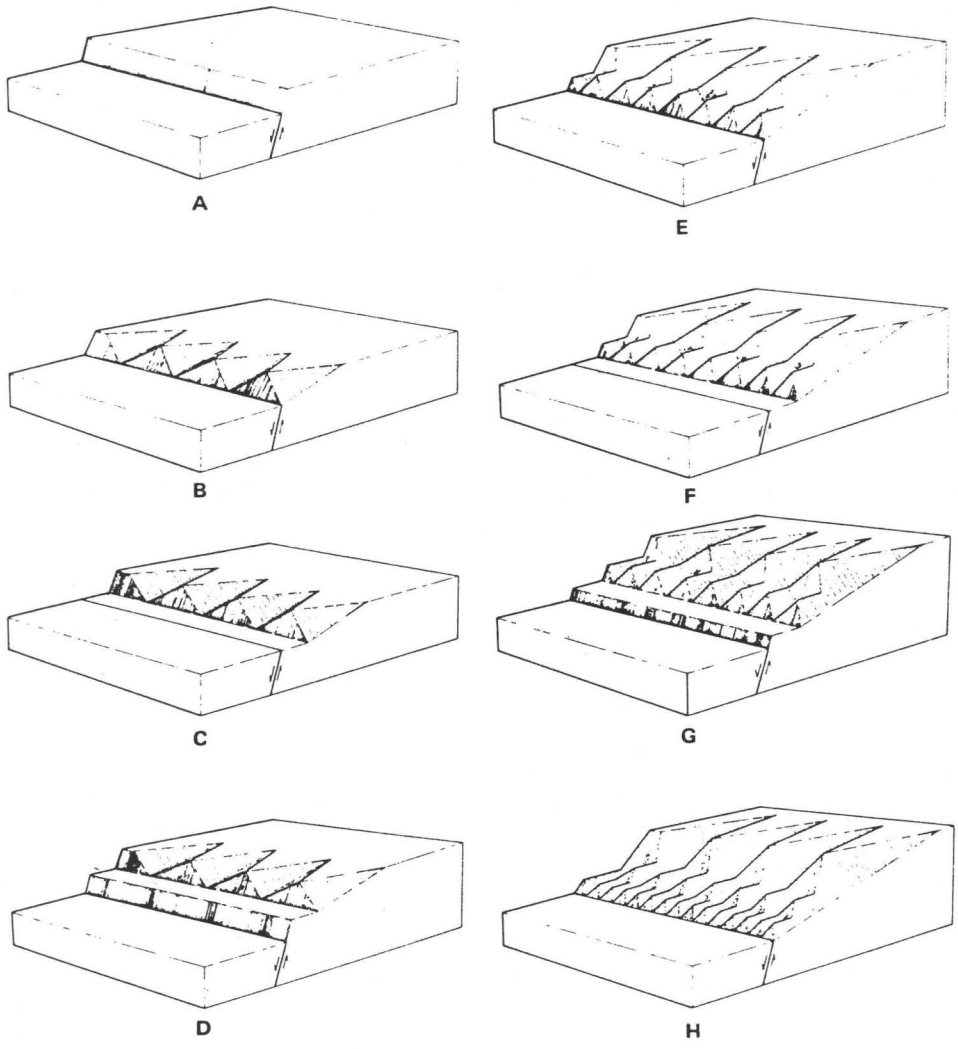

Fig. 4 - Diagrams showing evolution of faceted spurs produced by periods of movement separated by periods of stability. A, Undissected fault scarp; B, development of faceted spurs by streams cutting across scarp; C, period of stability with slope retreat and development of a narrow pediment; D, recurrent movement; E, dissection of new segment of scarp by major streams and by those developed on the face of faceted spurs formed in B; F, new period of stability with slope retreat and development of another narrow pediment at base of mountain front upthrown block; G, recurrent movement; H, dissection of scarp formed in G resulting in a line of small faceted spurs at base of mountain front. Remnants of narrow pediments are preserved at apices of each set of faceted spurs.

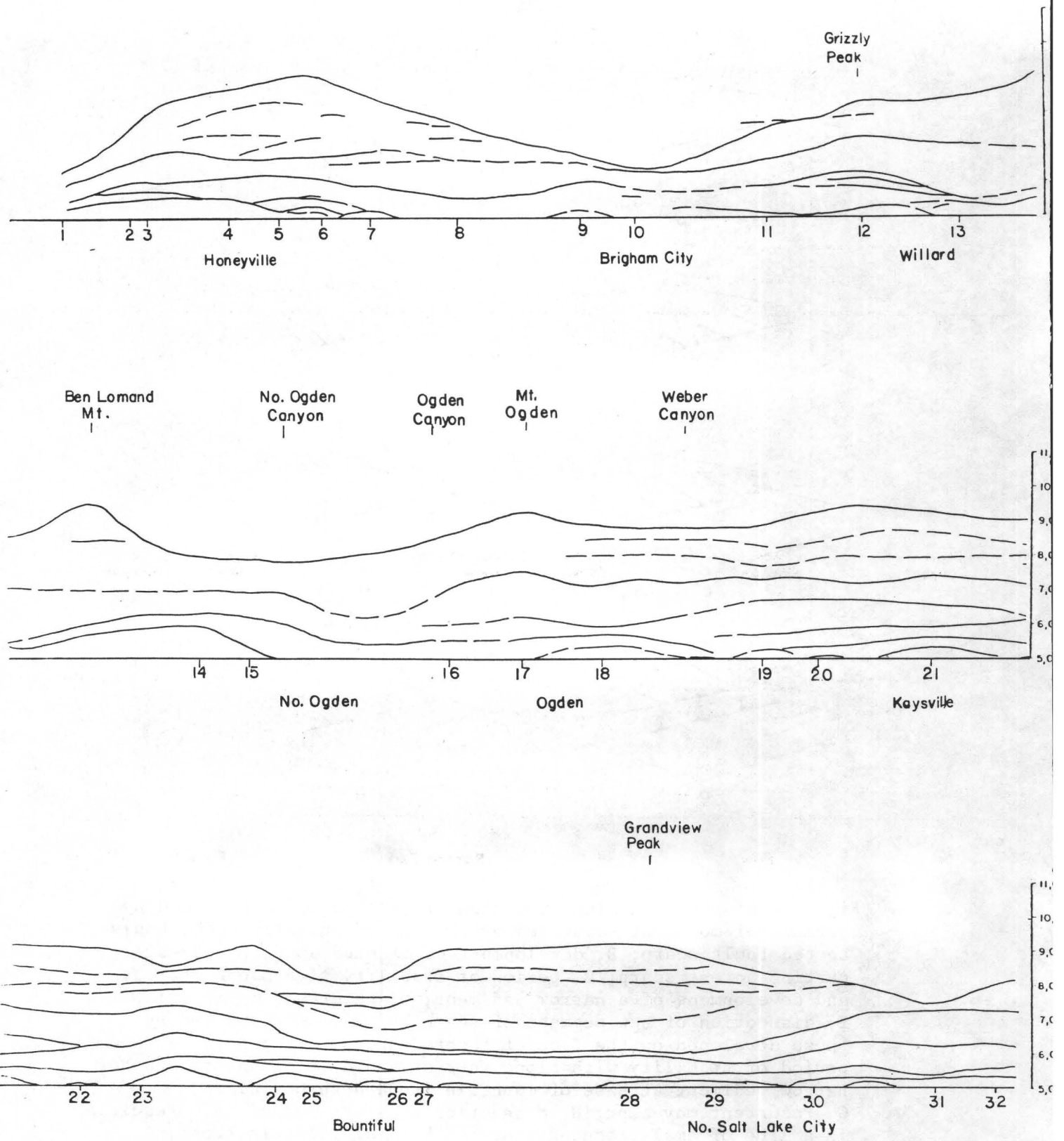

Figure 5 Diagram showing the elevations of the major erosional surfaces along the Wasatch Front

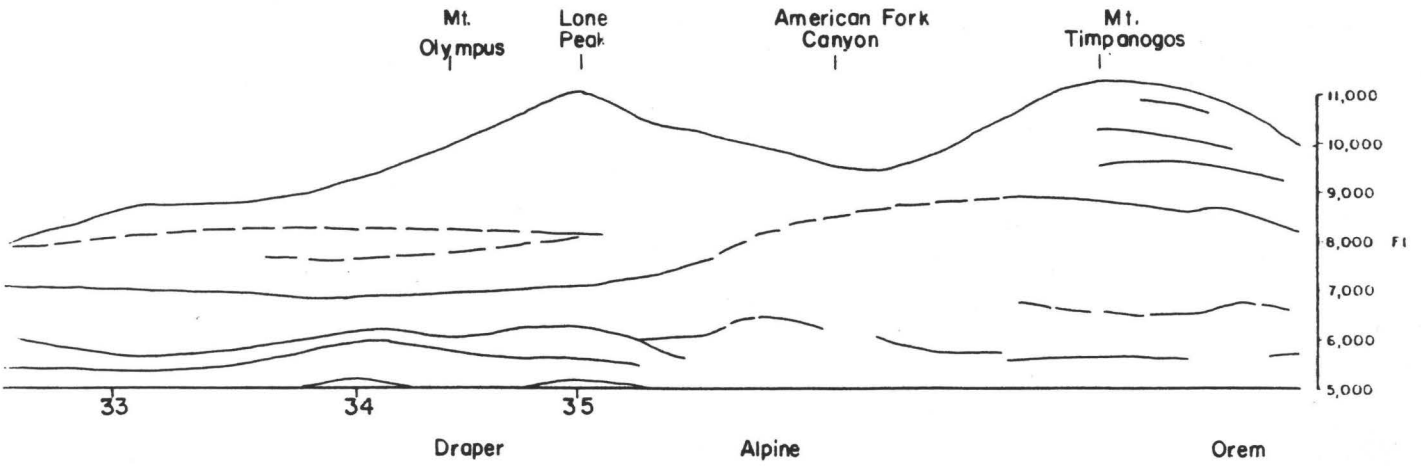

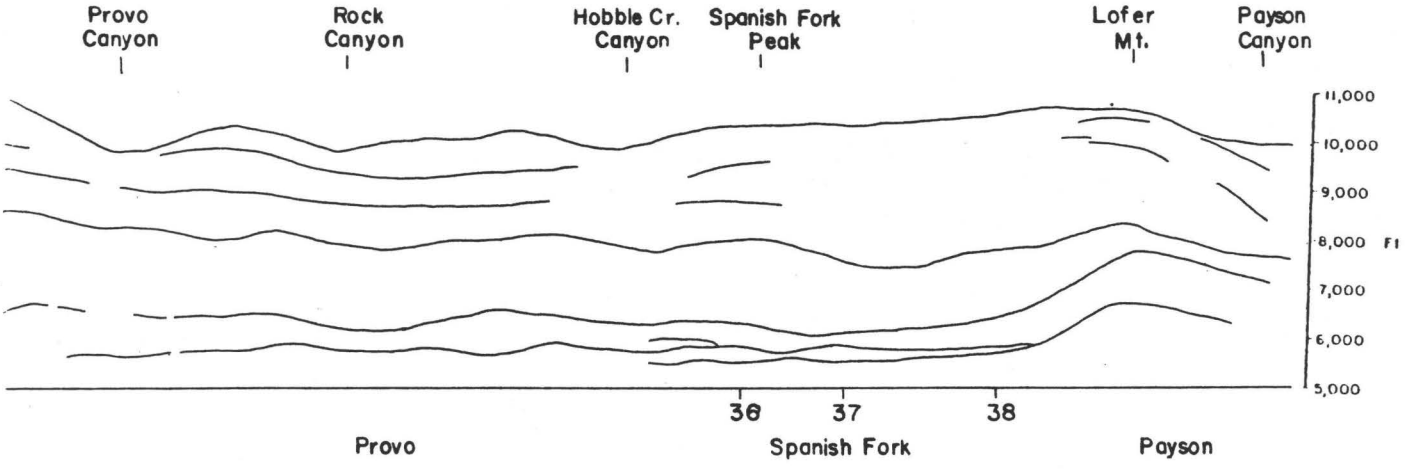

Figure 5 Cont.

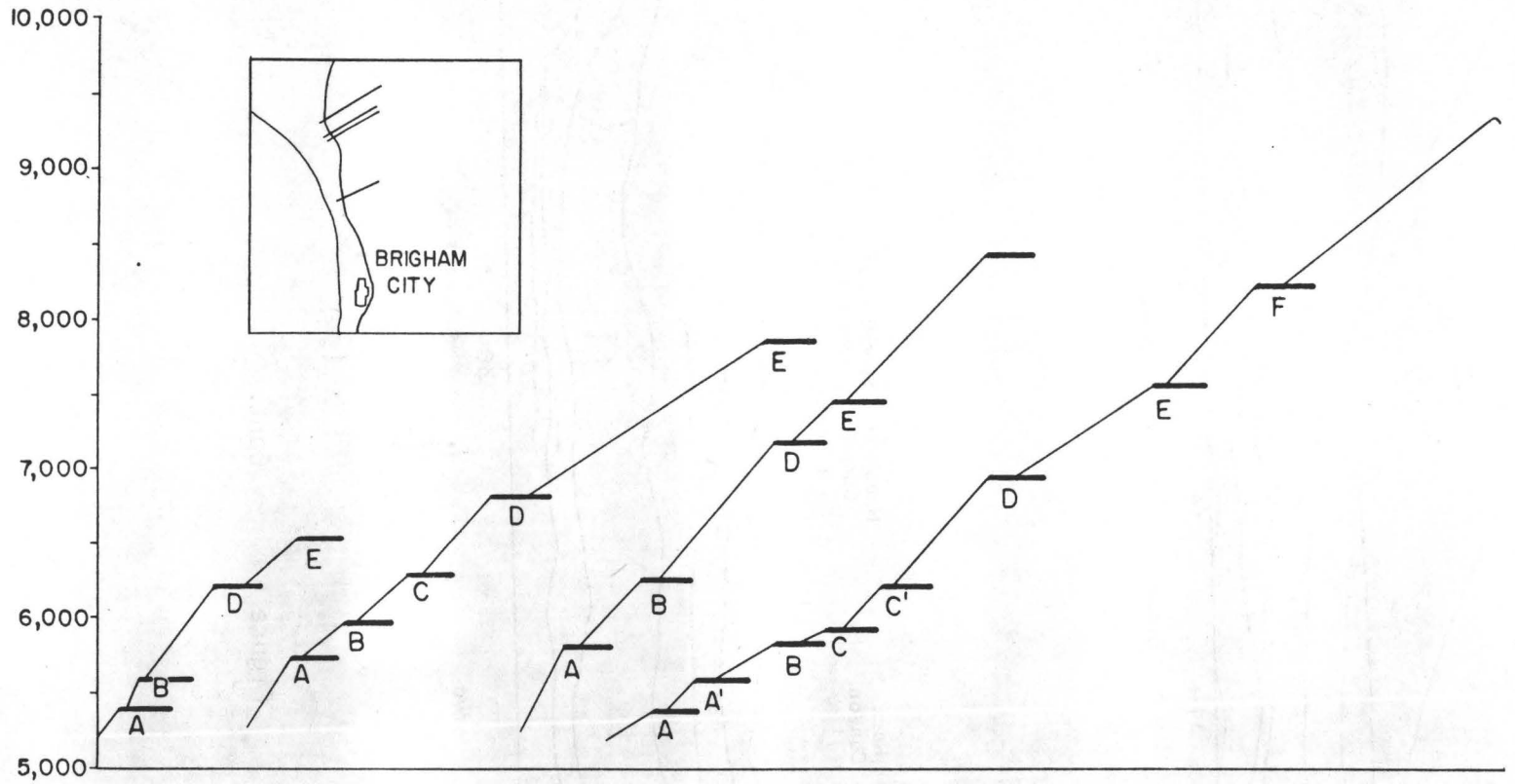

Figure 6 Profiles across the Wasatch Fault in the area north of Bountiful, Utah

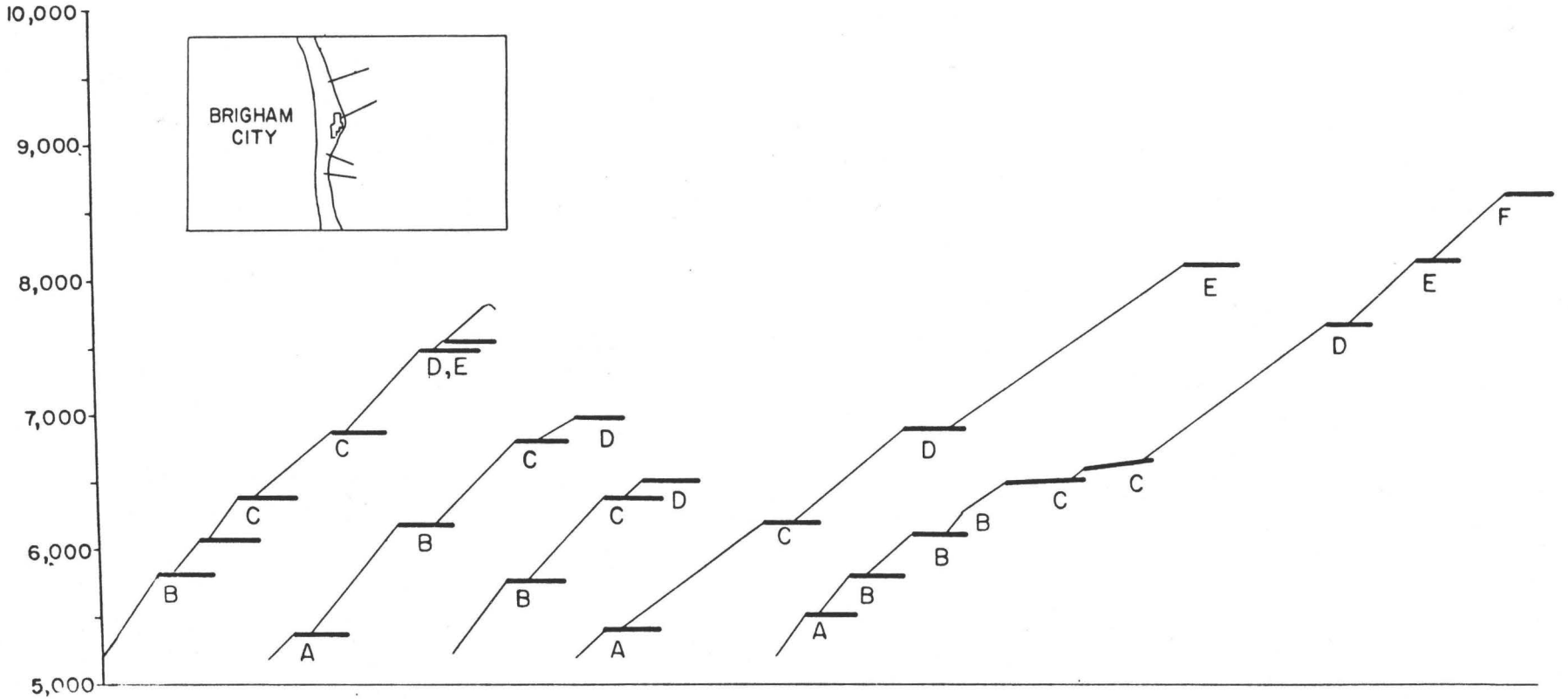

Figure 7 Profiles across the Wasatch Fault in the vicinity of Bountiful, Utah

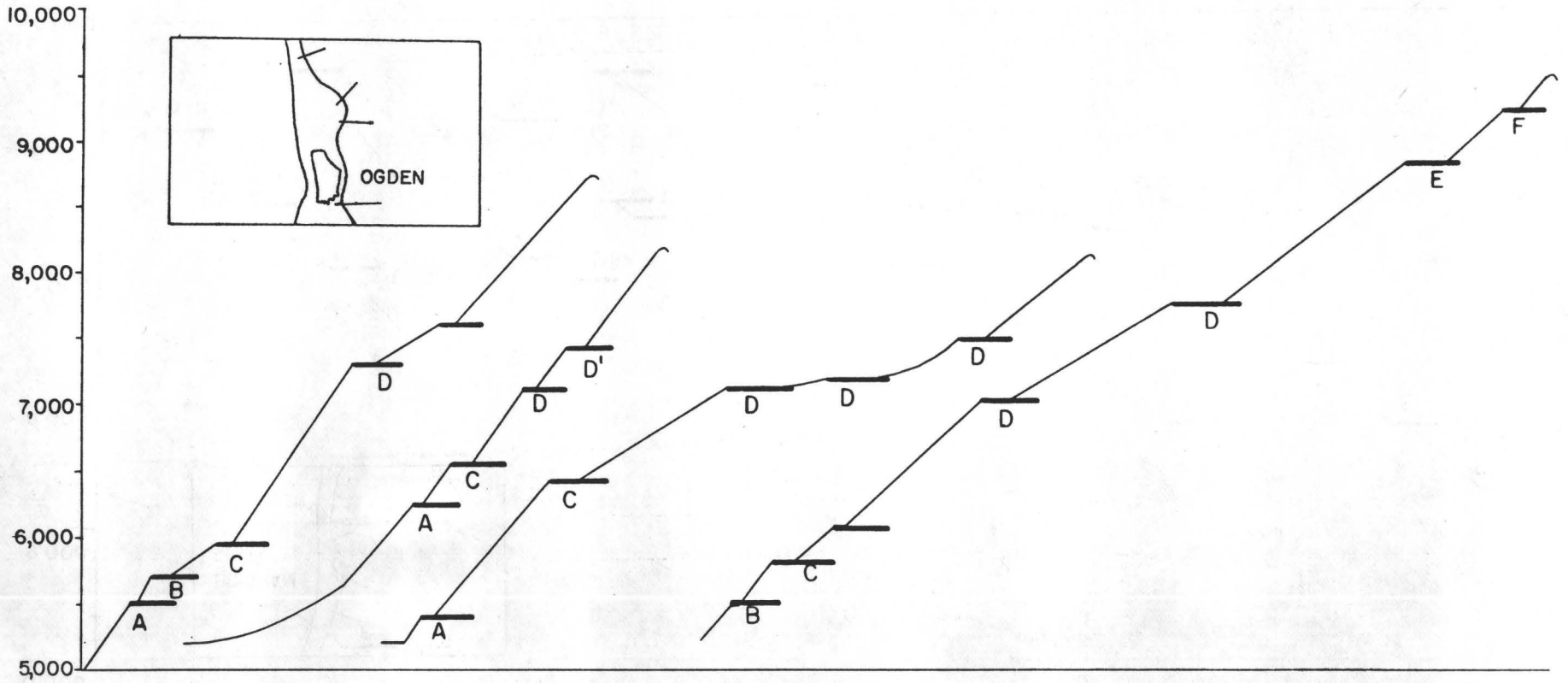

Figure 8 Profiles across the Wasatch Fault in the vicinity of Ogden, Utah

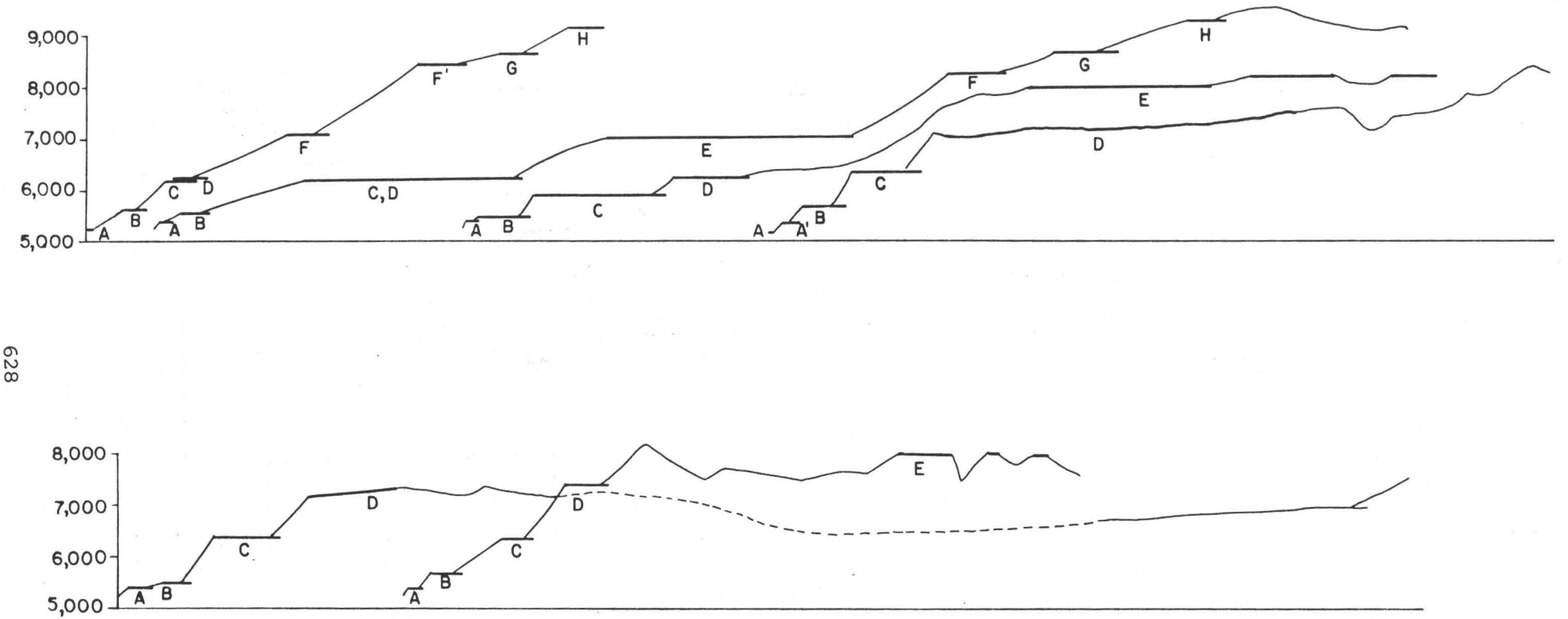

Figure 9 Profiles across the Wasatch Fault in the vicinity of Salt Lake City, Utah

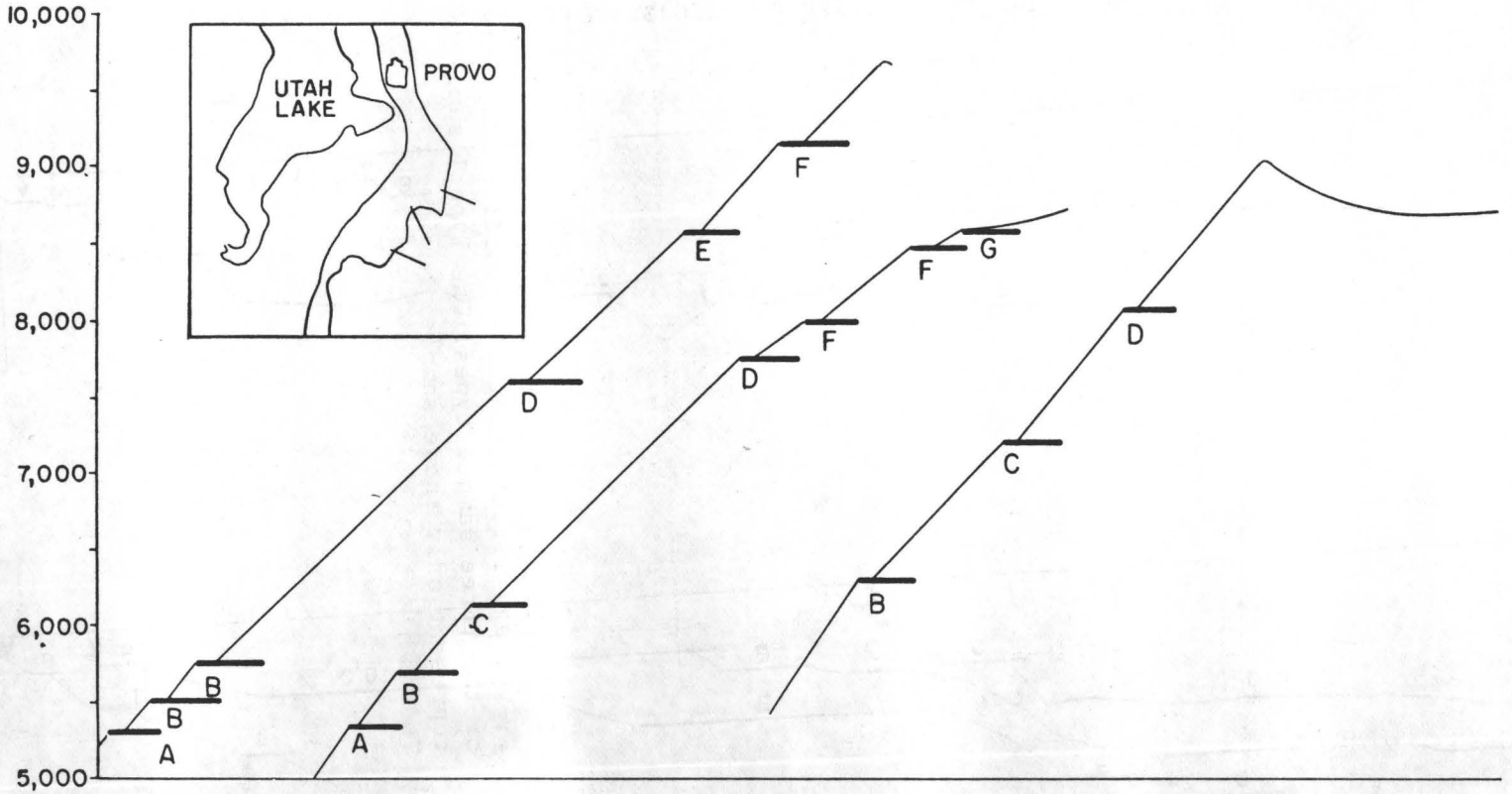

Figure 10 Profiles across the Wasatch Fault in the vicinity of Provo, Utah

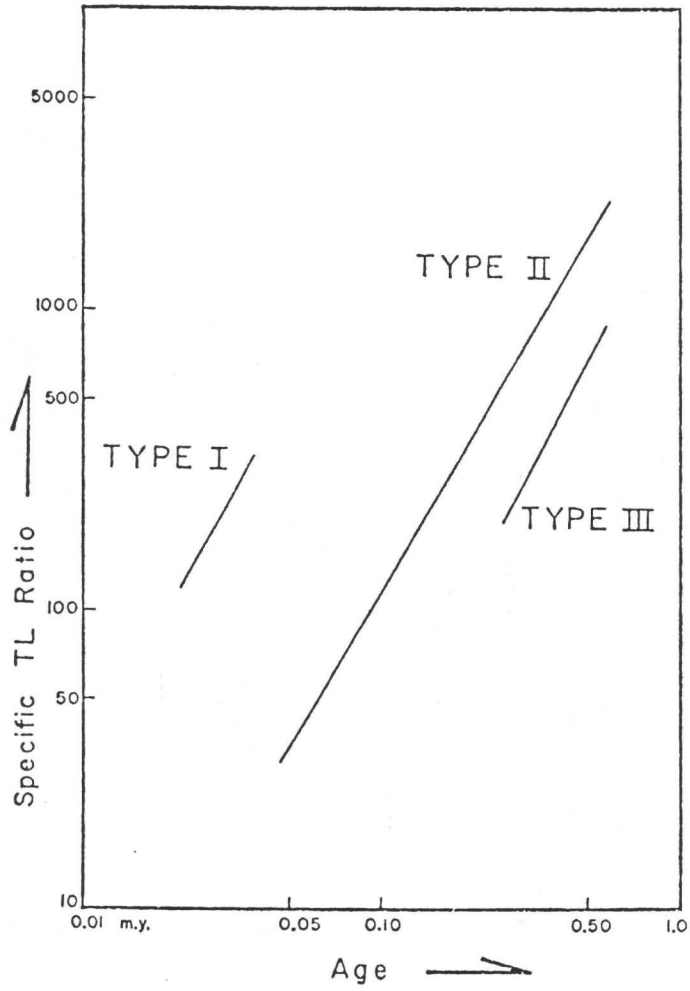

Figure 11.- Log-log plot of the specific TL ratio, R, vs. age illustrating the position and range of the three sample types. The Type I samples represent only those samples having the lowest TL and radiometric age uncertainties.

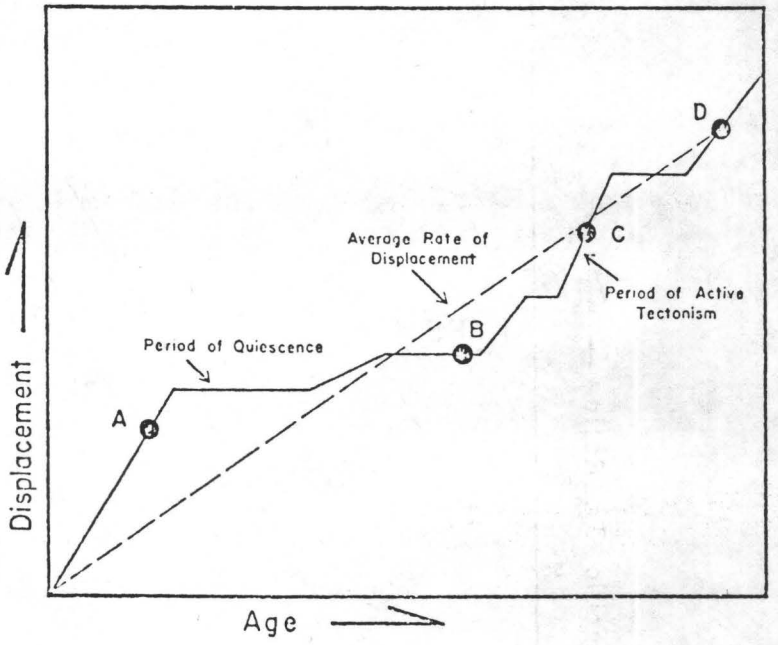

Figure 12 Hypothetical displacement history of a fault exhibiting alternating periods of recurrent movement and of tectonic quiescence. Events A-D represent points of known age and displacement (i.e. faulted lavas of known age).

a. Discontinuous scarps produced by several tectonic events.

b. Larger compound scarps produced by prolonged tectonism.

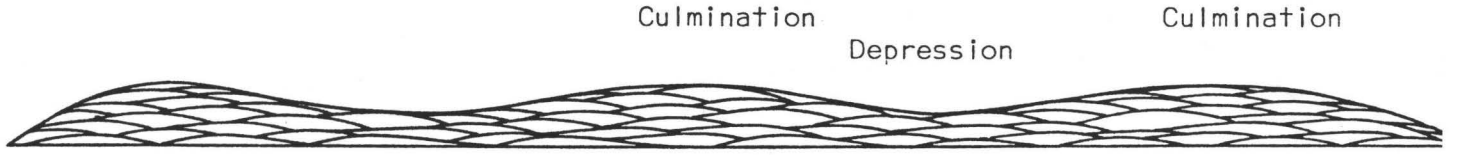

c. Continuous scarp produced by recurrent tectonism. Culminations and depressions occur in areas of previous tectonic stability.

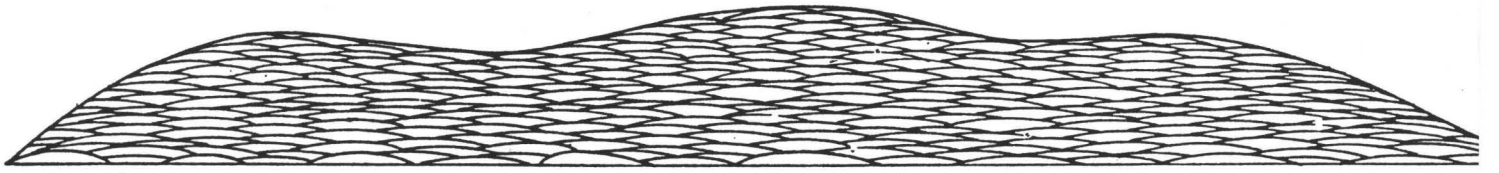

d. Mature scarp showing culminations and impressions.

Figure 13 Conceptual model showing the evolution of the normal faults.

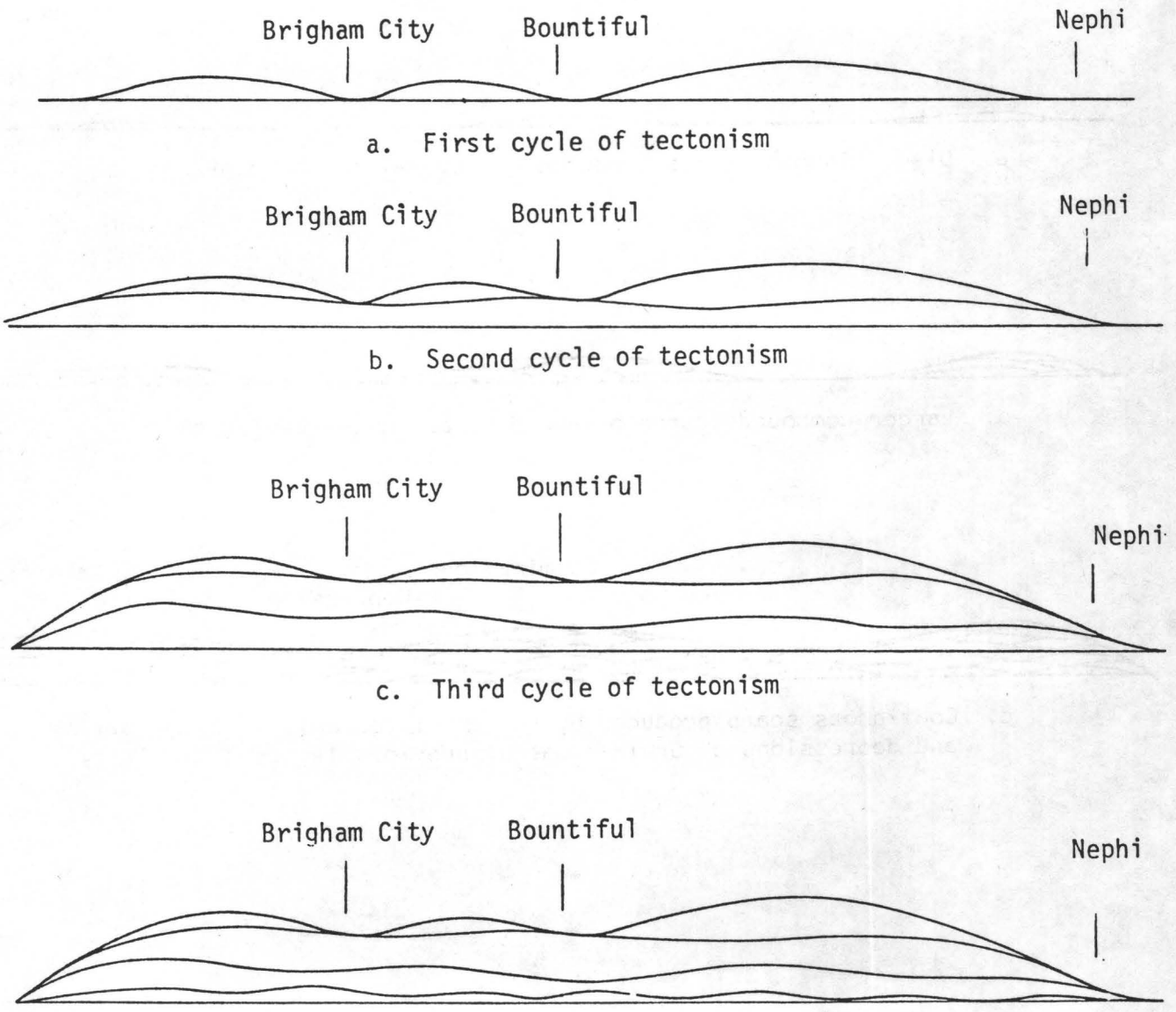

Figure 14 . Series of diagrams drawn parallel to the fault plane showing the cycles of recurrent tectonism.

Fission-track dating in the Wasatch Mts., Utah: an uplift study

by

C. W. Naeser[1], Bruce R. Bryant[1], M. D. Crittenden, Jr.[2] and M. L. Sorensen[2]

[1]U. S. Geological Survey, Denver, CO 80225

[2]U. S. Geological Survey, Menlo Park, CA 94025

Abstract

Apatite fission-track ages have been determined from forty-seven samples of the Archean Farmington Canyon Complex in the Wasatch Mts., Utah. These ages show a definite correlation with elevation on the mountain. The ages range from 7 m.y. near the Wasatch Fault at the base of the range to over 90 m.y. on the crest of the range. These data yield uplift rates of 0.012 mm/hr for the period from 90 m.y. to 10 m.y. and 0.4 mm/yr from 10 m.y. to the present.

Introduction:

Several studies over the last decade have shown the application of fission track dating of apatite to tectonic and uplift problems (Naeser and Faul, 1969; Wagner and Reimer, 1972; Wagner and others, 1977; and Naeser, 1979a, 1979b). Naeser and Fault (1969) showed that fission-tracks in apatite were annealed at temperatures as low as about 150°C if the sample was held at that temperature for at least 10^6 years. Their results came from extrapolating laboratory annealing data to times and temperatures of geologic significance. Naeser and Forbes (1976), Brookins and others (1977) and Naeser (unpublished data) have studied the change of apparent age of apatite in temperature increases with depth in a drillhole (Table 1). Both the laboratory and drill hole data show that the duration of the thermal event determines the temperature at which the apatite gives a "zero" apparent age. A rapid cooling rate (equivalent to a short-term thermal event) gives a higher temperature than a lower cooling rate. The drill hole data suggest somewhat lower annealing temperatures than those indicated by the laboratory experiments.

The apparent age of apatite records the time when the rock passed through the appropriate annealing temperature. It is therefore possible to calculate an uplift rate from the apatite age and the postulated geothermal gradient. Uplift rates can also be determined when more than one apatite data is available in vertical sequence; this calculation has the advantage that it does not require knowledge of either the geothermal gradient or annealing temperature.

The purpose of this paper is to present apatite fission-track ages from the Archean Farmington Canyon Complex of the Wasatch Mountains of Utah. These apatite ages will then be used to determine the post-Laramide uplift history of this large mountain block.

The area studied extends from Weber Canyon on the north to the head of Holbrook Canyon on the south (Figure 1). The general geology of the area is summarized by Arnow (1972). The Wasatch Mountains are bounded on the west by the Wasatch Fault, a major normal fault in north central Utah.

Relative displacements across the Wasatch Fault, from two trenching studies, has recently been determined for the Wasatch Fault (Swan and others, 1979; and Schwartz and others, 1979). These two studies have been able to determine vertical displacements for only the last 12,000 years. Swan and others (1979) reported 11 meters of displacement over the last 12,000 years at Kaysville, Utah. This is a differential uplift of 1.8 mm/year. Farther to the south at the mouth of Hobble Creek, Utah, Schwartz and others (1979) reported a maximum of 13.5 meters of apparent displacement over the last 12,000 years. This results in a rate of 1.1 mm/year.

Forty-nine apatite samples were dated in this study. Forty-seven of these were from the Archean Farmington Canyon Complex in the Wasatch Mountains and two were from an Archeozoic diamictite from Little Mt. (west of Ogden).

The procedures used to date the apatite are described in Naeser (1979a). All but two of the apatite concentrates were dated by using the population method, with the split used for the induced track density determination being annealed (500°C for 12 hr.) prior to irradiation. The two other samples, 41 and 42,

Table 1.--Fission-track annealing in apatite from deep drill holes

Drill Hole	Estimated duration of heating	Temperature at start of annealing	Temperature at completion of annealing	Reference
Eielson Air Force Base, Ak.	$>10^7$ years	--	105°C	Naeser and Forbes, 1976
EE-1 Los Alamos New Mexico	10^6 years	--	135°C	Brookins and others, 1977
Coso, Calif	10^5 years	120	145°C	Naeser, unpublished data

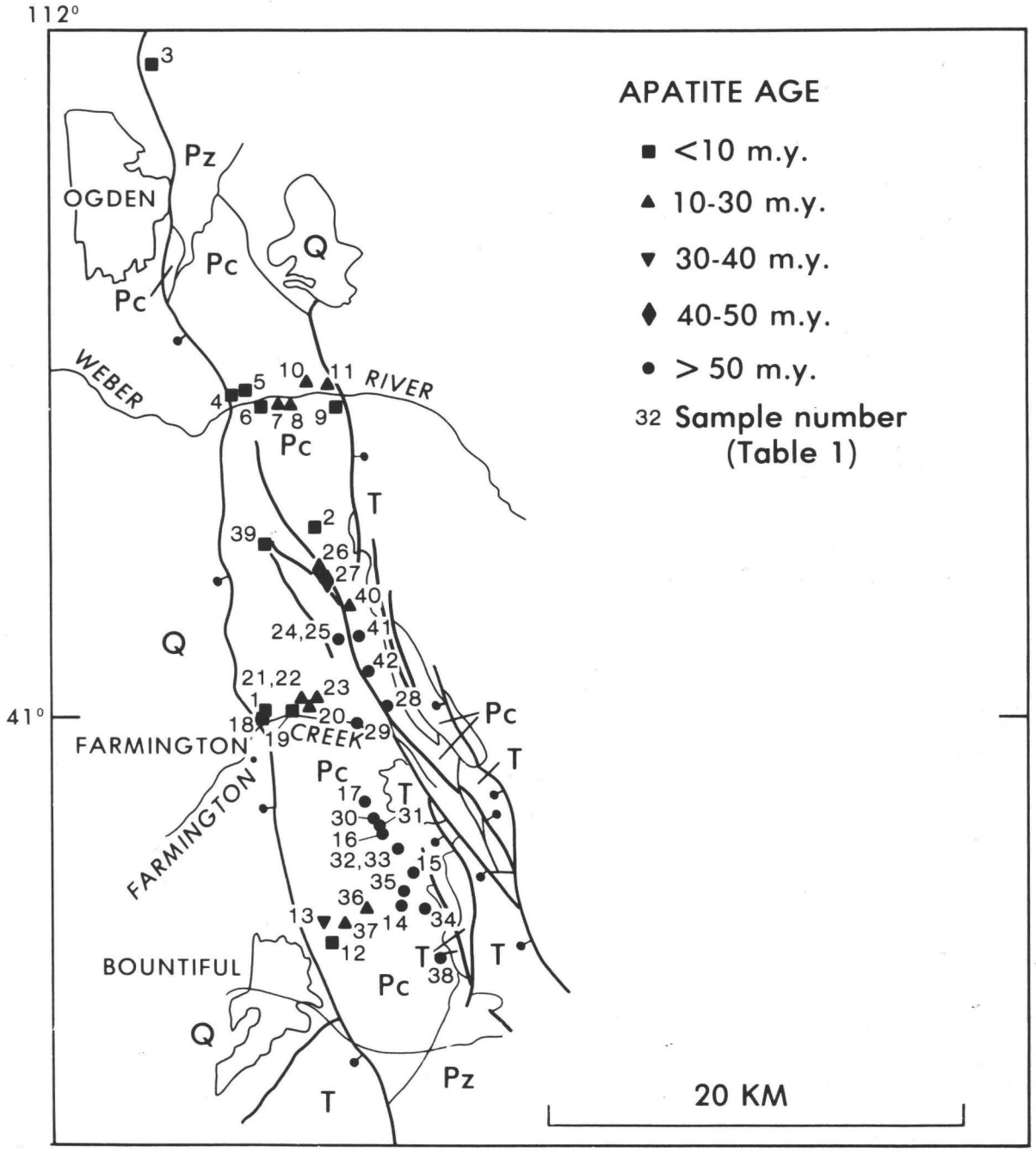

Figure 1.--Simplified geologic map of Wasatch Mts., Utah showing sample location and approximate ages of apatite. Samples 43 and 44 not shown.

were dated with the external detector method. The apatites were all etched in 7% HNO_3 for 30 seconds at 25°C. The neutron fluence was determined with National Bureau of Standards Standard Reference Materials 962 and 963, the primary copper activation calibration as determined by Carpenter and Reimer (1974) was used in calculating the doses used for calculating the ages reported in table 2. The constant for spontaneous fission of ^{238}U used in this report is $7.03 \times 10^{-17} yr^{-1}$.

Results:

The sample locations are shown on figure 1, and the analytical data for the samples are reported in table 2. The apatites studied range in age from 4.9 m.y. (#3) to 94.4 m.y. (#38). There is a general increase in age with elevation within the mountain block. The lower samples on the west near the Wasatch Fault have ages as young as 5 m.y. whereas most samples along the crest of the range have ages greater than 50 m.y. The oldest sample (#38) has an age of 94 m.y. and was collected at an elevation of 2615 meters. This sample lies directly beneath Tertiary sediments. Figure 2 shows a plot of the apparent apatite ages versus elevation. Three samples (#39, 2 and 40; circled on figure 2) appear to fall of the general trend. Two are from one fault block near the crest of the range south of Weber Canyon, the other is from an intermediate elevation west of the rnage crest in a much faulted area.

A series of samples collected along the Weber River in Weber Canyon (4-11) show an increase in age from west to east for the first 2 km. East of that point, ages seem more closely related to the fault block of the sample location, than to distance from the Wasatch fault. The easternmost samples (#9) from near the fault bounding the east margin of the mountain block, shows a decrease in age. These samples are not plotted on figure 2.

Two additional samples (43, 44) were collected from a diamictite of Proterozoic age exposed on Little Mountain west of Ogden.

Discussion of Results:

These apatite ages reflect the cooling (uplift) history of the Wasatch Mountain block. The cooling rate (indicated by the youngest samples on figure 2), is sufficiently high that a temperature of 120°C is taken as the apparent closing temperature. Thus these ages are recording the passage of these rocks through approximately the 120°C isotherm. Figure 2 shows that for the period prior to about 10 m.y. ago the region was undergoing a very slow (epirogenic) period of uplift (0.012 mm/yr; calculated from regression line through the data). Starting about 10 m.y. the rate of uplift accelerated. Assuming a temperature gradient of 30°C/km there has to have been at least 3-4 km of uplift during the last 5 m.y. in order to have the apatite near the base of the mountain exposed at the surface. Therefore the rate of uplift for the last 10 m.y. mus be on the order of .4 mm/year. If the uplift started later, for example about 5 m.y. ago the uplift rate would be about 0.8 mm/year.

The uplift rate of 0.4 mm/yr to 0.8 mm/yr for the last 5 to 10 m.y. is in good agreement with the rates of 1.1 to 1.8 mm/yr reported by Swan and others (1979), for the last 12,000 years. These apatite ages extend this latest uplift "event" back in time to 10 m.y.

Table 2.--Fission-track data for apatite from the Precambrian of the Wasatch Mts. and Little Mt., Utah

Map Number	Sample	Elevation meters	Number of grains counted	$\bar{s}$, r[1]	Fossil tracks/cm^2 X10^6	Induced tracks/cm^2 X10^6	Ø neutrons/cm^2 X10^{15}	T±2σ m.y.
Wasatch Mts.								
1	72MC113g DF-220	1454	50[2]	0.07($\bar{s}$)	0.122(254)[3]	1.09(2270)[3]	1.19	8.0± 1.1
2	72MC-116 DF-221	2958	50/40	0.06($\bar{s}$)	0.194(405)	1.44(2408)	1.19	9.6± 1.0
3	72MS-339 DF-222		50	0.09($\bar{s}$)	0.030(28)	0.441(408)	1.19	4.9± 1.9
4	73MS27a DF-606	1448	50	0.06($\bar{s}$)	0.164(152)	1.43(1323)	1.13	7.8± 1.3
4	73MS27b DF-607	1448	50	0.08($\bar{s}$)	0.131(121)	1.67(1546)	1.13	5.3± 1.0
5	73MS28a DF-608	1433	50	0.09($\bar{s}$)	0.238(220)	2.04(1887)	1.13	7.9± 1.1
5	73MS28b DF-609	1433	50	0.07($\bar{s}$)	0.136(126)	1.61(1487)	1.13	5.7± 1.1
6	73MS29a DF-610	1463	50	0.12($\bar{s}$)	0.104(96)	0.646(598)	1.13	10.8± 2.4
6	73MS29b DF-611	1463	50	0.10($\bar{s}$)	0.194(180)	1.75(1617)	1.13	7.5± 1.2
7	73MS30 DF-612	1433	50	0.08($\bar{s}$)	0.248(230)	1.16(1076)	1.13	14.4± 2.1
8	73MS31a DF-613	1463	50	0.08($\bar{s}$)	0.202(187)	1.15(1065)	1.13	11.9± 1.9
8	73MS31b DF-614	1463	50	0.14($\bar{s}$)	0.132(122)	0.717(664)	1.13	12.4± 2.4

Table 2.--Fission-track data for apatite from the Precambrian of the Wasatch Mts. and Little Mt., Utah (Cont'd)

Map Number	Sample	Elevation meters	Number of grains counted	$\bar{s}$, r^1	Fossil tracks/cm^2 X10^6	Induced tracks/cm^2 X10^6	Ø neutrons/cm^2 X10^{15}	T±2σ m.y.
Wasatch Mts. (Cont'd)								
9	73MS32 DF-615	1509	100/50	0.07($\bar{s}$)	0.076(141)	0.571(529)	1.13	9.0± 1.7
10	73MS33a DF-616	1463	50	0.06($\bar{s}$)	0.377(349)	1.72(1595)	1.13	14.7± 1.7
10	73MS33b DF-617	1463	50	0.11($\bar{s}$)	0.397(368)	1.43(1326)	1.13	18.7± 2.2
11	73MS34 DF-618	1463	50	0.08($\bar{s}$)	0.269(248)	0.909(842)	1.13	20.0± 2.9
12	73MS36 DF-619	1768	50	0.05($\bar{s}$)	0.181(168)	1.23(1138)	1.13	10.0± 1.6
13	73MS37 DF-620	1920	50	0.12($\bar{s}$)	0.149(138)	0.347(321)	1.22	31.3± 6.3
14	73MS39 DF-621	2377	50	0.07($\bar{s}$)	0.613(568)	0.733(679)	1.13	56.3± 6.4
15	73MS40 DF-622	2824	50	0.11($\bar{s}$)	0.172(159)	0.154(143)	1.13	74.8±17.2
16	73MS42 DF-623	2652	50	0.08($\bar{s}$)	1.10(1015)	1.06(985)	1.13	69.3± 6.2
17	73MS43b DF-624	2774	50	0.07($\bar{s}$)	0.953(882)	0.972(900)	1.13	65.9± 6.2
18	75MC7 DF-1027	1456	50	0.06($\bar{s}$)	0.252(525)	2.92(6078)	1.45	7.5± 0.7
19	75MC8 DF-1028	1646	50	0.09($\bar{s}$)	0.242(505)	2.18(4535)	1.45	9.7± 0.9

Table 2.--Fission-track data for apatite from the Precambrian of the Wasatch Mts. and Little Mt., Utah (Cont'd)

Map Number	Sample	Elevation meters	Number of grains counted	$\bar{s}$, r^1	Fossil tracks/cm^2 X10^6	Induced tracks/cm^2 X10^6	Ø neutrons/cm^2 X10^{15}	T±2σ m.y.
Wasatch Mts. (Cont'd)								
20	75MC9 DF-1029	1750	50	0.06($\bar{s}$)	0.708(656)	3.92(3630)	1.45	15.7± 1.3
21	75MC11 DF-1030	1839	50	0.07($\bar{s}$)	0.302(280)	1.50(1387)	1.45	17.5± 2.3
22	75MC12 DF-1031	1839	50	0.09($\bar{s}$)	0.231(482)	1.28(2656)	1.45	15.7± 1.5
23	75MC13 DF-1032	1890	50	0.09($\bar{s}$)	0.293(271)	1.49(1379)	1.45	17.0± 1.3
24	75MC14 DF-1033	2908	50	0.10($\bar{s}$)	0.113(236)	8.160(333)	1.45	61.2±10.4
25	75MC15 DF-1034	2908	50	0.10($\bar{s}$)	0.348(726)	0.460(958)	1.45	65.4± 3.2
26	75MC16 DF-1035	2893	50	0.07($\bar{s}$)	0.423(882)	0.777(1619)	1.45	47.1± 4.0
27	75MC18 DF-1036	2774	50	0.09($\bar{s}$)	0.728(674)	1.36(1264)	1.45	46.1± 4.4
28	75MC20 DF-1037	2512	50	0.08($\bar{s}$)	0.903(1881)	1.05(2186)	1.45	74.3± 4.6
29	75MC21 DF-1038	2012	50	0.13($\bar{s}$)	0.231(482)	0.505(1052)	1.45	39.6± 4.4
30	75MC23 DF-1039	2707	50	0.08($\bar{s}$)	0.333(693)	0.339(707)	1.45	84.5± 9.0
31	75MC24 DF-1040	2707	50	0.05($\bar{s}$)	0.724(1508)	1.04(2175)	1.45	59.9± 4.0

Table 2.--Fission-track data for apatite from the Precambrian of the Wasatch Mts. and Little Mt., Utah (Cont'd)

Map Number	Sample	Elevation meters	Number of grains counted	$\bar{s}$, r^1	Fossil tracks/cm^2 X10^6	Induced tracks/cm^2 X10^6	Ø neutrons/cm^2 X10^{15}	T±2σ m.y.
Wasatch Mts. (Cont'd)								
32	75MC25 DF-1041	2627	50	0.07($\bar{s}$)	0.305(635)	0.391(815)	1.45	67.3± 3.6
33	75MC26 DF-1042	2633	50	0.14($\bar{s}$)	0.883(818)	0.869(805)	1.45	87.6± 8.6
34	75MC28 DF-1043	2548	50	0.06($\bar{s}$)	1.47(1359)	1.77(1642)	1.45	31.4± 5.2
35	75MC29 DF-1044	2426	50	0.06($\bar{s}$)	0.154(321)	0.204(424)	1.45	65.4± 9.6
36	75MC31 DF-1045	2179	50	0.10($\bar{s}$)	0.091(190)	0.406(846)	1.45	19.5± 3.1
37	75MC32 DF-1046	2000	50	0.06($\bar{s}$)	0.107(222)	0.671(1397)	1.45	13.8± 2.0
38	B-112 DF-1873	2615	50	0.08($\bar{s}$)	0.839(777)	0.586(543)	1.11	94.4±10.5
39	K-12 DF-1874	2234	50	0.05($\bar{s}$)	0.084(176)	0.710(1479)	1.11	7.9± 1.3
40	P-77 DF-2164	2816	50	0.21($\bar{s}$)	0.059(74)	0.192(240)	0.961	17.7± 4.7
41	P-78 DF-2165	2816	6	0.89(r)	1.11(335)	5.81(853)	4.72	55.2± 4.0
42	P-79 DF-2166	2713	6	0.77(r)	1.52(400)	7.50(965)	4.69	56.7± 4.4

Table 2.--Fission-track data for apatite from the Precambrian of the Wasatch Mts. and Little Mt., Utah (Cont'd)

Map Number	Sample	Elevation meters	Number of grains counted	$\bar{s}$, r[1]	Fossil tracks/cm^2 X10^6	Induced tracks/cm^2 X10^6	Ø neutrons/cm^2 X10^{15}	T±2σ m.y.
Little Mt.								
43	72MC140a DF-223	1292	50	0.07($\bar{s}$)	0.605(1262)	0.571(1189)	1.19	75.2± 6.1
44	72MC140 DF-224	1292	50	0.10($\bar{s}$)	0.179(166)	0.190(176)	1.19	66.9±14.5

$\lambda_F = 7.03 \times 10^{-17} yr^{-1}$

[1]($\bar{s}$) = relative standard error of the mean of the induced count.
r = correlation coefficient.

[2]If one number present same number of grains counted for fossil and induced counts, if two numbers present first is number of grains counted for fossil, and second is number of grains counted for the induced count.

[3]Number of tracks counted is determining fossil or induced track density.

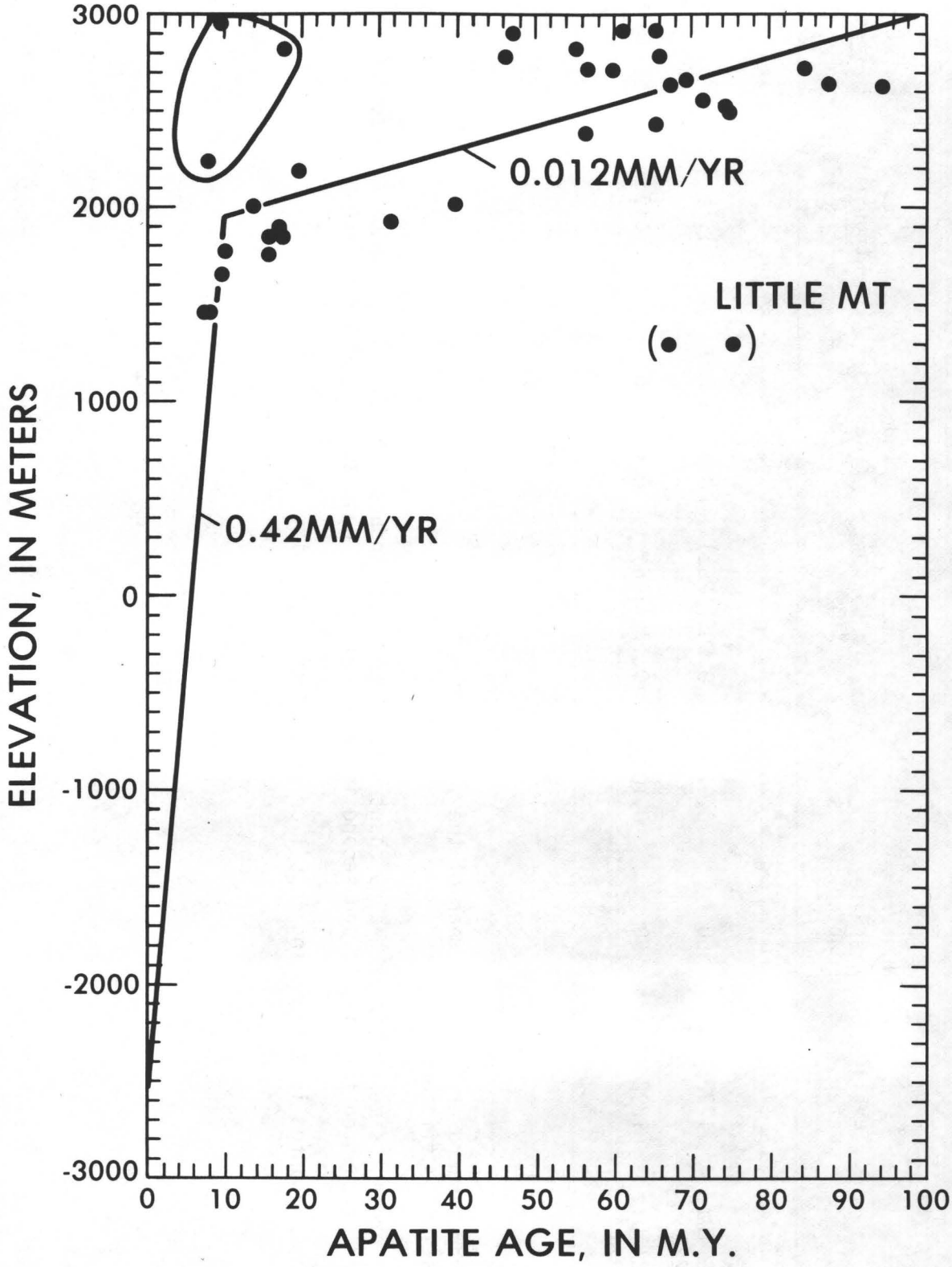

Figure 2.--Plot of apparent apatite age versus elevations for samples from central part of Wasatch Mts., Utah.

The two samples from Little Mt. have an average age of about 70 m.y. They outcrop at an elevation of about 1300 meters above sea level. Samples with a similar age occur at an elevation of about 2,600 meters in the Wasatch Mts. There has been a minimum amount of displacement of about 1300 meters between these two samples during the last 70 m.y.

Conclusion:

Apatite fission-track ages from the Farmington Canyon Complex in the Wasatch Mountains east of Ogden, Utah show that the mountain has been uplifting at a rate of about 0.4 mm/yr for the last 10 million years. Prior to that time the range was uplifting at a rate of only 0.012 mm/yr. The rocks were cooling at a rate of 0.36°C/m.y. between 90 and 10 m.y. ago. For the last 10 m.y. the cooling rate has been 12.6°C/m.y.

Two apatites from a Precambrian diamictite from Little Mt. west of Ogden have ages of about 70 m.y. These are from an elevation near which apatites on the east side of the Wasatch fault have ages of 7 m.y. and are 1300 m below elevations on the crest of the Wasatch mountains where apatites have 70 m.y. ages. There has been a minimum amount of 1300 meters of displacement during the last 70 m.y. A maximum amount of displacement could be in excess of 5 km.

References

Arnow, Ted, 1971, Geologic framework: in Environmental Geology of the Wasatch Front, 1971: Utah Geological Association Publication 1, p. B1-B6.

Brookings, D. G., Forbes, R. B., Turner, D. L., Laughlin, A. W., and Naeser, C. W., 1977, Rb-Sr, K-Ar, and fission-track geochronological studies from LASL drill holes GT-1, GT-2, and EE-1 Los Alamos Scientific Laboratories Informal Report LA-6829-MS, 27 p.

Carpenter, B. S., and Reimer, G. M., 1974, Calibrated glass standards for fission-track use: NBS Special Pub., 260-49, p. 1-16.

Naeser, C. W., 1979a, Fission-track dating and geologic annealing of fission-track; in Lectures in Isotope Geology edited by E. Jager and J. C. Hunziker: Springer-Verlag Berlin, p. 154-169.

Naeser, C. W., 1979b, Thermal history of sedimentary basin: Fission-track dating of subsurface rocks: SEPM Special Publication No. 26, p. 109-112.

Naeser, C. W., and Faul, H., 1969, Fission track annealing in apatite and sphene: J. Geophys. Res., v. 74, p. 705-710.

Naeser, C. W., and Forbes, R. B., 1976, Variation of fission-track ages with depth in two deep drill holes: EOS, Trans. Am. Geophys. Union, v. 57, p. 353.

Schwartz, D. P., Swan, F. H., III, Hanson, K. L., Knuepfer, P. L., and Cluff, L. S., 1979, Recurrence of surface faulting and large magnitude earthquakes along the Wasatch Front Zone near Provo, Utah: Geological Soceity of America Abstracts with Programs, v. 11, no. 6, p. 301.

Swan, F. H., III, Schwartz, D. P., Hanson, K. L., Knuepfer, P. D., and Cluff, L. S., 1979, Recurrence of surface faulting and large magnitude earthquakes along the Wasatch fault zone, Utah: Geological Society of America, Abstracts with Programs, v. 13, no. 3, p. 131.

Wagner, G. A., Reimer, G. M., and Jager, E., 1977, Cooling ages derived by apatite fission-track, mica Rb-Sr and K-Ar dating: The uplift and cooling history of the central Alps: Memorie degli Instituti Geologia a Mineralogia dell Universite di Padova, v. 30, p. 1-29.

Wagner, G. A., and Reimer, G. M., 1972, Fission-track tectonics: the tectonic interpretation of fission track apatite ages: Earth Planet. Sci. Letters, v. 14, p. 263-268.

Slip Vectors on Faults Near Salt Lake City, Utah, from Quaternary Displacements and Seismicity

by T. L. Pavlis and R. B. Smith

Introduction

The Salt Lake Valley (also known as Jordan Valley) in northern Utah has long been considered an area of relatively high seismic risk. Faults cut Holocene deposits in numerous localities along the Wasatch Front and attest to prehistoric seismic activity. Much of the southern Salt Lake Valley (Figure 1) is relatively aseismic, but a pronounced zone of seismicity extends through the populated and industrialized northeastern part of Salt Lake City and across western Salt Lake Valley (Smith, 1974; Arabasz et al., 1979). Within this zone of seismicity the Salt Lake salient, an elongate bedrock spur, extends westward approximately 6 km from the main front of the Wasatch Mountains. Two high-angle faults, the Warm Springs and Virginia Street faults, have been exposed by excavations on the western and southern margins of the Salt Lake salient respectively (Figure 1). The exposed fault surfaces are intensely striated and both faults show evidence for at least two distinct episodes of slip.

Discussion

The Warm Springs fault is a major normal fault that abruptly terminates the Salt Lake salient along its western margin (Figure 1). The fault can be traced as a bedrock escarpment from downtown Salt Lake City northward at least 8 km. Steep gravity gradients continue 13 km northward from the last mapped location of the fault suggesting a northward continuation of the fault to near Centerville, Utah (Cook and Berg, 1961). The contemporary epicenter distribution shows no clearcut relationship to the Warm Springs fault (Figure 1).

Approximately 12 m of post-Lake Bonneville (about 11,000 years B.P.) displacement has occurred on the Warm Springs fault (Gilbert, 1890). Most of this displacement is younger than post-Bonneville alluvial fans which are cut by the fault (Marsell, 1953). In the early 1920's excavations for gravel along one of these alluvial fans exposed the striated fault surface of brecciated Paleozoic and Tertiary sedimentary rocks (Pack, 1926; Schneider, 1925). Subsequent excavations have produced discontinuous exposures of the fault surface over a distance of approximately 5 km (Figure 2a). The westward dip of this fault surface is nearly constant at about 70° but the strike of the surface varies as much as 90°, from 305° to 35°. The variation in strike results in curvature of the fault trace on scales ranging from mesoscopic undulations with wavelengths from 1 to 10 m (Figure 2a) to macroscopic variations of the fault trace

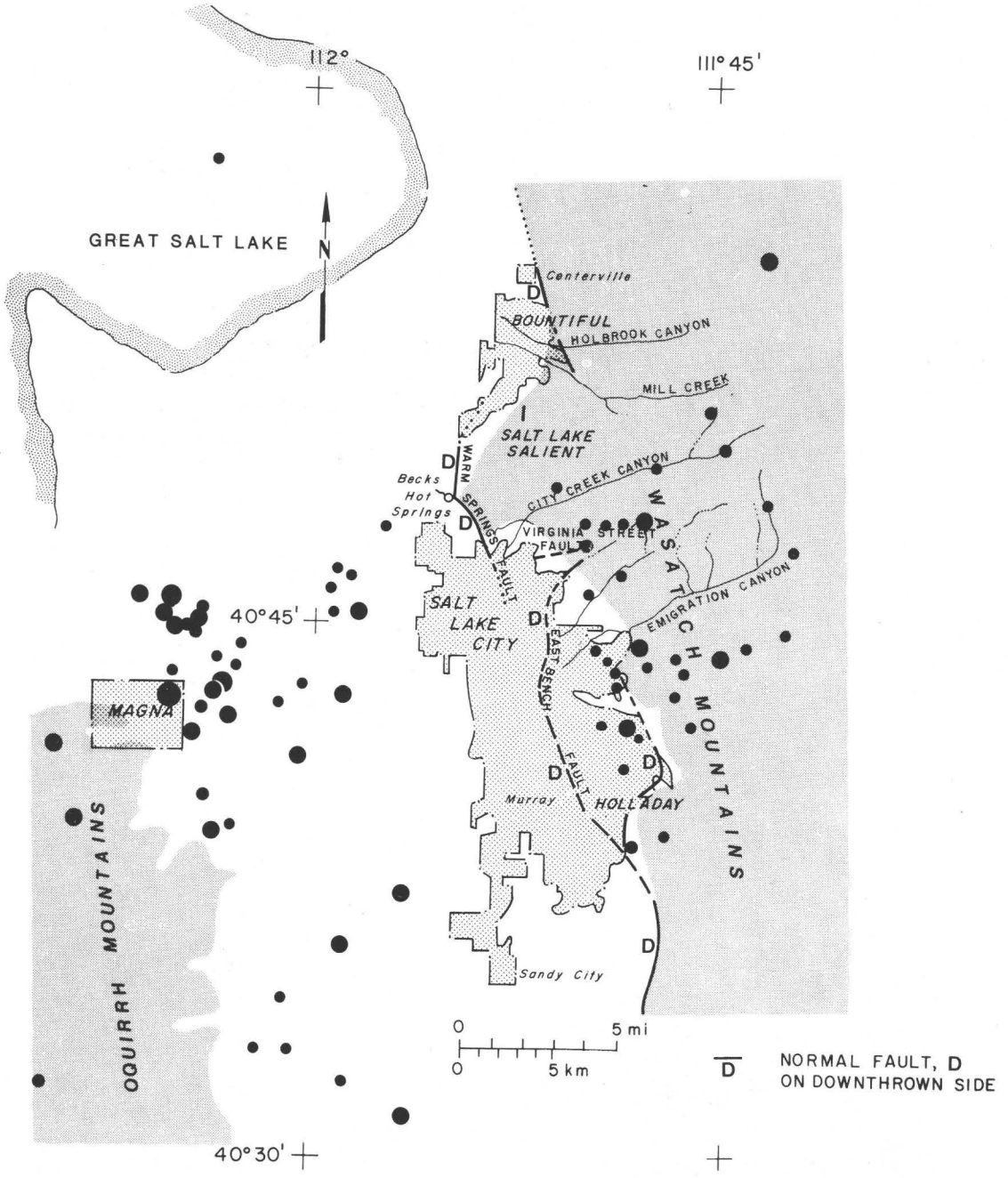

Fig. 1. Generalized Cenozoic fault map (after Marsell, 1953; Kaliser, 1976; and Cook and Berg, 1961) and contemporary seismicity (after Arabasz, et al., 1979) of the Salt Lake Valley. Dark shaded regions are bedrock exposures in mountain ranges.

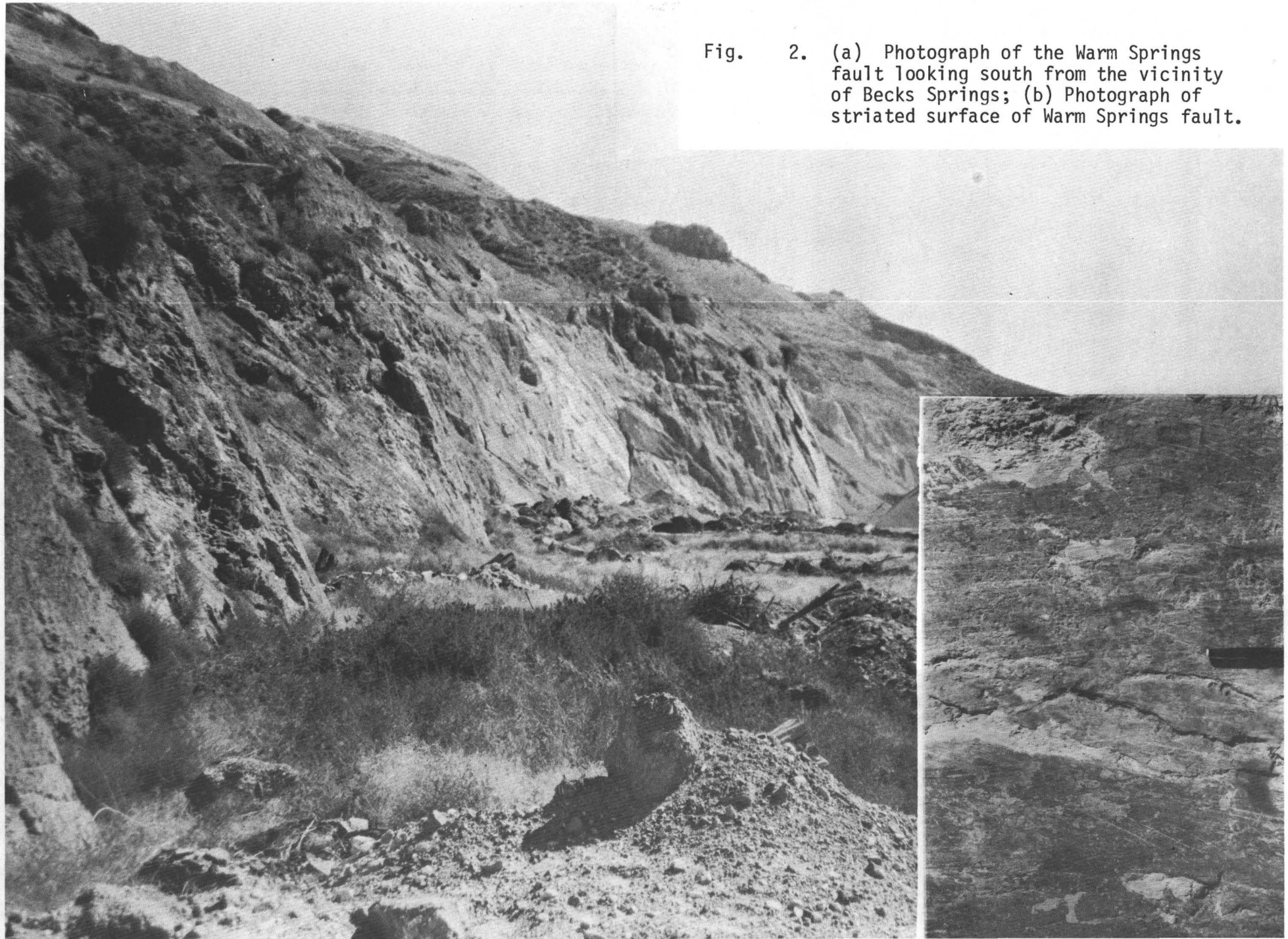

Fig. 2. (a) Photograph of the Warm Springs fault looking south from the vicinity of Becks Springs; (b) Photograph of striated surface of Warm Springs fault.

(Figure 1). The mesoscopic undulations are akin to large scale grooves, and although data are not abundant they suggest a bimodal grouping Figure 3i).

Exposures of the Warm Springs fault surface contain two distinct striation sets which are frequently superposed (Figure 2b). The trend of each striation set is independent of the orientation of the fault segment on which it occurs. Thompson and Burke (1973, p. 630) made a similar observation on a normal fault in Nevada and explained this observation by noting that "...when two blocks separated by a zigzag fault move apart, some fault segments would be expected to show lateral components of slip." On the Warm Springs fault, even stronger evidence for this type of slip is contained in the relative ages of the striations. The superposition of the two striation sets allowed a determination of relative age and consistently shows that for the data in Figure 3a the southwesterly trending (maximum at 239°) set is consistently superposed on the older, northwesterly trending (288°) set, regardless of the strike of the fault segment at a given locality.

On the southern margin of the Salt Lake salient, excavations near Virginia Streen in Salt Lake City have produced a small exposure of a very regular fault plane which strikes nearly east-west (80°) and dips steeply to the south (68°). The Virginia Street fault shows no clearcut displacement of Quaternary deposits but was labeled by Kaliser (1976) as a fault with "evidence of recent movement." The Virginia Street fault, like the Warm Springs fault, contains two independent striation sets (Figure 3b). Both striation sets show that the most recent movements on the Virginia Street fault have been dominantly strike slip. Unlike on the Warm Springs fault, however, superposed striations were not observed to allow determination of relative ages.

The striations on the exposed fault surfaces are interpreted as recording the slip directions during the last two major seismic events on the two faults. Then if an average fault plane orientation is chosen for each fualt from the mapped fault attitudes, hypothetical fault-plane solutions can be deduced for each fault and each assumed earthquake (Figure 2,3-f). Estimates of the inferred paleostress field (P and T axes) can then be added using a Coulomb failure criterion. The hypothetical fault-plane solutions for the Warm Springs fault (Figure 3, c and d) closely resemble a fault plane solution obtained from earthquakes 15 km west of the Salt Lake salient (Figure 3h) but differs from that obtained from earthquakes 20 km to the east of Salt Lake City (Figure 3g). The hypothetical fault plane solutions from the Virginia Street fault (Figure 3, e and f) are not similar to any of the observed fault plane solutions (Figure 3, h and g).

Conclusions

The similarity between fault plane solutions (Figure 3, g and h) from recorded earthquakes (M5.2 September 1962; a swarm of earthquakes up to M3.3, March 1978) and the hypotehtical fault plane solutions (Figure

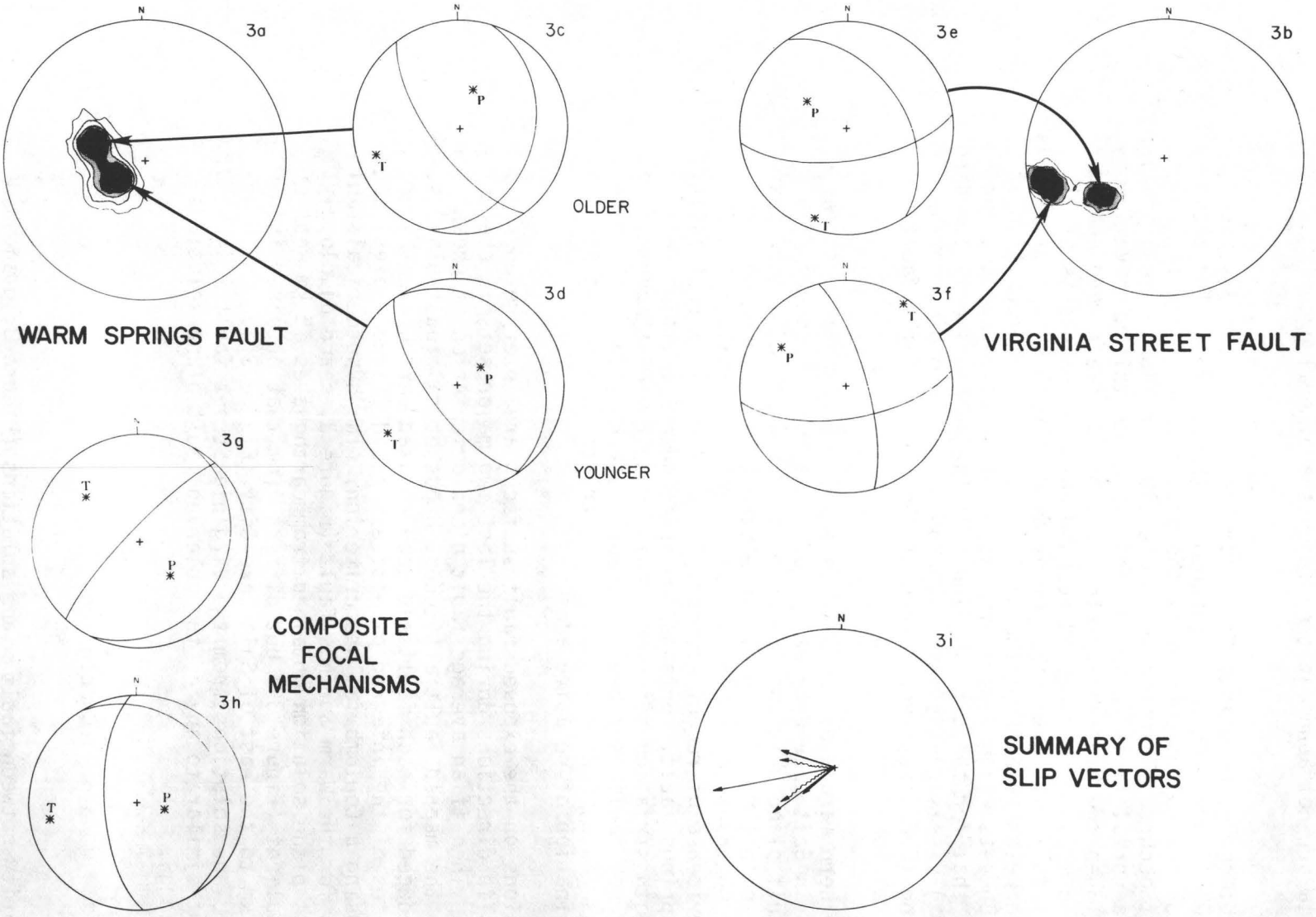

Fig. 3. Equal-area, lower-hemisphere projections of striation directions contoured by the Schmidt method. Contours are density intervals with the maximum greater than 25%. (a) Contours at 5% intervals from 274 slip directions on the Warm Springs fault. (b) Contours at 10% intervals from 18 slip directions on the Virginia Street fault. (c-f) Hypothetical fault-plane solutions produced from the data in a and b. (g,h) Observed fault-plane solutions from earthquakes 20 km east of Salt Lake City (g) and from 15 km west of the Salt Lake salient (h). (i) Summary of slip vectors from the Virginia Street fault (shown by thin solid lines), the Warm Springs fault (shown by heavy solid lines), and slip vectors based on mesoscopic undulations of the Warm Springs fault (shown by wavey lines).

3, c and d) on the Warm Springs fault suggests that the present stress field is similar to that which produced the 12 m of Holocene displacement on the Warm Springs fault. This suggests that the Warm Springs fault is probably still favorably oriented in the contemporary stress field for the generation of future surface faulting.

Comparison of slip vectors on the Virginia Street fault with those on the Warm Springs fault (Figure 3i) shows a close correpsondence between slip-vector trends on the two faults. This correspondence is independent of the fault attitude or relative displacement, i.e., the Virginia Street fault is a nearly EW-striking fault with dominantly strike-slip motion, whereas the Warm Springs fault is a NS-striking, dip-slip fault; yet the slip vectors have similar trends. This suggests that directions of surface displacements are the same on the margins of the salient, but stress fields (P and T axes on hypothetical fault-plane solutions) must vary markedly around the salient. The lack of clearcut Quaternary movement on the Virginia Street fault might suggest that the striations on the fault were produced during an earlier stress regime, but the close correspondence in slip vector trends between the Virginia Street and Warm Springs faults seems too coincidental for this explanation.

We suggest that the Salt Lake salient has behaved as a relatively cohesive crustal block. Surface faults on the margins of the salient, regardless of their orientation, would thus respond to a consistent displacement of the Salt Lake Valley relative to the Salt Lake salient and thus the apparent surface stress fields would be the product of a displacement, not vice-versa. If this motion of discrete crustal blocks is typical of faulting in the Great Basin, then orientations of P and T axes from fault plane solutions must be examined carefully since they could reflect only local displacements on oblique fault planes, and may not necessarily represent the regional stress field.

Acknowledgments

W. J. Arabasz and R. Bruhn critically reviewed the manuscript. This research was supported by U.S.G.S. Grant No. 14-08-0001-16725. We would like to thank Monroc, Inc., and Clark Tanklines, Inc., for allowing us access to their gravel pits to examine the Warm Springs fault.

References

Arabasz, W. J., Smith, R. B., and Richins, W. D. (1979). Earthquake Studies Along the Wasatch Front, Utah: Network monitoring, seismicity and seismic hazards: (preprint submitted to Bull. Seism. Soc. Am.).

Cook, K. L. and Berg, J. W. (1961). Regional gravity survey along the central and southern Wasatch Front, Utah: U.S. Geol. Survey Prof. Paper 316-E, 89 pp.

Gilbert, G. K. (1890). Lake Bonneville, U.S. Geol. Survey, Mon. 1, 438 pp.

Kaliser, B. N. (1976). Earthquake fault map of a portion of Salt Lake County, Utah, Utah Geological and Mineral Survey, Map 42.

Marsell, R. E. (1953). Geology of the central Wasatch Mountains near Salt Lake City, Compass 31, 3-22.

Pack, F. J. (1926). New discoveries relating to the Wasatch fault, Am. J. Sci. 11, 399-410.

Schneider, H. (1925). A discussion of certain geologic features of the Wasatch Mountains, J. Geology 33, 28-48.

Smith, R. B. (1974). Seismicity and earthquake hazards of the Wasatch Front, Utah, Earthquake Information Bull. 6, 12-17.

Thompson, G. A. and Burke, D. B. (1973). Rate and direction of spreading in Dixie Valley, Basin and Range Province, Nevada, Geol. Soc. Am. Bull. 84, 627-737.

T. L. Pavlis
Department of Geology and Geophysics
University of Utah
Salt Lake City, Utah 84112

R. B. Smith
Department of Geology and Geophysics
University of Utah
Salt Lake City, Utah 83112

Crustal Flexure And Earthquake-Generating Stress Along The Wasatch Front, Utah

George Zandt
Department of Geology and Geophysics
University of Utah
Salt Lake City, Utah 84112

ABSTRACT

A viscoelastic model of crustal deformation in Utah's Wasatch Front area predicts a stress field consistent with the observed pattern of seismicity. The seismicity bears no obvious relation to the mapped surface trace of the major Wasatch fault zone, which has recurrently ruptured during Holocene time. Seismicity is diffuse but locally intense throughout a 200-km-wide zone, approximately centered on the Wasatch fault; however, relatively few events are located near the fault. An intriguing aspect of the seismicity is the concentration of small earthquakes in discrete zones parallel to the Wasatch fault, but displaced about 30 km to the east. In an attempt to explain this "flanking seismicity", a model outlined by Vening Meinesz in 1958 and elaborated by Bott in 1976 was modified and applied to the Wasatch Front. The model consists of a viscoelastic crust overlying a substratum having long-term characteristics of a fluid. Normal faulting that penetrates the entire crust induces isostatic forces which produce upward flexure of the footwall side of the crust--thus uplifting the Wasatch Mountains. Initially, the uplifted crustal limb behaves elastically; bending stresses are produced on the flank away from the fault, causing small to moderate size earthquakes. However, after ~10^4 yrs, relaxation occurs and the bending stresses and corresponding seismicity decay. If uplift occurs episodically on the Wasatch fault (an episode encompasses several major earthquakes), there will be a cycle of generation and decay of the bending stresses. Interpreting the observed flanking seismicity in terms of this model indicates the uplifted crustal limb is currently behaving elastically.

INTRODUCTION

The Wasatch Front, Utah, is characterized by diffuse but locally intense seismicity throughout a 200-km-wide zone, roughly centered on the N-S Wasatch fault zone, with persistent quiescence along major sections of the Wasatch fault (Arabasz et al., 1979). Geological evidence of recurrent, large-displacement, Holocene faulting along the now seismically inactive segments of the Wasatch fault (Swan et al., 1978) clearly demonstrates the occurrence of large (M ~7-7.5) earthquakes as recently as several hundred years ago. Hence, in order to better evaluate earthquake hazards in this area the relationship between these major Wasatch fault

earthquakes and the small to moderate sized earthquakes occurring predominantly off the fault need to be clarified.

This paper includes an initial attempt to provide a framework for evaluating a large number of seismological, geophysical, and geological data that are now available for the Wasatch Front. The first part summarizes the available information pertinent to this study. The following section examines, in some detail, the applicability to the Wasatch Front of Vening Meinesz's graben formation model. A final section presents a modified model including a viscoelastic crust which better fits some of the geologic constraints.

THE WASATCH FRONT

The idea of the Wasatch Mountains as an uplifted crustal block due to Basin and Range faulting within an extensional stress regime was developed in the work of G. K. Gilbert (1928) and W. M. Davis (1903). This basic concept is now generally accepted although the details of the actual geometry and causal mechanisms are still debated.

Since the pioneering work of Gilbert, the work of A. J. Eardley stands out. He advanced the idea (Eardley, 1933) that a submature to mature surface with relief of about 900 m existed in the area before the Basin and Range faulting began. Eardley estimated the maximum fault displacement to be about 1800 m; however later studies (Crittenden, 1964) have placed the cumulative displacement as great as 4600 m. Using the physiography of the region, Eardley (1933) estimated the amount of eastward tilting of the Wasatch block at 2°-3° although the "Wasatch block suffered a warping deformation with tilting progressively greater toward the fault scarp." He also added that "neither block stood still in relation to sea level, one rose and the other sank, probably both tilting eastward".

Early geophysical work in Utah by K. L. Cook and J. W. Berg added the third dimension to the picture. Refraction studies in the Basin and Range province of Utah indicated a crustal thickness of about 25 km and an unusually low P_n velocity of 7.6 km/sec (Berg *et al.*, 1960). Regional gravity surveys along the central and southern Wasatch Front revealed the complexity of the crust (Cook and Berg, 1961). The gravity data were interpreted to reflect a north-south trend of major grabens west of the Wasatch Front.

High-resolution seismic refraction studies by R. B. Smith and colleagues have delineated the details of the crustal structure and the nature of the Basin and Range-Middle Rocky Mountains transition boundary. The refraction data indicate a crustal thickness of 28 km and a P_n velocity of 7.6 km/sec in the eastern Basin and Range, increasing to 40 km east of the Wasatch Front. A crustal low-velocity layer located between 10 and 15 km in depth appears to be continuous across the province boundary. Shear wave data suggest the low-velocity layer is a zone of low rigidity (Braile *et al.*, 1974). Further studies (Keller *et al.*, 1975) appear to confirm

the earlier interpretations outlining a similar transition from the Basin and Range to the Colorado Plateau. Smith et al. (1975) summarized data which indicated a major crustal - upper mantle boundary exists 40-50 km east of the Wasatch Front.

Earthquake hazard in Utah has stimulated a number of recent studies on Quaternary faults in the state. Hamblin (1976) studied the size and spacing of pediment remnants of faceted spurs along the Wasatch Front. These features were interpreted to be due to patterns of recurrent movement along the Wasatch fault. Periods of movement have produced 200 to 300 m of cumulative displacement separated by periods of quiescence of unknown duration. An episode of displacement results from a series of discrete displacements of a few meters each (a M~7 earthquake); however, in a geologic sense, the episode of displacement is essentially continuous. Also the history of movement differs from one segment of the fault to another.

An important element missing in the study by Hamblin is the timing. Dating of Quaternary faults from a scarp height-slope angle relationship appears promising (Bucknam and Anderson, 1979) but, as yet, has not been applied directly to the Wasatch Front. Trenching of the fault is providing important information on pre-historic earthquake recurrence intervals. These studies (Swan et al., 1978 and Schwartz et al., 1979) have confirmed the occurrence of M~7 earthquakes on the Wasatch fault as recently as within the past few hundred years. The recurrence interval of these scarp-forming earthquakes at a particular site is on the order of 1000 years. From these geologic studies an average uplift rate for the last 12,000 years for the Wasatch block appears to be about one millimeter per year. Preliminary results of fission track dating of rocks in the Wasatch Mountains indicate at least 3-4 km of uplift during the last 7 m.y. for an uplift rate of about 0.4 mm/yr for the last 10 m.y. (Naeser et al., 1979).

Earthquakes provide the most direct evidence of the current state of stress (or strain) in the crust. The seismicity of the Wasatch Front is discussed in detail by Arabasz et al. (1979). Figure 1 is from their paper and shows the seismicity of the region from 1974 to 1978. The quiescence of major segments of the Wasatch fault is evident, as well as the broad zone of intense activity a few tens of kilometers to the east. To the west of the Wasatch fault a more scattered zone of activity also exists. Arabasz et al. (1979) postulate that the observed spatial and temporal patterns of seismicity are related to discrete segments of the Wasatch fault passing through different stages of a seismic cycle. In the following section a mechanical, graben-formation model is described and analyzed as a possible explanation of the stress system in an isolated segment of the fault. Although there is undoubtedly a lateral coupling mechanism between segments of the fault, in the following, complete independence is assumed. The ultimate purpose is to understand the mechanism of the seismic cycle enough to predict the time and place of future large earthquakes along the Wasatch Front.

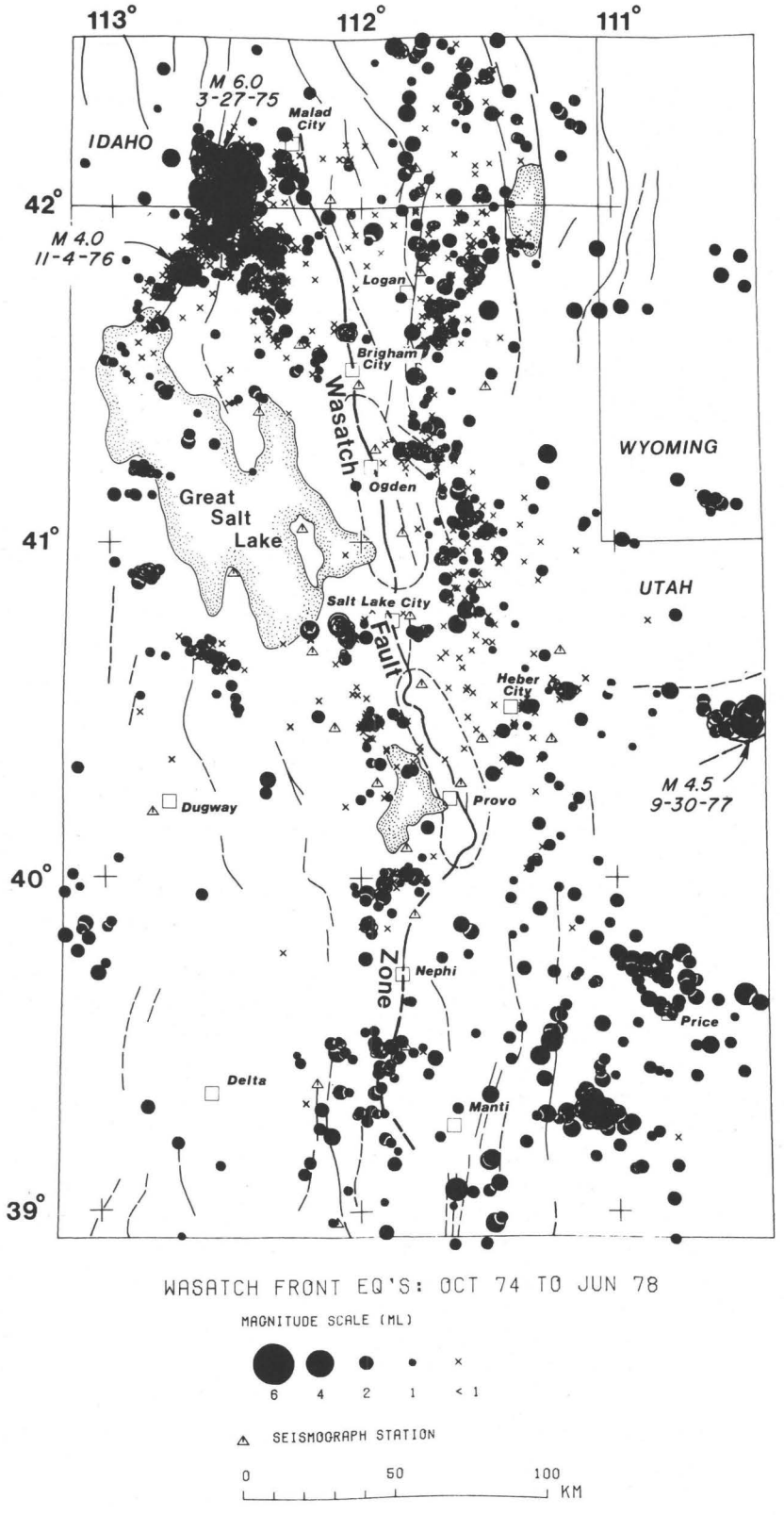

Fig. 1. Seismicity of the Wasatch Front, Utah: Oct. 1974 to June 1978. Dashed lines enclose "microseismic gaps".

APPLICATION OF VENING MEINESZ'S GRABEN FORMATION MODEL TO THE WASATCH FRONT

Description of model

A mechanism for the development of grabens was outlined by Vening Meinesz in Heiskanen and Vening Meinesz (1958) and further elaborated by Bott (1976). The model consists of an elastic layer overlying a ductile half-space with extensional forces acting on opposite ends of the elastic layer (Figure 2A). Assuming the deformations are small compared to the thickness of the elastic layer, the theory of thin plates or beams can be applied to this problem. The theory of thin plates with small deflection was developed with the following assumptions (Tismoshenko and Woinowsky-Krieger, 1959):

1) There is no deformation in the middle plane of the plate which remains neutral during bending. Stresses above and below the neutral line are equal and opposite in sign (Figure 2C).

2) Points of the plate lying initially on a line normal to the neutral line remain that way after bending.

3) The normal stresses in the direction transverse to the plate can be disregarded.

With these assumptions, all stress components can be expressed by the vertical deflection w of the plate which is a function of the x coordinate.

The sequence of hypothesized events is: (1) Horizontal extensional forces lead to the development of a normal fault along a tilted fault plane that penetrates the entire elastic layer. In theory the layer is now decoupled into two separate "limbs" and we can analyze the response of each separately (Figure 2B). (2) The dipping fault plane creates a lateral density contrast inducing isostatic forces which produce a downward pressure on the hanging wall plate and an upward pressure on the footwall plate (Figure 2B).

The problem is now reduced to that of analyzing the flexure of an elastic layer resting on a substratum that responds with bouyancy forces. The isostatic forces are represented by a point load p at x = 0. The governing differential equation is (Nadai, 1963)

$$N \frac{d^4w}{dx^4} + \rho_s g w = p \qquad (1)$$

$$N = \frac{Eh^3}{12(1-\nu^2)} \qquad \text{Layer modulus} \qquad (2)$$

Fig. 2. A. Initial configuration of an elastic layer resting on a "fluid" substratum. The elastic crust is subjected to horizontal extensional forces. Symbols are defined in the text.

B. Development of a through-going normal fault with hade $= \theta$ that induces isostatic forces p and -p.

C. Schematic perspective diagram of resulting flexure on both sides of main fault. Dashed line is the neutral axis. Outward pointing arrows represents tensional stresses. Inward pointing arrows represents compressional stresses.

A.

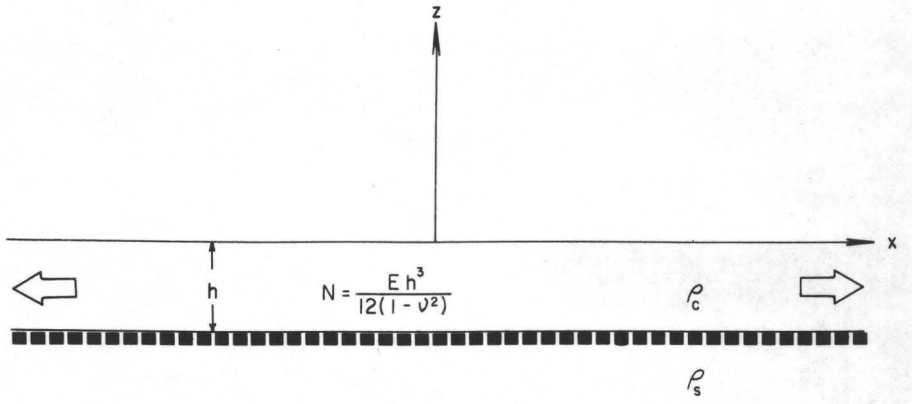
z
x
h
$N = \frac{E h^3}{12(1-\nu^2)}$
ρ_c
ρ_s

B.

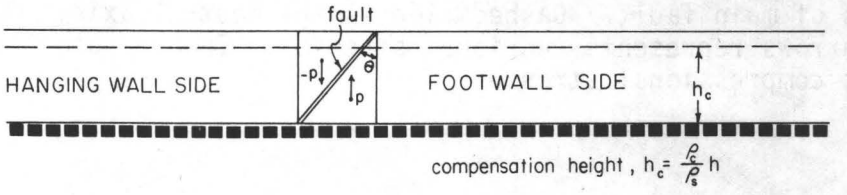
fault
HANGING WALL SIDE
FOOTWALL SIDE
-p
p
θ
h_c
compensation height, $h_c = \frac{\rho_c}{\rho_s} h$

C.

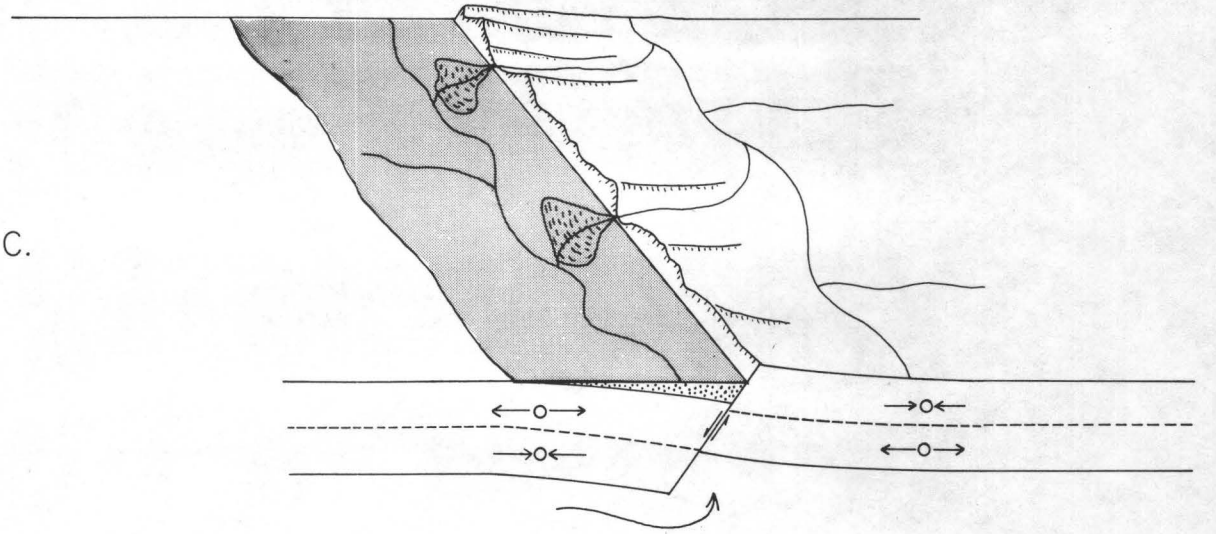

where w is the vertical displacement and

E = Young's modulus of layer

h = thickness of layer

ν = Poisson's ratio of layer

ρ_s = density of substratum

g = gravitational acceleration

p = point force

The general solution (excluding the exponentially growing solution) is given by a damped harmonic

$$w = w_0 e^{-x/\alpha} \cos\left(\frac{x}{\alpha} + \phi\right) \; ; \; x \geq 0 \tag{3}$$

$$\alpha^4 = \frac{4N}{\rho_s g} \tag{4}$$

where w_0 and ϕ are integration constants.

Walcott (1970) referred to α as the flexural parameter, which is related to the wavelength of the harmonic. The amplitude constant w_0 is the maximum deflection at $x = 0$ and is a function of the force p and inversely proportional to α. Thus, α is an important parameter which affects both the amplitude and wavelength of the flexure. The phase constant ϕ depends on the boundary condition at the origin $x = 0$. The boundary condition at $x = 0$ can be given either in terms of the dip of the layer $\left(\frac{dw}{dx}\right)$ or the moment $\left(\frac{d^2w}{dx^2}\right)$:

$$\frac{dw}{dx} = \frac{-w_0}{\alpha} e^{-x/\alpha} \left(\cos\left(\frac{x}{\alpha} + \phi\right) + \sin\left(\frac{x}{\alpha} + \phi\right)\right) \tag{5}$$

$$\frac{d^2w}{dx^2} = +2\frac{w_0}{\alpha^2} e^{-x/\alpha} \sin\left(\frac{x}{\alpha} + \phi\right) \tag{6}$$

For example, for the case of zero moment at the free end,

$$\left(\frac{d^2w}{dx^2}\right)_{x=0} = 0$$

$$\left(\frac{dw}{dx}\right)_{x=0} = 1$$

$$\phi = 0$$

The theoretical flexure curve and corresponding moment curve are illustrated in Figure 3.

The bending moment along the layer and corresponding stress at the surface and lower boundary of the layer are given by (Heiskanen and Vening Meinesz, 1958):

$$M = N \frac{d^2w}{dx^2} \tag{7}$$

$$\sigma_b = \pm \frac{6M}{h^2} \tag{8}$$

The dashed line in Figure 3 is $\frac{d^2w}{dx^2}$ and hence is proportional to the stresses along the surface of the layer and inversely proportional to the stresses along the bottom of the layer.

Another example of a flexure curve and the corresponding moment curve for a slightly different end condition is respresented in Figure 4. Notice that the stresses reverse in sign at some distance from the origin when the end is constrained. Figures 5 and 6 represent flexures and moments, respectively, for a family of different end conditions. Notice that even a small amount of constraint on the end induces relatively large stresses near the origin.

Predictions of model

In order to investigate the applicability of the model described above, predictions of the model are compared with observations for the Wasatch Front. Predictions for which there are observational data include: a) basement topography, b) wavelength of uplift/subsidence features, c) total amount of uplift/subsidence, and d) stress magnitudes and distribution. Each of these will be discussed in turn, but first we need to establish the applicability of the basic model and to assign some values to the constants in equations (3) and (4).

Models similar to the one described above have been used to explain other deformation processes of the Earth including glacial rebound (Nadai, 1963), sediment loading at a continental margin (Watts and Ryan, 1976), and the formation of the outer rise, oceanic trench bathymetry (Hanks, 1971). Most relevent to this paper are the studies of the response of the eastern Basin and Range to the loading of Pleistocene Lake Bonneville

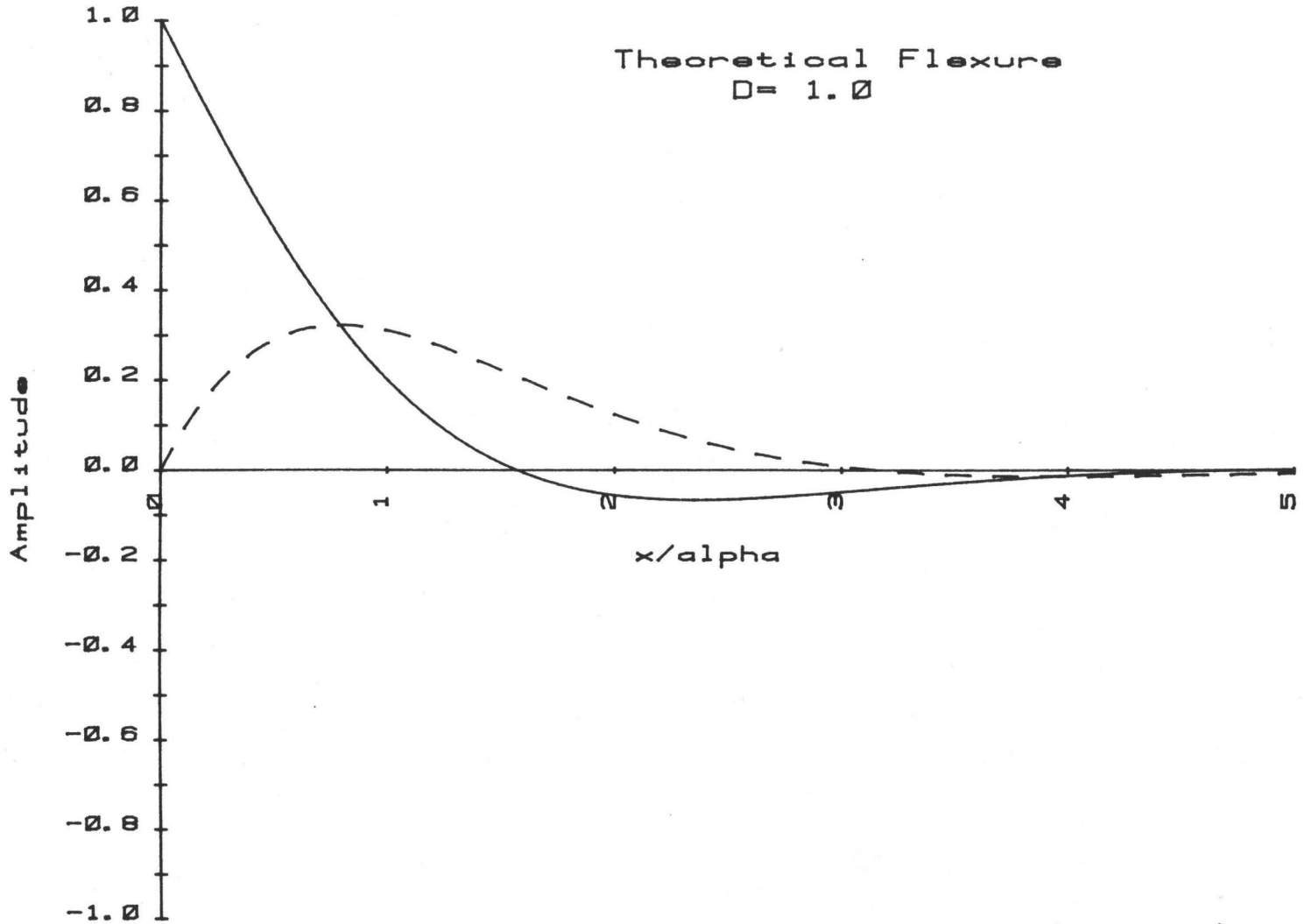

Fig. 3. Theoretical flexure (solid line) and moment (dashed line) for unconstrained end (ϕ = 0). D refers to the first derivative at the origin. Vertical exaggeration is 20:1.

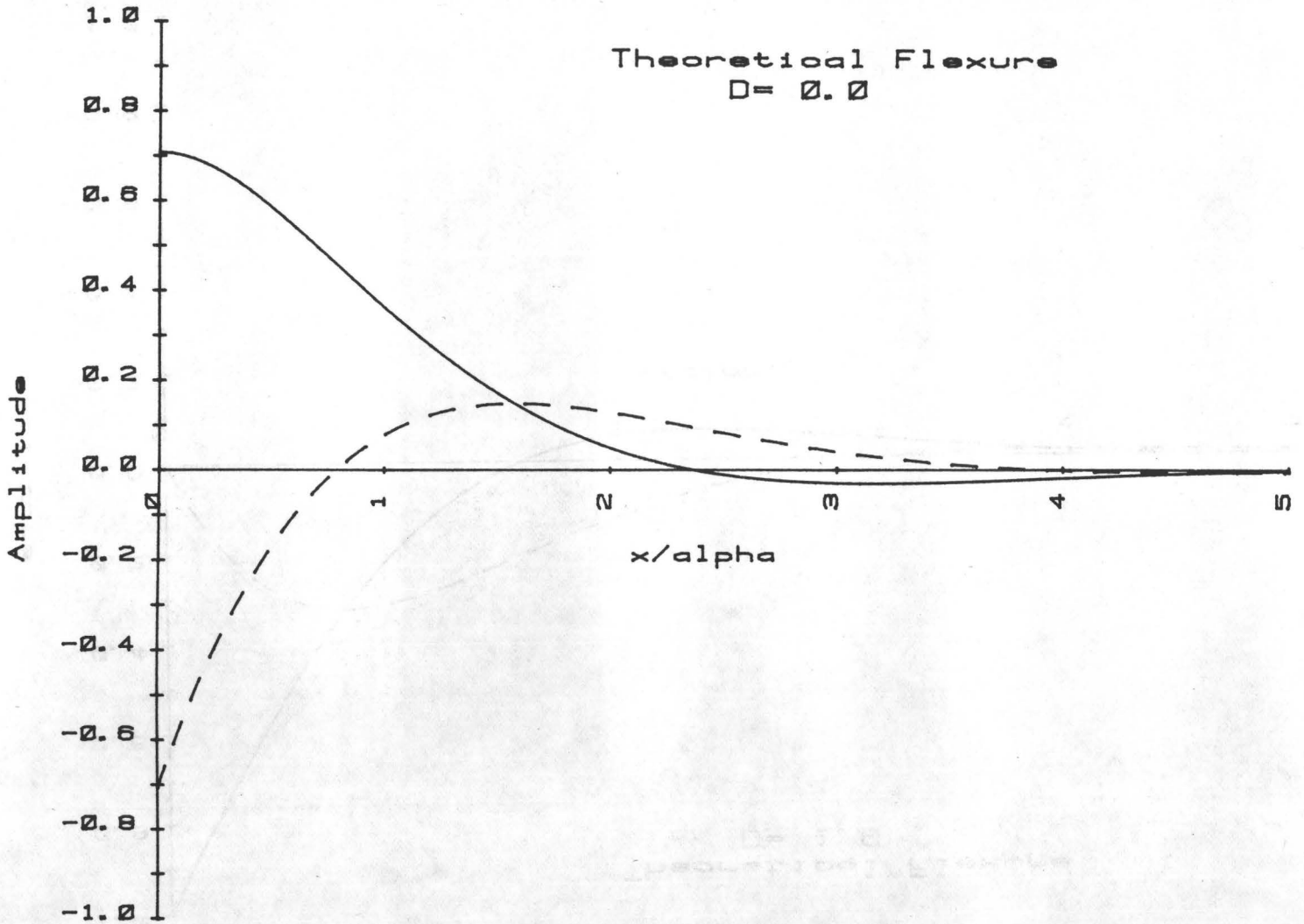

Fig. 4. Theoretical flexure (solid line) and moment (dashed line) for constrained end: D = 0. Vertical exaggeration is 20:1.

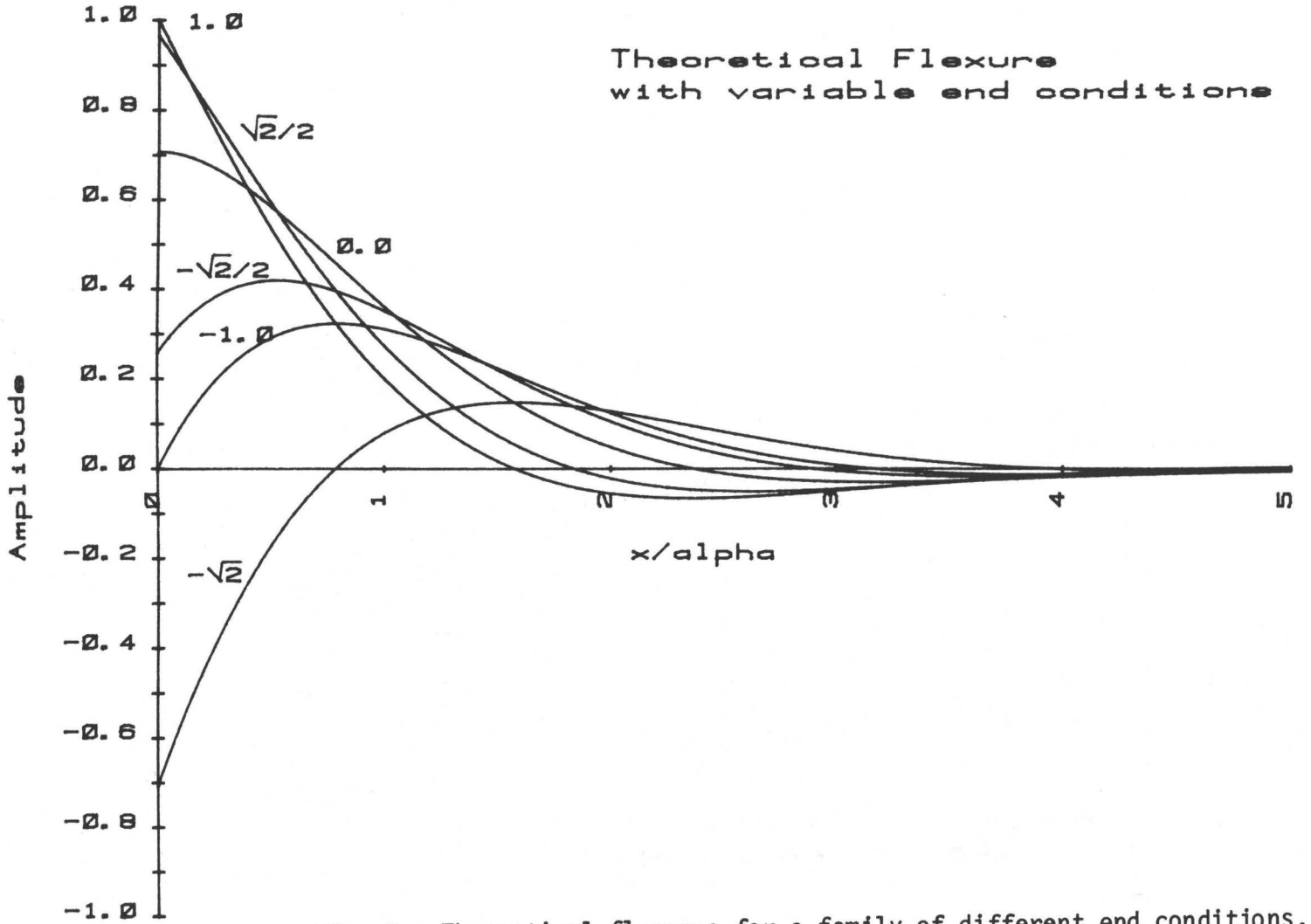

Fig. 5. Theoretical flexures for a family of different end conditions. Includes curves from Figs. 3 and 4. Numbers identifying curves refer to the value of the first derivative at the origin. Vertical exaggeration is 20:1.

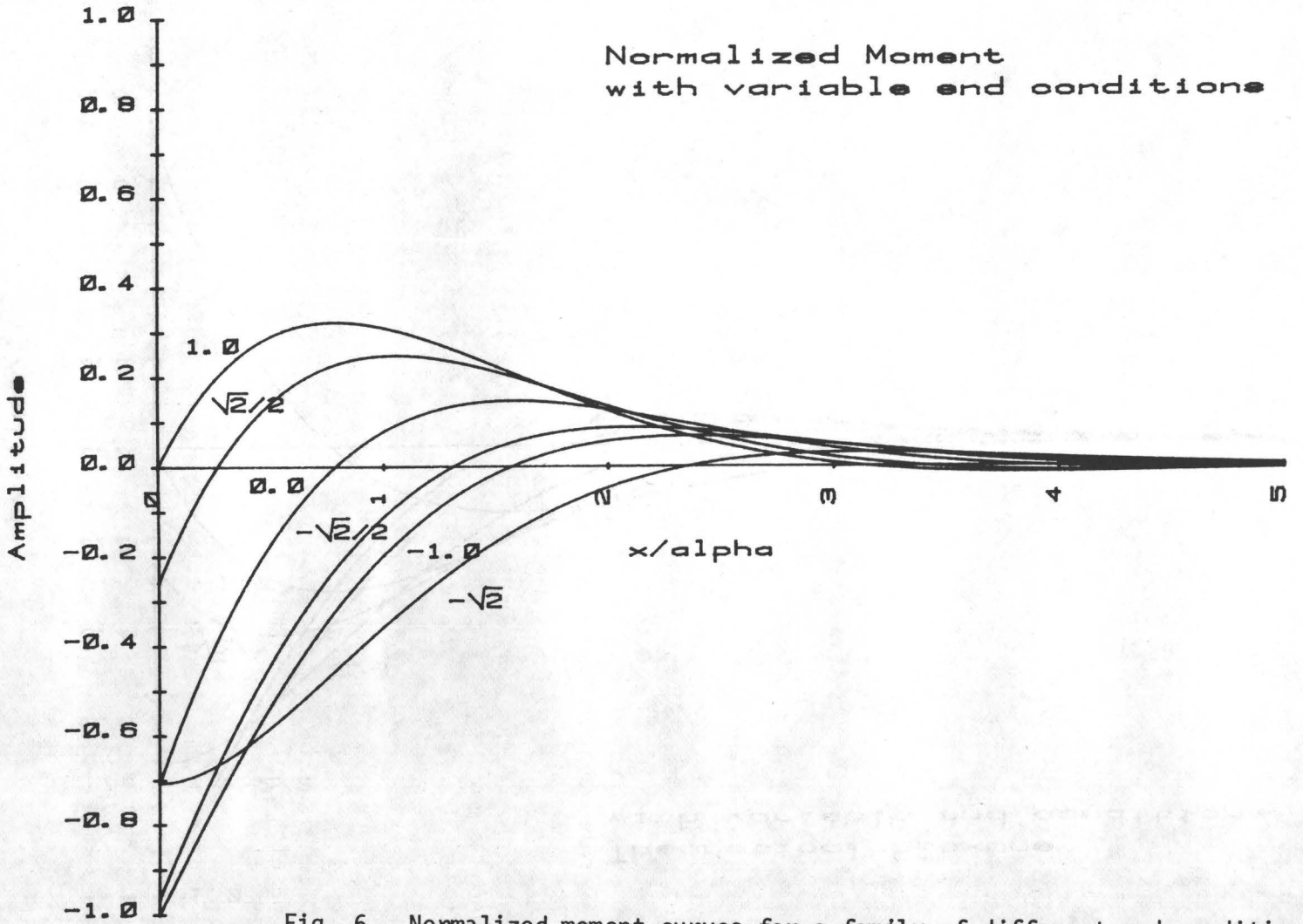

Fig. 6. Normalized moment curves for a family of different end conditions. Numbers identify corresponding curves in Fig. 5. Vertical exaggeration is 20:1.

999

(Crittenden, 1963, 1967; Walcott, 1970; Cathles, 1975). Crittenden's studies demonstrated that the rebound could be modelled by an elastic layer over a viscous half-space. His analysis indicated an elastic crustal thickness of only 10 km. Walcott's reanalysis of the same data showed that Crittenden's values provided a minimum estimate for the layer modulus (flexural rigidity) of 6×10^{21} newton-meters (nm). Walcott then provided a maximum estimate of 7×10^{22} nm, and a perferred value of 5×10^{22} nm. Using Poisson's ratio of 1/2 and Young's modulus between 5×10^{10} and 10^{11} n/m^2 in equation (2), Walcott showed the thickness of the elastic crust in the eastern Basin and Range is about 20 km. The other parameter required in equation (1) is the density of the substratum, ρ_s, which varies from 2800 kg/m^2 to 3300 kg/m^2 within the depth range of interest. With these numbers, the range in the parameter α is 30 - 50 km. Table 1 is a summary of the values assigned to constants used in this and following sections.

a) Basement Topography. Equation (3) represents the theoretical topography of Basin and Range mountain ranges (w_0 positive) and flanking valleys (w_0 negative). The real topography is complicated by preexisting topography, erosion, and deposition, and hence the comparison is not straightforward. Part of the difficulty is in specifying the end condition --different end conditions creating quite different profiles (Figure 5). However, as mentioned previously, even a minimal constraint on the end creates relatively large stresses near the end which would result in either slippage on the main fault or the creation of a new parallel fault. In either case the stress would be relieved and the end would become nearly, if not completely, unconstrained. Therefore, in the following the solution with $\phi = 0°$ is used for comparison.

Eardley's observations on the eastward tilting quoted in the introduction are correctly predicted by the model. Also the predicted tilting has been observed in several grabens in Oregon (Stewart, 1979), and reproduced in laboratory experiments (Figure 1-11 in Stewart, 1979). Although a more quantitative comparison is difficult due to the reasons mentioned above, it would be instructive, nonetheless, to compare some actual topographic profiles with a theoretical curve. Such a comparison is illustrated in Figure 7. The topographic profiles are taken from various locations perpendicular to the Wasatch Front. The theoretical curve is for $\phi = 0°$ and $\alpha = 32$ km. Considering the complicating factors, the match is satisfactory--at least east of the Wasatch fault. West of the Wasatch fault, the comparison is complicated by the sedimentary fill in the flanking valleys.

Another complicating factor is the partial development of graben and horst structures. Interpretation of gravity data (Cook and Berg, 1961) indicates that the flanking valleys west of the Wasatch range are partial grabens--bounded on the west by relatively small-displacement normal faults. The question of whether the Wasatch range is a horst depends on the reality of postulated faults in the "back valleys" of the range (Gilbert, 1928; Eardley, 1933). In both cases, however, the complementary faults are relatively minor and probably do not penetrate the entire elastic crust. If the complementary faults were through-going, the crust would become divided into independent blocks--rising and sinking until reaching

Table 1

Range and perferred values for parameters used in this paper

PARAMETER		RANGE	PERFERRED VALUE
Young's modulus	E	$5 \times 10^{10} - 1 \times 10^{11}$ n/m^2	1×10^{11} n/m^2
Poisson's ratio	ν	.25 - .50	.25
Layer thickness	h	10 - 20 km	20 km
Layer density	ρ_c	2600 - 2700 kg/m^2	2700 km/m^2
Substratum density	ρ_s	2800 - 3300 kg/m^2	2900 kg/m^2
Fault hade	θ	20° - 40°	30°
Layer modulus	N	$6 \times 10^{21} - 7 \times 10^{22}$ n-m	5×10^{22} n-m
Flexural Parameter	α	30 - 50 km	30 km
Isostatic force	p	$3 \times 10^{10} - 7 \times 10^{11}$ n	1×10^{11} n

g = 9.8 n/kg

1 bar = 10^5 n/m^2 = 10^6 dynes/cm^2

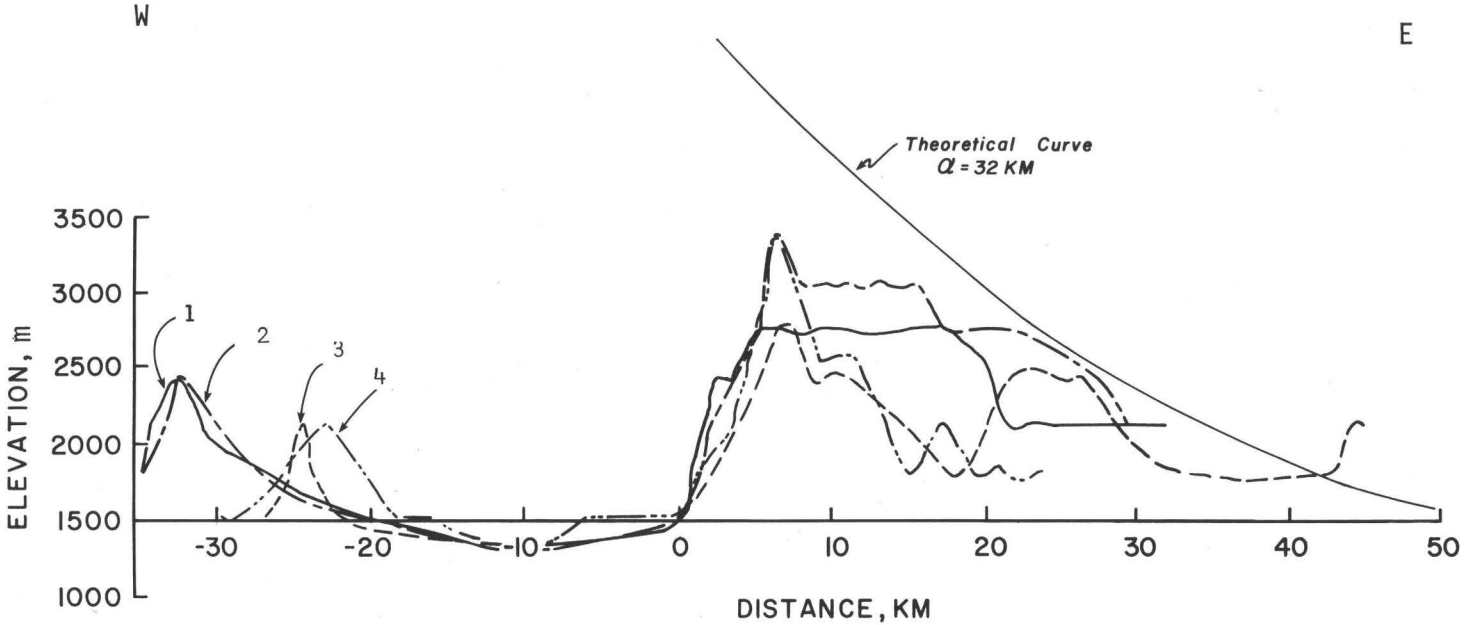

Fig. 7. Topographic profiles perpendicular to the Wasatch fault (fault at DISTANCE = 0). Numbers identify profiles named after major topographic feature on the profile: (1) Mr. Olympus profile; (2) Twin Peaks profile; (3) Bear Lake profile; (4) Mt. Timpanogos profile. Theoretical curve is displaced upward for clarity. Vertical exaggeration is 10:1.

isostatic equilibrium--resulting in a symmetrical graben and horst pair. The eastward tilt of both the mountain range and valley floor is evidence that either the complementary faults are minor, superficial features; or that they are young and represent the early stages of graben/horst forming faults. Either case is compatible with the model presented earlier.

b) Wavelength of Uplift/Subsidence Features. One method of overcoming the difficulty of comparing the observed and theoretical topography is to characterize the theoretical solution by some parameter that is easier to measure. The solution (3) is a damped cosine wave which can be characterized by the distance from the origin to the first zero: its quarter-wavelength referred to hereon as simply the wavelength. It is fixed by the flexural parameter α (equation 4) which is a function of the layer modulus N (equation 2). For the range in the value of α (30 to 50 km) the wavelength is $\pi\alpha/2$--that is the predicted widths of the mountain ranges and flanking valleys is 47 to 79 km. Another measure of the "width" is the theoretical graben width. Assuming faulting occurs at the point of maximum curvature, d^2w/dx^2, equation (6) and Figure 3 can be used to predict the resulting graben width as $\pi\alpha/4 \sim .80\alpha$. For the eastern Basin and Range the model predicts graben widths of 24 to 40 km.

Stewart (1978) stated in a review paper of Basin and Range structure that the mountain ranges are usually about 15 to 20 km across and are separated by alluviated valleys of comparable width. The regional gravity survey of the Wasatch Front by Cook and Berg (1961) delineated a structural trough more than 160 km in length comprising a belt of grabens between the Wasatch fault block to the east and a fault block to the west consisting of the Oquirrh Mountains, Boulter Ridge, and the East Tintic Mountains. From north to south the major grabens are the Farmington, Jordan (Salt Lake) Valley, Utah Valley, and Juab Valley grabens. The widths of these grabens range from about 8 km (Juab Valley) to 26 km (Salt Lake Valley). Hence, the elastic model predicts wavelengths of uplift/subsidence features in the correct range, although the predicted range is somewhat on the high side. A property of the elastic model is that the wavelength of the deflection curve is maintained as the amplitude grows. With this model, the only possible explanation for variations in graben widths is the variations of crustal parameters which influence the flexural parameter, α. We shall return to this point later and offer another viable explanation.

c) Total Amount of Uplift/Subsidence. Along with wavelength another characterization of the theoretical solution is the amplitude, w_o. If the flexure is due soley to isostatic forces, once isostatic equilibrium is reached, further movement on the fault will cease. Bott (1976) studied the case where the flexure induced further faulting and the formation of a graben-horst pair. His energy budget calculations showed that the maximum possible graben subsidence increased substantially with a sediment load and with the magnitude of the extensional forces acting on the crustal layer. The possible amount of subsidence is also greater for a narrower graben. For graben widths of 20 to 50 km--and ignoring the extreme models --Bott's calculations with sediment load have maximum graben subsidence

of 1.0 to 3.5 km. The amount of valley fill in the major grabens of the Great Basin range from a few hundred meters to over 3 km (Stewart, 1979). Total structural relief from the lowest bedrock units under the valleys to the highest adjacent mountains is generally from 2 to 5 km, although it is locally about 6 km (Stewart, 1979).

Bott's model, however, is not strictly applicable to the Wasatch Front where graben/horst structures are not completely developed. In order to compute the amplitude, w_o, the isostatic bouyancy force, p, must be computed. In equilibrium the bouyancy force of the lower, foot-wall block must equal the compensated weight of the upper, hanging-wall block (Figure 2B); hence (Heiskanen and Vening Meinesz, 1958)

$$p = \frac{1}{2} \frac{\rho_c}{\rho_s} (\rho_s - \rho_c) \, g \, h^2 \tan \theta \qquad (9)$$

where

ρ_c = crustal layer density

θ = hade (90° - dip) of the fault

Then the flexure, w, is related to p by

$$p = \rho_s g \int_{x=0}^{x=\infty} w dx \qquad (10)$$

Integration of equation (10) defines w_o,

$$w_o = \frac{2p}{\rho_s g \alpha} \qquad (11)$$

Using the parameters listed in Table 1, $p \sim 10^{11}$ n and the range of w_o is 140 m to 420 m. This is a minimum estimate because sediment loading and other possible forces were not considered. Even so, the model appears to severely underestimate the amplitude of uplift and subsidence along the Wasatch Front where total uplift and subsidence are an order of magnitude greater.

d) Stress Distribution and Magnitudes. As stated in the introduction, the primary purpose of this study was to analyze the flexure model as a stress-generating mechanism which could explain some of the perplexing features of the seismicity along the Wasatch Front. The evidence discussed so far, while far from conclusive, does suggest that elastic bending on both sides of a crustal-penetrating normal fault is at least a plausible mechanism to stress the region around the fault. Let us now consider some of the implications for the seismicity.

Seismicity on the major (through-going) normal fault is controlled by the interplay of three major forces. The regional extensional tectonic stress controls the extension rate of the brittle layer. The isostatic forces work in the vertical direction producing flexure in opposite directions on either side of the fault, and the frictional force on the fault surface resists the flexure. Major earthquakes on the fault occur sporadically as the tectonic and isostatic forces briefly overcome the friction. When the fault locks, the extensional forces build up until the fault slips again. Eventually the deflection increases to the point where bending stresses within the flexured crust become significant. The magnitude of the bending stresses peak at $x = \frac{\pi}{4}\alpha$ from the fault, but the peak is broad (see Figure 3) and may manifest itself as a broad zone of seismicity. Broad zones of seismicity centered near the predicted distance of 24-39 km (using α = 30 to 50 km) east and west of the Wasatch fault do exist (Figure 1). The reason for the lower intensity of the activity to the west may be related to the development of complementary, graben-forming faults. With the development of major, through-going faults, the seismicity may become more localized and sporadic.

The thin-plate model also predicts a vertically varying distribution of stress. Because of the neutral surface in the middle of the thin plate, stresses above and below will be equal and opposite in sign. For the Wasatch fault, the shallow seismicity to the east should be predominantly reverse faulting, while a deeper zone consists of normal faulting. To the west, the opposite should occur. A bimodal distribution of focal depths does exist for the Wasatch Front. A histogram of accurately determined focal depths peak at depths of 1-2 km and 7-9 km with a central minimum at 5 km (Arabasz et al., 1979). Focal mechanisms for the Wasatch Front include both normal and reverse faulting mechanisms (Arabasz et al., 1979), but the former predominate. The reverse faulting mechanisms may be confined to an area east of the Salt Lake Valley and be related to the intersection of the Wasatch Front and the Uinta Mountains. From the available fault-plane solutions there is no indication of the predicted depth separation of mechanism. However, at the present time, not enough focal mechanisms are available to make a definite conclusion. More precisely located mechanisms--as well as other source parameters such as moment and stress drop--are obviously crucial to further understanding of earthquake generating stresses on the Wasatch Front.

The magnitudes of the bending stresses caused by flexure can be calculated using equations (7) and (8). Combining equations (6), (7), (8), and (11) provides a simple expression for the maximum stress for a given load, p: $\sigma_{max} = 1.93\ \alpha\ p/h^2$. For the calculated isostatic force of 10^{11} n which produces an estimated 140-420 m of uplift, the induced bending stress is 140-240 bars. This magnitude of stress is probably sufficient to induce the flanking seismicity observed to the east of the Wasatch fault. However, the actual uplift is thought to be an order of magnitude greater than the calculated uplift. The corresponding stresses would then also be an order of magnitude greater; that is, in the kilobar range.

Limitations of Model

In summary, the major limitations of the elastic model are its overestimation of wavelength, underestimation of amplitude, and possibly overestimation of the magnitude of the stresses. The theoretical wavelengths are not greatly in error; however, in order to match the shorter observed wavelengths anomalous values would need to be assigned for some of the crustal parameters. Even more difficult to explain is the large variability in the observed wavelengths which would require correspondingly large variability in some of the crustal parameters.

The estimation of amplitude is closely related to the calculated bending stress magnitudes. Isostatic forces alone appear to be insufficient to produce the amount of uplift observed in the Wasatch mountains. On the other hand, given the amount of uplift (2-4 km), the magnitude of the bending stresses east of the Wasatch should be in the kilobar range (compressive near the surface and tensional near the bottom of the 20 km thick crustal layer). Because of the difficulty of measuring tectonic stress it is not known if such large tectonic stresses actually exist; however, the degree of seismicity observed probably could be explained by tectonic stress levels of an order of magnitude less.

The deficiencies of the elastic model are such as to suggest a viscoelastic model. The necessary modifications are described and analyzed in the following section.

VISCOELASTIC MODEL

The flexure, w, of a viscoelastic layer resting on a substratum that responds with bouyancy forces is determined from the differential equation (Nadai, 1963):

$$N \frac{d^4\dot{w}}{dx^4} = -\rho_s g \dot{w} + \frac{w}{t_e} + \dot{p} + \frac{p}{t_e} \qquad (12)$$

$$t_e = \frac{3\mu}{E} \qquad \text{Maxwell time constant} \qquad (13)$$

where μ = viscosity coefficient and the dot over the variable represents the time derivative. The general solution is (Nadai, 1963):

$$w = w_o e^{t/t_o} e^{-x/\lambda} \cos(x/\lambda + \phi) \tag{14}$$

$$t_o = (\beta - 1)t_e \tag{15}$$

$$\beta = \frac{4N}{\rho_s g \lambda^4} \tag{16}$$

The parameter λ is a measure of the wavelength of the flexure and is related at time $t = O(\lambda_o)$ to the flexural parameter α,

$$\lambda_o = \alpha \tag{17}$$

With equation (17) the parameter β can be rewritten,

$$\beta = (\lambda_o/\lambda)^4 \tag{18}$$

Examination of equations (14), (15), and (18) shows that under loading: $\beta>1$, t_o is positive and the deflections increase in amplitude and decrease in wavelength. For unloading: $0<\beta<1$, t_o is negative and the deflections decrease in amplitude and increase in wavelength. Hence, under a positive load p, the uplift increases in height and becomes narrower while the adjoining region on the flank is lowered and bulges down in a gentle valley.

Walcott (1970) demonstrated that it is possible to obtain an adequate match for the viscoelastic flexure with an elastic flexure with an appropriate "apparent" flexural parameter. Figure 8 is from Walcott's 1970 paper and is a plot of the change in apparent flexural parameter (α) against time where α_o now refers to the elastic flexural parameter. Because the flexures cannot be matched exactly, two curves are plotted: one on the basis of amplitude and the other on the basis of wavelength. The difference is insignificant within the context of the available data.

The implication of the curves in Figure 8 is that the value for α estimated from the Lake Bonneville data is in fact a value for the apparent flexural parameter. The characteristic (loading) time for Lake Bonneville is 10^4 yrs, and the time constant, t_e, for the continental lithosphere is 10^5 yrs (Walcott, 1970). The last figure, however, is probably an upper bound for the Basin and Range which is anomalous in almost all other parameters. Hence, t/t_e for Lake Bonneville lies somewhere between 10^{-1} and 10. That means the measured apparent flexural parameter is nearly the elastic flexural parameter. For the Wasatch Front, the characteristic loading time is 10^7 yrs, thus, t/t_e is a minimum of 100. Therefore, the value of α for the Wasatch Front problem should be .3 to .7 of the value obtained from the Lake Bonneville data (Figure 8). The maximum bounds on α for the Wasatch Front problem is reduced to 10 to 35 km and the corresponding bounds on amplitudes and wavelengths calculated in the previous

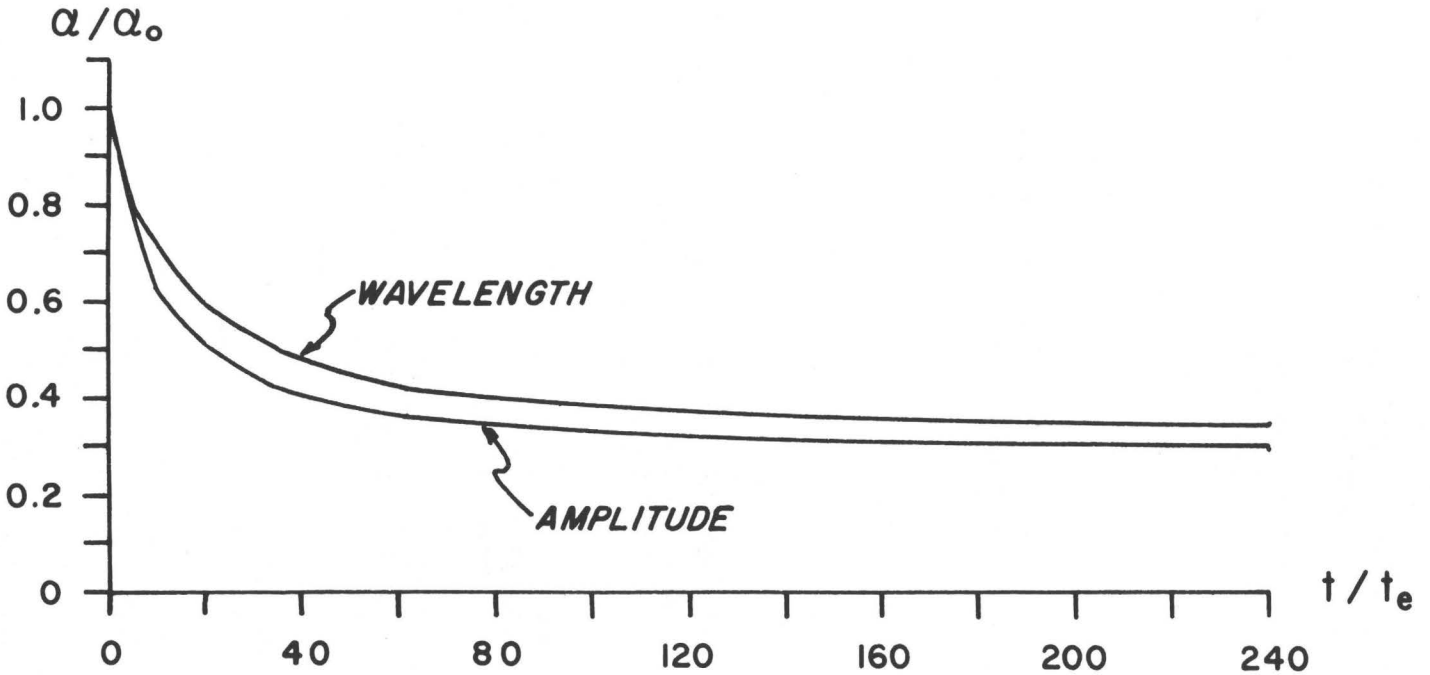

Fig. 8. Change in apparent flexural parameter against time. α_o is the elastic flexural parameter and t_e is the Maxwell time constant. The upper and lower curves are matches with the wavelength and amplitude, respectively of an equivalent elastic flexure (from Walcott, 1970).

section are changed. For example, predicted graben widths are now 8 to 28 km--much more in line with the observations. Maximum amplitudes are increased by as much as 3.3; so the maximum value for w_o computed for the purely elastic model is increased to about 1.4 km. Sediment loading would further increase the maximum amplitude.

Walcott (1970b) derived an amplification factor γ based on the loading of a harmonically varying topography, cos kx, by sediments of density ρ_a,

$$\gamma = \frac{Nk^4 + \rho_s g}{Nk^4 + (\rho_s - \rho_a)g} \qquad (19)$$

where $k = 2\pi/\text{wavelength}$. Applying this formula to the present case, a quarter-wavelength is equal to $(\pi/2)\alpha$, then $k = 1/\alpha$. Equation (19) simplifies to,

$$\gamma = \frac{5\rho_s}{5\rho_s - 4\rho_a} \qquad (20)$$

Using $\rho_a = 2.5$ g/cm^2 and $\rho_s = 2.9$ g/cm^2, $\gamma = 3.2$. Hence, sediment loading can increase maximum subsidence to nearly 4.5 km. The subsidence is likely to induce flow towards the uplift in the underlying substratum as depicted in Figure 2C. Perhaps such a flow can act as a mechanism for increasing the maximum uplift.

The viscoelastic model also provides a mechanism for producing major flexural structures in the crust without rupturing it with a major fault. The mechanism is relaxation. For a constant load, after enough time has passed--which depends on t_e--the stresses are dissipated and the deflected position becomes permanent. If the Wasatch range was uplifted episodically such that relaxation occurred at intervals, the total uplift need not have induced kilobars of stress on the flanks as predicted by the elastic model.

DISCUSSION

The eastern Basin and Range lithosphere behaves like a viscoelastic crust resting on a substratum that responds with bouyancy forces. Under regional extensional forces the brittle "crust" is penetrated by a through-going normal fault inducing isostatic forces which produce upward flexure of the footwall side and downward flexure of the hanging wall side. The upward flexure creates the Wasatch Mountains and the downward flexure becomes the site of the flanking alluvial valleys. During the initial, elastic portion of the flexure, bending stresses accumulate in a broad zone cenetered 10-30 km away from the main fault, causing small to

moderate size earthquakes. After 10^4-10^5 yrs the crust starts to behave viscously and the bending stresses and corresponding seismicity start to decay. If uplift occurs episodically on the Wasatch fault, there will be a cycle of generation and decay of the bending stresses. Interpreting the observed flanking seismicity in terms of this model indicates the uplifted crustal limb is currently behaving elastically. Hence, the Wasatch range is in an active uplift episode.

While still very speculative, the suggestion of a causal relationship between flanking seismicity and movement on the main Wasatch fault is an exciting concept. Similar relationships have been postulated along some plate boundaries (e.g. Kanamori, 1971). The intraplate setting of the Wasatch Front obscures the tectonic picture but there are some other similarities to a plate boundary. As in convergent plate boundaries the Wasatch fault appears segmented (Swan et al., 1978; Arabasz et al., 1979). The Wasatch fault is also characterized by seismic gaps (Figure 1)--although these are more accurately termed microseismic gaps. Because of the long recurrence intervals for large earthquakes (M>7) in the Wasatch Front area, the existence of gaps for large earthquakes can only be determined by trenching. However, the microseismic gaps may behave in a similar manner to plate boundary seismic gaps--identifying segments of the fault most likely to break next. On the other hand, if the microseismicity is a manifestation of bending stresses, the microseismic gaps may indicate fault segments which are unconstrained either because there is no uplift or the uplift is occurring aseismically (by creep). Whereas segments characterized by activity on or near the Wasatch fault may be an indication of a constrained segment which is accumulating strain on the fault. If such is the case, then the microseismic gaps would represent the "safest" segments of the fault. The resolution of the significance of the microearthquake gaps is obviously crucial to earthquake hazards evaluation along the Wasatch Front.

The mechanism described in this paper for earthquake-generating stress along the Wasatch Front is presented as a working hypothesis to be tested along with other hypotheses. The model is a simple one which can be extended once enough data are available to warrant it. One improvement would be to include the thermal aspects of uplift and subsidence. The importance of thermal stresses in generating earthquakes along the Wasatch Front is still one of many unanswered questions.

ACKNOWLEDGMENTS

I thank R. B. Smith and W. J. Arabasz for introducing me to the tectonics of the Wasatch Front and providing the opportunity to work on this project. K. Furlong listened with a critical ear to many of my early half-baked ideas. Discussions with R. Bruhn, D. Chapman, K. Furlong, and T. Owens on an earlier manuscript helped to improve this paper. Mardrene Robinson and Donna Leavitt typed the manuscript. This research was supported by the U.S. Department of the Interior, Geological Survey, Contract No. 14-08-0001-16725 as part of the Earthquake Hazards Reduction Program.

REFERENCES

Arabasz, W. J., Smith, R. B. Richins, W. D. Earthquake Studies Along the Wasatch Front, Utah: Network Monitoring, Seismicity, and Seismic Hazards, in this volume, 1979.

Berg, J. W., K. L. Cook, H. D. Narans, and W. M. Dolan. Seismic Investigation of Crustal Structure in the Eastern Part of the Basin and Range Province, BSSA, v. 50, p. 511-535. 1960.

Bott, M. H. P. Formation of Sedimentary Basins of Graben Type by Extension of the Continental Crust, Tectonophysics, 36, p. 77-86. 1976.

Braile, L. W., R. B. Smith, G. R. Keller, R. M. Welch, and R. P. Meyer. Crustal Structure Across the Wasatch Front From Detailed Seismic Refraction Studies. JGR, v. 79, p. 2669-2677. 1974.

Bucknam, R. C. and Anderson, R. E. Estimation of fault-scarp ages from a scarp-height-slope-angle relationship, Geology, v. 7, p. 11-14. 1979.

Cathles, L. M., III. Viscosity of the Earth's Mantle. Princton Univ. Press. 386 pp. 1975.

Cook, K. L., and Berg, Jr., J. W. Regional Gravity Survey Along the Central and Southern Wasatch Front, Utah, USGS Prof. Paper 316-E, p. 75-89, 1961.

Crittenden, M. D., Jr. Effective Viscosity of the Earth Derived from Isostatic Loading of Pleistocene Lake Bonneville. J.G.R. v. 68, p. 5517-5530. 1963.

Crittenden, M. D., Jr. General Geology of Salt Lake County, in Geology of Salt Lake County, Utah Geological and Mineralogical Survey, Bull. 69, p. 11-48. 1964.

Crittenden, M. D., Jr. Viscosity and Finite Strength of the Mantle as Determined from Water and Ice Loads, Geophys. J. R. Astron. Soc., v. 14, p. 261-279. 1967.

Davis, W. M. Mountain Ranges of the Great Basin, Harvard Coll. Mus. Comp. Zool. Bull. v. 42, p. 129-174. 1903.

Eardley, A. J. Strong Relief Before Block Faulting in the Vicinity of the Wasatch Mountains, Utah. Jour. Geology, v. 41, p. 243-267. 1933.

Gilbert, G. K. Studies of Basin-Range structure, USGS Prof. Paper 153, 89 p. 1928.

Hamblin, W. K. Patterns of displacement along the Wasatch fault, Geology 4, 619-622. 1976.

Hanks, T. C. The Kuril trench - Hokkaido rise system: Large shallow earthquakes and simple models of deformation. Geophys. J. Roy-Astron. Soc., v. 23, p. 173-189, 1971.

Heiskanen, W. A. and Vening Meinesz, F. A. The Earth and Its Gravity Field, McGraw-Hill Book Co., Inc. 470 pp. 1958.

Kanamori, H. Relation Between Tectonic Stress, Great Earthquakes and Earthquake Swarms. Tectonophysics, v. 14, p. 1-12. 1972.

Keller, G. R., R. B. Smith, and L. W. Braile. Crustal structure along the Great Basin-Colorado Transition from seismic refraction profiling, JGR, 80, p. 1093-1098. 1975.

Nadai, A. Theory of flow and fracture of solids. McGraw-Hill Book Company, Inc. 348 pp. 1963.

Naeser, C. W., Bryant, B. R., Crittenden, M. D., and Sorenson, M. L. Fission-track dating in the Wasatch Mountains, Utah: An uplift study. In this volume. 1979.

Schwartz, D. P., F. H. Swan, III, K. L. Hanson, P. L. Knuepfer, and L. S. Cluff. Recurrence of surface faulting and large magnitude earthquakes along the Wasatch fault zone near Provo, Utah, (abstract), Geol. Soc. Am. Abstracts with Programs, v. 11, p. 301, 1979.

Smith, R. B., Braile, L. W., and Keller, G. R., Upper Crustal Low-Velocity Layers: Possible Effect of High Temperatures Over a Mantle Upwarp at the Basin Range-Colorado Plateau Transition. Earth & Planet, Sci. Lett., v. 28, p. 197-204. 1975.

Stewart, J. H. Basin-range structure in western North America: A review, in Cenozoic Tectonics and Regional Geophysics of the Western Cordillera, R. B. Smith and G. P. Eaton, eds., Memoir 152, Geol. Soc. Am., 107-110. 1978.

Swan, F. H., III, D. P. Schwartz, K. L. Hanson, P. L. Kneupfer, and L. S. Cluff. Recurrence of surface faulting and large mangitude earthquakes along the Wasatch fault, Utah (abstract), EOS, Trans. Am. Geophys. Union, v. 59, p. 1126. 1978.

Timoshenko, S. and Woinowsky-Krieger, S. Theory of Plates and Shells, McGraw-Hill Book Co., Inc., 580 pp. 1959.

Walcott, R. I. Flexural Rigidity, Thickness, and Viscosity of the Lithosphere. JGR, v. 75, p. 3941-3954. 1970.

Walcott, R. I. An isostatic origin for basement uplifts, Can. J. of Earth Sciences, v. 7, p. 1-7. 1970b.

Watts, A. B., and Ryan, W. B. F. Flexure of the lithosphere and continental margin basins. Tectonophysics, v. 36, p. 25-44. 1976.